Scientific and Technical Aerospace Reports

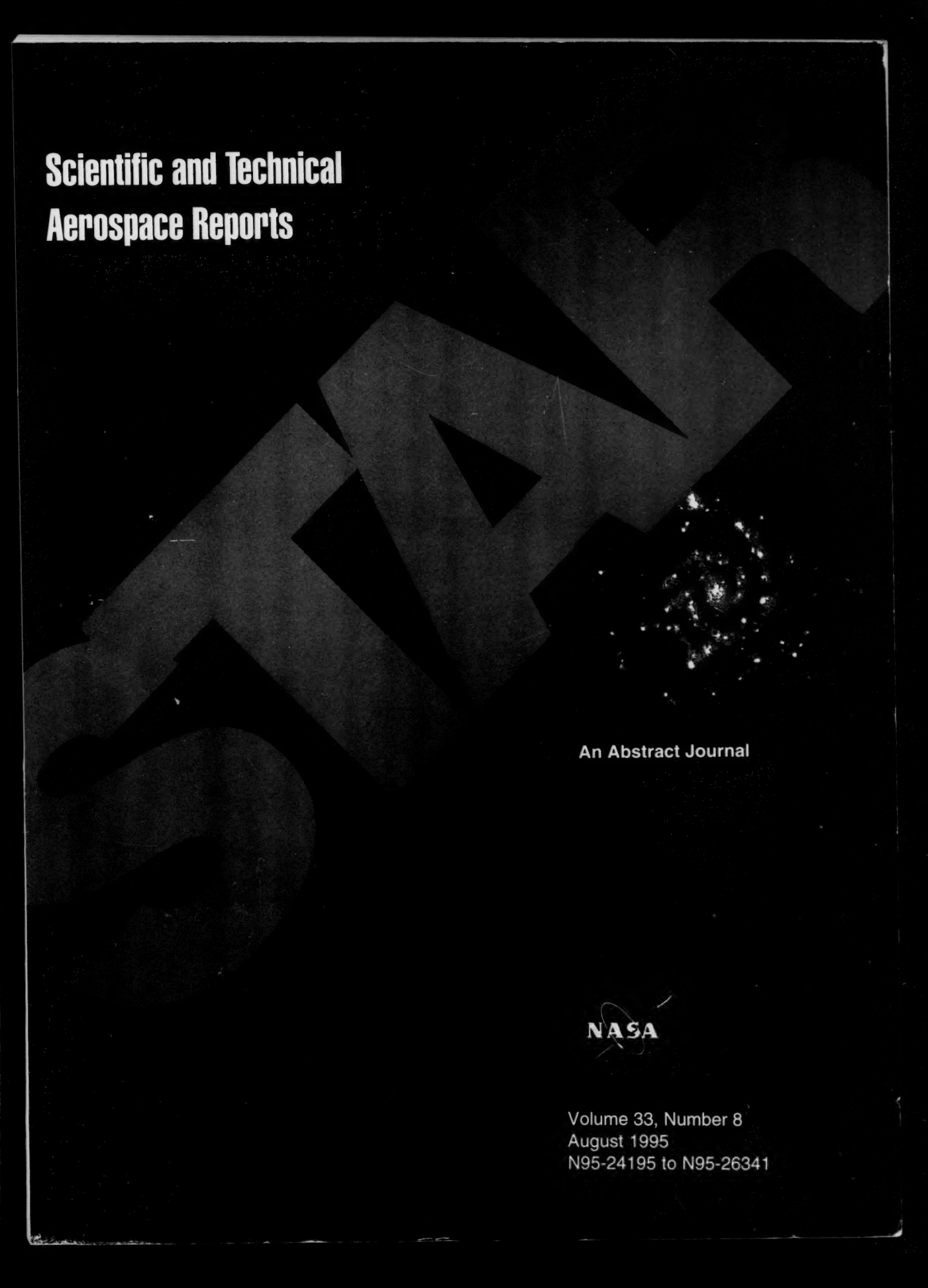

An Abstract Journal

NASA

Volume 33, Number 8
August 1995
N95-24195 to N95-26341

The NASA STI Office ... in Profile

Since its founding, NASA has been dedicated to the advancement of aeronautics and space science. The NASA Scientific and Technical Information (STI) Office plays a key part in helping NASA maintain this important role.

The NASA STI Office provides access to the NASA STI Database, the largest collection of aeronautical and space science STI in the world. The Office is also NASA's institutional mechanism for disseminating the results of its research and development activities.

Specialized services that help round out the Office's diverse offerings include creating custom thesauri, translating material to or from 34 foreign languages, building customized databases, organizing and publishing research results ... even providing videos.

For more information about the NASA STI Office, you can:

- **Phone** the NASA Access Help Desk at (301) 621-0390
- **Fax** your question to the NASA Access Help Desk at (301) 621-0134
- **E-mail** your question via the **Internet** to help@sti.nasa.gov
- **Write** to:

NASA Access Help Desk
NASA Center for AeroSpace Information
800 Elkridge Landing Road
Linthicum Heights, MD 21090-2934

Scientific and Technical Aerospace Reports

Scientific and Technical Aerospace Reports (STAR), is published each month as a major product of the NASA Scientific and Technical Information (STI) Office.

Inside this issue you will find:

- **Front Matter** containing a typical citation and abstract sample explaining the standard format, including codes for ordering reports
- **An Abstract Section** containing citations and abstracts of reports and publications that provide comprehensive coverage of worldwide aerospace-related topics including aeronautics and space science technology. *STAR* lists published and publicly available reports entered into the NASA STI Database during the four weeks preceding publication of this issue. These citations and abstracts are listed by subject categories.
- **An Index Section**
  - Subject
  - Personal author
  - Corporate source
  - Contract number
  - Report number
- **An Appendix** containing a guide for ordering cited reports, registering with the NASA STI Office, and using the available products and services. Additionally, price schedules, phone numbers, and addresses are included in this information packed section.

NASA also sponsors the companion journal, *NASA Open Volumes on Aerospace (NOVA)*, which lists abstracts of the open literature on aerospace subjects available worldwide. *NOVA* is for internal NASA use only, available from the NASA Center for AeroSpace Information (CASI).

Entries found in *STAR* are available through the NASA online retrieval service, RECON.

The NASA STI Office gathers information through national and international agreements and exchanges and makes this information available to the NASA community and to the public in many forms through various outlets.

For additional information on the NASA STI Office, call the NASA Access Help Desk at (301) 621-0390, or write to:

NASA Center for AeroSpace Information
800 Elkridge Landing Road
Linthicum Heights, Maryland 21090-2934

US ISSN 0036-8741

The New NASA Video Catalog is Here

Free!

To order your free copy call
the NASA Access Help Desk at
(301) 621-0390 or
fax to (301) 621-0134 or
e-mail to helpdesk@sti.nasa.gov

EXPLORE THE UNIVERSE

This publication was prepared by the NASA Center for AeroSpace Information,
800 Elkridge Landing Road, Linthicum Heights, MD 21090-2934, (301) 621-0390.

Volume 33 Number 8 / August 1995

TABLE OF CONTENTS

AERONAUTICS For related information see also *Astronautics.*

01 AERONAUTICS (GENERAL) **1905**

02 AERODYNAMICS **1906**
Includes aerodynamics of bodies, combinations, wings, rotors, and control surfaces; and internal flow in ducts and turbomachinery. For related information see also *34 Fluid Mechanics and Heat Transfer.*

03 AIR TRANSPORTATION AND SAFETY **1908**
Includes passenger and cargo air transport operations; and aircraft accidents. For related information see also *16 Space Transportation* and *85 Urban Technology and Transportation.*

04 AIRCRAFT COMMUNICATIONS AND NAVIGATION **1910**
Includes digital and voice communication with aircraft; air navigation systems (satellite and ground based); and air traffic control. For related information see also *17 Space Communications, Spacecraft Communications, Command and Tracking* and *32 Communications and Radar.*

05 AIRCRAFT DESIGN, TESTING AND PERFORMANCE **1910**
Includes aircraft simulation technology. For related information see also *18 Spacecraft Design, Testing and Performance* and *39 Structural Mechanics.* For land transportation vehicles see *85 Urban Technology and Transportation.*

06 AIRCRAFT INSTRUMENTATION **1912**
Includes cockpit and cabin display devices; and flight instruments. For related information see also *19 Spacecraft Instrumentation* and *35 Instrumentation and Photography.*

07 AIRCRAFT PROPULSION AND POWER **1913**
Includes prime propulsion systems and systems components, e.g., gas turbine engines and compressors; and onboard auxiliary power plants for aircraft. For related information see also *20 Spacecraft Propulsion and Power, 28 Propellants and Fuels,* and *44 Energy Production and Conversion.*

08 AIRCRAFT STABILITY AND CONTROL **1914**
Includes aircraft handling qualities; piloting; flight controls; and autopilots. For related information see also *05 Aircraft Design, Testing and Performance.*

09 RESEARCH AND SUPPORT FACILITIES (AIR) **1915**
Includes airports, hangars and runways; aircraft repair and overhaul facilities; wind tunnels; shock tubes; and aircraft engine test stands. For related information see also *14 Ground Support Systems and Facilities (Space).*

ASTRONAUTICS For related information see also *Aeronautics.*

12 ASTRONAUTICS (GENERAL) **1915**
For extraterrestrial exploration see *91 Lunar and Planetary Exploration.*

13 ASTRODYNAMICS ..... **N.A.**
Includes powered and free-flight trajectories; and orbital and launching dynamics.

14 GROUND SUPPORT SYSTEMS AND FACILITIES (SPACE) ..... **N.A.**
Includes launch complexes, research and production facilities; ground support equipment, e.g., mobile transporters; and simulators. For related information see also *09 Research and Support Facilities (Air).*

15 LAUNCH VEHICLES AND SPACE VEHICLES **1918**
Includes boosters; operating problems of launch/space vehicle systems; and reusable vehicles. For related information see also *20 Spacecraft Propulsion and Power.*

16 SPACE TRANSPORTATION **1918**
Includes passenger and cargo space transportation, e.g., shuttle operations; and space rescue techniques. For related information see also *03 Air Transportation and Safety* and *18 Spacecraft Design, Testing and Performance.* For space suits see *54 Man/System Technology and Life Support.*

17 SPACE COMMUNICATIONS, SPACECRAFT COMMUNICATIONS, COMMAND AND TRACKING **1920**
Includes telemetry; space communications networks; astronavigation and guidance; and radio blackout. For related information see also *04 Aircraft Communications and Navigation* and *32 Communications and Radar.*

N.A.—No abstracts were assigned to this category for this issue.

18 SPACECRAFT DESIGN, TESTING AND PERFORMANCE 1920
Includes satellites; space platforms; space stations; spacecraft systems and components such as thermal and environmental controls; and attitude controls. For life support systems see *54 Man/System Technology and Life Support.* For related information see also *05 Aircraft Design, Testing and Performance*, *39 Structural Mechanics*, and *16 Space Transportation.*

19 SPACECRAFT INSTRUMENTATION ..... N.A.
For related information see also *06 Aircraft Instrumentation* and *35 Instrumentation and Photography.*

20 SPACECRAFT PROPULSION AND POWER 1921
Includes main propulsion systems and components, e.g., rocket engines; and spacecraft auxiliary power sources. For related information see also *07 Aircraft Propulsion and Power*, *28 Propellants and Fuels*, *44 Energy Production and Conversion*, and *15 Launch Vehicles and Space Vehicles.*

CHEMISTRY AND MATERIALS

23 CHEMISTRY AND MATERIALS (GENERAL) 1923

24 COMPOSITE MATERIALS 1925
Includes physical, chemical, and mechanical properties of laminates and other composite materials. For ceramic materials see *27 Nonmetallic Materials.*

25 INORGANIC AND PHYSICAL CHEMISTRY 1928
Includes chemical analysis, e.g., chromatography; combustion theory; electrochemistry; and photochemistry. For related information see also *77 Thermodynamics and Statistical Physics.*

26 METALLIC MATERIALS 1933
Includes physical, chemical, and mechanical properties of metals, e.g., corrosion; and metallurgy.

27 NONMETALLIC MATERIALS 1939
Includes physical, chemical, and mechanical properties of plastics, elastomers, lubricants, polymers, textiles, adhesives, and ceramic materials. For composite materials see *24 Composite Materials.*

28 PROPELLANTS AND FUELS 1947
Includes rocket propellants, igniters and oxidizers; their storage and handling procedures; and aircraft fuels. For related information see also *07 Aircraft Propulsion and Power*, *20 Spacecraft Propulsion and Power*, and *44 Energy Production and Conversion.*

29 MATERIALS PROCESSING 1949
Includes space-based development of products and processes for commercial application. For biological materials see *55 Space Biology:*

ENGINEERING For related information see also *Physics.*

31 ENGINEERING (GENERAL) 1950
Includes vacuum technology; control engineering; display engineering; cryogenics; and fire prevention.

32 COMMUNICATIONS AND RADAR 1951
Includes radar; land and global communications; communications theory; and optical communications. For related information see also *04 Aircraft Communications and Navigation* and *17 Space Communications, Spacecraft Communications, Command and Tracking.* For search and rescue see *03 Air Transportation and Safety*, and *16 Space Transportation.*

33 ELECTRONICS AND ELECTRICAL ENGINEERING 1956
Includes test equipment and maintainability; components, e.g., tunnel diodes and transistors; microminiaturization; and integrated circuitry. For related information see also *60 Computer Operations and Hardware* and *76 Solid-State Physics.*

34 FLUID MECHANICS AND HEAT TRANSFER 1961
Includes boundary layers; hydrodynamics; fluidics; mass transfer and ablation cooling. For related information see also *02 Aerodynamics* and *77 Thermodynamics and Statistical Physics.*

35 INSTRUMENTATION AND PHOTOGRAPHY 1966
Includes remote sensors; measuring instruments and gauges; detectors; cameras and photographic supplies; and holography. For aerial photography see *43 Earth Resources and Remote Sensing.* For related information see also *06 Aircraft Instrumentation* and *19 Spacecraft Instrumentation.*

36 LASERS AND MASERS 1971
Includes parametric amplifiers. For related information see also *76 Solid-State Physics.*

37 MECHANICAL ENGINEERING **1974**
Includes auxiliary systems (nonpower); machine elements and processes; and mechanical equipment.

38 QUALITY ASSURANCE AND RELIABILITY **1978**
Includes product sampling procedures and techniques; and quality control.

39 STRUCTURAL MECHANICS **1979**
Includes structural element design and weight analysis; fatigue; and thermal stress. For applications see *05 Aircraft Design, Testing and Performance* and *18 Spacecraft Design, Testing and Performance.*

GEOSCIENCES For related information see also *Space Sciences.*

42 GEOSCIENCES (GENERAL) **1987**

43 EARTH RESOURCES AND REMOTE SENSING **1988**
Includes remote sensing of earth resources by aircraft and spacecraft; photogrammetry; and aerial photography. For instrumentation see *35 Instrumentation and Photography.*

44 ENERGY PRODUCTION AND CONVERSION **1990**
Includes specific energy conversion systems, e.g., fuel cells; global sources of energy; geophysical conversion; and windpower. For related information see also *07 Aircraft Propulsion and Power, 20 Spacecraft Propulsion and Power,* and *28 Propellants and Fuels.*

45 ENVIRONMENT POLLUTION **1996**
Includes atmospheric, noise, thermal, and water pollution.

46 GEOPHYSICS **2003**
Includes aeronomy; upper and lower atmosphere studies; ionospheric and magnetospheric physics; and geomagnetism. For space radiation see *93 Space Radiation.*

47 METEOROLOGY AND CLIMATOLOGY **2005**
Includes weather forecasting and modification.

48 OCEANOGRAPHY **2006**
Includes biological, dynamic, and physical oceanography; and marine resources. For related information see also *43 Earth Resources and Remote Sensing.*

LIFE SCIENCES

51 LIFE SCIENCES (GENERAL) **2007**

52 AEROSPACE MEDICINE **2009**
Includes physiological factors; biological effects of radiation; and effects of weightlessness on man and animals.

53 BEHAVIORAL SCIENCES **2012**
Includes psychological factors; individual and group behavior; crew training and evaluation; and psychiatric research.

54 MAN/SYSTEM TECHNOLOGY AND LIFE SUPPORT **2013**
Includes human engineering; biotechnology; and space suits and protective clothing. For related information see also *16 Space Transportation.*

55 SPACE BIOLOGY ..... **N.A.**
Includes exobiology; planetary biology; and extraterrestrial life.

MATHEMATICAL AND COMPUTER SCIENCES

59 MATHEMATICAL AND COMPUTER SCIENCES (GENERAL) **2014**

60 COMPUTER OPERATIONS AND HARDWARE **2015**
Includes hardware for computer graphics, firmware, and data processing. For components see *33 Electronics and Electrical Engineering.*

61 COMPUTER PROGRAMMING AND SOFTWARE **2015**
Includes computer programs, routines, algorithms, and specific applications, e.g., CAD/CAM.

62 COMPUTER SYSTEMS **2019**
Includes computer networks and special application computer systems.

63 CYBERNETICS **2022**
Includes feedback and control theory, artificial intelligence, robotics and expert systems. For related information see also *54 Man/System Technology and Life Support.*

64 NUMERICAL ANALYSIS **2027**
Includes iteration, difference equations, and numerical approximation.

65 STATISTICS AND PROBABILITY **2035**
Includes data sampling and smoothing; Monte Carlo method; and stochastic processes.

66 SYSTEMS ANALYSIS **2035**
Includes mathematical modeling; network analysis; and operations research.

67 THEORETICAL MATHEMATICS **2036**
Includes topology and number theory.

PHYSICS For related information see also *Engineering.*

70 PHYSICS (GENERAL) **2037**
For precision time and time interval (PTTI) see *35 Instrumentation and Photography*; for geophysics, astrophysics or solar physics see *46 Geophysics, 90 Astrophysics*, or *92 Solar Physics.*

71 ACOUSTICS **2039**
Includes sound generation, transmission, and attenuation. For noise pollution see *45 Environment Pollution.*

72 ATOMIC AND MOLECULAR PHYSICS **2040**
Includes atomic structure, electron properties, and molecular spectra.

73 NUCLEAR AND HIGH-ENERGY PHYSICS **2064**
Includes elementary and nuclear particles; and reactor theory. For space radiation see *93 Space Radiation.*

74 OPTICS **2072**
Includes light phenomena and optical devices. For lasers see *36 Lasers and Masers.*

75 PLASMA PHYSICS **2075**
Includes magnetohydrodynamics and plasma fusion. For ionospheric plasmas see *46 Geophysics.* For space plasmas see *90 Astrophysics.*

76 SOLID-STATE PHYSICS **2083**
Includes superconductivity. For related information see also *33 Electronics and Electrical Engineering* and *36 Lasers and Masers.*

77 THERMODYNAMICS AND STATISTICAL PHYSICS **2091**
Includes quantum mechanics; theoretical physics; and Bose and Fermi statistics. For related information see also *25 Inorganic and Physical Chemistry* and *34 Fluid Mechanics and Heat Transfer.*

SOCIAL SCIENCES

80 SOCIAL SCIENCES (GENERAL) **2100**
Includes educational matters.

81 ADMINISTRATION AND MANAGEMENT **2102**
Includes management planning and research.

82 DOCUMENTATION AND INFORMATION SCIENCE **2103**
Includes information management; information storage and retrieval technology; technical writing; graphic arts; and micrography. For computer documentation see *61 Computer Programming and Software.*

83 ECONOMICS AND COST ANALYSIS ..... **N.A.**
Includes cost effectiveness studies.

84 LAW, POLITICAL SCIENCE AND SPACE POLICY **2107**
Includes NASA appropriation hearings; aviation law; space law and policy; international law; international cooperation; and patent policy.

85 URBAN TECHNOLOGY AND TRANSPORTATION **2108**
Includes applications of space technology to urban problems; technology transfer; technology assessment; and surface and mass transportation. For related information see *03 Air Transportation and Safety, 16 Space Transportation,* and *44 Energy Production and Conversion.*

SPACE SCIENCES For related information see also *Geosciences.*

88 SPACE SCIENCES (GENERAL) **2108**

89 ASTRONOMY **2108**
Includes radio, gamma-ray, and infrared astronomy; and astrometry.

90 ASTROPHYSICS **2109**
Includes cosmology; celestial mechanics; space plasmas; and interstellar and interplanetary gases and dust. For related information see also *75 Plasma Physics.*

91 LUNAR AND PLANETARY EXPLORATION **2111**
Includes planetology; and manned and unmanned flights. For spacecraft design or space stations see *18 Spacecraft Design, Testing and Performance.*

92 SOLAR PHYSICS **2113**
Includes solar activity, solar flares, solar radiation and sunspots. For related information see also *93 Space Radiation.*

93 SPACE RADIATION **2114**
Includes cosmic radiation; and inner and outer earth's radiation belts. For biological effects of radiation see *52 Aerospace Medicine.* For theory see *73 Nuclear and High-Energy Physics.*

GENERAL

Includes aeronautical, astronautical, and space science related histories, biographies, and pertinent reports too broad for categorization; histories or broad overviews of NASA programs.

99 GENERAL **2114**

SUBJECT INDEX **I-1**

PERSONAL AUTHOR INDEX **I-97**

CORPORATE SOURCE INDEX **I-109**

CONTRACT NUMBER INDEX **I-127**

REPORT NUMBER INDEX **I-131**

APPENDIX **A-1**

TYPICAL CITATION AND ABSTRACT

NASA SPONSORED — ON MICROFICHE

ACCESSION NUMBER → **N95-10148*#** National Aeronautics and Space Administration. Lewis Research Center, Cleveland, OH. ← CORPORATE SOURCE

TITLE → **EFFECTS OF A FORWARD-SWEPT FRONT ROTOR ON THE FLOWFIELD OF A COUNTERROTATION PROPELLER**

AUTHORS → M. Nallasamy (NYMA, Inc., Brook Park, OH.) and Gary G. Podboy Aug. 1994 19 p Presented at the 30th Joint Propulsion Conference, Indianapolis, IN, 27-29 Jun. 1994; sponsored by AIAA, ASME, SAE, and ASEE ← PUBLICATION DATE

CONTRACT OR GRANT → (Contract NAS3-27186; RTOP 538-03-11)

REPORT NUMBERS → (NASA-TM-106671; E-8994; NAS 1.15:106671; AIAA Paper 94-2694) Avail: CASI HC A03/MF A01; 6 functional color pages ← AVAILABILITY SOURCE AND PRICE CODE

The effects of a forward-swept front rotor on the flowfield of a counterrotation model propeller at takeoff conditions at zero degree angle of attack are studied by solving the unsteady three-dimensional Euler equations. The configuration considered is an uneven blade count counterrotation model with twelve forward-swept blades on the fore rotor and ten aft-swept blades on the aft rotor. The flowfield is compared with that of a reference aft-swept counterrotation geometry and Laser Doppler Velocimeter (LDV) measurements. At the operating conditions considered, the forward-swept blade experiences a higher tip loading and produces a stronger tip vortex compared to the aft-swept blade, consistent with the LDV and acoustic measurements. Neither the solution nor the LDV data indicated the formation of a leading edge vortex. The predicted radial distribution of the circumferentially averaged axial velocity at the measurement station agreed very closely with LDV data, while crossflow velocities showed poor agreement. The discrepancy between prediction and LDV data of tangential and radial velocities is due in part to the insufficient mesh resolution in the region between the rotors and in the tip region to track the tip vortex. The vortex is diffused by the time it arrives at the measurement station. The uneven blade count configuration requires the solution to be carried out for six blade passages of the fore rotor and five passages of the aft rotor, thus making grid refinement prohibitive.

Author

VOLUME 33 NUMBER 8 / August 1995

Scientific and Technical Aerospace Reports

A Monthly Publication of the National Aeronautics and Space Administration

01 AERONAUTICS (GENERAL)

N95-24200 Defence Science and Technology Organisation, Melbourne (Australia). Airframes and Engines Div.
AN OVERVIEW OF HEALTH AND USAGE MONITORING SYSTEMS (HUMS) FOR MILITARY HELICOPTERS
Ken F. Fraser Sep. 1994 41 p
(DSTO-TR-0061; AR-008-923) Copyright Avail: Issuing Activity (DSTO Aeronautical nad Maritime Research Lab., GPO Box 4331, Melbourne, Victoria 3001, Australia)

The application of health and usage monitoring systems (HUMS) for military helicopters is lagging that for civil helicopters, but military operators are seriously examining the effectiveness of such systems for their fleets. The material presented in this document is based mainly on the author's recent discussions with researchers, manufacturers and military operators. It outlines some of the important issues which operators face and some initiatives in the area. Author

N95-24201 Defence Science and Technology Organisation, Melbourne (Australia). Airframes and Engines Div.
HELICOPTER LIFE SUBSTANTIATION: REVIEW OF SOME USA AND UK INITIATIVES
Ken F. Fraser Sep. 1994 26 p
(DSTO-TR-0062; AR-008-924) Copyright Avail: Issuing Activity (DSTO Aeronautical and Maritime Research Lab., GPO Gox 4331, Melbourne, Victoria 3001, Australia)

Military operators normally undertake programs to substantiate the fatigue lives of life-limited components in their major helicopter fleets. during recent visits to military helicopter representatives in the USA and the UK, the author discussed the motivation and the technical approach adopted by these operators for helicopter component life substantiation. Issues and programs of particular relevance to the Australian Defense Force are examined in this document. Author

N95-24295# Federal Aviation Administration, Cambridge, MA.
ESTIMATE OF PROBABILITY OF CRACK DETECTION FROM SERVICE DIFFICULTY REPORT DATA Final Report, Oct. 1992-1993
J. C. Brewer Sep. 1994 53 p Sponsored by Federal Aviation Administration Technical Center, Atlantic City, NJ
(Contract DOT-FA4H2/A4044)
(PB95-149381; DOT-VNTSC-FAA-94-4; DOT/FAA/CT-94/90) Avail: CASI HC A04/MF A01

The initiation and growth of cracks in a fuselage lap joint were simulated. Stochastic distributions of crack initiation and rivet interference were included. The simulation also contained a simplified crack link-up criterion and the effect of rivet interference on crack growth. Nominal crack growth behavior of large cracks was derived from the simulation results. These calculations implied that large cracks spend most of their lives as multiple small cracks and that the final growth and coalescence occur rapidly. The nominal crack growth histories were applied to 'C-check' crack detection data from the Service Difficulty Report (SDR) database to estimate the sizes of cracks when they were missed during previous inspections. These nondetection events were also estimated by assuming that each detected crack had always been a single crack. The results of each method were appropriately filtered and used to estimate probability of crack detection (POD) using the maximum likelihood technique. The POD estimates obtained from the single crack model are probably conservative, but the underlying assumption of slow crack growth (and therefore more inspection opportunities) might result in unconservative damage tolerance analyses. NTIS

N95-24465* National Aeronautics and Space Administration, Washington, DC.
AERONAUTICAL ENGINEERING: A CONTINUING BIBLIOGRAPHY WITH INDEXES (SUPPLEMENT 316)
Apr. 1995 146 p
(NASA-SP-7037(316); NAS 1.21:7037(316)) Avail: CASI HC A07

This bibliography lists 413 reports, articles, and other documents introduced into the NASA scientific and technical information system in April 1995. Subject coverage includes: aeronautics; mathematical and computer sciences; chemistry and material sciences; geosciences; design, construction and testing of aircraft and aircraft engines; aircraft components, equipment, and systems; ground support systems; and theoretical and applied aspects of aerodynamics and general fluid dynamics. Author

N95-25401 Sandia National Labs., Albuquerque, NM. Aging Aircraft NDI Validation Center.
EMERGING NONDESTRUCTIVE INSPECTION FOR AGING AIRCRAFT Final Report
Allan Beattie, Lutz Dahlke, John Gieske, Bruce Hansche, Gary Phipps, Dennis Roach, Rich Shagam, and Kyle Thompson Oct. 1994 167 p See also N92-33480 Limited Reproducibility: More than 20% of this document may be affected by microfiche quality
(Contract DTFA03-91-A-00018)
(PB95-143053; DOT/FAA/CT-94/11) Avail: CASI HC A08

The report identifies and describes emerging nondestructive inspection (NDI) methods that can potentially be used to inspect commercial transport and commuter aircraft for structural damage. The nine categories of emerging NDI techniques are acoustic emission, x-ray computed tomography, backscatter radiation, reverse geometry x-ray, advanced electromagnetics (including magneto-optic imaging and advanced eddy current techniques), coherent optics, advanced ultrasonics, and advanced visual and infrared thermography. NTIS

N95-25607 Science Applications International Corp., Dayton, OH.
VISUAL CONTRAST DETECTION THRESHOLDS FOR AIRCRAFT CONTRAILS Interim Report, Dec. 1993 - Jul. 1994
Jeffrey A. Doyal, David P. Ramer, Michael D. Stratton, and Bradley D. Purvis Jul. 1994 55 p Limited Reproducibility: More than 20% of this document may be affected by microfiche quality
(Contract F33615-92-D-2293)
(AD-A288618; AL-TR-1994-0116) Avail: Issuing Activity (Defense Technical Information Center (DTIC))

Twenty licensed pilots participated in a laboratory investigation of visual detection thresholds for simulated aircraft contrails. Subjects searched a projection screen for simulated contrails while maintaining a prescribed flight profile on a simple flight simulator. Simulated contrails varied in width from 5 arc min of visual angle to 25 arc min, and varied in length from 2 deg to 10 deg. Subjects performed the detection task in an uncued condition, in which they searched an area measuring 135 deg x 37 deg; and in a cued condition, in which they searched an area measuring 45 deg x 37 deg. Detection thresholds decreased with increasing widths and length, however, thresholds were found to be higher than those demonstrated in previous studies. This difference is attributed to the use of a large visual search area and a secondary task. Cued detection, as described above,

led to slightly lower detection thresholds. Psychometric functions were drawn that allow the reader to extrapolate the probability of detection associated with contrails of a given size and contrast. DTIC

N95-25798* National Aeronautics and Space Administration, Washington, DC.
AERONAUTICAL ENGINEERING: A CONTINUING BIBLIOGRAPHY WITH INDEXES (SUPPLEMENT 317)
May 1995 89 p
(NASA-SP-7037(317); NAS 1.21:7037(317)) Avail: CASI HC A05

This bibliography lists 224 reports, articles, and other documents introduced into the NASA scientific and technical information system in May 1995. Subject coverage includes: design, construction and testing of aircraft and aircraft engines; aircraft components, equipment, and systems; ground support systems; and theoretical and applied aspects of aerodynamics and general fluid dynamics. Author

02 AERODYNAMICS

Includes aerodynamics of bodies, combinations, wings, rotors, and control surfaces; and internal flow in ducts and turbomachinery.

For related information see also *34 Fluid Mechanics and Heat Transfer*.

N95-24210# Cambridge Univ., Cambridge (England). Dept. of Engineering.
THREE-DIMENSIONAL INTERACTION OF WAKE/BOUNDARY-LAYER AND VORTEX/BOUNDARY-LAYER DATA REPORT
C. P. Yeung and L. C. Squire 1993 141 p Sponsored by Croucher Foundation of Hong Kong
(ISSN 0309-7293)
(CUED/A-AEREO/TR-23) Avail: CASI HC A07/MF A02

In an attempt to study the three-dimensional interaction of wake and boundary-layer that commonly occurs on the suction surface of a high-lift multi-element aerofoil, an experimental test case has been established, which has a realistic slat/wing flow configuration under infinite swept wing conditions. This enables the effect of the crossflow induced by the wing sweep on the slat wake and the wing boundary-layer interaction process to be investigated. The measurements of the mean velocity and Reynolds stress components are carried out by an orthogonal triple hot-wire system developed by the authors. As well as the wake/boundary-layer interaction experiment, a three-dimensional boundary-layer experiment without the slat has also been conducted. As an extension of the project, the three-dimensional vortex/boundary-layer interaction which also commonly occurs on a high-lift aerofoil has been studied. The experimental configuration simulates the trailing vortices generated by two differentially-deflected slats which interact with an otherwise two-dimensional boundary-layer developed on the wing surface under a nominal zero pressure gradient. The mean and turbulent flowfields are measured by the same triple hot-wire system. This report essentially describes the experimental configurations of these three experiments and documents the triple-wire measurements of the mean and turbulent flowfields of the respective flow. Author

N95-24217*# Rockwell International Corp., Huntsville, AL. Space Systems Div.
HIGH FREQUENCY FLOW-STRUCTURAL INTERACTION IN DENSE SUBSONIC FLUIDS
Baw-Lin Liu and J. M. OFarrell Washington NASA Mar. 1995 216 p
(Contract NAS8-38187)
(NASA-CR-4652; M-773; NAS 1.26:4652) Avail: CASI HC A10/MF A03

Prediction of the detailed dynamic behavior in rocket propellant feed systems and engines and other such high-energy fluid systems requires precise analysis to assure structural performance. Designs sometimes require placement of bluff bodies in a flow passage. Additionally, there are flexibilities in ducts, liners, and piping systems. A design handbook and interactive data base have been developed for assessing flow/structural interactions to be used as a tool in design and development, to evaluate applicable geometries before problems develop, or to eliminate or minimize problems with existing hardware. This is a compilation of analytical/empirical data and techniques to evaluate detailed dynamic characteristics of both the fluid and structures. These techniques have direct applicability to rocket engine internal flow passages, hot gas drive systems, and vehicle propellant feed systems. Organization of the handbook is by basic geometries for estimating Strouhal numbers, added mass effects, mode shapes for various end constraints, critical onset flow conditions, and possible structural response amplitudes. Emphasis is on dense fluids and high structural loading potential for fatigue at low subsonic flow speeds where high-frequency excitations are possible. Avoidance and corrective measure illustrations are presented together with analytical curve fits for predictions compiled from a comprehensive data base. Author

N95-24308# Sandia National Labs., Albuquerque, NM.
VERIFICATION OF COMPUTATIONAL AERODYNAMIC PREDICTIONS FOR COMPLEX HYPERSONIC VEHICLES USING THE INCA(TRADEMARK) CODE
J. L. Payne and M. A. Walker 1995 11 p Presented at the 33rd AIAA Aerospace Sciences Meeting, Reno, NV, 9-12 Jan. 1995
(Contract DE-AC04-94AL-85000)
(DE95-004757; SAND-94-3190C; CONF-950130-3) Avail: CASI HC A03/MF A01

This paper describes a process of combining two state-of-the-art CFD tools, SPRINT and INCA, in a manner which extends the utility of both codes beyond what is possible from either code alone. The speed and efficiency of the PNS code, SPRING, has been combined with the capability of a Navier-Stokes code to model fully elliptic, viscous separated regions on high performance, high speed flight systems. The coupled SPRINT/INCA capability is applicable for design and evaluation of high speed flight vehicles in the supersonic to hypersonic speed regimes. This paper describes the codes involved, the interface process and a few selected test cases which illustrate the SPRINT/INCA coupling process. Results have shown that the combination of SPRINT and INCA produces correct results and can lead to improved computational analyses for complex, three-dimensional problems. DOE

N95-24379*# Overset Methods, Inc., Los Altos, CA.
AERODYNAMIC OPTIMIZATION STUDIES ON ADVANCED ARCHITECTURE COMPUTERS Final Report
Kalpana Chawla 28 Feb. 1995 31 p Original contains color illustrations
(Contract NCC2-806)
(NASA-CR-198045; NAS 1.26:198045; OMI-02-93) Avail: CASI HC A03/MF A01; 2 functional color pages

The approach to carrying out multi-discipline aerospace design studies in the future, especially in massively parallel computing environments, comprises of choosing (1) suitable solvers to compute solutions to equations characterizing a discipline, and (2) efficient optimization methods. In addition, for aerodynamic optimization problems, (3) smart methodologies must be selected to modify the surface shape. In this research effort, a 'direct' optimization method is implemented on the Cray C-90 to improve aerodynamic design. It is coupled with an existing implicit Navier-Stokes solver, OVERFLOW, to compute flow solutions. The optimization method is chosen such that it can accomodate multi-discipline optimization in future computations. In the work , however, only single discipline aerodynamic optimization will be included. Author

N95-24397*# National Aeronautics and Space Administration. Langley Research Center, Hampton, VA.
PERFORMANCE OF AN AERODYNAMIC YAW CONTROLLER MOUNTED ON THE SPACE SHUTTLE ORBITER BODY FLAP AT MACH 10
W. I. Scallion Feb. 1995 28 p
(RTOP 242-80-01-01)
(NASA-TM-109179; NAS 1.15:109179) Avail: CASI HC A03/MF A01

A wind-tunnel investigation of the effectiveness of an aerodynamic yaw controller mounted on the lower surface of a shuttle orbiter model body flap was conducted in the Langley 31-Inch Mach 10 Tunnel. The controller consisted of a 60 deg delta fin mounted perpendicular to the body flap lower surface and yawed 30 deg to the free stream direction. The control was tested at angles of attack from 20 deg to 40 deg at zero sideslip for a Reynolds number based on wing mean aerodynamic chord of 0.66 x 10(exp 6). The aerodynamic and control effectiveness characteristics are presented along with an analysis of the effectiveness of the controller in making a bank maneuver for Mach 18 flight conditions. The controller was

effective in yaw and produced a favorable rolling moment. The analysis showed that the controller was as effective as the reaction control system in making the bank maneuver. These results warrant further studies of the aerodynamic/aerothermodynamic characteristics of the control concept for application to future transportation vehicles. Author

N95-24443*# Bihrle Applied Research, Inc., Hampton, VA.
EXPERIMENTAL STUDY OF THE EFFECTS OF REYNOLDS NUMBER ON HIGH ANGLE OF ATTACK AERODYNAMIC CHARACTERISTICS OF FOREBODIES DURING ROTARY MOTION Final Report
H. Pauley, J. Ralston, and E. Dickes Jan. 1995 97 p Original contains color illustrations
(Contract NAS1-20228; RTOP 505-68-30-01)
(NASA-CR-195033; Rept-94-4; NAS 1.26:195033) Avail: CASI HC A05/MF A02; 32 functional color pages

The National Aeronautics and Space Administration and the Defense Research Agency (United Kingdom) have ongoing experimental research programs in rotary-flow aerodynamics. A cooperative effort between the two agencies is currently underway to collect an extensive database for the development of high angle of attack computational methods to predict the effects of Reynolds number on the forebody flowfield at dynamic conditions, as well as to study the use of low Reynolds number data for the evaluation of high Reynolds number characteristics. Rotary balance experiments, including force and moment and surface pressure measurements, were conducted on circular and rectangular aftbodies with hemispherical and ogive noses at the Bedford and Farnborough wind tunnel facilities in the United Kingdom. The bodies were tested at 60 and 90 deg angle of attack for a wide range of Reynolds numbers in order to observe the effects of laminar, transitional, and turbulent flow separation on the forebody characteristics when rolling about the velocity vector. Author

N95-24566*# Army Aviation Systems Command, Hampton, VA.
EXPLORATORY FLOW VISUALIZATION INVESTIGATION OF MAST-MOUNTED SIGHTS IN PRESENCE OF A ROTOR
Terence A. Ghee (Analytical Services and Materials, Inc., Hampton, VA.) and Henry L. Kelley Mar. 1995 36 p
(RTOP 505-59-36-01; RTOP 282-10-01-01)
(NASA-TM-4634; L-17409; NAS 1.15:4634; ATCOM-TR-95-A-001) Avail: CASI HC A03/MF A01

A flow visualization investigation with a laser light sheet system was conducted on a 27-percent-scale AH-64 attack helicopter model fitted with two mast-mounted sights in the langley 14- by 22-foot subsonic tunnel. The investigation was conducted to identify aerodynamic phenomena that may have contributed to adverse vibration encountered during full-scale flight of the AH-64D apache/longbow helicopter with an asymmetric mast-mounted sight. Symmetric and asymmetric mast-mounted sights oriented at several skew angles were tested at simulated forward and rearward flight speeds of 30 and 45 knots. A laser light sheet system was used to visualize the flow in planes parallel to and perpendicular to the free-stream flow. Analysis of these flow visualization data identified frequencies of flow patterns in the wake shed from the sight, the streamline angle at the sight, and the location where the shed wake crossed the rotor plane. Differences in wake structure were observed between the sight configurations and various skew angles. Analysis of lateral light sheet plane data implied significant vortex structure in the wake of the asymmetric mast-mounted sight in the configuration that produced maximum in-flight vibration. The data showed no significant vortex structure in the wake of the asymmetric and symmetric configurations that produced no increase in in-flight adverse vibration. Author

N95-24998# National Aerospace Lab., Tokyo (Japan). Aircraft Aerodynamics Div.
NUMERICAL AND EXPERIMENTAL STUDY OF DRAG CHARACTERISTICS OF TWO-DIMENSIONAL HLFC AIRFOILS IN HIGH SUBSONIC, HIGH REYNOLDS NUMBER FLOW
Yoji Ishida, Masayoshi Noguchi, Mamoru Sato, and Hiroshi Kanda Jul. 1994 14 p
(ISSN 0389-4010)
(NAL-TR-1244T) Avail: CASI HC A03/MF A01

Hybrid laminar flow control (HLFC) is one of the most promising aircraft drag reduction technologies. However, very few experimental and theoretical studies have been reported. We have investigated both numerically and experimentally the aerodynamic characteristics of an HLFC airfoil and wing at high subsonic, high Reynolds number conditions. In this paper, we report the results of the wind tunnel test on drag characteristics, with and without suction, of two-dimensional HLFC airfoils with porous and slot suction approach under some adverse factors against laminar flow, and a numerical analysis of the wind tunnel data, which is based on the boundary layer calculation with a new transition prediction method allowed for the adverse factors and the Squire-Young drag formula. The HLFC models achieved total drag reduction as high as 20% at realistic flight condition and the numerical methods has given satisfactory predictions. Author

N95-25105# National Aerospace Lab., Tokyo (Japan). Advanced Aircraft Research Group.
LOW SPEED AERODYNAMIC CHARACTERISTICS OF DELTA WINGS WITH VORTEX FLAPS: 60 DEG AND 70 DEG DELTA WINGS
Kenichi Rinoie (Tokyo Univ., Japan.), Toshimi Fujita, Akihito Iwasaki, and Hirotoshi Fujieda Jul. 1994 15 p In JAPANESE
(ISSN 0389-4010)
(NAL-TR-1245) Avail: CASI HC A03/MF A01

Low-speed wind tunnel tests have been made on a 70 deg delta wing model with tapered vortex flaps to investigate the effects of the swept-back angle on the performance of vortex flaps. The force, surface pressure measurements, and oil flow visualization tests were made on a 0.5 m span 70 deg delta wing model. The results were compared between 60 deg and 70 deg delta wing models. Flow patterns around the vortex flaps at the optimum lift/drag ratio flap configuration of 70 deg delta wing were found to be different from those of 60 deg delta wing. The maximum lift/drag ratio improvement for 70 deg delta wing is attained when a separated region is formed over the whole vortex flap surface. Author

N95-25338*# National Aeronautics and Space Administration. Langley Research Center, Hampton, VA.
INTERNAL PERFORMANCE CHARACTERISTICS OF THRUST-VECTORED AXISYMMETRIC EJECTOR NOZZLES
Milton Lamb Mar. 1995 227 p Prepared in cooperation with Pratt and Whitney (the Government Engines and Space Propulsion Div. of the United Technologies)
(RTOP 505-59-30-04)
(NASA-TM-4610; L-17386; NAS 1.15:4610) Avail: CASI HC A11/MF A03

A series of thrust-vectored axisymmetric ejector nozzles were designed and experimentally tested for internal performance and pumping characteristics at the Langley research center. This study indicated that discontinuities in the performance occurred at low primary nozzle pressure ratios and that these discontinuities were mitigated by decreasing expansion area ratio. The addition of secondary flow increased the performance of the nozzles. The mid-to-high range of secondary flow provided the most overall improvements, and the greatest improvements were seen for the largest ejector area ratio. Thrust vectoring the ejector nozzles caused a reduction in performance and discharge coefficient. With or without secondary flow, the vectored ejector nozzles produced thrust vector angles that were equivalent to or greater than the geometric turning angle. With or without secondary flow, spacing ratio (ejector passage symmetry) had little effect on performance (gross thrust ratio), discharge coefficient, or thrust vector angle. For the unvectored ejectors, a small amount of secondary flow was sufficient to reduce the pressure levels on the shroud to provide cooling, but for the vectored ejector nozzles, a larger amount of secondary air was required to reduce the pressure levels to provide cooling. Author

N95-25649# Defence Research Agency, Farnborough, Hampshire (England).
A THEORETICAL AND EXPERIMENTAL INVESTIGATION OF THE FLOW OVER SUPERSONIC LEADING EDGE WING/BODY CONFIGURATIONS
J. L. Fulker (Defence Research Agency, Bedford, England.), P. R. Ashill, and A. Shires Aug. 1993 42 p Presented at the 1993 European Forum on Recent Developments and Applications in Aeronautical CFD, Bristol, England, 1-3 Sep. 1993 Sponsored by Ministry of Defence Original contains color illustrations
(DRA-TM-AERO-PROP-41; DRA/AP/TM9341/1.0) Copyright Avail: CASI HC A03/MF A01

A theoretical and experimental study is described, of the flow over wing-body configurations with a supersonic component of free-stream normal to the leading edge, i.e. with a supersonic leading edge. The theoretical calculations have been performed using a code for solving Euler's equations for complex configurations known as SAUNA. An assessment is made of the predictions of this method, by comparison with the experimental results. Significant reductions in local pressure drag by the use of nose blunting are both predicted and measured over a substantial portion of the wing span. However, it is also shown that nose blunting results in a marked increase in local drag in the region of the wing/body junction. In this region the flow is complex, the bow shock having low local sweep and high strength. It is shown how the CFD method can be used both to identify this problem and to effect a redesign of the wing/body junction, for the blunt-nose configuration, with the aim of realizing the benefits of nose blunting. Significant drag reductions are obtained relative to the untreated configuration, indicating how advanced codes can provide a solution to problems of this kind without resort to further expensive wind-tunnel tests. Author

N95-25761# National Aerospace Lab., Tokyo (Japan). Aircraft Aerodynamics Div.

MEASUREMENTS OF LONGITUDINAL STATIC AERODYNAMIC COEFFICIENTS BY THE CABLE MOUNT SYSTEM

Katsuichi Murota and Masaaki Yanagihara Feb. 1994 22 p In JAPANESE

(ISSN 0389-4010)

(NAL-TR-1226) Avail: CASI HC A03/MF A01

The longitudinal static aerodynamic coefficients of an NAL spaceplane model were measured in the NAL 6.5 m x 5.5 m low-speed wind tunnel. The model was supported by a pair of cables, one spanned horizontally and the other vertically (cable mount system). The aerodynamic interference of the cable mount system is generally smaller than that of conventional model support systems such as the strut and sting system. This paper outlines the cable mount system, the cable mounted system, the method used to measure the trimmed longitudinal aerodynamic coefficients and the test results. Author

N95-25762# National Aerospace Lab., Tokyo (Japan). Airframe Div.

FUNDAMENTAL WIND TUNNEL EXPERIMENTS ON LOW-SPEED FLUTTER OF A TIP-FIN CONFIGURATION WING

Tetsuhiko Ueda, Tokuo Sotozaki, and Kazuo Iwasaki Mar. 1994 23 p In JAPANESE

(ISSN 0389-4010)

(NAL-TR-1228) Avail: CASI HC A03/MF A01

Wind tunnel tests were conducted to investigate the fundamental flutter characteristics of a tip-fin configuration wing. Two types of models were tested to provide experimental data for the flutter analysis of non-coplanar wings. One is a normally plain wing and the other has a cant angle of 15 deg at the tip-fin. They were tested in the 2m x 2m low-speed wind tunnel. On the tip-fin wing, mild flutter with limited amplitudes was observed in a certain range of speeds well below the typical violent flutter speed. It was caused by the coupling between wing torsion and the deflection of the rotationally free rudder with mass balance. The effects of mass balance of the rudder located at the tip-fin were also studied to confirm its role in flutter prevention. Modal tests on the models were performed automatically using the Dynamic Displacement Measurement System. Author

N95-25962*# National Aeronautics and Space Administration. Lewis Research Center, Cleveland, OH.

RECENT IMPROVEMENTS TO AND VALIDATION OF THE ONE DIMENSIONAL NASA WAVE ROTOR MODEL

Daniel E. Paxson and Jack Wilson (NYMA, Inc., Cleveland, OH.) May 1995 20 p

(Contract NAS3-25266; RTOP 505-62-50)

(NASA-TM-106913; E-9621; NAS 1.15:106913) Avail: CASI HC A03/MF A01

A numerical model has been developed at the NASA Lewis Research Center which can predict both the unsteady flow quantities within a wave rotor passage and the steady averaged flows in the ports. The model is based on the assumptions of one-dimensional, unsteady, perfect gas flow. The model assesses not only the dominant wave behavior, but the loss effects of finite passage opening time, leakage from the passage ends, viscosity, and heat transfer to and from the passages. The model operates in the rotor reference frame; however, until recently no account was made for the often significant effect of the rotor circumferential velocity component. The present model accounts for this by modifying the passage boundary conditions, allowing the internal computational scheme to remain the rotor reference frame, while quantities such as inlet duct stagnation properties may be specified in the fixed or absolute reference frame. Accurate modeling of this effect is critical to successful wave rotor analysis and design, particularly in off-design predictions where the flows in the inlet ducts are mismatched with the rotor passages and significant turning may take place (i.e., work is done on the gas). The relative simplicity of the model makes it useful for design and optimization, as well as analysis, of wave rotor cycles for many applications. This report, building on several earlier papers, describes the most recent modifications to the model. These include accounting for the relative/absolute transition at the passage boundaries and refinements to the viscous source term correlation which resulted from this accounting. Comparison of model predictions with measured data is then presented and discussed. Author

N95-26075*# National Aeronautics and Space Administration. Lewis Research Center, Cleveland, OH.

A COMBINED GEOMETRIC APPROACH FOR SOLVING THE NAVIER-STOKES EQUATIONS ON DYNAMIC GRIDS

John W. Slater May 1995 9 p Presented at the Conference on Numerical Methods for Fluid Dynamics, Oxford, England, United Kingdom, 3-6 Apr. 1995; sponsored by the University of Oxford and Reading

(RTOP 505-62-52)

(NASA-TM-106919; E-9630; NAS 1.15:106919) Avail: CASI HC A02/MF A01

A combined geometric approach for solving the Navier-Stokes equations is presented for the analysis of planar, unsteady flow about mechanisms with components in moderate relative motion. The approach emphasizes the relationships between the geometry model, grid, and flow model for the benefit of the total dynamics problem. One application is the analysis of the restart operation of a variable-geometry, high-speed inlet. Author

N95-26302*# National Aeronautics and Space Administration. Ames Research Center, Moffett Field, CA.

AERODYNAMICS MODEL FOR A GENERIC ASTOVL LIFT-FAN AIRCRAFT

Lourdes G. Birckelbaw, Walter E. McNeil, and Douglas A. Wardwell Apr. 1995 63 p

(RTOP 505-68-32)

(NASA-TM-110347; A-950051; NAS 1.15:110347) Avail: CASI HC A04/MF A01

This report describes the aerodynamics model used in a simulation model of an advanced short takeoff and vertical landing (ASTOVL) lift-fan fighter aircraft. The simulation model was developed for use in piloted evaluations of transition and hover flight regimes, so that only low speed (M approximately 0.2) aerodynamics are included in the mathematical model. The aerodynamic model includes the power-off aerodynamic forces and moments and the propulsion system induced aerodynamic effects, including ground effects. The power-off aerodynamics data were generated using the U.S. Air Force Stability and Control Digital DATCOM program and a NASA Ames in-house graphics program called VORVIEW which allows the user to easily analyze arbitrary conceptual aircraft configurations using the VORLAX program. The jet-induced data were generated using the prediction methods of R. E. Kuhn et al., as referenced in this report. Author

03 AIR TRANSPORTATION AND SAFETY

Includes passenger and cargo air transport operations; and aircraft accidents.

For related information see also *16 Space Transportation* and *85 Urban Technology and Transportation.*

N95-24206# National Transportation Safety Board, Washington, DC.

AIRCRAFT ACCIDENT REPORT: IMPACT WITH BLAST FENCE UPON LANDING ROLLOUT ACTION AIR CHARTERS FLIGHT 990 PIPER PA-31-350, N990RA, STRATFORD, CONNECTICUT,27 APRIL 1994

1994 75 p
(PB94-910410; NTSB/AAR-94/08) Avail: CASI HC A04/MF A01

On April 28, 1994, about 2256 eastern daylight time, Action Air Charters flight 990, a Piper PA-31-350 Navajo Chieftain, N990RA, crashed into a blast fence at the departure end of runway 6 after landing at Sikorsky Memorial Airport, Stratford, Connecticut. The flight originated in Atlantic City, New Jersey, and operated on a visual flight rules flight plan. The airplane was operating under Title 14 Code of Federal Regulations Part 135 as a single pilot, on-demand air carrier flight. Following handling touchdown and during rollout, the airplane collided with a blast deflector fence at the departure end of runway 6. The airplane was destroyed by impact forces and postcrash fire. Eight of the nine occupants sustained fatal injuries. One passenger was seriously injured. The National Transportation Safety Board determines that the probable causes of this accident were the failure of the captain to use the available instrument landing system (ILS) glideslope, his failure to execute a go-around when the conditions were not suitable for landing, and his failure to land the airplane on the runway at a point sufficient to allow for a safe stopping distance; the fatalities were caused by the presence of the nonfrangible blast fence and the absence of a safety area at the end of the runway. Safety issues in this report focused on the instrument landing system, runway safety areas, and runway lighting systems. Safety recommendations concerning these issues were made to the Federal Aviation Administration, the Connecticut Department of Transportation, the City of Bridgeport, and the Town of Stratford, Connecticut. Also, as a result of the investigation of this accident, on May 11, 1994, the Safety Board issued Urgent Action Safety Recommendations A-94-111 and A-94-112 to the Federal Aviation Administration concerning aircraft maintenance performed by Harrington Industries, Inc. Author

N95-24384# Civil Aeromedical Inst., Oklahoma City, OK.
DEVELOPMENT OF AN INTERVENTION PROGRAM TO ENCOURAGE SHOULDER HARNESS USE AND AIRCRAFT RETROFIT IN GENERAL AVIATION AIRCRAFT, PHASES 1 AND 2
James F. Parker, Jr. (BioTechnology, Inc., Falls Church, VA.), William T. Shepard (Federal Aviation Administration, Washington, DC.), Walter J. Gunn (Arlington Associates, Daytona Beach, FL.), and Diane G. Christensen (BioTechnology, Inc., Falls Church, VA.) Jan. 1995 63 p
(DOT/FAA/AM-95/2) Avail: CASI HC A04/MF A01

This report describes a study of shoulder harness installation and use rates in general aviation aircraft. Observations were made at six geographically separate areas to determine estimates of current installation and use rates. An expert panel was employed to identify important factors that affect installation and use of shoulder harness in general aviation aircraft. Analyses are presented to explain reasons for shoulder harness installation and use rates. An educational program is proposed to influence pilots to install and/or use shoulder harnesses in their general aviation aircraft. Author

N95-24391*# Clemson Univ., SC. Radar Systems Lab.
CHARACTERIZING THE WAKE VORTEX SIGNATURE FOR AN ACTIVE LINE OF SIGHT REMOTE SENSOR M.S. Thesis Technical Report No. 19
Robert Milton Heil 5 Aug. 1994 80 p
(Grant NGT-50975)
(NASA-CR-197697; NAS 1.26:197697; TR-080594-4871F) Avail: CASI HC A05/MF A01

A recurring phenomenon, described as a wake vortex, develops as an aircraft approaches the runway to land. As the aircraft moves along the runway, each of the wing tips generates a spiraling and expanding cone of air. During the lifetime of this turbulent event, conditions exist over the runway which can be hazardous to following aircraft, particularly when a small aircraft is following a large aircraft. Left to themselves, these twin vortex patterns will converge toward each other near the center of the runway, harmlessly dissipating through interaction with each other or by contact with the ground. Unfortunately, the time necessary to disperse the vortex is often not predictable, and at busy airports can severely impact terminal area productivity. Rudimentary methods of avoidance are in place. Generally, time delays between landing aircraft are based on what is required to protect a small aircraft. Existing ambient wind conditions can complicate the situation. Reliable detection and tracking of a wake vortex hazard is a major technical problem which can significantly impact runway productivity. Landing minimums could be determined on the basis of the actual hazard rather than imposed on the basis of a worst case scenario. This work focuses on using a windfield description of a wake vortex to generate line-of-sight Doppler velocity truth data appropriate to an arbitrarily located active sensor such as a high resolution radar or lidar. The goal is to isolate a range Doppler signature of the vortex phenomenon that can be used to improve detection. Results are presented based on use of a simplified model of a wake vortex pattern. However, it is important to note that the method of analysis can easily be applied to any vortex model used to generate a windfield snapshot. Results involving several scan strategies are shown for a point sensor with a range resolution of 1 to 4 meters. Vortex signatures presented appear to offer potential for detection and tracking. Author

N95-24631# Federal Aviation Administration, Atlantic City, NJ.
BIRD INGESTION INTO LARGE TURBOFAN ENGINES Final Report
Howard Banilower and Colin Goodall (Pennsylvania State Univ., University Park, PA.) Feb. 1995 139 p
(DOT/FAA/CT-93/14) Avail: CASI HC A07/MF A02

This final report contains findings from a study conducted by the Federal Aviation Administration (FAA) of bird ingestion into certain modern large high bypass turbofan engines. These engines were certified to current FAA standards and are installed in A-300, A-320, B-747, B-757, B-767, DC-10, and MD-11 aircraft in commercial service worldwide. Data pertaining to 644 aircraft ingestion events were collected for the FAA during 1989-1991 by the principal engine manufacturers. Topics addressed in the report include characteristics of ingested birds (numbers, species, and weights), ingestion rates, airports, aircraft parameters (flight phase, altitude, speed, engine position), and ingestion events which pose a potential threat to aircraft safety (multiple-engines or birds, transverse fracture of fan blades, power loss). Using statistical methods, the data are analyzed to determine the influence of flight phase (departure or arrival), bird weight, and bird numbers (single or multiple bird), both separately and in combination, on overall engine damage, fan blade damage, core damage, and other adverse effects on flight. A summary of all pertinent data from each ingestion is included in an appendix. Author

N95-24633*# National Aeronautics and Space Administration. Langley Research Center, Hampton, VA.
AVIATION SYSTEM CAPACITY IMPROVEMENTS THROUGH TECHNOLOGY
W. Don Harvey Mar. 1995 82 p
(RTOP 505-69-20-01)
(NASA-TM-109165; NAS 1.15:109165) Avail: CASI HC A05/MF A01

A study was conducted with the primary objective of determining the impact of technology on capacity improvements in the U.S. air transportation system and, consequently, to assess the areas where NASA's expertise and technical contributions would be the most beneficial. The outlook of the study is considered both near- and long-term (5 to 25 years). The approach was that of actively working with the Massachusetts Institute of Technology (MIT) Flight Transportation Laboratory and included interactions with 'users' outside of both agencies as well as with organizations within. This report includes an overall survey of what are believed to be the causes of the capacity problems, ongoing work with the Federal Aviation Administration (FAA) to alleviate the problems, and identifies improvements in technology that would increase capacity and reduce delays. Author

N95-25341*# Boeing Commercial Airplane Co., Seattle, WA.
CONSISTENT APPROACH TO DESCRIBING AIRCRAFT HIRF PROTECTION Final Report
P. R. Rimbey and D. B. Walen Mar. 1995 93 p
(Contract NAS1-19360; RTOP 538-01-13-01)
(NASA-CR-195067) Avail: CASI HC A05/MF A01

The high intensity radiated fields (HIRF) certification process as currently implemented is comprised of an inconsistent combination of factors that tend to emphasize worst case scenarios in assessing commercial airplane certification requirements. By examining these factors which include the process definition, the external HIRF environment, the aircraft coupling and corresponding internal fields, and methods of measuring equipment susceptibilities, activities leading to an approach to appraising airplane vulnerability to HIRF are proposed. This approach utilizes technically based criteria to evaluate the nature of the threat, including the probability of

encountering the external HIRF environment. No single test or analytic method comprehensively addresses the full HIRF threat frequency spectrum. Additional tools such as statistical methods must be adopted to arrive at more realistic requirements to reflect commercial aircraft vulnerability to the HIRF threat. Test and analytic data are provided to support the conclusions of this report. This work was performed under NASA contract NAS1-19360, Task 52. Author

04 AIRCRAFT COMMUNICATIONS AND NAVIGATION

Includes digital and voice communication with aircraft; air navigation systems (satellite and ground based); and air traffic control.

For related information see also *17 Space Communications, Spacecraft Communications, Command and Tracking* and *Communications and Radar.*

N95-25609 Army Engineer Waterways Experiment Station, Vicksburg, MS.

REAL-TIME TESTING AND DEMONSTRATION OF THE US ARMY CORPS OF ENGINEERS' REAL-TIME ON-THE-FLY POSITIONING SYSTEM

Sally L. Frodge, Benjamin W. Remondi, Dariusz Lapucha, and John E. Chance Sep. 1994 16 p Limited Reproducibility: More than 20% of this document may be affected by microfiche quality

(AD-A288624; WES/TN/DRP-4-10) Avail: Issuing Activity (Defense Technical Information Center (DTIC))

This technical note describes the U.S. Army Corps of Engineers' Real-Time On-the-Fly (OTF) positioning system and summarizes the results of testing and demonstrations conducted to date. DTIC

N95-25764# National Aerospace Lab., Tokyo (Japan). Advanced Aircraft Research Group

REENTRY GUIDANCE FOR HYPERSONIC FLIGHT EXPERIMENT (HYFLEX) VEHICLE Report No. 1

Hirokazu Suzuki Apr. 1994 19 p In JAPANESE

(ISSN 0389-4010)

(NAL-TR-1235) Avail: CASI HC A03/MF A01

This paper describes the design of the reentry guidance for Hypersonic Flight Experiment vehicle (HYFLEX), which is now under development at NAL and NASDA to prepare for its scheduled launch in 1996. First, the mission requirements of this flight experiment are described. Secondly, a reentry guidance based on the drag deceleration and the azimuth angle misalignment correction is suggested and its ability is evaluated. Consequently, the proposed reentry guidance is proved to have sufficient ability to satisfy the mission requirements. Author

05 AIRCRAFT DESIGN, TESTING AND PERFORMANCE

Includes aircraft simulation technology.

For related information see also *18 Spacecraft Design, Testing and Performance* and *39 Structural Mechanics.* For land transportation vehicles see *85 Urban Technology and Transportation.*

N95-24436*# Stanford Univ., CA. Dept. of Aeronautics and Astronautics.

NEW APPROACHES TO OPTIMIZATION IN AEROSPACE CONCEPTUAL DESIGN

Peter J. Gage Mar. 1995 186 p

(Grants NAG2-640; NAG1-1494; NAG1-1558; RTOP 505-69-50)

(NASA-CR-196695; A-950044; NAS 1.26:196695) Avail: CASI HC A09/MF A02

Aerospace design can be viewed as an optimization process, but conceptual studies are rarely performed using formal search algorithms. Three issues that restrict the success of automatic search are identified in this work. New approaches are introduced to address the integration of analyses and optimizers, to avoid the need for accurate gradient information and a smooth search space (required for calculus-based optimization), and to remove the restrictions imposed by fixed complexity problem formulations. (1) Optimization should be performed in a flexible environment. A quasi-procedural architecture is used to conveniently link analysis modules and automatically coordinate their execution. It efficiently controls a large-scale design tasks. (2) Genetic algorithms provide a search method for discontinuous or noisy domains. The utility of genetic optimization is demonstrated here, but parameter encodings and constraint-handling schemes must be carefully chosen to avoid premature convergence to suboptimal designs. The relationship between genetic and calculus-based methods is explored. (3) A variable-complexity genetic algorithm is created to permit flexible parameterization, so that the level of description can change during optimization. This new optimizer automatically discovers novel designs in structural and aerodynamic tasks. Author

N95-24541# Joint Publications Research Service, Arlington, VA.

JPRS REPORT: SCIENCE AND TECHNOLOGY. CENTRAL EURASIA

28 Feb. 1995 41 p Transl. into ENGLISH from various Central Eurasian articles

(JPRS-UST-95-011) Avail: CASI HC A03/MF A01

Translated articles cover the following topics: problems of constructing welded aircraft structures; automatic welding of aluminum and titanium alloy structures; fusion welding thin-sheet titanium alloys to corrosion-resistant steels; and reconditioning aircraft parts with laser-fused hard-facing coatings Author

N95-24582*# National Aeronautics and Space Administration. Langley Research Center, Hampton, VA.

A CREW-CENTERED FLIGHT DECK DESIGN PHILOSOPHY FOR HIGH-SPEED CIVIL TRANSPORT (HSCT) AIRCRAFT

Michael T. Palmer, William H. Rogers (Bolt, Beranek, and Newman, Inc., Cambridge, MA.), Hayes N. Press (Lockheed Engineering and Sciences Co., Hampton, VA.), Kara A. Latorella (State Univ. of New York, Buffalo, NY.), and Terence S. Abbott Jan. 1995 55 p

(RTOP 537-08-21-01)

(NASA-TM-109171; NAS 1.15:109171) Avail: CASI HC A04/MF A01

Past flight deck design practices used within the U.S. commercial transport aircraft industry have been highly successful in producing safe and efficient aircraft. However, recent advances in automation have changed the way pilots operate aircraft, and these changes make it necessary to reconsider overall flight deck design. The High Speed Civil Transport (HSCT) mission will likely add new information requirements, such as those for sonic boom management and supersonic/subsonic speed management. Consequently, whether one is concerned with the design of the HSCT, or a next generation subsonic aircraft that will include technological leaps in automated systems, basic issues in human usability of complex systems will be magnified. These concerns must be addressed, in part, with an explicit, written design philosophy focusing on human performance and systems operability in the context of the overall flight crew/flight deck system (i.e., a crew-centered philosophy). This document provides such a philosophy, expressed as a set of guiding design principles, and accompanied by information that will help focus attention on flight crew issues earlier and iteratively within the design process. This document is part 1 of a two-part set. Author

N95-24629*# National Aeronautics and Space Administration. Ames Research Center, Moffett Field, CA.

GEOMETRIC ANALYSIS OF WING SECTIONS

I.-Chung Chang, Francisco J. Torres, and Chee Tung (Army Aviation Systems Command, Moffett Field, CA.) Apr. 1995 18 p

(RTOP 505-10-11)

(NASA-TM-110346; A-950049; NAS 1.15:110346) Avail: CASI HC A03/MF A01

This paper describes a new geometric analysis procedure for wing sections. This procedure is based on the normal mode analysis for continuous functions. A set of special shape functions is introduced to represent the geometry of the wing section. The generators of the NACA 4-digit airfoils were included in this set of shape functions. It is found that the supercritical wing section, Korn airfoil, could be well represented by a set of ten shape functions. Preliminary results showed that the number of parameters to define a wing section could be greatly reduced to about ten. Hence, the present research clearly advances the airfoil design technology by reducing the number of design variables. Author

N95-24630*# Brown Univ., Providence, RI. Dept. of Engineering.
AERODYNAMIC PARAMETER ESTIMATION VIA FOURIER MODULATING FUNCTION TECHNIQUES
A. E. Pearson Hampton, VA NASA Apr. 1995 44 p
(Grant NAG1-1065; RTOP 505-64-52-01)
(NASA-CR-4654; NAS 1.26:4654) Avail: CASI HC A03/MF A01

Parameter estimation algorithms are developed in the frequency domain for systems modeled by input/output ordinary differential equations. The approach is based on Shinbrot's method of moment functionals utilizing Fourier based modulating functions. Assuming white measurement noises for linear multivariable system models, an adaptive weighted least squares algorithm is developed which approximates a maximum likelihood estimate and cannot be biased by unknown initial or boundary conditions in the data owing to a special property attending Shinbrot-type modulating functions. Application is made to perturbation equation modeling of the longitudinal and lateral dynamics of a high performance aircraft using flight-test data. Comparative studies are included which demonstrate potential advantages of the algorithm relative to some well established techniques for parameter identification. Deterministic least squares extensions of the approach are made to the frequency transfer function identification problem for linear systems and to the parameter identification problem for a class of nonlinear-time-varying differential system models. Author

N95-25334*# National Aeronautics and Space Administration. Ames Research Center, Moffett Field, CA.
AERODYNAMIC SHAPE OPTIMIZATION OF WING AND WING-BODY CONFIGURATIONS USING CONTROL THEORY
James Reuther and Antony Jameson (Princeton Univ., NJ.) Jan. 1995 33 p
(Contract NAS2-13721)
(NASA-CR-198024; NAS 1.26:198024; RIACS-TR-95-01) Avail: CASI HC A03/MF A01

This paper describes the implementation of optimization techniques based on control theory for wing and wing-body design. In previous studies it was shown that control theory could be used to devise an effective optimization procedure for airfoils and wings in which the shape and the surrounding body-fitted mesh are both generated analytically, and the control is the mapping function. Recently, the method has been implemented for both potential flows and flows governed by the Euler equations using an alternative formulation which employs numerically generated grids, so that it can more easily be extended to treat general configurations. Here results are presented both for the optimization of a swept wing using an analytic mapping, and for the optimization of wing and wing-body configurations using a general mesh. Author

N95-25578 Oklahoma City Air Logistics Center, Tinker AFB, OK.
PROCEEDINGS OF THE 2D USAF AGING AIRCRAFT CONFERENCE
C. I. Chang 19 May 1994 431 p Conference held in Del City, OK, 17-19 May 1994
(AD-A288217; AFOSR-94-0756TR) Avail: Issuing Activity (Defense Technical Information Center (DTIC))

The Air Force Office of Scientific Research gathered together representatives of universities funded under the University Research Institutes to present results of their Aging Aircraft research conducted over the preceding year. The purpose was to provide a forum for Technical Interchange and provide AFOSR an opportunity for the research community to interact with the applied engineering community and gain insight into the day to day problems experienced on Aging Aircraft. Technical presentations by-personnal from HO AFMC/EN Wright Labs, ASC, the five Air Logistics Centers, FAA and NASA were delivered on various topics including corrosion, corrosion fatique, multi-site damage and advanced non-destructive evaluation methods. Approximately 160 people attended the conference. DTIC

N95-25862# National Aerospace Lab., Tokyo (Japan). Aircraft Development Section.
A QUIET STOL RESEARCH AIRCRAFT DEVELOPMENT PROGRAM
Jan. 1994 35 p In JAPANESE
(ISSN 0389-4010)
(NAL-TR-1223) Avail: CASI HC A03/MF A01

This report presents a general account of a program undertaken by the National Aerospace Laboratory to develop a STOL research aircraft, designated ASKA. ASKA made its first flight on October 28, 1985. Descriptions of the development over the eight years from 1977 to 1985 are included along with descriptions of the aircraft and its systems, and various development tests. ASKA is a modified C-1 medium-sized troop and freight transport, manufactured by Kawaski Heavy Industries for the Air Self-Defence Force. The airframe was made anew and the two engines of C-1 were replaced with four FJR710/600S fan-jet engines arranged as in upper surface blowing system to provide powered lift for STOL operations. Author

N95-25935 Aeronautical Research Labs., Melbourne (Australia). Airframes and Engines Div.
CONFIGURATION AND OTHER DIFFERENCES BETWEEN BLACK HAWK AND SEAHAWK HELICOPTERS IN MILITARY SERVICE IN THE USA AND AUSTRALIA Abstract Only
R. W. Jackson Dec. 1993 1 p
(AR-008-386; ARL-GD-43) Avail: Issuing Activity (Aeronautical Research Labs., Melbourne, Australia)

Various versions of Black Hawk and Seahawk helicopters have been produced to match the requirements of different operators. Some of the differences between these versions, particularly those relevant to the dynamic system, are briefly reviewed. Author

N95-26009 Mechanical Engineering Lab., Sakura (Japan).
[LONG ENDURANCE STRATOSPHERIC SOLAR POWERED AIRSHIP]
Mar. 1994 71 p In JAPANESE
(PB95-178729) Avail: Issuing Activity (National Technical Information Service (NTIS))

This is a report on HALROP (High Altitude Long Range Observational Platform), a solar powered airship entitled 'Long Endurance Stratospheric Solar Powered Airship,' and was published by the New Airship System Study Group of the Japan Industrial Technology Promotion Association. The report covers history of previous research on stratospheric platform; the concept and design specifications of HALROP (a proposed model for 20 km altitude airship); relationship between the altitude and meteorological data; liftoff, descent, and recovery operations; design of high efficiency solar power system; structure and weight balance problems, a feasibility study of antarctic exploration by HALROP; the conceptual design of solar powered transport airship called JS-RESAT which makes use of the jet stream; and the feasibility study of stratospheric power generation. NTIS

N95-26062# University City Science Center, Philadelphia, PA.
WASTE MINIMIZATION ASSESSMENT FOR A MANUFACTURER OF PARTS FOR TRUCK ENGINES Environmental Research Brief
R. J. Jendrucko, K. Binkley, T. Thomas, S. Wilson, E. W. Daley (Tennessee Univ., Knoxville, TN.), and G. P. Looby (Tennessee Univ., Knoxville, TN.) Sep. 1994 7 p
(Grant EPA-R-914903)
(PB95-144481; EPA/600/S-94/019) Avail: CASI HC A02/MF A01

The Waste Minimization Assessment Center (WMAC) team at the University of Tennessee performed an assessment at a plant that manufactures turbochargers, fan drives, and vibration dampers for truck engines. Metal castings are machined and cleaned; degreased, coated and/or painted, if required; and assembled, inspected, packaged, and shipped. The team's report, detailing findings and recommendations, indicated that the plant could achieve significant cost savings by replacing its solvent-based painting system with an electrostatic powder coating system, thereby reducing paint overspray. NTIS

N95-26338# General Accounting Office, Washington, DC. National Security and International Affairs Div.
REPORT TO CONGRESSIONAL COMMITTEES. TACTICAL AIRCRAFT: CONCURRENCY IN DEVELOPMENT AND PRODUCTION OF F-22 AIRCRAFT SHOULD BE REDUCED
19 Apr. 1995 33 p
(GAO/NSIAD-95-59; B-259204) Avail: CASI HC A03/MF A01

The concurrency between the development and production phases of the Air Force's F-22 fighter program and the risk associated with that concurrency are assessed. Although the F-22 program involves considerable risk because it embodies important technological advances that are critical to its operational success, the F-22 program exhibits a high degree of concurrency because the program will enter production well before

commencement of initial operational testing and evaluation (IOT&E). The Air Force plans to procure 80 F-22s under low-rate initial production (LRIP), or 18 percent of the total planned procurement, at an estimated cost of $12.4 billion, before completing IOT&E. F-22 production rates in the LRIP phase are planned to accelerate so that 75 percent of the full-production rate, or 36 aircraft a year, will be achieved under the LRIP phase of the program. The planned rate of acceleration, it is believed, exceeds the amount that is needed to successfully complete the LRIP phase of the program and essentially represents a plan to commit to a full-rate production schedule before IOT&E is completed. The need for the F-22, based on analysis, is not urgent. Moreover, engine and stealthiness problems already disclosed by DOD, and the potential for avionics and software problems, underscore the need to demonstrate the weapon system's performance through flight testing before significant commitments are made to production. CASI

06 AIRCRAFT INSTRUMENTATION

Includes cockpit and cabin display devices; and flight instruments.

For related information see also *19 Spacecraft Instrumentation* and *35 Instrumentation and Photography.*

N95-24207*# National Aeronautics and Space Administration. Lewis Research Center, Cleveland, OH.

THE 1994 FIBER OPTIC SENSORS FOR AEROSPACE TECHNOLOGY (FOSAT) WORKSHOP

Robert Baumbick, comp., Grigory Adamovsky, comp., Meg Tuma, comp., Glenn Beheim, comp., and Jorge Sotomayor, comp. Feb. 1995 90 p Workshop held in Cleveland OH, 18-20 Oct. 1994

(RTOP 505-60-00)

(NASA-CP-10166; E-9426; NAS 1.55:10166) Avail: CASI HC A05/MF A01

The NASA Lewis Research Center conducted a workshop on fiber optic technology on October 18-20, 1994. The workshop objective was to discuss the future direction of fiber optics and optical sensor research, especially in the aerospace arena. The workshop was separated into four sections: (1) a Systems Section which dealt specifically with top level overall architectures for the aircraft and engine; (2) a Subsystems Section considered the parts and pieces that made up the subsystems of the overall systems; (3) a Sensor/Actuators section considered the status of research on passive optical sensors and optical powered actuators; and (4) Components Section which addressed the interconnects for the optical systems (e.g., optical connectors, optical fibers, etc.). This report contains the minutes of the discussion on the workshop, both in each section and in the plenary sessions. The slides used by a limited number of presenters are also included as presented. No attempt was made to homogenize this report. The view of most of the attendees was: (1) the government must do a better job of disseminating technical information in a more timely fashion; (2) enough work has been done on the components, and system level architecture definition must dictate what work should be done on components; (3) a Photonics Steering Committee should be formed to coordinate the efforts of government and industry in the photonics area, to make sure that programs complimented each other and that technology transferred from one program was used in other programs to the best advantage of the government and industry. Author

N95-24624*# National Aeronautics and Space Administration. Lewis Research Center, Cleveland, OH.

ASSESSMENT OF AVIONICS TECHNOLOGY IN EUROPEAN AEROSPACE ORGANIZATIONS Final Contractor Report

D. A. Martinec (Aeronautical Radio, Inc., Annapolis, MD.), Robert Baumbick, Ellis Hitt (Battelle Columbus Labs., OH.), Cornelius Leondes (Washington Univ., Bellingham, WA.), Monica Mayton (Air Force Systems Command, Wright-Patterson AFB, OH.), Joseph Schwind (Airline Pilots Association, Denison, TX.), and Joseph Traybar (Federal Aviation Administration, Atlantic City, NJ.) 21 Sep. 1992 179 p

(Contract NAS3-88622)

(NASA-CR-189201; E-9592; NAS 1.26:189201) Avail: CASI HC A09/MF A02

This report provides a summary of the observations and recommendations made by a technical panel formed by the National Aeronautics and Space Administration (NASA). The panel, comprising prominent experts in the avionics field, was tasked to visit various organizations in Europe to assess the level of technology planned for use in manufactured civil avionics in the future. The primary purpose of the study was to assess avionics systems planned for implementation or already employed on civil aircraft and to evaluate future research, development, and engineering (RD&E) programs, address avionic systems and aircraft programs. The ultimate goal is to ensure that the technology addressed by NASa programs is commensurate with the needs of the aerospace industry at an international level. The panel focused on specific technologies, including guidance and control systems, advanced cockpit displays, sensors and data networks, and fly-by-wire/fly-by-light systems. However, discussions the panel had with the European organizations were not limited to these topics. Author

N95-25005# National Aerospace Lab., Tokyo (Japan). Control Systems Div.

FLIGHT REFERENCE DISPLAY FOR POWERED-LIFT STOL AIRCRAFT

Keiji Tanaka, Kohei Funabiki, Masaru Nakamura, Yushi Terui, Toshiharu Inagaki, Hiroyasu Kawahara, Yukichi Tsukano, and Takatsugu Ono Oct. 1994 26 p

(ISSN 0389-4010)

(NAL-TR-1251) Avail: CASI HC A03/MF A01

This study deals with a proposed flight reference display for powered-lift STOL aircraft. The display design aims at providing pilots with new control cues for maintaining flight safety during low-speed high-power approach. The display utilizes angle of attack, pitch angle, and airspeed to indicate the flight reference for maintaining the flight safety margins. Piloted simulation using a moving-base flight simulator was conducted to verify the display scheme. The parameters of the display equations were designed on the basis of the flight test achievements of 'ASKA,' the experimental STOL aircraft of the National Aerospace Laboratory. This preliminary evaluation demonstrated that the display can be used for both flight reference tracking and safety margin monitoring, and provided appropriate values of coefficients of the display equations. The succeeding flight evaluation of the proposed flight reference display was conducted after installing the display upon an in-flight simulator, whose motion cues yield ultimate fidelity of flight simulation environment for the display evaluation. As the in-flight simulator, the variable stability and response airplane (VSRA) of the National Aerospace Laboratory was utilized for this experiment. The flight reference display for this flight evaluation was developed by using a color liquid crystal display. The results of the approach flight experiments provided proof of satisfactory performance of the display for pilots to monitor and regulate the safety margins, as well as suggestion for future improvement. Author

N95-26060 Pacific-Sierra Research Corp., Arlington, VA.

IMPLEMENTATION OF SCENE SHADOWS IN THE TARGET ACQUISITION TDA (TARGAC) Final Report

Ernest A. Carroll, Melanie J. Gouveia, Daniel A. DeBenedictis, Donald J. Hamann, Paul F. Hilton, Donald B. Hodges, Leigh N. Matheson, Steven J. McKay, Michael J. Oberlatz, and Kevin J. Rappoport et al White Sands Missile Range, NM Army Research Lab. Nov. 1994 317 p Prepared in cooperation with Hughes STX, Inc., Le xington, MA Limited Reproducibility: More than 20% of this document may be affected by microfiche quality

(Contract DAAL01-93-C-2002)

(AD-A288760; ARL-CR-194) Avail: Issuing Activity (Defense Technical Information Center (DTIC))

The performance of electro-optical weapon systems operating in the visible and near-infrared (IR) spectra depend on the illumination of the target and background. Scene shadows can decrease the illumination level of the target scene and alter the contrast characteristics between the target and background. Shadows are also an important source of clutter in a target scene. The primary objective of the first year of this Phase 2 SBIR is to (1) develop the partly cloudy shadowing model; (2) deliver the updated TARGAC software for the PC that implements the partly cloudy shadowing model; (3) determine the relationships between target acquisition, small-scale features, shadows, and clutter; and (4) develop a design approach for the incorporation into TARGAC of the temporal and spatial characteristics of clutter. DTIC

N95-26190 Organisatie voor Toegepast Natuurwetenschappelijk Onderzoek, Delft (Netherlands).
PARTIAL CAMERA AUTOMATION IN A SIMULATED UNMANNED AIR VEHICLE Interim Report
J. E. Korteling and W. vanderBorg 5 Oct. 1994 29 p Limited Reproducibility: More than 20% of this document may be affected by microfiche quality
(AD-A288786; TNO-TM-1994-B-16; TDCK-94-2179) Avail: Issuing Activity (Defense Technical Information Center (DTIC))

With the rapid development of automatic control techniques a central question is how the division of labor between the human operator and the automaton should be optimally distributed. In this connection, the present study focussed on an intelligent, semi-autonomous, interface for a camera operator of a simulated Unmanned Air Vehicle (UAV). This interface used inherent system knowledge concerning UAV motion in order to assist a camera operator in tracking an object moving through the landscape below. This landscape was sensored by the video camera attached to the UAV-platform and presented to the operator on a monitor display. The semi-automated system compensated for the translations of the UAV relative to the earth. This compensation was accompanied by the appropriate joystick movements ensuring tactile (haptic) feedback of these system interventions. The operator had to superimpose camera movements over these system actions required to track the motion of a target (a driving truck) relative to the terrain. Consequently, the operator remained in the loop; he still had total control of the camera-motion system. In order to investigate the effects of this semi-automation over a broad range of task situations, the tracking task was carried out under two conditions of update frequency of the monitor image and control mode difficulty. DTIC

07 AIRCRAFT PROPULSION AND POWER

Includes prime propulsion systems and systems components, e.g., gas turbine engines and compressors; and onboard auxilliary power plants for aircraft.

For related information see also *20 Spacecraft Propulsion and Power, 28 Propellants and Fuels,* and *44 Energy Production and Conversion.*

N95-24213*# Auburn Univ., AL. Dept. of Mechanical Engineering.
DYNAMIC BEHAVIOR OF A MAGNETIC BEARING SUPPORTED JET ENGINE ROTOR WITH AUXILIARY BEARINGS
Abdollah Homaifar, ed. (North Carolina Agricultural and Technical State Univ., Greensboro, NC.), John C. Kelly, Jr., ed. (North Carolina Agricultural and Technical State Univ., Greensboro, NC.), G. T. Flowers, H. Xie, and S. C. Sinha Albuquerque, NM 1994 7 p Presented at the First Industry/Academy Symposium on Research for Future Supersonic and Hypersonic Vehicles: Applications, Design, Development and Research, volume 1, Greensboro, NC, 4-6 Dec. 1994 *Its* TSI Press Series
(Grant NAG3-1507)
(NASA-CR-197860; NAS 1.26:197860) Avail: CASI HC A02/MF A01

This paper presents a study of the dynamic behavior of a rotor system supported by auxiliary bearings. The steady-state behavior of a simulation model based upon a production jet engine is explored over a wide range of operating conditions for varying rotor imbalance, support stiffness and damping. Interesting dynamical phenomena, such as chaos, subharmonic responses, and double-valued responses, are presented and discussed. Author

N95-24293 Northern Research and Engineering Corp., Woburn, MA.
SMALL GAS TURBINE COMPONENT EVALUATION STUDY Final Report, Jun. 1990-1992
J. B. Kesseli Jun. 1994 114 p Sponsored by Gas Research Inst. Limited Reproducibility: More than 20% of this document may be affected by microfiche quality
(Contract GRI-5089-291-2077)
(PB95-147542; NREC-1762; GRI-94/0350) Avail: CASI HC A06

The low pressure ratio, highly recuperated gas turbine engine is a candidate for future small (under 200 kW) cogeneration systems and other prime-mover applications. Existing gas engine equipment (cogeneration, chillers, pump and compressor-drives) based on spark ignition (Otto cycle) technology has not been successful enough to substantially expand the sale of natural gas. The small gas turbine is being considered for its potential economic advantages that stem from superior reliability (lower maintenance costs), increased shaft-power efficiency, less costly installation, and lower costs associated with meeting future emission standards. In this study and experimental program, the focus was in two areas of critical importance. These are the ability of the engine to meet future California State emission standards, and the cost-effectiveness of the recuperator. A complete engine test was performed based on non-developmental commercial components, including a non-optimum recuperator. NOx emissions were below 5 ppmv at 15% excess oxygen, while carbon monoxide was in the range of 25 ppmv. Engine electrical generation efficiency was 21% with a 71% effective recuperator, proving that the goal of 30 to 33% electrical efficiencies are attainable with an optimally sized recuperator. NTIS

N95-24304*# McDonnell-Douglas Aerospace, Long Beach, CA.
ADVANCED SUBSONIC AIRPLANE DESIGN AND ECONOMIC STUDIES Final Report
Robert H. Liebeck, Donald A. Andrastek, Johnny Chau, Raquel Girvin, Roger Lyon, Blaine K. Rawdon, Paul W. Scott, and Robert A. Wright Apr. 1995 37 p
(Contract NAS3-25965; RTOP 538-08-11)
(NASA-CR-195443; E-9488; NAS 1.26:195443) Avail: CASI HC A03/MF A01

A study was made to examine the effect of advanced technology engines on the performance of subsonic airplanes and provide a vision of the potential which these advanced engines offered. The year 2005 was selected as the entry-into-service (EIS) date for engine/airframe combination. A set of four airplane classes (passenger and design range combinations) that were envisioned to span the needs for the 2005 EIS period were defined. The airframes for all classes were designed and sized using 2005 EIS advanced technology. Two airplanes were designed and sized for each class: one using current technology (1995) engines to provide a baseline, and one using advanced technology (2005) engines. The resulting engine/airframe combinations were compared and evaluated on the basis on sensitivity to basic engine performance parameters (e.g. SFC and engine weight) as well as DOC+I. The advanced technology engines provided significant reductions in fuel burn, weight, and wing area. Average values were as follows: reduction in fuel burn = 18%, reduction in wing area = 7%, and reduction in TOGW = 9%. Average DOC+I reduction was 3.5% using the pricing model based on payload-range index and 5% using the pricing model based on airframe weight. Noise and emissions were not considered. Author

N95-24390*# National Aeronautics and Space Administration. Lewis Research Center, Cleveland, OH.
CROSSFLOW MIXING OF NONCIRCULAR JETS
D. S. Liscinsky (United Technologies Corp., East Hartford, CT.), B. True (United Technologies Corp., East Hartford, CT.), and J. D. Holdeman Feb. 1995 13 p Presented at the 33rd Aerospace Sciences Meeting and Exhibit, Reno, NV, 9-12 Jan. 1995; sponsored by AIAA Original contains color illustrations
(Contract NAS3-25954)
(NASA-TM-106865; E-9477; NAS 1.15:106865; AIAA Paper 95-0732)
Avail: CASI HC A03/MF A01; 5 functional color pages

An experimental investigation has been conducted of the isothermal mixing of a turbulent jet injected perpendicular to a uniform crossflow through several different types of sharp-edged orifices. Jet penetration and mixing was studied using planar Mie scattering to measure time-averaged mixture fraction distributions of circular, square, elliptical, and rectangular orifices of equal geometric area injected into a constant velocity crossflow. Hot-wire anemometry was also used to measure streamwise turbulence intensity distributions at several downstream planes. Mixing effectiveness was determined using (1) a spatial unmixedness parameter based on the variance of the mean jet concentration distributions and (2) by direct comparison of the planar distributions of concentration and of turbulence intensity. No significant difference in mixing performance was observed for the six configurations based on comparison of the mean properties. Author

N95-24392*# Iowa State Univ. of Science and Technology, Ames, IA.
STUDY OF COMPRESSIBLE FLOW THROUGH A RECTANGULAR-TO-SEMIANNULAR TRANSITION DUCT Final Report
Jeffry Foster, Theodore H. Okiishi, Bruce J. Wendt (Modern Technologies Corp., Middleburg Heights, OH.), and Bruce A. Reichert (Kansas State Univ., Manhattan, KS.) Cleveland, OH NASA Apr. 1995 61 p
(Grant NAG3-1561)
(NASA-CR-4660; E-9582; NAS 1.26:4660) Avail: CASI HC A04/MF A01

Detailed flow field measurements are presented for compressible flow through a diffusing rectangular-to-semiannular transition duct. Comparisons are made with published computational results for flow through the duct. Three-dimensional velocity vectors and total pressures were measured at the exit plane of the diffuser model. The inlet flow was also measured. These measurements are made using calibrated five-hole probes. Surface oil flow visualization and surface static pressure data were also taken. The study was conducted with an inlet Mach number of 0.786. The diffuser Reynolds based on the inlet centerline velocity and the exit diameter of the diffuser was 3,200,000. Comparison of the measured data with previously published computational results are made. Data demonstrating the ability of vortex generators to reduce flow separation and circumferential distortion is also presented. Author

N95-24561*# National Aeronautics and Space Administration. Lewis Research Center, Cleveland, OH.
THE EFFECT OF ALTITUDE CONDITIONS ON THE PARTICLE EMISSIONS OF A J85-GE-5L TURBOJET ENGINE
June Elizabeth Rickey Feb. 1995 52 p
(RTOP 505-62-00)
(NASA-TM-106669; E-9143; NAS 1.15:106669) Avail: CASI HC A04/MF A01

Particles from a J85-GE-5L turbojet engine were measured over a range of engine speeds at simulated altitude conditions ranging from near sea level to 45,000 ft and at flight Mach numbers of 0.5 and 0.8. Samples were collected from the engine by using a specially designed probe positioned several inches behind the exhaust nozzle. A differential mobility particle sizing system was used to determine particle size. Particle data measured at near sea-level conditions were compared with Navy Aircraft Environmental Support Office (AESO) particle data taken from a GE-J85-4A engine at a sea-level static condition. Particle data from the J85 engine were also compared with particle data from a J85 combustor at three different simulated altitudes. Author

N95-24990# National Aerospace Lab., Tokyo (Japan).
EFFECT OF FILM COOLING/REGENERATIVE COOLING ON SCRAMJET ENGINE PERFORMANCES
Fumiei Ono, Takeshi Kanda, Goro Masuya, Toshihito Saito, and Yoshio Wakamatsu Jul. 1994 16 p In JAPANESE
(ISSN 0389-4010)
(NAL-TR-1242) Avail: CASI HC A03/MF A01

Film cooling was modeled to allow performance prediction of scramjet engine design. The model was based on experimental results of compressible mixing layers for the vicinity of the injection slot, and on analytical results of the turbulent boundary layer in the region far from the slot. The film cooling model was integrated to a quasi one-dimensional scramjet performance prediction model. In the engine employing a combination of film cooling and regenerative cooling, coolant flow rate of the engine slightly exceeded the stoichiometric flow rate, even at high flight Mach numbers, and had the best specific impulse and system pressure performances. These advantages were achieved by increasing the volume flow rate and decreasing the velocity difference between the main flow and the coolant, both due to an increase in the film coolant temperature. The effective cooling system with a combination of film cooling and regenerative cooling was also advantageous in that excess cooling of the engine wall could be avoided. The combination of film cooling and regenerative cooling was also effective from the viewpoint of the propellant feed system. The turbine exhaust gas was suitable for the coolant of film cooling. Author

N95-25936 Aeronautical Research Labs., Melbourne (Australia). Airframes and Engines Div.
ASSESSMENT OF OVERHAUL SURGE MARGIN TESTS APPLIED TO THE T53 ENGINES IN ADF IROQUOIS HELICOPTERS Abstract Only
P. C. W. Frith Feb. 1994 1 p
(AR-008-389; ARL-TN-48) Avail: Issuing Activity (Aeronautical Research Labs., Melbourne, Australia)

The validity of the test procedures used at overhaul to establish the surge margin of Lycoming T53 engines installed in Australian Defence Force (ADF) Iroquois helicopters has been assessed. Recommendations are made on the use of wave-off tests, on the increased surge margin applied at overhaul to ADF T53 engines and on the implementation of improved inspection criteria at the unit level. Author

N95-25395*# Queensland Univ., Saint Lucia (Australia). Dept. of Mechanical Engineering.
THRUST MEASUREMENTS OF A COMPLETE AXISYMMETRIC SCRAMJET IN AN IMPULSE FACILITY
A. Paull, R. J. Stalker, and D. Mee *In its* Shock Tunnel Studies of Scramjet Phenomena 1993 Jan. 1995 p 15-18 Sponsored in cooperation with NASA. Langley Research Center and the Australian Research Council (For primary document see N95-25394 08-34)
Avail: CASI HC A01/MF A02

N95-25396*# Queensland Univ., Saint Lucia (Australia). Dept. of Mechanical Engineering.
SCRAMJET THRUST MEASUREMENT IN A SHOCK TUNNEL
A. Paull, R. J. Stalker, and D. J. Mee *In its* Shock Tunnel Studies of Scramjet Phenomena 1993 Jan. 1995 p 19-27 Sponsored in cooperation with the Australian Research Council (For primary document see N95-25394 08-34)
Avail: CASI HC A02/MF A02

N95-25397*# Queensland Univ., Saint Lucia (Australia). Dept. of Mechanical Engineering.
THRUST MEASUREMENT IN A 2-D SCRAMJET NOZZLE
Sean Tuttle *In its* Shock Tunnel Studies of Scramjet Phenomena 1993 Jan. 1995 p 29-36 (For primary document see N95-25394 08-34)
Avail: CASI HC A02/MF A02

08 AIRCRAFT STABILITY AND CONTROL

Includes aircraft handling qualities; piloting; flight controls; and autopilots.

For related information see also *05 Aircraft Design, Testing and Performance.*

N95-24260 National Defence Research Establishment, Linkoeping (Sweden).
INTERFACING A DIGITAL COMPASS TO A REMOTE-CONTROLLED HELICOPTER [INTERFACE MELLAN DIGITAL KOMPASS OCH RADIOSTYRD HELIKOPTER]
C. Ekstroem Jun. 1994 13 p In SWAHILI
(PB95-164927; FOA-C-30768-3.6) Avail: Issuing Activity (National Technical Information Service (NTIS))

One can use a digital compass as a tool to navigate a semiautonomous mini helicopter. This thesis describes how to create an interface between the digital compass (KVH C100) and the controlling servos in the mini helicopter. NTIS

09 RESEARCH AND SUPPORT FACILITIES (AIR)

Includes airports, hangars and runways; aircraft repair and overhaul facilities; wind tunnels; shock tubes; and aircraft engine test stands.

For related information see also *14 Ground Support Systems and Facilities (Space).*

N95-24302*# Purdue Univ., West Lafayette, IN. School of Aeronautical and Astronautical Engineering.

SUPERSONIC QUIET-TUNNEL DEVELOPMENT FOR LAMINAR-TURBULENT TRANSITION RESEARCH Final Report, Feb. 1994 - Feb. 1995

Steven P. Schneider Feb. 1995 172 p

(Grant NAG1-1607)

(NASA-CR-198040; NAS 1.26:198040) Avail: CASI HC A08/MF A02

This grant supported research into quiet-flow supersonic wind-tunnels, between February 1994 and February 1995. Quiet-flow nozzles operate with laminar nozzle-wall boundary layers, in order to provide low-disturbance flow for studies of laminar-turbulent transition under conditions comparable to flight. Major accomplishments include: (1) development of the Purdue Quiet-Flow Ludwieg Tube, (2) computational evaluation of the square nozzle concept for quiet-flow nozzles, and (3) measurement of the presence of early transition on the flat sidewalls of the NASA LaRC Mach 3.5 supersonic low-disturbance tunnel. Since items (1) and (2) are described in the final report for companion grant NAG1-1133, only item (3) is described here. A thesis addressing the development of square nozzles for high-speed, low-disturbance wind tunnels is included as an appendix. Author (revised)

N95-24380*# Cleveland State Univ., OH. Advanced Manufacturing Center.

AMC EN-1038: REDUCED SCALE SOLAR SIMULATOR SUPPLEMENTARY TEST REPORT Final Technical Report

Robert C. Biering [1994] 71 p

(Contract NCC3-143)

(NASA-CR-197988; NAS 1.26:197988) Avail: CASI HC A04/MF A01

The reduced scale solar simulator program conducted by the Advanced Manufacturing Center at Cleveland State University in 1992 provided sufficient data to support the selection of the uniform magnification solar simulator module for the Solar Dynamic Ground Test Demonstrator Program (SDGTD) at NASA LeRC. In 1993, additional testing of the reduced scale solar simulator was conducted to provide information to refine and improve the design of the full scale solar simulator. This report presents the results of these additional tests. Author

N95-24388*# North Carolina State Univ., Raleigh, NC.

DEVELOPMENT OF A MODEL PROTECTION AND DYNAMIC RESPONSE MONITORING SYSTEM FOR THE NATIONAL TRANSONIC FACILITY

Clarence P. Young, Jr., S. Balakrishna (Vigyan Research Associates, Inc., Hampton, VA.), and W. Allen Kilgore (Calspan Corp., Hampton, VA.) Feb. 1995 30 p Prepared in cooperation with ViGYAN, Inc. and Calspan Corp.

(Contract NCC1-141; RTOP 505-59-85-01)

(NASA-CR-195041; NAS 1.26:195041) Avail: CASI HC A03/MF A01

A state-of-the-art, computerized mode protection and dynamic response monitoring system has been developed for the NASA Langley Research Center National Transonic Facility (NTF). This report describes the development of the model protection and shutdown system (MPSS). A technical description of the system is given along with discussions on operation and capabilities of the system. Applications of the system to vibration problems are presented to demonstrate the system capabilities, typical applications, versatility, and investment research return derived from the system to date. The system was custom designed for the NTF but can be used at other facilities or for other dynamic measurement/diagnostic applications. Potential commercial uses of the system are described. System capability has been demonstrated for forced response testing and for characterizing and quantifying bias errors for onboard inertial model attitude measurement devices. The system is installed in the NTF control room and has been used successfully for monitoring, recording and analyzing the dynamic response of several model systems tested in the NTF. Author

N95-24424 Baker (Wilfred) Engineering, Inc., San Antonio, TX.

QUANTITY-DISTANCE REQUIREMENTS FOR EARTH-BERMED AIRCRAFT SHELTERS Final Technical Report, 22 May 1991 - 15 Feb. 1992

Mark G. Whitney and Kathy H. Spivey Jun. 1993 52 p Limited Reproducibility: More than 20% of this document may be affected by microfiche quality

(Contract F08635-91-C-0189)

(AD-A279692; WBE-228-001; AFCESA/ESL-TR-92-25) Avail: CASI HC A04

The subject work has been performed under Phase 1 of an SBIR program sponsored by Tyndall AFB. The effort concentrated on development of methods to quantify debris hazards from accidental explosions inside earth-bermed and unbermed aircraft shelters. The Phase 1 effort addressed shock loading, gas loading, debris breakup, and debris throw. The prediction model, Quantity-Distance Requirements for Aircraft Shelters (QDRACS), includes new programming which uses image charges and ray-tracing of shocks for the specific geometry of an aircraft shelter. Interior surfaces are divided into a grid of rectangular elements. Shock loads are calculated at each element for up to 20 munition stacks. Existing data were utilized to determine structural breakup dependence on load intensity and the formation of small or large debris. Venting is calculated using the FRANG program as a subroutine to QDRACS, but with special treatment for defining vent area and vent perimeter based on the breakup pattern, and venting provided by the door. The velocity of all missiles is calculated based on contributions from both the shock and gas pressure loading. Debris dispersion is calculated using MUDEMIMP as a subroutine. Model results were compared to the Q-D criteria based on DISTANT RUNNER tests. Hazard distances for Event 4 were predicted within 20 percent, and for Event 5, within 5 percent of the DISTANT RUNNER data. DTIC

N95-26053 Wright Lab., Wright-Patterson AFB, OH.

HEAT TRANSFER MEASUREMENTS IN SMALL SCALE WIND TUNNELS Final Report, 1 Nov. 1983 - 1 Sep. 1987

James R. Hayes Jun. 1994 36 p Limited Reproducibility: More than 20% of this document may be affected by microfiche quality

(AF Proj. 2404)

(AD-A288689; WL-TR-94-3097) Avail: Issuing Activity (Defense Technical Information Center (DTIC))

This report describes an effort at the Flight Dynamics Directorate to use small scale models, miniature instrumentation and small in-house hypersonic facilities to accomplish full configurational testing of vehicle concepts. The project included development of procedures for generating model geometry data and transmitting that data to 495th TW machine shops of model fabrication on NC machines. A discussion of problems peculiar to testing of small scale models is included. A comparison is presented of data taken under this effort with similar data taken in large production wind tunnels on large scale models. DTIC

N95-25399*# Queensland Univ., Saint Lucia (Australia). Dept. of Mechanical Engineering.

THE SUPERORBITAL EXPANSION TUBE CONCEPT, EXPERIMENT AND ANALYSIS

A. J. Neely and R. G. Morgan *In its* Shock Tunnel Studies of Scramjet Phenomena 1993 Jan. 1995 p 97-105 Sponsored in cooperation with the Australian Research Council (For primary document see N95-25394 08-34)

Avail: CASI HC A02/MF A02

12 ASTRONAUTICS (GENERAL)

For extraterrestrial exploration see *91 Lunar and Planetary Exploration.*

N95-24358# Joint Publications Research Service, Washington, DC.

JPRS REPORT: SCIENCE AND TECHNOLOGY. CENTRAL EURASIA: SPACE

5 Oct. 1994 34 p Transl. into ENGLISH from various Central Eurasian articles

(JPRS-USP-94-007) Avail: CASI HC A03/MF A01

Translated articles cover the following topics: psychological aspects of

theory and practice of manned cosmonautics; evaluation of characteristics of waves and tsunamis generated by the falling of asteroids and comets in oceans and seas; prominent role seen for small satellites; conversion of SS-18's for use as space launchers proposed; comparative assessment of effectiveness of data from ERS-1, almaz and landsat-TM satellites for documenting tundra ecosystems; accuracy in automated geographical referencing of meteor-3 satellite digital meteorological information; and monitoring atmospheric pollution using data from a territorial space survey. Author

N95-24359# Joint Publications Research Service, Washington, DC.
JPRS REPORT: SCIENCE AND TECHNOLOGY. CENTRAL EURASIA: SPACE
28 Dec. 1994 49 p Transl. into ENGLISH from various Central Eurasian articles
(JPRS-USP-94-008) Avail: CASI HC A03/MF A01

Translated articles cover the following topics: plasma instabilities and space vehicles, need discussed for protection against space catastrophes, Russians offer new energy concept for space stations, Russian space projects: Martian research, multi-impulse rendezvous trajectory for two spacecraft in circular orbit, placement of spacecraft into orbit around Mars with aerobraking, model of the shielding for the inhabited compartments of the base module of the Mir station, and measurement of the background electrostatic and variable electric fields on the outer surface of the Kvant module of the Mir orbital station. There are 25 translated articles in this 28 December 1994 edition. Author

N95-24467# Joint Publications Research Service, Washington, DC.
JPRS REPORT: SCIENCE AND TECHNOLOGY. CENTRAL EURASIA
16 Feb. 1995 47 p Transl. into ENGLISH from various Central Eurasian articles
(JPRS-UST-95-009) Avail: CASI HC A03/MF A01

Translated articles cover the following topics: microacceleration conditions, gravity sensitivity, and methods of analysis of production experiments performed in weightlessness; production equipment for the Unmanned Foton Satellite and some experimental results; producing layered semiconductor materials in microgravity and under slow cell rotation; convective flows in a cylindrical fluid zone in a high-frequency vibration field; study of the effect of weightlessness on convection and mass transfer when crystals are grown from aqueous solutions; convection in an oscillating field of forces and microgravity; features of the behavior of a fluid and a fluid-gas system under conditions close to weightlessness; natural convection and temperature stratification in a cryogenic fuel tank in microgravity; plans for manned flight to mars outlined; organizing test range for certifying satellite receiving-computation complexes; determining 'standard' positions of space vehicle; and organizing space images database. Author

N95-24621# Joint Publications Research Service, Washington, DC.
JPRS REPORT: SCIENCE AND TECHNOLOGY. CENTRAL EURASIA
13 Jan. 1995 63 p Transl. into ENGLISH from various Central Eurasian articles
(JPRS-UST-95-002) Avail: CASI HC A04/MF A01

Translated articles cover the following topics: analysis of accuracy characteristics and stability of nonlinear algorithms for evaluating parameters of motion of spacecraft encumbered by anomalous measurements; adaptive robust control of angular motion of space vehicle using predictive models; evaluating tensor of inertia of mir orbital station from measurements of kinetic moment of gyrodynes; attitude control of spacecraft by solar rudders; distribution of man-generated litter in circumterrestrial space and evaluation of its impact on spacecraft; modeling of anthropogenic effluent discharge into upper atmosphere; statistical characteristics of ULF and VLF electromagnetic emissions in upper ionosphere and magnetosphere over earthquake foci; analysis of measurements of absorbed doses on outer surface of mir station during June-July 1991; interaction between jet of electric rocket engines and spacecraft solar cells; stability of orientation system of deformable spacecraft with nonlinear correcting device; mathematical simulation of deployment of space structures by centrifugal forces; analysis of operation of solar cells on low-orbit spacecraft; clearing of near-space from space debris using large thin-film curtains without supporting structure formed by centrifugal forces; NASA uses full capacity of russian training center; and capacitive type stud welding in space technology production. CASI

N95-24847# Joint Publications Research Service, Arlington, VA.
JPRS REPORT: SCIENCE AND TECHNOLOGY. CENTRAL EURASIA: SPACE
28 Dec. 1994 49 p Transl. into ENGLISH from various Central Eurasian articles
(JPRS-USP-94-008) Avail: CASI HC A03/MF A01

Translated articles cover the following topics: plasma instabilities and space vehicles; need discussed for protection against space catastrophes; Russians offer new energy concept for space stations; investigation of the problem of estimating the inertial tensor of the Mir orbital station from the data of measurements of the angular momentum of the gyrodynes; multi-impulse rendezvous trajectory for two spacecraft in a circular orbit; placement of spacecraft into orbit around Mars with aerobraking; model of the shielding for the inhabited compartments of the base module of the Mir station; measurement of the background electrostatic and variable electric fields on the outer surface of the Kvant module of the Mir orbital station; planned communications satellites, projects at Khrunichev Center discussed; Russian booster to be used to launch Swedish satellite; and development of reusable air-launched booster systems urged. Author

N95-24872# European Space Agency. European Space Research and Technology Center, ESTEC, Noordwijk (Netherlands).
REFLECTIONS ON EUROPE IN SPACE
John Krige (European Univ. Inst., Florence, Italy.) and Arturo Russo (Palermo Univ., Italy.) Jan. 1994 52 p Original contains color illustrations
(ESA-HSR-11) Avail: CASI HC A04/MF A01

The ESA History Study Reports are preliminary reports of studies carried out within the framework of an ESA (European Space Agency) contract. They will form the basis of a comprehensive study of European Space activities covering the period 1959-1987. This report rings together four papers. The first attempts to think about ESRO in system terms. It is seen as an interlocking network of components including the organization itself, the Member States, industry, and scientists, and the relationships of power between these various elements are explored. The second paper is something of a tongue-in-cheek autocritique of work already done on the launch of ELDO, making particular use of some new results by two of the project's research assistants. The third paper details the emergence and development of ESRO's telecommunications satellite program in the late 1960s and early 1970s, placing it in the context of the process that led to the definition of a comprehensive European space policy and to the birth of ESA. The final paper uses the results of an interview program being conducted on the Giotto Halley probe to reflect on the meaning of the term 'big science' in the field of space research. Derived from text

N95-24892# European Space Agency. European Space Research and Technology Center, ESTEC, Noordwijk (Netherlands).
THE ORIGINS OF THE FEDERAL REPUBLIC OF GERMANY'S SPACE POLICY, 1959-1965: EUROPEAN AND NATIONAL DIMENSIONS
Peter Fischer (European Univ. Inst., Florence, Italy.) Jan. 1994 67 p Original contains color illustrations
(ESA-HSR-12) Avail: CASI HC A04/MF A01

The ESA History Study Reports are preliminary reports of studies carried out within the framework of an ESA (European Space Agency) contract. They will form the basis of a comprehensive study of European Space activities covering the period 1959-1987. The impressive, yet somewhat shady, political past of space research in Germany is discussed in this report. Germany's participation in the initial program of ELDO served to start an ambitious national space program denied to the country since 1945, first by allied prohibitions and then, after 1955, by self-exercised political restraints. German membership in ESRO and ELDO had the advantage that the Federal government would be locked into a structure from which it was extremely difficult to withdraw. Since any successful participation in these international organizations depended on the rapid national build-up of technological know-how and a functioning industrial and scientific infrastructure, the commitment for the Federal government to promote a national space program in parallel was an immediate consequence of the decision to join ESRO and ELDO. This assessment rapidly bore fruit and the Federal Republic soon became one of the major European space powers. Derived from text

N95-24896# European Space Agency. European Space Research and Technology Center, ESTEC, Noordwijk (Netherlands).
THE SCIENTIFIC PROGRAMME BETWEEN ESRO AND ESA: CHOOSING NEW PROJECTS (1973-1977)
Arturo Russo (Palermo Univ., Italy.) Feb. 1995 101 p Original contains color illustrations
(ESA-HSR-16) Avail: CASI HC A06/MF A02

The ESA History Study Reports are preliminary reports of studies carried out within the framework of an ESA (European Space Agency) contract. They will form the basis of a comprehensive study of European Space activities covering the period 1959-1987. The transformation of ESRO (European Space Research Organization) into ESA found the Organization's bodies involved in a new round of the decision-making process to select future scientific satellite projects. In this report, the three main phases of the decision-making process are discussed. The first, from June 1973 to April 1974, the European scientific community and their representatives in ESA's advisory committee structure were invited to agree on a set of space missions for which a definition study was recommended. At the end of this phase, thirteen missions were selected for such a definition study by ESRO's Scientific Program Board (SPB). The second phase covers the period from that decision up to March 1975, when a much more important decision was required, namely to select a restricted number of missions for which a feasibility study was to be performed. The aims of such feasibility studies were to establish the technical and financial feasibility of each project, to propose a well-defined project concept, to identify the research and technology effort required to support it, and to state a preliminary cost estimate to completion. The third phase covers the first two years of the new Agency's life, and concludes with the selection of the projects to be adopted in ESA's scientific program. Derived from text

N95-25424* National Aeronautics and Space Administration. Lyndon B. Johnson Space Center, Houston, TX.
APOLLO 12: PINPOINT FOR SCIENCE (Videotape)
30 Sep. 1991 Videotape: 28 min. playing time, in color and black and white, with sound
(NASA-TM-110576; JSC-536; NONP-NASA-VT-95-46065) Avail: CASI VHS A02/BETA A22

This video, using historical film footage, photography, and computer animation, describes the launch, flight, lunar landing and exploration, and return flight of Apollo 12, one of the manned lunar missions. The astronauts were Charles Conrad, Richard Gordon, and Allen Bean. Thirty-six seconds into the November 14, 1969 launch, the spacecraft was hit by lightning from the thunderstorm surrounding the launch site. In spite of this mishap, the vehicle and astronauts were not harmed and continued with their mission. The Yankee Clipper (command module) docked with the Intrepid (lunar module) and upon reaching the Moon, the Intrepid disconnected during lunar orbit and descended to the Moon's surface to a landing area previously marked by the Surveyor satellite. After lunar surface exploration, soil sample collection, satellite maintenance, and setting up various lunar surface monitoring equipment (a seismometer and two atmospheric monitors), the Intrepid launched back into lunar orbit, docked with the Yankee Clipper, and returned to Earth. There are both B/W and color photography and film footage, which includes the earth launch, lunar orbit, descent and ascent of Intrepid on the Moon, return flight, atmospheric reentry, and recovery on the Earth, and ground to air and space communication is shown. CASI

N95-25750 Japan Industrial Technology Association, Tokyo (Japan).
[FOURTH SYMPOSIUM OF THE GEOLOGICAL SURVEY OF JAPAN ON REMOTE SENSING OF SATELLITE GEOLOGY]
16 Jun. 1993 55 p In JAPANESE Symposium held in Japan, 1993
(PB95-178737) Copyright Avail: Issuing Activity (National Technical Information Service (NTIS))

This report is related to the 4th symposium of the geological survey of Japan on 'Remote Sensing of Satellite Geology.' The report contains five papers discussing the Japanese plan for satellite exploration, existence of water in satellites, remote sensing of earth and satellites, history of solar systems as viewed from isotopes, and satellite geology by remote sensing. NTIS

N95-26184*# National Aeronautics and Space Administration. Goddard Space Flight Center, Greenbelt, MD.
STEP: SATELLITE TEST OF THE EQUIVALENCE PRINCIPLE. REPORT ON THE PHASE A STUDY
J. P. Blaser (Paul Scherrer Inst., Villigen, Switzerland.), M. Bye (Stanford Univ., CA.), G. Cavallo (European Space Agency, Paris, France.), T. Damour (Institut des Hautes Etudes Scientifiques, Bures-sur-Yvette, France.), C. W. F. Everitt (Stanford Univ., CA.), A. Hedin, R. W. Hellings (Jet Propulsion Lab., California Inst. of Tech., Pasadena, CA.), Y. Jafry (European Space Agency. European Space Research and Technology Center, ESTEC, Noordwijk, Netherlands.), R. Laurance (European Space Agency. European Space Research and Technology Center, ESTEC, Noordwijk, Netherlands.), and M. Lee (National Aeronautics and Space Administration, Washington, DC.) et al Mar. 1993 136 p
(NASA-TM-110598; NAS 1.15:110598; SCI(93)4) Avail: CASI HC A07/MF A02

During Phase A, the STEP Study Team identified three types of experiments that can be accommodated on the STEP satellite within the mission constraints and whose performance is orders of magnitude better than any present or planned future experiment of the same kind on the ground. The scientific objectives of the STEP mission are to: test the Equivalence Principle to one part in 10(exp 17), six orders of magnitude better than has been achieved on the ground; search for a new interaction between quantum-mechanical spin and ordinary matter with a sensitivity of the mass-spin coupling constant g(sub p)g(sub s) = 6 x 10(exp -34) at a range of 1 mm, which represents a seven order-of-magnitude improvement over comparable ground-based measurements; and determine the constant of gravity G with a precision of one part in 10(exp 6) and to test the validity of the inverse square law with the same precision, both two orders of magnitude better than has been achieved on the ground. Author

N95-26205*# Georgia Inst. of Tech., Atlanta, GA. School of Aerospace Engineering.
OPTIMAL GUIDANCE LAW DEVELOPMENT FOR AN ADVANCED LAUNCH SYSTEM Final Report
Anthony J. Calise and Martin S. K. Leung Hampton, VA NASA Apr. 1995 107 p
(Grant NAG1-939; RTOP 232-01-04-05)
(NASA-CR-4667; NAS 1.26:4667) Avail: CASI HC A06/MF A02

The objective of this research effort was to develop a real-time guidance approach for launch vehicles ascent to orbit injection. Various analytical approaches combined with a variety of model order and model complexity reduction have been investigated. Singular perturbation methods were first attempted and found to be unsatisfactory. The second approach based on regular perturbation analysis was subsequently investigated. It also fails because the aerodynamic effects (ignored in the zero order solution) are too large to be treated as perturbations. Therefore, the study demonstrates that perturbation methods alone (both regular and singular perturbations) are inadequate for use in developing a guidance algorithm for the atmospheric flight phase of a launch vehicle. During a second phase of the research effort, a hybrid analytic/numerical approach was developed and evaluated. The approach combines the numerical methods of collocation and the analytical method of regular perturbations. The concept of choosing intelligent interpolating functions is also introduced. Regular perturbation analysis allows the use of a crude representation for the collocation solution, and intelligent interpolating functions further reduce the number of elements without sacrificing the approximation accuracy. As a result, the combined method forms a powerful tool for solving real-time optimal control problems. Details of the approach are illustrated in a fourth order nonlinear example. The hybrid approach is then applied to the launch vehicle problem. The collocation solution is derived from a bilinear tangent steering law, and results in a guidance solution for the entire flight regime that includes both atmospheric and exoatmospheric flight phases. Author

13 ASTRODYNAMICS

Includes powered and free-flight trajectories; and orbital and launching dynamics.

No abstracts in this category.

14 GROUND SUPPORT SYSTEMS AND FACILITIES (SPACE)

Includes launch complexes, research and production facilities; ground support equipment, e.g., mobile transporters; and simulators.

For related information see also *09 Research and Support Facilities (Air).*

N95-26305*# Vanderbilt Univ., Nashville, TN.
UNIVERSAL TEST FACILITY
Mike Laughery *In its* The 1994 NASA/USRA/ADP Design Projects 13 p(SEE N95-26304 08-80) 1994 (For primary document see N95-26304 08-80)
Avail: CASI HC A03/MF A02

N95-26306*# Vanderbilt Univ., Nashville, TN.
AUTOMATED PROTEIN CRYSTAL GROWTH FACILITY
Stacey Donald *In its* The 1994 NASA/USRA/ADP Design Projects 32 p(SEE N95-26304 08-80) 1994 (For primary document see N95-26304 08-80)
Avail: CASI HC A03/MF A02

15 LAUNCH VEHICLES AND SPACE VEHICLES

Includes boosters; operating problems of launch/space vehicle systems; and reusable vehicles.

For related information see also *20 Spacecraft Propulsion and Power.*

N95-24579*# McDonnell-Douglas Space Systems Co., Cocoa Beach, FL.
STUDY OF LAUNCH SITE PROCESSING AND FACILITIES FOR FUTURE LAUNCH VEHICLES Final Report, 21 Apr. 1993 - 31 Mar. 1995
Rex Shaffer Mar. 1995 167 p
(Contract NAS10-11999)
(NASA-CR-198025; NAS 1.26:198025) Avail: CASI HC A08/MF A02

The purpose of this research is to provide innovative and creative approaches to assess the impact to the Kennedy Space Center and other launch sites for a range of candidate manned and unmanned space transportation systems. The general scope of the research includes the engineering activities, analyses, and evaluations defined in the four tasks below: (1) development of innovative approaches and computer aided tools; (2) operations analyses of launch vehicle concepts and designs; (3) assessment of ground operations impacts; and (4) development of methodologies to identify promising technologies. Author

N95-26308*# Vanderbilt Univ., Nashville, TN.
LAUNCH SYSTEM DESIGN FOR ACCESS TO SPACE
Corbin Barnes *In its* The 1994 NASA/USRA/ADP Design Projects 20 p(SEE N95-26304 08-80) 1994 (For primary document see N95-26304 08-80)
Avail: CASI HC A03/MF A02

16 SPACE TRANSPORTATION

Includes passenger and cargo space transportation, e.g., shuttle operations; and space rescue techniques.

For related information see also *03 Air Transportation and Safety* and *18 Spacecraft Design, Testing and Performance.* For space suits see *54 Man/System Technology and Life Support.*

N95-24195* National Aeronautics and Space Administration. Lyndon B. Johnson Space Center, Houston, TX.
GO FOR EVA (Videotape)
5 Apr. 1995 *Its* Liftoff to Learning Series Videotape: 13 min. 48 sec. playing time, in color, with sound
(NASA-TM-110537; NONP-NASA-VT-95-43940) Avail: CASI VHS A02/BETA A22

In this educational video series, 'Liftoff to Learning', astronauts from the STS-37 Space Shuttle Mission (Jay Apt, Jerry Ross, Ken Cameron, Steve Nagel, and Linda Godwin) show what EVA (extravehicular activity) means, talk about the history and design of the space suits and why they are designed the way they are, describe different ways they are used (payload work, testing and maintenance of equipment, space environment experiments) in EVA work, and briefly discuss the future applications of the space suits. Computer graphics and animation is included. CASI

N95-24197* National Aeronautics and Space Administration. Lyndon B. Johnson Space Center, Houston, TX.
STS-66 MISSION HIGHLIGHTS RESOURCE TAPE (Videotape)
1995 Videotape: 54 min. playing time, in color, with sound
(NASA-TM-110550; VJSC-1448; NONP-NASA-VT-95-44679) Avail: CASI VHS A02/BETA A22

This video contains the mission highlights of the STS-66 Space Shuttle Atlantis Mission in November 1994. Astronauts included: Don McMonagle (Mission Commander), Kurt Brown, Ellen Ochoa (Payload Commander), Joe Tanner, Scott Parazynski, and Jean-Francois Clervoy (collaborating French astronaut). Footage includes: pre-launch suitup, entering Space Shuttle, countdown and launching of Shuttle, EVA activities (ATLAS-3, CRISTA/SPAS, SSBUV/A, ESCAPE-2), on-board experiments dealing with microgravity and its effects, protein crystal growth experiments, daily living and sleeping compartment footage, earthviews of various meteorological processes (dust storms, cloud cover, ocean storms), pre-landing and land footage (both from inside the Shuttle and from outside with long range cameras), and tracking and landing shots from inside Mission Control Center. Included is air-to-ground communication between Mission Control and the Shuttle. This Shuttle was the last launch of 1994. CASI

N95-24198* National Aeronautics and Space Administration. Lyndon B. Johnson Space Center, Houston, TX.
STS-67 POST FLIGHT PRESENTATION (Videotape)
3 Apr. 1995 Videotape: 41 min. 15 sec. playing time, in color, with sound
(NASA-TM-110552; JSC-1477; NONP-NASA-VT-95-45307) Avail: CASI VHS A02/BETA A22

This video is the post-flight presentation by the astronauts of the STS-67 Space Shuttle Mission. The astronauts were: Steve Oswald (Mission Commander), Bill Gregory (Shuttle Pilot), John Grunsfeld (Mission Specialist), Sam Durrance (Payload Specialist), Ron Parise (Payload Specialist), and Tammy Jernigan (Payload Commander). Footage includes: pre-launch suitup and launch (liftoff), the deployment of the telescope package payload (Hopkins UV telescope, Wisconsin UV polarimeter, and Astrostar Tracker) for their astronomical observations of different stellar objects, inside Shuttle shots of data collection stations, protein crystal growth experiments, medical BSO of head and eye functions in microgravity environment, storm activity over the United States and other Earth observation shots, Mid-deck Act Control Experiments, school-Shuttle direct radio communication, and descent and landing footage. This launch was a night launch and the flight was a 17 day flight (extended two days from original flight plan). CASI

N95-24215* National Aeronautics and Space Administration. Lyndon B. Johnson Space Center, Houston, TX.
APOLLO 13: HOUSTON, WE'VE GOT A PROBLEM (Videotape)
10 Apr. 1991 Videotape: 28 min. 30 sec. playing time, in color, with

sound
(NASA-TM-110551; JSC-548; NONP-NASA-VT-95-44678) Avail: CASI VHS A02/BETA A22

This video contains historical footage of the flight of Apollo-13, the fifth Lunar Mission and the third spacecraft that was to land on the Moon. Apollo-13's launch date was April 11, 1970. On the 13th of April, after docking with the Lunar Module, the astronauts, Jim Lovell, Fred Haise, and Jack Swiggert, discovered that their oxygen tanks had ruptured and ended up entering and returning to Earth in the Lunar Module instead of the Command Module. There is footage of inside module and Mission Control shots, personal commentary by the astronauts concerning the problems as they developed, national news footage and commentary, and a post-flight Presidential Address by President Richard Nixon. Film footage of the approach to the Moon and departing from Earth, and air-to-ground communication with Mission Control is included. CASI

N95-24466*# National Aeronautics and Space Administration, Washington, DC.

REPORT OF THE SPACE SHUTTLE MANAGEMENT INDEPENDENT REVIEW TEAM

Feb. 1995 40 p
(NASA-TM-110579; NAS 1.15:110579) Avail: CASI HC A03/MF A01

At the request of the NASA Administrator a team was formed to review the Space Shuttle Program and propose a new management system that could significantly reduce operating costs. Composed of a group of people with broad and extensive experience in spaceflight and related areas, the team received briefings from the NASA organizations and most of the supporting contractors involved in the Shuttle Program. In addition, a number of chief executives from the supporting contractors provided advice and suggestions. The team found that the present management system has functioned reasonably well despite its diffuse structure. The team also determined that the shuttle has become a mature and reliable system, and--in terms of a manned rocket-propelled space launch system--is about as safe as today's technology will provide. In addition, NASA has reduced shuttle operating costs by about 25 percent over the past 3 years. The program, however, remains in a quasi-development mode and yearly costs remain higher than required. Given the current NASA-contractor structure and incentives, it is difficult to establish cost reduction as a primary goal and implement changes to achieve efficiencies. As a result, the team sought to create a management structure and associated environment that enables and motivates the Program to further reduce operational costs. Accordingly, the review team concluded that the NASA Space Shuttle Program should (1) establish a clear set of program goals, placing a greater emphasis on cost-efficient operations and user-friendly payload integration; (2) redefine the management structure, separating development and operations and disengaging NASA from the daily operation of the space shuttle; and (3) provide the necessary environment and conditions within the program to pursue these goals. Author

N95-24765*# National Aeronautics and Space Administration. Langley Research Center, Hampton, VA.

SHUTTLE TO SPACE STATION TRANSFER OF THE MATERIALS EXPOSURE FACILITY

David T. Shannon, Jr. and Phillip J. Klich (Lockheed Engineering and Sciences Co., Hampton, VA.) Mar. 1995 26 p
(RTOP 963-89-00-01)
(NASA-TM-110156; NAS 1.15:110156) Avail: CASI HC A03/MF A01

The Materials Exposure Facility (MEF) is being proposed by LaRC as the first long-term space materials exposure facility with real-time interaction with materials experiments in actual conditions of orbital space flight. The MEF is proposed as a Space Station external payload dedicated to technology advancement in spacecraft materials and coatings research. This paper will define a set of potential logistics for removing the MEF from the Shuttle cargo bay and the process required for transferring the MEF to a specific external payload site on Space Station Freedom (SSF). The SSF UF-2 configuration is used for this study. The kinematics and ability to successfully perform the appropriate MEF maneuvers required were verified. During completion of this work, the Space Station was redesigned and the International Space Station Alpha (ISSA) configuration evolved. The transfer procedure for SSF was valid for ISSA; however, a verification of kinematics and clearances was essential. Also, SSF and ISSA robotic interfaces with the Orbiter were different. Author

N95-25747# Boeing Co., Seattle, WA.

COMMERCIAL SPACE TRANSPORTATION STUDY (CSTS) Final Report

May 1994 655 p Prepared in cooperation with Martin Marietta Corp., Bethesda, MD; General Dynamics Corp., Saint Louis, MO; McDonnell-Douglas Corp., Saint Louis, MO; Lockheed Corp., Calabasas, CA; and Rockwell International Corp., Pittsburgh, PA
(SSD94D0035) Avail: CASI HC A99/MF A06

The basis for this study was the perception held worldwide by government and industry that: (1) significant untapped markets exist or could be created if the costs for access to space could be reduced by an order of magnitude or more; (2) a new launch system can provide this order of magnitude reduction in launch costs; and (3) a reduction of that magnitude will cause the equivalent of a space industrial revolution with a tremendous increase in users and traffic. The conjecture is often stated but has never been proved. Phase 1 of the study identifies those new users and catagorizes their prospective payloads. Once the business opportunity has been identified, the best prospective launch system can be determined and the required technologies put in place. This is the linkage between phase 1 and the proposed phases 2 and 3. Author

N95-25874* National Aeronautics and Space Administration. Lyndon B. Johnson Space Center, Houston, TX.

STS-63 MISSION HIGHLIGHTS RESOURCE TAPE (Videotape)

1995 Videotape: 1 hr. playing time, in color, with sound
(NASA-TM-110562; JSC-1472; NONP-NASA-VT-95-45997) Avail: CASI VHS A01/BETA A22

This video (JSC1472) contains important visual events including launch, SPARTAN 204, SPACEHAB-03, CGP/ODERACS, and the rendezvous with the MIR Space Station, along with onboard activities, and landing. Also included are air-to-ground transmission between the crew and Mission, and various earthviews. JSC

N95-26189*# Lockheed Engineering and Management Services Co., Inc., Houston, TX. Flight Evaluation and Engineering Office.

STS-60 SPACE SHUTTLE MISSION REPORT

Robert W. Fricke, Jr. Apr. 1994 44 p Sponsored by NASA. Johnson Space Center
(NASA-CR-197233; JSC-08289; NSTS-08289; NAS 1.26:197233) Avail: CASI HC A03/MF A01

The STS-60 Space Shuttle Program Mission Report summarizes the Payload activities as well as the Orbiter, External Tank (ET), Solid Rocket Booster (SRB), Redesigned Solid Rocket Motor (RSRM), and the Space Shuttle main engine (SSME) systems performance during the sixtieth flight of the Space Shuttle Program and eighteenth flight of the Orbiter vehicle Discovery (OV-103). In addition to the Orbiter, the flight vehicle consisted of an ET designated at ET-61 (Block 10); three SSME's which were designated as serial numbers 2012, 2034, and 2032 in positions 1, 2, and 3, respectively; and two SRB's which were designated BI-062. The RSRM's that were installed in each SRB were designated as 360L035A (lightweight) for the left SRB, and 360Q035B (quarterweight) for the right SRB. This STS-60 Space Shuttle Program Mission Report fulfills the Space Shuttle Program requirement as documented in NSTS 07700, Volume VIII, Appendix E. That document requires that each major organizational element supporting the Program report the results of its hardware evaluation and mission performance plus identify all related in-flight anomalies. The primary objectives of the STS-60 mission were to deploy and retrieve the Wake Shield Facility-1 (WSF-1), and to activate the Spacehab-2 payload and perform on-orbit experiments. Secondary objectives of this flight were to activate and command the Capillary Pumped Loop/Orbital Debris Radar Calibration Spheres/Breman Satellite Experiment/Getaway Special (GAS) Bridge Assembly (CAPL/ODERACS/BREMSAT/GBA) payload, the Auroral Photography Experiment-B (APE-B), and the Shuttle Amateur Radio Experiment-II (SAREX-II). Derived from text

17 SPACE COMM., SPACECRAFT COMM., COMMAND & TRACKING

Includes telemetry; space communications networks; astronavigation and guidance; and radio blackout.

For related information see also *04 Aircraft Communications and Navigation* and *32 Communications and Radar.*

N95-25508 Science Applications International Corp., McLean, VA.
ASSESSMENT OF COMMERCIAL SATELLITE COMMUNICATIONS INITIATIVE (CSCI) STUDIES Final Report, Oct. 1992 - Dec. 1993
N. Smith, W. Kearns, and P. Chapell Jan. 1994 75 p Limited Reproducibility: More than 20% of this document may be affected by microfiche quality
(Contract DCA100-90-C-0056)
(AD-A288357; SAIC-MSO-93-205) Avail: Issuing Activity (Defense Technical Information Center (DTIC))

This report summarizes the fixed and mobile satellite services (FSS, MSS) as studied by three contractors: COMSAT, Hughes, and Space Systems/LORAL. Each contractor developed a commercial satellite communications initiative (CSCI) architecture based on the requirements provided them from DOD's Integrated Communications Data Base (ICDB). An implementation plan, recommending an acquisition, transition, logistics, and host nation approval plan, was developed according to each contractor's recommended architecture. In addition, this report summarizes the demonstrations conducted by each contractor and the vulnerabilities inherent in using commercial satellites. This summary information is provided as the foundation for the section on the government's assessment and critique of the CSCI study which emphasizes the highlights and remaining uncertainties from this program. DTIC

18 SPACECRAFT DESIGN, TESTING AND PERFORMANCE

Includes satellites; space platforms; space stations; spacecraft systems and components such as thermal and environmental controls; and attitude controls.

For life support systems see *54 Man/System Technology and Life Support.* For related information see also *05 Aircraft Design, Testing and Performance, 39 Structural Mechanics,* and *16 Space Transportation.*

N95-24505*# National Aeronautics and Space Administration, Washington, DC.
AEROSPACE SAFETY ADVISORY PANEL Annual Report, Feb. 1994 - Jan. 1995
Mar. 1995 66 p
(NASA-TM-110554; NAS 1.15:110554) Avail: CASI HC A04/MF A01

The Aerospace Safety Advisory Panel (ASAP) monitored NASA's activities and provided feedback to the NASA Administrator, other NASA officials and Congress throughout the year. Particular attention was paid to the Space Shuttle, its launch processing and planned and potential safety improvements. The Panel monitored Space Shuttle processing at the Kennedy Space Center (KSC) and will continue to follow it as personnel reductions are implemented. There is particular concern that upgrades in hardware, software, and operations with the potential for significant risk reduction not be overlooked due to the extraordinary budget pressures facing the agency. The authorization of all of the Space Shuttle Main Engine (SSME) Block II components portends future Space Shuttle operations at lower risk levels and with greater margins for handling unplanned ascent events. Throughout the year, the Panel attempted to monitor the safety activities related to the Russian involvement in both space and aeronautics programs. This proved difficult as the working relationships between NASA and the Russians were still being defined as the year unfolded. NASA's concern for the unique safety problems inherent in a multi-national endeavor appears appropriate. Actions are underway or contemplated which should be capable of identifying and rectifying problem areas. The balance of this report presents 'Findings and Recommendations' (Section 2), 'Information in Support of Findings and Recommendations' (Section 3) and Appendices describing Panel membership, the NASA response to the March 1994 ASAP report, and a chronology of the panel's activities during the reporting period (Section 4). Derived from text

N95-24581*# National Aeronautics and Space Administration. Langley Research Center, Hampton, VA.
EFFICIENT EIGENVALUE ASSIGNMENT BY STATE AND OUTPUT FEEDBACK WITH APPLICATIONS FOR LARGE SPACE STRUCTURES
Eric C. Vannell (George Washington Univ., Hampton, VA.), Sean P. Kenny, and Peiman G. Maghami Mar. 1995 69 p
(RTOP 233-01-01-03)
(NASA-TM-110155; NAS 1.15:110155) Avail: CASI HC A04/MF A01

The erection and deployment of large flexible structures having thousands of degrees of freedom requires controllers based on new techniques of eigenvalue assignment that are computationally stable and more efficient. Scientists at NASA Langley Research Center have developed a novel and efficient algorithm for the eigenvalue assignment of large, time-invariant systems using full-state and output feedback. The objectives of this research were to improve upon the output feedback version of this algorithm, to produce a toolbox of MATLAB functions based on the efficient eigenvalue assignment algorithm, and to experimentally verify the algorithm and software by implementing controllers designed using the MATLAB toolbox on the phase 2 configuration of NASA Langley's controls-structures interaction evolutionary model, a laboratory model used to study space structures. Results from laboratory tests and computer simulations show that effective controllers can be designed using software based on the efficient eigenvalue assignment algorithm. Author

N95-24711# Los Alamos National Lab., NM.
AN OVERVIEW OF THE NUCLEAR ELECTRIC PROPULSION SPACE TEST PROGRAM (NEPSTP) SATELLITE
Susan S. Voss and Edward L. Reynolds (Johns Hopkins Univ., Laurel, MD.) 1994 13 p Presented at the 29th Intersociety Energy Conversion Engineering Conference, Monterey, CA, 7-12 Aug. 1994
(Contract W-7405-eng-36)
(DE94-013121; LA-UR-94-1688; CONF-940812-4) Avail: CASI HC A03/MF A01

Early in 1992 the idea of purchasing a Russian designed and fabricated space reactor power system and integrating it with a US designed satellite went from fiction to reality with the purchase of the first two Topaz II reactors by the Strategic Defense Initiative Organization (now the Ballistic Missile Defense Organization (BMDO). The New Mexico Alliance was formed to establish a ground test facility in which to perform nonnuclear systems testing of the Topaz II, and to evaluate the Topaz 11 system for flight testing with respect to safety, performance, and operability. In conjunction, SDIO requested that the Applied Physics Laboratory in Laurel, MD propose a mission and design a satellite in which the Topaz II could be used as the power source. The outcome of these two activities was the design of the Nuclear Electric Propulsion Space Test Program (NEPSTP) satellite which combines a modified Russian Topaz II power system with a US designed satellite to achieve a specified mission. Due to funding reduction within the SDIO, the Topaz II flight program was postponed indefinitely at the end of Fiscal Year 1993. The purpose of this paper is to present an overview of the NEPSTP mission and the satellite design at the time the flight program ended. DOE

N95-24761# Joint Publications Research Service, Washington, DC.
JPRS REPORT: SCIENCE AND TECHNOLOGY. CENTRAL EURASIA: SEMINAR ON MATERIALS SCIENCE
14 Feb. 1995 45 p Transl. into ENGLISH from various Central Eurasian articles Presented at the Problems in Mechanics Under Conditions of Microgravity Conference, Moscow, Russia, 11 Nov. 1993.
(JPRS-UST-95-007) Avail: CASI HC A03/MF A01

Translated articles cover the following topics: mathematical modeling and measurement of microaccelerations aboard the Mir orbital station; system for protecting onboard production equipment from vibrations; seminar on numerical methods used in problems involving heat-and-mass transfer. CASI

N95-25337*# National Aeronautics and Space Administration. John F. Kennedy Space Center, Lompoc, CA.
DEBRIS/ICE/TPS ASSESSMENT AND INTEGRATED PHOTOGRAPHIC ANALYSIS OF SHUTTLE MISSION STS-63 Final Report, 1 Feb. - 13 Feb. 1995
Gregory N. Katnik, Barry C. Bowen, and J. Bradley Davis Mar. 1995 102 p Original contains color illustrations
(NASA-TM-110649; NAS 1.15:110649) Avail: CASI HC A06/MF A02; 43 functional color pages

A debris/ice/thermal protection system assessment and integrated photographic analysis was conducted for shuttle mission STS-63. Debris inspections of the flight elements and launch pad were performed before and after launch. Icing conditions on the external tank were assessed by the use of computer programs, monographs, and infrared scanner data during cryogenic loading of the vehicle followed by on-pad visual inspection. High speed photography of the launch was analyzed to identify ice/debris sources and evaluate potential vehicle damage and/or in-flight anomalies. This report documents the ice/debris/thermal protection system conditions and integrated photographic analysis of shuttle mission STS-63, and the resulting effect on the space shuttle program. Author

N95-25664# National Aerospace Lab., Tokyo (Japan). Aerodynamics Div.
AERODYNAMIC CHARACTERISTICS OF THE ORBITAL REENTRY VEHICLE EXPERIMENTAL PROBE FINS IN A SUPERSONIC FLOW
Mitsunori Watanabe, Hideo Sekine, Atsushi Tate, and Junichi Noda Apr. 1994 18 p In JAPANESE
(ISSN 0389-4010)
(NAL-TR-1232) Avail: CASI HC A03/MF A01

The aerodynamic characteristics of probe fins with a sweep angle of 60 deg, which are equipped on the Orbital Reentry Experiment (OREX) vehicle to measure the surrounding ionized gas temperature and electron number density distributions in the high temperature communication black out regions, have been measured in the supersonic wind tunnel of the National Aerospace Laboratory and compared with those of the fins of 0 deg sweep angles. Since the probes are to be embedded in the boundary layer where the local Mach number is less than 2.5 over the OREX surface at a hypersonic flight speed, the aerodynamic characteristics in supersonic regions are needed to estimate the rolling moments of fins caused by the error of the installation angles. The lift coefficient slope of the probe fins decreases as the Mach number increases, being less than the values for the 0 deg sweep fins. The drag coefficient depends highly on the sweep angle of the fins in Mach number regions less than 2.5. Author

N95-25875*# National Aeronautics and Space Administration. Marshall Space Flight Center, Huntsville, AL.
THE NATURAL SPACE ENVIRONMENT: EFFECTS ON SPACECRAFT
Bonnie F. James, O. W. Norton, comp., and Margaret B. Alexander, ed. Washington Nov. 1994 31 p Original contains color illustrations
(NASA-RP-1350; M-763; NAS 1.61:1350) Avail: CASI HC A03/MF A01; 4 functional color pages

The effects of the natural space environments on spacecraft design, development, and operation are the topic of a series of NASA Reference Publications currently being developed by the Electromagnetics and Environments Branch, Systems Analysis and Integration Laboratory, Marshall Space Flight Center. This primer provides an overview of the natural space environments and their effect on spacecraft design, development, and operations, and also highlights some of the new developments in science and technology for each space environment. It is hoped that a better understanding of the space environment and its effect on spacecraft will enable program management to more effectively minimize program risks and costs, optimize design quality, and successfully achieve mission objectives. Author

19 SPACECRAFT INSTRUMENTATION

For related information see also *06 Aircraft Instrumentation* and *35 Instrumentation and Photography.*

No abstracts in this category.

20 SPACECRAFT PROPULSION AND POWER

Includes main propulsion systems and components, e.g., rocket engines; and spacecraft auxiliary power sources.

For related information see also *07 Aircraft Propulsion and Power, 28 Propellants and Fuels, 44 Energy Production and Conversion,* and *15 Launch Vehicles and Space Vehicles.*

N95-24216*# McDonnell-Douglas Aerospace, Seabrook, MD.
SMALL SPACECRAFT POWER AND THERMAL SUBSYSTEMS Final Report
D. Eakman, R. Lambeck, M. Mackowski, and L. Slifer, Jr. Dec. 1994 124 p
(Contract NAS1-19244; RTOP 477-50-00)
(NASA-CR-195029; NAS 1.26:195029) Avail: CASI HC A06/MF A02

This white paper provides a general guide to the conceptual design of satellite power and thermal control subsystems with special emphasis on the unique design aspects associated with small satellites. The operating principles of these technologies are explained and performance characteristics of current and projected components are provided. A tutorial is presented on the design process for both power and thermal subsystems, with emphasis on unique issues relevant to small satellites. The ability of existing technology to meet future performance requirements is discussed. Conclusions and observations are presented that stress cost-effective, high-performance design solutions. Author

N95-24428*# McDonnell-Douglas Aerospace, Seabrook, MD.
SMALL SPACECRAFT POWER AND THERMAL SUBSYSTEMS
D. Eakman, R. Lambeck, M. Mackowski, and L. Slifer, Jr. Dec. 1994 125 p
(Contract NAS1-19244; RTOP 477-50-00)
(NASA-CR-195029; NAS 1.26:195029) Avail: CASI HC A06/MF A02

This white paper provides a general guide to the conceptual design of satellite power and thermal control subsystems with special emphasis on the unique design aspects associated with small satellites. The operating principles of these technologies are explained and performance characteristics of current and projected components are provided. A tutorial is presented on the design process for both power and thermal subsystems, with emphasis on unique issues relevant to small satellites. The ability of existing technology to meet future performance requirements is discussed. Conclusions and observations are presented that stress cost-effective, high-performance design solutions. Author

N95-24440*# United Technologies Corp., San Jose, CA.
BSM DELTA QUALIFICATION 2, VOLUME 1 Final Report
11 Nov. 1994 100 p Prepared in cooperation with United Space Boosters, Inc., Huntsville, AL
(Contract NAS8-36300)
(NASA-CR-196566-Vol-1; NAS 1.26:196566-Vol-1; CSD-5597-93-2) Avail: CASI HC A05/MF A02

This report, presented in three volumes, provides the results of a two-motor Delta Qualification 2 program conducted in 1993 to certify the following enhancements for incorporation into Booster Separation Motor (BSM) flight hardware: (1) vulcanized-in-place nozzle aft closure insulation; (2) new isostatic ATJ bulk graphite throat insert material; (3) adhesive EA 9394 for bonding the nozzle throat, igniter grain rod/centering insert/igniter case; (4) deletion of the igniter adapter insulator ring; (5) deletion of igniter adapter/igniter case interface RTV; and (6) deletion of Loctite from igniter retainer plate threads. The enhancements above directly resulted from (1) the BSM Total Quality Management (TQM) Team initiatives to enhance the BSM producibility, and (2) the necessity to qualify new throat insert and adhesive systems to replace existing materials that will not be available.

Testing was completed at both the component and motor levels. Component testing was accomplished to screen candidate materials (e.g., throat materials, adhesive systems) and to optimize processes (e.g., aft closure insulator vulcanization approach) prior to their incorporation into the test motors. Motor testing - consisting of two motors, randomly selected by USBI's onsite quality personnel from production lot AAY, which were modified to accept the enhancements - were completed to provide the final qualification of the enhancements for incorporation into flight hardware. It is concluded that all of the enhancements herein tested are qualified to be incorporated into flight hardware for the BSM. Author

N95-24626*# Alabama Univ., Huntsville, AL. Dept. of Electrical Engineering

AUTOMATION BASED ON KNOWLEDGE MODELING THEORY AND ITS APPLICATIONS IN ENGINE DIAGNOSTIC SYSTEMS USING SPACE SHUTTLE MAIN ENGINE VIBRATIONAL DATA M.S. Thesis

Jonnathan H. Kim Apr. 1995 66 p Sponsored by NASA. Marshall Space Flight Center

(CDDF Proj. 92-12)

(NASA-CR-197983; NAS 1.26:197983) Avail: CASI HC A04/MF A01

Humans can perform many complicated tasks without explicit rules. This inherent and advantageous capability becomes a hurdle when a task is to be automated. Modern computers and numerical calculations require explicit rules and discrete numerical values. In order to bridge the gap between human knowledge and automating tools, a knowledge model is proposed. Knowledge modeling techniques are discussed and utilized to automate a labor and time intensive task of detecting anomalous bearing wear patterns in the Space Shuttle Main Engine (SSME) High Pressure Oxygen Turbopump (HPOTP). Author

N95-24844*# United Technologies Corp., San Jose, CA.

BSM DELTA QUALIFICATION 2, VOLUME 2 Final Report

11 Nov. 1994 432 p

(Contract NAS8-36300)

(NASA-CR-196567; NAS 1.26:196567; CSD-5597-93-2) Avail: CASI HC A19/MF A04

This report, presented in three volumes, provides the results of a two-motor Delta Qualification 2 program conducted in 1993 to certify the following enhancements for incorporation into booster separation motor (BSM) flight hardware: vulcanized-in-place nozzle aft closure insulation; new iso-static ATJ bulk graphite throat insert material; adhesive EA 9394 for bonding the nozzle throat, igniter grain rod/centering insert/igniter case; deletion of the igniter adapter insulator ring; deletion of the igniter adapter/igniter case interface RTV; and deletion of loctite from igniter retainer plate threads. The enhancements above directly resulted from (1) the BSM total quality management (TQM) team initiatives to enhance the BSM producibility, and (2) the necessity to qualify new throat insert and adhesive systems to replace existing materials that will not be available. Testing was completed at both the component and motor levels. Component testing was accomplished to screen candidate materials (e.g., throat materials, adhesive systems) and to optimize processes (e.g., aft closure insulator vulcanization approach) prior to their incorporation into the test motors. Motor tests -- consisting of two motors, randomly selected by USBI's on-site quality personnel from production lot AAY, which were modified to accept the enhancements -- were completed to provide the final qualification of the enhancements for incorporation into flight hardware. Volume 2 details the environmental testing (vibration and shock) conducted at Marshall Space Flight Center (MSFC) to which the motors were subjected prior to static tests. Author

N95-24845*# United Technologies Corp., San Jose, CA.

BSA DELTA QUALIFICATION 2, VOLUME 3, BOOK 1 Final Report

11 Nov. 1994 424 p

(Contract NAS8-36300)

(NASA-CR-196565; NAS 1.26:196565; CSD-5597-93-2) Avail: CASI HC A18/MF A04

This report, presented in three volumes, provides the results of a two-motor Delta Qualification 2 program conducted in 1993 to certify the following enhancements for incorporation into booster separation motor (BSM) flight hardware: vulcanized-in-place nozzle aft closure insulation; new iso-static ATJ bulk graphite throat insert material; adhesive EA 9394 for bonding the nozzle throat, igniter grain rod/centering insert/igniter case; deletion of the igniter adapter insulator ring; deletion of the igniter adapter/igniter case interface RTV; and deletion of Loctite from igniter retainer plate threads. The enhancements above directly resulted from (1) the BSM total quality management (TQM) team initiatives to enhance the BSM producibility, and (2) the necessity to qualify new throat insert and adhesive systems to replace existing materials that will not be available. Testing was completed at both the component and motor levels. Component testing was accomplished to screen candidate materials (e.g., throat materials, adhesive systems) and to optimize processes (e.g., aft closure insulator vulcanization approach) prior to their incorporation into the test motors. Motor tests -- consisting of two motors, randomly selected by USBI's on-site quality personnel from production lot AAY, which were modified to accept the enhancements -- were completed to provide the final qualification of the enhancements for incorporation into flight hardware. Volume 3 book 1 provides supporting documentation to the analyses and plans of testing the two Delta Qualification units including thermal cycling planning/data acceptance records, environmental test procedures and pretest temperature conditioning history, Delta Qualification test plan, and specification SE0837 -- mix acceptance test specification. Author

N95-24854*# United Technologies Corp., San Jose, CA.

BSM DELTA QUALIFICATION 2, VOLUME 3, BOOK 2 Final Report

11 Nov. 1994 329 p

(Contract NAS8-36300)

(NASA-CR-196568; NAS 1.26:196568; CSD-5597-93-2) Avail: CASI HC A15/MF A03

This report, presented in three volumes, provides the results of a two-motor Delta Qualification 2 program conducted in 1993 to certify the following enhancements for incorporation into booster separation motor (BSM0 flight hardware: vulcanized-in-place nozzle aft closure insulation; new iso-static ATJ bulk graphite throat insert material, adhesive EA9394 for bonding the nozzle throat, igniter grain rod/centering insert/igniter case; deletion of the igniter adapter insulator ring; deletion of the igniter adapter/igniter case interface RTV; and deletion of loctite from igniter retainer plate threads. The enhancements above directly resulted from (1) the BSM total quality management (TQM) team initiatives to enhance the BSM producibility, and (2) the necessity to qualify new throat insert and adhesive systems to replace existing materials that will not be available. Testing was completed at both the component and motor levels. Component testing was accomplished to screen candidate materials (e.g., throat materials, adhesive systems) and to optimize processes (e.g., aft closure insulator vulcanization approach) prior to their incorporation into the test motors. Motor testing--consisting of two motors, randomly selected by USBI's on-site quality personnel from production lot AAY, which were modified to accept the enhancements -- was completed to provide the final qualification of the enhancements for incorporation into flight hardware. Volume 3, Book 2 provides various supporting documentation to the previous volumes with regards to the testing of the two Delta qualification units: data acceptance records, thermal conditioning analysis, igniter adapter thermal flake analysis, laboratory adhesive (EA-9394) qualification report, throat insert thermal/structural analysis, Delta Qualification Nonconformance Reports (NCR's), O-ring seating tests, and interim test report for vulcanization process qualification. Author

N95-24999# National Aerospace Lab., Tokyo (Japan). Rocket Propulsion Research Div.

DEVELOPMENT TEST OF A LIQUID APOGEE ENGINE FOR THE ETS-4

Oct. 1994 25 p Prepared in cooperation with Ishikawajima-Harima Heavy Industries Co., Ltd., Tokyo, Japan and National Space Development Agency, Tokyo, Japan

(ISSN 0389-4010)

(NAL-TR-1250) Avail: CASI HC A03/MF A01

A pressure-fed, full-blowdown, nitrogen tetroxide (NTO)/hydrazine (N2H4) bipropellant liquid apogee propulsion system was selected for Engineering Test Satellite - VI (ETS - VI), a 2000-kg Japanese Engineering Test Satellite. This 2000-kg mass geostationary satellite is scheduled to be launched by an H - II rocket in 1994. The apogee engine required a high reliability and a relatively high performance for a pressure fed system. In the preliminary development phase of the apogee engine, a peak vacuum specific impulse Ispv of 325 s was set as the initial development target. This performance requirement of the apogee engine is greater than that of the bipropellant engine using NTO/momomethyl hydrazine (MMH). To meet such high

performance requirements, we employed a NTO/N2H4 propellant system instead of NTO/MMH propellant and used a very large area ratio nozzle (nozzle area ratio is 200 to 300). To enhance the reliability of the apogee propulsion system, we selected a pressure-fed, full-blowdown system. Fundamental studies including hard-start, pop and thermal problems were also conducted during the development series of apogee engine started in 1983. Performance characteristics of apogee engine developed in 1990 were as follows: chamber pressure Pc = 0.97 approximately 0.63 MPa, mixture ratio MR = 0.85 approximately 1.05, vacuum thrust = 1980 approximately 1280 N, mean vacuum specific impulses Ispv = 320.0 +/- 2.7 s, and total burn time = 2900 s. Delivered peak Ispv was less than the initial development target, however, the engine performance was higher than that of the engine for NTO/MMH propellant. This paper describes mainly the development studies of the injectors used in the apogee engine. Author

N95-25103*# Engineering-Science, Inc., Huntsville, AL.
ADVANCED MULTI-PHASE FLOW CFD MODEL DEVELOPMENT FOR SOLID ROCKET MOTOR FLOWFIELD ANALYSIS Final Report
Paul Liaw and Yen-Sen Chen Mar. 1995 67 p
(Contract NAS8-39398)
(NASA-CR-198044; NAS 1.26:198044) Avail: CASI HC A04/MF A01

A Navier-Stokes code, finite difference Navier-Stokes (FDNS), is used to analyze the complicated internal flowfield of the SRM (solid rocket motor) to explore the impacts due to the effects of chemical reaction, particle dynamics, and slag accumulation on the solid rocket motor (SRM). The particulate multi-phase flowfield with chemical reaction, particle evaporation, combustion, breakup, and agglomeration models are included in present study to obtain a better understanding of the SRM design. Finite rate chemistry model is applied to simulate the chemical reaction effects. Hermsen correlation model is used for the combustion simulation. The evaporation model introduced by Spalding is utilized to include the heat transfer from the particulate phase to the gase phase due to the evaporation of the particles. A correlation of the minimum particle size for breakup expressed in terms of the Al/Al2O3 surface tension and shear force was employed to simulate the breakup of particles. It is assumed that the breakup occurs when the Weber number exceeds 6. A simple L agglomeration model is used to investigate the particle agglomeration. However, due to the large computer memory requirements for the agglomeration model, only 2D cases are tested with the agglomeration model. The VOF (Volume of Fluid) method is employed to simulate the slag buildup in the aft-end cavity of the redesigned solid rocket motor (RSRM). Monte Carlo method is employed to calculate the turbulent dispersion effect of the particles. The flowfield analysis obtained using the FDNS code in the present research with finite rate chemical reaction, particle evaporation, combustion, breakup, agglomeration, and VOG models will provide a design guide for the potential improvement of the SRM including the use of materials and the shape of nozzle geometry such that a better performance of the SRM can be achieved. The simulation of the slag buildup in the aft-end cavity can assist the designer to improve the design of the RSRM geometry. Author

N95-25877*# National Aeronautics and Space Administration. Lewis Research Center, Cleveland, OH.
CONTROLS CONCEPTS FOR NEXT GENERATION REUSEABLE ROCKET ENGINES
Carl F. Lorenzo, Walter C. Merrill, Jefferey L. Musgrave, and Asok Ray (Pennsylvania State Univ., University Park, PA.) Apr. 1995 11 p Presented at the 1995 American Control Conference, Seattle, WA, 21-23 Jun. 1995; sponsored by American Automatic Control Council
(RTOP 505-62-50)
(NASA-TM-106902; E-9594; NAS 1.15:106902) Avail: CASI HC A03/MF A01

Three primary issues will drive the design and control used in next generation reuseable rocket engines. In addition to steady-state and dynamic performance, the requirements for increased durability, reliability and operability (with faults) will dictate which new controls and design technologies and features will be brought to bear. An array of concepts which have been brought forward will be tested against the measures of cost and benefit as reflected in the above 'ilities'. This paper examines some of the new concepts and looks for metrics to judge their value. Author

N95-26310*# Vanderbilt Univ., Nashville, TN.
FEED SYSTEM DESIGN FOR A REDUCED PRESSURE TANK
Hurbert Lui *In its* The 1994 NASA/USRA/ADP Design Projects 19 p(SEE N95-26304 08-80) 1994 (For primary document see N95-26304 08-80)
Avail: CASI HC A03/MF A02

23 CHEMISTRY AND MATERIALS (GENERAL)

N95-24437*# National Aeronautics and Space Administration. Lewis Research Center, Cleveland, OH.
Au/Cr SPUTTER COATING FOR THE PROTECTION OF ALUMINA DURING SLIDING AT HIGH TEMPERATURES Final Report
Patricia A. Benoy (Saint Louis Univ., Cahokia, IL.) and Christopher DellaCorte Mar. 1995 15 p Presented at Joint Tribology Conference, Orlando, FL, 8-11 Oct. 1995; sponsored by Society of Tribologists, Lubrication Engineers and American Society of Mechanical Engineers
(Contracts NCC3-330; DE-AI01-91CE-50306; RTOP 505-63-5A)
(NASA-TM-106853; E-9442; NAS 1.15:106853; DOE/NASA/50306-7)
Avail: CASI HC A03/MF A01

A sputter deposited bilayer coating of gold and chromium was investigated as a potential solid lubricant to protect alumina substrates in applications involving sliding at high temperature. The proposed lubricant was tested in a pin-on-disk tribometer with coated alumina disks sliding against uncoated alumina pins. Three test parameters; temperature, load, and sliding velocity were varied over a wide range in order to determine the performance envelope on the gold/chromium (Au/Cr) solid lubricant film. The tribo-tests were run in an air atmosphere at temperatures of 25 to 1000 C, under loads of 4.9 to 49.0 N and at sliding velocities from 1 to 15 m/sec. Post test analyses included surface profilometry, wear factor determination and scanning electron microscopy/energy dispersive spectroscopy (SEM/EDS) examination of worn surfaces. Compared to unlubricated Al2O3 sliding, the use of the Au/Cr film reduced friction by 30 to 50 percent and wear by one to two orders of magnitude. Increases in test temperature resulted in lower friction and the Au/Cr film continued to provide low friction, about 0.3, even at 1000 C. Pin wear factors and friction were largely unaffected by increasing loads up to 29.4 N. Sliding velocity had essentially no effect on friction, however, increased velocity reduced coating life (total sliding distance). Based upon these research results, the Au/Cr film is a promising lubricant for moderately loaded, low speed applications operating at temperatures as high as 1000 C. Author

N95-24583*# Boeing Defense and Space Group, Seattle, WA.
COMPOSITE MATERIALS FLOWN ON THE LONG DURATION EXPOSURE FACILITY Report, Feb. 1990 - Feb. 1995
Pete E. George, Harry W. Dursch, and H. Gary Pippin Hampton, VA NASA Apr. 1995 65 p
(Contracts NAS1-18224; NAS1-19247; RTOP 506-43-61-02; RTOP 233-03-02-04)
(NASA-CR-4657; NAS 1.26:4657) Avail: CASI HC A04/MF A01

Organic composite test specimens were flown on several LDEF experiments. Both bare and coated composites were flown. Atomic oxygen eroded bare composite material, with the resins being recessed at a greater rate than the fibers. Selected coating techniques protected the composite substrate in each case. Tensile and optical properties are reported for numerous specimens. Fiberglass and metal matrix composites were also flown. Author

N95-24851# South Carolina Univ., Columbia, SC. Dept. of Chemistry.
THE TRANSFORMATION OF ORGANIC AMINES BY TRANSITION METAL CLUSTER COMPOUNDS Progress Report
Richard D. Adams Nov. 1994 41 p
(Contract DE-FG09-84ER-13296)
(DE95-004180; DOE/ER-13296/11) Avail: CASI HC A03/MF A01

Research during the current award period has covered several related topics which have emerged and grown as a consequence of the various discoveries that have been made during this award period. They have been divided into the following subsections for clarity and emphasis: The activation of tertiary amines by osmium cluster complexes; CH bond activation and ring opening of a nitrogen containing strained ring heterocycle

by an osmium cluster complex; Ring opening of cyclic thioethers; cyclooligomerization of Thietanes; Studies of the cyclobutyne ligand; Insertion of an alkynes into metal-metal bonds; and Energy storage in metal clusters. A summary of the results of these studies is given in the following sections of this report. These studies have resulted in 50 scientific publications over the last three years and details of their studies beyond that given in the following sections can be found in those reports. All of these reports are listed in the final section of this report by the author's name, title and journal citation. DOE

N95-25248# Pacific Northwest Lab., Richland, WA.
ELECTROCHEMICAL ORGANIC DESTRUCTION IN SUPPORT OF HANFORD TANK WASTE PRETREATMENT
W. E. Lawrence, J. E. Surma, K. L. Gervais, M. F. Buehler, G. Pillay, and A. J. Schmidt Oct. 1994 37 p Prepared for Westinghouse Hanford Co., Richland, WA
(Contract DE-AC06-76RL-01830)
(DE95-002854; PNL-10131; UC-800) Avail: CASI HC A03/MF A01

The US Department of Energy's Hanford Site in Richland, Washington, has 177 underground storage tanks that contain approximately 61 million gallons of radioactive waste. The current cleanup strategy is to retrieve the waste and separate components into high-level and low-level waste. However, many of the tanks contain organic compounds that create concerns associated with tank safety and efficiency of anticipated separation processes. Therefore, a need exists for technologies that can safely and efficiently destroy organic compounds. Laboratory-scale studies conducted during FY 93 have shown proof-of-principle for electrochemical destruction of organics. Electrochemical oxidation is an inherently safe technology and shows promise for treating Hanford complexant concentrate aqueous/ slurry waste. Therefore, in support of Hanford tank waste pretreatment needs, the development of electrochemical organic destruction (ECOD) technology has been undertaken. The primary objective of this work is to develop an electrochemical treatment process for destroying organic compounds, including tank waste complexants. Electroanalytical analyses and bench-scale flow cell testing will be conducted to evaluate the effect of anode material and process operating conditions on the rate of organic destruction. Cyclic voltammetry will be used to identify oxygen overpotentials for the anode materials and provide insight into reaction steps for the electrochemical oxidation of complexants. In addition, a bench-scale flow cell evaluation will be conducted to evaluate the influence of process operating conditions and anode materials on the rate and efficiency of organic destruction using the nonradioactive a Hanford tank waste simulant. DOE

N95-25286# Pacific Northwest Lab., Richland, WA.
MODELING OF THE SIMULATED COUNTERCURRENT MOVING-BED CHROMATOGRAPHIC REACTOR USED FOR THE OXIDATIVE COUPLING OF METHANE
Anna Lee Y. Tonkovich and Robert W. Carr Sep. 1994 20 p Presented at the 13th International Symposium on Chemical Reaction Engineering, Baltimore, MD, 25 Sep. 1994
(Contracts DE-AC02-76ER-02945; DE-AC06-76RL-01830)
(DE95-004930; PNL-SA-24416; CONF-940920-2) Avail: CASI HC A03/MF A01

The oxidative coupling reaction of methane (OCM) is a potential industrial reaction for the efficient production of ethylene. Replacement of current technologies requires significant product yield improvements. An experimental novel reactor design, the modified simulated countercurrent moving-bed chromatographic reactor (SCMCR), has reported improved ethane and ethylene product yields over other reported values. An understanding of the reactor operation is aided by concurrent mathematical modeling. The model mimics the exact experimental reactor configuration. Four sections are used; each section contains a reaction column and two separation columns connected in series. The feed is switched from section to section at discrete intervals. Reaction occurs in the first column and is followed by product and reactant separation in the ensuing section columns. Langmuir adsorption isotherms are used. The model does not incorporate the realistic and complex kinetics rising, from the OCM, rather a simplified reaction term is used to qualitatively gain insight into the operation of the modified SCMCR. A unimolecular reaction network is used in the model. The rate constants are set to permit a small fractional conversion, 5% per pass, at the concentrations during the first cycle. Similarly to the experimental reactor, the model adds a make-up feed (defined as percentage of the original feed, where excess methane is fed during the first cycle of the experimental reactor) to augment lost reactants. DOE

N95-25597# Los Alamos National Lab., NM.
SELECTIVE EXTRACTION OF TRIVALENT ACTINIDES FROM LANTHANIDES WITH DITHIOPHOSPHINIC ACIDS AND TRIBUTYLPHOSPHATE
G. Jarvinen, R. Barrans, N. Schroeder, K. Wade, M. Jones, B. F. Smith, J. Mills (Texas Technological Univ., Lubbock, TX.), G. Howard (Texas Technological Univ., Lubbock, TX.), H. Freiser (Arizona Univ., Tucson, AZ.), and S. Muralidharan (Arizona Univ., Tucson, AZ.) 1995 28 p Presented at the Spring National Meeting of the American Chemical Society (ACS), San Diego, CA, 13-18 Mar. 1994
(Contract W-7405-eng-36)
(DE95-005249; LA-UR-94-4350; CONF-940301-45) Avail: CASI HC A03/MF A01

A variety of chemical systems have been developed to separate trivalent actinides from lanthanides based on the slightly stronger complexation of the trivalent actinides with ligands that contain soft donor atoms. The greater stability of the actinide complexes in these systems has often been attributed to a slightly greater covalent bonding component for the actinide ions relative to the lanthanide ions. The authors have investigated several synergistic extraction systems that use ligands with a combination of oxygen and sulfur donor atoms that achieve a good group separation of the trivalent actinides and lanthanides. For example, the combination of dicyclohexyldithiophosphinic acid and tributylphosphate has shown separation factors of up to 800 for americium over europium in a single extraction stage. Such systems could find application in advanced partitioning schemes for nuclear waste. DOE

N95-25602 New Orleans Univ., LA. Dept. of Chemistry.
CONTINUED COMPUTATIONAL EVALUATION OF THE FEASIBILITY OF NITRATING PRECURSORS TO C12N12O12 Technical Report
Peter Politzeer and M. Edward Grice 5 Dec. 1994 4 p Limited Reproducibility: More than 20% of this document may be affected by microfiche quality
(Contract N00014-95-1-0028)
(AD-A288369; TR-76) Avail: Issuing Activity (Defense Technical Information Center (DTIC))

Extending the work reported in Technical Report No. 71 (October 20, 1994), we computed the average local ionization energies on the surfaces of two more possible precursors to 1. No minima were found at the positions to be nitrated, indicating that these are not favored sites for this purpose. DTIC

N95-25961*# National Aeronautics and Space Administration. Lewis Research Center, Cleveland, OH.
WEAR-RESISTANT, SELF-LUBRICATING SURFACES OF DIAMOND COATINGS
Kazuhisa Miyoshi May 1995 10 p Presented at the 1995 Applied Diamond Conference, Gaithersburg, MD, 21-24 Aug. 1995; sponsored by National Institute of Standards and Technology
(RTOP 505-63-5A)
(NASA-TM-106887; E-95-25; NAS 1.15:106887) Avail: CASI HC A02/MF A01

In humid air and dry nitrogen, as-deposited, fine-grain diamond films and polished, coarse-grain diamond films have low steady-state coefficients of friction (less than 0.1) and low wear rates (less than or equal to 10(exp -6) mm(exp 3)/N-m). In an ultrahigh vacuum (10(exp -7) Pa), however, they have high steady-state coefficients of friction (greater than 0.6) and high wear rates (greater than or equal to 10(exp -4) mm(exp 3)/N-m). Therefore, the use of as-deposited, fine-grain and polished, coarse-grain diamond films as wear-resistant, self-lubricating coatings must be limited to normal air or gaseous environments such as dry nitrogen. On the other hand, carbon-ion-implanted, fine-grain diamond films and nitrogen-ion-implanted, coarse-grain diamond films have low steady-state coefficients of friction (less than 0.1) and low wear rates (less than or equal to 10(exp -6) mm(exp 3)/N-m) in all three environments. These films can be effectively used as wear-resistant, self-lubricating coatings in an ultrahigh vacuum as well as in normal air and dry nitrogen. Author

N95-26072*# Boeing Defense and Space Group, Seattle, WA.
LONG DURATION EXPOSURE FACILITY MINI-DATA BASE USER'S GUIDE: IBM-COMPATIBLE PC COMPUTER VERSION (Diskette)
Gail Bohnhoff-Hlavacek, Gary Pippin, and Harry Dursch Hampton, VA NASA Apr. 1995 29 p Diskette: 3.5 inch IBM compatible diskette
(Contracts NAS1-18224; NAS1-19247; RTOP 506-43-61-02; RTOP 233-03-02-04)
(NASA-CR-4655; NAS 1.26:4655; NONP-NASA-DK-95-48160) Avail: CASI SET A09 (HC,DK)

One of the objectives of the LDEF Special Investigation Group (SIG) was to develop a LDEF data base that identifies the experiment objectives and hardware flown, summarizes results and conclusions, and provides a system analysis overview which would include spacecraft design guidelines and space environmental effects. Compiling this information into an easily accessible data base format and making it available to the space community was a major task accomplished by the System and Materials SIG effort beginning in 1991. Included in this document is a short user's manual for the LDEF Mini-Data Bases. The user's manual contains pertinent examples from the data base on specifically how to access and work with the LDEF information. Accompanying this document are the mini-data bases on disk. Author

24 COMPOSITE MATERIALS

Includes physical, chemical, and mechanical properties of laminates and other composite materials.

For ceramic materials see *27 Nonmetallic Materials*.

N95-24242 National Defence Research Establishment, Linkoeping (Sweden).
SIGNIFICANCE OF VARIED THICKNESS TO DAMAGE TOLERANCE OF CARBON FIBER/EPOXY LAMINATES [BALLISTISKA SKADORS INVERKAN PA RESTHALLFASTHETEN HOS KOLFIBER/EPOXI-LAMINAT MED VARIERAD TJOCKLEK]
L. Svensson Sep. 1994 18 p In SWAHILI; Text in SWEDISH; summary in ENGLISH. See also PB95-131611
(PB95-165460; FOA-R-94-00019-S.4-SE) Avail: Issuing Activity (National Technical Information Service (NTIS))

Carbon fiber/epoxy laminates loaded in compression were ballistically damaged. The laminates were 5.3 and 8.3 mm thick. If fracture did not occur at impact, the load was continuously increased until fracture. The results were compared with results from earlier tests with laminates of 10.6 mm thickness. The variation of compression strength between different thickness is small. Fracture occurs at impact, when strain is greater than 0.31% for 10.6 and 8.3 mm laminate, and strain greater than 0.39% for 5.3 mm laminate. Fracture does not occur without increased load when strain is less than 0.27% for 8.3 and 10.6 mm laminate, and strain less than 0.34% for 5.3 mm laminate. NTIS

N95-24365# Japan Atomic Energy Research Inst., Tokyo (Japan).
DEVELOPMENT OF OXIDATION RESISTANT SiC/C COMPOSITIONALLY GRADIENT MATERIALS
Kimio Fujii, Junichi Nakano, and Masami Shindo Jan. 1994 20 p
(DE94-785101; JAERI-M-94-001) Avail: CASI HC A03/MF A01

This report discusses the evaluation of oxidation characteristic for the trial production of SiC/C compositionally gradient carbon and SiC/C compositionally gradient carbon fiber reinforced carbon (CFRC) materials, which are composed of a surface SiC coating layer, an intermediate SiC/C layer and substrate material. An oxidation test (in air at 800 C for up to 100 h) was performed and the results were compared with each other (i.e., substrate material, one with intermediate SiC/C layer and one coated by SiC layer). It was shown that SiC/C compositionally gradient material exhibited the best oxidation resistance among each substrate series, and the conception of SiC/C compositionally gradient material could be applied to carbon and CFRC materials as well as graphite material. DOE

N95-24426# Burton Technologies, Inc., Raleigh, NC.
WEAR RESISTANT COMPOSITE STRUCTURE OF VITREOUS CARBON CONTAINING CONVOLUTED FIBERS
R. G. Burton 1 Feb. 1995 33 p
(Contract DE-FG01-94CE-15613)
(DE95-006255; DOE/CE-15613/T3) Avail: CASI HC A03/MF A01

Very good friction and wear measurements are reported for MRCC (metal reinforced carbon composites), made from low-wear non-graphitic carbon matrix with metal-fiber reinforcement. Counterfaces include austenitic and martensitic stainless steels, Si nitride, and alumina. Effects of high load, high temperature, and gaseous environments are reported: removal of humidity, atm. oxygen have little effect on friction, wear for MRCC sliding against ceramic or stainless steel. Wear of Al oxide riders on MRCC is very low, not affected by contact load. 260 C temperatures do not degrade performance of 440 C riders on MRCC disks or raise friction. In small or large sizes, MRCC is made in a single-pass process for about the same volume cost as cast iron. It can survive heating in nitrogen above 1600 C without loss of integrity or major change of dimensions. DOE

N95-24438*# Virginia Univ. Hospital, Charlottesville, VA. Dept. of Civil Engineering and Applied Mechanics.
AN EVALUATION OF A COUPLED MICROSTRUCTURAL APPROACH FOR THE ANALYSIS OF FUNCTIONALLY GRADED COMPOSITES VIA THE FINITE-ELEMENT METHOD Final Report
Marek-Jerzy Pindera and Patrick Dunn Cleveland, OH NASA Mar. 1995 23 p
(Grant NAG3-1377; RTOP 505-63-12)
(NASA-CR-195455; E-9546; NAS 1.26:195455) Avail: CASI HC A03/MF A01

A comparison is presented between the predictions of the finite-element analysis and a recently developed higher-order theory for functionally graded materials subjected to a thorough-thickness temperature gradient. In contrast to existing micromechanical theories that utilize classical (i.e., uncoupled) homogenization schemes to calculate micro-level and macro-level stress and displacement fields in materials with uniform or nonuniform fiber spacing (i.e., functionally graded materials), the new theory explicitly couples the microstructural details with the macrostructure of the composite. Previous thermo-elastic analysis has demonstrated that such coupling is necessary when: the temperature gradient is large with respect to the dimension of the reinforcement; the characteristic dimension of the reinforcement is large relative to the global dimensions of the composite and the number of reinforcing fibers or inclusions is small. In these circumstances, the standard micromechanical analyses based on the concept of the representative volume element used to determine average composite properties produce questionable results. The comparison between the predictions of the finite-element method and the higher-order theory presented herein establish the theory's accuracy in predicting thermal and stress fields within composites with a finite number of fibers in the thickness direction subjected to a thorough-thickness thermal gradient. Author

N95-24590# Los Alamos National Lab., NM.
COMPOSITE DUCTILITY: THE ROLE OF REINFORCEMENT AND MATRIX
N. Shi and R. J. Arsenault 1994 9 p Presented at the Annual Meeting and Exhibition of the Minerals, Metals and Materials Society, Las Vegas, NV, 12-16 Feb. 1995
(Contract W-7405-eng-36)
(DE95-003664; LA-UR-94-3958; CONF-950201-1) Avail: CASI HC A02/MF A01

The total ductility, i.e., the energy required to rupture a ductile solid is controlled by two factors: (1) ability to withstand strain hardening before initiation of critical nuclei for final rupture (microcracks or voids); (2) resistance to crack extension. The first group is related to the reinforcement; particle or whisker fracture, debonding and void nucleation and growth at the reinforcement-matrix interface. The second group is related to the matrix; triaxial stress state in matrix, the work hardened state of the matrix due to the (Delta)CTE effect, and localized matrix plastic flow. The experimental data and theoretical analysis show that the lack of strain hardening capacity of the matrix is the major contributing factor causing the low ductility of DMMCS (discontinuous metal matrix composites). This may be attributed intrinsically to the exhaustion of the strain hardening capacity from (Delta)CTE-induced work hardening and/or extrinsically to the high matrix triaxial stresses which induces rapid void growth. DOE

N95-24989# National Aerospace Lab., Tokyo (Japan). Airframe Div.
STUDY ON TENSILE FATIGUE TESTING METHOD OF UNIDIRECTIONAL FIBER-RESIN MATRIX COMPOSITES
Yoshio Noguchi Jul. 1994 13 p In JAPANESE
(ISSN 0389-4010)
(NAL-TR-1241) Avail: CASI HC A03/MF A01

The aim of the Versailles Project on advanced materials and standards (VAMAS) program is to evaluate the mechanical properties of advanced materials. In this study, as part of the polymer composites, the first phase of this round robin test was carried out to examine the tension-tension fatigue properties of unidirectional GFRP and CFRP. Fatigue tests were undertaken in a sinusoidal load-controlled testing mode, with a load ratio of 0.1. In the case of CFRP tests, the comparison of cold-setting epoxy resin and curing epoxy resin film as the end tab adhesive was made. It was found that the fatigue strength differed largely between the two types of tab adhesive. In another study, the effects of the end-tab configuration of the specimen and the testing frequency of fatigue behavior of unidirectional CFRP specimen were examined. As for the tab configuration, 10 deg tapered and untapered end-tab specimens were provided. On the testing frequency, fatigue tests were conducted with 2, 5 and 10Hz. The difference of fatigue strength under these testing conditions was found to be small in the present study. Author

N95-25111# National Inst. for Research in Inorganic Materials, Tsukuba (Japan).
STUDY OF COMPOSITE ZIRCONIUM OXIDE
25 Nov. 1993 56 p In JAPANESE
(DE95-730104; ETDE/JP-MF-95730104) Avail: CASI HC A04/MF A01

A collection of research reports regarding inorganic materials published by the Japan Science and Technology Agency are presented. The research subject is ZrO2-MOx. The principal component of the composite oxide under research, ZrO2, is multifunctional and is widely used as a structural material. It can be used as an optoceramics material such as PLZT or a material for intellectual functions. Unlike the existing techniques, excellent ceramic materials for fundamental study are produced and characterized by using a technique for synthesizing, characteristic composition, or nature (functions and properties). To summarize, the study includes the wet adjusting method of raw powder material, uniform melting method of impurities such as SiO2 and CaO, effects of Mn ion on diffusion coefficient and piezo-electric characteristics of PLZT ceramics, sintering structure of easily sinterable Mg powder, effective partial pressure of oxygen at HIP, multistep wet synthesis of SrZrO3, destructive observation and 500 C fatigue cracking of ZrO2, intelligent elements, heat transfer degradation in fine area, and self-return. As a result of these researches, about 90 reports were presented on the paper and 56 patents were applied in Japan and 4 in other countries. DOE

N95-25295# Sandia National Labs., Albuquerque, NM.
OPTICAL PROPERTIES OF FRACTAL NANOCOMPOSITES
V. A. Markel, W. Kim, R. Armstrong, V. Shalaev, and E. B. Stechel (New Mexico State Univ., Las Cruces, NM.) 1994 6 p Presented at the 1994 Fall Meeting of the Materials Research Society (MRS), Boston, MA, 28 Nov. - 2 Dec. 1994
(Contract DE-AC04-94AL-85000)
(DE95-005414; SAND-94-3070C; CONF-941144-43) Avail: CASI HC A02/MF A01

Optical processes in nanostructured fractal composites are shown to be strongly enhanced. The enhancement occurs because of a localization of dipolar eigenmodes in subwavelength areas. DOE

N95-25305* National Aeronautics and Space Administration. Langley Research Center, Hampton, VA.
METHOD AND APPARATUS FOR NON-DESTRUCTIVE EVALUATION OF COMPOSITE MATERIALS WITH CLOTH SURFACE IMPRESSIONS Patent
Eric I. Madras, inventor (to NASA) 21 Feb. 1995 13 p Filed 16 Jul. 1993 Supersedes N94-15878 (32 - 3, p 933)
(NASA-Case-LAR-14535-1; US-Patent-5,390,544;
US-Patent-Appl-SN-110278; US-Patent-Class-73/602;
Int-Patent-Class-G01N-9/24) Avail: US Patent and Trademark Office

A method and related apparatus for nondestructive evaluation of composite materials by determination of the quantity known as Integrated Polar Backscatter, which avoids errors caused by surface texture left by cloth impressions by identifying frequency ranges associated with peaks in a power spectrum for the backscattered signal, and removing such frequency ranges from the calculation of Integrated Polar Backscatter for all scan sites on the composite material is presented.
Official Gazette of the U.S. Patent and Trademark Office

N95-25505 Maryland Univ., College Park, MD. Metallurgical Materials Lab.
STRENGTHENING OF NiAl MATRIX COMPOSITES Annual Report, 1 Oct. 1993 - 30 Nov. 1994
R. J. Arsenault 30 Nov. 1994 86 p
(Contract N00014-94-1-0118)
(AD-A288923; MML-1-1994) Avail: Issuing Activity (Defense Technical Information Center (DTIC))

The significant result is that the observed strengthening due to various types of reinforcement (Al2O3 and TiB2) with the same size is almost identical. The smaller size reinforcement (5 micrometers versus 150 micrometers) produces greater strengthening. Also, the strengthening due to Al2O3 whiskers, which have long l/d (length to diameter) ratios of 10 to 100, is no greater than particulate Al2O3 and TiB2 of approximately the same size, which is a further indication that a load transfer mechanism is not applicable for these composites. A detailed examination of the data still suggests that the thermally-activated-rate controlling mechanism is the stress assisted motion of jogged screw dislocations. The specific details of the process must now be worked out to be able to obtain the proper stress and temperature dependence of the activation parameters. The strengthening observed in the composites at both high and low temperatures is due to an increase in the internal stress. This internal stress is independent of test temperature and stress. DTIC

N95-25546* National Aeronautics and Space Administration. Langley Research Center, Hampton, VA.
APPARATUS FOR CONSOLIDATING A PRE-IMPREGNATED, FILAMENT-REINFORCED POLYMERIC PREPREG MATERIAL Patent
Donald A. Sandusky, inventor (to NASA) (College of William and Mary, Williamsburg, VA.) 7 Mar. 1995 10 p Filed 20 Oct. 1993 Supersedes N94-29496 (32 - 8, p 3180)
(NASA-Case-LAR-15173-1-CU; US-Patent-5,395,477;
US-Patent-Appl-SN-141292; US-Patent-Class-156-441;
US-Patent-Class-156-180; US-Patent-Class-156-181;
US-Patent-Class-156-433; US-Patent-Class-118-124;
US-Patent-Class-264-136; US-Patent-Class-264-174) Avail: US Patent and Trademark Office

An apparatus and method were developed for providing a uniform, consolidated, unidirectional, continuous, fiber-reinforced polymeric material. The apparatus comprises a supply means, a forming means, a shaping means, and a take-up means. The forming means further comprises a pre-melting chamber and a stationary bar assembly. The shaping means is a loaded cooled nip-roller apparatus. Forming takes place by heating a polymeric prepreg material to a temperature where the polymer becomes viscous and applying pressure gradients at separate locations along the prepreg material. Upon exiting the forming means, the polymeric prepreg material is malleable, consolidated, and flattened. Shaping takes place by passing the malleable, consolidated, flattened prepreg material through a shaped, matched groove in a loaded, cooled nip-roller apparatus to provide the final solid product.
Official Gazette of the U.S. Patent and Trademark Office

N95-25596# Los Alamos National Lab., NM.
ISSUES RELATED TO PREDICTION OF RESIDUAL STRESSES IN TITANIUM ALLOY MATRIX COMPOSITES
P. Rangaswamy and N. Jayaraman (Cincinnati Univ., OH.) 1995 21 p Presented at the Life Prediction Methodology for Titanium Matrix Composites Symposium, Hilton Head, SC, 22-24 Mar. 1994
(Contract W-7405-eng-36)
(DE95-005243; LA-UR-94-4374; CONF-940399-2) Avail: CASI HC A03/MF A01

Recently, a detailed study of residual stresses on the as-processed SCS-6/Ti-24Al-11Nb (0)(sub 8) composite, and SCS-6/Beta-21S composites in unidirectional (0)(sub 4), cross-ply (0/90)s, and quasi-isotropic (0/(+/-)45/90)s lay-ups has been completed. In this study, residual stresses

have been measured using x-ray diffraction (Sin sq Psi) technique. We have shown that the use of conventional unit cell models consisting of a quarter fiber surrounded by the matrix material to predict residual stresses for verification of experimental results is inadequate. Such models have successfully predicted the stresses at the fiber-matrix interface. However, experimental work to measure residual stresses have always been on surfaces far away from the interface region. In this paper, the approach taken in extending the conventional unit cell model to the concept of multi-fiber models to predict average stresses are presented. In this process, several modeling issues have been identified. These issues are: (1) use of conventional unit models for prediction of average surface residual stresses; (2) effect of orientation of the sub-surface plies on the residual stresses in the surface ply; (3) residual stresses in the interior plies; and (4) constituent material properties. DOE

N95-25770# National Aerospace Lab., Tokyo (Japan). Airframe Div.
STUDY ON TENSILE FATIGUE TESTING METHOD OF UNIDIRECTIONAL FIBER-RESIN MATRIX COMPOSITES
Youshoi Noguchi Jul. 1994 14 p In JAPANESE
(ISSN 0389-4010)
(NAL-TR-1241) Avail: CASI HC A03/MF A01

The aim of the Versailles Project on Advanced Materials and Standards (VAMAS) program is to evaluate the mechanical properties of advanced materials. In this study, as a part of the polymer composites, the first phase of this round robin test was carried out to examine the tension-tension fatigue properties of unidirectional GFRP and CFRP. Fatigue tests were undertaken in a sinusoidal load-controlled testing mode, with a load ratio of 0.1. In the case of CFRP tests, the comparison of cold-setting epoxy resin and curing epoxy resin film as the end-tab adhesive was made. It was found that the fatigue strength differed largely between the two types of tab adhesive. In another study, the effects of the end-tab configuration of the specimen and the testing frequency of fatigue behavior of unidirectional CFRP specimen were examined. As for the tab configuration, 10 deg tapered and not tapered end-tab specimens were provided. On the testing frequency, fatigue tests were conducted with 2, 5 and 10Hz. The difference of fatigue strength under these testing conditions was found to be small in the present study. Author

N95-25859# National Aerospace Lab., Tokyo (Japan). Airframe Div.
STATIC AND FATIGUE PROPERTIES OF PIN-JOINT SPECIMENS OF A AS-4/PEEK THERMOPLASTIC COMPOSITE MATERIAL
Yoshiaki Kakuta, Toshiyuki Shimokawa, and Yasumasa Hamaguchi Oct. 1993 20 p In JAPANESE Original contains color illustrations
(ISSN 0389-4010)
(NAL-TR-1214) Avail: CASI HC A03/MF A01

The objective was to investigate static and fatigue strengths and damage around the hole of pin-joint specimens of an AS-4/PEEK thermoplastic material. Both static and fatigue tests were conducted at room temperature. Static tests clarified the relationship between load and deformation of a pin-joint hole and bearing strength. Fatigue tests clarified the relationships of load cycles and deformation of a pin-joint hole, S-N relationships, residual bearing strength, and the influence of the load cycle rate on fatigue life. Before and after static and fatigue tests, the edges around pin-joint holes were nondestructively tested by using an ultrasonic C-scan technology and a soft x-ray method to investigate damage growth. After fatigue and static tests, some specimens were sectioned and damage in the vicinity of the hole edge was observed by using a field-emmission-type scanning electron microscope. The test results are analyzed and discussed. Author

N95-25880*# NYMA, Inc., Brook Park, OH. Engineering Services Div.
THERMOMECHANICAL FATIGUE BEHAVIOR OF THREE CFCC'S Final Contractor Report
Dennis W. Worthem Cleveland, OH NASA Mar. 1995 25 p
(Contract NAS3-25266; RTOP 505-63-5B)
(NASA-CR-195441; E-9484; NAS 1.26:195441) Avail: CASI HC A03/MF A01

The thermomechanical fatigue (TMF) behavior of three continuous-fiber ceramic composites (CFCC's) was examined. The three matrices consisted of two different glass-ceramics and silicon carbide, respectively. The matrices of some of the specimens with the silicon carbide matrix were enhanced to improve oxidation resistance. All three were reinforced with Nicalon fibers with various fiber architectures. The thermoelastic properties of the matrix relative to the fibers, the elastic moduli and coefficients of thermal expansion (CTE), were different in each composite, providing a comparison of the effects of these critical properties. The specimens were tested under in-phase (IP) and out-of-phase (OP) cyclic loadings with respect to thermal cycling between 600 C and 1100 C. One of the glass-ceramic composites had greatly increased TMF lives compared to the other glass-ceramic matrix composites. This was probably caused by the reversal of the CTE mismatch between the fibers and the matrices and caused by the different oxidation resistances of the composites. For the same TMF lives a cross-ply reinforced composite had a maximum cyclic stress half as great, as that of unidirectionally reinforced composite. This indicated that the (0 deg) ply fibers had a strong influence of TMF life. Both the glass ceramic matrix composites had shallow-slope stress-life plots that indicated sensitivity to damage and therefore low damage tolerance. The composites with an unenhanced silicon carbide matrix experienced the shortest TMF lives of all the CFCC's tested. However, the enhanced composite had the longest. Also, the enhanced composite demonstrated the best damage tolerance as evidenced by a stress-life curve that curves sharply upward to the left. In all the composites, out-of-phase cyclic loading was worse than in-phase cyclic loadings despite the CTE mismatch between fiber and matrix. A damage investigation and a preliminary analysis of the stresses in the fibers and matrices taking into account their respective thermoelastic properties provided insight into the relative behavior of the glass-ceramic matrix composites under IP and OP TMF. Author

N95-25998# Materials Technologies of Virginia, Blacksburg, VA.
WHISKER REINFORCED GLASS CERAMIC Quarterly Progress Report No. 1, 27 Sep. 1994 - 27 Dec. 1994
G. R. Pickrell and J. J. Brown, Jr. 12 Jan. 1995 8 p
(Contract DE-FG01-94CE-15599)
(DE95-005568; DOE/CE-15599/T1) Avail: CASI HC A02/MF A01

The goal of this project is to investigate the physical properties of an in-situ whisker reinforced glass ceramic material and to produce prototype heat exchanger tubes for testing in a coal combustion environment. The in-situ whisker reinforced glass ceramic process was developed and patented at Virginia Tech and licensed to Materials Technologies of Virginia. Completion of this project will demonstrate the potential for this new material to replace existing heat exchanger materials due to its superior chemical and physical properties. The technical progress has been in three areas: Construction of a slurry filtration apparatus for preparation of glass ceramic samples, construction of a prototype heat exchanger preparation apparatus, and test melts of the glass powder with parameters for composition, heat treatments, quenching, and milling. DOE

N95-26083*# National Aeronautics and Space Administration. Langley Research Center, Hampton, VA.
SEPARATION OF CRACK EXTENSION MODES IN ORTHOTROPIC DELAMINATION MODELS
Jack L. Beuth (Carnegie-Mellon Univ., Pittsburgh, PA.) May 1995 26 p
(RTOP 505-63-50-04)
(NASA-TM-109180; NAS 1.15:109180) Avail: CASI HC A03/MF A01

In the analysis of an interface crack between dissimilar elastic materials, the mode of crack extension is typically not unique, due to oscillatory behavior of near-tip stresses and displacements. This behavior currently limits the applicability of interfacial fracture mechanics as a means to predict composite delamination. The Virtual Crack Closure Technique (VCCT) is a method used to extract mode 1 and mode 2 energy release rates from numerical fracture solutions. The mode of crack extension extracted from an oscillatory solution using the VCCT is not unique due to the dependence of mode on the virtual crack extension length, Delta. In this work, a method is presented for using the VCCT to extract Delta-independent crack extension modes for the case of an interface crack between two in-plane orthotropic materials. The method does not involve altering the analysis to eliminate its oscillatory behavior. Instead, it is argued that physically reasonable, Delta-independent modes of crack extension can be extracted from oscillatory solutions. Knowledge of near-tip fields is used to determine the explicit Delta dependence of energy release rate parameters. Energy release rates are then defined that are separated from the oscillatory dependence on Delta. A modified VCCT using these energy release rate definitions is applied to results from finite element analyses, showing that Delta-independent modes of crack extension result. The modified technique has potential as a consistent method for extracting crack extension modes

from numerical solutions. The Delta-independent modes extracted using this technique can also serve as guides for testing the convergence of finite element models. Direct applications of this work include the analysis of planar composite delamination problems, where plies or debonded laminates are modeled as in-plane orthotropic materials. Author

N95-26203*# Florida Univ., Gainesville, FL. Center for Studies of Advanced Structural Composites.
EFFECTS OF THROUGH-THE-THICKNESS STITCHING ON IMPACT AND INTERLAMINAR FRACTURE PROPERTIES OF TEXTILE GRAPHITE/EPOXY LAMINATES Final Report
Suresh K. Sharma and Bhavani V. Sankar Feb. 1995 132 p
(Grant NAG1-1226; RTOP 505-63-50-04)
(NASA-CR-195042; NAS 1.26:195042) Avail: CASI HC A07/MF A02

This study investigated the effects of through-the-thickness stitching on impact damage resistance, impact damage tolerance, and mode I and mode II fracture toughness of textile graphite/epoxy laminates. Uniweave resin-transfer-molded 48 ply graphite/epoxy (AS4/3501-6) laminates were stitched with Kevlar and glass yarns of different linear densities and stitch spacings. Delaminations were implanted during processing to simulate impact damage. Sublaminate buckling tests were performed to determine the effects of stitching on the compressive strength. The results showed outstanding improvements of up to 400 percent in the compression strength over the unstitched laminates. In impact and static indentation tests the onset of damage occurred at the same level, but the extent of damage was less in stitched laminates. Mode I fracture toughness of 24 ply Uniweave unidirectional (AS4/3501-6) stitched laminates was measured by conducting double-cantilever-beam tests. The critical strain energy release rate (G(sub Ic)) was found to be up to 30 times higher than the unstitched laminates. Mode II fracture toughness of the Uniweave laminates was measured by performing end-notched-flexure tests. Two new methods to compute the apparent G(sub IIc) are presented. The apparent G(sub IIc) was found to be at least 5-15 times higher for the stitched laminates. Author

N95-26251*# National Aeronautics and Space Administration. Langley Research Center, Hampton, VA.
DESIGN AND EVALUATION OF A FOAM-FILLED HAT-STIFFENED PANEL CONCEPT FOR AIRCRAFT PRIMARY STRUCTURAL APPLICATIONS
Damodar R. Ambur Jan. 1995 21 p Presented at the Third Advanced Composites Technology Conference, Jun. 1992
(RTOP 505-63-50-08)
(NASA-TM-109175; NAS 1.15:109175) Avail: CASI HC A03/MF A01

A structurally efficient hat-stiffened panel concept that utilizes a structural foam as stiffener core has been designed for aircraft primary structural applications. This stiffener concept utilizes a manufacturing process that can be adapted readily to grid-stiffened structural configurations which possess inherent damage tolerance characteristics due to their multiplicity of load paths. The foam-filled hat-stiffener concept in a prismatically stiffened panel configuration is more efficient than most other stiffened panel configurations in a load range that is typical for both fuselage and wing structures. The prismatically stiffened panel concept investigated here has been designed using AS4/3502 preimpregnated tape and Rohacell foam core and evaluated for its buckling and postbuckling behavior with and without low-speed impact damage. The results from single-stiffener and multi-stiffener specimens suggest that this structural concept responds to loading as anticipated and has good damage tolerance characteristics. Author

25 INORGANIC AND PHYSICAL CHEMISTRY

Includes chemical analysis, e.g., chromatography; combustion theory; electrochemistry; and photochemistry.

For related information see also *77 Thermodynamics and Statistical Physics.*.

N95-24222*# MVA, Inc., Norcross, GA.
TRANSMISSION ELECTRON MICROSCOPE STUDIES OF EXTRATERRESTRIAL MATERIALS Final Technical Report
Lindsay P. Keller 31 Jan. 1995 121 p
(Contract NAS9-18992)
(NASA-CR-188363; NAS 1.26:188363) Avail: CASI HC A06/MF A02

This two-section report describes research activities related to the analysis of extraterrestrial material using a transmission electron microscope (TEM). The first section is of carbon in interplanetary dust particles (IDP's). The section is divided into the following subsections: embedding IDP's in sulfur, preparing ultramicrotome thin sections, elimination of sulfur embedding media, carbon analysis using high-resolution transmission electron microscope (HRTEM), electron diffraction analysis of carbon in IDP's, carbon analysis by energy-dispersive x-ray spectrometry, carbon analysis by electron energy-loss spectroscopy, mineralogy and mineral chemistry of major phases, and reflectance spectroscopy of IDP's. The second section, an analysis of selected lunar samples using TEM, is divided into the following subsections: embedding and sectioning lunar samples, TEM studies of opaque assemblages in high-Ti basalts, analyzing blue rutiles in lunar basalt 70035, analysis of reaction rims on armalcolites, reduction microstructures in lunar soil grains, analyzing agglutinates in lunar soils, analyzing amorphous rims and vapor deposits, analyzing submicrometer glass spheres in soils, analyzing selected regolith grains for carbon, and analyzing selected lunar grains for reflectance spectra. The following publications are included within this report: The Oxidation State Of Altered Rims On Ilmenite From Lunar Soils ; Hydrated Cluster Particles: Chemical And Mineralogical Analyses Of Fragments From Two Interplanetary Dust Particles; The Nature Of Agglutinitic Glass In The Fine-Size Fraction Of Lunar Soil 10084; Electron Energy-Loss Spectroscopy Of Carbon In Interplanetary Dust Particles; The Anatomy Of A Cluster IDP (1): Carbon Abundance, Bulk Chemistry And Mineralogy Of Fragments From L2008#5; Anatomy Of A Cluster IDP (2): Noble Gas Abundances, Trace Element Geochemistry, Isotopic Abundances, And Trace Organic Chemistry Of Several Fragments From L2008#5; New Prospects For Analyzing Lunar Pyroclastic Glass; and The Contribution Of Vapor Deposition To Amorphous Rims On Lunar Soil Grains. CASI

N95-24257# Brookhaven National Lab., Upton, NY.
XAS STUDIES OF Ni(I), Ni(II), AND Ni(III) COMPLEXES
L. R. Furenlid, M. W. Renner, and E. Fujita 1995 11 p Presented at the 8th International Conference on X ray Absorption Fine Structure, Berlin, Germany, 28 Aug. - 2 Sep. 1994
(Contract DE-AC02-76CH-00016)
(DE95-004844; BNL-61084; CONF-9408131-5) Avail: CASI HC A03/MF A01

XAS techniques for studying structural and electronic changes taking place during oxidation and reduction reactions of nickel complexes are described and applied to selected models for Factor 430, a nickel containing cofactor catalyzing an important step in the conversion of carbon dioxide to methane by methanogenic bacteria. DOE

N95-24265 Brookhaven National Lab., Upton, NY.
FT-IR MICROSCOPICAL ANALYSIS WITH SYNCHROTRON RADIATION: THE MICROSCOPE OPTICS AND SYSTEM PERFORMANCE
J. A. Reffner (Spectra-Tech, Inc., Stamford, CT.), P. A. Martoglio (Spectra-Tech, Inc., Stamford, CT.), and G. P. Williams 1995 11 p Presented at the International Meeting on Synchrotron Radiation Instrumentation, Stony Brook, NY, 18-22 Jul. 1994 Limited Reproducibility: More than 20% of this document may be affected by microfiche quality
(Contract DE-AC02-76CH-00016)
(DE95-004834; BNL-61083; CONF-940714-47) Avail: CASI HC A03

When a Fourier transform infrared (FT-IR) microspectrometer was first interfaced with the National Synchrotron Light Source (NSLS) in September 1993, there was an instant realization that the performance at the diffraction limit had increased 40-100 times. The synchrotron source transformed the IR microspectrometer into a true IR microprobe, providing high-quality IR spectra for probe diameters at the diffraction limit. The combination of IR microspectroscopy and synchrotron radiation provides a powerful new tool for molecular spectroscopy. The ability to perform IR microspectroscopy with synchrotron radiation is still under development at Brookhaven National Laboratory, but several initial studies have been completed that demonstrate the broad-ranging applications of this technology and its potential for materials characterization. DOE

N95-24286# Massachusetts Inst. of Tech., Cambridge, MA.
DIRECT CATALYTIC DECOMPOSITION OF NITRIC OXIDE Quarterly Technical Progress Report Number 12, Jul. - Sep. 1994

M. Flytzani-Stephanopoulos (Tufts Univ., Medford, MA.), A. F. Sarofim, and Y. Zhang 1994 35 p
(Contract DE-FG22-91PC-91293)
(DE95-005202; DOE/PC-91293/12) Avail: CASI HC A03/MF A01

This project investigates a suitable catalyst system for the direct NO decomposition in post-combustion NO(sub x) control. The process does not use a reductant, such as ammonia used in the case of Selective Catalytic Reduction (SCR) of NO(sub x) to nitrogen. Therefore, it is a greatly simplified process basically involving passing the flue gas through a catalytic converter. Catalysts are prepared by incorporating metal cations into zeolite supports according to ion exchange procedures widely used in preparation of metal/zeolite catalysts. Particular emphasis is given in this work on promoted Cu-exchanged zeolites, especially the catalysts Mg/Cu-ZSM-5 and Ce/Cu-ZSM-5, which are promising for NO conversion to nitrogen at typical flue gas O2 and NO levels and over the temperature range of 723--873 K. Effects of zeolite modification, copper exchange level and catalyst preparation conditions on the catalyst activity are studied in a packed-bed microreactor. Kinetic and selectivity studies are conducted over a wide range of P(sub NO)/P(sub O2) and temperature with promoted and unpromoted Cu-ZSM-5. Structural characterization of the catalyst employs STEM/EDX analysis, XRD, XPS, EPR and luminescence analyses. A combination of techniques, including (27)Al NMR was used to identify the stabilization role of Ce(sup 3+) in Cu-ZSM-5 under wet NO decomposition conditions. DOE

N95-24341 Texas A&M Univ., College Station, TX.
FISCHER TROPSCH SYNTHESIS IN SUPERCRITICAL FLUIDS Quarterly Technical Progress Report, 1 Jul. 1994 - 30 Sep. 1994
A. Akgerman and D. B. Bukur 1995 53 p Limited Reproducibility: More than 20% of this document may be affected by microfiche quality
(Contract DE-FG22-92PC-92545)
(DE95-005206; DOE/PC-92545/8) Avail: CASI HC A04

In pursuit of the diffusion coefficients of Fischer-Tropsch products in supercritical fluids, the objectives for this quarter were to continue the work on effective density measurements. Some data were to be obtained and calculations of effective diffusivities were to be made. Once the effective diffusivity is known, then also knowing the molecular diffusivity, the tortuosity factor can be obtained. The porosity has been determined from independent experiments. Knowing the tortuosity and the porosity the only property that is needed to back calculate the effective diffusivity in a wide range of reactor conditions is the molecular diffusivity at those reaction conditions. DOE

N95-24345# Oak Ridge National Lab., TN.
SIMPLE CHEMICAL ASSAYS FOR PRESENCE OF S2F10 IN DECOMPOSED SF6
G. D. Griffin, M. R. Baker, and I. Sauers 1994 7 p Presented at the 7th International Symposium on Gaseous Dielectrics, Knoxville, TN, 4-28 Apr. 1994
(Contract DE-AC05-84OR-21400)
(DE95-001423; CONF-940414-6) Avail: CASI HC A02/MF A01

Disulfur decafluoride ((S2F10); also referred to as sulfur pentafluoride) is a highly toxic gas which can be produced by electrical discharges in SF6. It would be very useful, both for safety in handling decomposed SF6 and for diagnosis of fault conditions, to have a convenient, rapid and sensitive field assay for the presence of S2F10. A number of different assays for S2F10 with varying levels of sensitivity have been developed in the course of a CRADA initiative 'Investigation of S2F10 Production and Mitigation in Compressed SF6-Insulated power Systems.' These techniques include GC-MS, cryogenic GC enrichment and IR absorption. Although all of these procedures have been shown to have utility in detecting S2F10, and some have great sensitivity, they do not, in general, lend themselves to rapid field analyses. Ideally, one might wish to have an assay modeled after the 'Draeger Tubes,' where a gas sample is drawn through some chemical compound, and the resulting color change can be used to quantify the gas of interest. Disulfur decafluoride had been rather extensively studied in World War II as a candidate chemical warfare agent, and along with biological studies of its toxicity, chemical detection techniques had also been developed. Of the chemical assays described, two were particularly promising, one involving reaction of S2F10 with NaI to produce free I2 which could be titrated with sodium thiosulfate, and the other involving reaction of S2F10 with p-phenylenediamine to produce a pink/red color. This second assay appeared to hold some promise, and accordingly, experiments were carried out to see if this assay could be useful for detecting S2F10 in electrically decomposed SF6 samples. DOE

N95-24430# Westinghouse Savannah River Co., Aiken, SC.
CESIUM COBALTDICARBOLLIDE-SOLUBILITY, PRECIPITATION, AND REACTIVITY IN BASIC AQUEOUS SOLUTION
D. J. McCabe, J. C. Fanning, L. A. Hugg, W. A. Smith, A. S. Terrell, L. Yasinsac, L. J. Todd, and S. A. Jasper, Jr. 1994 20 p
(Contract DE-AC09-89SR-18035)
(DE95-005881; WSRC-RP-94-1272) Avail: CASI HC A03/MF A01

The title compound, Cs(+)(Co((3)-1, 2-C2B9H11)2)(-)(CsCDC), was precipitated with a NaCDC solution from solutions containing CsCl. The reaction was followed by measuring loss of light intensity as the precipitate formed. The (Cs(+)) and (CDC(-)) at the point of precipitation were estimated and approximate values of the K(sub sp) for CsCDC determined at room temperature: 8 x 10(exp -6) (water), 7 x 10(exp -6) (1 M NaOH), and 2 x 10(exp -6) (5M NaCl/0.1 M KOH/1.0 M NaOH). In some cases, NaCDC precipitated from solution when added to the latter salt solution. For the medium, 5 M NaNO3/0.1 M KOH/1.0 M NaOH a four-fold excess of NaCDC was added to a 10mM Cs(+) solution at 40 C and the (CDC(-)) measured spectrophotometrically. Only CsCDC precipitated, and a K(sub sp) of 3.9 x 10(exp -6) was determined. The solubilities of CsCDC were measured in NaNO3 and NaCl solutions at 30 C as a function of the Na salt concentration. Reaction of the CDC(-) with OH(-) slowly produces B(OH4)(-), H2, and CoO(OH). Reaction of 22 (mu)M CsCDC with 1M NaOH has a first order rate constant at 56 C of 8.8 x 10(exp -7) s(exp -1), while that for 14 mM NaCDC is 7.2 x 10(exp -7) s(exp -1). Activation energy for the reaction is 110 kJ. DOE

N95-24553# Department of Energy, Washington, DC. Div. of Chemical Sciences.
CARBONS AND HYDROGEN BY PERSISTENT METAL RADICALS Final Report, 1 Apr. 1993 - 31 Oct. 1994
1995 14 p
(Contract DE-FG06-92ER-14254)
(DE95-003834; DOE/ER-14254/2) Avail: CASI HC A03/MF A01

The synthesis of complexed rhenium radicals is demonstrated from the reaction of sterically demanding phosphine with the triphenylmethyl complex (n(sup 5)-CPh3)Re(CO)3. Low yields are experienced unless high concentrations of phosphine ligands are employed with the mechanism of this reaction yet unknown. A complexed rhenium dimer is also synthesized, but in low yield. X-ray crystallography reveals that the sixth coordination site of the electron deficient rhenium cation (an extremely strong Lewis acid) is occupied by an agostic interaction with one of the pendant C-H bonds of the cyclohexyl ring of the complex. Preliminary results show that the rhenium complexes have a significantly different chemistry from similar tungsten analogs in reactivity and isotope exchange rates. It is hypothesized that the rhenium complexes would be useful in catalyzing the isotope exchange between water and hydrogen. DOE

N95-24614# Sandia National Labs., Albuquerque, NM.
SYNTHESIS AND CHARACTERIZATION OF Fe COLLOID CATALYSTS IN INVERSE MICELLE SOLUTIONS
A. Martino, A. G. Sault, J. S. Kawola, M. Stoker (Brigham Young Univ., Provo, UT.), M. Hicks (Brigham Young Univ., Provo, UT.), and C. H. Bartholomew (Brigham Young Univ., Provo, UT.) 1995 11 p Presented at the American Chemical Society National Meeting, Anaheim, CA, 2-7 Apr. 1995
(Contract DE-AC04-94AL-85000)
(DE95-006313; SAND-94-3183C; CONF-950402-2) Avail: CASI HC A03/MF A01

Formation of Fe clusters in inverse micelles was studied. Iron salts are solubilized within the polar interior of inverse micelles, and addition of LiBH4 initiates reduction to produce monodisperse, nanometer-sized Fe based particles. The reaction sequence is sustained by material exchange between inverse micelles. Surfactant interface provides a spatial constraint on reaction volume, and reactions carried out in these micro-heterogeneous solutions produce colloidal sized particles (10-100 Angstrom) stabilized in solution against flocculation by surfactant. In this paper, the clusters were characterized using TEM, Moessbauer spectroscopy, electron diffraction, and x-ray photoelectron spectroscopy. DOE

N95-24686# Arizona State Univ., Tempe, AZ. Dept. of Chemistry and Biochemistry.

GENERATION, DETECTION AND CHARACTERIZATION OF GAS-PHASE TRANSITION METAL AGGREGATES AND COMPOUNDS Final Technical Report, 15 Sep. 1991 - 14 Jul. 1994

Timothy C. Steimle 12 Nov. 1994 11 p

(Contract DE-FG02-91ER-14227)

(DE95-004439; DOE/ER-14227/3) Avail: CASI HC A03/MF A01

The goal of this research project has been to identify and characterize small gas-phase metal containing molecules and relate these properties to proposed reaction mechanisms. Of particular emphasis has been the elucidation of the mechanism for activation of C-H, N-H, S-H, and C-C bonds in CH4, HCCH, H2S and NH3 by platinum, titanium, molybdenum, and niobium. DOE

N95-24840# Centro Brasileiro de Pesquisas Fisicas, Rio de Janeiro.

MOSSBAUER SPECTROSCOPY, X RAY DIFFRACTION AND MAGNETIC MEASUREMENTS OF IRON-NICKEL ULTRAFINE PARTICLES

R. B. Scorzelli, M. Elmassalami, E. G. daSilva, m1125797, C. Kaito (Kyoto Univ., Japan.), Y. Saito (Kyoto Univ., Japan.), and M. McElfresh (Purdue Univ., West Lafayette, IN.) 1993 12 p

(DE95-601136; CBPF-NF-067/93) Avail: CASI HC A03/MF A01 (US Sales Only)

Iron-nickel ultrafine particles with a composition in the Invar region (38-50% Ni) were prepared by the gas-evaporation-coalescence technique. The chemical composition was checked by electron probe microanalysis while X-ray diffraction Rietveld refinement was used to characterize the structure as well as to estimate the particle size. The temperature and field dependence of the magnetization M (B,T) was measured for 0 less than or equal to B less than or equal to 25 kOe in the temperature range 4.2 K less than or equal to T less than or equal to 400 K. Transmission Moessbauer spectra were taken at room temperature and at liquid helium temperature. The results obtained show that the predominant phase is a disordered Ni-rich alloy. DOE

N95-25097# Fernald Environmental Restoration Management Corp., Cincinnati, OH.

STANDARDIZATION OF EQUATIONS FOR RADIOCHEMICAL CALCULATIONS

Raymond J. Danahy, Thomas J. Dugan, F. Keith Tomlinson, and Hobert W. Jones (Labyrinth Group, Miamisburg, OH.) 1994 5 p Presented at the 40th Anniversary Conference on Bioassay, Analytical and Environmental Radiochemistry, Cincinnati, OH, 15-17 Nov. 1994

(Contract DE-AC24-92OR-21972)

(DE95-003028; FEMP-2387; CONF-9411105-1) Avail: CASI HC A01/MF A01

In mid-1993, the Fernald Environmental Restoration Management Corporation (FERMCO), with USEPA approval, implemented a project quality assurance plan containing performance-based specifications for radiochemical sample analyses conducted in support of the Fernald site remediation activities. FERMCO's initial approach to acquiring performance-based radioanalytical services was to provide limited guidance regarding equations for computation of the quantities required in each analysis report. It became evident that there was a significant divergence of opinion on how to compute some very basic radiochemical quantities. The use of a standardized set of equations was needed in order to ensure comparability of data from different laboratories. In a remediation project of this magnitude, use of multiple laboratories is a virtual necessity. Consequently comparability of data becomes an extremely important issue. A critical issue in the remedial investigation/feasibility study (RI/FS) phase of the clean up project is to avoid the occurrence of excessive false positive sample results. Such results could lead to unnecessary clean up and significant additional cost. This paper describes the specific formulas FERMCO is currently using to define such quantities as net sample count rate, sample radionuclide concentration, radiometric tracer and gravimetric carrier recovery. Equations have also been produced to define the uncertainty in each of the above quantities. Equations for the total propagated uncertainty (TPU) and for a sample-specific minimum detectable concentration (MDC) have also been specified. Generalized equations have been reformulated to address the specific conditions which apply to the analysis of FERMCO samples. In particular, FERMCO requires results which have been corrected for the radioactivity in the blank while in other instances, sample results without blank correction are required. DOE

N95-25098# Transducer Research, Inc., Naperville, IL.

FIELD-USABLE PORTABLE ANALYZER FOR CHLORINATED ORGANIC COMPOUNDS

William J. Buttner, Joseph R. Stetter, and Curtis V. Nakaishi (Department of Energy, Morgantown, WV.) 1994 14 p Presented at the International Nuclear and Hazardous Waste Management Conference, Atlanta, GA, 14-18 Aug. 1994

(Contract DE-AC21-92MC-29118)

(DE95-003127; DOE/METC-C/95/7163; CONF-940815-101) Avail: CASI HC A03/MF A01

A solid-state sensor was developed with selectivity for chlorinated organic vapors and sub-ppM sensitivity. DOE and TRI are currently developing an advanced chlorinated organic vapor monitor. The objective is to extend the analytical capabilities of this new sensing technology by designing and building an advanced instrument package. Design goals include a user-friendly, conveniently packaged instrument; a broad dynamic range provided by intelligent sampler systems including direct sampling, autodilution, and preconcentration; and an analytical capability for condensed media with a specialized sampler. Field testing of the advanced chlorinated organic vapor monitor has been completed and it was demonstrated that the advanced instrument system is capable of providing rapid, selective, on-site chemical analyses in a way that is not available by alternative techniques. For example, the soil around 100N Bunker C area at DOE Hanford has trace contamination levels of chlorinated solvents, but is also heavily contaminated by oils which will show up on the OVM. The advanced chlorinated organic vapor monitor performed soil gas analysis on five soil gas probes in less than 30 minutes with vapor levels ranging between 0 and 2 ppM without interference from oil. Area surveys were performed at Hanford by site personnel who received training sessions lasting less than five minutes, thus demonstrating ease of instrument operation. DOE

N95-25123# Brookhaven National Lab., Upton, NY.

A STUDY OF THE ELECTROCHEMICAL BEHAVIOR OF TUNGSTEN IN CAUSTIC SOLUTIONS AND PLATINUM/IRIDIUM IN CH LORIDE SOLUTIONS Informal Report

C. M. Vitus, H. S. Isaacs, and V. Schroeder (California Univ., Berkeley, CA.) 22 Nov. 1994 27 p

(Contract DE-AC02-76CH-00016)

(DE95-004951; BNL-61136) Avail: CASI HC A03/MF A01

Platinum/iridium and tungsten wires were electronically etched in chloride and caustic solution, respectively, to produce tips with high aspect ratio. A direct relationship between the meniscus and the aspect ratio of etched tips was established. Scanning electron micrographs indicated that higher aspect ratios were obtained by changing the geometry of the meniscus during the etch either by an increase in the applied a.c. voltage or with the addition of a nonpolar layer above the electrolytic solution during the etching process. Above the breakdown voltage, two possible mechanisms appeared to control the etching process by expediting chemical dissolution: cavitation and sparking. Cavitation caused erosion due to the force of evolved gases against the electrode and sparking attacked the surface by vaporizing the metal. Sparking commenced on both wires near 24V. This voltage corresponded to a minimum in the plot of total etch time versus voltage. From light emission studies, sparking on Pt/Ir was associated with the ionization of Pt, Ir, Ca, and Cl. A compositional analysis of insoluble black particles produced during a.c. and d.c. etching of Pt/Ir revealed Pt and Ir as the major constituents of the product. The sparking process was shown to have a potential use in micromachining. DOE

N95-25242# Sandia National Labs., Livermore, CA. Computational Mechanics Dept.

UNDERSTANDING AND IMPROVING MATERIALS PROCESSING THROUGH INTERPRETING AND MANIPULATING PREDICTIVE MODELS

Robert J. Kee, Aili Ting, and Paul A. Spence 1995 12 p Presented at the 1994 Fall Meeting of the Materials Research Society, Boston, MA, 28 Nov. - 2 Dec. 1994 Sponsored in cooperation with SEMATECH

(Contract DE-AC04-76DP-00789)

(DE95-004384; SAND-95-8455C; CONF-941144-19) Avail: CASI HC A03/MF A01

Most physically based modeling software accepts input in the form of

geometry definition, physical parameters, initial conditions, and boundary conditions; and then, on the basis of solving physical conservation equations, predicts the steady-state or transient behavior of a system or process. There is a growing need to create software tools that can themselves control or manipulate the physically based models in certain ways to enhance the usability of models for equipment design and process optimization. These required tools can be described broadly in the following categories: sensitivity analysis, parameter estimation, inverse problems, dynamic optimization, and real-time control. This paper discusses generally the development and application of such modeling tools, drawing examples from a specific RTP reactor design. These techniques accelerate significantly the optimal design of processes and the concurrent engineering of real-time process-control algorithms. DOE

N95-25252# Pacific Northwest Lab., Richland, WA.
A SOLUBILITY MODEL FOR AMORPHOUS SILICA IN CONCENTRATED ELECTROLYTES
A. R. Felmy, C. C. Schroeder, and M. J. Mason Aug. 1994 21 p Presented at the American Chemical Society National Meeting, Washington, DC, 21-26 Aug. 1994
(Contract DE-AC06-76RL-01830)
(DE95-004896; PNL-SA-25345; CONF-940813-33) Avail: CASI HC A03/MF A01

Silica is one of the major constituents of the earth's crust and is ubiquitously present in most natural materials. The solubility of silica and other silica-containing compounds is, therefore, of primary concern in geochemistry and in chemical processing applications where silica scale formation, resulting from changes in temperature and electrolyte composition, can cause problems in process design and operation. This paper describes the development of an aqueous thermodynamic model for accurately predicting the solubility of amorphous silica and other silica-containing compounds in the system Na(+)-H(+)-Mg(2+)-NO3(-)-SO4(2-)-Cl(-)-H2O to high concentration and across the temperature range 25 to 100 C. This model, which utilizes the aqueous thermodynamic model of Pitzer, includes only one dissolved silica species, H4SiO4(aq), and is valid in neutral to very acidic solutions. The model is parameterized from the extensive set of solubility data in the literature as well as from new experimental data on amorphous silica solubility in HNO3 and HCl developed as part of this study. The accuracy of the model is tested on solutions more complex than those used in model parameterization. DOE

N95-25291# Lawrence Livermore National Lab., Livermore, CA.
A HIGHER-ORDER PROJECTION METHOD FOR THE SIMULATION OF UNSTEADY TURBULENT NONPREMIXED COMBUSTION IN AN INDUSTRIAL BURNER
R. B. Pember, A. S. Almgren, J. B. Bell, P. Colella, L. Howell, and M. Lai Dec. 1994 19 p Presented at the 8th International Symposium on Transport Phenomena in Combustion, San Francisco, CA, 16-20 Jul. 1994
(Contract W-7405-eng-48)
(DE95-005919; UCRL-JC-118634; CONF-9407160-1) Avail: CASI HC A03/MF A01

The modeling of transient effects in burners is becoming increasingly important. The problem of ensuring the safe performance of an industrial burner, for example, is much more difficult during the startup or shutdown phases of operation. The peak formation of pollutants is also much more dependent on transient behavior, in particular, on peak temperatures, than on average operating conditions. In this paper we present a new methodology for the modeling of unsteady, nonpremixed, reacting flow in industrial burners. The algorithm uses a second-order projection method for unsteady, low-Mach number reacting flow and accounts for species diffusion, convective and radiative heat transfer, viscous transport, turbulence, and chemical kinetics. The time step used by the method is restricted solely by an advective CFL condition. The methodology is applicable only in the low-Mach number regime (M less than .3), typically met in industrial burners. The projection method for low-Mach number reacting flow is an extension of a higher-order projection method for incompressible flow to the low-Mach number equations of reacting flow. Our method is based on an approximate projection formulation. Radiative transport is modeled using the discrete ordinates method. The main goal of this work is to introduce and investigate the simulation of burners using a higher-order projection method for low-Mach number combustion. As such, the methodology is applied here only to axisymmetric flow in gas-fired burners for which the boundaries can be aligned with a rectangular grid. The perfect gas law is also assumed. In addition, we use a one-step reduced kinetics mechanism, a kappa minus epsilon model for turbulent transport, and a simple turbulent combustion model. DOE

N95-25356# National Lab. for High Energy Physics, Tsukuba (Japan).
PROCEEDINGS OF THE WORKSHOP ON DYNAMICS AND STRUCTURE OF DISORDERED SYSTEM
M. Arai, ed. (Kobe Univ., Japan.), K. Shibata, ed., and H. Ikeda, ed. Nov. 1993 138 p In JAPANESE Workshop held in Tsukuba, Japan, 17-18 Mar. 1993
(DE94-792685; KEK-PROC-93-14; CONF-9303298) Avail: CASI HC A07/MF A02

The workshop was held on March 17 and 18, 1993, at the National Laboratory for High Energy Physics. The topics were particularly limited to lattice system among the problems of the dynamics and structure of disordered system. The problems that became the focus were recent understanding of local structure and middle distance correlation in disordered system, universal thermal properties of disordered system and phonon state density, and further, problems related to fracton, and problems related to glass-transition. At the workshop, lectures were given on dynamic middle distance structure of amorphism, Raman scattering and middle distance correlation of germanium chalcogenide glass, universal thermal properties of glass near several K, low energy excitation of disordered system by photon echo spectroscopy, fracton computer experiment, sound wave absorption of SiO2-10% GeO2 glass, fracton in strong magnetic field, recent topics in Conference on Phonon Scattering, dynamic short distance structure of amorphism, structure of chalcogen nanodroplets, low energy excitation of polymers and glass-transition and so on. DOE

N95-25443# Swedish Inst. for Materials Testing, Boras (Sweden).
HEAT RELEASE RATE MEASUREMENTS IN TUNNEL FIRES
Haukur Ingason, Soren Gustavsson, and Martin Dahlberg 1994 61 p Sponsored by Swedish Fire Research Board, National Rescue Services Board and the Swedish Railway Co.
(Proj. BRANDFORSK 723-924)
(PB95-165106; SP-RAPP-1994:08) Avail: CASI HC A04/MF A01

This report describes measurements of heat release rates in tunnel fires by using the oxygen consumption technique. This technique is commonly used in fire laboratories to measure heat release rates up to 10 MW. Measured heat release rates from fire tests with vehicles (a train, a bus, a subway coach and a simulated truck load) and wood cribs are presented. The total heat release rate was determined by measuring oxygen concentrations and mass flow rates over the tunnel cross section at both sides of the fire. The convective fraction of the heat release rate was determined by measuring the temperature and the mass flow rate. The technique is found to work reasonably well for tunnel fires. However, the measured convective fraction of the heat release rate needs to be corrected for heat losses from the hot ceiling jet to the cold walls. The total heat release rate needs to be corrected for high yields of carbon monoxide (CO2) in the exhaust gases and for vitiation of the inflowing air in the lower part of the cross section. NTIS

N95-25447# International Centre for Theoretical Physics, Trieste (Italy).
TEMPERATURE BOUNDS IN A MODEL OF LAMINAR FLAMES
M. Kirane and S. Badraoui (Annaba Univ., Algeria.) Jun. 1994 4 p
(DE95-607048; IC-94/54) Avail: CASI HC A01/MF A01 (US Sales Only)

We consider reaction-diffusion equations coupling temperature and mass fraction in one-step-reaction model of combustion in R(sup N). Uniform temperature bounds are derived when the Lewis number is less than one. This result completes the case of Lewis number greater than one studied previously. DOE

N95-25492# Sandia Labs., Livermore, CA.
USER GUIDE TO THE BURNER ENGINEERING RESEARCH LABORATORY
Neal Fornaciari, Robert Schefer, Phillip Paul, Robert Sanford (Energy and Environmental Research Corp., Santa Ana, CA.), Lloyd Claytor (Energy and Environmental Research Corp., Santa Ana, CA.), and Christi Lubeck (California Univ., San Diego, CA.) Nov. 1994 27 p Presented at the International Conference on Environmental Control of Combustion Processes,

Honolulu, HI, 7-10 Oct. 1994
(Contract DE-AC04-94AL-85000)
(DE95-004191; SAND-94-8556; CONF-9410193-1) Avail: CASI HC A03/MF A01

The Burner Engineering Research Laboratory (BERL) was established with the purpose of providing a facility where manufacturers and researchers can study industrial natural gas burners using conventional and laser-based diagnostics. To achieve this goal, an octagonal furnace enclosure with variable boundary conditions and optical access that can accommodate burners with firing rates up to 2.5 MMBtu per hour was built. In addition to conventional diagnostic capabilities like input/output measurements, exhaust gas monitoring, suction pyrometry, and in-furnace gas sampling, laser-based diagnostics available at BERL include planar Mie scattering, laser Doppler velocimetry, and laser-induced fluorescence. This paper gives an overview of the operation of BERL and a description of the diagnostic capabilities and an estimate of the time required to complete each diagnostic for the potential user who is considering submitting a proposal. DOE

N95-25959 Polish Academy of Sciences, Warsaw (Poland). Inst. of Physical Acoustics.
THE CHARACTERISTICS AND DESIGN OF AN APPARATUS CONSTRUCTED BY THE INSTITUTE OF BASIC PROBLEMS OF TECHNOLOGY TO STUDY RELAXATION PHENOMENA IN LIQUIDS AT FREQUENCIES OF 10-150 MHz [CHARAKTERYSTYKA I KONSTRUKCJA ZBUDOWANEGO W IPPT STANOWISKA DO ULTRADZWIEKOWEGO BADANIA ZJAWISK RELAKSACYJNYCH W CIECZACH W ZAKRESIE CZESTOTLIWOSCI 10-150 MHZ]
A. Balczerak and R. Plowiec 1994 17 p In POLISH
(ISSN 0208-5658)
(IFTR-21/1994) Avail: Issuing Activity (Polish Academy of Sciences, Warsaw, Poland)

The principles of the operation and design of an apparatus to measure the velocity and damping of ultrasound waves in liquids is presented. These measurements are necessary to study relaxation phenomena in liquids. The apparatus described can be used to measure the phase velocities, group velocities, and damping coefficients of ultrasound waves in liquids with frequencies of 10 to 150 MHz.
Transl. by Schreiber Translations Inc.

N95-26000 Traeteknik Centrum, Stockholm (Sweden).
FIRE TEST OF SURFACE PRODUCTS: COMPARISON OF DATA FROM THE NORDIC BOX TEST AND THE CONE CALORIMETER [BRANDPROVNING AV YTMATERIAL: JAEMFOERELSE AV DATA FRAN LADMETODEN OCH KONKALORIMETERN]
L. Tsantaridis and B. Oestman Jul. 1994 38 p In SWAHILI
(PB95-165239; Traetek-R-94/040-SE) Avail: Issuing Activity (National Technical Information Service (NTIS))

New fire test methods, both in small and full scale, have been developed within ISO in order to determine and characterize the fire behavior in a more elaborate way than the present national test method. One of these new small scale tests is the Cone Calorimeter (ISO 5660). The national test method used in Sweden and in the other Nordic countries is the Box Test (NT Fire 004). Results from these two methods are compared for 49 surface products. NTIS

N95-26056 Naval Surface Warfare Center, Silver Spring, MD.
IN SITU XAFS STUDY OF OXIDES FORMED ON NICKEL THIN FILM ELECTRODES IN KOH SOLUTION
A. N. Mansour and C. A. Melendres 5 Dec. 1994 9 p Limited Reproducibility: More than 20% of this document may be affected by microfiche quality
(Contract N00014-94-WX-23074)
(AD-A288735) Avail: Issuing Activity (Defense Technical Information Center (DTIC))

The composition and structure of the oxides formed on nickel are of great interest for a number of technological applications, e.g., batteries and corrosion. In spite of the considerable research that has been done, there is still much uncertainty as to the stoichiometry and structure of the various oxides (hydroxides) that are formed during the anodic oxidation of the nickel. This is due largely to the highly disordered or amorphous nature of the phases formed which makes structural determination by X ray diffraction difficult. X ray absorption Fine Structure (XAFS) spectroscopy is an excellent technique for the characterization of such materials which have no long range order. In this paper, we present initial results of an 'in situ' study of the structure and composition of the oxides (hydroxides) formed on Ni thin film electrodes in 5M KOH solution as a function of the applied potential. DTIC

N95-26093# Air Products and Chemicals, Inc., Allentown, PA.
DEVELOPMENT OF NOVEL ACTIVE TRANSPORT MEMBRANE DEVICES Interim Report
Daniel V. Laciak Nov. 1994 98 p
(Contract DE-FC36-89ID-12779)
(DE95-002658; DOE/ID-12779/3) Avail: CASI HC A05/MF A02

Air Products has undertaken a research program to fabricate and evaluate gas separation membranes based upon promising 'active-transport' (AT) materials recently developed in our laboratories. Active Transport materials are ionic polymers and molten salts which undergo reversible interaction or reaction with ammonia and carbon dioxide. The materials are useful for separating these gases from mixtures with hydrogen. Moreover, AT membranes have the unique property of possessing high permeability towards ammnonia and carbon dioxide but low permeability towards hydrogen and can thus be used to permeate these components from a gas stream while retaining hydrogen at high pressure. DOE

N95-26107 Polish Academy of Sciences, Warsaw (Poland). Dept. of Aeroacoustics.
DYNAMIC METHODS FOR DETERMINING THE MATERIAL CHARACTERISTICS OF SATURATED PERMEABLE MEDIA [DYNAMICZNE METODY WYZNACZANIA CHARAKTERYSTYK MATERIALOWYCH NASYCONYCH OSRODKOW PRZEPUSZCZALNYCH]
Jozef Kubik and Mariusz Kaczmarek 1993 37 p In POLISH
(ISSN 0208-5658)
(IFTR-17/1993) Avail: Issuing Activity (Polish Academy of Sciences, Warsaw, Poland)

In addition to the effect of physical material characteristics, the many processes which take place in saturated permeable media (such as deformation, percolation, diffusion, and physical absorption) are significantly affected by the structure of the pores of the permeable skeleton, which is described by such macroparameters as porosity, sinuosity, and permeability. These parameters are explicitly contained in macrocontinual models of porous media and reflect such effects as the immiscibility effect, dynamic coupling caused by microvariations in the relative flow velocity field in the pore space, and hydrodynamic resistance caused by adhesive interaction of the phases at the very geometrically complex interface of the medium. That is why knowledge of these parameters and the availability of methods for determining them play a very important role in solving problems of permeable media mechanics. Transl. by SCITRAN

N95-26261# Melbourne Univ., Parkville (Australia).
CONDUCTIVITY IN INSULATORS DUE TO IMPLANTATION OF CONDUCTING SPECIES
S. Prawer, A. Hoffman (Australian Nuclear Science and Technology Organisation, Menai, Australia.), M. Petravic (Australian National Univ., Canberra, Australia.), and R. Kalish (Israel Inst. of Tech., Haifa, Israel.) 1993 19 p Sponsored by Dept. of Industry, Technology and Commerce
(DE95-607773; UM-P-92/77) Avail: CASI HC A03/MF A01 (US Sales Only)

Control of the surface conductivity of insulators can be accomplished by high dose ion implantation of conductive species. The use of C(+) as the implant species is particularly interesting because C can either form electrically insulating sp(sup 3) bonds or electrically conducting sp(sup 2) bonds. In the present work, fused quartz plates have been irradiated with 100 keV C(+) ions to doses up to 1 x 10(exp 17) ions/sq cm at room temperature and at 200 C. The ion beam induced conductivity was monitored in-situ and was found to increase by up to 8 orders of magnitude for the ion dose range studied. Xe implantations over a similar range did not induce any changes in the conductivity showing that the increase in conductivity is caused by the presence of the C in the fused quartz matrix and not by damage. The dependence of the conductivity on implantation temperature and on post implantation annealing sheds light on the clustering of the C implants. The temperature dependence of the conductivity for the highest doses employed (1 x 10(exp 17) C(+)/sq cm) can be described

very well by ln(sigma) (alpha) T. This is considered to be a peculiar dependence which does not comply with any of the standard models for conduction. DOE

N95-25398*# Queensland Univ., Saint Lucia (Australia). Dept. of Mechanical Engineering.
SCALING IN A SCRAMJET COMBUSTOR
M. V. Pulsonetti and R. J. Stalker *In its* Shock Tunnel Studies of Scramjet Phenomena 1993 Jan. 1995 p 37-40 (For primary document see N95-25394 08-34)
Avail: CASI HC A01/MF A02

26 METALLIC MATERIALS

Includes physical, chemical, and mechanical properties of metals, e.g., corrosion; and metallurgy.

N95-24220*# Virginia Univ., Charlottesville, VA. Dept. of Materials Science and Engineering.
NASA-UVA LIGHT AEROSPACE ALLOY AND STRUCTURES TECHNOLOGY PROGRAM (LA2ST) Progress Report, 1 Jul. - 31 Dec. 1994
Edgar A. Starke, Jr., Richard P. Gangloff, Carl T. Herakovich, John R. Scully, Gary J. Shiflet, Glenn E. Stoner, and John A. Wert Mar. 1995 209 p
(Grant NAG1-745)
(NASA-CR-198041; NAS 1.26:198041; UVA/528266/MSE94/117) Avail: CASI HC A10/MF A03

The NASA-UVa Light Aerospace Alloy and Structures Technology (LA2ST) Program was initiated in 1986 and continues with a high level of activity. Projects are being conducted by graduate students and faculty advisors in the Department of Materials Science and Engineering, as well as in the Department of Civil Engineering and Applied Mechanics, at the University of Virginia. Here, we report on progress achieved between July 1 and December 31, 1994. The objective of the LA2ST Program is to conduct interdisciplinary graduate student research on the performance of next generation, light-weight aerospace alloys, composites and thermal gradient structures in collaboration with NASA-Langley researchers. Specific technical objectives are presented for each research project. We generally aim to produce relevant data and basic understanding of material mechanical response, environmental/corrosion behavior, and microstructure; new monolithic and composite alloys; advanced processing methods; new solid and fluid mechanics analyses; measurement and modeling advances; and a pool of educated graduate students for aerospace technologies. Author

N95-24329# Lawrence Livermore National Lab., Livermore, CA.
CHARACTERIZATION OF ULTRADISPERSED ALUMINUM
R. L. Simpson, J. L. Maienschein, R. W. Swansiger, F. Garcia, and D. H. Darling Dec. 1994 20 p
(Contract W-7405-eng-48)
(DE95-006379; UCRL-ID-119235) Avail. CASI HC A03/MF A01

Samples of ultradispersed Al were received, which were produced by electrically exploding Al wires in argon. These samples comprised very small particles that were not significantly oxidized and that were stable in air. Particle morphology was studied with scanning electron microscopy, micropycnometry, and gas adsorption surface area. Composition was determined using various techniques, as were thermal stability and reaction exotherms. The inexplicable reports of an Al-Ar compound and of an exothermic reaction were not confirmed. The material is a stable, nonoxidized, small-particle, highly reactive form of aluminum that is of interest in energetic materials formulations. DOE

N95-24338# Japan Atomic Energy Research Inst., Tokyo (Japan).
CREEP PROPERTIES OF 20% COLD WORKED HASTELLOY XR
Yuji Kurata and Hajime Nakajima Feb. 1994 35 p
(DE94-785198; JAERI-M-94-022) Avail: CASI HC A03/MF A01

Creep properties of Hastelloy XR, in 20% cold worked or solution treated condition, were studied at 800, 900 and 1000 C. The results obtained are discussed as follows. (1) At 800 C, creep rupture time of 20% cold worked Hastelloy XR is longer than that of solution treated one. However, the effect disappears above 900 C. At 1000 C, it becomes shorter than that of solution treated Hastelloy XR. (2) Rupture elongation and reduction of area of 20% cold worked Hastelloy XR are smaller than those of solution treated one. While these values of 20% cold worked Hastelloy XR are lowest at 900 C, they recover considerably at 1000 C. (3) Nonclassical creep curves which have the region with low creep rate at an early stage of creep were observed at high temperatures for Hastelloy XR, in 20% cold worked or solution treated condition. (4) Minimum creep rate, epsilon(sub m), of 20% cold worked Hastelloy XR is decreased by as much at a factor of 20 to 50 at 800 and 900 C. On the other hand, epsilon(sub m) of 20% cold worked Hastelloy XR is increased by as much as a factor of 2 at 1000 C. (5) Although 20% cold work enhances creep resistance of Hastelloy XR at 800 and 900 deg C, the effect becomes detrimental at 1000 deg C where dynamic recrystallization occurs during creep. DOE

N95-24366# Instituto de Pesquisas Energeticas e Nucleares, Sao Paulo (Brazil).
PREPARATION OF STABILIZED ZIRCONIA (ZrO_2) WITH YTTERIA (Y_2O_3) BY SIMULTANEOUS PRECIPITATION
M. deCampos 1993 108 p
(DE95-600163; INIS-BR-3399) Avail: CASI HC A06/MF A02 (US Sales Only)

The preparation of cubic or tetragonal partially stabilized zirconia with Yttria by simultaneous precipitation was studied. The metals Zr and Y, in nitric acid and hydrogen peroxide medium, were precipitated with ammonia solution. The variables studied were: the pH of the aqueous medium (8, 9 and 10) and yttrium molar concentration (2, 3 and 5 mol %) in the final product. The resulting oxide samples were divided and calcined at 500, 700 and 900 C, separately. After that, all samples were sintered at 1500 C for one hour. For physico-chemical characterization, techniques such as ICP-AES, XRF, XRD, and SEM were used. The results show that by using this approach, predominant cubic and/or tetragonal phases can be reached with theoretical density over 92% and grain size lower than 1 micrometer. DOE

N95-24400*# California Univ., Santa Barbara, CA. Quantum Inst.
AN INVESTIGATION OF THE EFFECT OF SURFACE IMPURITIES ON THE ADSORPTION KINETICS OF HYDROGEN CHEMISORBED ONTO IRON Annual Status Report, 1 Jan. - 31 Dec. 1994
Mickey R. Shanabarger 31 Dec. 1994 22 p
(Contract NCC2-63)
(NASA-CR-197967; NAS 1.26:197967) Avail: CASI HC A03/MF A01

The goal of this program has been to develop an understanding of heterogeneous kinetic processes for those molecular species which produce gaseous hydrogen degradation of the mechanical properties of metallic structural materials. During the present program, the interaction of hydrogen with the surfaces of alpha-2 (Ti_3Al) titanium aluminide, gamma (TiAl) titanium aluminide, and beryllium were studied. The interaction of low pressure hydrogen with gamma titanium aluminide and beryllium was found to be relatively weak. Weak in the sense that adsorption leads to a low surface concentration of dissociated hydrogen, i.e., the chemisorption process is reversible at room temperature (300 K) for gamma titanium aluminide and the sticking coefficient for chemisorption is extremely small for beryllium. Hydrogen was found to interact readily with alpha-2 titanium aluminide to form a stable surface hydride at 300 K. These results correlate well with other recent studies which show that the mechanical properties for alpha-2 titanium aluminide are readily degraded in hydrogen while gamma titanium aluminide exhibits less degradation and beryllium essentially no degradation. The interaction of oxygen with the surface of several of these materials was studied. More recently, preliminary hydrogen permeation studies were completed for three high temperature alloys, Incoloy 909, Mo-47.5Re (wt. %), and this past year, Haynes 188. Author

N95-24432# Oak Ridge National Lab., TN.
TIME DEPENDENT INDENTATION TESTING AT NON-AMBIENT TEMPERATURES UTILIZING THE HIGH TEMPERATURE MECHANICAL PROPERTIES MICROPROBE
B. N. Lucas and W. C. Oliver (Nano Instruments, Inc., Knoxville, TN.) 1994 6 p Presented at the 1994 Fall Meeting of the Materials Research Society (MRS), Boston, MA, 28 Nov. - 2 Dec. 1994
(Contract DE-AC05-84OR-21400)
(DE95-005895; CONF-941144-53) Avail: CASI HC A02/MF A01

Time dependent indentation data for pure indium from -100 C to 75 C is presented. The properties reported include hardness, indentation strain rate, stress exponent and apparent activation energy for creep. These properties were measured using a depth-sensing indentation system capable of performing experiments between -100 C and 300 C in ultra-high vacuum. In addition, by employing laser interferometric techniques, this system can obtain displacement data with time constants as low as 50 ns. This allows the investigation of the material response to very fast stress changes over an extremely wide range of strain rates. The adverse and beneficial dynamic effects of step-loading the indenter into the surface of the material will be discussed. Initial results obtained from this type of experiment show that it is possible to obtain energy dissipation or damping information from the material being studied. DOE

N95-24433# Oak Ridge National Lab., TN.
SYNTHESIS OF Ni3Al AND NiAl INTERMETALLICS
V. K. Sikka and R. Cooper (Xform, Inc., Cohoes, NY.) 1994 13 p Presented at the Materials Week '94, Rosemont, IL, 3-7 Oct. 1994
(Contract DE-AC05-84OR-21400)
(DE95-005897; CONF-941016-5) Avail: CASI HC A03/MF A01

Intermetallics are an attractive class of advanced materials. The aluminide intermetallics offer advantages including: (1) lower density, (2) oxidation resistance, (3) carburization resistance, and (4) interesting mechanical properties because of their ordered crystal structure. Even though the attractive properties of the aluminides and other intermetallics have been known for nearly four decades, their practical applications have not been developed for two reasons: (1) poor ductility (in some cases at both ambient and high temperatures) and (2) lack of processability into meaningful components. Recent advances such as ductilization of Ni3Al by small additions of boron and the knowledge that environmental effects are the major cause of poor ductility in Fe3Al and FeAl systems have brought the intermetallics into the forefront of research and their commercial applications. This paper describes a method for melting Ni3Al-based alloys that successfully utilize the exotherm for formation of NiAl from elemental materials. The reaction-synthesis method has also been utilized for the production of NiAl and NiAl-based alloy powders from the elemental powders. Reaction-synthesized powders of NiAl and NiAl-based alloys were consolidated by hot extrusion and evaluated for tensile properties over a temperature range from room temperature to 1050 C. The powder-processing conditions have been found to have more influence on the ductile-to-brittle transition temperature of NiAl than the powder-production method. DOE

N95-24449# Pacific Northwest Lab., Richland, WA.
TEMPERATURE AND STRAIN-RATE EFFECTS ON DEFORMATION MECHANISMS IN IRRADIATED STAINLESS STEEL
J. L. Brimhall, J. I. Cole, J. S. Vetrano, and S. M. Bruemmer Nov. 1994 7 p Presented at the 1994 Fall Meeting of the Materials Research Society (MRS), Boston, MA, 28 Nov. - 2 Dec. 1994
(Contract DE-AC06-76RL-01830)
(DE95-004941; PNL-SA-25518; CONF-941144-31) Avail: CASI HC A02/MF A01

Analysis of the deformation microstructures in ion-irradiated stainless steel shows twinning to be the predominant deformation mode at room temperature. Dislocation channelling also occurs under slow strain rate conditions. Stresses required for twinning were calculated by the model of Venables and are compatible with observed yield stresses in neutron-irradiated material if loops are the principal twin source. Computation of the expected radiation hardening from the defect structure, based on a simple model, is consistent with yield strengths measured on neutron-irradiated steels. Lower yield stresses and greater thermal energy at 288 C lessen the probability of twinning and dislocation channeling becomes the primary deformation mode at the higher temperature. However, preliminary early results show that some twinning does occur in the irradiated stainless steel even at the higher temperature when higher strain rates are used. DOE

N95-24480# Westinghouse Savannah River Co., Aiken, SC.
CHARACTERIZING PRE-POLISHED TYPE 304L STAINLESS STEEL
Robert H. Hsu, Mike E. Summer, and W. Nevyn Rankin (Ebasco Services, Inc., Augusta, GA.) 1994 10 p Presented at the Joint Power Generation Conference, Phoenix, AZ, 2-6 Oct. 1994
(Contract DE-AC09-89SR-18035)
(DE95-001241; WSRC-MS-94-0437; CONF-941007-2) Avail: CASI HC A02/MF A01

Prepolished Type 304L stainless steel surfaces are being specified for replacement of some equipment in the 221-H Canyon Building at the Savannah River Site. A prepolished stainless steel surface picks up less contamination than a hot-rolled and pickled surface and is easier to decontaminate; therefore, less waste is generated. Surface-characterization techniques and specification for a prepolished surface were developed to ensure that prepolished items being obtained were properly electropolished. The use of this technology has resulted in obtaining prepolished items with an improved surface finish. DOE

N95-24615# Westinghouse Savannah River Co., Aiken, SC. Materials Technology Section.
STAINLESS STEEL RECYCLE Progress Report, 1994
K. J. Imrich 28 Oct. 1994 15 p
(Contract DE-AC09-89SR-18035)
(DE95-003905; WSRC-TR-94-0527) Avail: CASI HC A03/MF A01

The Materials Technology Section (MTS) of the Savannah River Technology Center (SRTC) was asked to demonstrate the practicality of recycling previously contaminated stainless steel components such as reactor heat exchanger heads, process water piping and slug buckets into 208 liters (55 gallon) drums and 2.8 cubic meter (100 cu ft) storage boxes. Radioactively contaminated stainless steel scrap will be sent to several industrial partners where it will be melted, decontaminated/cast into ingots, and rolled into plate and sheet and fabricated into the drums and boxes. As part of this recycle initiative, MTS was requested to demonstrate that radioactively contaminated Type 304L stainless steel could be remelted and cast to meet the applicable ASTM specification for fabrication of drums and boxes. In addition, MTS was requested to develop the technical basis of melt decontamination and establish practicality of using this approach for value added products. The findings presented in this investigation lead to the following conclusions: recycle of 18 wt% Cr - 8 wt% Ni alloy can be achieved by melting Type 304 stainless steel in an air vacuum induction furnace; limited melt decontamination of the contaminated stainless steel was achieved, surface contamination was removed by standard decontamination techniques; carbon uptake in the as-cast ingots resulted from the graphite susceptor used in this experiment and is unavoidable with this furnace configuration. A new furnace optimized for melting stainless steel has been installed and is currently being tested for use in this program. DOE

N95-24647# Tennessee Univ., Knoxville, TN. Dept. of Material Science and Technology.
LOCALIZED CORROSION AND STRESS CORROSION CRACKING CHARACTERISTICS OF A LOW-ALUMINUM-CONTENT IRON-ALUMINUM ALLOY
J. G. Kim and R. A. Buchanan Oct. 1994 26 p Prepared for Oak Ridge National Lab., TN
(Contract DE-AC05-84OR-21400)
(DE95-003259; ORNL/Sub-88-07685CT92/04) Avail: CASI HC A03/MF A01

The aqueous corrosion behavior of FAPY, a non-ordered Fe-Al alloy (Fe-16.1Al-5.4Cr-1.1Mo-0.11C-0.11Zr-0.06Y, at.%), was studied in various electrolytes and compared with reference materials. Corrosion rates for FAPY were much closer to that of 304L stainless steel than to the plain-carbon and low-alloy steels evaluated. Three-week crevice corrosion tests were performed in chloride-containing solutions on FAPY, and for comparison, on the Fe3Al-based iron aluminide FAL-Mo, and 304L stainless steel. The FAPY alloy was less resistant to crevice corrosion than FAL-Mo and 304L stainless steel. In the 3.5 wt% NaCl solution, the FAPY alloy was subject to severe crevice corrosion. Slow-strain-rate corrosion tests were conducted at the free-corrosion potential and at potentiostatically-controlled anodic and cathodic potentials to evaluate the environmental-embrittlement susceptibility. It was found that the FAPY alloy was susceptible to hydrogen embrittlement and anodic-dissolution stress corrosion cracking, but at the free-corrosion potential and the hydrogen-producing-cathodic potentials, the ductilities were significantly higher than those for Fe3Al-based iron aluminides. DOE

N95-24716# Sandia National Labs., Albuquerque, NM. Center for Solder Science and Technology.

CAPILLARY FLOW ON NARROW STRIPS AND IN V-SHAPED GROOVES

F. G. Yost and E. A. Holm 1995 21 p Presented at the InterPack 1995: International Electronic Packaging Conference, Maui, HI, 26-30 Mar. 1995

(Contract DE-AC04-94AL-85000)

(DE95-000543; SAND-94-2215C; CONF-950344-3) Avail: CASI HC A03/MF A01

Simple models for the flow of solder onto a copper metallized strip and into V-shaped grooves in copper were derived and compared to experimental results. The conditions for initiation of flow are established and followed by the determination of flow rates for the two geometrical configurations. The analysis leads to the conclusion that the standard approach to capillary flow is adequate for describing these kinetics. A computer simulation using the interfacial energy minimization code Surface Evolver, is also used to examine these systems and it is shown that it does predict the experimentally observed morphologies. The two approaches are compared and similarities are discussed. DOE

N95-24878*# Virginia Univ. Hospital, Charlottesville, VA. School of Engineering and Applied Science.

NASA-UVa LIGHT AEROSPACE ALLOY AND STRUCTURES TECHNOLOGY PROGRAM SUPPLEMENT: ALUMINUM-BASED MATERIALS FOR HIGH SPEED AIRCRAFT Semiannual Report, 1 Jul. - 31 Dec. 1992

E. A. Starke, Jr., ed. Feb. 1995 383 p

(Grant NAG1-745; RTOP 537-06-20-06)

(NASA-CR-4645; NAS 1.26:4645) Avail: CASI HC A17/MF A03

This report on the NASA-UVa light aerospace alloy and structure technology program supplement: Aluminum-Based Materials for High Speed Aircraft covers the period from July 1, 1992. The objective of the research is to develop aluminum alloys and aluminum matrix composites for the airframe which can efficiently perform in the HSCT environment for periods as long as 60,000 hours (certification for 120,000 hours) and, at the same time, meet the cost and weight requirements for an economically viable aircraft. Current industry baselines focus on flight at Mach 2.4. The research covers four major materials systems: (1) Ingot metallurgy 2XXX, 6XXX, and 8XXX alloys, (2) Powder metallurgy 2XXX alloys, (3) Rapidly solidified, dispersion strengthened Al-Fe-X alloys, and (4) Discontinuously reinforced metal matrix composites. There are ten major tasks in the program which also include evaluation and trade-off studies by Boeing and Douglas aircraft companies. Author

N95-25117 Polish Academy of Sciences, Warsaw (Poland). Dept. of the Strength of Materials.

THE EFFECT OF MULTIDIRECTIONAL CYCLICAL DEFORMATION ON THE EVOLUTION OF THE PLASTICITY SURFACE OF 18G2A STEEL [WPLYW ROZNOKIERUNKOWEJ DEFORMACJI CYKLICZNEJ NA EWOLUCJE POWIERZCHNI PLASTYCZNOSCI STALI 18G2A]

Zbigniew L. Kowalewski, Marek Sliwowski, and Grzegorz Socha Cooperative Publishing House Ltd. 1994 51 p In POLISH

(ISSN 0208-5658)

(IFTR-25/1994) Avail: Issuing Activity (Polish Academy of Sciences, Warsaw, Poland)

This article discusses experiments in a complex stress state conducted for the purpose of determining the effect of different forms of plastic deformation on the plastic properties of low-alloy 18G2A steel. The experiments involved the use of thin-walled tubular specimens in stress states which evenly covered the region of all four quadrants of the stress plane (sigma(sub x), tau(sub xy)). In the initial phase of the study the authors used a method which involved testing a large number of samples to determine the plasticity surface of the material as supplied, which constituted a reference point for comparisons of the changes in the properties of the material caused by intentional deformation. The program for testing materials with initial deformation included samples in which initial deformation was applied in the form of: (1) cyclical loading applied in selected directions in the stress plane (sigma(sub x), tau(sub xy)) and (2) monotonic loading. Deformation values were identical for the two deformation processes. Immediately after the initial deformation phase, the authors conducted tests to determine the plasticity surfaces of materials with a specific deformation history. In this case they used a method of successive piercing of the surface for each tested specimen. The authors indicate that the cyclical loading program they used weakened the material as evidenced by a reduction in the size of the material's plasticity surface after cycling as opposed to its size for the steel as supplied. The degree of weakening of the steel depends on the direction of the cyclical deformation and was greatest in the directions which coincided with the cycling directions. Deformation applied by monotonic tension with the same amplitude as in cyclical deformation resulted in greater weakening than the latter. Author

N95-25379# Los Alamos National Lab., NM.

ION BEAM MIXING OF TITANIUM OVERLAYERS WITH HYDROXYAPAPTITE SUBSTRATES

T. E. Levine, M. Nastasi, T. L. Alford (Arizona State Univ., Tempe, AZ.), C. Suchicital (Arizona State Univ., Tempe, AZ.), S. Russell (Arizona State Univ., Tempe, AZ.), K. Luptak (Arizona State Univ., Tempe, AZ.), V. Pizziconi (Arizona State Univ., Tempe, AZ.), and J. Mayer (Arizona State Univ., Tempe, AZ.) 1995 6 p Presented at the 1994 Fall Meeting of the Materials Research Society (MRS), Boston, MA, 28 Nov. - 2 Dec. 1994

(Contract W-7405-eng-36)

(DE95-005278; LA-UR-94-4364; CONF-941144-39) Avail: CASI HC A02/MF A01

The mixing of titanium overlayers with hydroxyapatite (HA) substrates via ion irradiation has been demonstrated. Analysis via secondary ion mass spectroscopy (SIMS) indicates an interfacial broadening of titanium and calcium of the implanted sample compared to that of the unimplanted sample. Attendant to the observed ion beam mixing of titanium into the HA, the oxygen signal of the titanium overlayer increases as a result of ion irradiation. It is supposed that this change is evident of diffusion through the metal layer and possibly from titania formation at the free surface and perovskite formation at the film/substrate interface. This possibility is consistent with thermodynamic predictions. Additionally, the force required to separate the film from the substrate increased as a result of ion irradiation, validating the continued study of ion beam processing of Ti/HA systems towards the improvement of long term fixation of implant devices. DOE

N95-25388# Oak Ridge National Lab., TN.

OXIDATION OF ION-IMPLANTED NiAl

R. J. Hanrahan, Jr., E. D. Verink, Jr., and S. P. Withrow 1994 7 p Presented at the Materials Week '94, Rosemont, IL, 3-7 Oct. 1994

(Contract DE-AC05-84OR-21400)

(DE95-005899; CONF-941016-3) Avail: CASI HC A02/MF A01

The oxidation of NiAl is complicated by the formation of transient alumina phases which result in convoluted scales which are prone to spallation. We have investigated high-dose implantation of oxygen as a technique for forming a protective oxide layer on the surface of NiAl and thereby bypassing the conditions that lead to transient oxide formation. Single crystal specimens of high purity NiAl were implanted with 1 x 10(exp 18) O-18 ions/sq cm at 160 keV. Implanted specimens were annealed for times ranging from 5 to 60 minutes in a reducing atmosphere. Oxidation experiments were conducted for periods ranging from 1 hour to 42 hours under both cyclic and isothermal conditions. Specimens in the as-implanted, annealed, and oxidized conditions were examined using Auger electron microscopy. Oxygen implantation followed by annealing was found to form an epitaxial oxide layer. This layer is stable for the duration of the oxidation experiments conducted in this study, and was found to result in reduced oxidation and improved resistance to scale spallation. DOE

N95-25390# Oak Ridge National Lab., TN.

PROCESSING AND PROPERTIES OF IRIDIUM ALLOYS FOR SPACE POWER APPLICATIONS

E. K. Ohriner 1994 7 p Presented at the 1994 International Conference on Tungsten and Refractory Metals, McLean, VA, 17-19 Oct. 1994

(Contract DE-AC05-84OR-21400)

(DE95-005902; CONF-9410213-4) Avail: CASI HC A02/MF A01

Iridium alloys are used as fuel cladding in radioisotope thermoelectric generators due to their high-melting point, high- temperature strength, and oxidation and corrosion resistance. Although iridium has a face-centered cubic crystal structure, it undergoes a distinct ductile-to-brittle transition characteristic of many body-centered cubic metals. Improved ductility in the alloys is achieved through material purification and controlled alloy additions at the parts per million (ppm) level. A vacuum arc remelt operation

produces a nearly defect-free casting, which is further processed to sheet products. A change in processing from drop castings of small arc-melted buttons to large arc-remelted ingots has substantially improved product yields. The effects of processing changes on alloy microstructure, sheet textures, oxidation effects, high-strain-rate ductility, and fabrication ability are discussed. DOE

N95-25502 SRI International Corp., Menlo Park, CA.
EVALUATION OF A DIFFUSION/TRAPPING MODEL FOR HYDROGEN INGRESS IN HIGH-STRENGTH ALLOYS Annual Report, 15 Sep. 1993 - 14 Sep. 1994
Bruce G. Pound Nov. 1994 69 p
(Contract N00014-91-C-0263)
(AD-A288447; SRI-PYU-2969) Avail: Issuing Activity (Defense Technical Information Center (DTIC))

The ingress of hydrogen in various high-strength alloys was investigated with a view to characterizing their susceptibility to hydrogen embrittlement (HE). A potentiostatic pulse technique was applied to two precipitation-hardened iron-base alloys (AerMet 100 and alloy A-286), two Cu-containing alloys (Be-Cu and alloy K-500), and a superferritic stainless steel (UNS 544660) in 1 mol/L acetic acid-1 mol/L sodium acetate. The data were analyzed using a diffusion/trapping model to obtain the irreversible trapping constant (k) and hydrogen entry flux for each alloy. Irreversible trapping was negligible in overaged AerMet 100 but pronounced in the aged alloy. The order of the k values for AerMet 100 and two steels (4340 and 1 18Ni) previously studied inversely parallels their threshold stress intensities for stress corrosion cracking. Likewise, the k values of alloy A-286, 18Ni steel, and also alloy 718 from earlier work are consistent with test data for their relative resistance to HE. The results for AerMet 100 and alloy A-286 extend the previously reported correlation between k and HE resistance. Unaged Be-Cu is intrinsically more susceptible to HE than unaged alloy K-500. The type of heat treatment has a marked effect on the trapping behavior of alloy K-500. The intrinsic susceptibility of the annealed and aged alloy is twice that of the direct-aged alloy. The propensity of the 544660 alloy to undergo HE at cathodic protection potentials can be attributed to the absence of an oxide and hence the relatively unrestricted entry of H. DTIC

N95-25529 Michigan State Univ., East Lansing, MI. Dept. of Physics and Astronomy.
STABILITY AND ELASTIC PROPERTIES OF HYDROGEN LOADED Ti(1-x)Al(x) ALLOYS: AN AB INITIO STUDY Annual Report
David Tomanek Dec. 1994 41 p
(Contract N00014-90-J-1396)
(AD-A288903; ORD-57810) Avail: Issuing Activity (Defense Technical Information Center (DTIC))

This study addresses on a microscopic level the mechanical failure of transition metals upon exposure to hydrogen. Using molecular dynamics computer simulations, the dependency of the critical tensile stress on hydrogen concentration and temperature in investigated in relation to the hydrogen embrittlement problem. DTIC

N95-25545* National Aeronautics and Space Administration. Marshall Space Flight Center, Huntsville, AL.
ROTARY ACTUATOR Patent
Myron Brudnicki, inventor (to NASA) (Allied-Signal Corp., Morristown, NJ.) 14 Mar. 1995 6 p Filed 12 Oct. 1993 Supersedes N94-29447 (32 - 8, p 3205)
(NASA-Case-MFS-28581-1; US-Patent-5,396,769;
US-Patent-Appl-SN-134441; US-Patent-Class-60-528;
US-Patent-Class-60-527; Int-Patent-Class-F03G-7/00) Avail: US Patent and Trademark Office

Rotary actuators and other mechanical devices incorporating shape memory alloys are provided herein. Shape memory alloys are a group of metals which when deformed at temperatures below their martensite temperatures, resume the shapes which they had prior to the deformation if they are heated to temperatures above their austensite temperatures. Actuators in which shape memory alloys are employed include bias spring types, in which springs deform the shape memory alloy (SMA), and differential actuators, which use two SMA members mechanically connected in series. Another type uses concentric cylindrical members. One member is in the form of a sleeve surrounding a cylinder, both being constructed of shape memory alloys. Herein two capstans are mounted on a shaft which is supported in a framework. Each capstan is capable of rotating the shaft. Shape memory wire, as two separate lengths of wire, is wrapped around each capstan to form a winding around that capstan. The winding on one capstan is so wrapped that the wire is in a prestretched state. The winding on the other capstan is so wrapped that the wire is in a taut, but not a prestretched, state. Heating one performs work in one direction, thus deforming the other one. When the other SMA is heated the action is reversed. Official Gazette of the U.S. Patent and Trademark Office

N95-25560# Cornell Univ., Ithaca, NY.
THE GEOMETRY OF DISORDER: THEORETICAL INVESTIGATIONS OF QUASICRYSTALS AND FRUSTRATED MAGNETS Annual Report, 1 Mar. 1994 - 28 Feb. 1995
C. L. Henley 1995 3 p
(Contract DE-FG02-89ER-45405)
(DE95-006641; DOE/ER-45405/8) Avail: CASI HC A01/MF A01

This annual report briefly discusses the findings for March 1994 to February 1995 for the theoretical investigations of quasicrystals and frustrated magnets. Random tilings, atomic structure models, and microscopic energies are briefly discussed. DOE

N95-25638 Polish Academy of Sciences, Warsaw (Poland). Department of the Strength of Materials.
A DESCRIPTION OF THE CYCLICAL PROPERTIES OF AN ALUMINUM ALLOY BASED ON COMPLEX STRESS STATE TESTS [CHARAKTERYSTYKA CYKLICZNYCH WLASCIWOSCI STOPU ALUMINIUM NA PODSTAWIE BADAN W ZLOZONYM STANIE NAPREZENIA]
Lech Dietrich, Zbigniew L. Kowalewski, Marek Sliwowski, and Grzegorz Socha 1994 61 p In POLISH
(ISSN 0208-5658)
(IFTR-29/1994) Avail: Issuing Activity (Polish Academy of Sciences, Warsaw, Poland)

The purpose of this study was to experimentally determine the properties of the aluminum alloy known as PA6 subjected to initial cyclical deformation in a complex stress state. These properties are characterized by skeleton curves plotted for different stress states. The tests were conducted using thin-walled tubular specimens in a planar stress state produced by different combinations of axial force and torque. The properties of the material as supplied were estimated in the stress space under consideration on the basis of the cross section of the plasticity surface determined on a large number of samples, each of which was subjected to loading in a different stress state. The experimentally determined forms of initial plasticity surfaces corresponding to different theoretical definitions of plasticization served as a reference point for comparing the changes in the properties of the material induced by intentional cyclical deformation. The skeleton curves plotted for different stress states were used to determine the so-called cyclical plasticity surface which describes the compliance of the material prior to changes in its properties in the plasticity range caused by cyclical loading applied in different directions of the stress space under consideration. The cyclical loading program used, which includes a fixed number of loading cycles in which the amplitude of total deformation is either constant or diminishes gradually in successive cycles, caused the aluminum alloy in question to grow stronger than it was originally. The tests revealed that the strengthening of the material in question, which has a very high initial anisotropy, varies significantly depending on the direction of application of the cyclical loading. Transl. by Schreiber Translations Inc.

N95-25677*# National Aeronautics and Space Administration. Marshall Space Flight Center, Huntsville, AL.
THE CORROSION PROTECTION OF AISI(TM) 1010 STEEL BY ORGANIC AND INORGANIC ZINC-RICH PRIMERS
M. D. Danford and M. J. Mendrek Washington Mar. 1995 18 p
(NASA-TP-3545; M-776; NAS 1.60:3545) Avail: CASI HC A03/MF A01

The behavior of zinc-rich primer-coated AISI 1010 steel in 3.5-percent Na-Cl was investigated using electrochemical techniques. The alternating current (ac) method of electrochemical impedance spectroscopy (EIS), in the frequency range of 0.001 to 40,000 Hz, and the direct current (dc) method of polarization resistance (PR), were used to evaluate the characteristics of an organic, epoxy zinc-rich primer and an inorganic, ethyl silicate zinc-rich primer. A dc electromechanical galvanic corrosion test

was also used to determine the corrosion current of each zinc-rich primer anode coupled to a 1010 steel cathode. Duration of the EIS/PR and galvanic testing was 21 days and 24 h, respectively. The galvanic test results demonstrated a very high current between the steel cathode and both zinc-rich primer anodes (38.8 and 135.2 microns A/sq cm for the organic and inorganic primers, respectively). The results of corrosion rate determinations demonstrated a much higher corrosion rate of the zinc in the inorganic primer than in the organic primer, due primarily to the higher porosity in the former. EIS equivalent circuit parameters confirmed this conclusion. Based on this investigation, the inorganic zinc-rich primer appears to provide superior galvanic protection and is recommended for additional study for application on solid rocket booster steel hardware. Author

N95-25751# Centro Brasileiro de Pesquisas Fisicas, Rio de Janeiro.
COERCIVE FIELD AND DOMAIN WALL PROPERTIES IN (Dy(x)Y(1-x))Fe2 AND (Er(x)Y(1-x))Fe2
K. M. B. Alves, L. C. Sampaio, A. P. Guimaraes, and S. F. daCunha 1993 17 p Submitted for publication
(ISSN 0029-3865)
(DE95-601135; CBPF-NF-020/93) Avail: CASI HC A03/MF A01 (US Sales Only)

Isothermal DC magnetization measurements were performed in (R(x), Y(1-X))Fe2 (with R = Dy and Er), in the range of 0 is less than x which is less than 1, for several temperatures. The observed pronounced decay of the coercive field H(sub c) with temperatures was fitted with an exponential. The coercive field H(sub c) and the propagation field H(sub p) show a maximum value in the range of 30-40% concentration for Dy or Er. At low temperatures, the coercive field H(sub c) decreases exponentially with temperature, near 50% R concentration. These results can be explained by intrinsic domain wall pinning. Time relaxations of the remanent magnetization are measured and attributed to domain wall surface deformations. DOE

N95-25775# Sandia National Labs., Albuquerque, NM.
SYNTHESIS AND PROCESSING OF Al2O3/Al COMPOSITES BY IN SITU REACTION OF ALUMINUM AND MULLITE
W. G. Fahrenholtz (New Mexico Univ., Albuquerque, NM.), K. G. Ewsuk, R. E. Loehman, and A. P. Tomsia (Pask Research and Engineering, Inc., Berkeley, CA.) 1995 11 p Presented at the In-situ Reactions for Synthesis of Composites, Ceramics, and Intermetallics, Las Vegas, NV, 12-16 Feb. 1995
(Contract DE-AC04-94AL-85000)
(DE95-006224; SAND-94-2833C; CONF-950263-1) Avail: CASI HC A03/MF A01

Al2O3/Al composites, were formed by reacting molten aluminum metal with dense mullite ceramic preforms. The composites produced by this reactive metal penetration process (RMP) have a two phase, interpenetrating microstructure in which both the ceramic and the metal are continuous in three dimensions. Scanning electron microscopy (SEM) micrographs of composites produced by RMP show a fine microstructure comprised of interlocked metal and ceramic phases, with a feature size of approximately 2 (mu)m. RMP is a relatively rapid process with metal penetration rates of nearly 5 mm/hour at 1100 C after a short incubation period. An activation energy of 92 kJ/mole was calculated from reaction rate data. Transmission electron microscopy (TEM) micrographs reveal that aluminum metal penetrates along the mullite grain boundaries before reaction with the mullite grains, indicating that diffusion along grain boundaries may be the rate limiting step for the reaction. Thermodynamic information, results of microstructure analyses, and kinetic data indicate that RMP proceeds in 4 stages: (1) Al melting and the formation of a thermodynamically stable metal/ceramic interface; (2) depletion of oxygen from the grain boundaries intersecting the ceramic/metal interface; (3) Al metal penetration into the ceramic preform along grain boundaries; (4) Al reaction with and conversion of individual mullite grains. DOE

N95-25977# International Centre for Theoretical Physics, Trieste (Italy).
THE (LAMBDA)-BAR EXPONENT FOR CONSERVATIVE SYSTEMS
M. Rao Jun. 1994 6 p
(DE95-607661; IC-94/137) Avail: CASI HC A02/MF A01 (US Sales Only)

Assuming the scaling form for the two-time correlation function, it follows that the nontrivial exponent (lambda)-bar is exactly equal to the spatial dimension d for any system with a conserved order parameter, as long as the initial variance of the magnetisation is nonzero. The result holds for conserved vector order parameters and for quenches to any temperature T less than or equal to T(sub c). DOE

N95-25983# International Centre for Theoretical Physics, Trieste (Italy).
STRUCTURAL AND THERMODYNAMIC PROPERTIES OF 3-D TRANSITION METALS: PSEUDOPOTENTIAL THEORY REVISITED
S. M. Osman and S. M. MujiburRahman Jun. 1994 13 p
(DE95-605639; IC-94/149) Avail: CASI HC A03/MF A01 (US Sales Only)

Structural and thermodynamic properties of 3d-transition metals are calculated in terms of the pseudopotential theory. The s-p and d-electrons are treated in a pseudoadiabatic approximation in such a way so that the s-p and d-electron are treated separately under the same footing. The s-p electrons are treated in terms of the conventional second-order pseudopotential theory, while the tightly bound d-electrons are treated in terms of the Wills-Harrison prescription that makes use of the Fridel rectangular electron-density of states (DOS) model. The predictions of the structural phase stability and other relevant thermodynamic properties are found to be consistent with experiments for almost all of the metals. DOE

N95-26007# Pacific Northwest Lab., Richland, WA.
RECENT PROGRESS IN SHEAR PUNCH TESTING
M. L. Hamilton, M. B. Toloczko (California Univ., Santa Barbara, CA.), and G. E. Lucas (California Univ., Santa Barbara, CA.) Sep. 1994 13 p Presented at the International Symposium on Miniaturized Specimens for Testing of Irradiated Materials, Julich, Germany, 22-23 Sep. 1994
(Contract DE-AC06-76RL-01830)
(DE95-005962; PNL-SA-24801; CONF-9409286-1) Avail: CASI HC A03/MF A01

The shear punch test was developed in response to the needs of the materials development community for small-scale mechanical properties tests. Such tests will be of great importance when a fusion neutron simulation device is built, since such a device is expected to have a limited irradiation volume. The shear punch test blanks a circular disk from a fixed sheet metal specimen, specifically a TEM disk. Load-displacement data generated during the test can be related to uniaxial tensile properties such as yield and ultimate strength. Shear punch and tensile tests were performed at room temperature on a number of unirradiated aluminum, copper, vanadium, and stainless steel alloys and on several irradiated aluminum alloys. Recent results discussed here suggest that the relationship between shear punch strength and tensile strength varies with alloy class, although the relationship determined for the unirradiated condition remains valid for the irradiated aluminum alloys. DOE

N95-26014 Los Alamos National Lab., NM.
ATOMISTIC STUDIES OF GRAIN BOUNDARIES IN NiAl
M. Yan, S. P. Chen, and V. Vitek (Pennsylvania Univ., Philadelphia, PA.) 1995 8 p Presented at the 1994 Fall Meeting of the Materials Research Society (MRS), Boston, MA, 28 Nov. - 2 Dec. 1994 Limited Reproducibility: More than 20% of this document may be affected by microfiche quality
(Contract W-7405-eng-36)
(DE95-005208; LA-UR-94-4218; CONF-941144-38) Avail: CASI HC A02

This paper presents the results of atomistic studies of grain boundaries in NiAl B2 alloy. The interatomic forces are described by Finnis-Sinclair type N-body potentials, and are fitted to properties of NiAl. The results show that the structure, energy and cohesive strength of a grain boundary depend strongly on its chemical configurations, and a grain boundary with surplus of Al is the weakest. Energies of antisite defects at the grain boundary (Sigma)5(210) are also calculated, and the results suggest that Al has much larger tendency to segregate at a grain boundary than Ni does. DOE

N95-26057 Naval Surface Warfare Center, Bethesda, MD. Carderock Div.
STATIC RECRYSTALLIZATION BEHAVIOR OF AUSTENITE IN HSLA 100 DURING THERMOMECHANICAL CONTROLLED PROCESSING (TMCP) Research and Development Report
E. M. Focht Nov. 1994 39 p Limited Reproducibility: More than 20%

of this document may be affected by microfiche quality
(AD-A288737; CARDIVNSWC-TR-61-94/28) Avail: Issuing Activity (Defense Technical Information Center (DTIC))

The austenite recrystallization behavior during the hot deformation of HSLA-100 was characterized in order to determine parameters for thermomechanical controlled processing. The steel was reheated to 2000 F (1093 C) and subjected to multiple isothermal deformations at 1800 F (982 C) and 1650 F (900 C) under various levels of deformation and hold times. At 10% deformation per hit, the steel took longer than 20 seconds to recrystallize at 1800 F (982 C) after three hits while at 1650 F (900 C) the steel did not recrystallize during the hold periods. At 20% deformation per hit, the steel began to recrystallize after the first hit after 20 seconds and recrystallized repeatedly after each subsequent hit during all of the hold periods at 1800 F (982 F) while at 1650 F (900 C), recrystallization occurred after three hits and the 20 second hold time. DTIC

N95-26064# Oak Ridge National Lab., TN.
ATOM PROBE FIELD ION MICROSCOPY OF TYPE 308 CRE STAINLESS STEEL WELDS
S. S. Babu, S. A. David, J. M. Vitek, and M. K. Miller 1995 3 p Presented at the 76th American Welding Society Convention, Cleveland, OH, 2-7 Apr. 1995 Sponsored in cooperation with Martin Marietta Energy Systems, Inc.
(Contract DE-AC05-84OR-21400)
(DE94-019161; CONF-950443-2) Avail: CASI HC A01/MF A01

Addition of controlled residual elements (CRE), such as 0.007 wt % B, to type 308 stainless steel welds, improved creep-rupture properties. In this paper, B distribution and microstructure development were studied. The microstructural evolution during high-temperature aging was found to similar to that of commercial SS308 welds. Atom probe analysis showed that B and C segregate to the ferrite-austenite interface. Thermodynamic calculations suggest that the segregation is due to preferential partitioning of B and C to the liquid during solidification. Further work is needed to study B redistribution in aging stages. DOE

N95-26068*# Precision Castparts Corp., Portland, OR.
AMCC CASTING DEVELOPMENT, VOLUME 2 Final Report
29 Mar. 1995 439 p
(Contract NAS8-39027)
(NASA-CR-197720; NAS 1.26:197720) Avail: CASI HC A19/MF A04

PCC successfully cast and performed nondestructive testing, FPI and x-ray, on seventeen AMCC castings. Destructive testing, lab analysis and chemical milling, was performed on eleven of the castings and the remaining six castings were shipped to NASA or Aerojet. Two of the six castings shipped, lots 015 and 016, were fully processed per blueprint requirements. PCC has fully developed the gating and processing parameters of this part and feels the part could be implemented into production, after four more castings have been completed to ensure the repeatability of the process. The AMCC casting has been a technically challenging part due to its size, configuration, and alloy type. The height and weight of the wax pattern assembly necessitated the development of a hollow gating system to ensure structural integrity of the shell throughout the investment process. The complexity in the jacket area of the casting required the development of an innovative casting technology that PCC has termed 'TGC' or thermal gradient control. This method of setting up thermal gradients in the casting during solidification represents a significant process improvement for PCC and has been successfully implemented on other programs. The alloy, JBK75, is a relatively new alloy in the investment casting arena and required our engineering staff to learn the gating, processing, and dimensional characteristics of the material. Author (revised)

N95-26179 Polish Academy of Sciences, Warsaw (Poland). Dept. of the Strength of Materials.
AN EXPERIMENTAL DETERMINATION OF THE PLASTIC ANISOTROPY OF METAL [DOSWIADCZALNE OKRESLENIE ANIZOTROPI PLASTYCZNEJ METALI]
Lech Dietrich 1994 21 p In POLISH
(ISSN 0208-5658)
(IFTR-33/1994) Avail: Issuing Activity (Polish Academy of Sciences, Warsaw, Poland)

The experimental determination of the type of anisotropy and its numerical coefficients depends on the type of semifinished metal products tested and is usually carried out under uni-axial tension applied at different angles relative to a specific axis of the semifinished product. Experiments such as these require the experimenter to fasten the specimen so as to avoid limiting its freedom of deformation when the main axes of anisotropy are not aligned with the axis of the specimen under tension. A good way to identify the anisotropy of metal is to test it in a complex stress state, which allows the experimenter to determine the shape and location of the metal's plasticity surface and thus determine the type and coefficients of plasticity. These tests should be conducted using specimens with the same orientation with regard to the axis of the semifinished product and subjected to a variety of stress states. In the case of semifinished products in rod or tube form, the experimenter should use thin-walled tubular samples subjected to different combinations of axial force, torque, and/or internal pressure. The basic problem of such tests for anisotropic materials is determining their theoretical yield limit and the associated curves of effective stress as a function of effective strains, because these quantities are associated with plasticity conditions. The author proposes a simple iterative procedure whose initial approximation consists of formulas for effective stresses and strains for an isotropic material described by a Huber-Mises condition and which then, for the thus transformed experimental material curves, proceeds to determine the initial approximations of the numerical values of plasticity coefficients in general form. Then the procedure determines successive approximations of the effective stress/strain function, from which new transformations of the experiment data are used to determine successive approximations of the numerical values of the plasticity coefficient. Computations are terminated as soon as the differences between the values of specific coefficients in successive iterations are sufficiently small. The author also presents the methods used to determine yield limits in previous studies in complex stress states for both anisotropic materials in their original condition and materials which were initially isotropic and then acquired anisotropic characteristics by virtue of their initial deformation.
Transl. by Schreiber Translations Inc.

N95-26333 Polish Academy of Sciences, Warsaw (Poland). Dept. of Strength of Materials.
CHANGES IN THE STRENGTH CHARACTERISTICS OF 15HM BOILER STEEL CAUSED BY INITIAL PLASTIC DEFORMATION UNDER CONSTANT AND MONOTONIC LOADS [PARAMETROW WYTRZYMALOSCIOWYCH STALI KOTLOWEJ 15HM POD WPLYWEM WSTEPNEJ DEFORMACJI PLASTYCZNEJ PRZY STALYCH I MONOTONICZNYCH OBCIAZENIACH]
Zbigniew L. Kowalewski 1994 41 p In POLISH
(ISSN 0208-5658)
(IFTR-30/1994) Avail: Issuing Activity (Polish Academy of Sciences, Warsaw, Poland)

In this study the author evaluated the properties of boiler steel known as 15M steel after creep and monotonic loading. The author used thin-walled tubular specimens prepared from finished pipes in a planar stress state produced by different combinations of axial force and torque. The properties of the material as supplied were estimated on the basis of the plasticity surface determined by a method of sequential loading of a single specimen and served as a reference point for comparing the changes in the properties of the material caused by intentional deformation under creep and monotonic loading. The loading program used, which included constant loads and monotonically increasing loads, caused the steel to weaken in the range of plastic deformations under consideration, with the most weakening occurring in directions opposite to the directions of the applied loading. After initial plastic deformation, the material exhibited a marked Bauschinger effect, regardless of the type of process used to induce the initial deformation. Transl. by Schreiber Translation, Inc.

27 NONMETALLIC MATERIALS

Includes physical, chemical, and mechanical properties of plastics, elastomers, lubricants, polymers, textiles, adhesives, and ceramic materials.

For composite materials see *24 Composite Materials.*

N95-24212*# National Aeronautics and Space Administration. Langley Research Center, Hampton, VA.

METHOD FOR MOLDING STRUCTURAL PARTS UTILIZING MODIFIED SILICONE RUBBER Patent Application

Erik S. Weisner, inventor (to NASA) (Weisner, Erik S., Santa Monica, CA.), Robert M. Baucom, inventor (to NASA), and John J. Snoha, inventor (to NASA) 12 Aug. 1994 14 p

(NASA-Case-LAR-15217-1; NAS 1.71:LAR-15217-1; US-Patent-Appl-SN-292621) Avail: CASI HC A03/MF A01

This invention improves upon a method for molding structural parts from preform material. Preform material to be used for the part is provided. A silicone rubber composition containing entrained air voids is prepared. The silicone rubber and preform material assembly is situated within a rigid mold cavity used to shape the preform material to the desired shape. The entire assembly is heated in a standard heating device so that the thermal expansion on the silicone rubber exerts the pressure necessary to force the preform material into contact with the mold container. The introduction of discrete air voids into the silicone rubber allows for accurately controlled pressure application on the preform material at the cure temperature. NASA

N95-24247# Oak Ridge National Lab., TN.

INVESTIGATION OF PROPERTIES AND PERFORMANCE OF CERAMIC COMPOSITE COMPONENTS Final Report

W. A. Curtin, K. L. Reifsnider, L. L. S. Oleksuk, and W. W. Stinchcomb (Virginia Polytechnic Inst., Blacksburg, VA.) 31 Oct. 1994 40 p

(Contract DE-AC05-84OR-21400)

(DE95-004737; ORNL/Sub-87-SA946C/04) Avail: CASI HC A03/MF A01

The purpose of Phase 2 of the Investigation of Properties and Performance of Ceramic Composite Components has been to build on and extend the work completed during Phase 1 to further advance the transition from properties of ceramic composite materials to performance of ceramic composite components used in fossil energy environments. The specific tasks of Phase 2 were: (1) develop and validate reliable and accurate high temperature, biaxial mechanical tests methods for structural ceramic composite components; (2) test and evaluate ceramic composite components, specifically tubes; (3) characterize long-term, mechanical performance of ceramic composite tubes at high temperatures; (4) develop a fundamental understanding of the mechanical degradation and performance limitations of ceramic composite components under service conditions; (5) develop predictive models for damage tolerance and reliability; and (6) relate component performance to microstructure and, thereby, provide feedback to the associated process-development effort, to improve performance. Accomplishments for each task are given. DOE

N95-24285# Lehigh Univ., Bethlehem, PA.

ROBOTIC WELD OVERLAY COATINGS FOR EROSION CONTROL Quarterly Technical Progress Report, Jul. - Sep. 1994

B. F. Levin, J. N. Dupont, and A. R. Marder 26 Oct. 1994 41 p

(Contract DE-FG22-92PC-92542)

(DE95-005187; DOE/PC-92542/T8) Avail: CASI HC A03/MF A01

Research is presently being conducted to develop a criteria for selecting weld overlay coatings for erosion mitigation in Circulated Fluidized Beds. Initially, eleven weld overlay alloys were selected for erosion testing based upon a literature review. All eleven coatings were deposited on 1018 steel substrates using the plasma arc welding process. Ten samples from each coating were prepared for erosion testing. All selected coatings were erosion tested at 400 C and their erosion resistance was evaluated by determining the steady state erosion rate. In addition, the microstructure of each coating was characterized before and after the erosion tests. No correlations were found between room temperature hardness of the weld overlay coatings and their erosion resistance at elevated temperature. It was suggested that weld overlays mechanical properties such as fracture strength, toughness and work hardening rates may contribute to their erosion resistance. During the previous two quarters, the microhardness tests were performed on the eroded samples in order to determine the size of the work hardened zone and the change in the coatings hardness due to erosion. As a result of these measurements it was established that one group of coatings deformed plastically, while another did not. In addition, the measurements of the weld overlays microhardness at 400 C were made. The coatings microhardness at 400 C was plotted versus their volume erosion rates. During the last quarter, erosion tests were performed for Inconel-625, 316L SS, and Iron-Aluminide wrought alloys in order to compare their erosion behavior with similar weld overlays. The results of microhardness profile measurements for all weld overlay coatings were analyzed. The factors that contribute to the erosion resistance of the coatings that deformed plastically are discussed in this progress report. DOE

N95-24300# Helsinki Univ. of Technology, Espoo (Finland).

MEASUREMENTS OF THERMAL CONDUCTIVITY OF DIAMOND THIN FILMS BY THE AC CALORIMETRIC METHOD

J. Kaitila, H. Isotalo, and P. Kuivalainen Sep. 1994 14 p Prepared in cooperation with Valtion Teknillinen Tutkimuskeskus

(ISSN 0355-5712)

(PB95-149746; ISBN-951-22-2185-3) Avail: CASI HC A03/MF A01

High thermal conductivity is one of the most interesting physical properties of diamond, when the potential applications of CVD diamond thin films in microelectronics are considered. In the report the authors describe the construction of a measuring system designed for the determination of the thermal diffusivity in thin films. The method is applied both to free standing films and to thin films deposited on various substrates. Reference measurements for metal thin films with well known thermal conductivities are also performed. The chosen method seems to work well for the free standing diamond and metal films, where as in the case of the thin films on substrates, the technique has to be developed further in order to increase the reliability of the method. NTIS

N95-24344# Westinghouse Savannah River Co., Aiken, SC.

SPEEDUP SIMULATION OF LIQUID WASTE BATCH PROCESSING, REVISION 1

K. L. Shannahan, J. E. Aull, R. A. Dimenna, G. K. Georgeton, M. Y. Gregory, T. Hang, T. E. Pate, P. K. Paul, F. G. Smith, and G. A. Taylor 1994 44 p Presented at ASPENWORLD 1994, Boston, MA, 6-9 Nov. 1994

(Contract DE-AC09-89SR-18035)

(DE95-001240; WSRC-MS-94-0246-Rev-1; CONF-9411135-1-Rev-1) Avail: CASI HC A03/MF A01

The Savannah River Site (SRS) has accumulated radioactive hazardous waste for over 40 years during the time SRS made nuclear materials for the United States Department of Energy (DOE) and its predecessors. This waste is being stored as caustic slurry in a large number of 1 million gallon steel tanks, some of which were initially constructed in the early 1950's. SRS and DOE intend to clean up the site and convert this waste into stable forms which then can be safely stored. The liquid waste will be separated into a partially decontaminated low-level and radioactive high-level waste in one feed preparation operation, In-Tank Precipitation. The low-level waste will be used to make a concrete product called saltstone in the Saltstone Facility, a part of the Defense Waste Processing Facility (DWPF). The concrete will be poured into large vaults, where it will be permanently stored. The high-level waste will be added to glass-formers and waste slurry solids from another feed preparation operation, Extended Sludge Processing. The mixture will then be converted to a stable borosilicate glass by a vitrification process that is the other major part of the DWPF. This glass will be poured into stainless steel canisters and sent to a temporary storage facility prior to delivery to a permanent underground storage site. DOE

N95-24373# Instituto de Pesquisas Energeticas e Nucleares, Sao Paulo (Brazil).

ANTIOXIDANT AND SENSITIZER EFFECT ON THE STABILITY OF NATURAL RUBBER LATEX VULCANIZED BY GAMMA RAYS

V. Canavel 1993 112 p

(DE94-636061; INIS-BR-3395) Avail: CASI HC A06/MF A02 (US Sales Only)

The natural rubber latex was vulcanized by gamma rays and electron

beams, in the presence and absence of sensitizers at room temperature. The sensitizers were the following: (1) n-butyl acrylate (n-BA)/t-butyl hydroperoxide (t-B H)/KOH; (2) CCl4/potassium laurate; and (3) n-BA/KOH. The antioxidants studied, Irganox 1520, Vulcanox SP and Vulcanox BKF, were added to the latex after irradiation. Among the antioxidants studied for tensile strength (TS) after the aging of rubber plates, Irganox was the most efficient during gamma vulcanization in the presence of n-BA/t-B H/KOH, was only 0.20 p hr was enough to obtain the greatest increase of TS, 34%, about 12 MPa to 16 MPa. The formulation method of latex with a sensitizer which established the results of 3.0 p hr of n-BA, 0.1 p hr of t-B H and 0.2 p hr of KOH, was evaluated in respect to the TS of the rubber plates. Electron beam vulcanization, which produces the greatest reversible perturbance in the colloidal stability of latex after irradiation, was caused by a radiolytic species absorption that promotes the increase of particle size. The antioxidant also contributes to reversible destabilization of the gamma irradiated latex, because it's adsorbed by surface particles. The relationship between the latex viscosity and the TS of the respective rubber plates is reversible, showing that latex stability affects the quality of rubber goods. DOE

N95-24456# Los Alamos National Lab., NM.
CHARACTERIZATION AND PERFORMANCE OF CARBON FILMS DEPOSITED BY PLASMA AND ION BEAM BASED TECHNIQUES
K. C. Walter, H. Kung, and T. Levine 1994 7 p Presented at the 1994 Fall Meeting of the Materials Research Society (MRS), Boston, MA, 28 Nov. - 2 Dec. 1994
(Contract W-7405-eng-36)
(DE95-005213; LA-UR-94-4179; CONF-941144-54) Avail: CASI HC A02/MF A01

Plasma and ion beam based techniques have been used to deposit carbon-based films. The ion beam based method, a cathodic arc process, used a magnetically mass analyzed beam and is inherently a line-of-sight process. Two hydrocarbon plasma-based, non-line-of-sight techniques were also used and have the advantage of being capable of coating complicated geometries. The self-bias technique can produce hard carbon films, but is dependent on rf power and the surface area of the target. The pulsed-bias technique can also produce hard carbon films but has the additional advantage of being independent of rf power and target surface area. Tribological results indicated the coefficient of friction is nearly the same for carbon films from each deposition process, but the wear rate of the cathodic arc film was five times less than for the self-bias or pulsed-bias films. Although the cathodic arc film was the hardest, contained the highest fraction of sp(sup 3) bonds and exhibited the lowest wear rate, the cathodic arc film also produced the highest wear on the 440C stainless steel counterface during tribological testing. Thus, for tribological applications requiring low wear rates for both counterfaces, coating one surface with a very hard, wear resistant film may detrimentally affect the tribological behavior of the counterface. DOE

N95-24554# Montana State Univ., Bozeman, MT. Dept. of Physics.
NMR AND OPTICAL STUDIES OF PIEZOELECTRIC POLYMERS Final Performance Report, 1 Apr. 1993 - 31 Mar. 1994
V. Hugo Schmidt and George F. Tuthill 1995 13 p
(Contract DE-FG06-87ER-45292)
(DE95-003836; DOE/ER-45292/15) Avail: CASI HC A03/MF A01

The piezoelectric liquid crystal mixtures ZLI-2861, E7, and the copolymers of vinylidene fluoride are investigated with a variety of instrumental techniques including optical studies, nuclear magnetic resonance, and neutron scattering/diffraction. A unique AC thermal diffusivity apparatus was built to determine the specific heat and thermal conductivity of the liquid crystals. Included is an elastic and surface hypothesis for droplets of the liquid crystals. Statistical mechanics, such as the Monte Carlo method, determined that the electrically active polymers showed no percolation transition and that electrical forces play a dominant role in determining chain conformations. A molecular dynamics simulation of PVF(sub 2) studied vibration spectrum, relaxation, and response to a switching field. DOE

N95-24562*# Alabama Univ., Huntsville, AL. Dept. of Biological Sciences.
FNAS PHASE PARTITIONS Final Progress Report
James M. VanAlstine 28 Aug. 1993 23 p
(Contract NAS8-36955)
(NASA-CR-193855; NAS 1.26:193855) Avail: CASI HC A03/MF A01

Project NAS8-36955 D.O. #100 initially involved the following tasks: (1) evaluation of various coatings' ability to control wall wetting and surface zeta potential expression; (2) testing various methods to mix and control the demixing of phase systems; and (3) videomicroscopic investigation of cell partition. Three complementary areas were identified for modification and extension of the original contract. They were: (1) identification of new supports for column cell partition; (2) electrokinetic detection of protein adsorption; and (3) emulsion studies related to bioseparations.
Derived from text

N95-24588# Oak Ridge National Lab., TN. Metals and Ceramics Div.
ACTIVITIES OF THE CERAMIC TECHNOLOGY PROJECT Semiannual Progress Report, Oct. 1993 - Mar. 1994
D. R. Johnson Sep. 1994 456 p
(Contract DE-AC05-84OR-21400)
(DE95-003394; ORNL/TM-12778) Avail: CASI HC A20/MF A04

The Ceramic Technology Project was originally developed by the Department of Energy's Office of Transportation Systems (OTS) in Conservation and Renewable Energy. Significant accomplishments in fabricating ceramic components for the Department of Energy (DOE), National Aeronautics and Space Administration (NASA), and Department of Defense (DOD) advanced heat engine programs have provided evidence that the operation of ceramic parts in high-temperature engine environments is feasible. An assessment of needs was completed, and a five-year project plan was developed with extensive input from private industry. In July 1990, the original plan was updated through the estimated completion of development in 1993. The original objective of the project was to develop the industrial technology base required for reliable ceramics for application in advanced automotive heat engines. During the course of the Ceramic Technology Project, remarkable progress has been made in the development of reliable structural ceramics. The direction of the Ceramic Technology Project is now shifting toward reducing the cost of ceramics to facilitate commercial introduction of ceramic components for near-term engine applications. In response to extensive input from industry, the plan is to extend the engine types which were previously supported (advanced gas turbine and low-heat-rejection diesel engines) to include near-term (5-10 years) applications in conventional automobile and diesel truck engines. To facilitate the rapid transfer of this technology to U.S. industry, the major portion of the work is being done in the ceramic industry, with technological support from government laboratories, other industrial laboratories, and universities. A systematic approach to reducing the cost of components is envisioned. DOE

N95-24717# Sandia National Labs., Albuquerque, NM.
FEASIBILITY OF CERAMIC JOINING WITH HIGH ENERGY ELECTRON BEAMS
B. N. Turman, S. J. Glass, J. A. Halbleib, D. R. Helmich, R. E. Loehman, and J. R. Clifford (Titan Technologies, Albuquerque, NM.) 1995 4 p Presented at the 19th Annual Conference on Advanced Ceramics, Materials and Structures, Cocoa Beach, FL, 8 Jan. 1995
(Contract DE-AC04-94AL-85000)
(DE95-004519; SAND-94-2056C; CONF-950129-1) Avail: CASI HC A01/MF A01

Joining structural ceramics is possible using high melting point metals such as Mo and Pt that are heated with a high energy electron beam, with the potential for producing joints with high temperature capability. A 10 MeV electron beam can penetrate through 1 cm of ceramic, offering the possibility of buried interface joining. Because of transient heating and the lower heat capacity of the metal relative to the ceramic, a pulsed high power beam has the potential for melting the metal without decomposing or melting the adjacent ceramic. The authors have demonstrated the feasibility of the process with a series of 10 MeV, 1 kW electron beam experiments. Shear strengths up to 28 NTa have been measured for Si3N4-Mo-Si3N4. These modest strengths are due to beam non-uniformity and the limited area of bonding. The bonding mechanism appears to be a thin silicide reaction layer. Si3N4-Si3N4 joints with no metal layer were also produced, apparently bonded an yttrium apatite grain boundary phase. DOE

N95-25237# Los Alamos National Lab., NM.
EVOLUTION OF PLASTIC ANISOTROPY FOR HIGH-STRAIN-RATE COMPUTATIONS
Sheila K. Schiferl and Paul J. Maudlin Dec. 1994 43 p
(Contract W-7405-eng-36)
(DE95-004220; LA-12858-MS) Avail: CASI HC A03/MF A01

A model for anisotropic material strength, and for changes in the anisotropy due to plastic strain, is described. This model has been developed for use in high-rate, explicit, Lagrangian multidimensional continuum-mechanics codes. The model handles anisotropies in single-phase materials, in particular the anisotropies due to crystallographic texture--preferred orientations of the single-crystal grains. Textural anisotropies, and the changes in these anisotropies, depend overwhelmingly on the crystal structure of the material and on the deformation history. The changes, particularly for a complex deformations, are not amenable to simple analytical forms. To handle this problem, the material model described here includes a texture code, or micromechanical calculation, coupled to a continuum code. The texture code updates grain orientations as a function of tensor plastic strain, and calculates the yield strength in different directions. A yield function is fitted to these yield points. For each computational cell in the continuum simulation, the texture code tracks a particular set of grain orientations. The orientations will change due to the tensor strain history, and the yield function will change accordingly. Hence, the continuum code supplies a tensor strain to the texture code, and the texture code supplies an updated yield function to the continuum code. Since significant texture changes require relatively large strains--typically, a few percent or more--the texture code is not called very often, and the increase in computer time is not excessive. The model was implemented, using a finite-element continuum code and a texture code specialized for hexagonal-close-packed crystal structures. The results for several uniaxial stress problems and an explosive-forming problem are shown. DOE

N95-25243# Air-Conditioning and Refrigeration Technology Inst., Inc., Arlington, VA.
MATERIALS COMPATIBILITY AND LUBRICANTS RESEARCH (MCLR) PROGRAM
S. R. Szymurski Dec. 1994 8 p Presented at the 1994 International Symposium on R-22 and R-502 Alternative Refrigerants, Kobe, Japan, 8-9 Dec. 1994
(Contract DE-FG02-91CE-23810)
(DE95-004862; DOE/CE-23810/49; CONF-941250-1) Avail: CASI HC A02/MF A01

Objective is to accelerate phaseout of CFC refrigerants. Since its start in 1991, the MCLR program has initiated twenty-five research projects and the ARTI Refrigerant Database. The MCLR program is now entering its final phase. This phase will include over a dozen new research projects which will be completed in the next two years. This presentation highlights accomplishments of the MCLR program and outlines new projects to be conducted in the final phase. DOE

N95-25342 National Inst. of Standards and Technology, Gaithersburg, MD. Building and Fire Research Lab.
INVESTIGATION INTO THE FLAMMABILITY PROPERTIES OF HONEYCOMB COMPOSITES
Marc R. Nyden and James E. Brown Oct. 1994 23 p Limited Reproducibility: More than 20% of this document may be affected by microfiche quality
(PB95-143293; NISTIR-5509) Avail: Issuing Activity (National Technical Information Service (NTIS))

The study was carried out in two stages. The objective of the first phase was to investigate the effect of electron beam irradiation and grafting on polymer flammability. The time to ignition and the rate-of-heat-release were measured for the combustion of a series of samples in which a fire resistant polymer was used to protect the surface of a more flammable polymer. The flammability properties of honeycomb composite materials, which are currently used in the interior cabin compartments of commercial aircraft, were examined in the second phase of this project. Analyses of the gases evolved during the thermal degradation of the components indicated that the phenol-formaldehyde resin makes a significant contribution to the flammability of these composites. The possibility that a more fire resistant formulation could be developed was examined by testing a series of resins which differed in the relative amounts of phenol and formaldehyde used in the reaction mixtures. The flammabilities of resins synthesized in excess phenol was measurably less than those synthesized in excess formaldehyde. NTIS

N95-25370# Sandia National Labs., Albuquerque, NM.
EFFECTS OF ACETYLACETONE ADDITIONS ON PZT THIN FILM PROCESSING
R. W. Schwartz, R. A. Assink, D. Dimos, M. B. Sinclair, T. J. Boyle, and C. D. Buchheit 1995 11 p Presented at the 1994 Fall Meeting of the Materials Research Society (MRS), Boston, MA, 28 Nov. - 2 Dec. 1994
(Contract DE-AC04-94AL-85000)
(DE95-006322; SAND-95-0091C; CONF-941144-35) Avail: CASI HC A03/MF A01

Sol-gel processing methods are frequently used for the fabrication of lead zirconate titanate (PZT) thin films for many electronic applications. Our standard approach for film fabrication utilizes lead acetate and acetic acid modified metal alkoxides of zirconium and titanium in the preparation of our precursor solutions. This report highlights some of our recent results on the effects of the addition of a second chelating ligand, acetylacetone, to this process. The authors discuss the changes in film drying behavior, densification, and ceramic microstructure which accompany acetylacetone additions to the precursor solution and relate the observed variations in processing behavior to differences in chemical precursor structure induced by the acetylacetone ligand. Improvements in thin film microstructure, ferroelectric properties, and optical properties are observed when acetylacetone is added to the precursor solution. DOE

N95-25382# Sandia National Labs., Albuquerque, NM.
RECIPROCAL SPACE ANALYSIS OF THE MICROSTRUCTURE OF LUMINESCENT AND NONLUMINESCENT POROUS SILICON FILMS
S. R. Lee, J. C. Barbour, J. W. Medernach, J. O. Stevenson, and J. S. Custer 1994 6 p Presented at the 1994 Fall Meeting of the Materials Research Society (MRS), Boston, MA, 28 Nov. - 2 Dec. 1994
(Contract DE-AC04-94AL-85000)
(DE95-005420; SAND-94-1736C; CONF-941144-42) Avail: CASI HC A02/MF A01

The microstructure of anodically prepared porous silicon films was determined using a novel X-ray diffraction technique. This technique uses double-crystal diffractometry combined with position-sensitive X-ray detection to efficiently and quantitatively image the reciprocal space structure of crystalline materials. Reciprocal space analysis of newly prepared, as well as aged, p(-) porous silicon films showed that these films exhibit a very broad range of crystallinity. This material appears to range in structure from a strained, single-crystal, sponge-like material exhibiting long-range coherency to isolated, dilated nanocrystals embedded in an amorphous matrix. Reciprocal space analysis of n(+) and p(+) porous silicon showed these materials are strained single-crystals with a spatially-correlated array of vertical pores. The vertical pores in these crystals may be surrounded by nanoporous or nanocrystalline domains as small as a few nm in size which produce diffuse diffraction indicating their presence. The photoluminescence of these films was examined using 488 nm Ar laser excitation in order to search for possible correlations between photoluminescent intensity and crystalline microstructure. DOE

N95-25386# Los Alamos National Lab., NM.
THERMOCHEMISTRY, KINETICS AND SPECTROSCOPY OF Kr AND Kr2F
D. W. Setser 1995 6 p
(Contract W-7405-eng-36)
(DE95-005732; LA-SUB-94-136) Avail: CASI HC A02/MF A01

The subcontract from Los Alamos National Laboratory to Kansas State University has been completed and this is the final report. The progress under this contract is described in three sections: (1) electronic quenching kinetics of KrF(B,C) and Kr2F(4(exp 2)Gamma) molecules; (2) photochemical excitation of van der Waals molecules containing Xe and Kr; and (3) cumulative listing of papers published with support of this contract. DOE

N95-25387# Oak Ridge National Lab., TN.
PROCESSING AND CHARACTERIZATION OF TRANSFORMATION-TOUGHENED CERAMICS WITH STRENGTH RETENTION TO ELEVATED TEMPERATURES Final Report
R. A. Cutler (Ceramatec, Inc., Salt Lake City, UT.), C. B. Brinkpeter

(Ceramatec, Inc., Salt Lake City, UT.), A. V. Vircar (Utah Univ., Salt Lake City, UT.), and D. K. Shetty (Utah Univ., Salt Lake City, UT.) Sep. 1994 72 p

(Contract DE-AC05-84OR-21400)

(DE95-005758; ORNL/Sub-85-22028/2) Avail: CASI HC A04/MF A01

Monolithic and three-layered Al2O3 -- 15 vol % ZrO2 composites were fabricated by slip casting aqueous slurries. The outer and inner layers of three-layer composites contained unstabilized and partially stabilized ZrO2, respectively. Transformation of part of the unstabilized ZrO2 led to surface compressive stresses in the outer layers. Strain gage, x-ray, indentation crack length, and strength measurements were used to determine the magnitude of residual stresses in the composites. The strength of the three-layer composites (approximately 1200 MPa) was 500-700 MPa higher than that of the monolithic outer layer composites at room temperature and 350 MPa higher at 750 C. The strength differential decreased rapidly above the m yields t transformation temperature. Three-layered composites showed excellent damage resistance and improved reliability. Cam follower rollers were fabricated to demonstrate the applicability of this technique for making automotive components. DOE

N95-25510 Army Tank-Automotive Systems Development Center, Warren, MI.

INFORMATION COMPENDIUM ON SOLID FILM LUBRICANTS Final Report, 1 Oct. 1992 - 31 Dec. 1993

Tonie S. Seide and Ellen M. Purdy Nov. 1994 24 p Limited Reproducibility: More than 20% of this document may be affected by microfiche quality

(AD-A288360; TARDEC-TR-13609) Avail: Issuing Activity (Defense Technical Information Center (DTIC))

This report has been prepared to aid in the investigation and development of environmentally compliant solid lubricants for future U.S. Army ground materiel lubricant needs. This paper covers the fundamentals of solid film lubricants and provides insight for basic research efforts being conducted. Topics discussed include the purpose, uses, formulation, application, and other factors which can influence the success or failure of thin film coatings applied to U.S. Army ground vehicle equipment. DTIC

N95-25633 Helsinki Univ. of Technology, Espoo (Finland). Electron Physics Lab.

POTENTIAL OF DIAMOND FOR APPLICATIONS IN MICROELECTRONICS

K. Grahn, S. Eraenen, P. Kuivalainen, I. Suni, and J. Kaitila 1993 59 p Prepared in cooperation with Valtion Teknillinen Tutkimuskeskus Limited Reproducibility: More than 20% of this document may be affected by microfiche quality

(PB95-141446; ISBN-951-22-1921-2) Avail: CASI HC A04

Diamond provides the highest figures of merit for any semiconductor materials for use in high power, high speed and high temperature device applications. However, fabrication of diamond devices is difficult and the devices made so far have shown rather poor performance. In the report the authors present a comprehensive review of the potential of diamond materials for various applications in microelectronics. Especially, by using a 2D-semiconductor device simulator the authors try to get a realistic view of the performance limits of diamond power devices, which could be fabricated by using the existing diamond and semiconductor technologies. The authors show that there are many unexpected difficulties in the design of optimum diamond power devices. The authors also present a summary of the diamond devices, which already have been fabricated in various laboratories. A conclusion drawn from these experimental and theoretical results and considerations is that simple figures of merit estimations give too optimistic a picture of the advantages in diamond power devices. Commercial level diamond devices seem to be available only far in the future. Instead of using diamond as an active material in semiconductor devices, a more straightforward application in microelectronics can be found in using diamond as a heat sink in the packaging technique of devices. Therefore the authors also review the progress obtained so far in these passive applications of diamond films. NTIS

N95-25760# National Aerospace Lab., Tokyo (Japan). Space Technology Research Group.

IMPROVED LUBRICATION PERFORMANCE OF SPUTTERED MoS2 FILM BY SURFACE TREATMENTS OF Ti-ALLOY SUBSTRATE

Makoto Nishimura (Hosei Univ., Tokyo, Japan.), Katsuhiro Kishi (Nissan Motor Co. Ltd., Tokyo, Japan.), Mineo Suzuki, Toshihiko Aikawa (Nissan Motor Co. Ltd., Tokyo, Japan.), and Masashi Arita (Nissan Motor Co. Ltd., Tokyo, Japan.) Oct. 1993 26 p In JAPANESE

(ISSN 0389-4010)

(NAL-TR-1213) Avail: CASI HC A03/MF A01

A molybdenum disulfide (MoS2) solid film lubricant and a stainless steel substrate are the most common combinations used in lubrication systems for aerospace applications. The use of a titanium (Ti) alloy as the substrate is very effective in reducing the weight of mechanical systems; however, it has not been applied for fear that it shortens the wear life of the solid lubricant film as compared with a stainless steel substrate. The aim of this work was to examine whether surface treatments applied to a Ti-alloy substrate are effective in improving the wear life of solid lubricant films, in particular, sputtered Mos2 film. Seventeen kinds of surface treatments were applied to a Ti-6Al-4V alloy substrate, and the lubrication performance and wear life of sputter-deposited MoS2 film on the substrate were evaluated. Tribological performance was investigated by conducting pin/disk sliding tests in a vacuum condition (10(exp -5)Pa). The test results indicated that the wear life of the MoS2 film was noticeably improved by applying some types of surface treatment to the Ti-alloy substrate. The MoS2 film deposited on the cyanate-bath-treated Ti-alloy substrate showed a 300-fold improvement in wear life compared with the film on an untreated substrate. This improvement is presumably caused by the increased affinity between the MoS2 film and Ti2O, which was formed on the substrate by the surface treatment. Author

N95-25898# Sandia National Labs., Albuquerque, NM.

NON-DESTRUCTIVE CHARACTERIZATION OF POROUS SILICON USING X RAY REFLECTIVITY

E. Chason, T. R. Guilinger, M. J. Kelly, T. J. Headley, and A. J. Howard 1995 7 p Presented at the 1994 Fall Meeting of the Materials Research Society (MRS), Boston, MA, 28 Nov. - 2 Dec. 1994

(Contract DE-AC04-94AL-85000)

(DE95-004766; SAND-94-1653C; CONF-941144-24) Avail: CASI HC A02/MF A01

Understanding the evolution of porous silicon (PS) layers at the early stages of growth is important for determining the mechanism of PS film growth and controlling the film properties. We have used X-ray reflectivity (XRR) to determine the evolution of layer thickness and interfacial roughness during the growth of thin PS layers (less than 200 mn) prepared by electrochemical anodization. The porous layer grows at a constant rate for films as thin as 15 mn indicating a very short incubation period during which the surface may be electropolished before the PS structure begins to form. Interface roughness measurements indicate that the top surface of the film remains relatively smooth during growth while the roughness of the PS/silicon interface increases only slightly with film thickness. The XRR results are compared with results obtained from the same films by cross-sectional transmission electron microscopy (XTEM), atomic force microscopy (AFM) and gravimetry. DOE

N95-26004# Lockheed Environmental Systems and Technologies Co., Las Vegas, NV.

PARTS WASHING ALTERNATIVES STUDY: UNITED STATES COAST GUARD. PROJECT SUMMARY AND REPORT

Brad Montgomery Jan. 1995 80 p

(Contract EPA-68-C4-0020)

(PB95-166146; EPA/600/R-95/006) Avail: CASI HC A05/MF A01

The report has been written to assist the United States Coast Guard (USCG) industrial managers in determining the most cost effective and environmentally acceptable parts washing alternatives for their specific applications. An evaluation was conducted on four different cleaners from three different USCG facilities. The following parts cleaners were evaluated: Bio seven, Penatone 724, Safety-Kleen 105, and Brulin 815GD. All four cleaners are effective cleaners for the specific applications described in this evaluation. The evaluation included the categories of process description; environmental, safety and health impacts; cost analysis; and the material and emission reduction opportunities. NTIS

N95-26049 Aerospace Corp., El Segundo, CA. Technology Operations.

SPACECRAFT MATERIALS STUDIES ON THE AEROSPACE CORPORATION TRAY ON EOIM-3

W. K. Stuckey, C. S. Hemminger, G. L. Steckel, M. M. Hills, and M. R. Hilton 15 Aug. 1994 28 p Sponsored by the Naval Surface Warfare Center; and the BMDO/WL PMA 1504 Materials and Structures Program Limited Reproducibility: More than 20% of this document may be affected by microfiche quality
(Contract F04701-93-C-0094)
(AD-A288682; TR-94(4935)-1; SMC-TR-94-41) Avail: Issuing Activity (Defense Technical Information Center (DTIC))

A passive tray was flown on the Effects of Oxygen Interaction with Materials experiment on STS-46 (EOIM-3) with 82 samples from The Aerospace Corporation. A variety of advanced materials related to potential uses on future spacecraft were included for evaluation representing optical coatings, lubricants, polymers, composites, carbon-carbon composite protective coatings, graphite protective coatings, thermal-control materials, and some samples of current materials. An overview of the available results from the investigations of these materials is presented. DTIC

N95-26081*# Puerto Rico Univ., Mayaguez. Dept. of Physics.
ENHANCEMENT OF THICKNESS UNIFORMITY OF THIN FILMS GROWN BY PULSED LASER DEPOSITION
Felix E. Fernandez Apr. 1995 8 p Repr. from Journal of Vacuum Science and Technology A, Second Series (Lancaster Press, Inc., Lancaster, PA), v. 13, no. 2, Mar.-Apr. 1995 p 421-427
(Contract NAG5-2188; DAAL03-G-0213; NSF EHR-91-08775)
(NASA-CR-197791; NAS 1.26:197791) Copyright Avail: CASI HC A02/MF A01

A peculiarity of the pulsed laser deposition technique of thin-film growth which limits its applicability is the very rapid drop of resulting film thickness as a function of distance from the deposition axis. This is due to the narrow forward peaking of the emission plume characteristic of the laser ablation process. The plume is usually modeled by a cos(sup n) theta function with n greater, and in some cases, much higher, than 1. Based on this behavior, a method is presented to substantially enhance coverage uniformity in substrate zones of the order of the target-substrate distance h, and to within a specified thickness tolerance. Essentially, target irradiation is caused to form an annular emission source instead of the usual spot. By calculating the resulting thickness profiles, an optimum radius s is found for the annular source, corresponding to a given power in the emission characteristic and a given value of h. The radius of this annulus scales with h. Calculated numerical results for optimal s/h ratios corresponding to a wide range of values for n are provided for the case of +/- 1% tolerance in deviation from the thickness at deposition axis. Manners of producing annular illumination of the target by means of conic optics are presented for the case of a laser beam with radially symmetric profile. The region of uniform coverage at the substrate can be further augmented by extension of the method to multiple concentric annular sources. By using a conic optic of novel design, it is shown also how a single-laser beam can be focused onto a target in the required manner. Applicability of the method would be limited in practice by the available laser power. On the other hand, the effective emitting area can be large, which favors extremely high growth rates, and since growth can occur uniformly over the whole substrate for each laser pulse, single-shot depositions with substantial thicknesses are possible. In addition, the simultaneity of growth over the complete substrate is desirable when monitoring the growth in situ.
Author

N95-26118* National Aeronautics and Space Administration. Langley Research Center, Hampton, VA.
METHOD AND APPARATUS FOR WEAVING CURVED MATERIAL PREFORMS Patent
Gary L. Farley, inventor (to NASA) 7 Mar. 1995 8 p Filed 10 Feb. 1993
(NASA-Case-LAR-14752-1; US-Patent-5,394,906;
US-Patent-Appl-SN-017205; US-Patent-Class-139-192;
US-Patent-Class-139-11; US-Patent-Class-139-384;
US-Patent-Class-139-305; US-Patent-Class-428-175;
Int-Patent-Class-D03D-3/08; Int-Patent-Class-D03D-41/00) Avail: US Patent and Trademark Office

A method and apparatus for fabricating straight or curved planar or three-dimensional (C channel, for example) fabric for fabrication into composite structures is presented. In the first embodiment, the fill yarns are inserted between layers of warp yarns, and a canted or curved reed, depending on the desired orientation of the fill yarns, is used to compact or 'beat-up' the fill yarns. In the second embodiment, the warp yarns of the fabric are curved using a conical or a combination of conical and cylindrical rollers to effect differential fabric take-up of the warp yarns for obtaining a constant radius of curvature of the warp yarns. In a third embodiment, a clamping bar fabric take-up device is used to effect the differential fabric take-up of the warp yarns for obtaining straight warp yarns, curved warp yarns with a constant radius of curvature, curved warp yarns with a non-contant radius of curvature, or some combinations of straight and curved warp yarns. In a fourth embodiment, for forming the flanges of the curved C channel, the warp yarns are alternately inserted through adjacent dent wires of the reed to permit vertical weaving of the flanges.
Author

N95-26119*# National Aeronautics and Space Administration. Lewis Research Center, Cleveland, OH.
THERMAL BARRIER COATING WORKSHOP Abstracts
W. J. Brindley, comp., W. Y. Lee, comp. (Oak Ridge National Lab., TN.), J. G. Goedjen, comp., and S. J. Dapkunas, comp. (National Inst. of Standards and Technology, Gaithersburg, MD.) Mar. 1995 31 p Workshop held in Westlake, OH, 27-29 Mar. 1995; cosponsored by NASA, DOE, and NIST
(RTOP 505-63-52)
(NASA-CP-10170; E-9509; NAS 1.55:10170) Avail: CASI HC A03/MF A01

This document contains the agenda and presentation abstracts for the Thermal Barrier Coating Workshop, sponsored by NASA, DOE, and NIST. The workshop covered thermal barrier coating (TBC) issues related to applications, processing, properties, and modeling. The intent of the workshop was to highlight the state of knowledge on TBC's and to identify critical gaps in knowledge that may hinder TBC use in advanced applications. The workshop goals were achieved through presentations by 22 speakers representing industry, academia, and government as well as through extensive discussion periods. For individual titles, see N95-26120 through N95-26140.

N95-26120*# Pratt and Whitney Aircraft, West Palm Beach, FL.
A DESIGN PERSPECTIVE ON THERMAL BARRIER COATINGS Abstract Only
F. O. Soechting *In* NASA. Lewis Research Center, Thermal Barrier Coating Workshop Mar. 1995 p 3 (For primary document see N95-26119 08-27)
Avail: CASI HC A01/MF A01

This technical paper addresses the challenges for maximizing the benefit of thermal barrier coatings for turbine engine applications. The perspective is from a customer's viewpoint, a turbine airfoil designer, who is continuously challenged to increase the turbine inlet temperature capability for new products while maintaining cooling flow levels or even reducing them. This is a fundamental requirement to achieve increased engine thrust levels. Developing advanced material systems for the turbine flowpath airfoils is one approach to solve this challenge, for example, high temperature nickel based superalloys or thermal barrier coatings to insulate the metal airfoil from the hot flowpath environment. The second approach is to increase the cooling performance of the turbine airfoil, which enables increased flowpath temperatures and reduced cooling flow levels. Thermal barrier coatings have been employed in jet engine applications for almost 30 years. The initial application was on augmenter lines to provide thermal protection during afterburner operation. However, the production use of thermal barrier coating in the turbine section has only occurred in the past 15 years. The application was limited to stationary parts, and only recently incorporated on the rotating turbine blades. This lack of endorsement of thermal barrier coatings resulted from the poor initial durability of these coatings in high heat flux environments. Significant improvements have been made to enhance spallation resistance and erosion resistance which has resulted in increased reliability of these coatings in turbine applications.
Author

N95-26121*# National Aeronautics and Space Administration. Lewis Research Center, Cleveland, OH.
THERMAL BARRIER COATINGS FOR AIRCRAFT ENGINES: HISTORY AND DIRECTIONS Abstract Only

R. A. Miller *In its* Thermal Barrier Coating Workshop Mar. 1995 p 5 (For primary document see N95-26119 08-27)
Avail: CASI HC A01/MF A01

Thin thermal barrier coatings for protecting aircraft turbine section airfoils are examined. The discussion focuses on those advances that led first to their use for component life extension and more recently as an integral part of airfoil design. It is noted that development has been driven by laboratory rig and furnace testing corroborated by engine testing and engine field experience. The technology has also been supported by performance modeling to demonstrate benefits and life modeling for mission analysis. Factors which have led to the selection of the current state-of-the-art plasma sprayed and physical vapor deposited zirconia-yttria/MCrAlY TBC's is emphasized in addition to observations fundamentally related to their behavior. Current directions in research into thermal barrier coatings and recent progress at NASA is also noted. Author

N95-26122*# Department of Energy, Washington, DC. Office of Industrial Technologies.
THERMAL BARRIER COATINGS ISSUES IN ADVANCED LAND-BASED GAS TURBINES Abstract Only
W. P. Parks, W. Y. Lee (Oak Ridge National Lab., TN.), and I. G. Wright (Oak Ridge National Lab., TN.) *In* NASA. Lewis Research Center, Thermal Barrier Coating Workshop Mar. 1995 p 7 (For primary document see N95-26119 08-27)
Avail: CASI HC A01/MF A01

The Department of Energy's Advanced Turbine System (ATS) program is aimed at forecasting the development of a new generation of land-based gas turbine systems with overall efficiencies significantly beyond those of current state-of-the-art machines, as well as greatly increased times between inspection and refurbishment, improved environmental impact, and decreased cost. The proposed duty cycle of ATS turbines will require the use of different criteria in the design of the materials for the critical hot gas path components. In particular, thermal barrier coatings will be an essential feature of the hot gas path components in these machines. While such coatings are routinely used in high-performance aircraft engines and are becoming established in land-based turbines, the requirements of the ATS turbine application are sufficiently different that significant improvements in thermal barrier coating technology will be necessary. In particular, it appears that thermal barrier coatings will have to function on all airfoil sections of the first stage vanes and blades to provide the significant temperature reduction required. In contrast, such coatings applied to the blades and vances of advanced aircraft engines are intended primarily to reduce air cooling requirements and extend component lifetime; failure of those coatings can be tolerated without jeopardizing mechanical or corrosion performance. A major difference is that in ATS turbines these components will be totally reliant on thermal barrier coatings which will, therefore, need to be highly reliable even over the leading edges of first stage blades. Obviously, the ATS program provides a very challenging opportunity for TBC's, and involves some significant opportunities to extend this technology. Author

N95-26123*# National Inst. of Standards and Technology, Gaithersburg, MD.
MEASUREMENT METHODS AND STANDARDS FOR PROCESSING AND APPLICATION OF THERMAL BARRIER COATINGS Abstract Only
S. J. Dapkunas *In* NASA. Lewis Research Center, Thermal Barrier Coating Workshop Mar. 1995 p 9 (For primary document see N95-26119 08-27)
Avail: CASI HC A01/MF A01

Application of thermal barrier coatings deposited by thermal spray, physical vapor and possibly other methods is expected to be extended from aircraft gas turbines to industrial and utility gas turbines as well as diesel engines. This increased usage implies the participation of greater numbers of processors and users, making the availability of standards for process control and property measurement more important. Available standards for processing and evaluation of thermal barrier coatings are identified as well as those needed in the future but currently unavailable. Author

N95-26124*# Department of Energy, Washington, DC. Office of Transportation Technologies.
THERMAL BARRIER COATINGS APPLICATION IN DIESEL ENGINES Abstract Only
J. W. Fairbanks *In* NASA. Lewis Research Center, Thermal Barrier Coating Workshop Mar. 1995 p 11 (For primary document see N95-26119 08-27)
Avail: CASI HC A01/MF A01

Commercial use of thermal barrier coatings in diesel engines began in the mid 70's by Dr,. Ingard Kvernes at the Central Institute for Industrial Research in Oslo, Norway. Dr. Kvernes attributed attack on diesel engine valves and piston crowns encountered in marine diesel engines in Norwegian ships as hot-corrosion attributed to a reduced quality of residual fuel. His solution was to coat these components to reduce metal temperature below the threshold of aggressive hot-corrosion and also to provide protection. The Department of Energy has supported thermal barrier coating development for diesel engine applications. In the Clean Diesel - 50 Percent Efficient (CD-50) engine for the year 2000, thermal barrier coatings will be used on piston crowns and possibly other components. The primary purpose of the thermal barrier coatings will be to reduce thermal fatigue as the engine peak cylinder pressure will nearly be doubled. As the coatings result in higher available energy in the exhaust gas, efficiency gains are achieved through use of this energy by turbochargers, turbocompounding or thermoelectric generators. Author

N95-26125*# Pratt and Whitney Aircraft, East Hartford, CT.
THERMAL BARRIER COATING EXPERIENCE IN THE GAS TURBINE ENGINE Abstract Only
S. Bose and J. DeMasi-Marcin *In* NASA. Lewis Research Center, Thermal Barrier Coating Workshop Mar. 1995 p 13 (For primary document see N95-26119 08-27)
Avail: CASI HC A01/MF A01

Thermal Barrier Coatings (TBC), provide thermal insulation and oxidation resistance in an environment consisting of hot combustion gases. TBC's consist of a two layer system. The outer ceramic layer provides good thermal insulation due to the low thermal conductivity of the ceramic coatings used, while the inner metallic bond coat layer provides needed oxidation resistance to the underlying superalloy. Pratt & Whitney has over a decade of experience with several generations of TBC systems on turbine airfoils. This paper will focus on the latest TBC field experience along with a proposed durability model. Author

N95-26126*# General Electric Co., Cincinnati, OH. Aircraft Engines.
PVD TBC EXPERIENCE ON GE AIRCRAFT ENGINES Abstract Only
A. Bartz, A. Mariocchi, and D. J. Wortman *In* NASA. Lewis Research Center, Thermal Barrier Coating Workshop Mar. 1995 p 15 (For primary document see N95-26119 08-27)
Avail: CASI HC A01/MF A01

The higher performance levels of modern gas turbine engines present significant challenges in the reliability of materials in the turbine. The increased engine temperatures required to achieve the higher performance levels reduce the strength of the materials used in the turbine sections of the engine. Various forms of Thermal Barrier Coatings (TBC's) have been used for many years to increase the reliability of gas turbine engine components. Recent experience with the Physical Vapor Deposition (PVD) process using ceramic material has demonstrated success in extending the service life of turbine blades and nozzles. Engine test results of turbine components with a 125 micrometer (0.005 in) PVD TBC have demonstrated component operating temperatures of 56-83 C (100-150 F) lower than uncoated components. Engine testing has also revealed the TBC is susceptible to high angle particle impact damage. Sand particles and other engine debris impact the TBC surface at the leading edge of airfoils and fracture the PVD columns. As the impacting continues the TBC erodes away in local areas. Analysis of the eroded areas has shown a slight increase in temperature over a fully coated area, however, a significant temperature reduction was realized over an airfoil without any TBC. Author

N95-26127*# General Electric Co., Schenectady, NY. Power Generation Engineering.
TBC EXPERIENCE IN LAND BASED GAS TURBINES Abstracct Only
W. A. Nelson and R. M. Orenstein *In* NASA. Lewis Research Center, Thermal Barrier Coating Workshop Mar. 1995 p 17 (For primary document see N95-26119 08-27)
Avail: CASI HC A01/MF A01

Prior and on-going machine evaluations of TBC coatings for power

generation applications are summarized. Rainbow testing of various TBC's on turbine nozzles, shrouds and buckets are described along with one test on combustor liners. GEPG has conducted over 15 machine tests with TBC coated turbine nozzles of various coatings. Rainbow test times generally range between 10,000 to 24,000 hours. TBC performance has been quite good and additional testing, including TBC's on shrouds and buckets is continuing. The results show that TBC's have the capability of surviving in power generation machines for the times required. The earlier rainbow tests which evaluated various top coat compositions resulted in confirmation of the superiority of YSZ and especially the 6-8 YSZ composition. On-going tests are more focused on TBC process and property variations. The prevalent failure modes seen thus far in the various rainbow tests are erosion, foreign object damage and buildup of deposits. Additional post test analysis is required to investigate bond coat oxidation and other time/temperature dependent changes to the system. Author

N95-26128*# Solar Turbines, Inc. San Diego, CA.
PERSPECTIVE ON THERMAL BARRIER COATINGS FOR INDUSTRIAL GAS TURBINE APPLICATIONS Abstract only
Z. Z. Mutasim, L. L. Hsu, and W. D. Brentnall *In* NASA. Lewis Research Center, Thermal Barrier Coating Workshop Mar. 1995 p 19 (For primary document see N95-26119 08-27)
Avail: CASI HC A01/MF A01

Thermal Barrier Coatings (TBC's) have been used in high thrust aircraft engines for many years, and have proved to be very effective in allowing higher turbine inlet temperatures. TBC life requirements for aircraft engines are typically less than those required in industrial gas turbines. The use of TBC's for industrial gas turbines can increase if durability and longer service life can be successfully demonstrated. This paper will describe current and future applications of TBC's in industrial gas turbine engines. Early testing and applications of TBC's will also be reviewed. This paper focuses on the key factors that are expected to influence utilization of TBC's in advanced industrial gas turbine engines. It is anticipated that reliable, durable and high effective coating systems will be produced that will ultimately improve engine efficiency and performance. Author

N95-26129*# Cummins Engine Co., Inc., Columbus, IN.
OVERVIEW OF THERMAL BARRIER COATINGS IN DIESEL ENGINES Abstract Only
T. M. Yonushonis *In* NASA. Lewis Research Center, Thermal Barrier Coating Workshop Mar. 1995 p 21 (For primary document see N95-26119 08-27)
Avail: CASI HC A01/MF A01

An understanding of delamination mechanisms in thermal barrier coatings has been developed for diesel applications through nondestructive evaluation, structural analysis modeling and engine evaluation of various thermal barrier coatings. This knowledge has resulted in improved thermal barrier coatings which survive abusive cyclic fatigue tests in high output diesel engines. Significant efforts are still required to improve the plasma spray processing capability and the economics for complex geometry diesel engine components. Data obtained from advanced diesel engines on the effect of thermal barrier coatings on engine fuel economy and emission has not been encouraging. Although the underlying metal component temperatures have been reduced through the use of thermal barrier coating, engine efficiency and emission trends have not been promising. Author

N95-26130*# State Univ. of New York, Stony Brook, NY.
THERMAL SPRAY PROCESSING Abstract Only
H. Herman and C. C. Berndt *In* NASA. Lewis Research Center, Thermal Barrier Coating Workshop Mar. 1995 p 23 (For primary document see N95-26119 08-27)
Avail: CASI HC A01/MF A01

Thermal spray processing has been used for a number of years to cost-effectively apply TBC's for a wide range of heat engine applications. In particular, bond coats are applied by plasma spray and HVOF techniques and partially-stabilized zirconia top coats are applied by plasma spray methods. Thermal spray involves melting and rapid transport of the molten particles to the substrate, where high-rate solidification and coating build-up occur. It is the very nature of this melt processing that leads to the unique layered microstructure, as well as the apparent imperfections, so readily identified with thermal spray. Modeling the process, process-induced residual stresses, and thermal conductivity will be discussed in light of a new understanding of porosity and its anisotropy. Microcracking can be understood using new approaches, allowing a fuller view of the processing-performance connection. Detailed electron microscopic, novel neutron diffraction and fracture analysis of the deposits can lead to a better understanding of how overall microstructure can be controlled to influence critical properties of the deposited TBC system. Author

N95-26131*# Pratt and Whitney Aircraft, West Palm Beach, FL.
JET ENGINE APPLICATIONS FOR MATERIALS WITH NANOMETER-SCALE DIMENSIONS Abstract Only
J. W. Appleby, Jr. *In* NASA. Lewis Research Center, Thermal Barrier Coating Workshop Mar. 1995 p 27 (For primary document see N95-26119 08-27)
Avail: CASI HC A01/MF A01

The performance of advanced military and commercial gas turbine engines is often linked to advances in materials technology. High performance gas turbine engines being developed require major material advances in strength, toughness, reduced density and improved temperature capability. The emerging technology of nanostructured materials has enormous potential for producing materials with significant improvements in these properties. Extraordinary properties demonstrated in the laboratory include material strengths approaching theoretical limit, ceramics that demonstrate ductility and toughness, and material with ultra-high hardness. Nanostructured materials and coatings have the potential for meeting future gas turbine engine requirements for improved performance, reduced weight and lower fuel consumption. Author

N95-26132*# Pratt and Whitney Aircraft, East Hartford, CT.
PROCESS, PROPERTIES AND ENVIRONMENTAL RESPONSE OF PLASMA SPRAYED THERMAL BARRIER COATINGS Abstract Only
R. C. Novak *In* NASA. Lewis Research Center, Thermal Barrier Coating Workshop Mar. 1995 p 29 (For primary document see N95-26119 08-27)
Avail: CASI HC A01/MF A01

Experimental results are shown which demonstrate that the properties of plasma sprayed fully stabilized zirconia are strongly influenced by the process parameters. Properties of the coatings in the as-sprayed condition are shown to be additionally influenced by environmental exposure. This behavior is dependent on raw material considerations and processing conditions as well as exposure time and temperature. Process control methodology is described which can take into consideration these complex interactions and help to produce thermal barrier coatings in a cost effective way while meeting coating technical requirements. Author

N95-26133*# Oak Ridge National Lab., TN.
THERMAL CONDUCTIVITY OF ZIRCONIA THERMAL BARRIER COATINGS Abstract Only
R. B. Dinwiddie, S. C. Beecher, B. A. Nagaraj (General Electric Co., Cincinnati, OH.), and C. S. Moore (General Electric Co., Cincinnati, OH.) *In* NASA. Lewis Research Center, Thermal Barrier Coating Workshop Mar. 1995 p 31 (For primary document see N95-26119 08-27)
Avail: CASI HC A01/MF A01

Thermal barrier coatings (TBC's) applied to the hot gas components of turbine engines lead to enhanced fuel efficiency and component reliability. Understanding the mechanisms which control the thermal transport behavior of the TBC's is of primary importance. Physical vapor description (PVD) and plasma spraying (PS) are the two most commonly used coating techniques. These techniques produce coatings with unique microstructures which control their performance and stability. The PS coatings were applied with either standard power or hollow sphere particles. The hollow sphere particles yielded a lower density and lower thermal conductivity coating. The thermal conductivity of both fully and partially stabilized zirconia, before and after thermal aging, will be compared. The thermal conductivity of the coatings permanently increase upon being exposed to high temperatures. These increases are attributed to microstructural changes within the coatings. Sintering of the as fabricated plasma sprayed lamellar structure is observed by scanning electron microscopy of coatings isothermally heat treated at temperatures greater than 1100 C. During this sintering process the planar porosity between lamella is converted to a series of small spherical pores. The change in pore morphology is the primary reason for the observed increase in thermal conductivity. This increase in thermal conductivity can be modeled using a relationship which depends on both the temperature

and time of exposure. Although the PVD coatings are less susceptible to thermal aging effects, preliminary results suggest that they have a higher thermal conductivity than PS coatings, both before and after thermal aging. The increases in thermal conductivity due to thermal aging for partially stabilized plasma sprayed zirconia have been found to be less than for fully stabilized plasma sprayed zirconia coatings. The high temperature thermal diffusivity data indicates that if these coatings reach a temperature above 1100 C during operation, they will begin to lose their effectiveness as a thermal barrier. Author

N95-26134*# Vanderbilt Univ., Nashville, TN.
MECHANICAL PROPERTIES TESTING AND RESULTS FOR THERMAL BARRIER COATINGS Abstract Only
T. A. Cruse and B. P. Johnsen *In* NASA. Lewis Research Center, Thermal Barrier Coating Workshop Mar. 1995 p 33 (For primary document see N95-26119 08-27)
Avail: CASI HC A01/MF A01

Thermal Barrier Coatings (TBC's) provide a significant challenge in the evaluation of their mechanical properties in ways that provide data that is not specimen dependent. The paper reviews various developments of the principal author over the past several years for both plasma sprayed and physical vapor deposited (PVD) materials, as well as new data on the fatigue behavior of one material system. The test methods that have been employed address tensile and compressive modulus and ultimate strength, tensile and compressive fatigue strength, and interfacial strength. This testing is now underway. Property testing is especially difficult for TBC's owing to the limitation on fabrication thickness of the coating. Bending tests are not used as these tests do not provide sufficiently uniform states of strain for property evaluations. Test specimens with uniform states of axial stress have been devised for each material system. The results show that the material property results between various experimenters and experimental methods are not yet consistent. However, the results provide critical design data at a suitable level of accuracy for life prediction. The paper will review both tensile and compressive mechanical testing of uniaxial specimens showing property dependencies on material density and temperatures for both material systems. Successful test results for both tensile and compressive fatigue loadings will be given. The test data shows that the fatigue strength of the TBC's is highly stress dependent in both loading conditions and is likely to depend on stress range and not mean stress. The fatigue strength of the plasma sprayed TBC's appears to increase with elevated temperatures in a range of temperatures below the creep activation temperature for the materials. The plasma sprayed TBC materials have been confirmed to have cyclic hysteresis at all temperature levels down to room temperature. Limited failure analysis data for various specimens suggest that the failure modes are driven by normal geometric discontinuities in the TBC's. Author

N95-26135*# National Aeronautics and Space Administration. Lewis Research Center, Cleveland, OH.
PROPERTIES OF PLASMA SPRAYED BOND COATS Abstract Only
W. J. Brindley *In its* Thermal Barrier Coating Workshop Mar. 1995 p 35 (For primary document see N95-26119 08-27)
Avail: CASI HC A01/MF A01

Increasing bond coat oxidation resistance has been clearly linked to increasing durability of the ceramic layer of TBC's. However, recent studies have shown that significant differences in TBC life can be achieved for different bond coats that have little or no difference in oxidation behavior. These results suggest bond coat properties other than oxidation resistance can also influence TBC life. A determination of which properties affect TBC life and an understanding of how these properties affect TBC life could be valuable in designing new, more durable TBC's. Unfortunately, there is little existing information on the physical and mechanical properties of bond coat materials and there are fewer comparative studies that can be used to determine which properties are important to TBC life. This paper compares the properties of three bond coat compositions that have similar oxidation behavior but different TBC lives. Analysis of the properties indicates that the coefficient of thermal expansion and stress relaxation (creep) behavior of the three alloys are strongly correlated to the observed differences in TBC life. Author

N95-26136*# Caterpillar Tractor Co., Peoria, IL.
THICK THERMAL BARRIER COATINGS FOR DIESEL ENGINES Abstract Only
M. B. Beardsley *In* NASA. Lewis Research Center, Thermal Barrier Coating Workshop Mar. 1995 p 37 (For primary document see N95-26119 08-27)
Avail: CASI HC A01/MF A01

Caterpillar's approach to applying Thick Thermal Barrier Coatings (TTBC's) to diesel engine combustion chambers has been to use advanced modeling techniques to predict engine conditions and combine this information with fundamental property evaluation of TTBC systems to predict engine performance and TTBC stress states. Engine testing has been used to verify the predicted performance of the TTBC systems and provide information on failure mechanisms. The objective of Caterpillar's subcontract with ORNL is to advance the fundamental understanding of thick thermal barrier coating systems. Previous reviews of thermal barrier coating technology concluded that the current level of understanding of coating system behavior is inadequate and the lack of fundamental understanding may impede the application of TTBC's to diesel engines. Areas of TTBC technology being examined in this program include powder characteristics and chemistry; bond coat composition; coating design, microstructure, and thickness as they affect properties, durability, and reliability; and TTBC 'aging' effects (microstructural and property changes) under diesel engine operating conditions. Methods to evaluate the reliability and durability of TTBC's have been developed that attempt to understand the fundamental strength of TTBC's for particular stress states. Author

N95-26137*# Naval Research Lab., Washington, DC.
SOME ASPECTS OF THE HOT CORROSION OF THERMAL BARRIER COATINGS Abstract Only
R. L. Jones *In* NASA. Lewis Research Center, Thermal Barrier Coating Workshop Mar. 1995 p 39 (For primary document see N95-26119 08-27)
Avail: CASI HC A01/MF A01

This paper provides a pro tem review of the hot corrosion of zirconia-based thermal barrier coatings for engine applications. Emphasis is placed on trying to understand the chemical reactions, and such other mechanisms as can be identified, that cause corrosive degradation of the thermal barrier coating. The various approaches taken in attempts to improve the hot corrosion resistance of thermal barrier coatings are also briefly described and critiqued. Author

N95-26138*# Purdue Univ., West Lafayette, IN.
THERMAL FRACTURE MECHANISMS IN CERAMIC THERMAL BARRIER COATINGS Abstract Only
K. Kokini, B. D. Choules, and Y. R. Takeuchi *In* NASA. Lewis Research Center, Thermal Barrier Coating Workshop Mar. 1995 p 41 (For primary document see N95-26119 08-27)
Avail: CASI HC A01/MF A01

Ceramic thermal barrier coatings represent an attractive method of increasing the high temperature limits for systems such as diesel engines, gas turbines and aircraft engines. However, the dissimilarities between ceramics and metal, as well as the severe temperature gradients applied in such systems, cause thermal stresses which can lead to cracking and ultimately spalling of the coating. This paper reviews the research which considers initiation of surface cracks, interfacial edge cracks and the effect of a transient thermal load on interface cracks. The results of controlled experiments together with analytical models are presented. The implications of these findings to the differences between diesel engines and gas turbines are discussed. The importance of such work for determining the proper design criteria for thermal barrier coatings is underlined. Author

N95-26139*# Deformation Control Technology, Inc., Cleveland, OH.
A SOFTWARE TOOL TO DESIGN THERMAL BARRIER COATINGS Abstract Only
G. Petrus and B. L. Ferguson *In* NASA. Lewis Research Center, Thermal Barrier Coating Workshop Mar. 1995 p 43 (For primary document see N95-26119 08-27)
Avail: CASI HC A01/MF A01

This paper summarizes work completed for a NASA Phase 1 SBIR program which demonstrated the feasibility of developing a software tool to aid in the design of thermal barrier coating (TBC) systems. Toward this

goal, three tasks were undertaken and completed. Task 1 involved the development of a database containing the pertinent thermal and mechanical property data for the top coat, bond coat and substrate materials that comprise a TBC system. Task 2 involved the development of an automated set-up program for generating two dimensional (2D) finite element models of TBC systems. Most importantly, Task 3 involved the generation of a rule base to aid in the design of a TBC system. These rules were based on a factorial design of experiments involving FEM results, and were generated using a Yates analysis. A previous study has indicated the suitability and benefit of applying finite element analysis to perform computer based experiments to decrease but not eliminate physical experiments on TBC's. This program proved feasibility by expanding on these findings by developing a larger knowledge base and developing a procedure to extract rules to aid in TBC design. Author

N95-26140*# Pratt and Whitney Aircraft, East Hartford, CT.
THERMAL BARRIER COATING LIFE MODELING IN AIRCRAFT GAS TURBINE ENGINES Abstract Only
D. M. Nissley *In* NASA. Lewis Research Center, Thermal Barrier Coating Workshop Mar. 1995 p 45 (For primary document see N95-26119 08-27)
Avail: CASI HC A01/MF A01

Analytical models useful for predicting ceramic thermal barrier coating (TBC) spalling life in aircraft gas turbine engines are presented. Electron beam-physical vapor deposited (EB-PVD) and plasma sprayed TBC systems are discussed. TBC spalling was attributed to a combination of mechanisms such as metal oxidation at the ceramic-metal interface, ceramic-metal interface stress concentrations at free surfaces due to dissimilar materials, ceramic-metal interface stresses caused by local radius of curvature and interface roughness, material properties and mechanical behavior, transient temperature gradients across the ceramic layer and component design features. TBC spalling life analytical models were developed based on observations of TBC failure modes and plausible failure theories. TBC failure was assumed to occur when the imposed stresses exceeded the material strength (at or near the ceramic-metal interface). TBC failure knowledge gaps caused by lack of experimental evidence and analytical understanding are noted. The analytical models are considered initial engineering approaches that capture observed TBC failure trends. Author

N95-26188 Aerospace Corp., El Segundo, CA. Technology Operations.
APPLICATIONS OF SOLID LUBRICANT FILMS IN SPACECRAFT
Michael R. Hilton and Paul D. Fleischauer Los Angeles Air Force Base, CA Space and Missile Systems Center 1 Sep. 1994 22 p Limited Reproducibility: More than 20% of this document may be affected by microfiche quality
(Contract F04701-88-C-0089)
(AD-A288784; TR-92(2935)-6; SMC-TR-94-45) Avail: Issuing Activity (Defense Technical Information Center (DTIC))

The use of solid (dry) lubricants, particularly solid lubricant thin films, in space systems, including satellites and launch vehicles, is reviewed. Various types of satellites and their generic mechanical requirements are outlined. Mechanisms that use solid lubricant films are described. The types of solid lubricant films available, including burnished, bonded, and sputter-deposited, are reviewed and their properties assessed relative to application requirements. Future opportunities for insertion of solid lubricants as replacements for liquid or grease lubricants are identified. DTIC

28 PROPELLANTS AND FUELS

Includes rocket propellants, igniters, and oxidizers; their storage and handling procedures; and aircraft fuels.

For related information see also *07 Aircraft Propulsion and Power, 20 Spacecraft Propulsion and Power,* and *44 Energy Production and Conversion.*

N95-24226*# Thiokol Corp., Huntsville, AL. Huntsville Div.
SPACE SHUTTLE PROPELLANT CONSTITUTIVE LAW VERIFICATION TESTS Final Technical Report, Oct. 1992 - Mar. 1995
James R. Thompson 31 Mar. 1995 37 p
(Contract NAS8-39619)
(NASA-CR-198047; NAS 1.26:198047; U-95-7007) Avail: CASI HC A03/MF A01

As part of the Propellants Task (Task 2.0) on the Solid Propulsion Integrity Program (SPIP), a database of material properties was generated for the Space Shuttle Redesigned Solid Rocket Motor (RSRM) PBAN-based propellant. A parallel effort on the Propellants Task was the generation of an improved constitutive theory for the PBAN propellant suitable for use in a finite element analysis (FEA) of the RSRM. The outcome of an analysis with the improved constitutive theory would be more reliable prediction of structural margins of safety. The work described in this report was performed by Materials Laboratory personnel at Thiokol Corporation/Huntsville Division under NASA contract NAS8-39619, Mod. 3. The report documents the test procedures for the refinement and verification tests for the improved Space Shuttle RSRM propellant material model, and summarizes the resulting test data. TP-H1148 propellant obtained from mix E660411 (manufactured February 1989) which had experienced ambient igloo storage in Huntsville, Alabama since January 1990, was used for these tests. Author

N95-24273# Department of Energy, Washington, DC.
ALTERNATIVES TO TRADITIONAL TRANSPORTATION FUELS 1993
Jan. 1995 90 p
(DE95-005445; DOE/EIA-0585(93)) Avail: CASI HC A05/MF A01

In recent years, gasoline and diesel fuel have accounted for about 80 percent of total transportation fuel and nearly all of the fuel used in onroad vehicles. Growing concerns about the environmental effects of fossil fuel use and the Nation's high level of dependence on foreign oil are providing impetus for the development of replacements or alternatives for these traditional transportation fuels. The Alternative Motor Fuels Act of 1988, the Clean Air Act Amendments of 1990 (CAAA90) and the Energy Policy Act of 1992 (EPACT) are significant legislative forces behind the growth of replacement fuel use. Alternatives to Traditional Transportation Fuels 1993 provides the number of on-road alternative fueled vehicles in use in the United States, alternative and replacement fuel consumption, and information on greenhouse gas emissions resulting from the production, delivery, and use of replacement fuels for 1992, 1993, and 1995. DOE

N95-24394 Defence Science and Technology Organisation, Melbourne (Australia). Explosives Ordance Div.
THE CRITICAL DIAMETER, DETONATION VELOCITY AND SHOCK SENSITIVITY OF AUSTRALIAN PBXW-115
G. Bocksteiner, Mike G. Wolfson, and Dan J. Whelan Oct. 1994 45 p
(DSTO-TR-0076; AR-008-944) Copyright Avail: Issuing Activity (DSTO Aeronautical and Maritime Research Lab., GPO Box 4331, Melbourne, Victoria 3001, Australia)

A study of the detonation performance of the insensitive explosive filling, PBXW-115 (Aust.), has been undertaken and the results compared to those from its American counterpart, PBXW-115 (USA) / PBXN-111, an explosive of the same nominal composition but formulated with biomodal RDX of different type and somewhat differing particle size distribution. The limiting value of the velocity of detonation at infinite diameter, D, of PBXW-115 (Aust.) is in the range 5.64 - 5.91 kms(exp -1), the actual value depending on the assumed relationship between the experimental V of D and the diameter of the charge. This range of values is slightly less than that calculated for PBXW-115 (USA), 5.76 - 6.19 kms(exp -1), using experimental data reported by Forbes et al. The major differences between the results from the two formulations, however, related not to values of D but to critical diameter and to relative shock sensitivity (as measured in the large Scale Gap Test). The critical diameter of unconfined PBXW-115 (Aust.) is ca. 80 mm; that of PBXW-115 (USA) is 38 plus or minus 2 mm; the differences are not as pronounced in charges confined in brass tubes, however - 24 plus or minus 2 mm (3 and 5 mm thick brass tubes) for PBXW-115 (Aust.) vs. 21 plus or minus 2 mm (2.5 mm thick brass tubes) and 17 plus or minus 2 mm (5 mm thick brass tubes) for PBXW-115 (USA). The shock sensitivity of PBXW-115 (Aust.) is 6.3 GPa, the explosive shock wave pressure which has been determined experimentally to result in a 50 percent probability of detonation in the Large Scale Gap Test. The corresponding figure for the US formulation is 4.7 GPa. Reasons for these differences are advanced. Author

N95-24498# Korea Inst. of Energy and Resources, Taejon, Chungchongnam (Republic of Korea).

STUDY ON THE PRODUCTION OF ALTERNATIVE FUELS BY CARBON DIOXIDE HYDROGENATION

K. S. Sim, Y. M. Son, J. W. Kim, Y. S. Kim, K. S. Myong, and J. M. Seo Dec. 1993 89 p

(DE95-744284; KE-93016G) Avail: CASI HC A05/MF A01 (US Sales Only)

The technologies of the separation and recovery of carbon dioxide, the most important greenhouse gas, from exhausted gases of the fuel production from carbon dioxide by catalytic hydrogenation were surveyed. For the catalytic hydrogenation we made the lab-scale reaction apparatus and carried out some basic experiments with several catalysts like CuO/ZnO/Al2O3, Raney nickel and other commercial catalysts. DOE

N95-24558*# National Aeronautics and Space Administration. Marshall Space Flight Center, Huntsville, AL.

SIMPLIFIED LIQUID OXYGEN PROPELLANT CONDITIONING CONCEPTS

N. L. Cleary, K. A. Holt, and R. H. Flachbart Washington Mar. 1995 66 p

(NASA-TM-108482; NAS 1.15:108482) Avail: CASI HC A04/MF A01

Current liquid oxygen feed systems waste propellant and use hardware, unnecessary during flight, to condition the propellant at the engine turbopumps prior to launch. Simplified liquid oxygen propellant conditioning concepts are being sought for future launch vehicles. During a joint program, four alternative propellant conditioning options were studied: (1) passive recirculation; (2) low bleed through the engine; (3) recirculation lines; and (4) helium bubbling. The test configuration for this program was based on a vehicle design which used a main recirculation loop that was insulated on the downcomer and uninsulated on the upcomer. This produces a natural convection recirculation flow. The test article for this program simulated a feedline which ran from the main recirculation loop to the turbopump. The objective was to measure the temperature profile of this test article. Several parameters were varied from the baseline case to determine their effects on the temperature profile. These parameters included: flow configuration, feedline slope, heat flux, main recirculation loop velocity, pressure, bleed rate, helium bubbling, and recirculation lines. The heat flux, bleed rate, and recirculation configurations produced the greatest changes from the baseline temperature profile. However, the temperatures in the feedline remained subcooled. Any of the options studied could be used in future vehicles. Author

N95-24608# Sandia National Labs., Albuquerque, NM.

NONEQUILIBRIUM MULTIPHASE MIXTURE MODELING OF ENERGETIC MATERIAL RESPONSE

M. R. Baer, E. Hertel, and R. Bell 1995 8 p Presented at the Nuclear Explosives Code Developers Conference (NECDC), Las Vegas, NV, 27 Oct. 1994

(Contract DE-AC04-94AL-85000)

(DE95-003353; SAND-94-2639C; CONF-9410254-1) Avail: CASI HC A02/MF A01

To model the shock-induced behavior of porous or damaged energetic materials, a nonequilibrium mixture theory has been developed and incorporated into the shock physics code, CTH. Foundation for this multiphase model is based on a continuum mixture formulation given by Baer and Nunziato. In this nonequilibrium approach, multiple thermodynamic and mechanics fields are resolved including the effects of material relative motion, rate-dependent compaction, drag and heat transfer interphase effects and multiple-step combustion. Benchmark calculations are presented which simulate low-velocity piston impact on a propellant porous bed and experimentally-measured wave features are well replicated with this model. This mixture model introduces micromechanical models for the initiation and growth of reactive multicomponent flow which are key features to describe shock initiation and self-accelerated deflagration-to-detonation combustion behavior. To complement one-dimensional simulation, two dimensional numerical simulations are presented which indicate wave curvature effects due to the loss of wall confinement. DOE

N95-24655# Lehigh Univ., Bethlehem, PA. Dept. of Chemistry

HIGH OCTANE ETHERS FROM SYNTHESIS GAS-DERIVED ALCOHOLS Final Technical Report, 25 Sep. 1990 - 24 Dec. 1993

Kamil Klier and Richard G. Herman May 1994 167 p

(Contract DE-AC22-90PC-90044)

(DE95-001146; DOE/PC-90044/T2) Avail: CASI HC A08/MF A02

The objective of the research was to develop the methodology for the catalytic synthesis of ethers, primarily methyl isobutyl ether (MIBE) and methyl tertiary butyl ether (MTBE), directly from alcohol mixtures that are rich in methanol and 2-methyl-1-propanol (isobutanol). The overall scheme involves gasification of coal, purification and shifting of the synthesis gas, higher alcohol synthesis, and direct synthesis of ethers. The last stage of the synthesis involves direct coupling of synthesis gas-derived methanol and isobutanol that has been previously demonstrated by us to occur over superacid catalysts to yield MIBE and smaller amounts of MTBE at moderate pressures and a mixture of methanol and isobutene at low pressures. A wide range of organic resin catalysts and inorganic oxide and zeolite catalysts have been investigated for activity and selectivity in directly coupling alcohols, principally methanol and isobutanol, to form ethers and in the dehydration of isobutanol to isobutene in the presence of methanol. All of these catalysts are strong acids, and it was found that the organic and inorganic catalysts operate in different, but overlapping, temperature ranges, i.e. mainly 60-120 C for the organic resins and 90-175 C for the inorganic catalysts. For both types of catalysts, the presence of strong acid centers is required for catalytic activity, as was demonstrated by lack of activity of fully K(+) ion exchanged Nafion resin and zirconia prior to being sulfated by treatment with sulfuric acid. DOE

N95-24670# Los Alamos National Lab., NM.

EXPLOSIVE PERFORMANCE MEASUREMENTS ON LARGE, MULTIPLE-HOLE ARRAYS AND LARGE MASSES OF CONVENTIONAL EXPLOSIVE

Thomas O. McKown, Donald D. Eilers (Raytheon Services Nevada, Las Vegas, NV.), and Pharis E. Williams 1994 14 p Presented at the 21st Annual Conference on Explosives and Blasting Techniques and 11th Annual Symposium on Explosives and Blasting Research, Nashville, TN, 5-9 Feb. 1995

(Contract W-7405-eng-36)

(DE95-002718; LA-UR-94-3490; CONF-950247-1) Avail: CASI HC A03/MF A01

The COntinuous Reflectometry for Radius vs. Time EXperiment (CORRTEX) system was developed by the Los Alamos National Laboratory for determining the energy released in a nuclear explosion by measuring the position of its shock front as a function of time. The CORRTEX system, fielding techniques, and the methods and software for data reduction and analysis were developed over a 15 year period with hundreds of measurements made on nuclear tests and high explosive experiments. CORRTEX is a compact, portable, fast-sampling, microprocessor-controlled system, based on time domain reflectometry, requiring only a 24 volt power source and a sensing element. Only the sensing element (a length of 50 ohm coaxial cable) is expended during the detonation. In 1979, the CORRTEX system was shown to be ideally suited for chemical explosive performance measurements. Its utility for diagnosing chemical explosives was further demonstrated with successful measurements on large multiple-hole chemical shots in rock quarries and strip mines. Accurate timing of the detonation of sequenced or ripple fired arrays, as well as data characterizing the initiation, explosive performance and detonation anomalies are obtained. This information can serve as the basis for empirical or modeled improvements to blasting operations. A summary of the special CORRTEX features and well developed analysis techniques together with the experiment designs, data, and conclusions regarding the measurements and explosive performance from several array detonations and the Chemical Kiloton Experiment, 2.9 million pounds of an ammonium nitrate-fuel oil (ANFO) and emulsion blend conducted on the Nevada Test Site in 1993, are presented. DOE

N95-24679# Department of Energy, Washington, DC. Office of Energy Efficiency and Renewable Energy.

FEDERAL ALTERNATIVE MOTOR FUELS PROGRAM: LIGHT DUTY FEDERAL VEHICLES, TRUCKS, AND BUSES Annual Report No. 3, fiscal year 1993

Sep. 1994 124 p

(DE95-003982; DOE/EE-0033) Avail: CASI HC A06/MF A02

This annual report to Congress details the Federal light-duty alternative fuel vehicle operations from October 1992 through September 1993 as

required by Section 400AA(b)(1)(B) of the Energy Policy and Conservation Act, 42 U.S.C. 6374(b)(1)(B). Also included are results of the first year of the Alternative Fuels Truck Commercial Application Program and the Alternative Fuels Bus Program activities required by sections 400BB and 400CC, respectively, of the Energy Policy and Conservation Act (42 U.S.C. 6374a and 6374b). The research that is associated with these projects is coordinated by the US Department of Energy (DOE), Office of Transportation Technologies, through the National Renewable Energy Laboratory (NREL). Significant expansion of the Alternative Motor Fuels Program data collection efforts occurred during fiscal year 1993 with the addition of more alternative fuel vehicles, test sites, and Federal agency involvement. In addition, the heavy-duty and bus projects required by the Energy Policy and Conservation Act have developed to the point where data are available for reporting. The locations of the Federal light-duty, heavy-duty truck, and bus vehicles that are participating in the data collection program are identified. DOE

N95-25244# Kauppa-ja Teollisuusministerio, Helsinki, Uudenmaa (Finland). Energy Dept.

JALO: FUEL CONVERSION Final Report on the Energy Research Program, 1988-1992

Kai Sipilae 1994 112 p

(DE95-737597; KTM/E-B-155) Avail: CASI HC A06/MF A02 (US Sales Only)

The Finnish research program on fuel conversion, JALO, was concerned with thermo-chemical conversion of spent pulping liquors, peat, wood, and industrial residues. The aim of the program was to develop innovative power plants based on integrated gasification combined-cycle (IGCC). The research activity was carried out within 13 projects and focused, in particular, on fundamentals of thermochemical conversion technologies as well as on laboratory and pilot tests. In addition, development work was carried out within 20 industrial joint-development projects. Experimental and theoretical know-how concerning the new processes was increased significantly and the knowledge was applied in experiments on pressurized gasification pilot rigs. Industrial pilot or demonstration plants are being operated or constructed by Kemira Corporation, A. Ahlstrom Corporation, Imatran Voima Oy and Tampella Power Ltd, and industrial-scale plants are being planned by A. Ahlstrom Corporation, Tampella Power Ltd and Neste Oy. The pressurized test rigs of both the companies and the research institutes are among the first ones of their kind in the world. International research co-operation has been very active within the frameworks of IEA, EU-JOULE and the Nordic Council of Ministers. The next phase of the national energy technology programs of Ministry of Trade and Industry started from the beginning of 1993 and is scheduled to continue until the end of 1998. Biomass conversion research will be done within BIOENERGY-program and gasification research within LIEKKI2-program. DOE

N95-25517 Prins Maurits Lab. TNO, Rijswijk (Netherlands).

CHARACTERIZATION OF PLASTIC BONDED EXPLOSIVES BY PYROLYSIS-GAS CHROMATOGRAPHY AND MULTIVARIATE DATA ANALYSIS. APPLICATIONS OF THE PROCEDURE Final Report [KARAKTERISERING VAN KUNSTSTOF GEBONDEN EXPLOSIEVEN MET PYROLYSE-GASCHROMATOGRAFIE EN MULTIVARIATE DATA ANALYSE. TOEPASSING VAN DE PROCEDURE]

M. Rietjens Oct. 1994 28 p

(AD-A288761; PML-1992-A79; TDCK-92-2406) Avail: Issuing Activity (Defense Technical Information Center (DTIC))

Applications of the developed procedure based on pyrolysis-gas chromatography (Py-GC) and principal component analysis (PCA) for the characterization of plastic bonded explosives (PBX's) are described. Due to difficulties with the commonly used normalization method a new normalization method was developed and applied in this investigation. The patterns in the score plots obtained after PCA of the Py-GC results appeared much clearer using this new method. PBX samples were examined on homogeneity, influence of the amount of antioxidant (Flexzone), and the crosslink density. It appears that PBX's were inhomogeneous despite a thorough mixing of the constituents during the preparation. Aging experiments were performed on samples which differed in the amount of Flexzone and in the crosslink density. As more Flexzone was added the change in the pattern of the GC-peaks became less. No relation could be found between the stability of PBX's and the crosslink density. Finally, a comparison was made between Dutch samples and samples from the UK and Norway. Small differences were observed between the samples from the three nations. DTIC

N95-25528 Prins Maurits Lab. TNO, Rijswijk (Netherlands).

CHARACTERIZATION OF PLASTIC BONDED EXPLOSIVES BY PYROLYSIS-GAS CHROMATOGRAPHY AND MULTIVARIATE DATA ANALYSIS. DEVELOPMENT OF THE PROCEDURE Final Report [KARAKTERISERING VAN KUNSTSOF GEBONDEN EXPLOSIEVEN MET PYROLYSE-GASCHROMATOGRAFIE EN MULTIVARIATE DATA ANALYSE. ONTWIKKELING VAN DE PROCEDURE]

M. Rietjens Oct. 1994 33 p

(AD-A288787; PML-1992-A78; TDCK-92-2398) Avail: Issuing Activity (Defense Technical Information Center (DTIC))

A further development of the procedure based on pyrolysis-gas chromatography (Py-GC) for the characterization of plastic bonded explosives (PBX's) is described. After grinding, the PBX samples were pressed on a pyrolysis wire followed by Py-GC analysis. The peak areas obtained were normalized and submitted to multivariate data analysis. The use of principal component analysis (PCA) was tested on five samples which differed slightly in composition and age. The results were promising and showed that PCA is a powerful tool for the differentiation between PBX samples. The pressure by which the samples were pressed on the pyrolysis wire appeared to be an important parameter. This parameter was optimized together with the pyrolysis temperature and the amount of sample. The optimization experiment was carried out with two PBX samples which differed only in crosslink density. It turned out that it was difficult to find optima in the parameters resulting in a maximal difference between the two samples. The following settings of the parameters were selected: 5.2 tonnes, 75 mg, and 610 C. DTIC

N95-25769# National Aerospace Lab., Tokyo (Japan). Rocket Propulsion Research Group.

COMBUSTION CHARACTERISTICS OF METALLIZED HYDROCARBON FUELS

Hiroshi Sakamoto, Kazuo Sato, and Nobuyuki Yatsuyanagi Jan. 1994 17 p In JAPANESE

(ISSN 0389-4010)

(NAL-TR-1224) Avail: CASI HC A03/MF A01

In this paper the combustion performance of tripropellants consisting of LOX/hydrocarbon fuel and solid metals was evaluated. Thermochemical calculations were performed to evaluate specific impulse, specific density impulse and the combustion properties of LOX/kerosene/Be, LOX/kerosene/B, LOX/kerosene/Mg and LOX/kerosene/Al tripropellants. The specific impulse advantage of LOX/kerosene/Be over bipropellants was demonstrated, and consideration of specific density impulse justifies the use of heavier elements such as aluminum, magnesium and boron. Experiments were conducted to evaluate the combustion characteristics of oxygen/kerosene/aluminum tripropellants using single-element injectors and a water-cooled combustion chamber. Two kinds of unlike-impinging element (F-O-F) injectors were tested using liquid oxygen, and one kind of coaxial injector was tested using gaseous oxygen. The fuel used was a kerosene/aluminum mixture which consisted of aluminum particles, with a mean diameter of approximately 1.9 to 3.1 micron, suspended in kerosene fuel. The aluminum concentration in the total fuel mass varied from approximately 1 to 20 Wt%. The tested combustion pressure was 4MPa, and the mixture ratios were from 1.4 to 5.1. Experimental results demonstrated a significant improvement in combustion stability with the use of the impinging type of injector, and an increase in C* efficiency was achieved with the use of the coaxial type injector by the addition of aluminum to kerosene fuel. Author

29 MATERIALS PROCESSING

Includes space-based development of products and processes for commercial applications.

For biological materials see *55 Space Biology*.

N95-24416*# National Aeronautics and Space Administration. Lewis Research Center, Cleveland, OH.

STEREO IMAGING VELOCIMETRY FOR MICROGRAVITY APPLICATIONS

Brian B. Miller (Miller, Brian, Mansfield, OH.), MaryJo B. Meyer, and Mark D. Bethea 1994 12 p Symposium held in Garmisch-parten Kirchen, 18-22 Apr. 1994

(NASA-TM-110494; NAS 1.15:110494) Avail: CASI HC A03/MF A01

Stereo imaging velocimetry is the quantitative measurement of three-dimensional flow fields using two sensors recording data from different vantage points. The system described in this paper, under development at NASA Lewis Research Center in Cleveland, Ohio, uses two CCD cameras placed perpendicular to one another, laser disk recorders, an image processing substation, and a 586-based computer to record data at standard NTSC video rates (30 Hertz) and reduce it offline. The flow itself is marked with seed particles, hence the fluid must be transparent. The velocimeter tracks the motion of the particles, and from these we deduce a multipoint (500 or more), quantitative map of the flow. Conceptually, the software portion of the velocimeter can be divided into distinct modules. These modules are: camera calibration, particle finding (image segmentation) and centroid location, particle overlap decomposition, particle tracking, and stereo matching. We discuss our approach to each module, and give our currently achieved speed and accuracy for each where available. Author

31 ENGINEERING (GENERAL)

Includes vacuum technology; control engineering; display engineering; cryogenics; and fire prevention.

N95-24472# Joint Publications Research Service, Washington, DC.

JPRS REPORT: SCIENCE AND TECHNOLOGY. CENTRAL EURASIA

9 Sep. 1994 184 p Transl. into ENGLISH from various Central Eurasian articles

(JPRS-UST-94-018) Avail: CASI HC A09/MF A02

Translated articles cover the following topics: estimating life of structural ceramic on basis of dynamic fatigue test results; numerical solution of 3-D problems of non-axisymmetrical deformation of laminated anisotropic rotation shells; edge effects in laminated plates; miniature high-temperature superconducting microwave antenna; device for diagnostic sounding of ionospheric plasma with neutralized effect of charge-carrying spacecraft; new types of diagnosis of ionospheric parameters by surface and remote radio sounding; development and use of new weldable structural alloys in the aircraft industry; aerodynamic characteristics of delta wing in hypersonic flow; interrelationship between acoustic properties of nozzle head and combustion chamber with exciting transverse gas oscillations; study of effect of refraction parallax on accuracy of measurements of angular coordinates of artificial earth satellite; assessment of possibility of observation of artificial earth satellite by passive optical means in a twilight and daylight conditions; experimental study of friction against fluid at high speeds; construction of airfoil profiles streamlined with separation of turbulent boundary layer; dependence of aerodynamic characteristics of circular cylinder in supersonic stream of ideal gas on temperature factor; optimum conditions for control of turbulence intensity in stream by means of honeycombs; ionospheric effects of spacecraft launches; and consequences of greenhouse effect: predictions and reality. Author

N95-24540# Joint Publications Research Service, Arlington, VA.

JPRS REPORT: SCIENCE AND TECHNOLOGY. CENTRAL EURASIA

9 Mar. 1995 93 p Transl. into ENGLISH from various Central Eurasian articles

(JPRS-UST-95-012) Avail: CASI HC A05/MF A01

Translated articles cover the following topics: Russian expectations from commercial space; Russian space activity in 1994; information security in data processing systems and networks; and volume interaction during the diffusion welding of boron carbide with titanium. Author

N95-24543*# National Aeronautics and Space Administration. John F. Kennedy Space Center, Cocoa Beach, FL.

METROLOGY: MEASUREMENT ASSURANCE PROGRAM GUIDELINES

W. G. Eicke, J. P. Riley, and K. J. Riley Mar. 1995 96 p

(RTOP 323-36-19)

(NASA-RP-1364; NAS 1.61:1364) Avail: CASI HC A05/MF A01

The 5300.4 series of NASA Handbooks for Reliability and Quality Assurance Programs have provisions for the establishment and utilization of a documented metrology system to control measurement processes and to provide objective evidence of quality conformance. The intent of these provisions is to assure consistency and conformance to specifications and tolerances of equipment, systems, materials, and processes procured and/or used by NASA, its international partners, contractors, subcontractors, and suppliers. This Measurement Assurance Program (MAP) guideline has the specific objectives to: (1) ensure the quality of measurements made within NASA programs; (2) establish realistic measurement process uncertainties; (3) maintain continuous control over the measurement processes; and (4) ensure measurement compatibility among NASA facilities. The publication addresses MAP methods as applied within and among NASA installations and serves as a guide to: control measurement processes at the local level (one facility); conduct measurement assurance programs in which a number of field installations are joint participants; and conduct measurement integrity (round robin) experiments in which a number of field installations participate to assess the overall quality of particular measurement processes at a point in time. Derived from text

N95-24559*# National Aeronautics and Space Administration. Langley Research Center, Hampton, VA.

INTEGRATION OF DESIGN, STRUCTURAL, THERMAL AND OPTICAL ANALYSIS: AND USER'S GUIDE FOR STRUCTURAL-TO-OPTICAL TRANSLATOR (PATCOD)

R. M. Amundsen, W. S. Feldhaus, A. D. Little, and M. V. Mitchum Mar. 1995 23 p

(RTOP 243-10-01-01)

(NASA-TM-110153; NAS 1.15:110153) Avail: CASI HC A03/MF A01

Electronic integration of design and analysis processes was achieved and refined at Langley Research Center (LaRC) during the development of an optical bench for a laser-based aerospace experiment. Mechanical design has been integrated with thermal, structural and optical analyses. Electronic import of the model geometry eliminates the repetitive steps of geometry input to develop each analysis model, leading to faster and more accurate analyses. Guidelines for integrated model development are given. This integrated analysis process has been built around software that was already in use by designers and analysis at LaRC. The process as currently implemented used Pro/Engineer for design, Pro/Manufacturing for fabrication, PATRAN for solid modeling, NASTRAN for structural analysis, SINDA-85 and P/Thermal for thermal analysis, and Code V for optical analysis. Currently, the only analysis model to be built manually is the Code V model; all others can be imported for the Pro/E geometry. The translator from PATRAN results to Code V optical analysis (PATCOD) was developed and tested at LaRC. Directions for use of the translator or other models are given. Author

N95-24731# Joint Publications Research Service, Washington, DC.

JPRS REPORT: SCIENCE AND TECHNOLOGY. CENTRAL EURASIA

13 Feb. 1995 74 p Transl. into ENGLISH from various Central Eurasian articles

(JPRS-UST-95-006) Avail: CASI HC A04/MF A01

Translated articles cover the following topics: laser-controlled rotary microwave waveguide junction; optical pulse-phase modulation of semiconductor laser; amplitude-phase distortions of light beam obliquely propagating through ground layer of troposphere; antenna arrays with ultrafast beam scanning; materials for a walk on moon; textile-wood-coal briquette path to capitalism; and development of automated system for scientific research and design of heat and mass transfer processes. CASI

N95-24759# Joint Publications Research Service, Washington, DC.

JPRS REPORT: SCIENCE AND TECHNOLOGY. CENTRAL EURASIA

25 Nov. 1994 79 p Transl. into ENGLISH from various Central Eurasian articles

(JPRS-UST-94-032) Avail: CASI HC A05/MF A01

Translated articles cover the following topics: synthesis of stabilization systems for unmanned aircraft using spatial states methods; synthesis of two-dimensional nonequidistant antenna arrays based on theory of difference sets; study of the stability of an elastic hull-fuel lines-engines system for liquid fuel packet arrangement rockets; determining parameters of strength kinetics and critical dimension of fracture of composite materials by recording electromagnetic radiation pulses recorded during fracture; air density distribution around supersonic cone at angle of attack; and transfer of laser energy through turbulent atmosphere to far moving objects. CASI

N95-25367# Oak Ridge National Lab., TN.
THERMODYNAMIC PROPERTY EVALUATION AND MAGNETIC REFRIGERATION CYCLE ANALYSIS FOR GADOLINIUM GALLIUM GARNET
R. W. Murphy Dec. 1994 37 p
(Contract DE-AC05-84OR-21400)
(DE95-005910; ORNL/TM-12664) Avail: CASI HC A03/MF A01

Based on relevant material property data and previous model formulations, a magnetothermodynamic property map for gadolinium gallium garnet (Gd3Ga5O12) was adapted for refrigeration cycle analysis in the temperature range 4-40 K and the magnetic field range 0-6 T. Employing methods similar to those previously developed for other materials and temperature ranges, assessments of limitations and relative performance were made for Carnot, ideal regenerative, and pseudo-constant field regenerative cycles. It was found that although Carnot cycle limitations on available temperature lift for gadolinium gallium garnet are not as severe as the limitations for materials previously examined, considerable improvement in cooling capacity and temperature lift combinations can be achieved by using regenerative cycles if serious loss mechanisms are avoided. DOE

N95-25513 Army Tank-Automotive Systems Development Center, Warren, MI.
EVALUATION OF COMMERCIAL FUEL TANK WATER ABSORBERS Final Report
William R. Williams Nov. 1994 18 p Limited Reproducibility: More than 20% of this document may be affected by microfiche quality
(AD-A288361; TARDEC-TR-13615) Avail: Issuing Activity (Defense Technical Information Center (DTIC))

This report describes the laboratory evaluation of three types of commercial fuel tank water absorber cartridges and a limited field test of one type. Evaluation included absorbance effectiveness, possible deleterious effects on the fuel, and design integrity. Results are discussed together with the potential for use by the Army. DTIC

N95-26109 Polish Academy of Sciences, Warsaw (Poland). Inst. of Basic Problems of Technology.
THE FUNDAMENTALS OF MODELLING HEAT AND MOISTURE PROCESSES IN STRUCTURES [PODSTAWY MODELOWANIA PROCESOW CIEPLNO-WILGOTNOSCIOWYCH W BUDYNKACH]
Dorota Bzowska, Stanislaw Chyrczakowski, Wojciech Dzieniszewski, Hana Jedrzejuk, Elzbieta Kossecka, Leszek Laskowski, and Joanna Moldach 1994 153 p In POLISH
(ISSN 0208-5658)
(IFTR-15/1994) Avail: Issuing Activity (Polish Academy of Sciences, Warsaw, Poland)

In this article the authors discuss a number of problems related to the basic aspects of modelling heat and moisture processes in structures from the standpoint of energy efficiency. The individual parts of the article discuss: physical and energy modelling of residential structures; the analysis of heat penetration through the walls of a structure; the effect of ventilation on an energy structure's thermal balance in different climatic zones; the problem of modelling heat pumps in heating systems used in residential construction; streamlined procedures for determining the heating requirements of energy-efficient buildings; and optimization of the heat insulation of structures buried in the ground so as to minimize heat loss.
Transl. by Schreiber Translations Inc.

32 COMMUNICATIONS AND RADAR

Includes radar; land and global communications; communications theory; and optical communications.

For related information see also *04 Aircraft Communications and Navigation* and *17 Space Communications, Spacecraft Communications, Command and Tracking.* For search and rescue see *03 Air Transportation and Safety,* and *16 Space Transportation.*

N95-24241 National Defence Research Establishment, Linkoeping (Sweden).
ARMDAT: A BRIEF DESCRIPTION OF A COMPUTERIZED TEST SYSTEM FOR BURST TRANSMISSION [ARMDAT: OEVERSIKTLIG BESKRIVNING AV ETT EXPERIMENTSYSTEM FOER SNABBSAENDNING]
M. Albinsson Aug. 1994 17 p In SWAHILI
(PB95-165452; FOA-R-00013-3.5-SE) Avail: Issuing Activity (National Technical Information Service (NTIS))

This report briefly presents a test system for burst transmission on the high frequency (HF) channel. The system employs the HF radio Ra 195 and the modulation and demodulation is performed in a computerized radio modem. The purpose of this work is to design a burst transmission system for tests with effective modulation and coding techniques. The radio modem is a personal computer (PC) plug-in card, based on a digital signal processor (DSP). The transmitted signal is created in the radio modem and the information is processed in the computer. The program for the DSP is stored in the computer and is easy to change or configurate. The protocol contains an error correcting code and the user interface is designed to simplify tests of the message error probability. Further, the work shows the advantages of using modern digital technology. NTIS

N95-24281 National Defence Research Establishment, Stockholm (Sweden). Huvudavdelning foer Informationsteknologi.
DETVAG-90: AN IMPLEMENTATION OF VOGLER'S METHOD FOR CALCULATION OF MULTIPLE KNIFE-EDGE DIFFRACTION [DETVAG-90: EN IMPLEMENTERING AV VOGLERS METOD FOER MULTIPEL KNIVEGGSDIFFRAKTION]
I. Svensson Jun. 1994 48 p In SWEDISH
(PB95-141859; FOA-C-30743-3.5) Avail: Issuing Activity (National Technical Information Service (NTIS))

This is a report within the Detvag-90 project with a description of an implementation of Vogler's method for calculation of multiple knife edge diffraction. The method is one of several for calculation of knife edge diffraction loss in the prediction model Detvag. Unlike earlier methods, Vogler's considers all obstacles at the same time. This method has been implemented into a computer program. The report treats problems arising in the implementation, like convergence and limits in the representation of large numbers in the computer. There is also a comparison between Vogler's method and Giovaneli's method, an earlier implemented method for knife edge diffraction. NTIS

N95-24289# Sandia National Labs., Albuquerque, NM.
OPTICAL GENERATION OF RADIO-FREQUENCY POWER
V. M. Hietala, G. A. Vawter, T. M. Brennan, B. E. Hammons, and W. J. Meyer Nov. 1994 38 p
(Contract DE-AC04-94AL-85000)
(DE95-005276; SAND-94-2761) Avail: CASI HC A03/MF A01

An optical technique for high-power radio-frequency (RF) signal generation is described. The technique uses a unique photodetector based on a traveling-wave design driven by an appropriately modulated light source. The traveling-wave photodetector (TWPD) exhibits simultaneously a theoretical quantum efficiency approaching 100% and a very large electrical bandwidth. Additionally, it is capable of dissipating the high-power levels required for the RF generation technique. The modulated light source is formed by either the beating together of two lasers or by the direct modulation of a light source. A system example is given which predicts RF power levels of 100's of mW's at millimeter wave frequencies with a theoretical 'wall-plug' efficiency approaching 34%. DOE

N95-24377# Joint Inst. for Nuclear Research, Dubna (USSR).
LIENARD-WIECHERT POTENTIALS AS A CONSEQUENCE OF LORENTZ TRANSFORMATION OF COULOMB POTENTIAL
V. N. Streltsov 1993 4 p
(DE94-636734; JINR-D-2-93-437) Avail: CASI HC A01/MF A01 (US Sales Only)

A derivation of the electric potential of a moving charge as a result of the 'relativization' of the Coulomb potential is considered. The account of the Lorentz covariance demand and the action retardation of the electromagnetic field with necessity leads to the Lienard-Wiechert potentials. DOE

N95-24395*# Illinois Univ., Chicago, IL.
GENERATION AND COMPUTERIZED SIMULATION OF MESHING AND CONTACT OF MODIFIED INVOLUTE HELICAL GEARS Final Contractor Report
Faydor L. Litvin, Ningxin Chen, and Jian Lu Jan. 1995 76 p
(RTOP 505-62-36; DA Proj. 1L1-62211-A-47-A)
(NASA-CR-4644; E-9410; NAS 1.26:4644; ARL-CR-221) Avail: CASI HC A05/MF A01

The design and generation of modified involute helical gears that have a localized and stable bearing contact, and reduced noise and vibration characteristics are described. The localization of the bearing contact is achieved by the mismatch of the two generating surfaces that are used for generation of the pinion and the gear. The reduction of noise and vibration will be achieved by application of a parabolic function of transmission errors that is able to absorb the almost linear function of transmission errors caused by gear misalignment. The meshing and contact of misaligned gear drives can be analyzed by application of computer programs that have been developed. The computations confirmed the effectiveness of the proposed modification of the gear geometry. A numerical example that illustrates the developed theory is provided. Author

N95-24403# International Centre for Theoretical Physics, Trieste (Italy).
OPTICAL SPACE COMMUNICATION: AN OVERVIEW
V. K. Jain Apr. 1994 19 p
(DE94-634314; LAMP-94/3) Avail: CASI HC A03/MF A01 (US Sales Only)

In this paper, importance of optical space communication has been highlighted. Its merits and demerits over conventional microwave systems has been presented. In contrast to coherent systems, use of an optical preamplifier in a direct detection system has been emphasized. Status of some of the ongoing/future space communication projects has been given. Author

N95-24445 National Defence Research Establishment, Linkoeping (Sweden). Huvudavdelning foer Informationsteknologi.
LASER BASED METHODS FOR RANGE, DOPPLER AND VIBRATION MEASUREMENTS [LASERBASERADE METODER FOER AVSTANDS-, DOPPLER- OCH VIBRATIONSMAETNING]
I. Renhorn May 1994 30 p In SWAHILI
(PB95-141958; FOA-C-30759-3.1) Avail: Issuing Activity (National Technical Information Service (NTIS))

Laser radar and electro-optics are being used in a great variety of tactical defense applications. Imaging systems can be supplemented with range, Doppler and vibration sensing capability. The large variation in applications is translated into a large variation in technology requirements. Apart from system parameters, the functionality depends on atmospheric transmission, turbulence and target decorrelation time. Different applications will put different requirements on updating frequency and for active systems pulse or modulation frequency. This report gives an introductory discussion of some basic technologies with emphasis on new technologies for range, Doppler and vibration sensing. Vibration sensing is a unique application for coherent detection. NTIS

N95-24491# Central Research Inst. of Electric Power Industry, Tokyo (Japan).
APPLICATION OF OPTICAL FIBER AMPLIFIER FOR WAVELENGTH DIVISION MULTIPLEXING COMMUNICATION SYSTEM. PART 2: DESIGN OF FOUR-CHANNEL TRANSMISSION SYSTEM USING TWO EDFA REPEATERS
Kiyoyuki Isawa, Masahiro Kurono, and Masayuki Kuribara Mar. 1994 34 p In JAPANESE
(DE95-730179; CRIE-R-93009) Avail: CASI HC A03/MF A01

Circuit design was made in case of applying an Er(3+)-doped fiber amplifier (EDFA) to the conventional one-wavelength optical communication system and four-wavelength division multiplexing optical communication system with two in-line amplifiers. Circuit-designed to use two EDFA's for amplifying an optical signal with a wavelength of 1540 nm, the one-wavelength optical communication system experimentally demonstrated that the circuit could be formed to the maximum length of 180 km. In the remote pumping through the signal transmission line used as a pumped optical supply line, the electric source is not necessary at the amplification point, so that the EDFA can be utilized under a good condition, if the pumped optical output is sufficiently high. The wavelength to pump the EDFA is 0.98 (mu)m and 1.48 (mu)m. Circuit-designed to multiplex wavelengths around 1555nm, the four-wavelength division multiplexing optical communication system with two in-line amplifiers gives the smallest difference in output among wavelengths on condition that the wavelength is set to equalize the amplified wavelength output at both transmission and reception points at the required input level. Mutual relation was elucidated among the in-line input level, working wavelength band and transmission distance. DOE

N95-24493# Central Research Inst. of Electric Power Industry, Tokyo (Japan).
SURVEY OF METHODS FOR SECURE CONNECTION TO THE INTERNET
Shouichi Matsui Apr. 1994 24 p In JAPANESE
(DE95-730185; CRIE-R-94001) Avail: CASI HC A03/MF A01

This paper describes a study of a security method of protecting inside network computers against outside miscreants and unwelcome visitors and a control method when these computers are connected with the Internet. In the present Internet, a method to encipher all data cannot be used, so that it is necessary to utilize PEM (Privacy Enhanced Mail) capable of the encipherment and conversion of secret information. For preventing miscreant access by eavesdropping password, one-time password is effective. The most cost-effective method is a firewall system. This system lies between the outside and inside network. By limiting computers that directly communicate with the Internet, control is centralized and inside network security is protected. If the security of firewall systems is strictly controlled under correct setting, security within the network can be secured even in open networks such as the Internet. DOE

N95-24503 Technical Univ. of Lublin, Lublin (Poland). Dept. of Fundamental Electrical Engineering.
ELECTROMAGNETIC DEVICES AND PROCESSES IN ENVIRONMENT PROTECTION. PROCEEDINGS OF INTERNATIONAL CONFERENCE ELMECO 1994
Sep. 1994 394 p Conference held in Lublin, Poland, 8-9 Sep. 1994 Limited Reproducibility: More than 20% of this document may be affected by microfiche quality
(Contract N68171-94-M-6201)
(AD-A286613; R/D-7463-CH-O2) Avail: CASI HC A17

The electrical power industry has contributed substantially to the destruction of the natural environment and that is why electrical engineers are particularly obliged to repair the damage and to reduce the risks as much as possible. For this reason, an approach to train specialists in the field of 'Electromagnetic processes and devices in environment protection' was undertaken by the Department of Fundamental Electrical Engineering, Lublin Technical University in 1990. Resulting research activities created the need to exchange the experience of specialists who deal with this field. The following categories were discussed at the conference and the papers that comprise them are presented within this report: ozone and plasma generators; materials and devices in environment protection; electromagnetic processes in environment protection; electromagnetic fields and devices; and noise and electromagnetic disturbance influence on human environment. CASI

N95-24506# Joint Inst. for Nuclear Research, Dubna (USSR). Theoretical Physics Lab.
LAGRANGIAN FORMULATION OF NJL MODEL WITH SE PARABLE INTERACTION

I. Anikin, M. Ivanov, N. Kulimanova (Ivanovo State Univ., Russia.), and V. Lyubovitskij (Tomsk State Univ., USSR.) 1993 20 p Submitted for publication
(DE94-628519; JINR-E-2-93-257) Avail: CASI HC A03/MF A01 (US Sales Only)

A Lagrangian formulation of the Nambu-Jona-Lasinio model with separable interaction is given. The electromagnetic interaction is introduced in a non-minimal way to the nonlocal quark current. We have calculated the pion weak decay constant, the two-photon decay width, as well as the form factor of the gamma(sup *) pi(sup 0) yields gamma-transition and the pion charge form factor. The two adjustable parameters, the range parameter appearing in the separable interaction and the constituent mass, m(sub q), have been fixed by fitting the experimental data for the pion decay constants. DOE

N95-24539# Joint Publications Research Service, Arlington, VA.
JPRS REPORT: SCIENCE AND TECHNOLOGY. CENTRAL EURASIA
17 Feb. 1995 41 p Transl. into ENGLISH from various Central Eurasian articles
(JPRS-UST-95-010) Avail: CASI HC A03/MF A01

Translated articles cover the following topics: new principle of detecting moving objects; Russian Federal space program for the period to year 2000: prospects for developing communication; systems for communication via low-orbit artificial earth satellites; and new communication and broadcasting satellites for economic purposes. Author

N95-24605# Sandia National Labs., Albuquerque, NM.
THE ACCIDENT SITE PORTABLE INTEGRATED VIDEO SYSTEM
D. P. Jones, D. L. Shirey, and W. A. Amai 1995 8 p Presented at the 6th American Nuclear Society Meeting on Robotics and Remote Systems, Monterey, CA, 5-10 Feb. 1995
(Contract DE-AC04-94AL-85000)
(DE95-000539; SAND-94-2394C; CONF-950232-2) Avail: CASI HC A02/MF A01

This paper presents a high bandwidth fiber-optic communication system intended for post accident recovery of weapons. The system provides bi-directional multichannel, and multi-media communications. Two smaller systems that were developed as direct spin-offs of the larger system are also briefly discussed. DOE

N95-24649 National Defence Research Establishment, Linkoeping (Sweden). Huvudavdelning foer Informationsteknologi.
WAVE-PROPAGATION ASPECTS ON VHF-RADAR APPLICATIONS [VAGUTBREDNINGSASPEKTER PA VHF-RADAR]
G. Eriksson Mar. 1994 43 p In SWAHILI
(PB95-141818; FOA-C-30754-3.5) Avail: Issuing Activity (National Technical Information Service (NTIS))

Within the project Technical-Strategical Study of Modern Concepts for Air Defense Radars (TSS/LFrr), some wave propagation aspects on radar applications at VHF have been studied. Comparisons are made with the conditions at more commonly used microwave frequencies. Interest is focused on the low-altitude radar coverage. Coverage behind obstacles is more easily obtained by diffraction at VHF than at microwave frequencies. This effect improves the possibilities of obtaining good coverage at low altitudes. Unfortunately, the high influence of the ground-reflected propagation component at VHF strongly counteracts this effect. By destructive interference, between the direct and the ground-reflected component, the attenuation will be high at low altitudes, even in cases when no obstruction occur. Furthermore, the accuracy of some terrain independent models (flat and spherical earth) for calculation of propagation loss is investigated along some obstructed paths. NTIS

N95-24835 National Defence Research Establishment, Linkoeping (Sweden). Huvudavdelning foer Informationsteknologi.
ANNUAL REPORT 1992/93, FOA 38. RADIO SYSTEMS AND WAVE PROPAGATION [ARSRAPPORT 1992/93 FOA 38. RADIOSYSTEM OCH VAGUTBREDNING]
I. M. Mildh Jan. 1994 66 p In SERBIAN; Text in SWEDISH and ENGLISH
(PB95-141735; FOA-C-30746-3.5) Avail: Issuing Activity (National Technical Information Service (NTIS))

The main objective of the division of Radio Systems and Wave Propagation is to carry out research and development in the field of secure and robust radio communications for Sweden's national defense. This is the Annual Report for fiscal year 1992/93 of the Division of Radio Systems and Wave Propagation. The division is responsible for research and development of secure radio communication for information transmission. We are also responsible for wave propagation research within a frequency range from LF to SHF. We carry out applied research in fields like antijamming systems, modulation, error correcting codes, wave propagation and digital signal processing. The wave propagation research is carried out by basic research so the demands from new techniques and new radio systems for accurate propagation models can be achieved. NTIS

N95-24836 National Defence Research Establishment, Linkoeping (Sweden). Huvudavdelning foer Informationsteknologi.
ANALYSIS OF DATA FROM A RADAR WARNING RECEIVER WITH THE ACCENT ON ASSOCIATION OF SENSOR REPORTS [ANALYS AV RADARVARNARDATA MED TONVIKT PA ASSOCIERING AV SENSORRAPPORTER]
L. Joensson and R. Roldan-Prado Mar. 1994 53 p In SWAHILI
(PB95-141768; FOA-C-30751-3.4) Avail: Issuing Activity (National Technical Information Service (NTIS))

Threat assessment, based on data from an airborne radar warning receiver, involves several difficult tasks. The main part of the report deals with the specific task of how to associate data from the same radar emitter. This association task can be difficult when several emitters of the same type are active in the same direction, especially when they suddenly change operation modes, which generates many possible candidates for data combinations. In these cases, data have to be fused with prior information/knowledge to make a successful association possible. In order to investigate this problem, sensor data in form of pulse chain reports have been simulated, and different association processes have been developed and tested. One of these seems to be an efficient way of associating reports in a correct manner. This process or concept includes limiting the number of candidates for report combination by constraints, estimating the likelihoods of possible pairs of reports, and clustering the reports directed by the estimates. The described concept can probably be used in other data fusion applications. In the initial parts of the report, examples are given of different problems of method concerning emitter assessment, as well as of different kinds of knowledge which could be used in this threat assessment application. NTIS

N95-24848# Central Research Inst. of Electric Power Industry, Tokyo (Japan).
STUDY ON PROPAGATION IMPAIRMENTS, DISTORTIONS AND UNAVAILABILITY ON DIGITAL MICROWAVE LINKS
Yoshizumi Serizawa Dec. 1993 153 p In JAPANESE
(DE95-723047; CRIE-R-01) Avail: CASI HC A08/MF A02

A study was made on propagation impairments (degradation) and distortions for design, route layout and operation of digital microwave links for information network basic telecommunication. As to multipath interference fading which causes distortions, a method to predict an outage probability of the link was introduced from in-band amplitude deviation. In the case of having system gains by influence of man-made structures, that is, in the case of the link in which the reflector is installed in the Fresnel region, in the reflector relay link, a precise measuring method to gain reflector was introduced. With the equivalent C/N degradation amount, a method was developed for estimation of influence quantity in the case of system loss (propagation impairments) caused by structures standing in the propagation path, and unnecessary reflection/scattered wave. With relation to CPM current differential teleprotection systems, a theoretical study was made on a relation between error ratio characteristics and relay motion at fading, indicating that the required bit error ratio is approximately 10(exp -6) - 10(exp -7). DOE

N95-24893# European Space Agency. European Space Research and Technology Center, ESTEC, Noordwijk (Netherlands).
ESRO'S TELECOMMUNICATIONS PROGRAMME AND THE OTS PROJECT (1970-1974)
Arturo Russo (Palermo Univ., Italy.) Feb. 1994 72 p Original contains color illustrations
(ESA-HSR-13) Avail: CASI HC A04/MF A01

The ESA History Study Reports are preliminary reports of studies carried

out within the framework of an ESA (European Space Agency) contract. They will form the basis of a comprehensive study of European Space activities covering the period 1959-1987. ESRO, the European Space Research Organization, had been formally established by ten European countries in 1964 as an organization solely devoted to space research. The first phase of implementation of ESRO's telecommunications program and the definition of the OTS (Orbital Test Satellite) project are discussed. The telecommunication program involved a large scale technological effort in key industrial sectors, with important financial investments and promising returns on the commercial level. The OTS project's industrial policy aspects involved the choice of the contractors for building the satellite and its earth control station. Derived from text

N95-25316* National Aeronautics and Space Administration. Pasadena Office, CA.

A SATELLITE-TRACKING MILLIMETER-WAVE REFLECTOR ANTENNA SYSTEM FOR MOBILE SATELLITE-TRACKING Patent

Arthur C. Densmore, inventor (to NASA) (Jet Propulsion Lab., California Inst. of Tech., Pasadena, CA.), Vahraz Jamnejad, inventor (to NASA) (Jet Propulsion Lab., California Inst. of Tech., Pasadena, CA.), and Kenneth E. Woo, inventor (to NASA) (Jet Propulsion Lab., California Inst. of Tech., Pasadena, CA.) 14 Mar. 1995 22 p Filed 30 Nov. 1992 Supersedes N93-28955 (31 - 11, p 3381)

(Contract NAS7-918)

(NASA-Case-NPO-18772-1-CU; US-Patent-5,398,035; US-Patent-Appl-SN-999794; US-Patent-Class-343-713; US-Patent-Class-343-786; US-Patent-Class-343-840; Int-Patent-Class-H01Q-19/12) Avail: US Patent and Trademark Office

A miniature dual-band two-way mobile satellite tracking antenna system mounted on a movable ground vehicle includes a miniature parabolic reflector dish having an elliptical aperture with major and minor elliptical axes aligned horizontally and vertically, respectively, to maximize azimuthal directionality and minimize elevational directionality to an extent corresponding to expected pitch excursions of the movable ground vehicle. A feed-horn has a back end and an open front end facing the reflector dish and has vertical side walls opening out from the back end to the front end at a lesser horn angle and horizontal top and bottom walls opening out from the back end to the front end at a greater horn angle. An RF circuit couples two different signal bands between the feed-horn and the user. An antenna attitude controller maintains an antenna azimuth direction relative to the satellite by rotating it in azimuth in response to sensed yaw motions of the movable ground vehicle so as to compensate for the yaw motions to within a pointing error angle. The controller sinusoidally dithers the antenna through a small azimuth dither angle greater than the pointing error angle while sensing a signal from the satellite received at the reflector dish, and deduces the pointing angle error from dither-induced fluctuations in the received signal. Official Gazette of the U.S. Patent and Trademark Office

N95-25393 Polish Academy of Sciences, Warsaw (Poland). Inst. of Electromagnetic Wave Theory.

THE DIFFRACTION OF ELECTROMAGNETIC WAVES BY SCREENS PLACED AT THE BOUNDARIES OF DIELECTRIC MEDIA Ph.D. Thesis [DYFRAKCJA FAL ELEKTROMAGNETYCZNYCH NA EKRANACH UMIESZCZONYCH NA GRANICY OSRODKOW DIELEKTRYCZNYCH]

Adam Ciarkowski Cooperative Publishing House Ltd. 1994 109 p In POLISH

(ISSN 0208-5658)

(IFTR-4/1994) Avail: Issuing Activity (Polish Academy of Sciences, Warsaw, Poland)

This dissertation concerns problems of the diffraction of electromagnetic waves by conductive infinitely thin screens situated at the interface of two different dielectric media. The author uses exact solutions of two-dimensional problems of the diffraction of E and H type plane waves on a half-plane to construct exact solutions for a three-dimensional case (oblique incidence of the plane wave relative to the edge of the half-plane). The author uses asymptotic analysis of contour integrals to obtain non-uniform and quasi-uniform high-frequency asymptotic expansions of this solution. The author provides a physical interpretation of the phenomena which accompany the diffraction of the incident wave and the relationship between the diffraction waves and transverse waves in the neighborhood of the interface. The asymptotic solutions for a particular form of screen which is a half-plane and physical analysis of wave phenomena are used to postulate and then find non-uniform and quasi- uniform asymptotic solutions for a screen with a curved edge. The author presents the procedure based on heuristic radial solutions which led to the construction of these solutions. The non-uniform solution is described by elementary functions and is applicable everywhere beyond the neighborhood of the boundaries of the shadow which figure in the wave problem and the neighborhood of the caustics of the diffraction waves. The quasi-uniform solution is expressed by means of a Fresnel integral and Weber function of the orders 1/2 and 3/2 and is continuous on the aforementioned boundaries. At a distance from these boundaries, it turns into a non-uniform solution. Like the non-uniform solution, it is not applicable in the neighborhood of the caustics of the diffraction waves, especially in the neighborhood of the edge of the screen. Author

N95-25482# Lund Univ. (Sweden). Research Policy Inst.

TOWARDS AN ERA OF GLOBAL VILLAGE: THE DYNAMICS OF WORLD TELECOMMUNICATIONS AND ITS IMPLICATIONS FOR THE FUTURE OF NATION STATE

Wang Yadong 1994 81 p Sponsored by OCB

(PB95-165064) Copyright Avail: CASI HC A05/MF A01

The paper on global telecommunications has been produced within a project called 'Identification of non-military security risks and analysis of security concepts in a geo-economic environment which is dominated by technological conversion of infrastructures'. The materials used were collected with a particular focus on satellite systems and optical fiber networks. The booklet can only scratch the surface of the fundamental changes which have taken place in the telecommunications sector. However, the technological change in the telecommunications sector is one of the fundamental changes which are affecting and drastically changing the character of the nation-state and its security. The selection of focus has been determined by an interest in gaining an understanding of the changing security situation of nations, in particular Sweden. NTIS

N95-25604 Massachusetts Univ., Amherst, MA. Dept. of Electrical and Computer Engineering.

DISCRETE-EVENT-DYNAMIC-SYSTEM-BASED APPROACHES FOR CONTROL IN INTEGRATED VOICE/DATA MULTIHOP RADIO NETWORKS Final Report, 1 Oct. 1992 - 30 Sep. 1993

Christos G. Cassandras and Vibhor Julka 7 Dec. 1994 34 p Limited Reproducibility: More than 20% of this document may be affected by microfiche quality

(Contract N00014-92-J-2017; ONR Proj. RR015-09-41)

(AD-A288389; NRL-MR/5520-94-7601) Avail: Issuing Activity (Defense Technical Information Center (DTIC))

We report accomplishments and new directions in our effort to develop and apply discrete-event-dynamic-system-based techniques for the transmission scheduling problem in Radio Networks (RN). First, we examine this problem in the context of data traffic in general topology networks. Next, we look at the scheduling problem when processing packetized voice calls, where Grade-of-Service (GOS) requirements are quite different. For data traffic, we formulate an optimization problem for the allocation of transmission time slots to different competing nodes and present a gradient-based algorithm suitable for on-line implementation without any assumptions on the nature of the data traffic processes. Examples illustrating the adaptive features of our approach and comparing it to other schemes are included. For voice traffic, we formulate the optimal scheduling problem as a stochastic discrete resource allocation problem, which is combinatorial hard. We describe a technique for transforming this to a continuous optimization problem and develop algorithms for minimizing the blocking probability of packetized voice traffic. DTIC

N95-25623 Research Inst. of National Defence, Linkoeping (Sweden). Huvudavdelning foer Informationsteknologi.

MULTISTATIC RADAR: SYNCHRONIZATION AND TIME REFERENCE SYSTEM [MULTISTATISK RADAR: SYNKRONISERING OCH REFERENSTIDSSYSTEM]

H. G. Jubrink Aug. 1994 31 p In SWAHILI

(PB95-165288; FOA-R-94-00015-3.2-SE) Avail: Issuing Activity (National Technical Information Service (NTIS))

A synchronization and time reference system for multistatic radar (MSR) is presented. The report also gives a summary of the most important parameter values of the synchronization process in MSR. Some reference oscillator systems using Loran C and global positioning system (GPS)

receivers have been briefly analyzed. The synchronization method is based on a multioscillator system from the HP time and frequency standard system, the HP 55000 system. The multioscillator concept gives a more robust and redundant solution of the synchronization problem. The synchronization system can also be given external support by other time precision systems, for instance the GPS system. NTIS

N95-25641 National Defence Research Establishment, Linkoeping (Sweden). Avdelningen foer Sensorteknik.

ANALYSIS OF WAVEFORMS FOR BISTATIC RADAR SYSTEMS [ANALYS AV VAGFORMER FOER BISTATISKA RADARSYSTEM]

U. Oreborn Jun. 1994 52 p In SWAHILI

(PB95-165098; FOA-C-30765-3.3) Avail: Issuing Activity (National Technical Information Service (NTIS))

The transmitter and receiver of Bistatic Radar Systems are located at different positions. It is therefore possible to transmit and receive simultaneously. This opens up the possibility of using continuous wave (CW) signals. This report shows how traditional pulse compression codes can be analyzed and enhanced, when adjusted to CW, with special attention paid to elude detection. NTIS

N95-25644 National Defence Research Establishment, Linkoeping (Sweden). Huvudavdelning foer Informationsteknologi.

EXPERIMENTAL STUDY OF TAPERED SLOT ELEMENTS [EXPERIMENTELL STUDIE AV TAPERADE SLITSELEMENT]

B. Carlegrim, L. Pettersson, and A. Vogel May 1994 89 p In SWAHILI

(PB95-165163; FOA-C-30758-3.2) Avail: Issuing Activity (National Technical Information Service (NTIS))

Experimental work to study conditions for realization of circular polarized broad band array antennas using microstrip fed slots as antenna elements is reported. Properties of the slot elements together with their fed networks have been studied in configurations such as a linear array, planar 2-dimensional linear polarized array, and elements in an orthogonal configuration to generate circular polarization. Properties such as antenna element gain, radiation characteristics, and polarization have been studied over the frequency range 6-18 GHz. Overcoming shortcomings of the used orthogonal slot elements, we have shown that it is possible to generate circular polarization, within limited scan angles, over a frequency range of 6-18 GHz. NTIS

N95-25648# International Centre for Theoretical Physics, Trieste (Italy).

A SUPERFIELD GENERALIZATION OF THE CLASSICAL ACTION-AT-A-DISTANCE THEORY

V. V. Tugai (Scientific Physicotechnological Center, Kharkov, Ukraine.) and A. A. Zheltukhin Jul. 1994 12 p Sponsored by International Science Foundation

(DE95-607084; IC-94/179) Avail: CASI HC A03/MF A01 (US Sales Only)

A generalization of the Fokker-Schwarzschild- Tetrode-Wheeler-Feynman electromagnetic theory onto superspace is considered. The classical vector and spinor fields belonging to the Maxwell supermultiplet are built of the world-line coordinates of the charged particles in superspace. DOE

N95-25710*# Jet Propulsion Lab., California Inst. of Tech., Pasadena, CA.

SPACEBORNE SYNTHETIC APERTURE RADAR: CURRENT STATUS AND FUTURE DIRECTIONS. A REPORT TO THE COMMITTEE ON EARTH SCIENCES, SPACE STUDIES BOARD, NATIONAL RESEARCH COUNCIL Report, Apr. 1994 - Feb. 1995

D. L. Evans, ed., J. Apel, R. Arvidson, R. Bindschadler, F. Carsey, J. Dozier, K. Jezek, E. Kasischke, F. Li, and J. Melack et al May 1995 183 p Original contains color illustrations

(NASA-TM-4679; NAS 1.15:4679) Avail: CASI HC A09/MF A02; 22 functional color pages

This report provides a context in which questions put forth by NASA's Office of Mission to Planet Earth (OMPTE) regarding the next steps in spaceborne synthetic aperture radar (SAR) science and technology can be addressed. It summarizes the state-of-the-art in theory, experimental design, technology, data analysis, and utilization of SAR data for studies of the Earth, and describes potential new applications. The report is divided into five science chapters and a technology assessment. The chapters summarize the value of existing SAR data and currently planned SAR systems, and identify gaps in observational capabilities needing to be filled to address the scientific questions. Cases where SAR provides complementary data to other (non-SAR) measurement techniques are also described. The chapter on technology assessment outlines SAR technology development which is critical not only to NASA's providing societally relevant geophysical parameters but to maintaining competitiveness in SAR technology, and promoting economic development. Author

N95-25749 Research Inst. of National Defence, Linkoeping (Sweden). Dept. of Command and Control Warfare Technology.

ORIENTATION DETERMINATION OF AIRCRAFT USING VISUAL 3D MATCHING AND RADAR. CASE STUDY 2

H. A. Olsson, M. Bengtsson, and P. Roivainen Aug. 1994 26 p

(PB95-165791) Avail: Issuing Activity (National Technical Information Service (NTIS))

This study is an application of a matching method using 3D models and images. In the earlier case study we combined radar data and visual matching for aircraft identification and orientation determination. We analyzed a video sequence of an aircraft together with radar data, where the radar has guided the tracking of the aircraft. The purpose of this case study is to test our new 3D model, composed of edge segments from the silhouette of an aircraft and to see if it is possible to analyze the video sequence only with visual matching, after the radar has given the initial start values. NTIS

N95-25876*# National Aeronautics and Space Administration. Lewis Research Center, Cleveland, OH.

FACILITY FOR THE EVALUATION OF SPACE COMMUNICATIONS AND RELATED SYSTEMS

Robert J. Kerczewski, James S. Svoboda (NYMA, Inc., Brook Park, OH.), and Brian A. Kachmar (Analex Corp., Brook Park, OH.) Apr. 1995 12 p Presented at the 41st International Instrumentation Symposium, Aurora, CO, 7-11 May 1995; sponsored by the Instrument Society of America

(Contracts NAS3-27186; NAS3-25776; RTOP 235-01-1E)

(NASA-TM-106904; E-9600; NAS 1.15:106904) Avail: CASI HC A03/MF A01

NASA Lewis Research Center's Communications Projects Branch has developed a facility for the evaluation of space communications systems and related types of systems, called the Advanced Space Communications (ASC) Laboratory. The ASC Lab includes instrumentation, testbed hardware, and experiment control and monitor software for the evaluation of components, subsystems, systems, and networks. The ASC lab has capabilities to perform radiofrequency (RF), microwave, and millimeter-wave characterizations as well as measurements using low, medium, or high data rate digital signals. In addition to laboratory measurements, the ASC Lab also includes integrated satellite ground terminals allowing experimentation and measurements accessing operational satellites through real space links. Author

N95-25891# Linkoeping Univ. (Sweden).

INVERSION OF CIRCULAR AVERAGES AND APPLICATION OF BACKPROJECTION METHODS TO RADAR IMAGING

S. Nilsson Feb. 1994 62 p

(ISSN 0347-3708)

(PB95-141578; FOA-C-30749-3.3) Avail: CASI HC A04/MF A01

In the report the authors study two mathematical inverse problems concerning the determination of a function from spherical averages, which appear in certain radar applications. The first inverse problem consists of determining a function from its spherical averages over all circles with center on a straight line and with arbitrary radius. In the second the authors have averages over discs instead of circles. They define the corresponding operators and their duals, called backprojection operators. They investigate the properties of these operators and also for which functions the resulting inversion formulas are valid. The inversion formula for the first problem can be expressed by the aid of a backprojection operator. This is used in order to obtain an approximate inversion formula for a perturbed problem where they know the averages over circles with center on a smooth curve deviating from the straight line. They describe the qualitative behavior of this approximative inversion formula contra the original one. Finally they present some numerical results obtained using a simulation program. NTIS

N95-26008 Communications Research Lab., Tokyo (Japan).
JOURNAL OF THE COMMUNICATIONS RESEARCH LABORATORY, VOLUME 41, NUMBER 1, MARCH 1994
Mar. 1994 49 p
(PB95-177606) Copyright Avail: Issuing Activity (National Technical Information Service (NTIS))

There are three technical papers with the following titles: H Alpha Solar Telescope for the Space Weather Forecast and its Initial Observations; Experimental Advanced Mobile Satellite Communications System in MM-Wave and Ka-Band Using Japan's COMETS; Data-driven Segmentation of Degraded Images Based on Markov Random Field Models. In addition, there are eight pages containing abstracts of recent papers published in the issues of 'Rev. Commun. Res. Lab.' NTIS

N95-26018 Polish Academy of Sciences, Warsaw (Poland). Inst. of Acoustic Phonetics.
A STUDY OF THE EFFECT OF VOICE PITCH ON THE PERCEPTION OF SYNTHETIC POLISH VOWELS [BADANIE WPLYWU WYSOKOSCI GLOSU NA PERCEPCJE SYNTETYCZNYCH SAMOGLOSEK POLISKICH]
Mariusz Owsianny 1994 20 p In POLISH
(ISSN 0208-5658)
(IFTR-10/1994) Avail: Issuing Activity (Polish Academy of Sciences, Warsaw, Poland)

The author studied the effect of the relationship between voice pitch and formant frequencies on the perception of synthetic vowels. The author used the SMOK software formant speech synthesizer in a serial-parallel system proposed by D. H. Klatt, which makes it possible to generate natural-sounding speech signals, to re-synthesize the Polish vowels /i/, /i(under bar)/, /e/, /a/, /o/, and /u/ uttered by female and male speakers. These prototype phones were then modified. The author varied the fundamental frequency F(sub 0) +/- 1 octave from its original value. Fifteen subjects, including 5 females and 10 males, took part in the hearing tests. The subjects had to identify vowels presented in random order. The results revealed that perceptual identification of vowels is greatly affected by the formants' relation to F(0) as well as their location on the frequency scale. The existence of a discrepancy between the formant frequencies and voice pitch leads to a change in phonetic category.
Transl. by Schreiber Translations Inc.

N95-26191 Defence Research Establishment Ottawa, Ottawa (Ontario). Electronic Warfare Div.
THE EFFECTS OF THE ENVIRONMENT ON AN EXPERIMENTAL VHF RADIO DIRECTION FINDING ANTENNA SYSTEM
William J. L. Read Aug. 1994 82 p Limited Reproducibility: More than 20% of this document may be affected by microfiche quality
(AD-A288791; DREO-1226) Avail: Issuing Activity (Defense Technical Information Center (DTIC))

This report discusses the results of VHF radio direction finding (DF) experiments carried out with an experimental linear eight antenna DF system. The main purpose of these experiments was to investigate the effect of the environment, in particular multipath propagation, on DF performance. A theoretical analysis of all known error mechanisms has also been carried out in order to better understand the measured results. This includes temporal noise, equipment errors, mutual coupling, and multipath. The analysis of multipath also includes the development of new models to predict statistical effects. The results of this investigation indicate that multipath effects are complex and may create difficulties in modern systems if improved accuracy is an objective. Further measurements will be required to verify these preliminary findings. DTIC

N95-26331 Polish Academy of Sciences, Warsaw (Poland). Inst. of Acoustic Phonetics.
AUTOMATIC CLASSIFICATION OF POLISH FRICATIVES ON THE BASIS OF OPTIMIZATION OF THE PARAMETER SPACE [AUTOMATYCZNA KLASYFIKACJA SPOLGLOSEK TRACYCH JEZYKA POLSKIEGO NA BAZIE OPTYMALIZACJI PRZESTRZENI PARAMETROW]
Piotr Domagala and Lutoslawa Richter Cooperative Publishing House Ltd. 1994 32 p In POLISH
(ISSN 0208-5658)
(IFTR-9/1994) Avail: Issuing Activity

The subject of this article is a study of the possibility of automatic classification and recognition of fricatives on the basis of a certain linear combination of values of an autocorrelation function. Automatic classification of fricative consonants constituted one phase of a study which involves the classification of all Polish phones for the purpose of enabling automatic speech recognition regardless of the phonetic context or the speaker. The study was conducted using phonetic material consisting of 166 nonsense syllables which included fricatives and had CVCV and VCCV structures. There were a total of about 20 contexts for each consonant. Separate classifications were performed for 5 female voices and 5 male voices and then both groups of voices were classified together. The three series of classifications had success rates of 60%, 69%, and 60% respectively. These results were about 10% better than the results obtained using classical discrimination analysis (CSS:Statistica 3.1 software). The use of cluster analysis and multidimensional scaling yielded information on the relative probabilities of the acoustic patterns of these phones in reference to perception tests. Transl. by Schreiber Translations Inc.

33 ELECTRONICS AND ELECTRICAL ENGINEERING

Includes test equipment and maintainability; components, e.g., tunnel diodes and transistors; microminiaturization; and integrated circuitry.

For related information see also *60 Computer Operations and Hardware* and *76 Solid-State Physics*.

N95-24245# International Centre for Theoretical Physics, Trieste (Italy).
CURRENT-VOLTAGE CHARACTERISTICS OF A TUNNEL JUNCTION WITH RESONANT CENTERS
T. Ivanov and V. Valtchinov (Northeastern Univ., Boston, MA.) May 1994 10 p Sponsored in part by Commission of the European Communities
(DE94-634530; IC-94/95) Avail: CASI HC A02/MF A01 (US Sales Only)

We calculated the I-V characteristics of a tunnel junction containing impurities in the barrier. We consider the indirect resonant tunneling involving the impurities. The Coulomb repulsion energy E(sub c) between two electrons with opposite spins simultaneously residing on the impurity is introduced by an Anderson Hamiltonian. At low temperatures T much less than E(sub c) the I-V characteristics is linear in V both for V less than E(sub c) and for V greater than E(sub c) and changes slope at V = E(sub c). This behavior reflects the energy spectrum of the impurity electrons - the finite value of the charging energy E(sub c). At T approximately E(sub c) the junction reveals an ohmic-like behavior as a result of the smearing out of the charging effects by the thermal fluctuations. DOE

N95-24447# QaRel Associates, Northampton (England).
FIFTH EUROPEAN SYMPOSIUM ON RELIABILITY OF ELECTRON DEVICES, FAILURE PHYSICS AND ANALYSIS
G. M. Brydon 7 Oct. 1994 559 p Symposium held in Glasgow, Scotland, 4-7 Oct. 1994
(AD-A286614) Avail: CASI HC A24/MF A04

Papers are grouped into the following sessions: failure analysis; characterization and modeling; hot carriers; oxide states; power devices; optoelectronics; microwave; reliability methodologies; electromigration; packaging; electrostatic discharges (ESD); design for reliability; and reliability evaluation. CASI

N95-24452# Department of Energy, Washington, DC.
SUPERCONDUCTIVITY PROGRAM FOR ELECTRIC POWER SYSTEMS: 1994 ANNUAL PEER REVIEW. VOLUME 1, MEETING PROCEEDINGS
29 Jul. 1994 690 p Conference held in Alexandria, VA, 19-20 Jul. 1994
(DE95-005058; CONF-9407153-Vol-1) Avail: CASI HC A99/MF A06

This is Volume 1 of information presented at the Annual Peer Review of the Superconductivity Program For Electric Power Systems. Topics include: Wire development; powder synthesis; characterization of superconducting materials; electric power applications; and motor cooling issues. Individual reports were processed separately for the database. DOE

N95-24453# Department of Energy, Washington, DC.
SUPERCONDUCTIVITY PROGRAM FOR ELECTRIC POWER SYSTEMS: 1994 ANNUAL PEER REVIEW. VOLUME 2, MEETING PROCEEDINGS
29 Jul. 1994 382 p Presented at conference held in Alexandria, VA, 19-20 Jul. 1994
(DE95-005059; CONF-9407153-Vol-2) Avail: CASI HC A17/MF A03

This is volume 2 of information that was presented at the 1994 Annual Peer Review, Superconductivity Program For Electric Power. Topics include component development; characterization of high-(Tc) Superconductors; wire development; coils; magnetic refrigerators; motor cooling issues; and magnetic separation. Individual projects were processed separately for the database. DOE

N95-24468# Joint Publications Research Service, Washington, DC.
JPRS REPORT: SCIENCE AND TECHNOLOGY. CENTRAL EURASIA
15 Feb. 1995 78 p Transl. into ENGLISH from various Central Eurasian articles
(JPRS-UST-95-008) Avail: CASI HC A05/MF A01

Translated articles cover the following topics: optical phonons and crystal lattice ordering of In(x)Ga(1-x)As solid solutions; radiation by dynamic conductivity of surface two-dimensional GaAs/AlGaAs superlattice by contactless SHF method in magnetic field; creation and study of optical properties in InGaAs/GaAs quantum wires; epitaxial growth of Si-Ge buffer layers with low dislocation density; ultrahigh-speed integrated circuits built with nonuniformly doped GaAs high-electron-mobility transistors; and depth of penetration into human skin of radio waves in the millimeter range. Author

N95-24470# Joint Publications Research Service, Washington, DC.
JPRS REPORT: SCIENCE AND TECHNOLOGY. CENTRAL EURASIA
31 Oct. 1994 48 p Transl. into ENGLISH from various Central Eurasian articles
(JPRS-UST-94-027) Avail: CASI HC A03/MF A01

Translated articles cover the following topics: delay effect and energy transfer through a turbulent atmosphere to a moving object; nonlinear phenomena in active phased arrays; linearizing modulation characteristics of microwave broadband avalanche transit time diode oscillators with varactor frequency turning; microwave radiation absorption by edge-type Josephson junctions in wide-band detection mode; and localization of vibrations in the shrouded blade assembly of the rotor wheel of a turbomachine. Author

N95-24476*# NYMA, Inc., Brook Park, OH.
BROADBAND UNIPLANAR MICROSTRIP TO SLOT-LINE TRANSITIONS Final Report
Nihad I. Dib (Michigan Univ., Ann Arbor, MI.), Rainee N. Simons, and Linda P. B. Katehi (Michigan Univ., Ann Arbor, MI.) CLEVELAND, OH NASA Mar. 1995 6 p Sponsored in cooperation with Army Research Office
(Contract NAS3-27186; RTOP 506-44-2C)
(NASA-CR-195448; E-9512; NAS 1.26:195448) Avail: CASI HC A02/MF A01

New in line uniplanar microstrip-to-slotline transitions for MIC/MMIC and phased array slotline antenna applications are described. Such transactions are compact and suitable to be used in an open environment or inside a package or a multichip module. The transitions share the concept of using a balun which consists of two microstrip lines connected to a slotline through a pair of coupled microstrips. The transitions are studied theoretically using the finite difference time domain (FDTD) technique and measured experimentally using an HP8510C Network Analyzer. For a back-to-back configuration, an insertion loss of less than 1.3 dB per transition is achieved over a 40% 3-dB bandwidth with a minimum of 0.6 dB at the design frequency. Author

N95-24482# Weizmann Inst. of Science, Rehovot (Israel). Dept. of Particle Physics.
ELECTRIC FIELD EFFECTS ON THE QUANTUM EFFICIENCY OF CESIUM-IODIDE PHOTOCATHODES IN GAS MEDIA
A. Breskin, A. Buzulutskov (Gosudarstvennyi Komitet po Ispolzovaniyu Atomnoi Energii, Protvino, USSR.), R. Chechik, D. Vartsky (Israel Atomic Energy Commission, Yavneh, Israel.), G. Malamud (Ecole Polytechnique, Palaiseau, France.), and P. Mine (Ecole Polytechnique, Palaiseau, France.) Dec. 1993 25 p Submitted for publication
(DE94-628176; WIS-PH-93-115) Avail: CASI HC A03/MF A01 (US Sales Only)

We have measured the quantum efficiency (QE) of Cesium iodide photocathodes as a function of the electric field strength in a parallel-plate geometry, in CH4, C2H6, and i-C4H10 both in charge collection and multiplication modes. It was found that in the collection mode the QE value in gases is lower compared to that of vacuum and is independent on the field; in gas media the QE starts to increase at the transition between collection and multiplication modes and reaches the vacuum value at high gas gain. We explain this effect by a decrease of the electron-molecule elastic backscattering while entering the multiplication mode. We conclude that the electric field effects observed here would also apply for other photocathodes and gas mixtures. An enhancement of the QE after micro discharges was observed and is discussed in detail. DOE

N95-24483# Weizmann Inst. of Science, Rehovot (Israel). Dept. of Particle Physics.
A CORRECTION OF THE QUANTUM EFFICIENCY OF CESIUM IODIDE AND OTHER PHOTOCATHODES DUE TO THE RECALIBRATION OF THE REFERENCE PHOTOMULTIPLIERS
A. Breskin, R. Chechik, D. Vartsky (Israel Atomic Energy Commission, Yavneh, Israel.), G. Malamud (Ecole Polytechnique, Palaiseau, France.), and P. Mine (Ecole Polytechnique, Palaiseau, France.) Dec. 1993 9 p Submitted for publication
(DE94-628177; WIS-PH-93-116) Avail: CASI HC A02/MF A01 (US Sales Only)

The quantum efficiency (QE) of four photomultipliers of the R1460 series of Hamammatsu, used in the last year as a reference in our ultraviolet-photocathode studies, was determined with the help of a calibrated vacuum ultraviolet-photodiode. Large discrepancies were found with respect to the quantum efficiency curves supplied for each tube by the manufacturer. The correction curves of the photomultipliers are presented and should be used to normalize our previously published quantum efficiency data for various photo-emissive materials. Corrected data of cesium iodide photocathodes are presented here. DOE

N95-24487# Joint Inst. for Nuclear Research, Dubna (USSR). Nuclear Problems Lab.
THE MEASUREMENT OF THE LOW FREQUENCY NOISE CHARACTERISTICS OF THE FIELD EFFECT TRANSISTORS FOR CRYOGENIC DETECTORS
V. A. Korobejnikov 1993 6 p In RUSSIAN; In RUSSIAN
(DE94-628257; JINR-R-13-93-331; Rept-P13-93-331) Avail: CASI HC A02/MF A01 (US Sales Only)

In this work low frequency noise characteristics of the Si field effect transistors at temperatures 300 and 77 K and GaAs transistors at temperatures 300, 77 and 4.2 K were measured. The lowest noise of 1.3 n V/radical Hz is provided by KP337g at room temperature. DOE

N95-24488# Sandia National Labs., Albuquerque, NM.
HIGH GAIN GaAs PHOTOCONDUCTIVE SEMICONDUCTOR SWITCHES (PCSS): DEVICE LIFETIME, HIGH CURRENT TESTING, OPTICAL PULSE GENERATORS
F. J. Zutavern, G. M. Loubriel, W. D. Helgeson, M. W. OMalley, R. R. Gallegos, H. P. Hjalmarson, A. G. Baca, and T. A. Plut 1995 9 p Presented at the Annual Conference of the Optical Society of America and Exhibit, Boston, MA, 30 Oct. - 4 Nov. 1994
(Contract DE-AC04-94AL-85000)
(DE95-003354; SAND-94-1186C; CONF-941006-3) Avail: CASI HC A02/MF A01

This paper presents results from three areas of GaAs PCSS research and development: device lifetime, high current switching, and PCSS-driven laser diode arrays (LDA). The authors have performed device lifetime tests on both lateral and vertical switches as a function of current amplitude, pulse width, and charging time. At present, their longest-lived switch reached 4 x 10(exp 6) pulses. Scanning electron microscope (SEM) images show damage near the contacts even after only 5 pulses. They are presently searching for the threshold at which no damage is evident after a single shot. In high current tests, they have reached 5.2 kA at 4.2 kV. This was achieved using twenty fiber-optic coupled lasers to distribute current filaments

over a 5 mm wide PCSS. Current waveforms and images of the current filaments as a function of current amplitude will be presented. The lasers used to trigger the high current PCSS were driven with a miniature PCSS. Low inductance, high speed GaAs PCSS are very effective as short pulse laser diode array drivers. Some types of arrays gain switch, producing a compressed optical pulse which is only 75 ps wide. Results from tests with a variety of laser diode arrays will be presented. DOE

N95-24532 Allied-Signal Aerospace Co., Kansas City, MO.
PIEZOELECTRIC MOTOR DEVELOPMENT AT ALLIEDSIGNAL INC., KANSAS CITY DIVISION
Robert B. Pressly and Charles P. Mentesana Nov. 1994 11 p Presented at the Technology 2004, Washington, DC, 8-10 Nov. 1994
(Contract DE-AC04-76DP-00613)
(DE95-003389; KCP-613-5515; CONF-9411151-1) Copyright Avail: Issuing Activity (Department of Energy (DOE))

The Kansas City Division of AlliedSignal Inc. has been investigating the fabrication and use of piezoelectric motors in mechanisms for United States Department of Energy (DOE) weapons applications for about four years. These motors exhibit advantages over solenoids and other electromagnetic actuators. Prototype processes have been developed for complete fabrication of motors from stock materials, including abrasive machining of piezoelectric ceramics and more traditional machining of other motor components, electrode plating and sputtering, electric poling, cleaning, bonding and assembly. Drive circuits have been fabricated and motor controls are being developed. Laboratory facilities have been established for electrical/mechanical testing and evaluation of piezo materials and completed motors. Recent project efforts have focused on the potential of piezoelectric devices for commercial and industrial use. A broad range of various motor types and application areas has been identified, primarily in Japan. The Japanese have been developing piezo motors for many years and have more recently begun commercialization. Piezoelectric motor and actuator technology is emerging in the United States and quickly gaining in commercial interest. The Kansas City Division is continuing development of piezoelectric motors and actuators for defense applications while supporting and participating in the commercialization of piezoelectric devices with private industry through various technology transfer and cooperative development initiatives. DOE

N95-24551# California Univ., Berkeley. Lawrence Berkeley Lab, CA. Accelerator and Fusion Research Div.
SUPERCONDUCTING MAGNETS, 1994
Aug. 1994 14 p
(Contract DE-AC03-76SF-00098)
(DE95-003813; LBL-35476) Avail: CASI HC A03/MF A01

This report discusses the following topics on superconducting magnets: D19B and -C: The next steps for a record-setting magnet; D20: The push beyond 10 T: Beyond D20: Speculations on the 16-T regime; other advanced magnets for accelerators; spinoff applications; APC materials development; cable and cabling-machine development; and high-(Tc) superconductor at low temperature. DOE

N95-24586# Sandia National Labs., Albuquerque, NM.
THE POTENTIAL OF VACUUM MICROELECTRONICS FOR SPACE REACTOR APPLICATIONS
Donald B. King, James G. Fleming, and Robert J. Walko 1994 6 p Presented at the 12th Symposium on Space Nuclear Power and Propulsion, Albuquerque, NM, 8-12 Jan. 1995
(Contract DE-AC04-94AL-85000)
(DE95-000542; SAND-94-2322C; CONF-950110-3) Avail: CASI HC A02/MF A01

This report discusses matrixed field emission devices which have been fabricated using a modification of standard integrated circuit fabrication techniques. The emitter-to-gate spacing is fixed by the thickness of a deposited oxide and not by photolithographic techniques. Functioning triodes have been fabricated using this deposited oxide spacer approach. Measured emission current to a collector electrically and physically separated from the matrixed emission array follows Fowler-Nordheim behavior. Modeling of the potential field near the emitter and gate structures as well as the emitted electron trajectories with a two-dimensional, Poisson solver, finite-difference code was used to evaluate and improve field emission structures. DOE

N95-24589# Los Alamos National Lab., NM.
EXPERIMENTAL AND THEORETICAL DEVELOPMENT TOWARDS A 500 MW, ONE-MICROSECOND, L-BAND RELATIVISTIC KLYSTRON AMPLIFIER
W. Brian Haynes, Michael V. Fazio, Bruce E. Carlsten, and Ray M. Stringfield 1994 9 p Presented at the Pulsed Radio Frequency Sources for Linear Colliders, Long Island, NY, 2-7 Oct. 1994
(Contract W-7405-eng-36)
(DE95-003682; LA-UR-94-4061; CONF-9410218-4) Avail: CASI HC A02/MF A01 (US Sales Only)

This paper describes the experimental development of a long pulse, high current, annular beam relativistic klystron amplifier. The desired performance parameters are 1 GW output power and 1 (mu)s pulse length with an operating frequency of 1.3 GHz. The electron beam voltage and current are nominally 600 kV and 5 kA. Peak powers approaching 500 MW have been achieved in pulses of 1 (mu)s nominal baseline-to-baseline duration. The half power pulse width is 0.5 (mu)s. These pulses contain an energy of about 160 J. The design of this class of tube presents some unique challenges, particularly in the output cavity. The output cavity must exhibit a very low gap shunt impedance in order to obtain reasonable conversion efficiency from the low impedance modulated electron beam to microwave power, while still maintaining a reasonable loaded Q for mode purity. The physics of this device is dominated by space charge effects which strongly impact the design. Current experimental results and theoretical design considerations for this class of tube, and scaling to higher frequency operation, suitable for the Next Linear Collider are discussed. DOE

N95-24620# Joint Publications Research Service, Washington, DC.
JPRS REPORT: SCIENCE AND TECHNOLOGY. CENTRAL EURASIA
17 Oct. 1994 104 p Transl. into ENGLISH from various Central Eurasian articles
(JPRS-UST-94-024) Avail: CASI HC A06/MF A02

Translated articles cover the following topics: study of the effect of nonlinear scattering of radio waves by metallic objects; estimating the directional vectors of an object's motion based on goniometricsystems; using modulation in microwave generators to produce a stochastic output signal; pulsed dense gas lasers pumped by self-sustained discharge; long-puls XeCl laser emission of ultrashort puls sequences with continuously tunable wavelengh; adaptive correction of direction of laser beam propagation in turbulent atmosphere. CASI

N95-24690# Bhabha Atomic Research Centre, Bombay (India). Radiation Safety Systems Div.
PC BASED ANALYSIS OF GAMMA RAY SPECTRA GENERATED BY SEMICONDUCTOR DETECTORS
M. C. Abani and V. K. Madan 1993 34 p
(DE94-628381; BARC-1993/E/025) Avail: CASI HC A03/MF A01 (US Sales Only)

This report describes a spectrum analysis method and computer program for analysis of gamma spectra obtained by using semiconductor detectors and multichannel analyzers. The analysis steps incorporated are: smoothing; peak location using signal processing method of convolution; selectable background subtraction viz linear; polynomial and step like; peak fitting both for singlets and doublets using Mukoyama's method for evaluation of full width at half maximum; and areaevaluation including errors in its evaluation. The program also provides a facility for energy calibration. Typical results of analysis for singlets and doublets are included. This report is based on Wilson's report which has been modified and extended. The program is written in BASIC and its listing is included in the appendices. DOE

N95-24701# National Lab. for High Energy Physics, Tsukuba (Japan).
HIGH-GRADIENT EXPERIMENT ON X-BAND DISK-LOADED STRUCTURES
T. Higo, T. Taniuchi, M. Yamamoto, J. Odagiri, S. Tokumoto, H. Mizuno, K. Takata, I. Wilson (European Organization for Nuclear Research, Geneva, Switzerland.), and W. Wuensch (European Organization for Nuclear Research, Geneva, Switzerland.) Sep. 1993 36 p
(DE94-765446; KEK-93-9) Avail: CASI HC A03/MF A01 (US Sales Only)

The high-gradient performance of two travelling-wave X-band accelerating structures 20 cm long has been studied. One of the structures, KEK, was

conditioned up to an average accelerating gradient (Eav) of 68 MV/m in 600 hours, while the other, CERN, reached 85 MV/m in 50 hours. In the latter case the maximum output power was fed from the SLED system and the maximum field inside the structure was 138 MV/m. This maximum level was limited by the available power from the klystron. Operation at the Eav=50 MV/m level was found to be stable for both structures. The associated dark current at this level was less than a few (mu)A for CERN but 20 to 30 (mu)A for KEK. Since the two electrical designs are almost the same the difference in dark current must be attributed to the difference in the two fabrication techniques. Modified Fowler-Northeim plots of downstream dark current showed a change of slope, a kink, around 50 to 60 MV/m above which the field enhancement factor was substantially increased. DOE

N95-24712# Sandia National Labs., Albuquerque, NM. Materials and Process Sciences Center.

ASSESSING CAPILLARY FLOW ON PRINTED WIRING BOARD SURFACES

F. M. Hosking, F. G. Yost, C. L. Hernandez, and S. J. Sackinger 1994 5 p Presented at the InterPack 1995: International Electronic Packaging Conference, Maui, HI, 26-30 Mar. 1995

(Contract DE-AC04-94AL-85000)

(DE94-015768; SAND-94-1112C; CONF-950344-1) Avail: CASI HC A01/MF A01

A solderability test for evaluating capillary flow on printed wiring boards is presented. The test measures the flow of molten solder from a pad of fixed diameter onto attached strips of different widths. The technique simulates capillary flow behavior, including wetting kinetics, during typical electronics soldering. A flow model is proposed. Computational and experimental data are compared. DOE

N95-24713# Sandia National Labs., Albuquerque, NM.

USING CONSUMER IC PACKAGES IN HARSH HIGH RELIABILITY APPLICATIONS

Cathleen A. Reber and David W. Palmer 1994 8 p Presented at the InterPack 1995: International Electronic Packaging Conference, Maui, HI, 26-30 Mar. 1995

(Contract DE-AC04-94AL-85000)

(DE94-016565; SAND-94-1982C; CONF-950344-2) Avail: CASI HC A02/MF A01

The improvements in purity of molding materials, the IC wafer passivation layers, and manufacturing quality have resulted over the last decade in extremely high reliability in commercial IC packages. In contrast the ceramic/hermetic package world is suffering from limited availability of the newest IC chips, higher cost, larger size, and decreasing quality and fewer manufacturing lines. Traditional manufacturing line qualification tests are a good start for conversion to commercial plastic parts. However, the use of standard sensitive test chips instead of product die is necessary to perform affordable, quantitative evaluations. These test chips have many integrated sensors measuring chemical, mechanical, thermal, and electrical degradation caused by manufacturing and the package environment. Besides visual, electrical test, and burn-in little has been documented on 100% nondestructive screening of plastic molded parts. Based on realistic process control and system engineer cultural expectations, user screening is necessary. Nondestructive tests of moisture and temperature excursion susceptibility are described. DOE

N95-24842# Centro Brasileiro de Pesquisas Fisicas, Rio de Janeiro.

INTRINSIC MAGNETIC TORQUE AT LOW MAGNETIC INDUCTION

M. M. Doria and I. G. deOliviera 1993 28 p

(DE95-601209; CBPF-NF-044/93) Avail: CASI HC A03/MF A01 (US Sales Only)

Using anisotropic London theory the intrinsic magnetic torque for extreme type 2 uniaxial superconductors for any value of the magnetic induction is obtained. It considered the vortex lines straight and takes into account the contribution of the supercurrents flowing inside the vortex core within the London theory. It is shown that the interline and intra line free energies give opposite torque contributions, the first drives the magnetic induction parallel to the superconductor's axis of symmetry and the second orthogonal to it. At high magnetic induction, torque expression obtained generalizes V. Kogan's formula since it has no free parameters other than the anisotropy (gamma) = m(sub 1)/m(sub 3) and the Ginzburg-Landau parameter (kappa). At low magnetic induction a way is proposed to observe vortex chain effects in the total torque based on the fact that London theory is linear and the energy to make a single vortex line in space is independent of the magnetic induction. DOE

N95-25116 Polish Academy of Sciences, Warsaw (Poland). Instytut Podstawowych Problemow Techniki.

TYPE P DISPERSIVE DELAY LINES [DYSPERSYJNE LINIE OPZNIAJACE TYPU P]

Eugeniusz Danicki 1993 25 p In POLISH

(ISSN 0208-5658)

Avail: Issuing Activity

Analysis and synthesis of dispersive interdigital transducers of surface acoustic waves and delay lines are presented. Some experimental and technological methods useful in designing Surface Acoustic Wave (SAW) devices for radar applications, spectral analyzers, etc. are described. The paper allows system designers to evaluate the parameters of SAW chirp filters required in designing amplifiers and electric circuits at both ends of DDLs. The main purpose of the paper is to provide system engineers with sufficient information for unaided designing of typical DDLs, and obtaining the working model with the help of enlisted institutions having corresponding technological facilities. Author

N95-25307* National Aeronautics and Space Administration. Pasadena Office, CA.

OPTICALLY-SWITCHED SUBMILLIMETER-WAVE OSCILLATOR AND RADIATOR HAVING A SWITCH-TO-SWITCH PROPAGATION DELAY

Patent

Michael G. Spencer, inventor (to NASA) (Jet Propulsion Lab., California Inst. of Tech., Pasadena, CA.) and Joseph Maserjian, inventor (to NASA) (Jet Propulsion Lab., California Inst. of Tech., Pasadena, CA.) 28 Mar. 1995 15 p Filed 23 Sep. 1993 Supersedes N94-17324 (32 - 3, p 1014)

(Contract NAS7-918)

(NASA-Case-NPO-18547-1-CU; US-Patent-5,401,953;

US-Patent-Appl-SN-125966; US-Patent-Class-250-208.4;

US-Patent-Class-330-4.5; US-Patent-Class-372-4;

US-Patent-Class-250-214.1; Int-Patent-Class-H01J-40/14) Avail: US Patent and Trademark Office

A submillimeter wave-generating integrated circuit includes an array of N photoconductive switches biased across a common voltage source and an optical path difference from a common optical pulse of repetition rate f sub 0 providing a different optical delay to each of the switches. In one embodiment, each incoming pulse is applied to successive ones of the N switches with successive delays. The N switches are spaced apart with a suitable switch-to-switch spacing so as to generate at the output load or antenna radiation of a submillimeter wave frequency f on the order of N f sub 0. Preferably, the optical pulse has a repetition rate of at least 10 GHz and N is of the order of 100, so that the circuit generates radiation of frequency of the order of or greater than 1 Terahertz.

Official Gazette of the U.S. Patent and Trademark Office

N95-25385# Los Alamos National Lab., NM.

RADIAL ELECTRON-BEAM-BREAKUP TRANSIT-TIME OSCILLATOR

M. A. Mostrom (Mission Research Corp., Albuquerque, NM.) and T. J. T. Kwan 1995 11 p

(Contract W-7405-eng-36)

(DE95-005731; LA-SUB-94-169) Avail: CASI HC A03/MF A01

A new radially-driven electron-beam-breakup transit-time oscillator has been investigated analytically and through computer simulation as a compact low-impedance high-power microwave generator. In a 1MV, 50kA device 35cm in radius and 15cm long, with no external magnetic field, 5GW of extracted power and a growth rate of 0.26/ns have been observed. Theoretical maximum efficiencies are several times higher. DOE

N95-25405# Centro Brasileiro de Pesquisas Fisicas, Rio de Janeiro.

Fe-57 AND Sn-119 MOESSBAUER STUDIES ON La(1.25)Nd(0.6)Sr(0.15)CuO4: EVIDENCE FOR LOCAL MAGNETIC ORDERING BELOW (APPROX. EQUAL) 32 K

M. Breuer (Cologne Univ., Germany.), B. Buechner (Cologne Univ., Germany.), H. Micklitz (Cologne Univ., Germany.), E. Baggio-Saitovitch, I. S. Azevedo, R. B. Scorzelli, and M. M. Abd-Elmguid (Ruhr Univ., Bochum,

Germany.) 1993 19 p Submitted for publication Sponsored by the Deutsche Forschungagermeinschaft
(DE95-601210; CBPF-NF-046/93) Avail: CASI HC A03/MF A01 (US Sales Only)

Fe-57 and Sn-119 Moessbauer effect studies on 0.5 at % Fe-57 (or Sn-119) doped non-superconducting La(1.25)Nd(0.6)Sr(0.15)CuO4 in the temperature region 300 K greater than or equal to T greater than or equal to 4.2 K reveal an onset of local magnetic ordering occurring at T(sub mu) approximately equal to 32 K for both Fe-57 as well as Sn-119 -doped samples. The local magnetic ordering shows up in the presence of a very large transferred hyperfine field at the Sn-119 nuclei. Since such a large field is neither present in antiferromagnetic La2CuO4 nor in superconducting La(1.85)Sr(0.15)CuO4 or overdoped La(2-x)Sr(x)CuO4 (x=0.4), the occurrence of such local spin correlations seems to be a signature of the non-superconducting low temperature tetragonal phase of La(1.25)Nd(0.6)Sr(0.15)CuO4. DOE

N95-25472# Swedish Inst. for Materials Testing, Boras (Sweden).
CROSSTALK ON PRINTED CIRCUIT BOARDS
Jan Carlsson 1994 44 p
(ISSN 0284-5172)
(PB95-165171; SP-RAPP-1994:14; ISBN-91-7848-473-1) Avail: CASI HC A03/MF A01

Crosstalk parallel conductors are examined in this document. The conductors can represent either conductors in a multiconductor cable or traces on a printed circuit board (PCB). An analysis method based on a lumped circuit equivalent for the problem as well as a method to calculate the per unit length parameters are presented. The computed results are validated by comparison with measurements as well as an exact solution of the multiconductor transmission line equations. Several PCB-layouts are analyzed to demonstrate how the crosstalk on a PCB can be minimized. NTIS

N95-25558# Sandia National Labs., Albuquerque, NM. Sensors and Electronics Dept.
THE IMPACT OF MULTIPLEXING ON THE DYNAMIC REQUIREMENTS OF ANALOG-TO-DIGITAL CONVERTERS
Tim J. Sobering and R. Rex Kay 1994 5 p Presented at the IEEE Instrumentation/Measurement Technology Conference: Annual Conference and Technical Meeting of the IEEE Instrumentation and Measurement Society: I3C - Integrating Intelligent Instrumentation and Control, Waltham, MA
(Contract DE-AC04-94AL-85000)
(DE95-006302; SAND-94-2577C; CONF-950436-1) Avail: CASI HC A01/MF A01

In data acquisition applications where the signals being digitized are produced in a time-division multiplexed system, the required dynamic performance of the analog-to-digital converter (ADC) is no longer bound by the conditions set forth in the Sampling Theorem. This results from the introduction of very high frequency information by the multiplexing process which, while not necessarily containing information of interest, must be processed by the input circuitry of the ADC. In this situation, signal bandwidths and slew rates can greatly exceed those produced in a Nyquist limited system and can surpass the capability of the ADC, thus degrading overall system performance. This paper will examine two common multiplexing schemes and their impact on ADC dynamic requirements. First, we will examine a simple voltage multiplexing scheme typically found in state-of-health or data-logging applications and develop the necessary equations to show how the ADC dynamic requirements are affected. Then, the analysis will then be extended to a multiplexed photodiode array readout to see how this application further challenges the dynamic performance of the ADC. Finally, the issues associated with developing dynamic test methodologies for assessing ADC performance in multiplexed systems will be discussed. DOE

N95-25889* National Aeronautics and Space Administration. Goddard Space Flight Center, Greenbelt, MD.
CIRCUIT FOR HIGH RESOLUTION DECODING OF MULTI-ANODE MICROCHANNEL ARRAY DETECTORS Patent
David B. Kasle, inventor (to NASA) 7 Mar. 1995 16 p Filed 7 May 1992
(NASA-Case-GSC-13478-1; US-Patent-5,396,073; US-Patent-Appl-SN-880099; US-Patent-Class-250-385.1; US-Patent-Class-250-214VT; US-Patent-Class-364-413.13; Int-Patent-Class-G01T-1/18) Avail: US Patent and Trademark Office

A circuit for high resolution decoding of multi-anode microchannel array detectors consisting of input registers accepting transient inputs from the anode array; anode encoding logic circuits connected to the input registers; midpoint pipeline registers connected to the anode encoding logic circuits; and pixel decoding logic circuits connected to the midpoint pipeline registers is described. A high resolution algorithm circuit operates in parallel with the pixel decoding logic circuit and computes a high resolution least significant bit to enhance the multianode microchannel array detector's spatial resolution by halving the pixel size and doubling the number of pixels in each axis of the anode array. A multiplexer is connected to the pixel decoding logic circuit and allows a user selectable pixel address output according to the actual multi-anode microchannel array detector anode array size. An output register concatenates the high resolution least significant bit onto the standard ten bit pixel address location to provide an eleven bit pixel address, and also stores the full eleven bit pixel address. A timing and control state machine is connected to the input registers, the anode encoding logic circuits, and the output register for managing the overall operation of the circuit. Author

N95-26038* National Aeronautics and Space Administration. Goddard Space Flight Center, Greenbelt, MD.
HIGH INPUT IMPEDANCE AMPLIFIER Patent
Leonard L. Kleinberg 21 Mar. 1995 6 p Filed 26 Aug. 1993
(NASA-Case-GSC-13571-1; US-Patent-5,399,993; US-Patent-Appl-SN-113373; US-Patent-Class-330-293; US-Patent-Class-330-291; US-Patent-Class-330-292; US-Patent-Class-330-294; US-Patent-Class-330-109; Int-Patent-Class-H03H-3/00) Avail: US Patent and Trademark Office

High input impedance amplifiers are provided which reduce the input impedance solely to a capacitive reactance, or, in a somewhat more complex design, provide an extremely high essentially infinite, capacitive reactance. In one embodiment, where the input impedance is reduced in essence, to solely a capacitive reactance, an operational amplifier in a follower configuration is driven at its non-inverting input and a resistor with a predetermined magnitude is connected between the inverting and non-inverting inputs. A second embodiment eliminates the capacitance from the input by adding a second stage to the first embodiment. The second stage is a second operational amplifier in a non-inverting gain-stage configuration where the output of the first follower stage drives the non-inverting input of the second stage and the output of the second stage is fed back to the non-inverting input of the first stage through a capacitor of a predetermined magnitude. These amplifiers, while generally useful, are very useful as sensor buffer amplifiers that may eliminate significant sources of error. Official Gazette of the U.S. Patent and Trademark Office

N95-26092# Westinghouse Hanford Co., Richland, WA.
NATIONAL STANDARD AND CODE COMPLIANCE FOR ELECTRICAL EQUIPMENT INSTALLED IN HAZARDOUS LOCATIONS FOR THE VOID FRACTION INSTRUMENT
J. H. Bussell, J. D. Martin, and T. I. Stokes 26 Sep. 1994 19 p
(Contract DE-AC06-87RL-10930)
(DE95-002158; WHC-SD-WM-DA-159) Avail: CASI HC A03/MF A01

The hazardous area classification is evaluated and defined for the void fraction instrument (VFI). The void fraction instrument is an instrument that is used to measure gas bubble concentration in tank waste. It is a 18.3 m (60-foot) long pipe with swivel sampling head. The assembly is lowered into tank waste via an available riser and waste sample is obtained. The sample is obtained and the sample chamber is pressurized from a fixed volume chamber. The pressure is then measured and then the VFI is moved to the next sample elevation. DOE

N95-26100# International Centre for Theoretical Physics, Trieste (Italy).
CONDENSATE LOCALIZATION BY MESOSCALE DISORDER IN HIGH-T(SUB c) SUPERCONDUCTORS
N. Kumar Jun. 1994 7 p
(DE95-607819; IC-94/133) Avail: CASI HC A02/MF A01 (US Sales Only)

We propose and solve approximately a phenomenological model for

Anderson localization of the macroscopic wavefunction for an inhomogeneous superconductor quench-disordered on the mesoscale of the order of the coherence length xi(sub 0). Our treatment is based on the nonlinear Schroedinger equation resulting from the Ginzburg-Landau free-energy functional having a spatially random coefficient representing spatial disorder of the pairing interaction. Linearization of the equation, valid close to the critical temperature T(sub c), or to the upper critical field H(sub c2) (T(sub c)) maps it to the Anderson localization problem with T(sub c) identified with the mobility edge. For the highly anisotropic high-T(sub c) materials and thin (2D) films in the quantum Hall geometry, we predict windows of reentrant superconductivity centered at integrally spaced temperature values. Our model treatment also provides a possible explanation for the critical current J(sub c perpendicular) becoming nonzero on cooling before J(sub c parallel) does in some high-T(sub c) superconductors. DOE

N95-26186 Office of Naval Research, Arlington, VA.
DIFFERENTIAL PREAMPLIFIER AND PRE-EMPHASIS NETWORK Patent Application
James D. Hagerty, inventor (to Navy) 7 Oct. 1994 16 p Filed 7 Oct. 1994 Limited Reproducibility: More than 20% of this document may be affected by microfiche quality
(AD-A288780; US-Patent-Appl-SN-319688; Navy-Case-75409) Avail: Issuing Activity (Defense Technical Information Center (DTIC))

A preamplifier and pre-emphasis network is provided having a differential amplifier exhibiting common mode noise rejection. The preamplifier is particularly suited for use with a double-sided sensor element and it includes a double-sided, balanced calibration circuit. First and second variable gain buffers are joined to the differential amplifier for preventing current noise degradation at the differential amplifier inputs. A pre-emphasis network is further provided in conjunction with the variable gain buffers for providing balanced differential ain of the sensor element signal. Further elements of the invention provide for high and low pass filtering, and differential buffering of the output signal. DTIC

34 FLUID MECHANICS AND HEAT TRANSFER

Includes boundary layers; hydrodynamics; fluidics; mass transfer; and ablation cooling.

For related information see also *02 Aerodynamics* and *77 Thermodynamics and Statistical Physics.*

N95-24221*# Rensselaer Polytechnic Inst., Troy, NY. Dept. of Materials Engineering.
KINETICS OF DIFFUSIONAL DROPLET GROWTH IN A LIQUID/LIQUID TWO-PHASE SYSTEM Final Technical Report
M. E. Glickman and V. E. Fradkov 1 Jan. 1995 26 p
(Grant NAG8-864)
(NASA-CR-198050; NAS 1.26:198050) Avail: CASI HC A03/MF A01

A new powerful experimental technique based on holographic observations, developed at the NASA Marshall Space Flight Center, now permits observation of small liquid droplets coarsening. This technique was developed and used for mixed-dimensional coarsening studies. Experiments were conducted on an isopycnic two-phase alloy of succinonitrile and water, annealed isothermally over a four-month period. The succinonitrile-rich droplets precipitate from a water-rich liquid matrix having a density very close to that of the droplets. The matrix and droplets, however, have different optical indices. The results of these experiments, along with the results of computer simulation based on the quasi-static diffusion approximation developed at Rensselaer are reported. These results were published recently. Copies of these papers are attached to this report. Derived from text

N95-24262# Sandia National Labs., Albuquerque, NM.
IMPLEMENTATION OF A PARALLEL ALGORITHM FOR THERMO-CHEMICAL NONEQUILIBRIUM FLOW SIMULATIONS
C. C. Wong, F. G. Blottner, J. L. Payne, and M. Soetrisno (Amtec Engineering, Inc., Bellevue, WA.) 1995 10 p Presented at the 33rd AIAA Aerospace Sciences Meeting, Reno, NV, 9-12 Jan. 1995
(Contract DE-AC04-94AL-85000)
(DE95-004758; SAND-94-1403C; CONF-950130-2) Avail: CASI HC A02/MF A01

Massively parallel (MP) computing is considered to be the future direction of high performance computing. When engineers apply this new MP computing technology to solve large-scale problems, one major interest is what is the maximum problem size that a MP computer can handle. To determine the maximum size, it is important to address the code scalability issue. Scalability implies whether the code can provide an increase in performance proportional to an increase in problem size. If the size of the problem increases, by utilizing more computer nodes, the ideal elapsed time to simulate a problem should not increase much. Hence one important task in the development of the MP computing technology is to ensure scalability. A scalable code is an efficient code. In order to obtain good scaled performance, it is necessary to first have the code optimized for a single node performance before proceeding to a large-scale simulation with a large number of computer nodes. This paper will discuss the implementation of a massively parallel computing strategy and the process of optimization to improve the scaled performance. Specifically, we will look at domain decomposition, resource management in the code, communication overhead, and problem mapping. By incorporating these improvements and adopting an efficient MP computing strategy, an efficiency of about 85% and 96%, respectively, has been achieved using 64 nodes on MP computers for both perfect gas and chemically reactive gas problems. A comparison of the performance between MP computers and a vectorized computer, such as Cray-YMP, will also be presented. DOE

N95-24396*# National Aeronautics and Space Administration. Langley Research Center, Hampton, VA.
DSMC CALCULATIONS FOR 70-DEG BLUNTED CONE AT 3.2 km/s IN NITROGEN
J. N. Moss, J. M. Price, and V. K. Dogra (Vigyan Research Associates, Inc., Hampton, VA.) Jan. 1995 54 p
(RTOP 242-80-01-01)
(NASA-TM-109181; NAS 1.15:109181) Avail: CASI HC A04/MF A01

Numerical results obtained with the direct simulation Monte Carlo (DSMC) method are presented for Mach 15.6 nitrogen flow about a 70-deg spherically blunted cone at zero incidence. This flow condition is one of several generated in the Large Energy National Shock (LENS) tunnel during tests of a 15.24 cm diameter model with an afterbody sting. The freestream Knudsen number, based on model diameter, is 0.0023. The focus of the DSMC calculations is to characterize the near wake flow under conditions where rarefaction effects may influence afterbody aerothermal loads. This report provides information concerning computational details along with flowfield and surface quantities. Calculations show that the flow enveloping the test model is in thermal nonequilibrium and a sizable vortex develops in the near wake. Along the model baseplane the heating rates are about 0.6 percent of the forebody stagnation value while the maximum heating along the sting is about 4.2 percent of the forebody stagnation value. Comparison of a Navier-Stokes solution with the present calculations show good agreement for surface heating, pressure, and skin friction results. Author

N95-24399*# National Aeronautics and Space Administration. Lewis Research Center, Cleveland, OH.
INVESTIGATION OF CONVECTION AND PRESSURE TREATMENT WITH SPLITTING TECHNIQUES
Siddharth Thakur (Florida Univ., Gainesville, FL.), Wei Shyy, and Meng-Sing Liou Mar. 1995 39 p
(Contract NCC3-370; RTOP 505-90-5K)
(NASA-TM-106868; E-9483; NAS 1.15:106868; ICOMP-95-3) Avail: CASI HC A03/MF A01

Treatment of convective and pressure fluxes in the Euler and Navier-Stokes equations using splitting formulas for convective velocity and pressure is investigated. Two schemes - controlled variation scheme (CVS) and advection upstream splitting method (AUSM) - are explored for their accuracy in resolving sharp gradients in flows involving moving or reflecting shock waves as well as a one-dimensional combusting flow with a strong heat release source term. For two-dimensional compressible flow computations, these two schemes are implemented in one of the pressure-based algorithms, whose very basis is the separate treatment of convective and pressure fluxes. For the convective fluxes in the momentum

equations as well as the estimation of mass fluxes in the pressure correction equation (which is derived from the momentum and continuity equations) of the present algorithm, both first- and second-order (with minmod limiter) flux estimations are employed. Some issues resulting from the conventional use in pressure-based methods of a staggered grid, for the location of velocity components and pressure, are also addressed. Using the second-order fluxes, both CVS and AUSM type schemes exhibit sharp resolution. Overall, the combination of upwinding and splitting for the convective and pressure fluxes separately exhibits robust performance for a variety of flows and is particularly amenable for adoption in pressure-based methods. Author

N95-24412*# California Univ., Los Angeles, CA. Dept. of Mechanical Aerospace and Nuclear Engineering.

EFFECT OF DENSITY GRADIENTS IN CONFINED SUPERSONIC SHEAR LAYERS, PART 1

Oshin Peroomian and R. E. Kelly 7 Nov. 1994 83 p

(Contract NCC2-374)

(NASA-CR-198029; NAS 1.26:198029) Avail: CASI HC A05/MF A01

The effect of density gradients on the supersonic wall modes (acoustic modes) of a 2-D confined compressible shear layer were investigated using linear analysis. Due to the inadequacies of the hyperbolic tangent profile, the boundary layer basic profiles were used. First a test case was taken with the same parameters as in Tam and Hu's analysis with convective Mach number M(sub c) = 1.836 and density ratio of 1.398. Three generalized inflection points were found giving rise to three modes. The first two show similar properties to the Class A and B modes, and the third is an 'inner mode' which will be called a Class C mode. As the density ratio is increased, the smallest of the three neutral phase speeds tends towards the speed of the lower velocity stream, and the other two eventually coalesce and then disappear. These two effects lead to a linear resonance between the Class B modes which increases the cutoff frequency and growth rate of the lowest mode. In fact, growth rates of 2-4 times the test case were found as the density ratio was increased to 7. A similar trend is observed for the Class A modes when the density ratio is decreased from the test case, but the growth rate is not changed by much from the test case.

Author

N95-24413*# California Univ., Los Angeles, CA. Dept. of Mechanical Aerospace and Nuclear Engineering.

EFFECT OF DENSITY GRADIENTS IN CONFINED SUPERSONIC SHEAR LAYERS. PART 2: 3-D MODES

Oshin Peroomian and R. E. Kelly 7 Nov. 1994 35 p

(Contract NCC2-374)

(NASA-CR-198030; NAS 1.26:198030) Avail: CASI HC A03/MF A01

The effect of basic flow density gradients on the supersonic wall modes were investigated in Part 1 of this analysis. In that investigation only the 2-D modes were studied. Tam and Hu investigated the 3-D modes in a confined vortex sheet and reported that the first 2-D Class A mode (A01) had the highest growth rate compared to all other 2-D and 3-D modes present in the vortex sheet for that particular set of flow patterns. They also showed that this result also held true for finite thickness shear layers with delta(sub w) less than 0.125. For free shear layers, Sandham and Reynolds showed that the 3-D K-H mode became the dominant mode for M(sub c) greater than 0.6. Jackson and Grosch investigated the effect of crossflow and obliqueness on the slow and fast odes present in a M(sub c) greater than 1 environment and showed that for certain combination of crossflow and wave angles the growth rates could be increased by up to a factor of 2 with respect to the 2-D case. The case studied here is a confined shear layer shown in Part 1. All solution procedures and basic low profiles are the same as in Part 1. The effect of density gradients on the 3-D modes present in the density ratios considered in Part 1 are investigated. Author

N95-24461*# Texas A&M Univ., College Station, TX. Dept. of Mechanical Engineering.

THERMOHYDRODYNAMIC ANALYSIS OF CRYOGENIC LIQUID TURBULENT FLOW FLUID FILM BEARINGS, PHASE 2 Annual Research Progress Report, 1 Jan. - 31 Dec. 1994

Luis SanAndres 31 Dec. 1994 211 p

(Grant NAG3-1434)

(NASA-CR-197412; NAS 1.26:197412) Avail: CASI HC A10/MF A03

The Phase 2 (1994) Annual Progress Report presents two major report sections describing the thermal analysis of tilting- and flexure-pad hybrid bearings, and the unsteady flow and transient response of a point mass rotor supported on fluid film bearings. A literature review on the subject of two-phase flow in fluid film bearings and part of the proposed work for 1995 are also included. The programs delivered at the end of 1994 are named hydroflext and hydrotran. Both codes are fully compatible with the hydrosealt (1993) program. The new programs retain the same calculating options of hydrosealt plus the added bearing geometries, and unsteady flow and transient forced response. Refer to the hydroflext & hydrotran User's Manual and Tutorial for basic information on the analysis and instructions to run the programs. The Examples Handbook contains the test bearing cases along with comparisons with experimental data or published analytical values. The following major tasks were completed in 1994 (Phase 2): (1) extension of the thermohydrodynamic analysis and development of computer program hydroflext to model various bearing geometries, namely, tilting-pad hydrodynamic journal bearings, flexure-pad cylindrical bearings (hydrostatic and hydrodynamic), and cylindrical pad bearings with a simple elastic matrix (ideal foil bearings); (2) improved thermal model including radial heat transfer through the bearing stator; (3) calculation of the unsteady bulk-flow field in fluid film bearings and the transient response of a point mass rotor supported on bearings; and (4) a literature review on the subject of two-phase flows and homogeneous-mixture flows in thin-film geometries. Derived from text

N95-24469# Joint Publications Research Service, Washington, DC.

JPRS REPORT: SCIENCE AND TECHNOLOGY. CENTRAL EURASIA

14 Nov. 1994 65 p Transl. into ENGLISH from various Central Eurasian articles

(JPRS-UST-94-030) Avail: CASI HC A04/MF A01

Translated articles cover the following topics: waves in an elastic prestressed compressible layer interacting with an ideal liquid; numerical solution of the 3D problem of high-speed interaction of a cylinder with a nondeformable barrier considering temperature effects; and mechanisms of the cytogenetic action of laser emissions. Author

N95-24489# Sandia National Labs., Albuquerque, NM.

SOLUTIONS OF TURBULENT BACKWARD-FACING STEP FLOW WITH HEAT TRANSFER USING THE FINITE VOLUME METHOD

R. H. Horstman (Boeing Commercial Airplane Co., Seattle, WA.), R. J. Cochran, and A. F. Emergy (Washington Univ., Seattle, WA.) 1995 9 p Presented at the American Society of Mechanical Engineers' Winter Annual Meeting, Chicago, IL, 9-11 Nov. 1994

(Contract DE-AC04-94AL-85000)

(DE95-003360; SAND-94-2264C; CONF-941142-26) Avail: CASI HC A02/MF A01

The heated turbulent flow over a backward-facing step is numerically solved using the commercial computational fluid dynamics program FLUENT. The methods used here consist of the default power-law upwinding scheme, default multigrid equation solution method and a standard k-epsilon turbulence model with wall functions. A total of four separate cases are reported. The four cases consist of combinations of partially and fully developed flow at the inlet with uniform or developed temperature profiles. Three mesh refinements are reported for each flow. DOE

N95-24580*# Institute for Computer Applications in Science and Engineering, Hampton, VA.

A REVIEW OF REYNOLDS STRESS MODELS FOR TURBULENT SHEAR FLOWS Final Report

Charles G. Speziale (Boston Univ., MA.) Mar. 1995 45 p Submitted for publication

(Contract NAS1-19480; RTOP 505-90-52-01; N00014-94-1-0088)

(NASA-CR-195054; NAS 1.26:195054; ICASE-95-15) Avail: CASI HC A03/MF A01

A detailed review of recent developments in Reynolds stress modeling for incompressible turbulent shear flows is provided. The mathematical foundations of both two-equation models and full second-order closures are explored in depth. It is shown how these models can be systematically derived for two-dimensional mean turbulent flows that are close to equilibrium. A variety of examples are provided to demonstrate how well properly calibrated versions of these models perform for such flows. However, substantial problems remain for the description of more complex

turbulent flows where there are large departures from equilibrium. Recent efforts to extend Reynolds stress models to nonequilibrium turbulent flows are discussed briefly along with the major modeling issues relevant to practical naval hydrodynamics applications. Author

N95-24584*# Institute for Computer Applications in Science and Engineering, Hampton, VA.
SPECTRUM AND ENERGY TRANSFER IN STEADY BURGERS TURBULENCE Final Report
Sharath S. Girimaji and Ye Zhou Mar. 1995 20 p Submitted for publication
(Contract NAS1-19480; RTOP 505-90-52-01)
(NASA-CR-195047; NAS 1.26:195047; ICASE-95-13) Avail: CASI HC A03/MF A01

The spectrum, energy transfer, and spectral interactions in steady Burgers turbulence are studied using numerically generated data. The velocity field is initially random and the turbulence is maintained steady by forcing the amplitude of a band of low wavenumbers to be invariant in time, while permitting the phase to change as dictated by the equation. The spectrum, as expected, is very different from that of Navier-Stokes turbulence. It is demonstrated that the far range of the spectrum scales as predicted by Burgers. Despite the difference in their spectra, in matters of the spectral energy transfer and triadic interactions Burgers turbulence is similar to Navier-Stokes turbulence. Author

N95-24628# Cleveland State Univ., OH. Dept. of Chemical Engineering.
NUMERICAL SIMULATION OF FLOW AND THE EFFECT OF BAFFLE ARRANGEMENT ON PRESSURE DROP AND TEMPERATURE PATTERN IN A CIRCULAR COMBUSTOR
Bahman Ghorashi and Sastry Taruvai [1991] 7 p
Avail: CASI HC A02/MF A01

A numerical simulation study was conducted to determine the effect of baffle arrangement on pressure drop in an experimental reverse-flow circular combustor with several mini-combustion zones (MCZ). The fluent computer code developed by Creare Inc., was used for this study. Three parameters which appeared to significantly affect the pressure drop were varied, and pressure drop for each case was numerically determined. The portion of the combustor volume that was investigated had two baffles on the upper face and two baffles on the lower face. Heated air at 1000 F with an inlet air velocity of 100 ft/sec and 1 atmosphere pressure was introduced into the combustor. Fuel (pentane) at 80 F was introduced via nozzles which were placed between the baffles. The following changes were then made in the baffle arrangement and the effects on the pressure drop and temperature distribution were evaluated for each of the following cases: (1) the positions of the baffles on the upper and lower face were changed; (2) the dimensions of the baffles were varied; (3) the shapes of the baffles were altered. The effects of the above mentioned design alterations are summarized. Author

N95-24678# California Univ., Santa Barbara, CA. Center for Risk Studies and Safety.
IGNITION OF EXPLODING ALUMINUM DROPLETS BEHIND SHOCK WAVES IN WATER
T. G. Theofanous, X. Chen, and P. DiPiazza Sep. 1994 29 p
(DE95-003975; DOE/ID-10456) Avail: CASI HC A03/MF A01 (US Sales Only)

This is an experimental study of the ignition of molten aluminum droplets in a well controlled and characterized simulated steam explosion environment. Ignition refers to the rapid oxidation of aluminum by steam, a reaction that can greatly augment the yield of the physical event (steam or thermal explosion). The simulated explosion environment was created in a hydrodynamic shock tube capable of producing sustained pressure pulses (2 ms duration) of amplitudes up to 50 MPa. The behavior of gram-quantities of molten aluminum droplets was studied as a function of their temperature in the 800 C (1073 K) to 1700 C (1973 K) range, and shock pressure, in the 6.8 to 40.8 MPa range. With the help of the resulting debris the authors have identified three main regimes of interaction: a 'chemical' one where 100% of the melt has been converted to finely pulverized (micron size) alpha-A2IO3 and gamma-AI2O3; a 'partially-chemical' one where only some fraction (10 to 40%) of the debris met the above 'chemical' characterization; and a 'physical' regime where no 'fines' or significant chemical oxidation of the melt was discernible. The work performed here involves extension of the working temperature range for shock tube research at UCSB to 1700 C and a breakthrough in demonstrating the effects of chemical reactions on the thermal interactions which had been the focus of fuel-coolant interaction (FCI) research. DOE

N95-24762# Cleveland State Univ., OH.
A REVIEW OF CHEMICALLY REACTIVE TURBULENT FLOW ANALYSIS, MIXING MECHANISMS AND MODELING, AND A NEW DESIGN OF LOW NOx COMBUSTOR FOR NON-PREMIXED REACTANTS
Giorgio McBeth and Bahman Ghorashi [1992] 13 p
Avail: CASI HC A03/MF A01

A review of chemically reactive flow analysis is presented. Key studies are reviewed. The approaches to modeling chemically reactive flows that are discussed are probability distribution function (PDF), conserved PDF, conserved scalar, stochastic, and mixing length. Turbulent mixing mechanisms are also discussed and a model is formulated that could be used for optimizing non-premixed gas reacting systems. Consequently, a re-examination of the NO(x) reduction concepts for non-premixed reactants is suggested, together with two new designs for low NO(x) subsonic combustor research. Author

N95-24906*# Houston Univ., TX. Dept. of Chemical Engineering.
STUDIES OF TWO-PHASE GAS-LIQUID FLOW IN MICROGRAVITY Ph.D. Thesis, Dec. 1994
William Scott Bousman Cleveland, OH NASA Feb. 1995 313 p
(Grant NAG3-510; RTOP 963-25-0A)
(NASA-CR-195434; E-9445; NAS 1.26:195434) Avail: CASI HC A14/MF A03

Two-phase gas-liquid flows are expected to occur in many future space operations. Due to a lack of buoyancy in the microgravity environment, two-phase flows are known to behave differently than those in earth gravity. Despite these concerns, little research has been conducted on microgravity two-phase flow and the current understanding is poor. This dissertation describes an experimental and modeling study of the characteristics of two-phase flows in microgravity. An experiment was operated onboard NASA aircraft capable of producing short periods of microgravity. In addition to high speed photographs of the flows, electronic measurements of void fraction, liquid film thickness, bubble and wave velocity, pressure drop and wall shear stress were made for a wide range of liquid and gas flow rates. The effects of liquid viscosity, surface tension and tube diameter on the behavior of these flows were also assessed. From the data collected, maps showing the occurrence of various flow patterns as a function of gas and liquid flow rates were constructed. Earth gravity two-phase flow models were compared to the results of the microgravity experiments and in some cases modified. Models were developed to predict the transitions on the flow pattern maps. Three flow patterns, bubble, slug and annular flow, were observed in microgravity. These patterns were found to occur in distinct regions of the gas-liquid flow rate parameter space. The effect of liquid viscosity, surface tension and tube diameter on the location of the boundaries of these regions was small. Void fraction and Weber number transition criteria both produced reasonable transition models. Void fraction and bubble velocity for bubble and slug flows were found to be well described by the Drift-Flux model used to describe such flows in earth gravity. Pressure drop modeling by the homogeneous flow model was inconclusive for bubble and slug flows. Annular flows were found to be complex systems of ring-like waves and a substrate film. Pressure drop was best fitted with the Lockhart- Martinelli model. Force balances suggest that droplet entrainment may be a large component of the total pressure drop. Author

N95-25001# National Aerospace Lab., Tokyo (Japan).
A STUDY OF THREE-DIMENSIONAL INTERACTION FLOW FIELDS BETWEEN SWEPT SHOCK WAVES AND TURBULENT BOUNDARY LAYERS. FLOW STRUCTURES AND EFFECTS OF BLEED
Masato Tamayama, Kimio Sakata, Ryouji Yanagi, Shigemi Shindo, Akira Murakami, and Shinji Honami (Tokyo Univ., Japan.) Mar. 1994 30 p In JAPANESE
(ISSN 0389-4010)
(NAL-TR-1227) Avail: CASI HC A03/MF A01

An experimental investigation of a three-dimensional flow field with a swept shock wave and a turbulent boundary layer interaction was made in

NAL's 1m x 1m Mach 4 supersonic wind tunnel. The emphasis of this study is placed on understanding the behaviors of the flow interactions with Mach number variation and the effects of bleed on the surface flow. A shock generator of 15 deg wedge placed normally on the flat plate was applied to generate an oblique shock wave. The experiments were conducted at Mach numbers of 3.25, 3.11, and 2.63. We adopted the conical coordinate system to analyze the flow. Air-bleed was also tested utilizing rows of bleed holes located at the foot print of the swept shock wave on the flat plate surface. It is generally accepted that the size and the strength of the separation vortex generated along the shock wave on the surface become wider and stronger as the Mach number increases. The corner flow around the leading edge of the shock generator was also clarified. As for the air-bleed, the suppression effects of the bleed on the separation vortex were also clarified at several bleed locations. The bleed upstream of the shock wave foot print effectively reduced the size of the vortex, while the downstream bleed suppressed the vortex strength. Therefore, it is concluded that the combination of the upstream and downstream bleed effectively suppresses the interaction between the shock wave and the boundary layer. Author

N95-25394*# Queensland Univ., Saint Lucia (Australia). Dept. of Mechanical Engineering.

SHOCK TUNNEL STUDIES OF SCRAMJET PHENOMENA 1993

R. J. Stalker, R. J. Bakos, R. G. Morgan, L. Porter, D. Mee, A. Paull, S. Tuttle, J. M. Simmons, M. Wendt, and K. Skinner et al Jan. 1995 108 p Sponsored in cooperation with the Australian Research Council and the Queen Elizabeth 2nd FellowshipScheme

(Grant NAGw-674; RTOP 505-70-62-04)

(NASA-CR-195038; NAS 1.26:195038) Avail: CASI HC A06/MF A02

Reports by the staff of the University of Queensland on various research studies related to the advancement of scramjet technology and hypervelocity pulse test facilities are presented. These reports document the tests conducted in the reflected shock tunnel T4 and supporting research facilities that have been used to study the injection, mixing, and combustion of hydrogen fuel in generic scramjets at flow conditions typical of hypersonic flight. In addition, topics include the development of instrumentation and measurement technology, such as combustor wall shear and stream composition in pulse facilities, and numerical studies and analyses of the scramjet combustor process and the test facility operation. This research activity is Supplement 10 under NASA Grant NAGw-674. For individual titles, see N95-25395 through N95-25400.

N95-25395*# Queensland Univ., Saint Lucia (Australia). Dept. of Mechanical Engineering.

THRUST MEASUREMENTS OF A COMPLETE AXISYMMETRIC SCRAMJET IN AN IMPULSE FACILITY **c07**

A. Paull, R. J. Stalker, and D. Mee *In its* Shock Tunnel Studies of Scramjet Phenomena 1993 Jan. 1995 p 15-18 Sponsored in cooperation with NASA. Langley Research Center and the Australian Research Council (For primary document see N95-25394 08-34)

Avail: CASI HC A01/MF A02

This paper describes tests which were conducted in the hypersonic impulse facility T4 on a fully integrated axisymmetric scramjet configuration. In these tests the net force on the scramjet vehicle was measured using a deconvolution force balance. This measurement technique and its application to a complex model such as the scramjet are discussed. Results are presented for the scramjet's aerodynamic drag and the net force on the scramjet when fuel is injected into the combustion chambers. It is shown that a scramjet using a hydrogen-silane fuel produces greater thrust than its aerodynamic drag at flight speeds equivalent to 260 m/s. Author

N95-25396*# Queensland Univ., Saint Lucia (Australia). Dept. of Mechanical Engineering.

SCRAMJET THRUST MEASUREMENT IN A SHOCK TUNNEL **c07**

A. Paull, R. J. Stalker, and D. J. Mee *In its* Shock Tunnel Studies of Scramjet Phenomena 1993 Jan. 1995 p 19-27 Sponsored in cooperation with the Australian Research Council (For primary document see N95-25394 08-34)

Avail: CASI HC A02/MF A02

This note reports tests in a shock tunnel in which a fully integrated scramjet configuration produced net thrust. The experiments not only showed that impulse facilities can be used for assessing thrust performance, but also were a demonstration of the application of a new technique to the measurement of thrust on scramjet configurations in shock tunnels. These two developments are of significance because scramjets are expected to operate at speeds well in excess of 2 km/sec, and shock tunnels offer a means of generating high Mach number flows at such speeds. Author

N95-25397*# Queensland Univ., Saint Lucia (Australia). Dept. of Mechanical Engineering.

THRUST MEASUREMENT IN A 2-D SCRAMJET NOZZLE **c07**

Sean Tuttle *In its* Shock Tunnel Studies of Scramjet Phenomena 1993 Jan. 1995 p 29-36 (For primary document see N95-25394 08-34)

Avail: CASI HC A02/MF A02

The two-dimensional thrust nozzle presents a challenging problem. The loading is not axisymmetric as in the case of a cone and the internal flow presents some design difficulties. A two-sting system has been chosen to accomodate the internal flow and achieve some symmetry. The situation is complicated by the fact that with the small ramp angle and the internal pressure on the nozzle walls, loading is predominantly transverse. Yet it is the axial thrust which is to be measured (i.e., the tensile waves propagating in the stings). Although bending stress waves travel at most at only 60% of the speed of the axial stress waves, the system needs to be stiffened against bending. The second sting was originally only used to preserve symmetry. However, the pressures on each thrust surface may be quite different at some conditions, so at this stage the signals from both stings are being averaged as a first order approximation of the net thrust. The expected axial thrust from this nozzle is not large so thin stings are required. In addition, the contact area between nozzle and sting needs to be maximized. The result was that it was decided to twist the stings through 90 deg, without distorting their cross-sectional shape, just aft of the nozzle. Finite element analysis showed that this would not significantly alter the propagation of the axial stress wave in the sting, while the rigidity of the system is greatly increased. A Mach 4 contoured nozzle is used in the experiments. The thrust calculated by integrating the static pressure measurements on the thrust surfaces is compared with the deconvolved strain measurement of the net thrust for the cases of air only and hydrogen fuel injected into air at approximately 9 MJ/kg nozzle supply enthalpy. The gain in thrust due to combustion is visible in this result. Derived from text

N95-25398*# Queensland Univ., Saint Lucia (Australia). Dept. of Mechanical Engineering.

SCALING IN A SCRAMJET COMBUSTOR **c25**

M. V. Pulsonetti and R. J. Stalker *In its* Shock Tunnel Studies of Scramjet Phenomena 1993 Jan. 1995 p 37-40 (For primary document see N95-25394 08-34)

Avail: CASI HC A01/MF A02

Studies of scramjet combustor scaling have been extended to include testing of a 'small' combustor, thereby allowing comparison with results obtained in a 'large' combustor of nearly identical configuration. The scale of the two combustors varied by a factor of 5. It was anticipated that the combustion process would scale as the product of pressure with length if the temperature, the Mach number, the velocity, the free stream composition and the equivalence ratio were the same. To achieve this while allowing for the necessary difference in pressure the two models were tested with different shock tunnel nozzles. The large was tested in a $M = 8$ nozzle, with an intake consisting of a pair of opposing wedges preceding the model, which produced shocks to reduce the Mach number to approximately 3.4 before the flow entered the model inlet. It was then expanded to raise the Mach number again. The small model was tested in a $M = 4$ nozzle, with the nozzle flow passing directly to the inlet of the model. The wedge intake for the large model was adjusted to yield similar combustion chamber Mach number for both models. Then, by matching the stagnation enthalpy, it was possible also to match the temperature and the velocity. The free stream composition was matched by operating at the same nozzle supply pressure. Wall pressure distributions were measured along each of the ducts. The pressure is normalized with respect to the pressure measured at the point opposite to the injector exit, and the distance downstream of the exit is normalized with respect to the height of the duct. It can be seen that, when normalized in this manner, both ducts produce quantitatively similar pressure distributions, confirming the initial hypothesis that the combustion process would scale as the product of pressure with length.

Derived from text

N95-25399*# Queensland Univ., Saint Lucia (Australia). Dept. of Mechanical Engineering.

THE SUPERORBITAL EXPANSION TUBE CONCEPT, EXPERIMENT AND ANALYSIS **c09**

A. J. Neely and R. G. Morgan *In its* Shock Tunnel Studies of Scramjet Phenomena 1993 Jan. 1995 p 97-105 Sponsored in cooperation with the Australian Research Council (For primary document see N95-25394 08-34)

Avail: CASI HC A02/MF A02

In response to the need for ground testing facilities for super orbital re-entry research, a small scale facility has been set up at the University of Queensland to demonstrate the superorbital expansion tube concept. This unique device is a free piston driven, triple diaphragm, impulse shock facility which uses the enthalpy multiplication mechanism of the unsteady expansion process and the addition of a secondary shock driver to further heat the driver gas. The pilot facility has been operated to produce quasi-steady test flows in air with shock velocities in excess of 13 km/s and with a usable test flow duration of the order of 15 micro sec. an experimental condition produced in the facility with total enthalpy of 108 MJ/kg and a total pressure of 335 MPa is reported. A simple analytical flow model which accounts for non-ideal rupture of the light tertiary diaphragm and the resulting entropy increase in the test gas is discussed. It is shown that equilibrium calculations more accurately model the unsteady expansion process than calculations assuming frozen chemistry. This is because the high enthalpy flows produced in the facility can only be achieved if the chemical energy stored in the test flow during shock heating of the test gas is partially returned to the flow during the process of unsteady expansion. Measurements of heat transfer rates to a flat plate demonstrate the usability of test flow for aerothermodynamic testing and comparison of these rates with empirical calculations confirms the usable accuracy of the flow model. Author

N95-25400*# Queensland Univ., Saint Lucia (Australia). Dept. of Mechanical Engineering.

BALANCES FOR THE MEASUREMENT OF MULTIPLE COMPONENTS OF FORCE IN FLOWS OF A MILLISECOND DURATION **c35**

D. J. Mee, W. J. Daniel, S. L. Tuttle, and J. M. Simmons *In its* Shock Tunnel Studies of Scramjet Phenomena 1993 Jan. 1995 p 107-112 Sponsored in cooperation with the Australian Research Council and the Queen Elizabeth 2nd FellowshipScheme (For primary document see N95-25394 08-34)

Avail: CASI HC A02/MF A02

This paper reports a new balance for the measurement of three components of force - lift, drag and pitching moment - in impulsively starting flows which have a duration of about one millisecond. The basics of the design of the balance are presented and results of tests on a 15 deg semi-angle cone set at incidence in the T4 shock tunnel are compared with predictions. These results indicate that the prototype balance performs well for a 1.9 kg, 220 mm long model. Also presented are results from initial bench tests of another application of the deconvolution force balance to the measurement of thrust produced by a 2D scramjet nozzle. Author

N95-25404# Oregon Univ., Eugene, OR. Dept. of Physics.

CRYOGENIC HELIUM GAS CONVECTION RESEARCH

Robert P. Behringer, Russell J. Donnelly, Michael McAshan, James Maddocks, Katepalli Sreenivasan, Chris Swanson, and Xaio-Zhong Wu Oct. 1994 202 p Prepared in cooperation with Yale Univ. and Duke Univ.

(Contracts DE-FG05-94ER-40878; DE-FG05-94ER-40876; DE-FG05-94ER-40877)

(DE95-004372; DOE/ER-40878/T1) Avail: CASI HC A10/MF A03

This is a report prepared by a group interested in doing research in thermal convection using the large scale refrigeration facilities available at the SSC Laboratories (SSCL). The group preparing this report consists of Michael McAshan at SSCL, Robert Behringer at Duke University, Katepalli Sreenivasan at Yale University, Xiao-Zhong Wu at Northern Illinois University and Russell Donnelly at the University of Oregon, who served as Editor for this report. This study reports the research and development opportunities in such a project, the technical requirements and feasibility of its construction and operation, and the costs associated with the needed facilities and support activities. The facility will be a unique national resource for studies of high-Reynolds-number and high-Rayleigh-number and high Rayleigh number turbulence phenomena, and is one of the six items determined as suitable for potential funding through a screening of Expressions of Interest. The proposed facility is possible only because of the advanced cryogenic technology available at the SSCL. Typical scientific issues to be addressed in the facility will be discussed. It devolved during our study, that while the main experiment is still considered to be the thermal convection experiment discussed in our original Expression of Interest, there are now a very substantial set of other, important and fundamental experiments which can be done with the large cryostat proposed for the convection experiment. We believe the facility could provide several decades of front-line research in turbulence, and shall describe why this is so. DOE

N95-25485# Sandia National Labs., Albuquerque, NM.

BENCHMARK TESTING AND INDEPENDENT VERIFICATION OF THE VS2DT COMPUTER CODE

James T. McCord and Michael T. Goodrich (IT Corp., Albuquerque, NM.) Nov. 1994 36 p

(Contract DE-AC04-94AL-85000)

(DE95-004386; SAND-91-1526; UC-403) Avail: CASI HC A03/MF A01

The finite difference flow and transport simulator VS2DT was benchmark tested against several other codes which solve the same equations (Richards equation for flow and the Advection-Dispersion equation for transport). The benchmark problems investigated transient two-dimensional flow in a heterogeneous soil profile with a localized water source at the ground surface. The VS2DT code performed as well as or better than all other codes when considering mass balance characteristics and computational speed. It was also rated highly relative to the other codes with regard to ease-of-use. Following the benchmark study, the code was verified against two analytical solutions, one for two-dimensional flow and one for two-dimensional transport. These independent verifications show reasonable agreement with the analytical solutions, and complement the one-dimensional verification problems published in the code's original documentation. DOE

N95-25895# Sandia National Labs., Albuquerque, NM.

A DOMAIN DECOMPOSITION STUDY OF MASSIVELY PARALLEL COMPUTING IN COMPRESSIBLE GAS DYNAMICS

C. C. Wong, F. G. Blottner, J. L. Payne, and M. Soetrisno (Amtec Engineering, Inc., Bellevue, WA.) 1995 16 p Presented at the 33rd American Institute of Aeronautics and Astronautics (AIAA) Aerospace Sciences Meeting, Reno, NV, 9-12 Jan. 1995

(Contract DE-AC04-94AL-85000)

(DE95-004759; SAND-94-1402C; CONF-950130-4) Avail: CASI HC A03/MF A01

The appropriate utilization of massively parallel computers for solving the Navier-Stokes equations is investigated and determined from an engineering perspective. The issues investigated are: (1) Should strip or patch domain decomposition of the spatial mesh be used to reduce computer time? (2) How many computer nodes should be used for a problem with a given sized mesh to reduce computer time? (3) Is the convergence of the Navier-Stokes solution procedure (LU-SGS) adversely influenced by the domain decomposition approach? The results of the paper show that the present Navier-Stokes solution technique has good performance on a massively parallel computer for transient flow problems. For steady-state problems with a large number of mesh cells, the solution procedure will require significant computer time due to an increased number of iterations to achieve a converged solution. There is an optimum number of computer nodes to use for a problem with a given global mesh size. DOE

N95-25960*# Institute for Computer Applications in Science and Engineering, Hampton, VA.

CLASSICAL CLOSURE THEORY AND LAM'S INTERPRETATION OF EPSILON-RNG Final Report

Ye Zhou Mar. 1995 11 p

(Contract NAS1-19480; RTOP 505-90-52-01)

(NASA-CR-195061; NAS 1.26;195061; ICASE-95-19) Avail: CASI HC A03/MF A01

Lam's phenomenological epsilon-renormalization group (RNG) model is quite different from the other members of that group. It does not make use of the correspondence principle and the epsilon-expansion procedure. We demonstrate that Lam's epsilon-RNG model is essentially the physical space version of the classical closure theory in spectral space and consider the corresponding treatment of the eddy viscosity and energy backscatter. Author

N95-25964*# Institute for Computer Applications in Science and Engineering, Hampton, VA.
A PSEUDO-SOUND CONSTITUTIVE RELATIONSHIP FOR THE DILATATIONAL COVARIANCES IN COMPRESSIBLE TURBULENCE: AN ANALYTICAL THEORY
J. R. Ristorcelli Mar. 1995 51 p Submitted for publication
(Contract NAS1-19480; RTOP 505-90-52-01)
(NASA-CR-195064; NAS 1.26:195064; ICASE-95-22) Avail: CASI HC A04/MF A01

The mathematical consequences of a few simple scaling assumptions about the effects of compressibility are explored using a simple singular perturbation idea and the methods of statistical fluid mechanics. Representations for the pressure-dilation and dilatational dissipation covariances appearing in single-point moment closures for compressible turbulence are obtained. While the results are expressed in the context of a second-order statistical closure they provide some interesting and very clear physical metaphors for the effects of compressibility that have not been seen using more traditional linear stability methods. In the limit of homogeneous turbulence with quasi-normal large-scales the expressions derived are - in the low turbulent Mach number limit - asymptotically exact. The expressions obtained are functions of the rate of change of the turbulence energy, its correlation length scale, and the relative time scale of the cascade rate. The expressions for the dilatational covariances contain constants which have a precise and definite physical significance; they are related to various integrals of the longitudinal velocity correlation. The pressure-dilation covariance is found to be a nonequilibrium phenomena related to the time rate of change of the internal energy and the kinetic energy of the turbulence. Also of interest is the fact that the representation for the dilatational dissipation in turbulence, with or without shear, features a dependence on the Reynolds number. This article is a documentation of an analytical investigation of the implications of a pseudo-sound theory for the effects of compressibility. Author

N95-26063# Lawrence Livermore National Lab., Livermore, CA.
VISCOELASTIC WAVES AND MULTIPLE SCALES
Gerald Hedstrom May 1994 10 p Presented at the 3rd International Conference on Mathematical and Numerical Aspects of Wave Propagation Phenomena, Juan-les-Pins, France, 24-28 Apr. 1995
(Contract W-7405-eng-48)
(DE94-014130; UCRL-JC-116569; CONF-950413-1) Avail: CASI HC A02/MF A01

A multiple-scales argument is used to obtain the speeds of the main shear and compressional waves in a general homogeneous viscoelastic medium. The rate of spreading by diffusion of these waves is also derived. These methods are also used to determine the speed of the main viscoelastic Rayleigh wave, as well as the rate of its energy decay. DOE

N95-26077*# National Aeronautics and Space Administration. Lewis Research Center, Cleveland, OH.
NUMERICAL CALCULATIONS OF SHOCK-WAVE/BOUNDARY-LAYER FLOW INTERACTIONS
P. G. Huang (Eloret Corp., Palo Alto, CA.) and W. W. Liou Aug. 1994 14 p Presented at the 1st International Conference on Flow Interactions, Hong Kong, 5-9 Sep. 1994; sponsored by Hong Kong Univ.
(Contract RTOP 505-90-5K; NCC3-233)
(NASA-TM-106694; ICOMP-94-16; CMOTT-94-4; E-9049; NAS 1.15:106694) Avail: CASI HC A03/MF A01

The paper presents results of calculations for 2-D supersonic turbulent compression corner flows. The results seem to indicate that the newer, improved kappa-epsilon models offer limited advantages over the standard kappa-epsilon model in predicting the shock-wave/boundary-layer flows in the 2-D compression corner over a wide range of corner angles and flow conditions. Author

N95-26161# Japan Atomic Energy Research Inst., Tokyo (Japan).
HEAT REMOVAL CAPABILITY OF DIVERTOR COAXIAL TUBE ASSEMBLY
Masanao Shibui, Masataka Nakahira, Eisuke Tada, and Hideyuki Takatsu May 1994 23 p
(DE95-709770; JAERI-M-94-073) Avail: CASI HC A03/MF A01

To deal with high power flowing in the divertor region, an advanced divertor concept with gas target has been proposed for use in ITER/EDA. The concept uses a divertor channel to remove the radiated power while allowing neutrals to recirculate. Candidate channel wall designs include a tube array design where many coaxial tubes are arranged in the toroidal direction to make louver. The coaxial tube consists of a Be protection tube encases many supply tubes wound helically around a return tube. V-alloy and hardened Cu-alloy have been proposed for use in the supply and return tubes. Some coolants have also been proposed for the design including pressurized He and liquid metals, because these coolants are consistent with the selection of coolants for the blanket and also meet the requirement of high temperature operation. In the coaxial tube design, the coolant area is restricted and brittle Be material is used under severe thermal cyclings. Thus, to obtain the coaxial tube with sufficient safety margin for the expected fusion power excursion, it is essential to understand its applicability limit. The paper discusses heat removal capability of the coaxial tube and recommends some design modifications. DOE

N95-26240 Sandia National Labs., Albuquerque, NM. Aerosciences and Fluid Dynamics Dept.
NUMERICAL SIMULATION OF LAMINAR FLOW IN A CURVED DUCT
Amalia R. Lopez and William L. Oberkampf 1995 18 p Presented at the 33rd American Institute of Aeronautics and Astronautics (AIAA) Aerospace Sciences Meeting, Reno, NV, 9-12 Jan. 1995 Limited Reproducibility: More than 20% of this document may be affected by microfiche quality
(Contract DE-AC04-94AL-85000)
(DE95-005427; SAND-95-0012C; CONF-950130-6) Avail: CASI HC A03

This paper describes numerical simulations that were performed to study laminar flow through a square duct with a 900 bend. The purpose of this work was two fold. First, an improved understanding was desired of the flow physics involved in the generation of secondary vortical flows in three-dimensions. Second, adaptive gridding techniques for structured grids in three- dimensions were investigated for the purpose of determining their utility in low Reynolds number, incompressible flows. It was also of interest to validate the commercial computer code CFD-ACE. Velocity predictions for both non-adaptive and adaptive grids are compared with experimental data. Flow visualization was used to examine the characteristics of the flow though the curved duct in order to better understand the viscous flow physics of this problem. Generally, moderate agreement with the experimental data was found but shortcomings in the experiment were demonstrated. The adaptive grids did not produce the same level of accuracy as the non-adaptive grid with a factor of four more grid points. DOE

N95-25868*# Brown Univ., Providence, RI. Dept. of Computer Science.
THE 3D WIDGETS FOR EXPLORATORY SCIENTIFIC VISUALIZATION
Kenneth P. Herndon and Tom Meyer *In its* Three-Dimensional User Interfaces for Scientific Visualization 20 Jan. 1995 2 p (For primary document see N95-25867 08-61)
(Contract N00014-91-J-4052; ARPA Order 8225)
Avail: CASI HC A01/MF A01; 9 functional color pages

N95-25869*# Digital Equipment Corp., Cambridge, MA.
AN ANNOTATION SYSTEM FOR 3D FLUID FLOW VISUALIZATION
Maria M. Loughlin and John F. Hughes (Brown Univ., Providence, RI.) *In* Digital Equipment Corp., Three-Dimensional User Interfaces for Scientific Visualization 20 Jan. 1995 8 p Sponsored in part by Digital Equipment Corp.; NSF; DARPA; IBM; NCR; Sun Microsystems; and Hewlett Packard (For primary document see N95-25867 08-61)
Avail: CASI HC A02/MF A01; 9 functional color pages

35 INSTRUMENTATION AND PHOTOGRAPHY

Includes remote sensors; measuring instruments and gages; detectors; cameras and photographic supplies; and holography.

For aerial photography see *43 Earth Resources and Remote Sensing*. For related information see also *06 Aircraft Instrumentation*, and *19 Spacecraft Instrumentation*.

N95-24203 Defence Science and Technology Organisation, Melbourne (Australia). Airframes and Engines Div.
A PORTABLE TRANSMISSION VIBRATION ANALYSIS SYSTEM FOR THE S-70A-9 BLACK HAWK HELICOPTER

D. M. Blunt, B. Rebbechi, B. D. Forrester, and K. W. Vaughan Sep. 1994 45 p Original contains color illustrations
(DSTO-TR-0072; AR-008-938) Copyright Avail: Issuing Activity (DSTO Aeronautical and Maritime Research Lab., GPO Box 4331, Melbourne, Victoria 3001, Australia)

The prototype portable transmission vibration analysis system developed by Aeronautical and Maritime Research Laboratory (AMRL) for the Black Hawk helicopter is described in detail, including the results of flight trials conducted at RAAF Base Edinburgh during July 1993. The results of these trials have proved the concept of the system and laid the foundations for the future development of smaller and lighter systems. Author

N95-24236* National Aeronautics and Space Administration. Ames Research Center, Moffett Field, CA.
LASER VELOCIMETER FOR NEAR-SURFACE MEASUREMENTS Patent
Dennis A. Johnson, inventor (to NASA) 25 Feb. 1992 7 p Filed 11 Oct. 1990
(NASA-Case-ARC-11917-1; US-Patent-5,090,801; US-Patent-Appl-SN-596105; US-Patent-Class-356-28.5; US-Patent-Class-356-28; Int-Patent-Class-B01P-3/36) Avail: US Patent and Trademark Office

The present invention relates to a laser Doppler velocimeter for near-wall measurements which includes at least one beam-turning device. The beam-turning device receives laser light, reflects and redirects the light at various angles in order to obtain measurements for all three velocity components at grazing incident angles. The beam-turning device includes a mirror or prism at one end which reflects the received light in a particular direction. A collector lens receives the particle scattered light from which the relevant velocity components are determined. The beam-turning device can also be a miniature fiber optic head which outputs laser light and can be turned in any direction. Author

N95-24259 Helsinki Univ. of Technology, Espoo (Finland).
RELATIVE ORIENTATION OF MULTIPLE IMAGES USING PROJECTIVE SINGULAR CORRELATION
I. Niini 14 Feb. 1994 66 p Limited Reproducibility: More than 20% of this document may be affected by microfiche quality
(ISSN 1237-5535)
(PB95-149936; ISBN-951-22-2205-1) Avail: Issuing Activity (National Technical Information Service (NTIS))

The singular correlation between two images contains all essential information about the relative orientation of the images but the relative orientation remains projectively deformed if the interior orientation is not known. The use of multiple singular correlations eliminates the deformation and is necessary for solving the unknown interior orientation, as well. The method is divided into three steps. First, all singular correlations of the images are computed. Second, the common interior orientation is computed using special quadratic equations derived from the relative orientation and singular correlation equations. Third, the relative orientations of the images are computed relative to one of the images. Finally, the model coordinates of the object are obtained from the relative orientation parameters. The shape of the model is correct but the scale of the model is arbitrary. The method needs at least three images taken with the same camera from distinct standpoints. The projection from the object to the images is assumed to be projectively linear or nonlinear image deformations are assumed to be corrected in advance. NTIS

N95-24280 National Defence Research Establishment, Stockholm (Sweden). Huvudavdelning foer Informationsteknologi.
READ OUT ELECTRONICS FOR THERMAL DETECTORS OF BOLOMETER TYPE [UTLAESNINGSELEKTRONIK FOER TERMISKA IR-DETEKTORER AV BOLOMETERTYP]
U. Ringh Jun. 1994 28 p In SWEDISH
(PB95-141842; FOA-C-30764-3.1) Avail: Issuing Activity (National Technical Information Service (NTIS))

Thermal infrared (IR) detectors can be used for imaging IR systems with high temperature resolution. One detector type which has shown high responsivity is the resistance bolometer. Radiometric calculations on the expected signal power for an IR camera with NETD = 0.1 K has been made. Traditional readout techniques for photon detectors is not directly applicable to bolometer detectors. During the read out of the signals from a bolometer, one has to consider the power dissipation due to bias current through the detector. Further on, the choice of bias resistor is important for stability reasons because it is possible to overheat the detector when using unsuitable resistance values. Elementary theory for bolometers is mentioned and an example is given with values published by the Honeywell Company. There is a demand for low noise in the read out electronics. Noise calculations have been made for transistors with varying dimensions less than 50 micrometers x 50 micrometers in a typical CMOS-process. The results show that the 1/f-noise is dominating at low frequencies. Noise calculations for BiC-MOS have not been made, however, due to the lack of process parameters. One conclusion when comparing the two techniques is that one has to compensate for the 1/f-noise when using CMOS in the actual application. NTIS

N95-24473*# United Technologies Corp., East Hartford, CT.
DEVELOPMENT OF SENSORS FOR CERAMIC COMPONENTS IN ADVANCED PROPULSION SYSTEMS. PHASE 2: TEMPERATURE SENSOR SYSTEMS EVALUATION Final Report
W. H. Atkinson, M. A. Cyr, and R. R. Strange Oct. 1994 158 p
(Contract NAS3-25141; RTOP 505-62-50)
(NASA-CR-195283; E-8627; NAS 1.26:195283; PWA-6113-55) Avail: CASI HC A08/MF A02

The 'development of sensors for ceramic components in advanced propulsion systems' program is divided into two phases. The objectives of Phase 1 were to analyze, evaluate and recommend sensor concepts for the measurement of surface temperature, strain and heat flux on ceramic components for advanced propulsion systems. The results of this effort were previously published in NASA CR-182111. As a result of Phase 1, three approaches were recommended for further development: pyrometry, thin-film sensors, and thermographic phosphors. The objective of Phase 2 were to fabricate and conduct laboratory demonstration tests of these systems. Six materials, mutually agreed upon by NASA and Pratt & Whitney, were investigated under this program. This report summarizes the Phase 2 effort and provides conclusions and recommendations for each of the categories evaluated. Author

N95-24484# Joint Inst. for Nuclear Research, Dubna (USSR).
ENERGY RESOLUTION OF A LEAD SCINTILLATING FIBER ELECTROMAGNETIC CALORIMETER
J. Budagov, I. Chirikov-Zorin, V. Glagolev, A. Jordanov, Yu Kharzheev, I. Liba, S. Malyukov, N. A. Russakovich, N. L. Russakovich, and A. Solovyev et al 1993 20 p Submitted for publication
(DE94-628253; JINR-E-13-93-308; Rept-E13-93-308) Avail: CASI HC A03/MF A01 (US Sales Only)

A calorimeter module was fabricated using profiled lead plates and scintillating fibers with diameter 1 mm and attenuation length about 80 cm. The absorber-to-fiber volume ratio was 1.17 and the module average radiation length X(sub 0) = 1.05 cm. The energy resolution of the module was investigated using the electron beams of U-70 at Serpukhov and of the SPS at CERN in the energy range 5-70 GeV. The energy resolution at theta = 3 deg (the angle between the fiber axis and the beam direction) may be expressed by the formula sigma/E(%) = 13.1/radical E + 1.7. The energy resolution was also simulated by Monte Carlo and good agreement with the experiment has been achieved. DOE

N95-24486# Joint Inst. for Nuclear Research, Dubna (USSR).
SOFTWARE OF A DISTRIBUTOR OF HIGH VOLTAGE OF THE H C-600 HADRONIC CALORIMETER
M. G. Kadykov and A. S. Shchelev 1993 3 p In RUSSIAN; In RUSSIAN
(DE94-628255; JINR-R-10-93-243; Rept-P10-93-243) Avail: CASI HC A01/MF A01 (US Sales Only)

The software to control the distribution block of high voltage hadron calorimeter H C-600 is described. This software permits to realize automatic control of high voltage for every spectrometric channel during preliminary calibration and exposition of the detector on the particles beam. DOE

N95-24596# Sandia National Labs., Albuquerque, NM.
RECIPES FOR HIGH RESOLUTION TIME-OF-FLIGHT DETECTORS
S. J. Anz (California Univ., Los Angeles, CA.), T. E. Felter, B. V. Hess, R. S. Daley (Lawrence Livermore National Lab., Livermore, CA.), M. L. Roberts (Lawrence Livermore National Lab., Livermore, CA.), and R. S. Williams

(California Univ., Los Angeles, CA.) Jan. 1995 60 p
(Contract DE-AC04-94AL-85000)
(DE95-006196; SAND-94-8251) Avail: CASI HC A04/MF A01

The authors discuss the dynamics, construction, implementation and benefits of a time-of-flight (TOF) detector with count rates an order of magnitude higher and resolution three to four times better than that obtainable with a surface barrier detector. The propose use of design criteria for a time-of-flight detector is outlined, and the determination of a TOF detector's total relative timing error and how this value determines the mass resolution are illustrated using a graphical analysis. They present simulation and experimental examples employing light ions and discuss advantages and pitfalls of medium-energy heavy ion TOF spectrometry. DOE

N95-24623# Brookhaven National Lab., Upton, NY.
THE DEVELOPMENT OF A POSITRON IONIZATION GAUGE
F. Jacobsen, M. Strongin, M. Ruckman, A. Wiess (Texas Univ., Arlington, TX.), and W. C. Turner (Superconducting Super Collider Lab., Dallas, TX.) Jan. 1994 11 p
(Contracts DE-AC02-76CH-00016; DE-AC35-89ER-40486)
(DE95-005958; BNL-61272; SSCL-N-846) Avail: CASI HC A03/MF A01

The authors present a method by which gas pressure (density) can be measured by positrons. The process to monitor is the formation of positronium, Ps, via electron capture by the e(+) from the rest gas molecules. The Ps signal which is proportional to the gas density is obtained from the annihilation photons which are emitted when the Ps atom decays. By this method it is not necessary to have access to the vacuum system in question other than having the possibility of passing a positron beam through it. Also the present method is fully UHV compatible. In its simplest version pressures below 10(sup -8) torr (at room temperature) can be measured within a reasonable time. Techniques are discussed which will significantly improve the sensitivity of the present ionization gauge. The specific reason for designing and using the positron ionization gauge is to be able to measure the pressure inside the Superconducting Super Collider beam tubing during simulated operation. DOE

N95-24625* Moore (Thomas C., Sr.), Poquoson, VA.
COMPENSATED HIGH TEMPERATURE STRAIN GAGE Patent
27 Dec. 1994 6 p Filed 12 Aug. 1992
(NASA-Case-LAR-14776-1; US-Patent-5,375,474;
US-Patent-Appl-SN-928865; US-Patent-Class-73-766;
US-Patent-Class-73-775; US-Patent-Class-29-621.1;
Int-Patent-Class-G01B-7/16) Avail: US Patent and Trademark Office

A device for measuring strain in substrates at high temperatures in which the thermally induced apparent strain is nulled is described. Two gages are used, one active gage and one compensating gage. Both gages are placed on the substrate to be gaged; the active gage is attached such that it responds to mechanical and thermally induced apparent strain while the compensating gage is attached such that it does not respond to mechanical strain and and measures only thermally induced apparent strain. A thermal blanket is placed over the two gages to maintain the gages at the same temperature. The two gages are wired as adjacent arms of a wheatstone bridge which nulls the thermally induced apparent strain giving a true reading of the mechanical strain in the substrate.
Official Gazette of the U.S. Patent and Trademark Office

N95-24635# Joint Inst. for Nuclear Research, Dubna (USSR).
ABSOLUTE CALIBRATION AND MONITORING OF A SPECTROMETRIC CHANNEL USING A PHOTOMULTIPLIER
E. H. Bellamy (Pisa Univ., Italy.), G. Bellettini (Pisa Univ., Italy.), F. Gervelli (Pisa Univ., Italy.), M. Incagli (Pisa Univ., Italy.), D. Lucchesi (Pisa Univ., Italy.), C. Pagliarone (Pisa Univ., Italy.), F. Zetti (Pisa Univ., Italy.), Yury Budagov (SSC Lab., Dallas, TX.), I. Chirikov-Zorin, and S. Tokar (Comenius Univ., Bratislava, Czechoslovakia.) 1993 16 p Submitted for publication
(DE94-628251; JINR-E-13-93-295) Avail: CASI HC A03/MF A01 (US Sales Only)

A method for measuring the photomultiplier gain using a realistic photomultiplier response function is described. A precision of about 1% for the deconvoluted gain parameter can be achieved. DOE

N95-24657# Lawrence Livermore National Lab., Livermore, CA. Nuclear Test/Environmental Sciences.
CHARACTERISTICS OF AN ULTRAFAST X-RAY STREAK CAMERA
Ronnie Shepherd, Rex Booth, Dwight Price, Mark Bowers, Don Swan, Jim Bonlie, Bruce Young, Jim Dunn, Bill White, and Richard Stewart Jun. 1994 9 p Presented at the Annual Meeting of the Society of Photo-Optical Instrumentation Engineers, San Diego, CA, 24-29 Jul. 1994
(Contract W-7405-eng-48)
(DE95-004210; UCRL-JC-116456; CONF-940723-32) Avail: CASI HC A02/MF A01

The detection and temporal dispersion of the x-rays using x-ray streak cameras has been limited to a resolution of 2 ps, primarily due to the transit time dispersion of the electrons between the photocathode and the acceleration grid. The transit time spread of the electrons traveling from the photocathode to the acceleration grid is inversely proportional to the accelerating field. By increasing the field by a factor of 7, we have minimized the effects of transit time dispersion in the photocathode/accelerating grid region and produce an x-ray streak camera with sub-picosecond temporal resolution (approximately 900 fs). The streak camera has been calibrated using a Michelson interferometer and 100 fs, 400 nm laser light. Time resolved x-ray data is shown from an aluminum target heated at 10(exp 18) W/cm(exp 2) with a 100 fs, 400 nm laser. DOE

N95-25118*# Virginia Polytechnic Inst., Blacksburg, VA. Dept. of Mechanical Engineering.
HEAT FLUX INSTRUMENTATION FOR HYFLITE THERMAL PROTECTION SYSTEM Final Report, 11 Jul. - 31 Dec. 1994
T. E. Diller 31 Dec. 1994 24 p
(Grant NAG3-1643)
(NASA-CR-197715; NAS 1.26:197715) Avail: CASI HC A03/MF A01

Tasks performed in this project were defined in a September 9, 1994 meeting of representatives of Vatell, NASA Lewis and Virginia Tech. The overall objective agreed upon in the meeting was 'to demonstrate the viability of thin film techniques for heat flux and temperature sensing in HYSTEP thermal protection systems'. We decided to attempt a combination of NASA's and Vatell's best heat flux sensor technology in a sensor which would be tested in the Vortek facility at Lewis early in 1995. The NASA concept for thermocouple measurement of surface temperature was adopted, and Vatell methods for fabrication of sensors on small diameter substrates of aluminum nitride were used to produce a sensor. This sensor was then encapsulated in a NARloy-Z housing. Various improvements to the Vatell substrate design were explored without success. The basic NASA and Vatell sensor layouts were analyzed by finite element modeling, in an attempt to better understand the effects of material properties, dimensions and thermal differential element location on sensor symmetry, bandwidth and sensitivity. This analysis showed that, as long as the thermal resistivity of the thermal differential element material is much larger (10X) than that of the substrate material, the simplest arrangement of layer is best. During calibration of the sensor produced in this project, undesirable side-effects of combining the heat flux and temperature sensor return leads were observed. The sensor did not cleanly separate the heat flux and temperature signals, as sensors with four leads have consistently done before. Task 7 and 8 discussed in the meeting will be performed with a continuation of funding in 1995. The following is a discussion of each of the tasks performed as outlined in the statement of work dated september 26, 1994. Task 1A was added to cover further investigation into the NASA sensor concept.
Author

N95-25330*# Connecticut Univ., Storrs, CT. Dept. of Mechanical Engineering/Physics.
X-RAY BASED DISPLACEMENT AND STRAIN MEASUREMENTS FOR HOSTILE ENVIRONMENTS Report, 17 Jul. 1992 - 20 Nov. 1993
Howard A. Canistraro, Eric H. Jordan, and Douglas M. Pease 30 Dec. 1993 54 p
(Contract NAS3-26619; RTOP 510-01-50)
(NASA-CR-194451; NAS 1.26:194451) Avail: CASI HC A04/MF A01

A completely new method of non-contacting, hostile environment displacement and strain measurement based on the focus and scanning of x-rays, has been developed and demonstrated. The new technique has the ability to overcome many of the limitations associated with available methods. The system is based on the focus and scanning of low energy, hard x-rays such as those emanating from table top copper or molybdenum

sources. The x-rays are focused into a narrow and intense line image which can be swept onto targets that fluoresce secondary x-ray radiation. By monitoring the secondary radiation intensity and comparing it with the focused x-ray image's position as it is swept over the target edge, the position of the target edge relative to the focused image can be determined. The present system has a resolution of 0.5 micron, which has been shown to be limited by bearing backlash (or 'yaw' error) in the linear translation table. Its use has been demonstrated in the presence of an open flame with a resultant target temperature in excess of 2000 degrees Fahrenheit (1000 degrees Celsius). Strain measurements have been conducted in a laboratory environment at both room temperature and at a specimen temperature of 1300 degrees Fahrenheit, with an accuracy of within 20 microstrain (primarily a function of the 0.5 micron resolution limit). The main advantage of the technique lies in the penetrating, non-refractive nature of x-rays, which are virtually immune to the presence of refracting gas layers, smoke, flame or intense thermal radiation. Author

N95-25381# Allied-Signal Aerospace Co., Kansas City, MO.
METROLOGY MEASUREMENT CAPABILITY
K. Shroyer Jan. 1995 91 p
(Contract DE-AC04-76DP-00613)
(DE95-005411; KCP-613-5411) Avail: CASI HC A05/MF A01

During the past 36 years, the Kansas City Division's (KCD) Metrology Department has developed measurement technology and calibration capability in four major areas of measurement: (1) Mechanical; (2) Environmental, Gas, Liquid; Electrical (D.C., A.C., RF/Microwave); and (3) Optical and Radiation. The capabilities developed include unique capabilities in many areas of measurement and engineering expertise to develop measurement techniques and resolve measurement problems in these major areas. KCD Metrology was established in 1958 to provide a measurement base for the Kansas City Plant. The Metrology Engineering Department provides the expertise to develop measurement capabilities for virtually any type of measurement which falls into the broad areas listed above. The engineering staff currently averages almost 19 years of measurement experience. A strong audit function has been developed to provide a means to evaluate the calibration programs of our suppliers and internal calibration organizations. This evaluation includes measurement audits and technical surveys. The requirements placed on Metrology require traceability of measurements to the National Institute of Standards and Technology or to nationally recognized methods or natural phenomena. A description of Metrology capabilities, traceability flow charts, and the measurement uncertainty of each of the measurement capabilities is contained in the following pages. DOE

N95-25384# Los Alamos National Lab., NM.
DEVELOPMENT OF A PORTABLE MASS SPECTROMETRIC SYSTEM FOR DETERMINATION OF ISOTOPIC COMPOSITION OF SOLID URANIUM SAMPLES USING FLUORINE VOLATILIZATION Final Report
G. Loge 30 Sep. 1994 9 p
(Contract W-7405-eng-36)
(DE95-005728; LA-SUB-95-1) Avail: CASI HC A02/MF A01

Using hardware and materials supplied by LANL, a prototype quadrupole mass spectrometer system designed for portable field analysis of isotopic composition of solid uranium samples was assembled and tested. The system contained the capability for fluorine volatilization of solid uranium samples with gas introduction, which was successfully tested and demonstrated using 100 mg samples of U3O8. Determination of precision and accuracy for measuring isotopic composition was performed using isotopic standards. Use with soil samples containing uranium were also attempted. Silicates in the soil forming SiF4 were found to be a kinetic bottleneck to the formation of UF6. This could be avoided by performing some sort of chemical separation as a pre-treatment step, which was demonstrated using nitric acid. DOE

N95-25544* National Aeronautics and Space Administration. Marshall Space Flight Center, Huntsville, AL.
SUSPENSION SYSTEM FOR GIMBAL SUPPORTED SCANNING PAYLOADS Patent
Michael E. Polites, inventor (to NASA) 14 Mar. 1995 9 p Filed 15 Sep. 1993 Supersedes N94-29358 (32 - 8, p 3287)
(NASA-Case-MFS-28817-1; US-Patent-5,396,815;
US-Patent-Appl-SN-123629; US-Patent-Class-74-61; US-Patent-Class-74-87;
US-Patent-Class-244-158R; US-Patent-Class-343-765;
US-Patent-Class-343-766; Int-Patent-Class-F16H-33/20;
Int-Patent-Class-B64G-1/66) Avail: US Patent and Trademark Office

Gimballed scanning devices or instruments are the subject of this invention. Scanning is an important aspect of space science. To achieve a scan pattern some means must be provided which impart to the payload an oscillatory motion. Various forms of machines have been employed for controllably conferring on scanning instruments predetermined scan patterns. They include control moment gyroscopes, reaction wheels, torque motors, reaction control systems, and the like. But rotating unbalanced mass (RUM) devices are a new and efficient way to generate scans in gimballed payloads. RUM devices are superior to previous scanning apparatus, but they require power consuming and frequently complex auxiliary control systems to position and reposition the particular scan pattern relative to a target or a number of targets. Herein the control system is simplified. The most frequently employed method for achieving the various scan patterns is to gimbal the scanning device. Gimbals are suspended in such a way that they can be activated to generate the scan pattern. The suspension means described is for payloads supported in gimbals wherein the payload rotation is restricted by a flex pivot so that the payload oscillates, thereby moving in a scan pattern. Official Gazette of the U.S. Patent and Trademark Office

N95-25547* National Aeronautics and Space Administration. Pasadena Office, CA.
ALTERNATE METHOD FOR ACHIEVING TEMPERATURE CONTROL IN THE -160 TO +90 CELCIUS RANGE Patent
Kenneth R. Johnson, inventor (to NASA) (Jet Propulsion Lab., California Inst. of Tech., Pasadena, CA.) 7 Mar. 1995 19 p Filed 4 Nov. 1993 Supersedes N94-29497 (32 - 8, p 3288)
(Contract NAS7-918)
(NASA-Case-NPO-18995-1-CU; US-Patent-5,394,704;
US-Patent-Appl-SN-152631; US-Patent-Class-62-51.1;
US-Patent-Class-62-50.2; US-Patent-Class-62-50.4; US-Patent-Class-62-122;
US-Patent-Class-62-159; Int-Patent-Class-F25B-19/00;
Int-Patent-Class-F17C-9/02) Avail: US Patent and Trademark Office

A single-pass method for accurate and precise temperature control in the -160 to +90 C range is discussed. The method exhibited minimal set-point overshoot during temperature transitions. Control to +/-2 C with transitions between set-points of 7 C per minute were achieved. The method uses commercially available temperature controllers and a gaseous nitrogen/liquid nitrogen mixer to dampen the amplitude of cold temperature spikes caused by liquid nitrogen pulsing.
Official Gazette of the U.S. Patent and Trademark Office

N95-25606 Army Research Lab., Aberdeen Proving Ground, MD.
WORKSHOP REPORT: MEASUREMENT TECHNIQUES IN HIGHLY TRANSIENT, SPECTRALLY RICH COMBUSTION ENVIRONMENTS Final Report, 1-30 Nov. 1993
Todd E. Rosenberger Sep. 1994 204 p Limited Reproducibility: More than 20% of this document may be affected by microfiche quality
(AD-A288395; ARL-SR-18) Avail: Issuing Activity (Defense Technical Information Center (DTIC))

With the emergence of advanced propulsion systems such as liquid propellant (LP), electrothermal-chemical (ETC), electromagnetic (EM), conventional hypervelocity, and in-bore ramjet, the measurement of combustion phenomena has become more complex. The data associated with these systems can be rich in high-frequency components, and share similar transient behavior. Measurement techniques associated with conventional solid propellant systems are not always capable of accurately recording these phenomena. The accuracy of pressure and acceleration measurements in combustion chambers, barrels, and on-board projectiles has been compromised by the lack of a fundamental understanding of the effects of the mounting configuration and the mechanical and electrical components of the transducer on the integrity of the measurement. Consequently, the system development and technical understanding of the physical processes involved in the ignition and combustion of such advanced propulsion systems have been compromised. A workshop was needed to bring together experts from the aforementioned and related communities to disseminate knowledge of lessons learned and to discuss the techniques necessary to make high-fidelity pressure measurements in these environments. This report will state the objectives, identify the participants who met to address them, provide a list of the technical presentations

made, present highlights from these presentations and the discussions that they prompted, and end with conclusions and recommendations which came out of the workshop. DTIC

N95-25699*# Old Dominion Univ., Norfolk, VA. Dept. of Aerospace Engineering.

HOT-WIRE CALIBRATION IN SUBSONIC/TRANSONIC FLOW REGIMES Research Report, 18 Nov. 1993 - 17 Nov. 1994

K. A. Nagabushana and Robert L. Ash Apr. 1995 101 p

(Grant NAG1-1552)

(NASA-CR-197725; NAS 1.26:197725) Avail: CASI HC A06/MF A02

A different approach for calibrating hot-wires, which simplifies the calibration procedure and reduces the tunnel run-time by an order of magnitude was sought. In general, it is accepted that the directly measurable quantities in any flow are velocity, density, and total temperature. Very few facilities have the capability of varying the total temperature over an adequate range. However, if the overheat temperature parameter, a(sub w), is used to calibrate the hot-wire then the directly measurable quantity, voltage, will be a function of the flow variables and the overheat parameter i.e., E = f(u,p,a(sub w), T(sub w)) where a(sub w) will contain the needed total temperature information. In this report, various methods of evaluating sensitivities with different dependent and independent variables to calibrate a 3-Wire hot-wire probe using a constant temperature anemometer (CTA) in subsonic/transonic flow regimes is presented. The advantage of using a(sub w) as the independent variable instead of total temperature, t(sub o), or overheat temperature parameter, tau, is that while running a calibration test it is not necessary to know the recovery factor, the coefficients in a wire resistance to temperature relationship for a given probe. It was deduced that the method employing the relationship E = f (u,p,a(sub w)) should result in the most accurate calibration of hot wire probes. Any other method would require additional measurements. Also this method will allow calibration and determination of accurate temperature fluctuation information even in atmospheric wind tunnels where there is no ability to obtain any temperature sensitivity information at present. This technique greatly simplifies the calibration process for hot-wires, provides the required calibration information needed in obtaining temperature fluctuations, and reduces both the tunnel run-time and the test matrix required to calibrate hotwires. Some of the results using the above techniques are presented in an appendix. Author

N95-25763# National Aerospace Lab., Tokyo (Japan). Computational Sciences Div.

VIDEO CAMERA AS A VISUAL SENSOR, PART 2

Hiromi Gomi Mar. 1994 25 p In JAPANESE

(ISSN 0389-4010)

(NAL-TR-1231-Pt-2) Avail: CASI HC A03/MF A01

A video camera was calibrated with one-to-one correspondence between picture elements of CCD and digital image by synchronizing VD/HD signals of video camera and an AD converter. Measurements were made on space resolution and sensitivity of the picture element, stability of the video signal, and on lens characteristics. A picture element leaked the output to the adjacent picture elements and the interference of outputs was linear. There were no defective picture elements. A focussing mechanism and 'contrast' algorithm made it possible to measure distance at a space resolution of 2 x 2 picture elements. Author

N95-25940# China Nuclear Information Centre, Beijing (China).

AN ION SENSITIVE PROBE AND ITS APPLICATION TO A MIRROR DEVICE

Duan Shuyun (Southwestern Inst. of Physics, Chengdu, China.) and Yang Zhigang (Southwestern Inst. of Physics, Chengdu, China.) Mar. 1994 8 p

(DE95-602307; CNIC-00817; SIP-0068) Avail: CASI HC A02/MF A01 (US Sales Only)

The basic principle and design parameters of an ion sensitive probe are introduced. The ion and electron temperature in a mirror are successfully measured by this probe. Discussions about the curves of ion temperature and density measured by the probe are also presented. DOE

N95-26059 Analytical Spectra Device, Inc., Boulder, CO.

FIELD-PORTABLE REFLECTANCE SPECTROMETER Final Report

Brian Curtiss and Alexander F. Goetz Hanover, NH U.S. Army Cold Regions Research and Engineering Lab. 5 Dec. 1994 33 p Limited Reproducibility: More than 20% of this document may be affected by microfiche quality

(Contract DACA33-94-C-0033)

(AD-A288750) Avail: Issuing Activity (Defense Technical Information Center (DTIC))

This study resulted in a design for an array detector based field spectroradiometer to be used for measurement of transmission and reflectance of man-made and natural materials using ambient solar illumination. This design is a significant advancement over currently available instrumentation. The design characteristics are: wavelength range from 0.35-2.5 micrometers spectral resolution of 4 nm (0.35-900 micrometers), 10 nm (0.9-2.5 micrometers); weight 15 pounds, exclusive of batteries; a minimum signal-to-noise ratio of 500:1 at 2200 nm under typical solar illumination; simultaneous acquisition of all wavelengths; operates at temperatures as low as -20 C; and, maintains radiometric calibration under field conditions. During Phase 1 a prototype was fabricated to test and validate this design. Government agencies using image data from high spectral resolution sensors will benefit. Additional applications include mineral resource evaluation, analytical chemistry and commercial remote sensing. DTIC

N95-26073*# National Aeronautics and Space Administration. Lewis Research Center, Cleveland, OH.

LIQUID CRYSTAL POINT DIFFRACTION INTERFEROMETER Ph.D. Thesis - Arizona Univ., 1995

Carolyn R. Mercer May 1995 109 p

(RTOP 505-62-50)

(NASA-TM-106899; E-9547; NAS 1.15:106899) Avail: CASI HC A06/MF A02

A new instrument, the liquid crystal point diffraction-interferometer (LCPDI), has been developed for the measurement of phase objects. This instrument maintains the compact, robust design of Linnik's point diffraction interferometer (PDI) and adds to it phase stepping capability for quantitative interferogram analysis. The result is a compact, simple to align, environmentally insensitive interferometer capable of accurately measuring optical wavefronts with very high data density and with automated data reduction. This dissertation describes the theory of both the PDI and liquid crystal phase control. The design considerations for the LCPDI are presented, including manufacturing considerations. The operation and performance of the LCPDI are discussed, including sections regarding alignment, calibration, and amplitude modulation effects. The LCPDI is then demonstrated using two phase objects: defocus difference wavefront, and a temperature distribution across a heated chamber filled with silicone oil. The measured results are compared to theoretical or independently measured results and show excellent agreement. A computer simulation of the LCPDI was performed to verify the source of observed periodic phase measurement error. The error stems from intensity variations caused by dye molecules rotating within the liquid crystal layer. Methods are discussed for reducing this error. Algorithms are presented which reduce this error; they are also useful for any phase-stepping interferometer that has unwanted intensity fluctuations, such as those caused by unregulated lasers. Author

N95-26113 University of South Florida, Saint Petersburg, FL. Dept. of Marine Science.

AVERAGE COSINE METER AND HIGH SPECTRAL RESOLUTION MEASUREMENTS AT THE MARINE LIGHT MIXED LAYER SITE Final Report, 1 Oct. 1990 - 30 Sep. 1994

Kendall L. Carder 30 Sep. 1994 125 p Limited Reproducibility: More than 20% of this document may be affected by microfiche quality

(Contract N00014-89-J-1091)

(AD-A288713) Avail: Issuing Activity (Defense Technical Information Center (DTIC))

The goals of this research have been to develop in situ optical instruments and computer models of the apparent and inherent optical properties of the submarine light field. The radiative transfer function in sea water is a complicated mix of signals caused by many component some of which are covarian. The approach taken in this research has been to measure by utilizing custom and commercial optical instrumentation as many of the components of light field at a single site rather than combine spotty information at many sites. A fundamental contribution to the program was our participation in the Marine Light Mixed Layer Experiment in the North Atlantic. This provided an opportunity to simultaneously measure the optical

components of the light field in a multi-investigator environment. We supported this project with state-of-the-art high spectral resolution optical field instrumentation and computer modelling of the submarine light field. The apparent optical properties of the MLML site were measured with the Spectral Transmissometer and Radiometer (STAR) and the Average Cosine Meter (ACM). Derived from text

N95-26182# National Inst. for Fusion Science, Nagoya (Japan).
HOLOGRAPY MACHINE HORN-1 FOR COMPUTER-AIDED RETRIEVE OF VIRTUAL THREE-DIMENSIONAL IMAGE
T. Yabe (Gunma Univ., Kiryu, Japan.), T. Ito (Gunma Univ., Kiryu, Japan.), and M. Okazaki (Gunma Univ., Kiryu, Japan.) Apr. 1993 16 p
(ISSN 0915-633X)
(NIFS-218) Avail: CASI HC A03/MF A01

We propose to retrieve the original 3-D objects as a virtual image by computers from a hologram created by real laser system. Then we can input the 3-D surface coordinates of a real object into computer memory. We may use these data as the boundaries to generate a body-fitted grid system for computer simulation, to modify these for computer animation, or to use these for pattern recognition of objects. HORN-1 (HOlographic ReconstructioN) specially prepared machine for this purpose enables us to do this work within quite short time. The machine has achieved a speed of 500 MFLOPS with one circuit. Massively parallel system combined into a LSI chip can work as a real-time recognition system. Author

N95-26340* National Aeronautics and Space Administration. Pasadena Office, CA.
CONTINUOUS PHASE AND AMPLITUDE HOLOGRAPHIC ELEMENTS Patent
Paul D. Maker, inventor (to NASA) and Richard E. Muller, inventor (to NASA) 28 Feb. 1995 13 p Filed 27 May 1993
(NASA-Case-NPO-18791-1; US-Patent-5,393,634;
US-Patent-Appl-SN-071131; US-Patent-Class-430-1;
US-Patent-Class-430-320; US-Patent-Class-430-2; US-Patent-Class-430-942;
US-Patent-Class-430-296; US-Patent-Class-250-492.22;
US-Patent-Class-250-492.3) Avail: US Patent and Trademark Office

A method for producing a phase hologram using e-beam lithography provides n-ary levels of phase and amplitude by first producing an amplitude hologram on a transparent substrate by e-beam exposure of a resist over a film of metal by exposing n is less than or equal to m x m spots of an array of spots for each pixel, where the spots are randomly selected in proportion to the amplitude assigned to each pixel, and then after developing and etching the metal film producing a phase hologram by e-beam lithography using a low contrast resist, such as PMMA, and n-ary levels of low doses less than approximately 200 micro-C/sq cm and preferably in the range of 20-200 micro-C/sq cm, and aggressive development using pure acetone for an empirically determined time (about 6 s) controlled to within 1/10 s to produce partial development of each pixel in proportion to the n-ary level of dose assigned to it.
Official Gazette of the U.S. Patent and Trademark Office

N95-25400*# Queensland Univ., Saint Lucia (Australia). Dept. of Mechanical Engineering.
BALANCES FOR THE MEASUREMENT OF MULTIPLE COMPONENTS OF FORCE IN FLOWS OF A MILLISECOND DURATION
D. J. Mee, W. J. Daniel, S. L. Tuttle, and J. M. Simmons *In its* Shock Tunnel Studies of Scramjet Phenomena 1993 Jan. 1995 p 107-112 Sponsored in cooperation with the Australian Research Council and the Queen Elizabeth 2nd FellowshipScheme (For primary document see N95-25394 08-34)
Avail: CASI HC A02/MF A02

36 LASERS AND MASERS

Includes parametric amplifiers.
For related information see also *76 Solid-State Physics.*

N95-24340# Japan Atomic Energy Research Inst., Tokyo (Japan).
SIMULATION STUDY OF TAPERED FEL AMPLIFIERS IN RAMAN AND COMPTON REGIMES
Mayuko Takahashi (Saitama Univ., Urawa, Japan.), Sunao Kawasaki (Saitama Univ., Urawa, Japan.), Keishi Sakamoto, Akihiko Watanabe, Yasuaki Kishimoto, and Makoto Shiho Mar. 1994 139 p
(DE94-785266; JAERI-M-94-048) Avail: CASI HC A07/MF A02

The magnetic taper of the wiggler field was studied numerically for an efficiency enhancement of mm wave free electron laser using the 3 dimensional analysis code. The linear taper seems effective to obtain an effective energy conversion. As the total conversion ratio increase as the K parameter increase, the large value of K parameter should be designed for high efficiency FEL. Prior to the simulation, the energy and its spread of the electron beam E(sub sp) were measured experimentally at the JAERI mm wave FEL (LAX-1). As a result, E(sub sp) = 15 keV at the beam energy of induction linac of 820 keV, which support that the JAERI FEL was operated at the Raman regime. DOE

N95-24371# California Univ., Los Angeles, CA. Flight Systems Research Center.
LASER BEAM LOG AMPLITUDE TEMPORAL SCINTILLATION SPECTRUM DUE TO CROSSWIND. PART 1: THEORY
A. V. Balakrishnan Sep. 1994 25 p
(TR-1-FSRC-1994-Pt-1) Avail: CASI HC A03/MF A01

We derive the temporal spectral density of the log-amplitude scintillation of a laser beam due to cross wind. The dependence on the velocity distribution along the propagation axis - magnitude and direction - in relation to the detector position vector in the plane normal to the axis is of main interest in addition to the usual turbulence parameters such as the inner and outer scales. Also studied are the moments of the (normalized) spectral density, which would appear to be less sensitive to these parameters, as providing possible means for monitoring changes in the wind velocity. We begin in Section 2 with a brief review of propagation theory essential for our purposes. The treatment is different from the standard textbook in that we make systematic use of the parabolic approximation of the Helmholtz equation rather than ad hoc arguments for simplification inside the solution integral. The main results, including the spectral density derivation, are in Section 3. Some approximations - which help avoid purely numerical computer evaluation of the integrals and provide some analytical insight - are studied in Section 4. Author

N95-24408# Sandia National Labs., Albuquerque, NM.
LASER BEAM CHARACTERIZATION RESULTS FOR A HIGH POWER CW Nd:YAG LASER
D. M. Keicher 1994 10 p Presented at the SPIE '95: SPIE Conference on Optics, Electro-optics, and Laser Application in Science, Engineering and Medicine, San Jose, CA, 5-10 Feb. 1995
(Contract DE-AC04-94AL-85000)
(DE95-006319; SAND-94-2206C; CONF-950226-1) Avail: CASI HC A02/MF A01

In an effort to understand multimode laser beam propagation characteristics for better development of laser material processing applications, beam diagnostic experiments were performed on a 1800 watt CW Nd:YAG laser. Beam diameter data were acquired at approximately 12 positions along the beam optical axis about the minimum waist created by a long focal length single element lens at several power levels. These data were then used to evaluate the laser output beam characteristics using two differing techniques. For the ISO technique, two data points from the beam diameter data were used in determining the output laser beam characteristics. These points were the beam minimum waist diameter and the diameter at a point along the beam optical axis where the beam diameter had increased to approximately 0.7 times that of the beam minimum waist diameter. The second analysis technique involved fitting the entire data set to theoretical equations used to describe the multimode laser beam propagation and points from the fitted curve fit were then used to determine the output beam characteristics from the laser. For all power levels evaluated, calculated results predicting the laser beam minimum waist location were in agreement with measured values and more consistent using the curve-fit technique than the two-point evaluation technique.
DOE

N95-24530*# National Aeronautics and Space Administration. Lewis Research Center, Cleveland, OH.
LASER LIGHT SCATTERING, FROM AN ADVANCED TECHNOLOGY DEVELOPMENT PROGRAM TO EXPERIMENTS IN A REDUCED GRAVITY ENVIRONMENT

William V. Meyer, Walther W. Tscharnuter (Brookhaven Instruments Corp., Holtsville, NY.), Andrew D. MacGregor (Edgerton, Germeshausen and Grier, Inc., Vaudreuil, Quebec.), Henri Dautet (Edgerton, Germeshausen and Grier, Inc., Vaudreuil, Quebec.), Pierre Deschamps (Edgerton, Germeshausen and Grier, Inc., Vaudreuil, Quebec.), Francois Boucher (Edgerton, Germeshausen and Grier, Inc., Vaudreuil, Quebec.), Jixiang Zuh (Princeton Univ., NJ.), Padetha Tin, Richard B. Rogers, and Rafat R. Ansari 22 Apr. 1994 16 p Presented at International Symposium on Space Optics, Garmisch-Partenkirchen, Germany, 18-22 Apr. 1994; sponsored by EOS and SPIE

(Contracts NCC3-208; NCC3-269; NCC3-166)

(NASA-TM-110496; NAS 1.15:110496; Paper-2210-21) Avail: CASI HC A03/MF A01

Recent advancements in laser light scattering hardware are described. These include intelligent single card correlators; active quench/active reset avalanche photodiodes; laser diodes; and fiber optics which were used by or developed for a NASA advanced technology development program. A space shuttle experiment which will employ aspects of these hardware developments is previewed. Author

N95-24707# Israel Atomic Energy Commission, Tel Aviv (Israel).

DECAY OF A LASER GENERATED SHOCK WAVE IN AN ALUMINIUM TARGET M.S. Thesis

Meir Werdiger Sep. 1993 118 p In HEBREW

(DE94-629014; IA-1482) Avail: CASI HC A06/MF A02 (US Sales Only)

When a shock wave arrives at the near surface of a solid material, a radical and fast change occurs in the reflection properties of the material. The phenomenon is used to develop a new way to measure the transit time of a shock wave in a target. A 10 milliwatt He:Ne laser is directed toward the rear surface of the target. The reflected beam arrives at a photo-diode with a fast rise time of 150 psec which detects the instant of the change in the reflection. This technique, called 'continuous back lightning', is used in experiments with aluminum foil thickness in the range of 40 micrometers less than or equal to x less than or equal to 1000 micrometers. The shock wave is induced by a laser pulse of an intensity of 3 x 10(exp 13) W/sq cm. The results show two main physical regimes: in the first one 40 micrometers less than or equal to x less than or equal to 210 micrometers, there is a constant shock wave velocity which in our experiments was measured to be (12.81 +/- 0.67)km/s. For x less than or equal to 210 micrometers the geometry is one dimensional for our experimental conditions, while for x greater than or equal to 300 micrometers the 1-D geometry changes to 2 dimensional (2-D) geometry. The 2-D shock wave decay asymptotically (x(yields)(infinity)) to an acoustic wave. Shock wave decay is described by a pressure scaling as x(sup -n) (n is a positive constant). The phenomenological equation of state is taken to be $P = A^{*} u(sub s)(sup 2) + B^{*} u(sub s)$, where P is the pressure, u(sub s) is the the shock velocity, A and B are constants. Applying our experimental results to the solution of the differential equation in this model $A^{*} x(exp 2) +/- B^{*} x = C^{*} x(sup -n)$ yields a value of n in the range 3.16 less than or equal to n less than or equal to 3.51. This pressure scaling law agrees with the self-similar solution of a concentrated impact on a surface between two media. This situation is well simulated by the laser deposition energy on a metal surface. In the experiment a 5% accuracy is achieved. Such a good accuracy has not been achieved so far in a laser induced shock-wave measurements in solids. DOE

N95-24709# General Atomics Co., San Diego, CA.

ENGINEERING AND DESIGN OF A CO2 PHASE CONTRAST INTERFEROMETER SYSTEM FOR DIII-D

R. D. Phelps and S. Coda (Massachusetts Inst. of Tech., Cambridge, MA.) Nov. 1994 19 p

(Contract DE-AC03-89ER-51114)

(DE95-004249; GA-A-21839; UC-420) Avail: CASI HC A03/MF A01

The development of a CO2 laser interferometer system, the engineering, design and installation of the hardware, and the selection of materials specific to the requirements of a CO2 laser diagnostic is discussed. A brief description of the system operation is included. A phase contrast interferometer diagnostic has been designed and installed on the DIII-D tokamak to enhance studies of the physical characteristics of plasma turbulence, and specifically to analyze plasma density fluctuations in the boundary region of the plasma. A 20 watt CO2 laser beam, operating at the 10.6 micron wavelength, is expanded to a diameter of 76 mm and directed through a series of mirrors which provide for entry of the beam into the vessel at a point 70 cm above the midplane at the 285 degree toroidal location. After being reflected from a mirror inside the vessel, the beam is directed downward so that it passes through the edge of the plasma immediately in front of a four-strap fast wave current drive RF antenna. The laser beam is then reflected by a second internal mirror and exits the vessel 70 cm below the midplane (also at 285 degrees) returning to an optical table through a final series of external steering mirrors. DOE

N95-24869# Fermi National Accelerator Lab., Batavia, IL.

THE KTeV PMT LASER MONITORING SYSTEM

Hogan H. Nguyen Nov. 1994 7 p Presented at the 5th International Conference on Calorimetry in High Energy Physics, Upton, NY, 25 Sep. - 1 Oct. 1994

(Contract DE-AC02-76CH-03000)

(DE95-004237; FNAL/C-94/398; CONF-9409268-2) Avail: CASI HC A02/MF A01

The KTeV (Kaons at the TeVatron) collaboration is currently building a high-precision, pure CsI electromagnetic calorimeter with sophisticated digital readout. The KTeV CsI electromagnetic calorimeter will be monitored in situ by a light pulser system. Pulsed light from a liquid dye scintillator, itself pumped by a Nd:YAG laser, will be injected into each Photomultiplier Tube (PMT) of the calorimeter. The system is designed to linearize the response of the combined PMT and readout electronics, as well as monitor the gains of the PMT's. DOE

N95-25100# Lawrence Livermore National Lab., Livermore, CA.

Na-LIKE AUTOIONIZING LEVELS: PLASMA DIAGNOSTICS AND PROSPECTS FOR PHOTOPUMPED SOFT X-RAY LASERS

A. L. Osterheld, J. Dunn, B. K. F. Young, S. B. Libby, A. Szoke, R. S. Walling, W. H. Goldstein, R. E. Stewart, A. Ya. Faenov (All-Union Research Inst. for Physical and Radiotechnical Measurements, Mendeleevo, USSR.), and I. Yu. Skobelev (All-Union Research Inst. for Physical and Radiotechnical Measurements, Mendeleevo, USSR.) Aug. 1994 7 p Presented at the 4th International Colloquium on X-ray Lasers, Williamsburg, VA, 16-20 May 1994

(Contract W-7405-eng-48)

(DE95-004207; UCRL-JC-117928; CONF-940592-10) Avail: CASI HC A02/MF A01

We have investigated the kinetics of doubly excited sodium-like copper states with 3131' and 3141' configurations, and the feasibility of photopumped x-ray lasing schemes and plasma diagnostics using transitions from these levels. These x-ray lasing schemes, like similar lasing schemes in Li-like ions, have high quantum efficiency and potentially reduced radiative trapping effects. In addition, the satellite transitions emitted by these sodium-like levels may provide valuable diagnostics of x-ray laser plasmas. DOE

N95-25491# Cape Coast Univ. (Ghana). Dept. of Physics.

THE THIRD INTERNATIONAL WORKSHOP ON THE PHYSICS AND MODERN APPLICATIONS OF LASERS

Aug. 1994 96 p Workshop held in Cape Coast, Ghana, 8-20 Aug. 1994

(DE95-606395; INIS-MF-14376; CONF-9408186) Avail: CASI HC A05/MF A01 (US Sales Only)

This document contains 31 abstracts and 7 papers on lasers and optical fibers presented at the third international workshop on the physics and modern applications of lasers. The main topics covered include: basics in lasers, geometrical, physical and quantum optics; optical techniques for research, education and development in Africa; application of lasers in optical fibre communication, environmental studies, bio medicine, chemistry, agriculture, engineering and industry. A list of lecturers, participants and programme of activities are also given. DOE

N95-25549# Sandia National Labs., Livermore, CA.

TUNABLE DIODE LASERS AS CONTINUOUS EMISSION MONITORS FOR THERMAL WASTE TREATMENT PROCESSES

S. W. Allendorf, D. K. Ottesen, H. A. Johnsen, J. Wang, M. D. Frish (PSI Technology Co., Andover, MA.), D. G. Trembley (PSI Technology Co., Andover, MA.), R. Severance (PSI Technology Co., Andover, MA.), and A. A. Boni, p6233502 1994 3 p Presented at the Incineration Conference:

13th International Symposium on Thermal Treatment Technologies, Houston, TX, 9-13 May 1994 Prepared in cooperation with PSI Technology Co., Andover, MA
(Contract DE-AC04-76DR-00789)
(DE95-004381; SAND-94-8699C; CONF-940528-7) Avail: CASI HC A01/MF A01

In this paper the ongoing program to develop and apply a family of on-line process monitors is described. This technique detects molecular gas-phase species by optical absorption using vibrational transitions in the near-infrared region. Near-infrared, tunable diode lasers are used that emit extremely narrow, single-mode radiation. Current efforts include laboratory work to identify the optimum absorption lines for the molecular species of interest. Sensors based on tunable diode lasers are being developed in parallel with this scoping work. One such instrument, designed to monitor ammonia, has been constructed and field-tested; its specification and performance are discussed. DOE

N95-25557# Los Alamos National Lab., NM.
TARGETS FOR LASER-DRIVEN OPACITY MEASUREMENTS
P. L. Gobby, H. Bush, Jr., V. A. Gurule, V. M. Gomez, J. E. Moore, and B. F. Henneke 1995 10 p Presented at the 17th Biennial World Conference ofthe International Nuclear Target Development Society: Targets, Research Materials and Related Topicsof Hadron Physics, Bloomington, IN, 17-21 Oct. 1994
(Contract W-7405-eng-36)
(DE95-006172; LA-UR-95-426; CONF-941041-1) Avail: CASI HC A02/MF A01

Special laser targets have been designed and fabricated which allow the opacity of materials to be experimentally determined at elevated temperatures (kT less than or equal to 200 eV). A general description of the technique is presented, as well as the fabrication steps necessary to produce the targets. A uniform high temperature environment is provided by the use of small millimeter-sized hohlraums driven by the Nova laser at Lawrence Livermore National Laboratory. The material sample is placed within the hohlraum and is further illuminated by the x-rays produced by one or two of the Nova beams incident on a second material known as a back lighter. Thus far, silver and niobium opacity samples have been used, and each has required a different fabrication technique. DOE

N95-25565# Los Alamos National Lab., NM.
AN FEL DESIGN CODE RUNNING ON MATHCAD(TRADEMARK)
D. C. Nguyen, S. M. Gierman, and P. G. OShea (Duke Univ., Durham, NC.) 1994 5 p Presented at the FEL '94: Nuclear Instrument Methods, Stanford, CA, 21-26 Aug. 1994
(Contract W-7405-eng-36)
(DE95-005279; LA-UR-94-4168; CONF-9408196-2) Avail: CASI HC A01/MF A01

We present a simple computer code called FEL-CAD that runs on the Mathcad(trademark) software. FEL-CAD gives estimates of the expected performance of a low-gain Compton FEL oscillator driven by an rf linac. The code provides fast, albeit approximate, answers to basic FEL design questions. Scaling can be done by varying the wiggler, the linac, the electron beam and the optical resonator parameters. DOE

N95-25622 Research Inst. of National Defence, Linkoeping (Sweden). Huvudavdelning foer Informationsteknologi.
DIODE LASER PUMPED SOLID STATE LASER WITH 2 MICROMETER WAVELENGTH [LASERDIODPUMPAD FASTA TILLSTANDSLASER MED VAGLAENGDEN 2 MU M]
G. Hansson and A. Callenas Jun. 1994 54 p In SWAHILI
(PB95-165270; FOA-C-30756-3.1) Avail: Issuing Activity (National Technical Information Service (NTIS))

Research at the FOA in the field diode laser pumped solid state lasers with 2 micrometer wavelength is presented. The research was made within the project Antisensor laser. Basic models for CW and pulsed lasers are presented together with results and experience from the design of a diode laser pumped CW laser based on Thulium (Tm), Holmium (Ho) doped Yttrium Lithium Fluoride (TLiF4), abbreviated Tm, Ho:YLF. Measurements on upconversion of energy from the upper laser level in the laser crystal has been made. The upconversion causes loss of energy which leads to higher laser threshold and lower upper state effective lifetime. The result shows less upconversion in Tm, Ho doped YLF than with the same active ions doped into Yttrium Aluminum Garnet (Tm, Ho: YAG). A simple pump configuration was assembled which produced a pump focus of about 200 micrometers radius. With 1 W pump power, an output power of 50 mW was achieved with the laser crystal at room temperature (25 C). With the crystal cooled to 5 C temperature, 77 mW output power was achieved. The measured laser threshold was in good agreement with the calculated value. The efficiency was only 10% compared to the predicted value of 50%. Measurements of laser beam cross section, wavelength and longitudinal laser modes have also been made and is presented in the report. NTIS

N95-25640 Rutherford Appleton Lab., Chilton (England).
CENTRAL LASER FACILITY. ANNUAL REPORT TO THE LASER FACILITY COMMITTEE Annual Report, 5 Apr. 1993 - 4 Apr. 1994
1994 272 p See also report for 1993, PB93-230456
(PB95-160511; RAL-94-042) Avail: Issuing Activity (National Technical Information Service (NTIS))

Contents include the following: High Power Laser Program: Laser Plasma Physics -- X-Ray Lasers, Short Pulse High Intensity Interactions, ICF (Inertial Confinement Fusion) Related Physics, Applications of Laser-Produced Plasmas, Theory and Computation; High Power Laser Program: High Power Lasers Development and Operations -- Glass Laser CPA (Chirped Pulse Amplification), KrF Laser CPA, KrF Raman, Titania Upgrade, Instrumentation and Other Developments, High Power Operations; Laser Support Facility (LSF) Program: LSF Experiments -- Chemistry, Biology, Physics; LSF Program: LSF Operations and Development; General Facility Publications -- High Power Laser Science, Laser Development, LSF Science; and Committee Membership. NTIS

N95-25973# International Centre for Theoretical Physics, Trieste (Italy).
CONSTRUCTION OF A NITROGEN LASER FOR PLASMA DIAGNOSTICS
G. C. Ishiekwene Jul. 1994 10 p
(DE95-607599; IC-94/200) Avail: CASI HC A02/MF A01 (US Sales Only)

The challenge faced in finding new sources of energy to bridge the gap between the availability and demand of energy is difficult to be overemphasized. Nuclear fusion seems to provide a potentially limitless source of energy which offers a bright prospect for solving this problem. Although an elaborate programme in fusion may be beyond the economic reach of most third world countries, some modest experiments are necessary to provide an indigenous expertise capable of enhancing international fusion studies. In order to initiate experimental research sufficient for plasma studies at an affordable cost to developing countries, this paper illustrates the construction of a simple, low cost, high power nitrogen laser and investigates some of its performance characteristics. Also, the laser is utilized as a source of illumination in the techniques of shadowgraphy. A series of shadowgrams depicting the temporal development of the plasma discharge is presented. The constructed laser is found to be cost-effective and useful in small-scale researches in laser-plasma diagnostics. DOE

N95-26112# Los Alamos National Lab., NM.
TIME-DEPENDENT NUMERICAL SIMULATION OF VERTICAL CAVITY LASERS
L. E. Thode, G. Csanak, L. L. So, T. J. T. Kwan, and M. Campbell (PASTDCO, Albuquerque, NM.) Feb. 1994 11 p Presented at the OE/LASE '94: Conference on Optics, Electro-optics, and Laser Applications in Science and Engineering, Los Angeles, CA, 22-29 Jan. 1994
(Contract W-7405-eng-36)
(DE95-006862; LA-UR-94-378; CONF-940142-48) Avail: CASI HC A03/MF A01

To simulate vertical cavity surface emitting lasers (VCSEL's), the authors are developing a three-dimensional, time-dependent field-gain model with absorption in bulk dielectric regions and gain in quantum well regions. Since the laser linewidth is narrow, the bulk absorption coefficient is assumed to be independent of frequency with a value determined by the material and the lattice temperature. In contrast, the frequency-dependent gain regions must be solved consistently in the time domain. Treatment of frequency-dependent media in a finite-difference time-domain code is computationally intensive. However, because the volume of the quantum well regions is small relative to the volume of the multilayer dielectric (MLD) mirror regions, the computational overhead is reasonable. A key

issue is the calculation of the fields in the MLD mirror regions. Although computationally intensive, good agreement has been obtained between simulation results and matrix equation solutions for the reflection coefficient, transmission coefficient, and bandwidth of MLD mirrors. The authors discuss the development and testing of the two-dimensional field-gain model. This field-gain model will be integrated with a carrier transport model to form the self-consistent laser code, VCSEL. DOE

N95-26114 Science Applications International Corp., McLean, VA. Applied Physics Operation.

NONLINEAR ANALYSIS OF MILLIMETER AND SUB-MILLIMETER WAVE SOURCES SUCH AS CERENKOV MASERS, OROTRONS, AND UBITRONS Final Report

Oct. 1994 172 p Sponsored by the Office of Naval Research Limited Reproducibility: More than 20% of this document may be affected by microfiche quality

(AD-A288777; SAIC-94/1150) Avail: Issuing Activity (Defense Technical Information Center (DTIC))

The research performed on the contract covers a broad range of topics related to coherent radiation sources. In general, the research can be divided into two broad categories: theoretical research into innovative concepts in the physics of ubitrons (or free-electron lasers), and in the application of this theory to the support of the experimental ubitron program in the Vacuum Electronics Branch of the Electronics Science and Technology Division at the Naval Research Laboratory. The general theory research covers a wide range of topics. Linearized analyses of the ubitron/free-electron laser (FEL) have been performed to study (1) thermal effects on the gain in both planar and helical wiggler geometries in ubitrons, and (2) the relationship between the variation in the relative phase and optical guiding. Nonlinear analyses have been conducted for a wide variety of configurations and purposes. These can be roughly categorized as studies of: (1) the effect of wiggler imperfections on ubitron operation, (2) space-charge effects in ubitrons, (3) slow-wave ubitrons, (4) tunability of tapered wiggler configurations in ubitrons, (5) a high-efficiency collective FEL experiment using a helical wiggler and an anti-parallel axial guide magnetic field, (6) the inclusion of a model of self-electric and magnetic fields in the nonlinear simulations of ubitrons, (7) a high power Cerenkov maser, and (8) the analysis of the Coaxial Hybrid Iron (CHI) wiggler.

Derived from text

37 MECHANICAL ENGINEERING

Includes auxiliary systems (nonpower); machine elements and processes; and mechanical equipment.

N95-24204*# Endorobotics Corp., Warren, NJ.

MILLI-ROBOTS FOR SURGICAL TELEOPERATION Progress Report, 19 Oct. 1994 - 19 Jan. 1995

19 Jan. 1995 10 p

(Contract NAS1-20288)

(NASA-CR-197378; NAS 1.26:197378) Avail: CASI HC A02/MF A01

A small hydraulic actuator with an integrated gripper has been constructed. This device is suitable as an end-effector for a laparoscopic surgical tool. Test results on the actuator prototype indicate that it exceeds, in some cases by a factor of three, the requirements of the application. The results reflect a slight modification relative to the proposed design that preserves the low-cost manufacturability of the original design, and that displays several other advantages in addition. Derived from text

N95-24218*# Georgia Inst. of Tech., Atlanta, GA. School of Mechanical Engineering.

ACTIVELY CONTROLLED SHAFT SEALS FOR AEROSPACE APPLICATIONS Final Report, 1 Jan. 1989 - 31 Dec. 1994

Richard F. Salant 31 Dec. 1994 189 p

(Grant NAG3-974)

(NASA-CR-198035; NAS 1.26:198035) Avail: CASI HC A09/MF A02

This study experimentally investigates an actively controlled mechanical seal for aerospace applications. The seal of interest is a gas seal, which is considerably more compact than previous actively controlled mechanical seals that were developed for industrial use. In a mechanical seal, the radial convergence of the seal interface has a primary effect on the film thickness. Active control of the film thickness is established by controlling the radial convergence of the seal interface with piezoelectric actuator. An actively controlled mechanical seal was initially designed and evaluated using a mathematical model. Based on these results, a seal was fabricated and tested under laboratory conditions. The seal was tested with both helium and air, at rotational speeds up to 3770 rad/sec, and at sealed pressures as high as 1.48 x 10(exp 6) Pa. The seal was operated with both manual control and with a closed-loop control system that used either the leakage rate or face temperature as the feedback. The output of the controller was the voltage applied to the piezoelectric actuator. The seal operated successfully for both short term tests (less than one hour) and for longer term tests (four hours) with a closed-loop control system. The leakage rates were typically 5-15 slm (standard liters per minute), and the face temperatures were generally maintained below 100 C. When leakage rate was used as the feedback signal, the setpoint leakage rate was typically maintained within 1 slm. However, larger deviations occurred during sudden changes in sealed pressure. When face temperature was used as the feedback signal, the setpoint face temperature was generally maintained within 3 C, with larger deviations occurring when the sealed pressure changed suddenly. Author

N95-24223*# Michigan State Univ., East Lansing, MI. Engine Research Lab.

STRATIFIED CHARGE ROTARY ENGINE COMBUSTION STUDIES Progress Report

H. Shock, F. Hamady, C. Somerton, T. Stuecken, E. Chouinard, T. Rachal, J. Kosterman, M. Lambeth, and C. Olbrich 6 Jul. 1989 186 p

(Grant NAG3-853)

(NASA-CR-197985; NAS 1.26:197985) Avail: CASI HC A09/MF A02

Analytical and experimental studies of the combustion process in a stratified charge rotary engine (SCRE) continue to be the subject of active research in recent years. Specifically to meet the demand for more sophisticated products, a detailed understanding of the engine system of interest is warranted. With this in mind the objective of this work is to develop an understanding of the controlling factors that affect the SCRE combustion process so that an efficient power dense rotary engine can be designed. The influence of the induction-exhaust systems and the rotor geometry are believed to have a significant effect on combustion chamber flow characteristics. In this report, emphasis is centered on Laser Doppler Velocimetry (LDV) measurements and on qualitative flow visualizations in the combustion chamber of the motored rotary engine assembly. This will provide a basic understanding of the flow process in the RCE and serve as a data base for verification of numerical simulations. Understanding fuel injection provisions is also important to the successful operation of the stratified charge rotary engine. Toward this end, flow visualizations depicting the development of high speed, high pressure fuel jets are described. Friction is an important consideration in an engine from the standpoint of lost work, durability and reliability. MSU Engine Research Laboratory efforts in accessing the frictional losses associated with the rotary engine are described. This includes work which describes losses in bearing, seal and auxillary components. Finally, a computer controlled mapping system under development is described. This system can be used to map shapes such as combustion chamber, intake manifolds or turbine blades accurately.

Author

N95-24356# Stanford Linear Accelerator Center, CA.

PEP-2 VACUUM SYSTEM: JOINING SS FLANGES TO COPPER BEAM CHAMBERS

S. Fetzko, E. Hoyt, and U. Cummings Jun. 1994 3 p Presented at the 4th European Particle Accelerator Conference, London, 27 Jun. - 1 Jul. 1994

(Contract DE-AC03-76SF-00515)

(DE95-006093; SU-SLAC-PUB-6566; CONF-940618-114) Avail: CASI HC A01/MF A01

Various methods of joining stainless steel flanges to the copper PEP-II high-energy ring vacuum chambers were investigated with regard to metallurgical soundness, reliability, complexity, and cost. The most promising method appears to be direct electron-beam welding. DOE

N95-24393 Defence Science and Technology Organisation, Melbourne (Australia). Airframes and Engines Div.
A REVIEW OF ROLLING ELEMENT BEARING VIBRATION DETECTION, DIAGNOSIS AND PROGNOSIS
Ian M. Howard Oct. 1994 109 p
(DSTO-RR-0013; AR-008-399) Copyright Avail: Issuing Activity (DSTO Aeronautical and Maritime Research Lab., GPO Box 4331, Melbourne, Victoria 3001, Australia)

Rolling element bearings are among the most common components to be found in industrial rotating machinery. They are found in industries from agriculture to aerospace, in equipment as diverse as paper mill rollers to the Space Shuttle Main Engine Turbomachinery. There has been much written on the subject of bearing vibration monitoring over the last twenty five years. This report attempts to summarize the underlying science of rolling element bearings across these diverse applications from the point of view of machine condition monitoring using vibration analysis. The key factors which are addressed in this report include the underlying science of bearing vibration, bearing kinematics and dynamics, bearing life, vibration measurement, signal processing techniques and prognosis of bearing failure. Author

N95-24462# Sandia National Labs., Albuquerque, NM.
THE ROLE OF FORCE MEASUREMENTS IN ADVANCED VIBRATION TEST METHODS
D. O. Smallwood 1994 6 p Presented at the International Modal Analysis Conference, Nashville, TN, 13-16 Feb. 1995
(Contract DE-AC04-94AL-85000)
(DE95-001833; SAND-94-2681C; CONF-950240-2) Avail: CASI HC A02/MF A01

The role of force measurements in vibration testing is discussed. The rational for a vibration test based on the extremal control of force and acceleration is developed. The differences between force measurements in vibration testing and modal testing is discussed. Several methods for estimating the input force in a vibration test are outlined. DOE

N95-24550# Lawrence Livermore National Lab., Livermore, CA.
OPTIMIZED HYDROGEN PISTON ENGINES
J. R. Smith 10 May 1994 8 p Presented at the 1994 Society of Automotive Engineers' Convergence, Detroit, MI, 18 Oct. 1994
(Contract W-7405-eng-48)
(DE95-003656; UCRL-JC-116894; CONF-9410256-1) Avail: CASI HC A02/MF A01

Hydrogen piston engines can be simultaneously optimized for improved thermal efficiency and for extremely low emissions. Using these engines in constant-speed, constant-load systems such as series hybrid-electric automobiles or home cogeneration systems can result in significantly improved energy efficiency. For the same electrical energy produced, the emissions from such engines can be comparable to those from natural gas-fired steam power plants. These hydrogen-fueled high-efficiency, low-emission (HELE) engines are a mechanical equivalent of hydrogen fuel cells. HELE engines could facilitate the transition to a hydrogen fuel cell economy using near-term technology. DOE

N95-24880# National Renewable Energy Lab., Golden, CO.
DEVELOPMENT OF A DEDICATED ETHANOL ULTRA-LOW EMISSION VEHICLE (ULEV) SYSTEM DESIGN
G. Bourn (Southwest Research Inst., San Antonio, TX.), T. Callahan (Southwest Research Inst., San Antonio, TX.), L. Dodge (Southwest Research Inst., San Antonio, TX.), J. Mulik (Southwest Research Inst., San Antonio, TX.), D. Naegeli (Southwest Research Inst., San Antonio, TX.), K. Shouse (Southwest Research Inst., San Antonio, TX.), L. Smith (Southwest Research Inst., San Antonio, TX.), and K. Whitney (Southwest Research Inst., San Antonio, TX.) Feb. 1995 90 p
(Contract DE-AC36-83CH-10093)
(DE95-004016; NREL/TP-425-6722) Avail: CASI HC A05/MF A01

The objective of this 3.5 year project is to develop a commercially competitive vehicle powered by ethanol (or ethanol blend) that can meet California's ultra-low emission vehicle (ULEV) standards and equivalent corporate average fuel economy (CAFE) energy efficiency for a light-duty passenger car application. The definition of commercially competitive is independent of fuel cost, but does include technical requirements for competitive power, performance, refueling times, vehicle range, driveability, fuel handling safety, and overall emissions performance. This report summarizes a system design study completed after six months of effort on this project. The design study resulted in recommendations for ethanol-fuel blends that shall be tested for engine low-temperature cold-start performance and other criteria. The study also describes three changes to the engine and two other changes to the vehicle to improve low-temperature starting, efficiency, and emissions. The three engine changes are to increase the compression ratio, to replace the standard fuel injectors with fine spray injectors, and to replace the powertrain controller. The two other vehicle changes involve the fuel tank and the aftertreatment system. The fuel tank will likely need to be replaced to reduce evaporative emissions. In addition to changes in the main catalyst, supplemental aftertreatment systems will be analyzed to reduce emissions before the main catalyst reaches operating temperature. DOE

N95-24991*# Auburn Univ., AL. Dept. of Civil Engineering.
EXPERIMENTAL ANALYSIS OF THREAD MOVEMENT IN BOLTED CONNECTIONS DUE TO VIBRATIONS Final Report
G. Ed Ramsey and Robert C. Jenkins Mar. 1995 176 p
(Contract NAS8-39131)
(NASA-CR-197705; NAS 1.26:197705) Avail: CASI HC A09/MF A02

This is the final report of research project NAS8-39131 #33 sponsored by NASA's George C. Marshall Space Flight Center (MSFC) and carried out by the Civil Engineering Department of Auburn University (Auburn, Alabama) and personnel of MSFC. The objective of this study was to identify the main design parameters contributing to the loosening of bolts due to vibration and to identify their relative importance and degree of contribution to bolt loosening. Vibration testing was conducted on a shaketable with a controlled-random input in the dynamic testing laboratory of the Structural Test Division of MSFC. Test specimens which contained one test bolt were vibrated for a fixed amount of time and a percentage of pre-load loss was measured. Each specimen tested implemented some combination of eleven design parameters as dictated by the design of experiment methodology employed. The eleven design parameters were: bolt size (diameter), lubrication on bolt, hole tolerance, initial pre-load, nut locking device, grip length, thread pitch, lubrication between mating materials, class of fit, joint configuration, and mass of configuration. These parameters were chosen for this experiment because they are believed to be the design parameters having the greatest impact on bolt loosening. Two values of each design parameter were used and each combination of parameters tested was subjected to two different directions of vibration and two different g-levels of vibration. One replication was made for each test to gain some indication of experimental error and repeatability and to give some degree of statistical credibility to the data, resulting in a total of 96 tests being performed. The results of the investigation indicated that nut locking devices, joint configuration, fastener size, and mass of configuration were significant in bolt loosening due to vibration. The results of this test can be utilized to further research the complex problem of bolt loosening due to vibration. Author

N95-24992 Institute of Sound and Vibration Research, Southampton (England). Structrural Dynamics Group.
THE TRANSMISSION AND CONTROL OF VIBRATIONAL POWER IN A TWO STAGE ISOLATION SYSTEM WITH A WATER-LOADED SUBSTRUCTURE
S. Shen and R. G. White Jun. 1994 43 p
(ISVR-TR-235) Copyright Avail: Issuing Activity (Director, Institute of Sound and Vibration Research, University of Southhampton, Southampton SO17 1BJ, England)

A theoretical analysis is carried out on the transmission of vibrational power from a source through a two stage isolation system to a fluid-loaded substructure. A viscoelastic sandwich damping treatment is introduced in the raft structure to control power transmission. The stiffness and mass matrices of a sandwich core are derived and a gradual approach algorithm is used to solve the eigenproblem with a large number of complex coefficients. The natural frequencies, mode shapes, and loss factors of a viscoelastic sandwich-type structure can be predicted. Results for unstiffened and stiffened plates are given for a range of boundary conditions, area ratio, and position of damping treatment. Some conclusions are drawn from the work which are useful in design. Author

N95-25101# Hansen Engine Corp., Minnetonka, MN.
INVESTIGATION OF A ROTARY VALVING SYSTEM WITH VARIABLE VALVE TIMING FOR INTERNAL COMBUSTION ENGINES Final Technical Report
Paul C. Cross and Craig N. Hansen 18 Nov. 1994 92 p
(Contract DE-FG01-89CE-90049)
(DE95-003831; DOE/CE-90049/T1) Avail: CASI HC A05/MF A01

The objective of the program was to provide a functional demonstration of the Hansen Rotary Valving System with Variable Valve Timing (HRVS/VVT), capable of throttleless inlet charge control, as an alternative to conventional poppet-valves for use in spark ignited internal combustion engines. The goal of this new technology is to secure benefits in fuel economy, broadened torque band, vibration reduction, and overhaul accessibility. Additionally, use of the variable valve timing capability to vary the effective compression ratio is expected to improve multifuel tolerance and efficiency. Efforts directed at the design of HRVS components proved to be far more extensive than had been anticipated, ultimately requiring that proof-trial design/development work be performed. Although both time and funds were exhausted before optical or ion-probe types of in-cylinder investigation could be undertaken, a great deal of laboratory data was acquired during the course of the design/development work. This laboratory data is the basis for the information presented in this final report. DOE

N95-25323# National Aerospace Lab., Tokyo (Japan).
PERFORMANCE OF SOLID LUBRICATED BALL BEARINGS AT HIGH-TEMPERATURES IN A VACUUM
Katsumi Seki (Hosei Univ., Tokyo, Japan.), Mineo Suzuki (Hosei Univ., Tokyo, Japan.), Makoto Nishimura (Hosei Univ., Tokyo, Japan.), Masaji Hasegawa, and Minoru Moriyama Jul. 1994 19 p In JAPANESE
(ISSN 0389-4010)
(NAL-TR-1243) Avail: CASI HC A03/MF A01

Ball bearings which can operate at high temperatures in a vacuum will be required with advances in technology. Among the issues for the operation of ball bearings at high temperatures, solid lubricants and bearing materials are crucial. The aim of this study was to develop ball bearings for use at high temperatures in a vacuum. The tested bearings were 20-mm bore-sized angular contact ball bearings. Three combinations of bearing materials were tested: M-50 bearings, hybrid bearings with M-50 races and Si3N4 balls, and Si3N4 bearings. M-50 bearings were lubricated with a silver film. Hybrid and ceramic bearings were lubricated with a pre-coated sputtered MoS2 film and a self-lubricating hot-pressed composite retainer. Tests were carried out at temperatures up to 500 C and a rotational speed of 600 rpm under an axial load of 50 N in a vacuum. Excellent performance at 500 C in a vacuum was obtained for Si3N4 bearings. Frictional torque was low and stable for more than 5x10(exp 7) revolutions. After the tests, the bearings were in very good condition with a small amount of wear. Hybrid bearings also showed very good performance at 350 C in a vacuum. M-50 steel bearings were operated without failure at 350 C in a vacuum, although frictional torque was rather high and unstable. X-ray photoelectron spectroscopy (XPS) analysis and scanning electron microscopy (SEM) observation revealed the existence of a film on the ball surface transferred from the composite retainer for both hybrid and ceramic bearings. Author

N95-25548* National Aeronautics and Space Administration. Marshall Space Flight Center, Huntsville, AL.
TERNARY GAS PLASMA WELDING TORCH Patent
Daniel J. Rybicki, inventor (to NASA) (Martin Marietta Corp., Huntsville, AL.), William F. McGee, inventor (to NASA) (Martin Marietta Corp., Huntsville, AL.), and Douglas J. Waldron, inventor (to NASA) (Palmdale, CA. Waldron, Douglas J.,) 21 Mar. 1995 5 p Filed 27 Dec. 1993 Supersedes N94-30173 (32 - 8, p 3303)
(NASA-Case-MFS-28857-1; US-Patent-5,399,831;
US-Patent-Appl-SN-172961; US-Patent-Class-219-121.45;
US-Patent-Class-219-121.5; US-Patent-Class-219-121.51;
US-Patent-Class-219-121.48; Int-Patent-Class-B23K-10/00) Avail: US Patent and Trademark Office

A plasma arc welding torch is discussed. A first plasma gas is directed through the body of the welding torch and out of the body across the tip of a welding electrode disposed at the forward end of the body. A second plasma gas is disposed for flow through a longitudinal bore in the electrode. The second plasma gas enters one end of the electrode and exits the electrode at the tip thereof for co-acting with the electric welding arc to produce the desired weld. A shield gas is directed through the torch body and circulates around the head of the torch adjacent to the electrode tip. Official Gazette of the U.S. Patent and Trademark Office

N95-25574 Environmental Protection Agency, Ann Arbor, MI. Office of Mobile Sources.
SPRAY CHARACTERISTICS OF SINGLE- AND THREE-HOLE NOZZLE INJECTORS IN AMBIENT AIR AND IN A MOTORED SINGLE-CYLINDER TEST ENGINE
J. P. Hahn, F. J. Hamady, and R. M. Schaefer Nov. 1994 14 p
Limited Reproducibility: More than 20% of this document may be affected by microfiche quality
(PB95-166286; EPA/AA/TDG-94/04) Avail: Issuing Activity (National Technical Information Service (NTIS))

The high-speed/high-resolution imaging system was used to evaluate two mid-pressure (15 MPa) fuel injector nozzles in ambient air and in a motored single-cylinder test engine. The nozzles are designed for use in the EPA/NVFEL program to develop clean and efficient engines that use alternative fuels. The report is part of an ongoing investigation to analyze the transient spray characteristics for direct-injection type fuel injectors. The experimental results compare a single-hole and a three-hole nozzle and conclude that both of these injector nozzles yield similar spray patterns and atomization and could be particularly useful for combustion systems where injection into a piston bowl is required. NTIS

N95-25592* National Aeronautics and Space Administration. Lyndon B. Johnson Space Center, Houston, TX.
PRELOAD RELEASE MECHANISM Patent
Robert M. Generoli, inventor (to NASA) (McDonnell-Douglas Corp., Houston, TX.) and Harry J. Young, inventor (to NASA) (McDonnell-Douglas Corp., Houston, TX.) 14 Mar. 1995 10 p Filed 20 Apr. 1994 Supersedes N94-36839 (32 - 12, p 4450)
(NASA-Case-MSC-22327-1; US-Patent-5,397,244;
US-Patent-Appl-SN-230571; US-Patent-Class-439-248;
Int-Patent-Class-H01R-13/629) Avail: US Patent and Trademark Office

This invention relates to a preload release mechanism comprising a preload spring assembly adapted to apply a preload to a first connector member which is mounted on a support structure and adapted for connection with a second connector member on an object. The assembly comprises telescoped bushings and a preload spring. A tubular shaft extends through the spring assembly and openings in the first connector member and support structure, on which it is clamped. A plunger rod in the shaft is provided with a tip end and a recess in the rod near the other end thereof. A retainer precludes passage of the rod through the shaft in one direction and an end cap closes the bore of the shaft at the other end and provides a shoulder which extends radially of the shaft. A plunger return spring biases the plunger rod against the plunger retainer with the plunger tip protruding from the shaft and a spring assembly return spring engages at its ends the shoulder of the end cap and one end of the spring assembly. Detents received in lateral openings in the tubular shaft are held captive by the plunger rod and one end of the spring assembly to lock the spring assembly on the tubular shaft and apply a preload to the first connector member. Upon completion of the connection, detents and spring assembly are released by plunger contact with the object to be connected, thereby releasing the preload while the connection is maintained. Official Gazette of the U.S. Patent and Trademark Office

N95-25595*# Applied Research, Inc., Huntsville, AL.
ACTIVE WELD CONTROL Final Report
Bradley W. Powell and Ivan A. Burroughs 31 Jan. 1994 120 p Prepared in cooperation with Science Applications International Corp., Huntsville, AL
(Contract NAS8-38551)
(NASA-CR-196588; NAS 1.26:196588) Avail: CASI HC A06/MF A02

Through the two phases of this contract, sensors for welding applications and parameter extraction algorithms have been developed. These sensors form the foundation of a weld control system which can provide action weld control through the monitoring of the weld pool and keyhole in a VPPA welding process. Systems of this type offer the potential of quality enhancement and cost reduction (minimization of rework on faulty welds) for high-integrity welding applications. Sensors for preweld and postweld inspection, weld pool monitoring, keyhole/weld wire entry monitoring, and seam tracking were developed. Algorithms for signal extraction were also

developed and analyzed to determine their application to an adaptive weld control system. The following sections discuss findings for each of the three sensors developed under this contract: (1) weld profiling sensor; (2) weld pool sensor; and (3) stereo seam tracker/keyhole imaging sensor. Hardened versions of these sensors were designed and built under this contract. A control system, described later, was developed on a multiprocessing/multitasking operating system for maximum power and flexibility. Documentation for sensor mechanical and electrical design is also included as appendices in this report. Author

N95-25672# National Aerospace Lab., Tokyo (Japan). Rocket Propulsion Research Div.

PERFORMANCE EVALUATION OF LE-7 HIGH PRESSURE PUMPS

Makoto Yoshida, Kenjiro Kamijo, and Takaharu Nagao Sep. 1993 10 p (ISSN 0389-4010)

(NAL-TR-1212T) Avail: CASI HC A02/MF A01

The LOX and LH2 pumps of the LE-7 rocket engine are characterized by high delivery pressure and a large flow rate. The hydrodynamic performance of these pumps was thermo-dynamically evaluated. The performance of the LOX pump was expressed by the adiabatic head and efficiency, because LOX is not particularly compressible. However, the efficiency was directly determined using the measured pressures and temperatures which were corrected to approximate the true efficiency, because there was internal leakage from the split pump to the main pump. For evaluation of the LH2 pump performance, the polytropic head and efficiency were used, because LH2 shows much greater compressibility than LOX. Comparison of the calculations and test results confirmed that they better approximated the true head and efficiency than the adiabatic head and efficiency. The efficiency of both pumps was fairly high compared with that of large rocket pumps which have been developed to date. Author

N95-26050 Imperial Coll. of Science and Technology, London (England). Dept. of Mechanical Engineering.

DEVELOPMENT OF A HIGH TEMPERATURE, HIGH SPEED DISC LUBRICANT TEST MACHINE Final Report, 1 Sep. 1987 - 30 Jun. 1994

David M. Nicolson and Richard S. Sayles Wright-Patterson Air Force Base, OH Wright Lab. Jun. 1994 97 p Limited Reproducibility: More than 20% of this document may be affected by microfiche quality

(Contract F49620-87-C-0084; AF Proj. 3048)

(AD-A288685; WL-TR-94-2069) Avail: Issuing Activity (Defense Technical Information Center (DTIC))

Scuffing and adhesive failure modes are outlined to provide the context for a more detailed review of gear lubrication distinguishing, in particular, elastohydrodynamic and boundary lubrication regimes. The major scuffing theories, are considered against the particular requirements of lubricating at high temperatures and entrainment speeds. Existing lubricant testers are classified and evaluated with respect to their correlation with field experience. The need for a disc machine utilizing mini-discs driven at high speeds is proposed to satisfy both existing and future test requirements. Details of rig design, commissioning and development are detailed together with prototype experience which dictated that improved repeatability and reproducibility over current methods outweighs incomplete reproduction of the contact cycle. Early failures of a similar nature to those experienced in high speed aerospace applications are being used to study the mechanism of high speed (high temperature) scuffing with synthetic lubricants. DTIC

N95-26074*# National Aeronautics and Space Administration. Lewis Research Center, Cleveland, OH.

COMPUTERIZED DESIGN AND GENERATION OF LOW-NOISE GEARS WITH LOCALIZED BEARING CONTACT

Faydor L. Litvin (Illinois Univ., Chicago, IL.), Ningxin Chen (Illinois Univ., Chicago, IL.), Jui-Sheng Chen (Illinois Univ., Chicago, IL.), Jian Lu (Illinois Univ., Chicago, IL.), and Robert F. Handschuh (Army Research Lab., Cleveland, OH.) Apr. 1995 16 p Presented at the 1994 Fall Technical Meeting, St. Louis, MO, 24-28 Oct. 1994; sponsored by American Gear Manufacturers Association

(RTOP 505-62-36; DA Proj. 1L1-62211-A-47-A)

(NASA-TM-106880; E-9516; NAS 1.15:106880; ARL-TR-760) Avail: CASI HC A03/MF A01

The results of research projects directed at the reduction of noise caused by misalignment of the following gear drives: double-circular arc helical gears, modified involute helical gears, face-milled spiral bevel gears, and face-milled formate cut hypoid gears are presented. Misalignment in these types of gear drives causes periodic, almost linear discontinuous functions of transmission errors. The period of such functions is the cycle of meshing when one pair of teeth is changed for the next. Due to the discontinuity of such functions of transmission errors high vibration and noise are inevitable. A predesigned parabolic function of transmission errors that is able to absorb linear discontinuous functions of transmission errors and change the resulting function of transmission errors into a continuous one is proposed. The proposed idea was successfully tested using spiral bevel gears and the noise was reduced a substantial amount in comparison with the existing design. The idea of a predesigned parabolic function is applied for the reduction of noise of helical and hypoid gears. The effectiveness of the proposed approach has been investigated by developed TCA (tooth contact analysis) programs. The bearing contact for the mentioned gears is localized. Conditions that avoid edge contact for the gear drives have been determined. Manufacturing of helical gears with new topology by hobs and grinding worms has been investigated. Author

N95-26076*# National Aeronautics and Space Administration. Lewis Research Center, Cleveland, OH.

TRANSMISSION DIAGNOSTIC RESEARCH AT NASA LEWIS RESEARCH CENTER

J. J. Zakrajsek, D. P. Townsend, D. G. Lewicki (Army Research Lab., Cleveland, OH.), H. J. Decker (Army Research Lab., Cleveland, OH.), and R. F. Handschuh (Army Research Lab., Cleveland, OH.) May 1995 13 p Presented at the Second International Conference on Gearbox Noise, Vibration, and Diagnostics, London, England, 16-17 Nov. 1995; sponsored by Institution of Mechanical Engineers

(RTOP 505-62-36; DA Proj. 1L1-62211-A-47-A)

(NASA-TM-106901; E-9590; NAS 1.15:106901; ARL-TR-748) Avail: CASI HC A03/MF A01

The NASA Lewis Research Center and the U.S. Army Research Laboratory are involved in a joint research program to advance the technology of aerospace transmissions. Within the last six years, a transmission diagnostics research team was formed to address current and future technology barriers in transmission diagnostics. The diagnostics team conducted a survey to determine critical needs of the diagnostics community. Survey results indicated that experimental verification of gear and bearing fault detection methods and damage magnitude assessment were considered the two most critical research areas of a highly reliable health and usage monitoring system. A plan was implemented by the diagnostics team to address these key research areas, by in-house research and university grants. A variety of transmission fault detection methods were applied to experimentally obtained fatigue data. Failure modes of the fatigue tests include a variety of gear pitting failures, tooth wear, tooth fracture, and bearing spalling failures. Accomplishments to date include verification of several specific gear diagnostic methods, verification of a new pattern recognition method to determine failure, and development of a new method to model gear tooth damage. This paper presents the results of these accomplishments in transmission diagnostics research at NASA Lewis Research Center. Author

N95-26172# Texas Univ., Austin, TX. Center for Electromechanics.

THE RAILPLUG: A NEW IGNITOR FOR INTERNAL COMBUSTION ENGINES

R. W. Faidley, M. H. Darden, and W. F. Weldon 1995 6 p Presented at the 6th Symposium on Electromagnetic Launch Technology, Austin, TX, 28-30 Apr. 1992

(Contract DE-FG05-91ER-12115)

(DE95-005487; CONF-9204102-11) Avail: CASI HC A02/MF A01

A miniaturized railgun, termed the 'railplug', has been developed for use as an ignitor of combustible mixtures in engines. The device drives a plasma armature in a multishot mode with the aim of creating a line-source for ignition rather than the point source provided by traditional spark plugs. Railplugs have been fabricated in both parallel rail and co-axial rail geometries. The railplug differs from most plasma armature railguns in two striking ways: (1) no fuse or pellet is used to initially establish the plasma (the armature is simply the arc created by a high-voltage pulse); and (2) it operates over a range of elevated pressures (up to 500 psi). Consequently, the railplug power supply must provide a high voltage spike to breakdown the gap between the rails followed by a sustaining voltage that supplies

current to drive the arc down the rails. Conceptually, this is the equivalent of combining the electrostatic problem of a sparkplug with the electrodynamic one of a railgun. Two power supply options that do this are outlined, as well as details of railplug geometries. Successes to date have demonstrated the firing of plugs for over 10(exp 4) shots at delivered arc energies of 1 J per shot. Rep rates have been demonstrated up to 50 Hz. DOE

N95-26286# National Renewable Energy Lab., Golden, CO.
DEVELOPING A STANDARDIZED TEST PROCEDURE FOR HYBRID VEHICLES: THE CHALLENGE OF THE SAE HEV TASK FORCE
Terry Penney, David Christensen, and Stephen Poulos (General Motors Corp., Warren, MI.) Nov. 1994 6 p Presented at the Society of Automotive Engineers' Convergence 1994, Detroit, MI, 18-27 Oct. 1994
(Contract DE-AC36-83CH-10093)
(DE95-000280; NREL/TP-473-7026; CONF-9410256-2) Avail: CASI HC A02/MF A01

In 1992, the Society of Automotive Engineers (SAE) established a task force to develop a procedure for measuring electric energy consumption, all-electric range, fuel economy, and exhaust emissions for hybrid vehicles; the procedure will be submitted to regulatory agencies as representing the automotive industry's recommendations. The draft procedure is currently being tested on hybrid vehicles. The University of Maryland's parallel hybrid was tested in September 1994, and the University of California-Davis' parallel hybrid and the University of Illinois' series hybrid will be tested in November 1994 and January 1995, respectively. The procedure is being modified to incorporate any lessons learned, and the task force hopes to recommend the final procedure to the SAE by mid 1995. DOE

N95-26282*# Virginia Univ., Hampton, VA. Center for Computational Structures Technology.
COMPUTATIONAL STRATEGIES FOR TIRE MONITORING AND ANALYSIS Abstract Only
Kent T. Danielson, Ahmed K. Noor, and James S. Green (Moravian Coll., Bethlehem, PA.) *In its* Center for Computational Structures Technology Apr. 1995 1 p (For primary document see N95-26263 08-39)
Avail: CASI HC A01/MF A01

N95-26307*# Vanderbilt Univ., Nashville, TN.
STIFFENING OF THE ACES DEPLOYABLE SPACE BOOM
Vince Sidwell *In its* The 1994 NASA/USRA/ADP Design Projects 13 p(SEE N95-26304 08-80) 1994 (For primary document see N95-26304 08-80)
Avail: CASI HC A03/MF A02

38 QUALITY ASSURANCE AND RELIABILITY

Includes product sampling procedures and techniques; and quality control.

N95-25304* National Aeronautics and Space Administration. Langley Research Center, Hampton, VA.
A QUALITY MONITOR AND MONITORING TECHNIQUE EMPLOYING OPTICALLY STIMULATED ELECTRON EMISSION Patent
William T. Yost, inventor (to NASA), Christopher S. Welch, inventor (to NASA) (College of William and Mary, Gloucester Point, VA.), Edmond J. Joe, inventor (to NASA) (AS&M, Inc., Hampton, VA.), and Bill Bryan Hefner, Jr., inventor (to NASA) (AS&M, Inc., Hampton, VA.) 28 Feb. 1995 21 p Filed 11 May 1993 Supersedes N93-30414 (31 - 11, p 3449)
(NASA-Case-LAR-15063-1-CU; US-Patent-5,393,980;
US-Patent-Appl-SN-060617; US-Patent-Class-250-306;
US-Patent-Class-250-305; US-Patent-Class-250-307;
US-Patent-Class-250-310; Int-Patent-Class-G01N-23/227) Avail: US Patent and Trademark Office

A light source directs ultraviolet light onto a test surface and a detector detects a current of photoelectrons generated by the light. The detector includes a collector which is positively biased with respect to the test surface. Quality is indicated based on the photoelectron current. The collector is then negatively biased to replace charges removed by the measurement of a nonconducting substrate to permit subsequent measurements. Also, the intensity of the ultraviolet light at a particular wavelength is monitored and the voltage of the light source varied to maintain the light a constant desired intensity. The light source is also cooled via a gas circulation system. If the test surface is an insulator, the surface is bombarded with ultraviolet light in the presence of an electron field to remove the majority of negative charges from the surface. The test surface is then exposed to an ion field until it possesses no net charge. The technique described above is then performed to assess quality.
Official Gazette of the U.S. Patent and Trademark Office

N95-25333*# Illinois Univ., Urbana, IL. Center for Reliable and High Performance Computing
FTAPE: A FAULT INJECTION TOOL TO MEASURE FAULT TOLERANCE
Timothy K. Tsai and Ravishankar K. Iyer American Inst. of Aeronautics and Astronautics, Inc. 1994 8 p Sponsored in cooperation with Tandem Computer, Inc. Prepared in cooperation with the Illinois Computer Laboratory for Aerospace Systems and Software
(Contract NAG1-613; DABT63-94-C-0045)
(NASA-CR-198000; NAS 1.26:198000) Copyright Avail: CASI HC A02/MF A01

The paper introduces FTAPE (Fault Tolerance And Performance Evaluator), a tool that can be used to compare fault-tolerant computers. The tool combines system-wide fault injection with a controllable workload. A workload generator is used to create high stress conditions for the machine. Faults are injected based on this workload activity in order to ensure a high level of fault propagation. The errors/fault ratio and performance degradation are presented as measures of fault tolerance.
Author

N95-25957 Polish Academy of Sciences, Warsaw (Poland). Inst. of Basic Problems of Technology.
MAGNETIC FLAW DETECTION STUDIES: METHODS AND EQUIPMENT [METODY I APARATURA DEFEKTOSKOPOWYCH BADAN MAGNETYCZNYCH]
Edmund Kania, Jerzy Ranachowski, and Andrzej Jedrzejewski (PASCAL Bureau, Poland.) 1994 56 p In POLISH
(ISSN 0208-5658)
(IFTR-38/1994) Avail: Issuing Activity (Polish Academy of Sciences, Warsaw, Poland)

The physical fundamental of magnetic testing concerning a non-destructive powder method is described. The authors discuss various procedures for testing specimens. They describe equipment designed and built at the Institute of Basic Problems of Technology of the Polish Academy of Sciences for these purposes, including a flux-type flaw detector, a current-type flaw detector, and a magnetic testing system.
Transl. bySchreiber Translations Inc.

N95-26002# Swedish National Testing and Research Inst., Tsoras (Sweden).
BACKGROUND INFORMATION TO RELIABILITY STRESS SCREENING OF COMPONENTS: A GUIDE FOR COMPONENT USERS. NORDTEST PROJECT 1140-93
A. Boerjesson and V. Loll 1994 44 p
(PB95-165775; SP-RAPP-1994:31) Avail: CASI HC A03/MF A01

A method for Reliability Stress Screening (RSS) of components has been developed and is proposed to form a baseline for a Nordtest-method. The baseline is described in SP-report 1994:30 (PB95-165783). The information in this report is intended to give extra information to the component user at the design of a RSS process. Further, the report gives reference information that makes further studies in the subject possible for the interested reader. NTIS

N95-26003# Swedish National Testing and Research Inst., Tsoras (Sweden).
PROPOSED NORDTEST METHOD: RELIABILITY STRESS SCREENING OF COMPONENTS. A GUIDE FOR COMPONENT USERS. NORDTEST PROJECT 1140-93
A. Boerjesson and V. Loll 1994 82 p
(PB95-165783; SP-RAPP-1994:30) Avail: CASI HC A05/MF A01

A method for reliability stress screening (RSS) of components has been developed and is proposed to be issued as a Nordtest-method. This baseline has now been supplemented, especially with more component studies and more examples of the application of RSS for different component

families. Further, the method has been restructured and all background information has been left out of the method itself. This background information has been collected in a separate report, SP report 1994:31 (PB95-165775). The RSS-method makes use of methods described in IEC standard 1163. It is complementary to Nordtest-method NT ELEC 018 which defines a method for RSS of printed wiring assemblies. With reference to the IEC standard this Nordtest-method RSS is extended to include removal of weak lots; it also describes procedures for lot acceptance.

NTIS

N95-26055 Army Research Lab., Watertown, MA. Materials Directorate.

AN OVERVIEW OF NDE METHODS FOR THICK COMPOSITES AND A PROPOSAL FOR ANALYSIS OF COMPUTED TECHNOLOGY DATA Final Report, Oct. 1993 - Oct. 1994

Kristen Weight Nov. 1994 18 p Limited Reproducibility: More than 20% of this document may be affected by microfiche quality

(AD-A288733; ARL-TR-516) Avail: Issuing Activity (Defense Technical Information Center (DTIC))

Non-Destructive Evaluation (NDE) techniques are used for detecting manufacturing flaws, detecting service induced damage, dimensioning of objects and characterizing materials. Many methods are available for composite materials inspection and yet no single method is able to resolve all the damage due to the complexity of the material. This report will review many of the techniques currently being used for the investigation of composite materials. The importance of determining the damage modes is critical to the effort for predicting the residual strength in thick composites. The study of composite materials is a multidisciplinary field, encompassing the study of mechanics, materials and NDE in order to effectively understand the damage accumulation process and the resulting behavior of composite structures. This report will discuss some of the information which can be gained from further study and analysis of Computed Tomography (CT) images representing the damage modes present in impact damaged thick composites, in particular, woven roving S-2 glass panels. A proposal for automating the calculation of the volume of damage in the composite panels will be presented as well as a proposal for separating the different damage modes corresponding to damage types such as matrix cracking, delaminations and fiber breakage. DTIC

39 STRUCTURAL MECHANICS

Includes structural element design and weight analysis; fatigue; and thermal stress.

For applications see *05 Aircraft Design, Testing and Performance* and *18 Spacecraft Design, Testing and Performance.*

N95-24208*# National Aeronautics and Space Administration. Langley Research Center, Hampton, VA.

INTEGRATED PASSIVE/ACTIVE VIBRATION ABSORBER FOR MULTI-STORY BUILDINGS

Gina J. Lee-Glauser, Goodarz Ahmadi (Clarkson Univ., Potsdam, NY.), and Lucas G. Horta Jan. 1995 22 p Sponsored by National Research Council

(RTOP 233-01-03)

(NASA-TM-109178; NAS 1.15:109178) Avail: CASI HC A03/MF A01

Passive isolator, active vibration absorber, and an integrated passive/active (hybrid) control are studied for their effectiveness in reducing structural vibration under seismic excitations. For the passive isolator, a laminated rubber bearing base isolator which has been studied and used extensively by researchers and seismic designers is considered. An active vibration absorber concept, which can provide guaranteed closed-loop stability with minimum knowledge of the controlled system, is used to reduce the passive isolator displacement and to suppress the top floor vibration. A three-story building model is used for the numerical simulation. The performance of an active vibration absorber and a hybrid vibration controller in reducing peak structural responses is compared with the passively isolated structural response and with absence of vibration control systems under the N00W component of El Centro 1940 and N90W component of the Mexico City earthquake excitation records. The results show that the integrated passive/active vibration control system is most effective in suppressing the peak structural acceleration for the El Centro 1940 earthquake when compared with the passive or active vibration absorber alone. The active vibration absorber, however, is the only system that suppresses the peak acceleration of the structure for the Mexico City 1985 earthquake. Author

N95-24211# Wichita State Univ., Wichita, KS. National Inst. for Aviation Research.

ANALYSIS OF WARPING EFFECTS ON THE STATIC AND DYNAMIC RESPONSE OF A SEAT-TYPE STRUCTURE Final Report

Steven J. Hooper and Manoj Rahematpura May 1994 97 p

(NIAR-94-12) Avail: CASI HC A05/MF A02

An experimental investigation was conducted to evaluate the significance of warping deformations in the dynamic response of a seat frame type structure subjected to impact loading. The test article design featured thin-walled open-section beams and was loaded inertially by a number of rigid weights which were attached to the 'seat frame' members. Strain gage data acquired during these tests were analyzed to whether these data are better represented by Vlasov beam theory or Euler-Bernoulli beam theory. Static tests of the test article were conducted to validate the data reduction techniques employed in the analysis of the dynamic data.

Derived from text

N95-24263# Sandia National Labs., Albuquerque, NM.

REDUCTION IN FIBER DAMAGE THRESHOLDS DUE TO STATIC FATIGUE

R. E. Setchell 1995 12 p Presented at the 26th Annual Symposium on Optical Materials for High Power Lasers: Boulder Damage Symposium, Boulder, CO, 24-26 Oct. 1994

(Contract DE-AC04-94AL-85000)

(DE95-004778; SAND-94-2617C; CONF-9410155-1) Avail: CASI HC A03/MF A01

Damage mechanisms may occur during the transmission of Q-switched, Nd/YAG laser pulses through fused silica fibers. Fiber end-face characteristics, laser characteristics, and aspects of the laser-to-fiber injection typically determine dominant damage mechanisms. However, an additional damage process has been observed at internal sites where fibers were experiencing significant local stresses due to fixturing or bends in the fiber path. A transmission reduction prior to damage was typically not measurable at these sites. Damage would not always occur during initial testing, but sometimes occurred later in time at laser levels that previously had been transmitted without damage. In these cases the time at stress appeared to be more important than the number of transmitted shots prior to damage. A possible relation between internal damage thresholds at stressed sites and the total time under stress is suggested by the fact that silica fibers experience static fatigue processes. These processes involve the slow growth of local defects under tensile stress at rates that depend upon environmental conditions. Defects reaching sufficient size and having appropriate location could be sites for reduced laser-induced damage thresholds. The present work looks into the possibility that static fatigue processes can affect damage thresholds. The experiments used a laser injection and fiber routing configuration that produced significantly elevated fluences within fiber core regions under tensile stress. In order to establish initial strength and fatigue properties for these fibers, a number of samples were used to generate time-to-failure data at various stress levels. Other fiber samples were subjected to conditions that greatly accelerated fatigue processes. Internal damage thresholds were then measured in these fibers and compared to thresholds measured in fresh fibers. Conclusive comparisons were frustrated by sample-to-sample and lot-to-lot variations in fiber defects. DOE

N95-24282# Office National d'Etudes et de Recherches Aerospatiales, Chatillon (France).

RESPONSE TO A LOCALIZED IMPACT LOADING OF A COMPOSITE MULTILAYERED ROTATIONAL SHELL STRUCTURE: THEORY AND NUMERICAL METHODS, VOLUME 1 [REPONSE A UN IMPACT LOCALISE D'UNE STRUCTURE COQUE COMPOSITE MULTICOUCHE ROTATIONNELLE: ETUDES THEORIQUES ET MISE AU POINT DE METHODES NUMERIQUES, VOLUME 1]

Thierry Kerber 1994 199 p In FRENCH

(ISSN 0078-3781)

(ONERA-NT-1994-10-Vol-1) Avail: CASI HC A09/MF A03

Solving problems of locally impacted composite multilayered shells is still a real challenge today. Computational and data storage costs are

indeed huge in industrial applications. Moreover, the problems of reliability appear crucial. Among these difficulties, shell modelling and solution of impact problems, with their delicate choice of space-time discretization, are prevalent. Whenever the structures studied admit symmetries, particularly axial, new opportunities arise. They consist in developing new specific procedures for taking advantage of solid properties to reduce computing costs. However, these methods, typically based on developments in Fourier series or decompositions using group theory, lead to new theoretical and practical problems, and published performance seems to be quite moderate so far. The behavior particularities due to symmetries, the risks of extreme sensitivity to imperfections with mode localization and eigenvalue loci veering phenomena, also bring to light theoretical difficulties which have not yet been overcome. Locally impacted composite multilayered rotational (i.e. admitting axial symmetries) shell structure therefore touches upon a number of distinct but interactive subjects. This is why the study has been divided into three basic themes: numerical solution of localized impacts; shell modelling, particularly composite multilayered ones; and theoretical and numerical analysis of axial symmetries including the influence of imperfections. The independently obtained and numerically validated pieces of knowledge are then combined in solving an industrial representative problem to bring out their interconnections. Author

N95-24283# Office National d'Etudes et de Recherches Aerospatiales, Chatillon (France).

RESPONSE TO A LOCALIZED IMPACT LOADING OF A COMPOSITE MULTILAYERED ROTATIONAL SHELL STRUCTURE: THEORY AND NUMERICAL METHODS, VOLUME 2 [REPONSE A UN IMPACT LOCALISE D'UNE STRUCTURE COQUE COMPOSITE MULTICOUCHE ROTATIONNELLE: ETUDES THEORIQUES ET MISE AU POINT DE METHODES NUMERIQUES, VOLUME 2]

Thierry Kerber 1994 364 p In FRENCH

(ISSN 0078-3781)

(ONERA-NT-1994-10-Vol-2) Avail: CASI HC A16/MF A03

Solving problems of locally impacted composite multilayered shells is still a real challenge today. Computational and data storage costs are indeed huge in industrial applications. Moreover, the problems of reliability appear crucial. Among these difficulties, shell modelling and solution of impact problems, with their delicate choice of space-time discretization, are prevalent. Whenever the structures studied admit symmetries, particularly axial, new opportunities arise. They consist in developing new specific procedures for taking advantage of solid properties to reduce computing costs. However, these methods, typically based on developments in Fourier series or decompositions using group theory, lead to new theoretical and practical problems, and published performance seems to be quite moderate so far. The behavior particularities due to symmetries, the risks of extreme sensitivity to imperfections with mode localization and eigenvalue loci veering phenomena, also bring to light theoretical difficulties which have not yet been overcome. Locally impacted composite multilayered rotational (i.e. admitting axial symmetries) shell structure therefore touches upon a number of distinct but interactive subjects. This is why the study has been divided into three basic themes: numerical solution of localized impacts; shell modelling, particularly composite multilayered ones; and theoretical and numerical analysis of axial symmetries including the influence of imperfections. The independently obtained and numerically validated pieces of knowledge are then combined in solving an industrial representative problem to bring out their interconnections. This is volume 2 of a three volume set. Volume 2 focuses on axial symmetric rotation. Author

N95-24284# Office National d'Etudes et de Recherches Aerospatiales, Chatillon (France).

RESPONSE TO A LOCALIZED IMPACT LOADING OF A COMPOSITE MULTILAYERED ROTATIONAL SHELL STRUCTURE: THEORY AND NUMERICAL METHODS, VOLUME 3 [REPONSE A UN IMPACT LOCALISE D'UNE STRUCTURE COQUE COMPOSITE MULTICOUCHE ROTATIONNELLE: ETUDES THEORIQUES ET MISE AU POINT DE METHODES NUMERIQUES, VOLUME 3]

Thierry Kerber 1994 134 p In FRENCH

(ISSN 0078-3781)

(ONERA-NT-1994-10-Vol-3) Avail: CASI HC A07/MF A02

Solving problems of locally impacted composite multilayered shells is still a real challenge today. Computational and data storage costs are indeed huge in industrial applications. Moreover, the problems of reliability appear crucial. Among these difficulties, shell modelling and solution of impact problems, with their delicate choice of space-time discretization, are prevalent. Whenever the structures studied admit symmetries, particularly axial, new opportunities arise. They consist in developing new specific procedures for taking advantage of solid properties to reduce computing costs, However, these methods, typically based on developments in Fourier series or decompositions using group theory, lead to new theoretical and practical problems, and published performance seems to be quite moderate so far. The behavior particularities due to symmetries, the risks of extreme sensitivity to imperfections with mode localization and eigenvalue loci veering phenomena, also bring to light theoretical difficulties which have not yet been overcome. Locally impacted composite multilayered rotational (i.e. admitting axial symmetries) shell structure therefore touches upon a number of distinct but interactive subjects. This is why the study has been divided into three basic themes: numerical solution of localized impacts; shell modelling, particularly composite multilayered ones; and theoretical and numerical analysis of axial symmetries including the influence of imperfections. The independently obtained and numerically validated pieces of knowledge are then combined in solving an industrial representative problem to bring out their interconnections. This is volume 3 of a three volume set. This volume focuses on industrial analysis. Author

N95-24296# Helsinki Univ. of Technology, Espoo (Finland).

SHELL DEFORMATION STATES AND THE FINITE ELEMENT METHOD: A BENCHMARK STUDY OF CYLINDRICAL SHELLS Research Report

J. Pitkaeranta, Y. Leino, O. Ovaskainen, and J. Piila May 1994 60 p

(ISSN 0784-3143)

(PB95-149621; RR-A333) Avail: CASI HC A04/MF A01

We demonstrate some of the basic mathematical characteristics of shell deformation states and shell models from the point of view of finite element approximation. As benchmark cases, we analyze in detail three simple cylindrical shell problems. These problems are seemingly similar but turn out to be quite different. We: (1) compute the exact displacement and strain fields in the model problems both numerically and symbolically using two variants of classical shell models; (2) for comparison, compute numerically the displacements and strains corresponding to certain higher-order dimension reduction models derived from the energy principle; (3) demonstrate the dissimilarity of the three benchmark problems as to their asymptotic behavior in the limit of zero thickness; and (4) show, both theoretically and experimentally, how this diversity is reflected in the accuracy of standard finite element approximations of both low and high order.

NTIS

N95-24383# Defence Research Agency, Farnborough, Hampshire (England).

THE DUAL BOUNDARY ELEMENT FORMULATION FOR ELASTOPLASTIC FRACTURE MECHANICS

V. Leitao (Wessex Inst. of Tech., Ashurst, England.), M. H. Aliabadi (Wessex Inst. of Tech., Ashurst, England.), and D. P. Rooke Aug. 1993 29 p Sponsored by Inst. Superior Tecnico

(DRA-TR-93062; ICAF-1949) Copyright Avail: CASI HC A03/MF A01

The extension of the dual boundary element method (DBEM) to the analysis of elastoplastic fracture mechanics (EPFM) problems is presented. The dual equations of the method are the displacement and the traction boundary integral equations. When the displacement equation is applied to one of the crack surfaces and the traction equation on the other, general mixed-mode crack problems can be solved with a single-region formulation. In order to avoid collocation at crack tips, crack kinks, and crack-edge corners, both crack surfaces are discretized with discontinuous quadratic boundary elements. The elastoplastic behavior is modeled through the use of an approximation for the plastic component of the strain tensor on the region expected to yield. This region is discretized with internal quadratic, quadrilateral, and/or triangular cells. A center-cracked plate and a slant edge-cracked plate subjected to tensile load are analyzed and the results are compared with others available in the literature. J-type integrals are calculated. Author

N95-24398*# Akron Univ., Akron, OH. Dept. of Civil Engineering.

ON THE FINITE ELEMENT IMPLEMENTATION OF THE GENERALIZED METHOD OF CELLS MICROMECHANICS CONSTITUTIVE MODEL Final Report

T. E. Wilt Cleveland, OH NASA Mar. 1995 61 p Original contains

color illustrations
(Contract NCC3-368; RTOP 505-63-12)
(NASA-CR-195451; E-9531; NAS 1.26:195451) Avail: CASI HC A04/MF A01; 3 functional color pages

The Generalized Method of Cells (GMC), a micromechanics based constitutive model, is implemented into the finite element code MARC using the user subroutine HYPELA. Comparisons in terms of transverse deformation response, micro stress and strain distributions, and required CPU time are presented for GMC and finite element models of fiber/matrix unit cell. GMC is shown to provide comparable predictions of the composite behavior and requires significantly less CPU time as compared to a finite element analysis of the unit cell. Details as to the organization of the HYPELA code are provided with the actual HYPELA code included in the appendix. Author

N95-24598# Westinghouse Savannah River Co., Aiken, SC.
RESIDUAL STRESS MEASUREMENTS WITH LASER SPECKLE CORRELATION INTERFEROMETRY AND LOCAL HEAT TREATING
M. J. Pechersky, R. F. Miller, and C. S. Vikram (Alabama Univ., Huntsville, AL.) Jan. 1994 26 p Presented at the SPIE '95: SPIE Conference on Optics, Electro-optics, and Laser Application in Science, Engineering and Medicine, San Jose, CA, 5-10 Feb. 1995
(Contract DE-AC09-89SR-18035)
(DE95-060082; WSRC-MS-94-0632; CONF-950226-3) Avail: CASI HC A03/MF A01

A new experimental technique has been devised to measure residual stresses in ductile materials with a combination of laser speckle pattern interferometry and spot heating. The speckle pattern interferometer measures in-plane deformations while the heating provides for very localized stress relief. The residual stresses are determined by the amount of strain that is measured subsequent to the heating and cool-down of the region being interrogated. A simple lumped parameter model is presented to provide a description of the method. This description is followed by presentations of the results of finite element analyses and experimental results with uniaxial test specimens. Excellent agreement between the experiments and the computer analyses were obtained. DOE

N95-24907*# Old Dominion Univ., Norfolk, VA. Dept. of Aerospace Engineering.
NUMERICAL SIMULATION OF THE NONLINEAR RESPONSE OF COMPOSITE PLATES UNDER COMBINED THERMAL AND ACOUSTIC LOADING Final Report, period ended 15 Mar. 1995
Chuh Mei and Jayashree Moorthy Jan. 1995 167 p
(Grant NAG1-1358)
(NASA-CR-197426; NAS 1.26:197426) Avail: CASI HC A08/MF A02

A time-domain study of the random response of a laminated plate subjected to combined acoustic and thermal loads is carried out. The features of this problem also include given uniform static inplane forces. The formulation takes into consideration a possible initial imperfection in the flatness of the plate. High decibel sound pressure levels along with high thermal gradients across thickness drive the plate response into nonlinear regimes. This calls for the analysis to use von Karman large deflection strain-displacement relationships. A finite element model that combines the von Karman strains with the first-order shear deformation plate theory is developed. The development of the analytical model can accommodate an anisotropic composite laminate built up of uniformly thick layers of orthotropic, linearly elastic laminae. The global system of finite element equations is then reduced to a modal system of equations. Numerical simulation using a single-step algorithm in the time-domain is then carried out to solve for the modal coordinates. Nonlinear algebraic equations within each time-step are solved by the Newton-Raphson method. The random gaussian filtered white noise load is generated using Monte Carlo simulation. The acoustic pressure distribution over the plate is capable of accounting for a grazing incidence wavefront. Numerical results are presented to study a variety of cases. Author

N95-24995 Institute of Sound and Vibration Research, Southampton (England). Structural Dynamics Group.
TUNABLE VIBRATION ABSORBERS: KEY DESIGN PARAMETERS
M. J. Brennan Mar. 1995 38 p
(ISVR-TR-244) Copyright Avail: Issuing Activity (Director, Institute of Sound and Vibration Research, University of Southampton, Southampton SO17 1BJ, England)

This report contains a theoretical investigation into the performance of a tunable vibration absorber when fitted to a machine. The steady-state behavior of a machine fitted with a tuned absorber is discussed, and simple formulae are derived that facilitate a prediction of the absorber's effectiveness using quantities that should be available to the systems designer. A bandwidth of operation is defined over which the absorber's effectiveness is at most 6 dB less than its maximum, and it is shown that this is equal to twice the absorber's damping ratio. Results from the analysis demonstrate that the only way to achieve high attenuation whilst maintaining a reasonable bandwidth is to increase the mass ratio. A study into the behavior of the machine-absorber system when the disturbance frequency changes with time is also conducted. It is shown that if we wish the response of the machine to be no worse when the absorber is fitted, then the maximum allowable control time delay between sensing a change in the excitation and re-tuning the absorber is dependent upon the rate of change of frequency variation and the mass ratio. Author

N95-24996 Polish Academy of Sciences, Warsaw (Poland). Mechanics Center.
DYNAMIC ANALYSIS OF TRUSS MEMBERS USING LONGITUDINAL WAVES [DYNAMICZNA ANALIZA PRETOW KRATOWNICY PRZY WYKORZYSTANIU FAL PODLUZNYCH]
Wladyslaw Nadolski and Amalia Pielorz Cooperative Publishing House Ltd. 1994 56 p In POLISH
(ISSN 0208-5658)
(IFTR-35/1994) Avail: Issuing Activity

This article pertains to the dynamic analysis of a plane truss whose members are only under tension and compression using discrete-continuous models. The authors assume that the external force is a variable force applied to a rigid body at one of the corners of the truss. In their equations the authors use a wave method which makes it possible to determine displacement, deformation, and velocity in any cross sections of the truss members at any moment in time. Numerical calculations were performed for two simple discrete-continuous models of a plane truss in a state of steady motion and in a state of variable motion. Author

N95-24997 Institute of Sound and Vibration Research, Southampton (England). Fluid Dynamics and Acoustics Group.
A TECHNIQUE FOR THE EVALUATION OF STRENGTH OF COUPLING BETWEEN SEA SUBSYSTEMS
P. James and F. J. Fahy Dec. 1994 76 p Sponsored by Societe Europeenne de Propulsion and Centre National d'Etudes Spatiales
(ISVR-TR-241) Copyright Avail: Issuing Activity (Director, Institute of Sound and Vibration Research, University of Southampton, Southampton SO17 1BJ, England)

One of the main requirements for the successful use of traditional Statistical Energy Analysis (SEA) is to have weakly coupled subsystems. In particular, the method of energy matrix inversion to determine loss factors can be subject to serious error if subsystems are strongly coupled. Unfortunately, there is neither a single definition of weak coupling nor a practical measure of the strength of coupling; but, recently, a very general definition of weak coupling, stemming from an exact derivation of the SEA fundamental equations, has been proposed by R.S. Langley. On the basis of this definition and the study of one-dimensional and two-dimensional coupled subsystems, a convenient way to measure the strength of coupling is described. It appears that, in the case of resonant coupling, when one subsystem is subject to impulsive excitation, the time delay in the rise of the kinetic energy in the indirectly excited subsystem can be used to define a good indicator of the strength of coupling for one and two-dimensional systems. Author

N95-25000# National Aerospace Lab., Tokyo (Japan). Structural Mechanics Div.
STRESS ANALYSIS OF A CRACK IN THE RESIDUAL STRESS FIELD BY WELDING AND ITS APPLICATION TO THE FATIGUE CRACK PROPAGATION
Hiroyuki Terada Sep. 1994 13 p In JAPANESE
(ISSN 0389-4010)
(NAL-TR-1248) Avail: CASI HC A03/MF A01

Structural failures often originate from weld joints. This is mainly due

to metallurgical deterioration by heating, high feasibility of defects and residual stress by welding. In such a situation, it seems to be very important to study the behavior of a crack around the welded joint. In this paper, an analytical study of a crack perpendicular to the welding bead subjected to the residual stress was carried out using a stress function. At first, the conditions which should be satisfied for the residual stress by welding were examined. Then the simulation function satisfying these conditions was proposed. Next, the stress intensity factors of an arbitrary crack perpendicular to the butt weld, which was subjected to the effect of residual stress, were derived by using the proposed function. The redistribution form of the residual stress near the crack was also evaluated and compared with the testing results obtained by Kanazawa, et al. Finally, the following effective stress intensity factor range delta K(sub eff), instead of conventional delta K, was proposed to evaluate the effect of residual stress on the fatigue crack propagation of a crack. Delta K(sub eff) = delta K(1 + (K(sub res)/delta K)), where, K(sub res) is the stress intensity factor induced by residual stress of welding. The effectiveness of delta K(sub eff) was proven by examining the experimental fatigue crack propagation data obtained by Glinka. Author

N95-25003 Institute of Sound and Vibration Research, Southampton (England). Structural Dynamics Group.

AN ANALYTICAL STUDY OF THE VIBRATION OF BEAMS FITTED WITH NEUTRALIZERS. PART 3: TORSIONAL WAVE MOTION

P. Clark and R. G. White Sep. 1994 36 p

(ISVR-TR-238-Pt-3) Copyright Avail: Issuing Activity (Director, Institute of Sound and Vibration Research, University of Southampton, Southampton SO17 1BJ, England)

With the majority of industrial machinery installations it is one-dimensional or beam-like structures - for example, pipework and other mechanical linkages - which form one of the main vibration paths which bypass isolator systems. It is of interest to consider the effects that the addition of certain discontinuities to this type of structure would have on the overall vibration transmission properties of the complete system. Previous work has considered the vibration neutralizer as one such discontinuity in terms of impinging axial and flexural wave motion. In this work, the analytical study is further extended to include the third major type of structural wave motion observed in one-dimensional structures: torsional motion. Author

N95-25332 Institute of Sound and Vibration Research, Southampton (England). Fluid Dynamics and Acoustics Group.

A TECHNIQUE FOR THE EVALUATION OF STRENGTH OF COUPLING BETWEEN SEA SUBSYSTEMS: EXPERIMENTS WITH TWO COUPLED PLATES AND TWO COUPLED ROOMS

P. J. James and F. J. Fahy Jan. 1995 58 p Sponsored by Societe Europeenne de Propulsion and Centre National d'Etudes Spatiales

(ISVR-TR-242) Copyright Avail: Issuing Activity (Director, Institute of Sound and Vibration Research, University of Southhampton, Southampton SO17 1BJ, England)

In ISVR Technical Report No. 241, a technique for the evaluation of strength of coupling between SEA subsystems is proposed on the basis of theoretical models. This report, No. 242, represents the results of an experimental application of the technique to two plates coupled by a variable number of straps to two rooms coupled by an aperture. Similar values for the coupling strength indicator C(sub s) to those theoretically evaluated are observed. It is seen that the C(sub s) depends on the frequency as well as on the physical strength of coupling but is fairly insensitive to damping. Author

N95-25444 Swedish Inst. for Metals Research, Stockholm (Sweden).

NEW TECHNIQUES TO TEST FATIGUE PROPERTIES OF COINED SHEET SPECIMENS. PART 2: COMPARISON OF DIFFERENT MATERIALS, FORMING OPERATIONS AND LIFE PREDICTION TECHNIQUES FOR A SIMPLE TEST GEOMETRY

A. Gustavsson, M. Larsson, A. Melander, and D. L. McDowell (Georgia Inst. of Tech., Atlanta, GA.) 1995 91 p See also PB95-165130 Sponsored by NUTEK Limited Reproducibility: More than 20% of this document may be affected by microfiche quality

(Proj. EUREKA-337)

(PB95-165122; IM-3145) Avail: CASI HC A05

The present research was devoted to the problem of fatigue of coinings in sheet steels. A typical application is in the automotive industry where coinings are introduced to increase the stiffness of sheet panels. The aim of the present work was to illuminate how the method of forming of the coinings influenced the fatigue life. The two forming methods investigated were bending and a deep-drawing like operation. The investigation was carried out for three high strength sheet steels: two dual-phase sheet steels and a Si-P alloyed sheet steel. The results indicate that the samples formed in the deep-drawing operation tend to carry somewhat higher local stresses than specimens formed in bending. However, if the life is assessed in terms of local bending moment, the results are reversed, which could be explained in terms of the locally reduced sheet thickness for deep-drawn specimens. NTIS

N95-25445# Swedish Inst. for Metals Research, Stockholm (Sweden).

NEW TECHNIQUES TO TEST FATIGUE PROPERTIES OF COINED SHEET SPECIMENS. PART 4: DEVELOPMENT OF EXPERIMENTAL TECHNIQUES

Anders Gustavsson and Arne Melander Sep. 1994 44 p See also PB95-165122 Sponsored by NUTEK

(Proj. EUREKA-337)

(PB95-165130; IM-3147-Pt-4) Avail: CASI HC A03/MF A01

The present work was directed to the development of laboratory specimens suitable for simulation of fatigue in coinings in sheet materials. This report describes the different steps taken to advance the test procedures towards the requirements formulated for the experiments. Two test geometries with corresponding test procedures were established. The two dimensional geometry loaded axially in the fatigue test benefits from its very simple form which results in ease of manufacture, testing and analysis. The more sophisticated three dimensional geometry developed resembles much of coinings in real automotive components - bending loading, geometry and similar fatigue failure site. However, due to its geometrical complexity it demands more when it comes to fatigue testing and analysis. NTIS

N95-25569# Swedish Inst. for Metals Research, Stockholm (Sweden).

NEW TECHNIQUES TO TEST FATIGUE PROPERTIES OF COINED SHEET SPECIMENS. PART 3: FATIGUE TESTING AND ANALYSIS OF A COMPONENT LIKE COINING IN SHEET STEEL MATERIALS

A. Gustavsson, M. Larsson, and A. Melander Sep. 1994 70 p

(Proj. EUREKA-337)

(PB95-165668; IM-3146-Pt-3) Avail: CASI HC A04/MF A01

Coinings are normally introduced in sheet components in order to increase the overall stiffness of the panel. In fatigue loaded components the coining may serve as a potential site for crack initiation. The reason is that bending stresses in the sheet are transferred up into the coining producing a stress concentration. Also, due to the forming of coining sheet thickness is often reduced, which increases the stresses locally. The present work is directed to the work of simulating the fatigue behavior of coinings in steel sheets. A specimen design was developed which comprises the main features of coinings in real life automotive components. Simultaneously to the experimental work, numerical work was done in order to predict the fatigue life of the coined geometry. The numerical models utilized finite element techniques with a non-linear kinematic hardening model to describe the behavior of the specimen both during forming and during fatigue loading. The local strain approach was adopted to estimate the fatigue life. NTIS

N95-25661# National Aerospace Lab., Tokyo (Japan). Structural Mechanics Div.

THERMOELASTIC EQUATIONS FOR MULTI-LAYERED CYLINDRICAL SHELL

Shuji Endo Jan. 1994 21 p In JAPANESE

(ISSN 0389-4010)

(NAL-TR-1222) Avail: CASI HC A03/MF A01

A governing equation for multi-layered cylindrical shells under combined thermal and mechanical loading is derived as a first approximation, consistent with the Kirchhoff-Love hypothesis, in the form of an eighth-order differential equation with respect to the lateral displacement. The shell structure is assumed to consist of homogeneous and isotropic layers having different material properties. It is also assumed that the material properties are constant for each layer. As an analytical example, the deformations and stresses of a multi-layered cylindrical shell under axisymmetric thermal load are analyzed. Author

N95-25796# National Aerospace Lab., Tokyo (Japan). Structural Mechanics Div.

STRESS ANALYSIS OF A CRACK IN THE RESIDUAL STRESS FIELD BY WELDING AND ITS APPLICATION TO THE FATIGUE CRACK PROPAGATION

Hiroyuki Terada Sep. 1994 13 p In JAPANESE

(ISSN 0389-4010)

(NAL-TR-1248) Avail: CASI HC A03/MF A01

Structural failures often originate from weld joints. This is mainly due to metallurgical deterioration by heating, high likelihood of defects and residual stress by welding. In such a situation, it seems to be very important to study the behavior of a crack around the welded joint. In this paper, an analytical study of a crack perpendicular to the welding bead subjected to the residual stress was carried out using a stress function. At first, the conditions which should be satisfied for the residual stress by welding were examined. Then the simulation function satisfying these conditions was proposed. Next, the stress intensity factors of an arbitrary crack perpendicular to the butt weld, which was subjected to the effect of residual stress most severely, were derived by using the proposed function. The redistribution form of the residual stress near the crack was also evaluated and compared with the testing results obtained by Kanazawa, et al. Finally, the following effective stress intensity factor range delta K(sub eff), instead of the conventional delta K, was proposed to evaluate the effect of residual stress on the fatigue crack propagation of a crack. Delta K(sub eff) = delta K(1 plus K(sub res) divided by delta K) where, K(sub res) is the stress intensity factor induced by residual stress by welding. The effectiveness of delta K(sub eff) was proved by examining the experimental fatigue crack propagation data obtained by Glinka. Author

N95-26078*# National Aeronautics and Space Administration. Lewis Research Center, Cleveland, OH.

A FULLY ASSOCIATIVE, NONISOTHERMAL, NONLINEAR KINEMATIC, UNIFIED VISCOPLASTIC MODEL FOR TITANIUM ALLOYS

S. M. Arnold, A. F. Saleeb (Akron Univ., Akron, OH.), and M. G. Castelli (NYMA, Inc., Brook Park, OH.) May 1995 31 p Presented at the Second Symposium on Thermomechanical Fatigue Behavior of Materials, Phoenix, AZ, 13-18 Nov. 1994; sponsored by the American Society for Testing and Materials

(Contract NAS3-27186; RTOP 505-63-12)

(NASA-TM-106926; E-9644; NAS 1.15:106926) Avail: CASI HC A03/MF A01

Specific forms for both the Gibb's and complementary dissipation potentials are chosen such that a complete (i.e., fully associative) potential base multiaxial, nonisothermal unified viscoplastic model is obtained. This model possesses one tensorial internal state variable (that is, associated with dislocation substructure) and an evolutionary law that has nonlinear kinematic hardening and both thermal and strain induced recovery mechanisms. A unique aspect of the present model is the inclusion of nonlinear hardening through the use of a compliance operator, derived from the Gibb's potential, in the evolution law for the back stress. This nonlinear tensorial operator is significant in that it allows both the flow and evolutionary laws to be fully associative (and therefore easily integrated), greatly influences the multiaxial response under non-proportional loading paths, and in the case of nonisothermal histories, introduces an instantaneous thermal softening mechanism proportional to the rate of change in temperature. In addition to this nonlinear compliance operator, a new consistent, potential preserving, internal strain unloading criterion has been introduced to prevent abnormalities in the predicted stress-strain curves, which are present with nonlinear hardening formulations, during unloading and reversed loading of the external variables. The specific model proposed is characterized for a representative titanium alloy commonly used as the matrix material in SiC fiber reinforced composites, i.e., TIMETAL 21S. Verification of the proposed model is shown using 'specialized' non-standard isothermal and thermomechanical deformation tests. Author

N95-26178 Polish Academy of Sciences, Warsaw (Poland). Dept. of Strength of Materials.

TECHNIQUES FOR STUDYING THE MECHANICAL PROPERTIES OF MATERIALS IN COMPLEX STRESS STATES [TECHNIKA BADAN WLASCIWOSCI MECHANICZNYCH MATERIALOW W ZLOZONYM STANIE NAPREZENIA]

Lech Dietrich, Karol Turski, Maciej Waniewski, Zygmunt Dziankowski, and Romuald Kiryk 1994 105 p In POLISH

(ISSN 0208-5658)

(IFTR-34/1994) Avail: Issuing Activity (Polish Academy of Sciences, Warsaw, Poland)

In this article the authors describe an experimental technique suitable for determining the mechanical properties of materials in complex stress states. The studies were conducted so as to allow determination of elastic characteristics defined by two elasticity constants, plastic flow coefficients defined by a hardening curve, mechanical property anisotropy characteristics defined by the form and values of material anisotropy constants, and the evolution of these properties under deformation. The realization of such an extensive program for materials in complex stress states requires very accurate measurements, precise and automatic control of the loading of the specimen, and the collection and processing of a large volume of digital measurements results. The program also requires the right instrumentation and computer software to control the strength testing machine for materials in a complex stress state and software to process and graph the measurement results and reflect them in a desired graphic form. These are extremely important elements of the article, which, in addition to the traditional mechanical element, also discusses preparing the specimens, fastening and loading them, measuring the components of stress and strain, and determining the quality of the research and the value of the results. This article covers all these aspects of testing materials in complex stress states in a planar stress state, while specific parts of the article include a discussion of the literature in the field, the method used for complex stress state tests, the software used to control the strength testing machine, the software used to process the measurement results, and the results obtained for several series of tests performed on tubular specimens of PA6 aluminum alloy and 18G2 steel.

Transl. by Schreiber Translation, Inc.

N95-26199*# Lockheed Engineering and Sciences Co., Hampton, VA.

A GENERIC INTERFACE ELEMENT FOR COMET-AR

Susan L. McCleary and Mohammad A. Aminpour NASA Mar. 1995 163 p Prepared in cooperation with Analytical Services and Materials, Inc., Hampton, VA

(Contracts NAS1-19000; NAS1-19700; RTOP 505-63-53-01)

(NASA-CR-195075; NAS 1.26:195075) Avail: CASI HC A08/MF A02

The implementation of an interface element capability within the COMET-AR software system is described. The report is intended for use by both users of currently implemented interface elements and developers of new interface element formulations. Guidance on the use of COMET-AR is given. A glossary is provided as an Appendix to this report for readers unfamiliar with the jargon of COMET-AR. A summary of the currently implemented interface element formulation is presented in Section 7.3 of this report. Author

N95-26263*# Virginia Univ., Hampton, VA.

CENTER FOR COMPUTATIONAL STRUCTURES TECHNOLOGY Semiannual Report

Ahmed K. Noor and Ferman W. Perry Apr. 1995 30 p Sponsored in cooperation with NASA. Langley Research Center

(Contract NCCw-11)

(NASA-CR-198028; NAS 1.26:198028) Avail: CASI HC A03/MF A01

The Center for Computational Structures Technology (CST) is intended to serve as a focal point for the diverse CST research activities. The CST activities include the use of numerical simulation and artificial intelligence methods in modeling, analysis, sensitivity studies, and optimization of flight-vehicle structures. The Center is located at NASA Langley and is an integral part of the School of Engineering and Applied Science of the University of Virginia. The key elements of the Center are: (1) conducting innovative research on advanced topics of CST; (2) acting as pathfinder by demonstrating to the research community what can be done (high-potential, high-risk research); (3) strong collaboration with NASA scientists and researchers from universities and other government laboratories; and (4) rapid dissemination of CST to industry, through integration of industrial personnel into the ongoing research efforts. For individual titles, see N95-26264 through N95-26283.

N95-26264*# Virginia Univ., Hampton, VA.

FINITE ELEMENT BUCKLING AND POSTBUCKLING SOLUTIONS FOR MULTILAYERED COMPOSITE PANELS Abstract only

Ahmed K. Noor and Jeanne M. Peters *In its* Center for Computational Structures Technology Apr. 1995 1 p (For primary document see N95-26263 08-39)
Avail: CASI HC A01/MF A01

A study is made of the buckling and postbuckling responses of flat, unstiffened composite panels subjected to various combinations of mechanical and thermal loads. The analysis is based on a first-order shear deformation von Karman-type plate theory. A mixed formulation is used with the fundamental unknowns consisting of the strain components, stress resultants and the generalized displacements of the plate. The stability boundary, postbuckling response and the sensitivity coefficients are evaluated. The sensitivity coefficients measure the sensitivity of the buckling and postbuckling responses to variations in the different lamination and material parameters of the panel. Numerical results are presented for both solid panels and panels with central circular cutouts. The results show the effects of the variations in the fiber orientation angels, aspect ratio of the panel, and the hole diameter (for panels with cutouts) on the stability boundary, postbuckling response and sensitivity coefficients. Author

N95-26265*# Virginia Univ., Hampton, VA. Center for Computational Structures Technology.
THREE-DIMENSIONAL SOLUTIONS FOR THERMOMECHANICAL STRESSES IN SANDWICH PANELS AND SHELLS Abstract Only
W. Scott Burton and Ahmed K. Noor *In its* Center for Computational Structures Technology Apr. 1995 1 p (For primary document see N95-26263 08-39)
Avail: CASI HC A01/MF A01

Analytic three-dimensional thermoelasticity solutions are presented for static problems of simply supported sandwich panels and cylindrical shells subjected to mechanical and thermal loads. The panels and shells have laminated composite face sheets of arbitrary thickness separated by a core. Each of the individual layers of the face sheets and the core is modeled as a three-dimensional continuum. Analytic first-order sensitivity coefficients are evaluated to assess the sensitivity of the responses to variations in material parameters of the face sheets and the core, as well as to variations in the curvatures and thicknesses of the sandwich and face sheets. Also, the strain energy associated with various stress components in the face sheets and core are calculated and compared. The information obtained in the present study can aid the development and assessment of two-dimensional models for sandwich structures and illuminate the role of particular material parameters in an equivalent model for the core. Author

N95-26266*# Virginia Univ., Hampton, VA. Center for Computational Structures Technology.
SENSITIVITY ANALYSIS OF THE NON-LINEAR DYNAMIC VISCOPLASTIC RESPONSE OF 2-D STRUCTURES WITH RESPECT TO MATERIAL PARAMETERS Abstract Only
Makarand Kulkarni and Ahmed K. Noor *In its* Center for Computational Structures Technology Apr. 1995 1 p (For primary document see N95-26263 08-39)
Avail: CASI HC A01/MF A01

A computational procedure is presented for evaluating the sensitivity coefficients of the viscoplastic response of structures subjected to dynamic loading. A state of plane stress is assumed to exist in the structure, a velocity strain-Cauchy stress formulation is used, and the geometric non-linearities arising from large strains are incorporated. The Jaumann rate is used as a frame indifferent stress rate. The material model is chosen to be isothermal viscoplasticity, and an associated flow rule is used with a von Mises effective stress. The equations of motion emanating from a finite element semi-discretization are integrated using an explicit central difference scheme with an implicit stress update. The sensitivity coefficients are evaluated using a direct differentiation approach. Since the domain of integration is the current configuration, the sensitivity coefficients of the spatial derivatives of the shape functions must be included. Numerical results are presented for a thin plate with a central cutout subjected to an in-plane compressive loading. The sensitivity coefficients are generated by evaluating the derivatives of the response quantities with respect to Young's modulus, and two of the material parameters characterizing the viscoplastic response. Time histories of the response and sensitivity coefficients, and spatial distributions at selected times are presented. Author

N95-26267*# National Aeronautics and Space Administration. Langley Research Center, Hampton, VA.
THERMOMECHANICAL POSTBUCKLING OF MULTILAYERED COMPOSITE PANELS WITH CUTOUTS Abstract Only
Ahmed K. Noor (Virginia Univ., Hampton, VA.), Jeanne M. Peters (Virginia Univ., Hampton, VA.), and James H. Starnes, Jr. *In* Virginia Univ., Center for Computational Structures Technology Apr. 1995 1 p (For primary document see N95-26263 08-39)
Avail: CASI HC A01/MF A01

The results of a study of the detailed thermomechanical postbuckling response characteristics of flat unstiffened composite panels with central circular cutouts are presented. The panels are subjected to combined temperature changes and applied edge loading (or edge displacements). The analysis is based on a first-order shear deformation plate theory. A mixed formulation is used with the fundamental unknowns consisting of the generalized displacements and the stress resultants of the plate. The postbuckling displacements, transverse shear stresses, transverse shear strain energy density, and their sensitivity coefficients are evaluated. The sensitivity coefficients measure the sensitivity of the post-buckling response to variations in the different lamination and material parameters of the panel. Numerical results are presented showing the effects of the variations in the hole diameter, laminate stacking sequence, fiber orientation, and aspect ratio of the panel on the thermomechanical postbuckling response and its sensitivity to changes in panel parameters. Author

N95-26268*# Virginia Univ., Hampton, VA. Center for Computational Structures Technology.
SENSITIVITY ANALYSIS FOR THE DYNAMIC RESPONSE OF VISCOPLASTIC SHELLS OF REVOLUTION Abstarct Only
Makarand Kulkarni and Ahmed K. Noor *In its* Center for Computational Structures Technology Apr. 1995 1 p (For primary document see N95-26263 08-39)
Avail: CASI HC A01/MF A01

A computational procedure is presented for evaluating the sensitivity coefficients of the dynamic axisymmetric response of viscoplastic shells of revolution. The analytical formulation is based on Reissner's large deformation shell theory with the effects of transverse shear deformation, rotatory inertia and moments turning around the normal to the middle surface included. The material model is chosen to be isothermal viscoplasticity, and an associated flow rule is used with a von Mises effective stress. A mixed formulation is used with the fundamental unknowns consisting of six stress resultants, three generalized displacements and three velocity components. Spatial discretization is performed using finite elements, with discontinuous stress resultants across element interfaces. The temporal integration is performed by using an explicit central difference scheme (leap-frog method) with an implicit constitutive update. The sensitivity coefficients are evaluated using a direct differentiation approach. Numerical results are presented for a spherical cap subjected to step loading, and a circular plate subjected to impulsive loading. The sensitivity coefficients are generated by evaluating the derivatives of the response quantities with respect to thickness, mass density, Young's modulus, and two of the material parameters characterizing the viscoplastic response. Time histories of the response and sensitivity coefficients are presented, along with spatial distributions of these quantities at selected times. Author

N95-26269*# Virginia Univ., Hampton, VA. Center for Computational Structures Technology.
NONLINEAR VIBRATIONS OF THIN-WALLED COMPOSITE FRAMES Abstract Only
Ahmed K. Noor and Jeanne M. Peters *In its* Center for Computational Structures Technology Apr. 1995 1 p (For primary document see N95-26263 08-39)
Avail: CASI HC A01/MF A01

A reduced basis technique and a computational procedure are presented for generating the nonlinear vibrational response, and evaluating the first-order sensitivity coefficients of thin-walled composite frames. The sensitivity coefficients are the derivatives of the nonlinear frequency with respect to the material and lamination parameters of the frame. A mixed formulation is used with the fundamental unknowns consisting of both the generalized displacements and stress resultants in the frame. The flanges and webs of the frames are modeled by using geometrically nonlinear two-dimensional shell and plate finite elements. The computational procedure

can be conveniently divided into three distinct steps. The first step involves the generation of various-order perturbation vectors, and their derivatives with respect to the material and lamination parameters of the frame, using the Linstedt-Poincare perturbation technique. The second step consists of using the perturbation vectors as basis vectors, computing the amplitudes of these vectors and the nonlinear frequency of vibration, via a direct variational procedure. The third step consists of using the perturbation vectors, and their derivatives, as basis vectors and computing the sensitivity coefficients of the nonlinear frequency via a second application of the direct variational procedure. Numerical results are presented for semicircular thin-walled frames with I and J section, showing the convergence of the nonlinear frequency and the sensitivity coefficients obtained by both the reduced-basis and perturbation techniques. Author

N95-26270*# Virginia Univ., Hampton, VA. Center for Computational Sructures Technology.

EFFECT OF MESH DISTORTION ON THE ACCURACY OF TRANSVERSE SHEAR STRESSES AND THEIR SENSITIVITY COEFFICIENTS IN MULTILAYERED COMPOSITES Abstract Only

Ahmed K. Noor and Yong H. Kim *In its* Center for Computational Structures Technology Apr. 1995 1 p (For primary document see N95-26263 08-39)

Avail: CASI HC A01/MF A01

A study is made of the effect of mesh distortion on the accuracy of transverse shear stresses and their first-order and second-order sensitivity coefficients in multilayered composite panels subjected to mechanical and thermal loads. The panels are discretized by using a two-field degenerate solid element, with the fundamental unknowns consisting of both displacement and strain components, and the displacement components having a linear variation throughout the thickness of the laminate. A two-step computational procedure is used for evaluating the transverse shear stresses. In the first step, the in-plane stresses in the different layers are calculated at the numerical quadrature points for each element. In the second step, the transverse shear stresses are evaluated by using piecewise integration, in the thickness direction, of the three-dimensional equilibrium equations. The same procedure is used for evaluating the sensitivity coefficients of transverse shear stresses. Numerical results are presented showing no noticeable degradation in the accuracy of the in-plane stresses and their sensitivity coefficients with mesh distortion. However, such degradation is observed for the transverse shear stresses and their sensitivity coefficients. The standard of comparison is taken to be the exact solution of the three-dimensional thermoelasticity equations of the panel. Author

N95-26271*# Virginia Univ., Hampton, VA. Center for Computational Structures Technology.

SENSITIVITY ANALYSIS OF FRICTIONAL CONTACT RESPONSE OF AXISYMMETRIC COMPOSITE STRUCTURES Abstract Only

I. Karaoglan and A. K. Noor *In its* Center for Computational Structures Technology Apr. 1995 1 p (For primary document see N95-26263 08-39)

Avail: CASI HC A01/MF A01

A computational procedure is presented for evaluating the sensitivity coefficients of the static frictional contact response of axisymmetric composite structures. The structures are assumed to consist of an arbitrary number of perfectly bonded homogeneous anisotropic layers. The material of each layer is assumed to be hyperelastic, and the effect of geometric nonlinearity is included. The sensitivity coefficients measure the sensitivity of the response variations in different material, lamination and geometric parameters of the structure. A displacement finite element model is used for the discretization. The normal contact conditions are incorporated into the formulation by using a perturbed Lagrangian approach with the fundamental unknowns consisting of nodal displacements, and Lagrange multipliers associated with the contact conditions. The Lagrange multipliers are allowed to be discontinuous at interelement boundaries. Tangential contact conditions are incorporated by using a penalty method in conjunction with the classical Coulomb's friction model. The Newton-Raphson iterative scheme is used for the solution of the resulting nonlinear algebraic equations, and for the determination of the contact region, contact conditions (sliding or sticking), and the contact pressures. The sensitivity coefficients are evaluated by using a direct differentiation approach. Numerical results are presented for the frictional contact of a composite spherical cap pressed against a rigid plate. Author

N95-26272*# Virginia Univ., Hampton, VA. Center for Computational Structures Technology.

NONLINEAR STRUCTURAL ANALYSIS ON DISTRIBUTED-MEMORY COMPUTERS Abstract Only

Brian C. Watson and Ahmed K. Noor *In its* Center for Computational Structures Technology Apr. 1995 1 p (For primary document see N95-26263 08-39)

Avail: CASI HC A01/MF A01

A computational strategy is presented for the nonlinear static and postbuckling analyses of large complex structures on massively parallel computers. The strategy is designed for distributed-memory, message-passing parallel computer systems. The key elements of the proposed strategy are: (1) a multiple-parameter reduced basis technique; (2) a nested dissection (or multilevel substructuring) ordering scheme; (3) parallel assembly of global matrices; and (4) a parallel sparse equation solver. The effectiveness of the strategy is assessed by applying it to thermo-mechanical postbuckling analyses of stiffened composite panels with cutouts, and nonlinear large-deflection analyses of HSCT models on Intel Paragon XP/S computers. The numerical studies presented demonstrate the advantages of nested dissection-based solvers over traditional skyline-based solvers on distributed memory machines. Author

N95-26273*# Virginia Univ., Hampton, VA. Center for Computational Structures Technology.

THREE-DIMENSIONAL SOLUTIONS FOR COUPLED THERMOELECTROELASTIC RESPONSE OF MULTILAYERED PLATES Abstract Only

Kangming Xu, Ahmed K. Noor, and Yvette Y. Tang *In its* Center for Computational Structures Technology Apr. 1995 1 p (For primary document see N95-26263 08-39)

Avail: CASI HC A01/MF A01

Analytic three-dimensional solutions are presented for the coupled thermoelectroelastic response of multilayered hybrid composite plates. The plates consist of a combination of fiber-reinforced cross-ply and piezothermoelastic layers. Both the thermoelectroelastic static response and its sensitivity coefficients are computed. The sensitivity coefficients measure the sensitivity of the response to variations in different mechanical, thermal and piezoelectric material properties of the plate. A linear constitutive model is used, and the material properties are assumed to be independent of the temperature and the electric field. The plates are assumed to have rectangular geometry and special material symmetries. A mixed formulation is used with the fundamental unknowns consisting of the three transverse stress components; three displacement components; transverse component of the electric displacement field; electric potential; transverse heat flux component, and temperature change. Each of the fundamental unknowns is expressed in terms of a double Fourier series in the Cartesian surface coordinates. A state space approach is used to generate the static response and to evaluate the sensitivity coefficients. Extensive numerical results are presented showing the effects of variation in the geometric parameters of the plate on the different response quantities and their sensitivity coefficients. Author

N95-26274*# Virginia Univ., Hampton, VA. Center for Computational Structures Technology.

RECENT ADVANCES IN THE SENSITIVITY ANALYSIS FOR THE THERMOMECHANICAL POSTBUCKLING OF COMPOSITE PANELS Abstract Only

Ahmed K. Noor *In its* Center for Computational Structures Technology Apr. 1995 1 p (For primary document see N95-26263 08-39)

Avail: CASI HC A01/MF A01

Three recent developments in the sensitivity analysis for thermomechanical postbuckling response of composite panels are reviewed. The three developments are: (1) effective computational procedure for evaluating hierarchical sensitivity coefficients of the various response quantities with respect to the different laminate, layer, and micromechanical characteristics; (2) application of reduction methods to the sensitivity analysis of the postbuckling response; and (3) accurate evaluation of the sensitivity coefficients to transverse shear stresses. Sample numerical results are presented to demonstrate the effectiveness of the computational procedures presented. Some of the future directions for research on sensitivity analysis for the thermomechanical postbuckling response of composite and smart structures are outlined. Author

N95-26275*# Virginia Univ., Hampton, VA. Center for Computational Structures Technology.

A HYBRID NEUROCOMPUTING/NUMERICAL STRATEGY FOR NONLINEAR STRUCTURAL ANALYSIS Abstract Only

Z. Peter Szewczyk and Ahmed K. Noor *In its* Center for Computational Structures Technology Apr. 1995 1 p (For primary document see N95-26263 08-39)

Avail: CASI HC A01/MF A01

A hybrid neurocomputing/numerical strategy is presented for geometrically nonlinear analysis of structures. The strategy combines model-free data processing capabilities of computational neural networks with a Pade approximants-based perturbation technique to predict partial information about the nonlinear response of structures. In the hybrid strategy, multilayer feedforward neural networks are used to extend the validity of solutions by using training samples produced by Pade approximations to the Taylor series expansion of the response function. The range of validity of the training samples is taken to be the radius of convergence of Pade approximants and is estimated by setting a tolerance on the diverging approximants. The norm of residual vector of unbalanced forces in a given element is used as a measure to assess the quality of network predictions. To further increase the accuracy and the range of network predictions, additional training data are generated by either applying linear regression to weight matrices or expanding the training data by using predicted coefficients in a Taylor series. The effectiveness of the hybrid strategy is assessed by performing large-deflection analysis of a doubly-curved composite panel with a circular cutout, and postbuckling analyses of stiffened composite panels subjected to an in-plane edge shear load. In all the problems considered, the hybrid strategy is used to predict selective information about the structural response, namely the total strain energy and the maximum displacement components only. Author

N95-26276*# Virginia Univ., Hampton, VA. Center for Computational Structures Technology.

POSTBUCKLING AND LARGE-DEFLECTION NONLINEAR ANALYSES ON DISTRIBUTED-MEMORY COMPUTERS Abstract Only

Brian C. Watson and Ahmed K. Noor *In its* Center for Computational Structures Technology Apr. 1995 1 p (For primary document see N95-26263 08-39)

Avail: CASI HC A01/MF A01

A computational strategy is presented for postbuckling and nonlinear static analyses of large complex structures on distributed-memory parallel computers. The strategy is designed for message-passing parallel computer systems. The key elements of the proposed strategy are: (1) a multiple-parameter reduced basis technique; (2) a nested dissection (or multilevel substructuring) ordering scheme; (3) parallel assembly of global matrices; and (4) a parallel sparse equation solver. The effectiveness of the strategy is assessed by performing thermomechanical postbuckling analyses of stiffened composite panels with cutouts, and nonlinear large-deflection analyses of High Speed Civil Transport models on three distributed-memory computers. The numerical studies presented demonstrate the advantages of nested dissection-based solvers over traditional skyline-based solvers on distributed-memory machines. Author

N95-26277*# Virginia Univ., Hampton, VA. Center for Computational Structures Technolology.

REDUCTION TECHNIQUE FOR TIRE CONTACT PROBLEMS Abstract Only

Ahmed K. Noor and Jeanne M. Peters *In its* Center for Computational Structures Technology Apr. 1995 1 p (For primary document see N95-26263 08-39)

Avail: CASI HC A01/MF A01

A reduction technique and a computational procedure are presented for predicting the tire contact response and evaluating the sensitivity coefficients of the different response quantities. The sensitivity coefficients measure the sensitivity of the contact response to variations in the geometric and material parameters of the tire. The tire is modeled using a two-dimensional laminated anisotropic shell theory with the effects of variation in geometric and material parameters, transverse shear deformation, and geometric nonlinearities included. The contact conditions are incorporated into the formulation by using a perturbed Lagrangian approach with the fundamental unknowns consisting of the stress resultants, the generalized displacements, and the Lagrange multipliers associated with the contact conditions. The elemental arrays are obtained by using a modified two-field, mixed variational principle. For the application of the reduction technique, the tire finite element model is partitioned into two regions. The first region consists of the nodes that are likely to come in contact with the pavement, and the second region includes all the remaining nodes. The reduction technique is used to significantly reduce the degrees of freedom in the second region. The effectiveness of the computational procedure is demonstrated by a numerical example of the frictionless contact response of the space shuttle nose-gear tire, inflated and pressed against a rigid flat surface. Author

N95-26278*# Virginia Univ., Hampton, VA. Center for Computational Structures Technology.

SENSITIVITY ANALYSIS FOR THE DYNAMIC RESPONSE OF THERMOVISCOPLASTIC SHELLS OF REVOLUTION Abstract Only

Makarand Kulkarni and Ahmed K. Noor *In its* Center for Computational Structures Technology Apr. 1995 1 p (For primary document see N95-26263 08-39)

Avail: CASI HC A01/MF A01

A computational procedure is presented for evaluating the sensitivity coefficients of the dynamic axisymmetric, fully-coupled, thermoviscoplastic response of shells of revolution. The analytical formulation is based on Reissner's large deformation shell theory with the effects of large-strain, transverse shear deformation, rotatory inertia and moments turning around the normal to the middle surface included. The material model is chosen to be viscoplasticity with strain hardening and thermal hardening, and an associated flow rule is used with a von Mises effective stress. A mixed formulation is used for the shell equations with the fundamental unknowns consisting of six stress resultants, three generalized displacements and three velocity components. The energy-balance equation is solved using a Galerkin procedure, with the temperature as the fundamental unknown. Spatial discretization is performed in one dimension (meridional direction) for the momentum and constitutive equations of the shell, and in two dimensions (meridional and thickness directions) for the energy-balance equation. The temporal integration is performed by using an explicit central difference scheme (leap-frog method) for the momentum equation; a predictor-corrector version of the trapezoidal rule is used for the energy-balance equation; and an explicit scheme consistent with the central difference method is used to integrate the constitutive equations. The sensitivity coefficients are evaluated by using a direct differentiation approach. Numerical results are presented for a spherical cap subjected to step loading. Author (revised)

N95-26279*# Virginia Univ., Hampton, VA. Center for Computational Structures Technology.

DYNAMIC SENSITIVITY ANALYSIS OF FRICTIONAL CONTACT/IMPACT RESPONSE OF AXISYMMETRIC COMPOSITE STRUCTURES Abstract Only

Levent Karaoglan and Ahmed K. Noor *In its* Center for Computational Structures Technology Apr. 1995 1 p Submitted for publication (For primary document see N95-26263 08-39)

Avail: CASI HC A01/MF A01

A computational procedure is presented for evaluating the sensitivity coefficients of the dynamic frictional contact/impact response of axisymmetric composite structures. The structures are assumed to consist of an arbitrary number of perfectly bonded homogeneous anisotropic layers. The material of each layer is assumed to be hyperelastic, and the effect of geometric nonlinearity is included. The sensitivity coefficients measure the sensitivity of the response to variations in different material, lamination and geometric parameters of the structure. A displacement finite element model is used for the discretization. The normal contact conditions are incorporated into the formulation by using a perturbed Lagrangian approach with the fundamental unknowns consisting of the nodal displacements, and the Lagrange multipliers associated with the contact conditions. The Lagrange multipliers are allowed to be discontinuous at interelement boundaries. Tangential contact conditions are incorporated by using a penalty method in conjunction with the classical Coulomb's friction model. Temporal integration is performed by using Newmark method. The Newton-Raphson iterative scheme is used for the solution of the resulting nonlinear algebraic equations, and for the determination of the contact region, contact conditions (sliding or sticking), and the contact pressures. The sensitivity coefficients

are evaluated by using a direct differentiation approach. Numerical results are presented from the frictional contact/impact response of a composite spherical cap impacting on a rigid plate. Author

N95-26280*# Virginia Univ., Hampton, VA. Center for Computational Structures Technology.
BUCKLING AND POSTBUCKLING OF COMPOSITE PANELS WITH CUTOUTS SUBJECTED TO COMBINED EDGE SHEAR AND TEMPERATURE CHANGE Abstract Only
Ahmed K. Noor and Yong H. Kim *In its* Center for Computational Structures Technology Apr. 1995 1 p (For primary document see N95-26263 08-39)
Avail: CASI HC A01/MF A01

The results of a detailed study of the buckling and postbuckling responses of composite panels with central circular cutouts are presented. The panels are subjected to combined edge shear and temperature change. The panels are discretized by using a two-field degenerate solid element with each of the displacement components having a linear variation throughout the thickness of the panel. The fundamental unknowns consist of the average mechanical strains through the thickness and the displacement components. The effects of geometric nonlinearities and laminated anisotropic material behavior are included. The stability boundary, postbuckling response and the hierarchical sensitivity coefficients are evaluated. The hierarchical sensitivity coefficients measure the sensitivity of the buckling and postbuckling responses to variations in the panel stiffnesses, and the material properties of both the individual layers and the constituents (fibers and matrix). Numerical results are presented for composite panels with central circular cutouts subjected to combined edge shear and temperature change, showing the effects of variations in the hole diameter, laminate stacking sequence and fiber orientation, on the stability boundary and postbuckling response and their sensitivity to changes in the various panel parameters. Author

N95-26281*# Virginia Univ., Hampton, VA. Center for Computational Structures Technology.
SENSITIVITY ANALYSIS FOR LARGE-DEFLECTION AND POSTBUCKLING RESPONSES ON DISTRIBUTED-MEMORY COMPUTERS Abstract Only
Brian C. Watson and Ahmed K. Noor *In its* Center for Computational Structures Technology Apr. 1995 1 p (For primary document see N95-26263 08-39)
Avail: CASI HC A01/MF A01

A computational strategy is presented for calculating sensitivity coefficients for the nonlinear large-deflection and postbuckling responses of laminated composite structures on distributed-memory parallel computers. The strategy is applicable to any message-passing distributed computational environment. The key elements of the proposed strategy are: (1) a multiple-parameter reduced basis technique; (2) a parallel sparse equation solver based on a nested dissection (or multilevel substructuring) node ordering scheme; and (3) a multilevel parallel procedure for evaluating hierarchical sensitivity coefficients. The hierarchical sensitivity coefficients measure the sensitivity of the composite structure response to variations in three sets of interrelated parameters; namely, laminate, layer and micromechanical (fiber, matrix, and interface/interphase) parameters. The effectiveness of the strategy is assessed by performing hierarchical sensitivity analysis for the large-deflection and postbuckling responses of stiffened composite panels with cutouts on three distributed-memory computers. The panels are subjected to combined mechanical and thermal loads. The numerical studies presented demonstrate the advantages of the reduced basis technique for hierarchical sensitivity analysis on distributed-memory machines. Author

N95-26282*# Virginia Univ., Hampton, VA. Center for Computational Structures Technology.
COMPUTATIONAL STRATEGIES FOR TIRE MONITORING AND ANALYSIS Abstract Only **c37**
Kent T. Danielson, Ahmed K. Noor, and James S. Green (Moravian Coll., Bethlehem, PA.) *In its* Center for Computational Structures Technology Apr. 1995 1 p (For primary document see N95-26263 08-39)
Avail: CASI HC A01/MF A01

Computational strategies are presented for the modeling and analysis of tires in contact with pavement. A procedure is introduced for simple and accurate determination of tire cross-sectional geometric characteristics from a digitally scanned image. Three new strategies for reducing the computational effort in the finite element solution of tire-pavement contact are also presented. These strategies take advantage of the observation that footprint loads do not usually stimulate a significant tire response away from the pavement contact region. The finite element strategies differ in their level of approximation and required amount of computer resources. The effectiveness of the strategies is demonstrated by numerical examples of frictionless and frictional contact of the space shuttle Orbiter nose-gear tire. Both an in-house research code and a commercial finite element code are used in the numerical studies. Author

N95-26283*# Virginia Univ., Hampton, VA. Center for Computational Structures Technology.
ASSESSMENT OF COMPUTATIONAL MODELS FOR THERMOELECTROELASTIC MULTILAYERED PLATES Abstract Only
Yvette T. Tang, Ahmed K. Noor, and Kangming Xu *In its* Center for Computational Structures Technology Apr. 1995 1 p (For primary document see N95-26263 08-39)
Avail: CASI HC A01/MF A01

A study is made of the accuracy of the steady-state (static) thermoelectroelastic response of multilayered hybrid composite plates predicted by five modeling approaches, based on two-dimensional plate theories. The plates consist of a combination of fiber-reinforced and piezothermoelastic layers. The standard of comparison is taken to be the exact three-dimensional thermoelectroelastic solutions, and the quantities compared include gross response characteristics (e.g., strain energy components, and average through-the-thickness displacements); detailed, through-the-thickness distributions of displacements and stresses; and sensitivity coefficients of the response quantities (derivatives of the response quantities with respect to material parameters of the plate). The modeling approaches considered include first-order theory; third-order theory; discrete-layer theory (with piecewise linear variation of the in-plane displacements, temperature and electric potential, in the thickness direction); and two predictor-corrector procedures. Author

N95-26309*# Vanderbilt Univ., Nashville, TN.
LH2 FUEL TANK DESIGN FOR SSTO
Geoff Wright *In its* The 1994 NASA/USRA/ADP Design Projects 31 p(SEE N95-26304 08-80) 1994 (For primary document see N95-26304 08-80)
Avail: CASI HC A03/MF A02

42 GEOSCIENCES (GENERAL)

N95-24538# Joint Publications Research Service, Arlington, VA.
JPRS REPORT: SCIENCE AND TECHNOLOGY. CENTRAL EURASIA
24 Mar. 1995 113 p Transl. into ENGLISH from various Central Eurasian articles
(JPRS-UST-95-013) Avail: CASI HC A06/MF A02

Translated articles cover the following topics: pragmatization of the Russian space program; results of lidar studies of aerosol in arctic-free troposphere; research on the dynamics of the development of optically dense winter hazes by inversion of atmospheric spectral transparency measurements method; dynamic structures in ocean waters and microphysical characteristics of suspended matter determined from hydrooptical measurements; comprehensive approach to solution of problems in wind sounding in cloudy atmospheres; lidar for sounding of tropospheric ozone using nonlinear converters of Cu vapor laser radiation; and laser sounding of mesosphere at the Siberian lidar station. Author

N95-24729# Joint Publications Research Service, Washington, DC.
JPRS REPORT: SCIENCE AND TECHNOLOGY. CENTRAL EURASIA
12 Dec. 1994 50 p Transl. into ENGLISH from various Central Eurasian articles
(JPRS-UST-94-034) Avail: CASI HC A03/MF A01

Translated articles cover the following topics: waveriders formed in currents behind shock waves in form of elliptical cones; features of solutions of aerodynamic problems of wing of finite span; manifestation of active

tectonic dislocations on space radar images and some results of lineament analysis of central part of greater caucasus; new applications of aerospace measurements to research on forest ecosystems; effect of space flight factors on regeneration in mammals and tailed amphibians; degradation of gallium arsenide low-noise microwave field transistors with Schottky barrier under impact of powerful pulsed microwave interference. CASI

N95-24730# Joint Publications Research Service, Washington, DC.
JPRS REPORT: SCIENCE AND TECHNOLOGY. CENTRAL EURASIA
1 Feb. 1995 71 p Transl. into ENGLISH from various Central Eurasian articles
(JPRS-UST-95-003) Avail: CASI HC A04/MF A01

Translated articles cover the following topics: history, outlook for Baykonur described; switching waves and autosolitons in wide-aperture lasers with saturating absorption; modular high-speed fiber-optic transmission system; apparatus and methods for strength tests of composite materials at temperatures to 3300 K; externally heated liquid-piston engine and areas of application; more precise determination of influence of eruptive volcanism on climate; laser beam propagation in stratosphere; optical sensing of the combustion products of a solid-fuel model motor; raman lidar detection range for trace atmospheric pollutants in the UV 'solar blind' region; lidar study of aerosol concentration fluctuations at earth's surface; cloud cover sounding with an orbital laser range finder; and new method to prepare initial information for long-term weather forecasting. CASI

N95-24760# Joint Publications Research Service, Washington, DC.
JPRS REPORT: SCIENCE AND TECHNOLOGY. CENTRAL EURASIA
23 Nov. 1994 81 p Transl. into ENGLISH from various Central Eurasian articles
(JPRS-UST-94-031) Avail: CASI HC A05/MF A01

Translated articles cover the following topics: comparative evaluation of formulas used in allowing for influence of troposphere and stratosphere on results of measurement of range to space objects by electronic devices; research on accuracy of translocation method when determining coordinates of points using GLONASS navigation satellites; combined method for automated interpretation of space images of snow-ice formations; model of global carbon cycle; estimate of the diurnal cycle of the CO2 greenhouse effect with 1D models of vertical atmospheric structure; and genesis of global climate fluctuations in the postglaciation epoch. CASI

N95-25440# Department of Energy, Washington, DC. Engineering and Geosciences Div.
SUMMARIES OF FY 1994 GEOSCIENCES RESEARCH
Dec. 1994 170 p
(DE95-005657; DOE/ER-0636) Avail: CASI HC A08/MF A02

The Geosciences Research Program is directed by the Department of Energy's (DOE's) Office of Energy Research (OER) through its Office of Basic Energy Sciences (OBES). Activities in the Geosciences Research Program are directed toward the long-term fundamental knowledge of the processes that transport, modify, concentrate, and emplace (1) the energy and mineral resources of the earth and (2) the energy byproducts of man. The Program is divided into five broad categories: Geophysics and earth dynamics; Geochemistry; Energy resource recognition, evaluation, and utilization; Hydrogeology and exogeochemistry; and Solar-terrestrial interactions. The summaries in this document, prepared by the investigators, describe the scope of the individual programs in these main areas and their subdivisions including earth dynamics, properties of earth materials, rock mechanics, underground imaging, rock-fluid interactions, continental scientific drilling, geochemical transport, solar/atmospheric physics, and modeling, with emphasis on the interdisciplinary areas. DOE

N95-26080# Joint Publications Research Service, Washington, DC.
JPRS REPORT: SCIENCE AND TECHNOLOGY. CENTRAL EURASIA
21 Apr. 1995 75 p Transl. into ENGLISH from various Central Eurasian articles
(JPRS-UST-95-017) Avail: CASI HC A04/MF A01

Translated articles cover the following topics: physical modeling of directed transport of laser radiation energy; spectrum of doppler shifts of coherent radiation scattered by oscillating rough surface; change in optical characteristics and destruction of glasses under influence of powerful laser radiation; comparative analysis of intraannual variation of total ozone content using data from satellite and surface observations; radar measurements of mesoscale fields of ocean currents made using Almaz-1 spacecraft SAR; evaluating possibility of increasing ocean surface temperature maps by joint use of on-line shipboard and satellite data; models of global communication satellite systems in elliptical orbits; morphostructural interpretation of data obtained by radar sensing from Almaz-1 spacecraft (exemplified by shelf of Helgoland Bay in North Sea); mathematical models of landscape patterns as one of bases for quantitative methods for interpreting aerospace survey materials; experience in use of multiband space information for evaluating condition of pastures and fields of agricultural crops in Rostov Oblast; coordinate systems in space photogrammetry; and state of the art in ecologic mapping. CASI

43 EARTH RESOURCES AND REMOTE SENSING

Includes remote sensing of earth resources by aircraft and spacecraft; photogrammetry; and aerial photography.

For instrumentation see *35 Instrumentation and Photography.*

N95-24240# National Defence Research Establishment, Linkoeping (Sweden).
USE OF VORONOI DIAGRAMS FOR QUALITATIVE MATCHING
S. Norrman and E. Jungert May 1994 36 p See also PB94-124443
(ISSN 0347-3708)
(PB95-165445; FOA-C-30761-3.4) Avail: CASI HC A03/MF A01

FOA (National Defense Research Establishment) has developed a system called FLASH (FOA Laser Airborne Sounder for Hydrography). FLASH is helicopter-borne and can determine x-, y- and z-coordinates by measuring height or depth with a laser while a global positioning system (GPS) takes care of the positioning. A question of interest is, can the FLASH system discover object movements on land, by flying over the same area at two different times and compare the z-values at each x- and y-coordinate, point of the two images, to see if something has changed. A problem with this approach is the position errors in the global positioning system. These errors are random with respect of their directions. This report investigates a method for correction of such errors. The method uses qualitative reasoning for matching of objects. These objects are polygons in a Voronoi diagram of the images from the FLASH system. The result showed that the method could not manage to correct the errors as the differences in the Voronoi diagrams of the two images were too big. NTIS

N95-24299 Helsinki Univ. of Technology, Espoo (Finland).
DIURNAL VARIATIONS OF BACKSCATTERING PROPERTIES OF PINE TREES AT C- AND X-BANDS
K. Heiska and M. Hallikainen May 1994 32 p Limited Reproducibility: More than 20% of this document may be affected by microfiche quality
(ISSN 0786-8154)
(PB95-149738; ISBN-951-22-2149-7) Avail: Issuing Activity (National Technical Information Service (NTIS))

The behavior of the backscattering coefficient of a pine tree canopy was monitored at C- and X-band, VV, HH, VH and HV polarizations over a period of 24 hours in August 1993. By using our HUTSCAT ranging scatterometer, we could measure separately the total backscattering coefficient, the ground contribution, and the canopy contribution. The incidence angle was 40 deg off nadir and the radar system was moved along a rail in order to obtain enough independent samples. The volumetric moisture of a tree trunk and ground surface (0 to 15 cm) along with the air temperature and total solar radiation was monitored as well. The backscattering coefficient for various frequency/polarization combination was compared with the ground truth. The results indicate that the diurnal behavior of the backscattering coefficient at C-band is different from that at X-band. NTIS

N95-24407# Department of Energy, Washington, DC.
IDENTIFICATION OF POTENTIAL GROUNDWATER FLOW PATHS USING GEOLOGICAL AND GEOPHYSICAL DATA
K. Pohlmann and R. Andricevic Sep. 1994 26 p
(Contract DE-AC08-90NV-10845)
(DE95-006253; DOE/NV-10845/49) Avail: CASI HC A03/MF A01

This project represents the first phase in the development of a methodology for generating three-dimensional equiprobable maps of hydraulic conductivity for the Nevada Test Site (NTS). In this study, potential

groundwater flow paths were investigated for subsurface tuffs at Yucca Flat by studying how these units are connected. The virtual absence of site-specific hydraulic conductivity data dictates that as a first step a surrogate attribute (geophysical logs) be utilized. In this first phase, the connectivity patterns of densely welded ash-flow tuffs were studied because these tuffs are the most likely to form zones of high hydraulic conductivity. Densely welded tuffs were identified based on the response shown on resistivity logs and this information was transformed into binary indicator values. The spatial correlation of the indicator data was estimated through geostatistical methods. Equiprobable three-dimensional maps of the distribution of the densely-welded and nonwelded tuffs (i.e., subsurface heterogeneity) were then produced using a multiple indicator simulation formalism. The simulations demonstrate that resistivity logs are effective as soft data for indicating densely welded tuffs. The simulated welded tuffs reproduce the stratigraphic relationships of the welded tuffs observed in hydrogeologic cross sections, while incorporating the heterogeneity and anisotropy that is expected in this subsurface setting. Three-dimensional connectivity of the densely welded tuffs suggests potential groundwater flow paths with lengths easily over 1 km. The next phase of this investigation should incorporate other geophysical logs (e.g., gamma-gamma logs) and then calibrate the resulting soft data maps with available hard hydraulic conductivity data. The soft data maps can then augment the hard data to produce the final maps of the spatial distribution of hydraulic conductivity that can be used as input for numerical solution of groundwater flow and transport. DOE

N95-24422 Naval Air Weapons Station, China Lake, CA.
COSO MONITORING PROGRAM, OCTOBER 1992 THROUGH SEPTEMBER 1993
S. C. Bjornstad, J. H. Monahan, and J. K. Sprouse Jan. 1994 128 p
Limited Reproducibility: More than 20% of this document may be affected by microfiche quality
(AD-A279147; NAWS-CL-TP-003) Avail: Issuing Activity (Defense Technical Information Center (DTIC))

The Coso Monitoring Program is a continuing effort in support of the Navy's geothermal resources within the Known Geothermal Resource Area (KGRA). Data are presented on the monitoring of steam flow rates and temperatures, water levels in ponds and wells, water chemistry, and rainfall in the Coso Hot Springs Resort Area. A monthly photographic essay of the mudfields and pools shows the variation of the surface water levels throughout the year. DTIC

N95-24441*# Colorado Univ., Boulder, CO. Cooperative Inst. for Research in Environmental Sciences.
ICE SURFACE TEMPERATURE RETRIEVAL FROM AVHRR, ATSR, AND PASSIVE MICROWAVE SATELLITE DATA: ALGORITHM DEVELOPMENT AND APPLICATION Annual Report No. 2
Jeff Key, James Maslanik, and Konrad Steffen 24 Mar. 1995 17 p
(Grant NAGw-3437)
(NASA-CR-198037; NAS 1.26:198037) Avail: CASI HC A03/MF A01

During the second phase project year we have made progress in the development and refinement of surface temperature retrieval algorithms and in product generation. More specifically, we have accomplished the following: (1) acquired a new advanced very high resolution radiometer (AVHRR) data set for the Beaufort Sea area spanning an entire year; (2) acquired additional along-track scanning radiometer(ATSR) data for the Arctic and Antarctic now totalling over eight months; (3) refined our AVHRR Arctic and Antarctic ice surface temperature (IST) retrieval algorithm, including work specific to Greenland; (4) developed ATSR retrieval algorithms for the Arctic and Antarctic, including work specific to Greenland; (5) developed cloud masking procedures for both AVHRR and ATSR; (6) generated a two-week bi-polar global area coverage (GAC) set of composite images from which IST is being estimated; (7) investigated the effects of clouds and the atmosphere on passive microwave 'surface' temperature retrieval algorithms; and (8) generated surface temperatures for the Beaufort Sea data set, both from AVHRR and special sensor microwave imager (SSM/I). Author

N95-24444 National Defence Research Establishment, Linkoeping (Sweden). Huvudavdelning foer Informationsteknologi.
RESEARCH IN THE SERVICE OF THE SWEDISH NATIONAL DEFENCE [FORSKARGAERNING I FOERSVARETS TJAENST]
T. Orhaug and E. B. Bjoerck Mar. 1994 34 p In SWAHILI
(PB95-141941; FOA-C-30750-3.4) Avail: Issuing Activity (National Technical Information Service (NTIS))

The document contains a list of documents and reports published 1956-1994 by Torleiv Orhaug, Director of Research at the National Defense Research Establishment in Sweden. Topics include: image processing; remote sensing; open skies; verification technology; and space technology. NTIS

N95-24502# Naval Aviation Systems Team, Arlington, VA.
MAPPING, CHARTING AND GEODESY HANDBOOK
John H. Harden, Jr. 15 Jul. 1994 69 p
(AD-A286558) Avail: CASI HC A04/MF A01

This handbook is for all members of the Naval Aviation Systems Team (TEAM). It is your initial reference for information about Mapping, Charting, and Geodesy (MC and G) support from the Defense Mapping Agency (DMA). This handbook will clarify MC and G relevance to TEAM systems development and your job, guide you in acquiring a necessary basic competence in MC and G, explain the process for you to get DMA MC and G data and services, and point you to help on MC and G within the TEAM, DMA, and elsewhere. DTIC

N95-24542*# National Aeronautics and Space Administration. Goddard Space Flight Center, Greenbelt, MD.
EOS DIRECTORY
Sep. 1994 298 p
(NASA-TM-110580; NAS 1.15:110580) Avail: CASI HC A13/MF A03

This Earth Observing System (EOS) directory is divided into two main sections: white and yellow pages. The white pages list alphabetically the names and addresses -- including e-mail, phone, and fax when available -- of all individuals involved with EOS, from graduate students to panel members to program management and more. The yellow pages list the names, affiliation, and phone number of participants divided by project management, program management, individual project participants, interdisciplinary investigations (listed alphabetically by PI), the Science Executive Committee, various panels, platforms, working groups, fellowships, and contractors. CASI

N95-24768# Joint Publications Research Service, Washington, DC.
JPRS REPORT: SCIENCE AND TECHNOLOGY. CENTRAL EURASIA. OTECHESTVENNAYA GEOLOGIYA: STUDIES IN AEROSPACE AND REMOTE SENSING
27 Jan. 1995 61 p Transl. into ENGLISH of Otechestvennaya Geologiya-Studies in Aerospace and Remote Sensing
(JPRS-UST-95-004) Avail: CASI HC A04/MF A01

Translated articles cover the following topics: Otechestvennaya Geologiya-studies in aerospace imaging and remote sensing; development of aerospace methods at the Laboratory of Aerial Methods of the All-Russian Scientific Research Institute of Satellite Aerogeological Methods; the place of remote methods in Russian geological research; infrared aerospace imaging: achievements and outlook; development of remote methods of studying petroleum and gas bearing territories at the Laboratory of Aerial Methods of the All-Russian Scientific Research Institute of Satellite Aerogeological Methods; remote-data study and prediction of material-structural inhomogeneities: petroleum and gas traps; remote sensing in forecasting and locating mineral ores in research by workers at VNIIKAM (the All-Russian Scientific Research Institute of Satellite Aerogeological Methods); using aerial and satellite imaging materials in geological research (status and outlook); and specifics of integrating GIS and remote sensing technologies in the study of natural resources. Author

N95-25110 EG and G Energy Measurements, Inc., Goleta, CA.
TURBINE-ENGINE APPLICATIONS OF THERMOGRAPHIC-PHOSPHOR TEMPERATURE MEASUREMENTS
Bruce W. Noel (Noel Associates, Espanola, NM.), W. Dale Turley, and Stephen W. Allison (Martin Marietta Energy Systems, Inc., Oak Ridge, TN.) 1995 24 p Presented at the Remote Temperature Sensing Workshop, Cleveland, OH, 27-28 Oct. 1994 Limited Reproducibility: More than 20% of this document may be affected by microfiche quality
(Contract DE-AC08-93NV-11265)
(DE95-003625; EGG-11265-3011; UC-706; CONF-9410259-1) Avail: CASI HC A03

The thermographic-phosphor (TP) method can measure temperature, heat flux, strain, and other physical quantities remotely in hostile and/or inaccessible environments such as the first-stage turbine components in turbine engines. It is especially useful in situations in which no other known method works well. This paper is a brief review of engine tests that demonstrated the utility of the TP method. For the most part, the results presented here are discussed only qualitatively. The papers in the bibliography describe these and other experiments and results in detail. The first viewgraph summarizes the many desirable features of the TP method. The second viewgraph describes TP's, and the third summarizes how the TP method works. To measure single-point temperatures in turbine-engine applications, we use the decay-time method, which depends on the fact that the luminescence following an impulse of ultraviolet excitation decays, with a characteristic decay time that is a monotonically decreasing function of temperature over some range of temperatures. The viewgraph is a set of calibration curves showing the behavior of some useful emission lines for ten important TP's. Consider LuPO4:Eu as an example. Below the 'quenching' temperature near 900 K, the decay time is nearly constant. Above it, the decay time decreases exponentially with the temperature. This strong functional dependence means that one can have a fairly large error in the lifetime measurement, as in environments with poor signal-to-noise ratios (SNR's), yet still obtain high accuracy in the temperature measurement. Our more-recent data up to 1900 K show the same behavior. DOE

N95-26040 Air Force Inst. of Tech., Wright-Patterson AFB, OH.
MULTISPECTRAL DETECTION OF GROUND TARGETS IN HIGHLY CORRELATED BACKGROUNDS M.S. Thesis
Jason E. Thomas Dec. 1994 114 p
(AD-A289292; AFIT/GEO/ENP/94D-06) Avail: Issuing Activity (Defense Technical Information Center (DTIC))

Multispectral detection methods attempt to discriminate targets in a dominant clutter background using multiple images of the same real-world scene taken in different narrow spectral bands in the infrared. Detection is possible due to the empirically-observed phenomenon that the radiance of man-made objects, such as a tank or truck, often lies off the main spectral correlation axis of that of natural backgrounds. Radiometric measurements of several vehicles and a tree canopy background taken over three days in June 1994 were used to examine the factors affecting multispectral detection. Results clearly showed that the processes which provide for higher spectral correlation of natural backgrounds tend to diminish the spectral separation between the background and target. Very high correlations between IR spectral bands for the targets and background were found to exist. The degree of correlation between bands in the LWIR was found to be higher than that for the MWIR for the correlation levels (p) of interest, p greater than or equal 0.99. The MW/LW combinations were found to almost never produce these high correlations. DTIC

44 ENERGY PRODUCTION AND CONVERSION

Includes specific energy conversion systems, e.g., fuel cells; global sources of energy; geophysical conversion; and windpower.

For related information see also *07 Aircraft Propulsion and Power, 20 Spacecraft Propulsion and Power,* and *28 Propellants and Fuels.*

N95-24199*# California State Univ., Los Angeles, CA. School of Engineering and Technology.
SOLAR EAGLE 2 Final Technical Report, 15 Sep. 1992 - 15 Nov. 1993
Richard D. Roberto Jan. 1995 58 p
(Contract NAG1-1455; Proj. Solar Eagle 2)
(NASA-CR-198043; NAS 1.26:198043) Avail: CASI HC A04/MF A01

During a 22-month period from February 1991 to December 1993, a dedicated group of students, faculty, and staff at California State University, Los Angeles completed a project to design, build, and race their second world class solar-powered electric vehicle, the Solar Eagle 2. This is the final report of that project. As a continuation of the momentum created by the success of the GM-sponsored Sunrayce USA in 1990, the U.S. Department of Energy (DOE) picked up the banner from General Motors as sponsors of Sunrayce 93. In February 1991, the DOE sent a request for proposals to all universities in North America inviting them to submit a proposal outlining how they would design, build, and test a solar-powered electric vehicle for a seven-day race from Arlington, Texas to Minneapolis, Minnesota, to be held in June 1993. Some 70 universities responded. At the end of a proposal evaluation process, 36 universities including CSLA were chosen to compete. This report documents the Solar Eagle 2 project--the approaches take, what was learned, and how our experience from the first Solar Eagle was incorporated into Solar Eagle 2. The intent is to provide a document that would assist those who may wish to take up the challenge to build Solar Eagle 3. Author

N95-24264# Sandia National Labs., Albuquerque, NM.
GaAsSb-BASED HETEROJUNCTION TUNNEL DIODES FOR TANDEM SOLAR CELL INTERCONNECTS
J. C. Zolper, J. F. Klem, T. A. Plut, and C. P. Tigges 1995 4 p
Presented at the 1st World Conference on Photovoltaic Energy Conversion, Waikoloa, HI, 5-9 Dec. 1994
(Contract DE-AC04-94AL-85000)
(DE95-004779; SAND-94-1597C; CONF-941203-13) Avail: CASI HC A01/MF A01

We report a new approach to tunnel junctions that employs a pseudomorphic GaAsSb layer to obtain a band alignment at a InGaAs or InAlAs p-n junction favorable for forward bias tunneling. Since the majority of the band offset between GaAsSb and InGaAs or InAlAs is in the valence band, when an GaAsSb layer is placed at an InGaAs or InAlAs p-n junction the tunneling distance is reduced and the tunneling current is increased. For all doping levels studied, the presence of the GaAsSb-layer enhanced the forward tunneling characteristics. In fact, in a InGaAs/GaAsSb tunnel diode a peak tunneling current sufficient for a 1000 sun intercell interconnect was achieved with p = 1.5 x l0(exp 18) cm(exp -3) while a similarly doped all-InGaAs diode was rectifying. This approach affords a new degree of freedom in designing tunnel junctions for tandem solar cell interconnects. Previously only doping levels could be varied to control the tunneling properties. Our approach relaxes the doping requirements by employing a GaAsSb-based heterojunction. DOE

N95-24305# National Renewable Energy Lab., Golden, CO.
NATIONAL RENEWABLE ENERGY LABORATORY INFORMATION RESOURCES CATALOGUE. A COLLECTION OF ENERGY EFFICIENCY AND RENEWABLE ENERGY INFORMATION RESOURCES
1994 80 p
(Contract DE-AC36-83CH-10093)
(DE94-011900; NREL/SP-336-7233) Avail: CASI HC A05/MF A01

NREL's first annual Information Resources Catalogue is intended to inform anyone interested in energy efficiency and renewable energy technologies of NREL's outreach activities, including publications and services. For ease of use, all entries are categorized by subject. The catalogue is separated into six main sections. The first section lists and describes services that are available through NREL and how they may be accessed. The second section contains a list of documents that are published by NREL on a regular or periodic basis. The third section highlights NREL's series publications written for specific audiences and presenting a wide range of subjects. NREL's General Interest Publications constitute the fourth section of the catalogue and are written for nontechnical audiences. Descriptions are provided for these publications. The fifth section contains Technical Reports that detail research and development projects. The section on Conference Papers/Journal Articles/Book Chapters makes up the sixth and final section of the catalogue. DOE

N95-24318# Allied-Signal Aerospace Co., Torrance, CA.
MONOLITHIC SOLID OXIDE FUEL CELL TECHNOLOGY ADVANCEMENT FOR COAL-BASED POWER GENERATION Final Report, Sep. 1989 - Mar. 1994
May 1994 377 p
(Contract DE-AC21-89MC-26006)
(DE94-012258; DOE/MC-26006/3824) Avail: CASI HC A17/MF A03

This project has successfully advanced the technology for MSOFC's for coal-based power generation. Major advances include: tape-calendering processing technology, leading to 3X improved performance at 1000 C; stack materials formulations and designs with sufficiently close thermal expansion match for no stack damage after repeated thermal cycling in air; electrically conducting bonding with excellent structural robustness; and sealants that form good mechanical seals for forming manifold structures.

A stack testing facility was built for high-spower MSOFC stacks. Comprehensive models were developed for fuel cell performance and for analyzing structural stresses in multicell stacks and electrical resistance of various stack configurations. Mechanical and chemical compatibility properties of fuel cell components were measured; they show that the baseline Ca-, Co-doped interconnect expands and weakens in hydrogen fuel. This and the failure to develop adequate sealants were the reason for performance shortfalls in large stacks. Small (1-in. footprint) two-cell stacks were fabricated which achieved good performance (average area-specific-resistance 1.0 ohm-sq cm per cell); however, larger stacks had stress-induced structural defects causing poor performance. DOE

N95-24355# Department of Energy, Washington, DC.
APPENDIX MODEL PERFORMANCE: MODEL DOCUMENTATION. RENEWABLE FUELS MODULE OF THE NATIONAL ENERGY MODELLING SYSTEM
Sep. 1994 12 p
(DE95-006080; DOE/EIA-M069-A) Avail: CASI HC A03/MF A01

Performance aspects of the Renewable Fuels Module (RFM) is discussed. The pattern of response of the RFM to typical changes in its major inputs from other NEMS modules is presented. The overall approach of this document, with the particular statistics presented, is designed to be comparable with similar analyses conducted for all of the modules of NEMS. While not always applicable, the overall approach has been to produce analyses and statistics that are as comparable as possible with model developer's reports for other NEMS modules. Those areas where the analysis is somewhat limited or constrained are discussed. Because the RFM consists of independent submodules, this appendix is broken down by submodule. DOE

N95-24369# Pacific Northwest Lab., Richland, WA.
SIMULATION OF DIURNAL THERMAL ENERGY STORAGE SYSTEMS: PRELIMINARY RESULTS
S. Katipamula, S. Somasundaram, and H. R. Williams (Alaska Univ., Fairbanks, AK.) Dec. 1994 43 p
(Contract DE-AC06-76RL-01830)
(DE95-005751; PNL-10222) Avail: CASI HC A03/MF A01

This report describes the results of a simulation of thermal energy storage (TES) integrated with a simple-cycle gas turbine cogeneration system. Integrating TES with cogeneration can serve the electrical and thermal loads independently while firing all fuel in the gas turbine. The detailed engineering and economic feasibility of diurnal TES systems integrated with cogeneration systems has been described in two previous PNL reports. The objective of this study was to lay the ground work for optimization of the TES system designs using a simulation tool called TRNSYS (TRaNsient SYstem Simulation). TRNSYS is a transient simulation program with a sequential-modular structure developed at the Solar Energy Laboratory, University of Wisconsin-Madison. The two TES systems selected for the base-case simulations were: (1) a one-tank storage model to represent the oil/rock TES system; and (2) a two-tank storage model to represent the molten nitrate salt TES system. Results of the study clearly indicate that an engineering optimization of the TES system using TRNSYS is possible. The one-tank stratified oil/rock storage model described here is a good starting point for parametric studies of a TES system. Further developments to the TRNSYS library of available models (economizer, evaporator, gas turbine, etc.) are recommended so that the phase-change processes is accurately treated. DOE

N95-24425# Department of Energy, Morgantown, WV.
MONOLITHIC SOLID OXIDE FUEL CELL TECHNOLOGY ADVANCEMENT FOR COAL-BASED POWER GENERATION Quarterly Technical Progress Report, Jan. - Mar. 1994
25 Oct. 1994 28 p
(Contract DE-AC21-89MC-26006)
(DE95-006152; DOE/MC-26006/3960) Avail: CASI HC A03/MF A01

The objective of this study is to advance materials and fabrication methods to develop a monolithic solid oxide fuel cell (MSOFC) system for coal-based power generation. Focus is on materials research and development (R and D), fabrication process development, cell/stack performance testing and characterization, cost and system analysis, and quality development. DOE

N95-24560*# National Aeronautics and Space Administration. Lewis Research Center, Cleveland, OH.
USE OF ADVANCED SOLAR CELLS FOR COMMERCIAL COMMUNICATION SATELLITES
Sheila G. Bailey and Geoffrey A. Landis (NYMA, Inc., Brook Park, OH.) Mar. 1995 6 p Presented at the First World Conference on Photovoltaic Energy Conversion, Waikoloa, HI, 5-9 Dec. 1994; cosponsored by IEEE, PVSEC-Japan and PVSEC-Europe
(Contract NAS3-25266; RTOP 233-01-00)
(NASA-TM-106879; E-9515; NAS 1.15:106879) Avail: CASI HC A02/MF A01

The current generation of communications satellites are located primarily in geosynchronous Earth orbit (GEO). Over the next decade, however, a new generation of communications satellites will be built and launched, designed to provide a world-wide interconnection of portable telephones. For this mission, the satellites must be positioned in lower polar and near-polar orbits. To provide complete coverage, large numbers of satellites will be required. Because the required number of satellites decreases as the orbital altitude is increased, fewer satellites would be required if the orbit chosen were raised from low to intermediate orbit. However, in intermediate orbits, satellites encounter significant radiation due to trapped electrons and protons. Radiation tolerant solar cells may be necessary to make such satellites feasible. We analyze the amount of radiation encountered in low and intermediate polar orbits at altitudes of interest to next-generation communication satellites, calculate the expected degradation for silicon, GaAs, and InP solar cells, and show that the lifetimes can be significantly increased by use of advanced solar cells. Author

N95-24607# Argonne National Lab., IL. Chemical Technology Div.
LIQUID-FUELED SOFC POWER SOURCES FOR TRANSPORTATION
K. M. Myles, R. Doshi, R. Kumar, and M. Krumpelt 1994 10 p Presented at the 1st European Solid Oxide Fuel Cell Forum: Engineering, Systems, Applications, Lucerne, Switzerland, 3-7 Oct. 1994
(Contract W-31-109-eng-38)
(DE95-002998; ANL/CMT/CP-84099; CONF-9410170-2) Avail: CASI HC A02/MF A01

Traditionally, fuel cells have been developed for space or stationary terrestrial applications. As the first commercial 200-kW systems were being introduced by ONSI and Fuji Electric, the potentially much larger, but also more challenging, application in transportation was beginning to be addressed. As a result, fuel cell-powered buses have been designed and built, and R&D programs for fuel cell-powered passenger cars have been initiated. The engineering challenge of eventually replacing the internal combustion engine in buses, trucks, and passenger cars with fuel cell systems is to achieve much higher power densities and much lower costs than obtainable in systems designed for stationary applications. At present, the leading fuel cell candidate for transportation applications is, without question, the polymer electrolyte fuel cell (PEFC). Offering ambient temperature start-up and the potential for a relatively high power density, the polymer technology has attracted the interest of automotive manufacturers worldwide. But the difficulties of fuel handling for the PEFC have led to a growing interest in exploring the prospects for solid oxide fuel cells (SOFCs) operating on liquid fuels for transportation applications. Solid oxide fuel cells are much more compatible with liquid fuels (methanol or other hydrocarbons) and are potentially capable of power densities high enough for vehicular use. Two SOFC options for such use are discussed in this report. DOE

N95-24666# National Renewable Energy Lab., Golden, CO.
BRAYTON-CYCLE SOLVENT RECOVERY HEAT PUMP. A TECHNICAL BRIEF
Nov. 1994 19 p
(Contracts DE-AC36-83CH-10093; DE-AC01-87CE-40762)
(DE94-000225; DOE/CH-10093/251) Avail: CASI HC A03/MF A01

The US Department of Energy's (DOE's) Office of Industrial Technologies (OIT) sponsors research and development (R & D) to improve the energy efficiency of American industry and to provide for fuel flexibility. Working closely with industry, OIT has successfully developed more than 50 new technologies that saved industry approximately 80 trillion Btu (84 quadrillion joules) of energy in 1992. More than 200 other projects are in various stages of development from laboratory research to field tests. The use of solvents in the industrial sector is widespread and results in the emission

of volatile organic compounds (VOC's) to the atmosphere. These VOC emissions represent an economic loss to industry and contribute significantly to air pollution. To comply with increasingly strict environmental regulations while keeping costs down, industry must find efficient and cost-effective ways to control emissions from solvent use. DOE

N95-24674# Sandia National Labs., Albuquerque, NM.
CO-VALIDATION OF THREE METHODS FOR OPTICAL CHARACTERIZATION OF POINT-FOCUS CONCENTRATORS
T. J. Wendelin (National Renewable Energy Lab., Golden, CO.) and J. W. Grossman 1994 11 p Presented at the American Society of Mechanical Engineers/Japanese Society of Mechanical Engineers/Japan Solar Energy Society International Solar Energy Conference, Maui, HI, 19-24 Mar. 1995
(Contracts DE-AC04-94AL-85000; DE-AC04-95DP-85000)
(DE95-001613; SAND-94-1839C; CONF-950336-2) Avail: CASI HC A03/MF A01

Three different methods for characterizing point-focus solar concentrator optical performance have been developed for specific applications. These methods include a laser ray trace technique called the Scanning Hartmann Optical Test, a video imaging process called the 2f Technique and actual on-sun testing in conjunction with optical computer modeling. Three concentrator test articles, each of a different design, were characterized using at least two of the methods and, in one case, all three. The results of these tests are compared in order to validate the methods. Excellent agreement is observed in the results, suggesting that the techniques provide consistent and accurate characterizations of solar concentrator optics. DOE

N95-24676# Sandia National Labs., Albuquerque, NM.
MIRROR ALIGNMENT AND FOCUS OF POINT-FOCUS SOLAR CONCENTRATORS
Richard B. Diver 1994 8 p Presented at the American Society of Mechanical Engineers/Japanese Society of Mechanical Engineers/Japan Solar Energy Society International Solar Energy Conference, Maui, HI, 19-24 Mar. 1995 Sponsored by Cummins Power Generations, Inc.
(Contract DE-AC04-94AL-85000)
(DE95-002609; SAND-94-2638C; CONF-950336-7) Avail: CASI HC A02/MF A01

Distributed point-focusing solar concentrators are being developed for dish-Stirling systems and other applications. Many of these concentrators make use of faceted mirrors that have to be accurately aligned. Some of the solar concentrator designs use stretched-membrane facets that also require focusing. Accurate mirror alignment and focus of faceted solar concentrators have two benefits. First, the concentration ratio of the concentrator/receiver (collector) system is improved with accurate alignment and focus. The receiver aperture diameter can therefore be smaller, thereby reducing thermal losses from the receiver and improving the overall efficiency of the collector. Second, and perhaps more importantly, flux intensities on the receiver can be sensitive to facet alignment and focus. In this paper, the theory and practical application of an alignment and focusing technique are presented. In the technique, light from an artificial source is reflected from the concentrator's facets to a target. From basic geometric principles, the shape and location of the reflected light on the target can be predicted. Alignment is accomplished by adjusting the facets' aim so that the reflected image falls on the predetermined location. To focus a stretched-membrane facet, the reflected image size is adjusted to match that of the target. The governing equations used to draw the alignment targets are developed and the practical application of the technique to the alignment and focus of the Cummins Power Generation, Inc. CPG-460 are presented. Alignment uncertainty associated with this technique on the CPG-460 is also discussed. DOE

N95-24682# Sandia National Labs., Albuquerque, NM.
FELT-METAL-WICK HEAT-PIPE SOLAR RECEIVER
Charles E. Andraka, Douglas R. Adkins, Timothy A. Moss, Howard M. Cole, and Nicos H. Andreas 1994 6 p Presented at the American Society of Mechanical Engineers/Japanese Society of Mechanical Engineers/Japan Solar Energy Society International Solar Energy Conference, Maui, HI, 19-24 Mar. 1995
(Contract DE-AC04-94AL-85000)
(DE95-004535; SAND-94-2682C; CONF-950336-13) Avail: CASI HC A02/MF A01

Reflux heat-pipe receivers have been identified as a desirable interface to couple a Stirling-cycle engine with a parabolic dish solar concentrator. The reflux receiver provides power nearly isothermally to the engine heater heads while decoupling the heater head design from the solar absorber surface design. The independent design of the receiver and engine heater head leads to higher system efficiency. Heat pipe reflux receivers have been demonstrated at approximately 65 kW(sub t) power throughput. Several 25 to 30 kW(sub e) Stirling-cycle engines are under development, and will soon be incorporated in commercial dish-Stirling systems. These engines will require reflux receivers with power throughput limits reaching 90 kW(sub t). The extension of heat pipe technology from 60 kW(sub t) to 100 kW(sub t) is not trivial. Current heat pipe wick technology is pushed to its limits. It is necessary to develop and test advanced wick structure technologies to perform this task. Sandia has developed and begun testing a Bekaert Corporation felt metal wick structure fabricated by Porous Metal Products Inc. This wick is about 95% porous, and has liquid permeability a factor of 2 to 8 times higher than conventional technologies for a given maximum pore radius. The wick has been successfully demonstrated in a bench-scale heat pipe, and a full-scale on-sun receiver has been fabricated. This report details the wick design, characterization and installation into a heat pipe receiver, and the results of the bench-scale tests are presented. The wick performance is modeled, and the model results are compared to test results. DOE

N95-24683# Missouri Univ., Rolla, MO. Dept. of Ceramic Engineering.
PROCESSING OF LaCrO3 FOR SOLID OXIDE FUEL CELL APPLICATIONS
Wayne Huebner and Harlen U. Anderson Sep. 1994 13 p
(Contract DE-FG21-93MC-29224)
(DE95-000024; DOE/MC-29224/3931) Avail: CASI HC A03/MF A01

The University of Missouri-Rolla is performing a 5 year research program dedicated towards the development of LaCrO3-based interconnect powders which densify when in contact with anode and cathode materials for solid oxide fuel cells (SOFC). During the course of this program the authors investigated compositions within the pseudo-ternary LaCrO3-LaMnO3-LaCoO3 system. Their expanded studies on the processing and sintering of LaCrO3 to make dense interconnects using LaCrO3-based oxides at temperatures less than 1,500 C in an air atmosphere and in contact with both anode and cathode oxides. The specific objectives of this research program are to: develop a novel technique which reproducibly yields LaCrO3-based powders with the desired particle characteristics; fully understand the liquid phase sintering mechanism; clearly identify the reason why LaCrO3 does not densify in the presence of electrolyte and cathode materials; systematically solve this problem through judicious control over the liquid phase; and incorporate materials developed in this program into planar cells and measure their performance. Results are discussed on porosity and skrinkage, and sintering and melting behaviors. DOE

N95-24684# National Renewable Energy Lab., Golden, CO.
DATA PREPARATION REQUIREMENTS FOR MODELING WIND TURBINES WITH ADAMS(R)
Marshall L. Buhl, Jr. Dec. 1994 4 p
(Contract DE-AC36-83CH-10093)
(DE95-000266; NREL/TP-442-7228) Avail: CASI HC A01/MF A01

This contains guidelines for the kind of information that designers need to model a complete wind turbine with ADAMS. The information here is not at all exhaustive. It does, however, represent the collective knowledge of two years of experience gained by National Renewable Energy Laboratory (NREL) engineers while using ADAMS to model wind turbines. If designers save the following information as they design a new turbine, they will have an excellent start on an ADAMS model. The more accurate the input data, the better the results will be. Designers will have to make the tradeoff between the required effort to improve their input data and the benefits of a more accurate simulation. The authors break the turbine into each of its major subsystems and describe them in detail. They attach a table of parameters to the end of the document to make it easier for one to keep track of data requirements. DOE

N95-24714# National Renewable Energy Lab., Golden, CO.
SOLAR THERMAL ELECTRIC HYBRIDIZATION ISSUES
Tom A. Williams, Mark S. Bohn, and Henry W. Price Oct. 1994 9 p Presented at the American Society of Mechanical Engineers/Japanese

Society of Mechanical Engineers/Japan Solar Energy Society International Solar Energy Conference, Maui, HI, 19-24 Mar. 1995
(Contract DE-AC36-83CH-10093)
(DE95-000217; NREL/TP-471-7019; CONF-950336-3) Avail: CASI HC A02/MF A01

Solar thermal electric systems have an advantage over many other renewable energy technologies because the former use heat as an intermediate energy carrier. This is an advantage, as it allows for a relatively simple method of hybridization by using heat from fossil-fuel. Hybridization of solar thermal electric systems is a topic that has recently generated significant interest and controversy and has led to many diverse opinions. This paper discusses many of the issues associated with hybridization of solar thermal electric systems such as what role hybridization should play; how it should be implemented; what are the efficiency, environmental, and cost implications; what solar fraction is appropriate; how hybrid systems compete with solar-only systems; and how hybridization can impact commercialization efforts for solar thermal electric systems. DOE

N95-24715# National Renewable Energy Lab., Golden, CO. Thermal Systems Branch.
FLUX ATTENUATION AT NREL'S HIGH-FLUX SOLAR FURNACE
Carl E. Bingham, Kent L. Scholl, and Allan A. Lewandowski Oct. 1994 7 p Presented at the American Society of Mechanical Engineers/Japanese Society of Mechanical Engineers/Japan Solar Energy Society International Solar Energy Conference, Maui, HI, 19-24 Mar. 1995
(Contract DE-AC36-83CH-10093)
(DE95-000219; NREL/TP-471-7294; CONF-950336-9) Avail: CASI HC A02/MF A01

The High-Flux Solar Furnace (HFSF) at the National Renewable Energy Laboratory (NREL) has a faceted primary concentrator and a long focal-length-to-diameter ratio (due to its off-axis design). Each primary facet can be aimed individually to produce different flux distributions at the target plane. Two different types of attenuators are used depending on the flux distribution. A sliding-plate attenuator is used primarily when the facets are aimed at the same target point. The alternate attenuator resembles a venetian blind. Both attenuators are located between the concentrator and the focal point. The venetian-blind attenuator is primarily used to control the levels of sunlight failing on a target when the primary concentrators are not focused to a single point. This paper will demonstrate the problem of using the sliding-plate attenuator with a faceted concentrator when the facets are not aimed at the same target point. We will show that although the alternate attenuator necessarily blocks a certain amount of incoming sunlight, even when fully open, it provides a more even attenuation of the flux for alternate aiming strategies. DOE

N95-24853# National Renewable Energy Lab., Golden, CO.
USING DIGITAL FILTERING TECHNIQUES AS AN AID IN WIND TURBINE DATA ANALYSIS
Teresa Young Nov. 1994 9 p Presented at the AIAA Region 5 Student Conference, Ft. Collins, CO, 21-24 Apr. 1993
(Contract DE-AC36-83CH-10093)
(DE94-011862; NREL/TP-441-7077; CONF-9304280-1) Avail: CASI HC A02/MF A01

Research involving very large sets of digital data is often difficult due to the enormity of the database. In the case of a wind turbine operating under varying environmental conditions, determining which data are representative of the blade aerodynamics and which are due to transient flow ingestion effects or errors in instrumentation, operation, and data collection is of primary concern to researchers. The National Renewable Energy Laboratory in Golden, Colorado collected extensive data on a downwind horizontal axis wind turbine (HAWT) during a turbine test project called the Combined Experiment. A principal objective of this experiment was to provide a means to predict HAWT aerodynamic, mechanical, and electrical operational loads based upon analytical models of aerodynamic performance related to blade design and inflow conditions. In a collaborative effort with the Aerospace Engineering Department at the University of Colorado at Boulder, a team of researchers has evolved and utilized various digital filtering techniques in analyzing the data from the Combined Experiment. A preliminary analysis of the data set was performed to determine how to best approach the data. The reduced data set emphasized selection of inflow conditions such that the aerodynamic data could be compared directly to wind tunnel data obtained for the same airfoil design as used for the HAWT's blades. It will be shown that this reduced data set has yielded valid, reproducible results that a simple averaging technique or a random selection approach cannot achieve. These findings provide a stable baseline against which operational HAWT data can be compared. DOE

N95-24862# Technical Research Centre of Finland, Jyvaskyla (Finland).
YEARBOOK 1993: BIOENERGY RESEARCH PROGRAMME. UTILIZATION OF BIOENERGY AND BIOMASS CONVERSION [VUOSIKIRJA 1993: BIOENERGIAN KAYTTO JA BIOMASSAN JALOSTUS]
Eija Alakangas, ed. 1994 239 p In FINNISH
(DE95-717518; VTT-Bioenergia-3-Pt-3) Avail: CASI HC A11/MF A03

BIOENERGIA Research Programme is one of the energy technology programs of the Finnish Ministry of Trade and Industry. The aim of the program is to increase the use of economically profitable and environmentally sound bioenergy by improving the competitiveness of present peat and wood fuels. R&D projects will also develop new economically competitive biofuels and new equipment and methods for production, handling, and utilization of biofuels. The total funding for 1993 was 45 million FIM and the number of projects 50. The research area of biomass conversion consists of 7 projects in 1993, and the research area of bioenergy utilization of 10 projects. The results of these projects carried out in 1993 and the plans for 1994 are presented in this publication. The aim of the biomass conversion research is to produce more bio-oils and electric power as well as wood processing industry and power plants than it is possible at present day appliances. The conversion research in 1993 was pointed at refining of the waste liquors of pulping industry and the extraction of them into fuel oil and liquid engine fuels, on production of wood oil via flash pyrolysis, and combustion tests. The target of the bioenergy utilization research is to demonstrate three to four new utilization technologies or methods. Each of these plants should have a potential of 0.2 - 0.3 million toe. The 1993 projects consisted of three main categories: reduction of emissions from small-scale combustion equipment, development of different equipment and methods for new power plant technologies, and the studies concerning additional usage of wood fuels in forest industry. DOE

N95-24865# National Renewable Energy Lab., Golden, CO.
NREL PHOTOVOLTAIC PROGRAM FY 1994 BIBLIOGRAPHY
Dec. 1994 21 p
(Contract DE-AC36-83CH-10093)
(DE95-000275; NREL/TP-410-7408) Avail: CASI HC A03/MF A01

This report lists all published documents of the Photovoltaic Program for FY 1994. Documents include conference papers, journal articles, book chapters, patents, etc. DOE

N95-24866# National Renewable Energy Lab., Golden, CO.
TITLE: ENVIRONMENTAL, HEALTH, AND SAFETY ISSUES OFFUEL CELLS IN TRANSPORTATION. VOLUME 1: PHOSPHORICACID FUEL-CELL BUSES
Shan Ring Dec. 1994 85 p
(Contract DE-AC36-83CH-10093)
(DE95-000289; NREL/TP-463-6831) Avail: CASI HC A05/MF A01

The U.S. Department of Energy (DOE) chartered the Phosphoric Acid Fuel-Cell (PAFC) Bus Program to demonstrate the feasibility of fuel cells in heavy-duty transportation systems. As part of this program, PAFC- powered buses are being built to meet transit industry design and performance standards. Test-bed bus-1 (TBB-1) was designed in 1993 and integrated in March 1994. TBB-2 and TBB-3 are under construction and should be integrated in early 1995. In 1987 Phase 1 of the program began with the development and testing of two conceptual system designs- liquid- and air-cooled systems. The liquid-cooled PAFC system was chosen to continue, through a competitive award, into Phase H, beginning in 1991. Three hybrid buses, which combine fuel-cell and battery technologies, were designed during Phase 3. After completing Phase 2, DOE plans a comprehensive performance testing program (Phase H1) to verify that the buses meet stringent transit industry requirements. The Phase 3 study will evaluate the PAFC bus and compare it to a conventional diesel bus. This NREL study assesses the environmental, health, and safety (EH&S) issues that may affect the commercialization of the PAFC bus. Because safety is a critical factor for consumer acceptance of new transportation-based technologies the study focuses on these issues. The study examines health

and safety together because they are integrally related. In addition, this report briefly discusses two environmental issues that are of concern to the Environmental Protection Agency (EPA). The first issue involves a surge battery used by the PAFC bus that contains hazardous constituents. The second issue concerns the regulated air emissions produced during operation of the PAFC bus. DOE

N95-24882# National Renewable Energy Lab., Golden, CO.
NREL AIRFOIL FAMILIES FOR HAWTs
J. L. Tangler and D. M. Somers (Airfoils, Inc., State College, PA.) Jan. 1995 10 p
(Contract DE-AC36-83CH-10093)
(DE95-000267; NREL/TP-442-7109) Avail: CASI HC A02/MF A01

The development of special-purpose airfoils for horizontal-axis wind turbines (HAWTs) began in 1984 as a joint effort between the National Renewable Energy Laboratory (NREL), formerly the Solar Energy Research Institute (SERI), and Airfoils, Incorporated. Since that time seven airfoil families have been designed for various size rotors using the Eppler Airfoil Design and Analysis Code. A general performance requirement of the new airfoil families is that they exhibit a maximum lift coefficient (c(sub l,max)) which is relatively insensitive to roughness effects. The airfoil families address the needs of stall-regulated, variable-pitch, and variable-rpm wind turbines. For stall-regulated rotors, better peak-power control is achieved through the design of tip airfoils that restrain the maximum lift coefficient. Restrained maximum lift coefficient allows the use of more swept disc area for a given generator size. Also, for stall-regulated rotors, tip airfoils with high thickness are used to accommodate overspeed control devices. For variable-pitch and variable-rpm rotors, tip airfoils having a high maximum lift coefficient lend themselves to lightweight blades with low solidity. Tip airfoils having low thickness result in less drag for blades having full-span pitch control. Annual energy improvements from the NREL airfoil families are projected to be 23% to 35% for stall-regulated turbines, 8% to 20% for variable-pitch turbines, and 8% to 10% for variable-rpm turbines. The improvement for stall-regulated turbines has been verified in field tests. DOE

N95-25109# Sandia National Labs., Albuquerque, NM.
AN EXAMINATION OF METAL FELT WICKS FOR HEAT-PIPE APPLICATIONS
Douglas R. Adkins, Timothy A. Moss, Charles E. Andraka, Nicos H. Andreas (Bekaert Fibre Technologies, Marietta, GA.), and Howard M. Cole (Porous Metal Products, Jacksboro, TX.) 1994 7 p Presented at the American Society of Mechanical Engineers/Japanese Society of Mechanical Engineers/Japan Solar Energy Society International Solar Energy Conference, Maui, HI, 19-24 Mar. 1995
(Contract DE-AC04-94AL-85000)
(DE95-002608; SAND-94-0657C; CONF-950336-6) Avail: CASI HC A02/MF A01

Precision metal felts are made of filaments of microndiameter wires that are chopped and layered onto a flat surface to form a wool-like material. Metal felts are commonly used as filters for micron-sized particles. The small diameters of the wires and the relatively open structure of these non-woven materials provide porosities on the order of 90% and greater. The high porosities of metal felts make them interesting candidate materials for heat pipe applications. Property measurements on selected samples of metal felts have demonstrated that typical effective pore radii range from 40 to 120 micrometers and the respective Darcy permeabilities range from 30 to 300 micrometers(exp 2). Through careful compaction of these materials, it is possible to tailor the flow characteristics of the materials to specific applications. Recently, a series of tests have been conducted at Sandia to measure the flow characteristics and pore structures of these materials as a function of compaction. Results from these tests and a discussion of the current applications of these materials in liquid-metal heat pipes for solar power conversion systems are presented. DOE

N95-25121# Pentastar Electronics, Inc., Huntsville, AL.
TEST PLAN/PROCEDURE FOR THE DPHV SYSTEM INTEGRATION
21 Oct. 1994 28 p
(Contract DE-AC02-94CE-50390)
(DE95-003414; DOE/CE-50390/3) Avail: CASI HC A03/MF A01

This is a test plan for the Direct Hydrogen-Fueled Proton-Exchange Membrane Fuel Cell powered Hybrid Vehicle (DPHV) system or subsystem to provide a documented approach to verify the feasibility of the hardware and software designs for that system. Performance of the testing described in this test plan will verify that the functional requirements of the system and subsystems making up that system have been met. DOE

N95-25309# National Renewable Energy Lab., Golden, CO.
COMPARISON OF THREE METHODS FOR OPTICAL CHARACTERIZATION OF POINT-FOCUS CONCENTRATORS
Timothy J. Wendelin and James W. Grossman (Sandia National Labs., Albuquerque, NM.) 1995 6 p Presented at the American Society of Mechanical Engineers/Japanese Society of Mechanical Engineers/Japan Solar Energy Society International Solar Energy Conference, Maui, HI, 19-24 Mar. 1995
(Contracts DE-AC36-83CH-10093; DE-AC04-94AL-85000)
(DE95-000282; NREL/TP-471-7296; CONF-950336-18) Avail: CASI HC A02/MF A01

Three different methods for characterizing point-focus solar concentrator optical performance have been developed for specific applications. These methods include a laser ray trace technique called the Scanning Hartmann Optical Test; a video imaging process called the 2f Test; and on-sun testing in conjunction with optical computer modeling. Three concentrator test articles, each of a different design, were characterized using at least two of the methods and, in one case, all three. The results of these tests are compared. Excellent agreement was observed in the results, suggesting that the techniques provide consistent and accurate characterizations of solar concentrator optics. DOE

N95-25360# Sandia National Labs., Albuquerque, NM.
A STATISTICAL ANALYSIS OF THE EFFECT OF PECVD DEPOSITION PARAMETERS ON SURFACE AND BULK RECOMBINATION IN SILICON SOLAR CELLS
D. S. Ruby, W. L. Wilbanks (New Mexico Univ., Albuquerque, NM.), and C. B. Fleddermann (New Mexico Univ., Albuquerque, NM.) 1995 5 p Presented at the 1st World Conference on Photovoltaic Energy Conversion, Waikoloa, HI, 5-9 Dec. 1994
(Contract DE-AC04-94AL-85000)
(DE95-004780; SAND-94-1557C; CONF-941203-16) Avail: CASI HC A01/MF A01

The authors performed a statistically designed multiparameter experiment using response surface methodology to determine the optimum deposition and anneal conditions for Plasma-Enhanced Chemical Vapor Deposition (PECVD) silicon-oxide and silicon-nitride films on Si solar cells. Their process included a unique in situ hydrogen plasma treatment to promote bulk defect passivation independently of surface effects. Their goal was to define a process to optimize cell performance by minimizing recombination while also providing an effective antireflection coating. Their initial results showed that excellent emitter-surface passivation, approaching that of the best thermally grown oxides, can be obtained using a single-layer nitride coating whose refractive index is optimized for antireflection purposes. Use of the PECVD-nitride instead of a TiO2 ARC resulted in an 11% increase in output power. DOE

N95-25501# Technische Univ., Delft (Netherlands). Inst. for Wind Energy.
FINITE ELEMENT METHODS IN A SIMULATION CODE FOR OFFSHORE WIND TURBINES M.S. Thesis
Wolfgang Kurz Jun. 1994 71 p
(PB95-164984; IW-94075R) Avail: CASI HC A04/MF A01

Offshore installation of wind turbines will become important for electricity supply in future. Wind conditions above sea are more favorable than on land and appropriate locations on land are limited and restricted. The dynamic behavior of advanced wind turbines is investigated with digital simulations to reduce time and cost in development and design phase. A wind turbine can be described and simulated as a multi-body system containing rigid and flexible bodies. Simulation of the non-linear motion of such a mechanical system using a multi-body system code is much faster than using a finite element code. However, a modal representation of the deformation field has to be incorporated in the multi-body system approach. The equations of motion of flexible bodies due to deformation are generated by finite element calculations. At Delft University of Technology the simulation code DUWECS has been developed which simulates the non-linear behavior

of wind turbines in time domain. The wind turbine is divided in subcomponents which are represented by modules (e.g. rotor, tower etc.). NTIS

N95-25566# Sandia National Labs., Albuquerque, NM.
BACK SURFACE CELL STRUCTURES FOR REDUCING RECOMBINATION IN CZ SILICON SOLAR CELLS
R. R. King (Siemens Solar Industries, Camarillo, CA.), K. W. Mitchell (Siemens Solar Industries, Camarillo, CA.), and J. M. Gee 1994 5 p Presented at the 1st World Conference on Photovoltaic Energy Conversion, Waikoloa, HI, 5-9 Dec. 1994
(Contract DE-AC04-94AL-85000)
(DE95-005423; SAND-94-1613C; CONF-941203-19) Avail: CASI HC A01/MF A01

Mass-produced terrestrial CZ silicon solar cells are currently entering the domain in which bulk diffusion length is comparable to the cell thickness, so that recombination at the back surface can have a significant effect on device performance. Three manufacturable processes that address the problem of back recombination are examined here: boron diffusion from a deposited doped SiO2, layer; Al-alloyed layers using screen-printed paste; and use of a collecting n* layer on the back interdigitated with the positive electrode. 104 sq cm cells fabricated at Siemens Solar Industries using these back surface structures are characterized by current-voltage, spectral response, photoconductivity decay, and SIMS measurements. DOE

N95-25758 Polish Academy of Sciences, Warsaw (Poland). Solar-Ecostructure Center of the Energy-Savings Construction Problems Lab.
THE ENERGY EFFICIENCY OF PASSIVE SOLAR HEATING SYSTEMS [EFEKTYWNOSC ENERGETYCZNA SYSTEMOW BIERNEGO OGRZEWANIA SLONECZNEGO]
Leszek Laskowski 1994 31 p In POLISH
(ISSN 0208-5658)
(IFTR-22/1994) Avail: Issuing Activity (Polish Academy of Sciences, Warsaw, Poland)

The author formulates 24-hour heat budget equations for mathematical models of passive solar heating systems. Taking into consideration the periodic pattern requirement, the author analyzes the thermal states of the structural partitions which act as heat reservoirs in the system. The author uses this as the basis to derive functions which define the solar heat used to heat interior spaces in combination with existing conventional heating systems. The author defines measures of the energy efficiency of passive solar heating and provides a method for calculating these measures. This article is a supplement to the author's monograph entitled 'Passive Solar Heating Systems: Problems of Operation and Energy Efficiency', which was published in 'Studii z Zakresu Inzynierii' (Studies in Engineering), No. 34 (1993). The author tests the formulas contained in this monograph which characterize the amount of solar heat used in the course of a 24-hour day to heat interior spaces and develops and generalizes his solutions for determining measures of the energy efficiency of heating systems. The author uses the same definitions of new concepts and notation for basic physical variables as he did in the monograph.
Transl. by Schreiber Translations Inc.

N95-25892# Swedish Inst. for Materials Testing, Boras (Sweden).
PERFORMANCE TESTS OF AIR SOURCE HEAT PUMPS UNDER FROSTING CONDITIONS. QUALITY OF RESULTS
P. Fahlen 1994 341 p
(PB95-141792; SP-RAPPORT-1994:01) Avail: CASI HC A15/MF A03

This report focuses on the analysis of uncertainties in research regarding air-source heat pumps. The principles recommended by the Western European Calibration Conference (WECC) are applied and the generated information is condensed in the form of uncertainty budgets. The ensuring discussion, and the Measurement Assurance Program that was applied during the research work are also relevant to general testing of cooling coils, e.g. for air source heat pumps. The general conclusion of the analysis is that the method of determining frost mass by continuous weighing and frost density by inference from pressure drop considerations, which is presented in the report, has the potential to produce results with an accuracy on a par with the best previously used techniques to investigate frosting and defrosting phenomena. Furthermore, the methodology has the distinct advantage of yielding online measuring possibilities and being much less time consuming than traditional techniques. NTIS

N95-25995# National Renewable Energy Lab., Golden, CO.
RENEWABLE ENERGY DEMONSTRATION PROJECT BY THE NATIONAL RENEWABLE ENERGY LABORATORY AND THE GENERAL SERVICES ADMINISTRATION
Nancy Carlisle, Ed Hoo, Robert Westby, Ed Hancock (Hancock, Ed and Associates, Boulder, CO.), and J. Lu (General Services Administration, Washington, DC.) Nov. 1994 7 p Presented at the 17th World Energy Engineering Congress and the 4th Environmental Technology Congress and Expo, Atlanta, GA, 7-9 Dec. 1994
(Contract DE-AC36-83CH-10093)
(DE95-000261; NREL/TP-472-7023; CONF-941218-2) Avail: CASI HC A02/MF A01

The Energy Policy Act of 1992 (EPACT) requires the General Services Administration (GSA) to implement a solar energy program to demonstrate and evaluate the performance of available technologies expected to have widespread commercial application. The GSA decided to carry out the project at the Denver Federal Center because of its proximity to the National Renewable Energy Laboratory (NREL). The location was thought to be of mutual benefit to NREL and the GSA: it provides NREL an opportunity to deploy technology and it provides the GSA an opportunity to gain a hands-on learning experience with renewables. The GSA plans to document their experience and use it as a case study in part of a larger training effort on renewable energy. This paper describes the technology selection process and provides an update on the status of the project. DOE

N95-26037# Sandia National Labs., Albuquerque, NM. Wind Energy Technology Dept.
USER'S MANUAL FOR FAROW: FATIGUE AND RELIABILITY OF WIND TURBINE COMPONENTS, VERSION 1.1
Paul S. Veers, Steven R. Winterstein (Stanford Univ., CA.), Clifford H. Lange (Stanford Univ., CA.), and Tracy A. Wilson (New Mexico Univ., Albuquerque, NM.) Nov. 1994 71 p
(Contract DE-AC04-94AL-85000)
(DE95-005530; SAND-94-2460; UC-1210) Avail: CASI HC A04/MF A01

FAROW is a Computer program that assists in the probabilistic analysis of the Fatigue and Reliability of wind turbines. The fatigue lifetime of wind turbine components is calculated using functional forms for important input quantities. Parameters of these functions are defined in an input file as either constants or random variables. The user can select from a library of random variable distribution functions. FAROW uses structural reli bility techniques to calculate the mean time to failure, probability of failure before a target lifetime, relative importance of each of the random inputs, and the sensitivity of the reliability to all input parameters. Monte Carlo simulation is also available. This user's manual is intended to provide sufficient information to knowledgeably run the program and meaningfully interpret the results. The first chapter provides an overview of the approach and the results. Chapter 2 describes the formulation and assumptions used in the fatigue life calculations. Each of the input parameters is described in detail in Chapter 3 along with hints and warnings on usage. An explanation of the outputs is provided in Chapter 4. Two example problems are described and solved in Chapter 5, one for the case where extensive data are available and the other with limited data where the uncertainty is higher. A typical input file and the output files for the example problems are included in the appendices. DOE

N95-26090# National Renewable Energy Lab., Golden, CO.
WIND TECHNOLOGY DEVELOPMENT: LARGE AND SMALL TURBINES
R. W. Thresher, S. M. Hock, R. R. Loose, and P. Goldman Dec. 1994 13 p Presented at the Power Generation Conference, Orlando, FL, 7-9 Dec. 1994
(Contract DE-AC36-83CH-10093)
(DE95-000286; NREL/TP-440-7224; CONF-941210-2) Avail: CASI HC A03/MF A01

Wind technology has developed rapidly over the last decade with the design and development of advanced systems with improved performance, higher reliability, and lower costs. During the past several years, substantial gains have been made in wind turbine designs, lowering costs to an average of $0.05/kWh while further technology development is expected to allow the cost to drop below $0.04/kWh by 2000. As a result, wind is expected to be one of the least expensive forms of new electric generation in the next century. This paper will present the technology developments

for both utility-scale wind turbines and remote, small-village wind turbines that are currently available or in development. Technology innovations are being adapted for remote and stand-alone power applications with smaller wind turbines. Hybrid power systems using smaller 1 to 50 (kW) wind turbines are being developed for non-grid-connected electrical generation applications. These village power systems typically use wind energy, photovoltaics, battery storage, and conventional diesel generators to power remote communities. Smaller turbines are being explored for application as distributed generation sources on utility grids to supply power during periods of peak demand, avoiding costly upgrades in distribution equipment. New turbine designs now account for turbulence-induced loads, unsteady aerodynamic stall effects, and complex fatigue loads, making use of new technology developments such as advanced airfoils. The new airfoils increase the energy capture, improve the operating efficiency, and reduce the sensitivity of the airfoils to operation roughness. Electronic controls are allowing variable rotor speed operation; while aerodynamic control devices, such as ailerons and flaps, are used to modulate power or stop the rotor in high-speed conditions. These technology trends and future turbine configurations are being sponsored and explored by the U.S. Department of Energy's Wind Energy Program. DOE

N95-26166# Sandia National Labs., Albuquerque, NM. Photovoltaic System Components Dept.

THE EFFECT OF ENCAPSULATION ON THE REFLECTANCE OF PHOTOVOLTAIC MODULES USING TEXTURED MULTICRYSTALLINE-SILICON SOLAR CELLS

James M. Gee, W. Kent Schubert, Herbert L. Tardy, Thomas D. Hund, and Gary Robison (Semiconductor Assembly Network, Prescott Valley, AZ.) 1995 4 p Presented at the 1st World Conference on Photovoltaic Energy Conversion, Waikoloa, HI, 5-9 Dec. 1994

(Contract DE-AC04-94AL-85000)

(DE95-004781; SAND-94-1571C; CONF-941203-15) Avail: CASI HC A01/MF A01

Texturing multicrystalline-silicon cells is a promising technique for reducing reflectance losses. We investigated two methods for texturing multicrystalline-silicon solar cells - anisotropic chemical etch and mechanical dicing saw. Our work emphasized reducing reflectance in the encapsulated module by using optical confinement in the module. We found that optical confinement in the module is very important in the optimization of texture geometries. DOE

N95-26171# Morgantown Technology Center, WV.

INTERMEDIATE-SIZED NATURAL GAS FUELED CARBONATE FUEL CELL POWER PLANTS

Frederick A. Sudhoff and Donald K. Fleming 1 Apr. 1994 4 p Prepared in cooperation with M-C Power Corp., Bur r Ridge, IL

(DE95-004990; DOE/METC-95-7169) Avail: CASI HC A01/MF A01

This executive summary of the report describes the accomplishments of the joint US Department of Energy's (DOE) Morgantown Energy Technology Center (METC) and M-C POWER Corporation's Cooperative Research and Development Agreement (CRADA) No. 93-013. This study addresses the intermediate power plant size between 2 megawatt (MW) and 200 MW. A 25 MW natural-gas, fueled-carbonate fuel cell power plant was chosen for this purpose. In keeping with recent designs, the fuel cell will operate under approximately three atmospheres of pressure. An expander/alternator is utilized to expand exhaust gas to atmospheric conditions and generate additional power. A steam-bottoming cycle is not included in this study because it is not believed to be cost effective for this system size. This study also addresses the simplicity and accuracy of a spreadsheet-based simulation with that of a full Advanced System for Process Engineering (ASPEN) simulation. The personal computer can fully utilize the simple spreadsheet model simulation. This model can be made available to all users and is particularly advantageous to the small business user. DOE

N95-26285# National Renewable Energy Lab., Golden, CO.

TECHNICAL EVALUATION OF A DUAL-JUNCTION SAME-BAND-GAP AMORPHOUS SILICON PHOTOVOLTAIC SYSTEM AT NREL

Troy Strand, Laxmi Mrig, Robert Hansen, and Keith Emery Dec. 1994 6 p Presented at the 1st World Conference on Photovoltaic Energy Conversion, Waikoloa, HI, 5-9 Dec. 1994

(Contract DE-AC36-83CH-10093)

(DE95-000277; NREL/TP-411-7402; CONF-941203-17) Avail: CASI HC A02/MF A01

On December 7, 1992, a 1.8-kW(sub ac) utility-interconnect photovoltaic (PV) system using amorphous silicon modules was brought on-line at the National Renewable Energy Laboratory's photovoltaic test site. This system was deployed to conduct an in-situ technical evaluation of the PV array (in a high voltage configuration) and system performance and reliability in a utility-interconnect application. The system is unique due to the installation of construction-grade insulation on the back of each PV module. This use of insulation is an attempt to levelize the annual array power output by elevating the operating temperature of the modules. This paper presents array and system performance data. Emphasis is placed on quantifying the effects of individual losses as well as seasonal changes on PV array and system performance. DOE

45 ENVIRONMENT POLLUTION

Includes atmospheric, noise, thermal, and water pollution.

N95-24274*# National Aeronautics and Space Administration, Washington, DC.

THE ATMOSPHERIC EFFECTS OF STRATOSPHERIC AIRCRAFT: A FOURTH PROGRAM REPORT

Richard S. Stolarski, ed. (National Aeronautics and Space Administration. Goddard Space Flight Center, Greenbelt, MD.), Howard L. Wesoky, ed., Steven C. Wofsy (Harvard Univ., Cambridge, MA.), A. R. Ravishankara (National Oceanic and Atmospheric Administration, Boulder, CO.), Jose M. Rodriguez (Atmospheric and Environmental Research, Inc., Cambridge, MA.), and William L. Grose (National Aeronautics and Space Administration. Langley Research Center, Hampton, VA.) Jan. 1995 234 p

(NASA-RP-1359; NAS 1.61:1359) Avail: CASI HC A11/MF A03

This document presents the fourth report from the Atmospheric Effects of Stratospheric Aircraft (AESA) component of NASA's High-Speed Research Program (HSRP). Market and technology considerations continue to provide an impetus for high-speed civil transport research. A recent AESA interim assessment report and a review of that report have shown that considerable uncertainty still exists about the possible impact of aircraft on the atmosphere. The AESA has been designed to develop the body of scientific knowledge necessary for the evaluation of the impact of stratospheric aircraft on the atmosphere. The first Program report presented the basic objectives and plans for AESA. This fourth report comes after the interim assessment and sets forth directions for the 1995 assessment at the end of AESA Phase 1. It also sets forth the goals and directions for AESA Phase 2, as reported at the 1994 Atmospheric Effects of Aviation Project (AEAP) annual meeting held in June. The focus of the Phase 2 effort is to obtain the best possible closure on the outstanding problems identified in the interim assessment and NASA/NRC review. Topics discussed in this report include how high-speed civil transports (HSCT) might affect stratospheric ozone, emissions scenarios and databases to assess potential atmospheric effects from HSCT's, calculated results from 2-D zonal mean models using emissions data, engine trace constituent measurements. Author

N95-24291# Mitsubishi Research Inst., Inc., Tokyo (Japan).

PREPARATORY RESEARCH FOR GLOBAL WARMING PRECAUTION SPREAD PROMOTION MANUAL AND EARLY SPREAD PLAN RESEARCH WORK Photovoltaic Power Generation Spread Plan Research Report

Mar. 1994 79 p

(DE95-730143; ETDE/JP-mf-95730143) Avail: CASI HC A05/MF A01

This is the report on the planning research in spread and promotion of solar cell generation (SCG) prepared by Japan Environmental Agency. The main subject that is detailed in the report includes the necessity and evaluation of effects of the SCG as a potential effective means against global warming, and the scenario of policy for multiplex spread of the system over a wide area. For references, the effects of the SCG system on CO2 reduction and other description in 20 items with different data are annexed to the report. For necessity, the process of the SCG system up to date in Japan is described, but no policy is given on high costs that is adversely affecting the spread of the system. The secondary effect on

cost reduction is expected to be enabled by increasing the ODA fund for developing countries. In other countries, such as the U.S.A., Germany, and Austria, the quick spread plan is being realized. For evaluation, three cases of demand forms are assumed to attempt to draw a future system and estimate the gradually increasing subsidy. The pattern of policy scenario was separately planned for up to 2000 and after 2000 and examination was conducted for each pattern. Both are based on the national consensus. DOE

N95-24294# Gas Research Inst., Chicago, IL.
RETROFIT NOx CONTROL TECHNOLOGIES FOR NATURAL GAS PRIME MOVERS Final Report, Sep. 1991 - Jul. 1992
S. Huey and C. Castaldini Mar. 1994 200 p Sponsored by Gas Research Inst.
(Contract GRI-5091-254-2209)
(PB95-149290; GRI-94/0329) Avail: CASI HC A09/MF A03

The subject of the report is to provide guidance on and estimates of the retrofit potential for the existing uncontrolled prime mover population. For existing natural gas prime movers, the report reviews the technical status of potential retrofit NOx control technologies, established which control technologies are feasible now and in the near term, and estimates reasonable NOx reduction goals. In addition to control performance and commercialization status, the review of control technologies includes discussions on energy, environmental, operational, and economic impacts based on retrofit experience on pipeline and other prime mover applications. NTIS

N95-24319# National Renewable Energy Lab., Golden, CO.
OVERVIEW OF SOLAR DETOXIFICATION ACTIVITIES IN THE UNITED STATES
M. Mehos, T. Williams, and C. Turchi Oct. 1994 7 p
(Contract DE-AC36-83CH-10093)
(DE95-000264; NREL/TP-471-7262) Avail: CASI HC A02/MF A01

The U.S. Department of Energy, through the National Renewable Energy Laboratory (NREL) and Sandia National Laboratories, has been investigating a process that uses solar energy to destroy hazardous wastes in air and water. The process, photocatalytic oxidation, uses ultraviolet light in conjunction with the semiconductor titanium dioxide to generate highly reactive hydroxyl radicals. Early research and development activities have demonstrated that photocatalysis may be cost effective for some applications. The Department of Energy is currently working to establish a commercial industry that uses solar energy to destroy hazardous wastes in air, water, and soil. To achieve this objective, NREL and Sandia are bringing together environmental firms, solar manufacturers, and organizations that have waste or remediation problems. DOE

N95-24334 Umweltbundesamt, Berlin (Germany).
RESPONSIBILITY MEANS DOING WITHOUT: HOW TO RESCUE THE OZONE-LAYER
1994 60 p Limited Reproducibility: More than 20% of this document may be affected by microfiche quality
(PB95-166807) Avail: CASI HC A04

The report summarizes the current state of knowledge and indicates what technical measures can be taken to reduce the use of ozone-depleting substances-which include the halons and some chlorinated hydrocarbons in addition to the CFCs--in all sectors. The necessary legal measures and supporting economic options for the Federal Republic of Germany are also indicated. NTIS

N95-24406# University of Western Kentucky, Bowling Green, KY.
CO-FIRING HIGH SULFUR COAL WITH REFUSE DERIVED FUELS Technical Progress Report No. 1
Wei-Ping Pan, J. T. Riley, and W. G. Lloyd 30 Nov. 1994 13 p
(Contract DE-FG22-94PC-94211)
(DE95-006243; DOE/PC-94211/T1) Avail: CASI HC A03/MF A01

This project is being coordinated with an ongoing project at Western Kentucky University that is being supported by the Southeastern Regional Biomass Energy Program through the Tennessee Valley Authority. Fluidized bed combustion tests will be performed on municipal solid waste blended with high-sulfur and high-chlorine coals in a laboratory scale combustor. The purpose of the tests is to evaluate combustion performance, the extent of the inorganic acid gases (HCl and SO(x)) and chlorinated organic compound formation, the effect of chlorine species on SO2 removal with a sorbent, and the effect of sulfur species on the formation of chlorinated organic compounds from MSW for a range of bed temperatures, excess air levels, municipal solid waste (MSW)/coal ratios, and S/Cl ratios. Flue gas samples will be collected and analyzed at three locations: free board, cyclone inlet, and cyclone outlet. Analytical methods used will include ion chromatography, gas chromatography, and mass spectrometry. Waste stream ash samples will be collected from the cyclone catch and analyzed for unburned carbon, chlorine, chlorinated benzenes, polychlorinated biphenyls, chlorinated phenols, dioxins, furans, and metal content. Major, minor, and trace elements in the ash will be determined by x-ray fluorescence and inductively coupled plasma-atomic emission spectroscopy. Accomplishments for the first quarter are presented. DOE

N95-24499# Korea Inst. of Energy and Resources, Taejon, Chungchongnam (Republic of Korea).
INVESTIGATION OF TECHNOLOGIES FOR CO2 SEPARATION, FIXATION AND DISPOSAL FOR THE PREVENTION OF GLOBAL WARMING
Y. M. Son, J. M. Auh, J. E. Son, K. S. Sim, S. H. Kim, J. W. Kim, B. M. Min, S. C. Park, and T. K. Lee Dec. 1993 164 p In ENGLISH and KOREAN
(DE95-744285; KE-93006B) Avail: CASI HC A08/MF A02 (US Sales Only)

Scientific assessments of global warming, which were discussed at various international forums, conferences and meetings, were introduced in this work. Also, various technologies of carbon dioxide treatment were investigated in order to study technical options for the prevention of global warming related on energy consumption. DOE

N95-24501*# Geo Eco Arc Research, La Canada, CA.
BIOSPHERIC EFFECTS OF A LARGE EXTRATERRESTRIAL IMPACT: CASE STUDY OF THE CRETACEOUS/TERTIARY BOUNDARY CRATER Annual Progress Report, 14 May 1994 - 13 May 1995
Kevin O. Pope 18 Mar. 1995 29 p
(Contract NASw-4812)
(NASA-CR-198015; NAS 1.26:198015) Avail: CASI HC A03/MF A01

The Chicxulub impact crater, buried in the Yucatan carbonate platform in Mexico, is the site of the impact purported to have caused mass extinctions at the Cretaceous/Tertiary (K/T) boundary. A recently discovered Chicxulub ejecta deposit in Belize contains evidence of carbonate vaporization and precipitation from the vapor plume. Sulfate clasts are almost absent in the Belize ejecta, but are abundant in the coarse ejecta near the crater rim, hwich may reflect the greater abundance of sulfates deep in the target section. The absence of sulfate precipitates in Belize may indicate that most of the vaporized sulfur was deposited in the upper atmosphere. Hydrocode modeling of the impact indicates that between 0.4 to 7.0 x 10(exp 17) g of sulfur were vaporized by the impact in sulfates. Laser experiments indicate that SO2, SO3, and SO4 are produced, and that complex chemical reactions between plume constituents occur during condensation. The sulfur released as SO3 or SO4 converted rapidly into H2HO4 aerosol. A radiative transfer model coupled with a model of coagulation predicts that the aerosol prolonged the initial blackout period caused by impact dust only if it contained impurities. The sulfur released as SO2 converted to aerosol slowly due to the rate limiting oxidation of SO2. Radiative transfer calculations combined with rates of acid production, coagulation, and diffusion indicate that solar transmission was reduced to 10-20 percent of normal for a period of 8-13 years. This reduction produced a climate forcing (cooling) of -300 Wm(exp -2), which far exceeded the +8 Wm(exp -2) greenhouse warming caused by the CO2 released through the vaporization of carbonates, and therefore produced a decade of freezing and near-freezing temperatures. Several decades of moderate warming followed the decade of severe cooling due to the long residence time of CO2. The prolonged impact winter may have been a major cause of the K/T extinctions. Derived from text

N95-24570# Brookhaven National Lab., Upton, NY.
MICROPHYSICAL AND COMPOSITIONAL INFLUENCES ON SHORTWAVE RADIATIVE FORCING OF CLIMATE BY SULFATE AEROSOLS
S. E. Schwartz, R. Wagener, and S. Nemesure 1995 6 p Presented at the 209th American Chemical Society National Meeting, Anaheim, CA,

2-7 Apr. 1995
(Contract DE-AC02-76CH-00016)
(DE95-005999; BNL-61230; CONF-950402-3) Avail: CASI HC A02/MF A01

Anthropogenic sulfate aerosols scatter shortwave (solar) radiation incident upon the atmosphere, thereby exerting a cooling influence on climate relative to pre-industrial times. Previous estimates of this forcing place its global and annual average value at about -1 W/sq M, uncertain to a factor of somewhat more than 2, comparable in magnitude to greenhouse gas forcing over the same period but opposite in sign and much more uncertain. Key sources of uncertainty are atmospheric chemistry factors (yield, residence time), and microphysical factors (scattering efficiency, upscatter fraction, and the dependence of these quantities on particle size and relative humidity, RH). This paper examines these microphysical influences to indentify properties required to obtain a more accurate description of this forcing. The mass scattering efficiency exhibits a maximum at a particle diameter approximately 0.5 micrometers roughly equal to the wavelength of maximum power in the solar spectrum and roughly equal to diameter typical of anthropogenic sulfate aerosols. Particle size, and hence mass scattering efficiency, increase with increasing on RH because of accretion of water by deliquescent salt aerosols. DOE

N95-24604 National Renewable Energy Lab., Golden, CO.
DIESEL FUEL COMPONENT CONTRIBUTION TO ENGINE EMISSIONS AND PERFORMANCE Final Report
Jimell Erwin, Thomas W. Ryan, III, and David S. Moulton (Southwest Research Inst., San Antonio, TX.) Nov. 1994 143 p Limited Reproducibility: More than 20% of this document may be affected by microfiche quality
(Contract DE-AC36-83CH-10093)
(DE95-000238; NREL/TP-425-6354) Avail: CASI HC A07

Contemporary diesel fuel is a blend of several refinery streams chosen to meet specifications. The need to increase yield of transportation fuel from crude oil has resulted in converting increased proportions of residual oil to lighter products. This conversion is accomplished by thermal, catalytic, and hydrocracking of high molecular weight materials rich in aromatic compounds. The current efforts to reformulate California diesel fuel for reduced emissions from existing engines is an example of another driving force affecting refining practice: regulations designed to reduce exhaust emissions. Although derived from petroleum crude oil, reformulated diesel fuel is an alternative to current specification-grade diesel fuel, and this alternative presents opportunities and questions to be resolved by fuel and engine research. Various concerned parties have argued that regulations for fuel reformulation have not been based on an adequate data base. Despite numerous studies, much ambiguity remains about the relationship of exhaust parameters to fuel composition, particularly for diesel fuel. In an effort to gather pertinent data, the automobile industry and the oil refiners have joined forces in the Air Quality Improvement Research Program (AUTO/OIL) to address this question for gasoline. The objective of that work is to define the relationship between gasoline composition and the magnitude and composition of the exhaust emissions. The results of the AUTO/OEL program will also be used, along with other data bases, to define the EPA 'complex model' for reformulated gasolines. Valuable insights have been gained for compression ignition engines in the Coordinating Research Council's VE-1 program, but no program similar to AUTO/OIL has been started for diesel fuel reformulation. A more detailed understanding of the fuel/performance relationship is a readily apparent need. DOE

N95-24606# Lovelace Biomedical and Environmental Research Inst., Albuquerque, NM. Inhalation Toxicology Research Inst.
EVALUATION OF THE PERFORMANCE OF AN ANNULAR DIFFUSION DENUDER
B. J. Fan, Y. S. Cheng, and Hsu-Chi Yeh 1994 12 p Presented at the Conferencce on Obscuration and Aerosol Research, Aberdeen, MD, 2-5 Jun. 1994
(Contract DE-AC04-76EV-01013)
(DE95-002258; CONF-9406275-1) Avail: CASI HC A03/MF A01

In air sampling, an annular diffusion denuder (ADD) is often used to trap specific gases from an air sample stream. The efficiency of an ADD in collecting a gas was considered in this study. A dimensional analysis showed that the collection efficiency depended on two parameters: the Peclet number and the annulus radii ratio. To determine collection efficiency, we calculated the fractional loss of the gas inside the denuder. In the calculation, the governing equations for gas concentration and flow field inside the annulus were solved numerically. After validating the methodology, a parametric calculation of the collection efficiency was made, and a one-equation model based on the calculation was developed. A comparison of the model and experimental data showed a variance coefficient of 3.26%. This confirmed that the performance of an annular denuder could be evaluated by this model. DOE

N95-24618# Argonne National Lab., IL.
METHODS OF VALUING AIR POLLUTION AND ESTIMATED MONETARY VALUES OF AIR POLLUTANTS IN VARIOUS US REGIONS
M. Q. Wang, D. J. Santini, and S. A. Warinner Dec. 1994 92 p
(Contract W-31-109-eng-38)
(DE95-006854; ANL/ESD-26) Avail: CASI HC A05/MF A01

Air pollutant emission values are used to determine the social costs of various technologies that cause air pollution and to estimate the benefits of emission control technologies. In this report, the authors present two methods of estimating air pollutant emission values--the damage value method and the control cost method--and review 15 recent studies in which these methods were employed to estimate emission values. The reviewed studies derived emission values for only a limited number of areas; emission value estimates are needed for other US regions. Using the emission values estimated in the reviewed studies, they establish regression relationships between emission values, air pollutant concentrations, and total population exposed, and apply the established relationships to 17 US metropolitan areas to estimate damage-based and control-cost-based emission values for reactive organic gases, nitrogen oxides, particulate matter measuring less than 10 microns, sulfur oxides, and carbon monoxide in these areas. Their estimates show significant variations in emission values across the 17 regions. DOE

N95-24653# Pacific Northwest Lab., Richland, WA.
SUPERCRITICAL CARBON DIOXIDE CLEANING MARKET ASSESSMENT AND COMMERCIALIZATION/DEPLOYMENT PLAN
L. J. Snowden-Swan Aug. 1994 24 p
(Contract DE-AC06-76RL-01830)
(DE94-017394; PNL-10044) Avail: CASI HC A03/MF A01

Through the US Department of Energy's Industrial Waste Program (IWP), work is being conducted to research, develop, and commercialize supercritical fluid cleaning for its potential as a safer technology in a wide range of industrial cleaning operations. Commercialization, which has not proceeded as quickly as expected, is being aided by the Joint Association for the Advancement of Supercritical Technology (JAAST), a research consortium made up of industry, university, and National Laboratory partners. Under the IWP, JAAST is facilitating interaction and communication among those involved in the technology and addressing specific issues slowing its growth and acceptance. As part of the IWP/JAAST effort, Pacific Northwest Laboratory conducted a study to: (1) identify and evaluate potential markets for supercritical fluids cleaning; (2) identify and address current perceptions that inhibit the acceptance of the technology into industrial cleaning operations; and (3) develop a plan that will lead to successful deployment and implementation in potential market areas. The approach to gathering the information needed for formulating the plan was to interview several individuals involved in developing, using, or commercializing the technology, specifically, supercritical carbon dioxide (SCCO2), the most commonly used fluid. Several potential markets were identified, including cleaning gyroscope and filling hardware; optical components; instrument bearings; computer disk drive components; medical devices; and fabrics, cloths, and rags. In cases where there are parts with intricate geometries, where water-based cleaning may corrode parts and materials, or where significant time and energy for drying is required, SCCO2 may be an especially attractive alternative. While pursuing these applications, certain barriers still need to be overcome. DOE

N95-24846*# Colorado Univ., Boulder, CO. Div. of Cryospheric and Polar Processes.
ASSESSMENT OF CLIMATE VARIABILITY OF THE GREENLAND ICE SHEET: INTEGRATION OF IN SITU AND SATELLITE DATA Annual Progress Report
K. Steffen, W. Abdalati, J. Stroeve, M. Stober, A. Nolin, and J. Key Apr. 1995 41 p Original contains color illustrations

(Grant NAGw-2158)
(NASA-CR-198020; NAS 1.26:198020) Avail: CASI HC A03/MF A01; 2 functional color pages

The proposed research involves the application of multispectral satellite data in combination with ground truth measurements to monitor surface properties of the Greenland ice sheet which are essential for describing the energy and mass of the ice sheet. Several key components of the energy balance are parameterized using satellite data and in situ measurements. The analysis will be done for a ten year time period in order to get statistics on the seasonal and interannual variations of the surface processes and the climatology. Our goal is to investigate to what accuracy and over what geographic areas large scale snow properties and radiative fluxes can be derived based upon a combination of available remote sensing and meterological data sets. Data analysis showed the following results: (1)cloud classification based on longwave sky radiation revealed that overcast sky occurred for 25% of the time in winter, and for 15% in spring and summer respectively (winter and summer both show the same occurrence of clear sky of approximately 26%); (2) comparison of aerodynamic profile method with eddy correlation method to derive sensible and latent heat flux showed good agreement in the diurnal cycle and the turbulent fluxes were underestimated with the aerodynamic method by 10 - 30% as compared to the in situ eddy flux method; (3) the katabatic wind shows a distinct diurnal cycle with a maximum in the morning (7-9 h solar time) and a minimum in the later afternoon (18 h solar time); (4) snow grain size was modeled with a surface energy balance model (SNTHERM) and compared with in situ measurements. Sharp decreases in the modeled snow grain size, caused by accumulation events such as precipitation and deposition, could be verified with observational data; (4) radiative transfer modeling of firn supports our beliefs that the observed trends in 18 and 19 GHz passive microwave brightness temperatures are attributable to accumulation rate changes (modeling also indicates the above relationship is detectable because of the presence of depth hoar; (5) snow melt can be detected by a distinct signal in the passive microwave cross-polarized gradient ratio (19h-37v)/(19h+37v) and has been used for wet/dry snow classification; (6) top of the atmosphere (TOA) broadband albedos were derived from AVHRR visible and near infrared reflectances for the entire ice sheet from May 1990 - June 1991, and the highest albedo values are found along the southeast coast of the ice sheet which is consistent with the summer peak of precipitation due to onshore flow loaded with high water vapor content (TOA albedo values dropped to around 40% along the south-western coast during July and August due to bare ice surfaces); and (7) the net all-wave radiation balance at the top of the atmosphere is negative over the entire ice sheet except for the summer months - June-July-August (in June, the net radiation balance is slightly positive over the dry snow areas--15 W/m2). Author

N95-24904# Finnish Association for Aerosol Research, Espoo (Finland).
REPORT SERIES IN AEROSOL SCIENCE
K. Haemeri, ed., P. Mikkanen, ed., and E. Kauppinen, ed. 1993 292 p Presented at the 5th Finnish National Aerosol Symposium, Espoo, Finland, 1-3 Jun. 1993 Prepared in cooperation with Technical Research Centre of Finland, Espoo, Finland
(DE95-737628; FAAR-23/1993; CONF-9306401) Avail: CASI HC A13/MF A03

The Fifth Finnish Aerosol Symposium was held June 1-3, 1993. The Symposium is jointly organized by FAAR (Finnish Association for Aerosol Research), Aerosol Technology Group of Technical Research Center of Finland and Helsinki University, Department of Physics. Aerosols, the suspensions of solid and liquid particles and gases, are receiving increasing importance in many areas of science and technology. These include industrial hygiene, ambient and indoor air pollution, pollution control technologies, cloud physics, nuclear safety engineering, combustion science and engineering, clean manufacturing technologies and material processing. The importance of aerosol issues during the development of advanced fuel conversion and material processing technologies can be realized when looking at the numerous papers presented on these topics at the Symposium. DOE

N95-25198# Los Alamos National Lab., NM.
PARALLEL PROCESSING OF ATMOSPHERIC CHEMISTRY CALCULATIONS: PRELIMINARY CONSIDERATIONS
S. Elliott and P. Jones Jan. 1995 29 p
(Contract W-7405-eng-36)
(DE95-005915; LA-12814-MS) Avail: CASI HC A03/MF A01

Global climate calculations are already saturating the class modern vector supercomputers with only a few central processing units. Increased resolution and inclusion of routines to deal with biogeochemical portions of the terrestrial climate system will soon demand massively parallel approaches. The atmospheric photochemistry ensemble is intimately linked to climate through the trace greenhouse gases ozone and methane and modules for representing it are being attached to global three dimensional transport and general circulation model (GCM) frameworks. Atmospheric kinetics involve dozen of highly interactive tracers and so will accentuate the need for parallel processing of earth system simulations. In the present text we lay some of the groundwork for addition of atmospheric kinetics packages to GCM and global scale atmospheric models on multiply parallel computers. The discussion is tailored for consumption by the photochemical modelling community. After a review of numerical atmospheric chemistry methods, we examine how kinetics can be implemented on a parallel computer. We concentrate especially on data layout and flexibility and how these can be implemented in various programming models. We conclude that chemistry can be implemented rather easily within existing frameworks of several parallel atmospheric models. However, memory limitations may preclude high resolution studies of global chemistry. DOE

N95-25199 Commonwealth Scientific and Industrial Research Organization, Mordialoc (Australia). Div. of Atmospheric Research.
FUTURE EMISSIONS AND CONCENTRATIONS OF CARBON DIOXIDE: KEY OCEAN/ATMOSPHERE/LAND ANALYSES
I. G. Enting, ed., T. M. L. Wigley, ed. (University Corp. for Atmospheric Research, Boulder, CO.), and M. Heimann, ed. (Max-Planck-Inst. fuer Meteorologie, Hamburg, Germany.) 1994 123 p
(CSIRO-TP-31; ISBN-0-643-05256-9) Copyright Avail: Issuing Activity (Commonwealth Scientific and Industrial Research Organization, Mordialloc, Australia)

Various projections of the relation between future CO2 concentrations and future emissions were undertaken as part of the scientific assessment for working group 1 of the intergovernmental panel on climate change. There were three types of calculation: (1) forward projections, calculating the atmospheric CO2 concentrations resulting from specified emission scenarios, (2) inverse calculations determining the emission rates that would be required to achieve stabilization of CO2 concentrations via specified pathways and (3) impulse response function calculations required for determining global warming potentials. The use of a standardized set of conditions allows an intercomparison of models. Sensitivity studies explore other aspects of the uncertainties of such projections. This report documents the specifications, the models that were used and the results that were obtained. Some preliminary interpretations of the results are included. Author

N95-25249# Pacific Northwest Lab., Richland, WA.
USE OF MASS SPECTROMETRIC METHODS FOR FIELD SCREENING OF VOC'S
John C. Evans Nov. 1994 27 p Presented at the Air and Waste Management Association Annual Conference, Eugene, OR, 16-18 Nov. 1994
(Contract DE-AC06-76RL-01830)
(DE95-004903; PNL-SA-25362; CONF-9411180-1) Avail: CASI HC A03/MF A01

While mass spectrometric (MS) methods of chemical analysis, particularly gas chromatography-mass spectrometry (GC/MS), have been the mainstay of environmental organic analytical techniques in the laboratory through the use of EPA and other standard methods, field implementation is relatively rare. Instrumentation and methods now exist for utilizing MS and GC/MS techniques in the field for analysis of VOC's in gas phase, aqueous, and soil media. Examples of field investigations utilizing HP 5971A and Viking SpectraTrak systems for analysis of VOC's in all three media will be presented. Mass spectral methods were found to offer significant advantages in terms of speed of analysis and reliability of compound identification over field gas chromatography (GC) methods while preserving adequate levels of detection sensitivity. The soil method in particular provides a method for rapid in-field analysis of methanol preserved samples thus

minimizing the problem of volatiles loss which typically occurs with routine use of the EPA methods and remote analysis. The high cost of MS instrumentation remains a major obstacle to more widespread use. DOE

N95-25278# Westinghouse Savannah River Co., Aiken, SC.
INTEGRATION OF HETEROGENEOUS DATA BASES FOR DEVELOPMENT OF A LARGE-SCALE ENVIRONMENTAL DATA ATLAS FOR MULTI-PLATFORM PC AND WORKSTATION USERS
P. J. Bresnaham (South Carolina Univ., Columbia, SC.), D. J. Cowen (South Carolina Univ., Columbia, SC.), J. R. Jensen (South Carolina Univ., Columbia, SC.), G. B. Ehler (South Carolina Univ., Columbia, SC.), and H. E. Mackey, Jr. 1994 14 p Presented at the 1994 Geographic Information Systems/Land Information Systems (GIS/LIS), Phoenix, AZ, 25-27 Oct. 1994
(Contract DE-AC09-89SR-18035)
(DE95-002689; WSRC-MS-94-0418; CONF-9410237-2) Avail: CASI HC A03/MF A01

Environmental monitoring and restoration at the Department of Energy's Savannah River Site (SRS) requires efficient access to large amounts of diverse spatial data. In order to handle this task the Environmental Sciences Section (ESS) of the Westinghouse Savannah River Company (WSRC) created an environmental data atlas that would use spatial keys to link all data sources to a common data base. These data include extensive information relating to both environmental and man-made features. The data were available in a multitude of different data structures, coordinate systems and formats. The final database also included multimedia information such as airborne multispectral scanner data, aircraft video, photography, bibliographic data, and scanned map bases. It was important that all of the data be readily accessible on the desktop of scientists regardless of the type of computer system they used. The purpose of this paper is to describe the creation of this extensive digital environmental data atlas. DOE

N95-25279# Lawrence Livermore National Lab., Livermore, CA.
GLOBAL OCEAN CIRCULATION AND EQUATOR-POLE HEAT TRANSPORT AS A FUNCTION OF OCEAN GCM RESOLUTION
C. Covey Jun. 1994 33 p
(Contract W-7405-eng-48)
(DE95-004198; UCRL-ID-117401) Avail: CASI HC A03/MF A01

To determine whether resolution of smaller scales is necessary to simulate large-scale ocean climate correctly, I examine results from a global ocean GCM run with horizontal grid spacings spanning a range from coarse resolutions traditionally used in climate modeling to nearly the highest resolution attained with today's computers. The experiments include four cases employing 4 degrees, 2 degrees, 1 degrees and 1/2 degrees spacing in latitude and longitude, which were run with minimal differences among them, i.e., in a controlled experiment. Two additional cases -- 1/2 degree spacing with a more scale-selective sub-gridscale mixing of heat and momentum, and approximate 1/4 degree spacing -- are also included. The 1/4 degree run resolves most of the observed mesoscale eddy energy in the ocean. Several artificial constraints on the model tend to minimize differences among the different resolution cases. Nevertheless, for quantities of interest to global climate studies,the simulations show significant changes as resolution increases. DOE

N95-25361# Department of Energy, Washington, DC.
VOLUNTARY REPORTING OF GREENHOUSE GASES UNDER SECTION 1605(b) OF THE ENERGY POLICY ACT OF 1992: GENERAL GUIDELINES
Oct. 1994 27 p
(DE95-003295; DOE/PO-0028-Vol-1) Avail: CASI HC A03/MF A01

Because of concerns with the growing threat of global climate change from increasing emissions of greenhouse gases, Congress authorized a voluntary program for the public to report achievements in reducing those gases. This document offers guidance on recording historic and current greenhouse gas emissions, emissions reductions, and carbon sequestration. Under the Energy Policy Act (EPAct) reporters will have the opportunity to highlight specific achievements. If you have taken actions to lessen the greenhouse gas effect, either by decreasing greenhouse gas emissions or by sequestering carbon, the Department of Energy (DOE) encourages you to report your achievements under this program. The program has two related, but distinct parts. First, the program offers you an opportunity to report your annual emissions of greenhouse gases. Second, the program records your specific projects to reduce greenhouse gas emissions and increase carbon sequestration. Although participants in the program are strongly encouraged to submit reports on both, reports on either annual emissions or emissions reductions and carbon sequestration projects will be accepted. These guidelines and the supporting technical documents outline the rationale for the program and approaches to analyzing emissions and emissions reduction projects. Your annual emissions and emissions reductions achievements will be reported. DOE

N95-25362# Department of Energy, Washington, DC.
SECTOR-SPECIFIC ISSUES AND REPORTING METHODOLOGIES SUPPORTING THE GENERAL GUIDELINES FOR THE VOLUNTARY REPORTING OF GREENHOUSE GASES UNDER SECTION 1605(B) OF THE ENERGY POLICY ACT OF 1992, VOLUME 1. PART 1: ELECTRICITY SUPPLY SECTOR. PART 2: RESIDENTIAL AND COMMERCIAL BUILDINGS SECTOR. PART 3: INDUSTRIAL SECTOR
Oct. 1994 239 p
(DE95-003296; DOE/PO-0028-Vol-1) Avail: CASI HC A11/MF A03

DOE encourages you to report your achievements in reducing greenhouse gas emissions and sequestering carbon under this program. Global climate change is increasingly being recognized as a threat that individuals and organizations can take action against. If you are among those taking action, reporting your projects may lead to recognition for you, motivation for others, and synergistic learning for the global community. This report discusses the reporting process for the voluntary detailed guidance in the sectoral supporting documents for electricity supply, residential and commercial buildings, industry, transportation, forestry, and agriculture. You may have reportable projects in several sectors; you may report them separately or capture and report the total effects on an entity-wide report. DOE

N95-25363# Argonne National Lab., IL.
CHELANT EXTRACTION AND REDOX MANIPULATION FOR MOBILIZATION OF HEAVY METALS FROM CONTAMINATED SOILS
Michael D. Brewster, Robert W. Peters, Gregory A. Miller, Terry L. Patton, and Louis E. Martino 1994 12 p Presented at the IGT Symposium on Gas, Oil, and Environmental Biotechnology, Colorado Springs, CO, 12-14 Dec. 1994
(Contract W-31-109-eng-38)
(DE95-004131; ANL/ES/CP-84872; CONF-941245-1) Avail: CASI HC A03/MF A01

As the result of open burning and open detonation of chemical agents and munitions in the Toxic Burning Pits area at J-Field, located in the Edgewood Area of Aberdeen Proving Ground in Harford County, Maryland, soils have been contaminated with heavy metals. Simultaneous extraction is complicated because of the multitude of contaminant forms that exist. This paper uses data from a treatability study performed at Argonne National Laboratory to discuss and compare several treatment methods that were evaluated for remediating metals-contaminated soils. J-Field soils were subjected to a series of treatability experiments designed to determine the feasibility of using soil washing/soil flushing, enhancements to soil washing/soil flushing, solidification/stabilization, and electrokinetics for remediating soils contaminated with metals. Chelating and mobilizing agents evaluated included ammonium acetate, ethylenediaminetetraacetic acid, citric acid, Citranox, gluconic acid, phosphoric acid, oxalic acid, and nitrilotriacetic acid, in addition to pH-adjusted water. REDOX manipulation can maximize solubilities, increase desorption, and promote removal of heavy metal contaminants. Reducing agents that were studied included sodium borohydride, sodium metabisulfite, and thiourea dioxide. The oxidants studied included hydrogen peroxide, sodium percarbonate, sodium hypochlorite, and potassium permanganate. This paper summaries the results from the physical/chemical characterization, soil washing/soil flushing, and enhancements to soil washing/soil flushing portions of the study. DOE

N95-25380# Oak Ridge National Lab., TN.
RESOLVING THE AMBIGUITIES: AN INDUSTRIAL HYGIENE INDOOR AIR QUALITY (IAQ) SYMPOSIUM
R. B. Gammage 1995 6 p Presented at the International Workshop on Indoor Air: An Integrated Approach, Gold Coast, Australia, 27 Nov. - 1 Dec. 1994

(Contract DE-AC05-84OR-21400)
(DE95-005391; CONF-941139-1) Avail: CASI HC A02/MF A01

Resolving the Ambiguities: An Industrial Hygiene (IAQ) Symposium was a one-day event designed to inform practicing industrial hygienists about highlight presentations made at Indoor Air '93. A broad range of topics was presented by invited speakers. Topics included were attempts to deal with guidelines and standards, questionnaires, odors and sensory irritation, respiratory allergies, neuroses, sick building syndrome (SBS), and multiple chemical sensitivity (MCS). DOE

N95-25442# Brookhaven National Lab., Upton, NY.
THE WHITEHOUSE EFFECT: SHORTWAVE RADIATIVE FORCING OF CLIMATE BY ANTHROPOGENIC AEROSOLS
S. E. Schwartz 1994 8 p Presented at the Conference on Aerosols and Atmospheric Optics: Radiation Balance and Visual Air Quality, Snowbird, UT, 25-30 Sep. 1994
(Contract DE-AC02-76CH-00016)
(DE95-005998; BNL-61220; CONF-9409255-2) Avail: CASI HC A02/MF A01

Increases in atmospheric concentrations of carbon dioxide and other infrared active gases over the industrial period are thought to have increased the average flux of longwave (thermal infrared) radiation between the surface of the earth and the lower atmosphere, leading to an increase in global mean temperature. Over the same period it is though that concentrations of aerosol particles in the troposphere have similarly increased as a consequence of industrial emissions and that these increased concentrations of particles have increased the earth's reflectivity of shortwave (solar) radiation incident on the planet both directly, by scattering radiation, and indirectly, by increasing the reflectivity of clouds. The term 'whitehouse effect' is introduced to refer to this increased scattering of shortwave radiation by analogy to the term 'greenhouse effect,' which refers to the enhanced trapping of longwave radiation resulting from increased concentrations of infrared active gases. Each of these phenomena is referred to as a 'forcing' of the earth's climate, that is a secular change imposed on the system; such a forcing is to be distinguished from a 'response' of the system, such as a change in global mean temperature or other index of global climate. The forcing due to the direct and indirect effects induced by anthropogenic aerosols has been estimated to be comparable in global-average magnitude to that due to increased concentrations of greenhouse gases, but it is of opposite direction, that is exerting a cooling influence. The shortwave radiative influence of anthropogenic aerosols may thus be considered to be offsetting some, perhaps a great fraction, of the longwave radiative influence of anthropogenic greenhouse gases. DOE

N95-25500# Finnish Association for Aerosol Research, Espoo (Finland).
EFFECTS OF NITRIC ACID VAPOR ON THE FORMATION OF CLOUD DROPLETS IN TROPOSPHERE [KAASUMAISEN TYPPIHAPON VAIKUTUS PILVIPISAROIDEN MUODOSTUMISEEN TROPOSFAARISSA]
Pekka Korhonen 1993 103 p In FINNISH
(DE95-744869; FAAR-24/1993) Avail: CASI HC A06/MF A02

The effects of nitric acid vapor on the formation of cloud droplets in tropospheric conditions are studied. The concentration of nitric acid in the polluted areas can be hundred times to that in the background areas. The effects of the changing cloud droplets concentration on the shortwave radiative properties of the cloud are also briefly studied. The formation of the cloud droplets is studied with an air parcel model describing the formation of a convective cloud. The simultaneous condensation of water and nitric acid vapour on the soluble sodium nitrate (NaNO3) particles is included in the model. The formation of the cloud droplets is simulated with different initial aerosol particle distributions and initial nitric acid concentrations. The concentrations of aerosol particles and nitric acid are varied from measured background values to values measured in heavily polluted areas. The properties of the simulated cloud, such as liquid water content, supersaturation of water vapor, the vertical velocity of rising air parcel and the amount of nitrate ions in the droplets, are compared to measured values and they have been found to be quite realistic. According to the obtained results the increase of the concentration of nitric acid vapor from background values (0.1 ppbv) ease remarkably the formation of cloud droplets. This leads to the higher amount of smaller cloud droplets in the forming cloud. The rise of the amount of nitric acid from the used background value to the 1 ppbv increased the amount of the cloud droplets so that the albedo of the thin cloud layer (less than 1 km) was clearly increased and its absorbtivity was somewhat decreased. DOE

N95-25521# International Centre for Theoretical Physics, Trieste (Italy).
A PHASE-TRANSITION INDUCED BY THE STRUGGLE FOR LIFE IN A COMPETITIVE COEXISTENCE MODEL IN ECOLOGY
Horacio S. Wio and M. N. Kuperman (Comision Nacional de Energia Atomica, San Carlos de Bariloche, Argentina.) Jul. 1994 8 p Sponsored by CONICET
(DE95-607047; IC-94/195) Avail: CASI HC A02/MF A01 (US Sales Only)

We have studied a spatially homogeneous model of an ecological system consisting of two species: a strong and a weak one, competing for a single food resource. The inclusion of a term corresponding to intraspecies competition, in particular for the strong species, shows that, it a certain threshold value is overcome, the classical result on extinction and coexistence of Lotka-Volterra type equations can drastically change yielding a kind of phase-transition to a coexistence phase. DOE

N95-25531# International Centre for Theoretical Physics, Trieste (Italy).
QUANTUM MECHANICAL ANALOGY FOR SOLVING A COMPETITIVE COEXISTENCE MODEL IN ECOLOGY
Horacio S. Wio, Marcelo N. Kuperman (Comision Nacional de Energia Atomica, San Carlos de Bariloche, Argentina.), and Bernardo vonHaeften Jul. 1994 19 p Sponsored by CONICET
(DE95-607046; IC-94/186) Avail: CASI HC A03/MF A01 (US Sales Only)

We have studied an ecological system of three species: a strong and a weak one, competing for a single food resource, modelled as a reaction-diffusion process. An exact analytical solution has been found through a quantum mechanical analogy. Such solution indicates that in certain situations the classical results on extinction and coexistence of Lotka-Volterra type equations are no longer valid, essentially, as a consequence of the weak species mobility. A stability analysis of this solution against changes in different parameters has been carried out. DOE

N95-25575# Environmental Protection Agency, Ann Arbor, MI. Office of Mobile Sources.
DRAFT REGULATORY IMPACT ANALYSIS: CONTROL OF AIR POLLUTION EMISSION STANDARDS FOR NEW NONROAD SPARK-IGNITION MARINE ENGINES
Bill Charmley, Deanne R. North, Michael Samulski, Sujan Srivastava, and Ken Zerafa Oct. 1994 92 p
(PB95-166294) Avail: CASI HC A05/MF A01

The document summarizes the results of the analyses performed in support for the Notice for Proposed Rulemaking for the establishment of emission standards for new nonroad spark-ignition marine engines (59 Federal Register 55930) November 9, 1994. The environmental impact, costs, and cost effectiveness of the proposal are assessed, as well as other associated benefits. NTIS

N95-25615# Skjoeldebrand (R.).
NUCLEAR ENERGY AND THE ENVIRONMENT
R. Skjoeldebrand 1994 18 p Presented at the National Seminar on Nuclear Energy in Everyday Life, Cairo, Egypt, 28-29 Jun. 1994
(DE95-600438; INIS-mf-13983; CONF-9406263) Avail: CASI HC A03/MF A01 (US Sales Only)

This paper's thesis is that the world will need more energy and not less in the coming decades and that this enormous energy consumption entails danger to the environment not just locally, but regionally and internationally through burned fossil fuel emissions which currently provide 85% of the world's commercial energy supply. The solution to this problem is nuclear power which does not contribute to global warming. DOE

N95-25629 Pacific Northwest Lab., Richland, WA.
CARBON TAXES AND INDIA
K. A. Fisher-Vanden, H. M. Pitcher, J. A. Edmonds, S. H. Kim, and P. R. Shukla (Indian Inst. of Management, Ahmedabad.) Jul. 1994 52 p Presented at the Snowmass 94: Particle and Astrophysics in the Next Millenium, Snowmass, CO, 29 Jun. - 14 Jul. 1994 Sponsored in cooperation with the United States Environmental Protection Agency Limited

Reproducibility: More than 20% of this document may be affected by microfiche quality
(Contract DE-AC06-76RL-01830)
(DE95-005401; PNL-SA-24842; CONF-9406269-4) Avail: CASI HC A04

Using the Indian module of the Second Generation Model 9SGM, we explore a reference case and three scenarios in which greenhouse gas emissions were controlled. Two alternative policy instruments (carbon taxes and tradable permits) were analyzed to determine comparative costs of stabilizing emissions at (1) 1990 levels (the 1 X case), (2) two times the 1990 levels (the 2X case), and (3) three times the 1990 levels (the 3X case). The analysis takes into account India's rapidly growing population and the abundance of coal and biomass relative to other fuels. We also explore the impacts of a global tradable permits market to stabilize global carbon emissions on the Indian economy under the following two emissions allowance allocation methods: (1) 'Grandfathered emissions': emissions allowances are allocated based on 1990 emissions. (2) 'Equal per capita emissions': emissions allowances are allocated based on share of global population. Tradable permits represent a lower cost method to stabilize Indian emissions than carbon taxes, i.e., global action would benefit India more than independent actions. DOE

N95-25745 Rijksinstituut voor Zuivering Afvalwater, Lelystad (Netherlands).
BIOLOGICAL MONITORING OF NATIONAL FRESHWATERS, 1992 [BIOLOGISCHE MONITORING ZOETE RIJKSWATEREN, 1992]
1994 43 p In DUTCH
(PB95-166690; RIZA-93.028) Avail: Issuing Activity (National Technical Information Service (NTIS))

This report offers a broad view on the present ecological status of large freshwater bodies in The Netherlands. Where sufficient information was available, trends were analyzed and information from various fields of study was matched. A numberof changes that have taken place in aquatic flora and fauna during the last few years are presented. NTIS

N95-25779# International Atomic Energy Agency, Vienna (Austria).
ENVIRONMENT, 1980-1993
Jan. 1994 42 p
(DE95-605240; INIS-mf-14358) Avail: CASI HC A03/MF A01 (US Sales Only)

This document lists all sales publications of the International Atomic Energy Agency dealing with Environment issued during the period 1980-1993. It gives a short abstract and contents of these issues along with their costs in Austrian Schillings. DOE

N95-25852# Executive Office of the President, Washington, DC. Office of Science and Technology Policy.
OUR CHANGING PLANET: THE FY 1995 U.S. GLOBAL CHANGE RESEARCH PROGRAM
1995 144 p Original contains color illustrations
Avail: CASI HC A07/MF A02

Described are the goals and activities of the U.S. Global Change Research Program (USGCRP), which supports research covering climate change and greenhouse warming, ozone depletion and ultraviolet radiation, desertification and forestry, and predicting significant variations of the seasonal to interannual climate. This research significantly contributes to the larger worldwide effort to study natural and human-induced changes in the earth system. The following topics are discussed: addressing critical global change issues through a research framework; the FY 1995 U.S. Global Change Research Program; linking to the international community; and global change education and public awareness. Appendices contain the FY 1995 USGCRP budget, agency program listings, and USGCRP management. CASI

N95-25899# Chemsyn Science Labs., Lenexa, KS.
THE EVALUATION OF POTENTIAL LIMONENE SCAVENGERS
Robert Roth, David Ebert, and Timothy J. Shepodd (Sandia National Labs., Albuquerque, NM.) Jan. 1995 35 p
(Contracts DE-AC04-94AL-85000; SANDIA-LA-3971; CSL Proj. 1061)
(DE95-006853; SAND-94-8238) Avail: CASI HC A03/MF A01

This work is the study of different scavengers of limonene. Limonene is a citrus-based, low toxicity, hydrocarbon solvent for cleaning circuit boards and other parts. Though almost all limonene evaporates after cleaning procedures, trace residual limonene would be a concern if allowed to migrate freely through a sealed system. This work was charted to investigate materials that would effectively scavenge and permanently immobilize trace limonene. The requirements of a successful scavenger are the following: it must remove greater than 90% of 30 mg/l limonene from asealed volume with 3 months, at 20-25 C; it must not release any volatiles over prolonged aging; it must be packaged such that limonene vapors can access the scavenger, but not such that the scavenging medium can migrate; and it must operate in the presence of water, oxygen, pentane, toluene, and carbon dioxide gases. A number of adsorbents were evaluated. Additionally, a scheme for scavenging limonene by chemical reaction was investigated at Sandia. This attempt was not successful. The details of this investigation are found at the end of this report. DOE

N95-25955*# Pennsylvania State Univ., University Park, PA. Dept. of Meteorology.
DEVELOPMENT OF A MODEL OF ATMOSPHERIC OXYGEN VARIATIONS TO ESTIMATE TERRESTRIAL CARBON STORAGE AND RELEASE Progress Report No.2, 1 May 1994 - 30 April 1995
Raymond G. Najjar, Ralph F. Keeling, and David J. Erickson, III Apr. 1995 13 p Original contains color illustrations
(Grant NAGw-3929)
(NASA-CR-198002; NAS 1.26:198002) Avail: CASI HC A03/MF A01; 4 functional color pages

Two years of work has been completed towards the development of a model of atmospheric oxygen variations on seasonal to decadal timescales. During the first year we (1) constructed a preliminary monthly-mean climatology of surface ocean oxygen anomalies, (2) began modeling studies to assess the importance of short term variability on the monthly-mean oxygen flux, and (3) conducted preliminary simulations of the annual mean cycle of oxygen in the atmosphere. Most of the second year was devoted to improving the monthly mean climatology of oxygen in the surface ocean. Derived from text

N95-26005# Radian Corp., Research Triangle Park, NC.
NITROGEN OXIDE EMISSIONS AND THEIR CONTROL FROM UNINSTALLED AIRCRAFT ENGINES IN ENCLOSED TEST CELLS: JOINT REPORT TO CONGRESS ON THE ENVIRONMENTAL PROTECTION AGENCY - DEPARTMENT OF TRANSPORTATION STUDY Final Report
Oct. 1994 196 p Prepared in cooperation with Energy and Environmental Research Corp., Durham, NC Sponsored in cooperation with FAA
(Contract EPA-68-D1-0177)
(PB95-166237; EPA/453/R-94/068) Avail: CASI HC A09/MF A03

The report was submitted to the Congress under mandate of Section 233 of the Clean Air Act Amendments of 1990. The report provides a characterization of aircraft engine test cells and their emissions. Various NOx control technologies that have been applied to combustion sources other than test cells are examined in the report for their applicability to test cells. Effects of NOx controls on the aircraft engine and aircraft engine test are also addressed. Finally, annual emissions from test cells are estimated and compared to total NOx emissions in the applicable ozone non-attainment areas. NTIS

N95-26047 Hokkaido National Industrial Research Inst., Sapporo (Japan).
[DISPOSAL OF ELECTRONIC EQUIPMENT]
Sep. 1994 56 p In JAPANESE
(PB95-177861) Copyright Avail: Issuing Activity (National Technical Information Service (NTIS))

The amount of electronic equipment that needs to be disposed is increasing. It contains toxic metals and there is a danger of these metals diffusing to our living space. To treat advanced technology products without releasing the toxic metals, this research involves the following, using printed wiring board with some circuits (PWBC): Combustion treatment to decrease their volume; Behavior of heavy metals during combustion; Feature of fluidized bed. In this report, the results are presented. NTIS

N95-26065# Department of Energy, Washington, DC.
SECTOR-SPECIFIC ISSUES AND REPORTING METHODOLOGIES SUPPORTING THE GENERAL GUIDELINES FOR THE VOLUNTARY REPORTING OF GREENHOUSE GASES UNDER SECTION 1605(B) OF THE ENERGY POLICY ACT OF 1992, VOLUME 2. PART 4: TRANSPORTATION SECTOR. PART 5: FORESTRY SECTOR. PART 6: AGRICULTURAL SECTOR
Oct. 1994 190 p
(DE95-003297; DOE/PO-0028-Vol-3) Avail: CASI HC A09/MF A02

This volume, the second of two such volumes, contains sector-specific guidance in support of the General Guidelines for the voluntary reporting of greenhouse gas emissions and carbon sequestration. This voluntary reporting program was authorized by Congress in Section 1605(b) of the Energy Policy Act of 1992. The General Guidelines, bound separately from this volume, provide the overall rationale for the program, discuss in general how to analyze emissions and emission reduction/carbon sequestration projects, and address programmatic issues such as minimum reporting requirements, time parameters, international projects, confidentiality, and certification. Together, the General Guidelines and the guidance in these supporting documents will provide concepts and approaches needed to prepare the reporting forms. This second volume of sector-specific guidance covers the transportation sector, the forestry sector, and the agricultural sector. DOE

N95-26091# Little (Arthur D.), Inc., Cambridge, MA.
CROSS-FLOW, FILTER-SORBENT-CATALYST FOR PARTICULATE, SO2 AND NO(x) CONTROL Final Report
Karen Benedek and Maria Flytzani-Stephanopoulos May 1994 119 p
(Contract DE-AC22-89PC-89805)
(DE95-001934; DOE/PC-89805/T9) Avail: CASI HC A06/MF A02

This report describes work performed on a new concept for integrated pollutant control: An active filter comprised of layered, gas permeable membranes that act as a particle filter, an SO2 sorbent, and a NO(x) reduction catalyst. The focus of the research program documented in this final report is the development of the sorbent/catalyst materials that are the basis of such an emission control system. The device investigated in this program will simultaneously remove particulates, SO2 and NO(x), from combustion exhaust gases. Sulfur dioxide capture and nitrogen oxide reduction are achieved with a reg le, mixed-metal oxide sorbent-catalyst. The device is a filter with layered walls: A small-pore layer is a barrier to particles, and a macroporus active layer is a SO2 sorbent and a catalyst for the selective catalytic reduction of NO(x). The small-pore layer could be an inert ceramic that provides structural strength to the unit and protects the active (sorbent-catalyst) material from abrasion or contamination from fly ash particles. We have found that 95-100% removal efficiency of SO2 and 60-90% removal of NO(x), is achievable with the use of mixed-metal oxide sorbent-catalysts in the device. The ceramic filters are barriers to particles and typically have removal efficiencies of 99.9%. DOE

46 GEOPHYSICS

Includes aeronomy; upper and lower atmosphere studies; ionospheric and magnetospheric physics; and geomagnetism.

For space radiation see *93 Space Radiation*.

N95-24336*# National Aeronautics and Space Administration. Goddard Space Flight Center, Greenbelt, MD.
AIRBORNE IMAGING OF TROPOSPHERIC EMISSION AT MILLIMETER AND SUBMILLIMETER WAVELENGTHS
J. R. Wang, P. E. Racette, A. J. Gasiewski (Georgia Inst. of Tech., Atlanta, GA.), D. M. Jackson (Georgia Inst. of Tech., Atlanta, GA.), and D. S. Zacharias (ZAX Millimeter Wane Corp., San Diamas, CA.) [1993] 3 p
(Grant NAG5-1490)
(NASA-TM-110498; NAS 1.15:110498) Avail: CASI HC A01/MF A01

In September 1993, the NASA Millimeter-wave Imaging Radiometer (MIR) flew on board the NASA ER-2 high-altitude aircraft during CAMEX, and obtained the first wideband millimeter- and submillimeter-wavelength images of tropospheric emission. The MIR is a cross-track radiometer with channels at 89, 150, 183 +/- 1, 3, 7, 220, and 325 +/- 1, 3, 8 GHz. This set provides upwelling brightness information at the two strong rotational water vapor lines at 183.310 and 325.153 GHz and three nearby atmospheric transmission windows. The wideband MIR images of convective raincells reveal unique cloud and precipitation mapping capabilities that are not available from lower frequency microwave channels. Comparisons between the 183 and 325 GHz spectra also reveal differential brightness temperature modes that are related to cloud water. Author

N95-24577# Stanford Linear Accelerator Center, CA.
CREATION OF A SCALAR POTENTIAL IN 2D DILATON GRAVITY
K. Behrndt Sep. 1994 4 p Presented at the 7th Marcel Grossman Meeting on General Relativity, Stanford, CA, 24-29 Jul. 1994
(Contract DE-AC03-76SF-00515)
(DE95-006066; SU-SLAC-PUB-6673; CONF-9407129-4) Avail: CASI HC A01/MF A01

The authors investigate quantum corrections of the 2D dilaton gravity near the singularity. Their motivation comes from a s-wave reduced cosmological solution which is classically singular in the scalar fields (dilaton and moduli). As a result they find, that the singularity disappears and a dilaton/moduli potential is created. DOE

N95-24763*# National Aeronautics and Space Administration. Marshall Space Flight Center, Huntsville, AL.
DYNAMICS EXPLORER 1, RETARDING ION MASS SPECTROMETER SUMMARY SPECTROGRAMS-82/110 TO 82/229 SPIN-TIME SPECTROGRAMS FOR H(+), He(+), O(+), N(+), O(++), M/Z = 2, AND MOLECULAR IONS
Washington Mar. 1995 388 p
(NASA-TM-108485; NAS 1.15:108485) Avail: CASI HC A17/MF A04

The retarding ion mass spectrometer (RIMS) experiment onboard the Dynamics Explorer 1 (DE 1) satellite was designed to perform energy and mass-per-charge analysis on low-energy ions (less than 50 eV) with mass/charge ratios ranging from 1 to 40 amu/Z. The DE 1 satellite, carrying the RIMS experiment, was launched into an elliptical polar orbit on August 3, 1981. The approximately 7.5 hour orbit has perigee of 675 km altitude and apogee of 24,875 km altitude. this document and those that following in this series, contains summary RIMS data spectrograms for each orbit for which RIMS data are available. The RIMS instrument began returning science data on day 280 of 1981 and continued to return usable data until the end of the DE mission in March 1991. It should be noted that studies of the RIMS data set should be conducted only with a thorough awareness of the material described in the introduction section presented here, or in collaboration with a scientist familiar with RIMS data analysis. Author

N95-24764*# National Aeronautics and Space Administration. Marshall Space Flight Center, Huntsville, AL.
DYNAMICS EXPLORER 1, RETARDING ION MASS SPECTROMETER SUMMARY SPECTROGRAMS-82/230 TO 82/265 SPIN-TIME SPECTROGRAMS FOR H(+), He(+), O(+), N(+), O(++), M/Z = 2, AND MOLECULAR IONS
Washington Mar. 1995 400 p
(NASA-TM-108486; NAS 1.15:108486) Avail: CASI HC A17/MF A04

The retarding ion mass spectrometer (RIMS) experiment onboard the Dynamics Explorer 1 (DE 1) satellite was designed to perform energy and mass-per-charge analysis on low-energy ions (less than 50 eV) with mass/charge ratios ranging from 1 to 40 amu/Z. the DE 1 satellite, carrying the RIMS experiment, was launched into an elliptical polar orbit on August 3, 1981. The approximately 7.5 hour orbit has perigee of 675 km altitude and apogee of 24,875 km altitude. This document and those that follow in this series, contain summary RIMS data spectrograms for each orbit for which RIMS data are available. The RIMS instrument began returning science data on day 280 of 1981 and continued to return usable data until the end of the DE mission in March 1991. It should be noted that studies of the RIMS data set should be conducted only with a thorough awareness of the material described in the introduction section presented here, or in collaboration with a scientist familiar with RIMS data analysis. Author

N95-24766*# National Aeronautics and Space Administration. Goddard Space Flight Center, Greenbelt, MD.
TECHNICAL REPORT SERIES ON GLOBAL MODELING AND DATA ASSIMILATION. VOLUME 5: DOCUMENTATION OF THE AIRES/GEOS DYNAMICAL CORE, VERSION 2
Max J. Suarez, ed. and Lawrence L. Takacs (General Sciences Corp.,

Laurel, MD.) Apr. 1995 51 p
(Contract NAS5-32332; RTOP 578-41-45-20)
(NASA-TM-104606-Vol-5; Rept-95B00069-Vol-5; NAS 1.15:104606-Vol-5)
Avail: CASI HC A04/MF A01

A detailed description of the numerical formulation of Version 2 of the ARIES/GEOS 'dynamical core' is presented. This code is a nearly 'plug-compatible' dynamics for use in atmospheric general circulation models (GCMs). It is a finite difference model on a staggered latitude-longitude C-grid. It uses second-order differences for all terms except the advection of vorticity by the rotation part of the flow, which is done at fourth-order accuracy. This dynamical core is currently being used in the climate (ARIES) and data assimilation (GEOS) GCMs at Goddard. Author

N95-24897# National Geophysical Data Center, Boulder, CO. World Data Center A for Solar-Terrestrial Physics.
GEOMAGNETIC POLAR CAP (PC) INDEX, 1975-1993
S. Vennerstrom (Danish Meteorological Inst., Copenhagen, Denmark.), E. Friis-Christensen (Danish Meteorological Inst., Copenhagen, Denmark.), O. A. Troshichev (Arctic and Antarctic Scientific Research Inst., Saint Petersburg, Leningradskaya, Russia.), and V. G. Andersen (Arctic and Antarctic Scientific Research Inst., Saint Petersburg, Leningradskaya, Russia.) Apr. 1994 284 p
(UAG-103) Avail: CASI HC A13/MF A03

The first series of PC index values were published by WDC B in Moscow for the years 1975-1982. Here we present a reprint of this data series, together with a continuation for the year 1983-1993. PC is an index for magnetic activity in the (P)olar (C)ap. It is based on data from a single nearpole station, and is aimed to monitor the polar cap magnetic activity. This activity is generated by such solar wind parameters as the southward component of the interplanetary magnetic field (IMF), the azimuthal component of the IMF (B(sub y)), and the solar wind velocity v. The station Thule, placed in the village Qaanaaq in Greenland at 86.5 deg geomagnetic invariant latitude, fulfills the requirement of being close to the magnetic pole in the northern hemisphere. The station Vostok at 83.3 deg does the same in the Southern Hemisphere. The PC index is derived independently for these two stations. Author

N95-25476# Sandia National Labs., Albuquerque, NM.
3-D SEISMIC IMAGING OF COMPLEX GEOLOGIES
David E. Womble, Sudip S. Dosanjh, John P. VanDyke, Ron A. Oldfield, and David S. Greenberg 1995 6 p Presented at the SMS Simulation Multiconference: Simulation As A Critical Technology, Phoenix, AZ, 9-13 Apr. 1995
(Contract DE-AC04-94AL-85000)
(DE95-006813; SAND-95-0169C; CONF-950439-6) Avail: CASI HC A02/MF A01

We present three codes for the Intel Paragon that address the problem of three-dimensional seismic imaging of complex geologies. The first code models acoustic wave propagation and can be used to generate data sets to calibrate and validate seismic imaging codes. This code reported the fastest timings for acoustic wave propagation codes at a recent SEG (Society of Exploration Geophysicists) meeting. The second code implements a Kirchhoff method for pre-stack depth migration. Development of this code is almost complete, and preliminary results are presented. The third code implements a wave equation approach to seismic migration and is a Paragon implementation of a code from the ARCO Seismic Benchmark Suite. DOE

N95-25666# Idaho National Engineering Lab., Idaho Falls, ID.
LONG-TERM FLOW TEST NUMBER 1: ROOSEVELT HOT SPRINGS, UTAH
D. D. Faulder 1994 8 p Presented at the 1994 Annual Meeting of the Geothermal Resources Council: Restructuring the Geothermal Industry, Salt Lake City, UT, 2-5 Oct. 1994 Sponsored in part by the California Energy Company, Inc.
(Contract DE-AC07-76ID-01570)
(DE95-004995; EGG-M-94230; CONF-941043-7) Avail: CASI HC A02/MF A01

The Roosevelt Hot Springs, Utah geothermal field has been the site of numerous investigations into the behavior of a geothermal system. However, a detailed description of the reservoir is lacking. This paper presents the results of the 237 day Long-Term Flow Test No. 1, conducted in 1977 and 1978, followed by a 100 day pressure buildup. The responses from one production well and three pressure observation wells, ranging 600 to 12,000 feet from the production well, were used. This study illustrates the utility of a reevaluation of a geothermal system using old, pre-exploitation data and is part of an ongoing case study of the Roosevelt Hot Springs system. Specific objectives are an improved interpretation of the geothermal reservoir, an estimate of aquifer behavior, and the primary reservoir volume. DOE

N95-25958 Polish Academy of Sciences, Warsaw (Poland). Inst. of Geophysics.
FRICTION ON GEOLOGICAL FAULTS MODELLING AND VARIATIONAL FORMULATION OF INITIAL BOUNDARY VALUE PROBLEMS [MODELOWANIE I WARIACYJNE SFORMULOWANIE ZAGADNIEN BRZEGOWO-POCZATKOWYCH]
Wlodzimierz Robert Bielski and Jozef Joachim Telega 1994 46 p In POLISH
(ISSN 0208-5658)
(IFTR-31/1994) Avail: Issuing Activity (Polish Academy of Sciences, Warsaw, Poland)

The authors review experimental and theoretical results in modeling friction on geological faults. They also propose a new approach by introducing a friction law in subdifferential form. Quasistatic and dynamic initial boundary value problems in two cases: (1) for a single slip sequence and (2) for friction described using internal parameters are formulated.
Transl. by Schreiber Translations Inc.

N95-26036# National Inst. for Fusion Science, Nagoya (Japan).
IMPULSIVE ALFVEN COUPLING BETWEEN THE MAGNETOSPHERE AND IONOSPHERE
R. V. Reddy, K. Watanabe (Indian Inst. of Geomagnetism, Bombay.), T. Sato, and T. H. Watanabe Apr. 1994 40 p Submitted for publication
(ISSN 0915-633X)
(NIFS-276) Avail: CASI HC A03/MF A01

Basic properties of the impulsive Alfven interaction between the magnetosphere and ionosphere have been studied by means of a three-dimensional self-consistent simulation of the coupled magnetosphere and ionosphere system. It is found that the duration time of an impulsive perturbation at the magnetospheric equator, the latitudinal distribution of the Alfven propagation time along the field lines, and the ratio between the magnetospheric impedance and the ionospheric resistance are the main key factors that determine the propagation dynamics and the ionospheric responses for an impulsive MHD perturbation in the magnetosphere. Author

N95-26089# California Univ., Berkeley, CA. Dept. of Materials Science and Mineral Engineering.
PREDICTING THE TRANSPORT PROPERTIES OF SEDIMENTARY ROCKS FROM MICROGEOMETRY
E. M. Schlueter Feb. 1995 92 p Prepared in cooperation with California Univ., Berkeley. Lawrence Berkeley Lab. CA
(Contracts DE-AC03-76SF-00098; DE-AC22-89BC-14475)
(DE95-000129; DOE/BC-95000129) Avail: CASI HC A05/MF A01

The author investigates through analysis and experiment how pore geometry, topology, and the physics and chemistry of mineral-fluid and fluid-fluid interactions affect the flow of fluids through consolidated/partially consolidated porous media. The approach is to measure fluid permeability and electrical conductivity of rock samples using single and multiple fluid phases that can be frozen in place (wetting and nonwetting) over a range of pore pressures. These experiments are analyzed in terms of the microphysics and microchemistry of the processes involved to provide a theoretical basis for the macroscopic constitutive relationships between fluid-flow and geophysical properties that the authors develop. The purpose of these experiments and their analyses is to advance the understanding of the mechanisms and factors that control fluid transport in porous media. This understanding is important in characterizing porous media properties and heterogeneities before simulating and monitoring the progress of complex flow processes at the field scale in permeable media. DOE

N95-26341*# National Aeronautics and Space Administration. Goddard Space Flight Center, Greenbelt, MD.

INTERCOMPARISON OF HYDROLOGIC PROCESSES IN GLOBAL CLIMATE MODELS

W. K.-M. Lau, Y. C. Sud, and J.-H. Kim (Applied Research Corp., Landover, MD.) May 1995 156 p Original contains color illustrations

(NASA-TM-104617; NAS 1.15:104617) Avail: CASI HC A08/MF A02; 6 functional color pages

In this report, we address the intercomparison of precipitation (P), evaporation (E), and surface hydrologic forcing (P-E) for 23 Atmospheric Model Intercomparison Project (AMIP) general circulation models (GCM's) including relevant observations, over a variety of spatial and temporal scales. The intercomparison includes global and hemispheric means, latitudinal profiles, selected area means for the tropics and extratropics, ocean and land, respectively. In addition, we have computed anomaly pattern correlations among models and observations for different seasons, harmonic analysis for annual and semiannual cycles, and rain-rate frequency distribution. We also compare the joint influence of temperature and precipitation on local climate using the Koeppen climate classification scheme. Author

47 METEOROLOGY AND CLIMATOLOGY

Includes weather forecasting and modification.

N95-24219*# North Dakota Univ., Grand Forks, ND. Dept. of Atmospheric Sciences.

PRELIMINARY ANALYSIS OF UNIVERSITY OF NORTH DAKOTA AIRCRAFT DATA FROM THE FIRE CIRRUS IFO-2 Final Report

Michael R. Poellot 30 Mar. 1995 14 p

(Grant NAG1-1351)

(NASA-CR-198038; NAS 1.26:198038) Avail: CASI HC A03/MF A01

The stated goals of the First ISCCP (International Satellite Cloud Climatology Project) Regional Experiment (FIRE) are 'to promote the development of improved cloud and radiation parameterization for use in climate models, and to provide for assessment and improvement of ISCCP projects'. FIRE Phase 2 has focused on the formation, maintenance and dissipation of cirrus and marine stratocumulus cloud systems. These objectives have been approached through a combination of modeling, extended-time observations and intensive field observation (IFO) periods. The work under this grant was associated with the FIRE Cirrus IFO 2. This field measurement program was conducted to obtain observations of cirrus cloud systems on a range of scales from the synoptic to the microscale, utilizing simultaneous measurements from a variety of ground-based, satellite and airborne platforms. By combining these remote and in situ measurements a more complete picture of cirrus systems can be obtained. The role of the University of North Dakota in Phase 2 was three-fold: to collect in situ microphysical data during the Cirrus IFO 2; to process and archive these data; and to collaborate in analyses of IFO data. This report will summarize the activities and findings of the work performed under this grant; detailed description of the data sets available and of the analyses are contained in the Semi-annual Status Reports submitted to NASA. Derived from text

N95-24411*# Desert Research Inst., Reno, NV. Atmospheric Sciences Center.

REPLICATOR FOR CHARACTERIZATION OF CIRRUS AND POLAR STRATOSPHERIC CLOUD PARTICLES Final Progress Report

John Hallett and Richard G. Purcell Mar. 1995 18 p Original contains color illustrations

(Contract NAG2-663; DE-FG08-90ER-61012)

(NASA-CR-197992; NAS 1.26:197992) Avail: CASI HC A03/MF A01; 2 functional color pages

A formvar replicator for installation in an aircraft pod has been designed, built, and flight tested on the NASA DC-8. The system incorporates a deicing capability (which can be pressure activated) to enable climb out through icing situations prior to deployment. The system can be operated at preselected speeds such that data can be recorded over a period of one to ten hours on 200 ft of 16mm film. A x2 speed control can be used during flight. Capability exists for detection of chemical constituents by appropriate doping of the formvar solution. An article entitled 'Measurements of ice particles in tropical cirrus anvils: importance in radiation balance' is attached as appendix A. Author

N95-24535*# Purdue Univ., West Lafayette, IN. Dept. of Earth and Atmospheric Sciences.

PASSIVE MICROWAVE ALGORITHM DEVELOPMENT AND EVALUATION Annual Progress Report No. 1, Apr. 1994 - Mar. 1995

Grant W. Petty 15 Mar. 1995 57 p

(Grant NAGw-3944)

(NASA-CR-197915; NAS 1.26:197915) Avail: CASI HC A04/MF A01

The scientific objectives of this grant are: (1) thoroughly evaluate, both theoretically and empirically, all available Special Sensor Microwave Imager (SSM/I) retrieval algorithms for column water vapor, column liquid water, and surface wind speed; (2) where both appropriate and feasible, develop, validate, and document satellite passive microwave retrieval algorithms that offer significantly improved performance compared with currently available algorithms; and (3) refine and validate a novel physical inversion scheme for retrieving rain rate over the ocean. This report summarizes work accomplished or in progress during the first year of a three year grant. The emphasis during the first year has been on the validation and refinement of the rain rate algorithm published by Petty and on the analysis of independent data sets that can be used to help evaluate the performance of rain rate algorithms over remote areas of the ocean. Two articles in the area of global oceanic precipitation are attached. Derived from text

N95-24613# State Univ. of New York, Albany, NY. Atmospheric Sciences Research Center.

USE OF CLOUD OBSERVATIONS AND MESOSCALE METEOROLOGY MODELS TO EVALUATE AND IMPROVE CLOUD PARAMETERIZATIONS Technical Progress Report, 1 Oct. 1993 - 30 Dec. 1994

C. J. Walcek 28 Dec. 1994 6 p

(Contract DE-FG02-92ER-61364)

(DE95-006256; DOE/ER-61364/3) Avail: CASI HC A02/MF A01

The main goal of this research effort is to improve methods for calculating cloud cover within climate models. Until now, cloud cover and heights have been diagnosed from the US Air Force RTNEPH and 3DNEPH archive, and recently, CART measurements are available for analysis. Improved cloud cover formulations have been compared with existing climate model algorithms. The authors earlier conclusions were that relative humidity and convective potential were the strongest factors influencing cloud cover on regional scales. Therefore, they are refining and validating an innovative Single Column Model (SCM) cumulus parameterization for calculating heating and moistening tendencies, and precipitation rates attributable to subgrid-scale convection not resolved by climate models. This SCM will be tested and evaluated using tropical convective measurements (GATE) and they will also be applied to the incoming measurements from the Oklahoma ARM site. Further development and testing of this SCM will improve their ability to predict convective effects and cloud cover in climate models. They will quantify the influence of convection on cloud cover using convective measures derived from this SCM. The output of this research will be a family of validated algorithms for assessing cloud cover under a variety of stable, unstable, continental or oceanic conditions, and an improved cumulus parameterization scheme. DOE

N95-25287# Lawrence Livermore National Lab., Livermore, CA.

IMPACTS OF MICROPHYSICS, RADIATION AND ENVIRONMENTAL WINDS IN MID-LATITUDE AND TROPICAL SQUALL-LINE SYSTEMS, AND THEIR CLIMATIC IMPLICATIONS

Steve Hung-Neng Chin Aug. 1994 6 p Presented at the 75th Annual Meeting of the American Meteorological Society: Diamond Anniversary, Dallas, TX, 15-20 Jan. 1995

(Contract W-7405-eng-48)

(DE95-004965; UCRL-JC-116574; CONF-950124-4) Avail: CASI HC A02/MF A01

Cloud-radiation feedback has been identified as the most important factor limiting general circulation models (GCM's) to further progress in climate change research. It is also regarded as a major uncertainty in estimating the impact of greenhouse gases on climate simulations. As a result, many GCM's showed high sensitivity to the treatment of clouds and cloud radiative properties. Therefore, a better understanding of cloud-radiation feedback on the large-scale environment is absolutely

essential to improve the representation of cloud processes in GCM's. To this end, a cloud model with enhanced model physics is used to study the impact of cloud-radiation interactions on mesoscale convective systems (MCS's). Case studies representing a variety of convective systems are important to generalize the overall effects of anvil clouds on the large-scale environment. Our primary interest is limited to the MCS's in an environment with substantial wind shear, such as squall-line systems, because they have longer lifetime and wider coverage to impact the earth radiation budget and climate. The objective of this study is to investigate the impacts of microphysics, radiation and environmental winds on mid-latitude continental and tropical oceanic squall-line systems. Comparisons between these two systems are presented. Recent studies indicated that the vertical shear of the environmental wind plays an important role in the formation of the anvil cloud through the tilting of MCS's. However, this process has not been represented in GCM's. A detailed investigation on the formation of anvil clouds and their relationship to cumulus portions of MCS's would help develop a better cloud parameterization for use in GCM's. Two important issues are addressed through these comparisons. First, what factors cause the differences between mid-latitude and tropical anvil clouds? Second, do these differences have climatic implications to improve our climate forecasting ability? DOE

N95-25635# Lawrence Livermore National Lab., Livermore, CA.
A NUMERICAL PREDICTION OF THE PRECIPITATION AND HYDROLOGY OF CALIFORNIA
Jinwon Kim, Norman Miller, S. T. Soong (California Univ., Davis, CA.), and Owen Rhea (California-Nevada River Forecast Center, Sacramento, CA.) Aug. 1994 7 p Presented at the 14th Conference on Weather Analysis and Forecasting, Dallas, TX, 15-20 Jan. 1995
(Contract W-7405-eng-48)
(DE95-004966; UCRL-JC-116575; CONF-950124-3) Avail: CASI HC A02/MF A01

A five day simulation of the precipitation over the southwestern United States using a RNWHPS (Regional Numerical Weather and Hydrology Prediction Systems) is presented. The MAS (Mesoscale Atmospheric Simulation) model accurately simulates the observed local precipitation, even though extreme values are somewhat underestimated. The precipitation at individual watersheds clearly indicates that the timing of local precipitation depends on the location of each watershed and the direction of the storm path. DOE

N95-26012 Science and Technology Corp., Hampton, VA.
DESIGN AND DEVELOPMENT OF A CLOUD REFERENCE LIBRARY AND SUPPORT FOR CLOUD AND SIMULATION COMMUNITIES. SUMMARY REPORT Final Report, Sep. 1989 - Sep. 1994
Paul D. Try, John Burgeson, Tom Piwowar, and Paul F. Twitchell Sep. 1994 89 p Limited Reproducibility: More than 20% of this document may be affected by microfiche quality
(Contract F19628-89-C-0190)
(AD-A288704; STC-TR-2855; PL-TR-94-2248) Avail: Issuing Activity (Defense Technical Information Center (DTIC))

This report summarizes the work accomplished under Contract No. F19628-89-C-0190. Three primary activities and products resulted from the work: (1) The development, implementation, and updating of the Cloud Information Reference Library and Archive (CIRLA). CIRLA provides information in cloud simulations, models, algorithms, analyses, and databases, and has recently been made accessible via Internet. (2) Three major conferences on Cloud Impacts on DOD Operations and Systems (CIDOS) - CIDOS-89/90, CIDOS-91, and CIDOS-93. The CIDOS conferences have evolved from evaluation by the DOD atmospheric science community of the impacts of clouds on military weapons systems, sensors, and operations, through the inclusion of civilian applications, to DOD simulation activities. (3) A survey of the DOD modeling and simulation (M&S) community's requirements for environmental models and databases. An overall strategy that planned and executed the survey task, including development of a comprehensive Requirements Questionnaire, was presented for Air Force and E2DIS Project approval. DTIC

N95-26043# International Centre for Theoretical Physics, Trieste (Italy).
MODELLING THE DAY TO DAY WIND VARIABILITY OFFSHORE CENTRAL CHILE AT ABOUT 30 DEG SOUTH
J. Rutllant Jul. 1994 19 p
(DE95-606032; IC-94/166) Avail: CASI HC A03/MF A01 (US Sales Only)

Cycles of strengthening and relaxation of the winds offshore 30 degrees S at central Chile, are related to the propagation of coastal-lows, a year-round phenomenon occurring with periodicities of about one in five days. Simple physical modelling of the day to day variability of the alongshore wind component at a coastal strip extending offshore up to the Rossby deformation radius of these wave perturbations, is presented in terms of the relevant horizontal pressure gradients and the ageostrophic components arising from the coastal-low propagation. The results of 5-day composites of 8 wind-events each, at the winter and summer halves of the annual cycle, respectively; lead to a good agreement between the observed phase-lag of the winds with respect to the pressure forcing field, stressing the importance of the ageostrophic wind components at the extremes of the pressure wave perturbation associated with the passage of coastal-lows over the Point Lengua de Vaca (30 15 S) area. A possible contribution of the upwelling-favorable wind enhancement at the time of the pressure rise and subsequent fall, ahead of the coastal-low, is postulated through an upwelling-front low-level jet, that would be carried onshore and closer to the surface by the combination of the enhanced coastal upwelling, the coastal depression of the subsidence inversion base and the coastal ageostrophic wind components during the passage of the leading edge of the coastal lows. DOE

N95-26197 Air Force Inst. of Tech., Wright-Patterson AFB, OH.
ON CONVERGENCE OF THE NELDER-MEAD SIMPLEX ALGORITHM FOR UNCONSTRAINED STOCHASTIC OPTIMIZATION Ph.D. Thesis
John J. Tomick May 1995 201 p Limited Reproducibility: More than 20% of this document may be affected by microfiche quality
(AD-A289453; AFIT/CI/CIA-94-151) Avail: Issuing Activity (Defense Technical Information Center (DTIC))

The Nelder-Mead simplex method is a direct search algorithm that has found widespread use in the optimization of nonlinear functions. Originally designed for deterministic optimization, the method is robust with respect to small perturbations in the function's values; and therefore, this method has been used for optimizing stochastic functions as well. However, if the random perturbations in the function's values are large enough the method may terminate before reaching the optimizer of the expected function. We prove convergence of the simplex to a point with probability 1 for constant functions with additive noise for 1- and 2-dimensional functions and provide empirical evidence for the same result in higher dimensions. This result implies that as the amount of noise increases, differences between the expected function's values at the vertices of the simplex become obscured and the probability of terminating early is increased. Also, we demonstrate empirically and analytically the probability of early termination on an unbounded univariate linear function with additive noise. We propose a new modification for the Nelder-Mead simplex method for use in stochastic optimization. This new method reduces to the original method when the noise level is negligible or nonexistent; and therefore, it is as efficient as the Nelder-Mead method when the noise level is low. And in Monte Carlo experiments, our proposed method continued to reduce the expected function for as long as the simulations were run; whereas the original method and the previously best know modified simplex methods terminated early. DTIC

48 OCEANOGRAPHY

Includes biological, dynamic, and physical oceanography; and marine resources.

For related information see also *43 Earth Resources and Remote Sensing.*

N95-25504 State Univ. of New York, Stony Brook, NY.
SHELF SEDIMENT DYNAMICS AND DEVELOPMENT OF LITHOSTRATIGRAPHY Report, 1 Jul. 1993 - 30 Jun. 1994
Charles A. Nittrouer 16 Nov. 1994 21 p
(Contract N00014-93-1-0799)
(AD-A288886) Avail: Issuing Activity (Defense Technical Information Center (DTIC))

This workshop designed an integrated investigation of the stratigraphic

signature that is created on the shelf and slope portions of continental margins. The goals of the overall program will: add geological perspective to shelf and slope studies of sediment transport, morphology, and fine-scale stratigraphy (time scales greater than 100 y); provide physical constraints on interpretation of high frequency seismic stratigraphy in the upper loom of the seabed (time scales of 10,000 y - 1,000,000 y); and develop approaches for interpolating between these time scales and obtaining stratigraphic insights. In order to reach these goals, field work will investigate the margins off northern California and New Jersey. Interdisciplinary studies will have a geologic focus designed to unravel the complex relationships between formative sedimentary processes and preserved strata. In the two diverse study areas, where much reconnaissance work already has been completed, a holistic approach to shelf and slope environments will observe and model sediment transport and accumulation and their relationships to resultant stratigraphy. DTIC

N95-25605 Naval Postgraduate School, Monterey, CA.
TECHNIQUES FOR THE INVESTIGATION OF WAVE TURBULENCE IN WATER WAVE DATA M.S. Thesis
John P. Davies Sep. 1994 78 p Limited Reproducibility: More than 20% of this document may be affected by microfiche quality
(AD-A288392) Avail: Issuing Activity (Defense Technical Information Center (DTIC))

Computer based tools were developed to search water wave data for a collective mode predicted by wave turbulence theory. A low frequency wave, the 'swell', can drive the collective mode by compressing and expanding the field of high frequency waves, the 'chop'. Through non-linear interactions, the chop responds with its own collective stiffness and inertia. This inertia should cause modulations of the chop amplitude to lag in phase behind the forcing from the swell. Two methods are presented for investigating the phase relationships between the chop amplitude and the swell. Method one employs the Fast Fourier Transform to examine directly the power levels at various frequencies. Method two employs digital signal processing to separate the swell and chop frequencies and the Hilbert Transform to compute the instantaneous phase of the swell and instantaneous amplitude of the chop. Various plotting techniques permit the examination of the relationships between the amplitude of the chop and the phase of the swell. The second method provided evidence of the collective mode when applied to data collected in a wave tank experiment described herein. DTIC

N95-26048 Institute for Defense Analyses, Alexandria, VA.
FLEXIBLE ARCHITECTURES FOR SENSOR FUSION IN THEATER MISSILE DEFENSE Final Report, Sep. 1993 - Apr. 1994
Gabriel Frenkel Apr. 1994 67 p Sponsored by the Ballistic Missile Defense Organization Limited Reproducibility: More than 20% of this document may be affected by microfiche quality
(Contract MDA903-89-C-0003)
(AD-A288666; IDA-Paper-P-2935) Avail: Issuing Activity (Defense Technical Information Center (DTIC))

This paper presents sensor fusion procedures and algorithms for tracking and intercept support. The effort was undertaken in support of Ballistic Missile Defense Office (BMDO) activities pertaining to the design of a effective Theater Ballistic Missile Defense (TBMD) Command and Control structure and associated Operational Control and Combat Command elements design. The following major issues are addressed: (1) Methods of sensor fusion and associated algorithms (their advantages and disadvantages and their dynamic utilization in the battle scenario). Issues of track fusion vs. data fusion are given particular attention; (2) The communication loads of particular sensor fusion architectures and of the associated operational control activities; (3) Algorithms for the effective utilization of sensor fusion for intercept support and for burnout point estimation. This paper addresses the simplest possible case: a single missile on a ballistic trajectory tracked by two radar sensors in a flat earth model. False signals, clutter, closely spaced objects, tumbling, and gravitational anomalies are not considered. We demonstrate that even this simple case is conducive for providing valuable answers in the broad areas listed above. Numerous graphs are included. These graphs are the results of simulation runs by the Sensor Fusion Architecture Model (SFAM) developed for this effort. DTIC

51 LIFE SCIENCES (GENERAL)

N95-24225# Georgia Univ., Athens, GA.
STRUCTURES AND FUNCTIONS OF OLIGOSACCHARINS
P. Albersheim Oct. 1994 6 p
(Contract DE-FG09-85ER-13425)
(DE95-003140; DOE/ER-13425/T3) Avail: CASI HC A02/MF A01

This paper contains abstracts of 10 papers published reporting work on the structure and functions of oligosaccharins. Topics include: Oligosaccharide regulatory molecules; Studies of the ability of xyloglucan oligosaccharides to inhibit auxin-stimulated growth; Oligosaccharins - oligosaccharides that regulate growth, development and defense responses in plants; Activation of a tobacco glycine-rich protein gene by a fungal glucan preparation; and Accumulation of PGIP in the cell wall reflects an active defense response of plants to fungal pathogens. DOE

N95-24306# National Renewable Energy Lab., Golden, CO.
BIOLOGICALLY PRODUCED SUCCINIC ACID: A NEW ROUTE TO CHEMICAL INTERMEDIATES
1995 3 p
(Contract DE-AC36-83CH-10093)
(DE95-000257; DOE/GO-10094-037) Avail: CASI HC A01/MF A01

The US Department of Energy (DOE) Alternative Feedstocks (AF) program is forging new links between the agricultural community and the chemicals industry through support of research and development (R & D) that uses 'green' feedstocks to produce chemicals. The program promotes cost-effective industrial use of renewable biomass as feedstocks to manufacture high-volume chemical building blocks. Industrial commercialization of such processes would stimulate the agricultural sector by increasing the demand of agricultural and forestry commodities. New alternatives for American industry may lie in the nation's forests and fields. The national laboratory consortium has undertaken a joint R&D project with the Michigan Biotechnology Institute to demonstrate the feasibility of producing a chemical intermediate, succinic acid, and various derivatives, from renewable agricultural resources. DOE

N95-24307# National Renewable Energy Lab., Golden, CO.
CLEAN FRACTIONATION OF BIOMASS
1995 3 p
(Contract DE-AC36-83CH-10093)
(DE95-000259; DOE/GO-10094-039) Avail: CASI HC A01/MF A01

The US Department of Energy (DOE) Alternative Feedstocks (AF) program is forging new links between the agricultural community and the chemicals industry through support of research and development (R & D) that uses 'green' feedstocks to produce chemicals. The program promotes cost-effective industrial use of renewable biomass as feedstocks to manufacture high-volume chemical building blocks. Industrial commercialization of such processes would stimulate the agricultural sector by increasing the demand of agricultural and forestry commodities. New alternatives for American industry may lie in the nation's forests and fields. The AF program is conducting ongoing research on a clean fractionation process. This project is designed to convert biomass into materials that can be used for chemical processes and products. Clean fractionation separates a single feedstock into individual components, cellulose, hemicellulose, and lignin. DOE

N95-24368 Georgia Univ., Athens, GA.
STRUCTURAL STUDIES OF COMPLEX CARBOHYDRATES OF PLANT CELL WALLS Progress Report, 15 Jun. 1992 - 14 Jun. 1993
A. G. Darvill Oct. 1994 8 p Limited Reproducibility: More than 20% of this document may be affected by microfiche quality
(Contract DE-FG09-85ER-13426)
(DE95-005545; DOE/ER-13426/T4) Avail: CASI HC A02

This report contains the abstracts of fourteen papers published, in press, or in preparation reporting on research activities to investigate the structure, as well as the function of cell walls in plants. This document also contains research on methods to determine the structure of complex carbohydrates of the cell walls. DOE

N95-24475*# Pennsylvania State Univ., University Park, PA. Center for Cell Research.

ELECTROPHORETIC SEPARATION OF CELLS AND PARTICLES FROM RAT PITUITARY Mid Term Progress Report

W. C. Hymer 20 Mar. 1995 78 p

(Grant NAG8-953)

(NASA-CR-197975; NAS 1.26:197975) Avail: CASI HC A05/MF A01

In spite of the fact that a vast majority of the electrophoresis effort (approximately 90%) could not be done on this mission (IML-2) due to failure of FFEU hardware, we find some interesting differences in flight samples obtained from other parts of the experiment. These differences are entirely novel and sometimes unexpected. This report is organized into 4 parts. Each part describes the data collected thus far from each of the 4 cell culture kits (CCK) which flew in space. Each CCK was loaded with 40x10(exp 6) fresh pituitary cells; all CCK's were identical at the start of the experiment because we prepared one pool of cells. Derived from text

N95-24531*# National Aeronautics and Space Administration. Marshall Space Flight Center, Huntsville, AL.

FUSION PROTEINS AS ALTERNATE CRYSTALLIZATION PATHS TO DIFFICULT STRUCTURE PROBLEMS

Daniel C. Carter, Florian Rueker (Bodenkultur Univ., Vienna, Austria.), Joseph X. Ho, Kap Lim, Kim Keeling, Gary Gilliland (Center for Advanced Research in Biotechnology, Rockville, MD.), and Xinhua Ji (Center for Advanced Research in Biotechnology, Rockville, MD.) [1994] 5 p

(NASA-TM-110497; NAS 1.15:110497) Avail: CASI HC A01/MF A01

The three-dimensional structure of a peptide fusion product with glutathione transferase from Schistosoma japonicum (SjGST) has been solved by crystallographic methods to 2.5 A resolution. Peptides or proteins can be fused to SjGST and expressed in a plasmid for rapid synthesis in Escherichia coli. Fusion proteins created by this commercial method can be purified rapidly by chromatography on immobilized glutathione. The potential utility of using SjGST fusion proteins as alternate paths to the crystallization and structure determination of proteins is demonstrated.

Author

N95-24600# Los Alamos National Lab., NM.

STAUROSPORINE ANALYSIS AND ITS PHARMACOKINETICS IN THE BLOOD OF RATS

L. R. Gurley, K. O. Umbarger, J. M. Kim, E. M. Bradbury, and B. E. Lehnert Jul. 1994 43 p

(Contract W-7405-eng-36)

(DE94-013857; LA-12788-MS) Avail: CASI HC A03/MF A01

Staurosporine (Stsp), a protein kinase inhibitor, has been found to have a differential effect on the proliferation of normal and transformed cells in vitro. Essentially nothing is known about the distribution and pharmacokinetics of Stsp in the body. To facilitate such investigations, we have developed a High-Performance Liquid Chromatography method for measuring the levels of Stsp in blood. Stsp was measured in both plasma and RBC of rat blood. In vivo, Stsp was rapidly sequestered in some other tissue compartment, which rapidly decreased the concentration of Stsp in plasma to nondetectable levels. Using a postchromatography computerized analysis program that amplified the Stsp UV absorption peak from the HPLC. nanogram levels of Stsp were detected in vivo. Using this detection system for pharmacokinetic studies it was found that, in vivo, Stsp had a half-life of 51.6 min in plasma and 75.3 min in RBC. Tissue adsorption studies demonstrated that up to 99% of the Stsp was adsorbed by the heart and lung tissue in one pass through these organs. Extrapolation of the data from these studies suggest that 1 micro g Stsp injections should produce a 2- to 7-ng/ml plasma Stsp level in vivo which is in the effective range to produce G1 arrest in normal cells. The short half-life of Stsp in plasma indicates that it will be necessary to infuse Stsp at some low level following the initial bolus injection in order to maintain Stsp levels in plasma at the 1- to 10-ng/ml level for the 2- to 3-day period necessary to achieve G1 arrest in vivo. DOE

N95-24843# Oak Ridge National Lab., TN.

BIOPROCESSING IN NONAQUEOUS MEDIA: CRITICAL NEEDS AND OPPORTUNITIES

C. D. Scott, T. C. Scott, H. W. Blanch (California Univ., Berkeley, CA.), A. M. Klibanov (Massachusetts Inst. of Tech., Cambridge, MA.), and A. J. Russell (Pittsburgh Univ., Pittsburgh, PA.) Jan. 1995 41 p

(Contract DE-AC05-84OR-21400)

(DE95-004878; ORNL/TM-12849) Avail: CASI HC A03/MF A01

Chemical conversion processes are pervasive in the U.S. industry. Whether they are used to make intermediate or final products or to remove hazardous materials from process waste streams, they are critical elements in the processing industries. Because of the mild reaction conditions, unique specificity, and selectivity, advanced processing concepts utilizing biocatalytic conversions are now being considered for many industrial uses, including those directly related to energy production and efficiency. Almost all bioprocessing systems currently used by industry utilize the biocatalysts (microorganisms or extracted enzymes) in a 'natural' aqueous environment. This has resulted in many important large-scale applications, particularly in the fermentation and pharmaceutical industries. An exciting new area of bioprocessing research is now evolving - the use of biocatalysts in contact with nonaqueous media such as organic liquids or gases, or supercritical fluids. Such approaches could result in additional bioprocessing concepts that would result in a much broader range of utility, especially in energy production and energy-efficient conversion processes in the chemical industry. In fact, a whole new industry may be evolving. DOE

N95-24850# Massachusetts Inst. of Tech., Cambridge, MA.

GENETIC AND BIOPHYSICAL STUDIES OF THE PHOTOSYNTHETIC REACTION CENTER Final Technical Report

Douglas C. Youvan 1994 11 p

(Contract DE-FG02-90ER-20019)

(DE95-004179; DOE/ER-20019/T1) Avail: CASI HC A03/MF A01

This research is aimed at understanding how critical amino acid residues (and peptides) interact to modify the chemistry of the prosthetic groups, for example: (1) in determining whether bacteriochlorophyll (BC) or bacteriopheophytin (BP) is bound at particular sites; (2) in facilitating electron transfer between prosthetic groups either by direct mechanisms or superexchange; (3) in modifying redox or spectral properties of the prosthetic groups; (4) in imparting resistance to certain quinone inhibitors, such as the triazine herbicides; and (5) in directing the path of the photoelectron down only one of two apparent pathways in the reaction center. A principal engineering goal of this research is to construct 'wrong-way' electron transfer mutants. This will be accomplished either by changing the specificity of tetrapyrrole binding sites (BC to BP (reverible reactions) interconversion) or by 'swapping' entire helices through the pseudo C2 symmetry axis. Such mutants are important for understanding pigment-protein assembly as well as mechanistic aspects of photochemistry. This report lists a point-by-point summary of the most important findings in the research over the past 4 years. More time and effort was dedicated to combinatorial mutagenesis on light harvesting antennae than initially proposed. The additional award from DOE for building a Digital Imaging Spectrophotometer (DIS) led to the development of general tools for studying the spectra of mutants directly on petri dishes. Applications of DIS should be even more general, including energy studies in plants and cyanobacteria. DOE

N95-25181# Argonne National Lab., IL.

OVERVIEW OF SELECTED MOLECULAR BIOLOGICAL DATABASES

K. D. Rayl and T. Gaasterland Nov. 1994 92 p

(Contract W-31-109-eng-38)

(DE95-005906; ANL/MCS-TM-200) Avail: CASI HC A05/MF A01

This paper presents an overview of the purpose, content, and design of a subset of the currently available biological databases, with an emphasis on protein databases. Databases included in this summary are 3D-ALI, Berlin RNA databank, Blocks, DSSP, EMBL Nucleotide Database, EMP, ENZYME, FSSP, GDB, GenBank, HSSP, LiMB, PDB, PIR, PKCDD, ProSite, and SWISS-PROT. The goal is to provide a starting point for researchers who wish to take advantage of the myriad available databases. Rather than providing a complete explanation of each database, we present its content and form by explaining the details of typical entries. Pointers to more complete 'user guides' are included, along with general information on where to search for a new database. DOE

N95-25383# Brookhaven National Lab., Upton, NY.

THE EFFECTS ON PHOTOSYNTHETIC CO2 ASSIMILATION TO LONG-TERM ELEVATION OF ATMOSPHERIC CO2 CONCENTRATION: AN ASSESSMENT OF THE RESPONSE OF TRIFOLIUM REPENS L. CV. BLANCA GROWN AT F.A.C.E

C. E. Lewis Nov. 1994 38 p
(Contract DE-AC02-76CH-00016)
(DE95-005687; BNL-61078) Avail: CASI HC A03/MF A01

Understanding how photosynthetic capacity acclimates to elevated CO2 concentrations is vital in predicting the response of important grassland species such as Trifolium repens. Previous studies of acclimatization have been carried out in artificial experimental conditions, such as acrylic greenhouses or controlled environment chambers. The advent of FACE technology has enabled a large area of crop to be fumigated in the field, providing more realistic growing conditions. Pure stands of Trifolium repens L. cv. Blanca grown at either 355 or 600 micromol/mol CO2 were examined, and their photosynthetic response to elevated c(sub a) a determined via gas exchange studies. Rates of photosynthesis of young, fully expanded leaves were increased between 21 and 36% when grown and measured at elevated CO2. This increase in A corresponded to a decrease in g(sub S) of between 18 and 52%. No acclimation effect was observed in the most frequently cut stands, whilst the response of stands clipped only 4 times per year was more variable. When down regulation of V(sub cmax) did occur, this was not nearly as marked as that which occurred in 3 other temperate species (Chrysanthemum leucanthemum, Ranunculus friesianus, Plantago lanceolata (L.) J. & C. Presl.), at similar growth regimes. No acclimation of stomatal frequency, SI or pore length was found to occur in the enriched clover stands. DOE

N95-25902# National Inst. of Radiological Sciences, Chiba (Japan).
ANNUAL REPORT OF NATIONAL INSTITUTE OF RADIOLOGICAL SCIENCES
Jul. 1993 127 p
(DE94-792664; NIRS-32) Avail: CASI HC A07/MF A02

This annual report is a compilation of the research activities and achievement in the National Institute of Radiological Sciences (NIRS) in Japan during the fiscal year 1992 (from April 1992 through March 1993). Construction of the Heavy Ion Medical Accelerator in Chiba (HIMAC) has reached semi-final stage. The research covers a wide range of radiological sciences from molecular biology to environmental studies and medicine including engineering for heavy ion therapy of cancer. Topics consists of physics, chemistry, biomedical science, clinical research, and environmental sciences, covering a total of 84 titles. A list of publications by staff members, activities of research divisions, and organization chart of the NIRS are given in Appendix. DOE

N95-26169# Pacific Northwest Lab., Richland, WA.
INTERACTION MECHANISMS AND BIOLOGICAL EFFECTS OF STATIC MAGNETIC FIELDS
T. S. Tenforde Jun. 1994 10 p Presented at the U.S.-Japan Seminar on Electromagnetic Fields Effects, Sapporo, Japan, 28 Jun. - 1 Jul. 1994
(Contract DE-AC06-76RL-01830)
(DE95-004929; PNL-SA-24930; CONF-9406207-2) Avail: CASI HC A02/MF A01

Mechanisms through which static magnetic fields interact with living systems are described and illustrated by selected experimental observations. These mechanisms include electrodynamic interactions with moving, ionic charges (blood flow and nerve impulse conduction), magnetomechanical interactions (orientation and translation of molecules structures and magnetic particles), and interactions with electronic spin states in charge transfer reactions (photo-induced electron transfer in photosynthesis). A general summary is also presented of the biological effects of static magnetic fields. There is convincing experimental evidence for magnetoreception mechanisms in several classes of lower organisms, including bacteria and marine organisms. However, in more highly evolved species of animals, there is no evidence that the interactions of static magnetic fields with flux densities up to 2 Tesla (1 Tesla(T) = 10(exp 4) Gauss) produce either behavioral or physiolocical alterations. These results, based on controlled studies with laboratory animals, are consistent with the outcome of recent epidemiological surveys on human populations exposed occupationally to static magnetic fields. DOE

N95-26193 Georgia Univ., Athens, GA. Research Foundation, Inc.
TESTING OF EXPERIMENTAL ANTILEISHMANIAL COMPOUNDS Final Report, 28 Mar. - 23 Sep. 1994
William L. Hanson 19 Oct. 1994 15 p Limited Reproducibility: More than 20% of this document may be affected by microfiche quality
(Contract DAMD17-94-V-4004)
(AD-A288807) Avail: Issuing Activity (Defense Technical Information Center (DTIC))

Six plant derivatives which were selected for in vivo study because of their in vitro antiLeishmanial activity and low toxicity were studied for activity against Leishmania Leishmania donovani and Leishmania Viannia brazitiensis in hamsters. The time interval between completion of treatment and evaluation of results was extended up to 4-6 weeks to evaluate any possible delayed antiLeishmanial activity by the compounds. None of the compounds studied were active in hamsters against either species of Leishmenia. Extension of time between treatment and evaluation of results did not increase the in vivo activity of any of the compounds studied. None of the compounds studied were toxic based on body weight loss, mortality, or clinical signs. DTIC

N95-25933*# San Francisco Univ., CA.
RADIOBIOLOGICAL EXPERIMENTS WITH PLANT SEEDS ABOARD THE BIOSATELLITE COSMOS 1887
E. V. Benton, I. D. Anikeeva (Academy of Sciences, USSR, Moscow, USSR.), Yu. A. Akatov (Institute of Biomedical Problems, Moscow, USSR.), E. N. Vaulina (Academy of Sciences, USSR, Moscow, USSR.), L. N. Kostina (Academy of Sciences, USSR, Moscow, USSR.), A. Marenny (Institute of Biomedical Problems, Moscow, USSR.), A. I. Portman (Institute of Biomedical Problems, Moscow, USSR.), and S. V. Rusin (Moscow Physical-Engineering Inst., Russia.) *In its* High LET, Passive Space Radiation Dosimetry and Spectrometry Mar. 1995 6 p (For primary document see N95-25911 08-72)
(Contract NCC2-521)
Avail: CASI HC A02/MF A03

N95-25934*# National Aeronautics and Space Administration. Marshall Space Flight Center, Huntsville, AL.
SPACE RADIATION DOSIMETRY ON US AND SOVIET MANNED MISSIONS
T. A. Parnell and E. V. Benton (San Francisco Univ., CA.) *In* San Francisco Univ., High LET, Passive Space Radiation Dosimetry and Spectrometry Mar. 1995 68 p (For primary document see N95-25911 08-72)
(Contract NAS9-17389; NAG8-071)
Avail: CASI HC A04/MF A03

52 AEROSPACE MEDICINE

Includes physiological factors; biological effects of radiation; and effects of weightlessness on man and animals.

N95-24227 Foerenade Fabriksverken, Linkoeping (Sweden). Huvudavdelning foer Informationsteknologi.
PREDICTION OF HUMANS IN VARIOUS ENVIRONMENTS USING GAS SENSORS AND NEURAL NETWORKS [PREDIKTION AV MAENNISKOR I OLIKA MILJOEER MED HJAELP AV GASSENSORER OCH NEURALA NAETVERK]
K. Gindahl, F. Winquist, and S. Oedman Mar. 1994 33 p In SWAHILI (PB95-141560; FOA-C-30757-3.1) Avail: Issuing Activity (National Technical Information Service (NTIS))

Humans excrete volatile compounds through pulmonary gases, mouth air and the surfaces of the skin. The presence of humans in small compartments could be predicted by gas sensors and neural networks. The experiments were made with volunteers sitting in a wardrobe from which the air was pumped into balloons. The content of the air was detected by gas sensors. Neural networks distinguished the sensor data taken in the presence of humans from those taken in absence of humans respectively. Various neural nets were examined. The results showed that the presence of humans could be predicted with a low percentage of error. Adults and children participated in the wardrobe experiments. Experiments in smoky environments, the training facility of a fire brigade, showed small changes induced in the sensitivity of the gas sensors. In spite of this, the neural network could predict the presence of humans in this environment. NTIS

N95-24309 Purdue Univ., West Lafayette, IN.
NON-INVASIVE DETECTION OF INCREASED INTRACRANIAL PRESSURE USING ACOUSTICAL TECHNIQUES Final Report, 8 Aug. 1992 - 7 Feb. 1994
George R. Wodicka 7 Mar. 1994 257 p Limited Reproducibility: More than 20% of this document may be affected by microfiche quality
(Contract DAMD17-92-J-2025)
(AD-A279292) Avail: Issuing Activity (Defense Technical Information Center (DTIC))

This study was undertaken to determine the relationships between intracranial pressure (ICP) and the acoustic response of the head. Potentially fatal increases in ICP can occur in soldiers afflicted with Acute Mountain Sickness at high-altitude, yet there is no reliable and noninvasive procedure to monitor ICP changes in uncontrolled conditions. In this investigation, an ovine animal model was used in which incremental increases in ICP were elicited and directly measured through intraventricular cannulae. At each ICP increment, a vibration source elicited a flexural response of the animal's head, and this acoustic response was measured at four locations on the skull using accelerometers. Spectral analysis of the response showed numerous changes in proportion to ICP up to roughly 20 CmH2O above normal; a clinically significant range. For example, changes in magnitude and phase at frequencies between 4 and 7 kHz each correlated well (greater than 0.92) with ICP across the study group. Thus, alterations in ICP give rise to measurable acoustic changes that can potentially be used to noninvasively monitor afflicted soldiers in uncontrolled environments. DTIC

N95-24310 Centre de Recherches du Service de Sante des Armees, La Tronche (France). Unite de Thermophysiologie.
THERMAL AND VASCULAR CHANGES INDUCED BY THE ACCLIMATION OF THE EXTREMITIES TO COLD IN MAN [MODIFICATIONS THERMIQUES ET VASCULAIRES INDUITES PAR L'ADAPTATION DES EXTREMITES AU FROID CHEZ L'HOMME]
G. Savourey, L. Clerc, A. M. Hanniquet, G. Livecchi-Gonnot, and J. Bittel Nov. 1994 67 p In FRENCH Sponsored by Direction des Recherches, Etudes et Techniques
(PB95-131587; CRSSA-8/FH/TP) Avail: Issuing Activity (National Technical Information Service (NTIS))

The acclimation of the extremities to cold, achieved through repeated immersion in cold water, will develop a local adaptation identical to that observed in some tribes (Lapps, Eskimos) or certain types of workers (Gaspe fishermen, fish fillet cutters). This adaptation translates, at the end of the immersion, into higher skin temperatures, enhanced dexterity, and an increased pain threshold. However, recovery is slower. The changes observed are more closely related to vascular changes than to local heat production. The spectroscopic analysis of P31 through nuclear magnetic resonance actually does not show any changes in the energetic substrates after immersion. On the other hand, exposure to cold prior to making an effort will alter the phosphocreatine metabolism and bring about alkalosis during recovery. NTIS

N95-24367# Instituto de Pesquisas Energeticas e Nucleares, Sao Paulo (Brazil).
APPLICATION OF COMPARTMENTAL METABOLIC MODELS FOR DETERMINATION OF RETENTION AND EXCRETION FUNCTIONS
O. RodriguesJunior 1994 99 p
(DE95-600249; INIS-BR-3412) Avail: CASI HC A05/MF A02 (US Sales Only)

After an intake of radioactive material, its behaviour in the human body can be described by mathematical models, where organs, tissues or regions of the body are treated as a chain of linked compartments. The mathematical approach for such metabolic models is usually done through a system of differential equations of first order with constant coefficients. The solutions of this system of equations associates the radionuclide intake, with the fraction excreted or retained in the organ of interest. A computer program - INCORP - was developed in order to find the solutions of this system of equations, using an analytical method based on expansion of a series of exponential matrices. The metabolic model presented in the ICRP-30 publication was simulated using the INCORP program, in order to find the respective retention and excretion curves for selected radionuclides. DOE

N95-24410*# Legacy Good Samaritan Hospital, Portland, OR. Clinical Vestibular Lab.
RELATION OF MOTION SICKNESS SUSCEPTIBILITY TO VESTIBULAR AND BEHAVIORAL MEASURES OF ORIENTATION Annual Status Report
Robert J. Peterka Apr. 1995 5 p
(Grant NAGw-3782)
(NASA-CR-198048; NAS 1.26:198048) Avail: CASI HC A03/MF A01

The objective is to determine the relationship of motion sickness susceptibility to vestibulo-ocular reflexes (VOR), motion perception, and behavioral utilization of sensory orientation cues for the control of postural equilibrium. The work is focused on reflexes and motion perception associated with pitch and roll movements that stimulate the vertical semicircular canals and otolith organs of the inner ear. This work is relevant to the space motion sickness problem since 0 g related sensory conflicts between vertical canal and otolith motion cues are a likely cause of space motion sickness. Derived from text

N95-24423 Prime Technology, Inc., Dayton, OH.
AVIATION EPIDEMIOLOGY DATA REGISTER Midterm Report, 1 Mar. 1992 - 1 Mar. 1994
Robert H. Schrimsher 15 Mar. 1994 8 p Limited Reproducibility: More than 20% of this document may be affected by microfiche quality
(Contract DAMD17-92-C-2062)
(AD-A279303) Avail: Issuing Activity (Defense Technical Information Center (DTIC))

The midterm report focuses only upon the research activity of this contract. Analytical support is the primary research activity, which consists of two areas: responding to data analysis requests and publications. Data analysis requests are mostly generated by researchers and scientists within USAARL (U.S. Army Aeromedical Research Laboratory). There have been 60 formal data analysis requests since the beginning of this contract and five publications by the Principal Investigator in conjunction with other USAARL investigators. One of the publications was in open literature, while the remaining were technical reports. The publications mainly were centered on Army aviator visual/refractive error concerns and Aviation Epidemiology Data Register (AEDR) monograms, which provide descriptive statistics of selected variables from an aviator's annual class 2 or 2A Flying Duty Medical Examination (FDME) for the applicable years. DTIC

N95-24427# Argonne National Lab., IL.
CONTRIBUTION OF ANKYRIN-BAND 3 COMPLEXES TO THE ORGANIZATION AND MECHANICAL PROPERTIES OF THE MEMBRANE SKELETON OF HUMAN ERYTHROCYTE
B. W. Shen 1995 28 p
(Contract W-31-109-eng-38)
(DE95-005835; ANL/BIM/PP-78964) Avail: CASI HC A03/MF A01

To understand the role of ankyrin-band 3 complexes in the organization of the spectrin-based membrane skeleton and its contribution to the mechanical properties of human erythrocytes, intact skeletons and single-layered skeleton leaflets were prepared from intact and physically sheared membrane ghosts, expanded in low salt buffer, and examined by transmission electron microscopy. While the structures of intact skeletons and single-layered skeleton leaflets shared many common features, including rigid junctional complexes of spectrin, actin, and band 4.1; short stretches (approximately 50 angstrom) of flexible spectrin filaments; and globular masses of ankyrin-band 3 complexes situated close to the middle of the spectrin filaments, the definition of structural units in the intact skeleton is obscured by the superposition of the two layers. However, the spatial disposition of structural elements can be clearly defined in the images of the single-layered skeleton leaflets. Partially expanded skeletal leaflets contain conglomerates of ankyrin-band 3 complexes arranged in a circular or clove-leaf configuration that straddles multiple strands of thick spectrin cables, presumably reflecting the association of ankyrin-band 3 complexes on neighboring spectrin tetramers as well as the lateral association of the spectrin filaments. Hyperexpansion of the skeleton leaflets led to dissociation of the conglomerates of ankyrin-band 3 complexes, full-extension of the spectrin tetramers, and separation of the individual strands of spectrin tetramers. Clearly defined stands of spectrin tetramers in the hyperexpanded single-layered skeletal leaflets often contained two sets of globular protein masses that divided the spectrin tetramers into three segments of approximately equal length. DOE

N95-24464* National Aeronautics and Space Administration, Washington, DC.

AEROSPACE MEDICINE AND BIOLOGY: A CONTINUING BIBLIOGRAPHY WITH INDEXES (SUPPLEMENT 400)

Apr. 1995 147 p

(NASA-SP-7011(400); NAS 1.21:7011(400)) Avail: CASI HC A07

This bibliography lists 397 reports, articles and other documents introduced into the NASA Scientific and Technical Information System during April 1995. Subject coverage includes: aerospace medicine and physiology, life support systems and man/system technology, protective clothing, exobiology and extraterrestrial life, planetary biology, and flight crew behavior and performance. Author

N95-24497# Los Alamos National Lab., NM.

INTERIM REPORT OF THE ADVISORY COMMITTEE ON HUMAN RADIATION EXPERIMENTS

21 Oct. 1994 118 p

(DE95-003265; ACHRE-95003265) Avail: CASI HC A06/MF A02

The Advisory Committee on Human Radiation Experiments was created by President Clinton to advise the Human Radiation Interagency Working Group on the ethical and scientific criteria applicable to human radiation experiments carried out or sponsored by the U.S. Government. The Committee seeks to answer several fundamental question: What ethics criteria should be used to evaluate human radiation experiments? What was the Federal Government's role in human radiation experiments? What are the criteria for determining appropriate Federal responses where wrongs or harms have occurred? What lessons learned from studying past and present research standards and practices should be applied to the future? The Committee has been gathering vast amounts of information and working to render it orderly and accessible. In the next six months, the Committee will continue with the tasks of data gathering and organizing. The focus of the work, however, will be developing criteria for judging historical and contemporary experiments, policies, and procedures, as well as criteria for remedies that may be appropriate where harms or wrongs have ocurred. Based on findings, the Committee will make specific recommendations regarding policies for the future. DOE

N95-24556*# Utah Univ., Salt Lake City, UT. Div. of Radiology.

HUMAN PARATHYROID HORMONE-(1-38) RESTORES CANCELLOUS BONE TO THE IMMOBILIZED, OSTEOPENIC PROXIMAL TIBIAL METAPHYSIS IN RATS

Y. F. Ma, W. S. S. Jee, H. Z. Ke (Pfizer Central Research, Groton, CT.), B. Y. Lin (Guangdong Medical Coll., Guangdong Province, China.), X. G. Liang (Helen Hayes Hospital, NY.), M. Li (Florida Univ., Gainesville, FL.), and N. Yamamoto (Niigata Univ., Niigata, Japan) 1 Sep. 1994 28 p

(Contract NAG2-435; DE-AC02-76EV-00119; NIH-AR-38346)

(NASA-CR-197709; NAS 1.26:197709) Avail: CASI HC A03/MF A01

The purpose of this study was to determine if human parathyroid hormone-(1-38) (PTH) can restore cancellous bone mass to the established osteopenic, immobilized proximal tibial metaphyses (PTM) of female rats. The right hindlimbs of six-month-old female Sprague-Dawley rats were immobilized by bandaging the right hindlimbs to the abdomen. After 30 days of right hindlimb immobilization (RHLI), the rats were subcutaneously injected with 200 microgram hPTH(1-38)/kg/day for 15 (short-term) or 75 (longer-term) days. Static bone histomorphometry was performed on the primary spongiosa, while both static and dynamic histomorphometry were performed on the secondary spongiosa of the right PTM. Immobilization for 30 days without treatment decreased trabecular bone area, number and thickness in both primary and secondary spongiosa, and induced an increase in eroded perimeter and a decrease in tissue referent-bone formation rate (BFR/TV) in the secondary spongios. These changes reached a new steady state thereafter. Treatment with 200 microgram hPTH(1-38)/kg/day for 15 days, beginning at 30 days post immobilization (IM), significantly increased trabecular bone area, thickness and number in both primary and secondary spongiosa despite continuous IM when compared to the age-related and IM controls. The short-term (15 days) PTH treatment significantly increased labeling perimeter, mineral apposition rate and BFR/TV in the secondary spongiosa and stimulated longitudinal bone growth as compared to the age-related and IM controls. PTH treatment for longer-term (75 days) further increased trabecular bone area, thickness and number as compared to aging and IM controls and short-term (15 days) PTH treated groups. The bone formation indices in the secondary spongiosa of these longer-term treated rats were lower than that of short-term (15 days) PTH treated group, but they were still higher than those of IM and age-related controls. Our findings indicate that PTH treatment stimulates cancellous bone formation, restores and adds extra cancellous bone to the established, disuse-osteopenic proximal tibial metaphysis of continuously RHLI female rats. These results suggest that PTH may be a useful agent in treatment disuse-induced osteoporosis in humans. Author

N95-24564*# Wisconsin Univ., Madison, WI. Waisman Center.

PSYCHOPHYSICAL EVALUATION OF THREE-DIMENSIONAL AUDITORY DISPLAYS Annual Progress Report, 1 May 1994 - 30 Apr. 1995

Frederic L. Wightman 30 Apr. 1995 27 p

(Contract NCC2-542)

(NASA-CR-198010; NAS 1.26:198010) Avail: CASI HC A03/MF A01

This report describes the progress made during the first year of a three-year cooperative research agreement (CRA NCC2-542). The CRA proposed a program of applied psychophysical research designed to determine the requirements and limitations of three-dimensional (3-D) auditory display systems. These displays present synthesized stimuli to a pilot or virtual workstation operator that evoke auditory images at predetermined positions in space. The images can be either stationary or moving. In previous years, we completed a number of studies that provided data on listeners' abilities to localize stationary sound sources with 3-D displays. the current focus is on the use of 3-D displays in 'natural' listening conditions, which include listeners' head movements, moving sources, multiple sources and 'echoic' sources. The results of our research on two of these topics, the role of head movements and the role of echoes and reflections, were reported in the most recent semi-annual progress report (Appendix A). In the period since the last progress report we have been studying a third topic, the localizability of moving sources. The results of this research are described. Author

N95-24863 National Defence Research Establishment, Stockholm (Sweden). Huvudavdelning foer Maensklig Prestation och Funktion.

MOTIONSICKNESS-SEASICKNESS: SUMMARY OF EXISTING KNOWLEDGE AND SUGGESTED LINES OF DEVELOPMENT [ROERELSESJUKA-SJOESJUKA: OEVERSIKT OCH UTVECKLINGSLINJER]

M. Magnusson and H. Oernhagen Jun. 1994 48 p In SWAHILI Prepared in cooperation with Lunds Lasarett, Sweden

(PB95-141495; FOA-C-50107-5.1) Avail: Issuing Activity (National Technical Information Service (NTIS))

Motion sickness causes decrement in human performance during several activities. At high velocities at sea, on the road, and in the air motion sickness can also be a risk factor. Drugs against motion sickness have side effects and in some cases these side effects can be as limiting to performance as the motion sickness itself. The report and the list of publications was produced to inform about motion sickness, give the background behind different kinds of treatment, and also point at some possible ways to counteract the performance reducing effects of motion sickness in the future. NTIS

N95-25336# Civil Aeromedical Inst., Oklahoma City, OK.

AN ASSESSMENT OF AVIATION ACCIDENT RISK OF APHAKIC CIVIL AIRMEN BY CLASS OF MEDICAL CERTIFICATE HELD AND BY AGE: 1982-1985 Final Report

Van B. Nakagawara, Ronald W. Montgomery, and Kathryn J. Wood Mar. 1995 12 p

(FAA Task AM-A-91-PHY-144)

(DOT/FAA/AM-95/11) Avail: CASI HC A03/MF A01

In the FY-92/93 annual program guidance and current policy statement, the federal air surgeon requested continued investigation of surgical procedures and ophthalmic devices, such as cataract surgery and artificial lens implants, as to their relevance to medical certification. No previous statistical studies of the aviation accident risk of civil airmen with aphakia and intraocular lens (IOL) by class of federal aviation administration (FAA) airman medical certificate held have been performed. We evaluated the accident frequency of aphakic airmen (with or without IOL) by effective class of medical certificate (first-, second-, third-class) and by age (less than 50 and greater than or equal to 50 years) versus similarly stratified non-aphakic airman populations for the period 1982-85. Medical records were evaluated for all certified airmen during the study period who were

carrying FAA-specific pathology codes for aphakia and/or artificial lens implant. Aviation accident and active airman population frequencies were obtained from FAA databases and used to calculate accident rates. Third-class total aphakia and IOL airmen and third-class aphakia and IOL airmen less than 50 years of age had significantly higher (p less than .05) accident rates compared to corresponding non-aphakic airman populations. Our findings suggest that medical impairment may be an important risk factor for aviation accidents. Aeromedical certification and safety program considerations of the study findings are discussed. This data may be used by the office of aviation medicine and the aeromedical certification division in future administrative considerations of airmen with aphakia and IOL's and in the reviews of medical standards concerning these eye pathology categories. Author

N95-25371# Department of Energy, Washington, DC.
HUMAN RADIATION EXPERIMENTS: THE DEPARTMENT OF ENERGY ROADMAP TO THE STORY AND THE RECORDS
Feb. 1995 302 p
(DE95-006364; DOE/EH-0445) Avail: CASI HC A14/MF A03

The role of the US Government in conducting or sponsoring human radiation experiments has become the subject of public debate. Questions have been raised about the purpose, extent, and health consequences of these studies, and about how subjects were selected. The extent to which subjects provided informed consent is also under scrutiny. To respond to these questions, the Clinton administration has directed the US Department of Energy (DOE), along with other Federal agencies, to retrieve and inventory all records that document human radiation experiments. Many such records are now publicly available and will permit an open accounting and understanding of what took place. This report summarizes the Department's ongoing search for records about human radiation experiments. It is also a roadmap to the large universe of pertinent DOE information. DOE is working to instill greater openness - consistent with national security and other appropriate considerations - throughout its operations. A key aspect of this effort is opening DOE's historical records to independent research and analysis. DOE

N95-25570# Research Inst. of National Defence, Stockholm (Sweden).
MEASUREMENT OF BLOOD NITROGEN CONTENT AFTER RAPID COMPRESSIONS TO ASSESS THE SPEED OF NITROGEN UPTAKE DURING THE COMPRESSION PHASE OF SUBMARINE ESCAPE. (INCLUDES MEASUREMENT OF NITROGEN CONCENTRATION IN BLOOD FOLLOWING RAPID COMPRESSION TO 5 BAR)
M. Gennser, H. Oernhagen, V. Flook, I. M. Holmen, and A. L. Ustad Aug. 1994 35 p Prepared in cooperation with Selskapet for Industriell og Teknisk Forskning, Trondheim, Norway
(PB95-165726; FOA-R-94-00008-5.1-SE) Avail: CASI HC A03/MF A01

Nitrogen concentration was measured in arterial blood during 4 minutes at 5 bar overpressure following rapid compression (10 seconds). The conclusions are as followed: the change of nitrogen in the arterial blood, following a 10 second compression to 5 bar overpressure, was rapid and was 95% complete by 7 seconds after reaching the final pressure; there was a range of time constants for the change between subjects but how this relates to blood flow is not known for this report; and the uptake in the tissues drained by the venous blood had a time constant of 4.3 minutes. NTIS

N95-25800* National Aeronautics and Space Administration, Washington, DC.
AEROSPACE MEDICINE AND BIOLOGY: A CONTINUING BIBLIOGRAPHY WITH INDEXES (SUPPLEMENT 401)
May 1995 66 p
(NASA-SP-7011(401); NAS 1.21:7011(401)) Avail: CASI HC A04

This bibliography lists 140 reports, articles and other documents introduced into the NASA Scientific and Technical Information System during May 1995. Subject coverage includes: aerospace medicine, behavioral sciences, man/system technology and life support, and space biology. Author

N95-25981# Australian Nuclear Science and Technology Organisation, Canberra (Australia).
THE USE OF RADIOISOTOPES IN HUMAN EXPERIMENTS: COMMENTS IN RESPONSE TO RECENT MEDIA ARTICLES
R. E. Boyd Apr. 1994 9 p
(DE95-605680; INIS-mf-14385) Avail: Issuing Activity (Department of Energy (DOE)) (US Sales Only)

Recent newspaper articles question the propriety and ethical foundation of early experimental programs in which radioisotopes were administered to human subjects. This paper describes the relevant activities of ANSTO's predecessor, the Australian Atomic Energy Commission, and provides an historical background to these and subsequent events. DOE

N95-26204# Civil Aeromedical Inst., Oklahoma City, OK.
SLEEP PATTERNS IN AIR TRAFFIC CONTROLLERS WORKING RAPIDLY ROTATING SHIFTS: A FIELD STUDY Final Report
Crystal E. Cruz and Pamela S. DellaRocco Apr. 1995 18 p
(DOT/FAA/AM-95/12) Avail: CASI HC A03/MF A01

This study was part of a research program in shift work and fatigue in the Air Traffic Control (ATC) environment. The purpose of the study was to investigate three different shift schedules in use at ATC facilities with respect to potential disruption of the sleep/wake cycle. A straight day schedule of early morning shifts (i.e., beginning before 0800), and two variations of counterclockwise, rapidly rotating shift schedules, the 2-2-1 and 2-1-2, were analyzed in terms of total sleep time, asleep and awake times, and subjective ratings of sleep quality and sleepiness. Data were collected in daily logbooks by air traffic control specialists (ATCS's). Total sleep time on the 2-2-1 schedule showed a characteristic decline from approximately 8 hours before the two afternoon shifts, to 5 hours before the two early morning shifts, to 2.4 hours before the midnight shift. Total sleep time on the 2-1-2 schedule decreased from 7.5-8 hours before the two afternoon shifts and one midday shift to approximately 6 hours before the two early morning shifts. Total sleep time on the straight day shift schedule was approximately 6 hours for each day of the week. The least amount of sleep was obtained before early morning shifts in all of the schedules and before the midnight shift in the 2-2-1 schedule. Disruptions in the timing of sleep were limited to changes in the timing of waking up associated with rotations into the early morning shifts for the 2-2-1 and 2-1-2 schedules and, of course, the afternoon sleep before the midnight shift. Neither subjective ratings of sleep quality or sleepiness were found to vary by schedule type. More 'high' ratings of sleepiness on the drive home, however, were reported following the midnight shift than any other shift. Author

53 BEHAVIORAL SCIENCES

Includes psychological factors; individual and group behavior; crew training and evaluation; and psychiatric research.

N95-24237# Civil Aeromedical Inst., Oklahoma City, OK.
A LONGEVITY AND SURVIVAL ANALYSIS FOR A COHORT OF RETIRED AIRLINE PILOTS Final Report
Robert O. Besco (Professional Performance Improvement, Inc., Dallas, TX.), Satya P. Sangal (Wright State Univ., Dayton, OH.), Thomas E. Nesthus, and Stephen J. H. Veronneau Feb. 1995 15 p
(DOT/FAA/AM-95/5) Avail: CASI HC A03/MF A01

There is a popular belief in the aviation industry that retired pilots die at a younger age than the general population. If this belief is, in fact, correct, research into the factors or events precipitating an early mortality among retired airline crew members could be of interest to the FAA. Few studies have addressed the question 'Do retired airline pilots die at a younger age than their 60 year-old counterparts in the U.S. population?' Airline pilots reach the mandatory retirement age of 60 after an entire career of active health monitoring and maintenance required by the Federal Aviation Administration (FAA). In this study, a preliminary survey was made to determine the mortality and survival profile of retired pilots from a major U.S. airline. An initial sample of 2209 retired pilots and flight engineers was surveyed. Early and late retirees were dropped from the sample, leaving us with 1494 pilots who retired at age 60 between the study dates of April 1968 to 1993. The Lift Table Method was identified as the most suitable approach to analyze the pattern of mortality for this data set. Life Table analysis provides estimates of probabilities of surviving a given number of years after retirement. This technique allows subjects to enter (i.e., retire at age 60) or leave the study (i.e., die) at different points in time and it utilizes all the data on partial exposure to the risk of dying. It is

non-parametric and requires no assumptions about the distribution of the survival function. Due to the anonymity of our sampling and other resultant assumptions, comparisons were made with the 1980 census of the U.S. general population of 60 year-old males. A difference in life expectancy of more than 5 years longer was found for our sample of retired airline cockpit crew members. Half of the pilots in this sample retiring at age 60 were expected to live past 83.8 years of age, compared to 77.4 years for the general population of 60 year-old white males in 1980. The authors concluded that the question of lowered life expectancy for airline cockpit crew was not supported by the results of this particular data set. Author

N95-24510 Foerenade Fabriksverken, Linkoeping (Sweden). Huvudavdelning foer Maensklig Prestation och Funktion.
VISUAL PERFORMANCE WITH OMNIBUS 3: A COMPARATIVE EVALUATION OF ENHANCED GENERATION THREE IMAGE INTENSIFIER TECHNOLOGY [MOERKERSEENDE MED OMNIBUS 3: JAEMFOERANDE PROV MED BILDFOERSTAERKARE AV GENERATION TRE]
S. Sandberg, L. Forsberg, F. Hultman, and M. Weideryd Jun. 1994 30 p In SWAHILI
(PB95-141891; FOA-A-50025-5.2) Avail: Issuing Activity (National Technical Information Service (NTIS))

Omnibus 3 Night Vision Goggles (NVG), with enhanced micro channel plates and a new optical layout, were compared to standard third generation NVG's. Visual resolution, contrast discrimination and usefulness for car driving were investigated. The Omnibus 3 enlarged ocular diameter, greater eye relief and adjustability facilitated observation and driving. The increased number of micro channels improved visual resolution and contrast discrimination. The Omnibus 3 display was brighter and more comfortable than that of the older NVG's. The enhanced performance is practically valuable. NTIS

N95-24864 Research Inst. of National Defence, Stockholm (Sweden).
COLOUR VISION DEFICIENCIES: MATCHING AND CONFUSION OF COMPUTER COLOURS
G. Derefeldt, C. E. Hedin, K. O. Skoog, and T. Swartling Apr. 1994 73 p Limited Reproducibility: More than 20% of this document may be affected by microfiche quality
(PB95-141925; FOA-A-50024-5.2) Avail: CASI HC A04

The report compares current methods of testing congenital color deficiencies with tests designed to employ color video display units (VDU's). Twelve persons with congential color vision deficiencies were asked to judge and match colors presented on a full color VDU. Color stimuli were selected from different 'chromaticity-confusion lines' within the CIE 1931 chromaticity diagram; colors were chosen from one tritan, three protan, and three deutan confusion lines. The results show that the ability to discriminate VDU color stimuli is greatly impaired in protanopes and deutranopes, compared with both normal and deuteranomalous observers. When pairs of color stimuli lay on a protan or deutan confusion line, protanopes and deuteranopes frequently accepted them as equivalent even when the stimuli were separated by large distances in the chromaticity diagram. Protanopes performed slightly better on color stimuli from deutan lines than on those from protan lines. Similarly, deuteranopes showed better performance on protan than on deutan pairs. Deutranomalous observers performed better than dichromats but less well than normals. Color confusions shown by dichromats are in agreement with those shown in standard tests of color vision. Since a full color VDU has a larger chromaticity gamut than the pseudo-isochromatic plates or the Farnsworth D-15 test, it can be a powerful tool for screening dichromats from normals and for illustrating the difficulties persons with color deficiency will have in discriminating colors. NTIS

N95-26010 Tennessee Univ., Knoxville, TN.
COGNITIVE DIAGNOSIS COMBINED WITH LATENT TRAIT THEORY AND MULTIPHASE RESPONSES Final Report, 1 Jan. 1990 - 31 Aug. 1994
Fumiko Samejima 25 Nov. 1994 47 p Limited Reproducibility: More than 20% of this document may be affected by microfiche quality
(Contract N00014-90-J-1456; RR04204)
(AD-A288701; R01-1069-25-001-95) Avail: Issuing Activity (Defense Technical Information Center (DTIC))

This is a summary of the research conducted in 1900-94 under the title, 'Cognitive diagnosis Combined with Latent Trait Theory and Multiphase Responses.' During this period, effort was focused on: (1) further development of the theory and methodologies in latent trait models, including the proposal of a new model, called acceleration models; (2) development of methodologies for cognitive diagnosis assessment applying and expanding latent trait models, which eventually integrated into the method, called competency space approach; (3) theoretical integration of the nonparametric approaches and methods developed in the past years; and (4) writing research outcomes in refereed journal papers and book chapters, and presenting them at international and domestic conferences.

Derived from text

N95-26041 Aerospace Medical Research Labs., Wright-Patterson AFB, OH. Crew Systems Directorate.
TEMPORAL PACING IN VISUAL ATTENTION Final Report, Dec. 91 - May 1991 - May 1994
June J. Skelly, Merry M. Roe, and Mari R. Jones Jun. 1994 70 p
(AF Proj. ILIR)
(AD-A289785; AL/CF-TR-1994-0087) Avail: Issuing Activity (Defense Technical Information Center (DTIC))

Viewers engaged in a continuous letter classification task involving selective attending to one of two information streams (relevant and irrelevant). Temporal and spatial relations were systematically varied between the two streams to address hypotheses about external control of attention in dynamic environments. Relative event timing was varied both within and between the two streams. Spatial relationships for relevant and irrelevant events was the same for experiments 1 & 3, but different for experiment 2. Contrary to predictions from either spatial or object oriented approaches, attending and hence, performance, to relevant events in all three experiments was dependent on the integrated rhythmic patterns that obtained between the two streams, rather than spatial location and event features. Several alternative hypotheses addressed the issue of non-spatial control of attending to dynamic displays, The best account assumes viewer attending is 'paced' by rhythms emerging from an integration of relevant and irrelevant event streams. DTIC

54 MAN/SYSTEM TECHNOLOGY AND LIFE SUPPORT

Includes human engineering; biotechnology; and space suits and protective clothing.

For related information see also *16 Space Transportation.*

N95-24627*# National Aeronautics and Space Administration. Lyndon B. Johnson Space Center, Houston, TX.
EVALUATION OF RESTRAINT SYSTEM CONCEPTS FOR THE JAPANESE EXPERIMENT MODULE FLIGHT DEMONSTRATION
Carlos E. Sampaio (Lockheed Engineering and Sciences Co., Houston, TX.), Terence F. Fleming (Lockheed Engineering and Sciences Co., Houston, TX.), Mark A. Stuart (Lockheed Engineering and Sciences Co., Houston, TX.), and Lynn A. Backemeyer (Lockheed Engineering and Sciences Co., Houston, TX.) Feb. 1995 15 p
(Contract NAS9-18800)
(NASA-TM-104808; S-791; NAS 1.15:104808) Avail: CASI HC A03/MF A01

The current International Space Station configuration includes a Japanese Experiment Module which relies on a large manipulator and a smaller dexterous manipulator to operate outside the pressurized environment of the experiment module. The module's flight demonstration is a payload that will be mounted in the aft flight deck on STS-87 to evaluate a prototype of the dexterous manipulator. Since the payload operations entail two 8-hour scenarios on consecutive days, adequate operator restraint at the workstation will be critical to the perceived success or failure of the payload. Simulations in reduced gravity environment on the KC-135A were the only way to evaluate the restraint systems and workstation configuration. Two astronaut and two non-astronaut operators evaluated the Advanced Lower Body Extremities Restraint Test and a foot loop restraint system by performing representative tasks at the workstation in each of the two restraint systems; at the end of each flight they gave their impressions of each system and the workstation. Results indicated

that access to the workstation switch panels was difficult and manipulation of the hand controllers forced operators too low for optimal viewing of the aft flight deck monitors. The workstation panel should be angled for better visibility, and infrequently used switches should be on the aft flight deck panel. Pitch angle and placement of the hand controllers should optimize the operator's eye position with respect to the monitors. The lower body restraint was preferred over the foot loops because it allowed operators to maintain a more relaxed posture during long-duration tasks, its height adjustability allowed better viewing of aft flight deck monitors, and it provided better restraint for reacting forces imparted on the operator at the workstation. The foot loops provide adequate restraint for the flight demonstration tasks identified. Since results will impact the design of the workstation, both restraints should be flown and used during operation of the flight demonstration payload to evaluate the effect of restraint during long-duration tasks. Author

N95-25306* National Aeronautics and Space Administration. Lyndon B. Johnson Space Center, Houston, TX.
INFLATABLE RESCUE DEVICE Patent
Scott A. Swan, inventor (to NASA) 28 Mar. 1995 9 p Filed 4 May 1993 Supersedes N94-15883 (32 - 3, p 1137)
(NASA-Case-MSC-22244-1; US-Patent-5,401,069;
US-Patent-Appl-SN-066274; US-Patent-Class-294-1.1;
US-Patent-Class-294-19.1; US-Patent-Class-244-158R;
Int-Patent-Class-B25J-1/00) Avail: US Patent and Trademark Office

This invention discloses, in one aspect, a personal rescue device for use in outer space which has an inflatable flexible tube with a shaper apparatus herein. Gas under pressure flows through the shaper apparatus and into the flexible tube. The flexible tube is mounted to the shaper so that as it inflates it expands and deploys lengthwise away from the shaper. In one embodiment a housing contains the shaper and the flexible tube and the housing is designed to facilitate movement of the expanding tube from the housing so the expanding tube does not bunch up in the housing. Official Gazette of the U.S. Patent and Trademark Office

N95-25483# Massachusetts Inst. of Tech., Cambridge, MA. Dept. of Nuclear Engineering.
THE DEPENDENCE OF HUMAN RELIABILITY UPON TASK INFORMATION CONTENT
E. M. Hermanson and M. W. Golay Sep. 1994 49 p
(Contract DE-FG02-92ER-75787)
(DE95-006645; DOE/ER-75787/3; MIT-ANP-TR-026) Avail: CASI HC A03/MF A01

The role of human error in safety mishaps is an important factor in system design. As systems become increasingly complex the capacity of the human to deal with the added complexity is diminished. It is therefore crucial to understand the relationship between system complexity and human reliability so that systems may be built in such a way as to minimize human error. One way of understanding this relationship is to quantify system complexity and then measure the human reaction in response to situations of varying complexity. The quantification of system complexity may be performed by determining the information content present in the tasks that the human must execute. The purpose of this work is therefore to build and perform a consistent experiment which will determine the extent to which human reliability depends upon task information content. Two main conclusions may be drawn from this work. The first is that human reliability depends upon task information content. Specifically, as the information content contained in a task increases, the capacity of a human to deal successfully with the task decreases monotonically. Here the definition of total success is the ability to complete the task at hand fully and correctly. Furthermore, there exists a value of information content below which a human can deal with the task successfully, but above which the success of an individual decreases monotonically with increasing information. These ideas should be generalizable to any model where system complexity can be clearly and consistently defined. DOE

N95-25610 Institute for Human Factors TNO, Soesterberg (Netherlands).
ON PRODUCING SEQUENTIAL MOVEMENTS AND ACTIONS. AN INTEGRATIVE REVIEW AND AN UPDATE OF THE GENERALIZED MOTOR PROGRAM Final Report [OVER HET UITVOEREN VAN SEQUENTIELE BEWEGINGEN EN ACTIES. EIN INTEGREREnde LITERATUURSTUDIE EN EEN AANPASSING VAN HET GENERALIZED MOTOR PROGRAM]
W. B. Verwey 29 Aug. 1994 95 p Limited Reproducibility: More than 20% of this document may be affected by microfiche quality
(AD-A288628; TNO-TM-1994-B-14; TDCK-TD94-0076) Avail: Issuing Activity (Defense Technical Information Center (DTIC))

This report presents a review of the literature on the rapid production of sequences of movements in general and the effects of practice on sequence production in particular. A basic notion in this chapter is that a sequence of up to five movement elements can be programmed in advance by loading information on each element into a short-term motor buffer in a step-by-step manner. Subsequently, the content of this motor buffer is used for rapidly executing the entire sequence. Evidence is discussed that the programming of individual sequence elements may also occur while earlier sequence elements are executed. Due to a limited processing capacity this shows as a reduction in sequence production rate unless the individual elements are already executed slowly because of biomechanical limitations. When a particular movement sequence is practiced extensively an integrated representation of the sequence develops. This representation is termed a motor chunk. Motor chunks facilitate sequence programming in that they allow the motor buffer to be loaded in a single processing step. Individual movements and movement sequences which are controlled by motor chunks are concatenated by action plans. A distinction is made between hierarchical action plans and hierarchical control in terms of processes at different stages that are simultaneously active. Together, these notions lead to the tentative Stage Model of Sequence Production. DTIC

55 SPACE BIOLOGY

Includes exobiology; planetary biology; and extraterrestrial life.

No abstracts in this category.

59 MATHEMATICAL AND COMPUTER SCIENCES (GENERAL)

N95-25119*# Institute for Computer Applications in Science and Engineering, Hampton, VA.
THE FIRST ICASE/LARC INDUSTRY ROUNDTABLE: SESSION PROCEEDINGS Final Report
Sharath Girimaji Feb. 1995 69 p
(Contract NAS1-19480; RTOP 505-90-52-01)
(NASA-CR-195040; NAS 1.26:195040; ICASE-26) Avail: CASI HC A04/MF A01

The first 'ICASE/LaRC Industry Roundtable' was held on October 3-4, 1994, in Williamsburg, Virginia. The main purpose of the roundtable was to draw attention of ICASE/LaRC scientists to industrial research agendas. The roundtable was attended by about 200 scientists, 30% from NASA Langley; 20% from universities; 17% NASA Langley contractors (including ICASE personnel); and the remainder from federal agencies other than NASA Langley. The technical areas covered reflected the major research programs in ICASE and closely associated NASA branches. About 80% of the speakers were from industry. This report is a compilation of the session summaries prepared by the session chairmen. Author

N95-26085*# Institute for Computer Applications in Science and Engineering, Hampton, VA.
CUMULATIVE REPORTS AND PUBLICATIONS THROUGH DECEMBER 31, 1994 Final Report, 1975 - Dec. 1994
Hampton, VA NASA Mar. 1995 109 p

(Contracts NAS1-19480; NAS1-18605; NAS1-17070; NAS1-17130; NAS1-15810; NAS1-16394; NAS1-14101; NAS1-14472; RTOP 505-90-52-01)
(NASA-CR-195043; NAS 1.26:195043) Avail: CASI HC A06/MF A02

This document contains a complete list of Institute for Computer Applications in Science and Engineering (ICASE) reports. Since ICASE reports are intended to be preprints of articles that will appear in journals or conference proceedings, the published reference is included when it is available. Author

60 COMPUTER OPERATIONS AND HARDWARE

Includes hardware for computer graphics, firmware, and data processing.

For components see *33 Electronics and Electrical Engineering.*

N95-24648# Stanford Linear Accelerator Center, CA.
ASIC IMPLEMENTATION OF A DATA-PUSH ARCHITECTURE FOR SILICON PIXEL READOUT
F. Lin (California Univ., Davis, CA.), P. Bloom (California Univ., Davis, CA.), E. Burlingame (California Univ., Davis, CA.), B. Holbrook (California Univ., Davis, CA.), S. Mani (California Univ., Davis, CA.), S. Rojas (California Univ., Davis, CA.), S. Shapiro, and D. Cords Oct. 1994 5 p Presented at the Meeting of the Division of Particles and Fields of the American Physical Society, Albuquerque, NM, 2-6 Aug. 1994
(Contracts DE-AC03-76SF-00515; DE-FG03-91ER-40674)
(DE95-003368; SU-SLAC-PUB-6680; CONF-940816-50) Avail: CASI HC A01/MF A01

A digital circuit for reading out a silicon pixel array consisting of 64 x 256 elements has been designed. The readout architecture has a data-push sequencing with a throughput of about 200ns/hit. The critical elements of this design have been fabricated through MOSIS using the HP 1.2 micron double-metal-single-polysilicon process. Design details of the ASIC and test results are presented. Measurements of interface effects (metastability) between the analog and digital circuit are also presented. DOE

N95-25773# California Univ., Berkeley. Lawrence Berkeley Lab, CA.
WIDE-AREA TRAFFIC: THE FAILURE OF POISSON MODELING
Vern Paxson and Sally Floyd Aug. 1994 12 p Presented at the SIGCOMM 1994 Conference, London, England, 27 Aug. - 4 Sep. 1994
(Contract DE-AC03-76SF-00098)
(DE95-004685; LBL-35238; CONF-9408202-2) Avail: CASI HC A03/MF A01

Network arrivals are often modeled as Poisson processes for analytic simplicity, even though a number of traffic studies have shown that packet interarrivals are not exponentially distributed. The authors evaluate 21 wide-area traces, investigating a number of wide-area (TCP) arrival processes (session and connection arrivals, Fault Tolerant Processor Data (FTPDATA) connection arrivals within FTP sessions, and TELNET packet arrivals) to determine the error introduced by modeling them using Poisson processes. The authors find that user-initiated TCP session arrivals, such as remote-login and file-transfer, are well-modeled as Poisson processes with fixed hourly rates, but that other connection arrivals deviate considerably from Poisson; that modeling TELNET packet interarrivals as exponential grievously underestimates the burstiness of TELNET traffic, but using the empirical Teplib(DJCME92) interarrivals preserves burstiness over many time scales; and that FTPDATA connection arrivals within FTP sessions come bunched into 'connection bursts', the largest of which are so large that they completely dominate FTPDATA traffic. Finally, they offer some preliminary results regarding how the findings relate to the possible self-similarity of wide-area traffic. DOE

N95-26192 Naval Research Lab., Washington, DC.
DESIGN DOCUMENTATION FOR THE SINTRA PREPROCESSOR
Myong H. Kang and Rodney Peyton (Kaman Sciences Corp., Alexandria, VA.) 12 Dec. 1994 23 p Prepared in cooperation with Kaman Sciences Corp., Alexandria, VA Limited Reproducibility: More than 20% of this document may be affected by microfiche quality
(AD-A288804; NRL/MR/5540-94-7640) Avail: Issuing Activity (Defense Technical Information Center (DTIC))

In this document, we present the detailed description of the Secure INformation Through Replicated Architecture (SINTRA) preprocessor. The SINTRA preprocessor is an implementation of the replicated data mode (CKF94). We describe the role of the preprocessor in the SINTRA system, the internal code structure, and high level specifications of the preprocessor. We have prepared this report for system designers and programmers who want to understand the structure of the SINTRA preprocessor. We also hope this report is also helpful to the people who will maintain the SINTRA preprocessor code. In this report, we assume that the reader is familiar with the material presented in (CKF94) and (Kan94). DTIC

61 COMPUTER PROGRAMMING AND SOFTWARE

Includes computer programs, routines, alogorithms, and specific applications, e.g., CAD/CAM.

N95-24209*# National Aeronautics and Space Administration. Langley Research Center, Hampton, VA.
REDUCING NEURAL NETWORK TRAINING TIME WITH PARALLEL PROCESSING
James L. Rogers, Jr. and William J. LaMarsh, II (Computer Sciences Corp., Hampton, VA.) Feb. 1995 21 p
(RTOP 505-53-50-12)
(NASA-TM-110154; NAS 1.15:110154) Avail: CASI HC A03/MF A01

Obtaining optimal solutions for engineering design problems is often expensive because the process typically requires numerous iterations involving analysis and optimization programs. Previous research has shown that a near optimum solution can be obtained in less time by simulating a slow, expensive analysis with a fast, inexpensive neural network. A new approach has been developed to further reduce this time. This approach decomposes a large neural network into many smaller neural networks that can be trained in parallel. Guidelines are developed to avoid some of the pitfalls when training smaller neural networks in parallel. These guidelines allow the engineer: to determine the number of nodes on the hidden layer of the smaller neural networks; to choose the initial training weights; and to select a network configuration that will capture the interactions among the smaller neural networks. This paper presents results describing how these guidelines are developed. Author

N95-24224*# Hawaii Univ., Honolulu, HI. Dept. of Electrical Engineering.
ON THE TRELLIS STRUCTURE OF A (64,40,8) SUBCODE OF THE (64,42,8) THIRD-ORDER REED-MULLER CODE
Hari T. Moorthy, Shu Lin, and Gregory Uehara 1 Mar. 1995 19 p
(Grant NAG5-2613)
(NASA-CR-198019; NAS 1.26:198019; Rept-95-001) Avail: CASI HC A03/MF A01

A (64,40,8) subcode of the (64,42,8) third-order Reed-Muller code is proposed to NASA for high-speed satellite communications. This code can be either used alone or used as an inner-code in a concatenated coding system with the NASA standard (255,223,33) Reed-Solomon code as the outer code to achieve high performance with reduced decoding complexity. This Reed-Muller subcode has a relatively simple and parallel trellis structure and consequently can be decoded with a group of identical and relatively simple Viterbi decoders in parallel to achieve high-speed decoding. In this report, the complexities of various sectionalized trellis diagrams are analyzed. Based on this analysis, the trellis diagram with the smallest overall complexity will be used for the implementation of a high-speed decoder. Author

N95-24346# Sandia National Labs., Albuquerque, NM.
PARALLEL ALGORITHMS FOR DYNAMICALLY PARTITIONING UNSTRUCTURED GRIDS
P. Diniz (California Univ., Santa Barbara, CA.), S. Plimpton, B. Hendrickson, and R. Leland 1994 6 p Presented at the 7th SIAM Conference on Parallel Processing for Scientific Computing, San Francisco, CA, 15-17 Feb. 1995
(Contract DE-AC04-94AL-85000)
(DE95-001616; SAND-94-2444C; CONF-950212-2) Avail: CASI HC A02/MF A01

Grid partitioning is the method of choice for decomposing a wide variety of computational problems into naturally parallel pieces. In problems where computational load on the grid or the grid itself changes as the simulation progresses, the ability to repartition dynamically and in parallel is attractive for achieving higher performance. We describe three algorithms suitable for parallel dynamic load-balancing which attempt to partition unstructured grids so that computational load is balanced and communication is minimized. The execution time of algorithms and the quality of the partitions they generate are compared to results from serial partitioners for two large grids. The integration of the algorithms into a parallel particle simulation is also briefly discussed. DOE

N95-24429# Joint Publications Research Service, Washington, DC.
JPRS REPORT: SCIENCE AND TECHNOLOGY. CENTRAL EURASIA
20 Dec. 1994 46 p Transl. into ENGLISH from various Central Eurasian articles
(JPRS-UST-94-035) Avail: CASI HC A03/MF A01

Translated articles cover the following topics: fuzzy set theory as an uncertainty theory and the problem of reaching solutions in a fuzzy experiment, theoretical study of the possibility of using bichromophores in optical information processing devices, and functional-logical combining of air- and rocket-borne subsystems in designing of air- and rocket-borne complexes. Author

N95-24536# Rochester Univ., NY. Dept. of Computer Science.
DIALOGUE TRANSCRIPTION TOOLS
Peter A. Heeman and James F. Allen Aug. 1994 59 p Sponsored by Natural Sciences and Engineering Research Council of Canada
(Contract NSF IRI-90-13160; N00014-92-J-1512)
(TN-94-1) Avail: CASI HC A04/MF A01

This document describes a toolkit and guidelines for the transcription of dialogues. The premise of these tools is that a dialogue between two people can be broken down into a series of utterance files, each spoken by one participant. This allows the transcription tools and standards already designed for single speaker speech to be used. Author

N95-24659# Sandia National Labs., Albuquerque, NM. Computational Mechanics and Visualization Dept.
EXODUS 2: A FINITE ELEMENT DATA MODEL
Larry A. Schoof and Victor R. Yarberry Sep. 1994 239 p
(Contract DE-AC04-94AL-85000)
(DE95-004267; SAND-92-2137) Avail: CASI HC A11/MF A03

EXODUS II is a model developed to store and retrieve data for finite element analyses. It is used for preprocessing (problem definition), postprocessing (results visualization), as well as code to code data transfer. An EXODUS II data file is a random access, machine independent, binary file that is written and read via C, C++, or Fortran library routines which comprise the Application Programming Interface (API). DOE

N95-24708# International Centre for Theoretical Physics, Trieste (Italy).
SEMI-INFINITE MATHEMATICAL PROGRAMMING: A COLLOCATION APPROACH
M. K. Luhandjula, M. Belhouas (Tizi-Ouzo Univ., Tizi-Ouzo, Algeria.), and M. Ouanes (Tizi-Ouzo Univ., Tizi-Ouzo, Algeria.) Mar. 1994 9 p Sponsored by the International Atomic Energy Agency and the United Nations Educational Scientific and Cultural Organization
(DE94-634273; IC-94/46) Avail: CASI HC A02/MF A01 (US Sales Only)

A semi-infinite mathematical program arises when an infinite number of constraints has to be incorporated into a mathematical program framework. In this paper a Galerkin approximation like method is used to derive a way for dealing with a semi-infinite non linear mathematical program. Convergence is guaranteed and it is shown that linear and geometric semi-infinite programs can be solved as particular cases. Salient features of the approach along with advantages over other discretization schemes are also pointed out. A numerical example is provided for the sake of illustration. DOE

N95-24876*# Alabama Univ., Huntsville, AL. Research Institute.
SOFTWARE ENGINEERING AND DATA MANAGEMENT FOR AUTOMATED PAYLOAD EXPERIMENT TOOL Final Technical Report, 4 May - 30 Nov. 1994
Gary A. Maddux, Anna Provancha, and David Chattam Nov. 1994 82 p
(Contract NAS8-38609)
(NASA-CR-197703; NAS 1.26:197703; UAH-TR-5-33534) Avail: CASI HC A05/MF A01

The Microgravity Projects Office identified a need to develop a software package that will lead experiment developers through the development planning process, obtain necessary information, establish an electronic data exchange avenue, and allow easier manipulation/reformatting of the collected information. An MS-DOS compatible software package called the Automated Payload Experiment Tool (APET) has been developed and delivered. The objective of this task is to expand on the results of the APET work previously performed by University of Alabama in Huntsville (UAH) and provide versions of the software in a Macintosh and Windows compatible format. Appendix 1 science requirements document (SRD) Users Manual is attached. Author

N95-24898# Lawrence Livermore National Lab., Livermore, CA.
DEBUGGING THE VIRTUAL MACHINE
P. Miller and R. Pizzi 2 Sep. 1994 15 p Presented at the Symposium on Applied Computing (SAC 1995), Nashville, TN, 26-28 Feb. 1995
(Contract W-7405-eng-48)
(DE95-002193; UCRL-JC-118448; CONF-950242-1) Avail: CASI HC A03/MF A01

A computer program is really nothing more than a virtual machine built to perform a task. The program's source code expresses abstract constructs using low level language features. When a virtual machine breaks, it can be very difficult to debug because typical debuggers provide only low level machine implementation in formation to the software engineer. We believe that the debugging task can be simplified by introducing aspects of the abstract design into the source code. We introduce object-oriented debugging interface extention (OODIE), an object-oriented language extension that allows programmers to specify a virtual debugging environment which includes the design and abstract data types of the virtual machine. DOE

N95-24993*# Illinois Univ., Urbana-Champaign, IL.
SOFTWARE FAULT TOLERANCE IN COMPUTER OPERATING SYSTEMS
Ravishankar K. Iyer and Inhwan Lee 1994 30 p Reprint Sponsored in cooperation with Tandem Computers Inc., IBM Poughkeepsie, and the Illinois Computer Lab. for Aerospace Systems and Software
(Contract NAG1-613; N00014-91-J-1116)
(NASA-CR-197999; NAS 1.26:197999) Copyright Avail: CASI HC A03/MF A01

This chapter provides data and analysis of the dependability and fault tolerance for three operating systems: the Tandem/GUARDIAN fault-tolerant system, the VAX/VMS distributed system, and the IBM/MVS system. Based on measurements from these systems, basic software error characteristics are investigated. Fault tolerance in operating systems resulting from the use of process pairs and recovery routines is evaluated. Two levels of models are developed to analyze error and recovery processes inside an operating system and interactions among multiple instances of an operating system running in a distributed environment. The measurements show that the use of process pairs in Tandem systems, which was originally intended for tolerating hardware faults, allows the system to tolerate about 70% of defects in system software that result in processor failures. The loose coupling between processors which results in the backup execution (the processor state and the sequence of events occurring) being different from the original execution is a major reason for the measured software fault tolerance. The IBM/MVS system fault tolerance almost doubles when recovery routines are provided, in comparison to the case in which no recovery routines are available. However, even when recovery routines are provided, there is almost a 50% chance of system failure when critical system jobs are involved. Author

N95-25392 Polish Academy of Sciences, Warsaw (Poland). Instytut Podstawowych Problemow Techniki.
COMPUTER ANALYSIS OF GRAPHICS FOR THE REQUIREMENTS OF COMPUTER-AIDED DESIGN SYSTEMS [KOMPUTEROWA ANALIZA RYSUNKOW NA POTRZEBY SYSTEMOW KOMPUTEROWEGO WSPOMAGANIA PROJEKTOWANIA]
Dariusz Madej 1992 156 p In POLISH
(ISSN 0208-5658)

(IPPT-29-1992) Avail: Issuing Activity (Polish Academy of Sciences, Warsaw, Poland)

This dissertation discusses the analysis of graphics and maps from the standpoint of automatic input in CAD systems. The dissertation includes an introduction to the conversion of graphics to meet the requirements of CAD systems and a description of the graphics conversion, recognition, and interpretation procedures used for this purpose. The author proposes a method for integrating the processes of interpretation and the approximation of selected elements in the low-level analysis phase. This makes it possible to improve the accuracy of analysis and ensure that the results are useful for CAD systems. In the process the need for traditional time-consuming filtration, segmentation, shading, and polygon approximation techniques is eliminated. The author also proposes a method for analyzing RLC graphics which speeds up the conversion process and reduces the amount of RAM required by an order of magnitude by comparison with the methods described in the literature while maintaining recognition accuracy. The author theoretically estimates the degree of data reduction in low-level analysis using RLC, point matrices, and chain codes and polygons to represent the graphic elements. The most important accomplishments of the dissertation include the author's development of an original method for segmenting RLC graphics, techniques for recognizing characters attached to lines, and the principles for determining the context of a symbol in relation to the line, methods of approximating and interpreting lines, an algorithm for recognizing geodetic symbols and interpreting boundary lines on geodetic maps, the principles for augmenting the description of a graphic in the low-level analysis phase, and procedures for inputting data into finite-element analysis systems by automatic recognition of discrete grid graphics. The dissertation also describes the implementation of systems for automatic input of geodetic maps onto CAD systems and inputting the discrete grids used in finite-element analysis into a computer. Author

N95-25448# Melbourne Univ., Parkville (Australia). School of Physics.

MONTE CARLO SIMULATIONS WITH INDEFINITE AND COMPLEX-VALUED MEASURES

T. D. Kieu and C. J. Griffin 1993 9 p Sponsored by Australian Research Council

(DE95-607056; UM-P-93/70) Avail: CASI HC A02/MF A01 (US Sales Only)

A method is presented to tackle the sign problem in the simulations of systems having indefinite or complex-valued measures. In general, this new approach is shown to yield statistical errors smaller than the crude Monte Carlo using absolute values of the original measures. Exactly solvable, one-dimensional Ising models with complex temperature and complex activity illustrate the considerable improvements and the workability of the new method even when the crude one fails. DOE

N95-25507 Massachusetts Inst. of Tech., Cambridge, MA. Research Lab. of Electronics.

NUMERICAL AND SYMBOLIC ALGORITHMS FOR APPLICATION SPECIFIC SIGNAL PROCESSING Semiannual Report, 5 Apr. - 30 Oct. 1994

Alan V. Oppenheim 21 Nov. 1994 11 p Limited Reproducibility: More than 20% of this document may be affected by microfiche quality

(Contract N00014-93-1-0686)

(AD-A288202) Avail: Issuing Activity (Defense Technical Information Center (DTIC))

The first step in one aspect of our research in the RASSP program involves evaluating the abilities and limitations of current digital signal processing (DSP) system design tools. We are concerned with what algorithms the tools support, and how the tool abilities might be expanded in the future to support emerging signal processing techniques. Major accomplishments in our recent approximate processing research include: (1) conceptual and mathematical elaboration of approximate processing concepts, (2) formulation and implementation of a class of incremental refinement algorithms for the short-time Fourier transform, (3) illustration of design issues in the context of incremental refinement algorithms, (4) continued development of the IPUS-C++ software environment for supporting the design of application systems with embedded approximate signal processing capabilities, and (5) initiation of a project to build a software environment to support algorithm design for approximate signal processing. DTIC

N95-25571 Research Inst. of National Defence, Linkoeping (Sweden). Huvudavdelning foer Informationsteknologi.

IMPLEMENTATION OF WAVE PROPAGATION MODEL FOR WINDOWS [WINDOWSIMPLEMENTERING AV VAGUTBREDNINGSMODELL]

C. Ekstroem Jun. 1994 28 p In SWAHILI

(Proj. FOA-518372)

(PB95-165742; FOA-C-30767-3.6) Avail: Issuing Activity (National Technical Information Service (NTIS))

This thesis describes how to implement a simple model of wave propagation for Windows. The model is implemented as a DLL-file (Dynamic Linked Library) and is therefore a general module for Windows. The intention is that when developing a program for Windows, e.g. Visual Basic or C, this module can be called when calculations of wave propagation are needed. NTIS

N95-25797*# Overset Methods, Inc., Los Altos, CA.

THE COUPLING OF FLUIDS, DYNAMICS, AND CONTROLS ON ADVANCED ARCHITECTURE COMPUTERS Final Report, 1 Jun. 1994 - 31 May 1995

Christopher Atwood May 1995 32 p Original contains color illustrations

(Contract NCC2-799)

(NASA-CR-197727; NAS 1.26:197727) Avail: CASI HC A03/MF A01; 1 functional color page

This grant provided for the demonstration of coupled controls, body dynamics, and fluids computations in a workstation cluster environment; and an investigation of the impact of peer-peer communication on flow solver performance and robustness. The findings of these investigations were documented in the conference articles.The attached publication, 'Towards Distributed Fluids/Controls Simulations', documents the solution and scaling of the coupled Navier-Stokes, Euler rigid-body dynamics, and state feedback control equations for a two-dimensional canard-wing. The poor scaling shown was due to serialized grid connectivity computation and Ethernet bandwidth limits. The scaling of a peer-to-peer communication flow code on an IBM SP-2 was also shown. The scaling of the code on the switched fabric-linked nodes was good, with a 2.4 percent loss due to communication of intergrid boundary point information. The code performance on 30 worker nodes was 1.7 (mu)s/point/iteration, or a factor of three over a Cray C-90 head. The attached paper, 'Nonlinear Fluid Computations in a Distributed Environment', documents the effect of several computational rate enhancing methods on convergence. For the cases shown, the highest throughput was achieved using boundary updates at each step, with the manager process performing communication tasks only. Constrained domain decomposition of the implicit fluid equations did not degrade the convergence rate or final solution. The scaling of a coupled body/fluid dynamics problem on an Ethernet-linked cluster was also shown. Derived from text

N95-25867*# Brown Univ., Providence, RI. Dept. of Computer Science.

THREE-DIMENSIONAL USER INTERFACES FOR SCIENTIFIC VISUALIZATION Status Report, Jan. 1994 - Jan. 1995

Andries vanDam 20 Jan. 1995 31 p Original contains color illustrations

(Grant NAG2-830)

(NASA-CR-197923; NAS 1.26:197923) Avail: CASI HC A03/MF A01; 9 functional color pages

The main goal of this project is to develop novel and productive user interface techniques for creating and managing visualizations of computational fluid dynamics (CFD) datasets. We have implemented an application framework in which we can visualize computational fluid dynamics user interfaces. This UI technology allows users to interactively place visualization probes in a dataset and modify some of their parameters. We have also implemented a time-critical scheduling system which strives to maintain a constant frame-rate regardless of the number of visualization techniques. In the past year, we have published parts of this research at two conferences, the research annotation system at Visualization 1994, and the 3D user interface at UIST 1994. The real-time scheduling system has been submitted to SIGGRAPH 1995 conference. Copies of these documents are included with this report. For individual titles, see N95-25868 through N95-25870.

N95-25868*# Brown Univ., Providence, RI. Dept. of Computer Science.
THE 3D WIDGETS FOR EXPLORATORY SCIENTIFIC VISUALIZATION
c34

Kenneth P. Herndon and Tom Meyer *In its* Three-Dimensional User Interfaces for Scientific Visualization 20 Jan. 1995 2 p (For primary document see N95-25867 08-61)
(Contract N00014-91-J-4052; ARPA Order 8225)
Avail: CASI HC A01/MF A01; 9 functional color pages

Computational fluid dynamics (CFD) techniques are used to simulate flows of fluids like air or water around such objects as airplanes and automobiles. These techniques usually generate very large amounts of numerical data which are difficult to understand without using graphical scientific visualization techniques. There are a number of commercial scientific visualization applications available today which allow scientists to control visualization tools via textual and/or 2D user interfaces. However, these user interfaces are often difficult to use. We believe that 3D direct-manipulation techniques for interactively controlling visualization tools will provide opportunities for powerful and useful interfaces with which scientists can more effectively explore their datasets. A few systems have been developed which use these techniques. In this paper, we will present a variety of 3D interaction techniques for manipulating parameters of visualization tools used to explore CFD datasets, and discuss in detail various techniques for positioning tools in a 3D scene. Derived from text

N95-25869*# Digital Equipment Corp., Cambridge, MA.
AN ANNOTATION SYSTEM FOR 3D FLUID FLOW VISUALIZATION
c34

Maria M. Loughlin and John F. Hughes (Brown Univ., Providence, RI.) *In* Digital Equipment Corp., Three-Dimensional User Interfaces for Scientific Visualization 20 Jan. 1995 8 p Sponsored in part by Digital Equipment Corp.; NSF; DARPA; IBM; NCR; Sun Microsystems; and Hewlett Packard (For primary document see N95-25867 08-61)
Avail: CASI HC A02/MF A01; 9 functional color pages

Annotation is a key activity of data analysis. However, current systems for data analysis focus almost exclusively on visualization. We propose a system which integrates annotations into a visualization system. Annotations are embedded in 3D data space, using the Post-it metaphor. This embedding allows contextual-based information storage and retrieval, and facilitates information sharing in collaborative environments. We provide a traditional database filter and a Magic Lens filter to create specialized views of the data. The system has been customized for fluid flow applications, with features which allow users to store parameters of visualization tools and sketch 3D volumes. Author

N95-25870*# Brown Univ., Providence, RI. NSF/ARPA Science and Technology Center for Computer Graphics and Scientific Visualization.
SCHEDULING TIME-CRITICAL GRAPHICS ON MULTIPLE PROCESSORS

Tom W. Meyer and John F. Hughes *In its* Three-Dimensional User Interfaces for Scientific visualization 20 Jan. 1995 5 p Sponsored in part my NSF/ARP; Sun Microsystems; Autodesk, Microsoft; and TACO Original contains color illustrations (For primary document see N95-25867 08-61)
Avail: CASI HC A02/MF A01; 9 functional color pages

This paper describes an algorithm for the scheduling of time-critical rendering and computation tasks on single- and multiple-processor architectures, with minimal pipelining. It was developed to manage scientific visualization scenes consisting of hundreds of objects, each of which can be computed and displayed at thousands of possible resolution levels. The algorithm generates the time-critical schedule using progressive-refinement techniques; it always returns a feasible schedule and, when allowed to run to completion, produces a near-optimal schedule which takes advantage of almost the entire multiple-processor system. Author

N95-25879*# National Aeronautics and Space Administration. Lewis Research Center, Cleveland, OH.
ESSENTIALLY NONOSCILLATORY (ENO) RECONSTRUCTIONS VIA EXTRAPOLATION

Ambady Suresh (NYMA, Inc., Brook Park, OH.) and Philip C. E. Jorgenson Apr. 1995 13 p Presented at the 33rd Aerospace Sciences Meeting and Exhibit, Reno, NV, 9-12 Jan. 1995; sponsored byAIAA
(Contract NAS3-25266; RTOP 505-62-52)
(NASA-TM-106907; E-9607; NAS 1.15:106907; AIAA Paper 95-0467)
Avail: CASI HC A03/MF A01

In this paper, the algorithm for determining the stencil of a one-dimensional Essentially Nonoscillatory (ENO) reconstruction scheme on a uniform grid is reinterpreted as being based on extrapolation. This view leads to another extension of ENO reconstruction schemes to two-dimensional unstructured triangular meshes. The key idea here is to select several cells of the stencil in one step based on extrapolation rather than one cell at a time. Numerical experiments confirm that the new scheme yields sharp nonoscillatory reconstructions and that it is about five times faster than previous schemes. Author

N95-26045# Finnish Centre for Radiation and Nuclear Safety, Helsinki (Finland).
RELIABILITY ANALYSIS OF SOFTWARE BASED SAFETY FUNCTIONS

U. Pulkkinen (Technical Research Centre of Finland, Espoo, Finland.) May 1993 65 p
(DE95-606516; STUK-YTO-TR-53) Avail: CASI HC A04/MF A01 (US Sales Only)

The methods applicable in the reliability analysis of software based safety functions are described in the report. Although the safety functions also include other components, the main emphasis in the report is on the reliability analysis of software. The check list type qualitative reliability analysis methods, such as failure mode and effects analysis (FMEA), are described, as well as the software fault tree analysis. The safety analysis based on the Petri nets is discussed. The most essential concepts and models of quantitative software reliability analysis are described. The most common software metrics and their combined use with software reliability models are discussed. The application of software reliability models in PSA is evaluated; it is observed that the recent software reliability models do not produce the estimates needed in PSA directly. As a result from the study some recommendations and conclusions are drawn. The need of formal methods in the analysis and development of software based systems, the applicability of qualitative reliability engineering methods in connection to PSA and the need to make more precise the requirements for software based systems and their analyses in the regulatory guides should be mentioned. DOE

N95-26058 Carnegie-Mellon Univ., Pittsburgh, PA. Software Engineering Inst.
QUARTERLY UPDATE Quarterly Report, Jul. - Sep. 1994

Sep. 1994 42 p Limited Reproducibility: More than 20% of this document may be affected by microfiche quality
(AD-A288743; SEI-94-CDRL-103-3) Avail: Issuing Activity (Defense Technical Information Center (DTIC))

The Software Engineering Institute (SBI) hosted its annual Software Engineering Symposium in August. This year's theme was '10 Years of Improving the State of the Practice.' The Empirical Methods Project and the Software Process Measurement Project completed a technical report on organizational gains associated with capability maturity model-based software process improvement. DTIC

N95-26167# Allied-Signal Aerospace Co., Kansas City, MO.
CMM FUNCTIONAL SOFTWARE EVALUATION (ALGORITHM QUALIFICATION) Final Report

J. L. Cummins Jan. 1995 5 p
(Contract DE-AC04-76DP-00613)
(DE95-006178; KCP-613-5452) Avail: CASI HC A01/MF A01

The mathematical algorithms for geometric features contained in proprietary coordinate measuring machine (CMM) vendor's software were tested by standardized data set applications and results were compared with known algorithm outputs. The CMM vendor's proprietary software requirements shield the user from visibility of the actual equations programmed into the coded software routines. All that is visible to the CMM inspector is the input data and the resulting output. Details of how those results were calculated from sample probing data would not typically be visible. Therefore, to gain rigorous confidence that the CMM inspection routines function as desired, independent testing was performed using sets of data with known results. Comparisons with the known results then verified functional algorithm acceptance. Agreement to the fifth and sixth decimal place was common. DOE

N95-26206*# Michigan Univ., Ann Arbor, MI. Dept. of Electrical Engineering and Computer Science.
INSTRUCTABLE AUTONOMOUS AGENTS Ph.D. Thesis
Scott Bradley Huffman Jan. 1994 151 p
(Contract NCC2-517)
(NASA-CR-197802; NAS 1.26:197802; CSE-TR-193-94) Avail: CASI HC A08/MF A02

In contrast to current intelligent systems, which must be laboriously programmed for each task they are meant to perform, instructable agents can be taught new tasks and associated knowledge. This thesis presents a general theory of learning from tutorial instruction and its use to produce an instructable agent. Tutorial instruction is a particularly powerful form of instruction, because it allows the instructor to communicate whatever kind of knowledge a student needs at whatever point it is needed. To exploit this broad flexibility, however, a tutorable agent must support a full range of interaction with its instructor to learn a full range of knowledge. Thus, unlike most machine learning tasks, which target deep learning of a single kind of knowledge from a single kind of input, tutorability requires a breadth of learning from a broad range of instructional interactions. The theory of learning from tutorial instruction presented here has two parts. First, a computational model of an intelligent agent, the problem space computational model, indicates the types of knowledge that determine an agent's performance, and thus, that should be acquirable via instruction. Second, a learning technique, called situated explanation specifies how the agent learns general knowledge from instruction. The theory is embodied by an implemented agent, Instructo-Soar, built within the Soar architecture. Instructo-Soar is able to learn hierarchies of completely new tasks, to extend task knowledge to apply in new situations, and in fact to acquire every type of knowledge it uses during task performance - control knowledge, knowledge of operators' effects, state inferences, etc. - from interactive natural language instructions. This variety of learning occurs by applying the situated explanation technique to a variety of instructional interactions involving a variety of types of instructions (commands, statements, conditionals, etc.). By taking seriously the requirements of flexible tutorial instruction, Instructo-Soar demonstrates a breadth of interaction and learning capabilities that goes beyond previous instructable systems, such as learning apprentice systems. Instructo-Soar's techniques could form the basis for future 'instructable technologies' that come equipped with basic capabilities, and can be taught by novice users to perform any number of desired tasks. Author

62 COMPUTER SYSTEMS

Includes computer networks and special application computer systems.

N95-24250# Oak Ridge National Lab., TN.
DOLIB: DISTRIBUTED OBJECT LIBRARY
E. F. DAzevedo and C. H. Romine Oct. 1994 49 p
(Contract DE-AC05-84OR-21400)
(DE95-004791; ORNL/TM-12744) Avail: CASI HC A03/MF A01

This report describes the use and implementation of DOLIB (Distributed Object Library), a library of routines that emulates global or virtual shared memory on Intel multiprocessor systems. Access to a distributed global array is through explicit calls to gather and scatter. Advantages of using DOLIB include: dynamic allocation and freeing of huge (gigabyte) distributed arrays, both C and FORTRAN callable interfaces, and the ability to mix shared-memory and message-passing programming models for ease of use and optimal performance. DOLIB is independent of language and compiler extensions and requires no special operating system support. DOLIB also supports automatic caching of read-only data for high performance. The virtual shared memory support provided in DOLIB is well suited for implementing Lagrangian particle tracking techniques. We have also used DOLIB to create DONIO (Distributed Object Network I/O Library), which obtains over a 10-fold improvement in disk I/O performance on the Intel Paragon. DOE

N95-24290# Department of Energy, Washington, DC. Office of Scientific Computing.
ESNET PROGRAM PLAN 1994
S. Merola 1 Nov. 1994 136 p
(DE95-005329; DOE/ER-0632) Avail: CASI HC A07/MF A02

This Program Plan characterizes ESnet with respect to the current and future needs of Energy Research programs for network infrastructure, services, and development. In doing so, this document articulates the vision and recommendations of the ESnet Steering Committee regarding ESnet's development and its support of computer networking facilities and associated user services. To afford the reader a perspective from which to evaluate the ever-increasing utility of networking to the Energy Research community, we have also provided a historical overview of Energy Research networking. Networking has become an integral part of the work of DOE principal investigators, and this document is intended to assist the Office of Scientific Computing in ESnet program planning and management, including prioritization and funding. In particular, we identify the new directions that ESnet's development and implementation will take over the course of the next several years. Our basic goal is to ensure that the networking requirements of the respective scientific programs within Energy Research are addressed fairly. The proliferation of regional networks and additional network-related initiatives by other Federal agencies is changing the process by which we plan our own efforts to serve the DOE community. ESnet provides the Energy Research community with access to many other peer-level networks and to a multitude of other interconnected network facilities. ESnet's connectivity and relationship to these other networks and facilities are also described in this document. Major Office of Energy Research programs are managed and coordinated by the Office of Basic Energy Sciences, the Office of High Energy and Nuclear Physics, the Office of Magnetic Fusion Energy, the Office of Scientific Computing, and the Office of Health and Environmental Research. Summaries of these programs are presented, along with their functional and technical requirements for wide-area networking. DOE

N95-24342# Argonne National Lab., IL.
COMPUTATIONAL LOAD IN MODEL PHYSICS OF THE PARALLEL NCAR COMMUNITY CLIMATE MODEL
J. G. Michalakes and R. S. Nanjundiah Nov. 1994 14 p
(Contract W-31-109-eng-38)
(DE95-005410; ANL/MCS-TM-186) Avail: CASI HC A03/MF A01

Maintaining a balance of computational load over processors is a crucial issue in parallel computing. For efficient parallel implementation, complex codes such as climate models need to be analyzed for load imbalances. In the present study we focus on the load imbalances in the physics portion of the community climate model's (CCM2) distributed-memory parallel implementation on the Intel Touchstone DELTA computer. We note that the major source of load imbalance is the diurnal variation in the computation of solar radiation. Convective weather patterns also cause some load imbalance. Land-ocean contrast is seen to have little effect on computational load in the present version of the model. DOE

N95-24343# Los Alamos National Lab., NM.
A PARALLEL, PORTABLE AND VERSATILE TREECODE
M. S. Warren and J. K. Salmon (Australian National Univ., Canberra, Australia.) 1994 7 p Presented at the 7th SIAM Conference on Parallel Processing for Scientific Computing, San Francisco, CA, 15-17 Feb. 1995
(Contract W-7405-eng-36)
(DE95-000842; LA-UR-94-3301; CONF-950212-1) Avail: CASI HC A02/MF A01

Portability and versatility are important characteristics of a computer program which is meant to be generally useful. We describe how we have developed a parallel N-body treecode to meet these goals. A variety of applications to which the code can be applied are mentioned. Performance of the program is also measured on several machines. A 512 processor Intel Paragon can solve for the forces on 10 million gravitationally interacting particles to 0.5% rms accuracy in 28.6 seconds. DOE

N95-24382*# National Aeronautics and Space Administration. Langley Research Center, Hampton, VA.
AN OPTIMIZED IMPLEMENTATION OF A FAULT-TOLERANT CLOCK SYNCHRONIZATION CIRCUIT
Wilfredo Torres-Pomales Feb. 1995 24 p
(RTOP 505-64-10-13)
(NASA-TM-109176; NAS 1.15:109176) Avail: CASI HC A03/MF A01

A fault-tolerant clock synchronization circuit was designed and tested. A comparison to a previous design and the procedure followed to achieve the current optimization are included. The report also includes a description of the system and the results of tests performed to study the synchronization and fault-tolerant characteristics of the implementation. Author

N95-24496# California Univ., Berkeley. Lawrence Berkeley Lab, CA.
A TOOL FOR DEBUGGING INTERNET MULTICAST ROUTING
Deborah Agarwal and Sally Floyd Mar. 1994 8 p Presented at the 1994 ACM Symposium on Applied Computing, Phoenix, AZ, 6-8 Mar. 1994
(Contract DE-AC03-76SF-00098)
(DE95-003433; LBL-34780; CONF-9403132-2) Avail: CASI HC A02/MF A01

The authors describe a debugging tool that is an effective means of analyzing problems with multicast packet routing in a network. Multicast packet routing is a source-driven distributed calculation performed by the routers in a multicast network. The routes taken by multicast packets are difficult to predict manually due to the large number of variables that must be considered. The multicast route debugging tool allows off-line investigation of the route taken by a multicast packet and the effects of network modifications on that route. The tool has already proved useful in debugging the problems that have occurred in the experimental Internet Multicast Backbone. The multicast route debugging tool currently predicts multicast routes of packets using the distance-vector truncated-broadcast algorithm implemented for Internet multicast traffic. They will be upgrading the tool to allow the user to choose other multicast routing algorithms. DOE

N95-24563*# Santa Clara Univ., CA. Dept. of Computer Engineering.
PARALLEL PROCESSING FOR SCIENTIFIC COMPUTATIONS Final Report
Hasan S. AlKhatib 29 Mar. 1995 49 p
(Contract NCC2-644)
(NASA-CR-198013; NAS 1.26:198013) Avail: CASI HC A03/MF A01

The scope of this project dealt with the investigation of the requirements to support distributed computing of scientific computations over a cluster of cooperative workstations. Various experiments on computations for the solution of simultaneous linear equations were performed in the early phase of the project to gain experience in the general nature and requirements of scientific applications. A specification of a distributed integrated computing environment, DICE, based on a distributed shared memory communication paradigm has been developed and evaluated. The distributed shared memory model facilitates porting existing parallel algorithms that have been designed for shared memory multiprocessor systems to the new environment. The potential of this new environment is to provide supercomputing capability through the utilization of the aggregate power of workstations cooperating in a cluster interconnected via a local area network. Workstations, generally, do not have the computing power to tackle complex scientific applications, making them primarily useful for visualization, data reduction, and filtering as far as complex scientific applications are concerned. There is a tremendous amount of computing power that is left unused in a network of workstations. Very often a workstation is simply sitting idle on a desk. A set of tools can be developed to take advantage of this potential computing power to create a platform suitable for large scientific computations. The integration of several workstations into a logical cluster of distributed, cooperative, computing stations presents an alternative to shared memory multiprocessor systems. In this project we designed and evaluated such a system. Author

N95-24597# Stanford Linear Accelerator Center, CA.
ADVENTURES IN THE EVOLUTION OF A HIGH-BANDWIDTH NETWORK FOR CENTRAL SERVERS
K. L. Swartz, L. Cottrell, and M. Dart Aug. 1994 8 p Presented at the 8th System Administration Conference, San Diego, CA, 21-23 Sep. 1994
(Contract DE-AC03-76SF-00515)
(DE95-006215; SU-SLAC-PUB-6567; CONF-9409186-2) Avail: CASI HC A02/MF A01

In a small network, clients and servers may all be connected to a single Ethernet without significant performance concerns. As the number of clients on a network grows, the necessity of splitting the network into multiple sub-networks, each with a manageable number of clients, becomes clear. Less obvious is what to do with the servers. Group file servers on subnets and multihomed servers offer only partial solutions. Many other types of servers do not lend themselves to a decentralized model, and tend to collect on another, well-connected but overloaded Ethernet. The higher speed of FDDI seems to offer an easy solution, but in practice both expense and interoperability problems render FDDI a poor choice. Ethernet switches appear to permit cheaper and more reliable networking to the servers while providing an aggregate network bandwidth greater than a simple Ethernet. This paper studies the evolution of the server networks at SLAC. Difficulties encountered in the deployment of FDDI are described, as are the tools and techniques used to characterize the traffic patterns on the server network. Performance of Ethernet, FDDI, and switched Ethernet networks is analyzed, as are reliability and maintainability issues for these alternatives. The motivations for re-designing the SLAC general server network to use a switched Ethernet instead of FDDI are described, as are the reasons for choosing FDDI for the farm and firewall networks at SLAC. Guidelines are developed which may help in making this choice for other networks. DOE

N95-24612# Los Alamos National Lab., NM.
A PRACTICAL APPROACH TO PORTABILITY AND PERFORMANCE PROBLEMS ON MASSIVELY PARALLEL SUPERCOMPUTERS
D. M. Beazley and P. S. Lomdahl (Utah Univ., Salt Lake City, UT.) Dec. 1994 10 p Presented at the Performance Tuning for Parallel Computing Systems, Cape Cod, MA, 3-5 Oct. 1994
(Contract W-7405-eng-36)
(DE95-005251; LA-UR-94-4339; CONF-9410291-1) Avail: CASI HC A02/MF A01

We present an overview of the tactics we have used to achieve a high-level of performance while improving portability for a large-scale molecular dynamics code SPaSM. SPaSM was originally implemented in ANSI C with message passing for the Connection Machine 5 (CM-5). In 1993, SPaSM was selected as one of the winners in the IEEE Gordon Bell Prize competition for sustaining 50 Gflops on the 1024 node CM-5 at Los Alamos National Laboratory. Achieving this performance on the CM-5 required rewriting critical sections of code in CDPEAC assembler language. In addition, the code made extensive use of CM-5 parallel I/O and the CMMD message passing library. Given this highly specialized implementation, we describe how we have ported the code to the Cray T3D and high performance workstations. In addition we will describe how it has been possible to do this using a single version of source code that runs on all three platforms without sacrificing any performance. Sound too good to be true? We hope to demonstrate that one can realize both code performance and portability without relying on the latest and greatest prepackaged tool or parallelizing compiler. DOE

N95-24634*# Odyssey Research Associates, Inc., Ithaca, NY.
TOWARDS A FORMAL SEMANTICS FOR Ada 9X Final Report
David Guaspari, John McHugh, Polak Wolfgang, and Mark Saaltink Mar. 1995 158 p
(Contract NAS1-18972; RTOP 505-64-10-56)
(NASA-CR-195037; NAS 1.26:195037; ORA-TM-95-0044) Avail: CASI HC A08/MF A02

The Ada 9X language precision team was formed during the revisions of Ada 83, with the goal of analyzing the proposed design, identifying problems, and suggesting improvements, through the use of mathematical models. This report defines a framework for formally describing Ada 9X, based on Kahn's 'natural semantics', and applies the framework to portions of the language. The proposals for exceptions and optimization freedoms are also analyzed, using a different technique. Author

N95-24658# Argonne National Lab., IL. Mathematics and Computer Science Div.
USERS MANUAL FOR KSP DATA-STRUCTURE-NEUTRAL CODES IMPLEMENTING KRYLOV SPACE METHODS
William Gropp and Barry Smith (California Univ., Los Angeles, CA.) Aug. 1994 41 p
(Contract W-31-109-eng-38)
(DE95-004265; ANL-93/30) Avail: CASI HC A03/MF A01

The combination of a Krylov space method and a preconditioner is at the heart of most modern numerical codes for the iterative solution of linear systems. This document contains both a users manual and a description of the implementation for the Krylov space methods package

KSP included as part of the Portable, Extensible Tools for Scientific computation package (PETSc). PETSc is a large suite of data-structure-neutral libraries for the solution of large-scale problems in scientific computation, in particular on massively parallel computers. The methods in KSP are conjugate gradient method, GMRES, BiCG-Stab, two versions of transpose-free QMR, and others. All of the methods are coded using a common, data-structure-neutral framework and are compatible with the sequential, parallel, and out-of-core solution of linear systems. The codes make no assumptions about the representation of the linear operator; implicitly defined operators (say, calculated using differencing) are fully supported. In addition, unlike all other iterative packages we are aware of, the vector operations are also data-structure neutral. Once certain vector primitives are provided, the same KSP software runs unchanged using any vector storage format. It is not restricted to a few common vector representations. The codes described are actual working codes that run on a large variety of machines including the IBM SP1, Intel DELTA, workstations, networks of workstations, the TMC CM-5, and the CRAY C90. New Krylov space methods may be easily added to the package and used immediately with any application code that has been written using KSP; no changes to the application code are needed. DOE

N95-24681# Sandia National Labs., Albuquerque, NM. Parallel Computing Scienes Dept.

DYNAMIC LOAD BALANCING FOR PARALLEL FINITE ELEMENT METHODS WITH ADAPTIVE h- AND p-REFINEMENT

Karen D. Devine and Joseph E. Flaherty (Rensselaer Polytechnic Inst., Troy, NY.) 1994 7 p Presented at the 7th SIAM Conference on Parallel Processing for Scientific Computing, San Francisco, CA, 15-17 Feb. 1995

(Contract DE-AC04-94AL-85000)

(DE95-004521; SAND-94-2420C; CONF-950212-4) Avail: CASI HC A02/MF A01

We describe a dynamic load-balancing strategy for parallel finite element methods with adaptive mesh (h-) and order (p-) refinement. The load-balancing algorithm is based on the tiling load-balancing system, where global balance is achieved by performing local balancing within overlapping neighborhoods of processors. Tiling is applied to each mesh level created by the adaptive h-refinement. Weights are used in the migration routines to reflect the nonuniform elemental work loads caused by adaptive p-refinement. The combination of adaptive refinement and tiling significantly reduces total execution time relative to fixed-mesh, fixed-order methods yielding comparable accuracy, as we demonstrate with experiments on an nCUBE/2. DOE

N95-24881# Pacific Northwest Lab., Richland, WA.

OBJECT-ORIENTED PARALLEL POLYGON RENDERING

Randy W. Heiland Sep. 1994 9 p Presented at the GVIS 1994: Graphics and Visualization Conference, Richland, WA, 8 Sep. 1994

(Contract DE-AC06-76RL-01830)

(DE95-004909; PNL-SA-25031; CONF-9409278-3) Avail: CASI HC A02/MF A01

Since many scientific datasets can be visualized using some polygonal representation, a polygon renderer has broad use for scientific visualization. With today's high performance computing applications producing very large datasets, a parallel polygon renderer is a necessary tool for keeping the compute-visualize cycle at a minimum. This paper presents a polygon renderer that combines the shared-memory and message-passing models of parallel programming. It uses the Global Arrays library, a shared-memory programming toolkit for distributed memory machines. The experience of using an object oriented approach for software design and development is also discussed. DOE

N95-25303# National Lab. for High Energy Physics, Tsukuba (Japan).

PROCEEDINGS OF WORKSHOP ON FUTURE IN HEP COMPUTING

Yukio Karita, ed., Katsuya Amako, ed., and Yoshiyuki Watase, ed. Dec. 1993 297 p In JAPANESE Workshop held in Tsukuba, Japan, 11-12 Mar. 1993

(DE94-792684; KEK-PROC-93-16; CONF-9303297) Avail: CASI HC A13/MF A03

The workshop was held on March 11 and 12, 1993, at the National Laboratory for High Energy Physics (KEK). The large flow from the conventional system centering around large versatile computers to the down-sizing taking distributed processing systems in it is formed, but its destination is not yet seen. As the concrete themes of 'future in HEP computing', problems toward down-sizing and the approach, future perspective of the networks, and adaptation of software engineering and pointing to object were taken up. At the workshop, lectures were given on requirements in HEP computing, possible solutions from Hitachi and Fujitsu, and network computing with workstations regarding down-sizing and HEP computing; approaches in INS and KEK regarding future computing system in HEP laboratories; user requirement for future network, network service available in 1995-2005, multimedia communication and network protocols regarding future networks; object-oriented approach for software development, OOP for real time data acquisition and accelerator control; ProdiG activities and future of FORTRAN, F90 and HPF regarding OOP and physics; and trends in software development methodology. DOE

N95-25359# California Univ., Berkeley. Lawrence Berkeley Lab, CA.

DYNAMICS OF TCP TRAFFIC OVER ATM NETWORKS

S. Floyd and A. Romanow (Sun Microsystems, Inc., Mountain View, CA.) Aug. 1994 10 p Presented at the SIGCOMM 1994 Conference, London, England, 27 Aug. - 4 Sep. 1994

(Contract DE-AC03-76SF-00098)

(DE95-004687; LBL-35179; CONF-9408202-1) Avail: CASI HC A02/MF A01

The authors investigate the performance of TCP (Transport Control Protocol) connections over ATM (Asynchronous Transfer Mode) networks without ATM-level congestion control, and compare it to the performance of TCP over packet-based networks. For simulations of congested networks, the effective throughput of TCP over ATM can be quite low when cells are dropped at the congested ATM switch. The low throughput is due to wasted bandwidth as the congested link transmits cells from 'corrupted' packets, i.e., packets in which at least one cell is dropped by the switch. This fragmentation effect can be corrected and high throughput can be achieved if the switch drops whole packets prior to buffer overflow; they call this strategy Early Packet Discard. They also discuss general issues of congestion avoidance for best-effort traffic in ATM networks. DOE

N95-25378# Idaho National Engineering Lab., Idaho Falls, ID.

LOW-COST IMAGE ANALYSIS SYSTEM

G. D. Lassahn 1995 12 p Presented at the 10th Conference on Geologic Remote Sensing: Exploration, Environment and Engineering, San Antonio, TX, 9-12 May 1994

(Contract DE-AC07-76ID-01570)

(DE95-005021; EGG-M-94084; CONF-940536-2) Avail: CASI HC A03/MF A01

The author has developed an Automatic Target Recognition system based on parallel processing using transputers. This approach gives a powerful, fast image processing system at relatively low cost. This system scans multi-sensor (e.g., several infrared bands) image data to find any identifiable target, such as physical object or a type of vegetation. DOE

N95-25477# Los Alamos National Lab., NM.

DESIGNING A STENCIL COMPILER FOR THE CONNECTION MACHINE MODEL CM-5

Ralph G. Brickner, Kathy Holian, Balaji Thiagarajan, and S. Lennart Johnsson (Thinking Machines Corp., Cambridge, MA.) 1994 19 p Submitted for publication

(Contract W-7405-eng-36)

(DE95-006861; LA-UR-94-3152) Avail: CASI HC A03/MF A01

In this paper the authors present the design of a stencil compiler for the Connection Machine system CM-5. The stencil compiler will optimize the data motion between processing nodes, minimize the data motion within a node, and minimize the data motion between registers and local memory in a node. The compiler will natively support two-dimensional stencils, but stencils in three dimensions will be automatically decomposed. Lower dimensional stencils are treated as degenerate stencils. The compiler will be integrated as part of the CM Fortran programming system. Much of the compiler code will be adapted from the CM-2/200 stencil compiler, which is part of CMSSL (the Connection Machine Scientific Software Library) Release 3.1 for the CM-2/200, and the compiler will be available as part of the Connection Machine Scientific Software Library (CMSSL) for the CM-5. In addition to setting down design considerations, they report on the implementation status of the stencil compiler. In particular, they discuss

optimization strategies and status of code conversion from CM-2/200 to CM-5 architecture, and report on the measured performance of prototype target code which the compiler will generate. DOE

N95-25625 Rutherford Appleton Lab., Oxford (England).
ALPHA(SUB CRITICAL) FOR PARALLEL PROCESSORS
D. Moncrieff, R. E. Overill, and S. Wilson Sep. 1994 10 p Prepared in cooperation with Florida State Univ., Tallahassee, FL; and Kings Coll., London, England
(PB95-165320; RAL-94-103) Avail: Issuing Activity (National Technical Information Service (NTIS))

Alpha(sub critical) is defined as the fraction of a computational task that must be executed in parallel for the theoretical peak performance for two parallel processors to be equal. Values of alpha(sub critical) are given for a number of contemporary high performance computing machines. Alpha prime(sub critical), the practical parallelization break-even fraction, is defined and discussed. NTIS

N95-26013# Pacific Northwest Lab., Richland, WA. Computer Science Dept.
FOUR-DIMENSIONAL INFORMATION VISUALIZATION AND ANALYSIS SYSTEM
Bruce Rex Sep. 1994 8 p Presented at the GVIS 1994: Graphics and Visualization Conference, Richland, WA, 8 Sep. 1994
(Contract DE-AC06-76RL-01830)
(DE95-004935; PNL-SA-24993; CONF-9409278-1) Avail: CASI HC A02/MF A01

The Four-Dimensional Information Visualization and Analysis System (4DIVAS) was conceived for two purposes. The first purpose was to fill the void between the current generation of geographic information systems (GIS) and high-end, image-only visualization systems. The gap existing between these two systems can be summarized as the limitation of relational database oriented GIS to deal with time and the poor connection in visualization systems to databases of any kind. The second purpose was to permit spatio-temporal modeling and query, functionalities currently underdeveloped in the commercial arena. At the Hanford Site, there are many potential applications for such a system, especially in the monitoring and modeling of potential constituent plumes in the subsurface hydrology over time, among others. In its current form, 4DIVAS exists as a proof-of-concept functional prototype and is, therefore, more of a technology than a product at this time. DOE

N95-26054 Secure Solutions, Inc., La Jolla, CA.
NAVAL NETWORK SECURITY REQUIREMENTS ANALYSIS Final Technical Report
Kym Blair Arlington, VA Space and Naval Warfare Systems Command 7 Dec. 1994 111 p Limited Reproducibility: More than 20% of this document may be affected by microfiche quality
(Contract N00039-93-C-0099)
(AD-A288692; Rept-102-94-022U) Avail: Issuing Activity (Defense Technical Information Center (DTIC))

Secure Solutions, Inc. was tasked by the Space and Naval Warfare Systems Command (SPAWAR) to perform a Small Business Innovation Research (SBIR) Phase II network security research effort. The report analyzes the DoD Goal Security Architecture (DGSA), Multilevel Information System Security Initiative (MISSI), and Navy Integrated Command and Control, Communications and Computers, and Intelligence (Integrated C4I) program areas in order to determine security implementation requirements for Navy networks. The report describes broad network security requirements for the Navy in light of emerging technologies. The analysis includes a brief review of the current environment, characterized by existing and emerging network Security products, and discusses possible deficiencies which may require the development of additional security products. These findings are preliminary and merit further investigation. DTIC

N95-26066# Los Alamos National Lab., NM.
CONVERTING MULTIPLE OC-3c ATM STREAMS TO HIPPI TO DRIVE AN HDTV FRAME BUFFER FROM A WORKSTATION CLUSTER
D. E. Tolmie, A. G. Dornhoff, and A. J. DuBois 1994 8 p Presented at the 9th International Parallel Processing Symposium (IPPS '95), Santa Barbara, CA, 25-28 Apr. 1995
(Contract W-7405-eng-36)
(DE95-003638; LA-UR-94-4127; CONF-950484-1) Avail: CASI HC A02/MF A01

A group of eight Digital Equipment Corporation Alpha workstations is interconnected with ATM to form a cluster with supercomputer power. For output, each workstation drives a single 'tile' on an 8-tile high-resolution frame buffer. A special purpose adapter is used to convert the workstation's ATM format to the frame buffer's HIPPI format. This paper discusses the rationale behind the workstation farm, and then describes the visualization output path in detail. To provide the system quickly, special emphasis was placed on making the design as simple as possible. The design choices are examined, and the resultant system is described. DOE

63 CYBERNETICS

Includes feedback and control theory, artificial intelligence, robotics and expert systems.

For related information see also *54 Man/System Technology and Life Support.*

N95-25253*# Jet Propulsion Lab., California Inst. of Tech., Pasadena, CA.
A DECADE OF NEURAL NETWORKS: PRACTICAL APPLICATIONS AND PROSPECTS
Sabrina E. Kemeny 11 May 1994 236 p Workshop held in Pasadena, CA, 11-13 May 1994; sponsored by NASA and DOD Sponsored in cooperation with Ballistic Missile Defense Organization; Army/All Source Analysis System Project Office; Communication and Electronic Command/Intelligence and Electronic Warfare Directorate; NSWC; and ONR
(Contract NAS7-918; RTOP 644-11-00)
(NASA-CR-197334; JPL-Publ-94-10; NAS 1.26:197334) Avail: CASI HC A11/MF A03

The Jet Propulsion Laboratory Neural Network Workshop, sponsored by NASA and DOD, brings together sponsoring agencies, active researchers, and the user community to formulate a vision for the next decade of neural network research and application prospects. While the speed and computing power of microprocessors continue to grow at an ever-increasing pace, the demand to intelligently and adaptively deal with the complex, fuzzy, and often ill-defined world around us remains to a large extent unaddressed. Powerful, highly parallel computing paradigms such as neural networks promise to have a major impact in addressing these needs. Papers in the workshop proceedings highlight benefits of neural networks in real-world applications compared to conventional computing techniques. Topics include fault diagnosis, pattern recognition, and multiparameter optimization. For individual titles, see N95-25254 through N95-25272.

N95-25254*# Naval Air Warfare Center, China Lake, CA. Weapons Div.
MISSILEBORNE ARTIFICIAL VISION SYSTEM (MAVIS)
David K. Andes, James C. Witham, and Michael D. Miles *In* JPL, A Decade of Neural Networks: Practical Applications and Prospects 11 May 1994 p 1-10 (For primary document see N95-25253 08-63)
Avail: CASI HC A02/MF A03

Several years ago when INTEL and China Lake designed the ETANN chip, analog VLSI appeared to be the only way to do high density neural computing. In the last five years, however, digital parallel processing chips capable of performing neural computation functions have evolved to the point of rough equality with analog chips in system level computational density. The Naval Air Warfare Center, China Lake, has developed a real time, hardware and software system designed to implement and evaluate biologically inspired retinal and cortical models. The hardware is based on the Adaptive Solutions Inc. massively parallel CNAPS system COHO boards. Each COHO board is a standard size 6U VME card featuring 256 fixed point, RISC processors running at 20 MHz in a SIMD configuration. Each COHO board has a companion board built to support a real time VSB interface to an imaging seeker, a NTSC camera, and to other COHO boards. The system is designed to have multiple SIMD machines each performing different corticomorphic functions. The system level software has been developed which allows a high level description of corticomorphic structures to be translated into the native microcode of the CNAPS chips. Corticomorphic structures are those neural structures with a form similar to

that of the retina, the lateral geniculate nucleus, or the visual cortex. This real time hardware system is designed to be shrunk into a volume compatible with air launched tactical missiles. Initial versions of the software and hardware have been completed and are in the early stages of integration with a missile seeker. Author

N95-25255*# Ford Motor Co., Dearborn, MI.
NEURAL NETWORK APPLICATION TO COMPREHENSIVE ENGINE DIAGNOSTICS
Kenneth A. Marko *In* JPL, A Decade of Neural Networks: Practical Applications and Prospects 11 May 1994 p 15-22 (For primary document see N95-25253 08-63)
Avail: CASI HC A02/MF A03

We have previously reported on the use of neural networks for detection and identification of faults in complex microprocessor controlled powertrain systems. The data analyzed in those studies consisted of the full spectrum of signals passing between the engine and the real-time microprocessor controller. The specific task of the classification system was to classify system operation as nominal or abnormal and to identify the fault present. The primary concern in earlier work was the identification of faults, in sensors or actuators in the powertrain system as it was exercised over its full operating range. The use of data from a variety of sources, each contributing some potentially useful information to the classification task, is commonly referred to as sensor fusion and typifies the type of problems successfully addressed using neural networks. In this work we explore the application of neural networks to a different diagnostic problem, the diagnosis of faults in newly manufactured engines and the utility of neural networks for process control. Derived from text

N95-25256*# Bell Telephone Labs., Inc., Holmdel, NJ.
DOCUMENT ANALYSIS WITH NEURAL NET CIRCUITS
Hans Peter Graf *In* JPL, A Decade of Neural Networks: Practical Applications and Prospects 11 May 1994 p 23-28 (For primary document see N95-25253 08-63)
Avail: CASI HC A02/MF A03

Document analysis is one of the main applications of machine vision today and offers great opportunities for neural net circuits. Despite more and more data processing with computers, the number of paper documents is still increasing rapidly. A fast translation of data from paper into electronic format is needed almost everywhere, and when done manually, this is a time consuming process. Markets range from small scanners for personal use to high-volume document analysis systems, such as address readers for the postal service or check processing systems for banks. A major concern with present systems is the accuracy of the automatic interpretation. Today's algorithms fail miserably when noise is present, when print quality is poor, or when the layout is complex. A common approach to circumvent these problems is to restrict the variations of the documents handled by a system. In our laboratory, we had the best luck with circuits implementing basic functions, such as convolutions, that can be used in many different algorithms. To illustrate the flexibility of this approach, three applications of the NET32K circuit are described in this short viewgraph presentation: locating address blocks, cleaning document images by removing noise, and locating areas of interest in personal checks to improve image compression. Several of the ideas realized in this circuit that were inspired by neural nets, such as analog computation with a low resolution, resulted in a chip that is well suited for real-world document analysis applications and that compares favorably with alternative, 'conventional' circuits.
Derived from text

N95-25257*# University of Southern California, Los Angeles, CA. Dept. of Electrical Engineering.
FROM NEURAL-BASED OBJECT RECOGNITION TOWARD MICROELECTRONIC EYES
Bing J. Sheu and Sa Hyun Bang *In* JPL, A Decade of Neural Networks: Practical Applications and Prospects 11 May 1994 p 29-37 (For primary document see N95-25253 08-63)
Avail: CASI HC A02/MF A03

Engineering neural network systems are best known for their abilities to adapt to the changing characteristics of the surrounding environment by adjusting system parameter values during the learning process. Rapid advances in analog current-mode design techniques have made possible the implementation of major neural network functions in custom VLSI chips. An electrically programmable analog synapse cell with large dynamic range can be realized in a compact silicon area. New designs of the synapse cells, neurons, and analog processor are presented. A synapse cell based on Gilbert multiplier structure can perform the linear multiplication for back-propagation networks. A double differential-pair synapse cell can perform the Gaussian function for radial-basis network. The synapse cells can be biased in the strong inversion region for high-speed operation or biased in the subthreshold region for low-power operation. The voltage gain of the sigmoid-function neurons is externally adjustable which greatly facilitates the search of optimal solutions in certain networks. Various building blocks can be intelligently connected to form useful industrial applications. Efficient data communication is a key system-level design issue for large-scale networks. We also present analog neural processors based on perceptron architecture and Hopfield network for communication applications. Biologically inspired neural networks have played an important role towards the creation of powerful intelligent machines. Accuracy, limitations, and prospects of analog current-mode design of the biologically inspired vision processing chips and cellular neural network chips are key design issues.
Author

N95-25258*# Jet Propulsion Lab., California Inst. of Tech., Pasadena, CA.
VLSI NEUROPROCESSORS
Sabrina E. Kemeny *In its* A Decade of Neural Networks: Practical Applications and Prospects 11 May 1994 p 39-51 Sponsored in cooperation with NASA; ASAS Program Office; ARPA; NSWC; BMDO; and ONR (For primary document see N95-25253 08-63)
Avail: CASI HC A03/MF A03

Electronic and optoelectronic hardware implementations of highly parallel computing architectures address several ill-defined and/or computation-intensive problems not easily solved by conventional computing techniques. The concurrent processing architectures developed are derived from a variety of advanced computing paradigms including neural network models, fuzzy logic, and cellular automata. Hardware implementation technologies range from state-of-the-art digital/analog custom-VLSI to advanced optoelectronic devices such as computer-generated holograms and e-beam fabricated Dammann gratings. JPL's concurrent processing devices group has developed a broad technology base in hardware implementable parallel algorithms, low-power and high-speed VLSI designs and building block VLSI chips, leading to application-specific high-performance embeddable processors. Application areas include high throughput map-data classification using feedforward neural networks, terrain based tactical movement planner using cellular automata, resource optimization (weapon-target assignment) using a multidimensional feedback network with lateral inhibition, and classification of rocks using an inner-product scheme on thematic mapper data. In addition to addressing specific functional needs of DOD and NASA, the JPL-developed concurrent processing device technology is also being customized for a variety of commercial applications (in collaboration with industrial partners), and is being transferred to U.S. industries. This viewgraph p resentation focuses on two application-specific processors which solve the computation intensive tasks of resource allocation (weapon-target assignment) and terrain based tactical movement planning using two extremely different topologies. Resource allocation is implemented as an asynchronous analog competitive assignment architecture inspired by the Hopfield network. Hardware realization leads to a two to four order of magnitude speed-up over conventional techniques and enables multiple assignments, (many to many), not achievable with standard statistical approaches. Tactical movement planning (finding the best path from A to B) is accomplished with a digital two-dimensional concurrent processor array. By exploiting the natural parallel decomposition of the problem in silicon, a four order of magnitude speed-up over optimized software approaches has been demonstrated. Author

N95-25259*# Martin Marietta Corp., Denver, CO. Photonic Systems Div.
PHOTONICS: FROM TARGET RECOGNITION TO LESION DETECTION
E. Michael Henry *In* JPL, A Decade of Neural Networks: Practical Applications and Prospects 11 May 1994 p 53-63 Prepared in cooperation with Rose Medical Center, Denver, CO (For primary document see N95-25253 08-63)
Avail: CASI HC A03/MF A03

Since 1989, Martin Marietta has invested in the development of an innovative concept for robust real-time pattern recognition for any

two-dimensioanal sensor. This concept has been tested in simulation, and in laboratory and field hardware, for a number of DOD and commercial uses from automatic target recognition to manufacturing inspection. We have now joined Rose Health Care Systems in developing its use for medical diagnostics. The concept is based on determining regions of interest by using optical Fourier bandpassing as a scene segmentation technique, enhancing those regions using wavelet filters, passing the enhanced regions to a neural network for analysis and initial pattern identification, and following this initial identification with confirmation by optical correlation. The optical scene segmentation and pattern confirmation are performed by the same optical module. The neural network is a recursive error minimization network with a small number of connections and nodes that rapidly converges to a global minimum. Derived from text

N95-25260*# Irvine Sensors Corp., Costa Mesa, CA.
THREE-D ARTIFICIAL NEURAL NETWORK (3DANN) TECHNOLOGY. BLUEPRINT FOR THE FUTURE Status Report
John Carson *In* JPL, A Decade of Neural Networks: Practical Applications and Prospects 11 May 1994 p 65-74 (For primary document see N95-25253 08-63)
Avail: CASI HC A02/MF A03

Irvine Sensors Corporation (ISC), working closely with JPL under BMDO/ONR sponsorship, is developing a radically new neural computing technology. Primarily aimed at discrimination and target recognition for BMDO missile interceptor applications, it appears to have near term commercial applicability to such problems as handwriting and face recognition, just to name two. In its earliest form it will be able to perform inner product computation using 262 thousand 64x64 templates (weighted synapse arrays) where the 64(exp 5) weights can all be changed every millisecond. Internal switching provides an inherent capability to zoom, translate, or rotate the templates. The 3D silicon architecture is manufactured on a commercial, high volume DRAM production line at very low cost, enabling its commercialization. Two technology thrusts are beginning: in the first, the 64 layer capability of 3DANN-I will be extended to 1024 layers and beyond. In the second layer size will be shrunk to 2-3 millimeters to reduce layer costs. Our workshop goal is to expose this technology to the neural network community as an emerging tool for their use and to obtain their desire for its future development. Author

N95-25261*# Jet Propulsion Lab., California Inst. of Tech., Pasadena, CA.
HIDDEN MARKOV MODELS AND NEURAL NETWORKS FOR FAULT DETECTION IN DYNAMIC SYSTEMS
Padhraic Smyth *In its* A Decade of Neural Networks: Practical Applications and Prospects 11 May 1994 p 75-89 (For primary document see N95-25253 08-63)
Avail: CASI HC A03/MF A03

Neural networks plus hidden Markov models (HMM) can provide excellent detection and false alarm rate performance in fault detection applications, as shown in this viewgraph presentation. Modified models allow for novelty detection. Key contributions of neural network models are: (1) excellent nonparametric discrimination capability; (2) a good estimator of posterior state probabilities, even in high dimensions, and thus can be embedded within overall probabilistic model (HMM); and (3) simple to implement compared to other nonparametric models. Neural network/HMM monitoring model is currently being integrated with the new Deep Space Network (DSN) antenna controller software and will be on-line monitoring a new DSN 34-m antenna (DSS-24) by July, 1994. Derived from text

N95-25262*# Dortmund Univ. (Germany). Faculty of Electrical Engineering.
INNOVATION AND APPLICATION OF ANN IN EUROPE DEMONSTRATED BY KOHONEN MAPS
Karl Goser *In* JPL, A Decade of Neural Networks: Practical Applications and Prospects 11 May 1994 p 91-93 (For primary document see N95-25253 08-63)
Avail: CASI HC A01/MF A03

One of the most important contributions to neural networks comes from Kohonen, Helsinki/Espoo, Finland, who had the idea of self-organizating maps in 1981. He verified his idea by an algorithm of which many applications make use of. The impetus for this idea came from biology, a field where the Europeans have always been very active at several research laboratories. The challenge was to model the self-organization found in the brain. Today one goal is the development of more sophisticated neurons which model the biological neurons more exactly. They should come to a better performance of neural nets with only a few complex neurons instead of many simple ones. A lot of application concepts arise from this idea: Kohonen himself applied it to speech recognition, but the project did not overcome much more than the recognition of the numerals one to ten at that time. A more promising application for self-organizing maps is process control and process monitoring. Several proposals were made which concern parameter classification of semiconductor technologies, design of integrated circuits, and control of chemical processes. Self-organizing maps were applied to robotics. The neural concept was introduced into electric power systems. At Dortmund we are working on a system which has to monitor the quality and the reliability of gears and electrical motors in equipment installed in coal mines. The results are promising and the probability to apply the system in the field is very high. A special feature of the system is that linguistic rules which are embedded in a fuzzy controller analyze the data of the self-organizing map in regard to life expectation of the gears. It seems that the fuzzy technique will introduce the technology of neural networks in a tandem mode. These technologies together with the genetic algorithms start to form the attractive field of computational intelligence. Author (revised)

N95-25263*# Alacron, Inc., Nashua, NH.
NEURAL NETWORK CLASSIFICATION OF CLINICAL NEUROPHYSIOLOGICAL DATA FOR ACUTE CARE MONITORING
Joseph Sgro *In* JPL, A Decade of Neural Networks: Practical Applications and Prospects 11 May 1994 p 95-106 Prepared in cooperation with Neurological Inst. of New York, New York, NY (For primary document see N95-25253 08-63)
Avail: CASI HC A03/MF A03

The purpose of neurophysiological monitoring of the 'acute care' patient is to allow the accurate recognition of changing or deteriorating neurological function as close to the moment of occurrence as possible, thus permitting immediate intervention. Results confirm that: (1) neural networks are able to accurately identify electroencephalogram (EEG) patterns and evoked potential (EP) wave components, and measuring EP waveform latencies and amplitudes; (2) neural networks are able to accurately detect EP and EEG recordings that have been contaminated by noise; (3) the best performance was obtained consistently with the back propagation network for EP and the HONN for EEG's; (4) neural network performed consistently better than other methods evaluated; and (5) neural network EEG and EP analyses are readily performed on multichannel data. Derived from text

N95-25264*# Air Force Academy, CO.
APPLICATION OF NEURAL NETWORKS TO UNSTEADY AERODYNAMIC CONTROL
William E. Faller, Scott J. Schreck, and Marvin W. Luttges (Colorado Univ., Boulder, CO.) *In* JPL, A Decade of Neural Networks: Practical Applications and Prospects 11 May 1994 p 107-126 (For primary document see N95-25253 08-63)
Avail: CASI HC A03/MF A03

The problem under consideration in this viewgraph presentation is to understand, predict, and control the fluid mechanics of dynamic maneuvers, unsteady boundary layers, and vortex dominated flows. One solution is the application of neural networks demonstrating closed-loop control. Neural networks offer unique opportunities: simplify modeling of three dimensional, vortex dominated, unsteady separated flow fields; are effective means for controlling unsteady aerodynamics; and address integration of sensors, controllers, and time lags into adaptive control systems. CASI

N95-25265*# California Inst. of Tech., Pasadena, CA.
SMART VISION CHIPS: AN OVERVIEW
Christof Koch *In* JPL, A Decade of Neural Networks: Practical Applications and Prospects 11 May 1994 p 127-135 (For primary document see N95-25253 08-63)
Avail: CASI HC A02/MF A03

This viewgraph presentation presents four working analog VLSI vision chips: (1) time-derivative retina, (2) zero-crossing chip, (3) resistive fuse, and (4) figure-ground chip; work in progress on computing motion and neuromorphic systems; and conceptual and practical lessons learned.
CASI

N95-25266*# Jet Propulsion Lab., California Inst. of Tech., Pasadena, CA.
PREDICTABILITY IN SPACE LAUNCH VEHICLE ANOMALY DETECTION USING INTELLIGENT NEURO-FUZZY SYSTEMS
Sandeep Gulati, Nikzad Toomarian, Jacob Barhen, Ayanna Maccalla, Raoul Tawel, Anil Thakoor, and Taher Daud *In its* A Decade of Neural Networks: Practical Applications and Prospects 11 May 1994 p 137-162 Prepared in cooperation with NASA. Johnson Space Center, Houston, TX; McDonnell-Douglas Corp., Saint Louis, MO; and LMSC, Palo Alto, CA (For primary document see N95-25253 08-63)
Avail: CASI HC A03/MF A03

Included in this viewgraph presentation on intelligent neuroprocessors for launch vehicle health management systems (HMS) are the following: where the flight failures have been in launch vehicles; cumulative delay time; breakdown of operations hours; failure of Mars Probe; vehicle health management (VHM) cost optimizing curve; target HMS-STS auxiliary power unit location; APU monitoring and diagnosis; and integration of neural networks and fuzzy logic. CASI

N95-25267*# University of South Florida, Tampa, FL. Coll. of Medicine.
NEURAL NETWORKS: APPLICATION TO MEDICAL IMAGING
Laurence P. Clarke *In* JPL, A Decade of Neural Networks: Practical Applications and Prospects 11 May 1994 p 163-170 (For primary document see N95-25253 08-63)
Avail: CASI HC A02/MF A03

The research mission is the development of computer assisted diagnostic (CAD) methods for improved diagnosis of medical images including digital x-ray sensors and tomographic imaging modalities. The CAD algorithms include advanced methods for adaptive nonlinear filters for image noise suppression, hybrid wavelet methods for feature segmentation and enhancement, and high convergence neural networks for feature detection and VLSI implementation of neural networks for real time analysis. Other missions include (1) implementation of CAD methods on hospital based picture archiving computer systems (PACS) and information networks for central and remote diagnosis and (2) collaboration with defense and medical industry, NASA, and federal laboratories in the area of dual use technology conversion from defense or aerospace to medicine. Derived from text

N95-25268*# Duke Univ., Durham, NC. Dept. of Electrical Engineering.
LEARNING RANDOM NETWORKS FOR COMPRESSION OF STILL AND MOVING IMAGES
Erol Gelenbe, Mert Sungur (Middle East Technical Univ., Ankara, Turkey.), and Christopher Cramer *In* JPL, A Decade of Neural Networks: Practical Applications and Prospects 11 May 1994 p 171-189 Sponsored in cooperation with a NATO science fellowship (For primary document see N95-25253 08-63)
Avail: CASI HC A03/MF A03

Image compression for both still and moving images is an extremely important area of investigation, with numerous applications to videoconferencing, interactive education, home entertainment, and potential applications to earth observations, medical imaging, digital libraries, and many other areas. We describe work on a neural network methodology to compress/decompress still and moving images. We use the 'point-process' type neural network model which is closer to biophysical reality than standard models, and yet is mathematically much more tractable. We currently achieve compression ratios of the order of 120:1 for moving grey-level images, based on a combination of motion detection and compression. The observed signal-to-noise ratio varies from values above 25 to more than 35. The method is computationally fast so that compression and decompression can be carried out in real-time. It uses the adaptive capabilities of a set of neural networks so as to select varying compression ratios in real-time as a function of quality achieved. It also uses a motion detector which will avoid retransmitting portions of the image which have varied little from the previous frame. Further improvements can be achieved by using on-line learning during compression, and by appropriate compensation of nonlinearities in the compression/decompression scheme. We expect to go well beyond the 250:1 compression level for color images with good quality levels. Author

N95-25269*# Ford Motor Co., Dearborn, MI.
LEARNING TO TRAIN NEURAL NETWORKS FOR REAL-WORLD CONTROL PROBLEMS Abstract Only
Lee A. Feldkamp, G. V. Puskorius, L. I. Davis, Jr., and F. Yuan *In* JPL, A Decade of Neural Networks: Practical Applications and Prospects 11 May 1994 p 191 (For primary document see N95-25253 08-63)
Avail: CASI HC A01/MF A03

Over the past three years, our group has concentrated on the application of neural network methods to the training of controllers for real-world systems. This presentation describes our approach, surveys what we have found to be important, mentions some contributions to the field, and shows some representative results. Topics discussed include: (1) executing model studies as rehearsal for experimental studies; (2) the importance of correct derivatives; (3) effective training with second-order (DEKF) methods; (4) the efficacy of time-lagged recurrent networks; (5) liberation from the tyranny of the control cycle using asynchronous truncated backpropagation through time; and (6) multistream training for robustness. Results from model studies of automotive idle speed control serve as examples for several of these topics. Author

N95-25270*# Bell Communications Research, Inc., Morristown, NJ.
NEURAL NETWORK APPLICATIONS IN TELECOMMUNICATIONS
Joshua Alspector *In* JPL, A Decade of Neural Networks: Practical Applications and Prospects 11 May 1994 p 209-218 (For primary document see N95-25253 08-63)
Avail: CASI HC A02/MF A03

Neural network capabilities include automatic and organized handling of complex information, quick adaptation to continuously changing environments, nonlinear modeling, and parallel implementation. This viewgraph presentation presents Bellcore work on applications, learning chip computational function, learning system block diagram, neural network equalization, broadband access control, calling-card fraud detection, software reliability prediction, and conclusions. CASI

N95-25271*# McDonnell-Douglas Aerospace, Saint Louis, MO. New Aircraft and Missile Products.
A NEURAL NETWORK CONTROLLER FOR AUTOMATED COMPOSITE MANUFACTURING
Peter F. Lichtenwalner *In* JPL, A Decade of Neural Networks: Practical Applications and Prospects 11 May 1994 p 219-230 (For primary document see N95-25253 08-63)
Avail: CASI HC A03/MF A03

At McDonnell Douglas Aerospace (MDA), an artificial neural network based control system has been developed and implemented to control laser heating for the fiber placement composite manufacturing process. This neurocontroller learns an approximate inverse model of the process on-line to provide performance that improves with experience and exceeds that of conventional feedback control techniques. When untrained, the control system behaves as a proportional plus integral (PI) controller. However after learning from experience, the neural network feedforward control module provides control signals that greatly improve temperature tracking performance. Faster convergence to new temperature set points and reduced temperature deviation due to changing feed rate have been demonstrated on the machine. A Cerebellar Model Articulation Controller (CMAC) network is used for inverse modeling because of its rapid learning performance. This control system is implemented in an IBM compatible 386 PC with an A/D board interface to the machine. Author

N95-25272*# Air Force Inst. of Tech., Wright-Patterson AFB, OH. Dept. of Electrical and Computer Engineering.
HOW CAPTAIN AMERIKA USES NEURAL NETWORKS TO FIGHT CRIME
Steven K. Rogers, Matthew Kabrisky, Dennis W. Ruck, and Mark E. Oxley *In* JPL, A Decade of Neural Networks: Practical Applications and Prospects 11 May 1994 p 231-235 (For primary document see N95-25253 08-63)
Avail: CASI HC A01/MF A03

Artificial neural network models can make amazing computations. These models are explained along with their application in problems associated with fighting crime. Specific problems addressed are identification of people using face recognition, speaker identification, and fingerprint and handwriting analysis (biometric authentication). Author (revised)

N95-25335*# Ohio State Univ., Columbus, OH. Cognitive Systems Engineering Lab.

GROUNDING EXPLANATIONS IN EVOLVING, DIAGNOSTIC SITUATIONS Final Report

Leila J. Johannesen, Richard I. Cook, and David D. Woods Dec. 1994 85 p

(Grant NAG9-390; RF Proj. 760678/727376)

(NASA-CR-198027; NAS 1.26:198027; CSEL-1994-TR-03) Avail: CASI HC A05/MF A01

Certain fields of practice involve the management and control of complex dynamic systems. These include flight deck operations in commercial aviation, control of space systems, anesthetic management during surgery or chemical or nuclear process control. Fault diagnosis of these dynamic systems generally must occur with the monitored process on-line and in conjunction with maintaining system integrity.This research seeks to understand in more detail what it means for an intelligent system to function cooperatively, or as a 'team player' in complex, dynamic environments. The approach taken was to study human practitioners engaged in the management of a complex, dynamic process: anesthesiologists during neurosurgical operations. The investigation focused on understanding how team members cooperate in management and fault diagnosis and comparing this interaction to the situation with an Artificial Intelligence(AI) system that provides diagnoses and explanations. Of particular concern was to study the ways in which practitioners support one another in keeping aware of relevant information concerning the state of the monitored process and of the problem solving process. Author

N95-25368# Brookhaven National Lab., Upton, NY.

NEURAL NETWORK TECHNIQUE FOR ORBIT CORRECTION IN ACCELERATORS/STORAGE RINGS

E. Bozoki and A. Friedman 1995 8 p Presented at the Orbit Correction and Analysis in Circular Accelerators Workshop, Upton, NY, 1-3 Dec. 1993

(Contract DE-AC02-76CH-00016)

(DE95-005955; BNL-61253; CONF-931254-10) Avail: CASI HC A02/MF A01

The authors are exploring the use of Neural Networks, using the SNNS simulator, for orbit control in accelerators (primarily circular accelerators) and storage rings. The orbit of the beam in those machines are measured by orbit monitors (input nodes) and controlled by orbit corrector magnets (output nodes). The physical behavior of an accelerator is changing slowly in time. Thus, an adoptive algorithm is necessary. The goal is to have a trained net which will predict the exact corrector strengths which will minimize a measured orbit. The relationship between 'kick' from the correctors and 'response' from the monitors is in general non-linear and may slowly change during long-term operation of the machine. In the study, several network architectures are examined as well as various training methods for each architecture. DOE

N95-25568# Research Inst. of National Defence, Linkoeping (Sweden). Huvudavdelning foer Informationsteknologi.

CLUSTERING USING WINNER-TAKE-ALL UNITS

Mats Bengtsson and Pertti Roivainen Aug. 1993 37 p

(PB95-165403; FOA-C-30723-3.4) Avail: CASI HC A03/MF A01

We present an application of a Potts glass to the clustering problem. Simulated annealing in the mean field approximation is used in order to avoid local minima. The resulting updating equations are completely parallel, and very simple and easy to implement. The model has no free parameters except for the annealing parameters. We demonstrate how it can be designed for some special clustering problems. The T approaches 0 limit of the Potts glass is identical to the vector quantization algorithm with certain step lengths. A comparative study of the Potts glass and vector quantization is made. For difficult clustering problems the Potts glass is far better than vector quantization. NTIS

N95-25603 Institute of Electrical and Electronics Engineers, New York, NY.

PROCEEDINGS OF THE 4TH IEEE WORKSHOP ON NEURAL NETWORKS FOR SIGNAL PROCESSING

John Vlontzos, Jenq-Neng Hwang, and Elizabeth Wilson 8 Sep. 1994 715 p Workshop held in Ermioni, Greece, 6-8 Sep. 1994 Limited Reproducibility: More than 20% of this document may be affected by microfiche quality

(AD-A288383) Avail: Issuing Activity (Defense Technical Information Center (DTIC))

This document contains papers presented at the fourth IEEE workshop on Neural Network for Signal Processing (NNSP'94). The workshop is designed to serve as a regular forum for researchers from universities and industry who are interested in interdisciplinary research on neural networks for signal processing applications. In the present scope, the workshop encompasses up-to-date research results in several key areas, including: learning algorithms, network architectures, speech processing, image processing, adaptive signal processing, medical signal processing, and other applications. The conference Proceedings is crafted to be an archival reference in the rapidly growing field of Neural Networks for Signal Processing. Derived from text

N95-25801*# Texas Technological Univ., Lubbock, TX.

HIERARCHICAL CONTROL AND TRAJECTORY PLANNING Annual Report, 2 Jan. - 31 Dec. 1994

Clyde F. Martin and P. W. Horn 31 Dec. 1994 201 p

(Grant NAG2-902)

(NASA-CR-197922; NAS 1.26:197922) Avail: CASI HC A10/MF A03

Most of the time on this project was spent on the trajectory planning problem. The construction is equivalent to the classical spline construction in the case that the system matrix is nilpotent. If the dimension of the system is n then the spline of degree 2n-1 is constructed. This gives a new approach to the construction of splines that is more efficient than the usual construction and at the same time allows the construction of a much larger class of splines. All known classes of splines are reconstructed using the approach of linear control theory. As a numerical analysis tool control theory gives a very good tool for constructing splines. However, for the purposes of trajectory planning it is quite another story. Enclosed in this document are four reports done under this grant. For individual titles, see N95-25802 through N95-25805.

N95-25802*# Texas Technological Univ., Lubbock, TX.

SPLINES AND CONTROL THEORY

Zhimin Zhang, John Tomlinson, and Clyde Martin *In its* Hierarchical Control and Trajectory Planning 31 Dec. 1994 29 p (For primary document see N95-25801 08-63)

Avail: CASI HC A03/MF A03

In this work, the relationship between splines and the control theory has been analyzed. We show that spline functions can be constructed naturally from the control theory. By establishing a framework based on control theory, we provide a simple and systematic way to construct splines. We have constructed the traditional spline functions including the polynomial splines and the classical exponential spline. We have also discovered some new spline functions such as trigonometric splines and the combination of polynomial, exponential and trigonometric splines. The method proposed in this paper is easy to implement. Some numerical experiments are performed to investigate properties of different spline approximations. Author

N95-25803*# Texas Technological Univ., Lubbock, TX.

A BRIEF SURVEY OF CONSTRAINED MECHANICS AND VARIATIONAL PROBLEMS IN TERMS OF DIFFERENTIAL FORMS

Robert Hermann *In its* Hierarchical Control and Trajectory Planning 31 Dec. 1994 15 p (For primary document see N95-25801 08-63)

Avail: CASI HC A03/MF A03

There has been considerable interest recently in constrained mechanics and variational problems. This is in part due to applied interests (such as 'non-holonomic mechanics in robotics') and in other part due to the fact that several schools of 'pure' mathematics have found that this classical subject is of importance for what they are trying to do. I have made various attempts at developing these subjects since my Lincoln lab days of the late 1950's. In this Chapter, I will sketch a Unified point of view, using Cartan's approach with differential forms. This has the advantage from the C-O-R viewpoint being developed in this Volume that the extension from 'smooth' to 'generalized' data is very systematic and algebraic. (I will only deal with the 'smooth' point of view in this Chapter; I will develop the 'generalized function' material at a later point.) The material presented briefly here about Variational Calculus and Constrained Mechanics can be

found in more detail in my books, 'Differential Geometry and the Calculus of Variations', 'Lie Algebras and Quantum Mechanics', and 'Geometry, Physics and Systems'. Author

N95-25804*# Texas Technological Univ., Lubbock, TX.
CONTROL THEORY AND SPLINES, APPLIED TO SIGNATURE STORAGE
Per Enqvist *In its* Hierarchical Control and Trajectory Planning 31 Dec. 1994 45 p (For primary document see N95-25801 08-63)
Avail: CASI HC A03/MF A03

In this report the problem we are going to study is the interpolation of a set of points in the plane with the use of control theory. We will discover how different systems generate different kinds of splines, cubic and exponential, and investigate the effect that the different systems have on the tracking problems. Actually we will see that the important parameters will be the two eigenvalues of the control matrix. Author

N95-25805*# Texas Technological Univ., Lubbock, TX.
HOW TO FLY AN AIRCRAFT WITH CONTROL THEORY AND SPLINES
Anders Karlsson *In its* Hierarchical Control and Trajectory Planning 31 Dec. 1994 108 p (For primary document see N95-25801 08-63)
Avail: CASI HC A06/MF A03

When trying to fly an aircraft as smoothly as possible it is a good idea to use the derivatives of the pilot command instead of using the actual control. This idea was implemented with splines and control theory, in a system that tries to model an aircraft. Computer calculations in Matlab show that it is impossible to receive enough smooth control signals by this way. This is due to the fact that the splines not only try to approximate the test function, but also its derivatives. A perfect traction is received but we have to pay in very peaky control signals and accelerations. Author

N95-26086*# Joint Inst. for Advancement of Flight Sciences, Hampton, VA.
SIMULATING THE DYNAMIC INTERACTION OF A ROBOTIC ARM AND THE SPACE SHUTTLE REMOTE MANIPULATOR SYSTEM M.S. Thesis - George Washington Univ., Dec. 1994
Steven L. Garrahan, Robert H. Tolson, and Robert L. Williams, II (Ohio Univ., Athens, OH.) Apr. 1995 108 p
(Contract NCC1-104; RTOP 233-03-03-02)
(NASA-CR-195076; NAS 1.26:195076) Avail: CASI HC A06/MF A02

Industrial robots are usually attached to a rigid base. Placing the robot on a compliant base introduces dynamic coupling between the two systems. The Vehicle Emulation System (VES) is a six DOF platform that is capable of modeling this interaction. The VES employs a force-torque sensor as the interface between robot and base. A computer simulation of the VES is presented. Each of the hardware and software components is described and Simulink is used as the programming environment. The simulation performance is compared with experimental results to validate accuracy. A second simulation which models the dynamic interaction of a robot and a flexible base acts as a comparison to the simulated motion of the VES. Results are presented that compare the simulated VES motion with the motion of the VES hardware using the same admittance model. The two computer simulations are compared to determine how well the VES is expected to emulate the desired motion. Simulation results are given for robots mounted to the end effector of the Space Shuttle Remote Manipulator System (SRMS). It is shown that for fast motions of the two robots studied, the SRMS experiences disturbances on the order of centimeters. Larger disturbances are possible if different manipulators are used. Author

N95-26330 Polish Academy of Sciences, Warsaw (Poland). Inst. of Basic Problems of Technology.
ACTUATING SIGNALS IN ADAPTIVE CONTROL SYSTEMS [SYGNALY POBUDZAJACE W ADAPTACYJNYCH UKLADACH STEROWANIA]
Dariusz Janecki 1994 180 p In POLISH
(ISSN 0208-5658)
(IFTR-13/1994) Avail: Issuing Activity (Polish Academy of Sciences, Warsaw, Poland)

This dissertation discusses the properties of selected adaptive control systems and describes the methods used to analyze these systems. The author places particular emphasis on the theoretical problems associated with the stability, convergence, and immunity of adaptive systems, especially on the significance of uniform actuation of a controlled system for the properties in question. In addition to existing results which are already rooted in the theory, the author presents new results concerning the immunity of adaptive systems published for the first time. The author supplements and illustrates his theoretical solutions with an example of the use of adaptive controllers to control the vibrations of flexible rotors.
Transl. by SCITRAN

64 NUMERICAL ANALYSIS

Includes iteration, difference equations, and numerical approximation.

N95-24214*# Research Inst. for Advanced Computer Science, Moffett Field, CA.
PERFORMANCE ISSUES FOR ITERATIVE SOLVERS IN DEVICE SIMULATION
Qing Fan, P. A. Forsyth (Waterloo Univ., Ontario.), J. R. F. McMacken (Goal Electronics Inc.), and Wei-Pai Tang (Waterloo Univ., Ontario.) Dec. 1994 21 p Sponsored in part by Natural Sciences and Engineering Research Council of Canada and by Information Technology Research Center
(Contract NAS2-13721)
(NASA-CR-197952; NAS 1.26:197952; RIACS-TR-94-21) Avail: CASI HC A03/MF A01

Due to memory limitations, iterative methods have become the method of choice for large scale semiconductor device simulation. However, it is well known that these methods still suffer from reliability problems. The linear systems which appear in numerical simulation of semiconductor devices are notoriously ill-conditioned. In order to produce robust algorithms for practical problems, careful attention must be given to many implementation issues. This paper concentrates on strategies for developing robust preconditioners. In addition, effective data structures and convergence check issues are also discussed. These algorithms are compared with a standard direct sparse matrix solver on a variety of problems. Author

N95-24228# International Centre for Theoretical Physics, Trieste (Italy).
FINITE QUANTUM PHYSICS AND NONCOMMUTATIVE GEOMETRY
A. P. Balachandran (Syracuse Univ., NY.), G. Bimonte, E. Ercolessi (Syracuse Univ., NY.), G. Landi (Syracuse Univ., NY.), F. Lizzi (Istituto Nazionale di Fisica Nucleare, Naples, Italy.), G. Sparano (Istituto Nazionale di Fisica Nucleare, Naples, Italy.), and P. Teotonio-Sobrinho (Syracuse Univ., NY.) Apr. 1994 40 p Sponsored by the International Atomic Energy Agency and the United Nations Educational Scientific and Cultural Organization
(DE94-634282; IC-94/38; DSF-T-2/94; SU-4240-567) Avail: CASI HC A03/MF A01 (US Sales Only)

Conventional discrete approximations of a manifold do not preserve its nontrivial topological features. In this article we describe an approximation scheme due to Sorkin which reproduces physically important aspects of manifold topology with striking fidelity. The approximating topological spaces in this scheme are partially ordered sets (posets). Now, in ordinary quantum physics on a manifold M, continuous probability densities generate the commutative C(sup *)-algebra C(M) of continuous functions on M. It has a fundamental physical significance, containing the information to reconstruct the topology of M, and serving to specify the domains of observables like the Hamiltonian. For a poset, the role of this algebra is assumed by a noncommutative C(sup *)-algebra A. As noncommutative geometries are based on noncommutative C(sup *)-algebra, we therefore have a remarkable connection between finite approximations to quantum physics and noncommutative geometries. Varies methods for doing quantum physics using A are explored. Particular attention is paid to developing numerically viable approximation schemes which at the same time preserve important topological features of continuum physics. DOE

N95-24229# International Centre for Theoretical Physics, Trieste (Italy).
DISTANCES ON A LATTICE FROM NONCOMMUTATIVE GEOMETRY
G. Bimonte, F. Lizzi (Istituto Nazionale di Fisica Nucleare, Naples, Italy.), and G. Sparano (Istituto Nazionale di Fisica Nucleare, Naples, Italy.) Apr. 1994 12 p Sponsored by the International Atomic Energy Agency and the United Nations Educational, Scientific and Cultural Organization
(DE94-634327; IC-94/76; DSF-T-7/94) Avail: CASI HC A03/MF A01 (US Sales Only)

Using the tools of noncommutative geometry we calculate the distances between the points of a lattice on which the usual discretized Dirac operator has been defined. We find that these distances do not have the expected behaviour, revealing that from the metric point of view the lattice does not look at all as a set of points sitting on the continuum manifold. We thus have an additional criterion for the choice of the discretization of the Dirac operator. DOE

N95-24243# Institut des Hautes Etudes Scientifiques, Bures-sur-Yvette (France).

UNIFORM RECTIFIABILITY AND SINGULAR SETS

G. David and S. Semmes Sep. 1994 51 p

(PB95-165502; IHES/M/94/52) Avail: CASI HC A04/MF A01

The authors consider under what conditions can one say something about the geometric structure of the singular set of a function. A famous result of this type states that the singular set (= set of non-Lebesgue points) of a function of bounded variation on R(sup n) is (countably) rectifiable. In this paper we shall be concerned with quantitative forms of rectifiability, and we give a quantitative version of this theorem. We also give uniform rectifiability results for the singular sets of minimizers of higher-dimensional versions of the Mumford-Shah functional. Along the way we shall encounter some generalizations of the usual topological notion of a set 'separating' points in the complement, including one which is based on the failure of Poincare inequalities on the complement of the given set. NTIS

N95-24251 Institut des Hautes Etudes Scientifiques, Bures-sur-Yvette (France).

SEMICLASSICAL ASYMPTOTICS ON COVERING MANIFOLDS AND MORSE INEQUALITIES

M. A. Shubin Sep. 1994 52 p Prepared in cooperation with Northeastern Univ. Limited Reproducibility: More than 20% of this document may be affected by microfiche quality

(Grant NSF DMS-92-22491)

(PB95-165510; IHES/M/94/51) Avail: CASI HC A04

This paper contains some results about semi-classical asymptotics of spectra of second order elliptic self-adjoint operators. The paper begins with the classical example of the quantum harmonic oscillator. NTIS

N95-24255# Institut des Hautes Etudes Scientifiques, Bures-sur-Yvette (France).

CONSTRUCTION OF THE MODULI SPACE OF MONOPOLES

R. G. Wang Sep. 1994 29 p See also PB94-167756

(PB95-165528; IHES/M/94/50) Avail: CASI HC A03/MF A01

Yang-Mills-Higgs theory in the Euclidean space R(sup 3) has been studied in various points of view for many years. A unifying theme of Yang-Mills-Higgs theory is the moduli space M(sup k) of charge k monopoles on M. It gives a cobordism of the moduli spaces M(sup k, sub m) of large and small mass monopoles both of which seem to have a rich geometry. In this paper, however, we begin with the moduli space M(sup k, sub m) of medium mass as it is the most general. By investigating the structure of M(sup k, sub m) of medium mass and constructing rather explicitly the 'stratification' of the end of M(sup k, sub m) we prove in (a paper in preparation) that M(sup k, sub m) has a standard compactification. It would lead to a definition of Donaldson-type invariants for closed 3-manifolds. Throughout the paper, M is assumed to be a metric connected sum of an oriented, rational homology 3-sphere X and R(sup 3) and the gauge group is taken as SU2. The main purpose of the paper is to give a detailed construction of the end M(sup k, sub m, infinity) of the moduli space M(sup k, sub m). NTIS

N95-24276# International Centre for Theoretical Physics, Trieste (Italy).

A FUNCTIONAL INTEGRAL APPROACH WITHOUT SLAVE BOSONS TO THE ANDERSON MODEL

Ngoc Thuan Nguyen (Institute of Theoretical Physics, Hanoi, Viet Nam.), Toan Thang Nguyen (Institute of Theoretical Physics, Hanoi, Viet Nam.), B. Coqblin (Paris Univ., France.), A. Bhattacharjee (Paris Univ., France.), and Anh Tuan Hoang Jun. 1994 6 p Sponsored in cooperation with the National Basic Research Program on Natural Sciences

(Contract KT-04)

(DE94-634858; IC-94/110) Avail: CASI HC A02/MF A01 (US Sales Only)

We developed the technique of the functional integral method without slave bosons for the periodic Anderson model (PAM) suggested by Sarker for treating the Hubbard model. This technique allowed us to obtain an analytical expression of Green functions containing U-dependence that is omitted in the formalism with slave bosons. DOE

N95-24301 Institut des Hautes Etudes Scientifiques, Bures-sur-Yvette (France).

PERIODIC SOLUTIONS OF HAMILTONIAN PERTURBATIONS OF 2D LINEAR SCHROEDINGER EQUATIONS

J. Bourgain Sep. 1994 8 p Limited Reproducibility: More than 20% of this document may be affected by microfiche quality

(PB95-165536; IHES/M/94/48) Avail: CASI HC A02

The purpose of this note is to construct periodic solutions of nonlinear 2D Schroedinger equations, which equations have a parameter corresponding to a perturbation of the linear equation. We consider the case of periodic boundary conditions. Our aim is to study the persistency of time periodic solutions of the linear equation, in the perturbed equation. We follow a method for 1-D equations, which is an infinite dimensional phase space version of the Liapounov-Schmidt argument for the construction of periodic solutions. More recently, the author extended this method to deal also with 1D-quasi periodic problems. In 2D, no such results seem to be known at all, and it seems thus natural to start investigating the periodic case, which is considerably easier. NTIS

N95-24321 Institut des Hautes Etudes Scientifiques, Bures-sur-Yvette (France).

BEHAVIOR OF A TRIGONOMETRIC POLYNOMIAL WITH GIVEN NUMBER OF TERMS ON SMALL SUBSETS OF THE UNIT CIRCUMFERENCE (NORM DUPLICATION PROBLEM)

F. Nazarov Aug. 1994 21 p Limited Reproducibility: More than 20% of this document may be affected by microfiche quality

(PB95-165544; IHES/M/94/47) Avail: CASI HC A03

This paper can be considered as an appendix to the author's previous paper 'Local estimates of exponential polynomials and their applications to inequalities of the Uncertainty Principle type', where the author obtained some rather sharp estimates for the norm of an exponential polynomial on the interval I (included in) R through its number of terms and its norm on some small measurable subset E (included in) I. The question arose whether one can obtain some good estimates in the case when the measure of E is not small, but, inversely, very close to the measure of I. It turns out that it is rather difficult and one still cannot answer it in the general case. Nevertheless, one particular problem can be solved which seems to be of special interest for applications: the so-called 'norm duplication' problem. Roughly speaking, the question is how close must the measure of E be to that of I to guarantee that the norm of the polynomial on the whole interval I does not exceed more than twice its norm on E. This is discussed in this document. NTIS

N95-24322 Institut des Hautes Etudes Scientifiques, Bures-sur-Yvette (France).

CONSTRUCTION OF QUASI-PERIODIC SOLUTIONS FOR HAMILTONIAN PERTURBATIONS OF LINEAR EQUATIONS AND APPLICATIONS TO NONLINEAR PDE

J. Bourgain Aug. 1994 18 p Limited Reproducibility: More than 20% of this document may be affected by microfiche quality

(PB95-165551; IHES/M/94/46) Avail: Issuing Activity (National Technical Information Service (NTIS))

Our aim is to develop a new approach to prove persistency of quasi-periodic low dimensional tori in large (possibly infinite) dimensional systems, avoiding some of the limitations inherent to the usual KAM procedures. We proceed along the lines of the Liapounov-Schmidt method for the periodic case, recently developed further and used successfully in constructing periodic solutions of certain nonlinear wave and Schroedinger equations. The main new problem in the quasi-periodic case is a control of the inverses of certain linear operators arising from solving the 'P-equation' by a Newton iteration scheme. This issue is more delicate than in the periodic setting. We succeeded in extending Kuksin's work to Hamiltonian perturbations of 1D-nonlinear Schroedinger and wave equations under periodic boundary conditions. We consider here only the nonresonnant case, i.e., the situation of normal frequencies that are nonresonnant with those of the persistent torus. NTIS

N95-24323 Institut des Hautes Etudes Scientifiques, Bures-sur-Yvette (France).
INTRINSIC HEIGHTS OF STABLE VARIETIES. APPLICATION TO ABELIAN VARIETIES
J. B. Bost Sep. 1994 56 p Limited Reproducibility: More than 20% of this document may be affected by microfiche quality
(PB95-165577; IHES/M/94/49) Avail: CASI HC A04

For any (d,delta) (a member of) N* x N*, let nu(d,delta) be the set of isomorphism classes of pairs (X,L) where X is a projective variety of dimension d over Q(bar) and L is an ample line bundle over X of degree delta. In this paper, we develop a construction of natural heights on some subsets of V(d,delta) based on the geometric invariant theory of Mumford, combined with the higher dimensional Arakelov theory of Gillet and Soule. This construction completes our earlier work and turns out to have various applications. In particular, it applies to abelian varieties, to which it associates heights which are closely related to Faltings heights. NTIS

N95-24325 Institut des Hautes Etudes Scientifiques, Bures-sur-Yvette (France).
DISTRIBUTION OF THE ERROR TERM FOR THE NUMBER OF LATTICE POINTS INSIDE A SHIFTED BALL Preliminary Technical Report
J. Bourgain Jul. 1994 22 p Limited Reproducibility: More than 20% of this document may be affected by microfiche quality
(PB95-165569; IHES/M/94/45) Avail: Issuing Activity (National Technical Information Service (NTIS))

The problem defined here is F(sub x)(R) = (N(sub x)(R) - R(sup d) Vol(sub d) B(1))/R(sup (d-1)/2), where N(sub x)(R) = the set (n belonging to Z(sup d) such that the absolute value of (x-n) is less than or equal to R). Analogues of results for d greater than 2, at least in partial form, are obtained in this report. NTIS

N95-24375# Joint Inst. for Nuclear Research, Dubna (USSR).
SYSINT(SYSINTM)-PROGRAM COMPLEX FOR NUMERICAL SOLUTION OF THE EIGENVALUE PROBLEM FOR SYSTEM OF INTEGRAL EQUATIONS
E. V. Zemlyanaya 1994 10 p
(DE94-636729; JINR-R-11-94-120) Avail: CASI HC A02/MF A01 (US Sales Only)

SYSINT (SYSINTM) - program complex for numerical solution of the eigenvalue problem for a system of integral equations is described. The iterative scheme is realized on the basis of the modified continuous analogue of Newton method. The programs are written in Fortran. The description of algorithms and parameters of programs is presented. The examples illustrating the use of the program are given. DOE

N95-24387# Joint Inst. for Nuclear Research, Dubna (USSR).
NUMERICAL INVESTIGATION OF SCHWINGER-DYSON AND BETHE-SALPETER EQUATIONS WITH GAUSS POTENTIAL IN THE FRAMEWORK OF THE QUARKONIUM MODEL
I. V. Amirkhanov, E. V. Zemlyanaya, V. N. Pervushin, I. V. Puzynin, T. B. Puzynina, N. A. Sarikov, and T. A. Strizh 1994 18 p
(DE94-636730; JINR-R-11-94-74) Avail: CASI HC A03/MF A01 (US Sales Only)

The mathematical model 'quarkonium' is considered on the basis of the Schwinger-Dyson equation for the quark mass function and the Bethe-Salpeter equation for the bound states. The software for the numerical investigations of the model is constructed and the solutions to the boundary problems for these equations with the Gauss potential for pion are obtained. Several renormalization schemes of the quark wave function 'inside' the meson are considered. It is shown in the considered renormalization schemes that the model with the Gauss potential describes the quark dynamical mass, due to the spontaneous chiral symmetry breaking, as well as the mass and the leptonic decay constant of the pion. DOE

N95-24389*# Institute for Computer Applications in Science and Engineering, Hampton, VA.
SEPARATION ANALYSIS, A TOOL FOR ANALYZING MULTIGRID ALGORITHMS Final Report
Sorin Costiner and Shlomo Taasan (Carnegie-Mellon Univ., Pittsburgh, PA.) Feb. 1995 21 p Submitted for publication
(Contracts NAS1-18605; NAS1-19480; RTOP 505-90-52-01)
(NASA-CR-195036; NAS 1.26:195036; ICASE-95-8) Avail: CASI HC A03/MF A01

The separation of vectors by multigrid (MG) algorithms is applied to the study of convergence and to the prediction of the performance of MG algorithms. The separation operator for a two level cycle algorithm is derived. It is used to analyze the efficiency of the cycle when mixing of eigenvectors occurs. In particular cases the separation analysis reduces to Fourier type analysis. The separation operator of a two level cycle for a Schridubger eigenvalue problem, is derived and analyzed in a Fourier basis. Separation analysis gives information on how to choose performance relaxations and inter-level transfers. Separation analysis is a tool for analyzing and designing algorithms, and for optimizing their performance. Author

N95-24401# International Centre for Theoretical Physics, Trieste (Italy).
OPTICAL DIFFRACTION FROM FRACTALS WITH A STRUCTURAL TRANSITION
F. PerezRodriguez, Wei Wang (Nanjing Univ., China.), and E. Canessa Apr. 1994 19 p
(DE94-634311; IC-94/77) Avail: CASI HC A03/MF A01 (US Sales Only)

A macroscopic characterization of fractals showing up a structural transition from dense to multibranched growth is made using optical diffraction theory. Such fractals are generated via the numerical solution of the 2D Poisson and biharmonic equations and are compared to more 'regular' irreversible clusters such as diffusion limited and Laplacian aggregates. The optical diffraction method enables to identify a decrease of the fractal dimension above the structural point. Author

N95-24421*# Institute for Computer Applications in Science and Engineering, Hampton, VA.
COVOLUME SOLUTIONS OF THREE DIMENSIONAL DIV-CURL EQUATIONS Final Report
R. A. Nicolaides (Carnegie-Mellon Univ., Pittsburgh, PA.) and X. Wu (Hong Kong Baptist Univ.,, Hong Kong.) Jan. 1995 14 p Submitted for publication
(Contracts NAS1-19480; RTOP 505-90-52-01; F49620-92-J-0133; F49620-92-J-0133)
(NASA-CR-195031; NAS 1.26:195031; ICASE-95-4) Avail: CASI HC A03/MF A01

Delaunay-Voronoi mesh systems provide a generalization of the classical rectangular staggered meshes to unstructured meshes. It is shown how such 'covolume' discretizations may be applied to div-curl systems in three dimensions. Error estimates are proved and confirmed by a numerical illustration. Author

N95-24458# Cornell Univ., Ithaca, NY.
LINEAR NON-MODAL PHENOMENA IN NUMERICAL ANALYSIS AND APPLIED MATHEMATICS First Annual Performance Report, 15 Feb. 1994 - 15 Nov. 1994
L. N. Trefethen 14 Nov. 1994 9 p
(Contract DE-FG02-94ER-25199)
(DE95-005495; DOE/ER-25199/T1) Avail: CASI HC A02/MF A01

This report contains information on the following topics: pseudospectra of an operator of Hille and Phillips; Schwarz- Christoffel toolbox user's guide; a matlab toolbox for Schwarz- Christoffel mapping; spectra and pseudospectra for pipe poiseuille flow; faster SVD for matrices with small m/n; calculation of pseudospectra by the Arnoldi iteration; and mostly linear model of transition to turbulence. DOE

N95-24474*# National Aeronautics and Space Administration. Lewis Research Center, Cleveland, OH.
THE METHOD OF SPACE-TIME CONSERVATION ELEMENT AND SOLUTION ELEMENT: DEVELOPMENT OF A NEW IMPLICIT SOLVER
S. C. Chang, X. Y. Wang (Colorado Univ., Boulder, CO.), C. Y. Chow (Colorado Univ., Boulder, CO.), and A. Himansu (Cleveland Telecommunications Corp., Solon, OH.) Apr. 1995 14 p Presented at the Ninth International Conference on Numerical Methods in Laminar and Turbulent Flow, Atlanta, GA, 10-14 Jul. 1995; sponsored by Georgia Institute of Technology
(RTOP 505-62-52)

(NASA-TM-106897; E-9545; NAS 1.15:106897) Avail: CASI HC A03/MF A01

The method of space-time conservation element and solution element is a nontraditional numerical method designed from a physicist's perspective, i.e., its development is based more on physics than numerics. It uses only the simplest approximation techniques and yet is capable of generating nearly perfect solutions for a 2-D shock reflection problem used by Helen Yee and others. In addition to providing an overall view of the new method, we introduce a new concept in the design of implicit schemes, and use it to construct a highly accurate solver for a convection-diffusion equation. It is shown that, in the inviscid case, this new scheme becomes explicit and its amplification factors are identical to those of the Leapfrog scheme. On the other hand, in the pure diffusion case, its principal amplification factor becomes the amplification factor of the Crank-Nicolson scheme. Author

N95-24557# Illinois Univ., Urbana-Champaign, IL. Center for Supercomputing Research and Development.

VISIBILITY ORDERING MESHED POLYHEDRA

Peter L. Williams Feb. 1992 31 p Sponsored by Sun Microsystems
(Contract DE-FG02-85ER-25001; AF-AFOSR-0044-91; NSF MIP-84-10110)
(CSRD-1097) Avail: CASI HC A03/MF A01

A visibility ordering of a set of objects from some viewpoint is an ordering such that if object a obstructs object b, then b precedes a in the ordering. An algorithm is presented that generates a visibility ordering of an acyclic convex set of meshed convex polyhedra. This algorithm takes time linear in the size of the mesh. Modifications to this algorithm and/or preprocessing techniques are described which permit nonconvex cells, nonconvex meshes (meshes with cavities and/or voids), meshes with cycles, and sets of disconnected meshes to be ordered. Visibility ordering of polyhedra is applicable to scientific visualization, particularly direct volume rendering. It is shown how the ordering algorithms can be used for domain decomposition of finite element meshes for parallel processing, and how the data structures used by these algorithms can be used to solve the spatial point location problem. The effects of cyclically obstructing polyhedra are discussed, and methods for their elimination are described, including the use of the Delaunay triangulation. Methods for converting nonconvex meshes into convex meshes are described. Author

N95-24592# Oak Ridge National Lab., TN.

BOUNDS FOR DEPARTURE FROM NORMALITY AND THE FROBENIUS NORM OF MATRIX EIGENVALUES

S. L. Lee Dec. 1994 22 p
(Contract DE-AC05-84OR-21400)
(DE95-006144; ORNL/TM-12853) Avail: CASI HC A03/MF A01

New lower and upper bounds for the departure from normality and the Frobenius norm of the eigenvalues of a matrix are given. The significant properties of these bounds are also described. For example, the upper bound for matrix eigenvalues improves upon the one derived by Kress, de Vries and Wegmann. The upper bound for departure from normality is sharp for any matrix whose eigenvalues are collinear in the complex plane. Moreover, the latter formula is a practical estimate that costs (at most) 2m multiplications, where m is the number of nonzeros in the matrix. In terms of applications, the results can be used to bound from above the sensitivity of eigenvalues to matrix perturbations or bound from below the condition number of the eigenbasis of a matrix. DOE

N95-24609# Los Alamos National Lab., NM.

THE GEOMETRY OF WEAK SOLUTIONS OF CERTAIN INTEGRABLE NONLINAR PDE'S

M. S. Alber (Notre Dame Univ., IN.), R. Camassa, D. D. Holm (California Univ., Berkeley, CA.), and J. E. Marsden (California Univ., Berkeley, CA.) 1994 6 p Presented at the NEEDS '94, Los Alamos, NM, 12-16 Sep. 1994
(Contract W-7405-eng-36)
(DE95-005241; LA-UR-94-4382; CONF-9409241-5) Avail: CASI HC A02/MF A01

We investigate the geometry of new classes of soliton-like weak solutions for integrable nonlinear equations. One example is the class of peakons introduced by Camassa and Holm (1993) for their integrable shallow water equation. Alber, Camassa, Holm and Marsden (1994a) put this shallow water equation into the framework of complex integrable Hamiltonian systems on Riemann surfaces and use special limiting procedures to obtain new solutions such as quasiperiodic solutions, n-solitons, solitons with quasiperiodic background, billiard, and n-peakon solutions and complex angle representations for them. They also obtain explicit formulas for phase shifts of interacting soliton solutions using the method of asymptotic reduction of the corresponding angle representations. The method they use for the shallow water equation also leads to a link between one of the members of the Dym hierarchy and geodesic flow on N-dimensional quadrics. Amongst these geodesics, particularly interesting ones are the umbilic geodesics, which generate the class of umbilic soliton solutions. Umbilic solitons have the property that as the space variable x tends to infinity, the solution tends to a periodic wave, and as x tends to minus infinity, it tends to the same periodic wave with a phase shift. Elliptic billiards may be obtained from the problem of geodesics on quadrics by collapsing along the shortest semiaxis. The corresponding Hamiltonian billiard flows are associated to new classes of solutions of equations in the Dym hierarchy. Such billiard type solutions have discontinuous spatial derivative and, thus, are weak solutions for this class of PDE's. DOE

N95-24632*# National Aeronautics and Space Administration. Langley Research Center, Hampton, VA.

A CONSERVATIVE STAGGERED-GRID CHEBYSHEV MULTIDOMAIN METHOD FOR COMPRESSIBLE FLOWS Final Report

David A. Kopriva (Florida State Univ., Tallahassee, FL.) and John H. Kolias (Florida State Univ., Tallahassee, FL.) Mar. 1995 49 p Submitted for publication
(Contracts NAS1-19480; RTOP 505-90-52-01; DE-FC05-85ER-25000; NSF DMS-94-04322)
(NASA-CR-195060; NAS 1.26:195060; ICASE-95-18) Avail: CASI HC A03/MF A01

We present a new multidomain spectral collocation method that uses staggered grids for the solution of compressible flow problems. The solution unknowns are defined at the nodes of a Gauss quadrature rule. The fluxes are evaluated at the nodes of a Gauss-Lobatto rule. The method is conservative, free-stream preserving, and exponentially accurate. A significant advantage of the method is that subdomain corners are not included in the approximation, making solutions in complex geometries easier to compute. Author

N95-24636# Joint Inst. for Nuclear Research, Dubna (USSR).

OSCILLATOR POLY SPHEROIDAL FUNCTIONS

N. F. Truskova 1993 14 p
(DE94-628440; JINR-R-5-93-169) Avail: CASI HC A03/MF A01 (US Sales Only)

Necessary in a number of physical problems, new special functions are obtained. Solutions of the Schroedinger equation of the N-dimensional (N greater than or equal to 4) harmonic oscillator in Euclidean and pseudo Euclidean spaces in the poly spheroidal coordinate systems are expressed via functions, particular cases of which are Coulomb spheroidal and wave poly spheroidal functions. Analytical expressions are found, main properties and particular cases of new functions are considered and an algorithm for their computer calculation is prepared. DOE

N95-24645# Joint Inst. for Nuclear Research, Dubna (USSR).

ADAPTIVE PROJECTIVE FILTERS

N. D. Dikusar 1993 22 p
(DE94-628374; JINR-E-5-93-314) Avail: CASI HC A03/MF A01 (US Sales Only)

A new approach to the solving of the finding problem is proposed. The method is based on the Discrete Projective Transformations (DPT), the List Square Fitting (LSF) and uses feedback information tracing for linear or quadratic track segments (TS). It's fast and stable with respect to measurement errors and a background points recurrent algorithm is suggested. The algorithm realizes the family of digital adaptive projective filters (APF) with known nonlinear weight functions-projective invariants. APF can be used in adequate control systems for collection, processing, and compression of data, including tracking problems for a wide class of detectors. DOE

N95-24691# Joint Inst. for Nuclear Research, Dubna (USSR).

ASYS2: A NEW VERSION OF COMPUTER ALGEBRA PACKAGE ASYS FOR ANALYSIS AND SIMPLIFICATION OF POLYNOMIAL SYSTEMS

V. P. Gerdt, N. V. Khutornoj, and A. Yury Zharkov (Saratov Univ., USSR.)

1993 20 p Presented at The Rhine Workshop on Computer Algebra, Karlsruhe, Germany, 22-24 Mar. 1994
(DE94-628384; JINR-E-11-93-468) Avail: CASI HC A03/MF A01 (US Sales Only)

In this paper a new version of a package ASYS for analysis of nonlinear algebraic equations based on the Groebner basis technique is described. In addition to the first version ASYS1 of the package, the current one has a number of new facilities which provide its higher efficiency. Some examples and results of comparison between ASYS2, ASYS1 and two other REDUCE packages GROEBNER and CALI included in REDUCE 3.5, are given. DOE

N95-24694# Joint Inst. for Nuclear Research, Dubna (USSR).
GENERATORS OF MATRIX FACTORABLE REPRESENTATIONS OF BLOCK-TRIDIAGONAL AND INVERSE MATRICES
G. A. Emelyanenko and T. T. Rakhmonov 1993 26 p In RUSSIAN Submitted for publication
(DE94-628387; JINR-R-11-93-265) Avail: CASI HC A03/MF A01 (US Sales Only)

The generators of set of matrix-factorable representations of general block-tridiagonal and inverse to them matrices both in case of zero main block-angular minors and nonzero ones are obtained. DOE

N95-24695# Joint Inst. for Nuclear Research, Dubna (USSR).
DOMAIN DECOMPOSITION AND GENERATORS OF DIRECT METHODS OF THE SOLUTION OF LINEAR EQUATION SYSTEMS WITH GENERAL BLOCK-TRIDIAGONAL MATRICES
G. A. Emelyanenko and T. T. Rakhmonov 1993 22 p In RUSSIAN Submitted for publication
(DE94-628388; JINR-R-11-93-266) Avail: CASI HC A03/MF A01 (US Sales Only)

The generators of direct decomposition methods of the solution of linear equations systems with general block-tridiagonal matrices are obtained. This investigation has been performed at the laboratory of computing Techniques and automation, JINR. DOE

N95-24697# International Centre for Theoretical Physics, Trieste (Italy).
CYCLIC SUBGROUPS IN CLASS GROUPS OF REAL QUADRATIC FIELDS
Lawrence C. Washington (Maryland Univ., College Park, MD.) and Zhang Xianke Jan. 1994 11 p Sponsored by the International Atomic Energy Agency and the United Nations Educational Scientific and Cultural Organization
(DE94-628407; IC-92/393) Avail: CASI HC A03/MF A01 (US Sales Only)

While examining the class numbers of the real quadratic field Q(radical(n(exp 2) + 3n + 9)), we observed that the class number is often a multiple of 3. There is a simple explanation for this, namely -27 = (2n + 3)(exp 2) - 4(n(exp 2) + 3n + 9), so the cubes of the prime ideals above 3 are principal. If the prime ideals themselves are non-principal then 3 must divide the class number. In the present paper, we study this idea from a couple different directions. In the first section we present a criterion that allows us to show that the ideal class group of a real quadratic field has a cyclic subgroup of a given order n. We then give several families of fields to which this criterion applies, hence in which the ideal class groups contain elements of order n. In the second section, we discuss the situation where there is only a potential element of order p (=an odd prime) in the class group, such as the situation described above. We present a modification of the Cohen-Lenstra heuristics for the probability that in this situation the class number is actually a multiple of p. We also extend this idea to predict how often the potential element of order p is actually non-trivial. Both of these predictions agree fairly well with the numerical data. DOE

N95-24698# Joint Inst. for Nuclear Research, Dubna (USSR).
GEOMETRIC QUANTIZATION OF SYMPLECTIC MANIFOLDS WITH SYMMETRY
A. D. Popov 1993 20 p
(DE94-628435; JINR-E-2-93-292) Avail: CASI HC A03/MF A01 (US Sales Only)

The finite-dimensional phase manifolds M, the Marsden-Weinstein reduction of these manifolds by the Hamiltonian action of the connected Lie group G and the geometric quantization of the reduced manifolds M(sub G) are considered. The algorithm of the geometric quantization of the manifolds M provided with a complex structure J invariant with respect to the action of the subgroup tau(G) in the group AutP of the automorphisms of the symplectic frame bundle P over M is described. DOE

N95-24704# Joint Inst. for Nuclear Research, Dubna (USSR).
QUASI-GENERALIZED MATRIX PROCESSES AND REPRESENTATIONS OF GENERAL BLOCK TRIDIAGONAL MATRICES
G. A. Emelyanenko and T. T. Rakhmonov 1993 15 p In RUSSIAN
(DE94-628377; JINR-R-11-93-249) Avail: CASI HC A03/MF A01 (US Sales Only)

The multiplicity of the matrix-factorable representations of the general block-tridiagonal matrices on the basis of the quasi-generalized matrix processes is obtained. DOE

N95-24705# Joint Inst. for Nuclear Research, Dubna (USSR).
NATURAL ELEMENTARY FACTORIZATION OF GENERAL BLOCK-TRIDIAGONAL MATRICES IN CASE OF ZERO MINORS OF BOTH TYPES
G. A. Emelyanenko and T. T. Rakhmonov 1993 23 p In RUSSIAN
(DE94-628378; JINR-R-11-93-250) Avail: CASI HC A03/MF A01 (US Sales Only)

The multiplicity of the factorable representations of the general block-tridiagonal matrices in the case of zero minors of both types is obtained. DOE

N95-24856*# Institute for Computer Applications in Science and Engineering, Hampton, VA.
EXPONENTIALLY ACCURATE APPROXIMATIONS TO PIECE-WISE SMOOTH PERIODIC FUNCTIONS Final Report
James Greer and Saheb Banerjee (Binghamton Univ., NY.) Mar. 1995 41 p Submitted for publication
(Contract NAS1-19480; RTOP 505-90-52-01)
(NASA-CR-195059; NAS 1.26:195059; ICASE-95-17) Avail: CASI HC A03/MF A01

A family of simple, periodic basis functions with 'built-in' discontinuities are introduced, and their properties are analyzed and discussed. Some of their potential usefulness is illustrated in conjunction with the Fourier series representations of functions with discontinuities. In particular, it is demonstrated how they can be used to construct a sequence of approximations which converges exponentially in the maximum norm to a piece-wise smooth function. The theory is illustrated with several examples and the results are discussed in the context of other sequences of functions which can be used to approximate discontinuous functions. Author

N95-24857*# Institute for Computer Applications in Science and Engineering, Hampton, VA.
MULTIGRID SOLUTION STRATEGIES FOR ADAPTIVE MESHING PROBLEMS Final Report
Dimitri J. Mavriplis Mar. 1995 40 p Submitted for publication
(Contract NAS1-19480; RTOP 505-90-52-01)
(NASA-CR-195049; NAS 1.26:195049; ICASE-95-14) Avail: CASI HC A03/MF A01

This paper discusses the issues which arise when combining multigrid strategies with adaptive meshing techniques for solving steady-state problems on unstructured meshes. A basic strategy is described, and demonstrated by solving several inviscid and viscous flow cases. Potential inefficiencies in this basic strategy are exposed, and various alternate approaches are discussed, some of which are demonstrated with an example. Although each particular approach exhibits certain advantages, all methods have particular drawbacks, and the formulation of a completely optimal strategy is considered to be an open problem. Author

N95-24859# Joint Inst. for Nuclear Research, Dubna (USSR).
ON THE STRUCTURE OF DIRECT REPRESENTATIONS OF INVERSE MATRICES TO THE BLOCK-TRIDIAGONAL ONES IN CASE OF ZERO MAIN BLOCK ANGULAR MINORS
G. A. Emelyanenko and T. T. Rakhmonov 1993 16 p In RUSSIAN Submitted for publication
(DE94-628376; JINR-R-11-93-248) Avail: CASI HC A03/MF A01 (US Sales Only)

The multiplicity of the direct representations of the inverse matrices to the general nonsingular block-tridiagonal ones in the case of some zero main block angular minors is obtained. The structure of these representations is investigated. DOE

N95-24860# Joint Inst. for Nuclear Research, Dubna (USSR).
ASYMPTOTIC PROPERTIES OF THE OSCILLATOR POLY SPHEROIDAL FUNCTIONS
N. F. Truskova 1993 8 p
(DE94-628441; JINR-R-5-93-170) Avail: CASI HC A02/MF A01 (US Sales Only)

Asymptotics of the oscillator poly spheroidal eigenfunctions and their eigenvalues as p approaches 0 and p approaches infinity are obtained. They generate corresponding asymptotics of the Coulomb spheroidal and wave poly spheroidal functions and are reduced to these for special parameters. DOE

N95-25106*# Institute for Computer Applications in Science and Engineering, Hampton, VA.
IMPLEMENTATION OF A PARALLEL UNSTRUCTURED EULER SOLVER ON THE CM-5
Eric Morano (Institut National de Recherche d'Informatique d'Automatique, Cote d'Azur, France.) and D. J. Mavriplis Mar. 1995 22 p Submitted for publication
(Contract NAS1-19480; RTOP 505-90-52-01)
(NASA-CR-195056; NAS 1.26:195056; ICASE-95-16) Avail: CASI HC A03/MF A01

An efficient unstructured 3D Euler solver is parallelized on a Thinking Machine Corporation Connection Machine 5, distributed memory computer with vectoring capability. In this paper, the single instruction multiple data (SIMD) strategy is employed through the use of the CM Fortran language and the CMSSL scientific library. The performance of the CMSSL mesh partitioner is evaluated and the overall efficiency of the parallel flow solver is discussed. Author

N95-25114*# Institute for Computer Applications in Science and Engineering, Hampton, VA.
A WELL-POSED NUMERICAL METHOD TO TRACK ISOLATED CONFORMAL MAP SINGULARITIES IN HELE-SHAW FLOW Final Report
Gregory Baker (Ohio State Univ., Columbus, OH.), Michael Siegel (Ohio State Univ., Columbus, OH.), and Saleh Tanveer (Ohio State Univ., Columbus, OH.) Feb. 1995 51 p Submitted for publication
(Contract NAS1-19480; RTOP 505-90-52-01)
(NASA-CR-195035; NAS 1.26:195035; ICASE-95-7) Avail: CASI HC A04/MF A01

We present a new numerical method for calculating an evolving 2D Hele-Shaw interface when surface tension effects are neglected. In the case where the flow is directed from the less viscous fluid into the more viscous fluid, the motion of the interface is ill-posed; small deviations in the initial condition will produce significant changes in the ensuing motion. This situation is disastrous for numerical computation, as small round-off errors can quickly lead to large inaccuracies in the computed solution. Our method of computation is most easily formulated using a conformal map from the fluid domain into a unit disk. The method relies on analytically continuing the initial data and equations of motion into the region exterior to the disk, where the evolution problem becomes well-posed. The equations are then numerically solved in the extended domain. The presence of singularities in the conformal map outside of the disk introduces specific structures along the fluid interface. Our method can explicitly track the location of isolated pole and branch point singularities, allowing us to draw connections between the development of interfacial patterns and the motion of singularities as they approach the unit disk. In particular, we are able to relate physical features such as finger shape, side-branch formation, and competition between fingers to the nature and location of the singularities. The usefulness of this method in studying the formation of topological singularities (self-intersections of the interface) is also pointed out. Author

N95-25251# Oak Ridge National Lab., TN.
A NOTE ON THE TOTAL LEAST SQUARES PROBLEM FOR COPLANAR POINTS
S. L. Lee Sep. 1994 14 p
(Contract DE-AC05-84OR-21400)
(DE95-004876; ORNL/TM-12852) Avail: CASI HC A03/MF A01

The total least squares (TLS) fit to the points (x(sub k), y(sub k)), k = 1, ..., n, minimizes the sum of the squares of the perpendicular distances from the points to the line. This sum is the TLS error, and minimizing its magnitude is appropriate if x(sub k) and y(sub k) are uncertain. A priori formulas for the TLS fit and TLS error to coplanar points were originally derived by Pearson, and they are expressed in terms of the mean, standard deviation, and correlation coefficient of the data. In this note, these TLS formulas are derived in a more elementary fashion. The TLS fit is obtained via the ordinary least squares problem and the algebraic properties of complex numbers. The TLS error is formulated in terms of the triangle inequality for complex numbers. DOE

N95-25427# International Centre for Theoretical Physics, Trieste (Italy).
QUANTUM SYMPLECTIC GEOMETRY. 1: THE MATRIX HAMILTONIAN FORMALISM
A. E. F. Djemai Jul. 1994 80 p
(DE95-607009; IC-94/204) Avail: CASI HC A05/MF A01 (US Sales Only)

The main purpose of this work is to describe the quantum analogue of the usual classical symplectic geometry and then to formulate the quantum mechanics as a (quantum) non-commutative symplectic geometry. In this first part, we define the quantum symplectic structure in the context of the matrix differential geometry by using the discrete Weyl-Schwinger realization of the Heisenberg group. We also discuss the continuous limit and give an expression of the quantum structure constants. DOE

N95-25452# International Centre for Theoretical Physics, Trieste (Italy).
NONLINEARITY INDUCED NONTRIVIAL DYNAMICS IN THE JAYNES-CUMMINGS HAMILTONIAN
J. L. Gruver, J. Aliaga, Hilda A. Cerdeira, and A. N. Proto (Buenos Aires Univ., Argentina.) Jun. 1994 15 p Sponsored by Comision de Investigaciones Cientificas de las Provincia de Buenos Aires, International Centre for Theoretical Physics, and Istituto Nazionale de Fisica Nucleare
(DE95-607004; IC-94/158) Avail: CASI HC A03/MF A01 (US Sales Only)

The addition of a nonlinear term to the Jaynes-Cummings Hamiltonian induced a nontrivial discrete dynamics for the number of possible transitions of a given order, represented by a Fibonacci series. We describe the physics of the problem in terms of relevant operators which close a semi-Lie algebra under commutation with the Hamiltonian and therefore extending the generalized Bloch equations, already obtained for the linear case, to the non-linear one. The initial conditions as well as a thermodynamical treatment of the problem is analyzed via the maximum entropy principle density operator. Finally, a generalized solution for the time-dependent case is obtained and the solution for the field in a thermal state is recovered. DOE

N95-25457# International Centre for Theoretical Physics, Trieste (Italy).
INVOLUTIVE CO-DISTRIBUTIONS PRESERVED BY TRANSITIVE FAMILIES OF VECTOR FIELDS
Victor Ayala Bravo Jun. 1994 16 p
(DE95-607078; IC-94/144) Avail: CASI HC A03/MF A01 (US Sales Only)

This paper leads with integrability conditions of involutive co-distributions defined on co-tangent bundle of a differentiable manifold M. Via Frobenius's integrability theorem, the analysis is aimed at the search for conditions so that this type of co-distributions preserved by transitive families of vector fields in M. We rely on the work of Lobry, Sussmann, Matsuda and Stefan. The type of situation studies comes up naturally in weak-observability problems and weakly-minimal realizations of arbitrary control systems. DOE

N95-25480# Utah State Univ., Logan, UT. Dept. of Mathematics and Statistics.
NEWTON ITERATIVE METHODS FOR LARGE SCALE NONLINEAR SYSTEMS Final Report, Aug. 1992 - Jul. 1994
Homer F. Walker and Kathryn Turner 1995 7 p
(Contract DE-FG02-92ER-25136)
(DE95-007067; DOE/ER-25136/2) Avail: CASI HC A02/MF A01

Newton iterative methods, also known as truncated Newton methods, are implementations of Newton's method in which an iterative linear solver is used to solve approximately the linear systems that characterize Newton steps. These methods are particularly appropriate for large-scale problems in which iterative linear algebra methods are preferred. They are currently used in many important scientific applications, including many of major industrial importance. In addition to their effectiveness on important problems, these methods also offer a nonlinear 'framework' within which to transfer to the nonlinear setting any advances in linear system solving, such as new iterative methods for nonsymmetric linear systems, new preconditioning techniques, or new algorithms that exploit advanced machine architectures. DOE

N95-25509 Army Armament Research, Development and Engineering Center, Watervliet, NY.
ADAPTIVE FINITE ELEMENT METHOD 2: ERROR ESTIMATION Final Report
J. M. Coyle and J. E. Flaherty Sep. 1994 31 p Limited Reproducibility: More than 20% of this document may be affected by microfiche quality
(AD-A288358; ARCCB-TR-94034) Avail: Issuing Activity (Defense Technical Information Center (DTIC))

An adaptive finite element method is developed to solve initial boundary value problems for vector systems of parabolic partial differential equations in one space dimension and time. The differential equations are discretized in space using piecewise linear finite element approximations. Superconvergence properties and quadratic polynomials are used to derive a computationally inexpensive approximation to the spatial component of the error. This technique is coupled with time integration schemes of successively higher orders to obtain an approximation of the temporal and total discretization errors. Computational results indicate that these approximations converge to the exact discretization errors as the mesh is refined. DTIC

N95-25532# International Centre for Theoretical Physics, Trieste (Italy).
ON EXOTIC SUPERSYMMETRIES OF THE PHI(1,3) DEFORMATION OF MINIMAL MODELS
A. Kadiri (Mohammed V Univ., Rabat, Morocco.), E. H. Saidi (Mohammed V Univ., Rabat, Morocco.), S. J. Zerouaoui (Mohammed V Univ., Rabat, Morocco.), and M. B. Sedra Jul. 1994 40 p
(DE95-607088; IC-94/216) Avail: CASI HC A03/MF A01 (US Sales Only)

Using algebraic and field theoretical methods, the fractional spin symmetries of the (phi)(sub 1,3) deformation of minimal models is studied. The particular example of the D = 2 three state tricritical Potts model is examined in detail. Various models based on subalgebras and appropriate discrete automorphism groups of the two dimensional fractional spin algebra are obtained. General features such as superspace and superfield representations, the U(sub q)(sl(sub 2)) symmetry, the spontaneous exotic supersymmetry breaking, relations with the N = 2 Landau Ginzburg models as well as other things are discussed. DOE

N95-25539 Joint Inst. for Nuclear Research, Dubna (USSR).
VARIATIONAL METHOD FOR THE CALCULATION OF THE SURFFACE HYPERSPHERICAL FUNCTIONS FOR THE SYSTEMS OF ZH(mu)-TYPE. THE TEST CALCULATION OF THE dt(mu)-SYSTEM
V. B. Belyaev, O. I. Kartavtsev, and V. I. Kochkin 1993 7 p In RUSSIAN
(DE94-628905; JINR-R-4-93-460) Copyright Avail: Issuing Activity (Department of Energy (DOE)) (US Sales Only)

The variational approach is applied for calculation of the 'surface' hyperspherical function for the three-body problem with Coulomb interaction. The variational 'surface' function is applied for the construction of the matrix of the effective potentials in the systems of the hyper radial differential equations. The numerical calculation has been performed for the dt(mu)-system. DOE

N95-25601 Pittsburgh Univ., Pittsburgh, PA. Dept. of Mathematics and Statistics.
SINGULARLY PERTURBED DIFFERENTIAL/ALGEBRAIC EQUATIONS
Xiaopu Yan Oct. 1994 44 p Limited Reproducibility: More than 20% of this document may be affected by microfiche quality
(Contract N00014-90-J-1025; NSF OCR-92-03488)
(AD-A288365; TR-ICMA-94-192) Avail: Issuing Activity (Defense Technical Information Center (DTIC))

In this paper, singularly perturbed nonlinear differential/algebraic equations (DAE's) are considered and a proof of the existence and uniqueness of a solution is given. Asymptotic expansions for such a solution are obtained and proved to be uniformly convergent. This generalizes known results about asymptotic expansions of singularly perturbed ordinary differential equations. DTIC

N95-25627 Rutherford Appleton Lab., Chilton (England). Central Computing Dept.
USE OF MULTIPLE FRONTS IN GAUSSIAN ELIMINATION
I. S. Duff and J. A. Scott 13 Sep. 1994 16 p
(PB95-165353; RAL-94-040) Avail: Issuing Activity (National Technical Information Service (NTIS))

The authors examine a method for extending a frontal solution scheme principally, so that parallelism can be exploited in the solution process. This technique can reduce the amount of work required and enable the solution of very large problems even on uniprocessors. NTIS

N95-25645# International Centre for Theoretical Physics, Trieste (Italy).
NONEXISTENCE OF GLOBAL SOLUTIONS TO SOME QUASILINEAR HYPERBOLIC EQUATIONS WITH DYNAMIC BOUNDARY CONDITIONS
M. Kirane, S. Kouachi (Ecole Normale Superieure de Mecanique, Oum El Bouaghi, Algeria.), and N. Tatar (Annaba Univ., Algeria.) Mar. 1994 7 p
(DE95-607010; IC-94/53) Avail: CASI HC A02/MF A01 (US Sales Only)

The nonexistence of the global solutions to two fourth-order hyperbolic equations with dynamic boundary conditions is considered. The method of proof makes use of the generalized convexity method due to Ladyzhenskaya and Kalantarov. DOE

N95-25676# Los Alamos National Lab., NM. Inst. for Geophysics and Planetary Physics.
NONLINEAR DIFFERENCE APPROXIMATIONS FOR EVOLUTIONARY PDE'S
Donald A. Jones, Len G. Margolin, and Andrew C. Poje 1995 15 p Presented at the NEEDS '94 Conference, Los Alamos, NM, 12-16 Sep. 1994
(Contract W-7405-eng-36)
(DE95-005260; LA-UR-94-4035; CONF-9409241-6) Avail: CASI HC A03/MF A01

The authors describe a procedure to improve both the accuracy and computational efficiency of finite difference schemes used to simulate nonlinear partial differential equations (PDE's). The underlying idea is that of enslaving, which is the estimation of the small unresolved scales in terms of the larger resolved scales. They discuss details of the procedure and illustrate them in the context of the forced Burgers' equation in one dimension. They present computational examples that demonstrate the predicted increases in accuracy and efficiency. DOE

N95-25748# International Centre for Theoretical Physics, Trieste (Italy).
BEHAVIOUR AT X= +/- INFINITY OF SOLUTIONS TO A PR EDATOR-PREY MODEL
M. Kirane, S. Badraoui (Annaba Univ., Algeria.), and M. Guedda (Picardie Univ., Amiens, France.) Jun. 1994 13 p
(DE95-607049; IC-94/55) Avail: CASI HC A03/MF A01 (US Sales Only)

We consider the behavior at x= +/- infinity of solutions to a system of reaction diffusion equations modelling two species in a predator-prey relationship. We show that if the initial data have limits at +/- infinity, then at +/- infinity the solutions will satisfy the free diffusion system for all positive time. DOE

N95-25767# Los Alamos National Lab., NM.
THE HARD TRUTH
Kenneth M. Hanson and Gregory S. Cunningham 1994 9 p Presented at the Maximum Entropy and Bayesian Methods Workshop, Cambridge, UK, 1-4 Aug. 1994 Submitted for publication
(Contract W-7405-eng-36)

(DE95-005240; LA-UR-94-4385; CONF-9408207-1) Avail: CASI HC A02/MF A01

In the Bayesian methodology, the posterior probability combines uncertainty about prior knowledge, and available data about alternative models of reality. The posterior quantifies the degree of certainty one has in inferring the truth in terms of those models. We propose a method to determine the reliability of a specific feature of a Bayesian solution. Our approach is based on an analogy between the negative logarithm of the posterior and a physical potential. This analogy leads to the interpretation of gradient of this potential as a force that acts on the model. As model parameters are perturbed from their maximum a posteriori (MAP) values, the strength of the restoring force that drives them back to the MAP solution is directly related to the reliability of those parameter estimates. The correlations between the uncertainties of parameter estimates can be elucidated. DOE

N95-25782# Joint Inst. for Nuclear Research, Dubna (USSR).
ELLIPSOIDAL BASIS FOR ISOTROPIC OSCILLATOR
W. Kallies (Humboldt Univ., Berlin, German D.R.); I. Lukac, G. S. Pogosyan, and A. N. Sisakyan 1994 12 p
(DE95-605253; JINR-E-2-94-230) Avail: CASI HC A03/MF A01 (US Sales Only)

The solutions of the Schroedinger equation are derived for the isotropic oscillator potential in the ellipsoidal coordinate system. The explicit expression is obtained for the ellipsoidal integrals of motion through the components of the orbital moment and Demkov's tensor. The explicit form of the ellipsoidal basis is given for the lowest quantum numbers. DOE

N95-25783# Joint Inst. for Nuclear Research, Dubna (USSR).
QUANTIZATION OF A HAMILTONIAN SYSTEM WITH AN INFINITE NUMBER OF DEGREES OF FREEDOM
P. E. Zhidkov 1994 14 p
(DE95-605279; JINR-E-5-94-172) Avail: CASI HC A03/MF A01 (US Sales Only)

We propose a method of quantization of a discrete Hamiltonian system with an infinite number of degrees of freedom. Our approach is analogous to the usual finite-dimensional quantum mechanics. We construct an infinite-dimensional Schroedinger equation. We show that it is possible to pass from the finite-dimensional quantum mechanics to our construction in the limit when the number of particles tends to infinity. In the paper rigorous mathematical methods are used. DOE

N95-25860# National Aerospace Lab., Tokyo (Japan). Control Systems Div.
NONLINEAR SYSTEM ANALYSIS USING SLOWLY-VARYING COMPLEX FREQUENCY METHOD
Hiroshi Yamada Dec. 1993 16 p In JAPANESE
(ISSN 0389-4010)
(NAL-TR-1217) Avail: CASI HC A03/MF A01

This paper presents a new method that can be used in the analysis of nonlinear equations. The report also contains four examples of this new method being applied. In this new method, the author analyses a nonlinear equation by dividing the solution into terms with different complex frequencies separated from each other. This is conducted in a manner where the complex frequencies in the two terms forming the fundamental solution have been assumed to vary slowly with time in the vicinity of certain constant frequencies. The purpose of the new method is to clarify the physical concept of each equation. For example, this aids in simplifying the analysis of a nonlinear control system in which the damping factor is extremely large in the vibrating system. Furthermore this method makes it possible to formulate many different solutions to any particular equation. In the four examples presented the author has analyzed equations utilizing a technique based on feedback theory, thus illustrating the method applied to a 'real' physical concept. Author

N95-25893# Linkoeping Univ. (Sweden).
HEURISTIC APPROACH TO THE PATH PLANNING PROBLEM IN A RASTER MAP
E. Toller Apr. 1994 85 p
(PB95-141826; FOA-C-30748-3.4) Avail: CASI HC A05/MF A01

This report describes a method of finding an obstacle-free, reasonably short (not shortest) path between two locations in an image. The method operates directly on a binary image, and uses a set of 17 heuristic rules. The results of the method were compared with the results of a graph-based method that guarantees that it is the shortest path that is generated. The work was implemented in the Common Lisp language, on a Texas Instruments Explorer Lisp machine. NTIS

N95-25906# Joint Inst. for Nuclear Research, Dubna (USSR).
ON THE NUMERICAL METHOD FOR ANALYSIS OF THE DYNAMICS OF THE CLASSICAL HAMILTONIAN SYSTEMS
P. G. Akishin, I. V. Puzynin, V. V. Starkov, and S. I. Vinitskij 1994 12 p
(DE95-605218; JINR-E-11-94-140) Avail: CASI HC A03/MF A01 (US Sales Only)

The numerical algorithm of analysis of the dynamics of the classical Hamiltonian systems with pair potentials is proposed. The method uses the Taylor expansions of solution. The main supposition is: the terms of this Taylor's series may be expressed analytically. There are such potentials which are important in physics. The proposed algorithm allows one to choose efficiently the integration step depending on the behavior of the truncation error of the series, and also to carry out the parallel analysis of evaluation of the small perturbation of solution, which, in turn, makes it possible to reason about such properties of the system as the stability and the transition to chaotic regime. The codes realizing the proposed method have been created. The results of the numerical calculations for some Hamiltonian systems are given. DOE

N95-25982# International Centre for Theoretical Physics, Trieste (Italy).
NUMERICAL SOLUTION OF THE OPTIMIZED RANDOM PHASE APPROXIMATION
G. Pastore (Trieste Univ., Italy.), F. Matthews, O. Akinlade, and Z. Badirkhan Jun. 1994 14 p
(DE95-605636; IC-94/196) Avail: CASI HC A03/MF A01 (US Sales Only)

An accurate, efficient and robust numerical method for the solution of the Optimized Random Phase Approximation (ORPA) of classical liquids is presented. The uniqueness of the solution of the ORPA is rigorously proved. The method, hinging on the characterization of the generating functions, significantly improves on previous algorithms. Higher accuracy is obtained by using the values of the unknown functions on the grid points as independent variables instead of the usual coefficients of an expansion in orthogonal polynomials. It is shown that minimizing a suitably modified functional with a conjugate-gradient algorithm results in a very efficient and robust algorithm. DOE

N95-25989# International Centre for Theoretical Physics, Trieste (Italy).
ON THE COHEN-MACAULAYNESS AND GORENSTEINNESS OF INTEGRAL CLOSURE FILTRATIONS REES ALGEBRAS OF HEIGHT-TWO EQUIMULTIPLE IDEALS
Duong Quoc Viet Jun. 1994 12 p
(DE95-607000; IC-94/136) Avail: CASI HC A03/MF A01 (US Sales Only)

In this paper we give the criteria for an integral closure filtration Rees algebra R(I)-bar of height-two equimultiple ideal I in terms of a basic ring and an ideal I. From these criteria we obtain interesting information on the structure of a basic ring and an ideal I, when Rees algebra R(I)-bar is a Cohen-Macaulay or Gorenstein ring. DOE

N95-25992# International Centre for Theoretical Physics, Trieste (Italy).
THE CRITERIA FOR THE COHEN-MACAULAYNESS AND GORENSTEINESS OF REES ALGEBRAS OF IDEALS HAVING POSITIVE ANALYTIC DEVIATION
Duong Quoc Viet Jun. 1994 13 p
(DE95-607003; IC-94/153) Avail: CASI HC A03/MF A01 (US Sales Only)

This paper investigates the relationships between the maximal reduction number and q-invariant of a graded ring in the case of Rees ring being a Cohen-Macaulay or Gorenstein ring. From these relationships we give the criteria for Rees algebra of the ideal I having arbitrary analytic deviation to be Cohen-Macaulay and Gorenstein in terms of associated graded ring and maximal reduction number of I. DOE

N95-26051 Army Research Lab., Aberdeen Proving Ground, MD.
DYNAMIC MATRICES AND THEIR APPLICATION TO THE CONCEPT OF A SEMI-SPARSE MATRIX Final Report, Jan. 1987 - May 1994
Daniel M. Pressel Nov. 1994 66 p Limited Reproducibility: More than 20% of this document may be affected by microfiche quality
(AD-A288688; ARL-MR-198) Avail: Issuing Activity (Defense Technical Information Center (DTIC))

This report primarily describes research performed by the author while he was still employed by the U.S. Army Chemical Research, Development and Engineering Center, as well as continuing research being conducted by the author at the U.S. Army Research Laboratory, Aberdeen, MD. In a number of cases (e.g., tridiagonal matrices, triangular matrices, and the production of raster images from wireframe CAD data), one is left with the problem of efficiency storing and accessing matrices which are large enough to worry about, and have regions of a meaningful size with no data (or if one prefers, some default value, usually zero), and other regions with at least some data. In many cases, these matrices contain too much data to be efficiently handled using the linked lists commonly used with sparse matrices. On the other hand, they may be too large and too sparse to be efficiently handled using normal methods. The author has named the matrices which fall into this category, SEMI-SPARSE MATRICES. While it is true that there are well-known application-specific methods for dealing with some types of matrices in this category (e.g., triangular matrices), there appears to be no standard mend for dealing with this category as a whole. In response to some of the problems this caused, the author has developed and implemented the concept which he refers to as a DYNAMIC MATRIX. DTIC

N95-26106 Polish Academy of Sciences, Warsaw (Poland). Dept. of Structural Theory.
SPLINES IN TWO-DIMENSIONAL PROBLEMS [SPLINE'Y W ZAGADNIENIACH]
Zdzislaw Iwanow, Jacek Bauer, and Jacek Ronda (Cape Town Univ., South Africa.) 1993 38 p In POLISH
(ISSN 0208-5658)
(IFTR-2/1993) Avail: Issuing Activity (Polish Academy of Sciences, Warsaw, Poland)

The authors describe the use of splines to determine the first derivatives of functions which transform an initial region into a rectangle relative to the independent variables of the initial system. Because in many cases it is difficult to determine the transformation of the initial region into a rectangle, the authors limit themselves to finding the transformation of the rectangle into the initial region by interpreting it as an implicit representation of the opposite transformation (region into rectangle). The corresponding derivatives are determined as for an implicit function. The authors illustrate the appropriateness and numerical efficiency of the algorithm for cases in which the analytical form of the first transformation and its opposite are known and thus the corresponding derivatives of these transformations are also known. The authors compare their analytically determined values with numerically determined values obtained with the aforementioned algorithm. Transl. by SCITRAN

65 STATISTICS AND PROBABILITY

Includes data sampling and smoothing; Monte Carlo method; and stochastic processes.

N95-24278*# Clemson Univ., SC. Radar Systems Lab.
ON THE JOINT SPECTRAL DENSITY OF BIVARIATE RANDOM SEQUENCES Thesis Technical Report No. 21
David D. Aalfs 17 Jan. 1995 111 p
(Grants NAG1-928; NGT-50414)
(NASA-CR-197698; NAS 1.26:197698; TR-011795-3570P) Avail: CASI HC A06/MF A02

For univariate random sequences, the power spectral density acts like a probability density function of the frequencies present in the sequence. This dissertation extends that concept to bivariate random sequences. For this purpose, a function called the joint spectral density is defined that represents a joint probability weighing of the frequency content of pairs of random sequences. Given a pair of random sequences, the joint spectral density is not uniquely determined in the absence of any constraints. Two approaches to constraining the sequences are suggested: (1) assume the sequences are the margins of some stationary random field, (2) assume the sequences conform to a particular model that is linked to the joint spectral density. For both approaches, the properties of the resulting sequences are investigated in some detail, and simulation is used to corroborate theoretical results. It is concluded that under either of these two constraints, the joint spectral density can be computed from the non-stationary cross-correlation. Author

N95-24643# Joint Inst. for Nuclear Research, Dubna (USSR).
UNFOLDING OF TRUE DISTRIBUTIONS FROM EXPERIMENTAL DATA DISTORTED BY DETECTORS WITH FINITE RESOLUTIONS
N. D. Gagunashvili 1993 14 p Submitted for publication
(DE94-628372; JINR-E-10-93-311) Avail: CASI HC A03/MF A01 (US Sales Only)

A new procedure for unfolding the true distribution from experimental data distorted by a detector is proposed. For the given detector a result can be found by the least squares method, hence, without bias and involving minimal statistical errors. Stability of the result is achieved at the expense of its information content and/or using additional information on the shape of the distributions to be measured. The method may be applied for detectors with linear or nonlinear distortions. DOE

N95-24693# Joint Inst. for Nuclear Research, Dubna (USSR).
INTRODUCTION TO THE MONTE CARLO METHODS
V. V. Uzhinskij 1993 20 p
(DE94-628386; JINR-E-2-93-462) Avail: CASI HC A03/MF A01 (US Sales Only)

Codes illustrating the use of Monte Carlo methods in high energy physics such as the inverse transformation method, the ejection method, the particle propagation through the nucleus, the particle interaction with the nucleus, etc. are presented. A set of useful algorithms of random number generators is given (the binomial distribution, the Poisson distribution, beta-distribution, gamma-distribution and normal distribution). DOE

N95-24858# Joint Inst. for Nuclear Research, Dubna (USSR).
MULTIDIMENSIONAL DATA ANALYSIS ON THE BASIS OF INTEGRAL NONPARAMETRIC STATISTICS AND MULTILAYER PERCEPTRONS
V. V. Ivanov 1993 16 p In RUSSIAN Submitted for publication
(DE94-628375; JINR-R-10-93-348) Avail: CASI HC A03/MF A01 (US Sales Only)

A comparative study of powers of multidimensional classifiers on the basis of integral nonparametric goodness-off-fit criteria omega(sub n)(sup k) and multilayer perceptrons was carried out in the cases where investigated distributions present simultaneous measurements of the same physical values in some detectors of experimental set-up. With the help of a numerical experiment it has been shown that multilayer perceptron provides the power close to limit if the identification of events is carried out in the space of effective variables. A procedure of transformation to such variables is described. Recommendations for the joint usage of the omega(sub n)(sup k) criteria and multilayer perceptrons are given. DOE

N95-24883# Joint Inst. for Nuclear Research, Dubna (USSR).
ON AN EXPANSION OF THE FERMI FUNCTION
V. K. Lukyanov 1993 3 p
(DE94-628494; JINR-R-4-93-300) Avail: CASI HC A01/MF A01 (US Sales Only)

An expansion is obtained of the Fermi-function in the 'diffuseness' parameter where the corresponding coefficients are proportional to derivatives of the delta-function. DOE

66 SYSTEMS ANALYSIS

Includes mathematical modeling; network analysis; and operations research.

N95-24248# Westinghouse Hanford Co., Richland, WA.
WORKFLOW AUTOMATION ARCHITECTURE STANDARD
R. P. Moshofsky and W. T. Rohen (Boeing Computer Services Co., Richland,

WA.) 14 Nov. 1994 66 p
(Contract DE-AC06-87RL-10930)
(DE95-004748; WHC-SD-TD-CSWD-002) Avail: CASI HC A04/MF A01

This document presents an architectural standard for application of workflow automation technology. The standard includes a functional architecture, process for developing an automated workflow system for a work group, functional and collateral specifications for workflow automation, and results of a proof of concept prototype. DOE

N95-25894# Linkoeping Univ. (Sweden).
ASPECT ESTIMATION OF AN AIRCRAFT USING LIBRARY MODEL SILHOUETTES
A. Lauberts Jun. 1994 23 p
(PB95-141834; FOA-C-30763-8.4,3.4) Avail: CASI HC A03/MF A01

This matching method uses a library of silhouettes of a model aircraft with 512 uniformly distributed orientations. The library contains silhouettes of aircraft aspects stored as chain code in a look-up table. Scaled model silhouettes are matched to a distance transform map of the object silhouette. The scaling is according to the apparent major diameter, being a relatively rotation invariant quantity. After translation to a common center of area, the silhouettes are rotated in discrete angular steps until best fit model-object. The best matched views, constrained within a small group of nearby aspect directions, are added vectorially using inverse fit errors as weights to yield an optimum aspect direction. The corresponding aspect angles define the model orientation, and therefore give an estimate of the object orientation. Optionally, radar gives position and velocity of the object, restricting the number of possible views. However, only the aspect matching method supplies the instantaneous 3D orientation needed for accurate prediction of an evasive flight maneuver. NTIS

67 THEORETICAL MATHEMATICS

Includes topology and number theory.

N95-24504# Joint Inst. for Nuclear Research, Dubna (USSR). Theoretical Physics Lab.
ON SQUARING THE PRIMARY CONSTRAINTS IN A GENERALIZED HAMILTONIAN DYNAMICS
V. V. Nesterenko 1993 12 p Submitted for publication
(DE94-628500; JINR-E-2-93-328) Avail: CASI HC A03/MF A01 (US Sales Only)

Consideration of the model of the relativistic particle with curvature and torsion in the three-dimensional space-time shows that the squaring of the primary constraints entails a wrong result. The complete set of the Hamiltonian constraints arising here corresponds to another model with an action similar but not identical with the initial action. DOE

N95-24688# Joint Inst. for Nuclear Research, Dubna (USSR). Theoretical Physics Lab.
SADDLE-POINT METHOD IN PATH INTEGRALS
A. L. Koshkarov 1993 10 p In RUSSIAN Submitted for publication
(DE94-628379; JINR-R-2-93-321) Avail: CASI HC A02/MF A01 (US Sales Only)

Functional saddle-point approximation is developed to evaluate the quantum-mechanical path integral for the probability amplitude of a particle propagating in an arbitrary potential V(x). This method is analogous to the conventional saddle-point approximation for the ordinary finite dimensional integrals, but it does not require the transition to the Euclidean form of the theory. The consideration is essentially based on the notion of functional Cauchy-Riemann conditions and the Cauchy theorem. After choosing the proper steepest-descent contour original path integral is reduced to that of the cutting exponent. The results obtained may provide a ground for constructing functional measures for the Feynman path integrals. DOE

N95-24699# Joint Inst. for Nuclear Research, Dubna (USSR).
EQUIVARIANT LOCALIZATION: BV-GEOMETRY AND SUPERSYMMETRIC DYNAMICS
A. P. Nersesyan 1993 11 p
(DE94-628436; JINR-E-2-93-358) Avail: CASI HC A03/MF A01 (US Sales Only)

It is shown, that the geometrical objects of Batalin-Vilkovisky formalism - odd symplectic structure and nulpotent operator delta can be naturally incorporated in Duistermaat-Heckman localization procedure. The presence of the supersymmetric bi-Hamiltonian dynamics with even and odd symplectic structure in this procedure is established. These constructions can be straightly generalized for the path-integral case. DOE

N95-25434# International Centre for Theoretical Physics, Trieste (Italy).
TWO DIMENSIONAL SIMPLICIAL PATHS
M. I. Piso Jul. 1994 6 p Sponsored by Romanian Space Agency
(DE95-607087; IC-94/207) Avail: CASI HC A02/MF A01 (US Sales Only)

Paths on the R(sup 3) real Euclidean manifold are defined as 2-dimensional simplicial strips which are orbits of the action of a discrete one-parameter group. It is proven that there exists at least one embedding of R(sup 3) in the free Z-module generated by S(sup 2)(x(sub 0)). The speed is defined as the simplicial derivative of the path. If mass is attached to the simplex, the free Lagrangian is proportional to the width of the path. In the continuum limit, the relativistic form of the Lagrangian is recovered. DOE

N95-25439# International Centre for Theoretical Physics, Trieste (Italy).
SYMBOLIC DYNAMICS OF THE LORENZ EQUATIONS
Hai-Ping Fang and Bai-Lin Hao Jul. 1994 31 p Sponsored by Chinese Natural Science Foundation and the Academia Sinica
(DE95-607045; IC-94/184) Avail: CASI HC A03/MF A01 (US Sales Only)

The Lorenz equations are investigated in a wide range of parameters by using the method of symbolic dynamics. First, the systematics of stable periodic orbits in the Lorenz equations is compared with that of the one-dimensional cubic map, which shares the same discrete symmetry with the Lorenz model. The systematics is then 'corrected' in such a way as to encompass all the known periodic windows of the Lorenz equations with only one exception. Second, in order to justify the above approach and to understand the exceptions, another 1D map with a discontinuity is extracted from an extension of the geometric Lorenz attractor and its symbolic dynamics is constructed. All this has to be done in light of symbolic dynamics of two-dimensional maps. Finally, symbolic dynamics for the actual Poincare return map of the Lorenz equations is constructed in a heuristic way. New periodic windows of the Lorenz equations and their parameters can be predicted from this symbolic dynamics in combination with the 1D cubic map. The extended geometric 2D Lorenz map and the 1D antisymmetric map with a discontinuity describe the topological aspects of the Lorenz equations to high accuracy. DOE

N95-25455# International Centre for Theoretical Physics, Trieste (Italy).
EQUIVARIANT KAEHLER GEOMETRY AND LOCALIZATION IN THE G/G MODEL
Matthias Blau and George Thompson Jun. 1994 39 p
(DE95-607073; IC-94/108; ENSLAPP-L-469/94) Avail: CASI HC A03/MF A01 (US Sales Only)

We analyze in detail the equivariant supersymmetry of the G/G model. In spite of the fact that this supersymmetry does not model the infinitesimal action of the group of gauge transformations, localization can be established by standard arguments. The theory localizes onto reducible connections and a careful evaluation of the fixed point contributions leads to an alternative derivation of the Verlinde formula for the G(sub k) WZW model. We show that the supersymmetry of the G/G model can be regarded as an infinite dimensional realization of Bismut's theory of equivariant Bott-Chern currents on Kaehler manifolds, thus providing a convenient cohomological setting for understanding the Verlinde formula. We also show that the supersymmetry is related to a non-linear generalization (q-deformation) of the ordinary moment map of symplectic geometry in which a representation of the Lie algebra of a group G is replaced by a representation of its group algebra with commutator (g,h) = gh - hg. In the large k limit it reduces to the ordinary moment gap of two-dimensional gauge theories. DOE

N95-25522# International Centre for Theoretical Physics, Trieste (Italy).
ON D=2 (1/3, 1/3) SUPERSYMMETRIC THEORIES 1
E. H. Saidi (Mohammed V Univ., Rabat, Morocco.), J. Zerouaoui (Mohammed V Univ., Rabat, Morocco.), and M. B. Sedra Jun. 1994 20 p
(DE95-607075; IC-94/130) Avail: CASI HC A03/MF A01 (US Sales Only)

Denoting by D=2 (1/k,1/k) superalgebra the two dimensional generalized supersymmetry generated by spin s=1/k and -1/k; k=2,3,4, ... charge operators Q and Q-bar satisfying among other things Q(sup k)=P and Q-bar(sup k)=P-bar where P and P-bar are the light components of the energy momentum operator, we build a superspace representation of this exotic symmetry. This realization generalizing the usual D=2 (1/2,1/2) supersymmetric one is based on the use of parafermionic variables theta and theta-bar of spin s=-1/k and 1/k obeying theta(sup k)=theta-bar(sup k)=0 as well as generalized commutation relation rules. Two-dimensional (1/3,0) and (1/3,1/3) invariant scalar superfield models extending the well-known D=2 (1/2,0) and (1/2,1/2) supersymmetric models are given. The link between this exotic symmetry and the periodic representation of U(sub q)(sl(sub 2)) with q(sup k)=I is worked out. Other features are also discussed. DOE

N95-25523# International Centre for Theoretical Physics, Trieste (Italy).
ON D=2 (1/3,1/3) SUPERSYMMETRIC THEORIES 2
E. H. Saidi (Mohammed V Univ., Rabat, Morocco.), J. Zerouaoui (Mohammed V Univ., Rabat, Morocco.), and M. B. Sedra Jun. 1994 18 p
(DE95-607076; IC-94/131) Avail: CASI HC A03/MF A01 (US Sales Only)

Denoting by D=2 (1/3,1/3) superalgebra; the off critical symmetry of the Phi(sub 5/7,5/7) perturbation of the C=6/7 conformal theory, we build a new superspace solution of the (1/3,1/3)(sup -) subalgebra generated by spin +/- 1/3 charge operators extending the usual (1/2,1/2) supersymmetry generated by spin +/- 1/2 charges. This solution is based on the use of two Grassmann variables instead of one parafermionic variable theta(sub +/- 1/3) satisfying the cubic nilpotency condition (theta(sub +/-1/3))(sup 3)=0. Known results on the C=6/7 tricritical Potts model are recovered as special features. A relation with N=2 Landau-Ginzburg models is also discussed. DOE

N95-25599# International Centre for Theoretical Physics, Trieste (Italy).
CENTRAL EXTENSION OF A NEW W(INFINITY)-TYPE ALGEBRA
M. N. Stoilov and R. P. Zaikov (Institute for Nuclear Research and Nuclear Energy, Sofia, Bulgaria.) Jul. 1994 6 p Sponsored by Bulgarian National Scientific Foundation
(DE95-607086; IC-94/201) Avail: CASI HC A02/MF A01 (US Sales Only)

The central extension of a new infinite dimensional algebra which has both W(infinity) and affine sl(2, R) as subalgebras is found. The critical dimension of the corresponding string model is D = 5. DOE

N95-25781# Joint Inst. for Nuclear Research, Dubna (USSR).
CONSTRAINTS, COMPLEX STRUCTURES AND QUANTIZATION
A. D. Popov 1994 23 p
(DE95-605252; JINR-E-2-94-174) Avail: CASI HC A03/MF A01 (US Sales Only)

The finite-dimensional phase manifolds M, the Marsden-Weinstein reduction of these manifolds by the Hamiltonian action of a connected Lie group G and the geometric quantization of the reduced manifolds M(sub G) are considered. We study geometry of a Kaehler manifolds for which the action of G on M does not preserve a complex structure J on M, but preserves some family of complex structures. The algorithm of the geometric quantization of such classical systems is described. We discuss in detail the quantization of the flat phase space R(sup 2n) for the cases when the group G is generated by quadratic first-class constraints. DOE

70 PHYSICS (GENERAL)

For precision time and time interval (PTTI) see *35 Instrumentation and Photography;* for geophysics, astrophysics or solar physics see *46 Geophysics, 90 Astrophysics,* or *92 Solar Physics.*

N95-24363# Joint Inst. for Nuclear Research, Dubna (USSR).
A COMPUTING PROGRAM OF SAMPLE MAGNETIC MOMENTS RECOGNITION FOR SQUID-MAGNETOMETER MEASUREMENTS
E. I. Litvinenko and Yu. V. Obukhov 1994 15 p
(DE94-637073; JINR-R-10-94-44) Avail: CASI HC A03/MF A01 (US Sales Only)

A method of SQUID-magnetometer signal analysis, based on the convolution equation solution is proposed. This method allows one to obtain the local contribution of magnetic moments by coordinates for a sample to be under investigation. The errors of the method are estimated. A computing program with a user friendly interface has been developed for Micro soft Windows 3.1 application. DOE

N95-24479# Oak Ridge National Lab., TN.
SPIN CORRELATIONS IN PERCOLATING NETWORKS WITH FRACTAL GEOMETRY
H. Ikeda (Keio Univ., Hiyoshi, Japan.), K. Iwasa (Keio Univ., Hiyoshi, Japan.), J. A. FernandezBaca, and R. M. Nicklow 28 Jul. 1994 23 p Presented at the Neutron Scattering, Sendai, Japan, 11-14 Oct. 1994
(Contract DE-AC05-84OR-21400)
(DE95-001074; CONF-9410165-6) Avail: CASI HC A03/MF A01

Using neutron scattering techniques, the authors investigated the magnetic correlations in diluted antiferromagnets close to the percolation threshold in which the magnetic connectivity takes a fractal form. Recent experimental results concerning the self-similarity of the magnetic order, and magnetic excitations in two-dimensional Ising and three-dimensional Heisenberg antiferromagnets are presented. DOE

N95-24696# Joint Inst. for Nuclear Research, Dubna (USSR).
TOROIDAL RESPONSE IN MAGNETIC RESONANCE
V. M. Dubovik, I. V. Lunegov, and M. A. Martsenyuk 1993 22 p In RUSSIAN Submitted for publication
(DE94-628406; JINR-R-6-93-244) Avail: CASI HC A03/MF A01 (US Sales Only)

Toroidal response of a nuclear spin system to the pulse of a uniform ratio frequency magnetic field is considered. It is shown that the toroidal moment of the system induces an electrical field response which may be measured together with the magnetic field response (that is induced by the magnetic moment of the system and it is usually observed in NMR). An example of a system of three nuclear spins is examined in detail by the direct solution of the Schroedinger equation. Both responses-magnetic and toroidal-are evaluated and compared with each other. The general approach based on SO(4)group representation of spin dynamics is also used. It allows one to take into consideration the toroidal moment of the system and gives the possibility to clarify the origin of toroidal response. The general scheme of the device for registering the electric component of the response is discussed. DOE

N95-24732# Joint Publications Research Service, Washington, DC.
JPRS REPORT: SCIENCE AND TECHNOLOGY. CENTRAL EURASIA
9 Dec. 1994 79 p Transl. into ENGLISH from various Central Eurasian articles
(JPRS-UST-94-033) Avail: CASI HC A05/MF A01

Translated articles cover the following topics: rotation of a body revolving around a center of mass; possible applications of self-channeling in the matter of strong ultrashort laser pulses; new method of aerospace photography and problems in photogrammetry. CASI

N95-25339 Polish Academy of Sciences, Warsaw (Poland). Inst. of Basic Problems of Technology.
AN ANALYSIS OF HYPERCRITICAL STATES IN ELASTIC AND INELASTIC SYSTEMS [ANALIZA STANOW POKRYTYCZNYCH W UKLADACH SPREZYSTYCH I NIESPREZYSTYCH]
Maciej Kowalczk 1994 163 p In POLISH
(ISSN 0208-5658)
(IFTR-1/1994) Avail: Issuing Activity (Polish Academy of Sciences, Warsaw, Poland)

The author raises a wide range of problems whose common characteristic is an analysis of hypercritical states in elastic and inelastic systems. the article consists of two basic parts. The first part primarily discusses problems of modelling hypercritical states, while the second analyzes numerical methods (so-called continuation methods) used to solve non-linear problems. The original approaches for modelling hypercritical states found in this article include the combination of plasticity theory and an energy condition for cracking, accounting for the variability and cyclical nature of the forms of fracture of a brittle material under a die, and the combination of plasticity theory and a simplified description of the phenomenon of localization along a discontinuity line. The author presents analytical solutions of three non-linear problems for systems made of

elastic/brittle/plastic and elastic/ideally plastic materials. The author proceeds to discuss the analytical basics of continuation methods and analyzes the significance of the parameterization of non-linear problems, provides a method for selecting control parameters based on an analysis of the rank of a rectangular matrix of a uniform system of increment equations, and also provides a new method for selecting an equilibrium path originating from a bifurcation point. The author provides a general outline of continuation methods based on an analysis of the rank of a matrix of a corrective system of equations. The author supplements his theoretical solutions with numerical solutions of non-linear problems for rod systems and problems of the plastic disintegration of a notched rectangular plastic plate. Author

N95-25408# Stanford Linear Accelerator Center, CA.
FASTER MAGNET SORTING WITH A THRESHOLD ACCEPTANCE ALGORITHM
S. Lidia (California Univ., Davis, CA.) and R. Carr Aug. 1994 4 p Presented at the International Meeting on Synchrotron Radiation Instrumentation, Stony Brook, NY, 18-22 Jul. 1994
(Contract DE-AC03-76SF-00515)
(DE95-006487; SU-SLAC-PUB-6632; SLAC/SSRL-0091; CONF-940714-48) Avail: CASI HC A01/MF A01

The authors introduce here a new technique for sorting magnets to minimize the field errors in permanent magnet insertion devices. Simulated annealing has been used in this role, but they find the technique of threshold acceptance produces results of equal quality in less computer time. Threshold accepting would be of special value in designing very long insertion devices, such as long FEL's. Their application of threshold acceptance to magnet sorting showed that it converged to equivalently low values of the cost function, but that it converged significantly faster. They present typical cases showing time to convergence for various error tolerances, magnet numbers, and temperature schedules. DOE

N95-25430# Melbourne Univ., Parkville (Australia). School of Physics.
ON THE EFFECTS OF GRAVITATIONAL FIELDS ON THE ELECTRICAL PROPERTIES OF MATTER
Geoffrey I. Opat 1993 9 p Sponsored by Australian Research Council
(DE95-607022; UM-P-93/61) Avail: CASI HC A02/MF A01 (US Sales Only)

A discussion of the electrical state of a conducting solid in a static gravitational field is presented. The analysis of the stress-gravitational force balance inside the solid is complicated; however, outside the solid, in the evanescent electron field, the analysis of such a balance simplifies greatly. As a consequence of this external analysis, an expression for the electric field external to the body is presented which includes the direct effect of gravity on the electrons, as well as the indirect effect due to the stress induced by gravity acting on the bulk solid. Such fields are an important determinant of the gravitational motion of charged particles within metallic shields. DOE

N95-25458# Melbourne Univ., Parkville (Australia). School of Physics.
STAGGERED MAGNETIZATION IN THE HEISENBERG ANTIFERROMAGNET
Lloyd C. L. Hollenberg and Michael J. Tomlinson 1993 13 p Sponsored by Australian Research Council
(DE95-607102; UM-P-93/72) Avail: CASI HC A03/MF A01 (US Sales Only)

In the presence of a staggered magnetic field, the plaquette expansion of the Lanczos matrix elements are obtained for the antiferromagnetic 2D Heisenberg model up to order 1/N(sub p) (N(sub p) is the number of plaquettes on the lattice). The resulting approximate tri-diagonal form of the Hamiltonian is diagonalized for various values of the field strength in the N(sub p) (approaches) (infinity) limit for the ground state energy density. From the behaviour of the ground state energy density at weak fields, the staggered magnetization at this order in the plaquette expansion is found to be 0.647 (in units where the Neel state staggered magnetization is 1.0). The estimated error is only a few percent. DOE

N95-25524# International Centre for Theoretical Physics, Trieste (Italy).
HYPERKAEHLER METRICS BUILDING AND INTEGRABLE MODELS
E. H. Saidi (Mohammed V Univ., Rabat, Morocco.) and M. B. Sedra Jun. 1994 11 p
(DE95-607077; IC-94/132) Avail: CASI HC A03/MF A01 (US Sales Only)

Methods developed for the analysis of integrable systems are used to study the problem of hyperKaehler metrics building as formulated in D=2 N=4 supersymmetric harmonic superspace. We show, in particular, that the constraint equation (beta)(delta)(sup ++2)(omega)-(xi)(sup ++2) exp2(beta)(omega)=0 and its Toda like generalizations are integrable. Explicit solutions together with the conserved currents generating the symmetry responsible of the integrability of these equations are given. Other features are also discussed. DOE

N95-25552 Academy of Sciences of the Ukraine, Kiev (Ukraine). Inst. Teoreticheskoj Fiziki.
PHYSICS IN UKRAINE INTERNATIONAL CONFERENCE. VOLUME 3: STATISTICAL PHYSICS AND PHASE TRANSITIONS
A. Sitenko, ed. 1993 188 p Conference held in Kiev, Ukraine, 22-27 Jun. 1993
(DE95-605765; INIS-UA-004-Vol-3; CONF-9306388) Copyright Avail: Issuing Activity (Department of Energy (DOE)) (US Sales Only)

Problems of modern physics and the situation with physical research in Ukraine are considered. Program of the conference includes scientific and general problems. Its proceedings are published in six volumes. The papers presented in this volume refer to statistical physics and phase transition theory. DOE

N95-25553 Academy of Sciences of the Ukraine, Kiev (Ukraine). Inst. Teoreticheskoj Fiziki.
PHYSICS IN UKRAINE INTERNATIONAL CONFERENCE. VOLUME 5: LOW TEMPERATURE PHYSICS
A. Sitenko, ed. 1993 271 p Conference held in Kiev, Ukraine, 22-27 Jun. 1993
(DE95-605800; INIS-UA-004-Vol-5; CONF-9306388) Copyright Avail: Issuing Activity (Department of Energy (DOE)) (US Sales Only)

Problems of modern physics and the situation with physical research in Ukraine are considered. The program of the conference includes scientific and general problems. Its proceeding are published in six volumes. The papers presented in this volume refer to low-temperature physics. DOE

N95-25600# Oak Ridge National Lab., TN.
SUPERCONDUCTIVITY, MAGNETISM AND METAL-INSULATOR TRANSITIONS IN SOME TERNARY AND PSEUDOTERNARY 3D-, 4D- AND 5D-METAL OXIDES
D. C. Johnston (Iowa State Univ. of Science and Technology, Ames, IA.), T. Ami (Du Pont de Nemours, E. I. and Co., Wilmington, DE.), F. Borsa (Iowa State Univ. of Science and Technology, Ames, IA.), M. K. Crawford (Du Pont de Nemours, E. I. and Co., Wilmington, DE.), J. A. Fernandez-Baca, K. H. Kim (Iowa State Univ. of Science and Technology, Ames, IA.), R. L. Harlow (Du Pont de Nemours, E. I. and Co., Wilmington, DE.), A. V. Manajan (Iowa State Univ. of Science and Technology, Ames, IA.), L. L. Miller (Iowa State Univ. of Science and Technology, Ames, IA.), and M. A. Subramanian (Du Pont de Nemours, E. I. and Co., Wilmington, DE.) et al 1994 23 p Presented at the 17th International Taniguchi Symposium on Theoretical Physics on Spectroscopy of Mott Insulators and Correlated Metals, Shima, Japan,24-29 Oct. 1994 Submitted for publication
(Contract DE-AC05-84OR-21400)
(DE95-005904; CONF-9410283-1) Avail: CASI HC A03/MF A01

Electron conduction effects have been found to be particularly important in the metallic compounds LiV2O4 and possibly Sr2l(1-x)Ru(x)O4 (x greater than 0.7), but not in metallic Sr(1-x)La(x)VO3 (x less than 0.7), and they cause the compounds Sr2lrO4 and ZnV2O4 to be (Mott-Hubbard) insulators. The LiV2O4 spinel compound is especially interesting, because the V ions exhibit rather clear local moment (S = 1/2) behavior even though the compound is a metal. DOE

N95-25616 Academy of Sciences of the Ukraine, Kiev (Ukraine). Inst. Teoreticheskoj Fiziki.
PHYSICS IN UKRAINE INTERNATIONAL CONFERENCE. VOLUME 4: RADIOPHYSICS AND ELECTRONICS
A. Sitenko, ed. 1993 294 p Conference held in Kiev, Ukraine, 22-27 Jun. 1993

(DE95-605570; INIS-UA-004-Vol-4; CONF-9306388) Copyright Avail: Issuing Activity (Department of Energy (DOE)) (US Sales Only)

Problems of modern physics and the situation with physical research in Ukraine are considered. The areas covered in the conference include: (1) physics of elementary particles and quantum field theory; (2) nuclear physics; (3) solid state physics; (4) statistical physics and phase transitions; (5) plasma physics; (6) radiophysics and electronics; and (7) low temperature physics. The proceedings are published in 6 volumes. The papers presented in this volume refer to radio physics and electronics. DOE

N95-25646# International Centre for Theoretical Physics, Trieste (Italy).

THE GEODESIC MOTION IN KALUZA-KLEIN SPINNING SPACE

Dumitru Baleanu Apr. 1994 13 p

(DE95-607070; IC-94/84) Avail: CASI HC A03/MF A01 (US Sales Only)

The geodesic motion of pseudo-classical spinning particles in the space of a Kaluza-Klein monopole in the presence of a scalar sigma field coupled to the metric tensor is analysed. The generalized equations for spinning space are investigated and the constants of motion are derived in terms of the solutions of these equations. The motion on a cone and on a plane is analyzed. DOE

N95-26332 Polish Academy of Sciences, Warsaw (Poland). Inst. of Basic Problems of Technology.

THE ROTATIONS OF DEFORMABLE BODIES. PART 1: GEOMETRY AND KINEMATICS [OBROTY CIAL ODKSZTALCALNYCH CZESC I GEOMETRIA I KINAMATYKA]

Andrzej Blinowski 1994 114 p In POLISH

(ISSN 0208-5658)

(IFTR-7/1994) Avail: Issuing Activity (Polish Academy of Sciences, Warsaw, Poland)

This treatise contains a geometry and kinematic description of the rotation of material objects and non-material objects coupled with a deformable material medium. The rotations of rigid bodies and their kinematics are examined as a special case of the motions of deformable bodies. In order to standardize the terminology used to describe rotations and major deformations of the medium, the description involves the successive use of orthogonal tensors and their time derivatives. In order to make it easier for the reader, the treatise contains a large number of references which point out, reinterpret, and comment on the important relations of the broadly comprehended tensor calculus, several of which are derived in full with the exception of its two introductory paragraphs, the first part contains a description of the geometry of the orientation space (the set of rotation tensors) as a three-dimensional submanifold of a nine-dimensional linear space of second-rank tensors. The author also studies both the local and global properties of the orientation space, the functions defined on this space, and the differential operators. The second, kinematic part of the treatise contains a description of time derivatives of the rotation tensors and their location in the space adjacent to the rotation manifold. The author also examines kinematics in the orientation space and in particular introduces a local balance law for the orientation decomposition function. Part 3 is devoted to the geometry and kinematics of objects coupled with a deformable continuum such as fibers and material surfaces and so-called Mandel reference points, which are introduced for the purpose of describing rotations in plasticity theory. The author also examines the rotation velocities of the sets of main directions of symmetric tensors, for which he introduces closed formulas. The last section is devoted to a description of the evolution of the curvatures of fibers and material surfaces (bending and the rate of bending) using the characteristics of the motion of the medium (the second gradients of deformation and velocity fields). The configuration and choise of material and the method of explaining it were intended more for purposes of interpreation and illustration than mathematical rigor. Transl. by Schreiber Translations Inc.

71 ACOUSTICS

Includes sound generation, transmission and attenuation.
For noise pollution see *45 Environmental Pollution.*

N95-24879*# Georgia Tech Research Inst., Atlanta, GA. Acoustics, Aerodynamics, and Advanced Vehicles Div.

EFFECTS OF CAVITY DIMENSIONS, BOUNDARY LAYER, AND TEMPERATURE ON CAVITY NOISE WITH EMPHASIS ON BENCHMARK DATA TO VALIDATE COMPUTATIONAL AEROACOUSTIC CODES

K. K. Ahuja and J. Mendoza Apr. 1995 278 p

(Contract NAS1-19061; RTOP 505-59-52-01)

(NASA-CR-4653; NAS 1.26:4653) Avail: CASI HC A13/MF A03

This report documents the results of an experimental investigation on the response of a cavity to external flowfields. The primary objective of this research was to acquire benchmark of data on the effects of cavity length, width, depth, upstream boundary layer, and flow temperature on cavity noise. These data were to be used for validation of computational aeroacoustic (CAA) codes on cavity noise. To achieve this objective, a systematic set of acoustic and flow measurements were made for subsonic turbulent flows approaching a cavity. These measurements were conducted in the research facilities of the Georgia Tech research institute. Two cavity models were designed, one for heated flow and another for unheated flow studies. Both models were designed such that the cavity length (L) could easily be varied while holding fixed the depth (D) and width (W) dimensions of the cavity. Depth and width blocks were manufactured so that these dimensions could be varied as well. A wall jet issuing from a rectangular nozzle was used to simulate flows over the cavity. Author

N95-25115 Polish Academy of Sciences, Warsaw (Poland). Instytut Podstawowych Problemow Techniki.

THE USE OF ACOUSTIC SURFACE WAVES TO ANALYZE GASES APPARATUS AND EXPERIMENTS [WYKORZYSTANIE AKUSTYCZNYCH FAL POWIERZCHNIOWYCH DO ANALIZY GAZOW APARATURA I DOSWIADCZENIA]

Jerzy Ranachowski, Eugeniusz Adamczyk, Jadwiga Rzeszotarska, Aleksander Opilski, Marian Urbanczyk, and Wieslaw Jakubik Dec. 1994 25 p In POLISH

(ISSN 0208-5658)

Avail: Issuing Activity (Polish Academy of Sciences, Warwaw, Poland)

Recent years have witnessed the rapid development of new methods for diagnosing man's natural environment. Especially noteworthy are the acoustic methods based on the use of surface acoustic wave (SAW) propagation in layered systems in which a macromolecular compound is the chemically active layer. This article presents the results of studies of the effects of a selected group of gases and organic solvent vapors on the acoustic properties of a thin film of copper phthalocyanine CuPc. The authors also describe the apparatus developed and built for this method by the Institute of Basic Problems of Technology of the Polish Academy of Sciences. Author

N95-25503 Salford Univ. (England).

ATMOSPHERIC AND TERRAIN EFFECTS ON ACOUSTIC PROPAGATION Final Report

M. West 1 Oct. 1994 14 p

(Contract DAJA45-93-C-0033)

(AD-A288727; USARL/O3; R/D-6968-EN-01) Avail: Issuing Activity (Defense Technical Information Center (DTIC))

Three computer models have been configured to give predictions under a range of atmospheric and terrain conditions which have allowed comparisons with measurements. A new parabolic equation (PE) model, (HIPEDEM) which uses the robust Crank Nicholson (CN) algorithm and which includes novel procedures for treating the ground and upper atmospheric boundaries, has been developed together with a new turbulent atmosphere front end processor which can be coupled to the high atmosphere PE to give turbulent atmosphere predictions. A new generalized terrain PE model (GT-PE) has been developed which is capable of predictions over any smooth two dimensional terrain profile in the presence of a moving atmosphere. A feasibility study on the split step high speed PE has also been completed and a tutorial code for testing it has been written. Some interesting insights into the operational requirements of the Greens function PE (GF-PE) have been gained. DTIC

N95-26071 Polish Academy of Sciences, Warsaw (Poland). Inst. of Basic Problems of Technology.
AN ANALYSIS OF THE FEASIBILITY OF USING THE HSU-NIELSEN CALIBRATION METHOD IN SYSTEMS FOR MEASURING ACOUSTIC EMISSION FROM PARTIAL DISCHARGES [ANALIZA MOZLIWOSCI WYKORZYSTANIA METODY WZORCOWANIA HSU-NIELSENA W UKLADACH DO POMIARU EA OD WYLADOWAN NIEZUPELNYCH]
Jerzy Skubis (Technical Univ. of Opole, Poland.), Zbigniew Ranachowski, T. Boczar (Technical Univ. of Opole, Poland.), and M. Lorenc (Technical Univ. of Opole, Poland.) 1994 39 p In POLISH
(ISSN 0208-5658)
(IFTR-20/1994) Avail: Issuing Activity (Polish Academy of Sciences, Warsaw, Poland)

The subject of this article is an analysis of the feasibility of using the Hsu-Nielsen calibration method to measure acoustic emission from partial discharges. In the first part of the article the authors present a concept and method of calibration which makes it possible to calibrate the measuring circuit properly. The second part contains the results of experiments which involved calibrating two different acoustic emission analyzers, namely the Izold and the Demy 34 models. In conclusion the authors discuss the practical requirements for proper calibration of the systems in a technical environment. Transl. by Schreiber Translations Inc.

N95-26108 Polish Academy of Sciences, Warsaw (Poland). Aeroacoustics Inst.
THE PHENOMENON OF NON-LINEARITY ACCOMPANYING THE ACTION OF ACOUSTIC PRESSURE ON A HELMHOLTZ RESONATOR [ZJAWISKO NIELINIOWOSCI PRZY ODDZIALYWANIU CISNIENIA AKUSTYCZNEGO NA REZONATOR HELMHOLTZA]
Miroslaw Meissner 1994 51 p In POLISH
(ISSN 0208-5658)
(IFTR-19/1994) Avail: Issuing Activity (Polish Academy of Sciences, Warsaw, Poland)

The purpose of this study was to conduct a theoretical and experimental analysis of the phenomenon of non-linearity which accompanies high acoustic pressure acting on a Helmholtz resonator. In Part 2 of the study the author presents a theoretical model of the phenomenon which accounts for the effect of narrowing the current line downstream of the opening of the resonator during the generation of turbulence. The author derived an equation to describe the oscillations of the system from the balance of pressures on both sides of the opening. In this equation non-linearity losses are defined by a resistance proportional to the amplitude of acoustic velocity in the resonator opening. In Part 3 the author presents the results of measurements of the resonantor's absorption coefficient under a constant incident wave pressure and resistance and reactance under a constant pressure at the base of the resonator. The author's measurement procedure allowed him to determine the general relationship between loss resistance and the amplitude of velocity in the opening. The results revealed that the pressure acting on the resonator may have a major effect on its absorption properties, while the experimentally observed decrease in the absorption coefficient at high pressures is a result of an increase in losses due to non-linearity. Transl. by SCITRAN

N95-26160*# McDonnell-Douglas Aerospace, Long Beach, CA.
NOISE IMPACT OF ADVANCED HIGH LIFT SYSTEMS Final Report
Kevin R. Elmer and Mahendra C. Joshi Mar. 1995 66 p
(Contract NAS1-20103; RTOP 538-03-15-01)
(NASA-CR-195028; NAS 1.26:195028; CRAD-9310-TR-0127) Avail: CASI HC A04/MF A01

The impact of advanced high lift systems on aircraft size, performance, direct operating cost and noise were evaluated for short-to-medium and medium-to-long range aircraft with high bypass ratio and very high bypass ratio engines. The benefit of advanced high lift systems in reducing noise was found to be less than 1 effective-perceived-noise decibel level (EPNdB) when the aircraft were sized to minimize takeoff gross weight. These aircraft did, however, have smaller wings and lower engine thrusts for the same mission than aircraft with conventional high lift systems. When the advanced high lift system was implemented without reducing wing size and simultaneously using lower flap angles that provide higher L/D at approach a cumulative noise reduction of as much as 4 EPNdB was obtained. Comparison of aircraft configurations that have similar approach speeds showed cumulative noise reduction of 2.6 EPNdB that is purely the result of incorporating advanced high lift system in the aircraft design. Author

N95-26180 Polish Academy of Sciences, Warsaw (Poland). Inst. of Basic Problems of Technology.
MEASUREMENTS OF ACOUSTIC EMISSION ON A LASER CERAMIC TREATMENT LINE [POMIARY EMISJI AKUSTYCZNEJ (EA) W TRAKCIE LASEROWEJ OBROBKI CERAMIKI]
Jerzy Ranachowski, Zbigniew Ranachowski, and Adam Zaboklicki (Fraunhofer-Inst. fuer Produktionstechnologie, Aachen, Germany.) Cooperative Publishing House Ltd. 11 Oct. 1994 13 p In POLISH
(ISSN 0208-5658)
(IFTR-28/1994) Avail: Issuing Activity (Polish Academy of Sciences, Warsaw, Poland)

This article describes the results of measurements of the acoustic emission generated on a laser treatment line by three ceramic materials. In their analysis of the results, the authors distinguished two different ranges of thermal loading of the material, with the first not causing any macroscopic structural changes and the second causing local fusion and cracking. The authors compare the energies of the acoustic emission signals generated by the laser beam in ceramic structures characterized by different radiation absorption coefficients in the two ranges of thermal energies. They also describe the method they used to calculate the energy of the acoustic emission detected in the process of subjecting a ceramic specimen to heat shock. Author

N95-26187* National Aeronautics and Space Administration. Lewis Research Center, Cleveland, OH.
JET MIXER NOISE SUPPRESSOR USING ACOUSTIC FEEDBACK Patent
Edward J. Rice, inventor (to NASA) 28 Feb. 1995 12 p Filed 10 Feb. 1994 Division of US-Patent-5,325,661 (US Patent-Appl-SN-46256, filed 14 Apr. 1993)
(NASA-Case-LEW-15170-2; US-Patent-5,392,597;
US-Patent-Appl-SN-194654; US-Patent-Appl-SN-046256;
US-Patent-Class-60-204; US-Patent-Class-60-271;
Int-Patent-Class-F02C-7/00) Avail: US Patent and Trademark Office

The present invention generally relates to providing an improved jet mixer noise suppressor for high speed jets that rapidly mixes high speed air flow with a lower speed air flow, and more particularly, relates to an improved jet mixer noise suppressor that uses feedback of acoustic waves produced by the interaction of shear flow instability waves with an obstacle downstream of the jet nozzle.
Official Gazette of the U.S. Patent and Trademark Office

72 ATOMIC AND MOLECULAR PHYSICS

Includes atomic structure, electron properties, and molecular spectra.

N95-24230# International Atomic Energy Agency, Vienna (Austria). Atomic and Molecular Data Unit.
INTERNATIONAL BULLETIN ON ATOMIC AND MOLECULAR DATA FOR FUSION, NO. 47
Javier Botero, ed. Dec. 1993 146 p
(DE94-634442; IBAMD-47) Avail: CASI HC A07/MF A02 (US Sales Only)

This bulletin, published by the IAEA, provides atomic and molecular data references relevant to fusion research and technology. In part 1 the indexation of the papers is provided separately for: (1) structure and spectra; (2) atomic and molecular collisions; and (3) surface interactions. Part 2 contains the bibliographic data for the above-listed topics and for high-energy laser and beam-matter interaction of atomic particles with fields. Also included are sections on atomic and molecular data needs for fusion research and on news about ALADDIN (A Labelled Atomic Data INterface) and evaluated data bases. DOE

N95-24231# International Atomic Energy Agency, Vienna (Austria). Nuclear Data Section.
ATOMIC MASSES 1993. THE 1993 ATOMIC MASS EVALUATION

G. Audi and A. H. Wapstra 4 Nov. 1993 8 p Revised
(DE94-634462; IAEA-NDS-47-Rev-2) Avail: CASI HC A02/MF A01 (US Sales Only)

The 1993 atomic mass evaluation by G. Audi and A.H. Wapstra is documented. The resulting data files containing recommended values of atomic masses, obtained by experiment of systematics, and related data such as reaction and separation energies are described. The data files can be obtained through online services from several nuclear data centers or on magnetic tape, free of charge. DOE

N95-24232# International Centre for Theoretical Physics, Trieste (Italy).
FRACTAL STUDIES ON THE POSITRON ANNIHILATION IN METALS
C. W. Lung Jun. 1994 7 p Sponsored by the International Atomic Energy Agency, the United Nations Educational Scientific and Cultural Organization, and the National Natural Science Foundation of China
(DE94-634488; IC-94/125) Avail: CASI HC A02/MF A01 (US Sales Only)

Traditionally, the Euclidean lines, circles and spheres have served as the basis of the intuitive understanding of the geometry of nature. Recently, the concept of fractals caught the imagination of scientists in many fields. This paper continues our previous work on position annihilation near fractal surfaces and demonstrates that the concept of fractals provides a powerful tool for understanding the structure and properties of defects and rough surfaces in relation to positron annihilation studies. Some problems on Berry geometrical phase are also discussed. DOE

N95-24252# Fermi National Accelerator Lab., Batavia, IL.
STUDY OF THE STRUCTURE OF THE EVENTS PRODUCED IN SOFT (BAR p)p INTERACTIONS OF (RADICAL)s = 1800 GeV
F. Rimondi Dec. 1994 10 p Presented at the 24th International Symposium on Multiparticle Dynamics, Vietri sul Mare, Italy, 12-19 Sep. 1994
(Contract DE-AC02-76CH-03000)
(DE95-004851; FNAL/C-94/404-E; CONF-9409257-3) Avail: CASI HC A02/MF A01

In this note preliminary results on a systematic study of the event structure dependence on the event multiplicity and/or event average p(sub t) are presented. The mean p(sub t), the short range pseudorapidity correlations and the mean sphericity are analysed as a function of the event multiplicity. The mean sphericity and the mean multiplicity are studied as a function of the event average p(sub t). DOE

N95-24253# Fermi National Accelerator Lab., Batavia, IL.
MEASUREMENT OF THE SS-OS DIJET CROSS-SECTION RATIO
Jun. 1994 14 p Presented at the ICHEP '94, Glasgow, England, 20-27 Jul. 1994
(Contract DE-AC02-76CH-03000)
(DE95-004852; FNAL/C-94/144-E; CONF-9407142-7) Avail: CASI HC A03/MF A01

The authors present a measurement of the same-side to opposite side dijet cross section ratio in p(bar p) collisions at (radical)s = 1.8 TeV, using approximately 19 pb(exp -1) of data collected by the Collider Detector at Fermilab during the 1992-93 run of the Fermilab Tevatron. They show that, for large pseudorapidities and small transverse energies, this ratio is sensitive to the gluon distribution at small x. They compare the measured values of the ratio with the theoretical predictions, smeared to incorporate detector effects, for a variety of parton distributions. Overall, They find very good agreement between the data and the predictions for a wide range of jet energies and pseudorapidities. At low transverse energies, there are some minor discrepancies between the data and the predictions that could arise from the effects of a more singular gluon distribution. DOE

N95-24254# Fermi National Accelerator Lab., Batavia, IL.
TOP QUARK KINEMATICS AND MASS DETERMINATION
H. H. Williams Oct. 1994 9 p Presented at the ICHEP '94, Glasgow, England, 20-27 Jul. 1994
(Contract DE-AC02-76CH-03000)
(DE95-004853; FNAL/C-94/368-E; CONF-9407142-5) Avail: CASI HC A02/MF A01

An analysis is presented of 10 W + greater than or equal to 3 jet events, each with evidence for the presence of a b quark, that were recently observed by the CDF collaboration. Seven of these events include a fourth jet and can be explicitly reconstructed as t(bar t) production. The best estimate of the top quark mass is M(sub t) = 174 +/- 10(sub -12, sup +13) GeV/c(exp 2). A study has also been performed to see if the kinematical properties of events with W + greater than or equal to 3 jets gives evidence for top production. An excess of events with large jet energies, compared to that expected from direct production of W + greater than or equal to 3 jets, is observed. A large fraction of these events also contain a b-quark and a fourth jet. DOE

N95-24256# Fermi National Accelerator Lab., Batavia, IL.
W-CHARGE ASYMMETRY AT CDF, TESTS OF STRUCTURE FUNCTIONS
H. S. Budd Sep. 1994 3 p Presented at the ICHEP '94, Glasgow, England, 20-27 Jul. 1994
(Contract DE-AC02-76CH-03000)
(DE95-004855; FNAL/C-94/337-E; CONF-9407142-6) Avail: CASI HC A01/MF A01

The charge asymmetry of W-bosons produced in p(bar p) collisions has been measured using 19,039 W (yields) e(nu) and W (yields) (mu)(nu) decays recorded by the CDF detector during the 1992-93 Tevatron collider run. The asymmetry is sensitive to the slope of the proton's d/u quark distribution ratio down to x less than 0.01 at Q(sup 2) (approx) M(sub W, sup 2), where nonperturbative QCD effects are minimal. Of recent parton distribution functions, those of Martin, Roberts and Stirling are favored over those of the CTEQ collaboration. This difference is seen even though both sets agree, at the level of the nuclear shadowing corrections, with the recent NMC measurements of F(sub 2, sup (mu)n)/F(sub 2, sup (mu)p). DOE

N95-24258# Los Alamos National Lab., NM.
LAWRENCE LIVERMORE PULSED SPHERE BENCHMARK ANALYSIS OF MCNP(TRADEMARK) ENDF/B-VI
J. D. Court, R. C. Brockhoff, and J. S. Hendricks Dec. 1994 142 p
(Contract W-7405-eng-36)
(DE95-004864; LA-12885) Avail: CASI HC A07/MF A02

Twenty-eight Lawrence Livermore pulsed sphere experiments were modeled using MCNP for the purpose of bench-marking the new MCNP ENDF/B-VI data library. The twenty-eight pulsed sphere experiments contain thirty-four of the 124 isotopic or elemental evaluations contained in the new ENDF/B-VI set. The ENDF/B-VI results are compared to experimental neutron time-of-flight data, the results obtained from using ENDF/B-V, and against an additional data set, the MCNP Recommended Library, which includes Los Alamos group T-2 evaluations. The results show that ENDF/B-VI results give better or comparable results in comparison to experiment to ENDF/B-V in many cases, and do not deviate grossly in the other cases. DOE

N95-24267# Academy of Sciences (USSR), Novosibirsk (USSR).
ON THE POSSIBILITY OF OBTAINING THE POLARIZED PROTONS BY THE METHOD OF DIRECT OPTIC PUMPING OF A FAST ATOMIC BEAM
V. G. Shamovsky 1993 8 p
(DE94-634309; BUDKERINP-93-40; IYaF-93-40) Avail: CASI HC A02/MF A01 (US Sales Only)

The direct optic pumping of accelerated hydrogen atoms is shown to be really possible. The method allows to obtain a spin polarized H ion beam with the polarization degree = 1 and the real intensity which is close to the currently attained intensity of nonpolarized ion beams. DOE

N95-24268# International Centre for Theoretical Physics, Trieste (Italy).
LASER COOLING OF NEUTRAL ATOMS BY RED-SHIFTED DIFFUSE LIGHT IN AN OPTICAL INTEGRAL SPHERE CAVITY
Yuzhu Wang, Hongxin Chen (Academia Sinica, Shanghai, China.), Weiquan Cai (Academia Sinica, Shanghai, China.), Liang Liu (Academia Sinica, Shanghai, China.), Shanyu Zhou (Academia Sinica, Shanghai, China.), Wei Shu (Academia Sinica, Shanghai, China.), and Fosheng Li (Academia Sinica, Shanghai, China.) May 1994 12 p
(DE94-634310; LAMP-94/5) Avail: CASI HC A03/MF A01 (US Sales Only)

In this paper, we report a cooling and deceleration experiment of a thermal beam by using a nearly resonant red-shifted diffuse light in an

optical integral sphere cavity. With this red-shifted diffuse light, a part of thermal sodium atoms is cooled to 380 m/s and the velocity width of cooled atoms is about 20 m/s. The mechanism of this kind of laser cooling and the experimental results are discussed. DOE

N95-24269# Bhabha Atomic Research Centre, Bombay (India).
DETERMINATION OF TRACE ELEMENTS IN PLUTONIUM BY SOLVENT EXTRACTION AND ICP-ATOMIC EMISSION SPECTROMETRY
A. B. Patwardhan, M. V. Joshi, V. T. Kulkarni, Radhakrishnan, S. Sumathi, and Mary Jacob (Bhabha Atomic Research Centre, Bombay, India.) 1993 16 p
(DE94-634887; BARC-1993/E/027) Avail: CASI HC A03/MF A01 (US Sales Only)

This report describes the studies carried out for the determination of trace metallic impurities in plutonium solutions. Plutonium is separated from the impurity elements by the selective extraction of plutonium in tri-butyl-phosphate. The aqueous phase containing the impurities is fed to the high temperature source of excitation such as inductively coupled argon plasma and the analysis is carried out employing computer controlled multichannel direct reading spectrometer. Based on the above studies a method has been standardized for the analysis of sixteen elements in plutonium oxide/nitrate samples. The relative standard deviation of the method for various elements is in the range of +/- 1 to 5%. The method offers distinct advantages over the conventional carrier distillation technique in terms of precision, range, and sensitivity. DOE

N95-24292# Argonne National Lab., IL.
POLARIZATION AND N-N ELASTIC SCATTERING AMPLITUDES
G. P. Ramsey Oct. 1994 10 p Presented at the International Symposia on High Energy Spin Physics and Polarization Phenomena in Nuclear Physics, Bloomington, IN, 15-22 Sep. 1994
(Contract W-31-109-eng-38)
(DE95-004648; ANL-HEP-CP-94-66; CONF-9409103-9) Avail: CASI HC A02/MF A01

We discuss the role of polarization measurements and scattering amplitudes for elastic nucleon-nucleon processes at high energy. The relative normalization of these amplitudes involves a 'leading order form factor' which we determine empirically. These amplitudes provide an economical description of a large body of existing data and make some nontrivial predictions for spin observables. In particular, we have investigated cross sections and asymmetry data at large angles (including 90 deg c.m.) and the fixed absolute value of t, large s region, dominated by the three-gluon exchange mechanism. Our results indicate that polarization experiments can test basic Quantum Chromodynamics (QCD) elements such as helicity conservation, wave function properties and the interplay between various interaction mechanisms. The significance of this analysis will be discussed in terms of specific polarization experiments. DOE

N95-24297 Helsinki Univ. of Technology, Espoo (Finland).
EXPERT SYSTEM FOR NUCLIDE IDENTIFICATION IN GAMMA SPECTRUM ANALYSIS
P. A. Aarnio, J. J. Ala-Heikkilae, T. T. Hakulinen, and J. T. Routti 1994 12 p Presented at the Conference on Methods and Applications of Radioanalytical Chemistry - 3, Kailua-Kona, Hawaii, 10-16 Apr. 1994 Limited Reproducibility: More than 20% of this document may be affected by microfiche quality
(ISSN 0355-7790)
(PB95-149712; TKK-F-A731) Avail: CASI HC A03

An expert system coupled with the gamma spectrum analysis system SAMPO has been developed for automating the qualitative identification of radionuclides as well as for determinating the quantitative parameters of the spectrum components. The program is written in C-language and runs in various environments ranging from PC's to UNIX workstations. The expert system utilizes a complete gamma library with over 2600 nuclides and 80,000 lines, and a rule base of about fifty criteria including energies, relative peak intensities, genesis modes, half-lives, parent-daughter relationships etc. The rule base is furthermore extensible by the user. The performance of the expert system has been evaluated using test cases from environmental samples, sets of standard sources and activation analysis measurements, which have been carefully analyzed manually. Also synthesized spectra have been used, where the exact composition of the sample is known in advance. Results from these tests show that the expert system performs very well even for difficult spectra. NTIS

N95-24298 Helsinki Univ. of Technology, Espoo (Finland).
GAMMA SPECTRUM ANALYSIS INCLUDING NAA WITH SAMPO FOR WINDOWS
P. A. Aarnio, M. T. Nikkinen, and J. T. Routti 1994 14 p Presented at the Conference on Methods and Applications of Radioanalytical Chemistry - 3, Kailua-Kona, Hawaii, 10-16 Apr. 1994 Limited Reproducibility: More than 20% of this document may be affected by microfiche quality
(ISSN 0355-7790)
(PB95-149720; TKK-F-A730) Avail: CASI HC A03

SAMPO for Windows is a high performance gamma spectrum analysis program. All the measurement, analysis and neutron activation analysis (NAA) phases can be done either under full interactive user control or user defined tasks can be used for automated measurement and analysis sequences including control of Multichannel Analyzers (MCA's) and sample changers. High resolution gamma-ray spectroscopy together with the possibility to resolve complex multiplets with high accuracy makes SAMPO very suitable for INAA. On the other hand, the possibility to automate analysis sequences allows its use effectively also all routine NAA measurements. NAA in SAMPO is accomplished using comparative methods. Spectra of standards, flux monitors, controls and actual samples are analyzed normally to obtain the peak areas which are optionally corrected for decay. In the comparison the flux monitor results are used to correct for variations in the effective neutron flux. An optional irradiation position correction can also be applied. The controls are used to alarm for possible deviations in the results. The sophisticated spectrum analysis methods used together with the comparative NAA and monitors give accurate results limited by the systematic effects only. The Windows environment provides ease of use and further processing power is available through the interface to expert system identification of nuclides. NTIS

N95-24314# Joint Inst. for Nuclear Research, Dubna (USSR).
BOUND STATES OF 'DRESSED' PARTICLES
M. I. Shirokov 1994 6 p
(DE94-636773; JINR-E-2-94-82) Avail: CASI HC A02/MF A01 (US Sales Only)

A new approach to the problem of bound states in relativistic quantum field theories is suggested. It uses the creation - destruction operators of 'dressed' particles which have been granted by Faddeev's (1963) 'dressing' formalism. Peculiarities of the proposed approach as compared to the known ones are discussed. DOE

N95-24315# Joint Inst. for Nuclear Research, Dubna (USSR).
DEFICIENCY OF THE GROSS-LLEWELLYN SMITH SUM RULE AND QCD VACUUM POLARIZATION EFFECT
A. E. Dorokhov 1994 7 p
(DE94-636790; JINR-E-2-94-103) Avail: CASI HC A02/MF A01 (US Sales Only)

From the analysis of the recent CCFR Collaboration data for the structure function x F(sub 3)(x, Q(sup 2)) (0.015 is less than x which is less than 0.65 and 1.2 GeV(sup 2) is less than Q(sup 2) which is less than 501 GeV(sup 2)) of the deep inelastic neutrino-nucleon scattering we conclude that probably part of the nucleon baryon number is due to the vacuum polarization effects. DOE

N95-24316# Joint Inst. for Nuclear Research, Dubna (USSR).
LOW ENERGY THEOREMS IN QUARK POTENTIAL MODELS
W. Kallies, V. N. Pervushin, and N. A. Sarikov 1994 8 p
(DE94-636791; JINR-E-2-94-42) Avail: CASI HC A02/MF A01 (US Sales Only)

Low energy theorems for pion decays (pi yields mu nu, pi yields gamma gamma) are considered in the framework of the quark potential models. It is shown that the separable approximation to the class of potentials leads to self-consistent reproducing of these theorems. It is found that the generalization of the approach to the arbitrary potential of the quark interaction requires redefinition of the quark condensate by taking into account the form of the potential. DOE

N95-24326# Argonne National Lab., IL.
PROTON-PROTON INTERACTIONS USING THE RHIC POLARIZED COLLIDER
A. Yokosawa 1994 9 p Presented at the International Seminar on High-energy Physics Problems: Relativistic Nuclear Physics and QCD, Dubna, Russian Federation, 13-17 Sep. 1994
(Contract W-31-109-eng-38)
(DE95-005839; ANL-HEP-CP-94-68; CONF-940963-1) Avail: CASI HC A02/MF A01

The first polarized collider where we collide 250-GeV/c beams of 70% polarized protons at high luminosity is under construction. This will allow a determination of the nucleon spin-dependent structure functions over a large range in x and a collection of sufficient W and Z events to investigate extremely interesting spin-related phenomena. DOE

N95-24332# Argonne National Lab., IL.
NEW RESULTS IN NUCLEON-NUCLEON SCATTERING AT INTERMEDIATE ENERGIES
H. Spinka 1995 16 p Presented at the International Symposia on High Energy Spin Physics and Polarization Phenomena in Nuclear Physics, Bloomington, IN, 15-22 Sep. 1994
(Contract W-31-109-eng-38)
(DE95-004594; ANL-HEP-CP-94-76; CONF-9409103-12) Avail: CASI HC A03/MF A01

Many np elastic scattering spin observables have recently been measured between kinetic energies of about 500 and 1100 MeV at Saclay and LAMPF. These data are summarized and some new results are presented. Evidence for structure in pp observables near 2100 MeV is reviewed, and new data in this energy region are shown from SATURNE. DOE

N95-24337# Japan Atomic Energy Research Inst., Tokyo (Japan).
STRUCTURE AND MANUAL OF RADIOISOTOPE-PRODUCTION DATA BASE, ISOP
Kentaro Hata and Kusuo Terunuma Feb. 1994 43 p
(DE94-785197; JAERI-M-94-012) Avail: CASI HC A03/MF A01

We planned on collecting the information of radioisotope production which was obtained from research works and tasks at the Department of Radioisotopes in JAERI, and constructed a proto-type data base ISOP after discussion of the kinds and properties of the information available for radioisotope production. In this report the structure and the manual of ISOP are described. DOE

N95-24339# Japan Atomic Energy Research Inst., Tokyo (Japan).
DESIGN STUDY OF A NEGATIVE-ION BASED NBI SYSTEM FOR JT-60U
Noboru Akino, Masanori Araki, and Noboru Ebisawa Mar. 1994 431 p
(DE94-785265; JAERI-M-94-072) Avail: CASI HC A19/MF A04

A high energy negative-ion based NBI system for JT-60U has been designed. The objective of the NBI system is to demonstrate mega-ampere level NB current drive and plasma core heating in a reactor-grade high density plasma. This is the first negative-ion based NBI system in the world. The required specifications of the NBI system are: a beam energy of 500 keV, an injection power of 10 MW, a beam pulse duration of 10 sec with a duty cycle of 1/60 and a beam species of deuterium or hydrogen. The neutral beam power of 10 MW is injected tangentially using one beam-line with two large negative-ion sources. The construction of the NBI system has been started, and will be operational in 1996. DOE

N95-24350# Centro Brasileiro de Pesquisas Fisicas, Rio de Janeiro.
ANIONIC CONSTRUCTION OF THE sl(SUB q, s)(2) ALGEBRA
J. L. Matheus-Valle and M. R. Monteiro 1993 18 p
(DE95-600838; CBPF-NF-062/93) Avail: CASI HC A03/MF A01 (US Sales Only)

Considering anionic oscillators in a two-dimensional lattice, the quantum semi-group sl(sub (q,s)) (2) is realized by means of a generalized Schwinger construction. It is found that the parameter q of the algebra is connected to the statistical parameter, whereas the s parameter is related to a s-deformed oscillator introduced at each point of the lattice. DOE

N95-24354# Stanford Linear Accelerator Center, CA.
TEST OF AN ARRAY OF CsI(Tl) CRYSTAL TOWERS FOR A LOW OR MEDIUM ENERGY e(+)e(-) COLLIDER CALORIMETER
M. E. King Oct. 1994 3 p Presented at the International Europhysics Conference on High-energy Physics, Marseille, France, 22-28 Jul. 1993
(Contract DE-AC03-76SF-00515)
(DE95-006068; SU-SLAC-PUB-6701; CONF-930761-1) Avail: CASI HC A01/MF A01

Energy and position resolution results of a test of an array of CsI(Tl) crystal towers in an e-/ (pi)(-) beam (120 to 400 MeV) at TRIUMF are presented. The array was designed to study the effects of longitudinal and transverse crystal segmentation on energy and position resolution, and background rejection. The author also studied a wavelength-shifter and multi-photodiode readout system suitable for use in an electromagnetic CsI calorimeter in a detector at low and medium energy, high-luminosity e+ e- storage rings. Energy resolution of (1.69 +/- 0.08)%/(radical)E and (1.83 +/- 0.05)%/(radical)E were obtained for two different crystal tower configurations. Position resolution of 6.5 (9.0) mm was obtained at 300 (120) MeV for four 4 x 4 sq cm, 4 radiation length CsI crystals. DOE

N95-24360# Joint Inst. for Nuclear Research, Dubna (USSR).
ON LEADING CHARMED MESON PRODUCTION IN PI-NUCLEON INTERACTIONS
V. A. Bednyakov 1994 6 p
(DE94-636797; JINR-E-2-94-79) Avail: CASI HC A02/MF A01 (US Sales Only)

It is shown that the D-meson, whose light quark is the initial-pion valence quark and whose charmed quark is produced in annihilation of valence quarks and has got a large enough momentum, is really a leading meson in reactions like pi(-) p yields DX. If such annihilation of valence quarks from initial hadrons is impossible, there must be no distinct leading effect. DOE

N95-24361# Joint Inst. for Nuclear Research, Dubna (USSR).
INVESTIGATION OF THE GROSS STRUCTURE OF SPECTRA AND MASS DISTRIBUTIONS OF HADRONIC RESONANCES
F. A. Gareev, G. S. Kazacha, Yu. L. Ratis, and E. A. Strokovskij 1994 14 p
(DE94-636799; JINR-E-2-94-131) Avail: CASI HC A03/MF A01 (US Sales Only)

The systematical investigation of the gross structure of spectra and mass distributions of all known hadronic resonances starting from light mesons and ending with bottomonium resonances is carried out. The regular periodic structures in the invariant mass distributions of resonances is established. They have the period Delta(sub m) approx equal to 200 MeV in regions of the light unflavored, psi and Upsilon mesons and Delta(sub m) approx equal to 100 MeV for baryon resonances. It is demonstrated that the three-meson (1(sup --)) molecular states in decay channels should play an essential role in understanding of mass distributions of the psi and Upsilon mesons. We predict the existence of new regions of (1(sup --)) resonances: 27-33 GeV, 81-100 GeV (W and Z boson region), 240-300 GeV and so on. DOE

N95-24364# Joint Inst. for Nuclear Research, Dubna (USSR).
STRUCTURE OF LIQUID He-4 EXCITATIONS SPECTRUM
N. M. Blagoveshchenskij, A. V. Puchkov, A. N. Skomorokhov, I. V. Bogoyavlenskij, L. V. Karnatsevich, and Kolobrodov 1994 22 p
(DE94-637113; JINR-R-3-94-125) Avail: CASI HC A03/MF A01 (US Sales Only)

Experimental data of the excitations spectrum structure of the He 1 and He 2 are obtained. At t greater than T(sub lambda) the collective excitations of the zero sound type at the wave vectors q is less than 0.65 A(sup -1) and the excitations at the wide q-range, which may be explained as 'normal' (classical) phonons, connected with the quasicrystal liquid structure are observed. In the superfluid phase the additional excitations branch appears. The intensities of these excitations increase rapidly with the decrease T. This branch may be identified as the Landau elementary excitation curve. There are main transformations of the excitation spectrum at the temperatures near the lambda-point and at the narrow range where q is approximately 0.5-0.65 A(sup -1). Bose condensate density estimate is presented. DOE

N95-24404# International Centre for Theoretical Physics, Trieste (Italy).
NEUTRINO MASSES AND b - TAU UNIFICATION IN THE SUPERSYMMETRIC STANDARD MODEL

F. Vissani (International School for Advanced Studies, Trieste, Italy.) and A. Yu. Smirnov May 1994 14 p
(DE94-634361; IC-94/102; SISSA-63/94/EP) Avail: CASI HC A03/MF A01 (US Sales Only)

There are several indications that the Majorana masses of the right-handed neutrino components, M(sub R), are at the intermediate scale: M(sub R) approx. (10(sup 10) - 10(sup 12)) GeV or even lighter. The renormalization effects due to large Yukawa couplings of neutrinos from region of momenta M(sub R) less than or approx. q less than or approx. M(sub G) are studied in the supersymmetric standard model. It is shown that neutrino renormalization effect can increase the m(sub b)/m(sub tau) ratio up to (10/15)%. This strongly disfavors m(sub b) - m(sub tau) unification for low values of tan beta less than 10 especially at large values of alpha(sub s). Lower bound on M(sub R) and tan beta from the b - tau unification condition were found. The implications of the results to the see-saw mechanism of the neutrino mass generation are discussed.
Author

N95-24414# Stanford Linear Accelerator Center, CA.
THE DISCOVERY OF THE TAU LEPTON: PART 1, THE EARLY HISTORY THROUGH 1975; PART 2, CONFIRMATION OF THE DISCOVERY AND MEASUREMENT OF MAJOR PROPERTIES, 1976-1982
M. L. Perl Aug. 1994 18 p Presented at the International Conference on the History of Original Ideas and Basic Discoveries in Particle Physics, Erice, Italy, 29 Jul. - 4 Aug. 1994
(Contract DE-AC03-76SF-00515)
(DE95-005945; SU-SLAC-PUB-6584; CONF-9407157-2) Avail: CASI HC A03/MF A01

Several previous papers have given the history of the discovery of the tau lepton at the Stanford Linear Accelerator Center (SLAC). These papers emphasized: (1) the experiments which led to our 1975 publication of the first evidence for the existence of the tau; (2) the subsequent experiments which confirmed the existence of the tau, and (3) the experiments which elucidated the major properties of the tau. That history will be summarized in Part 2 of this talk. In this Part 1, I describe the earlier thoughts and work of myself and my colleagues at SLAC in the 1960's and early 1970's which led to the discovery. I also describe the theoretical and experimental events in particle physics in the 1960's in which our work was immersed. I will also try to describe for the younger generations of particle physicists, the atmosphere in the 1960's. That was before the elucidation of the quark model of hadrons, before the development of the concept of particle generations The experimental paths to program we hot as clear as they are today and we had to cast a wide experimental net. DOE

N95-24415# Stanford Linear Accelerator Center, CA.
EXTENDING THE KINEMATIC RANGE FOR W(SUB R) SEARCHES IN e(-)e(-) COLLISIONS AT THE NLC
T. G. Rizzo Jul. 1994 6 p Presented at the Meeting of the Division of Particles and Fields of the American Physical Society, Albuquerque, NM, 2-6 Aug. 1994
(Contract DE-AC03-76SF-00515)
(DE95-005946; SU-SLAC-PUB-6591; CONF-940816-80) Avail: CASI HC A02/MF A01

While the much discussed lepton-number violating process e(-) e(-) yields W(sub R)(-) W(sub R)(-) provides an excellent probe of both the Majorana nature of the right-handed neutrino and the symmetry breaking sector of the Left-Right Symmetric Model, it is likely that W(sub R)'s are too massive to be pair produced at the NLC with radical s in the 1-1.5 TeV range. The author is thus lead to consider the single W(sub R) production process e(-) e(-) yields W(sub R)(-) W(sub R)(-) (sup *) yields W(sub R)(-) + jj in order to expand the collider's kinematic reach. After pointing out that W(sub R)'s with masses of order 1 TEV may be missed by future hadron collider searches, the author demonstrates that this three-body process possesses a significant cross section, of order several fb, at the NLC with radical s in the range above. The angular distribution of the produced W(sub R)'s is shown to be essentially flat and the potential backgrounds from standard model processes are shown to be small.
DOE

N95-24417# Stanford Linear Accelerator Center, CA.
A MEASUREMENT OF QUARK AND GLUON JET DIFFERENCES AT THE Z(SUP 0) RESONANCE
Yoshihito Iwasaki (Tohoku Univ., Sendai, Japan.) Aug. 1994 6 p Presented at the Meeting of the Division of Particles and Fields of the American Physical Society, Albuquerque, NM, 2-6 Aug. 1994
(Contract DE-AC03-76SF-00515)
(DE95-005947; SU-SLAC-PUB-6597; CONF-940816-79) Avail: CASI HC A02/MF A01

The authors have studied differences between quark and gluon jets using 3-jet events in hadronic decays of Z(sup 0) bosons collected by the SLD experiment at SLAC. Gluon jets were identified in symmetric 3-jet events containing one jet tagged as a heavy quark jet and compared with a mixed sample of quark and gluon jets and also with a mixed sample of light quark (u, d and s) and gluon jets. Their preliminary results show that the particle multiplicity in gluon jets is higher than that in light quark jets. These results are in qualitative agreement with QCD expectations. Differences are also observed in particle energy spectra and the jet widths, consistent with QCD expectations. DOE

N95-24418# Stanford Linear Accelerator Center, CA.
A TEST OF THE FLAVOR INDEPENDENCE OF STRONG INTERACTIONS
M. D. Hildreth Aug. 1994 6 p Presented at the Meeting of the Division of Particles and Fields of the American Physical Society, Albuquerque, NM, 2-6 Aug. 1994
(Contract DE-AC03-76SF-00515)
(DE95-005948; SU-SLAC-PUB-6598; CONF-940816-76) Avail: CASI HC A02/MF A01

The authors present a comparison of the strong couplings of b, c, and light (u, d, and s) quarks derived from multi-jet rates in flavor-tagged samples of hadronic Z(sup 0) decays recorded with the SLC Large Detector at the SLAC Linear Collider. By comparing the rates of 3-jet events in these three samples they have extracted (Preliminary) values of: alpha(sub s)(uds)/alpha(sub s)(all) = 0.96 +/- 0.03(stat.) +/- 0.04(syst.) +/- 0.02(theory), alpha(sub s)(c)/alpha(sub s)(all) = 1.16 +/- 0.11(stat.) +/- 0.10(syst.) +/- 0.07(theory), alpha(sub s)(b)/alpha(sub s)(all) = 0.98 +/- 0.04(stat.) +/- 0.08(syst.) +/- 0.02(theory). DOE

N95-24419# Jagellonian Univ., Cracow (Poland).
ELECTRONIC STRUCTURE AND PAIRING OF STRONGLY CORRELATED FERMIONS: FERMI LIQUID VERSUS SPIN LIQUID
K. Byczuk, J. Karbowski (Warsaw Univ., Warsaw, Poland.), J. Spalek, and W. Wojcik Apr. 1994 13 p Presented at the International Conference on Superconductivity and Strongly Correlated Electron Systems, Amalfi, Italy, 14-16 Oct. 1993
(Contract DE-FG02-90ER-45427)
(DE95-005929; CONF-931077-1) Avail: CASI HC A03/MF A01

We summarize recent theoretical results of our group concerning the electronic states of the strongly correlated fermions at nonzero temperature. The state of almost localized fermions is discussed within a mean-field approach for auxiliary bosons, both in the narrow-band (Section 1) and in the hybridized band (Section 3) cases. This state represents a metallic state of correlated fermion systems (such as V2O3) below the Mott-Hubbard localization threshold. The Fermi liquid state does not describe properly the properties of narrow band electrons in the large Hubbard -- U limit beyond the localization threshold. Therefore, in Section 4 and 5 we introduce a phenomenological concept of statistical spin liquid which describes principal features of a crossover from a high-temperature superconductor to the Mott insulator for a two-dimensional system. It also reproduces the main features of the phase diagram for La(2-x)Sr(x)CuO4 system, which is modelled by a planar structure. DOE

N95-24420# Brookhaven National Lab., Upton, NY.
PROBING ANOMALOUS GAUGE BOSON COUPLINGS AT LEP
S. Dawson and G. Valencia 1994 12 p Presented at the Joint US/Polish Workshop on Physics From Planck Scale To Electroweak Scale; Meeting of the Division of Particles and Fields of the American Physical Society, Warsaw, Poland; Albuquerque, NM, 21-24 Sep. 1994; 2-6 Aug.
(Contract DE-AC02-76CH-00016)
(DE95-005934; BNL-61179; CONF-9409287-1; CONF-940816-88) Avail: CASI HC A03/MF A01

We bound anomalous gauge boson couplings using LEP data for the Z yields bar-ff partial widths. We use an effective field theory formalism to compute the one-loop corrections resulting from non-standard model three and four gauge boson vertices. We find that measurements at LEP constrain the three gauge boson couplings at a level comparable to that obtainable at LEPII. DOE

N95-24434# Stanford Univ., CA.
MEASUREMENT OF ALPHA(SUB s)FROM HADRONIC EVENT OBSERVABLES AT THE Z(SUP 0) RESONANCE
Jul. 1994 35 p Presented at the 27th International Conference on High Energy Physics, Glasgow, England, 21-27 Jul. 1994
(Contracts DE-AC03-76SF-00515; DE-FG02-91ER-40676; DE-FG03-92ER-40701; DE-FG03-91ER-40618; DE-FG03-92ER-40689; DE-FG03-93ER-40788; DE-FG02-91ER-40672; DE-FG02-91ER-40677; DE-AC03-76SF-00098; DE-FG02-92ER-40715)
(DE95-005943; SU-SLAC-PUB-6549; CONF-940722-38) Avail: CASI HC A03/MF A01

The strong coupling alpha(sub s) has been measured using hadronic decays of Z(sup 0) bosons collected by the SLD experiment at SLAC. The data were compared with QCD predictions both at fixed order, O(alpha(sub s)(sup 2)), and including resummed analytic formulae based on the leading and next-to-leading logarithm approximation. The authors studied event shapes, jet rates, particle correlations, and energy fraction and checked the consistency between alpha(sub s) extracted from these different measures. Combining all results they obtain alpha(sub s)(M(sub Z(sup 0))(sup 2)) = 0.120 +/- 0.003(exp.) +/- 0.009(theor.), where the dominant uncertainty in alpha(sub s) is from uncalculated higher order contributions. DOE

N95-24435# Stanford Linear Accelerator Center, CA.
A SEARCH FOR JET HANDEDNESS IN HADRONIC Z(SUP 0) DECAYS
Jul. 1994 10 p Presented at the 27th International Conference on High Energy Physics, Glasgow, England, 21-27 Jul. 1994
(Contracts DE-AC03-76SF-00515; DE-FG02-91ER-40676; DE-FG03-92ER-40701; DE-FG03-91ER-40618; DE-FG03-92ER-40689; DE-FG03-93ER-40788; DE-FG02-91ER-40672; DE-FG02-91ER-40677; DE-AC03-76SF-00098; DE-FG02-92ER-40715)
(DE95-005944; SU-SLAC-PUB-6550; CONF-940722-37) Avail: CASI HC A02/MF A01

The authors have searched for signatures of polarization in hadronic jets from Z(sup 0) yields q bar-q decays using the 'jet handedness' method. The charge asymmetry induced by the high SLC electron beam polarization was used to select quark or antiquark jets, expected to be left- and right-polarized, respectively. They find no evidence for jet handedness in their global sample nor in a sample of light quark jets. They set upper limits of 5.1% and 9.1% respectively on the magnitude of the analyzing power of this technique at the 95% C.L. They have studied several alternative definitions of jet handedness and find no signal by any method. DOE

N95-24459# Argonne National Lab., IL.
PULSE RADIOLYSIS OF ALKANES: A TIME-RESOLVED ELECTRON PARAMAGNETIC RESONANCE STUDY
I. A. Shkrob and A. D. Trifunac 14 Feb. 1994 42 p
(Contract W-31-109-eng-38)
(DE95-005831; ANL/CHM/PP-82180) Avail: CASI HC A03/MF A01

Time-resolved spin-echo-detected electron paramagnetic resonance (EPR) was applied to examine short-lived alkyl radicals formed in pulse radiolysis of liquid alkanes. It was found that the ratio of yields of penultimate and interior radicals in n-alkanes at the instant of their generation is temperature-independent and is ca. 1.25 times greater than the statistical quantity. This higher-than-statistical production of penultimate radicals indicates that the fast ion molecule reactions involving radical cations are a significant route of radical generation. The analysis of spin-echo kinetics in n-alkanes suggests that the alkyl radicals are emissively polarized in spur reactions. This initial polarization rapidly increases with shortening of the aliphatic chain. Another finding is that a long-chain structure of these radicals results in much higher rate of Heisenberg spin exchange relative to the recombination rate. The relative yields of hydrogen abstraction and fragmentation for various branched alkanes are estimated. It is concluded that the fragmentation occurs prior to the formation of radicals in an excited precursor species. Effects of phenolic and alkene additives in radiolysis of n-alkanes are examined. It is demonstrated that phenoxy radicals are produced in dissociative capture of electrons and alkane holes. Another route is a reaction of phenols with free hydrogen atoms. A rapid transfer of singlet correlation from the geminate radical ion pairs is responsible for unusual polarization patterns in the phenoxy and cyclohexadienyl radicals. The significance of these results in the context of cross-linking in polyethylene and higher paraffins is discussed. DOE

N95-24471# Joint Publications Research Service, Washington, DC.
JPRS REPORT: SCIENCE AND TECHNOLOGY. CENTRAL EURASIA: INSTITUTE OF GENERAL AND NUCLEAR PHYSICS: 1993 STATUS AND PROSPECTS
24 Oct. 1994 96 p Transl. into ENGLISH from various Central Eurasian articles Conference held in Russia on 23 Apr. 1993; sponsored by the Kurchatovskiy Inst. Russian Scientific Center
(JPRS-UST-94-025) Avail: CASI HC A05/MF A01

Translated articles cover the following topics: low-energy physics; relativistic nuclear physics; physics of weak interactions; applied nuclear physics; and synchrotron radiation. Author

N95-24485# Joint Inst. for Nuclear Research, Dubna (USSR).
MUON IDENTIFIER EFFICIENCY OF THE GINES DETECTO R IN THE UNK NEUTRINO BEAM
A. P. Nagajtsev, S. N. Plyashkevich, M. I. Solovev, N. G. Fadeev, and A. P. Cheplakov 1993 10 p In RUSSIAN; In Russian
(DE94-628254; JINR-R-1-93-285; Rept-P1-93-285) Avail: CASI HC A02/MF A01 (US Sales Only)

The method and the calculated results of the muon identification efficiency for the GINES experiment at UNK are presented. The identifier is assembled from drift tubes and is supposed to be exposed to neutrino beams produced by primary protons of 500 GeV energy. The identification of muons is based on a high space resolution of the drift tube coordinate detector designed at JINR. A value better than 95% was obtained for the highest expected intensity of background particles. DOE

N95-24512# California Univ., Berkeley. Lawrence Berkeley Lab, CA.
A DISCRETE VARIABLE REPRESENTATION FOR ELECTRON-HYDROGEN ATOM SCATTERING Ph.D. Thesis
Lionel Francis Gaucher Aug. 1994 152 p
(Contract DE-AC03-76SF-00098)
(DE95-003436; LBL-36080) Avail: CASI HC A08/MF A02

A discrete variable representation (DVR) suitable for treating the quantum scattering of a low energy electron from a hydrogen atom is presented. The benefits of DVR techniques (e.g. the removal of the requirement of calculating multidimensional potential energy matrix elements and the availability of iterative sparse matrix diagonalization/inversion algorithms) have for many years been applied successfully to studies of quantum molecular scattering. Unfortunately, the presence of a Coulomb singularity at the electrically unshielded center of a hydrogen atom requires high radial grid point densities in this region of the scattering coordinate, while the presence of finite kinetic energy in the asymptotic scattering electron also requires a sufficiently large radial grid point density at moderate distances from the nucleus. The constraints imposed by these two length scales have made application of current DVR methods to this scattering event difficult. DOE

N95-24533# California Univ., Berkeley. Lawrence Berkeley Lab, CA. Chemical Sciences Div.
STUDY OF RADICALS, CLUSTERS AND TRANSITION STATE SPECIES BY ANION PHOTOELECTRON SPECTROSCOPY Ph.D. Thesis
Don Wesley Arnold Aug. 1994 481 p
(Contract DE-AC03-76SF-00098)
(DE95-003438; LBL-36079) Avail: CASI HC A21/MF A04

Free radicals, elemental and van der Waals clusters and transition state species for bimolecular chemical reactions are investigated using anion photoelectron spectroscopy. Several low-lying electronic states of ozone have been identified via photoelectron spectroscopy of O3(-). A characterization of these states is important to models for atmospheric ozone reaction kinetics. The fluoroformyloxyl radical, FCO2, has been investigated, providing vibrational frequencies and energies for two electronic states. The technique has also been employed to make the first direct observation and characterization of the NNO2 molecule. Several electronic

states are observed for this species which is believed to play a role as a reactive intermediate in the N + NO2 reaction. The experimental results for all three of these radicals are supplemented by ab initio investigations of their molecular properties. The clusters investigations include studies of elemental carbon clusters (C2(-) - C11(-)), and van der Waals clusters (X(-))(CO2)(sub n), X = I, Br, Cl; n less than or equal to 13 and I(-)(N2O)(sub n=1-11). Primarily linear clusters are observed for the smaller carbon clusters, while the spectra of the larger clusters contain contribution from cyclic anion photodetachment. Very interesting ion-solvent interactions are observed in the X(-)(CO2)(sub n) clusters. The transition state regions for several bimolecular chemical reactions have also been investigated by photodetachment of a negative ion precursor possessing a geometry similar to that of the transition state species. These spectra show features which are assigned to motions of the unstable neutral complex existing between reactants and products. DOE

N95-24547# Michigan Univ., Ann Arbor, MI. High Energy Spin Physics Group.

ACCELERATOR PHYSICS R AND D

A. D. Krisch 22 Aug. 1994 10 p

(Contract DE-FG02-94ER-40822)

(DE95-003624; DOE/ER-40822/1) Avail: CASI HC A02/MF A01

This report discusses the NEPTUN-A experiment that will study spin effects in violent proton-proton collisions; the Siberian snake tests at IUCF cooler ring; polarized gas jets; and polarized proton acceleration to 1 TeV at Fermilab. DOE

N95-24549# Lawrence Livermore National Lab., Livermore, CA.

TOWARD IMPROVED PHOTON-ATOM SCATTERING PREDICTIONS

Lynn Kissel 21 Oct. 1994 12 p Presented at the 13th International Conference on the Application of Accelerators in Research and Industry, Denton, TX, 7-10 Nov. 1994

(Contract W-7405-eng-48)

(DE95-003651; UCRL-JC-117932; CONF-941129-10) Avail: CASI HC A03/MF A01

Photon-atom scattering is important in a variety of applications, but scattering from a composite system depends on the accurate characterization of the scattering from an isolated atom or ion. We have been examining the validity of simpler approximations of elastic scattering in the light of second-order S-matrix theory. Partitioning the many-body amplitude into Rayleigh and Delbrueck components, processes beyond photoionization contribute. Subtracted cross sections for bound-bound atomic transitions, bound pair annihilation, and bound pair production are required in anomalous scattering factors for: (1) convergence of the dispersion integral; (2) agreement with predictions of the more sophisticated S-matrix approach; (3) satisfying the Thomas-Reiche-Kuhn sum rule. New accurate tabulations of anomalous scattering factors have been prepared for all Z, for energies 0-10,000 keV, within the independent particle approximation (IPA) using a Dirac-Slater model of the atom. Separately, experimental atomic photoabsorption threshold information has been used to modify these IPA predictions for improved comparison with experiment. DOE

N95-24571# Stanford Linear Accelerator Center, CA.

MEASUREMENT OF THE CHARGED MULTIPLICITY OF Z(SUP 0) (YIELDS) b(BAR b) EVENTS

P. N. Burrows (Massachusetts Inst. of Tech., Cambridge, MA.) Aug. 1994 6 p Presented at the Meeting of the Division of Particles and Fields of the American Physical Society, Albuquerque, NM, 2-6 Aug. 1994

(Contract DE-AC03-76SF-00515)

(DE95-006051; SU-SLAC-PUB-6602; CONF-940816-75) Avail: CASI HC A02/MF A01

Using an impact parameter tag to select an enriched sample of Z(sup 0) (yields) b(bar b) events, the authors have measured the difference between the average charged multiplicity of Z(sup 0) (yields) b(bar b) and Z(sup 0) (yields) hadrons to be (bar n)(sub b) - (bar n)(sub had) = 2.24 +/- 0.30(stat.) +/- 0.33(syst.) tracks per event. From this, they have derived (bar n)(sub b) - (bar n)(sub uds) = 3.31 +/- 0.41 +/- 0.79. Comparing this measurement with those at lower center-of-mass energies, the authors find no evidence that (bar n)(sub b) - (bar n)(sub uds) depends on energy, in agreement with a precise prediction of perturbative QCD. DOE

N95-24575# Stanford Linear Accelerator Center, CA.

A MEASUREMENT OF THE LEFT-RIGHT, FORWARD-BACKWARD ASYMMETRY FOR CHARM QUARKS USING D(*+) AND D(+) MESONS

M. E. King Sep. 1994 4 p Presented at the Meeting of the Division of Particles and Fields of the American Physical Society, Albuquerque, NM, 2-6 Aug. 1994

(Contract DE-AC03-76SF-00515)

(DE95-006061; SU-SLAC-PUB-6653; CONF-940816-73) Avail: CASI HC A01/MF A01

Longitudinal polarization of the SLC e(-) beam allows a direct measurement of the left-right, forward-backward asymmetry of c-quarks to be made with the SLD. Events from Z(sup 0) (yields) c(bar c) are tagged using fully and partially reconstructed decays of D(*+) mesons, and fully reconstructed decays of D(+) mesons. The authors measure A(sub c) = 0.77 +/- 0.22(stat.) +/- 0.10(syst.). DOE

N95-24576# Stanford Linear Accelerator Center, CA.

A TEST OF THE FLAVOR INDEPENDENCE OF STRONG INTERACTIONS

T. W. Markiewicz Sep. 1994 6 p Presented at the QCD 94: Nuclear Physics B, Montpellier, France, 7-13 Jul. 1994

(Contract DE-AC03-76SF-00515)

(DE95-006063; SU-SLAC-PUB-6659; CONF-9407135-3) Avail: CASI HC A02/MF A01

The authors present a comparison of the strong couplings of b, c, and light (u, d, and s) quarks derived from multi-jet rates in flavor-tagged samples of hadronic Z(sup 0) decays recorded with the SLC Large Detector at the SLAC Linear Collider. By comparing the rates of 3-jet events in these three samples they have extracted the Preliminary values of: (alpha)(sub s)(uds)/(alpha)(sub s)(all) = 0.96 +/- 0.03(stat.) +/- 0.04(syst.) +/- 0.02(theory), (alpha)(sub s)(c)/(alpha)(sub s)(all) = 1.16 = +/-0.11(stat.) +/- 0.10(syst.) +/- 0.07(theory), (alpha)(sub s)(b)/(alpha)(sub s)(all) = 0.98 +/- 0.04(stat.) +/- 0.08(syst.) +/- 0.02(theory). DOE

N95-24591# Stanford Linear Accelerator Center, CA.

TAU PHYSICS AT FUTURE FACILITIES

M. L. Perl Dec. 1994 14 p Presented at the 3rd Workshop on Tau Lepton Physics, Montreux, Switzerland, 19-22 Sep. 1994

(Contract DE-AC03-76SF-00515)

(DE95-006071; SU-SLAC-PUB-6730; CONF-9409277-1) Avail: CASI HC A03/MF A01

This paper discusses and projects the tau research which may be carried out at CESR, at BEPC, at the SLC, in the next few years at LEP 1, at the asymmetric B-factories under construction in Japan and the United States and, if built, a tau-charm factory. As the size of tau data sets increases, there is an increasing need to reduce the effects of systematic errors on the precision and search range of experiments. In most areas of tau physics there is a large amount of progress to be made, but in a few areas it will be difficult to substantially improve the precision of present measurements. DOE

N95-24593# Stanford Linear Accelerator Center, CA.

THE LEFT-RIGHT FORWARD-BACKWARD ASYMMETRY OF HEAVY QUARKS MEASURED WITH JET CHARGE AND WITH LEPTONS AT THE SLD

D. C. Williams Oct. 1994 7 p Presented at the Meeting of the Division of Particles and Fields of the American Physical Society, Albuquerque, NM, 2-6 Aug. 1994

(Contract DE-AC03-76SF-00515)

(DE95-006145; SU-SLAC-PUB-6648; CONF-940816-71) Avail: CASI HC A02/MF A01

The authors present direct measurements of the left-right asymmetry of b- and c-quarks from the decay of Z(sup 0) bosons produced in the annihilation of longitudinally polarized electrons and unpolarized positrons. Two complementary techniques are presented: (1) Z(sup 0) (yields) b(bar b) decays are tagged using track impact parameters with b(bar b) discrimination provided by momentum-weighted track charge; (2) semileptonic b-decays are tagged using high p and p(sub T) muons and electrons. The preliminary results from their 1993 data sample are: A(sub b) = 0.93 +/- 0.13 +/- 0.13 for the jet charge and A(sub b) = 0.93 +/- 0.14 +/- 0.09, and A(sub c) = 0.40 +/- 0.23 +/- 0.20 for the leptons, where the first error is statistical and the second systematic. DOE

N95-24595# Los Alamos National Lab., NM.
CORRELATIONS FOR THE NO A(SUP 2)(SIGMA)(+) ELECTRONIC QUENCHING CROSS-SECTION
P. H. Paul, C. D. Carter, J. A. Gray, J. L. Durant, Jr., J. W. Thoman, and M. R. Furlanetto Jan. 1995 21 p
(Contract DE-AC04-94AL-85000)
(DE95-006195; SAND-94-8237) Avail: CASI HC A03/MF A01

This report summarizes recent progress in the development of a model for collisional electronic quenching of NO A(sup 2)(Sigma)(+) by a number of molecules commonly found in combustion and aerodynamic systems. The model provides a means to reliably extend the measurement data base as well as suggesting simple analytic forms which can be used to provide physically plausible fits to the measurements. This report also contains a compilation of the available experimental data for collisional electronic quenching of NO A(sup 2)(Sigma)(+). DOE

N95-24622# Stanford Linear Accelerator Center, CA.
MEASUREMENT OF ALPHA(SUB s) FROM HADRONIC EV ENT OBSERVABLES AT THE Z(SUP 0) RESONANCE
Yukiyoshi Ohnishi Aug. 1994 6 p Presented at the Meeting of the Division of Particles and Fields of the American Physical Society, Albuquerque, NM, 2-6 Aug. 1994
(Contract DE-AC03-76SF-00515)
(DE95-005949; SU-SLAC-PUB-6599; CONF-940816-77) Avail: CASI HC A02/MF A01

The authors have measured the strong coupling alpha(sub s) using hadronic decays of Z(sup 0) bosons collected by the SLD experiment at SLAC. The data were compared with QCD predictions both at fixed order, O(alpha(sub s)(sup 2)), and including resumed analytic formulae based on the leading and next-to-leading logarithm approximation. The study includes event shapes, jet rates, and particle correlations. They checked the consistency between alpha(sub s) extracted from these different measures and found the dominant uncertainty on alpha(sub s) to be from uncalculated higher order contributions. DOE

N95-24640# Joint Inst. for Nuclear Research, Dubna (USSR). Lab. of Theoretical Physics.
COVARIANT SINGLE-TIME EQUATIONS FOR A SYSTEM OF N SPINOR PARTICLES
E. A. Dej (Gomel State Univ., Gomel, Byelarus.), V. N. Kapshaj (Gomel State Univ., Gomel, Byelarus.), and N. B. Skachkov 1993 20 p Submitted for publication
(DE94-628587; JINR-E-2-93-340) Avail: CASI HC A03/MF A01 (US Sales Only)

Based on the field-theoretical Green functions that describe a system of N fermions in terms of single-time variables we have derived covariant equations for the wave function of a bound state. The interaction operators in these equations and normalization conditions for the wave function are determined. As an example, the baryon is considered as a bound state of three quarks. DOE

N95-24641# Stanford Linear Accelerator Center, CA.
MULTIPLICITY MOMENTS IN e(+)e(-) ANNIHILATION INTO HADRONS AT THE Z(SUP 0) RESONANCE
J. Zhou (Oregon Univ., Eugene, OR.) Aug. 1994 6 p Presented at the Meeting of the Division of Particles and Fields of the American Physical Society, Albuquerque, NM, 2-6 Aug. 1994
(Contracts DE-AC03-76SF-00515; DE-FG06-85ER-40224)
(DE95-005950; SU-SLAC-PUB-6600; CONF-940816-78) Avail: CASI HC A02/MF A01

The authors present the ratio of cumulant to factorial moments of multiplicity distributions in hadronic events from Z(sup 0) decays. Their preliminary result show that this ratio, as a function of moment rank q, decreases sharply to a negative minimum at q approximately 5, followed by a sequence of quasi-oscillations. These observed features are in qualitative agreement with expectations from higher-order perturbative QCD. DOE

N95-24644# Joint Inst. for Nuclear Research, Dubna (USSR).
THE EMISSION OF PARTICLE IDENTIFICATION EFFICIENCY IN THE EXCHARM EXPERIMENT
A. F. Kamburyan, M. N. Kapishin, V. D. Kekelidze, Yury K. Potrebennikov, and E. A. Chudakov (Moscow State Univ., Russia.) 1993 10 p In RUSSIAN
(DE94-628258; JINR-R-13-93-362) Avail: CASI HC A02/MF A01 (US Sales Only)

The method to calculate the efficiency at the charged hadrons identification in experiment EXCHARM is proposed. The calculations have been performed simulating experimental conditions of the multichannel threshold gas Cherenkov counter and using the developed identification algorithms to select events of desired configurations. By the example of the decay anti (Lambda)(sup 0) (yields) anti p(pi)(sup +) it is shown that the proposed technique allows one to determine the efficiency of the decay selection rather precisely over the wide range of identification criteria for antiproton. DOE

N95-24660# Stanford Linear Accelerator Center, CA.
A STUDY OF K(SUB s) (LAMBDA) AND (BAR (LAMBDA)) PRODUCTION IN HADRONIC Z(SUP 0) DECAYS
K. G. Baird (Rutgers - The State Univ., New Brunswick, NJ.) Aug. 1994 4 p Presented at the Meeting of the Division of Particles and Fields of the American Physical Society, Albuquerque, NM, 2-6 Aug. 1994
(Contract DE-AC03-76SF-00515)
(DE95-004280; SU-SLAC-PUB-6601; CONF-940816-54) Avail: CASI HC A01/MF A01

We present a preliminary measurement of the inclusive production rates of K(sub s), A and X hadrons produced in e(+)e(-) annihilation at the Z(sup 0) pole. The analysis is based upon approximately 50K Z(sup 0) decays collected in the SLD experiment at SLAC in 1993. The observed rates of (K(sub s)) = 1.02 +/- 0.02 +/- 0.09 and (Lambda) + (bar-Lambda) = 0.38 +/- 0.01 +/- 0.04 are consistent with previous measurements. Our differential cross section peak-position results are shown to be consistent with QCD predictions based on the modified leading logarithm approximation and local parton-hadron duality. DOE

N95-24662# Stanford Linear Accelerator Center, CA.
SPIN STRUCTURE OF THE NUCLEON AND POLARIZATION
Charles Y. Prescott Sep. 1994 4 p Presented at the Conference on Physics in Collision, Tallahassee, FL, 15-17 Jun. 1994
(Contract DE-AC03-76SF-00515)
(DE95-004282; SU-SLAC-PUB-6620; CONF-940693-5) Avail: CASI HC A01/MF A01

Recent experiments at CERN and SLAC have added new knowledge about the spin structure of the proton and the deuteron. A brief historical background is presented, the status of experiments is discussed, and progress in the understanding of the spin of the nucleon in the context of the quark parton model is summarized. DOE

N95-24663# Stanford Linear Accelerator Center, CA.
GEOMETRY OF MULTIHADRON PRODUCTION
James D. Bjorken Oct. 1994 9 p Presented at the 24th International Symposium on Multiparticle Dynamics, Vietri sul Mare, Italy, 12-19 Sep. 1994
(Contract DE-AC03-76SF-00515)
(DE95-004290; SU-SLAC-PUB-6707; CONF-9409257-1) Avail: CASI HC A02/MF A01

This summary talk only reviews a small sample of topics featured at this symposium: introduction; the geometry and geography of phase space; space-time geometry and HBT; multiplicities, intermittency, correlations; disoriented chiral condensate; deep inelastic scattering at HERA; and other contributions. DOE

N95-24668# Joint Inst. for Nuclear Research, Dubna (USSR). Lab. of Theoretical Physics.
ON A POSSIBILITY FOR A MEASUREMENT OF THE TRANSVERSAL PROTON POLARIZATION IN THE DIFFRACTIVE PION PRODUCTION IN pp AND pe HIGH ENERGY COLLISIONS
A. B. Arbuzov, V. A. Vasendina, Eh. A. Kuraev, and V. A. Nikitin 1993 14 p In RUSSIAN Submitted for publication
(DE94-628598; JINR-R-2-93-304) Avail: CASI HC A03/MF A01 (US Sales Only)

A mechanism of an asymmetry arising of the fragmentation products of a transversely polarized proton in processes of diffractive pion productions in pp and pe high energy collisions is considered. The asymmetry arises

due to an interference of amplitudes, containing resonant state in the intermediate state pp yields pN* yields pN(pi), ep yields e(delta) yields eN(pi), with non-resonant background. The asymmetry has magnitude of tenths percents in the case of completely polarized proton, when the invariant mass of the (N(pi)) system is close to the resonant mass. DOE

N95-24669# Joint Inst. for Nuclear Research, Dubna (USSR). Lab. of Computing Techniques and Automation.
SOME REMARKS TO THE PROBLEM OF NEUTRINO OSCILLATION
Kh. M. Beshtoev 1993 6 p Submitted for publication
(DE94-628599; JINR-E-2-93-297) Avail: CASI HC A02/MF A01 (US Sales Only)

The paper deals with the analysis of possible neutrino oscillation types. The conclusion drawn is that if masses of different type neutrinos are equal, then real oscillation of different type neutrinos is possible by analogy with K(sup 0), antikaons neutral oscillation. If masses of different type neutrinos are different then only virtual neutrino oscillation is possible, and real oscillation of neutrinos requires their participation in interactions for transition to the appropriate mass shells by analogy with the gamma quantum transition to the rho(sup 0)-meson in the vector dominance model. This neutrino oscillation will occur when neutrinos produced inside the Sun are passing through the Sun or when they are passing through the Earth. DOE

N95-24671# Columbia Univ., New York, NY.
THEORY OF ULTRA DENSE MATTER AND THE DYNAMICS OF HIGH ENERGY INTERACTIONS INVOLVING NUCLEI Progress Report, 15 Dec. 1993 - 14 Dec. 1994
Miklos Gyulassy 12 Sep. 1994 13 p
(Contract DE-FG02-93ER-40764)
(DE95-004114; DOE/ER-40764/3) Avail: CASI HC A03/MF A01

This report summarizes the progress made during the second year of the three year DOE agreement DE-FG02-93ER40764 on theoretical nuclear physics research performed at the Columbia University and presents a detailed budget adjustment for the third year period December 15, 1994 to December 14, 1995. Sections 1.1 to 1.8 highlight the technical progress made on the following general areas: multiple scattering and radiative processes in QCD; the quark-gluon plasma transition in nuclear matter; QCD transport theory and dissipative mechanism in dense matter; phenomenological models of high energy interactions involving nuclei; signatures of quark-gluon plasma formation in A+A; neurocomputation theory. Section 2 contains a bibliography of published papers and invited conference papers. Section 3 lists the Columbia nuclear theory members for the December 15, 1994 to December 14, 1995 period. Finally, the budget adjustment requesting $319,830 for the third year relative to the original $320,000 is presented in section 6. Copies of the research papers accompany this report. DOE

N95-24677# Brookhaven National Lab., Upton, NY.
SEARCH FOR TOP IN LEPTON + JETS IN D0 USING A TOPOLOGICAL TAG
Serban Protopopescu 1994 5 p Presented at the 27th International Conference on High Energy Physics, Glasgow, Scotland, 21-27 Jul. 1994
(Contract DE-AC02-76CH-00016)
(DE95-003929; BNL-60981; CONF-940722-36) Avail: CASI HC A01/MF A01

We have searched for production of t(bar t) pairs in p(bar p) interactions at 1.8 TeV center-of-mass energy at the FNAL Tevatron collider. The search assumes standard model decay for top quark into W + b quark. We observe in (mu) + jets and 14 + jets final states a small, not statistically significant, excess above the background estimated by two different methods. The results presented are preliminary. DOE

N95-24687# State Univ. of New York, Stony Brook, NY.
DESIGN OF SUPRAMOLECULAR ORDERED SYSTEMS FOR MESOSCOPIC COLLOIDS AND MOLECULAR COMPOSITES Progress Report, 10 Nov. 1993 - 10 Jun. 1994
1995 6 p
(Contract DE-FG02-86ER-45237)
(DE95-004448; DOE/ER-45237/T3) Avail: CASI HC A02/MF A01

During this reporting period, the authors group has been active in five areas of research: (1) improvements on their x-ray instrumentation at the SUNY Beamline, National Synchrotron Light Source (NSLS) so that they can perform new experiments which are not accessible otherwise; (2) characterization of functionalized hairy rod polymers designed for studying the macromolecular structures in molecular composites; (3) investigation of supramolecular ordered systems composed mainly of block copolymers from dilute to concentrated solutions, including the gel state; (4) evolution of crystalline structures in polymer blends and melts; and (5) multiphase structure of segment polyurethanes. DOE

N95-24689# Joint Inst. for Nuclear Research, Dubna (USSR).
IONIZATION POTENTIAL DATA LIBRARY OF ATOMS AND IONS
K. Mule, E. Eh. Shirkova, and G. D. Shirkov 1993 6 p In RUSSIAN
(DE94-628380; JINR-R-9-93-307) Avail: CASI HC A02/MF A01 (US Sales Only)

The general principles of the library construction of data files for the atomic and ionic ionization potentials are described. Each file relates to one atom and contains the information of the structure of atom electron shells, the ionization potentials for all subshells of neutral atom and the energy shifts of potentials for all ionization states of given element. The library files have been used in the mathematical simulation of processes connected with the ion formation and confinement in the sources of multicharged ions. DOE

N95-24692# Joint Inst. for Nuclear Research, Dubna (USSR).
THE DETERMINATION OF THE MAIN PARAMETERS OF THE BACKWARD SPECTROMETER OF THE 0(SUP 0) FACILITY
P. G. Akishin, V. I. Komarov, and A. I. Puzynin 1993 18 p
(DE94-628385; JINR-E-13-93-339) Avail: CASI HC A03/MF A01 (US Sales Only)

The main parameters (dimensions, momentum and angular-momentum acceptances) of the backward spectrometer of the '0(sup 0) Facility' set-up installed at the internal cooled beam of the proton synchrotron COSY (Juelich, Germany) were determined. The estimation of the angular and momentum resolution was performed. The comparison of two methods for calculation of track parameters in the magnetic field was realized. DOE

N95-24700# Joint Inst. for Nuclear Research, Dubna (USSR).
ELASTIC FORM FACTORS OF HYDROGEN-LIKE ATOMS IN nS-STATES
L. G. Afanasev and A. V. Tarasov 1993 4 p
(DE94-628437; JINR-E-4-93-293) Avail: CASI HC A01/MF A01 (US Sales Only)

The exact analytical formula for elastic form factors of the hydrogenlike atoms in the n S-states is given. The formula has a quite simple form. DOE

N95-24702# National Lab. for High Energy Physics, Tsukuba (Japan).
CURRENT STATUS AND FUTURE PROSPECT OF SPACE AND TIME REVERSAL SYMMETRY VIOLATION ON LOW ENERGY NEUTRON REACTIONS
Yasuhiro Masuda, ed. Jan. 1993 88 p
(DE94-765589; KEK-PROC-92-18) Avail: CASI HC A05/MF A01 (US Sales Only)

In this report the following papers are collected: symmetry violation under space reflection and time reversal and neutron spin; neutron spin rotation and P-violation; parity nonconservation in neutron capture reaction; some advantage of the search for CP-violation in neutron scattering; dynamic polarization of La-139 target; alexandrite laser for optical pumping; polarized He-3 system for T- and P-violation neutron experiments; control of neutron spin in T-violation neutron experiment; symmetry regarding time and space and angular distribution and angular correlation of radiation and particle beams; and T-violation due to low temperature nuclear polarization and axion exploration using nuclear transition. DOE

N95-24718# International Centre for Theoretical Physics, Trieste (Italy).
SEMICLASSICAL HYPERSPHERICAL MATRIX ELEMENTS FOR HELIUM DOUBLY EXCITED STATES
J. MahechaGomez Jan. 1994 17 p
(DE94-628867; LAMP-94/1) Avail: CASI HC A03/MF A01 (US Sales Only)

A classical description of the two-electron atom, analogous to the quantum adiabatic hyperspherical channel approach, is presented. The

classical problems, analogue to the quantum eigenvalue problem for the great angular momentum operator, and the separated dynamical systems defined by each of the other constants of the motion of the non-interacting system are solved, using the Hamiltonian-Jacobi method. Some matrix elements of the Coulomb interaction terms of the Hamilton for doubly excited helium atom using the Heisenberg correspondence principle are calculated. DOE

N95-24719# Joint Inst. for Nuclear Research, Dubna (USSR). Lab. of Theoretical Physics.

PRESENT EXPERIMENTAL DATA ON CROSS CHANNEL DEEP-INELASTIC PROCESSES AND THE GRIBOV-LIPATOV RELATION

V. F. Konoplyanikov (Gomel State Univ., Gomel, Byelarus.) and N. B. Skachkov 1993 10 p Submitted for publication

(DE94-628605; JINR-E-2-93-294) Avail: CASI HC A02/MF A01 (US Sales Only)

The validity of Gribov-Lipatov relation is studied on the basis of the existing experimental data for deep inelastic process e(-)p yields e(-)+X and its analog in a cross channel e(+)e(-) yields p+X. DOE

N95-24720# Joint Inst. for Nuclear Research, Dubna (USSR). Lab. of Theoretical Physics.

REALISTIC NN POTENTIAL FOR THE LOW APPROACH

A. J. Chelidze and L. A. Slepchenko 1993 14 p Submitted for publication

(DE94-628606; JINR-E-2-93-357) Avail: CASI HC A03/MF A01 (US Sales Only)

A realistic NN potential for the Low equation including contact interaction of four nucleons is constructed. All possible characteristic contributions to the potential are calculated and estimated. DOE

N95-24722# Weizmann Inst. of Science, Rehovot (Israel). Dept. of Physics.

NEW PHYSICS EFFECTS ON CP VIOLATION IN B DECAYS

Yosef Nir Aug. 1993 22 p Presented at the Workshop on B Physics At Hadron Accelerators, Snowmass, CO, 21 Jun. - 2 Jul. 1993

(DE94-628617; WIS-PH-93-94; CONF-9306258) Avail: CASI HC A03/MF A01 (US Sales Only)

We review new physics effects on C P violation in B decays. We discuss the Standard Model picture of CP violations in B decays, with special emphasis on the clenliness of the predictions. We point out the ingredients in the analysis that are sensitive to new physics and deduce the type of new physics that is most likely to modify the Standard Model predictions. DOE

N95-24724# China Nuclear Information Centre, Beijing (China).

KORP-1: A PROGRAM FOR CALCULATING THE DIRECT (n, p) OR (p, n) REACTION BY USING DWBA METHOD

Ziqiang Yu and Yixin Zuo Apr. 1993 7 p

(DE94-628768; CNIC-00736; NKU-0002) Avail: CASI HC A02/MF A01 (US Sales Only)

KORP-1 is used to calculate the direct (n,p) or (p,n) reaction differential cross section and its Legendre coefficients as well as the integral cross section. The direct process for (n,p) or (p,n) reaction is treated as a knock-out reaction and calculated by conventional DWBA (distorted wave Born approximation) theory in the zero-range approximation. In general, the calculated results of angle distribution are in agreement with the experimental data. DOE

N95-24877*# Massachusetts General Hospital, Boston, MA. Statistics Research Lab.

ON THE UNCERTAINTY IN SINGLE MOLECULE FLUORESCENT LIFETIME AND ENERGY EMISSION MEASUREMENTS

Emery N. Brown, Zhenhua Zhang, and Alex D. McCollom 6 Apr. 1995 24 p Revised Sponsored by the Robert Wood Johnson Foundation (Grant NAGw-4061)

(NASA-CR-198009; NAS 1.26:198009; TR-94-03-Rev) Avail: CASI HC A03/MF A01

Time-correlated single photon counting has recently been combined with mode-locked picosecond pulsed excitation to measure the fluorescent lifetimes and energy emissions of single molecules in a flow stream. Maximum likelihood (ML) and least square methods agree and are optimal when the number of detected photons is large however, in single molecule fluorescence experiments the number of detected photons can be less than 20, 67% of those can be noise and the detection time is restricted to 10 nanoseconds. Under the assumption that the photon signal and background noise are two independent inhomogeneous poisson processes, we derive the exact joint arrival time probably density of the photons collected in a single counting experiment performed in the presence of background noise. The model obviates the need to bin experimental data for analysis, and makes it possible to analyze formally the effect of background noise on the photon detection experiment using both ML or Bayesian methods. For both methods we derive the joint and marginal probability densities of the fluorescent lifetime and fluorescent emission. the ML and Bayesian methods are compared in an analysis of simulated single molecule fluorescence experiments of Rhodamine 110 using different combinations of expected background nose and expected fluorescence emission. While both the ML or Bayesian procedures perform well for analyzing fluorescence emissions, the Bayesian methods provide more realistic measures of uncertainty in the fluorescent lifetimes. The Bayesian methods would be especially useful for measuring uncertainty in fluorescent lifetime estimates in current single molecule flow stream experiments where the expected fluorescence emission is low. Both the ML and Bayesian algorithms can be automated for applications in molecular biology. Author

N95-24887# Joint Inst. for Nuclear Research, Dubna (USSR). Lab. of Nuclear Problems.

NOTION OF THE INCLUSIVE SPECTRA AND CROSS SECTIONS OF B-MESON PRODUCTION IN HADRONIC INTERACTIONS OF HIGH ENERGIES

O. I. Piskunova 1993 7 p Submitted for publication

(DE94-628628; JINR-E-2-93-309) Avail: CASI HC A02/MF A01 (US Sales Only)

B-meson hadro-production cross sections obtained by the Monte Carlo generating program PYTHIA 5.3 are compared to the results of calculations within the framework of Quark-Gluon String Model (QGSM). The Model is based on the phenomenological description of soft peripheral hadronic interactions whereas the considered Lund-type program takes into account the hard subprocesses described by perturbation theory diagrams of QCD (Quantum Chromodynamics). Such comparison allows one to define the possibilities for the development of both approaches. DOE

N95-24888# Joint Inst. for Nuclear Research, Dubna (USSR).

MESON PROPERTIES AT FINITE TEMPERATURE AND DENSITY WITHIN NAMBU-JONA-LASINIO MODEL

T. I. Gulamov (Academy of Sciences of the Uzbek SSR, Tashkent, Uzbekistan.) and A. I. Titov 1993 26 p In RUSSIAN Submitted for publication

(DE94-628630; JINR-R-2-93-463) Avail: CASI HC A03/MF A01 (US Sales Only)

The properties of mesons at finite temperature and density are studied within the Nambu-Jona-Lasinio model. The analysis is done by means of the self consistent way, which is equivalent to the standard one only at zero temperature and density. As a result, a qualitative and quantitative difference in sigma, pi, rho, and a(sub 1) meson masses in comparison with previous works is found. Also the temperature dependence of the effective coupling constant of rho yields pi pi decay is studied. DOE

N95-24889# Joint Inst. for Nuclear Research, Dubna (USSR).

SEARCH FOR THE PROMPT MUON ANTINEUTRINO FROM CHARM PARTICLE DECAYS AT THE IHEP-JINR NEUTRINO DETECTOR IN 70 GeV PROTON BEAM-DUMP EXPERIMENT

L. S. Barabash, S. A. Baranov, and Yu. A. Batusov 1993 16 p In RUSSIAN Submitted for publication

(DE94-628772; JINR-R-1-93-327) Avail: CASI HC A03/MF A01 (US Sales Only)

Data from the 70 GeV proton beam-dump experiment have been analyzed with the aim of the detection of signal from the prompt muon antineutrino. The 'equilibrium' mu(+) and mu(-) muons, produced in the interactions of neutrinos and antineutrinos in muon iron filter, placed in front of the detector have been registered by the IHEP-JINR Neutrino detector. The upper limit for total cross section of charm particle production at 70 GeV pN-interactions has been obtained: sigma(sub cc) less than 4.7 micro b/nucl. (90% C.L.). Results are compared with the data received in other experiments. The

anomaly high charm production cross section has not been observed near a threshold. The upper limit of the charm production cross section doesn't contradict to the theoretical calculations based on QCD. DOE

N95-24890# Joint Inst. for Nuclear Research, Dubna (USSR). Lab. of Theoretical Physics.

MESIC MOLECULES OF LIGHT NUCLEI IN THE OSCILLATOR REPRESENTATION

M. Dinejkhan (Academy of Sciences, USSR, Alma-Ata, USSR.) and G. V. Efimov 1993 8 p Submitted for publication

(DE94-628904; JINR-E-4-93-465) Avail: CASI HC A02/MF A01 (US Sales Only)

The mesic molecules (H(mu)N(sub z)), where H is the hydrogen isotopes (p,d,t) and N(sub z) are nuclei with charges Z = 2,3,4,... and masses M(sub z) = 2Zm(sub p), are studied. The energy values of the ground state for the molecules of light nuclei have been calculated by using the oscillator representation method. The dependence of the binding energies of the muonic molecules on nuclear charges and the critical values of nuclear charges are obtained. DOE

N95-24901# Fermi National Accelerator Lab., Batavia, IL.

THE CDF SILICON VERTEX DETECTOR SVX AND ITS UPGRADES

Sally Seidel (New Mexico Univ., Albuquerque, NM.) Nov. 1994 16 p Presented at the 2nd Workshop on Vertex Detectors, Lake Bohinji, Slovenia, 12-17 Jun. 1993

(Contract DE-AC02-76CH-03000)

(DE95-003743; FNAL/C-94/377-E; CONF-9306398-1) Avail: CASI HC A03/MF A01

The three generations of Collider Detector at Fermilab (CDF) silicon vertex detectors, SVX, SVX(prime), and SVX II, are described. SVX, which operated during Tevatron run Ia, achieved 10.6 (mu)m resolution in r (minus) (phi). SVX(prime) is a radiation-hard device for run Ib with a similar but improved mechanical design and improved signal/noise. SVX II, which will be installed for run II, will track in three dimensions with radiation tolerance and electronics appropriate to a Main Injector environment. DOE

N95-24902# State Univ. of New York, Binghamton, NY. Dept. of Physics.

TESTS FOR LEPTONIC CP VIOLATION IN TAU DECAYS

C. A. Nelson, M. Kim, and Hui-Chun Yang 1994 9 p Presented at the 27th International Conference on High Energy Physics, Glasgow, England, 21-27 Jul. 1994

(Contract DE-FG02-86ER-40291)

(DE95-005927; DOE/ER-40291/25; CONF-940722-40) Avail: CASI HC A02/MF A01

At the Z(sup o) or a B factory, there are two tests for non-CKM-type leptonic CP violation in the tau yields rho(nu)(a(sub 1)(sup -)nu) decay channel by inclusion of rho(a(sub 1)) polarimetry. By CP invariance, the moduli ratio of, and the phase difference between, the two helicity amplitudes for tau(sup -) yields rho(sup -)(nu)(a(sub 1)(sup -)nu) decay should equal those for tau(sup +) yields rho(sup +)(anti nu)(a(sub 1)(sup +)(anti nu)) decay. Formulas are given for a L-handed nu(sub tau), and also for an arbitrary mixture of nu(sub L) and nu(sub R) neutrino helicities. Statistical errors are listed for both the case that the tau(sup -) momentum direction is not known, and when it is known via a silicon vertex detector. DOE

N95-24903# Stanford Linear Accelerator Center, CA.

PROBING NEW PHYSICS IN RARE CHARM PROCESSES

J. L. Hewett Sep. 1994 6 p Presented at the Meeting of the Division of Particles and Fields of the American Physical Society, Albuquerque, NM, 2-6 Aug. 1994

(Contract DE-AC03-76SF-00515)

(DE95-006067; SU-SLAC-PUB-6674; CONF-940816-69) Avail: CASI HC A02/MF A01

The possibility of using the charm system to search for new physics is addressed. Phenomena such as D(exp 0) - (bar D)(exp 0) mixing and rare decays of charmed mesons are first examined in the Standard Model to test the present understanding and to serve as benchmarks for signals from new sources. The effects of new physics from various classes of non-standard dynamical models on D(exp 0) - (bar D)(exp 0) mixing are investigated. DOE

N95-25094# Joint Inst. for Nuclear Research, Dubna (USSR). Theoretical Physics Lab.

THE EXISTENCE OF ANTIPARTICLES SEEMS TO FORBID VIOLATIONS OF STATISTICS

A. B. Govorkov 1993 15 p Submitted for publication

(DE94-628523; JINR-E-2-93-53) Avail: CASI HC A03/MF A01 (US Sales Only)

The impossibility of small violations of Fermi- and Bose-statistics even within the nonlocal quantum field theory corresponding to the infinite statistics is evident. The existence of antiparticles plays the crucial role in this proof. DOE

N95-25099# Oak Ridge National Lab., TN.

A HIGH INTENSITY SLOW POSITRON FACILITY FOR THE ADVANCED NEUTRON SOURCE

L. D. Hulett, Jr. and C. C. Eberle 1994 4 p Presented at the 10th International Conference on Positron Annihilation, Beijing, China, 23-29 May 1994

(Contract DE-AC05-84OR-21400)

(DE94-014108; CONF-9405170-3) Avail: CASI HC A01/MF A01

A slow positron spectroscopy facility, based on (sup 64)Cu activation, has been designed for incorporation in the Advanced Neutron Source (ANS). The ANS is a reactor-based research center planned for construction at Oak Ridge, Tennessee. Multiple sources of slow positron beams will be available. One-half mm diameter, copper-coated aluminum microspheres will be activated and transported to a positron spectroscopy building, where they will be dispersed over the surfaces of horizontal pans, 0.1 m(sup 2) in area, located in source chambers. Fast positions from the pans will be intercepted by cylinders coated inside with inert gas moderators. Yields will approach 10(sup 12) positrons per second before brightness enhancement. Beams will be transported to multiple experiment stations, which will include a 50 meter diameter, 20-detector angular correlation of annihilation radiation (ACAR) spectrometer, and other equipment for materials analysis and fundamental science. DOE

N95-25112# State Univ. of New York, Buffalo, NY. Dept. of Chemistry.

GROUP TRANSFER AND ELECTRON TRANSFER REACTIONS OF ORGANOMETALLIC COMPLEXES

Jim D. Atwood 1994 4 p

(Contract DE-FG02-87ER-13775)

(DE95-003732; DOE/ER-13775/6) Avail: CASI HC A01/MF A01

During 1994, despite the disruptions, the authors have made progress in several aspects of their research on electron transfer reactions between organometallic complexes. This summary covers three areas that are relatively complete: (1) reactions between metal carbonyl anions and metal carbonyl halides, (2) reactions of hydrido- and alkyl-containing anions (RFe(CO)4(-) and RW(CO)5(-) with metal carbonyl cations; and (3) reactions of a seventeen-electron complex (Cp* Cr(CO)3*) with metal carbonyl derivatives. Two areas of examination that have just begun (possible carbene transfer and the possible role of metal carbonyl anions in carbon-hydrogen bond activation) will also be described. DOE

N95-25180# General Atomics Co., San Diego, CA.

EXPERIMENTAL CONSTRAINTS ON TRANSPORT

T. C. Luce, K. H. Petty, K. H. Burrell, C. B. Forest, P. Gohil, R. J. Groebner, J. C.M. DeHaas, R. A. James, and M. A. Makowski Dec. 1994 12 p Presented at the 15th International Conference on Plasma Physics and Controlled Nuclear Fusion Research, Seville, Spain, 26 Sep. - 1 Oct. 1994

(Contract DE-AC03-89ER-51114)

(DE95-004962; GA-A-21834; CONF-940933-24) Avail: CASI HC A03/MF A01

Characterization of the cross-field energy transport in magnetic confinement experiments in a manner applicable to the accurate assessment of future machine performance continues to be a challenging goal. Experimental results from the DIII-D Tokamak in the areas of dimensionless scaling and non-diffusive transport represent progress toward this goal. Dimensionless scaling shows how beneficial the increase in machine size and magnetic field is for future devices. The experiments on DIII-D are the first to determine separately the electron and ion scaling with normalized gyroradius rho(sub *); the electrons scale as expected from gyro-Bohm class theories, while the ions scale consistent with the Goldston empirical scaling. This result predicts an increase in transport relative to Bohm

diffusion as rho(sub *) decreases in future devices. The existence of distinct rho(sub *) scalings for ions and electrons cautions against a physical interpretation of one-fluid or global analysis. The second class of experiments reported here are the first to demonstrate the existence of non-diffusive energy transport. Electron cyclotron heating was applied at the half radius; the electron temperature profile remains substantially peaked. Power balance analysis indicates that heat must flow in the direction of increasing temperature, which is inconsistent with purely diffusive transport. The dynamics of electron temperature perturbations indicate the presence in the heat flux of a term dependent on temperature rather than its gradient. These two observations strongly constrain the types of models which can be applied to cross-field heat transport. DOE

N95-25241# Texas Univ. at Dallas, Richardson, TX. Dept. of Physics.
ELEMENTARY PARTICLE PHYSICS Progress Report, Jul. 1992 - Oct. 1994
Joseph M. Izen Oct. 1994 60 p
(Contract DE-FG05-92ER-40736)
(DE95-004376; DOE/ER-40736/T1) Avail: CASI HC A04/MF A01

The University of Texas at Dallas (UTD) is participating in two e(+)e(-), experiments, Beijing Spectrometer (BES) and BABAR, the PEP-11 B Factory detector. Associated production of tau and charmed mesons allow for absolute branching fraction measurements with good control of backgrounds. BES is uniquely positioned to study the leptonic and hadronic decays of quarkonia. The Beijing Electron Positron Collider (BEPC) delivers luminosities an order of magnitude higher than earlier facilities. BES and BEPC will be upgraded following the 1994-5 run, and will resume data taking in Fall, 1996 with an improved detector and a Three-fold increase in luminosity. The raison d'etre of BABAR is the exploration of CP violation in the B meson system. An asymmetric storage ring is required to observe the time-dependence of the CP asymmetry. Other BABAR physics includes measurements of CKM matrix elements, rare B decays, penguin diagrams, B(sub s) decays, and precision measurements of tau and D meson decays. The scheduled BABAR turn-on in 1999 provides the UTD group with a natural evolution with continuous physics during this period. DOE

N95-25290# International Centre for Theoretical Physics, Trieste (Italy).
LOW ENERGY PROPERTIES OF THE HEAVY VECTOR FERMIONS
Hanqing Zheng Jun. 1994 18 p
(DE94-634362; IC-94/121) Avail: CASI HC A03/MF A01 (US Sales Only)

We discuss the properties of the heavy vector fermions with bare Dirac mass terms and a SU(2) x SU(2) global symmetry in the Yukawa interaction Lagrangian. Using the heat kernel expansion method we calculate their contributions to the low energy observables. We argue that these heavy fermions may be responsible for a soft dynamical symmetry breaking through their condensation. We also discuss the possibility to consider the ordinary fermions as one part of the vector fermions within our model. Author

N95-25292# State Univ. of New York, Binghamton, NY.
CP VIOLATION TESTS FOR TAU/TOP PROCESSES
C. A. Nelson 1994 11 p Presented at the La Thuile Conference on Elementary Particles, Aosta Valley, Italy, 7-12 Mar. 1994
(Contract DE-FG02-86ER-40291)
(DE95-005924; DOE/ER-40291/22; CONF-9403198-1) Avail: CASI HC A03/MF A01

This paper reviews the following topics: tests for CP violation in top-quark production and decay processes. In particular, m(sub t) = 174 +/- 17 GeV implies good top-quark polarimetry because the W bosons in t-quark decays must be predominantly longitudinally polarized (Gamma(sub L)/Gamma(sub T) = 2.4). Tests for CP violation in tau lepton decays by the tau approachs (rho)(nu) decay mode by usage of rho polarimetry signatures. Tests for complete measurement of the Z(exp 0), gamma (*) approachs tau(-)tau(+) vertex, including tests for CP violation in tau production processes. DOE

N95-25294# State Univ. of New York, Binghamton, NY.
q-BOSONS AND THE q-ANALOGUE QUANTIZED FIELD
C. A. Nelson 1994 7 p Presented at the Workshop on Harmonic Oscillators, Cocoyoc, Mexico, 23-25 Mar. 1994
(Contract DE-FG02-86ER-40291)
(DE95-005925; DOE/ER-40291/23; CONF-9403139-2) Avail: CASI HC A02/MF A01

The q-analogue coherent states (vert bar)z greater than (sub q) are used to identify physical signatures for the presence of a q-analogue quantized radiation field in the (vert bar) greater than (sub q) classical limit where absolute value of z is large. In this quantum-optics-like limit, the fractional uncertainties of most physical quantities (momentum, position, amplitude, phase) which characterize the quantum field are O(1). They only vanish as O(1/absolute value of z) when q = 1. However, for the number operator, N, and the N-Hamiltonian for a free q-boson gas, H(sub N) = Dirac-h omega(N + 1/2), the fractional uncertainties do still approach zero. A signature for q-boson counting statistics is that (Delta)N (exp 2)/less than N greater than approaches 0 as absolute value approaches infinity. Except for its O(1) fractional uncertainty, the q-generalization of the Hermitian phase operator of Pegg and Barnett, phi(sub q), still exhibits normal classical behavior. The standard number-phase uncertainty-relation, Delta-N Delta phi(sub q) = 1/2, and the approximate commutation relation, (N, phi(sub q)) = i, still hold for the single-mode q-analogue quantized field. So, N and phi(sub q) are almost canonically conjugate operators in the (vert bar)z greater than (sub q) classical limit. The (vert bar)z greater than (sub q) CS's minimize this uncertainty relation for moderate absolute value of z(exp 2). DOE

N95-25296# State Univ. of New York, Binghamton, NY.
TAU AS A PROBE FOR NEW PHYSICS
C. A. Nelson 1994 15 p Presented at the 3rd Workshop on Tau Lepton Physics, Montreux, Switzerland, 19-22 Sep. 1994
(Contract DE-FG02-86ER-40291)
(DE95-005928; DOE/ER-40291/26; CONF-9409277-3) Avail: CASI HC A03/MF A01

The usage of polarimetry and spin-correlation tests to determine the complete Lorenz structure of the tau lepton's charged and neutral-current couplings is reviewed. The emphasis is on tests for 'something' in a (V-A)+ 'something' structure in J(sup charged) Lepton current, so as to bound the scales (lambda) for 'new physics' such as arising from tau weak magnetism, weak electricity, and/or second-class currents. Tests for T and for CP violation are discussed. DOE

N95-25372# Fermi National Accelerator Lab., Batavia, IL.
B PHYSICS WITH CDF: RECENT RESULTS AND FUTURE PROSPECTS
J. A. Mueller (Rutgers Univ., Piscataway, NJ.) Aug. 1994 28 p Presented at the 2nd International Workshop on B-physics At Hadron Machines (Beauty '94), Le Mont St. Michel, France, 24-29 Apr. 1994
(Contract DE-AC02-76CH-03000)
(DE95-004793; FNAL/C-94/252-E; CONF-9404228-1) Avail: CASI HC A03/MF A01

Using data collected during the 1992-1993 collider run, we report on measurements of the B(sup o), B(+), and B(sub s) lifetimes. We also present our revised measurement of the B(sub s) mass. Production studies involving inclusive modes decaying into J/psi or psi(2S), semileptonic decays involving D(sup o) or D*(+) mesons, and fully reconstructed B mesons are also presented. We present the prospects for future work with this data, as well as that being collected in the 1994-1995 collider run. Upgrades to the detector and estimates of physics capabilities for future collider runs are also presented. DOE

N95-25373# Oak Ridge Associated Universities, Inc., TN.
BIOLOGICAL EFFECTIVENESS OF NEUTRONS: RESEARCH NEEDS
G. W. Casarett, L. A. Braby, J. J. Broerse, M. M. Elkind, D. T. Goodhead, and N. L. Oleinick Feb. 1994 194 p
(Contract DE-AC05-76OR-00033)
(DE95-004795; ORAU-94/D-58) Avail: CASI HC A09/MF A03

The goal of this report was to provide a conceptual plan for a research program that would provide a basis for determining more precisely the biological effectiveness of neutron radiation with emphasis on endpoints relevant to the protection of human health. This report presents the findings of the experts for seven particular categories of scientific information on neutron biological effectiveness. Chapter 2 examines the radiobiological mechanisms underlying the assumptions used to estimate human risk from neutrons and other radiations. Chapter 3 discusses the qualitative and quantitative models used to organize and evaluate experimental observations and to provide extrapolations where direct observations cannot be made.

Chapter 4 discusses the physical principles governing the interaction of radiation with biological systems and the importance of accurate dosimetry in evaluating radiation risk and reducing the uncertainty in the biological data. Chapter 5 deals with the chemical and molecular changes underlying cellular responses and the LET dependence of these changes. Chapter 6, in turn, discusses those cellular and genetic changes which lead to mutation or neoplastic transformation. Chapters 7 and 8 examine deterministic and stochastic effects, respectively, and the data required for the prediction of such effects at different organizational levels and for the extrapolation from experimental results in animals to risks for man. Gaps and uncertainties in this data are examined relative to data required for establishing radiation protection standards for neutrons and procedures for the effective and safe use of neutron and other high-LET radiation therapy. DOE

N95-25374# Brookhaven National Lab., Upton, NY.
BARYON SPECTROSCOPY AND THE OMEGA MINUS
N. P. Samios 1994 22 p Presented at the International Conference on the History of Original Ideas and Basic Discoveries in Particle Physics, Erice, Italy, 29 Jul. - 4 Aug. 1994
(Contract DE-AC02-76CH-00016)
(DE95-004838; BNL-61099; CONF-9407157-1) Avail: CASI HC A03/MF A01

In this report, I will mainly discuss baryon resonances with emphasis on the discovery of the Omega(-). However, for completeness, I will also present some data on the meson resonances which together with the baryons led to the uncovering of the SU(3) symmetry of particles and ultimately to the concept of quarks. DOE

N95-25375# Brookhaven National Lab., Upton, NY.
TAU PHYSICS 1994: A THEORETICAL PERSPECTIVE
W. J. Marciano Nov. 1994 12 p Presented at the 3rd Workshop on Tau Lepton Physics, Montreux, Switzerland, 19-22 Sep. 1994
(Contract DE-AC02-76CH-00016)
(DE95-004840; BNL-61141; CONF-9409277-2) Avail: CASI HC A03/MF A01

In this paper I describe some recent advances in tau physics and discuss their implications from a theoretical perspective. The examples I have chosen include e-mu-tau universality, QCD studies, anomalous electroweak dipole moments, and forbidden decays. That list is by no means exhaustive. It should, however, demonstrate the breath of tau physics, describe some interesting new results, and point out the potential for future advances. DOE

N95-25377# Fermi National Accelerator Lab., Batavia, IL.
PHOTON-CHARM PRODUCTION IN p(ANTI p) COLLISIONS AT RADICAL s = 1.8 TeV
R. T. Hamilton (Harvard Univ., Cambridge, MA.) Aug. 1994 3 p Presented at the Meeting of the Division of Particles and Fields of the American Physical Society, Albuquerque, NM, 2-6 Aug. 1994
(Contract DE-AC02-76CH-03000)
(DE95-004850; FNAL/C-94/209-E; CONF-940816-82) Avail: CASI HC A01/MF A01

The authors present preliminary results of a measurement of inclusive photon-charm production in (anti p)p collisions. Using data collected by the CDF experiment during the 1992-1993 Tevatron collider run, the authors have measured the inclusive photon-muon cross section, and estimated the decay-in-flight and punchthrough backgrounds. They compare the measured photon-muon cross section and photon E(sub T) spectrum to Pythia predictions for the charm Compton contribution. DOE

N95-25402# Fermi National Accelerator Lab., Batavia, IL.
A SEARCH FOR t(ANTI t) (YIELDS) LEPTON + E(SUB T) + JETS SIGNATURE IN p(ANTI p) COLLISIONS AT (RADICAL)S = 1.8 TeV WITH THE DO DETECTOR
Dhiman Chakraborty Sep. 1994 7 p Presented at the 8th Meeting of the Division of Participles and Fields, Albuquerque, NM, 1-8 Aug. 1994; sponsored by the American Physical Society Prepared in cooperation with State Univ. of New York, Stony Brook, NY
(Contract DE-AC02-76CH-03000)
(DE95-004239; FNAL/C-94/294-E; CONF-940816-65) Avail: CASI HC A02/MF A01

The authors report the results from a search for t(anti t) production in p(anti p) collisions at (radical)s = 1.8 TeV with the D0 detector at Fermilab in the final states consisting of one isolated high p(sub T) lepton (e or mu), multiple jets and a substantial missing transverse energy (E(sub T)), excluding the events that have mu-tagged jets. Two independent analysis approaches lead them to similar estimates for the cross-section. They see no conclusive evidence for top production in the 13.5 pb(sup -1) of data taken during the 1992--1993 run of the Tevatron. DOE

N95-25403# Washington Univ., Seattle, WA. Inst. for Nuclear Theory.
NEUTRINO OSCILLATIONS FROM DISCRETE NON-ABELIAN FAMILY SYMMETRIES
Martin Schmaltz Nov. 1994 10 p
(Contract DE-FG06-90ER-40561)
(DE95-004355; DOE/ER-40561/168) Avail: CASI HC A02/MF A01

The author discusses a SUSY-GUT model with a non-Abelian discrete family symmetry that explains the observed hierarchical pattern of quark and lepton masses. This SO(10) x Delta(75) model predicts modified quadratic seesaw neutrino masses and mixing angles which are interesting for three reasons: (1) they offer a solution to the solar neutrino problem; (2) the tau neutrino has the right mass for a cosmologically interesting hot dark matter candidate; and (3) they suggest a positive result for the nu(sub mu) yields nu(sub tau) oscillation searches by the CHORUS and NOMAD collaborations. However, the model shares some problems with many other predictive GUT models of quark and lepton masses. Well-known and once successful mass and angle relations, such as the SU(5) relation lambda(sub b)(exp GUT) = lambda(sub t)(exp GUT), are found to be in conflict with the current experimental status. Attempts to correct these relations seem to lead to rather contrived models. DOE

N95-25407# Stanford Linear Accelerator Center, CA.
EXTENDED GAUGE SECTORS
T. G. Rizzo 1995 9 p Presented at the 4th International Conference on Physics Beyond the Standard Model, Lake Tahoe, CA, 13-18 Dec. 1994
(Contract DE-AC03-76SF-00515)
(DE95-006485; SU-SLAC-PUB-95-6741; CONF-941251-1) Avail: CASI HC A02/MF A01

Present and future prospects for the discovery of new gauge bosons, Z' and W', are reviewed. Particular attention is paid to hadron and e(+)e(-) collider searches for the W' of the Left-Right Symmetric Model. DOE

N95-25436# International Centre for Theoretical Physics, Trieste (Italy).
CRITICAL PARAMETERS OF QUARK-HADRON PHASE TRANSITION WITH INTERACTING AND MASSIVE QUARKS
C. P. Singh and B. K. Patra (Banaras Hindu Univ., Varanasi, India.) Jun. 1994 11 p Sponsored by Department of Science and Technology
(DE95-607143; IC-94/119) Avail: CASI HC A03/MF A01 (US Sales Only)

Current techniques to simulate the dynamical behaviour of Quark-Gluon Plasma (QGP) reveal that the order of the phase transition as well as the values of the critical parameters depend on the number of quark flavors as well as on the quark-masses included in the simulation. We attempt to show here the effects of the number of quark flavors and quark-masses on critical parameters by using the perturbative, finite temperature field theory to g(exp 3)(sub s) order in the strong coupling g(sub s). We treat the hadrons as particles with finite size and its implications on the equation of state for hadron gas are studied. We find that the critical temperature T(sub c) is lowered by 9 MeV as we move from two to three quark flavors. The nature of the phase transition always remains as first order. However, the inclusion of quark-masses in our calculation does not affect the result much. DOE

N95-25437# International Centre for Theoretical Physics, Trieste (Italy).
THE TWIST-3 SINGLE SPIN ASYMMETRIES OF PION PRODUCTION
A. Efremov (Joint Inst. for Nuclear Research, Dubna, USSR.), O. Teryaev, and V. Korotkiyan (Joint Inst. for Nuclear Research, Dubna, USSR.) Jul. 1994 7 p Sponsored by International Science Foundation and the Russian Foundation for Fundamental Researches
(DE95-607144; IC-94/169) Avail: CASI HC A02/MF A01 (US Sales Only)

Single spin parton asymmetries for the high p(sub T) gluon and quark production are calculated. Using the sum rules, relating twist-3 quark-gluon

correlators with twist-2 distribution function, we propose an explanation of the difference in the sign of the asymmetries for pi(+), pi(0), and pi(-) productions. DOE

N95-25438# International Centre for Theoretical Physics, Trieste (Italy).
SCALAR THREE BODY DECAYS AND SIGNALS FOR NEW PHYSICS
Rathin Adhikari (Mehta Research Inst. of Mathematics and Mathematical Physics, Allahabad, India.) and Biswarup Mukhopadhyaya Jul. 1994 12 p
(DE95-607188; IC-94/174) Avail: CASI HC A03/MF A01 (US Sales Only)

If massive invisible particles are pair-produced in a three-body decay, then the energy distribution of the other (visible) product is sensitive to the mass of the invisible pair. We use this fact in the context of a Higgs boson decaying into (1) a Z-boson and two massive neutrinos of a fourth generation, and (2) a Z and two lightest supersymmetric particles in the minimal supersymmetric standard model. We discuss how the Z-energy spectrum in each case can reflect the values of the parameters of such models. DOE

N95-25449# International Centre for Theoretical Physics, Trieste (Italy).
ON THE FIELD THEORY OF THE EXTENDED-TYPE ELECTRON
Giovanni Salesi and Erasmo Recami Jul. 1994 20 p Sponsored by INFN-Sezione di Catania, INFN-Sezione di Milano, CNR, MURST, and CNPq
(DE95-607069; IC-94/185) Avail: CASI HC A03/MF A01 (US Sales Only)

In a recent paper, the classical theory of Barut and Zhanghi (BZ) for the electron spin (which interpreted the Zitterbewegung (zbw) motion as an internal motion along helical paths) and its 'quantum' version have been investigated by using the language of Clifford algebras. In so doing, a new nonlinear Dirac-like equation (NDE) was derived. We want to readdress the whole subject, and 'complete' it, by adopting - for the sake of physical clarity - the ordinary tensorial language, within the frame of a first quantization formalism. In particular, we rederive here the NDE for the electron field, show it to be associated with a new conserved probability current which allows us to work out a quantum probability interpretation of NDE. Actually, we propose this equation in substitution for the Dirac equation, which is obtained from the former by averaging over a zbw cycle. We then derive a new equation of motion for the four-velocity field which will allow us to regard the electron as an extended object with a classically intelligible internal structure (thus overcoming some known, long-standing problems). We carefully study the solutions of the NDE, with special attention to those implying (at the classical limit) light-like helical motions, since they appear to be the most adequate solutions for the electron description from a kinematical and physical point of view, and to cope with the electromagnetic properties of the electron. DOE

N95-25450# International Centre for Theoretical Physics, Trieste (Italy).
MASSES OF HEAVY FERMIONS AND HIGGS BOSON IN FOUR-GENERATION FERMION CONDENSATE SCHEME
Bang-Rong Zhou (China Center for Advanced Science and Technology, Beijing, China.) Jul. 1994 12 p Sponsored by National Science Foundation of China
(DE95-607124; IC-94/202) Avail: CASI HC A03/MF A01 (US Sales Only)

The renormalization group analyses based on low-energy effective Lagrangian indicate that a model of electroweak breaking of Nambu-Jona-Lasinio (NJL) type with four generations of quarks and leptons could accommodate itself to the top-quark mass (approx) 174 GeV for the acceptable momentum cut-off and (approx) 10(exp 6) - 5 x 10(exp 3) GeV. The fourth generation of quarks will always be heavier than the top-quark but the corresponding leptons, though being heavier than the Z boson, can be either lighter or heavier than the top-quark depending on (Lambda) being either greater or less than (approx) 2.5 x 10(exp 4) GeV. The mass of the Higgs boson is predicted to be in the region 287-481 GeV which could provide an important experimental test of the model. DOE

N95-25459# International Centre for Theoretical Physics, Trieste (Italy).
ZERO SOUND VELOCITY IN pi, rho MESONS AT DIFFERENT TEMPERATURES
Jishnu Dey, Mira Dey, Lauro Tomio (Instituto de Fisica Teorica, Sao Paulo, Brazil.), and Carlos F. deAraujo, Jr. (Instituto de Fisica Teorica, Sao Paulo, Brazil.) Jul. 1994 12 p Sponsored by DST, Government of India, CPq of Brazil
(DE95-607145; IC-94/191) Avail: CASI HC A03/MF A01 (US Sales Only)

Sharp transitions are perhaps absent in QCD, so that one looks for physical quantities which may reflect the phase change. One such quantity is the sound velocity which was shown in lattice theory to become zero at the transition point for pure glue. We show that even in a simple bag model the sound velocity goes to zero at temperature T = T(sub nu) when it is different than zero and that the numerical value of this T(sub nu) depends on the nature of the meson. The average thermal energy of mesons go linearly with T near T(sub nu), with much smaller slope for the pion. The T(sub nu) - s can be connected with the Boltzmann temperatures obtained from transverse momentum spectrum of these mesons in heavy ion collision at mid-rapidity. It would be interesting to check the presence of different T(sub nu) - s in present day finite T lattice theory. DOE

N95-25460# International Centre for Theoretical Physics, Trieste (Italy).
HEAVY QUARK EFFECTIVE THEORY, INTERPOLATING FIELDS AND BETHE-SALPETER AMPLITUDES
F. Hussain and G. Thomspon Jul. 1994 12 p Submitted for publication
(DE95-607146; IC-94/64; HEP-PH-9407330) Avail: CASI HC A03/MF A01 (US Sales Only)

We use the LSZ reduction theorem and interpolating fields, along with the heavy quark effective theory, to investigate the structure of the Bethe-Salpeter amplitude for heavy hadrons. We show how a simple form of this amplitude, used extensively in heavy hadron decay calculations, follows naturally up to O(1/M) from these field theoretic considerations. DOE

N95-25461# Melbourne Univ., Parkville (Australia). Research Centre for High Energy Physics.
STUDY OF THE SIMPLEST REALISTIC HIGGS SECTOR IN QUARK-LEPTON SYMMETRIC MODELS
Y. Levin and R. R. Volkas 1993 25 p
(DE95-607159; UM-P-93/51; OZ-93/11) Avail: CASI HC A03/MF A01 (US Sales Only)

A discrete symmetry between quarks and (generalized) leptons can exist in nature, and its spontaneous symmetry breaking scale can be as low as a few TeV. Such discrete symmetry also has interesting implications for how electroweak symmetry is spontaneously broken, because the simplest version of the theory requires two electroweak Higgs doublets rather than one in order to provide acceptable values for quark and lepton masses. The effective theory generated at electroweak-scale energies is thus a particular type of two-Higgs-doublet model. We point out in this paper that the broken discrete symmetry imposes very interesting constraints on the form of the Yukawa couplings between physical Higgs bosons and quarks and leptons. In particular, we find that the flavor-changing neutral Higgs couplings to down-sector quarks are proportional to the neutrino Dirac mass matrix. If neutrinos are Dirac particles, then the severe experimental upper bounds on their mass values renders tree-level neutral flavor-changing Higgs effects on down-quark systems like K(sup 0) - bar-K(sup 0) bar negligibly small. DOE

N95-25462# International Centre for Theoretical Physics, Trieste (Italy).
RADIATIVE CORRECTIONS FOR PION POLARIZABILITY EXPERIMENTS
A. A. Akhundov, S. Gerzon (Tel-Aviv Univ., Ramat-Aviv, Tel-Aviv, Israel.), S. Kananov (Tel-Aviv Univ., Ramat-Aviv, Tel-Aviv, Israel.), and M. A. Moinester (Tel-Aviv Univ., Ramat-Aviv, Tel-Aviv, Israel.) Aug. 1994 12 p Sponsored by Ministry of Absorption, Israel Ministry of Science, Wolfson Foundation, US-Israel Binational Science Foundation
(DE95-607177; IC-94/203; TAUP-2183-94) Avail: CASI HC A03/MF A01 (US Sales Only)

We use the semi-analytical program RCFORGV to evaluate radiative corrections to one-photon radiative emission in the high-energy scattering of pions in the Coulomb field of a nucleus with atomic number Z. It is shown that radiative corrections can simulate a pion polarizability effect. The average effect is alpha(sup rc)(sub pi) = -beta(sup rc)(sub pi) =

(0.20 +/- 0.05) x 10(exp -43) cu cm, for pion energies 40-600 GeV. We also study the range of applicability of the equivalent photon approximation in describing one-photon radiative emission. DOE

N95-25463# International Centre for Theoretical Physics, Trieste (Italy).
ANNIHILATION DIAGRAMS IN TWO-BODY NONLEPTONIC DECAYS OF CHARMED MESONS
P. Bedaque, A. Das, and V. S. Mathur (Rochester Univ., NY.) Jun. 1994 9 p
(Contract DE-FG02-91ER-40685)
(DE95-607181; IC-93/216; UR-1316; ER-40685-766) Avail: CASI HC A02/MF A01 (US Sales Only)

In the pole-dominance model for the two-body nonleptonic decays of charmed mesons D yields PV and D yields VV, it is shown that the contributions of the intermediate pseudoscalar and the axial-vector meson poles cancel each other in the annihilation diagrams in the chiral limit. In the same limit, the annihilation diagrams for the D yields PP decays vanish independently. DOE

N95-25464# Melbourne Univ., Parkville (Australia). Research Centre for High Energy Physics.
ANOMALOUS WWZ COUPLINGS AND K(SUB L) YIELDS mu(+) mu(-)
Xiao-Gang He 1993 9 p Sponsored by Australian Research Council
(DE95-607190; UM-P-93/58; OZ-93/13) Avail: CASI HC A02/MF A01 (US Sales Only)

The author analyzed contributions to K(sub L) yields mu(+) mu(-) from anomalous WWZ interactions. There are, in general, seven anomalous couplings. Among the seven anomalous couplings, only two of them contribute significantly. The others are suppressed by factors like m(sup 2)(sub s)/M(sup 2)(sub W), m(sup 2)(sub d)/M(sup 2)(sub W), or M(sup 2)(sub K)/M(sup 2)(sub W). Using the experimental data on K(sub L) yields mu(+) mu(-), it is possible to obtain strong bounds on the two anomalous couplings. DOE

N95-25465# Melbourne Univ., Parkville (Australia). Research Centre for High Energy Physics.
CAN THE ELECTRIC CHARGES OF ELEMENTARY PARTICLES CHANGE WITH TIME?
A. Yu. Ignatiev and G. C. Joshi 1993 9 p Sponsored by Australian Research Council
(DE95-607194; UM-P-93/42) Avail: CASI HC A02/MF A01 (US Sales Only)

This paper presents the limits on possible time variation of the electric charges of quarks and leptons at the time of primordial nucleosynthesis within a model with dequantized electric charges which allows for the case of charged neutrino and neutron. DOE

N95-25466# International Centre for Theoretical Physics, Trieste (Italy).
NEUTRINO MASS AND OSCILLATION ANGLE PHENOMENA WITHIN THE ASYMMETRIC LEFT-RIGHT MODELS
O. Boyarkin and D. Rein (Technische Hochschule, Aachen, Germany.) Jul. 1994 21 p Sponsored by German Bundesministerium fur Forschung und Technologie
(DE95-607201; IC-94/163) Avail: CASI HC A03/MF A01 (US Sales Only)

The light and heavy Majorana neutrinos which appear naturally in SU(2)(sub L) x SU(2)(sub R) x U(1)(sub B-L) model are investigated. The exact solutions are presented for the system of two neutrinos with multipole moments propagating through magnetic and matter fields. The cross section of the reaction e(-) e(-) yields W(-)(sub k) W(-)(sub n) calculated and its dependence on the mass of the right-handed neutrino and the oscillation angle is investigated. The process e(+) e(-) yields W(+)(sub k) W(-)(sub n) is also included in our analysis. DOE

N95-25470# Sandia National Labs., Albuquerque, NM.
RECENT ADVANCES IN LITHIUM ION TECHNOLOGY
S. C. Levy 1995 7 p Presented at the Portable By Design Conference, Santa Clara, CA, 15-17 Feb. 1995
(Contract DE-AC04-94AL-85000)
(DE95-004769; SAND-94-2763C; CONF-950259-1) Avail: CASI HC A02/MF A01

Lithium ion technology is based on the use of lithium intercalating electrodes. Carbon is the most commonly used anode material, while the cathode materials of choice have been layered lithium metal chalcogenides (LiMX(sub 2)) and lithium spinel-type compounds. Electrolytes may be either organic liquids or polymers. Although the first practical use of graphite intercalation compounds as battery anodes was reported in 1981 for molten salt cells and in 1983 for ambient temperature systems, it was not until Sony Energytech announced a new lithium ion rechargeable cell containing a lithium ion intercalating carbon anode in 1990, that interest peaked. The reason for this heightened interest is that these cells have the high energy density, high voltage and light weight of metallic lithium systems plus a very long cycle life, but without the disadvantages of dendrite formation on charge and the safety considerations associated with metallic lithium. DOE

N95-25474# Melbourne Univ., Parkville (Australia). School of Physics.
STATISTICAL MECHANICS OF RELATIVISTIC SPIN-1 BOSONS IN A MAGNETIC FIELD
J. Daicic and N. E. Frankel 1993 18 p Sponsored by Australian Postgraduate Research Program
(DE95-607100; UM-P-93/65) Avail: CASI HC A03/MF A01 (US Sales Only)

This paper investigates the statistical mechanics of a gas of spin-1 particles with pair creation in a homogeneous magnetic field. It is shown that expansions for the thermodynamic potential and magnetization in fields below the mass scale of the constituent particles are well behaved. However, when the field is at or above the mass scale, an intrinsic pathology of the single-particle energy spectrum manifests itself in the statistical mechanics of the system. Whilst for the spin-0 and spin-1/2 analog of this system there seemed to be no barrier ab initio to the field strength. The nature of the vacuum and the role of interactions were always borne in mind as matters to be considered in a high-order treatment, particularly when the field was at or above the mass scale. In the spin-1 case, the pathology in the single-particle energy spectrum heralds this from the beginning, and seems to be a warning that a single particle non-interacting picture of physics at high energies needs some reconsideration. DOE

N95-25479# Colorado Univ., Denver, CO. Dept. of Mathematics.
FAST ALGORITHMS FOR TRANSPORT MODELS Final Report, 1 Jun. 1993 - 31 May 1994
Tom Manteuffel Dec. 1994 4 p
(Contract DE-FG03-93ER-25165)
(DE95-007064; DOE/ER-25165/T1) Avail: CASI HC A01/MF A01

The focus of this project is the study of multigrid and multilevel algorithms for the numerical solution of Boltzmann models of the transport of neutral and charged particles. In previous work a fast multigrid algorithm was developed for the numerical solution of the Boltzmann model of neutral particle transport in slab geometry assuming isotropic scattering. The new algorithm is extremely fast in the thick diffusion limit; the multigrid v-cycle convergence factor approaches zero as the mean-free-path between collisions approaches zero, independent of the mesh. Also, a fast multilevel method was developed for the numerical solution of the Boltzmann model of charged particle transport in the thick Fokker-Plank limit for slab geometry. Parallel implementations were developed for both algorithms. DOE

N95-25481# Brandeis Univ., Waltham, MA. Dept. of Physics.
RESEARCH IN ELEMENTARY PARTICLE PHYSICS Technical Progress Report, 1 Jun. 1993 - 31 May 1994
James R. Bensinger, Craig A. Blocker, Lawrence E. Kirsch, and Howard J. Schnitzer 1995 32 p
(Contract DE-FG02-92ER-40706)
(DE95-007323; DOE/ER-40706/2) Avail: CASI HC A03/MF A01

The Brandeis experimental particle physics group has for many years pursued an understanding of physical interactions at the highest available energies. To this end they have been active in the development of the Collider Detector at Fermilab (CDF) and in the development of detectors that were planned for the SSC. They have also had an active program of analysis to understand the data and its implications from these detectors. Brandeis remains fully engaged in the understanding of physical interactions at the highest available energies. While pursuing physics analysis, detector support activities and detector upgrades at CDF, they are also exploring the physics potential of the LHC. Pending overall agreements between the Department of Energy and CERN, the authors have joined the ATLAS

experiment at CERN. The expertise gained in planning SSC detectors is directly applicable there. During the past year, the theoretical physics group pursued research in quantum field theory, with the 1/N expansion and other non-perturbative methods providing a unifying theme of much of this work. Activities centered on large N limit in scalar field theories, and two-dimensional Yang-Mills theories. DOE

N95-25484# Los Alamos National Lab., NM.
THE NJOY NUCLEAR DATA PROCESSING SYSTEM: VERSION 91
R. E. MacFarlane and D. W. Muir Oct. 1994 580 p
(Contract W-7405-eng-36)
(DE95-006764; LA-12740-M) Avail: CASI HC A25/MF A06

The NJOY nuclear data processing system is a comprehensive computer code package for producing pointwise and multigroup cross sections and related quantities from elevated nuclear data in the ENDF format, including the latest US library, ENDF/B-VI. The NJOY code can work with neutrons, photons, and charged particles, and it can produce libraries for a wide variety of particle transport and reactor analysis codes. DOE

N95-25493# Joint Inst. for Nuclear Research, Dubna (USSR).
INELASTIC COLLISIONS OF NEGATIVE MUONS AND HADRONS WITH HELIUM METASTABLE ATOMS
G. Ya. Korenman, O. Lkhagva, and Kh. Tsookhuu 1994 15 p Submitted for publication
(DE95-607538; JINR-R-4-94-146) Avail: CASI HC A03/MF A01 (US Sales Only)

We consider inelastic collisions of slow negative muons and hadrons on He(2(sup 1) S, 2(sup 3) S) atoms at velocity upsilon less than 1 a.u. The semiclassical solution of the problem of two- and three-particle close coupled channels is used. Diabatic terms for excited states pass to continuum at the distances R(sub *) approx. 5-10 a.u. which are greater essentially of those for ground state term (approx. 1 a.u.). These distances play the role of inelastic interaction radii. The inelastic cross sections are at least one order of magnitude greater than that for ground state. They depend appreciably on the spin of initial state. Kinetic characteristics of slowing-down and capture of the particles are acutely sensitive to presence of metastable atoms. Slowing-down time in the energy range under study is reduced by factor 2-3 at 100% concentration of metastable atoms. Primary distribution of captured particles on orbits hits to the binding energy region epsilon less than or equal 0.15 a.u. whereas for ordinary He target epsilon less than or equal 0.9 a.u. Circular orbits with principal quantum number up to n = 156 are populated when antiproton is captured by metastable atom. It offers a possibility to study new region of metastable states of hadrons in helium. DOE

N95-25494# Tokyo Univ., Tanashi (Japan). Inst. for Nuclear Study.
A SIMPLE RELATION AMONG THE QUARK MASSES
Hidezumi Terazawa Mar. 1994 12 p
(DE95-703783; INS-1028) Avail: CASI HC A03/MF A01

Based on our recent suggestion that the first and second generations of quarks and leptons can be taken as almost and quasi Nambu-Goldstone fermions, respectively, derived is a simple relation among the quark masses, m(sub u)m(sub s)(sup 3)m(sub t)(sup 2)(approx equal)m(sub d)m(sub c)(sup 3)m(sub b)(sup 2), from which the top quark mass is predicted to be m(sub t) approx.equal (180 +/- 100) - (200 +/- 110)GeV. DOE

N95-25496# Japan Atomic Energy Research Inst., Tokyo (Japan). Dept. of Chemistry and Fuel Research.
MOLECULAR DYNAMICS CALCULATION OF SHEAR VISCOSITY FOR MOLTEN SALT
Yoshihiro Okamoto, Mitsuo Yokokawa, and Toru Ogawa Dec. 1993 35 p In JAPANESE
(DE95-703970; JAERI-M-93-242) Avail: CASI HC A03/MF A01

A computer program of molecular dynamics simulation has been made to calculate shear viscosity of molten salt. Correlation function for an off-diagonal component of stress tensor can be obtained as the results of calculation. Shear viscosity is calculated by integration of the correlation function based on the Kubo-type formula. Shear viscosities for a molten KCl ranging in temperature from 1047 K to 1273 K were calculated using the program. Calculation of 10(exp 5) steps (1 step corresponds to 5 x 10(exp -15)s) was performed for each temperature in the 216 ions system. The obtained results were in good agreement with the reported experimental values. The program has been vectorized to achieve a faster computation in supercomputer. It makes possible to calculate the viscosity using a large number of statistics amounting to several million MD steps. DOE

N95-25497# Japan Atomic Energy Research Inst., Tokyo (Japan). Dept. of Reactor Engineering.
BENCHMARK EXPERIMENT ON A COPPER SLAB ASSEMBLY BOMBARDED BY D-T NEUTRONS
Fujio Maekawa, Yukio Oyama, Chikara Konno, Yujiro Ikeda, Hiroshi Maekawa, and Kazuaki Kosako (Nuclear Energy Data Center, Japan.) Mar. 1994 83 p
(DE95-709764; JAERI-M-94-038) Avail: CASI HC A05/MF A01

Copper is a very important material for fusion reactor because it is used in superconducting magnets or first walls and so on. To verify nuclear data of copper, a benchmark experiment was performed using the D-T neutron source of the FNS facility in Japan Atomic Energy Research Institute. An cylindrical experimental assembly of 629 mm in diameter and 608 mm in thickness made of pure copper was located at 200 mm from the D-T neutron source. In the assembly, the following quantities were measured: (1) neutron spectra in energy regions of MeV and keV, (2) neutron reaction rates, (3) prompt and decay gamma-ray spectra, and (4) gamma-ray heating rates. The obtained experimental data were compiled in this report. DOE

N95-25499# Institute of Nuclear Chemistry and Technology, Warsaw (Poland).
ELECTRON SPIN RESONANCE OF RADICALS AND METAL COMPLEXES
1993 55 p Presented at the 1st International Conference of the Polish ESR Group, Zakopane, Poland, 31 May - 4 Jun. 1993; sponsored by State Committee for Scientific Research, National Atomic Energy Agency, Polish Academy of Sciences, The British Council, Bruke
(DE95-605640; INIS-MF-14387; CONF-9305384) Avail: CASI HC A04/MF A01

The materials are a collection of extended synopsis of papers presented at the conference sessions. The broad area of magnetic technique applications has been described as well as their spectra interpretation methods. The ESR, NMR, ENDOR, and spin echo were applied for studying the radiation and UV induced radicals in chemical and biological systems. Also in the study of complexes of metallic ions (having the paramagnetic properties) and their interaction with the matrix, the magnetic techniques have been commonly used. They are also very convenient tool for the study of reaction kinetics and mechanism as well as interaction of paramagnetic species with themselves and crystal lattice or with the surface as for the catalytic processes. DOE

N95-25537 Joint Inst. for Nuclear Research, Dubna (USSR). Lab. of Theoretical Physics.
MULTICHANNEL RESONANCES AND CLOSED CHANNELS (SCALAR SECTOR)
D. Krupa, V. A. Meshcheryakov, and Yu. S. Surovtsev 1993 12 p
(DE94-628629; JINR-E-2-93-461) Copyright Avail: Issuing Activity (Department of Energy (DOE)) (US Sales Only)

The problem of multichannel resonances is discussed in the 2 and 3-channel approaches on the basis of analyticity and unitarity. A model-independent pole representation of multichannel resonances is obtained as a realization of the idea of dominance of the nearest singularities on all corresponding sheets of the Riemann surface of the S-matrix. The role of closed channels in forming the resonances is irvestigated in both the K and S-matrix approaches. The method is illustrated for coupled processes (pi)(pi) (approaches) (pi)(pi), K bar K, (eta)(eta) in the isoscalar s-wave (with the (chi)(exp 2) analysis of experimental data on (pi)(pi) scattering in the energy region below 1.6 GeV). DOE

N95-25538 Joint Inst. for Nuclear Research, Dubna (USSR). Lab. of Neclear Reactions.
STUDY OF PROPERTIES OF Ne - Al NEUTRON RICH ISOTOPES AT AND NEAR N = 20 MAGIC SHELL USING ELASTIC SCATTERING IN INVERSE KINEMATICS
A. G. Artyukh, S. N. Ershov, and F. A. Gareev 1993 12 p
(DE94-628655; JINR-E-7-93-74) Copyright Avail: Issuing Activity (Department of Energy (DOE)) (US Sales Only)

The problem of the existence of the ground-state deformation for

neutron-rich nuclei near closed shell N = 20 for Na element has been discussed. For experimental study of the evolution of the nuclear shapes of these nuclides versus increase of neutron excess, we propose using a three-dimensional tracking detector multiplicity (time-projection chamber) in the regime of detector-target-detector. The analysis of the elastic scattering of Na nuclei in the inverse kinematics has been given. Estimation of the effect of elastic scattering of Na nuclei, which is expected to have a low intensity, has been presented. DOE

N95-25554 Academy of Sciences of the Ukraine, Kiev (Ukraine). Inst. Teoreticheskoj Fiziki.
PHYSICS IN UKRAINE INTERNATIONAL CONFERENCE. VOLUME 1: PHYSICS OF ELEMENTARY PARTICLES AND QUANTUM FIELD THEORY. GENERAL PROBLEMS
A. Sitenko, ed. 1993 192 p Conference held in Kiev, Ukraine, 22-27 Jun. 1993
(DE95-606413; INIS-UA-004-Vol-1; CONF-9306388) Copyright Avail: Issuing Activity (Department of Energy (DOE)) (US Sales Only)

Problems of modern physics and the situation with physical research in Ukraine are considered. Program of the conference includes scientific and general problems. Its proceedings are published in six volumes. The papers presented in this volume refer to elementary particle physics and quantum field theory. The main attention is paid to the following problems: development of science in Ukraine and its role in the state structures; modern state of scientific research in Ukraine; education and training of specialists; history of Ukrainian physics and contribution of Ukrainian scientists in the world science; and problems of the Ukrainian scientific terminology. DOE

N95-25563# Fermi National Accelerator Lab., Batavia, IL.
ELECTROWEAK BOSON PAIR PRODUCTION AT THE TEVATRON
Steven M. Errede (Illinois Univ., Urbana-Champaign, IL.) Sep. 1994 7 p Presented at the 27th International Conference on High Energy Physics, Glasgow, Scotland, 20-27 Jul.1994
(Contracts DE-AC02-76CH-03000; DE-FG02-91ER-40677)
(DE95-004234; FNAL/C-94/306-E; CONF-940722-35) Avail: CASI HC A02/MF A01

Preliminary results from CDF and D(O) on W(gamma), Z(gamma) and WW, WZ, ZZ boson pair production in (radical)s = 1.8 TeV (anti p)-p collisions from the 1992-93 collider run are presented. Direct limits on CP-conserving and CP-violating WW(gamma), WWZ, ZZ(gamma) and Z(gamma)(gamma) anomalous couplings have been obtained. The results are consistent with Standard Model expectations. In the static limit, the direct experimental limits on WW(gamma) and ZZ(gamma) anomalous couplings are related to bounds on the higher-order static (transition) EM moments of the W(Z) bosons. Expectations from the on-going and future Tevatron collider runs are discussed. DOE

N95-25567 Rutherford Appleton Lab., Oxford (England).
FURTHER WAYS TO DISTINGUISH SINGLE-LEPTON TOP QUARK SIGNALS FROM BACKGROUND AT THE TEVATRON
V. Barger, E. Mirkes, J. Ohnemus, and R. J. N. Phillips Sep. 1994 13 p Prepared in cooperation with Wisconsin Univ., Madison, WI; California Univ., Davis, CA; and DOE, Washington, DC
(Contract DE-AC02-76ER-00881)
(PB95-165395; RAL-94-099) Avail: Issuing Activity (National Technical Information Service (NTIS))

Further kinematical variables are suggested, in which to compare the putative leptonic W plus 4-jet top quark signal with the QCD background. The authors show that the lepton rapidity asymmetry, the p(sub T)-ranking of the tagged b-jet, the double-tag probability, the reconstructed t+t(bar) invariant mass, and the lepton energy in the parent top quark restframe, all display interesting differences between signal and background. NTIS

N95-25614# Japan Atomic Industrial Forum, Inc. (Japan).
PROCEEDINGS OF THE 21ST JAPAN CONFERENCE ON RADIATION AND RADIOISOTOPES
1994 596 p In JAPANESE and ENGLISH Conference held in Tokyo, Japan, 2-4 Feb. 1994 Prepared in cooperation with Japan Radioisotope Association, Inc., Tokyo, Japan, and Japan Atomic Energy Research Inst., Tokyo, Japan
(DE94-785275; INIS-JP-024; CONF-940268) Avail: CASI HC A25/MF A06

This publication is the collection of papers presented at the title conference. The 54 presented papers are indexed individually. DOE

N95-25619 Rutherford Appleton Lab., Chilton (England).
PARTON DISTRIBUTIONS FOR LOW Q2
A. D. Martin, W. J. Stirling, and R. G. Roberts Sep. 1994 24 p Prepared in cooperation with Durham Univ., England
(PB95-165213; RAL-94-104) Avail: Issuing Activity (National Technical Information Service (NTIS))

The authors extend the MRS(A) set of parton distributions, which provides an up-to-date description of the structure of the proton probed by hard interactions, into the region of Q(sup 2) below 5 GeV(sup 2). After physically-motivated modifications, the authors obtain a smooth description of the data on the structure function F(sub 2)(x, Q(sup 2)) all the way from Q(sup 2) = 0.1 to 1000 GeV(sup 2). NTIS

N95-25620 Rutherford Appleton Lab., Chilton (England).
DIAGRAMMATIC MANY-BODY PERTURBATION EXPANSION FOR ATOMS AND MOLECULES
J. Lyons, D. Moncrieff, and S. Wilson Oct. 1994 208 p Prepared in cooperation with Florida State Univ., Tallahassee, FL
(Contract DE-FC05-85ER-25000)
(PB95-165221; RAL-94-108) Avail: Issuing Activity (National Technical Information Service (NTIS))

A complete list of connectivity matrices for the fifth-order Hugenholtz energy diagrams for a closed shell system described in zero-order by a single determinant constructed from canonical Hartree-Fock orbitals has been automatically generated. From these matrices, the Hugenholtz diagrams have been automatically drawn and the corresponding algebraic expressions printed. NTIS

N95-25624 Rutherford Appleton Lab., Oxford (England).
MuSR USER GUIDE
S. H. Kilcoyne, S. R. Brown, S. P. Cottrell, S. D. Johnston, and C. A. Scott Oct. 1994 29 p
(PB95-165304; RAL-94-109) Avail: Issuing Activity (National Technical Information Service (NTIS))

Contents include: Layout of ISIS muon facility; Setting up--Instrument geometry, Sample environment, Magnetic fields, Selecting the beam size, Setting the steering magnet, Photomultiplier tubes; Sample environment control, data collection--(mu)SR control system, Writing a command file to control the experiment; Computing--General information, Data files, Printers; Troubleshooting--No muons, Computer problems, Temperature control and MTEMP, Double pulse-failure of the electrostatic kicker; Telephone numbers; Appendix 1--The (mu)SR data analysis program-UDA; Appendix 2--Rotating MuSR; MuSR mini guide. NTIS

N95-25626 Rutherford Appleton Lab., Oxford (England).
HEAVY-NEUTRINO EFFECTS ON TAU-LEPTON DECAYS
A. Pilaftsis Nov. 1994 16 p
(PB95-165346; RAL-94-113) Avail: Issuing Activity (National Technical Information Service (NTIS))

Minimal extensions of the Standard Model that are motivated by grand unified theories or superstring models with an E(6) symmetry can naturally predict heavy neutrinos of a Dirac or Majorana nature. Such heavy neutral leptons violate the decoupling theorem at the one-loop electroweak order and hence offer a unique chance for possible lepton-flavor decays of the tau lepton, e.g. tau to eee or tau to (mu)(mu)(mu), to be seen in LEP experiments. We analyze such decays in models with three and four generations. NTIS

N95-25668# Joint Inst. for Nuclear Research, Dubna (USSR). Lab. of Theoretical Physics.
INELASTIC COLLISIONS OF NEGATIVE MUONS AND HADRONS WITH METASTABLE HYDROGEN ATOMS
G. Ya. Korenman, O. Lkhagva, Kh. Tsookhuu, and R. Badamdamdin 1994 15 p In RUSSIAN Submitted for publication
(DE95-607537; JINR-R-4-94-143) Avail: CASI HC A03/MF A01 (US Sales Only)

We consider inelastic collisions of slow negative muons and hadrons

on a hydrogen atom in metastable 2 s-state. The calculations were using both diabatic and adiabatic bases. It is shown that both approaches reproduce similar qualitative peculiarities of ionization and Coulomb capture for collisions between M(sup -) particle and metastable atom. Ionization and Coulomb capture cross sections exceed the corresponding values for ground state by more than one order of magnitude. Slowing-down and capture kinetic characteristics also depend on the presence of metastable atoms essentially. DOE

N95-25669# Tokyo Univ., Tanashi (Japan). Inst. for Nuclear Study.
ON ANALYSIS OF RESONANCE NEUTRON DEPOLARIZATION IN UNIAXIAL MEDIA
E. I. Sharapov Feb. 1994 11 p Sponsored by Ministry of Education, Science and Culture of Japan
(DE95-703782; INS-1027) Avail: CASI HC A03/MF A01

Quantum mechanical general formalism of the neutron depolarization in a magnetically anisotropic media is reviewed and is applied to the analysis of recent TRIPLE data on holmium single crystal prepared for the test of time-reversal-invariance. Information on magnetic domain parameters is obtained for this sample. DOE

N95-25768# Stanford Univ., CA. Stanford Linear Accelerator Center.
ELECTROWEAK COUPLING MEASUREMENTS FROM POLARIZED BHABHA SCATTERING AT THE Z(EXP 0) RESONANCE Ph.D. Thesis - Univ. of Oregon
Kevin T. Pitts Mar. 1994 172 p
(Contracts DE-AC03-76SF-00515; DE-FG06-85ER-40224)
(DE95-006090; SU-SLAC-446; UC-414) Avail: CASI HC A08/MF A02

The cross section for Bhabha scattering (e(+)e(-) yields e(+)e(-)) with polarized electrons at the center of mass energy of the Z(exp 0) resonance has been measured with the SLD experiment at the Stanford Linear Accelerator Center during the 1992 and 1993 runs. The electroweak couplings of the electron are extracted. At small angles the measurement is done in the SLD Silicon/Tungsten Luminosity Monitor (LMSAT). A detailed description of the design, construction, commissioning and operation of the LMSAT is provided. The integrated luminosity for 1992 is measured to be L = 420.86 +/- 2.56 (stat) +/- 4.23 (sys) nb(exp -1). The luminosity asymmetry for polarized beams is measured to be A(sub LR)(LUM) = (1.7 +/- 6.4) x 10(exp -3). The large angle polarized Bhabha scattering reveals the effective electron vector and axial vector couplings to the Z(exp 0) through the measurement of the Z(exp 0) yields e(+)e(-) partial width, Gamma(sub ee), and the parity violation parameter, A(sub e). From the combined 1992 and 1993 data the effective electron vector and axial vector couplings are measured to be bar g(sub v)(exp e) = -0.0495 +/- 0.0096 +/- 0.0030, and bar g(sub (alpha)(exp e) = -0.4977 +/- 0.0035 +/- 0.0064 respectively. The effective weak mixing angle is measured to be sin(exp 2)theta(sub W)(exp eff) = 0.2251 +/- 0.0049 +/- 0.0015. These results are compared with other experiments. DOE

N95-25778# Joint Inst. for Nuclear Research, Dubna (USSR).
DYNAMICS OF NONADIABATIC CHARGED PARTICLES IN THE MAGNETIC DIPOLE FIELD WITH IMPOSED HOMOGENEOUS MAGNETIC FIELD
I. V. Amirkhanov, E. P. Zhidkov, Yu. G. Dzyuba (Moscow State Univ., Russia.), A. N. Ilina (Moscow State Univ., Russia.), and V. D. Ilin (Moscow State Univ., Russia.) 1994 34 p
(DE95-605222; JINR-R-10-94-105) Avail: CASI HC A03/MF A01 (US Sales Only)

The model of charged particles motion in the summary dipole and external uniform, parallel to dipole, field is considered. External field associates with the effect of magnetic perturbation. Such problem appears, for example, for protons in geomagnetic field during the magnetic storm. In contrast to traditional model, not the line of force, but the so-called Central Trajectory (CT-trajectory which passes through the dipole centre) is used as the leading centre's trajectory. It allows to save the basic ideas of adiabatic theory for the nonadiabatic case in modified form. CT was constructed with the help of numerical experiments and its characteristics are described. DOE

N95-25784# Joint Inst. for Nuclear Research, Dubna (USSR).
EXISTENCE DOMAINS AND SOME PROPERTIES OF A PARTICLE BOUND STATE IN FIELDS WITH HOMOGENEOUS DEPENDENCE OF ITS POTENTIAL ENERGY ON COORDINATES
I. M. Matora 1994 10 p
(DE95-605280; JINR-R-4-94-115) Avail: CASI HC A02/MF A01 (US Sales Only)

The nonrelativistic bound state problem for a particle embedded in the field, being a homogeneous function of the spatial coordinates, is investigated. On the basis of the Virial theorem general properties of the total energy eigenvalue spectra and the corresponding expectation values of the kinetic and potential energy operators are derived. The analytical solution of the nonrelativistic Schroedinger equation is obtained and the wave functions of bound states for the known problem 'fall on centre' are determined. DOE

N95-25896# Washington Univ., Seattle, WA.
THE OFF-SHELL AXIAL ANOMALY VIA THE (GAMMA)*(PI)(SUP 0) (YIELDS) (GAMMA) TRANSITION
M. R. Frank, K. L. Mitchell (Kent State Univ., OH.), P. C. Tandy (Kent State Univ., OH.), and C. D. Roberts (Argonne National Lab., IL.) 1995 10 p
(Contracts DE-FG06-90ER-40561; W-31-109-eng-38)
(DE95-004762; DOE/ER-40561/172) Avail: CASI HC A02/MF A01

The (gamma)*(pi)(sup 0) (yields) (gamma) form factor, including the extension off the pion mass-shell, is obtained from a generalized impulse approximation within a QCD-based model field theory known to provide an excellent description of the pion charge form factor. This approach implements dressing of the vertex functions and propagators consistent with dynamical chiral symmetry breaking, gauge invariance, quark confinement and perturbative QCD. Soft nonperturbative behavior, dictated by the axial anomaly, is found to evolve to the perturbative QCD limit only for Q(sup 2) greater than or equal to 20 GeV(sup 2). DOE

N95-25900 Rutherford Appleton Lab., Oxford (England).
HET MINI-MANUAL
R. S. Eccleston and R. Osborn Nov. 1994 35 p
(PB95-165338; RAL-94-117) Avail: Issuing Activity (National Technical Information Service (NTIS))

Inelastic neutron scattering may be successfully performed on a pulsed source using direct geometry or chopper spectrometers. One may use the chopper spectrometer HET, in which a single incoming energy is selected, and the final energy and momentum transfer is analyzed by time-of-flight and detector angle. The document is designed to get one started planning an experiment and analyzing the data. Chapter headings include the following: (1) An Introduction to HET; (2) Controlling the Instrument; (3) Sample Environment Equipment; (4) Data Analysis and Visualization; (5) Summaries; (6) Heat Instrument Parameters; and (7) HET Detector Angles. NTIS

N95-25901# Kyoto Univ., Uji (Japan).
QUASI TWO BODY DECAYS OF CHARM MESONS
K. Terasaki Apr. 1994 19 p
(DE94-792634; YITP/U-94-10) Avail: CASI HC A03/MF A01

Quasi two body decays of charm mesons are studied by using a hard meson approximation in which the amplitude M is approximated by M(approximately equal)M(sub ETC)+M(sub S). The surface term M(sub S) is given by a sum of all the possible pole amplitudes involving contributions of four-quark and hybrid mesons in addition to ground-state (QQ-bar)(sub 0) mesons to the intermediate states. Contributions of multi-hadron intermediate states are taken in the form of M(sub ETC). In the annihilation type of decays, hybrid mesons play an important role. The spectator type of decays can have significant contributions of four-quark mesons. The mixed type of decays are a little complicated since they can have all the contributions of possible hybrid and four-quark mesons in addition to the ground-state (QQ-bar)(sub 0). The calculated branching ratios, (beta)D(+)(yields)K-bar(sup 0)(rho)(+) and (beta)D(sup 0)(yields)K(-)(rho)(+), are of ordinary size in contrast with the factorization which predicts very large rates for these decays. The predicted (beta)(D(sub s)(+)(yields)(pi)(+)(omega)) is very small. The D(sub s)(+)(yields)(pi)(+)(rho)(sup 0) decay can be suppressed in consistency with the other decays. DOE

N95-25905# Joint Inst. for Nuclear Research, Dubna (USSR).
THE TRACK SYSTEM OF THE MODERNIZED HYPERON SPECTROMETER
A. G. Volodko, Yu. I. Davydov (Tbilisi State Univ., USSR.), and D. G. Dzhincharadze 1994 11 p
(DE95-604003; JINR-R-13-94-114) Avail: CASI HC A03/MF A01 (US Sales Only)

The description of the multiwire proportional chambers of the 'Hyperon' facility aimed at research of the rare kaon decays is presented. The setup includes 39 multiwire chambers with areas from 128-128 sq mm up to 90-130 sq cm which contain about 9500 channels. Two magnetic spectrometers based on these multiwire chambers provide the momentum resolution 0.5% and 1.1% consequently at momentum 10 GeV/c. DOE

N95-25908# Joint Inst. for Nuclear Research, Dubna (USSR).
MASS SPLITTING OF THE PSEUDOSCALAR AND VECTOR MESONS INDUCED BY THE HOMOGENEOUS VACUUM GLUON FIELD
Ya. V. Burdanov, S. A. Solunin, G. V. Efimov, and S. N. Nedelko 1994 16 p
(DE95-605322; JINR-E-2-94-88) Avail: CASI HC A03/MF A01 (US Sales Only)

Masses of the pseudoscalar and vector mesons are calculated within the generalized Nambu-Jona-Lasinio model taking into account homogeneous vacuum gluon field. This vacuum provides an analytical quark confinement. Colorless modes are determined by the confined gluons and are described by the nonlocal quark currents with appropriate radial and angular quantum numbers. An interaction of the quark spin with the vacuum gluon field arises naturally within the model under consideration. It is shown that this spin-field interaction leads to mass splitting between vector and pseudoscalar mesons with identical quark structure ((rho) - (pi), K-K(sup *) and so on). In contrast to the standard NJL model, this allows to use the four-fermion coupling constant being common for both nonets. DOE

N95-25909# Joint Inst. for Nuclear Research, Dubna (USSR).
EXCITED STATES OF MESONS WITHIN THE NJL MODEL WITH THE HOMOGENEOUS VACUUM GLUON FIELD
Ya. V. Burdanov, S. A. Solunin, G. V. Efimov, and S. N. Nedelko 1994 15 p
(DE95-605323; JINR-E-2-94-89) Avail: CASI HC A03/MF A01 (US Sales Only)

Excited states of mesons are considered within generalization of the Nambu-Jona(sub L)asinio model taking into account the (anti)self-dual homogeneous background gluon field. This vacuum configuration ensures an analytical quark confinement. Colorless models are determined by the confined gluons and are described by the nonlocal quark currents with appropriate radial and orbital quantum numbers. The effective meson Lagrangian corresponds to ultraviolet finite theory. Spectrum of radial and orbital meson excitations predicted by the model is asymptotically equidistant, i.e., it has the Regge behavior. For real values of the orbital momentum it describes experimental data quantitatively. DOE

N95-25910# Joint Inst. for Nuclear Research, Dubna (USSR).
VACUUM POLARIZATION EFFECTS IN LOW-ENERGY MUONIC ATOM COLLISIONS
V. S. Melezhik 1994 11 p
(DE95-605393; JINR-E-4-94-141) Avail: CASI HC A03/MF A01 (US Sales Only)

We estimate the vacuum polarization (V P) correction to the Coulomb interaction in collisions of muonic atoms. It is shown that the V P effect, amplified by the low-lying virtual state (epsilon)(sub (epsilon)) (approximately) 10 eV, is of the order (approximately) 1-2% in the S-wave cross sections for p(mu) + p collisions as (epsilon)less than or equal to (epsilon)(sub (upsilon)). The V P amplitude becomes comparable to the anomalously small pure Coulomb amplitude for the singlet t(mu) + t scattering as (epsilon) approaches 0 and near the Ramsauer-Townsend minima in the d(mu) + p and t(mu) + p scattering. DOE

N95-25911*# San Francisco Univ., CA. Dept. of Physics.
HIGH LET, PASSIVE SPACE RADIATION DOSIMETRY AND SPECTROMETRY Final Report
E. V. Benton, A. L. Frank, E. R. Benton, R. P. Keegan, L. A. Frigo, D. Sanner, and V. Rowe Mar. 1995 356 p
(Grant NAG9-235)
(NASA-CR-197694; NAS 1.26:197694; USF-TR-82) Copyright Avail: CASI HC A16/MF A03

The development of high linear energy transfer (LET), passive radiation dosimetry and spectrometry is needed for the purpose of accurate determination of equivalent doses and assessment of health risks to astronauts on long duration missions. Progress in the following research areas is summerized: intercomparisons of cosmic ray equivalent dose and LET spectra measurements between STS missions and between astronauts; increases LET spectra measurement accuracy with ATAS; space radiation measurements for intercomparisons of passive (PNTD, TLD, TRND, Emulsion) and active (TEPC, RME-111) dosimeters; interaction of cosmic ray particles with nuclei in matter; radiation measurements after long duration space exposures; ground based dosimeter calibrations; neutron detector calibrations; radiation measurements on Soviet/Russian spacecraft; space radiation measurements under thin shielding; and space radiation. For individual titles, see N95-25912 through N95-25934.

N95-25912*# San Francisco Univ., CA.
LET SPECTRA MEASUREMENTS FROM THE STS-35 CPDs
In its High LET, Passive Space Radiation Dosimetry and Spectrometry Mar. 1995 6 p (For primary document see N95-25911 08-72)
Avail: CASI HC A02/MF A03

Linear energy transfer (LET) spectra derived form automated track analysis system (ATAS) track parameter measurements for crew passive dosimeters (CPD's) flown with the astronauts on STS-35 are plotted. The spread between the seven individual spectra is typical of past manual measurements of sets of CPD's. This difference is probably due to the cumulative net shielding variations experienced by the CPD's as the astronauts carrying them went about their activities on the Space Shuttle. The STS-35 mission was launched on Dec. 2, 1990, at 28.5 degrees inclination and 352-km altitude. This is somewhat higher than the nominal 300-km flights and the orbit intersects more of the high intensity trapped proton region in the South Atlantic Anomaly (SAA). However, in comparison with APD spectra measured on earlier lower altitude missions (STS-26, -29, -30, -32), the flux spectra are all roughly comparable. This may be due to the fact that the STS-35 mission took place close to solar maximum (Feb. 1990), or perhaps to shielding differences. The corresponding dose and dose equivalent spectra for this mission are shown. The effect of statistical fluctuations at the higher LET values, where track densities are small, is very noticeable. This results in an increased spread within the dose rate and dose equivalent rate spectra, as compared to the flux spectra. The contribution to dose and dose equivalent per measured track is much greater in the high LET region and the differences, though numerically small, are heavily weighted in the integral spectra. The optimum measurement and characterization of the high LET tails of the spectra represent an important part of the research into plastic nuclear track detector (PNTD) response. The integral flux, dose rate, dose equivalent rate and mission dose equivalent for the seven astronauts are also given.
Derived from text

N95-25913*# San Francisco Univ., CA.
SUMMARY OF LET SPECTRA AND DOSE MEASUREMENTS ON TEN STS MISSIONS
In its High LET, Passive Space Radiation Dosimetry and Spectrometry Mar. 1995 22 p (For primary document see N95-25911 08-72)
Avail: CASI HC A03/MF A03

A comparison of linear energy transfer (LET) spectra measurements made with plastic nuclear track detectors (PNTD's) from area passive dosimeters (APD's), was made for ten different STS missions under similar shielding. The results show that integral flux, dose rate and equivalent dose rate values follow a general increase with respect to increasing orbital inclination and altitude but that there are large variations from a simple relationship. This is to be expected since it has been shown that Shuttle attitude variations, combined with the anisotropic particle flux at the South Atlantic Anomaly (SAA), can result in differences of a factor of 2 in dose rate inside the Shuttle (Badhwar et al., 1995). Solar cycle and shielding differences also result in variations in radiation dose between STS missions. Spaceflight dosimeters from the STS missions are also being used in the development of a method for increasing LET spectra measurement accuracy by extending LET measurements to particle tracks of ranges 10-80 microns. Refinements in processing and measurement

techniques for the flight PNTD's have yielded increased detection efficiencies for the short tracks when LET spectra determined by using the standard and refined methods were intercompared. Derived from text

N95-25914*# National Aeronautics and Space Administration. Lyndon B. Johnson Space Center, Houston, TX.
A STUDY OF THE RADIATION ENVIRONMENT ON BOARD THE SPACE SHUTTLE FLIGHT STS-57
G. D. Badhwar, W. Atwell (Rockwell Space Operations Co., Houston, TX.), E. V. Benton (San Francisco Univ., CA.), A. L. Frank (San Francisco Univ., CA.), R. P. Keegan (San Francisco Univ., CA.), V. E. Dudkin (Research Center of Space Craft Radiation Safety, Moscow, Russia.), O. N. Karpov (Research Center of Space Craft Radiation Safety, Moscow, Russia.), V. Potapov (Research Center of Space Craft Radiation Safety, Moscow, Russia.), A. B. Akopova (Research Center of Space Craft Radiation Safety, Moscow, Russia.), and N. V. Magradze (Academy of Sciences of the Armenian SSR, Erivan, Armenia.) et al *In* San Francisco Univ., High LET, Passive Space Radiation Dosimetry and Spectrometry Mar. 1995 24 p (For primary document see N95-25911 08-72)
Avail: CASI HC A03/MF A03

A joint NASA-Russian study of the radiation environment inside a SPACEHAB 2 locker on space shuttle flight STS-57 was conducted. The shuttle flew in a nearly circular orbit of 28.5 deg inclination and 462 km altitude. The locker carried a charged particle spectrometer, a tissue equivalent proportional counter (TEPC), and two area passive detectors consisting of combined NASA plastic nuclear track detectors (PNTD's) and thermoluminescent detectors (TLD's), and Russian nuclear emulsions, PNTD's, and TLD's. All the detector systems were shielded by the same shuttle mass distribution. This makes possible a direct comparison of the various dose measurement techniques. In addition, measurements of the neutron energy spectrum were made using the proton recoil technique. The results show good agreement between the integral LET spectrum of the combined galactic and trapped particles using the tissue equivalent proportional counter and track detectors between about 15 keV/micron and 200 keV/micron. The LET spectrum determined from nuclear emulsions was systematically lower by about 50%, possibly due to emulsion fading. The results show that the TEPC measured an absorbed dose 20% higher than TLD's, due primarily to an increased TEPC response to neutrons and a low sensitivity of TLD's to high LET particles under normal processing techniques. There is a significant flux of high energy neutrons that is currently not taken into consideration in dose equivalent calculations. The results of the analysis of the spectrometer data will be reported separately. Author

N95-25915*# San Francisco Univ., CA.
USF/RUSSIAN DOSIMETRY ON STS-57
In its High LET, Passive Space Radiation Dosimetry and Spectrometry Mar. 1995 14 p (For primary document see N95-25911 08-72)
Avail: CASI HC A03/MF A03

The major purpose of this experiment was to conduct an international comparison of passive dosimetry methods in space. Two APD's were flown in the charged particle directional spectrometer (CPDS)/tissue equivalent proportional counter (TEPC) locker on the space shuttle during the STS-57 mission. Due to placement, the shielding and radiation environment of the APD's were nearly the same and the dosimeters distributed in the two boxes can be considered equally exposed. The dosimeter types included plastic nuclear track detectors (PNTD's), thermoluminescent detectors (TLD), nuclear emulsions, and thermal/resonance neutron detectors (TRND's). The USF dosimeters included PNTD's, TLD's, and TRND's, while the Russian dosimeters included PNTD's, TLD's, and nuclear emulsions.
Derived from text

N95-25916*# San Francisco Univ., CA.
DOSIMETRY ON STS-42 WITH THE RME APD
In its High LET, Passive Space Radiation Dosimetry and Spectrometry Mar. 1995 4 p (For primary document see N95-25911 08-72)
Avail: CASI HC A01/MF A03

Beginning with the STS-42 mission, this laboratory began participating in instrument comparison studies in which space radiation was measured contiguously by passive and active methods. The active instrument was the RME-3 microdosimeter. This instrument measures four-channel LET spectra and employs a tissue-equivalent proportional counter. It is sensitive to the full LET range of ionizing radiation present. Our area passive dosimeter, the RME APD, contained arrays of plastic nuclear track detectors (PNTD's) and thermoluminescent detectors (TLD's). The PNTD's measure LET spectra, while the TLD's measure total absorbed dose. The object of this experiment is to compare the active and passive measurements on the basis of LET spectra, total absorbed dose, and dose equivalent. The STS-42 mission was launched on January 22, 1992, with a flight duration of 8.052 days. The orbit had an inclination of 57 deg and an altitude of 302 km. The shuttle in this orbit is expected to encounter radiation levels dominated by galactic cosmic rays (GCR's) with a lesser contribution from trapped protons in the lower region of the South Atlantic Anomaly (SAA).
Derived from text

N95-25917*# San Francisco Univ., CA.
MULTIPLICITIES OF SECONDARIES IN INTERACTIONS OF 1.8 GeV/NUCLEON Fe-56 NUCLEI WITH PHOTOEMULSION AND THE CASCADE EVAPORATION MODEL
V. E Dudkin (Institute of Biomedical Problems, Moscow, USSR.), E. E. Kovalev (Institute of Biomedical Problems, Moscow, USSR.), N. A. Nefedov (Institute of Biomedical Problems, Moscow, USSR.), V. A. Antonchik (Leningrad State Univ., USSR.), S. D. Bogdanov (Leningrad State Univ., USSR.), V. I. Ostroumov (Leningrad State Univ., USSR.), H. J. Crawford (California Univ., Berkeley, CA.), and E. V. Benton *In its* High LET, Passive Space Radiation Dosimetry and Spectrometry Mar. 1995 18 p (For primary document see N95-25911 08-72)
Avail: CASI HC A03/MF A03

A nuclear photographic emulsion method was used to study the charge-state, ionization, and angular characteristics of secondaries produced in inelastic interactions of Fe-56 nuclei at 1.8 GeV/nucleon with H, CNO, and AgBr nuclei. The data obtained are compared with the results of calculations made in terms of the Dubna version of the cascade evaporation model (DCM). The DCM has been shown to satisfactorily describe most of the interaction characteristics for two nuclei in the studied reactions. At the same time, quantitative differences are observed in some cases.
Author

N95-25918*# San Francisco Univ., CA.
TARGET FRAGMENTS IN COLLISIONS OF 1.8 GeV/NUCLEON Fe-56 NUCLEI WITH PHOTOEMULSION NUCLEI, AND THE CASCADE-EVAPORATION MODEL
V. E. Dudkin (Institute of Biomedical Problems, Moscow, USSR.), E. E. Kovalev (Institute of Biomedical Problems, Moscow, USSR.), N. A. Nefedov (Institute of Biomedical Problems, Moscow, USSR.), V. A. Antonchik (Leningrad State Univ., USSR.), S. D. Bogdanov (Leningrad State Univ., USSR.), V. I. Ostroumov (Leningrad State Univ., USSR.), E. V. Benton, and H. J. Crawford (California Univ., Berkeley, CA.) *In its* High LET, Passive Space Radiation Dosimetry and Spectrometry Mar. 1995 12 p (For primary document see N95-25911 08-72)
Avail: CASI HC A03/MF A03

Nuclear photographic emulsion is used to study the dependence of the characteristics of target-nucleus fragments on the masses and impact parameters of interacting nuclei. The data obtained are compared in all details with the calculation results made in terms of the Dubna version of the cascade-evaporation model (DCM). Author

N95-25919*# San Francisco Univ., CA.
DEPENDENCE OF THE MULTIPLICITIES OF SECONDARY PARTICLES ON THE IMPACT PARAMETER IN COLLISIONS OF HIGH-ENERGY NEON AND IRON NUCLEI WITH PHOTOEMULSION NUCLEI
V. E. Dudkin (Research Center of Space Craft Radiation Safety, Moscow, Russia.), E. E. Kovalev (Research Center of Space Craft Radiation Safety, Moscow, Russia.), N. A. Nefedov (Research Center of Space Craft Radiation Safety, Moscow, Russia.), V. A. Antonchik (Saint Petersburg State Univ., Saint Petersburg, Russia.), S. D. Bogdanov (Saint Petersburg State Univ., Saint Petersburg, Russia.), V. F. Kosmach (Saint Petersburg State Univ., Saint Petersburg, Russia.), A. Yu. Likhachev (Saint Petersburg State Univ., Saint Petersburg, Russia.), E. V. Benton, and H. J. Crawford (California Univ., Berkeley, CA.) *In its* High LET, Passive Space Radiation Dosimetry and Spectrometry Mar. 1995 12 p (For primary document see N95-25911 08-72)
Avail: CASI HC A03/MF A03

A method is proposed for finding the dependence of mean multiplicities

of secondaries on the nucleus-collision impact parameter from the data on the total interaction ensemble. The impact parameter has been shown to completely define the mean characteristics of an individual interaction event. A difference has been found between experimental results and the data calculated in terms of the cascade-evaporation model at impact-parameter values below 3 fm. Author

N95-25920*# San Francisco Univ., CA.
MULTIPLICITIES OF SECONDARIES IN NUCLEAR INTERACTIONS, INDUCED BY Ne-20, Ar-40 AND Fe-56 NUCLEI AT 0.1-0.5 GeV/NUCLEON

V. E. Dudkin (Research Center of Space Craft Radiation Safety, Moscow, Russia.), E. E. Kovalev (Research Center of Space Craft Radiation Safety, Moscow, Russia.), N. A. Nefedov (Research Center of Space Craft Radiation Safety, Moscow, Russia.), V. A. Antonchik (Saint Petersburg State Univ., Saint Petersburg, Russia.), S. D. Bogdanov (Saint Petersburg State Univ., Saint Petersburg, Russia.), V. F. Kosmach (Saint Petersburg State Univ., Saint Petersburg, Russia.), A. Yu. Likhachev (Saint Petersburg State Univ., Saint Petersburg, Russia.), J. Hasan (Saint Petersburg State Univ., Saint Petersburg, Russia.), E. V. Benton, and H. J. Crawford (California Univ., Berkeley, CA.) *In its* High LET, Passive Space Radiation Dosimetry and Spectrometry Mar. 1995 12 p (For primary document see N95-25911 08-72)

Avail: CASI HC A03/MF A03

Multiplicities of various species of charged secondaries produced in inelastic interactions of Ne-20, Ar-40, and Fe-56 nuclei with emulsion nuclei, at 0.1-0.5 GeV/nucleon have been measured. The data obtained are compared with the results for interactions of higher energy nuclei with emulsion nuclei. The dependences of the nucleus-nucleus interaction parameters on masses and energies of colliding nuclei are examined. Author

N95-25921*# San Francisco Univ., CA.
FRAGMENTATION CROSS SECTIONS OF O-16 BETWEEN 0.9 AND 200 GeV/NUCLEON

S. E. Hirzebruch (Siegen Univ.,, Germany.), W. Heinrich (Siegen Univ.,, Germany.), K. D. Tolstov (Joint Inst. for Nuclear Research, Dubna, USSR.), A. D. Kovalenko (Joint Inst. for Nuclear Research, Dubna, USSR.), and E. V. Benton *In its* High LET, Passive Space Radiation Dosimetry and Spectrometry Mar. 1995 9 p (For primary document see N95-25911 08-72)

Avail: CASI HC A02/MF A03

Inclusive cross sections for high energy interactions at 0.9, 2.3, 3.6, and 13.5 GeV/nucleon of O-16 with C, CR-39 (C12H18O7), CH2, Al, Cu, Ag, and Pb targets were measured. The total charge-changing cross sections and partial charge-changing cross sections for the production of fragments with charge $Z = 6$ and $Z = 7$ are compared to previous experiments at 60 and 200 GeV/nucleon. The contributions of Coulomb dissociation to the total cross sections are calculated. Using factorization rules the partial electromagnetic cross sections are separated from the nuclear components. Energy dependence of both components are investigated and discussed. Author

N95-25922*# National Aeronautics and Space Administration. Langley Research Center, Hampton, VA.
HZE BEAM TRANSPORT IN MULTILAYERED MATERIALS

J. L. Shinn, J. W. Wilson, F. F. Badavi (Christopher Newport Coll., Newport News, VA.), E. V. Benton (San Francisco Univ., CA.), I. Csige (Institute of Nuclear Research, Debrecen, Hungary.), A. L. Frank (San Francisco Univ., CA.), and E. R. Benton (San Francisco Univ., CA.) *In* San Francisco Univ., High LET, Passive Space Radiation Dosimetry and Spectrometry Mar. 1995 9 p (For primary document see N95-25911 08-72)

Avail: CASI HC A02/MF A03

A nonperturbative analytic solution of the high charge and energy (HZE) Green's function is used to implement a computer code for laboratory ion beam transport in multiple-layered materials. The code is established to operate on the Langley nuclear fragmentation model used in space engineering applications. Computational procedures are established to generate linear energy transfer (LET) distributions for a specified ion beam and target for comparison with experimental measurement. Comparison with Fe-56 ion with Pb-Al and Pb-(CH2)(x) targets shows reasonable agreement. Author

N95-25923*# San Francisco Univ., CA.
PRELIMINARY RESULTS OF RADIATION MEASUREMENTS ON EURECA

E. V. Benton and A. L. Frank *In its* High LET, Passive Space Radiation Dosimetry and Spectrometry Mar. 1995 10 p Presented at the 3rd Post-Retrieval LDEF Symposium, Williamsburg, VA, 8-12 Nov. 1993 (For primary document see N95-25911 08-72)

Avail: CASI HC A02/MF A03

The eleven-month duration of the EURECA mission allows long-term radiation effects to be studied similarly to those of the Long Duration Exposure Facility (LDEF). Basic data can be generated for projections to crew doses and electronic and computer reliability on spacecraft missions. A radiation experiment has been designed for EURECA which uses passive integrating detectors to measure average radiation levels. The components include a Trackoscope, which employs fourteen plastic nuclear track detector (PNTD) stacks to measure the angular dependence of high LET (greater than or equal to 6 keV/micro m) radiation. Also included are TLD's for total absorbed doses, thermal/resonance neutron detectors (TRND's) for low energy neutron fluences and a thick PNTD stack for depth dependence measurements. LET spectra are derived from the PNTD measurements. Preliminary TLD results from seven levels within the detector array show that integrated does inside the flight canister varied from 18.8 +/- 0.6 cGy to 38.9 +/- 1.2 cGy. The TLD's oriented toward the least shielded direction averaged 53% higher in dose than those oriented away from the least shielded direction (minimum shielding toward the least shielded direction varied from 1.13 to 7.9 g/cm(exp 2), Al equivalent). The maximum dose rate on EURECA (1.16 mGy/day) was 37% of the maximum measured on LDEF and dose rates at all depths were less than measured on LDEF. The shielding external to the flight canister covered a greater solid angle about the canister than the LDEF experiments. Author

N95-25924*# San Francisco Univ., CA.
FISSION FOIL DETECTOR CALIBRATIONS WITH HIGH ENERGY PROTONS

E. V. Benton and A. L. Frank *In its* High LET, Passive Space Radiation Dosimetry and Spectrometry Mar. 1995 10 p (For primary document see N95-25911 08-72)

Avail: CASI HC A02/MF A03

Fission foil detectors (FFD's) are passive devices composed of heavy metal foils in contact with muscovite mica films. The heavy metal nuclei have significant cross sections for fission when irradiated with neutrons and protons. Each isotope is characterized by threshold energies for the fission reactions and particular energy-dependent cross sections. In the FFD's, fission fragments produced by the reactions are emitted from the foils and create latent particle tracks in the adjacent mica films. When the films are processed surface tracks are formed which can be optically counted. The track densities are indications of the fluences and spectra of neutrons and/or protons. In the past, detection efficiencies have been calculated using the low energy neutron calibrated dosimeters and published fission cross sections for neutrons and protons. The problem is that the addition of a large kinetic energy to the (n,nucleus) or (p,nucleus) reaction could increase the energies and ranges of emitted fission fragments and increase the detector sensitivity as compared with lower energy neutron calibrations. High energy calibrations are the only method of resolving the uncertainties in detector efficiencies. At high energies, either proton or neutron calibrations are sufficient since the cross section data show that the proton and neutron fission cross sections are approximately equal. High energy proton beams have been utilized (1.8 and 4.9 GeV, 80 and 140 MeV) for measuring the tracks of fission fragments emitted backward and forward. Derived from text

N95-25925*# San Francisco Univ., CA.
PROTON CALIBRATION OF LOW ENERGY NEUTRON DETECTORS CONTAINING (6)LiF

E. V. Benton and A. L. Frank *In its* High LET, Passive Space Radiation Dosimetry and Spectrometry Mar. 1995 5 p (For primary document see N95-25911 08-72)

Avail: CASI HC A01/MF A03

The purpose of the present calibrations is to measure the proton response of the detectors with accelerated beams having energies within the region of maximum intensities in the trapped proton spectrum encountered in near-Earth orbit. This response is compared with the responses of the

spaceflight detectors when related to proton exposures. All of the spaceflight neutron measurements have been accompanied by TLD absorbed doses measurements in close proximity within the spacecraft. For purposes of comparison, the spaceflight TLD doses are assumed to be proton doses. Author

N95-25926*# National Aeronautics and Space Administration. Marshall Space Flight Center, Huntsville, AL.

LINEAR ENERGY TRANSFER (LET) SPECTRA OF COSMIC RADIATION IN LOW EARTH ORBIT **c93**

T. A. Parnell, J. W. Watts, Jr., A. B. Akopova (Academy of Sciences of the Armenian SSR, Erivan, Armenia.), N. V. Magradze (Academy of Sciences of the Armenian SSR, Erivan, Armenia.), V. E. Dudkin (Institute of Biomedical Problems, Moscow, USSR.), E. E. Kovalev (Institute of Biomedical Problems, Moscow, USSR.), Yu. V. Potapov (Institute of Biomedical Problems, Moscow, USSR.), E. V. Benton (San Francisco Univ., CA.), A. L. Frank (San Francisco Univ., CA.), and E. R. Benton (San Francisco Univ., CA.) *In* San Francisco Univ., High LET, Passive Space Radiation Dosimetry and Spectrometry Mar. 1995 6 p (For primary document see N95-25911 08-72)

(Contract NCC2-521; NAG8-071)

Copyright Avail: CASI HC A02/MF A03

Integral linear energy transfer (LET) spectra of cosmic radiation (CR) particles were measured on five Cosmos series spacecraft in low Earth orbit (LEO). Particular emphasis is placed on results of the Cosmos 1887 biosatellite which carried a set of joint U.S.S.R.-U.S.A. radiation experiments involving passive detectors that included thermoluminescent detectors (TLD's), plastic nuclear track detectors (PNTD's), fission foils, nuclear photo-emulsions, etc. which were located both inside and outside the spacecraft. Measured LET spectra are compared with those theoretically calculated. Results show that there is some dependence of LET spectra on orbital parameters. The results are used to estimate the CR quality factor (QF) for the COSMOS 1887 mission. Author

N95-25927*# National Aeronautics and Space Administration. Marshall Space Flight Center, Huntsville, AL.

DEPTH DISTRIBUTION OF ABSORBED DOSE ON THE EXTERNAL SURFACE OF COSMOS 1887 BIOSATELLITE

J. W. Watts, Jr., T. A. Parnell, Yu. A. Akatov (Institute of Biomedical Problems, Moscow, USSR.), V. E. Dudkin (Institute of Biomedical Problems, Moscow, USSR.), E. E. Kovalev (Institute of Biomedical Problems, Moscow, USSR.), E. V. Benton (San Francisco Univ., CA.), and A. L. Frank (San Francisco Univ., CA.) *In* San Francisco Univ., High LET, Passive Space Radiation Dosimetry and Spectrometry Mar. 1995 4 p (For primary document see N95-25911 08-72)

(Contract NCC2-521)

Avail: CASI HC A01/MF A03

Significant absorbed dose levels exceeding 1.0 Gy day(exp -1) have been measured on the external surface of the Cosmos 1887 biosatellite as functions of depth in stacks of thin thermoluminescent detectors (TLD's) made in U.S.S.R. and U.S.A. The dose was found to decrease rapidly with increasing absorber thickness, thereby indicating the presence of intensive fluxes of low-energy particles. Comparison between the U.S.S.R. and U.S.A. results and calculations based on the Vette Model environment are in satisfactory agreement. The major contribution to the dose under thin shielding thickness is shown to be from electrons. The fraction of the dose due to protons and heavier charged particles increases with shielding thickness. Author

N95-25928*# San Francisco Univ., CA.

NEUTRON INFLUENCES AND ENERGY SPECTRA IN THE COSMOS-2044 BIOSATELLITE ORBIT

V. E. Dudkin (Research Center of Space Craft Radiation Safety, Moscow, Russia.), Yu. V. Potapov (Research Center of Space Craft Radiation Safety, Moscow, Russia.), A. B. Akopova (Academy of Sciences of the Armenian SSR, Erivan, Armenia.), L. V. Melkumyan (Academy of Sciences of the Armenian SSR, Erivan, Armenia.), Sh. B. Rshtuni (Academy of Sciences of the Armenian SSR, Erivan, Armenia.), E Benton, V., and A. L. Frank *In its* High LET, Passive Space Radiation Dosimetry and Spectrometry Mar. 1995 4 p (For primary document see N95-25911 08-72)

(Contract NCC2-521)

Avail: CASI HC A01/MF A03

Joint Soviet-American measurements of the neutron component of space radiation (SR) were carried out during the flight of the Soviet biosatellite Cosmos-2044. Neutron flux densities and differential energy spectra were measured inside and on the external surface of the spacecraft. Three energy intervals were employed: thermal (E(sub n) less than or equal to 0.2 eV), resonance (0.2 eV less than E(sub n) less than 1.0 MeV) and fast (E(sub n) greater than or equal to 1.0 MeV) neutrons. The first two groups were measured with U.S. (6)LiF detectors, while fast neutrons were recorded both by U.S. fission foils and Soviet nuclear emulsions. Estimations were made of the contributions to absorbed and equivalent doses from each neutron energy interval and a correlation was presented between fast neutron fluxes, measured outside the satellite, and the phase of solar activity (SA). Average dose equivalent rates of 0.018 and 0.14 mrem d(exp -1) were measured for thermal and resonance neutrons, respectively, outside the spacecraft. The corresponding values for fast neutrons were 3.3 (U.S.) and 1.8 (U.S.S.R.) mrem d(exp -1). Inside the spacecraft, a value of 3.5 mrem d(exp -1) was found. Author

N95-25929*# National Aeronautics and Space Administration. Marshall Space Flight Center, Huntsville, AL.

EXPERIMENTAL AND CALCULATED LET DISTRIBUTIONS IN THE COSMOS-2044 BIOSATELLITE ORBIT

J. W. Watts, Jr., V. E. Dudkin (Research Center of Space Craft Radiation Safety, Moscow, Russia.), O. N. Karpov (Research Center of Space Craft Radiation Safety, Moscow, Russia.), Yu. V. Potapov (Research Center of Space Craft Radiation Safety, Moscow, Russia.), A. B. Akopova (Academy of Sciences of the Armenian SSR, Erivan, Armenia.), N. V. Magradze (Academy of Sciences of the Armenian SSR, Erivan, Armenia.), A. A. Moiseenko (Academy of Sciences of the Armenian SSR, Erivan, Armenia.), E. V. Benton (San Francisco Univ., CA.), and A. L. Frank (San Francisco Univ., CA.) *In* San Francisco Univ., High LET, Passive Space Radiation Dosimetry and Spectrometry Mar. 1995 6 p (For primary document see N95-25911 08-72)

(Contract NCC2-521)

Avail: CASI HC A02/MF A03

During the flight of the Cosmos-2044 biosatellite, joint U.S.S.R.-U.S.A. investigations of different characteristics of cosmic radiation (CR) in the near-Earth environment were carried out. The U.S. dielectric track detectors CR-39 and Soviet BYa- and BR-type nuclear photo-emulsions were used as detectors. The present work shows some results of experimental measurements of linear energy transfer (LET) spectra of CR particles obtained with the use of these detectors, which were placed both inside and outside the satellite. The LET spectra measurements with plastic detectors is composed of two parts: the measurement of galactic cosmos rays (GCR) particles, and of short-range particles. The contributions of these components to the total LET distribution at various thicknesses of the shielding were analyzed and the results of these studies are presented. Calculated LET spectra in the Cosmos-2044 orbit were compared with experimental data. On the basis of experimental and calculated values of the LET spectra, absorbed and equivalent CR doses were calculated. In the shielding range of 1-1.5 g cm(exp -2), outside the spacecraft, the photo-emulsions yielded 10.3 mrad d(exp -1) and 13.4 mrem d(exp -1) (LET greater than or equal to 40 MeV cm(exp -1)). Inside the spacecraft (greater than or equal to 10 g cm(exp -2) the photo-emulsions yielded 8.9 mrad d(exp -1) and 14.5 mrem d(exp -1). Author

N95-25930*# National Aeronautics and Space Administration. Marshall Space Flight Center, Huntsville, AL.

COSMIC RAY LET SPECTRA AND DOSES ON BOARD COSMOS-2044 BIOSATELLITE

J. W. Watts, Jr., T. A. Parnell, V. E. Dudkin (Research Center of Space Craft Radiation Safety, Moscow, Russia.), E. E. Kovalev (Research Center of Space Craft Radiation Safety, Moscow, Russia.), Yu. V. Potapov (Research Center of Space Craft Radiation Safety, Moscow, Russia.), E. V. Benton (San Francisco Univ., CA.), A. L. Frank (San Francisco Univ., CA.), E. R. Benton (San Francisco Univ., CA.), R. Beaujean (Kiel Univ., Germany.), and C. Heilmann (Centre de Recherches Nucleaires, Strasbourg, France.) et al *In* San Francisco Univ., High LET, Passive Space Radiation Dosimetry and Spectrometry Mar. 1995 8 p (For primary document see N95-25911 08-72)

(Contract NCC2-521)

Avail: CASI HC A02/MF A03

Results of the experiments on board Cosmos-2044 (Biosatellite 9) are presented. Various nuclear track detectors (NTD) (dielectric, AgCl-based, nuclear emulsions) were used to obtain the Linear Energy Transfer (LET) spectra inside and outside the satellite. The spectra from the different NTDs have proved to be in general agreement. The results of LET spectra calculations using two different models are also presented. The resultant LET distributions are used to calculate the absorbed and equivalent doses and the orbit-averaged quality factors (QF) of the cosmic rays (CR). Absorbed dose rates inside (approximately 20 g cm (exp -2) shielding) and outside (1 g cm(exp -2) the spacecraft, omitting electrons, were found to be 4.8 and 8.6 mrad d (exp -1), respectively, while the corresponding equivalent doses were 8.8 and 19.7 mrem d(exp -1). The effects of the flight parameters on the total fluence of, and on the dose from the CR particles are analyzed. Integral dose distributions of the detected particles are also determined. The LET values which separate absorbed and equivalent doses into 50% intervals are estimated. The CR-39 dielectric NTD is shown to detect 20-30% of the absorbed dose and 60-70% of the equivalent dose in the Cosmos-2044 orbit. The influence of solar activity phase on the magnitude of CR flux is discussed. Author

N95-25931*# San Francisco Univ., CA.

COSMIC RAY PARTICLES WITH DIFFERENT LET VALUES UNDER VARIOUS THICKNESSES OF SHIELDING IN LOW ALTITUDE ORBITS: CALCULATIONS AND COSMOS-2044 MEASUREMENTS **c93**

E. V. Benton, A. L. Frank, E. R. Benton, A. M. Marenny (Research Center of Space Craft Radiation Safety, Moscow, Russia.), R. A. Nymmik (Moscow State Univ., Russia.), and A. A. Suslov (Moscow State Univ., Russia.) *In its* High LET, Passive Space Radiation Dosimetry and Spectrometry Mar. 1995 5 p (For primary document see N95-25911 08-72)

(Contract NCC2-521)

Avail: CASI HC A01/MF A03

Fluxes of cosmic ray particles with different LET values were measured on board the COSMOS-2044 biosatellite under various thicknesses of shielding by stacks of CR-39 and nitrocellulose plastic nuclear track detectors (mounted outside the satellite). The component composition of the particles detected under shieldings of 0.1-2.5 g cm(exp -2) is verified by comparing experimental data with the results of model simulations of the fluxes of galactic cosmic ray particles and of radiation belt protons. Author

N95-25932*# San Francisco Univ., CA.

DIFFERENTIAL NEUTRON ENERGY SPECTRA MEASURED ON SPACECRAFT LOW EARTH ORBIT

E. V. Benton, A. L. Frank, E. V. Dudkin (Institute of Biomedical Problems, Moscow, USSR.), Yu. V. Potapov (Institute of Biomedical Problems, Moscow, USSR.), A. B. Akopova (Academy of Sciences of the Armenian SSR, Erivan, Armenia.), and L. V. Melkumyan (Academy of Sciences of the Armenian SSR, Erivan, Armenia.) *In its* High LET, Passive Space Radiation Dosimetry and Spectrometry Mar. 1995 6 p (For primary document see N95-25911 08-72)

Avail: CASI HC A02/MF A03

Two methods for measuring neutrons in the range from thermal energies to dozens of MeV were used. In the first method, alpha-particles emitted from the (sup 6) Li(n,x)T reaction are detected with the help of plastic nuclear track detectors, yielding results on thermal and resonance neutrons. Also, fission foils are used to detect fast neutrons. In the second method, fast neutrons are recorded by nuclear photographic emulsions (NPE). The results of measurements on board various satellites are presented. The neutron flux density does not appear to correlate clearly with orbital parameters. Up to 50% of neutrons are due to albedo neutrons from the atmosphere while the fluxes inside the satellites are 15-20% higher than those on the outside. Estimates show that the neutron contribution to the total equivalent radiation dose reaches 20-30%. Author

N95-25933*# San Francisco Univ., CA.

RADIOBIOLOGICAL EXPERIMENTS WITH PLANT SEEDS ABOARD THE BIOSATELLITE COSMOS 1887 **c51**

E. V. Benton, I. D. Anikeeva (Academy of Sciences, USSR, Moscow, USSR.), Yu. A. Akatov (Institute of Biomedical Problems, Moscow, USSR.), E. N. Vaulina (Academy of Sciences, USSR, Moscow, USSR.), L. N. Kostina (Academy of Sciences, USSR, Moscow, USSR.), A. Marenny (Institute of Biomedical Problems, Moscow, USSR.), A. I. Portman (Institute of Biomedical Problems, Moscow, USSR.), and S. V. Rusin (Moscow Physical-Engineering Inst., Russia.) *In its* High LET, Passive Space Radiation Dosimetry and Spectrometry Mar. 1995 6 p (For primary document see N95-25911 08-72)

(Contract NCC2-521)

Avail: CASI HC A02/MF A03

The effects of spaceflight factors on the seeds of Arabidopsis thaliana and Crepis capillaris were studied. The seeds were located inside the satellite in an open space, protected with aluminum foil and also exposed without the foil cover. When the seeds were in open space without any protection, their viability was found to be suppressed; the survival rate and fertility of plants grown from these seeds were also diminished. An increase in the frequency of chromosome aberrations (CA) and in the number of multiple injuries was registered in this case. Experiments with the aluminum foil shielding showed a decrease in the suppression of the seeds' viability, but mutational changes were found to be even more increased, while the survival rate and fertility of the plants decreased. An increase in the thickness of shielding resulted in a decrease in the effects up to the level of the control, except for the effects connected with CA and fertility of the plants. Analysis of the results shows that these impairments can be ascribed to the action of single heavy charged particles (HCP). The seeds can thus be regarded as an integral biological 'dosimeter' which allows estimation of the total effects of radiation, ecological and biological factors. Author

N95-25934*# National Aeronautics and Space Administration. Marshall Space Flight Center, Huntsville, AL.

SPACE RADIATION DOSIMETRY ON US AND SOVIET MANNED MISSIONS **c51**

T. A. Parnell and E. V. Benton (San Francisco Univ., CA.) *In* San Francisco Univ., High LET, Passive Space Radiation Dosimetry and Spectrometry Mar. 1995 68 p (For primary document see N95-25911 08-72)

(Contract NAS9-17389; NAG8-071)

Avail: CASI HC A04/MF A03

Radiation measurements obtained on board U.S. and Soviet spacecraft are presented and discussed. A considerable amount of data has now been collected and analyzed from measurements with a variety of detector types in low-Earth orbit. The objectives of these measurements have been to investigate the dose and Linear Energy Transfer (LET) spectra within the complex shielding of large spacecraft. The shielding modifies the external radiation (trapped protons, electrons, cosmic ray nuclei) which, in turn, is quite dependent on orbital parameters (altitude, inclination). For manned flights, these measurements provide a crew exposure record and a data base for future spacecraft design and flight planning. For the scientific community they provide useful information for planning and analyzing data from experiments with high sensitivity to radiation. In this paper, results of measurements by both passive and active detectors are described. High-LET spectra measurements were obtained by means of plastic nuclear track detectors (PNTD's) while thermoluminescent dosimeters (TLD's) measured the dose. Author (revised)

N95-25944# European Organization for Nuclear Research, Geneva (Switzerland).

A NORMAL FORM APPROACH TO THE THEORY OF NONLINEAR BETATRONIC MOTION

A. Bazzani and E. Todesco (European Organization for Nuclear Research, Geneva, Switzerland.) 24 Mar. 1994 225 p

(DE95-603831; CERN-94-02) Avail: CASI HC A10/MF A03 (US Sales Only)

The betatronic motion of a particle in a circular accelerator is analyzed using the transfer map description of the magnetic lattice. In the linear case the transfer matrix approach is shown to be equivalent to the Courant-Snyder theory: in the normal coordinates' representation the transfer matrix is a pure rotation. When the nonlinear effects due to the multipolar components of the magnetic field are taken into account, a similar procedure is used: a nonlinear change of coordinates provides a normal form representation of the map, which exhibits explicit symmetry properties depending on the absence or presence of resonance relations among the linear tunes. The use of normal forms is illustrated in the simplest but significant model of a cell with a sextupolar nonlinearity which is described by the quadratic Henon map. After recalling the basic theoretical results in Hamiltonian dynamics, we show how the normal forms describe the different topological structures of phase space such as KAM tori, chains of islands

and chaotic regions; a critical comparison with the usual perturbation theory for Hamilton equations is given. The normal form theory is applied to compute the tune shift and deformation of the orbits for the lattices of the SPS and LHC accelerators, and scaling laws are obtained. Finally, the correction procedure of the multipolar errors of the LHC, based on the analytic minimization of the tune shift computed via the normal forms, is described and the results for a model of the LHC are presented. This application, relevant for the lattice design, focuses on the advantages of normal forms with respect to tracking when parametric dependences have to be explored. DOE

N95-25963*# Case Western Reserve Univ., Cleveland, OH.
MOLECULAR DYNAMICS SIMULATION OF A PISTON DRIVEN SHOCK WAVE IN A HARD SPHERE GAS Final Contractor Report Ph.D. Thesis
Myeung-Jouh Woo and Isaac Greber Cleveland, OH NASA Apr. 1995 123 p
(Grant NAG3-795; RTOP 233-01-0E)
(NASA-CR-195463; E-9603; NAS 1.26:195463) Avail: CASI HC A06/MF A02

Molecular dynamics simulation is used to study the piston driven shock wave at Mach 1.5, 3, and 10. A shock tube, whose shape is a circular cylinder, is filled with hard sphere molecules having a Maxwellian thermal velocity distribution and zero mean velocity. The piston moves and a shock wave is generated. All collisions are specular, including those between the molecules and the computational boundaries, so that the shock development is entirely causal, with no imposed statistics. The structure of the generated shock is examined in detail, and the wave speed; profiles of density, velocity, and temperature; and shock thickness are determined. The results are compared with published results of other methods, especially the direct simulation Monte-Carlo method. Property profiles are similar to those generated by direct simulation Monte-Carlo method. The shock wave thicknesses are smaller than the direct simulation Monte-Carlo results, but larger than those of the other methods. Simulation of a shock wave, which is one-dimensional, is a severe test of the molecular dynamics method, which is always three-dimensional. A major challenge of the thesis is to examine the capability of the molecular dynamics methods by choosing a difficult task. Author

N95-25965# Joint Inst. for Nuclear Research, Dubna (USSR).
ON A NEW TYPE OF LONG-RANGE FORCES
V. S. Barashenkov, A. B. Pestov, and M. Z. Yurev 1994 6 p
(DE95-605286; JINR-E-2-94-132) Avail: CASI HC A02/MF A01 (US Sales Only)

It is shown that systems with non fixed (precessing) spin can generate long-range forces, though particle components constituting the system do not possess this property. The equations of motion describing the connection of a new field with its sources are derived. DOE

N95-25968# Joint Inst. for Nuclear Research, Dubna (USSR).
ON A POSSIBLE EXPLANATION OF THE ORIGIN OF THE QUARK MASS SPECTRUM
D. I. Kazakov 1994 7 p
(DE95-605315; JINR-E-2-94-162) Avail: CASI HC A02/MF A01 (US Sales Only)

Contrary to the usual case when the quark mass spectrum is defined by that of the quark Yukawa couplings while the vacuum expectation value of the Higgs field remains universal, we suggest to consider the opposite situation. Each generation of quarks and leptons is associated with its own Higgs doublet, while the Yukawa couplings are the same. This situation naturally arises in the framework of finite supersymmetric Grand Unification scenario. Non degeneracy of the quark mass spectrum is then due to asymmetric vacuum expectation values which spontaneously break the discrete flavor symmetry in the Higgs sector. DOE

N95-25969# Melbourne Univ., Parkville (Australia). School of Physics.
STATISTICAL MECHANICS OF MAGNETIZED PAIR FERMI GAS
J. Daicic, N. E. Frankel, and V. Kowalenko 1993 28 p Sponsored by Australian Postgraduate Research Award Program
(DE95-607097; UM-P-93/45) Avail: CASI HC A03/MF A01 (US Sales Only)

Following previous work on the magnetized pair Bose gas this contribution presents the statistical mechanics of the charged relativistic Fermi gas with pair creation in d spatial dimensions. Initially, the gas in no external fields is studied. As a result, expansions for the various thermodynamic functions are obtained in both the (mu)/m(yields)0 (neutrino) limit, and about the point (mu)/m =1, where (mu) is the chemical potential. The thermodynamics of a gas of quantum-number conserving massless fermions is also discussed. Then a complete study of the pair Fermi gas in a homogeneous magnetic field, is presented investigating the behavior of the magnetization over a wide range of field strengths. The inclusion of pairs leads to new results for the net magnetization due to the paramagnetic moment of the spins and the diamagnetic Landau orbits. DOE

N95-25971# International Centre for Theoretical Physics, Trieste (Italy).
DYNAMIC JAHN-TELLER-INDUCED INFRARED ABSORPTION OF A CHARGED C60(-) MOLECULE
Wen-Zheng Wang, A. R. Bishop, and Yu Lu Jun. 1994 14 p
(DE95-607577; IC-94/148) Avail: CASI HC A03/MF A01 (US Sales Only)

The observable consequences of the dynamic Jahn-Teller effect due to quantum-fluctuations between the six degenerate D(sub 5d) polaronic configurations on a singly charged C60(-) molecule ar e considered. The multi-phonon infrared absorption spectrum is calculated taking into account the dynamic symmetry breaking. Some of the Jahn-Teller active (also Raman-active) modes are predicted to be observable as multi-phonon overtones in the infrared absorption. DOE

N95-25991# International Centre for Theoretical Physics, Trieste (Italy).
STRONG PHASE CORRELATIONS OF SOLITONS OF NONLINEAR SCHROEDINGER EQUATION
A. G. Litvak, V. A. Mironov (Academy of Sciences, USSR, Nizhny Novgorod, USSR.), and A. P. Protogenov Jun. 1994 11 p
(DE95-607002; IC-94/152) Avail: CASI HC A03/MF A01 (US Sales Only)

We discuss the possibility to suppress the collapse in the nonlinear 2+1 D Schroedinger equation by using the gauge theory of strong phase correlations. It is shown that invariance relative to q-deformed Hopf algebra with deformation parameter q being the fourth root of unity makes the values of the Chern-Simons term coefficient, k=2, and of the coupling constant, g=1/2, fixed; no collapsing solutions are present at those values. DOE

N95-25993# Melbourne Univ., Parkville (Australia). School of Physics.
STATISTICAL MECHANICS OF THE MAGNETIZED PAIR BOSE GAS
J. Daicic, N. E. Frankel, R. M. Gailis, and V. Kowalenko 1993 63 p Sponsored by Australian Postgraduate Research Award Program
(DE95-607096; UM-P-93/44) Avail: CASI HC A04/MF A01 (US Sales Only)

The statistical mechanics of the charged relativistic Bose gas with pair creation in d spatial dimensions is studied. It begins with the case of a gas with no external fields present, and investigate the nature of the phase transition at the critical temperature for Bose-Einstein condensation, and also the behaviour of the specific heat in the ultra-relativistic (photon) limit. An extensive study of the pair Bose gas in an external homogeneous magnetic field is then presented, employing a Mellin transform technique to obtain high-temperature expansions for the thermodynamic potential and magnetization of this system for a wide range of field strengths. It is shown that Bose-Einstein condensation does occur in the relativistic regime for d (greater than or equal to) 5, and that for d (greater than or equal to) 3 the magnetization has a remarkably different form to that of the non-relativistic gas, but that the Meissner effect is still exhibited. The pair Bose gas is therefore shown to be a relativistic superconductor. DOE

N95-25994# International Centre for Theoretical Physics, Trieste (Italy).
OPTICAL INSTABILITIES AND CHAOS DUE TO THE VIRTUAL FORMATION OF BIEXCITONS
Nguyen Trung Dan Jul. 1994 10 p
(DE95-607664; IC-94/190) Avail: CASI HC A02/MF A01 (US Sales Only)

Optical instabilities and chaos due to virtual formation of biexcitons in optically excited semiconductors are investigated. A complete linear stability analysis of steady-state bistable solutions of nonlinear coupled differential

equations describing the nonlinear dynamics of semiconductors is carried out. The dynamical solutions are studied numerically using an iterative procedure. DOE

N95-26001 Rutherford Appleton Lab., Oxford (England).
SEARCHING FOR EXOTIC MESONS IN e(+)e(-) ANNIHILATION AT DA(PHI)NE
F. E. Close and G. J. Gounaris Sep. 1994 13 p Prepared in cooperation with Thessaloniki Univ., Salonika, Greece
(PB95-165379; RAL-94-107) Avail: Issuing Activity (National Technical Information Service (NTIS))

DA(phi)Ne should be useful for testing the nature of the vector mesons directly produced in e(-)e(+) annihilation, as well as the nature of the C=+ states produced in the radiative decays of these vector mesons. In the DA(Phi)NE energy range, these latter states may have spin up to two and any parity. Provided the background can be handled and the spin of the produced state is known, the study of the angular distributions in these decays can measure the parity of the produced meson as well as the ratios of the independent production helicity amplitudes. These ratios provide sensitive tests for quark model classification of the states, in particular the enigmatic f1(1420). Thus, they can be used to indicate whether the mesons involved are consistent with the usual qq(bar) interpretation, or whether other interpretations like e.g. hybrid, glueball or multiquark, are more favorable for some of them. NTIS

N95-26006# Brookhaven National Lab., Upton, NY.
RESULTS/PROSPECTS IN E777/851/865
D. M. Lazarus Dec. 1994 16 p Presented at the 2nd International Workshop on Heavy Quark Physics in Fixed Targets, Charlottesville, VA, 6-10 Oct. 1994; sponsored by the Univ. of Virginia
(Contract DE-AC02-76CH-00016)
(DE95-005959; BNL-61258; CONF-9410285-1) Avail: CASI HC A03/MF A01

E777 has set 90% C.L. branching ratio upper limits of 2.1 x 10(exp -10) for the decays K(+) yields pi(+)mu(+)e(-) and 4.5 x 10(exp -7) for K(+) yields pi(+)A(0), where A(0) is any particle of mass less than 100 MeV/sq c decaying into e(+)e(-) with lifetime less than 10(exp -13) s. E851 measured the BR(K(+) yields pi(+)e(+)e(-)) = 2.97(sub -0.22)(+0.19) x 10(exp -7) and BR(pi(0) yields e(+)e(-)) = (8.0 +/- 2.6 +/- 0.6) x 10(exp -8). E865 is preparing to take data in 1995 which should greatly improve these results. DOE

N95-26096 Rutherford Appleton Lab., Oxford (England).
HEAVY-NEUTRINO CHIRALITY ENHANCEMENT OF THE DECAY K(L) YIELDS e(mu) IN LEFT-RIGHT SYMMETRIC MODELS
Z. Gagyi-Palffy, A. Pilaftsis, and K. Schilcher Aug. 1994 18 p Prepared in cooperation with Mainz Univ., Germany
(PB95-165387; RAL-94-090) Avail: Issuing Activity (National Technical Information Service (NTIS))

The decay K(sub L) yields e(mu) in minimal extensions of the Standard Model based on the gauge groups SU(2)(sub L) (circle multiply) U(1)(sub Y) and SU(2)(sub R) (circle multiply) SU(2)(sub L) (circle multiply) U(1)(sub B-L), in which heavy Majorana neutrinos are present, is studied. In SU(2)(sub L) (circle multiply) U(1)(sub Y) models with chiral neutral singlets, B(K(sub L) yields e(mu)) cannot be much larger than 5 x 10(exp -15) without violating other low-energy constraints. In SU(2)(sub L) (circle multiply) SU(2)(sub R) (circle multiply) U(1)(sub B-L) models, we find the heavy-neutrino-chirality enhancements due to the presence of left-handed and right-handed currents can give rise to a branching ratio close to the present experimental limit B(K(sub L) yields e(mu)) less than 3.3 x 10(exp -11). NTIS

N95-26168# Sandia National Labs., Albuquerque, NM.
ATOMIC FORCE MICROSCOPY AS A PROCESS CHARACTERIZATION TOOL FOR GaAs-BASED INTEGRATED CIRCUIT FABRICATION
A. J. Howard, A. G. Baca, R. J. Shul, J. C. Zolper, M. E. Sherwin, and D. J. Rieger 1995 5 p Presented at the Workshop on Semiconductor Characterization, Gaithersburg, MD, 30 Jan. - 2 Feb. 1995
(Contract DE-AC04-94AL-85000)
(DE95-006223; SAND-94-2426C; CONF-950117-2) Avail: CASI HC A01/MF A01

While developing the fabrication process for GaAs-based integrated circuits numerous situations have been encountered where an in-line and post-process characterization tool which operates in a non-destructive manner was required. We will report several examples which demonstrate that the atomic force microscope (AFM) fills this characterization void in our laboratory. The AFM is extremely useful where the unintentional removal of small amounts of GaAs can be detrimental in the fabrication of devices with very thin active layers, e.g., FET channels within 30 nm of the GaAs surface. We have also characterized the use of AFM as a non-destructive tool to determine complete etching of 1.25 micro m Si3N4 via holes for a two-level interconnect process. The AFM has been useful in optimizing the ion implant activation anneal conditions of Al(0.75)Ga(0.25)Sb epitaxial layers by comparing the morphology through RMS roughness measurements. Finally we have observed differences in wet etch results based on prior process history, such as 1-5 nm differences in etch depth and morphological differences of ion implanted vs. non-implanted areas. The results and implications from these various AFM processing studies will be presented in this paper. DOE

N95-26256# California Univ., Berkeley. Lawrence Berkeley Lab, CA. Life Science Div.
LuAlO3: A HIGH DENSITY, HIGH SPEED SCINTILLATOR FOR GAMMA DETECTION
W. W. Moses, S. E. Derenzo, A. Fyodorov (Akademiya Nauk BSSR, Minsk, Russia.), M. Korzhik (Akademiya Nauk BSSR, Minsk, Russia.), A. Gektin (Academy of Sciences of the Ukraine, Kharkov, Ukraine.), B. Minkov (Academy of Sciences of the Ukraine, Kharkov, Ukraine.), and V. Aslanov (SCITEC RI and NC, Minsk, Belarus.) Nov. 1994 5 p Presented at the IEEE Nuclear Science Symposium, Norfolk, VA, 1-5 Nov. 1994 Sponsored by Public Health Service
(Contract DE-AC03-76SF-00098)
(DE95-004678; LBL-36273; CONF-9411173-2) Avail: CASI HC A01/MF A01

We present measurements of the scintillation properties cerium doped lutetium aluminum perovskite, LuAlO3:Ce, new dense ((rho)=8.34 g/cm(sup 3)) inorganic scintillator. This material has a 511 keV interaction length and photoelectric fraction 1.1 cm and 32% respectively, which are well suited to gamma ray detection. In powdered form with 0.5% cerium concentration, the scintillation light output is estimated to be 9,600 photons/MeV of deposited energy, the emission spectrum is a single peak centered at 390 nm, and the fluorescence lifetime is described by the sum of 3 exponential terms, with 60% of the light being emitted with a 11 ns decay time, 26% with a 28 ns decay time, and 13% with a 835 ns decay time. Single crystals contaminated with =10% lutetium aluminum garnet (Lu3Al5Ol2) have significantly altered scintillation properties. The light output is 26,000 photons/MeV (3.2 times that of BGO), but the decay time increases significantly (1% of the light is emitted with a 10 ns decay time, 15% with a 245 ns decay time, and 85% with a 2010 ns decay time) and the emission spectrum is dominated by a peak centered at 315 nm with a secondary peak centered at 500 rum. The short decay lifetime, high density, and reasonable light output of LuAlO3:Ce (the perovskite phase) suggest that it is useful for applications where high counting rates, good stopping power, good energy resolution, and fast timing are important. However, it is necessary to grow single crystals that are uncontaminated by the garnet phase to realize these properties. DOE

73 NUCLEAR AND HIGH-ENERGY PHYSICS

Includes elementary and nuclear particles; and reactor theory. For space radiation see *93 Space Radiation.*

N95-24267# Brookhaven National Lab., Upton, NY.
THE AGS GAMMA(SUB t)-JUMP SYSTEM
M. J. Syphers, L. Ahrens, W. vanAsselt, and J. M. Brennan 12 Sep. 1994 21 p
(Contract DE-AC02-76CH-00016)
(DE95-003170; BNL-60824; AGS/AD-94-5) Avail: CASI HC A03/MF A01

In an attempt to generate a lossless crossing of an accelerator's transition energy, one procedure is to alter the transition energy of the accelerator quickly as the beam passes through this energy region by changing the optics of the lattice -- a so-called 'transition jump,' or 'gamma(sub t)-jump'

scheme. Such a system was first implemented at CERN and later adopted at other accelerator laboratories. A scheme for the AGS was developed in 1986. A description of the AGS gamma(sub t)-jump system, and recent results from its commissioning are presented in this report. DOE

N95-24317# Colorado State Univ., Fort Collins, CO.
MEASUREMENT OF THE MAGNETICALLY-INDUCED QED BIREFRINGENCE OF THE VACUUM AND AN IMPROVED SEARCH FOR LABORATORY AXIONS: PROJECT DEFINITION STUDY OF THE USE OF ASSETS AND FACILITIES OF THE SUPERCONDUCTING SUPER COLLIDER LABORATORY Technical Report
S. A. Lee, W. M. Fairbank, Jr., W. H. Toki, and J. L. Hall (Colorado Univ., Boulder, CO.) 31 Oct. 1994 107 p
(Contract DE-FG05-94ER-40880)
(DE95-005110; DOE/ER-40880/1) Avail: CASI HC A06/MF A02

The Colorado State Collaboration has studied the feasibility of a high sensitivity Quantum Electrodynamics (QED) birefringence/axion search measurement. The objective of this work is to measure, for the first time, the birefringence induced in the vacuum on a light beam travelling in a powerful magnetic field. The same experimental setup also allows a highly sensitive search for axion or axion-like particles. The experiment would combine custom-designed optical heterodyne interferometry with a string of six SSC prototype superconducting dipole magnets at the N-15 site of the SSC Laboratory. With these powerful laser tools, sensitivity advances of 10(exp 7) to 10(exp 9) over previous optical experiments will be possible. The proposed experiment will be able to measure the QED light-by-light scattering effect with a 0.5% accuracy. The increased sensitivity for the axion-two photon interaction will result in a bound on this process rivaling the results based on astrophysical arguments. In the technical report the authors address the scientific significance of these experiments and examine the limiting technical parameters which control their feasibility. The proposed optical/electronic scheme is presented in the context of a background of the known and projected systematic problems which will confront any serious attempt to make such measurements. DOE

N95-24320# California Univ., Berkeley. Lawrence Berkeley Lab, CA.
THE COOLING OF PARTICLE BEAMS
A. M. Sessler Oct. 1994 17 p Presented at the 4th Tamura Symposium on Accelerator Physics, Austin, TX, 14-16 Nov. 1994
(Contract DE-AC03-76SF-00098)
(DE95-004669; LBL-36302; CONF-9411120-3) Avail: CASI HC A03/MF A01

A review is given of the various methods which can be employed for cooling particle beams. These methods include radiation damping; stimulated radiation damping; ionization cooling; stochastic cooling; electron cooling; laser cooling; and laser cooling with beam coupling. Laser Cooling has provided beams of the lowest temperatures, namely 1 mK, but only for ions and only for the longitudinal temperature. Recent theoretical work has suggested how laser cooling, with the coupling of beam motion, can be used to reduce the ion beam temperature in all three directions. The majority of this paper is devoted to describing laser cooling and laser cooling with beam coupling. DOE

N95-24331# Los Alamos National Lab., NM.
SELF-CONSISTENT BEAM HALO STUDIES & HALO DIAGNOSTIC DEVELOPMENT IN A CONTINUOUS LINEAR FOCUSING CHANNEL
R. A. Jameson 1994 25 p Presented at the Joint US-CERN-Japan Topical Course on Accelerator Physics and Technology: Frontiers of Accelerator Technology, Maui, HI, 3-9 Nov. 1994
(Contract W-7405-eng-36)
(DE95-003706; LA-UR-94-3753; CONF-941186-1) Avail: CASI HC A03/MF A01

Beam halos are formed via self-consistent motion of the beam particles. Interactions of single particles with time-varying density distributions of other particles are a major source of halo. Aspects of these interactions are studied for an initial equilibrium distribution in a radial, linear, continuous focusing system. When there is a mismatch, it is shown that in the self-consistent system, there is a threshold in space-charge and mismatch, above which a halo is formed that extends to (approximately) 1.5 times the initial maximum mismatch radius. Tools are sought for characterizing the halo dynamics. Testing the particles against the width of the mismatch driving resonance is useful for finding a conservative estimate of the threshold. The exit, entering and transition times, and the time evolution of the halo, are also explored using this technique. Extension to higher dimensions is briefly discussed. DOE

N95-24335*# Fermi National Accelerator Lab., Batavia, IL.
ON CORRECTIONS TO THE NAMBU ACTION
Vanda Silveira (Brasilia Univ., Brasilia, Brazil.) and M. D. Maia (Brasilia Univ., Brasilia, Brazil.) 13 Jan. 1994 11 p
(Grant NAGw-2381)
(NASA-CR-197625; FERMILAB-Pub-94/027-A; NAS 1.26:197625) Avail: CASI HC A03/MF A01

We analyze the thickness-corrections to the Nambu walls, focussing on recent discussions on the subject. The presence of corrections depending on the Gaussian curvature and its implications are reviewed. We also highlight the consistency of the calculations, its limitations and the connection between alternative derivations. Author

N95-24348# Joint Inst. for Nuclear Research, Dubna (USSR).
FIELD EQUIPOTENTIALS OF A FAST-MOVING CHARGE IN MEDIUM
V. N. Streltsov 1994 3 p
(DE94-636737; JINR-D-2-94-85) Avail: CASI HC A01/MF A01 (US Sales Only)

The Lienard-Wiechert field equipotentials of an uniformly moving charge in a medium are presented. At one time, based on the Lienard-Wiechert potentials, it was found that the equipotential surfaces of a uniformly moving charge have the form of revolution ellipsoids stretched in the direction of motion. With growing speed the field stretches more and more forward and acts on greater distances. One can that there is a kind of relativistic long-range effect occurring. Presented in this document from an analogous view is the behavior of field equipotentials for a charge moving in a refractive medium, which we feel reflects the peculiarity of radiation behavior. Stressed is the fact that the obtained curves describe the angular dependence of the formation way of the radiation, in particular, the infinite formation way for the Cherenkov radiation. Derived from text

N95-24351# Instituto de Fisica Teorica, Sao Paulo (Brazil).
LIMITING ANALYTIC FORM FOR AHARONOV-BOHM DIFFRACTION PATTERN
V. C. Aguilera-Navarro and R. M. Quick (Pretoria Univ., South Africa.) Apr. 1994 24 p
(DE95-600839; IFT-P-014/94) Avail: CASI HC A03/MF A01 (US Sales Only)

A two-slit diffraction experiment with a magnetic flux confined to an unaccessible region between two rectangular slits is considered. A leading order analytic form for the asymmetry in the resulting diffraction pattern is obtained. The corrections to the expressions are bounded and disappear in the limit of long wavelengths and/or infinite source-slit-screen spacing. Using the analytic form derived, the authors obtain a non-zero value for the asymmetry in the number of electrons scattered to the left and to the right, and a zero value for their average displacement. DOE

N95-24357# Brookhaven National Lab., Upton, NY.
A HIGH-ENERGY HIGH-LUMINOSITY (MU)(+) - (MU)(-) COLLIDER
D. V. Neuffer (Continuous Electron Beam Accelerator Facility, Newport New, VA.) and R. Palmer Jun. 1994 4 p Presented at the 4th European Particle Accelerator Conference, London, 27 Jun. - 1 Jul. 1994
(Contract DE-AC02-76CH-00016)
(DE95-006097; BNL-61267; CONF-940618-116; CAP-109-MUON-94C)
Avail: CASI HC A01/MF A01

We present a candidate design for a high-energy high luminosity (mu)(+)-(mu) collider, with E(sub cm) = 4 TeV, L = 10(exp 34) cm(exp -2) s(exp -1), using only existing technology. The design uses a rapid-cycling medium-energy proton synchrotron, which produces proton beam pulses which are focused onto two (pi)- producing targets, with two (pi)-decay transport lines producing (mu)(+)(prime)s and (mu)(-)(prime)s. The (mu)(prime)s are collected, rf-rotated, cooled and compressed into a recirculating linac for acceleration, and then transferred into a storage ring collider. The keys to high luminosity are maximal (mu) collection and cooling; innovations with these goals are included. DOE

N95-24409# Stanford Linear Accelerator Center, CA.
DEPOLARIZATION IN THE SLC COLLIDER ARCS

P. Emma, T. Limberg, and R. Rossmanith (Continuous Electron Beam Accelerator Facility, Newport New, VA.) Jun. 1994 4 p Presented at the 4th European Particle Accelerator Conference, London, 27 Jun. - 1 Jul. 1994

(Contracts DE-AC03-76SF-00515; DE-AC05-84ER-40150)

(DE95-005942; SU-SLAC-PUB-6527; CONF-940618-115) Avail: CASI HC A01/MF A01

In the 1993 running cycle of the Stanford Linear Collider, electron spin polarization measurements with a Moller polarimeter at the end of the linac and a Compton polarimeter near the interaction point (IP) indicated a relative polarization loss of up to 20% across the arc. The authors present calculations of the depolarizing effects where variations in energy, energy spread and transverse emittance as well as changes in orbit and initial spin orientation are taken into account. They compare their results with measurements and conclude that, in standard operating conditions, the relative polarization loss is only 3 +/- 2%. DOE

N95-24448# Tampere Univ. of Technology (Finland).

AVAILABILITY ANALYSIS OF A 100 kWh SUPERCONDUCTING MAGNETIC ENERGY STORAGE

H. Maekinen and R. Mikkonen 1994 87 p

(DE95-737621; TTKK/TST-2/94) Avail: CASI HC A05/MF A01

Superconducting Magnetic Energy Storage (SMES) is one of the possible and useful applications of modern superconducting technology. It is known that some loads on electricity distribution networks are particularly sensitive to short power interruptions and voltage sags. Different ranges of SMES applications have been widely discussed for large scale units (1 MWh - 1 GWh) as well as for small and medium scale units (1 kWh - 1 MWh). The major components of a SMES system are the superconducting magnet winding, the cryogenic refrigeration system and the power conditioning system, which interfaces the coil to the utility grid and applied load. The SMES winding is cooled by a cryogenic coolant: liquid helium for LTS (low temperature superconductor) wires; gaseous helium, liquid hydrogen or liquid nitrogen for HTS (high temperature superconductor) wires. In addition the higher operating temperature of HTS materials also means higher refrigeration efficiencies, greater reliability and easier acceptance within the utility community. It has been estimated that applying HTS materials in a SMES system will reduce the capital costs some 14-26 %. In this calculation it has been assumed that the price of HTS material is equivalent to that of LTS material. This report deals with the availability aspects of a 100 kWh SMES. A conceptual design of a reference unit has been used as a basis of the study. Therefore the lack of the detailed design leads to uncertainty in evaluating the failure data for single components. The failure rate data are mainly adopted from fusion data sources. This extrapolation is problematic, but in most cases the only way to get results at all. The method used is based on the failure modes, effects and criticality analysis, FMECA. Fault trees describe the outage logic based on the functional analysis. Event trees clarify the consequences of the primary events and the criticality of these consequences are expressed as system down times. DOE

N95-24495# California Univ., Berkeley. Lawrence Berkeley Lab, CA.

THE PHYSICS AND EXPERIMENTAL PROGRAM OF THE RELATIVISTIC HEAVY ION COLLIDER (RHIC)

John W. Harris Sep. 1994 12 p Presented at the NATO Advanced Research Workshop on Hot Hadronic Matter: Theory and Experiment, Divonne-les-Baines, 27 Jun. - 1 Jul. 1994 Sponsored by Alexander von Humboldt Foundation

(Contract DE-AC03-76SF-00098)

(DE95-003416; LBL-36250; CONF-9406274-2) Avail: CASI HC A03/MF A01

The primary motivation for studying nucleus-nucleus collisions at relativistic and ultrarelativistic energies is to investigate matter at high energy densities (epsilon much greater than 1 GeV/fm(sup 3)). Early speculations of possible exotic states of matter focused on the astrophysical implications of abnormal states of dense nuclear matter. Field theoretical calculations predicted abnormal nuclear states and excitation of the vacuum. This generated an initial interest among particle and nuclear physicists to transform the state of the vacuum by using relativistic nucleus-nucleus collisions. Extremely high temperatures, above the Hagedorn limiting temperature, were expected and a phase transition to a system of deconfined quarks and gluons, the Quark-Gluon Plasma (QGP), was predicted. Such a phase of matter would have implications for both early cosmology and stellar evolution. The understanding of the behavior of high temperature nuclear matter is still in its early stages. However, the dynamics of the initial stages of these collisions, which involve hard parton-parton interactions, can be calculated using perturbative QCD. Various theoretical approaches have resulted in predictions that a high temperature (T (approximately) 500 MeV) gluon gas will be formed in the first instants (within 0.3 fm/c) of the collision. Furthermore, QCD lattice calculations exhibit a phase transition between a QGP and hadronic matter at a temperature near 250 MeV. Such phases of matter may have existed shortly after the Big Bang and may exist in the cores of dense stars. An important question is whether such states of matter can be created and studied in the laboratory. The Relativistic Heavy Ion Collider (RHIC) and a full complement of detector systems are being constructed at Brookhaven National Laboratory to investigate these new and fundamental properties of matter. DOE

N95-24500# Sandia National Labs., Albuquerque, NM.

PULSED POWER DRIVERS FOR ICF AND HIGH ENERGY DENSITY PHYSICS

Juan J. Ramirez, M. Keith Matzen, and Dillon H. McDaniel 1995 17 p Presented at the International Atomic Energy Agency (IAEA) Technical Committee Meeting on Drivers for Inertial Confinement Fusion, Paris, France, 14-18 Nov. 1994

(Contract DE-AC04-94AL-85000)

(DE95-003361; SAND-94-1419C; CONF-9411152-1) Avail: CASI HC A03/MF A01

Nanosecond Pulsed Power Science and Technology has its origins in the 1960s and over the past decade has matured into a flexible and robust discipline capable of addressing key physics issues of importance to Inertial Confinement Fusion (ICF) and high Energy Density Physics. The major leverage provided by pulsed power is its ability to generate and deliver high energy and high power at low cost and high efficiency. A low-cost, high-efficiency driver is important because of the very large capital investment required for multi-megajoule ignition-class systems. High efficiency is of additional importance for a commercially viable inertial fusion energy option. Nanosecond pulsed power has been aggressively and successfully developed at Sandia over the past twenty years. This effort has led to the development of unique multi-purpose facilities supported by highly capable diagnostic, calculational and analytic capabilities. The Sandia Particle-beam Fusion Program has evolved as part of an integrated national ICF Program. It applies the low-cost, high-efficiency leverage provided by nanosecond pulsed power systems to the longer-term goals of the national program, i.e., the Laboratory Microfusion Facility and Inertial Fusion Energy. A separate effort has led to the application of nanosecond pulsed power to the generation of intense, high-energy laboratory x-ray sources for application to x-ray laser and radiation effects science research. Saturn is the most powerful of these sources to date. It generates (approximately) 500 kilojoules of x-rays from a magnetically driven implosion (Z-pinch). This paper describes results of x-ray physics experiments performed on Saturn, plans for a new Z-pinch drive capability for PBFA-2, and a design concept for the proposed (approximately) 15 MJ Jupiter facility. The opportunities for ICF-relevant research using these facilities will also be discussed. DOE

N95-24572# Stanford Linear Accelerator Center, CA.

OVER-COMPRESSION, A METHOD TO SHAPE THE LONGITUDINAL BUNCH DISTRIBUTION FOR A REDUCED ENERGY SPREAD

F. J. Decker, R. Holtzapple, and T. Raubenheimer Jul. 1994 4 p Presented at the 17th International LINAC Conference, Tsukuba, Japan, 21-26 Aug. 1994

(Contract DE-AC03-76SF-00515)

(DE95-006052; SU-SLAC-PUB-6604; CONF-9408125-46) Avail: CASI HC A01/MF A01

In the Stanford Linear Collider the energy spread of the bunches at the end of the linac is dominated by longitudinal wakefields. A short, high current bunch with a Gaussian shape will produce a double-horned energy distribution. It can be shown that certain charge distributions with a sharp rise time (about rectangular or half-Gaussian) will give no additional energy spread due to the linac, since the generated wakefield and the rf-curvature cancel each other exactly. In this paper different methods are presented on how to achieve such distributions by using non-linear dependences in the RTL (Ring-To-Linac) compression region. A simple and effective method to achieve such a distribution is by over-compression. When not fully

compressing the bunch, there are two settings of the compressor voltage, under and over-compression, which give the same core bunch length in the linac. By switching from the under to the over-compressed setting, the tails are reduced from more than Gaussian to less than Gaussian beam tails. This results in a roughly rectangular shape which will give the wakefield-rf cancellation. Simulations, measurements and their implications are discussed. DOE

N95-24573# Stanford Linear Accelerator Center, CA.
TUTORIAL ON BEAM-BASED FEEDBACK SYSTEMS FOR LINACS
L. Hendrickson, S. Allison, T. Gromme, P. Grossberg, T. Himel, K. Krauter, R. MacKenzie, M. Ross, R. Sass, and H. Shoaee Aug. 1994 5 p Presented at the 17th International LINAC Conference, Tsukuba, Japan, 21-26 Aug. 1994
(Contract DE-AC03-76SF-00515)
(DE95-006054; SU-SLAC-PUB-6621; CONF-9408125-48) Avail: CASI HC A01/MF A01

A generalized fast feedback system stabilizes beams in the SLC. It performs measurements and modifies actuator settings to control beam states such as position, angle, energy and intensity on a pulse to pulse basis. An adaptive cascade feature allows communication between a series of linac loops, avoiding overcorrection problems. The system is based on the state space formalism of digital control theory. Due to the database-driven design, new loops are added without requiring software modifications. Recent enhancements support the monitoring and control of nonlinear states such as beam phase using excitation techniques. In over three years of operation, the feedback system has grown from its original eight loops to more than fifty loops, and it has been invaluable in stabilizing the machine. DOE

N95-24574# Stanford Linear Accelerator Center, CA.
ELECTROWEAK COUPLING MEASUREMENTS FROM POLARIZED BHABHA SCATTERING AT THE Z(SUP 0) RESONANCE
K. T. Pitts (Oregon Univ., Eugene, OR.) Aug. 1994 5 p Presented at the Meeting of the Division of Particles and Fields of the American Physical Society, Albuquerque, NM, 2-6 Aug. 1994
(Contracts DE-FG06-85ER-40224; DE-AC03-76SF-00515)
(DE95-006056; SU-SLAC-PUB-6639; CONF-940816-81) Avail: CASI HC A01/MF A01

The cross section for Bhabha scattering e(+)e(-) (yields) e(+)e(-) with polarized electrons at the center of mass energy of the Z(sup 0) resonance has been measured with the SLD experiment at the SLAC Linear Collider (SLC) during the 1992 and 1993 runs. The first measurement of the left-right asymmetry in Bhabha scattering (A(sub LR)e(+)e(-)(theta) is presented. From A(sub LR)e(+)e(-)(theta) the effective weak mixing angle is measured to be sin(sup 2)(theta)(sub W)(sup eff) = 0.2245 +/- 0.0049 +/- 0.0010. The effective electron vector and axial vector couplings to the Z(sup 0) are extracted from a combined analysis of the polarized Bhabha scattering data and the left-right asymmetry (A(sub LR)) previously published by this collaboration. From the combined 1992 and 1993 data the effective electron couplings are measured to be v(sub e) = -0.0414 +/- 0.0020 and a(sub e) = -0.4977 +/- 0.0045. DOE

N95-24601# Fermi National Accelerator Lab., Batavia, IL.
MEASUREMENT OF THE WW GAMMA, ZZ GAMMA AND Z GAMM A GAMMA COUPLINGS AT THE FERMILAB TEVATRON
John Ellison (California Univ., Riverside, CA.) Sep. 1994 7 p Presented at the Meeting of the Division of Particles and Fields of the American Physical Society, Albuquerque, NM, 2-6 Aug. 1994
(Contract DE-AC02-76CH-03000)
(DE95-003495; FNAL/C-94/329-E; UCR/DO/94-20; CONF-940816-59) Avail: CASI HC A02/MF A01

The processes p p-bar yields ell nu-bar(sub gamma) + X and p p-bar yields ell(+) ell(-)(sub gamma) + X (ell = e, mu) have been observed using the DO detector at the Fermilab Tevatron Collider at radical s = 1.8 TeV. The observed signals in the electron and muon decay channels are used as a probe of the WW gamma, ZZ gamma, and Z gamma gamma vertex couplings. By comparing the event rates and shapes of the photon ET distributions with theoretical predictions, 95% confidence limits are obtained on the WW gamma, ZZ gamma, and Z gamma gamma vertex coupling parameters. DOE

N95-24651# Lawrence Livermore National Lab., Livermore, CA.
TARGET INJECTION METHODS FOR INERTIAL FUSION ENERGY
Ronald W. Petzoldt and Ralph W. Moir Jun. 1994 12 p Presented at the 11th Topical Meeting on the Technology of Fusion Energy, New Orleans, LA, 19-24 Jun. 1994
(Contract W-7405-eng-48)
(DE95-003654; UCRL-JC-116030; CONF-940630-52) Avail: CASI HC A03/MF A01

We have studied four methods to inject IFE targets: the gas gun, electrostatic accelerator, induction accelerator, and rail gun. We recommend a gas gun for indirect drive targets because they can support a gas pressure load on one end and can slide along the gun barrel without damage. With the gas gun, the amount of gas required for each target (about 10 to 100 mg) is acceptable; for other types of targets, a sabot would be necessary. A cam and poppet valve arrangement is recommended for gas flow control. An electrostatic accelerator is attractive for use with lightweight spherical direct drive targets. Since there is no physical contact between the target and the injector, there will be no wear of either component during the injection process. An induction accelerator has an advantage of no electrical contact between the target and the injector. Physical contact is not even necessary, so the wear should be minimal. It requires a cylindrical conductive target sleeve which is a substantial added mass. A rail gun is a simpler device than an electrostatic accelerator or induction accelerator. It requires electrical contact between the target and the rails and may have a significant wear rate. The wear in a vacuum could be reduced by use of a solid lubricant such as MoS2. The total required accuracy of target injection, tracking and beam pointing of +/- 0.4 mm appears achievable but will require development and experimental verification. DOE

N95-24652# California Univ., Berkeley. Lawrence Berkeley Lab, CA.
CURRENT EXPERIMENTS IN ELEMENTARY PARTICLE PHYSICS. REVISION
H. Galic (Stanford Linear Accelerator Center, CA.), F. E. Armstrong, B. vonPrzewoski (Indiana Univ., Bloomington, IN.), V. I. Klyukhin (Gosudarstvennyi Komitet po Ispolzovaniyu Atomnoi Energii, Protvino, USSR.), Yu. G. Ryabov (Gosudarstvennyi Komitet po Ispolzovaniyu Atomnoi Energii, Protvino, USSR.), S. V. Bilak (Academy of Sciences, USSR, Moscow, USSR.), N. S. Illarionova (Academy of Sciences, USSR, Moscow, USSR.), O. B. VanDyck (Lawrence Livermore National Lab., Livermore, CA.), R. Frosch (Paul Scherrer Inst., Villigen, Switzerland.), and F. Lehar (Commissariat a l'Energie Atomique, Saclay, France.) Aug. 1994 174 p
(Contracts DE-AC03-76SF-00098; DE-AC03-76SF-00515)
(DE95-003797; LBL-91-Rev-8/94) Avail: CASI HC A08/MF A02

This report contains summaries of 568 current and recent experiments in elementary particle physics. Experiments that finished taking data before 1988 are excluded. Included are experiments at BEPC (Beijing), BNL, CEBAF, CERN, CESR, DESY, FNAL, INS (Tokyo), ITEP (Moscow), IUCF (Bloomington), KEK, LAMPF, Novosibirsk, PNPI (St. Petersburg), PSI, Saclay, Serpukhov, SLAC, and TRIUMF, and also several underground and underwater experiments. Instructions are given for remote searching of the computer database (maintained under the SLAC/SPIRES system) that contains the summaries. DOE

N95-24661# Stanford Linear Accelerator Center, CA.
STUDIES OF STRONG ELECTROWEAK SYMMETRY BREAKING AT FUTURE e(+)e(-) LINEAR COLLIDERS
T. L. Barklow Aug. 1994 4 p Presented at the Meeting of the Division of Particles and Fields of the American Physical Society, Albuquerque, NM, 2-6 Aug. 1994
(Contract DE-AC03-76SF-00515)
(DE95-004281; SU-SLAC-PUB-6618; CONF-940816-53) Avail: CASI HC A01/MF A01

Methods of studying strong electroweak symmetry breaking at future e(+)e(-) linear colliders are reviewed. Specifically, we review precision measurements of triple gauge boson vertex parameters and the rescattering of longitudinal W bosons in the process e(+)e(-) yields W(+)W(-). Quantitative estimates of the sensitivity of each technique to strong electroweak symmetry breaking are included. DOE

N95-24664# Stanford Linear Accelerator Center, CA.
A FAST TRACKING METHOD USING RESONANCE BASIS HAMILTONIANS
J. Irwin, T. Chen, and Y. T. Yan Dec. 1994 5 p Presented at the Workshop on Nonlinear Dynamics in Particle Accelerators: Theory and Experiments, Arcidosso, Italy, 4-9 Sep. 1994
(Contract DE-AC03-76SF-00515)
(DE95-004292; SU-SLAC-PUB-6727; CONF-9409258-1) Avail: CASI HC A01/MF A01

A resonance basis map is an important way of analyzing lattice properties in circular accelerators. A method is developed to do tracking with resonance basis maps. The speed of this method is faster than other map tracking methods, and can be dramatically increased by dropping insignificant resonance terms. This mapping method enables us to simulate and study the interplay between lattice nonlinearities and other effects such as the beam-beam interaction. DOE

N95-24665# California Univ., Berkeley. Lawrence Berkeley Lab, CA.
PROCEEDINGS OF THE 1994 CONFERENCE ON COMPUTING IN ENERGY PHYSICS
S. C. Loken, ed. 1994 532 p Conference held in San Francisco, CA, 21-27 Apr. 1994
(Contract DE-AC03-76SF-00098)
(DE95-004442; LBL-35822; CONF-940492) Avail: CASI HC A23/MF A04

This report contains papers on the following topics: Triggering, data acquisition, online and control systems; hardware architectures; networks and interconnections; data handling and storage systems; software methodologies, languages and tools; user interfaces and visualization; computation; and information systems and multimedia. The individual papers have been indexed and cataloged elsewhere. DOE

N95-24680# Argonne National Lab., IL. High Energy Physics Div.
HIGH ENERGY PHYSICS DIVISION RESEARCH ACTIVITIES Semiannual Report, 1 Jan. - 30 Jun. 1994
Sep. 1994 72 p
(Contract W-31-109-eng-38)
(DE95-003985; ANL-HEP-TR-94-60) Avail: CASI HC A04/MF A01

This report describes the research conducted in the High Energy Physics Division of Argonne National Laboratory during the period of January 1, 1994-June 30, 1994. Topics covered here include experimental and theoretical particle physics, advanced accelerator physics, detector development, and experimental facilities research. Lists of division publications and colloquia are included. DOE

N95-24685 Brookhaven National Lab., Upton, NY.
CRYSTALLINE BEAMS: THEORY, EXPERIMENTS, AND PROPOSALS
Alessandro G. Ruggiero 1995 23 p Presented at the INFN Elosiatron Workshop on Quantum-like Models and Coherent Effects, Erice, Italy, 13-20 Jun. 1994 Limited Reproducibility: More than 20% of this document may be affected by microfiche quality
(Contract DE-AC02-76CH-00016)
(DE95-003955; BNL-61007; CONF-9406292-1) Avail: CASI HC A03

Crystalline beams are an ordered state of an ensemble of ions, circulating in a storage ring, with very small velocity fluctuations. They can be obtained from ordinary warm ion beams with the application of intense cooling techniques (stochastic, electron, laser). A phase transition occurs when sufficiently small velocity spreads are reached, freezing the particle-to-particle spacing in strings, Zigzags, and helices. The properties and the feasibility of Crystalline Beams depend on the choice of the lattice of the Storage Ring. There are three issues closely related to the design of the Storage Ring; namely: the determination of equilibrium configurations, confinement conditions, and stability conditions. Of particular concern is the effect of the trajectory curvature and of the beam momentum spread, since they set the requirements on the amount of momentum cooling, on the focussing, and on the distribution of bending in the lattice of the storage ring. The practical demonstration of crystalline beams may create the basis for an advanced technology for particle accelerators, where the limitations due to Coulomb intrabeam scattering and space-charge forces would finally be brought under control, so that beams of ions, more dense than normal, can be achieved for a variety of new applications. DOE

N95-24728# Fermi National Accelerator Lab., Batavia, IL.
EVIDENCE FOR TOP QUARK PRODUCTION IN 1.8 TEV P-BAR P COLLISIONS
Hans B. Jensen Sep. 1994 12 p Presented at the 27th International Conference on High Energy Physics, Glasgow, Scotland, 21-27 Jul. 1994
(Contract DE-AC02-76CH-03000)
(DE95-003496; FNAL/C-94/339-E; CONF-940722-33) Avail: CASI HC A03/MF A01

This report is a summary of the evidence for top quark production in p-bar p collisions at a center of mass energy of 1.8 TeV which was obtained by the CDF Collaboration earlier this year. The data analyzed corresponds to an integrated luminosity of 19.3 pb(sup -1), recorded with the CDF Detector at the Fermilab Tevatron Collider during 1992-1993. Three different search channels for t t-bar production are used. A search for dilepton events finds 2 events, while two different methods of identifying b-quark jets in events with W+ greater or equal 3 jets finds 6 and 7 events, respectively. The probability that the observed total yield is consistent with the estimated background of 5.96(sub -0.44)(sup +0.49) is 0.26%. Though the statistics are too limited to firmly establish the existence of the top quark, a natural interpretation of the excess is that it is due to t t-bar production. Under this assumption, constrained mass fitting of a subset of events yields a top quark mass of 174 +/-10(sub -12)(sup +13) GeV/c(sup 2) and a t t-bar production cross section of 13.9(sub -4.8)(sup +6.1) pb. DOE

N95-24852# Hawaii Univ., Honolulu, HI.
DOE-HIGH ENERGY PHYSICS CONTRACT WITH THE UNIVERSITY OF HAWAII Final Technical Report, 1 Jul. 1983 - 28 Feb. 1994
1995 46 p
(Contract DE-AC03-83ER-40103)
(DE95-004214; DOE/ER-40103/T6) Avail: CASI HC A03/MF A01

This report is divided into two sections: (1) experimental program; and (2) theoretical program. In each case the report includes a highly condensed summary of the major developments on various Hawaii projects. The various experimental programs in which Hawaii played a significant role during this period are: (1) neutrino bubble chamber experiments; (2) electron-positron colliding beams; (3) development of silicon particle-position detectors for HEP; (4) proton decay search; (5) high energy gamma-ray astronomy; and (6) DUMAND project. The theoretical programs are: (1) research in neutrino physics; (2) supernova neutrinos; (3) solar neutrinos; (4) atmospheric neutrinos; (5) searching for supersymmetry; (6) Higgs boson searches; (7) simulation of supersymmetry; (8) signals of R-parity violation; (9) leptoquarks, stable heavy particles and other exotica; (10) CP non conservation; (11) neutron electron dipole moment; (12) heavy quark physics; and (13) hadron spectroscopy. DOE

N95-24899# Department of Energy, Washington, DC. High Energy Physics Div.
HIGH ENERGY PHYSICS ADVISORY PANEL'S SUBPANEL ON VISION FOR THE FUTURE OF HIGH-ENERGY PHYSICS
May 1994 157 p
(DE94-013641; DOE/ER-0614P) Avail: CASI HC A08/MF A02

This report was requested by the Secretary of Energy to (1) define a long-term program for pursuing the most important high-energy physics goals since the termination of the Superconducting Super Collider (SSC) project, (2) assess the current US high-energy physics program, (3) make recommendations regarding the future of the field. Subjects on which recommendations were sought and which the report addresses were: high-energy physics funding priorities; facilitating international collaboration for future construction of large high-energy physics facilities; optimizing uses of the investment made in the SSC; how to encourage displaced scientists and engineers to remain in high-energy physics and to attract young scientists to enter the field in the future. The report includes a description of the state of high-energy physics research in the context of history, a summary of the SSC project, and documentation of the report's own origins and development. DOE

N95-25238# Fermi National Accelerator Lab., Batavia, IL.
DOUBLE-SIDED SILICON MICROSTRIP SENSORS FOR THE CDF SVX 2 DETECTOR
Sally Seidel (New Mexico Univ., Albuquerque, NM.) Nov. 1994 7 p Presented at the Meeting of the Division of Particles and Fields of the

American Physical Society, Albuquerque, NM, 2-6 Aug. 1994
(Contract DE-AC02-76CH-03000)
(DE95-004235; FNAL/C-94/375-E; CONF-940816-66) Avail: CASI HC A02/MF A01

The SVX II is the planned third-generation silicon vertex detector in the Collider Detector at Fermilab. Now in the prototyping phase, it is scheduled for operation in Tevatron Run II. This document describes aspects of the detector related to the design of the silicon microstrip sensors. DOE

N95-25281# Argonne National Lab., IL.
THE INTERACTIONS OF HIGH-ENERGY, HIGHLY CHARGED Xe IONS WITH BUCKYBALLS
R. Ali, H. G. Berry, and S. Cheng 1994 13 p Presented at the Interaction of Charged Particles and Radiation With Matter, Oak Ridge, TN, 23-25 Oct. 1994
(Contract W-31-109-eng-38)
(DE95-004597; ANL/PHY/CP-84104; CONF-9410275-1) Avail: CASI HC A03/MF A01

Ionization and fragmentation have been measured for C(60) molecules bombarded by highly charged (up to 35+) xenon ions with energies ranging up to 625 MeV. The observed mass distribution of positively charged fragments is explained in terms of a theoretical model indicating that the total interaction cross section contains roughly equal contributions from (1) excitation of the giant plasmon resonance, and (2) large-energy-transfer processes that lead to multiple fragmentation of the molecule. Preliminary results of measurements on VUV photons emitted in these interactions are also presented. DOE

N95-25297# Stanford Univ., CA.
TESTING SUPERSYMMETRY AT THE NEXT LINEAR COLLIDER
J. L. Feng Sep. 1994 4 p Presented at the Meeting of the Division of Particles and Fields of the American Physical Society, Albuquerque, NM, 2-6 Aug. 1994
(Contract DE-AC03-76SF-00515)
(DE95-006064; SU-SLAC-PUB-6662; CONF-940816-70) Avail: CASI HC A01/MF A01

If new particles are discovered, it will be important to determine if they are the supersymmetric partners of standard model bosons and fermions. Supersymmetry predicts relations among the couplings and masses of these particles. The authors discuss the prospects for testing these relations at a future e(+)e(-) linear collider with measurements that exploit the availability of polarized beams. DOE

N95-25300# Argonne National Lab., IL.
BREMSSTRAHLUNG SCATTERING CALCULATIONS FOR THE BEAM STOPS AND COLLIMATORS IN THE APS INSERTION-DEVICE BEAMLINES
P. K. Job, D. R. Haeffner, and D. Shu Dec. 1994 27 p
(Contract W-31-109-eng-38)
(DE95-005471; ANL/APS/TB-20) Avail: CASI HC A03/MF A01

Bremsstrahlung is produced in the APS storage ring by the interaction of positrons with the residual gas molecules in the vacuum chamber of the storage ring. The bremsstrahlung production causes a serious challenge in shielding the insertion-device beamlines because the entire straight section (15 meters) is in the line of sight of the beamline. The radiation emerges in a narrow cone tangential to the beam path with the characteristic emission angle 1/gamma, where gamma is E/mc(exp 2) which is the ratio of the kinetic energy to the rest mass for the positrons. This high-energy gamma radiation has an approximate 1/E spectrum with the maximum energy extending up to the particle energy (7 GeV for the APS). Bremsstrahlung, being high-energy photons, produces an electromagnetic shower when it encounters the beamline elements. A beamline element not thick enough to fully contain an electromagnetic shower can cause considerable scatter of the high-energy bremsstrahlung radiation. The low-energy component of the bremsstrahlung can also be scattered and create high dose rates in the first-optical and white-beam enclosures. The fully developed electromagnetic shower will have a photon spectrum almost independent of the material. The electromagnetic showers in the high-Z materials can also produce photoneutrons. This note reports the summary of EGS4 calculations performed on bremsstrahlung scattering from different beamline components in a typical APS insertion-device beamline. The related recommendations for shielding are also given. The shielding criterion adopted is a total dose rate of 2.5 micro Sv/h (0.25 mrem/h) at 30 cm from the shield. DOE

N95-25358# California Univ., Berkeley. Lawrence Berkeley Lab, CA.
ELISE: THE NEXT STEP IN DEVELOPMENT OF INDUCTION HEAVY ION DRIVERS FOR INERTIAL FUSION ENERGY
E. Lee, R. O. Bangerter, C. Celata, A. Faltens, T. Fessenden, C. Peters, J. Pickrell, L. Reginato, P. Seidl, and S. Yu et al Nov. 1994 10 p Presented at the International Atomic Energy Agency (IAEA) Technical Committee Meeting on Drivers for Inertial Confinement Fusion, Paris, France, 14-18 Nov. 1994
(Contract DE-AC03-76SF-00098)
(DE95-004679; LBL-35635; CONF-9411152-3) Avail: CASI HC A02/MF A01

LBL, with the participation of LLNL and industry, proposes to build Elise, an electric-focused accelerator as the next logical step towards the eventual goal of a heavy-ion induction linac powerful enough to implode or 'drive' inertial-confinement fusion targets. Elise will be at full driver scale in several important parameters-most notably line charge density (a function of beam size), which was not explored in earlier experiments. Elise will be capable of accelerating and electrostatically focusing four parallel, full-scale ion beams and will be designed to be extendible, by successive future construction projects, to meet the goal of the USA DOE Inertial Fusion Energy program (IFE). This goal is to address all remaining issues in heavy-ion IFE except target physics, which is currently the responsibility of DOE Defense Programs, and the target chamber. Thus Elise is the first step of a program that will provide a solid foundation of data for further progress toward a driver, as called for in the National Energy Strategy and National Energy Policy Act. DOE

N95-25365# Idaho National Engineering Lab., Idaho Falls, ID.
COBALT RELEASE FROM PCA STEEL DURING POSSIBLE FUSION REACTOR ACCIDENTS
G. R. Smolik, K. A. McCarthy, D. L. Hagrman, and E. B. McNew 1995 4 p Presented at the 18th European Symposium on Fusion Technology, Karlsruhe, Germany, 22-26 Aug. 1994
(Contract DE-AC07-76ID-01570)
(DE95-005019; EGG-M-94129; CONF-940843-13) Avail: CASI HC A01/MF A01

Possible accident scenarios for a fusion reactor include breaches in the vacuum or cooling system. Intruding air or steam could react with structural or plasma facing materials, possibly mobilizing radioactive isotopes. Safety assessments must consider the early dose at the site boundary from the release of these activated materials. Previous calculations have indicated that cobalt isotopes dominate dose calculations for designs using stainless steel. Values used in these calculations, however, had been largely determined by the measurement limits of the chemical analysis methodology instead of measured releases. The purpose of the current study was to refine the analytical method to reduce the limit for detecting cobalt, and then test PCA steel in air and steam between 973 and 1473 K. Goals were to obtain more accurate measurements of cobalt mobilization in terms of g/sq m.h and insight into the mobilization mechanisms. DOE

N95-25366# Los Alamos National Lab., NM.
NEUTRAL CURRENT NEUTRINO-NUCLEON SCATTERING
G. T. Garvey 1995 16 p Presented at the 3rd School on Astrofundamental Physics, Erice, Italy, 15-22 Sep. 1994
(Contract W-7405-eng-36)
(DE95-005027; LA-UR-94-4124; CONF-9409270-2) Avail: CASI HC A03/MF A01

It may appear unusual to have a contribution on neutrino scattering at a school devoted to electromagnetic probes, as the neutrino has no known electromagnetic couplings. However, as a means to examine the hidden flavor currents in the nucleon, the recent results observed for the spin structure function of the nucleon have focused attention on the nucleon's neutral weak currents (NWC). When an electromagnetic probe is scattered elastically from a nucleon, the NWC interactions are observable only through the detection of very small (less than 10(exp -6)) parity-violating processes. In the case of neutrino scattering, the NWC is the dominant coupling. In what follows it will be shown how the nucleon's vector and axial vector form factors arising from strange quark currents can be measured via

neutrino elastic scattering. Preliminary results from the Large Scintillation Neutrino Detector (LSND) at LAMPF will be presented as well as a recent analysis of an earlier experiment (E734) carried out at Brookhaven. DOE

N95-25369# Brookhaven National Lab., Upton, NY.
COUPLING CORRECTION USING CLOSED ORBIT MEASUREMENTS
J. Safranek and S. Krinsky 18 Feb. 1994 7 p Presented at the Orbit Correction and Analysis in Circular Accelerators Workshop, Upton, NY, 1-3 Dec. 1993
(Contract DE-AC02-76CH-00016)
(DE95-005957; BNL-61246; CONF-931254-9) Avail: CASI HC A02/MF A01

The authors describe a coupling correction scheme they have developed and used to successfully reduce the vertical emittance of the NSLS X-Ray ring by a factor of 6 to below 2 A. This gives a vertical to horizontal emittance ratio of less than 0.2%. They find the strengths of 17 skew quadrupoles to simultaneously minimize the vertical dispersion and the coupling. As a measure of coupling they utilize the shift in vertical closed orbit resulting from a change in strength of a horizontal steering magnet. Experimental measurements confirm the reduced emittance. DOE

N95-25406# Stanford Linear Accelerator Center, CA.
RF PULSE COMPRESSION IN THE NLC TEST ACCELERATOR AT SLAC
T. L. Lavine 1995 6 p Presented at the Pulsed Radio Frequency Sources for Linear Colliders, Long Island, NY, 2-7 Oct. 1994
(Contract DE-AC03-76SF-00515)
(DE95-006478; SU-SLAC-PUB-95-6742; CONF-9410218-6) Avail: CASI HC A02/MF A01

At the Stanford Linear Accelerator Center (SLAC), the authors are designing a Next Linear Collider (NLC) with linacs powered by x-band klystrons with RF pulse compression. The design of the linac RF system is based on x-band prototypes which have been tested at high power, and on a systems-integration test - the Next Linear Collider Test Accelerator (NLCTA) - which is currently under construction at SLAC. This paper discusses some of the systems implications of RF pulse compression, and the use of pulse compression in the NLCTA, both for peak power multiplication and for controlling, by RF phase modulation, intrapulse variations in the linac beam energy. DOE

N95-25441# Brookhaven National Lab., Upton, NY.
CLOSED ORBIT RELATED PROBLEMS: CORRECTION, FEEDBACK, AND ANALYSIS
E. S. Bozoki 1995 10 p Presented at the Orbit Correction and Analysis in Circular Accelerators Workshop, Upton, NY, 1-3 Dec. 1993
(Contract DE-AC02-76CH-00016)
(DE95-005969; BNL-61251; CONF-931254-8) Avail: CASI HC A02/MF A01

Orbit correction - moving the orbit to a desired orbit, orbit stability - keeping the orbit on the desired orbit using feedback to filter out unwanted noise, and orbit analysis - to learn more about the model of the machine, are strongly interrelated. They are the three facets of the same problem. The better one knows the model of the machine, the better the predictions that can be made on the behavior of the machine (inverse modeling) and the more accurately one can control the machine. On the other hand, one of the tools to learn more about the machine (modeling) is to study and analyze the orbit response to 'kicks'. DOE

N95-25478# California Univ., Berkeley. Lawrence Berkeley Lab, CA.
CONFERENCE ON PHYSICS FROM LARGE GAMMA-RAY DETEC TOR ARRAYS. VOLUME 2: PROCEEDINGS
1995 356 p Presented at the Physics With Large Gamma Ray Detector Arrays Conference, Berkley, CA, 2-6 Aug. 1994
(Contract DE-AC03-76SF-00098)
(DE95-006900; LBL-35687-Vol-2; CONF-940888-Vol-2) Avail: CASI HC A16/MF A03

The conference on 'Physics from Large gamma-ray Detector Arrays' is a continuation of the series of conferences that have been organized every two years by the North American Heavy-ion Laboratories. The aim of the conference this year was to encourage discussion of the physics that can be studied with such large arrays. This volume is the collected proceedings from this conference. It discusses properties of nuclear states which can be created in heavy-ion reactions, and which can be observed via such detector systems. DOE

N95-25594# Los Alamos National Lab., NM.
MAGNETIZED TARGET FUSION: AN OVERVIEW OF THE CONCEPT
Ronald C. Kirkpatrick 1994 20 p Presented at the 1st International Symposium for Evaluation of Current Trends in Fusion Research, Washington, DC, 14-18 Nov. 1994 Submitted for publication
(Contract W-7405-eng-36)
(DE95-005247; LA-UR-94-4354; CONF-9411182-1) Avail: CASI HC A03/MF A01

Magnetized target fusion (MTF) seeks to take advantage of the reduction of thermal conductivity through the application of a strong magnetic field and thereby ease the requirements for reaching fusion conditions in a thermonuclear (TN) fusion fuel. A potentially important benefit of the strong field in the partial trapping of energetic charged particles to enhance energy deposition by the TN fusion reaction products. The essential physics is described. MTF appears to lead to fusion targets that require orders of magnitude less power and intensity for fusion ignition than currently proposed (unmagnetized) inertial confinement fusion (ICF) targets do, making some very energetic pulsed power drivers attractive for realizing controlled fusion. DOE

N95-25631# Japan Atomic Energy Research Inst., Tokyo (Japan).
A NEW METHOD OF EMITTANCE MEASUREMENT FOR ELECTRON BEAMS FROM THE MICRO-EMITTER
Hiroshi Ishizuka (Fukuoka Inst. of Tech., Fukuoka, Japan.), Yuriko Nakahara (Fukuoka Inst. of Tech., Fukuoka, Japan.), Sunao Kawasaki (Saitama Univ., Urawa, Japan.), Stephen Musyoki, Hiroshi Shimizu, Akihiko Watanabe, and Makoto Shiho Mar. 1994 25 p In JAPANESE
(DE94-792657; JAERI-M-94-047) Avail: CASI HC A03/MF A01

Recently a new type of cathode called Micor-emitter has been put in progress. This cathode is a microfabricated field emitter having the characteristics of very low emittance and high brightness. We cannot measure the emittance of the cathode with conventional methods like the pepper-pot method. The reasons are: (1) the angle between the electron orbit and the axis is very small and (2) we cannot focus the electron beam in the vacuum or on the surface of the material since the current density of the cathode is extremely high. For the emittance measurement for such low emittance and high brightness cathode, we need to expand the beam, and measure the beam's cross section without any slits or apertures. We studied and proposed a new emittance measurement method for the Micro-emitter. DOE

N95-25634# Joint Inst. for Nuclear Research, Dubna (USSR). Bogolubov Lab. of Theoretical Physics.
ANISOTROPY OF DILEPTON EMISSION FROM NUCLEAR COLLISIONS
E. L. Bratkovskaya, O. V. Teryaev, and V. D. Toneev (Washington Univ., Seattle, WA.) Nov. 1994 11 p Sponsored in cooperation with the International Science Foundation
(Contract DE-FG06-90ER-40561)
(DE95-004354; DOE/ER-40561/167) Avail: CASI HC A03/MF A01

Attention is paid to studying the angular characteristics of e(+)e(-) pairs created in collisions with nuclear targets at intermediate and relativistic energies. Arising due to general spin and angular momentum constraints, the dilepton anisotropy seems to be quite sensitive to the contribution of different sources and may be used for disentangling these sources (or models) as well as an additional signature of a possible chiral symmetry restoration and phase transition of hadrons into the quark-gluon plasma. An anisotropy estimate for some dilepton sources is given and its relevance to the problems mentioned is discussed. DOE

N95-25772# Tokyo Univ. (Japan). Inst. for Nuclear Study.
A GREEN'S FUNCTION METHOD FOR HADRONS IN NUCLEI
Osamu Morimatsu and Koichi Yazaki Feb. 1994 52 p
(DE94-792620; INS-1026; JP9407200) Avail: CASI HC A04/MF A01

A partial review is given of the Green's function method for calculating inclusive and semi-inclusive cross sections for quasi-free processes where various hadrons are produced in nuclear targets. The general properties of the Green's function related to the energy spectrum of the system is discussed. It is shown that the method provides us with a unique way of

studying hadrons in nuclei in the form of the final state interaction between the produced hadron and the residual nucleus. The method is applied to the Sigma-hyperon production by (K(-), pi(-)) reactions on nuclei in connection with the possibility of observing Sigma-hypernuclear states, the production of hadronic atoms where the strong interaction interferes with the Coulomb interaction giving rise to interesting phenomena and the high energy electron scattering in the quasi-elastic region associated with the nuclear or color transparency. DOE

N95-25785# Brookhaven National Lab., Upton, NY. National Synchrotron Light Source.

EIGENVECTOR METHOD FOR OPTIMIZED ORBIT CORRECTION

Aharon Friedman and Eva Bozoki 1995 8 p Presented at the Orbit Correction and Analysis in Circular Accelerators Workshop, Upton, NY, 1-3 Dec. 1993

(Contract DE-AC02-76CH-00016)

(DE95-005967; BNL-61252; CONF-931254-11) Avail: CASI HC A02/MF A01

The task of the orbit correction is to find the kick vector (Theta) for a given measured orbit vector (bar-X). The authors are presenting a method, in which the kick vector is expressed as a linear combination of the eigenvectors. An additional advantage of this method is that it yields the smallest possible kick vector to correct the orbit. They will illustrate the application of the method to the NSLS X-ray and UV storage rings and the resulting measurements. It will be evident that the accuracy of this method allows the combination of the global orbit correction and local optimization of the orbit for beam lines and insertion devices. The eigenvector decomposition can also be used for optimizing kick vectors, taking advantage of the fact that eigenvectors with corresponding small eigenvalues generate negligible orbit changes. Thus, one can reduce a kick vector calculated by any other correction method and still stay within the tolerance for orbit correction. The response matrix A is defined by the equation (bar-X) = A(bar-Theta), where (bar-Theta) is the kick vector and (bar-X) is the resulting orbit vector. Since A is not necessarily a symmetric or even a square matrix the authors symmetrize it by using A(sup T)A. Then they find the eigenvalues and eigenvectors of this A(sup T)A matrix. The physical interpretation of the eigenvectors for circular machines is discussed. DOE

N95-25855# National Inst. for Fusion Science, Nagoya (Japan).

NEW EVALUATION METHOD OF SUPERCONDUCTOR CHARACTERISTICS FOR REALIZING THE LARGE HELICAL DEVICE

J. Yamamoto, O. Motojima, T. Mito, K. Takahata, N. Yanagi, S. Yamada, H. Chikaraishi, S. Imagawa, A. Iwamoto, and H. Kaneko et al Aug. 1994 18 p Presented at the 15th International Conference on Plasma Physics and Controlled Nuclear Fusion Research, Seville, Spain, 26 Sep. - 1 Oct. 1994; sponsored by the International Atomic Energy Agency

(ISSN 0915-633X)

(NIFS-297; IAEA-CN-60/F-P-3) Avail: CASI HC A03/MF A01

It is necessary to apply extra large scale superconducting magnets for a fusion device like a Large Helical Device (LHD). Because of the relatively larger current (l0 kA or more), new evaluation methods to determine the fundamental characteristics of superconductors have to be developed, which are already established for thin superconducting wires. In this paper, a measuring method for the critical current, stability margin, and current distribution are mainly discussed. Bath-cooled composite type and supercritical helium force-cooled type NbTi conductors have been chosen for the helical coils and poloidal coils of the LHD, respectively. The critical current of a conductor was measured as follows: (1) Two 2-m long parallel conductors, which were connected to each other at the bottom, were inserted in a 9 T split coil; (2) Fifty percent of the surface of the conductor was covered by spacers in order to simulate heat transfer conditions; and (3) The time dependent transition phenomena between the normal and superconducting states were observed by the voltage distribution along the conductor. On the study of the forced flow cooled conductors, the current transfer from a quenching strand to another strand was measured by the pick-up coils on a conduit. We measured the stability margin by using a pancake-type coil as a long sample test. The major measurement results of bath- and forced-cooled LHD conductors using this system have given enough fundamental data of high current multistrand conductors for the LHD. Author

N95-26011 Fermi National Accelerator Lab., Batavia, IL.

PRELIMINARY RESULTS ON THE DECAYS D(+) YIELDS K(+)pi(+)pi(-), D(+) YIELDS K(+)K(+)K(-)

Milind Purohit (Princeton Univ., NJ.) and James Wiener (Princeton Univ., NJ.) Dec. 1994 7 p Presented at the Meeting of the Division of Particles and Fields of the American Physical Society, Albuquerque, NM, 2-6 Aug. 1994 Limited Reproducibility: More than 20% of this document may be affected by microfiche quality

(Contract DE-AC02-76CH-03000)

(DE95-004865; FNAL/C-94/408-E; CONF-940816-83) Avail: CASI HC A02

Preliminary results on the Doubly Cabibbo Suppressed Decays (DCSD) D(+) (yields) K(+)pi(+)pi(-) and D(+) (yields) K(+)K(+)K(-) from roughly 40% of the E791 data set are summarized. The authors present an analysis of candidate events from E791 data in these decay modes. They show that there is a clear signal in the D(+) (yields) K(+)pi(+)pi(-) mode and discuss backgrounds and sources of error in the results. They disagree with a published signal level in the D(+) (yields) K(+)K(+)K(-) mode. DOE

N95-26029# National Inst. for Fusion Science, Nagoya (Japan).

A POSSIBILITY OF pi(-) MESON PRODUCTION BY A LOW ENERGY ELECTRON BUNCH AND POSITIVE ION BUNCH

Joshin Uramoto Apr. 1994 27 p

(ISSN 0915-633X)

(NIFS-277) Avail: CASI HC A03/MF A01

A low energy electron beam (less than or equal to 1200 eV) is injected perpendicularly to a uniform magnetic field, together with a low energy positive ion beam which is stopped electrically. On these magnetic mass analyses (using the uniform magnetic field), two peaks of secondary electrons to the beam collector appear at two analyzing magnetic field intensities which correspond to two relations of microns(-) muon (the mass m(sub 1) = 207 m(sub e) and the charge q(sub 1) = e) and pi(-) meson (the mass m(sub 2) = 273 m(sub e) and the charge q(2) = 3, where m(sub e) and e are mass and charge of electron). We consider that the pi(-) meson may be produced by a coherent interaction between the magnetically bunched beam electrons and the electrically bunched beam ions, and that the negative muon micron(-) may be produced through the decay of pi(-) meson. Author

N95-26031# National Inst. for Fusion Science, Nagoya (Japan).

HIGH-BETA DISCHARGES WITH NEUTRAL BEAM INJECTION IN CHS

S. Okamura, K. Matsuoka, K. Nishimura, K. Tsumori, R. Akiyama, S. Sakakibara, H. Yamada, S. Morita, T. Morisaki, and N. Nakajima et al May 1994 43 p

(ISSN 0915-633X)

(NIFS-280) Avail: CASI HC A03/MF A01

High-beta plasmas with a volume-averaged equilibrium beta value 2.1% were produced in CHS using tangential neutral beam injection. This beta value was achieved with the confinement improvement (reheat mode) observed after turning off a strong gas puffing. The wall conditioning with titanium gettering was used to make a high density operation (bar n(sub e) less than 8 x 10(exp 19) m(exp -3)) possible for low magnetic field (B(sub t) = 0.6 T). The discharges start with the magnetic hill configuration (in vacuum) and finally get Mercier stable equilibrium due to the shelf-stabilization effect given by the magnetic well which is produced by the plasma pressure. The Shafranov shift was about 40% of a plasma minor radius. Magnetic fluctuations did not increase with increasing plasma pressure when beta value exceeded 1%. The dynamic poloidal field control was applied to suppress the outward plasma shift with increasing plasma pressure. Such operation gave an additional increase of beta value compared with the constant poloidal field operation. Author

N95-26079# Joint Publications Research Service, Washington, DC.

JPRS REPORT: SCIENCE AND TECHNOLOGY. CENTRAL EURASIA

24 Apr. 1995 75 p Transl. into ENGLISH from various Central Eurasian articles

(JPRS-UST-95-018) Avail: CASI HC A04/MF A01

Translated articles cover the following topics: advantages of a positive temperature effect to ensure space nuclear power supply safety; and verification of nuclear safety assessment programs for space nuclear power supply reactors. CASI

N95-26095# China Nuclear Information Centre, Beijing (China).
EMITTANCE GROWTH CAUSED BY NONUNIFORM CHARGE DISTRIBUTION OF BUNCHED BEAM IN LINAC
Yinbao Chen and Zhenhai Zang Sep. 1993 8 p
(DE95-602121; CNIC-00797; IAE-0127) Avail: CASI HC A02/MF A01 (US Sales Only)

The nonlinear space charge effect of bunched beams in linac is one of the important actions that induce emittance growth because of the conversion of the field energy to kinetic energy. The authors have worked out the internal field energies associated with some nonuniform space change distributions of a bunched beam, such as Gaussian distribution, waterbag distribution and parabolic distribution. The emittance growths caused by these nonuniformities are obtained. DOE

N95-26110# National Inst. for Fusion Science, Nagoya (Japan).
CHARACTERISTICS OF D(-3)He FUELED FRC REACTOR: ARTEMIS-L
H. Momota, O. Motojima, M. Okamoto, S. Sudo, Y. Tomita, S. Yamaguchi, A. Iiyoshi, M. Onozuka (Mitsubishi Heavy Industries Ltd., Tokyo, Japan.), M. Ohnishi (Kyoto Univ., Uji, Japan.), and C. Uenosono (Kansai Electric Power Co., Inc., Osaka, Japan.) Nov. 1993 17 p Original contains color illustrations
(ISSN 0915-633X)
(NIFS-251) Avail: CASI HC A03/MF A01

The characteristics of D(-3)He fueled commercial fusion reactor ARTEMIS-L are discussed. By using favorable characteristics of a field-reversed configuration, the fusion plasma of ARTEMIS-L becomes compact and its veta-value is extremely high. Consequently, it is possible to construct an economical fusion power plant based on this concept. The life of the structural materials is found during the full reactor life (30 years) and the safety of the reactor is intrinsic to D(-3)He fuels. The amount of disposed materials is rather small and the level of the intruder dose is so low that the plant appears to be acceptable in regards to the environment. Author (revised)

N95-26111# National Inst. for Fusion Science, Nagoya (Japan).
INNOVATIVE ENERGY PRODUCTION IN FUSION REACTORS
A. Iiyoshi, H. Momota, O. Motojima, M. Okamoto, S. Sudo, Y. Tomita, S. Yamaguchi, M. Ohnishi (Kyoto Univ., Uji, Japan.), M. Onozuka (Mitsubishi Heavy Industries Ltd., Tokyo, Japan.), and C. Uenosono (Kansai Electric Power Co., Inc., Osaka, Japan.) Oct. 1993 22 p Original contains color illustrations
(ISSN 0915-633X)
(NIFS-250) Avail: CASI HC A03/MF A01

Concepts of innovative energy production in neutron-lean fusion reactors without having the conventional turbine-type generator are proposed for improving the plant efficiency. These concepts are: (1) traveling wave direct energy conversion of 14.7 MeV protons; (2) cusp type direct energy conversion of charged particles; (3) efficient use of radiation with semiconductor and supplying clean fuel in a form of hydrogen gas; and (4) direct energy conversion from deposited heat to electric power with semiconductor utilizing Nernst effect. The candidates of reactors such as a toroidal system and an open system are also studied for application of the new concepts. The study shows the above concepts for a commercial reactor are promising. Author

N95-26162# Rikkyo Univ., Yokosuka (Japan). Inst. for Atomic Energy.
PROCEEDINGS OF THE INTERNATIONAL SEMINAR ON THE CHEMISTRY OF HIGH ENERGY ATOMS
Dec. 1993 270 p Seminar held in Tokyo, Japan, 28-30 Oct. 1992
(DE95-709895; IAERU-9304; CONF-9210482) Avail: CASI HC A12/MF A03

This issue is the collection of the papers presented at the title meeting. Sixteen of the presented papers are indexed individually. DOE

N95-26163# Kyoto Univ. (Japan).
[ACTIVITIES OF THE RADIATION LABORATORY DEPARTMENT OF NUCLEAR ENGINEERING KYOTO UNIVERSITY] Annual Report, fiscal year 1993
Jul. 1994 163 p In JAPANESE
(DE95-709896; INIS-JP-029) Avail: CASI HC A08/MF A02

This publication is the collection of the papers which present research activities of Radiation Laboratory, Department of Nuclear Engineering, Kyoto University during the 1993 academic/fiscal year (April, 1993 - March, 1994). The 47 papers presented are indexed individually. DOE

N95-26164# Kyoto Univ. (Japan).
[ACTIVITIES OF THE RADIATION LABORATORY DEPARTMENT OF NUCLEAR ENGINEERING FACULTY OF ENGINEERING, KYOTO UNIVERSITY] Annual Report
Jul. 1993 156 p In JAPANESE
(DE95-709897; INIS-JP-028) Avail: CASI HC A08/MF A02

This publication is the collection of the papers presenting research activities of the Radiation Laboratory, Department of Nuclear Engineering, Kyoto University during the 1992 academic/fiscal year (April, 1992 - March, 1993). The 48 papers presented are indexed individually. DOE

N95-26165# National Inst. of Radiological Sciences, Chiba (Japan).
[ACTIVITIES OF THE NATIONAL INSTITUTE OF RADIOLOGICAL SCIENCES] Annual Report, fiscal year 1992
Jan. 1994 262 p In JAPANESE
(DE95-709916; NIRS-AR-36) Avail: CASI HC A12/MF A03

This annual report presents activities at the National Institute of Radiological Sciences (NIRS) in Japan during the period April 1992-March 1993. The activities are divided into research, technical aids, training, medical services, management, library or editing, and international cooperation. Research activities are arranged with twelve sections. The first section on special researches deals with continuing research projects entitled: (1) 'Biological Risk Evaluation in Public Exposure'; (2) 'Exposure Assessment in the Environment and the Public Through Food Chain'; (3) 'Medical Use of Accelerated Heavy Ions'; and (4) 'Preliminary Study for the Demonstration of Dose-Response Relationships in Low-Dose Range'. All projects except for project (4) will be finished up to March 1993. The section of assigned researches covers four titles. The section of ordinary researches covers physics (four titles), pharmacochemistry (four), biology (three), genetics (four), physiopathology (four), cytological radiation injuries (three), internal exposure (four), environmental science (four), clinical research (four), clinical research for radiation injuries (three), medical use of heavy particles (three), environmental radiation ecology (three), and aquatic radiation ecology (two). The section on technical aids gives an overview of technical services, radiation safety, animal and plant management, and cyclotron management. Appendices give the information on personnel in NIRS. DOE

N95-26250# National Inst. for Fusion Science, Nagoya (Japan).
DIRECT ENERGY CONVERSION OF RADIATION ENERGY IN FUSION REACTOR
S. Yamaguchi, A. Iiyoshi, O. Motojima, M. Okamoto, S. Sudo, M. Ohnishi (Kyoto Univ., Japan.), M. Onozuka (Mitsubishi Heavy Industries Ltd., Tokyo, Japan.), and C. Uenosono (Kansai Electric Power Co., Inc., Osaka, Japan.) Nov. 1993 17 p
(ISSN 0915-633X)
(NIFS-254) Avail: CASI HC A03/MF A01

Direct energy conversion from plasma heat flux has been studied. Since major parts of fusion energy in the advanced fusion reactor are radiation and charged particle energies, the flexible design of the blanket is possible. We discuss the potentiality of the thermoelectric element that generates electricity by temperature gradient in conductors. A strong magnetic field is used to confine the fusion plasma, therefore, it is appropriate to consider the effect of the magnetic field. We propose a new element which is called Nernst element. The new element needs the magnetic field and the temperature gradient. We compare the efficiency of these two elements in a semiconductor model. Finally, a direct energy conversion are mentioned. Author

74 OPTICS

Includes light phenomena; and optical devices.
For lasers see *36 Lasers and Masers.*

N95-24386*# National Aeronautics and Space Administration. Lewis Research Center, Cleveland, OH.
A PREVIEW OF A MODULAR SURFACE LIGHT SCATTERING INSTRUMENT WITH AUTOTRACKING OPTICS

William V. Meyer, Padetha Tin, J. Adin Mann, Jr. (Case Western Reserve Univ., Cleveland, OH.), H. Michael Cheung (Akron Univ., Akron, OH.), Richard B. Rogers, and Lars Lading (National Lab., Roskilde, Denmark.) 22 Apr. 1994 12 p Presented at International Symposium on Space Optics, Garmisch-Partenkirchen, Germany, 18-22 Apr. 1994; sponsored by EOS and SPIE
(Contracts NCC3-266; NCC3-269; NCC3-208)
(NASA-TM-110495; NAS 1.15:110495; Paper-2210-29) Avail: CASI HC A03/MF A01

NASA's Advanced Technology Development (ATD) program is sponsoring the development of a new generation of surface light scattering hardware. This instrument is designed to non-invasively measure the surface response function of liquids over a wide range of operating conditions while automatically compensating for a sloshing surface. The surface response function can be used to compute surface tension, properties of monolayers present, viscosity, surface tension gradient and surface temperature. The instrument uses optical and electronic building blocks developed for the laser light scattering program at NASA Lewis along with several unique surface light scattering components. The emphasis of this paper is the compensation for bulk surface motion (slosh). Some data processing background information is also included. Author

N95-24402# International Centre for Theoretical Physics, Trieste (Italy).
NUMERICAL SIMULATION METHODS FOR WAVE PROPAGATION THROUGH OPTICAL WAVEGUIDES
A. Sharma Aug. 1993 30 p
(DE94-634313; LAMP-93/4) Avail: CASI HC A03/MF A01 (US Sales Only)

The simulation of the field propagation through waveguides requires numerical solutions of the Helmholtz equation. For this purpose a method based on the principle of orthogonal collocation was recently developed. The method is also applicable to nonlinear pulse propagation through optical fibers. Some of the salient features of this method and its application to both linear and nonlinear wave propagation through optical waveguides are discussed in this report. DOE

N95-24545*# Alabama Univ., Huntsville, AL. Center for Applied Optics.
DEVELOPMENT OF OPTICAL SYSTEMS Final Report, 3 Sep. 1994 - 1 Aug. 1995
Chandra S. Vikram Jan. 1995 30 p
(Contract NAS8-38609)
(NASA-CR-197702; NAS 1.26:197702; UAH-5-33475; UAH-5-33477)
Avail: CASI HC A03/MF A01

Several key aspects of multi-color holography and laser speckle technique to study holographic reconstructions are considered in the report. Holographic fringe contrast in two-color holography in the presence of a fluid cell in the object beam is discussed in detail. A specific example of triglycine sulfate crystal growth is also considered. A breadboard design using fiber optics and diode lasers for three-color holography for fluid experiments is presented. A possible role of multi-color holography in various new applications is summarized. Finally, the use of a a laser speckle technique is demonstrated for the study of holographic reconstructions. The demonstration is performed using a Spacelab 3 hologram. Author

N95-24546# California Univ., Berkeley. Lawrence Berkeley Lab, CA.
ADVANCED LIGHT SOURCE REPORT
Sep. 1994 12 p
(Contract DE-AC03-76SF-00098)
(DE95-003449; LBL-PUB-601-Vol-7-No-1) Avail: CASI HC A03/MF A01

The exceptional science already emerging from the user program at the Advanced Light Source (ALS) shows that the promises of 'unique research opportunities' and 'experiments not possible anywhere else' made at the inception of the ALS are indeed coming true. In less than a year of beamline operations, the ALS has produced numerous high-quality results and achieved an enviable level of performance. Since the beginning of 1994, the ALS has operated for 92% of its scheduled hours, an outstanding achievement for a new machine. The ALS' ability to deliver the brightest light in the world in the ultraviolet and soft x-ray regions of the spectrum has attracted a who's who of synchrotron research to the experiment floor. These users have produced a variety of scientifically significant results during the ALS' first year of operation, a few of which are highlighted in this article. DOE

N95-24642# Joint Inst. for Nuclear Research, Dubna (USSR).
DETECTOR FOR TRANSIT TIME MEASUREMENT OF PHOTOMULTIPLIER SINGLE-PHOTOELECTRON PULSES
O. A. Zajmidoroga and A. A. Kulkov 1993 4 p In RUSSIAN; In RUSSIAN Submitted for publication
(DE94-628256; JINR-R-13-93-326) Avail: CASI HC A01/MF A01 (US Sales Only)

The detector time transit measurement of PMT single-photoelectron pulses is been presented. The Cherenkov light produced by electrons in the radiator is observed by two PMT. One is used for triggering the system and the tested one is used for working in single-photoelectron mode. DOE

N95-24673 Swedish Inst. for Materials Testing, Boras (Sweden).
CALIBRATION OF OPTICAL TIME DOMAIN REFLECTOMETERS USING TIME DELAY GENERATOR
Magnus Holmsten and Roland Andersson 1994 46 p Limited Reproducibility: More than 20% of this document may be affected by microfiche quality
(ISSN 0284-5172)
(PB95-141776; SP-RAPPORT-1993:29; ISBN-91-7848-414-6) Avail: CASI HC A03

A calibration method called 'external source method' for measuring Optical Time Domain Reflectometers (OTDR) is evaluated. The work is based on one of the proposed methods in IEC/TC86/WG4/SWG2 'Calibration of optical time-domain reflectometer'. The method simulates an optical fiber in terms of length and attenuation. This is done with a set of instruments which are described and evaluated in this report. The optical pulse from the test object is delayed and attenuated with the instruments. This corresponds to a certain length with a certain attenuation of a fiber. The OTDR is then calibrated with the set of instruments which simulate known length and attenuation. The report describes the instrument set-up and evaluates it. The proposed calibration procedure is also described, uncertainty calculation of the instrument set-up and of a complete calibration are evaluated. A short description of the computer control system is also given where the program language is written in visual basic. NTIS

N95-25004# National Aerospace Lab., Tokyo (Japan). Control Systems Div.
PRELIMINARY EXPERIMENTS OF AN OPTICAL FIBER DISPLAY
Kaoru Wakairo, Akira Watanabe, and Hiroyasu Kawahara Jan. 1995 20 p In JAPANESE
(ISSN 0389-4010)
(NAL-TR-1257) Avail: CASI HC A03/MF A01

At the National Aerospace Laboratory, the technological feasibility study of a dome screen display, which is able to give simulator pilots a very wide field of outside view, has been conducted. To provide this wide field of view, we designed a new display screen which itself could emit the light. We call this kind of screen 'a self-luminescence display.' For the self-luminescence display, we can use not only a CRT or a liquid crystal display, but also optical fibers. To investigate the applicability of plastic fibers for a self-luminescence display for use in flight simulators, we prepared a trial display. We made two displays of the same size, both of which were 900 mm in height and 1200 mm in length. The fiber's diameter is 0.75 mm, and the total number of fibers is 34,400 per display. We tested the validities of a fiber display and reached the following conclusions: (1) brightness is sufficient; (2) angle of view is limited and too narrow for practical use; and (3) picture quality is inferior. Author

N95-25239# Fermi National Accelerator Lab., Batavia, IL.
NEUTRINO OPTICS
David C. Carey Oct. 1994 32 p Presented at the 4th International Conference on Charged Particle Optics, Tsukuba, Japan, 3-6 Oct. 1994
(Contract DE-AC02-76CH-03000)
(DE95-004236; FNAL/C-94/356-E; CONF-9410229-2) Avail: CASI HC A03/MF A01

Neutrinos are produced by the in-flight decay of (pi) and k mesons. Neutrinos are uncharged and cannot be focused directly. However, the transverse momentum of the neutrino due to the decay is typically much smaller than the transverse momentum spread of the parent meson. The focusing of the meson beam will then significantly enhance the neutrino flux at a distant detector. Neutrino beams can effectively be focused in

the same manner as other charged particle beams, by means of quadrupoles and bending magnets. The bending magnets also can serve to define the momentum of the neutrino beams. Alternatively, neutrino beams can be focused by the use of magnetic horns. Both systems are described here. Proposed experiments with neutrinos to detect neutrino oscillations place the detector hundreds of kilometers away from the source. The flux of neutrinos through the detector then becomes very small. The calculation of the flux by conventional Monte Carlo or numerical integration techniques becomes prohibitively difficult. An alternate mathematical technique can be used to give results which are reliable to about 10%. DOE

N95-25357# California Univ., Berkeley. Lawrence Berkeley Lab, CA.
NONLINEAR OPTICS AND ORGANIC MATERIALS
Y. R. Shen Jul. 1994 15 p Presented at the 4th IKETANI Conference on Optically Nonlinear Organic Materials and Applications, Kamuela, HI, 16-18 May 1994
(Contract DE-AC03-76SF-00098)
(DE95-004677; LBL-36050; CONF-9405275-1) Avail: CASI HC A03/MF A01

We shall consider an interesting topic relating nonlinear optics and organic materials: how nonlinear optics can be used to study organic materials. One of the 'main differences between linear and nonlinear responses of a medium to incoming radiation is in their symmetries. It leads to the possibility that some properties of the medium could be more sensitively probed by nonlinear, rather than linear, optical means, or vise versa. A well-known example is that some vibrational modes of a medium could be Raman-active but infrared-inactive, and would be more readily observed by Raman scattering, which is a two-photon transition process. In this paper, we shall discuss, with the help of three examples, how we can use second harmonic generation (SHG) and sum frequency generation (SFG) to obtain unique information about a material. We shall focus on thin films, surfaces, and interfaces. DOE

N95-25506 Irvine Sensors Corp., Costa Mesa, CA.
MULTI-SPECTRAL SMART RETINA
David R. Shostak, David E. Ludwig, and Chris Saunders 1994 6 p Sponsored by Army
(AD-A288950) Avail: Issuing Activity (Defense Technical Information Center (DTIC))

To make focal plane arrays (FPA's) 'smart' is to associate analog and digital signal processing electronics as intimately as possible with the detector arrays. The challenge is that there isn't enough room for the amount of signal processing required. With system requirements advancing to even higher resolution, planar FPA technologies have only the detector area available and this area is as low as one thousandth of an inch (one mil) on a side. Z-plane technology overcomes this problem by providing 2000 mil of area in the Z-direction behind each detector. However, Z-plane technology can currently only achieve four mil resolution. Thus, the challenge: a compromise must be found between the degree of parallelism in the signal processing and the resolution achievable. Irvine Sensors has achieved the first step of a two stage process. A new IC for improving detector resolution for multispectral imaging has been made and is called the Multispectral Smart Retina (MSSR). The second step is to bump bond this detector to a Z-plane module that has large processing power. The purpose of this paper is to report on the initial technical results of the Multispectral Smart Retina. DTIC

N95-25559# Sandia National Labs., Albuquerque, NM.
PHASE CORRECTION IN TWO-CRYSTAL OPTICAL PARAMETRIC OSCILLATORS
D. J. Armstron, W. J. Alford, T. D. Raymond, and A. V. Smith 1995 11 p Presented at the SPIE '95: SPIE Conference on Optics, Electro-optics, and Laser Application in Science, Engineering and Medicine, San Jose, CA, 5-10 Feb. 1995
(Contract DE-AC04-94AL-85000)
(DE95-006317; SAND-95-0093C; CONF-950226-5) Avail: CASI HC A03/MF A01

The effect of the pump, signal, and idler wave phases on three-wave nonlinear parametric mixing is investigated in a series of single-pass-gain experiments. Measurements are made with two angle-tuned KTP crystals in a 532 nm pumped, walkoff-compensated, optical parametric amplifier that is seeded by an 800 nm CW diode laser. In one of the measurements the second crystal is orientated to have its effective nonlinearity d(sub eff.) of opposite sign to that of the first crystal, so that all mixing that occurred in the first crystal is cancelled by the second when the phase mismatch Delta k(sub crystal 1) = Delta k (sub crystal 2) = 0. Efficient two-crystal amplification is subsequently restored by selecting the correct phase relationship for the three waves entering the crystal by inserting a dispersive plate between the crystals. The experimental results are explained in a straightforward manner with diagrams involving the three input wave polarizations. These results demonstrate that walkoff-compensated geometries require phase correction to achieve efficient mixing in the second crystal whenever the nonlinear interaction involves two extraordinary waves (e-waves). One practical application of this work may be lower oscillation thresholds and enhanced performance in walkoff-compensated optical parametric oscillators which use two e-waves. DOE

N95-25573 Rutherford Appleton Lab., Oxford (England).
USER GUIDE FOR THE POLARIS POWDER DIFFRACTOMETER AT ISIS. VERSION 2.1
R. I. Smith and S. Hull Oct. 1994 29 p
(PB95-165767; RAL-94-115) Avail: Issuing Activity (National Technical Information Service (NTIS))

The POLARIS instrument at ISIS is scheduled as a high intensity, medium resolution powder diffractometer. The high incident neutron flux on POLARIS, combined with a large detector coverage, enables experiments to be performed with comparatively short counting times or where very little sample is available. This guide is intended to give a short description of the POLARIS diffractometer and to provide the basic information required to perform a powder diffraction experiment. To keep this guide as brief as possible the text contains several references to appropriate manuals, where more detailed information may be found. NTIS

N95-25999 Swedish National Testing and Research Inst., Tsoras (Sweden).
AUTOMATIC MEASUREMENT SYSTEM FOR MEASURING OF THE NONLINEARITY OF PHOTO DETECTORS [AUTOMATISERAT MAETSYSTEM FOER MAETNING AV OLINJAERITET HOS OPTISKA DETEKTORER]
C. Martinsson 1994 50 p In SWAHILI
(PB95-165197; SP-RAPP-1994:37) Avail: Issuing Activity (National Technical Information Service (NTIS))

A computer controlled measurement system for measuring of the nonlinearity of photodetectors has been developed. The measurement system can be used with wavelengths ranging from 380 nm to 2.0 micrometers. The method which has been used is based on superposition of two beams. Both coherent and non-coherent radiation sources have been used. The radiation power level is controlled using different transmission filters. Three different ways of measuring the photo current has been studied. Firstly it has been measured using a current amplifier connected to a voltmeter and secondly directly using a current meter and thirdly using a lock-in-amplifier having a current measurement input. The nonlinearities of the measurement instruments are not known or small. They are included in the nonlinearity measurement i.e. the nonlinearity of the combination of photo detector and measurement instrument is measured. Nonlinearity measurements have been made on silicon and germanium detectors and on a photomultiplier. At the most, six decades has been covered. The smallest obtained uncertainties are in the order 10(exp -5). NTIS

N95-26015* National Aeronautics and Space Administration. Ames Research Center, Moffett Field, CA.
ANGULAR DISPLACEMENT MEASURING DEVICE Patent
H. Lee B. Seegmiller, inventor (to NASA) 11 Aug. 1992 7 p Filed 10 Oct. 1991
(NASA-Case-ARC-11937-1; US-Patent-5,137,353;
US-Patent-Appl-SN-774490; US-Patent-Class-356-152;
US-Patent-Class-356-34; US-Patent-Class-250-225;
Int-Patent-Class-G01B-11/16) Avail: US Patent and Trademark Office

A system for measuring the angular displacement of a point of interest on a structure, such as aircraft model within a wind tunnel, includes a source of polarized light located at the point of interest. A remote detector arrangement detects the orientation of the plane of the polarized light received from the source and compares this orientation with the initial

orientation to determine the amount or rate of angular displacement of the point of interest. The detector arrangement comprises a rotating polarizing filter and a dual filter and light detector unit. The latter unit comprises an inner aligned filter and photodetector assembly which is disposed relative to the periphery of the polarizer so as to receive polarized light passing the polarizing filter and an outer aligned filter and photodetector assembly which receives the polarized light directly, i.e., without passing through the polarizing filter. The purpose of the unit is to compensate for the effects of dust, fog and the like. A polarization preserving optical fiber conducts polarized light from a remote laser source to the point of interest.
Official Gazette of the U.S. Patent and Trademark Office

N95-26039 Wright Lab., Wright-Patterson AFB, OH.
MICROSCAN SIMULATION Final Report, 1 Apr. - 1 May 1994
Brian Yasuda Sep. 1994 76 p
(AF Proj. 2004)
(AD-A289139; WL-TR-94-1149) Avail: Issuing Activity (Defense Technical Information Center (DTIC))
This report investigates the effects of detector shape, detector size, fill factor, array size, optical MTF, image reconstruction techniques, and microscan steps on aliasing and image quality using computer simulations.
DTIC

N95-26117* National Aeronautics and Space Administration. Ames Research Center, Moffett Field, CA.
METHOD FOR DETERMINING SHEAR DIRECTION USING LIQUID CRYSTAL COATINGS Patent
Daniel C. Reda 7 Mar. 1995 6 p Filed 16 Mar. 1993
(NASA-Case-ARC-11995-1; US-Patent-5,394,752;
US-Patent-Appl-SN-031972; US-Patent-Class-73-800;
US-Patent-Class-356-32; Int-Patent-Class-G01B-11/16;
Int-Patent-Class-C09K-19/00) Avail: US Patent and Trademark Office
A method is provided for determining shear direction wherein a beam of white light is directed onto the surface of a liquid crystal coating to cause the white light to be dispersed (reflected) from the surface in a spectrum having bands of different colors in a fixed spatial 2 (angular) sequence. The system is calibrated by locating an observer, e.g., a video and movie camera, such that a particular color band (preferably at or near the center of the reflected spectrum) is observed to thereby provide a reference color band. Because the application of shear causes either clockwise or counterclockwise rotation of the reflected spectrum dependent on the direction of the shear, a determination is then made of the reflected color band observed by the observer when the surface of the liquid crystal is subjected to shear to thereby determine the direction of the shear based on the directional (rotation) relation of the observed color band with respect to the reference color band in the spatial sequence of color bands. Official Gazette of the U.S. Patent and Trademark Office

N95-26173 Environmental Research Inst. of Michigan, Ann Arbor, MI.
INFRARED MULTISPECTRAL SENSOR PROGRAM, PHASE 2. FIELD MEASUREMENTS, ANALYSIS AND MODELING. VOLUME 1: FOURIER TRANSFORM SPECTROMETER SENSOR CHARACTERIZATION Final Technical Report, 1 Jan. - 31 Dec. 1993
J. N. Cederquist, M. T. Eismann, C. R. Schwartz, J. H. Selding, and A. D. Stocker May 1994 158 p
(Contract F33615-90-C-1441)
(AD-A288888; ERIM-232300-54-F-Vol-1; WL-TR-94-1095-Vol-1) Avail: Issuing Activity (Defense Technical Information Center (DTIC))
A data collection sensor based on a Bomem Fourier transform spectrometer was used to measure infrared multispectral target/background signatures. This report describes the data collection sensor, including data processing software for quick look data analysis, gives the sensor characteristics test procedures and their results, and analyzes the effect of the sensor characteristics on the quality of the measured signatures.The sensor gives a very high level of performance including noise equivalent spectral radiances of 1 nW/sq cm sr cm-1 in the MWIR (3 to 5 micrometers) region and 6 nW/sq cm sr cm-1 in the LWIR (8 to 12 micrometers region), a relative calibration accuracy to less than 0.25% above 4 micrometers, and spectral band-to-band correlation preservation greater than 0.9999 in the LWIR, and greater than 0.9995 between MWIR and LWIR and within the 4 to 5 micrometers region of the MWIR. DTIC

N95-26198# Aerospace Corp., El Segundo, CA. Engineering and Technology Group.
CALCULATION OF LIGHT SCATTERING FROM A SPHERICAL PARTICLE ON A SURFACE BY THE MULTIPOLE EXPANSION METHOD
B. R. Johnson 30 Apr. 1995 39 p
(ATR-95(9558)-2) Avail: CASI HC A03/MF A01
The multipole expansion method for calculating light scattering from a spherical particle on or near a smooth surface is reviewed and presented, with special attention to symmetry, to reduce the computational effort. Formulas for the scattering amplitude and the differential scattering cross section are presented. In addition, useful new formulas are derived for the absorption and extinction cross sections. The theory is exact in the limiting case that the substrate is a perfect conductor, but an approximation is needed at a crucial stage of the calculation to handle problems with dielectric substrates. To test the approximation, a series of test calculations for particles on dielectric substrates was carried out. The results of these tests are presented and compared to previously published 'benchmark' calculations for the same problems. Author

75 PLASMA PHYSICS

Includes magnetohydrodynamics and plasma fusion.
For ionospheric plasmas see *46 Geophysics*. For space plasmas see *90 Astrophysics*.

N95-24270# Japan Atomic Energy Research Inst., Naka (Japan). Fusion Plasma Research Dept.
FUSION-NEUTRON DIAGNOSTIC ON THE MICROWAVE TOKAMAK EXPERIMENT
Toshihide Ogawa, Kazumi Oasa, Katsumichi Hoshino, Kazuo Odajima, and Hikosuke Maeda Feb. 1994 50 p Sponsored by the DOE-JAERI collaborative program for the MTX project
(Contract W-7405-eng-48; Proj. MTX)
(DE94-777530; JAERI-M-94-021) Avail: CASI HC A03/MF A01
A neutron diagnostic system, which was designed and constructed for the Microwave Tokamak Experiment (MTX) at the Lawrence Livermore National Laboratory, has been installed and operated on that experiment. The system consisted of two different types of neutron detectors. A plastic scintillator with a nanosecond response was used for high-speed neutron measurements for the purpose of studying the intense FEL microwave absorption process. The temporal resolution of this system was limited to 2 kHz by counting statistics for standard ohmic plasma. A proportional counter array with a polyethylene neutron moderator was used to determine global neutron production for a wide range of source strengths above 10(exp 8) n/s. This system was calibrated with a Cf-252 neutron source in the MTX vacuum vessel. The time behavior of ion temperature was evaluated from the neutron production rates using line-averaged electron densities for each MTX shot. DOE

N95-24271# Japan Atomic Energy Research Inst., Naka (Japan). Fusion Plasma Research Dept.
DEVELOPMENT OF A FAST RESPONSE ROTATING POLARIMETER FOR A FARADAY ROTATION MEASUREMENT
Masaki Maeno, Norio Ogiwara, Hiroaki Ogawa, and Toshiaki Matsuda 2 Feb. 1994 22 p
(DE94-777532; JAERI-M-94-039) Avail: CASI HC A03/MF A01
This paper describes a method for using a spindle sustained with active magnetic bearing to make a rotating half waveplate frequency more fast. The time interval of the zero-cross phase measurement is 189 microseconds in this experiment. The magnetic bearing is applicable to increase the rotating waveplate frequency by a factor of 2-3 compared with the conventional one. The waveplate speed as well as the deviation with respect to the stationary laser beam has no influence on the amplitude and phase shift of the rotating polarized beam signal. There is also no influence of the mirror reflections on the phase shift. The overall phase resolution is estimated to be about 0.1 degrees. DOE

N95-24272# Japan Atomic Energy Research Inst., Naka (Japan). Fusion Plasma Research Dept.
A PROPOSAL TO INTRODUCE A TURBULENCE FACTOR INTO A

DIFFUSION COEFFICIENT OF A TOKAMAK PLASMA
Hiroshi Aikawa 1 Feb. 1994 17 p
(DE94-777533; JAERI-M-94-035) Avail: CASI HC A03/MF A01

It is proposed that a diffusion coefficient (D), which is well known to be anomalous in usual Tokamak plasmas as a result of the turbulences caused by the several instabilities, can be expressed with a measure of turbulence, i.e. a so-called 'Reynolds number' (R(sub e)), in the following manner, D approximately (omega/k(sub perpendicular)(exp 2)) R(sub e)(exp 1/(R(sub e) + beta)) where R(sub e) approximately (gamma/omega), and (omega), (gamma), (k(sub perpendicular)) are respectively a representative frequency, a growth rate, and a wave number in the radial direction of the responsible instability, beta being a numerical factor around 0 - 0.5, introduced for the sake of adjustment caused by unsolved ambiguities. As sample cases of the instabilities, various types of the drift waves are studied. The proposal is discussed from the viewpoint of a general stochasticity on the basis of the simplified nonlinear oscillator model with use of the mixing-length argument to find the aforementioned relation by a heuristic way. It should be noticed that the proposal is still not definite, including the intrinsic ambiguities resulting from nonlinearity, and should be modified by more advanced nonlinear studies in the future. DOE

N95-24311# Japan Atomic Energy Research Inst., Naka (Japan). Fusion Plasma Research Dept.
OUTLINE OF FAST ANALYZER FOR MHD EQUILIBRIUM FAME
Shinya Sakata, Hirofumi Haginoya, Takuya Tsuruoka, Tetsuo Aoyagi, Naoyuki Saito, Hiroo Harada, Keiji Tani, and Hideto Watanabe 14 Feb. 1994 38 p In JAPANESE; In Japanese Original contains color illustrations
(DE94-777540; JAERI-M-94-050) Avail: CASI HC A03/MF A01

The FAME (Fast Analyzer for Magnetohydrodynamic (MHD) Equilibrium) system has been developed in order to provide more than 100 MHD equilibria in time series which are enough for the non-stationary analysis of the experimental data of JT-60 within about 20 minutes shot interval. The FAME is an MIMD type small scale parallel computer with 20 microprocessors which are connected by a multi-stage switching system. The maximum theoretical speed is 250 MFLOPS. For the software system of FAME, MHD equilibrium analysis code SELENE and its input data production code FBI are tuned up taking the parallel processing into consideration. Consequently, the computational performance of the FAME system becomes more than 7 times faster than the existing general purpose computer FACOM M780-10s. This report summarizes the outline of the FAME system including hardware, soft-ware and peripheral equipments. DOE

N95-24490# Lawrence Livermore National Lab., Livermore, CA.
UEDGE AND DEGAS MODELING OF THE DIII-D SCRAPE-OFF LAYER PLASMA
M. E. Genstermacher, G. D. Porter, M. E. Rensink, T. D. Rognlien, S. L. Allen, D. N. Hill, C. J. Lasnier, T. Leonard (General Atomics Co., San Diego, CA.), and T. Petrie (General Atomics Co., San Diego, CA.) May 1994 63 p Presented at the 11th International Conference on Plasma Surface Interactions in Controlled Fusion Devices, Mito, Japan, 23-27 May 1994
(Contracts W-7405-eng-48; DE-AC03-89ER-51114)
(DE95-003652; UCRL-JC-115491; CONF-940580-23) Avail: CASI HC A04/MF A01

This paper presents the results of work to develop benchmarked theoretical models of scrape-off-layer (SOL) characteristics in diverted tokamaks by comparing shot simulations using the UEDGE plasma fluid and DEGAS Monte-Carlo neutral particle transport codes to measurements of the DIII-D SOL plasma. The available experimental data include the radial profiles of electron density and temperature, the ion temperature, the divertor exhaust power, the intensity of H(sub alpha) emission, and profiles of the radiated power. A very simple model of the anomalous perpendicular transport rates produces consistency between the calculated and measured radial profiles of the divertor power, and of the midplane densities and temperatures. Experimentally, measured exhaust power is now typically 80-90% of the input power. The simulated peak power on the outer leg of the divertor floor is now within about 20% of the measured power. Various sensitivities of the simulation and measurement comparisons to model assumptions are described. Finally, these benchmarked models have been used to examine the effects of various baffle configurations for the Radiative Divertor Upgrade in DIII-D. DOE

N95-24511# Japan Atomic Energy Research Inst., Tokyo (Japan).
PHASE 3 EXPERIMENTS OF THE JAERI/USDOE COLLABORATIVE PROGRAM ON FUSION BLANKET NEUTRONICS. VOLUME 1: EXPERIMENT
Yukio Oyama, ed., Chikara Konno, Yujiro Ikeda, Fujio Maekawa, Kazuaki Kosako, Tomoo Nakamura, Hiroshi Maekawa, Mahmoud Z. Youssef (California Univ., Los Angeles, CA.), Anil Kumar (California Univ., Los Angeles, CA.), and Mohamed A. Abdou (California Univ., Los Angeles, CA.) et al Feb. 1994 212 p
(DE94-777528; JAERI-M-94-015-Vol-1) Avail: CASI HC A10/MF A03

A pseudo-line source has been realized by using an accelerator based D-T point neutron source. The pseudo-line source is obtained by time averaging of continuously moving point source or by superposition of finely distributed point sources. The line source is utilized for fusion blanket neutronics experiments with an annular geometry so as to simulate a part of a tokamak reactor. The source neutron characteristics were measured for two operational modes for the line source, continuous and step-wide modes, with the activation foil and the NE213 detectors, respectively. In order to give a source condition for a successive calculational analysis on the annular blanket experiment, the neutron source characteristics was calculated by a Monte Carlo code. The reliability of the Monte Carlo calculation was confirmed by comparison with the measured source characteristics. The shape of the annular blanket system was a rectangular with an inner cavity. The annular blanket was consist of 15 mm-thick first wall (SS304) and 406 mm-thick breeder zone with Li2O at inside and Li2CO3 at outside. The line source was produced at the center of the inner cavity by moving the annular blanket system in the span of 2 m. Three annular blanket configurations were examined; the reference blanket, the blanket covered with 25 mm thick graphite armor and the armor-blanket with a large opening. The neutronics parameters of tritium production rate, neutron spectrum and activation reaction rate were measured with specially developed techniques such as multi-detector data acquisition system, spectrum weighting function method and ramp controlled high voltage system. The present experiment provides unique data for a higher step of benchmark to test a reliability of neutronics design calculation for a realistic tokamak reactor. DOE

N95-24544# Lawrence Livermore National Lab., Livermore, CA.
FLOW-THROUGH Z-PINCH STUDY FOR RADIATION GENERATION AND FUSION ENERGY PRODUCTION
Charles W. Hartman, James L. Eddleman, Ralph Moir, and U. Shumlak (Phillips Lab., Kirtland AFB, NM.) 20 Jun. 1994 5 p Presented at the 11th Topical Meeting on the Technology of Fusion Energy, New Orleans, LA, 19-24 Jun. 1994
(Contract W-7405-eng-48)
(DE95-004209; UCRL-JC-117669; CONF-940630-51) Avail: CASI HC A01/MF A01

We discuss a high-density fusion reactor which utilizes a flow-through Z pinch magnetic confinement configuration. Assessment of this reactor system is motivated by simplicity and small unit size (few hundred MWe) and immunity to plasma contamination made possible at high density. The type reactor discussed here would employ a liquid Li vortex as the first wall/blanket to capture fusion neutrons with minimum induced radioactivity and to achieve high wall loading and a power density of 200 w/cm(exp 3). DOE

N95-24548# Lawrence Livermore National Lab., Livermore, CA.
THE PHYSICS DESIGN OF THE TOKAMAK PHYSICS EXPERIMENT
K. I. Thomassen, D. B. Batchelor, and J. Bialek Aug. 1994 9 p Presented at the 15th International Conference on Plasma Physics and Controlled Nuclear Fusion Research, Seville, Spain, 26 Sep. - 1 Oct. 1994
(Contract W-7405-eng-48)
(DE95-003649; UCRL-JC-118496; IAEA-CN-60-I-2; CONF-940933-16)
Avail: CASI HC A02/MF A01

The physics approaches to improved, steady-state tokamak reactors, as evolved through reactor design studies, ideas based on experimental results, and better theoretical understanding, are the foundation for the mission and physics design of the Tokamak Physics Experiment (TPX). The mission of TPX is to develop the scientific basis for cost-competitive, continuously operating tokamak power plants. We report here the design status of TPX, a device optimized to achieve improved performance through strong plasma shaping, recycling control, and current profile shaping, while

operating continuously. The design incorporates poloidal field flexibility for a wide range of operation in normalized beta and internal inductance, a double-null 'Vee' divertor configuration for power and particle control, internal and external n (ne) 0 coils, as well as passive stabilizers, for control of MHD activity, and remote maintenance for continuous high-power operation in deuterium. Having superconducting poloidal and toroidal coils, the TPX device itself is capable of continuous operation, although initially auxiliary equipment limits the pulse length to 1000 sec. DOE

N95-24552# Idaho National Engineering Lab., Idaho Falls, ID.
MAGNETICALLY CONTROLLED DEPOSITION OF METALS USING GAS PLASMA Quarterly Progress Report, Jul. - Sep. 1994
1995 23 p
(Contract DE-FG07-93ID-13220)
(DE95-003827; DOE/ID-13220/T2) Avail: CASI HC A03/MF A01

This document reports the status of grant DE-FE07-93ID13220 for the July-September, 1994 quarter. The objective of this grant is to develop a method of spraying materials on a substrate in a controlled manner to eliminate the waste inherent in the present process. Thin layers of secondary material are plated on substrates either by plating or spraying processes. Plating operations produce large amounts of hazardous liquid waste. Spraying, while one of the less waste intensive methods, produces 'over spray' which is waste that is a result of the uncontrolled nature of the spray stream. In many cases the over spray produces a hazardous waste. DOE

N95-24585# Japan Atomic Energy Research Inst., Tokyo (Japan).
HIGH HEAT FLUX EXPERIMENT ON B4C-CONVERTED CARBON BASED MATERIALS FOR PLASMA FACING MATERIALS OF JT-60U
Kazuyuki Nakamura, Hiroshi Ishikawa (Power Reactor and Nuclear Fuel Development Corp., Tokyo, Japan.), Toshiro Ando, Kazuyoshi Satoh, Kenji Yokoyama, Satoshi Suzuki, Masayuki Dairakum, Masanori Araki, and Masato Akiba Mar. 1994 35 p In ENGLISH and JAPANESE
(DE94-777545; JAERI-M-94-046) Avail: CASI HC A03/MF A01

High heat flux experiments have been previously carried out on three kinds, namely low pressure plasma spray (LPPS), chemical vapor deposition (CVD) and conversion (CVR) methods, of B4C-overlaid CFC's using the JAERI electron beam irradiation system (JEBIS). As a result, it turned out that CVR method has the best adhesion property between B4C layer and bulk carbon. However, thicker B4C layer is necessary to use in long period as the divertor tiles of JT-60U. The purpose of this experiment is to investigate the thermal property of B4C-converted carbon based materials which have thicker B4C layer than the previous experiments. Irradiations were performed under two different heating conditions, namely in the normal condition (5-20 MW/m(exp 2), 5 s) and in the disruption conditions (1100-1600 MW/m(exp 2), 2-3 ms). The dimensions of the samples were 25 mm x 25 mm x 25 mm, and B4C-converted layers were made on the three kinds of CFC's and fifth kinds of isotropic graphites. The thickness of B4C layer was 150-1300 (mu)m. Measurements were made with respect to the weight loss, changes of the surface morphology and the surface temperature. In the normal condition, the damages such as surface melting and exfoliation were not observed on the samples which have B4C layer below 600 (mu)m in thickness. In the disruption condition, melting and exfoliation were observed on the surfaces of the samples whose substrates were PD-330S, PD-600S and HCB-5S, and melting was observed on the surfaces of the samples whose substrates were PCC-2S, MFC-1, MCI-felt, ETP-10 and STP-60. It is considered that the porous layer in the B4C layer caused the severe exfoliation from the measurement of the surface composition. DOE

N95-24587# Texas Univ., Austin, TX.
TRANSPORT SUPPRESSION BY DIAMAGNETIC PHASE SHIFT AS A POSSIBLE MECHANISM TO THE L TO H TRANSITION
M. B. Isichenko and P. H. Diamond (California Univ., San Diego, La Jolla, CA.) 28 Sep. 1994 10 p
(Contracts DE-FG05-88ER-53266; DE-FG03-94ER-54241)
(DE95-003345; DOE/ER-53266/48; FRCR-451) Avail: CASI HC A02/MF A01

In the presence of a pressure gradient, the phase velocity of drift-wave or ITG-mode turb ice is different from the poloidal E x B rotation velocity of guiding centers. This results in an E x B turbulent particle diffusion being suppressed by the phase shift due to the diamagnetic rotation velocity upsilon(sub theta) = (c/enB)dP/dr. This shift cannot be eliminated by a frame change and affects the plasma transport. For upsilon(sub theta) well above the turbulent velocity v = -c grad phi x B/B(exp 2), the radial diffusivity is suppressed as D proportional to upsilon(sub theta)(exp -3). This results in a non-monotonous particle flux Gamma(grad n) approx equal - D(sub 0) grad n (1 + alpha(grad n)(exp 2))(sup 3/2) such as the transport can develop a bifurcation at a realistic density gradient. DOE

N95-24602# Wisconsin Univ., Madison, WI.
ADVANCES AND PROSPECTS IN REVERSED FIELD PINCH RESEARCH
S. C. Prager Dec. 1994 6 p Presented at the 6th International Toki Conference on Plasma Physics and Controlled Nuclear Fusion: Research for Advanced Concepts in Magnetic Fusion, Toki-city, Japan, 29 Nov. - 2 Dec. 1994
(Contract DE-FG02-85ER-53198)
(DE95-007017; DOE/ER-53198/254; CONF-941182-1) Avail: CASI HC A02/MF A01

The reactor attributes of the compact, high beta RFP are as needed today as when the RFP was conceived. Confinement is a dominant scientific issue at present. In the past several years magnetic fluctuations have been shown experimentally to drive anomalous transport. From an understanding of the cause of transport, it is expected that flattening of the current density profile should suppress fluctuations and transport. Inductive current profile control has succeeded in reducing fluctuations, and doubling the energy and particle confinement times. For steady state current profile control, electrostatic current injection (dc helicity injection) is under preparation and rf current drive (fast wave and lower hybrid) has been shown to be feasible. DOE

N95-24619# Wisconsin Univ., Madison, WI.
TRANSPORT REDUCTION BY CURRENT PROFILE CONTROL IN THE REVERSED FIELD PINCH
J. S. Sarff, A. F. Almagri, and M. Cekic Nov. 1994 28 p
(Contract DE-FG02-85ER-53198)
(DE95-007016; DOE/ER-53198/253) Avail: CASI HC A03/MF A01

An auxiliary poloidal inductive electric field applied to a reversed field pinch (RFP) plasma reduces the current density gradient, slows the growth of m = 1 tearing fluctuations, suppresses their associated sawteeth, and doubles the energy confinement time. This experiment attacks the dominant RFP plasma loss mechanism of parallel streaming in a stochastic magnetic field. The auxiliary electric field flattens the current profile and reduces the magnetic fluctuation level. Since a toroidal flux change linking the plasma is required to generate the inductive poloidal electric field, the current drive is transient to avoid excessive perturbation of the equilibrium. To sustain and enhance the improved state, electrostatic and RF current drivers are being developed. A novel electrostatic current drive scheme uses a plasma source for electron injection, and the lower-hybrid wave is a good candidate for RF current drive. DOE

N95-24646# General Atomics Co., San Diego, CA.
EXPERIMENTAL AND THEORETICAL BASIS FOR ADVANCED TOKAMAKS
V. S. Chan Sep. 1994 15 p Presented at the ISPP Workshop on Tokamak Concept Improvement, Varenna, Italy, 29 Aug. - 3 Sep. 1994 Submitted for publication
(Contracts DE-AC03-89ER-51114; DE-FG03-92ER-54150; DE-AC05-84OR-21400; W-7405-eng-48)
(DE95-003255; GA-A-21813; CONF-9408189-1) Avail: CASI HC A03/MF A01

In this paper, arguments will be presented to support the attractiveness of advanced tokamaks as fusion reactors. The premise that all improved confinement regimes obtained to date were limited by magnetohydrodynamic stability will be established from experimental results. Accessing the advanced tokamak regime, therefore, requires means to overcome and enhance the beta limit. We will describe a number of ideas involving control of the plasma internal profiles, e.g. to achieve this. These approaches will have to be compatible with the underlying mechanisms for confinement improvement, such as shear rotation suppression of turbulence. For steady-state, there is a trade-off between full bootstrap current operation and the ability to control current profiles. The coupling between current drive and stability dictates the choice of sources and suggests an optimum for the bootstrap fraction. We summarize by presenting the future plans of

the US confinement devices, DIII-D, PBX-M, C-Mod, to address the advanced tokamak physics issues and provide a database for the design of next-generation experiments. DOE

N95-24650# Lawrence Livermore National Lab., Livermore, CA.
DIVERTOR DESIGN FOR THE TOKAMAK PHYSICS EXPERIMENT
D. N. Hill, B. Braams (New York Univ., New York, NY.), J. N. Brooks (Argonne National Lab., IL.), D. N. Ruzic (Illinois Univ., Urbana, IL.), M. Ulrickson (Sandia National Labs., Albuquerque, NM.), K. A. Werley (Los Alamos National Lab., NM.), R. Campbell (Sandia National Labs., Albuquerque, NM.), R. Goldston (Princeton Univ., NJ.), T. Kaiser, and G. H. Nellson (Oak Ridge National Lab., TN.) et al May 1994 39 p Presented at the 11th International Conference on Plasma Surface Interactions in Controlled Fusion Devices, Mito, Japan, 23-27 May 1994
(Contracts W-7405-eng-48; DE-AC02-76CH-03073)
(DE95-003653; UCRL-JC-115492; CONF-940580-22) Avail: CASI HC A03/MF A01

In this paper we discuss the present divertor design for the planned TPX tokamak, which will explore the physics and technology of steady-state (1000s pulses) heat and particle removal in high confinement (2-4 x L-mode), high beta (beta(sub N) greater than or equal to 3) divertor plasmas sustained by non-induct ive current drive. The TPX device will operate in the double-null divertor configuration, with actively cooled graphite targets forming a deep (0.5 m) slot at the outer strike point. The peak heat flux on, the highly tilted (74 deg) from normal) re-entrant (to recycle ions back toward the separatrix) will be in the range of 4-6 MW/sq m with 18 MW of neutral beams and RF heating power. The combination of active pumping and gas puffing (deuterium plus impurities), along with higher heating power (45 MW maximum) will allow testing of radiative divertor concepts at ITER-like power densities. DOE

N95-24667# Los Alamos National Lab., NM.
HYDRODYNAMIC INSTABILITIES IN INERTIAL CONFINEMENT FUSION
N. M. Hoffman 1994 36 p Presented at the 45th Scottish Universities Summer School in Physics, Fife, England, 7-20 Aug. 1994
(Contract W-7405-eng-36)
(DE95-003663; LA-UR-94-3945; CONF-9408127-5) Avail: CASI HC A03/MF A01

The focus of the paper is on buoyancy-driven instabilities of the Rayleigh-Taylor type, which are commonly regarded as the most important kind of hydrodynamic instability in inertial-confinement-fusion implosions. The paper is intended to be pedagogical rather than research-oriented, and so is by no means a comprehensive review of work in this field. Rather, it is hoped that the student will find here a foundation on which to build an understanding of current research, and the experienced researcher will find a compilation of useful results. The aim of the paper is to discuss the evolution of a single Rayleigh-Taylor unstable mode, from its linear phase to its late-stage constant-velocity bubble growth, with a brief consideration of the saturation of linear growth. The influence of other modes in invoked only in the short-range sense (in wavenumber space) of the Haan saturation model. Owing to limitations of space, the treatment of other instabilities such as Richtmyer-Meshkov and Kelvin-Helmholtz is necessarily very brief, and entirely inadequate as an introductory discussion. Likewise, there is no reference to the effect of convergent geometry, to long-range mode coupling, or to shape effects in three-dimensional growth. Furthermore, there is no reference to the large body of experimental research related to hydrodynamic instabilities. DOE

N95-24706# Israel Atomic Energy Commission, Yavneh (Israel). Nuclear Research Center.
EXPERIMENTAL AND THEORETICAL STUDY OF PLASMA-WATER INTERACTION IN ELECTROTHERMAL GUNS Ph.D. Thesis
Alex Arensburg May 1993 122 p
(DE94-628961; IA-1479) Avail: CASI HC A06/MF A02 (US Sales Only)

This thesis comprises an experimental and theoretical study of the plasma-jet-water interaction in electrothermal guns. In the present work the plasma jet was produced by high current pulsed discharge in a plasma injector consisting of polyethylene capillary, closed at one end by a metallic anode and supported at the other end with a hollow cathode. A thin aluminium fuse placed inside the capillary and connecting both electrodes, provided an initial conducting element. A pulse forming network delivering a high current pulse through the fuse, exploded it and produced an aluminium plasma. Subsequently, ablation of the capillary wall begun as a result of its exposure to radiation from the fuse plasma. The ablation products were heated by the pulse current until ionized, replacing the fuse plasma by a polyethylene plasma thus sustaining the ablation process. The experimental investigation reported here used x-ray shadowgraphy to observe the plasma-working fluid interaction process. The working fluid was an aqueous solution of 92% water and 8% lead acetate gelatinized with agar. The penetration of the plasma jet into the working fluid was exposed on films at successive time intervals by means of x-ray shadowgraphy. When the water interacts with the plasma it also ablates. This ablation rate was estimated from energy conservation considerations. Peak pressures up to 3.5 x 10(exp 8) Pa were measured during the process. At such pressure, water does not undergo phase transformation when heated. Thus the mass density at the plasma water interface should be regarded as a continuous function of temperature. The determination of the temperature profile at the interface between the capillary plasma and the water requires the solution of the heat transfer and radiative transfer equations under ablation conditions. This constituted the main theoretical part of the present work. DOE

N95-24861# Argonne National Lab., Idaho Falls, ID.
MODELING PLASMA/MATERIAL INTERACTIONS DURING A TOKAMAK DISRUPTION
Ahmed Hassanein and Isak K. Konkashbaev (Troitsk Inst. for Innovation, Troitsk, Russia.) Oct. 1994 20 p
(Contract W-31-109-eng-38)
(DE95-004247; ANL/FPP/TM-271) Avail: CASI HC A03/MF A01

Disruptions in tokamak reactors are still of serious concern and present a potential obstacle for successful operation and reliable design. Erosion of plasma-facing materials due to thermal energy dump during a disruption can severely limit the lifetime of these components, therefore diminish the economic feasibility of the reactor. A comprehensive disruption erosion model which takes into account the interplay of major physical processes during plasma-material interaction has been developed. The initial burst of energy delivered to facing-material surfaces from direct impact of plasma particles causes sudden ablation of these materials. As a result, a vapor cloud is formed in front of the incident plasma particles. Shortly thereafter, the plasma particles are stopped in the vapor cloud, heating and ionizing it. The energy transmitted to the material surfaces is then dominated by photon radiation. It is the dynamics and the evolution of this vapor cloud that finally determines the net erosion rate and, consequently, the component lifetime. The model integrates with sufficient detail and in a self-consistent way, material thermal evolution response, plasma-vapor interaction physics, vapor hydrodynamics, and radiation transport in order to realistically simulate the effects of a plasma disruption on plasma-facing components. Candidate materials such as beryllium and carbon have been analyzed. The dependence of the net erosion rate on disruption physics and various parameters was analyzed and is discussed. DOE

N95-25102# General Atomics Co., San Diego, CA.
THE ROLE OF SHAPING IN ACHIEVING HIGH PERFORMANCE IN DIII-D
E. A. Lazarus (Oak Ridge National Lab., TN.), A. W. Hyatt, T. H. Osborne, S. E. Attenberger (Oak Ridge National Lab., TN.), M. E. Austin (Maryland Univ., College Park, MD.), K. H. Burrell, T. A. Casper (Lawrence Livermore National Lab., Livermore, CA.), M. S. Chu, J. W. Cuthbertson (Sandia National Labs., Albuquerque, NM.), and E. J. Doyle (California Univ., Los Angeles, CA.) et al Oct. 1994 16 p Presented at the 15th International Conference on Plasma Physics and Controlled Nuclear Fusion Research, Seville, Spain, 26 Sep. - 1 Oct. 1994
(Contracts DE-AC03-89ER-51114; DE-AC05-84OR-21400; W-7405-eng-48; DE-AC04-94AL-85000; DE-FG03-89ER-51121; GA Proj. 3466)
(DE95-003877; GA-A-21807; IAEA-CN-60/A-5-I-1; CONF-940933-23)
Avail: CASI HC A03/MF A01

Experiments to study the effect of plasma shape on performance show that the high performance levels characteristic of VH-mode plasmas are only obtained for high triangularity (delta). A characteristic difference in central heating efficiency is observed when high and low (delta) plasmas are compared. The authors find this difference to correlate well with the attainment of Mercier stability. The core plasma for the high (delta) cases achieves Mercier stability when q(sub 0) rises above a critical value which depends on (delta), providing direct access to the second-stable regime.

Other attributes of the VH-mode commence after a delay. The rise in q(sub 0) is attributable to the radial gradients in the neutral beam and bootstrap current sources. Simulation indicates that such plasmas would persist for many seconds if the rise in density could be controlled, maintaining a centrally peaked neutral beam deposition profile. DOE

N95-25108# General Atomics Co., San Diego, CA.
A VACUUM WINDOW FOR A 1 MW CW 110 GHz GYROTRON
C. P. Moeller, J. L. Doane, and M. DiMartino Jul. 1994 3 p Presented at the 19th International Conference on Infrared and Millimeter Waves, Sendai, Japan, 17-21 Oct. 1994
(Contracts DE-AC03-89ER-51114; DE-AC03-89ER-52153)
(DE94-016584; GA-A-21741; CONF-9410163-1) Avail: CASI HC A01/MF A01

Development of high power microwave sources for fusion applications is limited by the availability of suitable vacuum windows in the 100 to 200 GHz frequency range. A novel vacuum window uses water cooled sapphire as the dielectric. Heat removal is achieved by using thin slats of sapphire interleaved and brazed to niobium hexagonal tubes in which the cooling water flows. Analysis indicates a window 100 cm(sup 2) in area can readily pass 1 MW in the HE(sub 11) mode at 110 GHz for current experimental applications and 1 MW with a HE(sub 11)(sup 0)-HE(sub 12)(sup 0) mixture at 170 GHz, the projected international thermonuclear fusion experimental reactor (ITER) frequency. DOE

N95-25120# General Atomics Co., San Diego, CA.
RESULTS OBTAINED USING THE PELLET CHARGE EXCHANGE DIAGNOSTIC ON TFTR
J. M. McChesney, R. K. Fisher, P. B. Parks, H. H. Duong (California Univ., Irvine, CA.), D. K. Mansfield (Princeton Univ., NJ.), S. S. Medley (Princeton Univ., NJ.), A. L. Roquemore (Princeton Univ., NJ.), and M. P. Petrov (Ioffe, A. F. Physical-Technical Inst., Saint Petersburg, Russia.) May 1994 15 p Presented at the 10th Topical Conference on High-temperature Plasma Diagnostics, Rochester, NY, 8-12 May 1994
(Contracts DE-FG03-92ER-54150; DE-AC02-76CH-03073)
(DE95-003254; GA-A-21709; CONF-940552-33) Avail: CASI HC A03/MF A01

Experiments are underway on TFTR to measure the confined alpha particle distribution functions using small low-Z pellets injected into the plasma. Upon entering the plasma, the pellet ablates, forming a plasma ablation cloud, elongated in the magnetic field direction, that travels alongside the pellet. A small fraction of the fusion produced 3.5 MeV alpha particles incident on the cloud are converted to helium neutrals. By measuring the resultant helium neutrals escaping from the plasma by means of a mass and energy resolving charge exchange analyzer, the energy distribution of the alpha particles incident on the cloud can be inferred. Preliminary experiments to observe neutrals from the 100-1000 keV He-3 tail produced during ICRF minority heating experiments were successful. However, no significant alpha particle signals have been observed during D-T operation on TFTR. The authors attribute this lack of signal to stochastic toroidal field ripple loss in the outer regions of the plasma. They are studying ways to improve the pellet penetration so that the pellet penetrates into the central regions of the plasma where ripple induced losses are small and the alpha population is high. DOE

N95-25216# Texas Univ., Austin, TX. Inst. for Fusion Studies.
ENERGETIC PARTICLE DRIVE FOR TOROIDICITY-INDUCED ALFVEN EIGENMODES AND KINETIC TOROIDICITY-INDUCED ALFVEN EIGENMODES IN A LOW-SHEAR TOKAMAK
B. N. Breizman and S. E. Sharapov (Joint European Torus Project, Abingdon, England.) Oct. 1994 31 p Revised
(Contract DE-FG05-80ET-53088)
(DE95-003222; DOE/ET-53088/671; IFSR-671) Avail: CASI HC A03/MF A01

The structure of toroidicity-induced Alfven eigenmodes (TAE) and kinetic TAE (KTAE) with large mode numbers is analyzed and the linear power transfer from energetic particles to these modes is calculated in the low shear limit when each mode is localized near a single gap within an interval whose total width Delta(sup out) is much smaller than the radius r(sub m) of the mode location. Near its peak where most of the mode energy is concentrated, the mode has an inner scalelength Delta(sup in), which is much smaller than Delta(sup out). The scale Delta(sup in) is determined by toroidicity and kinetic effects, which eliminate the singularity of the potential at the resonant surface. This work examines the case when the drift orbit width of energetic particles Delta(sub b) is much larger than the inner scalelength Delta(sup in), but arbitrary compared to the total width of the mode. It is shown that the particle-to-wave linear power transfer is comparable for the TAE and KTAE modes in this case. The ratio of the energetic particle contributions to the growth rates of the TAE and KTAE modes is then roughly equal to the inverse ratio of the mode energies. It is found that, in the low shear limit the growth rate of the KTAE modes can be larger than that for the TAE modes. DOE

N95-25250# General Atomics Co., San Diego, CA.
EVIDENCE FOR MODIFIED TRANSPORT DUE TO SHEARED E X B FLOWS IN HIGH-TEMPERATURE PLASMAS
R. J. Groebner, K. H. Burrell, and M. E. Austin (Maryland Univ., College Park, MD.) Nov. 1994 9 p Presented at the International Conference on Plasma Physics, Foz do Igacu, Brazil, 31 Oct. - 4 Nov. 1994
(Contracts DE-AC03-89ER-51114; DE-AC05-84OR-21400; DE-AC04-76DP-00789; DE-FG03-86ER-53225; DE-FG02-91ER-54109; W-7405-eng-48)
(DE95-004870; GA-A-21872; CONF-9410249-2) Avail: CASI HC A02/MF A01

Sheared mass flows are generated in many fluids and are often important for the dynamics of instabilities in these fluids. Similarly, large values of the E x B velocity have been observed in magnetic confinement machines and there is theoretical and experimental evidence that sufficiently large shear in this velocity may stabilize important instabilities. Two examples of this phenomenon have been observed in the D3-D Tokamak. In the first example, sufficient heating power can lead to the L-H transition, a rapid improvement in confinement in the boundary layer of the plasma. For discharges with heating power close to the threshold required to get the transition, changes in the edge radial electric field are observed to occur prior to the transition itself. In the second example, certain classes of discharges with toroidal momentum input from neutral beam injection exhibit a further improvement of confinement in the plasma core leading to a regime called the VH-mode. In both examples, the region of improved confinement is characterized by an increase of shear in the radial electric field E(sub r), reduced levels of turbulence, and increases in gradients of temperatures and densities. These observations are consistent with the hypothesis that the improved confinement is caused by an increase in shear of the E x B velocity which leads to a reduction of turbulence. For the VH-mode, the dominant term controlling E(sub r) is the toroidal rotation v(sub phi), indicating that the E(sub r) profile is controlled by the source and transport of toroidal momentum. DOE

N95-25283# Argonne National Lab., IL.
US TECHNICAL REPORT FOR THE ITER BLANKET/SHIELD Topical Report, Jul. - Nov. 1990
1995 257 p
(Contracts W-31-109-eng-38; DE-AC05-84OR-21400)
(DE95-004667; ITER-TN-BL-5-0-3) Avail: CASI HC A12/MF A03

Three solid-breeder water-cooled blanket concepts have been developed for ITER based on a multilayer configuration. The primary difference among the concepts is in the fabricated form of breeder and multiplier. All the concepts have beryllium for neutron multiplication and solid-breeder temperature control. The blanket design does not use helium gaps or insulator material to control the solid breeder temperature. Lithium oxide (Li2O) and lithium zirconate (Li2ZrO3) are the primary and the backup breeder materials, respectively. The lithium-6 enrichment is 95%. The use of high lithium-6 enrichment reduces the solid breeder volume required in the blanket and consequently the total tritium inventory in the solid breeder material. Also, it increases the blanket capability to accommodate power variation. The multilayer blanket configuration can accommodate up to a factor of two change in the neutron wall loading without violating the different design guidelines. The blanket material forms are sintered products and packed bed of small pebbles. The first concept has a sintered product material (blocks) for both the beryllium multiplier and the solid breeder. The second concept, the common ITER blanket, uses a packed bed breeder and beryllium blocks. The last concept is similar to the first except for the first and the last beryllium zones. Two small layers of beryllium pebbles are located behind the first wall and the back of the last beryllium zone to reduce the total inventory of the beryllium material and to improve the

blanket performance. The design philosophy adopted for the blanket is to produce the necessary tritium required for the ITER operation and to operate at power reactor conditions as much as possible. Also, the reliability and the safety aspects of the blanket are enhanced by using low-pressure water coolant and the separation of the tritium purge flow from the coolant system by several barriers. DOE

N95-25289# Los Alamos National Lab., NM.
MAGNETIZED TARGET FUSION: AN ULTRA HIGH ENERGY APPROACH IN AN UNEXPLORED PARAMETER SPACE
I. R. Lindemuth 1994 25 p Presented at the 1st International Symposium for Evaluation of Current Trends in Fusion Research, Washington, DC, 14-18 Nov. 1994
(Contract W-7405-eng-36)
(DE95-005252; LA-UR-94-4333; CONF-9411182-2) Avail: CASI HC A03/MF A01

Magnetized target fusion is a concept that may lead to practical fusion applications in a variety of settings. However, the crucial first step is to demonstrate that it works as advertised. Among the possibilities for doing this is an ultrahigh energy approach to magnetized target fusion, one powered by explosive pulsed power generators that have become available for application to thermonuclear fusion research. In a collaborative effort between Los Alamos and the All-Russian Scientific Institute for Experimental Physics (VNIIEF) a very powerful helical generator with explosive power switching has been used to produce an energetic magnetized plasma. Several diagnostics have been fielded to ascertain the properties of this plasma. We are intensively studying the results of the experiments and calculationally analyzing the performance of this experiment. DOE

N95-25325*# Aerospace Corp., El Segundo, CA. Space and Environment Technology Center.
PARTICLE ACCELERATION VERY NEAR AN X-LINE IN A COLLISIONLESS PLASMA
L. R. Lyons and D. C. Pridmore-Brown 15 Mar. 1995 13 p
(Grant NAGw-2126)
(ATR-92(7251)-4) Avail: CASI HC A03/MF A01

In a previous paper, we applied a simplified model for particle motion in the vicinity of a magnetic X-line that had been introduced by Dungey. We used the model to quantitatively show that an electric force along an X-line can be balanced by the gyroviscous force associated with the off-diagonal elements of the pressure tensor. Distribution functions near the X-line were shown to be skewed in azimuth about the magnetic field and to include particles accelerated to very high energies. In the present paper, we apply the previous model and use the distribution functions to evaluate the energization that results from particle interactions with the X-line. We find that, in general, this interaction gives a spectrum of energized particles that can be represented by a Maxwellian distribution. A power-law, high-energy tail does not develop. The thermal energy, K, of the Maxwellian can be expressed simply in terms of the field parameters and particle mass and charge. It is independent of the thermal energy, K(sub i), of the particle distribution incident upon the region of the X-line, provided that K(sub i) is less than K. Significant energization is not found for K(sub i) is greater than K. Author

N95-25340 Polish Academy of Sciences, Warsaw (Poland). Instytut Podstawowych Problemow Techniki.
SELECTED PROBLEMS OF THE INTERACTION OF ELECTROMAGNETIC WAVES AND A TURBULENT PLASMA [WYBRANE ZAGADNIENIA ODDZIALYWANIA FAL ELEKTROMAGNETYCZNYCH Z TURBLENTNA PLAZMA]
Barbara Atamaniuk Sep. 1993 31 p In POLISH
(ISSN 0208-5658)
(IFTR-9-1993) Avail: Issuing Activity (Polish Academy of Sciences, Warsaw, Poland)

The interaction of electromagnetic waves in a plasma may be considered a problem of non-linear electrodynamics. The electrodynamics of material media are in reality non-linear because of the non-linearity of the material equations. In this article we shall limit ourselves to the effects associated with the relatively low non-linearity of the medium, i.e. with the fact that a material equation may be represented as a series in terms of electromagnetic field intensities and limited to a finite, small number of terms. Non-linear electrodynamics has undergone especially rapid development in two fields. The first area is the theory of a slightly turbulent plasma or the non-linear interaction of the free oscillations of the plasma. The other is non-linear optics. The similarity between the two is based on the use of non-linear material (constituent) equations and approximate electromagnetic field equations to describe non-linear phenomena. The only essential difference between the two lies in the fact that turbulent plasma theory is based on the solution of problems of statistical electrodynamics in which the phase relations between the interacting waves are not fixed, while in non-linear optics the phases of the waves are fixed. We shall represent material equations as a series of multiple integrals. The construction of approximate solutions is based on the use of a finite number of terms from this series. This type of procedure is characteristic, for example, of problems of non-linear optics, the non-linear mechanics of shape memory materials (polymers), plasma electrodynamics, and so forth. In the material medium, current and charge density are induced by external sources. Author

N95-25344# Lawrence Livermore National Lab., Livermore, CA.
USING AND PROGRAMMING THE SUPERCODE
Scott W. Haney Jun. 1994 304 p
(Contract W-7405-eng-48)
(DE95-004342; UCRL-ID-118982) Avail: CASI HC A14/MF A03

SUPERCODE is a systems code used in designing tokamak devices and reactors. This report is divided into 4 chapters. Chapter one covers installing the code and directory organization. The execution of the code, command line editing and history, the shell language, classes, and shell input and output are discussed in chapter two. Chapter three covers the writing modules. In chapter four, the Consts module, Sys module, and Plot module are covered. At the end of the report, the need and use of SUPERCODE are summarized. DOE

N95-25471# Japan Atomic Energy Research Inst., Tokyo (Japan). Dept. of Fusion Plasma Research.
NUMERICAL ANALYSIS OF ELECTRON CYCLOTRON RESONANCE HEATING ON JT-60U AND JFT-2M
Kiyotaka Hamamatsu and Masafumi Azumi Mar. 1994 26 p In JAPANESE
(DE95-709766; JAERI-M-94-062) Avail: CASI HC A03/MF A01

To analyze electron cyclotron heating (ECH) in tokamak plasmas, the computational code has been developed using the ray tracing method. The propagation and absorption of electron cyclotron waves are numerically analyzed on JT-60U and JFT-2M plasmas. ECH by the extraordinary wave is studied in the frequency range of second harmonic resonance on JFT-2M plasmas. The dependence of the power absorption on plasma parameters, electron density and temperature, is obtained. On JT-60U, the ordinary and extraordinary waves are numerically analyzed in the fundamental resonance frequency range. In the case of the ordinary wave heating, it is shown that the location of power deposition can be scanned along a minor radius by controlling the horizontal angle of beam injection. As for the extraordinary wave heating, the down shift of effective cyclotron resonance frequency due the relativistic effect is investigated. In the case of that the electron temperature exceeds about 10keV, the following is cleared: The wave frequency can be sifted down to 80GHz, where the cyclotron resonance frequency is 120GHz at the plasma center, and the heating of central region is possible. DOE

N95-25495# Japan Atomic Energy Research Inst., Tokyo (Japan). Dept. of Fusion Engineering Research.
DESIGN OF FUSION SAFETY DATA BASE
Isao Aoki and Yasushi Seki Mar. 1994 68 p In JAPANESE
(DE95-703897; JAERI-M-94-044) Avail: CASI HC A04/MF A01

This report presents a data base architecture with its circumstance which is designed to be used for safety design and analysis studies. Design of Fusion Safety Data Base has been carried out to take into account a great number of published references on operation and control of fusion energy and engineering features to secure safety of fusion devices. Data Base of Fiscal Year 1993 - which has been established over an extended year - realized on PC (Personal Computer) peripherals is reported. The concept of data base architecture with its attributive issues and a manipulating way for users are also shown. DOE

N95-25498# Japan Atomic Energy Research Inst., Tokyo (Japan). Dept. of Chemistry and Fuel Research.

MEASUREMENT OF KINETIC ENERGY OF IONS COLLECTED FROM LASER RESONANCE PHOTOIONIZED PLASMA BY TIME-OF-FLIGHT METHOD

Yukinori Aishima (Ibaraki Univ., Hitachi, Japan.), Takashi Ikehata (Ibaraki Univ., Hitachi, Japan.), Hiroshi Mase (Ibaraki Univ., Hitachi, Japan.), Koichi Ogura, and Takemasa Shibata Mar. 1994 16 p In JAPANESE

(DE95-709767; JAERI-M-94-056) Avail: CASI HC A03/MF A01

Neodymium plasma was produced between parallel electrodes by laser resonance photoionization. Ions were extracted and collected on a negative electrode by applying an electric field across the electrodes. Kinetic energy of ions collected at arbitrary time during ion collection was measured by the time-of-flight method using a gate electrode set behind negative electrode. It was confirmed that the kinetic energy of ions collected is equal to V(sub 0)(eV) at any time during ion collection when electric potential V(sub 0)(V) is applied between the parallel electrodes. This method will be used for measuring the kinetic energy of ions collected by improved methods such as by applying a electric potential to a wire electrode or by applying a radio frequency voltage. DOE

N95-25555 Academy of Sciences of the Ukraine, Kiev (Ukraine). Inst. Teoreticheskoj Fiziki.

PHYSICS IN UKRAINE INTERNATIONAL CONFERENCE. VOLUME 6: PLASMA PHYSICS

A. Sitenko, ed. 1993 222 p Conference held in Kiev, Ukraine, 22-27 Jun. 1993

(DE95-606422; INIS-UA-004-Vol-6; CONF-9306388) Copyright Avail: Issuing Activity (Department of Energy (DOE)) (US Sales Only)

Problems of modern physics and the situation with physical research in Ukraine are considered. Program of the conference includes scientific and general problems. Its proceeding are published in six volumes. The papers presented in this volume refer to plasma physics. DOE

N95-25556 Academy of Sciences of the Ukraine, Kiev (Ukraine). Teoreticheskoj Fiziki.

DYNAMICS OF STRUCTURE FORMATION IN NONEQUILIBRIUM SYSTEMS (WAVE MEDIA)

A. G. Zagorodnij, A. V. Kirichok, V. M. Kuklin, and I. P. Panchenko 1994 28 p In UKRAINIAN Submitted for publication

(DE95-607609; ITF-94-4) Copyright Avail: Issuing Activity (Department of Energy (DOE)) (US Sales Only)

Structures play a significant role in the processes of energy transfer in nonequilibrium dissipative systems. The processes of dissipative structure formation and evolution in both weak nonequilibrium and strong nonequilibrium systems are described. DOE

N95-25561# Maryland Univ., College Park, MD.

MARYLAND CONTROLLED FUSION RESEARCH PROGRAM Progress Report, 1 Nov. 1993 - 31 Oct. 1994

T. M. Antonsen, Jr., J. F. Drake, J. M. Finn, P. N. Guzdar, A. Hassam, C. S. Liu, and E. Ott Jul. 1994 6 p

(Contract DE-FG02-93ER-54197)

(DE95-006642; DOE/ER-54197/2) Avail: CASI HC A02/MF A01

The theoretical research activity at the University of Maryland supported by the Department of Energy focuses on two major tasks. They are: (1) Transport, generation of shear flow and L-H transitions in Tokamaks; and (2) MHD stability of Tokamaks. Titles of specific research projects under these fields carried out in this period include: (1) Poloidal rotation of tokamak plasmas at super-poloidal-sonic speeds; (2) Rotation of plasmas in neoclassical regimes; (3) New unstable branch of drift resistive ballooning modes in tokamaks; (4) 3D fluid simulations of the drift resistive ballooning modes - twisted coordinate system; (5) Disintegration of ion banana orbits in tokamak edge plasmas; (6) Fast reconnection in high temperature plasmas; (7) Dynamics of sawtooth collapse in tokamak plasmas; (8) Effect of trapped particles on MHD modes; and (9) MHD stability of high beta toroidal equilibria. DOE

N95-25617 Academy of Sciences of the Ukraine, Kiev (Ukraine). Inst. for Theoretical Physics.

FLUCTUATIONS AND ELECTROMAGNETIC WAVE SCATTERING IN MACROSCOPICALLY AGITATED PLASMA: EFFECTS OF TURBULENT DIFFUSION

P. P. Sosenko and D. Gresillon 1994 15 p Submitted for publication

(DE95-607612; ITP-94-9) Copyright Avail: Issuing Activity (Department of Energy (DOE)) (US Sales Only)

In order to explain some observations of space and fusion plasmas, it is possible to assume that fluid-like plasma motion occurs. In this paper, fluctuation spectral distributions in such plasmas are investigated, when the renormalization of the test-particle transition probability and test-particle shielding are important. It is demonstrated that in the case of small correlation lengths for fluid-like motion, as compared to the fluctuation scale lengths, transformations of fluctuation spectral distributions are subordinated to the magnitude of a turbulent diffusion coefficient. This peculiarity can be exploited in plasma diagnostics as a tool for measuring the diffusion coefficient. This peculiarity can be exploited in plasma diagnostics as a tool for measuring the diffusion coefficient. DOE

N95-25632 Academy of Sciences of the Ukraine, Kiev (Ukraine). Inst. for Theoretical Physics.

QUASIPARTICLES IN MAGNETIZED PLASMA

P. P. Sosenko and V. K. Decyk 1994 17 p Submitted for publication

(DE95-607610; ITP-94-10) Copyright Avail: Issuing Activity (Department of Energy (DOE)) (US Sales Only)

The quasiparticle approach to the description of the magnetized plasma is reviewed. DOE

N95-25651# National Inst. for Fusion Science, Nagoya (Japan).

MEASUREMENT OF PROFILES OF THE SPACE POTENTIAL IN JIPP T-IIU TOKAMAK PLASMAS BY SLOW POLOIDAL AND FAST TOROIDAL SWEEPS OF A HEAVY ION BEAM

Y. Hamada, A. Nishizawa, Y. Kawasumi, K. Narihara, K. Sato, T. Seki, K. Toi, H. Iguchi, A. Fujisawa, and K. Adachi et al Feb. 1994 36 p

(ISSN 0915-633X)

(NIFS-273) Avail: CASI HC A03/MF A01

The use of simultaneous fast toroidal and slow poloidal sweeps of a heavy ion beam, plasma potential profiles in JIPP T-IIU Tokamak are measured at the rate of 120 spatial profiles per second. A new method to eliminate the error due to the change of out-of-plane entrance angle caused by large plasma current is successfully applied. One of the key factors is the very homogeneous characteristics of the energy analyzer along the wide slit length. A shaped electrode system, instead of guard rings with a resistor chain, successfully increases the homogeneity of an analyzer. The error due to the significant change of an in-plane entrance angle during a poloidal sweep is carefully minimized and calibrated by a secondary beam ionized by neutral gas introduced in a vacuum vessel. The depth of the measured potential at the plasma center reaches more than 1.5 keV in ohmic plasmas with the ion temperature of 600 eV. In some cases, a rather wide region of positive potential and a sharp decrease of the potential in the center of the plasma are observed. Author

N95-25653# National Inst. for Fusion Science, Nagoya (Japan).

NEW MODULAR HELIOTRON SYSTEM COMPATIBLE WITH CLOSED HELICAL DIVERTOR AND GOOD PLASMA CONFINEMENT

K. Yamazaki and K. Y. Watanabe Apr. 1995 26 p

(ISSN 0915-633X)

(NIFS-279) Avail: CASI HC A03/MF A01

A new helical system ('Modular Heliotron') with improved modular coils compatible with efficient closed helical divertor and good plasma confinement property is proposed based on a Heliotron system with continuous helical coils and one pair of poloidal coils. The physics optimization of this system as a function of the gap angle between adjacent modular coils has been carried out by means of vacuum magnetic surface calculations and finite-beta plasma analyses, and a new improved coil system is invented by combining sectored helical field coils with sectored returning poloidal field coils. The Modular Heliotron with standard coil winding law (reference Modular Heliotron) was previously proposed, but it is found that this is not appropriate to keep clean helical divertor and high beta configuration when the coil gap becomes large. By modulating the modular coil winding with outside-plus and inside-minus pitch modulation, almost the same good magnetic

configuration as that of a conventional Heliotron can be produced. The optimal gap angle is determined as a function of the modulation parameter. This improved Modular Heliotron permits larger gap angle between adjacent modules and produces more clean helical divertor configuration than the reference Modular Heliotron. All these helical system are created by only modular coils without poloidal coils. Author

N95-25759# National Inst. for Fusion Science, Nagoya (Japan).
SELF-SUSTAINED TURBULENCE AND L-MODE CONFINEMENT IN TOROIDAL PLASMAS 2
K. Itoh, S.-I. Itoh (Kyushu Univ., Kasuga, Japan), A. Fukuyama (Okayama Univ., Japan.), M. Yagi (Japan Atomic Energy Research Inst., Naka, Japan.), and M. Azumi (Japan Atomic Energy Research Inst., Naka, Japan.) 1994 42 p
(ISSN 0915-633X)
(NIFS-278) Avail: CASI HC A03/MF A01

A theory of the anomalous transport coefficient in toroidal helical systems (such as, stellarators, torsatron, and Heliotron devices) is developed. The theoretical formalism of self-sustained turbulence is applied to the interchange mode turbulence and ballooning mode turbulence. The nonlinear destabilization of microscopic modes by current diffusivity is the key for the anomalous transport. A general form of the anomalous transport coefficient in the toroidal plasmas is derived. The intrinsic importance of the pressure gradient, collisionless skin depth, and Alfven transit time is confirmed. The geometrical factors which characterize the magnetic configurations are also obtained. The theory is extended to study the influence of parallel compressibility. The ion viscosities of the perpendicular and parallel momenta, electron viscosity, and energy diffusion coefficient are obtained. A comparison with the experimental results is also given. Author

N95-25777 Academy of Sciences of the Ukraine, Kiev (Ukraine). Inst. for Theoretical Physics.
FLUCTUATIONS IN MACROSCOPICALLY AGITATED PLASMA: QUASIPARTICLES AND EFFECTIVE TEMPERATURE
P. P. Sosenko and D. Gresillon 1994 9 p Submitted for publication
(DE95-607611; ITP-94-8) Copyright Avail: Issuing Activity (Department of Energy (DOE)) (US Sales Only)

Fluctuations in the plasma, in which macroscopic fluid-like motion is agitated due to large-scale and low-frequency electro-magnetic fields, are studied. Such fields can be produced by external factors or internally, for example due to turbulence. Fluctuation spectral distributions are calculated with regard to the renormalization of the transition probability for a test-particle and of the test-particle shielding. If the correlation length for the random fluid-like motion is large as compared to the fluctuation scale lengths, then the fluctuation spectral distributions can be explained in terms of quasiparticles originating from macroscopic plasma agitation and of an effective temperature. DOE

N95-25903# Tokyo Univ. (Japan). Nuclear Engineering Research Lab.
PROCEEDINGS OF THE 2ND INTERNATIONAL WORKSHOP ON ELECTROMAGNETIC FORCES AND RELATED EFFECTS ON BLANKETS AND OTHER STRUCTURES SURROUNDING THE FUSION PLASMA TORUS
T. Takagi, ed. (Tohoku Univ., Sendai, Japan.), I. Nishiguchi, ed. (Kanagawa Univ., Japan.), and Y. Yoshida, ed. 1993 291 p Workshop held in Tokai, Japan, 15-17 Sep. 1993
(DE94-792667; UTNL-R-0302; CONF-9309405) Avail: CASI HC A13/MF A03

This publication is the collection of the papers presented at the title meeting. The subjects of the papers presented were categorized in six parts and are contained in this volume. In the first part, the valuable experiences are presented concerning electromagnetic phenomena in existing large devices or those under construction. In the 2nd part, the papers are mainly concerning on the evaluation of the electromagnetic fields and forces for the next experimental reactors. In the 3rd part, electromagnetomechanical coupling problems were treated by numerical and experimental approaches. In the part 4, numerical and experimental approaches for ferromagnetic structures are performed. In the 5th part, papers related to the structural integrity evaluation are presented. The part 6 is devoted to the proposal of the intelligent material system. A summary of the panel discussion held at the final session of the workshop is also included at the end of this volume. The 22 of the presented papers are indexed individually. DOE

N95-25904# National Inst. for Fusion Science, Nagoya (Japan).
REPORT ON THE MEETING ON CHAOTIC PHENOMENA IN PLASMA
Apr. 1994 110 p
(DE94-792670; NIFS-PROC-16) Avail: CASI HC A06/MF A02

This is a report on the meeting on Chaotic Phenomena in Plasma, held at NIFS on December 1, 1993. Eight of the present papers are indexed individually. DOE

N95-25942# China Nuclear Information Centre, Beijing (China).
PLASMA BURNING AND CONTROL IN REACTOR CORE
Qiang Xu and Yiping Chen Dec. 1993 8 p
(DE95-602882; CNIC-00808; ASIPP-0039) Avail: CASI HC A02/MF A01 (US Sales Only)

A zero-dimensional, three-fluids, time-dependent, particle and power balance code is developed. The dynamics of plasma and results of neo-classical transport theory are combined. The code is used to study control of plasma burning by auxiliary heating power, fuel injection and toroidal field ripple modulation. Results show that plasma stable burning and removing ashes can be realized. DOE

N95-25943# China Nuclear Information Centre, Beijing (China).
OPERATING LEVEL OF HT-6B TOKAMAK DEVICE
Linzhong Li, Chuanbao Deng, and Dequan Guo Sep. 1993 14 p
(DE95-602999; CNIC-00789; ASIPP-0038) Avail: CASI HC A03/MF A01 (US Sales Only)

The operating status of HT-6B tokamak device has been introduced. The extending processes of HT-6B operating regions have been analyzed. The developing cases of main parameters are discussed. By comparison with some international famous tokamak devices on normalized operating map, it has been shown that under the condition of ohmic heating the operating region of HT-6B device has achieved the same level. DOE

N95-25972# International Centre for Theoretical Physics, Trieste (Italy).
EVOLUTION OF SPARK PLASMA USING NITROGEN LASER SHADOWGRAPHY SYSTEM
G. C. Ishiekwene Jul. 1994 13 p
(DE95-607598; IC-94/142) Avail: CASI HC A03/MF A01 (US Sales Only)

A simple, low cost, home built high power nitrogen laser is used as the light source for a shadowgraphy system. A series of shadowgrams depicting the temporal growth of a spark plasma discharge is obtained. The results could be useful in plasma diagnostic studies. DOE

N95-25974# International Centre for Theoretical Physics, Trieste (Italy).
SOLITONS IN ELECTRON-POSITRON PLASMA
G. Carlini (Trieste Univ., Italy.) and V. I. Berezhiani Jul. 1994 8 p
(DE95-607608; IC-94/157) Avail: CASI HC A02/MF A01 (US Sales Only)

The nonlinear propagation of 'ordinary' electromagnetic waves in electron-positron plasma is considered. The possibility to find soliton solitons in such a plasma is explored. DOE

N95-25975# International Centre for Theoretical Physics, Trieste (Italy).
SELF-FOCUSING OF ELECTROMAGNETIC RADIATION IN ELECTRON-POSITRON ION PLASMA
V. I. Berezhiani and S. M. Mahajan Jun. 1994 8 p
(DE95-607626; IC-94/134) Avail: CASI HC A02/MF A01 (US Sales Only)

We consider the self-focusing of electromagnetic (EM) radiation in electron-positron plasmas with a small fraction of ions. It is shown that in such a plasma EM pulses may form and propagate like oscillatory waveguides. DOE

N95-25976# Melbourne Univ., Parkville (Australia).
TWO DIMENSIONAL BOSE PLASMA IN A MAGNETIC FIELD
D. C. Bardos, D. F. Hines, and N. E. Frankel 1993 25 p
(DE95-607629; UM-P-93/04) Avail: CASI HC A03/MF A01 (US Sales Only)

The dielectric response of a planar Bose plasma is investigated in the presence of a constant external magnetic field. The conductivity tensor is derived in the self-consistent Random Phase Approximation. The tensor components are evaluated at zero temperature, leading to explicit dispersion relations for the electrodynamic models of the plasma. For plasma layers, longitudinal and transverse modes are in general coupled. These coupled modes are investigated in detail. DOE

N95-26019 Polish Academy of Sciences, Warsaw (Poland). Physical Acoustics Inst.
THE EFFECT OF THE IMPEDANCE OF THE GENERATOR AND INTERMEDIATE CIRCUITS ON THE IMPEDANCE OF PLASMA AS IT APPLIES TO MAGNETRON SPUTTERING OF THIN FILMS IN A RADIO-FREQUENCY FIELD [WPLYW IMPEDANCJE GENERATORA I OBWODOW POSREDNICH NA IMPEDANCJE PLAZMY W ZASTOSOWANIU DO NAPYLANIA MAGNETRONOWEGO CIENKICH WARSTW W POLU WIELKIEJ CZESTOTLIWOSCI]
Wojciech Ciecwierz and Ryszard Plowiec 1994 15 p In POLISH
(ISSN 0208-5658)
(IFTR-8-1994) Avail: Issuing Activity

On the basis of measurements of the parameters of magnetron sputtering in a radio-frequency field, namely the capacitance and conductivity of the plasma during a plasma discharge as a function of the partial pressure of organ and the power delivered by a radio-frequency generator, the authors calculated the elements of a system which matches the magnetron gun to the wave impedance of the cable which conducts the RF power of the generator. The authors describe the matching system they built and its practical operation. Transl. by Screiber Translations Inc.

N95-26082*# Hughes STX, Inc., Lanham, MD.
PARTICLE-MESH TECHNIQUES
Peter MacNeice Washington NASA May 1995 67 p
(Contract NAS5-32350)
(NASA-CR-4666; Rept-95B00072; NAS 1.26:4666) Avail: CASI HC A04/MF A01

This is an introduction to numerical Particle-Mesh techniques, which are commonly used to model plasmas, gravitational N-body systems, and both compressible and incompressible fluids. The theory behind this approach is presented, and its practical implementation, both for serial and parallel machines, is discussed. This document is based on a four-hour lecture course presented by the author at the NASA Summer School for High Performance Computational Physics, held at Goddard Space Flight Center. Author

N95-26185# Argonne National Lab., IL. Fusion Power Program/Technology Development Div.
SUMMARY REPORT FOR ITER TASK D10: UPDATE AND IMPLEMENTATION OF NEUTRON TRANSPORT AND ACTIVATION CODES AND PROCESSED LIBRARIES
Hosny Attaya Jan. 1995 25 p
(Contract W-31-109-eng-38)
(DE95-007631; ANL/FPP/TM-277; ITER/US-95/IV-BL-17) Avail: CASI HC A03/MF A01

The primary goal of this task is to provide the capabilities in the activation code RACC, to treat pulsed operation modes. In addition, it is required that the code utilize the same spatial mesh and geometrical models as employed in the one or multidimensional neutron transport codes used in ITER design. This would ensure the use of the same neutron flux generated by those codes to calculate the different activation parameters. It is also required to have the capabilities for generating graphical outputs for the calculated activation parameters. DOE

N95-26326# National Inst. for Fusion Science, Nagoya (Japan).
ISOTOPE EFFECT ON CONFINEMENT IN DT PLASMAS
A. Fukuyama (Okayama Univ., Japan.), K. Itoh, S. I. Itoh (Kyushu Univ., Kasuga, Japan), M. Yagi (Japan Atomic Energy Research Inst., Ibaraki, Japan.), and M. Azumi (Japan Atomic Energy Research Inst., Ibaraki, Japan.) Mar. 1994 13 p Sponsored in part by the Grant-in-Aid for Scientific Research of Ministry of Education Japan Submitted for publication
(ISSN 0915-633X)
(NIFS-275) Avail: CASI HC A03/MF A01

Isotope effect on the energy confinement time is discussed for the DT plasma. The transport theory which is based on the ballooning mode turbulence is applied. When the DT plasma is produced under the condition of beta(sub p) greater than 1, the energy confinement time of DT plasma (50% mixture) is expected to be about 1.2 times better than the D plasma with the same operation condition. Author

N95-26337# National Inst. for Fusion Science, Nagoya (Japan).
MAGNETIC MIRROR EFFECT AS A TRIGGER OF COLLISIONLESS MAGNETIC RECONNECTION
Sergey Bazdenkov, Tetsuya Sato, Ritoku Horiuchi, and Kunihiko Watanabe Aug. 1994 17 p
(ISSN 0915-633X)
(NIFS-295) Avail: CASI HC A03/MF A01

A new mechanism of collisionless magnetic reconnection is proposed. It is based on the current density redistribution along the magnetic field lines caused by the reflection of meandering particles due to the magnetic mirror effect from the would-be reconnection region. Author

N95-26339# National Inst. for Fusion Science, Nagoya (Japan).
A MECHANISM OF COLLISIONLESS MAGNETIC RECONNECTION
Motohiko Tanaka Mar. 1994 25 p Submitted for publication
(ISSN 0915-633X)
(NIFS-274) Avail: CASI HC A03/MF A01

Forced reconnection in a collisionless magnetized plasma is studied using an implicit particle simulation. A coalescence of magnetic islands induces the electric field E(sub t) at the x-point via the displacement current. A quasi-steady reconnection is achieved with E(sub t) does not equal 0, the poloidal electric field E(sub p) generated by electrostatic shielding, and the current J(sub t) continuously removed via the E(sub p) x B plasma convection. Transit acceleration of electrons by unshielded parallel electric field E(sub parallel) approximately equals E(sub t) at the x-point yields the Ohm's law E(sub t) approx. equals eta(sub eq)J(sub t) with eta(sub eq) the inertia (kinetic) resistivity. Author

76 SOLID-STATE PHYSICS

Includes superconductivity.

For related information, see also *33 Electronics and Electrical Engineering* and *36 Lasers and Masers.*

N95-24205 Polish Academy of Sciences, Warsaw (Poland).
ELECTROMAGNETIC WAVES AND PHOTOACOUSTIC TRANSFORMATION IN GYROTROPIC SUPERLATTICES
E. G. Starodubtesev (Gomel State Univ., Gomel, Byelarus.), G. S. Mityurich (Gomel State Univ., Gomel, Byelarus.), and J. Ranachowski 1994 30 p
(ISSN 0208-5658)
Avail: Issuing Activity

The optical properties, photoacoustic (PA) transformation, and possibilities of PA measurements in short-period superlattices (SL) originated by nonmagnetic absorbing gyrotropic crystals of various classes of symmetry are investigated. Calculations have been made at arbitrary combinations of effects of optical anisotropy, absorption, gyrotropy, and multibeam optical interference in plane wave approximation. At typical parameters the models advanced predict some characteristic optical properties of the gyrotropic SL satisfying the long wavelength approximation. It is shown that photoacoustic transformation in short-period SL originated by cubic gyrotropic crystals has the peculiarities connected with the effect on PA response of multibeam optical interference, SL constants effective character, circular dichroism, and exciting radiation polarization. The analysis allows the definition of the conditions of experimental investigation and control of SL optical, thermal, and geometrical properties by the PA spectroscopy method. Derived from text

N95-24233# Los Alamos National Lab., NM.
THE TEMPERATURE AND STRAIN RATE DEPENDENCE OF THE FLOW STRESS OF SINGLE CRYSTAL NiAl DEFORMED ALONG THE ZONE GROUP AXES (110)
S. A. Maloy and G. T. Gray, III 1995 6 p Presented at the 1994 Fall Meeting of the Materials Research Society (MRS), Boston, MA, 28 Nov. - 2 Dec. 1994

(Contract W-7405-eng-36)
(DE95-003634; LA-UR-94-4081; CONF-941144-6) Avail: CASI HC A02/MF A01

Single crystal NiAl and Ni-49.75Al-0.25Fe have been deformed along the zone group axes (110) at temperatures of 77, 298 and 773K and strain rates of 0.001/s, and 2000/s. The flow stress of the zone group axes (110) NiAl is rate and temperature sensitive. The 0.25 at.% Fe addition resulted in a small increase in flow stress at strain rates of 0.001 and 0.1/s at 298 and 77K. A significant decrease in the work hardening rate is observed after deformation at 77K and a strain rate of 2000/s. Coarse zone axes (110) slip traces are observed after deformation at a strain rate of 2000/s at 77K, while no slip traces were observed after deformation under all other conditions. TEM observations reveal distinct zone axes (110) slip bands after deformation at 77K and a strain rate of 2000/s. DOE

N95-24244# International Centre for Theoretical Physics, Trieste (Italy).
TEMPERATURE DEPENDENCE OF MAGNETIC ANISOTROPY AND MAGNETOSTRICTION: BEYOND THE MEAN-FIELD THEORY
Yonko Millev and M. Faehnle (Max-Planck-Inst. fuer Metallforschung, Stuttgart, Germany.) May 1994 25 p Sponsored in cooperation with Commission of the European Communities
(Contract F205/BSF)
(DE94-634529; IC-94/106) Avail: CASI HC A03/MF A01 (US Sales Only)

The first nonvanishing magnetic anisotropy coefficient is calculated as a function of temperature for any spin quantum number and all temperatures below the Curie temperature for the case of face-centred cubic symmetry within the random-phase approximation (RPA). A detailed and instructive comparison between the mean-field and the RPA predictions is carried out. The RPA magnetization curves are also given for the first time for spins S greater than 1/2. Most of the theoretical considerations are quite general as regard lattice type and even decoupling scheme and can thus be applied straightforwardly to other cases of interest. The progress reported here has been attained with the help of a new simplified and improved parametric approach and of a recent calculation of the average occupation number of magnons within the RPA. In particular, the new approach makes unnecessary the solving of integral equations so that the proposed procedure is especially simple and practically versatile in applications to any particular anisotropic material. DOE

N95-24246# International Centre for Theoretical Physics, Trieste (Italy).
ON THE CALCULATION OF LATTICE SUMS ARISING IN BOSE-EINSTEIN STATISTICS OF QUASIPARTICLE EXCITATIONS
Y. Millev and M. Faehnle (Max-Planck-Inst. fuer Metallforschung, Stuttgart, Germany.) May 1994 17 p Sponsored by Commission of the European Communities
(Contract F205/BSF)
(DE94-634531; IC-94/99) Avail: CASI HC A03/MF A01 (US Sales Only)

A new method for the calculations of the average occupation number of bosonic quasi-particle excitations valid for any type of lattice is proposed. The method is based on the recognition of the connection with lattice Green's functions and generalized Watson integrals, on one hand, and on a very simple differentiation technique which renders unnecessary and artificial to this problem more sophisticated Laplace transform summation procedures. The mean-field approximation to Green's function theories of ferromagnetism arises naturally as the zeroth term in the obtained summation formulae. The results have been specified completely for the three cubic lattices. They are new for the simple cubic and face-centered cases, whereas certain redundancy is removed form the known body-centered cubic results. Applications of the method to more complex sums as, for instance, the thermodynamic sum for the total energy of the quasiparticles, are straightforward. There has also been found a new three-position recursion relation for the calculation of frequently occurring triple geometric integrals in the face-centred cubic case. It originates from a corresponding relation for a relevant Heun function. DOE

N95-24261*# Alabama Univ., Huntsville, AL.
ESTIMATES OF EFFECTS OF RESIDUAL ACCELERATION ON USML-1 EXPERIMENTS Final Report
Robert J. Naumann 1995 158 p
(Contract NAS8-36955)
(NASA-CR-197964; NAS 1.26:197964) Avail: CASI HC A08/MF A02

The purpose of this study effort was to develop analytical models to describe the effects of residual accelerations on the experiments to be carried on the first U.S. Microgravity Lab mission (USML-1) and to test the accuracy of these models by comparing the pre-flight predicted effects with the post-flight measured effects. After surveying the experiments to be performed on USML-1, it became evident that the anticipated residual accelerations during the USML-1 mission were well below the threshold for most of the primary experiments and all of the secondary (Glovebox) experiments and that the only set of experiments that could provide quantifiable effects, and thus provide a definitive test of the analytical models, were the three melt growth experiments using the Bridgman-Stockbarger type Crystal Growth Furnace (CGF). This class of experiments is by far the most sensitive to low level quasi-steady accelerations that are unavoidable on space craft operating in low earth orbit. Because of this, they have been the drivers for the acceleration requirements imposed on the Space Station. Therefore, it is appropriate that the models on which these requirements are based are tested experimentally. Also, since solidification proceeds directionally over a long period of time, the solidified ingot provides a more or less continuous record of the effects from acceleration disturbances. Derived from text

N95-24279# Argonne National Lab., IL.
DEVICE-QUALITY TUNNEL JUNCTIONS ON THE HIGH (T(SUB c)) SUPER CONDUCTOR HgBa2CuO(4+DELTA)
J. Zasadzinski (Illinois Inst. of Tech., Chicago, IL.), J. Chen, P. Romano, K. E. Gray, J. L. Wagner, and D. G. Hinks 1995 14 p Presented at the 7th Conference on Superconductivity and Applications, Buffalo, NY, 7-9 Sep. 1994
(Contract W-31-109-eng-38)
(DE95-004646; ANL/MSD/CP-84398; CONF-940926-3) Avail: CASI HC A03/MF A01

Superconductor insulator normal metal (SIN) and superconducting insulator superconducting (SIS) tunnel junction devices (e.g. photon detectors, logic elements) require quasiparticle characteristics that exhibit sharp current onsets at the gap voltage and very low subgap conductances. Progress is reported on the development of such junctions on High T(sub c) cuprates using mechanical point contacts. In general, these contacts display the optimum characteristics that can be obtained from high temperature superconductors (HTS) native-surface tunnel barriers. Most cuprates display a subgap conductance which monotonically increases with voltage about the minimum value at zero bias. However, tunneling data of unusually high quality have been obtained for the recently discovered Hg-based cuprate, HgBa2CuO4 (T(sub c) = 96K). SIS(prime) tunneling data using a Nb tip are presented which exhibit very low and flat subgap conductances and sharp conductance peaks as expected from a BCS density of states. These results are slightly improved over earlier published results with SIN junctions. Use of the experimental data to simulate the performance of a quasiparticle mixer demonstrates that noise temperatures approaching the quantum limit are possible for SIS and SIN mixers in the range 1-5 THz. DOE

N95-24324# International Centre for Theoretical Physics, Trieste (Italy).
ONE-STEP IN-DIFFUSION AS A RESULT OF MULTIPULSE LASER IRRADIATION OF LiNbO3 SINGLE-CRYSTALLINE SUBSTRATES COVERED WITH THIN Ti DEPOSITS ON THE EFFECT OF THE RADIATION WAVELENGTH
A. Ferrari (La Sapienza Univ., Rome, Italy.), L. Schirone (La Sapienza Univ., Rome, Italy.), G. Maiello (La Sapienza Univ., Rome, Italy.), C. DeCesare (La Sapienza Univ., Rome, Italy.), F. Carassitti (La Sapienza Univ., Rome, Italy.), M. Bertolotti (La Sapienza Univ., Rome, Italy.), M. A. Caponero (Energia Nucleare e Delle Energie Alternative, Rome, Italy.), A. Luches (Lecce Univ., Italy.), M. Martino (Lecce Univ., Italy.), and M. Dinescu et al May 1994 10 p Submitted for publication
(DE94-634524; IC-94/100) Avail: CASI HC A02/MF A01 (US Sales Only)

We studied Ti in-diffusion as an effect of multiple laser irradiation, in either visible or ultraviolet (u.v.) spectral ranges, of LiNbO3 single-crystalline structures with Ti coatings of two different thickness. It is shown that while u.v. (excimer, lambda approx. 308 nm) laser irradiation causes a complete

expulsion of the Ti deposit, the visible (ruby, lambda approx. 694.3 nm) laser irradiation at intermediate incident laser fluence (up to approx. 0.7J cm(sup -2)) promotes efficient Ti in-diffusion from the thin (400 A width) Ti deposit down to a micrometer range implantation depth. DOE

N95-24362# Joint Inst. for Nuclear Research, Dubna (USSR).
THERMAL DIFFUSE SCATTERING IN TIME-OF-FLIGHT NEUTRON DIFFRACTION STUDIED ON SBN SINGLE CRYSTALS
F. Prokert, B. N. Savenko, and A. M. Balagurov 1994 14 p
(DE94-637054; JINR-E-14-94-99) Avail: CASI HC A03/MF A01 (US Sales Only)

At time-of-flight (TOF) diffractometer D N-2, installed at the pulsed reactor IBR-2 in Dubna, Sr(x)Ba(1-x)Nb2O6 mixed single crystals (SBN-x) of different compositions (0.50 less than x less than 0.75) were investigated between 15 and 773 K. The diffraction patterns were found to be strongly influenced by the thermal diffuse scattering (TDS). The appearance of the TDS from the long wavelength acoustic models of vibration in single crystals is characterized by the ratio of the velocity of sound to the velocity of neutron. Due to the nature of the TOF Laue diffraction technique used on D N-2, the TDS around Bragg peaks has rather a complex profile. An understanding of the TDS close to Bragg peaks is essential in allowing the extraction of the diffuse scattering occurring at the diffuse ferroelectric phase transition in SBN crystals. DOE

N95-24374# Joint Inst. for Nuclear Research, Dubna (USSR).
THE FACILITY FOR COMMERCIAL DOPING OF SILICON BY THERMAL NEUTRONS IN CHANNEL 3 AT THE IBR-2
V. V. Golikov, V. L. Kamionskij, E. N. Kulagin, V. I. Lushchikov, and E. P. Shabalin 1994 20 p
(DE94-636293; JINR-18-94-108) Avail: CASI HC A03/MF A01 (US Sales Only)

The possibility of thermal neutron doping large silicon single crystals of up to 150 mm (6 in) in diameter by means of the formation of the spatial and energy spectrum neutrons in irradiation channel 3 at IBR-2 is demonstrated. On the basis of theoretical and experimental work, a facility has been created for the commercial production of doped silicon. This facility has the following parameters: (1) the average density of thermal neutron flux for the volume of 5 x 10(exp 3)cu cm is 3.0 x 10(exp 12) n/sq cm sec; (2) the maximal size of ingots under doping is -127 mm (5 in.) in diameter and 360 mm long; (3) the doping inhomogeneity is not worse than 5%; (4) the temperature of the ingots during irradiation is less than 100 C; and (5) the annual production rate of ingots doped to have a specific resistivity of 100 Om(center dot)cm (from the initial of 1000 Om(center dot)cm) is 1200 kg. DOE

N95-24431# Oak Ridge National Lab., TN.
NEUTRON DIFFRACTION FROM HoNi2B2C, VERSION 1
C. V. Tomy, L. J. Chang, D. M. Paul, N. H. Andersen (Risoe National Lab., Roskilde, Denmark.), and M. Yethiraj Feb. 1994 9 p Presented at the Neutron Scattering, Sendai, Japan, 11-14 Oct. 1994
(Contract DE-AC05-84OR-21400)
(DE95-005894; CONF-9410165-10) Avail: CASI HC A02/MF A01

RENi2B2C (RE=Rare Earth) are quaternary compounds which exhibit a considerable degree of interaction between their superconducting and magnetic properties. The Ho variant is found to become superconducting at T(sub c)= 9 K, but anomalous behaviour is observed in the low field magnetic properties at T less than 7 K (increasing susceptibility with decreasing temperature); at temperatures less than 5.6 K more conventional behaviour is regained. Neutron diffraction measurements demonstrate that at low temperatures (T less than 5K) the magnetic order consists of ferromagnetic planes antiferromagnetically coupled up the c-axis with a Ho moment of 8.9 +/- 0.2 (mu)(sub B) canted at 15 degrees +/- 5 from the a-b plane. At high temperatures (7 less than T less than 8.5 K) satellites, together with the principal Bragg reflections, are observed which correspond to a modulation of the magnetic order with a wavelength of approximately 136 Angstrom up the c-axis. In the intermediate temperature (5 less than T less than 7 K) range further Bragg reflections become evident. An additional modulation along the a-axis becomes important in this temperature range. DOE

N95-24451# Brookhaven National Lab., Upton, NY.
UPDATE ON B(SUB K) WITH WILSON FERMIONS
C. Bernard and A. Soni Dec. 1994 3 p Presented at the Lattice '94, Bielefeld, Germany, 25 Sep. - 1 Oct. 1994
(Contracts DE-AC02-76CH-00016; DE-FG02-91ER-40628)
(DE95-004953; BNL-61139; CONF-9409269-2) Avail: CASI HC A01/MF A01

The K-(anti K) mixing matrix element is a hadronic matrix element that is of crucial importance to electroweak phenomenology. For convenience, the authors introduce the so called bag parameter, B(sub K). It has been known for a long time that B(sub K) is amenable to lattice Monte-Carlo methods. Indeed, recently Sharpe and collaborators, using staggered formulation for fermions have made remarkable progress in calculating B(sub K) and have reported a result with an impressive accuracy. In this work the authors will present their results for B(sub K) using the Wilson formulation for fermions. DOE

N95-24460# Loyola Coll., Baltimore, MD. International Technology Reseach Inst.
DISPLAY TECHNOLOGIES IN RUSSIA, UKRAINE, AND BELARUS Final Report
William J. Doane, Patricia E. Cladis, Christopher Curtin, James Larimer, Marko Slusarczuk, Jan B. Talbot, and Ziv Yaniv Dec. 1994 289 p
(Grant NSF ENG-92-17849)
(ISBN-1-883712-36-X) Avail: CASI HC A13/MF A03

This report is a review of advanced display research, development, and manufacturing activity in Belarus, Russia, and Ukraine. Topics covered include: liquid crystal display materials and related technologies; liquid crystal and other non-emissive displays; vacuum fluorescent, electroluminescent, field emission, and other emissive displays; and phosphors and other emissive materials. Also included is a review of infrastructure and business issues related to the display industry in the former Soviet Union. The panel found promising technologies in projection systems (e.g., the 'quantoscope' - utilizing an e-beam pumped laser), Supertwisted Nematic (STN) Liquid Cristal Displays (LCD) manufacturing at several locations in Russia and Belarus, developing capabilities and plans for future Active Matrix Liquid Cristal Display (AMLCD) production in all three countries, and a strong vacuum-fluorescent production capability in Saratov, Russia. Most significantly, the panel found many advanced concepts under development at basic research laboratories throughout the three countries visited; these research efforts are now in jeopardy due to insufficient funding, an uncertain business climate and deteriorating infrastructure. Nevertheless, there are many promising opportunities for foreign investment in display technology and manufacturing in Russia, Ukraine, and Belarus. Author

N95-24463# Stanford Linear Accelerator Center, CA.
A PHOTOEMISSION STUDY OF THE DIAMOND AND THE SINGLE CRYSTAL C(60) Ph.D. Thesis
Jin Wu Mar. 1994 104 p
(Contract DE-AC03-76SF-00515)
(DE95-006149; SU-SLAC-450; SLAC/SSRL-0089) Avail: CASI HC A06/MF A02

This report studied the electronic structure of diamond (100) and diamond/metal interface and C(60), using angle-resolved and core level photoemission. The C(100)-(2X1) surface electronic structure was studied using both core level and angle resolved valence band photoemission spectroscopy. The surface component of the C 1s core level spectrum agrees with theoretical existence of only symmetrical dimers. In the case of metal/diamond interfaces, core level and valence photoelectron spectroscopy and LEED studies were made of B and Sb on diamond (100) and (111) surfaces. In the case of single-crystal C(60), photoemission spectra show sharp molecular features, indicating that the molecular orbitals are relatively undisturbed in solid C(60). DOE

N95-24478*# Desert Research Inst., Reno, NV. Atmospheric Sciences Center.
NUCLEATION AND GROWTH OF CRYSTALS UNDER CIRRUS AND POLAR STRATOSPHERIC CLOUD CONDITIONS Final Report
John Hallett, Brian Queen (Prodata, Inc., Burlingame, CA.), Edward Teets (National Aeronautics and Space Administration. Hugh L. Dryden Flight Research Center, Edwards, CA.), and James Fahey Mar. 1995 58 p
(Grant NAGw-2572)
(NASA-CR-197991; NAS 1.26:197991) Avail: CASI HC A04/MF A01

Laboratory studies examine phase changes of hygroscopic substances

which occur as aerosol in stratosphere and troposphere (sodium chloride, ammonium sulfate, ammonium bisulfate, nitric acid, sulfuric acid), under controlled conditions, in samples volume 1 to 10(exp -4) ml. Crystallization of salts from supersaturated solutions is examined by slowly evaporating a solution drop on a substrate, under controlled relative humidity, until self nucleation occurs; controlled nucleation of ice in a mm capillary U-tube gives a measured ice crystallization velocity at known supercooling. Two states of crystallization occur for regions where hydrates exist. It is inferred that all of the materials readily exist as supersaturated/supercooled solutions; the degree of metastability appears to be slightly enhanced by inclusion of aircraft produced soot. The crystallization velocity is taken as a measure of viscosity. Results suggest an approach to a glass transition at high molality, supersaturation and/or supercooling within the range of atmospheric interest. It is hypothesized that surface reactions occur more readily on solidified particles - either crystalline or glass, whereas volume reactions are more important on droplets with sufficiently low viscosity and volume diffusivity. Implications are examined for optical properties of such particles in the atmosphere. In a separate experiment, crystal growth was examined in a modified thermal vapor diffusion chamber over the range of cirrus temperature (-30 to -70 C) and under controlled supersaturation and air pressure. The crystals grew at a velocity of 1-2 microns/s, thickness 60-70 micron, in the form of thin column crystals. Design criteria are given for a system to investigate particle growth down to -100 C, (PSC temperatures) where nitric acid particles can be grown under similar control and in the form of hydrate crystals. Author

N95-24513# Los Alamos National Lab., NM.
THEORETICAL AND EXPERIMENTAL STUDIES ON THE C15 INTERMETALLIC COMPOUND NbCr2
F. Chu, D. J. Thoma, Y. He, T. E. Mitchell, S. P. Chen, and J. H. Perepezko (Wisconsin Univ., Madison, WI.) 1994 7 p Presented at the 1994 Fall Meeting of the Materials Research Society (MRS), Boston, MA, 28 Nov. - 2 Dec. 1994
(Contract W-7405-eng-36)
(DE95-003665; LA-UR-94-3956; CONF-941144-10) Avail: CASI HC A02/MF A01

The electronic structure and total energy of the C15 NbCr2 have been calculated using the linear muffin-tin orbital (LMTO) method with the atomic sphere approximation (ASA). The total energy vs. volume curve, band structure, density of states and Fermi surface were obtained. The calculated results were used to examine several features of the C15 phase, including the elastic properties, phase formation and stability, and solubility of the C15 phase. The theoretical results are compared to experimental studies on the C15 NbCr2 phase. For example, the elastic moduli, phase stability, and homogeneity range have been characterized with a variety of experimental techniques. Comparison of the experimental and theoretical results will be discussed. DOE

N95-24514# Los Alamos National Lab., NM.
THIN FILM IONIC CONDUCTORS BASED ON CERIUM OXIDE
P. Haridoss (Wisconsin Univ., Madison, WI.), E. Hellstrom (Wisconsin Univ., Madison, WI.), F. H. Garzon, D. R. Brown, and M. Hawley 1994 4 p Presented at the 1994 Fall Meeting of the Materials Research Society (MRS), Boston, MA, 28 Nov. - 2 Dec. 1994
(Contract W-7405-eng-36)
(DE95-003668; LA-UR-94-3966; CONF-941144-9) Avail: CASI HC A01/MF A01

Fluorite and perovskite structure cerium oxide based ceramics are a class of materials that may exhibit good oxygen ion and/or protonic conductivity. The authors have successfully deposited thin films of these materials on a variety of substrates. Interesting orientation relationships were noticed between cerium oxide films and strontium titanate bi-crystal substrates. Near lattice site coincidence theory has been used to study these relationships. DOE

N95-24534*# Alabama Univ., Huntsville, AL. Center for Microgravity and Materials Research.
CONVECTIVE FLOW EFFECTS ON PROTEIN CRYSTAL GROWTH
Semiannual Progress Report No. 4, 1 Aug. 1994 - 31 Jan. 1995
Franz Rosenberger and Lisa A. Monaco 31 Jan. 1995 46 p
(Grant NAG8-950)
(NASA-CR-197891; NAS 1.26:197891) Avail: CASI HC A03/MF A01

During the fourth semi-annual period under this grant we have pursued the following activities: (1) crystal growth morphology and kinetics studies with tetragonal lysozyme. These clearly revealed the influence of higher molecular weight protein impurities on interface shape; (2) characterization of the purity and further purification of lysozyme solutions. These efforts have, for the first time, resulted in lysozyme free of higher molecular weight components; (3) continuation of the salt repartitioning studies with Seikagaku lysozyme, which has a lower protein impurity content that Sigma stock. These efforts confirmed our earlier findings of higher salt contents in smaller crystals. However, less salt is in corporated into the crystals grown from Seikagaku stock. This strongly suggests a dependence of salt repartitioning on the concentration of protein impurities in lysozyme. To test this hypothesis, repartitioning studies with the high purity lysozyme prepared in-house will be begun shortly; (4) numerical modelling of the interaction between bulk transport and interface kinetics. These simulations have produced interface shapes which are in good agreement with out experimental observations; and (5) light scattering studies on under- and supersaturated lysozyme solutions. A consistent interpretation of the static and dynamic data leaves little doubt that pre-nucleation clusters, claimed to exist even in undersaturated solutions, are not present. The article: 'Growth morphology response to nutrient and impurity nonuniformities' is attached. Derived from text

N95-24537# Joint Inst. for Nuclear Research, Dubna (USSR). Neutron Physics Lab.
COPPER TRANSPORT ON OXYGEN ANNEALING OF A SUPERCONDUCTING FILM Y-Ba-Cu-O
D. M. Shirokov, A. P. Kobzev, D. A. Korneev, and L. P. Chernenko 1993 10 p In RUSSIAN; In RUSSIAN
(DE94-627566; JINR-R-3-93-242) Avail: CASI HC A02/MF A01 (US Sales Only)

With the help of an improved method of helium ion backscattering it is found that the heating up of a superconducting film Y-Ba-Cu-O in oxygen at 400 C results in a strongly inhomogeneous distribution of both oxygen and copper ions. It is explained by oxygen involving of copper ions into the process of preferred intergranular diffusion causing a change in the superconducting properties of the film. Strong oxygen enrichment is observed in the near-surface layer of superconducting, polycrystal textured film Y-Ba-Cu-O at normal keeping conditions. DOE

N95-24594# Los Alamos National Lab., NM.
SOLUTION BASED SYNTHESIS OF PEROVSKITE-TYPE OXIDE FILMS AND POWDERS Ph.D. Thesis
J. M. McHale, Jr. Jan. 1995 210 p
(Contract W-7405-eng-36)
(DE95-006170; LA-UR-95-440) Avail: CASI HC A10/MF A03

Conventional solid state reactions are diffusion limited processes that require high temperatures and long reaction times to reach completion. In this work, several solution based methods were utilized to circumvent this diffusion limited reaction and achieve product formation at lower temperatures. The solution methods studied all have the common goal of trapping the homogeneity inherent in a solution and transferring this homogeneity to the solid state, thereby creating a solid atomic mixture of reactants. These atomic mixtures can yield solid state products through diffusionless mechanisms. The effectiveness of atomic mixtures in solid state synthesis was tested on three classes of materials, varying in complexity. A procedure was invented for obtaining the highly water soluble salt, titanyl nitrate, TiO(NO3)2, in crystalline form, which allowed the production of titanate materials by freeze drying. The freeze drying procedures yielded phase pure, nanocrystalline BaTiO3 and the complete SYNROC-B phase assemblage after ten minute heat treatments at 600 C and 1,100 C, respectively. Two novel methods were developed for the solution based synthesis of Ba2YCu3O(7-x) and Bi2Sr2Ca2Cu3O10. Thin and thick films of Ba2YCu3O(7-x) and Bi2Sr2Ca2Cu3O10 were synthesized by an atmospheric pressure, chemical vapor deposition technique. Liquid ammonia solutions of metal nitrates were atomized with a stream of N2O and ignited with a hydrogen/oxygen torch. The resulting flame was used to coat a substrate with superconducting material. Bulk powders of Ba2YCu3O(7-x) and Bi2Sr2Ca2Cu3O10 were synthesized through a novel acetate glass method. The materials prepared were characterized by XRD, TEM, SEM, TGA, DTA, magnetic susceptibility and electrical resistivity measurements. DOE

N95-24611# Oak Ridge National Lab., TN. Solid State Div.
[ACTIVITIES OF THE SOLID STATE DIVISION] Progress Report, period ending 30 Sep. 1993
P. H. Green, ed. and L. W. Hinton, ed. Aug. 1994 301 p
(Contract DE-AC05-84OR-21400)
(DE95-003900; ORNL-6816) Avail: CASI HC A14/MF A03

This report covers research progress in the Solid State Division from April 1, 1992, to September 30, 1993. During this period, the division conducted a broad, interdisciplinary materials research program with emphasis on theoretical solid state physics, neutron scattering, synthesis and characterization of materials, ion beam and laser processing, and the structure of solids and surfaces. This research effort was enhanced by new capabilities in atomic-scale materials characterization, new emphasis on the synthesis and processing of materials, and increased partnering with industry and universities. The theoretical effort included a broad range of analytical studies, as well as a new emphasis on numerical simulation stimulated by advances in high-performance computing and by strong interest in related division experimental programs. Superconductivity research continued to advance on a broad front from fundamental mechanisms of high-temperature superconductivity to the development of new materials and processing techniques. The Neutron Scattering Program was characterized by a strong scientific user program and growing diversity represented by new initiatives in complex fluids and residual stress. The national emphasis on materials synthesis and processing was mirrored in division research programs in thin-film processing, surface modification, and crystal growth. Research on advanced processing techniques such as laser ablation, ion implantation, and plasma processing was complemented by strong programs in the characterization of materials and surfaces including ultrahigh resolution scanning transmission electron microscopy, atomic-resolution chemical analysis, synchrotron x-ray research, and scanning tunneling microscopy. DOE

N95-24616# Sandia National Labs., Albuquerque, NM.
EFFECT OF He PRESSURE ON THE SUPERCONDUCTING TRANSITION TEMPERATURES OF Na2CsC60 AND (NH3)4Na2CsC60
J. E. Schirber, W. R. Bayless, M. J. Rosseinsky (Bell Telephone Labs., Inc., Murray Hill, NJ.), O. Zhou (Bell Telephone Labs., Inc., Murray Hill, NJ.), R. M. Fleming (Bell Telephone Labs., Inc., Murray Hill, NJ.), D. Murphy (Bell Telephone Labs., Inc., Murray Hill, NJ.), and J. E. Fischer (Pennsylvania Univ., Philadelphia, PA.) 1994 6 p Presented at the 1994 Fall Meeting of the Materials Research Society (MRS), Boston, MA, 28 Nov. - 2 Dec. 1994
(Contract DE-AC04-94AL-85000)
(DE95-006320; SAND-94-1703C; CONF-941144-33) Avail: CASI HC A02/MF A01

The Na based mixed alkali doped C60 superconductors show anomalous behavior with respect to the 'universal' superconducting transition temperature (Tc) vs lattice constant a(sub 0) relation followed by most of the fcc A3C60 superconductors. We have measured dT(sub c)/dP for Na2CsC60 and (NH3)4Na2CsC60 using solid He as the pressure medium to approximately 6 kbar finding dT(sub c)/dP equal to -0.8 +/- (0.01) K/kbar and -1.0 +/- (0.1)K/kbar for Na 2CsC60 and Na2(NH3)4C60 respectively. Our value for Na2CsC60 differs markedly from that obtained by Mizuki et al of about -1.3 K/kbar. However, using N2 or Ar, we obtain values for dT(sub c)/dP in substantial agreement with Mizuki et al who used fluorinert to generate their pressure. This work emphasizes the need for compressibility measurements with the same pressure medium in the appropriate temperature range so that meaningful comparisons can be made between various pressure measurements and models which are based on lattic spacing. DOE

N95-24617# Sandia National Labs., Albuquerque, NM.
DISILENE ADDITION TO C70
S. J. Jacobs, P. A. Cahill, and C. M. Rohlfing (Sandia National Labs., Livermore, CA.) 1994 7 p Presented at the 1994 Fall Meeting of the Materials Research Society (MRS), Boston, MA, 28 Nov. - 2 Dec. 1994
(Contract DE-AC04-94AL-85000)
(DE95-006321; SAND-94-1693C; CONF-941144-37) Avail: CASI HC A02/MF A01

Semiempirical and ab initio Hartree Fock computational results indicate that the highly reactive dienophile tetramethyldisilene, Me2Si=SiMe2, is an excellent candidate for a novel functionalization of the equator of C70 via a (2+4) cycloaddition to the 21, 22, 23, 42 carbons. Thermal or photochemical generation of tetramethyldisilene in the presence of C70 results in similar complex mixtures in which the major product appears to be that of (2+2) cycloaddition to the 7,8 carbons of C70. A minor product clearly results from (2+2) cycloaddition to the 1,9 carbons. Both of these products are hydrolytically unstable and are converted nonspecifically to mixtures of 1,9- and 7,8-C70H2 which are also present in HPLC traces of the reaction mixtures. DOE

N95-24849# Brookhaven National Lab., Upton, NY. Physics Dept.
CHIRAL SYMMETRY ON THE LATTICE
Michael Creutz Nov. 1994 11 p Presented at the Lattice 1994, Bielefeld, Germany, 25 Sep. - 1 Oct. 1994
(Contract DE-AC02-76CH-00016)
(DE95-003962; BNL-61011; CONF-9409269-1) Avail: CASI HC A03/MF A01

The author reviews some of the difficulties associated with chiral symmetry in the context of a lattice regulator. The author discusses the structure of Wilson Fermions when the hopping parameter is in the vicinity of its critical value. Here one flavor contrasts sharply with the case of more, where a residual chiral symmetry survives anomalies. The author briefly discusses the surface mode approach, the use of mirror Fermions to cancel anomalies, and finally speculates on the problems with lattice versions of the standard model. DOE

N95-24855# Argonne National Lab., IL. Materials Science Div.
BCS-LIKE GAP STRUCTURE OF HgBa2CuO(4+DELTA) TUNNEL JUNCTIONS
J. Chen, J. F. Zasadzinski, K. E. Gray, J. L. Wagner, D. G. Hinks, K. Kouznetsov (Illinois Inst. of Tech., Chicago, IL.), and L. Coffey (Illinois Inst. of Tech., Chicago, IL.) 1994 5 p Presented at the Applied Superconductivity Conference, Boston, MA, 16-21 Oct. 1994
(Contract W-31-109-eng-38)
(DE95-004125; ANL/MSD/CP-83118; CONF-941013-16) Avail: CASI HC A01/MF A01

The authors report point-contact tunneling into polycrystalline HgBa2CuO(4+delta) superconductors with a T(sub c) onset of 97 K using a superconducting Nb counterelectrode. These SIS tunnel junctions are of unusually high quality for cuprate superconductors, exhibiting low and flat sub-gap conductances and sharp conductance peaks as expected from a BCS density of states. These features are obtained reproducibly and are consistent with earlier published SIN results using an Au counterelectrode. Use of experimental data to simulate the performance of a quasiparticle mixer indicates that HgBa2CuO(4+delta) may be suitable for use in low noise heterodyne receivers operating at a few THz. DOE

N95-24868# Argonne National Lab., IL. Materials Science Div.
MELTING OF THE MOVING VORTEX LATTICE IN THE PRESENCE OF DISORDER
A. E. Koshelev (Academy of Sciences, USSR, Moscow, USSR.) and V. M. Vinokur Jul. 1994 3 p Presented at the 4th International Conference on Materials and Mechanisms of Superconductivity, High Temperture Superconductors (M2-HTSC IV), Grenoble, France, 5-9 Jul. 1994
(Contract W-31-109-eng-38; NSF DMR-91-20000)
(DE95-004126; ANL/MSD/CP-84784; CONF-940701-22) Avail: CASI HC A01/MF A01

The authors investigate the melting of the two-dimensional vortex lattice moving in an inhomogeneous environment under the applied current j. They predict the existence of a dynamic phase transition at some current j = j(sub t) (crystallization current) from the motion of the amorphous configuration at j less than j(sub t) to the motion of the crystal at j greater than j(sub t). j(sub t) exceeds essentially the critical current j(sub c) for strongly disordered systems and approaches j(sub c) with the decrease of the degree of disorder. They find that j(sub t) diverges as temperature approaches the melting temperature of the undisturbed lattice. DOE

N95-24891# Joint Inst. for Nuclear Research, Dubna (USSR). Lab. of Nuclear Reactions.
HIGH-ENERGY IONOLUMINESCENCE OF LIF
V. A. Skuratov, A. Yu. Didyk, and S. M. AbuAlAzm 1994 11 p Submitted for publication

(DE94-629015; JINR-E-14-94-20) Avail: CASI HC A03/MF A01 (US Sales Only)

The luminescence of pure crystals of lithium fluoride during irradiation by the ions B (13.6 MeV), Ne (26.7 MeV), Ar (46.3 MeV), Kr (210 MeV) and Xe (158 MeV) is investigated. Spectra were registered at the temperature of 80 - 300 K in the wavelength range of 250 - 700 nm. Spectral distribution is characterized by a set of wide bands with maximum of 670, 525, 330 and 296 nm. Possible reasons of the luminescence yield of ultraviolet band of 296 nm dependence on ion type and energy at liquid nitrogen temperature with regard to radiation damaging of LiF are discussed. DOE

N95-24900# National Inst. for Research in Inorganic Materials, Tsukuba (Japan).

STUDY OF VERY HIGH TEMPERATURE TECHNOLOGY, 2

25 Nov. 1993 52 p In JAPANESE
(DE95-730105; ETDE/JP-MF-95730105) Avail: CASI HC A04/MF A01

This paper is a collection of research reports of 1993 regarding very high temperature technology published by Japan Science and Technology Agency. High-frequency thermal plasmas (RF plasma), under the very high temperature generation method in the very high temperature (4000-10000 C) processing technology that has recently been attracting attention of the industry, have various features. The highly-reactive chemical species in plasma have the same important reaction as found in diamond thin film synthesis. As an application technology, the torch is essential for generating plasma for a long time. The torch for creating the characteristic chemical species should be developed as an important factor. The measurement technologies were developed involving these generation technologies. The main study of the very high temperature station is the development of the very high temperature generation mechanism and the application technologies. The study overview presents the development of generation system, plasma stability, measurement control, application technologies, simultaneous emission of RF plasma and UV laser, phase transfer of alpha-alumina in plasma, and more. Related research is separately collected and attached to the paper as the supplement. As a result of this research, 43 reports were presented and 4 patents were applied for in Japan. DOE

N95-24988# National Inst. for Research in Inorganic Materials, Tsukuba (Japan).

STUDY OF COPPER PEROVSKITE

25 Nov. 1993 68 p In JAPANESE
(DE95-730106; ETDE/JP-MF-95730106) Avail: CASI HC A04/MF A01

This paper describes the research reports of 1993 regarding Cu Perovskite SC (Superconductor) published by Japan Science and Technology Agency. This is the study of superconductivity at a high critical temperature (Tc = 30 K or more) of copper-containing K2NiF4 type oxide. The study includes synthesis, characterization, and examination of substantial nature of this superconductor. Synthesis was conducted by applying the very fast cooling thick film synthesis method and some other methods. Characterization was achieved by observing the newly designed SXDM/XPD. The substantial nature was verified by using the Meissner effect measurement method. Amorphous film of Bi series oxide SC was created by applying the very fast cooling method for the first time in the world. Bi-Pb thick film was created, and high-orientation film was produced on the trial basis. The complete C-axis orientation film of (Nd - Ce)2CuO4 could be produced on the trial basis by using the sputtering method. Copper-containing oxide was synthesized at a high oxygen pressure, and the substantial nature of magnetic oxide was examined at a high pressure. The quality of lead germanate could also be improved by using the very fast cooling method. Each study subject is partially successful through the newly proposed techniques, but many issues needing to be corrected are still part of each study. DOE

N95-25002# Pacific Northwest Lab., Richland, WA.

PROCESSING AND ELECTROCHEMICAL PROPERTIES OF MIXED CONDUCTING La(1-x)A(x)Co(1-y)Fe( )O(3-DELTA) (A=Sr, Ca)

W. J. Weber, J. W. Stevenson, T. R. Armstrong, and L. R. Pederson

Nov. 1994 7 p Presented at the 1994 Fall Meeting of the Materials Research Society (MRS), Boston, MA, 28 Nov. - 2 Dec. 1994
(Contract DE-AC06-76RL-01830)
(DE95-004910; PNL-SA-25465; CONF-941144-32) Avail: CASI HC A02/MF A01

Powder compositions in the series La(1-x)A(x)Co(1-y)Fe(y)O(3-delta) (A = Sr, Ca) have been prepared by a combustion synthesis method. Sintering of pressed powders produced high-density test specimens with the perovskite structure. The specimens exhibited high electrical conductivities with appreciable oxygen-ion conductivity that increased with Co content for the compositions studied. Oxygen permeation studies showed a significant flux of oxygen that increased with temperature for specimens in a P(O2) gradient with no applied field. Thermogravimetric studies of the La(1-x)Sr(x)Co(0.2)Fe(0.8)O(3-delta) system indicated a reversible mass loss with increasing temperature that increased with Sr content. DOE

N95-25280# Argonne National Lab., IL.

NANOSTRUCTURED MATERIALS

R. W. Siegel Nov. 1994 10 p Presented at the Nanoparticulates '94 Conference, Monterey, CA, 14-15 Nov. 1994
(Contract W-31-109-eng-38)
(DE95-004595; ANL/MSD/CP-84768; CONF-9411172-1) Avail: CASI HC A02/MF A01

Interest in the physics of condensed matter at size scales larger than that of atoms and smaller than that of bulk solids has grown rapidly over the past two decades owing to the increasing realization that the properties of these mesoscopic atomic ensembles are different than those of conventional solids. As a consequence, interest in artificially assembling materials from nanometer sized building blocks, whether layers or clusters of atoms, arose from discoveries that by controlling the sizes in the range of 1-100 nm and the assembly of such constituents one could begin to alter and prescribe the properties of the assembled nanostructures. Nature had already learned the value of nanostructuring, since many examples of naturally formed nanostructures can be found in biological systems from sea shells to the human body. Nanostructured materials are modulated over nanometer length scales in from zero to three dimensions. They can be assembled with modulation dimensionalities of zero (atom clusters or filaments), one (multilayers), two (ultrafine-grained overlayers or coatings or buried layers), and three (nanophase materials), or also with intermediate dimensionalities. Thus, nanocomposite materials containing multiple phases can range from the most conventional case in which a nanoscale phase is embedded in a phase of conventional sizes to the case in which all the constituent phases are of nanoscale dimensions. All nanostructured materials share three features: atomic domains (grains, layers or phases) spatially confined to less than 100 nm in at least one dimension, significant atom fractions associated with interfacial environments, and interactions between their constituent domains. DOE

N95-25282# Argonne National Lab., IL.

OXYGEN STOICHIOMETRY AND ITS INFLUENCE ON SUPERCONDUCTIVITY IN Bi2Sr2CaCu2O(8+x)

P. Krishnaraj, M. Lelovic, N. G. Eror, and U. Balachandran 1994 11 p Presented at the Physics and Materials Science of High-temperature Superconductors, Porto Carras, Greece, 10-23 Jul. 1994
(Contract W-31-109-eng-38)
(DE95-004660; ANL/ET/CP-84649; CONF-9407156-1) Avail: CASI HC A03/MF A01

Bi2Sr2CaCu2O(8+x) (2212) was synthesized from freeze-dried precursors. The oxygen content of 2212 was determined as a function of temperature and oxygen partial pressure and the variation of Tc with oxygen content was determined. It was found that 2212 without excess oxygen (x = 0) is superconducting. This points to the role of the (Bi-O)(sub infinity) layers as a source for holes in 2212. Four probe resistivity measurements were also performed on 2212. The nature of oxygen intercalation and oxygen removal in 2212 was studied by thermogravimetry and resistivity. It was also found that samples of 2212 with the same oxygen content had different (Tc)'s depending on thermal history. This difference in (Tc) is thought to arise from oxygen occupying different sites in the lattice while maintaining the same total oxygen content. DOE

N95-25288# Pacific Northwest Lab., Richland, WA.

TEMPERATURE AND DOSE DEPENDENCE OF METAL COLLOID PRODUCTION IN ALPHA-IRRADIATED CaF2

W. J. Weber, G. J. Exarhos, and L. M. Wang Nov. 1994 7 p Presented at the 1994 Fall Meeting of the Materials Research Society (MRS), Boston, MA, 28 Nov. - 2 Dec. 1994
(Contract DE-AC06-76RL-01830)

(DE95-004907; PNL-SA-25425; CONF-941144-26) Avail: CASI HC A02/MF A01

Single crystals of CaF2 were irradiated with 5.8 MeV alpha particles from a Cm-244 source. The absorbance spectra were recorded as a function of dose and temperature. At low doses, the absorbance from the colloid band increased with dose to saturation values that changed with temperature. The colloid band exhibited a sharp increase in rate of growth over a narrow temperature range with a peak at 150 C. The intensity of the colloid band after a dose of 1.4 x 10(exp 16) alpha/sq cm is a factor of 7 to 8 higher than the intensity at 100 and 200 C. The temperature (150 C) for the maximum rate of colloid growth in CaF2 under the alpha irradiation conditions (approximately 5 x 10(exp 8) rad/h) of this study is significantly higher than the peak temperature (60 C) reported for colloid production in CaF2 under electron irradiation at slightly higher dose rates (approximately 10(exp 9) rad/h). Cryogenic transmission electron microscopy of the irradiated crystals revealed dislocation loops and small dark clusters as the dominant microstructural features. DOE

N95-25353# Sandia National Labs., Albuquerque, NM.

OPTICAL DETERMINATIONS OF ENERGY-BAND DISPERSION CURVES IN NOVEL COMPOUND SEMICONDUCTOR MATERIALS

E. D. Jones 1995 9 p Presented at the SPIE '95: SPIE Conference on Optics, Electro-optics, and Laser Application in Science, Engineering and Medicine, San Jose, CA, 5-10 Feb. 1995

(Contract DE-AC04-94AL-85000)

(DE95-006318; SAND-95-0094C; CONF-950226-2) Avail: CASI HC A02/MF A01

We present magnetoluminescence data which provides a quantitative measure of the energy-band dispersion curves of novel compound semiconductor optoelectronic materials. Data for a n-type strained-layer InGaAs/GaAs (quantum-well width approximately 8 nm) and a n-type 4.5-nm-wide GaAs/AlGaAs lattice-matched single-quantum well are presented. We find that the conduction bands are almost parabolic, with a mass of about 0.068 m(sub 0) for InGaAs/GaAs and 0.085 m(sub 0) for the GaAs/AlGaAs structure. The valence-bands are nonparabolic with wave vector dependent in-plane valence-band masses varying from about 0.1 m(sub 0) at zone center to about 0.3 m(sub 0) for 20 meV energies. DOE

N95-25389# Oak Ridge National Lab., TN.

FORMATION OF THALLIUM BASED HIGH TEMPERATURE SUPERCONDUCTORS USING AEROSOL FLOW REACTED PRECURSOR POWDERS

J. Brynestad, M. Paranthaman, A. Goyal, D. E. Heatherly, and D. M. Kroeger 1995 5 p Presented at the Harold A. Oeye International Symposium, Trondheim, Norway, 2-3 Feb. 1995

(Contract DE-AC05-84OR-21400)

(DE95-005901; CONF-950265-1) Avail: CASI HC A01/MF A01

Highly anisotropic particles of various thallium containing superconductors were grown. The Tl free precursor powders with the nominal compositions BaCa2Cu3Ag(0.37)O6 and Ba2Ca2Cu3Ag(0.37)O7 were prepared using an aerosol flow reactor. These precursor powders were post-annealed in 0.1 atm oxygen at 700 C for 4h to reduce the carbon present, and subsequently mixed with Tl2O3 (typical composition of Tl(x); x = 0.6 - 1.0). The Tl-containing powders were heat-treated in semi-sealed gold tubes between 650-890 C with various short and long heat-treatments. X-ray diffraction showed that the TlBa2CaCu2O7 (referred to as Tl-1212) and TlBa2Ca2Cu3O9 (Tl-1223) phases formed below 700 C while Tl2Ba2CaCu2O8 (Tl-2212) formed between 700-830 C, and Tl2Ba2Ca2Cu3O10 (Tl-2223) formed above 830 C. Scanning electron microscopy showed evidence for the presence of high aspect-ratio particles. These highly anisotropic particles may be of interest for the preparation of powder-in-tube and other powder-deposited conductors, for current leads, and for grain alignment studies. DOE

N95-25391# Oak Ridge National Lab., TN.

KINETIC MODELING OF THE ATOMIC LAYER EPITAXY WINDOW IN GROUP 4 SEMICONDUCTOR GROWTH

G. Eres 1995 3 p Presented at the Optical Society of America Winter Topical Meeting, Santa Fe, NM, 9-11 Feb. 1995

(Contract DE-AC05-84OR-21400)

(DE95-005903; CONF-950262-1) Avail: CASI HC A01/MF A01

Atomic layer epitaxy (ALE) is a method for epitaxial growth of semiconductor thin films that utilized adsorption kinetics of source gases for external control of the film growth process. ALE takes advantage of the self-limiting nature of the chemiadsorption process for achieving layer-by-layer growth of semiconductors with uniform film thickness, ideally, 1 ML per each adsorption cycle. The 1 ML/cycle film growth is a uniquely distinguishing feature that makes ALE high attractive for preparation of ultrathin films of precisely controlled thickness. Other unique characteristics of ALE growth are that the spatial homogeneity of this film, and the film thickness per cycle are insensitive to small variations in the external process parameters. The parameter space in which ALE is independent of external conditions is known as the ALE window. This paper is concerned with the modeling and kinetics associated with the ALE window in Group 4 compound semiconductors. Derived from text

N95-25409*# Teledyne Brown Engineering, Huntsville, AL.

CRYSTAL GROWTH FURNACE (CGF) Final Report, 11 Jun. 1987 - 30 Dec. 1992

Charles E. Billingsley and Larry Frederick 2 Feb. 1993 16 p

(Contract NAS8-36637)

(NASA-CR-196591; NAS 1.26:196591; Rept-210RPT0046) Avail: CASI HC A03/MF A01

The contract baseline, contract requirements review, contract modifications, contract problem areas and conclusions are addressed. Contract baseline was established 11 June 1987 and updated 1 December 1989. Significant changes were introduced into the 1989 baseline as compared to the original baseline. Contract modifications were made to add requirements as the program matured and as definition of requirements were completed. Problems were solved in real time through the contractor/customer team involvement and relationship to assure a timely and successful mission. The conclusion is that the CGF performed as designed and the experiments performed during the USML-1 Mission supports the conclusion. Author

N95-25598# Los Alamos National Lab., NM.

TEMPERATURE-DEPENDENT GROWTH OF LaAlO3 FILMS ON YBa2CuO7 C-AXIS FILMS FOR MULTILAYER STRUCTURES

M. E. Hawley, R. J. Houlton, I. A. Raistrick, and F. H. Garzon 1995 7 p Presented at the 1994 Fall Meeting of the Materials Research Society (MRS), Boston, MA, 28 Nov. - 2 Dec. 1994

(Contract W-7405-eng-36)

(DE95-005257; LA-UR-94-4295; CONF-941144-34) Avail: CASI HC A02/MF A01

Fabrication of ultra smooth films, free of micro-shorts, is essential to the development of High Temperature Superconducting (HTS) thin film devices. One such example is a SNS junction consisting of two HTS layers separated by a uniformly smooth continuous barrier material. Other schemes under consideration require multilayer structures of up to 5 - 7 epitaxially grown layers of complex oxide material. Successful fabrication of such devices necessitates understanding the epitaxial growth of polycrystalline oxide films on polycrystalline film templates. Toward this end we have developed a set of deposition parameters that produce high quality epitaxial insulating layers suitable for HTS device applications. All films in this study were grown by off-axis RF magnetron sputter deposition. LaAlO3 films were deposited over MgO grown YBa2Cu3O7 (YBCO) c-axis thin films at temperatures ranging from 200 to 700C and on virgin substrates at 600C. Atomic Force Microscopy, eddy current measurements, and x-ray diffraction techniques were used to monitor the effect of growth conditions on the resulting film crystallinity, nanostructure, and electrical properties. Ex-situ interrupted growth characterization of these materials has yielded new insight into the processes that control the growth mechanism and resulting microstructure. All films were polycrystalline. Below 600C, LaAlO3 films were not epitaxial while films grown at 650C showed some zone group axes(200) orientation. The shape of the underlying YBCO film is most clearly evident for the film grown at 400C. Surface roughness depended on the appearance of crystals on the film surface. The superconducting properties of the underlying YBCO film required O2 annealing prior to deposition of the LaAlO3 layer. DOE

N95-25776# Academy of Sciences of the Ukraine, Kiev (Ukraine). Inst. Teoreticheskoj Fiziki.
POLARIZATION AND INTENSITY OF dd-TRANSITIONS IN SUPERCONDUCTING COPPER OXIDES
V. M. Loktev 1994 5 p Submitted for publication Sponsored by Interntional Science Foundation
(DE95-605886; ITP-94-1) Avail: CASI HC A01/MF A01 (US Sales Only)

The simple explanation of experimentally observed dipole character and plane polarization of lowest dd-transitions which is based on pd-hybridization effects is proposed. DOE

N95-25851 Joint Inst. for Nuclear Research, Dubna (USSR).
ACCURATE DETERMINATION OF IC MODULATION PARAMETER IN Sr(x)Ba(1-x)Nb2O6 FROM SECOND ORDER SATELLITES OF NEUTRON DIFFRACTION TOF (TIME-OF-FLIGHT) SPECTRA
F. Prokert (Research Centre Rossendorf, Rossendorf, Germany.), B. N. Savenko, and A. M. Balagurov 1993 10 p Sponsored by BMFT
(DE94-629003; JINR-E-14-93-279) Copyright Avail: Issuing Activity (Department of Energy (DOE)) (US Sales Only)

The nature of the incommensurate structure modulation in niobates of the tungsten bronze type has been dealt with in numerous investigations. The influence of the crystal imperfections upon the incommensurate modulation was discovered in barium sodium niobate. Our neutron diffraction investigations show that a similar effect is also observed in strontium barium niobate. Near the known phase transitions at approximately 200 and approximately 60 K slight anomalies are seen in two regions of the temperature dependence of the modulation parameter delta. This behavior of delta gives grounds for the conclusion that the order relationship of the two inter-growing orthorhombic structures changes in these phase transitions. This fits with the electron diffraction data. DOE

N95-25897# Sandia National Labs., Albuquerque, NM.
THE EFFECT OF O2 INTERCALATION ON THE ROTATIONAL DYNAMICS AND THE ORDERING TRANSITION OF C60
S. A. Myers, R. A. Assink, J. E. Schirber, and D. A. Loy 1995 6 p Presented at the 1994 Fall Meeting of the Materials Research Society (MRS), Boston, MA, 28 Nov. - 2 Dec. 1994
(Contract DE-AC04-94AL-85000)
(DE95-004765; SAND-94-3147C; CONF-941144-27) Avail: CASI HC A02/MF A01

We have used C-13 magic-angle spinning (MAS) nuclear magnetic resonance (NMR) to characterize the structure and rotational dynamics of C60 containing oxygen molecules located in the interstitial sites of the fcc lattice. Under normal conditions, a narrow peak at 143.7 ppm is observed for C60. When exposed to oxygen at moderate pressures, several additional resonances appear in the C-13 MAS NMR spectrum. These secondary resonances are shifted downfield from the main peak at 143.7 ppm and are due to the Fermi-contact interaction of the paramagnetic oxygen molecules with the C-13 nuclear spins. The presence of oxygen depresses the orientational ordering transition by ca. 20 K as observed by DSC. The spin-lattice relaxation time (T(sub 1)) of each secondary peak shows a minimum near the ordering transition, indicating that this transition is not dependent on the number of oxygen molecules surrounding an individual C60 molecule. The T(sub 1), due to paramagnetic relaxation, normalized by the number of surrounding oxygen molecules, is constant. This observation demonstrates that within a given sample, the dynamics of C60 molecules are independent of the number of surrounding oxygen molecules. DOE

N95-25978# International Centre for Theoretical Physics, Trieste (Italy).
DYNAMICS OF PHASE ORDERING OF NEMATICS IN A PORE
A. Bhattacharya, M. Rao, and A. Chakrabarti (Kansas State Univ., Manhattan, KS.) Jun. 1994 16 p
(DE95-607662; IC-94/138) Avail: CASI HC A03/MF A01 (US Sales Only)

We study the kinetics of phase ordering of a nematic liquid crystal, modeled by a spin-rotor Hamiltonian, confined within a parallel piped pore. The dynamics of the rotor obeys the time-dependent Ginzburg-Landau equation. We study the generation and evolution of a variety of defect structures, and the growth of domains, with different anchoring conditions at the pore surface. Unlike in binary fluids, mere confinement with no anchoring field, does not result in slow dynamics. Homeotropic anchoring, however, leads to slow logarithmic growth. Interestingly, homogeneous anchoring dynamically generates wall defects, resulting in an Ising like structure factor at late times. DOE

N95-25979# International Centre for Theoretical Physics, Trieste (Italy).
DOMAIN GROWTH IN WEAKLY DISORDERED MAGNETS: A COUPLED MAP LATTICE APPROACH
B. Biswal, S. Puri (Jawaharlal Nehru Univ., New Delhi, India.), and D. Chowdhury Jun. 1994 16 p
(DE95-607663; IC-94/145) Avail: CASI HC A03/MF A01 (US Sales Only)

We developed a novel numerical method of studying domain growth in the Ising-type models. Using this method we investigate the laws of domain growth in random-exchange Ising model. DOE

N95-25984# Melbourne Univ., Parkville (Australia).
APPLICATION OF EXTENDED-CRYSTAL DIFFRACTION TECHNIQUES TO THE SYMMETRY AND STRUCTURE ANALYSIS OF 221-PbBiSrCaCuO
P. Goodman and P. Miller (Commonwealth Scientific and Industrial Research Organization, Parkville, Australia.) 1993 13 p
(DE95-605913; UM-P-93/64) Avail: CASI HC A03/MF A01 (US Sales Only)

The discovery of a series of layer-perovskite superconducting compounds presented a challenge for present day electron diffraction techniques, due to their common occurrence as mixed phases, and the existence of complex structural modulations of more than one type. Cowley's theory developed specifically for describing diffraction effects from layered crystals having a micro-domainal sub-structure seems particularly well suited to the task of solving these structures, while the technique of extended-crystal diffraction is shown here to be capable of providing data of sufficient precision for this analysis. The present study is made on the 221 compound of PbBiSrCaCuO. Using the above diffraction techniques it is shown that the true symmetry of the whole structure is orthorhombic, Amaa, and not monoclinic as previously assumed, and that the superlattice reflections arise as a result of a basic microdomainal constitution, rather than from a uniform and incommensurate modulation. DOE

N95-25985# Melbourne Univ., Parkville (Australia).
PULSED LASER ANNEALING OF P IMPLANTED DIAMOND
M. G. Allen, S. Prawer, D. N. Jameison, and R. Kalish (Technion - Israel Inst. of Tech., Haifa, Israel.) 1993 16 p
(DE95-605947; UM-P-93/49) Avail: CASI HC A03/MF A01 (US Sales Only)

Diamond deeply implanted with 4 MeV P to a dose of 1 x 10(exp 15) atoms/sq cm is annealed by a focused pulsed laser that is selectively absorbed by the implanted damaged layer. Laser treatment with multiple pulses at ever increasing power effects excellent regrowth as measured by channeling RBS, surface profilometry, and by optical transmission. The importance of the deep implantation and the potential of this method for doping diamond is demonstrated. DOE

N95-26061 Virginia Univ., Charlottesville, VA. School of Engineering and Applied Science.
A THEORETICAL ANALYSIS OF STRAIN IN GaN AND ITS EFFECTS ON CARRIER CONDUCTIVITY Final Report, 1 May 1992 - 30 Apr. 1994
Michael Shur and John Marshall Money Dec. 1994 17 p Limited Reproducibility: More than 20% of this document may be affected by microfiche quality
(Contract N00014-92-J-1580)
(AD-A288769; UVA/525467/EE95/101) Avail: Issuing Activity (Defense Technical Information Center (DTIC))

We performed an ensemble Monte Carlo simulation of the electron transport in gallium nitride (GaN). Our calculation showed that intervalley electron transfer plays a dominant role in GaN in high electric fields leading to a strongly inverted electron distribution and to a large negative differential conductance. We found that, in a GaN-AlN-GaN SIS structure, the strain-induced electric fields can shift the flat band voltage and produce an accumulation region on one side and the depletion region on the other side of the AlN insulator. We used our theory, the current-voltage measurements, and the capacitance-voltage measurements of the GaN-AlN-GaN SIS structures for quantitative characterization of the degree

of the AlN film relaxation depending on the film thickness. Our results show that the 30 A AlN film is slightly relaxed, the 60 A film data show well-developed relaxation process, and the 100 A structure is almost fully relaxed. Out data indicate that the low bound of the conduction band offset for the AlN/GaN heterointerface is close to 1 eV. DTIC

N95-26087# Oak Ridge National Lab., TN.
RAMAN STUDY OF DAMAGE PROCESSES IN Si(+)-IMPLANTED GaAs
M. Ivanda (Wuerzburg Univ., Germany.), U. V. Desnica (Institut Rudjer Boskovic, Zagreb, Yugoslavia.), T. E. Haynes, I. Hartmann (Wuerzburg Univ., Germany.), and W. Kiefer (Wuerzburg Univ., Germany.) Sep. 1994 5 p Presented at the 22nd European Conference on Molecular Spectroscopy, Essen, Germany, 11-16 Sep. 1994 Submitted for publication
(Contract DE-AC05-84OR-21400)
(DE95-005898; CONF-940903-1) Avail: CASI HC A01/MF A01

Ion-induced damage in GaAs as a function of ion dose following 100 keV Si(+) implants has been investigated by Raman spectroscopy. A new approach for decomposition of Raman scattering intensity on to the crystalline and amorphous phase components has been used in analysis of Raman spectra. With increasing ion dose the following was observed: (1) the widths of vibrational bands of a-phase significantly increase, while the width of the LO(Gamma) phonon band of c-phase remains unchanged; (2) the longitudinal optical phonon band of c-phase completely disappears, while the transverse optical phonon mode evolves in to a new band of a-phase; (3) the wavenumbers of all vibrational bands of a- and c-phase shift to lower values by (approximately) 10--15 cm(exp -1). A number of mechanisms possibly accountable for these shifts were analysed and evaluated. DOE

N95-26101# International Centre for Theoretical Physics, Trieste (Italy).
COHERENT STATE PATH-INTEGRAL REPRESENTATION OF SUPERSYMMETRIC LATTICE MODELS
Zhe Chang Jul. 1994 31 p
(DE95-607820; IC-94/159) Avail: CASI HC A03/MF A01 (US Sales Only)

A kind of high temperature superconductivity related lattice model is investigated within the framework of supergroup coherent state path-integral representation. Symmetry properties are analyzed and the Hamiltonians are written in the symmetric form explicitly in terms of generators of the supergroup U(N/M). By a standard approach, general supergroup coherent states are constructed. Holstein-Primakoff realizations of the supergroup U(N/M) on the coset space U(N/M)/(U(1) x U(N-1/M)) are obtained. Vacuum persistence amplitudes are expressed in terms of parameters on the coset space U(2/M)/(U(1) x U(1/M)). Symmetry-breaking terms in the Hamiltonian are taken into account separately. The Lagrangians of these models are quadratic in Grassmann variables. Thus fermionic fields can be integrated out. Nonlinear sigma model is arrived at as effective continuum field theory describing the low energy excitations of the supersymmetric lattice models. DOE

N95-26103# International Centre for Theoretical Physics, Trieste (Italy).
QUANTUM GROUP RANDOM WALKS IN STRONGLY CORRELATED 2+1 D SPIN SYSTEMS
A. P. Protogenov, Yu. V. Rostovtsev (Academy of Sciences, USSR, Nizhny Novgorod, USSR.), and V. A. Verbus (Academy of Sciences, USSR, Nizhny Novgorod, USSR.) Jun. 1994 9 p Sponsored by American Physical Society
(DE95-607844; IC-94/151) Avail: CASI HC A02/MF A01 (US Sales Only)

We consider the temporal evolution of strong correlated degrees of freedom in 2+1 D spin systems using the Wilson operator eigenvalues as variables. It is shown that the quantum-group diffusion equation at deformation parameter q being the k-th root of unity has the polynomial solution of degree k. DOE

N95-26170# Lawrence Livermore National Lab., Livermore, CA.
ELECTRONIC STRUCTURE OF (La,Sr)2CuO4 AND Ba(0.6)K(0.4)BiO3
R. H. Howell, P. A. Sterne, M. J. Fluss, J. H. Kaiser (Texas Univ., Arlington, TX.), K. Kitazawa (Tokyo Univ., Japan.), H. Kojima (Yamanashi Univ., Kofu, Japan.), W. D. Mosley (California Univ., Davis, CA.), J. W. Dykes (California Univ., Davis, CA.), and R. N. Shelton (California Univ., Davis, CA.) May 1994 8 p Presented at the 10th International Conference on Positron Annihilation, Beijing, China, 23-29 May 1994 Sponsored in part by the Robert A. Welch Foundation
(Contract W-7405-eng-48)
(DE95-004963; UCRL-JC-116558; CONF-9405170-8) Avail: CASI HC A02/MF A01

We have measured and calculated the electron-positron momentum distribution of La(2-x)Sr(x)CuO4 samples for Sr concentration of 0, 0.1,0.13, and 0.2 and Ba(0.6)K(0.4)BiO3. The momentum distribution of all samples contained features derived from the overlap of the positron distribution with the valence electrons. In addition, discontinuities typical of a Fermi surface are seen in the superconducting samples. The form and position of these features are in general agreement with band theory for both La(2-x)Sr(x)CuO4 and Ba(0.6)K(0.4)BiO3. However, the evolution of the Fermi surface with doping in La(2-x)Sr(x)CuO4 differed significantly from expectations based on single electron band theories. DOE

N95-26252# International Centre for Theoretical Physics, Trieste (Italy).
ROTATIONAL MELTING IN DISPLACIVE QUANTUM PARAELECTRICS
R. Martonak and E. Tosatti Jun. 1994 43 p Submitted for publication
(DE95-607804; IC-94/139) Avail: CASI HC A03/MF A01 (US Sales Only)

Displacive quantum paraelectrics are discussed as possible realizations of rotational quantum melting. The phenomenology of SrTiO3 and KTaO3 is discussed in this light. Both old and fresh theoretical work on two-dimensional lattice models for quantum paraelectricity is reviewed. DOE

N95-26260# Ecole Polytechnique Federale de Lausanne (Switzerland). Laboratoire de Ceramique.
SURFACE PLASMON OBSERVED FOR CARBON NANOTUBES
L. A. Bursill, P. A. Stadelmann, J. L. Peng (Melbourne Univ., Parkville, Australia.), and S. Prawer (Melbourne Univ., Parkville, Australia.) 1993 15 p Sponsored by Swiss National Funds for Research, and Australian Research Council
(DE95-607769; UM-P-93/73) Avail: CASI HC A03/MF A01 (US Sales Only)

Parallel electron energy loss spectra (PEELS) results obtained for individual carbon nanotubes, using nanoprobe techniques (1-2 nm diameter electron beam), energy resolution 0.5 eV and collection times of 4-25 sec are presented. The aim was to use a nanoprobe to compare PEELS spectra from different parts of a tube, in order to search for variations in sp(exp 2)/sp(exp 3) bonding ratios as well as to look for orientation dependent plasmon and core-loss phenomena. It also seemed interesting to compare results for nanotubes with those for other varieties of graphitized carbons. The most interesting result so far was the appearance of a 15 eV plasmon peak, which appeared only for tubes containing less than or equal to about 12 graphite-like layers. This peak did not shift significantly with tube size. A low-loss peak at 6 eV of variable relative intensity was also observed. This peak was relatively very weak for amorphous tubes; it appears to be characteristic of graphite-like layers, as found for nanotubes and, of course, graphite itself. This paper is restricted to discussion of the low-loss results. The experimental techniques are first described, including some details of the methods which may be used to disperse and support sooty carbons for high-resolution transmission electron microscopy. The results are then presented, followed by an interpretation of all the low-loss PEELS results. DOE

77 THERMODYNAMICS AND STATISTICAL PHYSICS

Includes quantum mechanics; theoretical physics; and Bose and Fermi statistics.

For related information see also *25 Inorganic and Physical Chemistry* and *34 Fluid Mechanics and Heat Transfer.*

N95-24235# Los Alamos National Lab., NM.
THEORETICAL MOTIVATION FOR GRAVITATION EXPERIMENTS ON ULTRA-LOW ENERGY ANTIPROTONS AND ANTIHYDROGEN
M. M. Nieto 1995 6 p Presented at the Low-energy Antiproton Physics, Bled, Slovenia, 12-17 Sep. 1994

(Contract W-7405-eng-36)
(DE95-003662; LA-UR-94-3953; CONF-9409264-1) Avail: CASI HC A02/MF A01

It is known that the generally accepted theories of gravity and quantum mechanics are fundamentally incompatible. Thus, when one tries to combine these theories, one must beware of physical pitfalls. Modern theories of quantum gravity are trying to overcome these problems. Any ideas must confront the present agreement with general relativity, but yet be free to wonder about not understood phenomena, such as the dark matter problem. This all has led some 'intrepid' theorists to consider a new gravitational regime, that of antimatter. Even more 'daring' experimentalists are attempting, or considering attempting, the measurement of the gravitational force on antimatter, including low-energy antiprotons and, perhaps most enticing, antihydrogen. DOE

N95-24266# International Centre for Theoretical Physics, Trieste (Italy).
QUANTUM MECHANICS WITH SPONTANEOUS LOCALIZATION AND EXPERIMENTS
F. Benatti (Trieste Univ., Italy.), G. C. Ghirardi, and R. Grassi (Udine Univ., Italy.) May 1994 20 p
(DE94-634285; IC-94/93) Avail: CASI HC A03/MF A01 (US Sales Only)

We examine from an experimental point of view the recently proposed models of spontaneous reduction. We compare their implications about decoherence with those of environmental effects. We discuss the treatment, within the considered models, of the so called quantum telegraph phenomenon and we show that, contrary to what has been recently stated, no problems are met. Finally, we review recent interesting work investigating the implications of dynamical reduction for the proton decay. DOE

N95-24275# International Centre for Theoretical Physics, Trieste (Italy).
SUPERCONDUCTING IN THE NEAR HALF-FILLING HUBBARD MODEL
Anh Tuan Hoang, Toan Thang Nguyen (Institute of Theoretical Physics, Hanoi, Viet Nam.), and Ngoc Thuan Nguyen (Institute of Theoretical Physics, Hanoi, Viet Nam.) Jun. 1994 7 p
(Grant KC-05-01)
(DE94-634857; IC-94/109) Avail: CASI HC A02/MF A01 (US Sales Only)

The near half-filling Hubbard model of strongly correlated electron systems is considered within the framework of the new functional integral method without slave boson. A dynamical system of equations determining the superconducting phase of the Hubbard model is derived. Both singlet and triplet Cooper pairings are studied. DOE

N95-24277# International Centre for Theoretical Physics, Trieste (Italy).
ELECTRON-PHONON INTERACTION IN THE HUBBARD MODEL
Anh Tuan Hoang, Toan Thang Nguyen (Institute of Theoretical Physics, Hanoi, Viet Nam.), and Ngoc Thuan Nguyen (Institute of Theoretical Physics, Hanoi, Viet Nam.) Jun. 1994 8 p
(Grant KC-05-01)
(DE94-634859; IC-94/111) Avail: CASI HC A02/MF A01 (US Sales Only)

Superconductivity existence in the Hubbard model is studied, taking into account both electron-phonon and electron-electron interactions. Using Sarker's functional integral formalism a system of equations for the dynamical order parameters is derived. DOE

N95-24288# International Centre for Theoretical Physics, Trieste (Italy).
T=0 FINITE-SIZE SCALING FOR A QUANTUM SYSTEM WITH LONG-RANGE INTERACTION
H. Chamati May 1994 17 p
(DE94-634528; IC-94/103) Avail: CASI HC A03/MF A01 (US Sales Only)

The general idea of finite-size scaling is tested by the example of the pure quantum version of an exactly solvable model of structural phase transition with long range interactions decaying at large distances tau as tau(sup -d-sigma), where d is the space dimensionality and sigma greater than 0. The finite size shift of the quantum parameter (playing the same role as that of the temperature for classical systems) is calculated for the general geometry L(sup d-d') x infinity(sup d'), with 0 less than or equal d' less then d. The root mean square order parameter is evaluated for 0 less then or equal to d' less then sigma/2. DOE

N95-24312# Joint Inst. for Nuclear Research, Dubna (USSR).
ANHARMONIC POTENTIAL IN THE OSCILLATOR REPRESENTATION
M. Dineykhan and G. V. Efimov 1994 26 p
(DE94-636740; JINR-E-4-94-75) Avail: CASI HC A03/MF A01 (US Sales Only)

In the non relativistic and relativized Schroedinger equation the Wick ordering method called the oscillator representation is proposed to calculate the energy spectrum for a wide class of potentials allowing the existence of a bound state. The oscillator representation method gives a unique regular way to describe and calculate the energy levels of ground as well as orbital and radial excitation states for a wide class of potentials. The results of the zeroth approximation oscillator representation are in good agreement with the exact values for the anharmonic potentials. The oscillator representation method was applied to the relativized Schroedinger equation too. The perturbation series converges fairly fast, i.e., the highest perturbation corrections over the interaction Hamiltonian are small enough. DOE

N95-24313# Joint Inst. for Nuclear Research, Dubna (USSR).
ELLIPTIC DEFORMED NEWTON MECHANICS IN THE THREE-DIMENSIONAL PHASE SPACE
R. M. Yamaleev 1994 6 p
(DE94-636741; JINR-R-2-94-109) Avail: CASI HC A02/MF A01 (US Sales Only)

We formulate the basic notions of mechanics in three-dimensional phase space, which is obtained as elliptic deformation of Newton mechanics. It is shown that in that mechanics the Nambu equations will play the role of the Hamilton equations. DOE

N95-24328# Stanford Linear Accelerator Center, CA.
RECENT PROGRESS IN ONE-LOOP MULTI-PARTON CALCULATIONS
Z. Bern (California Univ., Los Angeles, CA.), L. Dixon, D. C. Dunbar (University Coll. of Swansea, Wales.), and D. A. Kosower Sep. 1994 5 p Presented at the QCD 94: Nuclear Physics B, Montpellier, France, 7-13 Jul. 1994
(Contracts DE-AG03-76SF-00515; DE-FG03-91ER-40662)
(DE95-006062; SLAC-PUB-6658; CONF-9407135-2) Avail: CASI HC A01/MF A01

The authors describe techniques that simplify the calculation of one-loop QCD amplitudes with many external legs, which are needed for next-to-leading-order (NLO) corrections to multi-jet processes. The constraints imposed by perturbative unitarity, collinear singularities and a supersymmetry-inspired organization of helicity amplitudes are particularly useful. Certain sequences of one-loop helicity amplitudes may be obtained for an arbitrary number of external gluons using these techniques. They also report on progress in completing the set of one-loop helicity amplitudes required for NLO three-jet production at hadron colliders, namely the amplitudes with two external quarks and three gluons. DOE

N95-24333# California Univ., Berkeley. Lawrence Berkeley Lab, CA.
SUPERSYMMETRY
Hitoshi Murayama Jun. 1994 25 p Presented at the INS Symposium, Tokyo, Japan, 8-10 Mar. 1994
(Contract DE-AC03-76SF-00098)
(DE95-004670; LBL-36175; CONF-9403122-4) Avail: CASI HC A03/MF A01

The author reviews phenomenologically interesting aspects of supersymmetry. First he points out that the discovery of the positron can be regarded as a historic analogue to the would-be discovery of supersymmetry. Second he reviews the recent topics on the unification of the gauge coupling constants, m(sub b)-M(sub (tau)) relation, proton decay, and baryogenesis. The author also briefly discusses the recent proposals to solve the problem of flavor changing neutral currents. Finally he argues that the measurements of supersymmetry parameters may probe the physics at the Planck scale. DOE

N95-24347# Joint Inst. for Nuclear Research, Dubna (USSR).
MOVING SCALES CONTRACTION CONTRADICTS INTERVAL INVARIANCE
M. S. Khvastunov and V. N. Streltsov 1994 3 p
(DE94-636736; JINR-D-2-94-72) Avail: CASI HC A01/MF A01 (US Sales Only)

The traditional definition of the moving scale length is analyzed from

the viewpoint of a 'strong' condition of the interval (s) invariance which means s independence of the motion velocity. It is stressed that the simultaneity of the scale end marks contradicts this condition. DOE

N95-24349# Joint Inst. for Nuclear Research, Dubna (USSR).
ON A GENERALIZED KEPLER-COULOMB SYSTEM: INTER BASIS EXPANSIONS
M. Kibler (Lyon-1 Univ., Lyon, France.), L. G. Mardoyan (Erivan State Univ., USSR.), and G. S. Pogosyan 1994 18 p
(DE94-636739; JINR-E-2-94-107) Avail: CASI HC A03/MF A01 (US Sales Only)

This paper deals with a dynamic system that generalizes the Kepler-Coulomb system and the Hartmann system. It is shown that the Schroedinger equation for the generalized Kepler-Coulomb system can be separated in prolate spheroidal coordinates. The coefficients of the inter basis expansions between three bases (spherical, parabolic and spheroidal) are studied in detail. It is found that the coefficients for the expansion of the parabolic basis in terms of the spherical basis, and vice versa, can be expressed through the Clebsch-Gordan coefficients for the group SU (2) analytically continued to real values of their arguments. The coefficients for the expansions of the spheroidal basis in terms of the spherical and parabolic bases are proved to satisfy three term recursion relations. DOE

N95-24352# Centro Brasileiro de Pesquisas Fisicas, Rio de Janeiro.
ON THE CENTRAL CHARGE IN 3 D-SUPERSYMMETRY
L. P. Colatto Jan. 1994 13 p
(DE95-600851; CBPF-NF-010/94) Avail: CASI HC A03/MF A01 (US Sales Only)

A matter self-interacting model with N = 1-supersymmetry in 3D is discussed in connection with the appearance of a central charge in the algebra of the supersymmetry generators. The result is extended to include gauge fields with a Chern-Simons term. DOE

N95-24353# Centro Brasileiro de Pesquisas Fisicas, Rio de Janeiro.
CONSTRAINTS AND HAMILTONIAN IN LIGHT-FRONT QUANTIZED FIELD THEORY
P. P. Srivastava 1993 16 p
(DE95-600852; CBPF-NF-032/93; DFPF-92/TH/58) Avail: CASI HC A03/MF A01 (US Sales Only)

Self-consistent Hamiltonian formulation of scalar theory on the null plane is constructed and quantized following the Dirac procedure. The theory also contains constraint equations which would give, if solved, a nonlocal Hamiltonian. In contrast to the equal-time formulation, we obtain a different description of the spontaneous symmetry breaking in the continuum, and the symmetry generators are found to annihilate the light-front vacuum. Two examples are given where the procedure cannot be applied self-consistently. The corresponding theories are known to be ill-defined from the equal-time quantization. DOE

N95-24376# Joint Inst. for Nuclear Research, Dubna (USSR).
THE LIENARD-WIECHERT POTENTIALS AND RELATIVISTIC LENGTH
V. N. Streltsov 1993 6 p
(DE94-636733; JINR-D-2-93-381) Avail: CASI HC A02/MF A01 (US Sales Only)

Additional arguments in favor of the relativistic length concept and the elongation formula that follows from it are presented. The formula is obtained as a direct consequence of the Feynman-Wheeler presentation (the 'mean' Lienard-Wiechert potential). It is shown that the relativization of the radar measuring procedure also leads to the elongation formula. The deduction of the Lienard-Wiechert potential based on the Lorentz transformation of the Coulomb potential is given. The relationship of the formation way of radiation with the electric field sizes of a moving charge (that are in fact defined by the Lienard-Wiechert equipotential) is discussed. DOE

N95-24378# Joint Inst. for Nuclear Research, Dubna (USSR).
THE FITZGERALD-LORENTZ HYPOTHESIS FROM THE VIEWPOINT OF RELATIVITY THEORY
V. N. Streltsov 1994 2 p
(DE94-636735; JINR-D-2-94-11) Avail: CASI HC A01/MF A01 (US Sales Only)

The notions of resting and moving reference systems change places when treated by the known Michelson-Morley experiment in the relativity theory (in comparison with the other theory). Taking this into account, the Fitzgerald-Lorentz formula should mean lengthen the longitudinal arm of an interferometer when it's in motion. DOE

N95-24405# International Centre for Theoretical Physics, Trieste (Italy).
Z FLUX-LINE LATTICES AND SELF-DUAL EQUATIONS IN THE STANDARD MODEL
G. Bimonte and G. Lozano Apr. 1994 9 p
(DE94-634364; IC-94/65; DSF-T-5/94; INFN-NA-IV-5/94) Avail: CASI HC A02/MF A01 (US Sales Only)

We derive gauge covariant self-dual equations for the SU(2) x U(1)(sub y) theory of electroweak interactions and show that they admit solutions describing a periodic lattice of Z-strings. Author

N95-24446# Centro Brasileiro de Pesquisas Fisicas, Rio de Janeiro.
RELATIONS AMONG SOLUTIONS FOR WAVE AND KLEIN-GORDON EQUATIONS FOR DIFFERENT DIMENSIONS
J. J. Giambiagi (Centro Latinoamericano de Fisica, Rio de Janeiro, Brazil.) Aug. 1993 15 p
(ISSN 0029-3865)
(DE95-600853; CBPF-NF-043/93) Avail: CASI HC A03/MF A01 (US Sales Only)

Relations between solutions of homogeneous wave equations for different dimensions are discussed. Idem for Green's functions. A similar discussion is given for the Klein Gordon equations. Relations with solutions for powers of D'Alembertian and Kleinian are also discussed. The importance of understanding the relations between analytic and dimensional regularization is briefly mentioned. DOE

N95-24450# Brookhaven National Lab., Upton, NY.
THE 24TH ORDER HIGH TEMPERATURE EXPANSION FOR THE 3-D ISING MODEL
U. Glaessner (Wuppertal Univ., Germany.), K. Schilling (Wuppertal Univ., Germany.), G. Bhanot (Institute for Advanced Study, Princeton, NJ.), and M. Creutz Dec. 1994 5 p Presented at the Lattice '94, Bielefeld, Germany, 25 Sep. - 1 Oct. 1994
(Contract DE-AC02-76CH-00016)
(DE95-004952; BNL-61142; CONF-9409269-3) Avail: CASI HC A01/MF A01

The authors present the series for the free energy and their estimate for the critical exponent (alpha), as computed by a recursive bookkeeping algorithm on the CM5. They begin with a discussion of the algorithm to compute the High-Temperature expansion on finite 3-D Ising lattices. DOE

N95-24457# Los Alamos National Lab., NM.
COMPLEX SCATTERING DYNAMICS AND THE QUANTUM HALL EFFECT
S. A. Trugman 16 Dec. 1994 31 p Presented at the Quantum Complexity in Mesoscopic Systems, Los Alamos, NM, 16-20 May 1994
(Contract W-7405-eng-36)
(DE95-005239; LA-UR-94-4386; CONF-9405204-3) Avail: CASI HC A03/MF A01

We review both classical and quantum potential scattering in two dimensions in a magnetic field, with applications to the quantum Hall effect. Classical scattering is complex, due to the approach of scattering states to an infinite number of dynamically bound states. Quantum scattering follows the classical behavior rather closely, exhibiting sharp resonances in place of the classical bound states. Extended scatterers provide a quantitative explanation for the breakdown of the QHE at a comparatively small Hall voltage as seen by Kawaji et al., and possibly for noise effects. DOE

N95-24481# Joint Inst. for Nuclear Research, Dubna (USSR). Nuclear Reactions Lab.
ENTROPY AND ENTHALPY OF ADSORPTION OF GASEOUS CHLORIDES OF METALS ON QUARTZ GLASS AS A FUNCTION OF THE MOLECULAR COMPOSITION
Yury T. Chuburkov, Kho Seb Nam, L. K. Alpert, and I. Zvara 1993 19 p In RUSSIAN; In RUSSIAN
(DE94-627162; JINR-R-6-93-289; Rept-P6-93-289) Avail: CASI HC A03/MF A01 (US Sales Only)

Adsorption of Cs, Au, Tb, Tm, Pb, Zr, Hf, Sb, Bi, Nb chlorides has been studied using micro quantities of radionuclides. The experiments have been performed in a thermochromatographic column with SOCl2 as a chlorinating agent at some 'perfect' purification of the carrier-gas and the surface of the quartz glass as well as at less through one. It has been found from the temperature dependence of the Henry constant that Delta S(sup 0)(sub alpha) values (for a certain standard state) of chloride fall in a narrow range of (130-170) J.mol(sup -1).K(sup -1). After introducing the data for Pb free atoms the correlation with the number of atoms in a molecule, m, has been found Delta S(sup 0)(sub alpha) = -184+8.5 m. Then the adsorption enthalpy can be estimated from a single experimental point for the adsorption equilibrium using the formula Delta H(sup 0)(sub alpha) = (8.5 m - 184 - R 1 n K(sup 0)(sub alpha))T, as well as from the temperature of the maximum of the thermochromatographic peak, using the basic equation of thermochromatography and substituting the above formula for Delta S(sup 0) (sub alpha). For the conditions of the perfect cleaning the rule -Delta H(sup 0)(sub alpha) less than or equal Delta H(sub vap), is usually satisfied, which can be useful for identifying the chemical state of elements in gas phase and estimating the degree of modification of the sorbent surface. DOE

N95-24507# Joint Inst. for Nuclear Research, Dubna (USSR). Theoretical Physics Lab.

HEAT KERNEL EXPANSION ON A CONE AND QUANTUM FIELDS NEAR COSMIC STRINGS

D. V. Fursaev 1993 19 p Presented at the Friedman International Seminar on Gravitation and Cosmology, St. Petersburg, Russia, 12-19 Sep. 1993 Submitted for publication

(DE94-628520; JINR-E-2-93-291) Avail: CASI HC A03/MF A01 (US Sales Only)

An asymptotic expansion of the trace of the heat kernel on a cone where the heat coefficients have a delta function behaviour at the apex is obtained. It is used to derive the renormalized effective action and total energy of a self-interacting quantum scalar field on the cosmic string space-time. Analogy is pointed out with quantum theory with boundaries. The surface infinities in the effective action are shown to appear and are removed by renormalization of the string tension. Besides the total renormalized energy turns out to be finite due to cancellation of the known non-integrable divergence in the energy density of the field with a counterterm in the bare string tension. DOE

N95-24508# Joint Inst. for Nuclear Research, Dubna (USSR). Theoretical Physics Lab.

THE LATTICE SPINOR QED HAMILTONIAN CRITIQUE OF THE CONTINUOUS SPACE APPROACH

A. V. Sidorov and L. G. Zastavenko 1993 20 p Submitted for publication

(DE94-628521; JINR-E-2-93-315) Avail: CASI HC A03/MF A01 (US Sales Only)

We give the irreproachable, from the point of view of gauge invariance, derivation of the lattice spinor QED Hamiltonian. Our QED Hamiltonian is manifestly gauge invariant. We point out important defects of the continuous space formulation of the QED that make, in our opinion, the lattice QED obviously preferable to the continuous space QED. We state that it is impossible to give a continuous space QED formulation which is compatible with the condition of gauge invariance. DOE

N95-24509# Joint Inst. for Nuclear Research, Dubna (USSR). Lab. of Theoretical Physics.

QUANTUM GROUP GAUGE THEORIES AND COVARIANT QUANTUM ALGEBRAS

A. P. Isaev and Z. Popowicz (Wroclaw Univ., Poland.) 1993 11 p Submitted for publication

(DE94-628524; JINR-E-2-93-54) Avail: CASI HC A03/MF A01 (US Sales Only)

The algebraic formulation of the quantum group gauge models in the framework of the R-matrix approach to the theory of quantum groups is given. Gauge groups taking values in the quantum groups and noncommutative gauge fields transformed as comodules under the coaction of the gauge quantum group G(sub q) are considered. Using this approach the quantum deformations of the topological Chern-Simons models, non-Abelian gauge theories and the Einstein gravity are constructed. The noncommutative fields in these models generate G(sub q)-covariant quantum algebras. DOE

N95-24578# Stanford Linear Accelerator Center, CA.

DECOHERENCE, DETERMINISM AND CHAOS REVISITED

H. P. Noyes 15 Nov. 1994 18 p Presented at the Law and Prediction in Natural Science in the Light of New Knowledge From Chaos Research, Salzburg, Austria, 7-10 Jul. 1994

(Contract DE-AC03-76SF-00515)

(DE95-006070; SU-SLAC-PUB-6718; CONF-9407158-1) Avail: CASI HC A03/MF A01

We suggest that the derivation of the free space Maxwell Equations for classical electromagnetism, using a discrete ordered calculus developed by L. H. Kauffman and T. Etter, necessarily pushes the discussion of determinism in natural science down to the level of relativistic quantum mechanics and hence renders the mathematical phenomena studied in deterministic chaos research irrelevant to the question of whether the world investigated by physics is deterministic. We believe that this argument reinforces Suppes' contention that the issue of determinism versus indeterminism should be viewed as a Kantian antinomy incapable of investigation using currently available scientific tools. DOE

N95-24610# Los Alamos National Lab., NM.

CHIRAL LIMIT OF QCD

R. Gupta 1994 11 p Presented at the Lattice '94, Bielefeld, Germany, 25 Sep. - 1 Oct. 1994

(Contract W-7405-eng-36)

(DE95-005245; LA-UR-94-4365; CONF-9409269-4) Avail: CASI HC A03/MF A01

This talk contains an analysis of quenched chiral perturbation theory and its consequences. The chiral behavior of a number of quantities such as the pion mass m(sub pi)(exp 2), the Bernard-Golterman ratios R and chi, the masses of nucleons, and the kaon B-parameter are examined to see if the singular terms induced by the additional Goldstone boson, eta', are visible in present data. The overall conclusion of this analysis is that even though there are some caveats attached to the indications of the extra terms induced by eta' loops, the standard expressions break down when extrapolating the quenched data with m(sub q) is less than m(sub s)/2 to physical light quarks. I then show that due to the single and double poles in the quenched eta', the axial charge of the proton cannot be calculated using the Adler-Bell-Jackiw anomaly condition. I conclude with a review of the status of the calculation of light quark masses from lattice QCD. DOE

N95-24637# Joint Inst. for Nuclear Research, Dubna (USSR). Lab. of Theoretical Physics.

GENERALIZATION OF THE RAYLEIGH FORMULA TO THE MODEL WITH RING-SHAPED POTENTIALS

L. G. Mardoyan (Erivan State Univ., USSR.), V. M. Ter-Antonyan, T. A. Chatrchyan (Erivan State Univ., USSR.), and A. N. Sisakyan (Erivan State Univ., USSR.) 1993 7 p Presented at the International Workshop Symmetry Methods in Physics, Dubna, Russia, 6-10 Jul. 1993

(DE94-628578; JINR-E-2-93-290) Avail: CASI HC A02/MF A01 (US Sales Only)

The motion of a quantum particle is investigated in the ring-shaped model when the 'bare' potential is equal to zero. Factorized in the spherical and cylindrical coordinates bases of this model are derived. The generalization of the Rayleigh expression for the plane wave expansion in the spherical waves is derived. DOE

N95-24638# Joint Inst. for Nuclear Research, Dubna (USSR). Lab. of Theoretical Physics.

ON THE PROBLEM OF UNBOUNDEDNESS FROM BELOW OF THE SPINOR QED HAMILTONIAN

L. G. Zastavenko 1993 15 p Submitted for publication

(DE94-628579; JINR-E-2-93-71) Avail: CASI HC A03/MF A01 (US Sales Only)

It is shown that the Hamiltonian H(sub QED) + H(sub 2), where H(sub QED) is the spinor QED Hamiltonian and H(sub 2) is the positive transversal photon mass term, is unbounded from below if the electromagnetic coupling constant e(exp 2) is small enough, e(exp 2) less than e(sub 0)(exp 2), and

the transversal photon squared mass parameter M(exp 2) is not too large: 0 less than M(exp 2) less than ce(exp 2)(1 - e(exp 2)/e(sub 0)(exp 2))l(exp 2). Here, l is the cut-off parameter; and c and e(sub 0)(exp 2), positive constants which do not depend on any parameters. DOE

N95-24639# Joint Inst. for Nuclear Research, Dubna (USSR). Lab. of Theoretical Physics.
DRESSING AND BOUND STATES IN QUANTUM FIELD THEORY
M. I. Shirokov 1993 18 p Submitted for publication
(DE94-628580; JINR-E-4-93-55) Avail: CASI HC A03/MF A01 (US Sales Only)

The program of introducing 'dressed' particles (instead of 'bare' ones) was suggested earlier by L. Faddev et al. It is modified here for the case when 'dressed' states can decay. On the basis of this 'dressing' formalism, a new approach is proposed to the problem of bound states in field theories such as the hydrogen atom and the positronium in QED or hadrons in QCD. Peculiarities of this approach as compared to the known ones are discussed. DOE

N95-24723# Weizmann Inst. of Science, Rehovot (Israel).
THE DETERMINATION OF V(SUB cb) AND QCD SUM RULES IN HEAVY QUARK EFFECTIVE THEORY
Zoltan Ligeti Oct. 1993 18 p Presented at the Advanced Study Conference On Heavy Flavours, Pavia, Italy, 3-7 Sep. 1993
(DE94-628636; WIS-PH-93-103) Avail: CASI HC A03/MF A01 (US Sales Only)

I review recent development in Heavy Quark Effective Theory that leads to an almost model-independent determination of the V(sub cb) element of the Cabibbo-Kobayashi-Maskawa matrix from exclusive semileptonic B yields D(sup *) decays. In particular, I compare the theoretical uncertainties in the B yields D(sup *l(nu)) and the B yields D(sup *l(nu)) decay modes. I discuss the applications of QCD sum rules within the Heavy Quark Effective Theory to semileptonic heavy mesons decays and gives predictions for the form factors measurable in B yields D(sup *l(nu)) decays. DOE

N95-24727# Joint Inst. for Nuclear Research, Dubna (USSR). Lab. of Theoretical Physics.
ON THE COMPTON NON-ABELIAN TWIST-3 ASYMMETRY
V. M. Korotkiyan and O. V. Teryaev 1993 7 p Submitted for publication
(DE94-628586; JINR-E-2-93-286) Avail: CASI HC A02/MF A01 (US Sales Only)

The 'fermion poles' contribution to the twist-3 single asymmetry in the gluon Compton process is calculated. The 'gluon poles' contribution appeared to be equal to zero. Qualitative predictions for the direct photon and jets asymmetries are presented. DOE

N95-24767# International Centre for Theoretical Physics, Trieste (Italy).
QUANTUM GROUP AND QUANTUM SYMMETRY
Zhe Chang May 1994 128 p Submitted for publication Sponsored by the International Atomic Energy Agency and the United Nations Educational Scientific and Cultural Organization
(DE94-634329; IC-94/89) Avail: CASI HC A07/MF A02 (US Sales Only)

This is a self-contained review on the theory of quantum group and its applications to modern physics. A brief introduction is given to the Yang-Baxter equation in integrable quantum field theory and lattice statistical physics. The quantum group is primarily introduced as a systematic method for solving the Yang-Baxter equation. Quantum group theory is presented within the framework of quantum double through quantizing Lie bi-algebra. Both the highest weight and the cyclic representations are investigated for the quantum group and emphasis is laid on the new features of representations for q being a root of unity. Quantum symmetries are explored in selected topics of modern physics. For a Hamiltonian system the quantum symmetry is an enlarged symmetry that maintains invariance of equations of motion and allows a deformation of the Hamiltonian and symplectic form. The configuration space of the integrable lattice model is analyzed in terms of the representation theory of quantum group. By means of constructing the Young operators of quantum group, the Schroedinger equation of the model is transformed to be a set of coupled linear equations that can be solved by the standard method. Quantum symmetry of the minimal model and the WZNW model in conformal field theory is a hidden symmetry expressed in terms of screened vertex operators, and has a deep interplay with the Virasoro algebra. In quantum group approach a complete description for vibrating and rotating diatomic molecules is given. The exact selection rules and wave functions are obtained. The Taylor expansion of the analytic formulas of the approach reproduces the famous Dunham expansion. DOE

N95-24833# Centro Brasileiro de Pesquisas Fisicas, Rio de Janeiro.
NONLINEAR THEORIES OF SPIN-2 FIELD IN TERMS OF FIERZ VARIABLES
L. R. deFreitas, M. Novello, and N. Pinto-Neto 1993 33 p
(DE95-600854; CBPF-NF-055/93) Avail: CASI HC A03/MF A01 (US Sales Only)

Exceptional non linear Lagrangians for a spin-two field in terms of the Fierz variables are obtained using the method proposed by Lax. They are equivalent to the Born-Infeld Lagrangian for a spin-one field theory and are free from unbounded growth of wave velocities. DOE

N95-24834# Centro Brasileiro de Pesquisas Fisicas, Rio de Janeiro.
PROBING THE FROISSART BOUND FOR MODELS WITH CHARGED VECTOR FIELDS IN D = 3
O. M. DelCima 1993 10 p
(DE95-600855; CBPF-NF-064/93) Avail: CASI HC A02/MF A01 (US Sales Only)

The tree-level unitarity is discussed and the asymptotic behavior of scattering amplitudes for 3-dimensional gauge-invariant models is presented, where complex Chern-Simons-Maxwell fields (with and without a Proca-like mass) are coupled to an Abelian gauge field. DOE

N95-24837# Centro Brasileiro de Pesquisas Fisicas, Rio de Janeiro.
LIGHT-FRONT QUANTIZED FIELD THEORY: AN INTRODUCTION. SPONTANEOUS SYMMETRY BREAKING. PHASE TRANSITION IN (PHI)(SUP 4) THEORY
P. P. Srivastava 1993 34 p
(DE95-600856; CBPF-NF-075/93) Avail: CASI HC A03/MF A01 (US Sales Only)

The field theory quantized on the light-front is compared with the conventional equal-time quantized theory. The arguments based on the micro causality principle would imply that the light-front field theory may become nonlocal with respect to the longitudinal coordinate even though the corresponding equal-time formulation is local. This is found to be the case for the scalar theory. The conventional instant form theory is sometimes required to be constrained by invoking external physical considerations; the analogous conditions seem to be already built in the theory on the light-front. In spite of the different mechanisms of the spontaneous symmetry breaking in the two forms of dynamics they result in the same physical content. The phase transition in ((phi)(sup 4))(sub 2) theory is also discussed. The symmetric vacuum state for vanishingly small couplings is found to turn into an unstable symmetric one when the coupling is increased and may result in a phase transition of the second order in contrast to the first order transition concluded from the usual variational methods. DOE

N95-24838# Centro Brasileiro de Pesquisas Fisicas, Rio de Janeiro.
ON q-DEFORMED SUPERSYMMETRIC CLASSICAL MECHANICAL MODELS
L. P. Colatto and J. L. Matheus-Valle Jan. 1994 13 p
(DE95-600864; CBPF-NF-008/94) Avail: CASI HC A03/MF A01 (US Sales Only)

Based on the idea of quantum groups and para-Grassmann variables, a generalization of supersymmetric classical mechanics with a deformation parameter q = exp(sup 2(pi)i)/(kappa) and work with the (kappa) = 3 case is presented. The coordinates of the q-superspace are a commuting parameter t and a para-Grassmann variable (theta), where (theta)(sup 3) = O. The generator and covariant derivative are obtained, as well as the action for some possible superfields. DOE

N95-24839# Instituto de Fisica Teorica, Sao Paulo (Brazil).
PARITY DOUBLING FROM THERMODYNAMICS OF EXPERIMENTAL HADRON SPECTRUM
J. Dey, G. Krein, L. Tomio, and T. Frederico (Centro Tecnico Aerospacial, San Jose dos Campos, Brazil.) Mar. 1994 10 p

(DE95-600934; IFT-P-012/94) Avail: CASI HC A02/MF A01 (US Sales Only)

Parity doubling is a way of recovering chiral symmetry, and one gets this behaviour in the real world of heavy ion collisions at mid-rapidity. Both the odd and even parity baryons show a tendency to be degenerate at a mass 3(pi) T at the freeze-out temperature of about 140-160 MeV. It is also shown that strange baryons, the (Lambda) and (Sigma), are above the value 3(pi) T by about 100 MeV. DOE

N95-24867# Florida Univ., Gainesville, FL. Dept. of Physics.

A QUANTUM GRAVITATIONAL MECHANISM FOR EXITING INFLATION

R. P. Woodard Aug. 1994 11 p Presented at the Workshop on Quantum Infrared Physics, Paris, France, 6-10 Jun. 1994
(Contract DE-FG05-86ER-40272; NATO-CRG-910627)
(DE95-003342; DOE/ER-40272/206; CONF-9406248-5) Avail: CASI HC A03/MF A01

I discuss the proposal by Nick Tsamis and myself that quantum gravity may mediate a naturally slow exit from inflation. The emphasis is on our recently completed two loop computation of the effective Hubble constant. When this result is properly checked and independently confirmed it will provide a proof that the mechanism functions in perturbation theory. DOE

N95-25095# Weizmann Inst. of Science, Rehovot (Israel). Dept. of Physics.

TeV SCALE LEPTOQUARKS AS A SIGNATURE OF STANDARD-LIKE SUPERSTRING MODELS

Edi Halyo Dec. 1993 15 p Sponsored by Feinberg Fellowship
(DE94-628529; WIS-PH-93-114) Avail: CASI HC A03/MF A01 (US Sales Only)

We show that there can be TeV scale scalar and fermionic leptoquarks with very weak Yukawa couplings in a generic standard-like superstring model. Leptoquark (down-like) quark mixing though present, is not large enough to violate the unitary bounds on the CKM matrix. The constraints on the leptoquark masses and couplings from flavor changing neutral currents (FCNC) are easily satisfied whereas those from baryon number violation may cause problems. The leptoquarks of the model are compared to the ones in the E(sub 6) Calabi-Yau models. DOE

N95-25096# Weizmann Inst. of Science, Rehovot (Israel). Dept. of Physics.

SUPERSYMMETRY AND LIGHT QUARK MASSES IN A REALISTIC SUPERSTRING MODEL

Edi Halyo Oct. 1993 24 p Sponsored by Feinberg Fellowship
(DE94-628530; WIS-PH-93-98) Avail: CASI HC A03/MF A01 (US Sales Only)

We examine the light quark masses in a standard-like superstring model in the four dimensional free fermionic formulation. We find that the supersymmetry constraints in the observable and hidden sectors eliminate all large contributions to m(sub u) and m(sub d) and force them to be much smaller than the other quark masses. The requirement for an acceptable Higgs doublet spectrum results in m(sub u) much less than m(sub d). In these models a realistic m(sub d) can always be obtained whereas m(sub u) is at most 10(sup -5) MeV. For particular choices on flat direction or vacua m(sub u) can be as small as 10(sup -7) MeV but cannot vanish. DOE

N95-25107# International Centre for Theoretical Physics, Trieste (Italy).

VORTEX SOLUTIONS IN TWO-HIGGS-DOUBLET SYSTEMS

G. Bimonte and G. Lozano Apr. 1994 9 p
(DE94-634363; IC-94/18; DSF-T-1/94; INFN-NA-IV-1/94) Avail: CASI HC A02/MF A01 (US Sales Only)

We analyze the existence of string-like defects in a two-Higgs-doublet system having SU(2) x U(1)(sub y) x U(1)(sub y), as gauge group. We are able to show that, when certain relations among the parameters hold, these configurations satisfy a set of first order differential equations (Bogomol'nyi equations) and their energy is proportional to their topological charge. Author

N95-25215# Weizmann Inst. of Science, Rehovot (Israel). Dept. of Physics.

R PARITY IN STANDARD-LIKE SUPERSTRING MODELS

Edi Halyo Jan. 1994 12 p Sponsored by Feinberg Fellowship
(DE94-628531; WIS-PH-94-4) Avail: CASI HC A03/MF A01 (US Sales Only)

We investigate the R symmetries of standard-like superstring models. At the level of the cubic superpotential there are three global U(1) R symmetries. These are broken explicitly by N greater than 3 terms in the superpotential and spontaneously by scalar Vacuum Expectation Values (VEV) necessary to preserve supersymmetry at M(sub p). A Z(sub 2) discrete symmetry remains but is equivalent to fermion number modulo 2. These models possess an effective R parity which arises from the interplay between the gauged U(1)(sub B - L) and U(1)(sub r(sub j + 3)). DOE

N95-25293# Los Alamos National Lab., NM.

STATISTICAL MECHANICS OF NONLINEAR COHERENT STRUCTURES: KINKS IN THE PHI(SUP 6) MODEL

S. Habib and A. Saxena 1994 13 p Presented at the NEEDS '94, Los Alamos, NM, 12-16 Sep. 1994
(Contract W-7405-eng-36)
(DE95-005253; LA-UR-94-4318; CONF-9409241-7) Avail: CASI HC A03/MF A01

We study the thermodynamics of kinks in the Phi(sup 6) model using a Langevin code implemented on a massively parallel computer. This code can be used to study first order dynamical phase transitions which exhibit multiple length and time scales. The classical statistical mechanics of a 1 + 1-dimensional field theory reduces to a time-independent quantum problem in one dimension via the transfer integral method. Exact solutions of the Schroedinger equation exist for the Phi(sup 6) potential (unlike the case for Phi(sup 4)) and can be used to check results from the simulations. The Phi(sup 6) model is also much richer than the Phi(sup 4) model in terms of the variety of coherent structures and possible phases accompanying a phase transition. Specifically, we have calculated (in a one dimensional model) such quantities as the probability density function (PDF) and field-field correlation functions. These quantities help us understand the contribution to the specific heat from coherent structures such as domain walls (kinks) and other transformation structures as opposed to the contribution from lattice vibrations. We have calibrated our results against known exact solutions for limiting cases with very high accuracy. Having understood this problem, we are now extending our Langevin code to higher dimensions. DOE

N95-25425# International Centre for Theoretical Physics, Trieste (Italy).

ON CONNECTION OF q-DEFORMED PARA OSCILLATORS WITH PARA OSCILLATORS

Ha Huy Bang Jul. 1994 7 p
(DE95-607007; IC-94/189) Avail: CASI HC A02/MF A01 (US Sales Only)

The connection of q-deformed para-Bose oscillators with para-Bose oscillators is determined. From this, the most general commutation relations for q-deformed para-Bose oscillator are constructed. DOE

N95-25426# International Centre for Theoretical Physics, Trieste (Italy).

DISSIPATIVE QUANTUM MECHANICS: THE GENERALIZATION OF THE CANONICAL QUANTIZATION AND VON NEUMANN EQUATION

Vasily E. Tarasov Jul. 1994 18 p Sponsored by Russian Fund for Fundamental Researches
(DE95-607008; IC-94/192) Avail: CASI HC A03/MF A01 (US Sales Only)

Sedov variational principle, which is the generalization of the least actional principle for the dissipative processes is used to generalize the canonical quantization and von Neumann equation for dissipative systems (particles and strings). DOE

N95-25428# Australian National Univ., Canberra (Australia). Dept. of Applied Mathematics.

ASYMPTOTICS FOR THE KUMMER FUNCTION OF BOSE PLASMAS

Victor Kowalenko and N. E. Frankel 1993 31 p
(DE95-607019; UM-P-93/46) Avail: CASI HC A03/MF A01 (US Sales Only)

The asymptotic expansions for the Kummer function obtained in the study of the linear response of magnetized Bose plasmas at T = 0 K are presented for large and small values of its parameter, thereby displaying the function's asymptotic nonuniformity. The large parameter expansion

plays a determining role in the behavior of these Bose systems in the limit that the external magnetic field B approaches 0. This particular expansion is generalized herein and its validity tested by determining the asymptotic expansion for the Hurwitz zeta function. DOE

N95-25429# Melbourne Univ., Parkville (Australia). Research Center for High Energy Physics.
CAN WE TEST THE MANY-HILBERT-SPACE APPROACH TO QUANTUM MECHANICS?
Mark J. Thomson 1993 10 p
(DE95-607021; UM-P-93/53) Avail: CASI HC A02/MF A01 (US Sales Only)

The differences between the many-Hilbert-space (MHS) and the von Neumann theories of quantum measurement are clarified. In particular, it is shown that recent claims that certain neutron optics experiments indicate in favor of the MHS theory at the expense of the von Neumann theory are mistaken. The question of whether the MHS theory can be falsified is also discussed. It is concluded that the principle difference between the MHS approach to the quantum measurement problem, and the usual von Neumann theory, is the absence of wave function collapse in the former and the essential role of random processes in the later. DOE

N95-25432# International Centre for Theoretical Physics, Trieste (Italy).
RELEVANCE OF INDUCED GAUGE INTERACTIONS IN DECOHERENCE
Dhurjati Prasad Datta Jul. 1994 10 p
(DE95-607082; IC-94/168) Avail: CASI HC A02/MF A01 (US Sales Only)

Decoherence in quantum cosmology is shown to occur naturally in the presence of induced geometric gauge interactions associated with particle production. A new 'gauge'-variant form of the semiclassical Einstein equations is also presented which makes the non-gravitating character of the vacuum polarization energy explicit. DOE

N95-25435# Melbourne Univ., Parkville (Australia). Research Centre for High Energy Physics.
A PARTIAL UNIFICATION MODEL IN NON-COMMUTATIVE GEOMETRY
B. E. Hanlon and G. C. Joshi 1993 23 p Sponsored by Australian Postgraduate Research Award
(DE95-607129; UM-P-93/54; OZ-93/12) Avail: CASI HC A03/MF A01 (US Sales Only)

The SU(2)(sub L) product SU(2)(sub R) product SU(4) partial unification models is presented as an example of phenomenologically acceptable unification models in the absence of supersymmetry in non-commutative geometry. The authors exploit the Chamseddine, Felder and Froehlich generalization of the Connes and Lott model building prescription. By introducing a bi-module structure and appropriate permutation symmetries a model is constructed with triplet Higgs fields in the SU(2) sectors and spontaneous breaking of SU(4). It was found that a very natural model emerges without the need to introduce singlet spinors or additional set of conjugate fermions. The symmetry breaking scales, corresponding to the 'distance' between copies of space-time, can now find a geometrical basis. DOE

N95-25446# Melbourne Univ., Parkville (Australia). School of Physcis.
OBSERVATION OF THE SCALAR AHARONOV-BOHM EFFECT BY NEUTRON INTERFEROMETRY
B. E. Allman, A. Cimmino, A. G. Klein, G. I. Opat, H. Kaiser (Missouri Univ., Columbia, MO.), and S. A. Werner (Missouri Univ., Columbia, MO.) 1993 30 p Sponsored by Australian Research Grants Scheme
(Grant NSF PHY-90-24608)
(DE95-607020; UM-P-93/50) Avail: CASI HC A03/MF A01 (US Sales Only)

A phase shift for de Broglie waves due to the action of a scalar potential in an otherwise field-free (i.e. force-free) region of space is known as the scalar Aharonov-Bohm (AB) effect. Unlike the more familiar AB effect due to the magnetic vector potential, the scalar effect has hitherto remained unverified due, presumably, to technical difficulties in electron interferometry. An analogous interferometric experiment was performed with thermal neutrons subject to pulsed magnetic fields. The observations were carried out at the University of Missouri Research Reactor, using a skew-symmetric perfect silicon crystal neutron interferometer. The expected phase shifts have been observed to a high degree of accuracy. A detailed description of the experiment and its interpretation is given. DOE

N95-25453# International Centre for Theoretical Physics, Trieste (Italy).
TESTING QUANTUM BEHAVIOUR AT THE MACROSCOPIC LEVEL
GianCarlo Ghirardi (Trieste Univ., Italy.) Jul. 1994 14 p Presented at the 1st International Conference on Phenomonology of Verification from Present to Future, Rome, Italy, 23-26 Mar. 1994 Sponsored by INFN
(DE95-607005; IC-94/165) Avail: CASI HC A03/MF A01 (US Sales Only)

We reconsider recent proposals to test macro realism versus quantum mechanics in experiments involving noninvasive measurement processes on a Squid. In spite of the fact that we are able to prove that the proposed experiments do not represent a test of macro realism but simply of macroscopic quantum coherence we call attention to their extreme conceptual relevance. We also discuss some recent criticisms which have been raised against the considered proposal and we show that they are not relevant. DOE

N95-25454# International Centre for Theoretical Physics, Trieste (Italy).
RECOIL EFFECTS IN QUANTUM TOPOLOGICAL SOLITONS
Fermin Aldabe Jul. 1994 6 p
(DE95-607006; IC-94/171) Avail: CASI HC A02/MF A01 (US Sales Only)

We enlarge the space of dynamical variables to include the collective coordinate defining the position of the quantum topological soliton. The leading order correction arising from this treatment allows us to confirm that the energy of the soliton varies covariantly to lowest order for certain types of self interacting potentials. Upon imposing conservation of statistics we find that the allowed momenta is quantized. A Yukawa coupling appears as a consequence of diagonalizing the Hamiltonian of the mesons. These results along with its quantum nature proposes the quantum topological solitons as excellent candidates for nuclear physics at intermediate energies. DOE

N95-25456# International Centre for Theoretical Physics, Trieste (Italy).
TACHYON CONDENSATES AND ANISOTROPIC UNIVERSE
Swapna Mahapatra and Sudipta Mukherji Aug. 1994 15 p
(DE95-607074; IC-94/116; IMSC-94-31; HEPTH-9408063) Avail: CASI HC A03/MF A01 (US Sales Only)

We investigate the cosmological solutions in closed bosonic string theory in the presence of non zero tachyon condensate. We specifically obtain time dependent solutions which describe an anisotropic universe. We also discuss the nature of such time dependent solutions when small tachyon fluctuations around the condensate are taken into account. DOE

N95-25468# International Centre for Theoretical Physics, Trieste (Italy).
PHOTOIONIZATION OF SHALLOW DONOR IMPURITIES IN FINITE-BARRIER QUANTUM WELLS
K. F. Ilaiwi Jul. 1994 9 p
(DE95-607521; IC-94/177) Avail: CASI HC A02/MF A01 (US Sales Only)

The dependence of the photoionization cross-section on photon energy is calculated for shallow donors in finite-barrier GaAs/Ga(1-x)Al(x)As quantum well as well as the binding energy as a function of well width. The effect of magnetic field is also considered. DOE

N95-25473# Melbourne Univ., Parkville (Australia). School of Physics.
MATRIX ELEMENT AND COMPLEX l-PLANE EVALUATION OF TWO-LOOP VACUUM AMPLITUDES IN QED ON S4
B. A. Harris and G. C. Joshi 1993 50 p
(DE95-607099; UM-P-93/63) Avail: CASI HC A03/MF A01 (US Sales Only)

This paper further develops the matrix element and complex angular momentum summation techniques of the authors, in order to calculate both the one-loop free field, and two-loop interacting vacuum diagrams in field theory on a four-sphere. In the case of the free field diagrams, it is shown how the sums may be evaluated by integrating over an analytic function with both poles and branch cuts where the discontinuity across the cuts determines the result. Then, the matrix element formalism is extended to multiple angular momenta involving the addition of angular momenta and the associated Clebsch-Gordon type selection rules. This

then allows the evaluation of matrix elements of two-loop diagrams in spherical QED as a function of the three angular momenta in the diagram. The selection rules allows to cast the triple angular momentum sum into a form which enables evaluation again by contour integrated. The result is obtained in analytic form using dimensional regularization for the previously obtained spinor case, and also for scalar QED which is believed to be a new result. Finally, the applicability of this method for calculations in non-Abelian field theory is discussed. DOE

N95-25475# Melbourne Univ., Parkville (Australia). Research Centre for High Energy Physics.
THE HAMILTONIAN OF SU(2) LATTICE GAUGE THEORY IN APPROXIMATE TRI-DIAGONAL FORM
Lloyd C. L. Hollenberg 1993 16 p
(DE95-607101; UM-P-93/71; OZ-93/15) Avail: CASI HC A03/MF A01 (US Sales Only)

Employing Hamiltonian moments of SU(2) lattice gauge theory, with respect to the strong coupling vacuum, the matrix elements of the Lanczos tri-diagonal form are written down from the palquette expansion to order 1/N(sup 2)(sub p) in the number of plaquettes, N(sub p). The consequences of this approximate tri-diagonal form are studied by computing the vacuum energy density and the specific heat in the infinite lattice limit, for strong to weak coupling. The results at this order appear to reach beyond the strong to weak transition point at g(sup 1/2)(sub c) (approx) 2.0, as indicated by the peaking behaviour of the specific heat. The results demonstrate that the plaquette expansion method to the order considered here is able to describe the physics of the vacuum at the strong to weak transition and just beyond. Whilst the accuracy of the results presented here are not quite of the caliber of the t-expansion or Monte-Carlo calculations, the method used here is simpler and, since it is semi-analytic and not dependent on extrapolation, is to a large extent cleaner. In principle, the results can be improved by increasing the plaquette expansion order and/or choosing a better trial state. Furthermore, unlike a variational approach, this framework allows for the calculation of excited states and so physically interesting quantities such as glueball masses and the string tension, could be calculated by diagonalizing the plaquette expansion in the relevant sector. DOE

N95-25525# International Centre for Theoretical Physics, Trieste (Italy).
GEOMETRIC GAUGE FIELDS IN SEMICLASSICAL GRAVITY
Dhujati Prasad Datta Jun. 1994 14 p
(DE95-607079; IC-94/146) Avail: CASI HC A03/MF A01 (US Sales Only)

Some non-trivial applications of the geometric gauge fields in semiclassical gravity are studied in the framework of the Starobinsky model coupled to quantized matter fields. DOE

N95-25526# International Centre for Theoretical Physics, Trieste (Italy).
BOUNDARY DYNAMICS IN DILATON GRAVITY
Sumit R. Das (Tata Inst. of Fundamental Research, Bombay, India.) and Sudipta Mukherji Jun. 1994 18 p
(DE95-607080; IC-94/147; TIFR/TH-94-24; HEP-TH-9407015) Avail: CASI HC A03/MF A01 (US Sales Only)

We study the dynamics of the boundary in two dimensional dilaton gravity coupled to N massless scalars. We rederive the boundary conditions in a way which makes the requirement of reparametrization invariance and the role of conformal anomaly explicit. We then study the semiclassical behavior of the boundary in the N=24 theory in the presence of an incoming matter wave with a constant energy flux spread over a finite interval. There is a critical value of the matter energy density below which the boundary is stable and all the matter is reflected back. For energy densities greater than this critical value there is a similar behavior for small values of the total energy thrown in. However, when the total energy exceeds another critical value the boundary exhibits a runaway behavior and the spacetime develops in singularities and horizons. DOE

N95-25527# International Centre for Theoretical Physics, Trieste (Italy).
SEMIGLOBAL ALICE STRINGS
G. Dvali (Pisa Univ., Italy.) and G. Senjanovic Jul. 1994 8 p
(DE95-607081; IC-94/156; IFUP-TH-39/94) Avail: CASI HC A02/MF A01 (US Sales Only)

We show that in certain theories with topologically trivial quotient space of spontaneously broken gauge symmetry there can exist topologically stable strings that carry nonabelian gauge flux. These objects result from the 'accidental' global degeneracy of the vacuum which makes it topologically nontrivial. In particular, some models contain the semiglobal analog of the Alice strings. DOE

N95-25530# Stanford Linear Accelerator Center, CA.
MEASUREMENT ACCURACY, BIT-STRINGS, MANTHEY'S QUATERNIONS, AND RRQM
H. P. Noyes 1995 12 p Presented at the 16th Annual International Meeting of the Alternative Natural Philosophy Association, Cambridge, England, 10-13 Sep. 1994
(Contract DE-AC03-76SF-00515)
(DE95-006211; SU-SLAC-PUB-95-6750; CONF-9409283-1) Avail: CASI HC A03/MF A01

The author continues the discussion started last year. By now three potentially divergent research programs have surfaced in ANPA: (1) the Bastin-Kilmister understanding of the combinatorial hierarchy (Clive's 'Menshevik' position); (2) the author's bit-string 'Theory of Everything' (which Clive has dubbed 'Bolshevik'); (3) Manthey's cycle hierarchy based on co-occurrence and mutual exclusion that Clive helped him map onto quaternions (an as yet unnamed heresy?). Unless a common objective can be found, these three points of view will continue to diverge. The authors suggests the reconstruction of relativistic quantum mechanism (RRQM) as a reasonable, and attainable goal that might aid convergence rather than divergence. DOE

N95-25533# Melbourne Univ., Parkville (Australia). Research Centre for High Energy Physics.
TEN DIMENSIONAL SO(10) G.U.T. MODELS WITH DYNAMICAL SYMMETRY BREAKING
B. E. Hanlon and G. C. Joshi 1993 25 p Submitted for publication Sponsored by Australian Postgraduate Research Award
(DE95-607093; UM-P-93/01; OZ-93/01) Avail: CASI HC A03/MF A01 (US Sales Only)

To date, considerations on SO (10) models within Coset Space Dimensional Reduction (CSDR) have been diagonalized to the standard model or rely upon imaginative applications of Wilson lines so as to avoid the problem of the nonexistence of an intermediate Higgs mechanism. However, there is an alternative approach involving four fermion condensates, breaking symmetries by a dynamical mechanism. Indeed, dynamical symmetry breaking has been the direction taken in some SU(5) models within this framework in order to avoid the problems of electroweak symmetry breaking at the compactification scale. This paper presents realistic models which utilize this mechanism. It is shown that the appropriate fermionic representations can emerge from CSDR and the construction of such condensates within the constraints of this scheme is presented. By introducing discrete symmetries onto the internal manifold a strong breaking of the SO(10) G.U.T. is produced and, more importantly, eliminate Higgs fields of geometrical origin. DOE

N95-25534# Kings Coll., London (England). Dept. of Mathematics.
A COVARIANT CANONICAL DESCRIPTION OF LIOUVILLE FIELD THEORY
G. Papadopoulos and B. Spence (Melbourne Univ., Parkville, Australia.) Mar. 1993 12 p Sponsored by Commission of European Communities and Australian Government
(DE95-607094; UM-P-93/33) Avail: CASI HC A03/MF A01 (US Sales Only)

A new parametrisation of the space of solutions of Liouville field theory on a cylinder is presented. In this parametrisation, the solutions are well-defined and manifestly real functions over all space-time and all of parameter space. It is shown that the resulting covariant phase space of the Liouville theory is diffeomorphic to the Hamiltonian one, and to the space of initial data of the theory. The Poisson brackets are derived and shown to be those of the co-tangent bundle of the loop group of the real line. Using Hamiltonian reduction, it is shown that this covariant phase space formulation of Liouville theory may also be obtained from the covariant phase space formulation of the Wess-Zumino-Witten model. DOE

N95-25562# Maryland Univ., College Park, MD. Dept. of Physics.
THEORETICAL STUDIES IN HADRONIC AND NUCLEAR PHYSICS
Progress Report, 1 Dec. 1993 - 30 Jun. 1994

Thomas D. Cohen and Manoj K. Banerjee Jul. 1994 52 p
(Contract DE-FG02-93ER-40762)
(DE95-006643; DOE/ER-40762/042) Avail: CASI HC A04/MF A01

Under Hadrons in Nuclei and Nuclear Matter the authors research the ways in which the properties of nucleons and mesons are modified in the nuclear medium. Research progress is reported on a number of topics in this general area, including studies of the role of chiral symmetry for finite density or temperature nuclear matter, the use of QCD sum rules to describe baryons in nuclear matter, and color transparency. In the general field of Hadron Physics broad progress included studies of perturbative QCD, heavy quark physics, QCD sum rules, and QCD-based models. Notable progress was also achieved in Relativistic Dynamics in Quark, Hadron, and Nuclear Physics, where an explicit model of composite particles shows how the z-graph physics (which is an essential part of Dirac phenomenology) comes about. In addition, calculations of elastic electron-deuteron scattering based on two-body relativistic dynamics and meson exchange currents were completed, as were studies of quark-anti-quark bound states based on a relativistic quark model. Progress is also reported on the relativistic few-body problem. In the area of Heavy Ion Dynamics and Sharp Lepton Pairs, work continues on the Composite Particle Scenario for the 'Sharp Lepton Problem'. In particular, the scenario can now encompass the anomalous sharp leptons reported from positron irradiation of heavy neutral atoms, establishing such irradiations as an alternative experimental window to the heavy ion experiments. DOE

N95-25628 Rutherford Appleton Lab., Oxford (England).
COSMOLOGICAL CONSTRAINTS ON PERTURBATIVE SUPERSYMMETRY BREAKING
S. A. Abel and S. Sarkar Sep. 1994 12 p Prepared in cooperation with Oxford Univ., Oxford, England
(PB95-165361; RAL-94-094) Avail: Issuing Activity (National Technical Information Service (NTIS))

The authors discuss the cosmology of string models with perturbative supersymmetry breaking at a scale of O(TeV). Such models exhibit Kaluza-Klein like spectra and contain unstable massive gravitinos/gravitons. The authors find that considerations of primordial nucleosynthesis constrain the maximum temperature following inflation to be not much larger than the supersymmetry breaking scale. This imposes conflicting requirements on the scalar field driving inflation, making it rather difficult to construct a consistent cosmological history for such models. NTIS

N95-25650# Kings Coll., London (England). Dept. of Mathematics.
THE SPACE OF SOLUTIONS OF TODA FIELD THEORY
G. Papadopoulos and B. Spence (Melbourne Univ., Parkville, Australia.) May 1993 14 p Sponsored by Commission of European Communities and the Australian Government
(DE95-607095; UM-P-93/38; KCL-93/7; HEP-TH-9306088) Avail: CASI HC A03/MF A01 (US Sales Only)

A new parameterization of the solutions of Toda field theory is introduced. In this parameterization, the solutions of the field equations are real, well-defined functions on space-time, which is taken to be two-dimensional Minkowski space or a cylinder. The global structure of the covariant phase space of Toda theory is examined and it is shown that it is isomorphic to the Hamiltonian phase space. The Poisson brackets of Toda theory are then calculated. Finally, using the methods developed to study the Toda theory, these results are extended to the non-Abelian Toda field theories. DOE

N95-25667# Academy of Sciences of the Ukraine, Kiev (Ukraine). Inst. Teoreticheskoj Fiziki.
DYNAMICAL CHIRAL SYMMETRY BREAKING IN SCALE INVARIANT QUANTUM ELECTRODYNAMICS IN SIXTH DIMENSIONS
Eh. V. Gorbar and Eh. Sausedo 1993 13 p In UKRAINIAN
(DE95-607133; ITF-93-38) Avail: CASI HC A03/MF A01 (US Sales Only)

The scale invariant extension of quantum electrodynamics on six-dimensional space-time is considered. This model extension permits to show that essentially non analytical dependence of the chiral order parameter observing in ladder approximation of quantum electrodynamics and corresponded non triviality of the local limit of the theory are connected with exact scale invariance of theory in ladder approximation. DOE

N95-25780# Joint Inst. for Nuclear Research, Dubna (USSR).
WORMHOLE ON THE LOBACHEVSKY BACKGROUND
M. N. Tentyukov 1994 6 p
(DE95-605251; JINR-E-2-94-153) Avail: CASI HC A02/MF A01 (US Sales Only)

The exact spherical symmetric static solution of Rosen like equations of the bi metric theory is investigated. The background metric is not flat, but curved, with the Lobachevsky spatial sections and 'cosmic time' c(sup 2) derivative of t(sup 2). There are two branches of the solution. The first is similar to the Schwarzschild solution and turns to it when the Lobachevsky constant goes to infinity, while the second describes the traversable wormhole and has no Einstein limit. DOE

N95-25878*# National Aeronautics and Space Administration. Lewis Research Center, Cleveland, OH.
ELECTRIC FIELD EFFECTS ON A NEAR-CRITICAL FLUID IN MICROGRAVITY
G. Zimmerli (NYMA, Inc., Brook Park, OH.), R. A. Wilkinson, R. A. Ferrell (Maryland Univ., College Park, MD.), H. Hao (Maryland Univ., College Park, MD.), and M. R. Moldover (National Inst. of Standards and Technology, Gaithersburg, MD.) Apr. 1994 8 p Presented at the National Heat Transfer Conference, Portland, OR, 5-9 Aug, 1995; sponsored by the American Society of Mechanical Engineers
(Contract NAS3-27186; NAG3-1395; RTOP 963-50-0A)
(NASA-TM-106894; E-9540; NAS 1.15:106894) Avail: CASI HC A02/MF A01

The effects of an electric field on a sample of SF6 fluid in the vicinity of the liquid-vapor critical point is studied. The isothermal increase of the density of a near-critical sample as a function of the applied electric field was measured. In agreement with theory, this electrostriction effect diverges near the critical point as the isothermal compressibility diverges. Also as expected, turning on the electric field in the presence of density gradients can induce flow within the fluid, in a way analogous to turning on gravity. These effects were observed in a microgravity environment by using the Critical Point Facility which flew onboard the Space Shuttle Columbia in July 1994 as part of the Second International Microgravity Laboratory Mission. Both visual and interferometric images of two separate sample cells were obtained by means of video downlink. The interferometric images provided quantitative information about the density distribution throughout the sample. The electric field was generated by applying 500 Volts to a fine wire passing through the critical fluid. Author

N95-25966# Joint Inst. for Nuclear Research, Dubna (USSR).
ON FRACTAL STRUCTURE OF QUANTUM GRAVITY AND RELIC RADIATION ANISOTROPY
M. V. Altajskij, V. A. Bednyakov, and S. G. Kovalenko 1994 10 p
(DE95-605306; JINR-E-2-94-170) Avail: CASI HC A02/MF A01 (US Sales Only)

It is argued that cosmic microwave background large scale (greater than 7(sup 0)) anisotropy detected in COBE cosmic experiment can be considered as a trace of the quantum gravity fractal structure. DOE

N95-25967# Joint Inst. for Nuclear Research, Dubna (USSR).
EXACT SOLUTION OF 2 D POINCARE GRAVITY COUPLED WITH FERMION MATTER
S. N. Solodukhin 1994 16 p
(DE95-605314; JINR-E-2-94-117) Avail: CASI HC A03/MF A01 (US Sales Only)

The 2 D model of gravity with dyad e(sup a) and the Lorentz connection one-form (omega) as independent gravitational variables coupled with rd massless Dirac matter is considered. It is shown that the classical equations of motion are exactly integrated. DOE

N95-25970# Melbourne Univ., Parkville (Australia). School of Physics.
A NEW FORMULATION OF QUANTUM FIELD THEORY ON S4
B. A. Harris and G. Joshi 1993 42 p Supersedes UM-P-91/50 and UM-P-92/72
(DE95-607098; UM-P-93/62; UM-P-91/50; UM-P-92/72) Avail: CASI HC A03/MF A01 (US Sales Only)

Recent developments in quantum gravity suggest that wormholes may influence the observed values of the constants of nature. The Euclidean formulation of quantum gravity predicts that wormholes induce a probability

distribution in the space of possible fundamentals constants. In particular, the effective action on a large spherical space may lead to the vanishing of the cosmological constant and possibly determine the values of other constants of nature. The ability to perform calculations involving interacting quantum fields, particularly non-Abelian models, on a four-sphere is vital if one is to investigate this possibility. In this paper, a new formulation of field theory on a four-sphere is presented using the angular momentum space representation of SO(5). A review of field theory on a sphere is given and then show how a matrix element prescription in angular momentum space and a new summation technique based on the complex l-plane, overcome previous limitations in calculation techniques. The standard one-loop graphs of QED are given as examples. DOE

N95-25987# International Centre for Theoretical Physics, Trieste (Italy).
CHARGE-DYON SYSTEM AS THE REDUCED OSCILLATOR
A. Nersessian and V. Antonian (Joint Inst. for Nuclear Research, Dubna, USSR.) Jun. 1994 4 p
(DE95-606998; IC-94/128) Avail: CASI HC A01/MF A01 (US Sales Only)

It is shown, that in the general case the Kustaanheimo-Stiefel transformation (reduction of 4d oscillator on the Twistor space by the Hamiltonian action of U(1) with further time-reparametrization) leads to the integrable system, describing the motion of a spinless electrically charged particle in the Dyon field. DOE

N95-25988# International Centre for Theoretical Physics, Trieste (Italy).
ON SEGAL-WILSON'S CONSTRUCTION FOR THE (TAU)-FUNCTIONS OF THE CONSTRAINED KP HIERARCHIES
You-jin Zhang Jun. 1994 15 p
(DE95-606999; IC-94/135) Avail: CASI HC A03/MF A01 (US Sales Only)

In this letter we study the constrained KP hierachies by employing Segal-Wilson's theory on the (tau)-functions of the KP hierarchy. We first describe the elements of the Grassmannian which correspond to solutions of the constrained KP hierarchy, and then we show how to construct its rational and soliton solutions from these elements of the Grassmannian. DOE

N95-26046# International Centre for Theoretical Physics, Trieste (Italy).
DESCRIBING THE MACROSCOPIC WORLD: CLOSING THE CIRCLE WITHIN THE DYNAMICAL REDUCTION PROGRAM
G. C. Ghirardi, R. Grassi (Udine Univ., Italy.), and F. Benatti (Trieste Univ., Italy.) Jun. 1994 37 p
(DE95-606997; IC-94/107) Avail: CASI HC A03/MF A01 (US Sales Only)

With reference to recently proposed theoretical models accounting for reduction in terms of a unified dynamics governing all physical processes we analyze the problem of working out a world view accommodating our knowledge about natural phenomena. We stress the relevant conceptual differences between the considered models and standard quantum mechanics. In spite of the fact that both theories describe systems within a genuine Hilbert space framework, the peculiar features of the spontaneous reduction models limit drastically the states which are dynamically stable. This fact by itself allows one to work out an interpretation of the formalism which makes possible to give a satisfactory description of the world in terms of the values taken by an appropriately defined mass density function in ordinary configuration space. A topology based on this function and which is radically different from the one characterizing the Hilbert space is introduced and in terms of it the ideal of similarity of macroscopic situations is precisely defined. Finally, the formalism and the interpretation are shown to yield a natural criterion for establishing the psycho-physical parallelism. The conclusion is that, within the considered theories and at the nonrelativistic level, one can satisfy all sensible requirements for a completely satisfactory macro-objective description of reality. DOE

N95-26102# International Centre for Theoretical Physics, Trieste (Italy).
CORRELATED DENSITY MATRIX THEORY OF SPATIALLY INHOMOGENEOUS BOSE FLUIDS
K. A. Gernoth, J. W. Clark (Washington Univ., Saint Louis, MO.), and M. L. Ristig (Cologne Univ., Germany.) Jun. 1994 13 p Sponsored by Deutsche Forschungsgemeinschaft, European Research Office, and Army Research Office
(Grant NSF PHY-93-07484)
(DE95-607840; IC-94/129) Avail: CASI HC A03/MF A01 (US Sales Only)

The variational Hartree-Jastrow theory of the ground state of spatially inhomogeneous Bose systems is extended to finite temperatures. The theory presented here is a generalization also in the sense that it extends the correlated density matrix approach, formulated previously for uniform Bose fluids, to systems with nonuniform density profiles. The method provides a framework in which the effects of thermal excitations on the spatial structure of a Bose fluid, as represented by the density profile and the two-body distribution functions, may be discussed on the basis of an ab initio microscopic description of the system. Thermal excitations make their appearance through self-consistently determined one-body and two-body potentials which enter the nonlinear, coupled Euler-Lagrange equations for the one-body density and for the pair distribution function. Since back-flow correlations are neglected, the excitations are described by a Feynman eigenvalue equation, suitably generalized to nonzero temperatures. The only external quantities entering the correlated density matrix theory elaborated here are the bare two-body interaction potential and, in actual applications, the boundary conditions to be imposed on the one-body density. DOE

N95-26104# Melbourne Univ., Parkville (Australia).
MAGNETIZED PAIR BOSE GAS: RELATIVISTIC SUPERCONDUCTOR
J. Daicic, N. E. Frankel, and V. Kowalenko 31 May 1993 10 p
Sponsored by Australian Postgraduate Research Program, and Australian Research Fellowship
(DE95-607846; UM-P-93/56) Avail: CASI HC A02/MF A01 (US Sales Only)

The magnetized Bose gas at temperatures above pair threshold is investigated. New magnetization laws are obtained for a wide range of field strengths, and the gas is shown to exhibit the Meissner effect. Some related results for the Fermi gas, a relativistic paramagnet, are also discussed. It is concluded that the pair gases, through the interplay between pair creation, temperature, field strength, statistics, and, in the case of fermions, spin, have remarkable magnetic properties. DOE

N95-26105# International Centre for Theoretical Physics, Trieste (Italy).
CALCULATING THE THERMODYNAMIC PROPERTIES OF PLANAR AND SPHERICAL LIQUID-VAPOUR INTERFACE
S. M. Osman Jun. 1994 18 p
(DE95-608777; IC-94/150) Avail: CASI HC A03/MF A01 (US Sales Only)

We present results of calculations of the equilibrium density profile and related surface properties for liquid-vapor interface of simple fluids. The interface has been considered (1) planar and (2) spherical, with some attention to the stability of small liquid droplets. These calculations are based on the density functional theory (DFT), in particular, the gradient approximation, in conjunction with the simplified random phase approximation (RPA) Bhatia-Young model for the bulk liquid. DOE

80 SOCIAL SCIENCES (GENERAL)

Includes educational matters.

N95-25643*# National Aeronautics and Space Administration, Washington, DC.
PERSPECTIVES FROM SPACE: NASA CLASSROOM INFORMATION AND ACTIVITIES
[1992] 35 p
(NASA-TM-110577; NAS 1.15:110577) Avail: CASI HC A03/MF A01

This booklet contains the information and classroom activities included on the backs of the eight poster series, 'Perspectives From Space'. The first series, Earth, An Integrated System, contains information on global ecology, remote sensing from space, data products, earth modeling, and international environmental treaties. The second series, Patterns Among Planets, contains information on the solar system, planetary processes, impacts and atmospheres, and a classroom activity on Jupiter's satellite system. The third series, Our Place In The Cosmos, contains information on the scale of the universe, origins of the universe, mission to the universe, and three classroom activities. The fourth series, Our Sun, The Nearest

Star, contains information on the Sun. The fifth series, Oasis Of Life, contains information on the development of life, chemical and biological evolution on Earth and the search for other life in the universe. The sixth series, The Influence Of Gravity, contains information on Newton's Law of Gravity, space and microgravity, microgravity environment, and classroom activities on gravity. The seventh series, The Spirit Of Exploration, contains information on space exploration, the Apollo Program, future exploration activities, and two classroom activities. The eighth series, Global Cooperation, contains information on rocketry, the space race, and multi-nation exploration projects. CASI

N95-26304*# Vanderbilt Univ., Nashville, TN. Dept. of Mechanical Engineering.
THE 1994 NASA/USRA/ADP DESIGN PROJECTS Final Report
Thomas Cruse, Joseph Richardson, and Robert Tryon 1994 135 p Original contains color illustrations
(Contract NASw-4435)
(NASA-CR-197415; NAS 1.26:197415) Avail: CASI HC A07/MF A02; 7 functional color pages

The NASA/USRA/ADP Design Projects from Vanderbilt University, Department of Mechanical Engineering (1994) are enclosed in this final report. Design projects include: (1) Protein Crystal Growth, both facilities and methodology; (2) ACES Deployable Space Boom; (3) Hybrid Launch System designs for both manned and unmanned systems; (4) LH2 Fuel Tank design (SSTO); (5) SSTO design; and (6) Pressure Tank Feed System design. For individual titles, see N95-26305 through N95-26310.

N95-26305*# Vanderbilt Univ., Nashville, TN.
UNIVERSAL TEST FACILITY **c14**
Mike Laughery *In its* The 1994 NASA/USRA/ADP Design Projects 13 p(SEE N95-26304 08-80) 1994 (For primary document see N95-26304 08-80)
Avail: CASI HC A03/MF A02

A universal test facility (UTF) for Space Station Freedom is developed. In this context, universal means that the experimental rack design must be: automated, highly marketable, and able to perform diverse microgravity experiments according to NASA space station requirements. In order to fulfill these broad objectives, the facility's customers, and their respective requirements, are first defined. From these definitions, specific design goals and the scope of the first phase of this project are determined. An examination is first made into what types of research are most likely to make the UTF marketable. Based on our findings, the experiments for which the UTF would most likely be used included: protein crystal growth, hydroponics food growth, gas combustion, gallium arsenide crystal growth, microorganism development, and cell encapsulation. Therefore, the UTF is designed to fulfill all of the major requirements for the experiments listed above. The versatility of the design is achieved by taking advantage of the many overlapping requirements presented by these experiments. Author

N95-26306*# Vanderbilt Univ., Nashville, TN.
AUTOMATED PROTEIN CRYSTAL GROWTH FACILITY **c14**
Stacey Donald *In its* The 1994 NASA/USRA/ADP Design Projects 32 p(SEE N95-26304 08-80) 1994 (For primary document see N95-26304 08-80)
Avail: CASI HC A03/MF A02

A customer for the protein crystal growth facility fills the specially designed chamber with the correct solutions, fills the syringes with their quenching solutions, and submits the data needed for the proper growth of their crystal. To make sure that the chambers and syringes are filled correctly, a NASA representative may assist the customer. The data needed is the approximate growth time, the growth temperature, and the desired crystal size, but this data can be changed anytime from the ground, if needed. The chambers are gathered and placed into numbered slots in special drawers. Then, data is entered into a computer for each of the chambers. Technicians map out when each chamber's growth should be activated so that all of the chambers have enough time to grow. All of this data is up-linked to the space station when the previous growth session is over. Anti-vibrational containers need to be constructed for the high forces encountered during the lift off and the landing of the space shuttle, and though our team has not designed these containers, we do not feel that there is any reason why a suitable one could not be made. When the shuttle reaches the space station, an astronaut removes a drawer of quenched chambers from the growth facility and inserts a drawer of new chambers. All twelve of the drawers can be replaced in this fashion. The optical disks can also be removed this way. The old drawers are stored for the trip back to earth. Once inside the growth facility, a chamber is removed by the robot and placed in one of 144 active sites at a time previously picked by a technician. Growth begins when the chamber is inserted into an active site. Then, the sensing system starts to determine the size of the protein crystal. All during the crystal's growth, the customer can view the crystal and read all of the crystal's data, such as growth rate and crystal size. When the sensing system determines that the crystal has reached the predetermined size, the robot is told to pick up a syringe filled with the correct quenchant solution and inject it into the chamber to stop the crystal growth. The chamber is then removed from the active site and placed into its original storage slot. Another chamber is then placed into the active site and the process is repeated in all of the active sites until all of the chambers have complted their growth. After ninety days (the scheduled time between shuttle visits), the crystal growth is completed, and the old drawers are replaced with new ones. Once the customer extracts the crystals, the chambers are retrieved for future customers. Author

N95-26307*# Vanderbilt Univ., Nashville, TN.
STIFFENING OF THE ACES DEPLOYABLE SPACE BOOM **c37**
Vince Sidwell *In its* The 1994 NASA/USRA/ADP Design Projects 13 p(SEE N95-26304 08-80) 1994 (For primary document see N95-26304 08-80)
Avail: CASI HC A03/MF A02

The purpose of this design project was to design an active planar stiffening device for the existing ACES (Acoustic Containerless Experiment System) structure. the ACES structure was modeled using simple beam theory. Various concepts were generated about how the stiffening device should be configured in order to perform at an optimum level. The optimum configuration was selected to be a single set of spreaders located approximately 63% of the distance down the beam. Actuation was to be provided by a DC electric motor. From the test results, the design group was able to draw conclusions and make recommendations about the utility of further research into this area. Author

N95-26308*# Vanderbilt Univ., Nashville, TN.
LAUNCH SYSTEM DESIGN FOR ACCESS TO SPACE **c15**
Corbin Barnes *In its* The 1994 NASA/USRA/ADP Design Projects 20 p(SEE N95-26304 08-80) 1994 (For primary document see N95-26304 08-80)
Avail: CASI HC A03/MF A02

Here, a hybrid launch system is developed. The hybrid launch system combines the lower operating cost advantage of an non-man-rated SSTO (Single Stage to Orbit) MLV (Medium Launch Vehicle) with the crew survivability advantage of a ballistic escape pod. Ultimately, it was found that a non-man-made MLV is configured the same as a man-rated MLV and offers no significant savings in operational cost. However, addition of the proposed escape system would increase the crew survivability rate of the SSTO while incurring only a small cost per pound payload penalty. Author

N95-26309*# Vanderbilt Univ., Nashville, TN.
LH2 FUEL TANK DESIGN FOR SSTO **c39**
Geoff Wright *In its* The 1994 NASA/USRA/ADP Design Projects 31 p(SEE N95-26304 08-80) 1994 (For primary document see N95-26304 08-80)
Avail: CASI HC A03/MF A02

This report will discuss the design of a liquid hydrogen fuel tank constructed from composite materials. The focus of this report is to recommend a design for a fuel tank which will be able to withstand all static and dynamic forces during manned flight. Areas of study for the design include material selection, material structural analysis, heat transfer, thermal expansion, and liquid hydrogen diffusion. A structural analysis FORTRAN program was developed for analyzing the buckling and yield characteristics of the tank. A thermal analysis Excel spreadsheet was created to determine a specific material thickness which will minimize heat transfer through the wall of the tank. The total mass of the tank was determined by the combination of both structural and thermal analyses. The report concludes with the recommendation of a layered material tank

construction. The designed system will include exterior insulation, combination of metal and organize composite matrices and honeycomb. Author

N95-26310*# Vanderbilt Univ., Nashville, TN.
FEED SYSTEM DESIGN FOR A REDUCED PRESSURE TANK c20
Hurbert Lui *In its* The 1994 NASA/USRA/ADP Design Projects 19 p(SEE N95-26304 08-80) 1994 (For primary document see N95-26304 08-80)
Avail: CASI HC A03/MF A02

Three designs were considered to satisfy the design objective. These designs were the current design, a Land Based Pressurized Feed System, and a fuel recirculation system. A computer code was developed to analyze the current feed system and assist in the analysis of the two experimental systems. After comparing the three concepts, the land Based Pressurized Feed System seemed to be the most promising new development. This design coupled with the piping configuration described in the report provides a justifiable fuel feed system which satisfies all the necessary requirements. Author

81 ADMINISTRATION AND MANAGEMENT

Includes management planning and research.

N95-24202# Federal Aviation Administration, Washington, DC.
FEDERAL AVIATION ADMINISTRATION PLAN FOR RESEARCH, ENGINEERING AND DEVELOPMENT, 1995
Dec. 1994 216 p
Avail: CASI HC A10/MF A03

The Federal Aviation Administration (FAA) manages and operates the National Airspace System (NAS), a significant national resource. However, the demands on this system are continuously growing, and changing technologies provide the opportunity to improve system effectiveness and efficiency. Today, 23 of the country's largest airports are plagued by more than 20,000 hours of delay per year, which is projected to grow to 40 major airports by 2000. Nationally, air traffic delays cost the economy an estimated $6 billion in passenger delays and $3 billion in airline operating costs in 1990. At current trends, these costs will increase 50 percent within 10 years. The FAA must accommodate the increasing demand on limited airport and airspace capacity, deal with crucial airport security issues, and cope with the unforeseen problems of an aging aircraft fleet. These requirements pose unprecedented challenges, which can only be met through a major investment in research, engineering and development (R,E&D). The projects in this Plan are those needed to bring the FAA's vision of the future system to reality in the context of a continuing top-level system engineering process. The Plan has enjoyed contributions from across the spectrum of scientific, operational, and user communities.Plan contents: capacity and air traffic management technology; communications, navigation, and surveilance; weather; airport technology; aircraft safety technology; system security technology; human factors and aviation medecine; environment and energy,and innovative/cooperative research. Derived from text

N95-24442*# Procurement Automation Inst., Arlington, VA.
AUTOMATED PROCUREMENT SYSTEM (APS): PROJECT MANAGEMENT PLAN (DS-03), VERSION 1.2 Final Report
Diane R. Murphy 30 Sep. 1994 41 p
(Contract NAS8-39897)
(NASA-CR-196576; NAS 1.26:196576) Avail: CASI HC A03/MF A01

The National Aeronautics and Space Administration (NASA) Marshall Space Flight Center (MSFC) is implementing an Automated Procurement System (APS) to streamline its business activities that are used to procure goods and services. This Project Management Plan (PMP) is the governing document throughout the implementation process and is identified as the APS Project Management Plan (DS-03). At this point in time, the project plan includes the schedules and tasks necessary to proceed through implementation. Since the basis of APS is an existing COTS system, the implementation process is revised from the standard SDLC. The purpose of the PMP is to provide the framework for the implementation process. It discusses the roles and responsibilities of the NASA project staff, the functions to be performed by the APS Development Contractor (PAI), and the support required of the NASA computer support contractor (CSC). To be successful, these three organizations must work together as a team, working towards the goals established in this Project Plan. The Project Plan includes a description of the proposed system, describes the work to be done, establishes a schedule of deliverables, and discusses the major standards and procedures to be followed. Author

N95-24565*# National Aeronautics and Space Administration, Washington, DC.
ISSUES IN NASA PROGRAM AND PROJECT MANAGEMENT
Edward J. Hoffman, ed. 1994 67 p
(NASA-SP-6101(08); NAS 1.21:6101(08)) Avail: CASI HC A04/MF A01

This volume is the sixth in an ongoing series on aerospace project management at NASA. Articles in this volume cover the following topics: (1) evolution of NASA cost estimating; (2) SAM 2; (3) National Space Science Program: strategies to maximize science return; and (4) human needs, motivation, and results of the NASA culture surveys. A section on resources for NASA managers rounds out the publication. Author

N95-24905# Fernald Environmental Restoration Management Corp., Cincinnati, OH.
INTEGRATED PLANNING: A BASELINE DEVELOPMENT PERSPECTIVE
Lloyd Clauss and David Chang 8 Dec. 1994 9 p Presented at the 2nd Annual EM Cost Management Conference, San Francisco, CA, 5-9 Dec. 1994; sponsored by the U.S. Department of Energy
(Contract DE-AC05-92OR-21972)
(DE95-004945; FEMP-2396; CONF-941246-6) Avail: CASI HC A02/MF A01

The FEMP (Fernald Environmental Management Project) Baseline establishes the basis for integrating environmental activity technical requirements with their cost and schedule elements. The result is a path forward to successfully achieving the FERMCO (Fernald Environmental Restoration Management Corporation) mission. Specific to cost management, the FEMP Baseline has been incorporated into the FERMCO Project Control System (PCS) to provide a time-phased budget plan against which contractor performance is measured with an earned value management system. The result is the Performance Measurement Baseline (PMB), an important tool for keeping cost under control. DOE

N95-25642 National Defence Research Establishment, Stockholm (Sweden).
PLANNING FOR THE UNKNOWN: COPING WITH UNCERTAINTY [PLANERA FOER DET OKAENDA: OM HANTERING AV OSAEKERHET]
K. H. Dreborg, E. A. Eriksson, U. Jeppsson, and M. Jungmar Aug. 1994 104 p In SWAHILI
(PB95-165114; FOA-R-94-00005-1.2-SE) Avail: Issuing Activity (National Technical Information Service (NTIS))

This report deals with the problem of uncertainty in connection with long range planning. Key issues are: (1) Is it possible to strengthen the ability of an organization to cope with the unexpected; and (2) How could one plan in face of the (partly) unknown. The report is based on experience of Swedish defense analysis, mainly from the field of civil preparedness planning. Four cases for Swedish defense planning are included. The aim of the report is to develop a conceptual framework and formulate a set of principles useful for long range societal planning. One conclusion is that it is necessary to accept a certain amount of uncertainty as inevitable. Creating action space for the future becomes an important concern--to successively make decisions and to develop the ability to act on unexpected situations as they emerge. This ability could be developed through games and exercises. Another conclusion is that uncertainties relevant to a decision situation should be made explicit and understandable to the decision makers. When many factors are uncertain, a simple systems model is often preferable to a more complex one. NTIS

N95-25771*# National Aeronautics and Space Administration. Goddard Space Flight Center, Greenbelt, MD.
COMPUTER SUPPORT FOR COOPERATIVE TASKS IN MISSION OPERATIONS CENTERS
Jeffrey Fox (Pacific Northwest Lab., Richland, WA.) and Mike Moore Oct. 1994 12 p Presented at the Computer Supported Cooperative Symposium, Chapel Hill, NC, 22-26 Oct. 1994
(Contract DE-AC06-76RL-01830)

(DE95-004928; PNL-SA-23824; CONF-941070-2) Avail: CASI HC A03/MF A01

Traditionally, spacecraft management has been performed by fixed teams of operators in Mission Operations Centers. The team cooperatively: (1) ensures that payload(s) on spacecraft perform their work; and (2) maintains the health and safety of the spacecraft through commanding and monitoring the spacecraft's subsystems. In the future, the task demands will increase and overload the operators. This paper describes the traditional spacecraft management environment and describes a new concept in which groupware will be used to create a Virtual Mission Operations Center. Groupware tools will be used to better utilize available resources through increased automation and dynamic sharing of personnel among missions. DOE

N95-25849*# National Aeronautics and Space Administration, Washington, DC.

CONTINUAL IMPROVEMENT PLAN

Aug. 1994 49 p

(NASA-TM-110574; NAS 1.15:110574) Avail: CASI HC A03/MF A01

NASA's approach to continual improvement (CI) is a systems-oriented, agency-wide approach that builds on the past accomplishments of NASA Headquarters and its field installations and helps achieve NASA's vision, mission, and values. The NASA of the future will fully use the principles of continual improvement in every aspect of its operations. This NASA CI plan defines a systematic approach and a model for continual improvement throughout NASA, stressing systems integration and optimization. It demonstrates NASA's constancy of purpose for improvement - a consistent vision of NASA as a worldwide leader in top-quality science, technology, and management practices. The CI plan provides the rationale, structures, methods, and steps, and it defines NASA's short term (1-year) objectives for improvement. The CI plan presents the deployment strategies necessary for cascading the goals and objectives throughout the agency. It also provides guidance on implementing continual improvement with participation from top leadership and all levels of employees. Derived from text

N95-25850*# National Aeronautics and Space Administration, Washington, DC.

ACQUISITION FORECAST: FISCAL YEAR 1995

15 May 1995 165 p

(NASA-TM-110575; NAS 1.15:110575) Avail: CASI HC A08/MF A02

This volume includes projections of all anticipated FY95, and beyond, NASA contract actions above $25,000 that small and small disadvantaged businesses may be able to perform under direct contract with the government or as subcontractors. The forecast consolidates anticipated procurements at each NASA center into an agencywide report, with the aim of increasing industries' advance knowledge of NASA requirements and enhancing competition in contracting. Each center forecast report is divided into three principal categories of procurement: research and development, services, and supplies and equipment. Derived from text

N95-26262*# National Aeronautics and Space Administration, Washington, DC.

NASA STRATEGIC PLAN

Feb. 1995 28 p

(NASA-TM-110592; NAS 1.15:110592) Avail: CASI HC A03/MF A01

NASA's Plan summarizes the Agency's vision, mission, and values. Specific goals are listed for each externally focused Enterprise: Mission to Planet Earth, Aeronautics, Human Exploration and Development of Space, Space Science, and Space Technology. These Enterprises satisfy the needs of customers external to NASA. The Strategic Functions (Space Communications, Human Resources, and Physical Resources) are necessary in order to meet the goals of the Enterprises. The goals of these Functions are also presented. All goals must be met while adhering to the discussed values and operating principles of NASA. A final section outlines the implementing strategy. CASI

82 DOCUMENTATION AND INFORMATION SCIENCE

Includes information management; information storage and retrieval technology; technical writing; graphic arts; and micrography.

For computer documentation see *61 Computer Programming and Software.*

N95-24238*# National Aeronautics and Space Administration, Washington, DC.

NASA VIDEO CATALOG

1995 69 p

(NASA-SP-7109(01); NAS 1.21:7109(01)) Avail: CASI HC A04

This issue of the NASA Video Catalog lists 463 video productions announced in the NASA STI Database. The videos listed in this catalog have been developed by the NASA Centers covering Shuttle mission press conferences; fly-bys of planets; aircraft design, testing and performance; environmental pollution; lunar and planetary exploration; and many other categories related to manned and unmanned space exploration. Each entry in the publication consists of a standard bibliographic citation accompanied by an abstract. The listing of the entries is arranged by STAR categories. A complete Table of contents describes the scope of each entry. Three indexes - title, report number, and accession number - are included. NASA guidelines, ordering information, and order form are located at the back of this issue. Derived from text

N95-24330# Argonne National Lab., IL.

RAISING THE IQ IN FULL-TEXT SEARCHING VIA INTELLIGENT QUERYING

R. Kero, L. Russell, C. Swietlik, C. Morgan (Department of Energy, Washington, DC.), C. Clayton (Department of Energy, Washington, DC.), and K. Dunlap (Department of Energy, Washington, DC.) 1994 13 p Presented at the Office of Scientific and Technical Information INFOTECH '94, Oak Ridge, TN, 25-26 Oct. 1994

(Contract W-31-109-eng-38)

(DE95-002981; ANL/DIS/CP-84374; CONF-9410141-4) Avail: CASI HC A03/MF A01

Current Information Retrieval (IR) technologies allow for efficient access to relevant information, provided that user selected query terms coincide with the specific linguistical choices made by the authors whose works constitute the text-base. Therefore, the challenge is to enhance the limited searching capability of state-of-the-practice IR. This can be done either with augmented clients that overcome current server searching deficiencies, or with added capabilities that can augment searching algorithms on the servers. The technology being investigated is that of deductive databases, with a set of new techniques called cooperative answering. This technology utilizes semantic networks to allow for navigation between possible query search term alternatives. The augmented search terms are passed to an IR engine and the results can be compared. The project utilizes the OSTI Environment, Safety and Health Thesaurus to populate the domain specific semantic network and the text base of ES&H related documents from the Facility Profile Information Management System as the domain specific search space. DOE

N95-24370# Pacific Northwest Lab., Richland, WA.

FINAL REPORT AND RECOMMENDATIONS OF THE ESnet AUTHENTICATION PILOT PROJECT

G. R. Johnson, J. P. Moore, C. L. Athey (Lawrence Livermore National Lab., Livermore, CA.), D. E. Engert (Argonne National Lab., IL.), and J. E. Ramus (National Energy Research Supercomputer Center, Livermore, CA.) Jan. 1995 49 p

(Contract DE-AC06-76RL-01830)

(DE95-005755; PNL-10382) Avail: CASI HC A03/MF A01

To conduct their work, U.S. Department of Energy (DOE) researchers require access to a wide range of computing systems and information resources outside of their respective laboratories. Electronically communicating with peers using the global Internet has become a necessity to effective collaboration with university, industrial, and other government partners. DOE's Energy Sciences Network (ESnet) needs to be engineered to facilitate this 'collaboratory' while ensuring the protection of government computing resources from unauthorized use. Sensitive information and

intellectual properties must be protected from unauthorized disclosure, modification, or destruction. In August 1993, DOE funded four ESnet sites (Argonne National Laboratory, Lawrence Livermore National Laboratory, the National Energy Research Supercomputer Center, and Pacific Northwest Laboratory) to begin implementing and evaluating authenticated ESnet services using the advanced Kerberos Version 5. The purpose of this project was to identify, understand, and resolve the technical, procedural, cultural, and policy issues surrounding peer-to-peer authentication in an inter-organization internet. The investigators have concluded that, with certain conditions, Kerberos Version 5 is a suitable technology to enable ESnet users to freely share resources and information without compromising the integrity of their systems and data. The pilot project has demonstrated that Kerberos Version 5 is capable of supporting trusted third-party authentication across an inter-organization internet and that Kerberos Version 5 would be practical to implement across the ESnet community within the U.S. The investigators made several modifications to the Kerberos Version 5 system that are necessary for operation in the current Internet environment and have documented other technical shortcomings that must be addressed before large-scale deployment is attempted. DOE

N95-24372# Japan Atomic Energy Research Inst., Tokyo (Japan).
PROCEEDINGS OF THE 1993 SYMPOSIUM ON NUCLEAR DATA
M. Kawai, ed. (Toshiba Corp., Tokyo, Japan.) and T. Fukahori, ed. Feb. 1994 425 p Symposium held in Tokai, Japan, 18-19 Nov. 1993
(DE94-012554; JAERI-M-94-019; INDC(JPN)-169/L; CONF-9311139)
Avail: CASI HC A18/MF A04 (US Sales Only)

The 1993 Symposium on Nuclear Data was held at Tokai Research Establishment, Japan Atomic Energy Research Institute (JAERI), on the 18th and 19th of November, 1993. The symposium was organized by Japanese Nuclear Data Committee (JNDC) and Nuclear Data Center, JAERI. Celebrating the 30th anniversary of JNDC, two special sessions were held; the review of foreign activities by invited foreign scientists and the panel discussion on the future of nuclear data activity. In the oral session, a total of 14 papers was presented under sessions termed foreign activities, JENDL and intermediate energy shielding experiments, nuclear data needs in non-energy applications, and unstable nuclei beam. The panel discussion was held with a keynote address and seven panelists' presentations. Presented in the poster session were 29 papers concerning experiments, evaluations and benchmark tests of nuclear data. All of the 43 papers and reports in the panel discussion are compiled in this proceedings. DOE

N95-24439*# Native American Services, Huntsville, AL.
NLS FLIGHT SIMULATION LABORATORY (FSL) DOCUMENTATION Final Report
[1995] 24 p
(Contract NAS8-37925)
(NASA-CR-196564; NAS 1.26:196564) Avail: CASI HC A03/MF A01

The Flight Simulation Laboratory (FSL) Electronic Documentation System design consists of modification and utilization of the MSFC Integrated Engineering System (IES), translation of the existing FSL documentation to an electronic format, and generation of new drawings to represent the Engine Flight Simulation Laboratory design and implementation. The intent of the electronic documentation is to provide ease of access, local print/plot capabilities, as well as the ability to correct and/or modify the stored data by network users who are authorized to access this information.
Derived from text

N95-24454# Oak Ridge National Lab., TN.
CD-ROM IN THE AGE OF INTERNET
B. Conrad and D. Depp 1994 10 p Presented at the Office of Scientific and Technical Information INFOTECH '94, Oak Ridge, TN, 25-26 Oct. 1994
(Contract DE-AC05-84OR-21400)
(DE95-005067; CONF-9410141-6) Avail: CASI HC A02/MF A01

Networks are hot and CD-ROM is also hot, but how do they mix? CD-ROM is a relatively inexpensive medium for storing and delivering information, and increasingly, users are connected to networks. But the technologies have developed separately, and there are obstacles to their integration. Drawing on their experience networking CD-ROMs at Oak Ridge National Laboratory, the authors discuss CD-ROM's strengths and weaknesses as a technology for delivering information to the desktop. CD-ROM networking solutions are LAN-based, not 'open systems'. Despite this limitation, due to the large number of information resources available on CD-ROM and the relative ease of installing and maintaining databases on CD-ROM, CD-ROMs remain an essential piece of the electronic information puzzle. DOE

N95-24477*# Alabama Univ., Huntsville, AL. Research Inst.
SOFTWARE ENGINEERING AND DATA MANAGEMENT FOR AUTOMATED PAYLOAD EXPERIMENT TOOL Final Technical Report, 4 May - 30 Nov. 1994
Gary A. Maddux, Anna Provancha, and David Chattam Nov. 1994 82 p
(Contract NAS8-38609)
(NASA-CR-196562; NAS 1.26:196562; UAH-5-33534) Avail: CASI HC A05/MF A01

The Microgravity Projects Office identified a need to develop a software package that will lead experiment developers through the development planning process, obtain necessary information, establish an electronic data exchange avenue, and allow easier manipulation/reformatting of the collected information. An MS-DOS compatible software package called the Automated Payload Experiment Tool (APET) has been developed and delivered. The objective of this task is to expand on the results of the APET work previously performed by UAH and provide versions of the software in a Macintosh and Windows compatible format. Author

N95-24492# Central Research Inst. of Electric Power Industry, Tokyo (Japan).
INTEGRATED RESOURCE MANAGEMENT DATABASE FOR A DISTRIBUTED INFORMATION SYSTEM
Atsushi Futakata Mar. 1994 24 p In JAPANESE
(DE95-730180; CRIE-R-93015) Avail: CASI HC A03/MF A01

An integrated resource management database was reported which was developed for the distributed information system. In that system, various systems fluctuate fluidly with dispersion of information resources such as data and process. Therefore, relation is difficult to grasp among those resources, and the information system is also difficult to manage. In order to express those resources and their mutual relation, a business information model which could give both data-oriented and process-oriented views was developed and so hierarchically structured as to detail the description. Based on that model, an integrated resource management database was further developed which generalized and managed the information resources. Thus, the influence analysis of change in system and maintenance of data conformity are expected to be eased. A system was also experimentally prepared which supported the structure based on a proposed methodology to structure the business information model. As a result, it was confirmed that the present database is easy to grasp by the managers and excellent in maintenance properties. DOE

N95-24494# Central Research Inst. of Electric Power Industry, Tokyo (Japan).
DOWNSIZING SYSTEMS AND EXPECTED OPPOSITION TO INTRODUCTION
Ken-Ichi Tokoro Apr. 1994 27 p In JAPANESE
(DE95-730186; CRIE-R-94002) Avail: CASI HC A03/MF A01

The proper use of downsizing systems and mainframe systems was studied for the purpose of introducing advantages of downsizing while utilizing existing information systems. Downsizing has four features: high cost performance, high flexibility and expandability, highly functional interface, and a horizontal linkage system. But compared with centralized systems, downsizing systems entail higher operation and control costs. Downsizing introduction technology has not yet been established in the field of systematization where renewal of corporate data, high security, and mass high-speed printing are required. Downsizing is suitable for fields where systematization is difficult with centralized systems, characteristics of downsizing can be fully demonstrated, and advanced and established technology is not needed. Specific examples of its application are the support of decision making, creative work, and group operation. For improving the performance of the downsizing system as a whole, its application to computers on the network, and distributed data arrangement are important. DOE

N95-24603# Westinghouse Hanford Co., Richland, WA.
MEASURING THE STRATEGIC VALUE OF INFORMATION TECHNOLOGY INVESTMENTS

Kurt W. Conrad (Boeing Computer Services Co., Richland, WA.) Aug. 1994 38 p Presented at the 11th Office Information Technology Conference, Chicago, IL, 23-25 Aug. 1994
(Contract DE-AC06-87RL-10930)
(DE94-018160; WHC-SA-2594; CONF-940873-3) Avail: CASI HC A03/MF A01

Value is often perceived differently by the proponents of new information technologies and those who allocate resources and define priorities. Such differences often become a roadblock to meeting true business needs. Project justifications regularly rely on calculated cost savings, which rarely measure the full benefit of new technologies. In fact, if cost savings provide a complete picture, then the organization is probably just automating routine clerical operations and has abandoned efforts that would provide significant strategic value. Strategic value is not limited to financial calculations, but includes quality, time and risk criteria. This paper describes approaches for measuring strategic value that can provide organizations with proven techniques to improve performance, reengineer processes, benchmark performance against other suppliers, identify outsourcing opportunities, or defend themselves from pressures to outsource. Many organizations respond to tightening budgets by cutting overhead. These measurement approaches can demonstrate how overhead is critical to organizational effectiveness and how cost savings can be found, instead, by measurably improving performance throughout the organization. Finally, the paper describes efforts underway within the Department of Energy and at the Hanford Site to implement the approaches described in this paper. DOE

N95-24654# Westinghouse Hanford Co., Richland, WA.
ACTIVITY MANAGEMENT SYSTEM USER REFERENCE MANUAL
T. A. Gates and M. B. Burdick 22 Sep. 1994 105 p Revised
(Contract DE-AC06-87RL-10930)
(DE95-000989; WHC-SD-HWV-UM-004-Rev-1) Avail: CASI HC A06/MF A02

The Activity Management System (AMS) was developed in response to the need for a simple-to-use, low-cost, user interface system for collecting and logging Hanford Waste Vitrification Plant Project (HWVP) activities. This system needed to run on user workstations and provide common user access to a database stored on a local network file server. Most important, users wanted a system that provided a management tool that supported their individual process for completing activities. Existing system treated the performer as a tool of the system. All AMS data is maintained in encrypted format. Users can feel confident that any activities they have entered into the database are private and that, as the originator, they retain sole control over who can see them. Once entered into the AMS database, the activities cannot be accessed by anyone other than the originator, the designated agent, or by authorized viewers who have been explicitly granted the right to look at specific activities by the originator. This user guide is intended to assist new AMS users in learning how to use the application and, after the initial learning process, will serve as an ongoing reference for experienced users in performing infrequently used functions. Online help screens provide reference to some of the key information in this manual. Additional help screens, encompassing all the applicable material in this manual, will be incorporated into future AMS revisions. A third, and most important, source of help is the AMS administrator(s). This guide describes the initial production version of AMS, which has been designated Revision 1.0. DOE

N95-24656# Oak Ridge National Lab., TN. Environmental Restoration Div.
INFORMATION MANAGEMENT ARCHITECTURE FOR AN INTEGRATED COMPUTING ENVIRONMENT FOR THE ENVIRONMENTAL RESTORATION PROGRAM. ENVIRONMENTAL RESTORATION PROGRAM, VOLUME 3: INTERIM TECHNICAL ARCHITECTURE
Sep. 1994 119 p
(Contract DE-AC05-84OR-21400)
(DE95-001386; ES/ER/TM-120/V3) Avail: CASI HC A06/MF A02

This third volume of the Information Management Architecture for an Integrated Computing Environment for the Environmental Restoration Program--the Interim Technical Architecture (TA) (referred to throughout the remainder of this document as the ER TA)--represents a key milestone in establishing a coordinated information management environment in which information initiatives can be pursued with the confidence that redundancy and inconsistencies will be held to a minimum. This architecture is intended to be used as a reference by anyone whose responsibilities include the acquisition or development of information technology for use by the ER Program. The interim ER TA provides technical guidance at three levels. At the highest level, the technical architecture provides an overall computing philosophy or direction. At this level, the guidance does not address specific technologies or products but addresses more general concepts, such as the use of open systems, modular architectures, graphical user interfaces, and architecture-based development. At the next level, the technical architecture provides specific information technology recommendations regarding a wide variety of specific technologies. These technologies include computing hardware, operating systems, communications software, database management software, application development software, and personal productivity software, among others. These recommendations range from the adoption of specific industry or Martin Marietta Energy Systems, Inc. (Energy Systems) standards to the specification of individual products. At the third level, the architecture provides guidance regarding implementation strategies for the recommended technologies that can be applied to individual projects and to the ER Program as a whole. DOE

N95-24675# Sandia National Labs., Albuquerque, NM.
THE ENERGY INTELLIGENCE INFORMATION SYSTEM
Leonard Malczynski 1994 11 p Presented at the 1994 Geographic Information Systems/Land Information Systems (GIS/LIS), Phoenix, AZ, 25-27 Oct. 1994
(Contract DE-AC04-94AL-85000)
(DE95-002184; SAND-94-2764C; CONF-9410237-1) Avail: CASI HC A03/MF A01

The safety and security of foreign nuclear facilities is an important topic for intelligence services. This has been made more important by the breakup of the Former Soviet Union. The major requirement of intelligence analysts is rapid information retrieval after the report of an incident at a foreign facility. Sandia National Laboratories is developing a GIS-based Energy Intelligence Information System (EIIS) to help analysts at The Office of Energy Intelligence of the Department of Energy formulate a response to a nuclear incident. The Vital Issues process was used to determine which information might be the most important to collect. Joint Applications Design and prototyping sessions were held to establish EIIS requirements and refine the user interface. EIIS was built to access any point on the globe or to move directly to a site, facility, or city. The EIIS version 1.0 concentrates on commercial reactors, version 2.0 will include other nuclear fuel cycle sites and release 3.0 will include waste and disposal information. The system runs on a SUN workstation using ARC/INFO(trademark) and Informix as the RDBMS. The map system relies upon the Digital Chart of the World from the Defense Mapping Agency. DOE

N95-24710# Energy Information Administration, Washington, DC.
DIRECTORY OF ENERGY DATA COLLECTION FORMS: FORMS IN USE AS OF OCTOBER 1994
15 Dec. 1994 67 p
(DE95-004329; DOE/EIA-0249(94)) Avail: CASI HC A04/MF A01

This 18th edition directory provides an overview of DOE's energy information collection programs for decisionmakers in Government and industry; selected public use forms currently used as basic energy information gathering tools by DOE are covered. For each form, an abstract is included that describes the form's uses, its respondents, and the data collected. Also shown are frequently requested items: energy sources and functions covered by the form, general categories of respondents, collection frequency, public laws and regulations, reporting requirement, name and phone number of the data collection manager, and the publications resulting from the data collection. Indexes, arranged according to energy source/function, publications, respondent categories, former EIA form number designations, and collection authorities, are provided. DOE

N95-25240# Prairie View Agricultural and Mechanical Coll., TX. Dept. of Physics.
A REPORT: A PLAN TO ESTABLISH INTERNET ACCESS POINTS AT MINORITY CAMPUS SITES FOR CONNECTION TO A CENTRAL COMPUTING FACILITY
31 Oct. 1994 64 p Sponsored by Rice Univ., Texas A and M Univ., Texas A and I Univ., Lincoln Univ., Cheyney Univ., Univ. of Pennsylvania, Howard Univ., The Johns Hopkins Univ., Southern Univ., Louisiana State Univ., Langston Univ., Univ. of Oklahoma, Morgan State Univ., Univ. of

Maryland, Paul Quinn College, and Southern Methodist Univ.
(Contracts DE-FG05-94ER-40879; DE-PS05-94ER-40863)
(DE95-004374; DOE/ER-40879/T1) Avail: CASI HC A04/MF A01

In 1989, as the SSC was just getting under way, many of the HBCU/MI's experienced deep research and communications infrastructure problems as they attempted to find the necessary resources to link through the Internet to the Central Facility at the Superconducting Super Collider Laboratory (SSCL). The Internet was to many of the minority universities indeed a new and vital research support and information retrieval tool. Many minority researchers were unable to capitalize on these newly formed and rapidly evolving SSC projects. It was not necessarily because of heavy teaching loads alone but more because of a lack of resources and an academic infrastructure that could not generate the needed resources. Federal research dollars are most difficult to come by in an environment like this. We have learned over the years and across several minority institutions that internecine feuding between academic and administrative units, coupled with both physical and social isolation, are in part responsible for the weak rate of evolution at most minority institutions as compared with majority universities of comparable size and mission. The Tuples concept was a way to increase the minority researcher's productivity. DOE

N95-25376# Fermi National Accelerator Lab., Batavia, IL.
A GENERIC DATA EXCHANGE SCHEME BETWEEN FITS FORMAT AND C STRUCTURES
Peng Wei and T. Nicinski Nov. 1994 4 p Presented at the Astronomical Data Acquisition Software System Conference, Baltimore, MD, 25-28 Sep. 1994
(Contract DE-AC02-76CH-03000)
(DE95-004849; FNAL/C-94/397; CONF-9409280-1) Avail: CASI HC A01/MF A01

A flexible and efficient scheme allowing arbitrary FITS Binary and ASCII Tables to be converted to arbitrary C structures at runtime is presented. This scheme has been successfully implemented and used with Shiva (Survey Human Interface and Visualization Environment), a package developed by Fermilab for the analysis of Sloan Digital Sky Survey data. DOE

N95-25410*# NASA Center for AeroSpace Information, Linthicum Heights, MD.
MACHINE-AIDED INDEXING AT NASA
June P. Silvester, Michael T. Genuardi, and Paul H. Klingbiel 1994 15 p Repr. from Information Processing and Management (England, Pergamon), v. 30, no. 5 p 631-645 Sponsored by NASA
(ISSN 0306-4573)
(NASA-CR-197796; NAS 1.26:197796) Copyright Avail: CASI HC A03/MF A01

This report describes the NASA Lexical Dictionary (NLD), a machine-aided indexing system used online at the National Aeronautics and Space Administration's Center for AeroSpace Information (CASI). This system automatically suggests a set of candidate terms from NASA's controlled vocabulary for any designated natural language text input. The system is comprised of a text processor that is based on the computational, nonsyntactic analysis of input text and an extensive knowledge base that serves to recognize and translate text-extracted concepts. The functions of the various NLD system components are described in detail, and production and quality benefits resulting from the implementation of machine-aided indexing at CASI are discussed. Author

N95-25572 Research Inst. of National Defence, Linkoeping (Sweden). Huvudavdelning foer Informationsteknologi.
GEOGRAPHICAL INFORMATION SYSTEMS AND OTHER TOOLS FOR SPATIAL INFORMATION MANAGEMENT [GEOGRAFISKA INFORMATIONSSYSTEM OCH ANDRA VERKTYG FOER HANTERING AV RUMSLIG INFORMATION]
A. Brama Jun. 1994 39 p In SWAHILI
(PB95-165759; FOA-C-30766-3.4) Avail: Issuing Activity (National Technical Information Service (NTIS))

The use of spatial information management tools in defense related applications is increasing. Tools exist for all levels of application, from relatively simple display systems to very advanced geographical information systems. In this report a selection of systems and tools developed and/or used by the Swedish Defense is described. NTIS

N95-25608 Defense Mapping Agency Aerospace Center, Saint Louis, MO.
HARDCOPY EXTRACTION CONSIDERATIONS FOR VECTOR PRODUCT FORMAT (VPF) PRODUCTS
Kimberly H. Berger Oct. 1994 15 p Limited Reproducibility: More than 20% of this document may be affected by microfiche quality
(AD-A288620) Avail: Issuing Activity (Defense Technical Information Center (DTIC))

Vector Product Format (VPF) is a standard format, structure, and organization developed by the Defense Mapping Agency (DMA) and intended to be used for large geographic product data bases. VPF product data-bases are often initially populated with data taken from existing hardcopy map source of the appropriate scale. Military Specifications are written for each new VPF product defining, among other things, the product's features, their attributes, and valid attribute values. The Military Specifications do not, however, address the issues introduced by the practice of feature collection from existing cartographic source. This paper addresses data collection and organizational issues from the production standpoint. Particular attention is given to VMap Level 1 experience. DTIC

N95-25765# Idaho National Engineering Lab., Idaho Falls, ID.
APPLICATIONS FOR ELECTRONIC DOCUMENTS
George A. Beitel 1995 5 p Presented at the 1994 Annual Meeting of the American Nuclear Society, Stanford, CA, 19-23 Jun. 1994
(Contract DE-AC07-76ID-01570)
(DE95-005036; EGG-M-94071; CONF-9406297-1) Avail: CASI HC A01/MF A01

This paper discusses the application of electronic media to documents, specifically Safety Analysis Reports (SARs), prepared for Environmental Restoration and Waste Management (ER&WM) programs being conducted for the Department of Energy (DOE) at the Idaho National Engineering Laboratory (INEL). Efforts are underway to upgrade our document system using electronic format. To satisfy external requirements (DOE, State, and Federal), ER&WM programs generate a complement of internal requirements documents including a SAR and Technical Safety Requirements along with procedures and training materials. Of interest is the volume of information and the difficulty in handling it. A recently prepared ER&WM SAR consists of 1000 pages of text and graphics; supporting references add 10,000 pages. Other programmatic requirements documents consist of an estimated 5000 pages plus references. DOE

N95-25774# Pacific Northwest Lab., Richland, WA.
MULTIDIMENSIONAL VISUALIZATION AND BROWSING FOR INTELLIGENCE ANALYSIS
Vern Crow, Marc Pottier, Jim Thomas, David Lantrip (Michigan Univ., Ann Arbor, MI.), Craig Struble, Kelly Pennock, Anne Schur, Jim Wise, Tarra Fiegel, and Jeremy York Sep. 1994 9 p Presented at the GVIS 1994: Graphics and Visualization Conference, Richland, WA, 8 Sep. 1994
(Contract DE-AC06-76RL-01830)
(DE95-004901; PNL-SA-24870; CONF-9409278-2) Avail: CASI HC A02/MF A01

Visualization tools have been invaluable in the process of scientific discovery by providing researchers with insights gained through graphical tools and techniques. At Pacific Northwest Laboratory (PNL), the Multidimensional Visualization and Advanced Browsing (MVAB) project is extending visualization technology to the problems of intelligence analysis of textual documents by creating spatial representations of textual information. By representing an entire corpus of documents as points in a coordinate space of two or more dimensions, the tools developed by the MVAB team give the analyst the ability to quickly browse the entire document base and determine relationships among documents and publication patterns not readily discernible through traditional lexical means. DOE

N95-25907# Joint Inst. for Nuclear Research, Dubna (USSR).
THE USE OF DBMS AND DOCUMENT ORIENTED INTERFACE IN THE TPLAN-SYSTEM
F. N. Fernandez 1994 10 p
(DE95-605219; JINR-E-11-94-204) Avail: CASI HC A02/MF A01 (US Sales Only)

The paper describes the user-friendly input/output interface (DOI) for the TPLAN database management system that includes high quality output in Latex format from databases and retrieves selected information from

Latex document (according to a specific grammar that includes a subset of the Latex grammar) to be stored in the databases. The TPLAN system was developed to manage the annual Topical Plan of JINR. It was written in 'C' and DOS Fox Base/Fox Pro for IBM comparable personal computer. It was also prototyped in Visual Basic and Windows Access using standard V B controls. DOE

N95-25941# International Atomic Energy Agency, Vienna (Austria).
ONLINE NUCLEAR DATA SERVICE
C. L. Dunford and T. W. Burrows Mar. 1994 91 p
(DE95-602487; IAEA-NDS-150-(Rev-94/3); NNDC/ONL-94/3) Avail: CASI HC A05/MF A01 (US Sales Only)

The U.S. National Nuclear Data Center and the IAEA Nuclear Data Section offer online computer access through international networks to their nuclear-physics and photoatomic numeric databases, related bibliographic systems and other related information of interest to basic and applied research and technology. A detailed description of the access procedures, the technical requirements, and the available databases is given. DOE

N95-25980# International Atomic Energy Agency, Vienna (Austria).
INDEX OF NUCLEAR DATA LIBRARIES AVAILABLE FROM THE IAEA NUCLEAR DATA SECTION
H. D. Lemmel Mar. 1994 39 p
(DE95-605213; IAEA-NDS-7(Rev-94/3)) Avail: CASI HC A03/MF A01 (US Sales Only)

This document lists more than 100 nuclear data libraries together with references that give more detailed information about these libraries. The data libraries include neutron cross-sections, resonance parameters, fission-product yields, nuclear structure and decay data, gamma-rays from radionuclides, data of nuclear reactions induced by charged particles or heavy ions, photonuclear data, photoatomic interaction data, and many others, partly with related data processing computer codes. All data and documentation references are available upon request from the IAEA Nuclear Data Section, free of charge on magnetic tape, PC diskettes, or online through the INTERNET computer network: either menu driven within the Nuclear Data Information System (NDIS), or through FTP file transfer. DOE

N95-26084*# National Aeronautics and Space Administration. Marshall Space Flight Center, Huntsville, AL.
THE SPACELAB SCIENTIFIC MISSIONS: A COMPREHENSIVE BIBLIOGRAPHY OF SCIENTIFIC PUBLICATIONS
Marsha Torr, comp. Washington Apr. 1995 136 p
(NASA-TM-108487; NAS 1.15:108487) Avail: CASI HC A07/MF A02

November 1993 represented the 10-year anniversary of the flight of Spacelab 1 mission, with the first precursor mission (OSTA-1) being launched 2 years earlier. Since that time, a total of 27 Shuttle missions has been flown, using the Spacelab system as a facility for conducting scientific research in space. The missions flown to date have allowed a total of approximately 500 Principle Investigator class investigations to be conducted in orbit. These investigations have constituted major scientific efforts in astronomy/astrophysics, atmospheric science, Earth observation, life sciences, microgravity science, and space plasma physics. An initial survey of the scientific products gleaned from Spacelab missions already flown was sent to the Principle Investigators. In that survey, information was gathered from the investigators on the scientific highlights of their investigations and statistical measurements of overall success -- such as papers published. This document is a compilation of the papers that have been published to date in referred literature. Author

N95-26334# Advisory Group for Aerospace Research and Development, Neuilly-Sur-Seine (France). Technical Information Panel.
DIRECTORY OF DEFENCE AND AEROSPACE INFORMATION CENTERS [ANNUAIRE DES CENTRES DE LAS DEFENSE ET DE L'AEROSPATIALE CIVILE]
Mar. 1995 101 p
(AGARD-R-802; ISBN-92-836-1015-6) Copyright Avail: CASI HC A06/MF A02

The Directory of Defense and Aerospace Information Centers is a reference guide to information centers located in NATO nations. The information provided represents submissions from forty eight information centers across fourteen countries. The guide provides assistance in locating scientific and technical information resources from several countries' information centers. Points of contact are provided for each center. The directory includes information on: points of contact, subject coverage, description of major products and services, access limitations where applicable, e-mail addresses, and phone and fax numbers. An index to centers by organizational title is included for quick reference. Author

83 ECONOMICS AND COST ANALYSIS

Includes cost effectiveness studies.

No abstracts in this category.

84 LAW, POLITICAL SCIENCE AND SPACE POLICY

Includes NASA appropriation hearings; aviation law; space law and policy; international law; international cooperation; and patent policy.

N95-24894# European Space Agency. European Space Research and Technology Center, ESTEC, Noordwijk (Netherlands).
UNITED STATES-EUROPEAN COOPERATION IN SPACE DURING THE SIXTIES
Lorenza Sebesta (European Univ. Inst., Florence, Italy.) Jul. 1994 62 p Original contains color illustrations
(ESA-HSR-14) Avail: CASI HC A04/MF A01

The ESA History Study Reports are preliminary reports of studies carried out within the framework of an ESA (European Space Agency) contract. They will form the basis of a comprehensive study of European Space activities covering the period 1959-1987. Euro-American relationships in space have passed through several phases. According to the ex-director general of ESA, Reimar Lust, during the first, from the early 1960s to the early 1970s, the US exercized 'tutorship' of Europe. During the second, which lasted until the beginning of the mid-1980s, Europe became America's 'junior partner' while during the third, and current, phase there has been both 'partnership and competition'. This paper deals with the first phase, analyzing the fields of cooperation and the underlying changing patterns of cooperative policy between NASA and ESRO/ELDO from 1958 to 1973. Derived from text

N95-24895# European Space Agency. European Space Research and Technology Center, ESTEC, Noordwijk (Netherlands).
UNITED STATES-EUROPEAN SPACE COOPERATION IN THE POST-APOLLO PROGRAMME
Lorenza Sebesta (European Univ. Inst., Florence, Italy.) Feb. 1995 92 p Original contains color illustrations
(ESA-HSR-15) Avail: CASI HC A05/MF A01

The ESA History Study Reports are preliminary reports of studies carried out within the framework of an ESA (European Space Agency) contract. They will form the basis of a comprehensive study of European Space activities covering the period 1959-1987. Discussions that took place during the second part of the sixties, even if unfruitful, set the stage for a broadening of perspective within US-Euopean cooperation. Negotiations on the post-Apollo program showed how painful and controversial this process could be. This paper analyzes the various interlocking elements that influenced the outcome of these negotiations and the content of the two 1973 agreements which set the legal framework for cooperation on Spacelab. Derived from text

85 URBAN TECHNOLOGY AND TRANSPORTATION

Includes applications of space technology to urban problems; technology transfer; technology assessment; and surface and mass transportation.

For related information see also *03 Air Transportation and Safety, 16 Space Transportation,* and *44 Energy Production and Conversion.*

N95-26183*# National Aeronautics and Space Administration, Washington, DC.

OFFICE OF SPACE SCIENCE: INTEGRATED TECHNOLOGY STRATEGY

Wesley T. Huntress, Jr. and Gregory M. Reck [1994] 49 p

(NASA-TM-110578; NAS 1.15:110578) Avail: CASI HC A03/MF A01

This document outlines the strategy by which the Office of Space Science, in collaboration with the Office of Advanced Concepts and Technology and the Office of Space Communications, will meet the challenge of the national technology thrust. The document: highlights the legislative framework within which OSS must operate; evaluates the relationship between OSS and its principal stakeholders; outlines a vision of a successful OSS integrated technology strategy; establishes four goals in support of this vision; provides an assessment of how OSS is currently positioned to respond to the goals; formulates strategic objectives to meet the goals; introduces policies for implementing the strategy; and identifies metrics for measuring success. The OSS Integrated Technology Strategy establishes the framework through which OSS will satisfy stakeholder expectations by teaming with partners in NASA and industry to develop the critical technologies required to: enhance space exploration, expand our knowledge of the universe, and ensure continued national scientific, technical and economic leadership. Derived from text

88 SPACE SCIENCES (GENERAL)

N95-24196* National Aeronautics and Space Administration. Lyndon B. Johnson Space Center, Houston, TX.

SPACE BASIC (Videotape)

Dexter Herbert, ed. 2 Jan. 1991 *Its* Liftoff to Learning Series Videotape: 20 min. 55 sec. playing time, in color, with sound

(NASA-TM-110540; NONP-NASA-VT-95-43943) Avail: CASI VHS A02/BETA A22

In this education video series, 'Liftoff to Learning', astronauts (Bruce Melnick, Thomas Akers, William Shepherd, Robert Cabana, and Richard Richards) describe the historical beginnings of space exploration from the time of Robert H. Goddard (considered the Father of Rocketry), who, in 1929, invented the first propellant rocket, the prototype of modern liquid propellant rockets, up to the modern Space Shuttles. The questions - where is space, what is space, and how do astronauts get to, stay in, and come back from space are answered through historical footage, computer graphics, and animation. The space environment effects, temperature effects, and gravitational effects on the launching, orbiting, and descent of the Shuttles are discussed. Included is historical still photos and film footage of past space programs and space vehicles. CASI

N95-25746*# National Aeronautics and Space Administration. Goddard Space Flight Center, Greenbelt, MD.

FROM SUPERCONDUCTIVITY TO SUPERNOVAE: THE GINZBURG SYMPOSIUM. REPORT ON THE SYMPOSIUM HELD IN HONOR OF VITALY L. GINZBURG

Alan F. Clark (National Inst. of Standards and Technology, Gaithersburg, MD.), Vitaly L. Ginzburg (Academy of Sciences, USSR, Moscow, USSR.), L. P. Gorkov (Illinois Univ., Urbana, IL.), W. A. Little (Stanford Univ., CA.), K. Kellermann (National Radio Astronomy Observatory, Charlottesville, VA.), V. Z. Kresin (California Univ., Berkeley. Lawrence Berkeley Lab, CA.), J. D. Kurfess (Naval Research Lab., Washington, DC.), and R. Ramaty Nov. 1994 79 p Symposium held in Gaithersburg, MD, 22 May 1992

(NASA-TM-110596; NAS 1.15:110596; PB95-171963; NISTIR-5556) Avail: CASI HC A05/MF A01

A one day symposium honoring Professor Vitaly L. Ginzburg and his many contributions to the world of physics was held at the National Institute of Standards and Technology. An additional purpose was to explore future directions for research in the context of his extensive involvement in the rapid developments in physics in the last fifty years. This transcription of the proceedings includes invited talks on some of those recent developments in such fields as superconductivity and astrophysics. Prof. Ginzburg's own address 'What problems of physics and astrophysics seem now to be especially important and interesting' was the focus for discussion on the future directions of physics research. Titles of the other papers given at the symposium are as follows: New Phenomena in Proximity Effect Tunneling in High TC Superconductors; Radio Galaxies, Quasars, and Superluminal Radio Sources; Exotic Properties of High TC Materials and the Ginzburg Parameter; Gamma Ray Astrophysics and early results of the Compton Observatory; Some Puzzles of the Normal State of High TC Oxides; Galactic Annihilation Radiation. NTIS

89 ASTRONOMY

Includes radio, gamma-ray, and infrared astronomy, and astrometry.

N95-24385*# Applied Research Corp., Landover, MD.

ASCA SOLID STATE IMAGING SPECTROMETER OBSERVATIONS OF O STARS Final Report, 4 Feb. 1994 - 31 Jan. 1995

M. F. Corcoran, W. L. Waldron, J. J. MacFarlane (Wisconsin Univ., Madison, WI.), W. Chen (National Aeronautics and Space Administration. Goddard Space Flight Center, Greenbelt, MD.), A. M. T. Pollock (Computer and Scientific Co. Ltd., Sheffield, England.), K. Torrii (Osaka Univ., Toyonaka, Japan.), S. Kitamoto (Osaka Univ., Toyonaka, Japan.), N. Muira (Osaka Univ., Toyonaka, Japan.), M. Egoshi (Osaka Univ., Toyonaka, Japan.), and Y. Ohno (Osaka Univ., Toyonaka, Japan.) 2 Feb. 1995 5 p

(NASA Order S-14645-F; NASA Order S-14626-F; NASA Order S-14648-F) (NASA-CR-197281; NAS 1.26:197281; R95-232) Avail: CASI HC A01/MF A01

We report ASCA Solid State Imaging Spectrometer (SIS) x-ray observations of the O stars delta Ori and lambda Ori. The energy resolution of the SIS allows us to resolve features in the O star x-ray spectra which are not apparent in spectra obtained by x-ray spectrometers with lower energy resolution. SIS spectra from both stars show evidence of line emission, suggesting the thermal nature of the x-ray source. However, the observed line strengths are different for the two stars. The observed stellar x-ray spectra are not well described by isothermal models although absorbed thermal emission models with two or more temperatures can provide an adequate fit to the data. For both stars we present evidence of absorbing columns significantly larger than the known ISM columns, indicative of absorption by a circumstellar medium, presumably the stellar winds. In addition, the lambda Ori spectrum shows the presence of emission at energies greater than 3 keV which is not seen in the delta Ori spectrum. Author

N95-25104*# Columbia Univ., New York, NY. Dept. of Astronomy and Physics.

LARGE-FORMAT HIGH RESOLUTION MICROCHANNEL PLATE DETECTORS FOR ULTRAVIOLET ASTRONOMY Final Technical Report, 31 Dec. 1994

Christopher Martin 31 Mar. 1995 28 p

(Grant NAGw-2593)

(NASA-CR-197993; NAS 1.26:197993; CAL-2294) Avail: CASI HC A03/MF A01

This report includes work on two types of two-dimensional position-sensitive detectors that were developed in this lab under this award. We worked to develop and optimize the wire-wound helical delay line detector (HDL) in the first and second years. Some early work on the HDL is contained in a paper included as Appendix A. In the second and third years we developed the concept for, then successfully designed and tested, both a lab prototype, and a flight prototype of the first, crossed delay line detector based on two orthogonal serpentine delay lines (SDL). Some of the work on the SDL is contained in a paper included as Appendix B. Appendix C contains copies of the invention report and record. Derived from text

90 ASTROPHYSICS

Includes cosmology; celestial mechanics; space plasmas; and interstellar and interplanetary gases and dust.

For related information see also *75 Plasma Physics*.

N95-24234# Los Alamos National Lab., NM.
RESOLUTION OF THE CLASSICAL HYADES LITHIUM PROBLEM
J. Faulkner and F. J. Swenson 1995 9 p Presented at the Light Element Abundances, Elba, Italy, 23-28 May 1994
(Contract W-7405-eng-36)
(DE95-003661; LA-UR-94-3937; CONF-9405264-1) Avail: CASI HC A02/MF A01

For the very first time, it has recently proved possible to make a well-motivated, physically plausible, and self-consistent prediction of the Hyades G- and K-dwarf (Li,T(sub eff)) relationship that matches the long-unexplained observations. The method employs the latest Iglesias &, Rogers (OPAL) interior opacities and Alexander surface opacities (whose respective values are now themselves close to empirical predictions or estimates made earlier in this Hyades project), King's recently discovered (O/Fe) enhancement (another prediction) and utterly conventional PMS (pre-main-sequence) evolution unaided by arbitrary and ad hoc adjustable parameters. Thus, the following assumptions form a self-consistent set explaining the Hyades G- and K-dwarf (Li,T(sub eff)) observations: (1) Pop. I interior opacities are now essentially correct; (2) Pop. I surface opacities are now essentially correct; (3) The Hyades distance is now essentially correct; (4) The Hyades (Fe/H) and (O/Fe) are now essentially correct, and possible changes in (Ne, Mg, or Si/Fe) are likely to have only a small effect; (5) Convective envelope overshooting is negligible; and (6) Quarreling with the above means finding at least two compensating errors in assumptions (1) through (5). DOE

N95-24327# Stanford Linear Accelerator Center, CA.
QUANTUM CORRECTIONS FOR A COSMOLOGICAL STRING SOLUTION
K. Behrndt Aug. 1994 6 p Presented at the Symposium on Particles, Strings and Cosmology, Syracuse, NY, 19-24 May 1994
(Contract DE-AC03-76SF-00515)
(DE95-006057; SLAC-PUB-6640; HEP-TH-9408137; CONF-9405162-2) Avail: CASI HC A02/MF A01

The author investigates quantum corrections for a cosmological solution of the string effective action. Starting point is a classical solution containing an antisymmetric tensor field, a dilaton and a modulus field which has singularities in the scalar fields. As a first step he quantizes the scalar fields near the singularity with the result that the singularities disappear and that in general non-perturbative quantum corrections form a potential in the scalar fields. DOE

N95-24455# Los Alamos National Lab., NM.
THE INFLUENCE OF CDM ON THE DYNAMICAL ESTIMATE OF (OMEGA) IN THE LOCAL NEIGHBORHOOD
A. M. Dunn and R. Laflamme 1994 5 p Presented at the 5th Astrophysics Conference, College Park, MD, 10-12 Oct. 1994
(Contract W-7405-eng-36)
(DE95-005212; LA-UR-94-4196; CONF-9410287-3) Avail: CASI HC A01/MF A01

Peebles has suggested an interesting method to trace back in time positions of galaxies called the least action method. This method applied on the Local Group galaxies seems to indicate that we live in an (Omega)(approx) 0.1 Universe. We have studied a cold dark matter (CDM) N-body simulation with (Omega) = 0.2 and H = 50 kms(exp -1)/Mpc and compare trajectories traced back from the Least Action Principle and the center of mass of the particle forming CDM halos. We have shown that the agreement between these set of trajectories is at best qualitative. We have also shown that the line of sight peculiar velocities are underestimated. This discrepancy is due to orphans, CDM particles which do not end up in halos. By varying the density parameter (Omega) in the least action principle we show that using this method we would underestimate the density of the Universe by a factor of 4--5. DOE

N95-24884# International Centre for Theoretical Physics, Trieste (Italy).
CREATION AND DEVELOPMENT OF THE UNIVERSE (SYMMETRY APPROACH)
I. S. Zheludev (Academy of Sciences, USSR, Moscow, USSR.) Sep. 1993 38 p
(DE94-628558; IC-92/332) Avail: CASI HC A03/MF A01 (US Sales Only)

The model according to which space subreality and time subreality are created during Big Bang is introduced. The first one is centrosymmetrical, the second anticentrosymmetrical. One to another they are transformed by mutual 'replacement' space and time. Such subrealities are not antisubrealities and their elementary particles (appeared through Big Bang) are not able to annihilate completely because of symmetry conditions. This leads to the appearance of condensed matter. The model of two subrealities gives the possibility to explain without 'parity violation' any physical phenomena. Four macroscopic rules of symmetry (scale, corkscrew, gyroscope and right (left) hand) reflect four fundamental interactions of our reality. DOE

N95-24885# Joint Inst. for Nuclear Research, Dubna (USSR). Nuclear Problems Lab.
POSSIBLE CONSTRAINTS ON SUSY-MODEL PARAMETERS FROM DIRECT DARK MATTER SEARCH
V. A. Bednyakov, S. G. Kovalenko, and H. V. Klapdor-Kleingrothaus (Max-Planck-Inst. fuer Kernphysik, Heidelberg, Germany.) 1993 8 p Submitted for publication Sponsored by Russian Foundation for Fundamental Research
(DE94-628561; JINR-E-2-93-447) Avail: CASI HC A02/MF A01 (US Sales Only)

We consider the SUSY-model neutralino as a dominant Dark Matter (DM) particle in the galactic halo and investigate some general issues of direct DM searches via elastic neutralino-nucleus scattering. On the basis of conventional assumptions about the nuclear and nucleon structure, without referring to a specific SUSY-model, we prove that it is impossible in principle to extract more than three constrains on fundamental supersymmetry (SUSY) - model parameters from the direct Dark Matter searches. Three types of Dark Matter detector probing different groups of parameters are recognized. DOE

N95-24886# Joint Inst. for Nuclear Research, Dubna (USSR). Nuclear Problems Lab.
ON SUSY DARK MATTER DETECTION WITH SPINLESS NUCLEI
V. A. Bednyakov, S. G. Kovalenko, and H. V. Klapdor-Kleingrothaus (Max-Planck-Inst. fuer Kernphysik, Heidelberg, Germany.) 1993 16 p Submitted for publication Sponsored by Russian Foundation for Fundamental Research
(DE94-628562; JINR-E-2-93-448) Avail: CASI HC A03/MF A01 (US Sales Only)

We investigate the role of nuclear spin in elastic scattering of Dark Matter (DM) neutralinos from nuclei in the framework of the Minimal Supersymmetry (SUSY) standard model (MSSM). The relative contribution of spin-dependent axial-vector and spin-independent scalar interactions to the event rate in a DM detector has been analyzed for various nuclei. Within general assumptions about the nuclear and nucleon structure we find that for nuclei with atomic weights A greater than 50 the spin-independent part of the event rate R(sub si) is larger than the spin-dependent one R(sub sd) in the domain of the MSSM parameter space allowed by the known experimental data and where the additional constraint for the total event rate R=R(sub sd)+R(sub si) greater than 0.01 is satisfied. The latter reflects realistic sensitivities of present and near future DM detectors. Therefore we expect equal chances for discovering the DM event either with spin-zero or with spin-non-zero isotopes if their atomic weights are A(sub 1) approx A(sub 2) greater than 50. DOE

N95-25122*# Washington Univ., Seattle, WA. Inst. for Nuclear Theory.
CORE-COLLAPSE SUPERNOVAE AND NUCLEOSYNTHESIS
W. C. Haxton 1994 15 p Presented at the 3rd School on Astrofundamental Physics, Erice, Italy, Sep. 1994
(Contract NAGw-2523; DE-FG06-90ER-40561)
(NASA-CR-197731; NAS 1.26:197731; DE95-004357; DOE/ER-40561/170; CONF-9409270-1) Avail: CASI HC A03/MF A01

The author discusses some of the physics that govern the collapse

and explosion of a massive star, including issues such as lepton number losses in the infall stage and neutrino heating and convection following the core bounce. Recent work on the neutrino process and the r-process is reviewed. The author describes how the nucleosynthesis depends on the explosion mechanism. Some of the interesting possibilities for oscillations of closure mass (nu)(sub (tau))s are discussed, along with their signatures in terrestrial detectors and in nucleosynthesis. DOE

N95-25343# State Univ. of New York, Stony Brook, NY. Dept. of Earth and Space Sciences.
RESEARCH IN NUCLEAR ASTROPHYSICS: STELLAR COLLAPSE AND SUPERNOVAE Continuation Progress Report, 1 Dec. 1994 - 30 Nov. 1995
James M. Lattimer and Amos Yahil 30 Nov. 1995 9 p
(Contract DE-FG02-87ER-40317)
(DE95-004300; DOE/ER-40317/13) Avail: CASI HC A02/MF A01

This progress report describes the nuclear astrophysics research activities in the Earth and Space Sciences Department at Stony Brook during the last year. The research focuses on three aspects of nuclear astrophysics: (1) the equation of state of hot, dense matter; (2) the origin of supernovae and neutron stars; and (3) the early cooling epoch of neutron stars. Ongoing projects are first described individually, and are followed by a series of detailed reports, which summarize each project completed within the last year. DOE

N95-25431# International Centre for Theoretical Physics, Trieste (Italy).
FLARE STARS AND PASCAL DISTRIBUTION
R. Muradian (Joint Inst. for Nuclear Research, Dubna, USSR.) Jul. 1994 6 p
(DE95-607044; IC-94/175) Avail: CASI HC A02/MF A01 (US Sales Only)

Observed statistics of stellar flares are described by Pascal or negative binomial distribution. The analogy with other classes of chaotic production mechanisms such as hadronic particle multiplicity distributions and photoelectron counts from thermal sources is noticed. DOE

N95-25433# International Centre for Theoretical Physics, Trieste (Italy).
STRING-LOOP CORRECTIONS TO EFFECTIVE ACTION AND BLACK-HOLE INSTABILITIES
V. V. Belokurov and M. Z. Iofa (Moscow State Univ., Russia.) Jul. 1994 10 p Sponsored by Russian Fund for Fundamental Researches
(DE95-607085; IC-94/193) Avail: CASI HC A02/MF A01 (US Sales Only)

Following the ideas of Ellis, Mavromatos and Nanopoulos, to account for instability of 2D black-hole solution, we discuss possible imaginary string-loop corrections to the coefficient at the Einstein term in string effective action. In closed bosonic string theory, such corrections appear because of the tachyon contribution to the integration measure over the moduli. In superstring theory (in critical as well as in non-critical dimensions), no one-string-loop complex corrections to the Einstein term are generated and the mechanism for generating black-hole instabilities proposed above fails. DOE

N95-25467# International Centre for Theoretical Physics, Trieste (Italy).
FAR-INFRARED AND SUBMILLIMETER SPECTROSCOPY OF PHOTODISSOCIATION REGIONS
Abdul Qaiyum Dec. 1993 22 p
(DE95-607520; IC-93/424) Avail: CASI HC A03/MF A01 (US Sales Only)

The physical properties of the galactic and extragalactic photodissociation regions, warm gas components molecular clouds are, generally, derived through the far-infrared (FIR) fine structure and submillimeter line emissions arising out of these regions. In the theoretical studies of these lines the model of Tielens and Hollenbach (herein after referred as TH) are usually employed in which all the opacity is assumed local in escape probability formalism and inward directed photons do not escape. These assumptions are contrary to the observational facts, where most of the lines are found optically thin except OI (63 micro m) and low rotational transitions of CO and some other molecules. The optically thin medium will allow the radiation to escape through any face of the region. These observational evidences let us to assume finite parallel plane slab, instead of semi-infinite parallel slab, in which the photons are allowed to escape from both surfaces (back and front). In the present study an attempt has been made to incorporate the two sided escape of photons from the PDR's and to study its effect on the FIR and submillimeter line emission from the PDR's/molecular clouds. Further the present formalism is also employed to study the clumpy PDR's/molecular clouds. The preliminary results show that now serious consequences are found on the thermal and chemical structure of the regions but individual line emissions are modified by differing factors. Particularly at low density and low kinetic temperature the change is substantial but at density greater than the critical density of the line and temperature close to the excitation temperature its effect is almost negligible. An attempt has also been made to study the physical conditions of the M17 region employing the present formalism. DOE

N95-25469# International Centre for Theoretical Physics, Trieste (Italy).
VALENCIA 1993: THE SUMMARY OF PARTICLE THEORY
Goran Senjanovic Jul. 1994 12 p Presented at The International School on Cosmological Dark Matter, Valencia, Italy
(DE95-607121; IC-94/155) Avail: CASI HC A03/MF A01 (US Sales Only)

The International School on Cosmological Dark Matter held in Valencia in the fall of 1993 was devoted to the interplay of cosmology and particle physics, with the obvious emphasis on the Dark Matter issue. The author presents the expanded version of his summary regarding the particle physics theory session of the School. DOE

N95-25647# International Centre for Theoretical Physics, Trieste (Italy).
HOMOGENEOUS ANISOTROPIC COSMOLOGICAL MODELS IN THE MINIMUM QUADRATIC POINCARE GAUGE THEORY OF GRAVITY
A. V. Minkevich (Belorussian State Univ., Minsk, Byelarus.), Nguyen Van Hoang (Center for Cosmic Physics and Remote Sensing, Hochiminh, Viet Nam.), and Nguyen Hong Chuong Jul. 1994 17 p
(DE95-607083; IC-94/173) Avail: CASI HC A03/MF A01 (US Sales Only)

In the present article we resume some of our results on homogeneous anisotropic models of the Poincare gauge theory of gravity based on the Riemann-Cartan spacetime. Namely, within the framework of the minimum quadratic Poincare gauge theory of gravity the dynamics of homogeneous anisotropic Bianchi types I-IX spinning-fluid cosmological models is studied. A basic equation set for these models is obtained and analyzed. In particular, exact solutions for the Bianchi type-I spinning-fluid and Bianchi type-V perfect-fluid models are found in integral form. DOE

N95-25675# Los Alamos National Lab., NM.
MILAGRO: A LOW ENERGY THRESHOLD EXTENSIVE AIR SHOWER ARRAY
C. Sinnis 1994 5 p Presented at the Trends in Astrophysics Conference, Stockholm, Sweden, 22-25 Sep. 1994 Submitted for publication
(Contract W-7405-eng-36)
(DE95-005246; LA-UR-94-4361; CONF-9409284-1) Avail: CASI HC A01/MF A01

Observations of high-energy gamma rays from astronomical sources have revolutionized our view of the cosmos. Gamma rays with energies up to approximately 10 GeV can be observed directly with space-based instruments. Above 100 GeV the low flux of gamma rays requires one to utilize ground-based instruments. Milagro is a new type of gamma-ray detector based on water Cerenkov technology. This new design will enable to continuously observe the entire overhead sky, and be sensitive to cosmic rays with energies above approximately 250 GeV. These attributes make Milagro an ideal detector for the study of high-energy transient phenomenon. DOE

N95-25766# Los Alamos National Lab., NM. Theoretical Astrophysics.
RICH CLUSTER SIMULATION: DYNAMICS AND MASS ESTIMATES
Benjamin Bromley, Michael Warren, Wojciech Zurek, and P. J. Quinn 1994 5 p Presented at the 5th Annual Astrophysics Conference, College Park, MD, 10-12 Oct. 1994 Submitted for publication Sponsored in part by the Aspen Center for Physics and the NASA HPCC program
(Contract W-7405-eng-36)
(DE95-005233; LA-UR-94-4163; CONF-9410287-1) Avail: CASI HC A01/MF A01

We present an analysis of a simulated rich cluster dominated by cold

dark matter. We focus on the dynamics of collapsed dark matter halos which may be associated with galaxies. We use projected positions and velocities of both dark matter particles and of halos to assess several conventional measures of cluster mass. The results indicate that the measures give reasonable results for dark matter particles but cause overestimates when applied to halos. In searching for the source of the discrepancies, we find that tidal disruption and dynamical friction do not induce a significant bias in the projected velocity dispersion of halos; however, an antibias in the spatial distribution of halos relative to that of the total mass appears to be most problematic for cluster mass estimates. DOE

N95-25990# International Centre for Theoretical Physics, Trieste (Italy).
REGGE IN THE SKY: ORIGIN OF THE COSMIC ROTATION
R. Muradian Jun. 1994 8 p
(DE95-607001; IC-94/143) Avail: CASI HC A02/MF A01 (US Sales Only)

Observed universal spin and mass relationship for a wide range of astronomical objects are described by two extended Regge trajectories: disc-trajectory for stars and planets, and ball-trajectory for galaxies and their clusters. The cosmic Chew-Frautschi plot is presented and two fundamental points are revealed on it: Eddington and Chandrasekhar points with coordinates expressed via combinations of the fundamental constants. DOE

N95-26044# International Centre for Theoretical Physics, Trieste (Italy).
THE USE OF EMPIRICAL MODELS TO INVESTIGATE GPS DERIVED TOTAL ELECTRON CONTENT
S. Kartal, S. M. Radicella, and P. Spalla (Consiglio Nazionale delle Ricerche, Florence, Italy.) Jul. 1994 6 p
(DE95-606045; IC-94/180) Avail: CASI HC A02/MF A01 (US Sales Only)

Hourly values of two months of Total Electron Content (TEC) calculated from Global Positioning System (GPS) Satellites observations of Doppler effect using a technique developed at the IROE of Florence, Italy (Ciraolo, 1993) are studied together with simultaneous measurements of Geostationary Satellite Faraday TEC obtained at a different location in Europe. These experimental data are compared with TEC values calculated by using DGR and IRI-90 empirical models of the electron density in the ionosphere based on ionospheric characteristics obtained from vertical sounding at locations near the two places where TEC from satellite observations are obtained. The results show that the correlation of experimental and model data is good in daytime. Night-time values of GPS (TEC) is not well correlated with the model calculations possible indicating that this technique sees an additional distribution of ionization from the one obtained by Faraday observations and the empirical models used. DOE

N95-26195# Iowa Univ., Iowa City, IA. Dept. of Physics and Astronomy.
THE WHISTLER-MODE BOW WAVE OF AN ASTEROID
Donald A. Gurnett Mar. 1995 33 p
(U-OF-IOWA-95-2) Avail: CASI HC A03/MF A01

The Galileo spacecraft has flown by two asteroids, Gaspra in 1990, and Ida in 1993. In both cases, the magnetometer detected magnetic field perturbations that are believed to be produced by an interaction of the asteroid with the solar wind. Kivelson et al. have proposed that these perturbations are caused by whistler-mode waves excited by the solar wind flow around the asteroid. This paper presents an analysis of whistler-mode waves generated by the interaction of a small object with the solar wind. Three cases are considered, with the solar wind magnetic field (1) parallel, (2) perpendicular, and (3) at an arbitrary angle to the velocity vector. Using the Cerenkov condition and the quasi-longitudinal approximation for the whistler mode, the angular limits of the wave pattern are determined. For the parallel case, the waves are confined to the upstream region, and for the perpendicular case, the waves are confined to two wedge-shaped regions extending downstream from the magnetic field line through the object. For intermediate magnetic field orientations, the accessibility region maintains the wedge-shaped configuration, with the leading edge of the wedge roughly following the direction of the magnetic field. The outer boundary of the accessibility region is a caustic surface, along which large field amplitudes are expected, similar to the bow wave of a ship. In all cases the interaction involves a characteristic wavelength, lambda(sub c) = (f(sub c) c-squared)/(f(sub p)-squared V), that is comparable to the size of an asteroid. Author

N95-26196# Iowa Univ., Iowa City, IA. Dept. of Physics and Astronomy.
ON A REMARKABLE SIMILARITY BETWEEN THE PROPAGATION OF WHISTLERS AND THE BOW WAVE OF A SHIP
Donald A. Gurnett Dec. 1994 20 p
(U-OF-IOWA-94-22) Avail: CASI HC A03/MF A01

It is well known that lightning-generated whistlers propagate along the Earth's magnetic field lines within a cone that at low frequencies makes an angle of 19 deg 28 min with respect to the local magnetic field. This angle turns out to be exactly the same as the half-angle of the bow wave of a ship in deep water. Both problems are complicated by the fact that the wave propagation is dispersive. In this paper we show that these two seemingly unrelated problems can be understood using the same basic approach, which is to analyze the group velocity direction as a function of the wave normal angle. This approach may have applications to other problems of geophysical interest, such as the bow wave generated by the interaction of an asteroid with the solar wind. Author

N95-26284# Fermi National Accelerator Lab., Batavia, IL.
A SURVEY OF SURVEYS
S. M. Kent Nov. 1994 9 p Presented at the IAU169 Conference on Unsolved Problems of the Milky Way, The Hague, Netherlands, 23-27 Aug. 1994
(Contract DE-AC02-76CH-03000)
(DE95-004238; FNAL/C-94/373; CONF-9408198-1) Avail: CASI HC A02/MF A01

A new era for the field of Galactic structure is about to be opened with the advent of wide-area digital sky surveys. In this article, the author reviews the status and prospects for research for 3 new ground-based surveys: the Sloan Digital Sky Survey (SDSS), the Deep Near-Infrared Survey of the Southern Sky (DENIS) and the Two Micron AU Sky Survey (2MASS). These surveys will permit detailed studies of Galactic structure and stellar populations in the Galaxy with unprecedented detail. Extracting the information, however, will be challenging. DOE

91 LUNAR AND PLANETARY EXPLORATION

Includes planetology; and manned and unmanned flights.

For spacecraft design or space stations see *18 Spacecraft Design, Testing and Performance.*

N95-24239*# Pennsylvania State Univ., Erie, PA. Div. of Science.
INFRARED SPECTROSCOPY OF JUPITER AND SATURN Final Technical Report
Roger F. Knacke [1994] 3 p
(Grant NAGw-2194)
(NASA-CR-198034; NAS 1.26:198034) Avail: CASI HC A01/MF A01

Infrared spectroscopy provides unique insights into the chemistry and dynamics of the atmospheres of Jupiter and Saturn -- and of Titan, the enigmatic satellite of Saturn. The 5 micron spectral region of these objects is transparent to deep levels, and is therefore particularly useful for the identification of molecules in the deep atmosphere at very low (parts per billion) concentrations. In 1991 we obtained data at J, H, K, and M and made repeated observations of Titan's albedo as the satellite orbited Saturn. The J albedo is 12 + -3% greater than the albedo measured in 1979; the H and K albedos are the same. There was no evidence for variations at any wavelength over the eastern hali of Titan's orbit. We also obtained low resolution (R = 50) spectra of Titan between 3.1 and 5.1 microns. The spectra contain evidence for CO and CH3D absorptions. Spectra of Callisto and Ganymede in the 4.5 micron spectral region are featureless and give albedos of 0.08 and 0.04 respectively. If Titan's atmosphere is transparent near 5 microns, its surface albedo there is similar to Callisto's. In 1992 and 1993 we obtained further spectroscopic data of Titan with the UKIRT CGS4 spectrometer. We discovered two unexpected and unexplained spectral features in the 3-4 micron /spectrum of Titan. An apparent emission feature near the 3 micron (nu3) band of methane indicates temperatures higher than known to be present in Titan's upper stratosphere and may be caused by unexpected non-LTE emission. An absorption feature near 3.47

microns may be caused by absorption in solid grains or aerosol's in Titan's clouds. The feature is similar, but not identical to organics in the interstellar matter and in comets. Derived from text

N95-24303*# University of Southern California, Los Angeles, CA. Dept. of Earth Sciences.

GEOLOGIC MAPPING OF ARGYRE PLANITIA Final Technical Report

Donn S. Gorsline and Timothy J. Parker (Jet Propulsion Lab., California Inst. of Tech., Pasadena, CA.) Mar. 1995 46 p

(Grant NAGw-2902)

(NASA-CR-197986; NAS 1.26:197986) Avail: CASI HC A03/MF A01

This report describes the results from the geologic mapping of the central and southern Argyre basin of Mars. At the Mars Geologic Mapper's Meeting in Flagstaff during July, 1993, Dave Scott (United States Geological Survey, Mars Geologic Mapping Steering Committee Chair) recommended that all four quadrangles be combined into a single 1:1,000,000 scale map for publication. It was agreed that this would be cost-effective and that the decrease in scale would not compromise the original science goals of the mapping. Tim Parker completed mapping on the 1:500,000 scale base maps, for which all the necessary materials had already been produced, and included the work as a chapter in his dissertation, which was completed in the fall of 1994. Geologic mapping of the two southernmost quadrangles (MTM -55036 and MTM -55043; MTM=Mars Transverse Mercator) was completed as planned during the first year of work. These maps and a detailed draft of the map text were given a preliminary review by Dave Scott during summer, 1993. Geologic mapping of the remaining two quadrangles (MTM -50036 and MTM -50043) was completed by summer, 1994. Results were described at the Mars Geologic Mappers Meeting, held in Pocatello, Idaho, during July, 1994. Funds for the third and final year of the project have been transferred to the Jet Propulsion Laboratory, where Tim Parker will revise and finalize all maps and map text for publication by the United States Geological Survey at the 1:1,000,000 map scale. Derived from text

N95-24672* Jet Propulsion Lab., California Inst. of Tech., Pasadena, CA.

MARS OBSERVER MISSION: MAPPING THE MARTIAN WORLD (Videotape)

1992 Videotape: 7 min. 14 sec. playing time, in color, with sound

(NASA-CR-110585; AVC-92-193; NONP-NASA-VT-95-47244) Avail: CASI VHS A02/BETA A22

The 1992 Mars Observer Mission is highlighted in this video overview of the mission objectives and planning. Using previous photography and computer graphics and simulation, the main objectives of the 687 day (one Martian year) consecutive orbit by the Mars Observer Satellite around Mars are explained. Dr. Arden Albee, the project scientist, speaks about the pole-to-pole mapping of the Martian surface topography, the planned relief maps, the chemical and mineral composition analysis, the gravity fields analysis, and the proposed search for any Mars magnetic fields. CASI

N95-24987*# Jet Propulsion Lab., California Inst. of Tech., Pasadena, CA.

USER GUIDE TO THE MAGELLAN SYNTHETIC APERTURE RADAR IMAGES Reference Publication

Stephen D. Wall, Shannon L. McConnell, Craig E. Leff, Richard S. Austin, Kathi K. Beratan, and Mark J. Rokey Mar. 1995 204 p

(Contract NAS7-1260)

(NASA-RP-1356; NAS 1.61:1356) Avail: CASI HC A10/MF A03

The Magellan radar-mapping mission collected a large amount of science and engineering data. Now available to the general scientific community, this data set can be overwhelming to someone who is unfamiliar with the mission. This user guide outlines the mission operations and data set so that someone working with the data can understand the mapping and data-processing techniques used in the mission. Radar-mapping parameters as well as data acquisition issues are discussed. In addition, this user guide provides information on how the data set is organized and where specific elements of the set can be located. Author

N95-24994*# National Aeronautics and Space Administration. Goddard Space Flight Center, Greenbelt, MD.

THE CLEMENTINE MISSION: INITIAL RESULTS FROM LUNAR MAPPING

P. D. Spudis (Lunar and Planetary Inst., Houston, TX.), E. Shoemaker (Lowell Observatory, Flagstaff, AZ.), C. Acton (Jet Propulsion Lab., California Inst. of Tech., Pasadena, CA.), B. Burratti (Jet Propulsion Lab., California Inst. of Tech., Pasadena, CA.), T. Duxbury (Jet Propulsion Lab., California Inst. of Tech., Pasadena, CA.), D. Baker, D. Smith, J. Blamont (Centre National d'Etudes Spatiales, Paris, France.), M. Davies (RAND Corp., Santa Monica, CA.), and E. Eliason (Geological Survey, Flagstaff, AZ.) et al [1994] 12 p LIMITED REPRODUCIBILITY: More than 20% of this document may be affected by color photographs Original contains color illustrations

(NASA-TM-110555; NAS 1.15:110555; ESA-SP-1170) Avail: CASI HC A03/MF A01; 3 functional color pages

Clementine was a mission designed to test the space-worthiness of a variety of advanced sensors for use on military surveillance satellites while, at the same time, gathering useful scientific information on the composition and structure of the Moon and a near-Earth asteroid. Conducted jointly by the Ballistic Missile Defense Organization (BMDO, formerly the Strategic Defense Initiative Organization) of the US Department of Defense and NASA, Clementine was dispatched for an extended stay in the vicinity of Earth's moon on 25 January 1994 and arrived at the Moon on 20 February 1994. The spacecraft started systematic mapping on 26 February, completed mapping on 22 April, and left lunar orbit on 3 May. The entire Clementine project, from conception through end-of-mission, lasted approximately 3 years. Author

N95-25854*# Jet Propulsion Lab., California Inst. of Tech., Pasadena, CA.

VOYAGER: THE GRANDEST TOUR. THE MISSION TO THE OUTER PLANETS

Apr. 1991 43 p Original contains color illustrations

(NASA-CR-197708; JPL-400-445; NAS 1.26:197708) Avail: CASI HC A03/MF A01; 35 functional color pages

A history and general accomplishments of the Voyager 1 and 2 missions to the outer planets are presented. Over the course of 12 years, these spacecraft drew back the curtain on nearly half the solar system. They brought into sharp focus the faces of the four giant outer planets - Jupiter, Saturn, Uranus, and Neptune - and their families of disparate moons. The Voyagers showed us unimagined worlds: frozen beauty in the rings of Saturn, and molten violence in the explosive sulfur volcanoes on Jupiter's moon Io. They brought us close-ups of the florid and intricate storms of Jupiter itself. Voyager 2 went on to reveal the peculiarities of cockeyed Uranus and its equally skewed rings and moons. Then finally, Neptune, nearly invisible from earth, was unveiled in all its big, blue splendor, circled by shadowy rings and a bright pastel moon called Triton. Both Voyagers are headed toward the outer boundary of the solar system in search of the heliopause, the region where the sun's influence wanes and the beginning of interstellar space can be sensed. CASI

N95-26116*# Southwest Research Inst., Boulder, CO. Geophysical, Astrophysical, and Planetary Sciences Section.

DISTRIBUTION AND NATURE OF UV ABSORBERS ON TRITION'S SURFACE Semiannual Report

S. Alan Stern 28 Feb. 1995 48 p

(Grant NAGw-3402; SwRI Proj. 15-5653)

(NASA-CR-198008; NAS 1.26:198008) Avail: CASI HC A03/MF A01

Substantial evidence suggests that a UV (ultraviolet) Spectrally Absorbing Material (UV-SAM) exists on Triton's surface. This evidence is found in the positive slope in Triton's spectrum from the UV to the near-IR, and the increasing contrast in Triton's light curve in the blue and UV. Although it is now widely-thought that UV-SAM's exist on Triton, little is known about their distribution and spectral properties. The goal of this NDAP Project is to determine the spatial distribution and geological context of the UV-SAM material. We hope to determine if UV-SAM's on Triton are correlated with geologic wind streaks, craters, calderas, geomorphic/topographic units, regions containing (or lacking) volatile frosts, or some other process (e.g., magnetospheric interactions). Once the location and distribution of UV-SAM's has been determined, further constraints on their composition can be made by analyzing the spectrographic data set. To accomplish these goals, various data sets will be used, including Voyager 2 UV and visible images of Triton's surface, IUE and HST spectra of Triton, and a geologic map of the surface based on Voyager 2 and spectrophotometric data. The results

of this research will be published in the planetary science literature.
Derived from text

N95-26336*# Jet Propulsion Lab., California Inst. of Tech., Pasadena, CA.
RETURN TO THE RED PLANET: THE MARS OBSERVER MISSION
Bevan M. French and Carolynn Young, ed. Aug. 1993 66 p Original contains color illustrations
(NASA-CR-197707; JPL-400-504; NAS 1.26:197707) Avail: CASI HC A04/MF A01; 1 functional color page

An overview of the Mars Observer Mission is discussed. Highlights include: (1) the spacecraft; (2) the instrumentation and science experiments; (3) the countries involved; (4) the flight teams; and (5) the planet Mars itself (a brief history). Photographs and flow charts are included, along with diagrams of instrumentation and a brief historical narrative of space observation and exploration. CASI

92 SOLAR PHYSICS

Includes solar activity, solar flares, solar radiation and sunspots. For related information see *93 Space Radiation.*

N95-24249# Washington Univ., Seattle, WA.
LANDAU-ZENER TREATMENTS OF SOLAR NEUTRINO OSCILLATIONS
M. Bruggen (Cambridge Univ., Cambridge, England.), W. C. Haxton, and Y. Z. Qian 1995 21 p
(Contract DE-FG06-90ER-40561)
(DE95-004761; DOE/ER-40561/164) Avail: CASI HC A03/MF A01

The authors present a simple derivation of Landau-Zener formulae for nonadiabatic level crossings for linear and exponential density profiles. The derivation depends on a single assumption that applies somewhat differently to the exponential and linear cases, providing some insight into the relationship between the respective formulae. They note that one exponential Landau-Zener formula in common use is only approximately correct. Comparisons with exact calculations are made. DOE

N95-25364# Brookhaven National Lab., Upton, NY.
UPDATE OF GALLEX SOLAR NEUTRINO RESULTS AND IMPLICATIONS
T. Kirsten (Max-Planck-Inst. fuer Kernphysik, Heidelberg, Germany.) 1995 9 p Presented at the Neutrino 1994: 16th International Conference on Neutrino Physics and Astrophysics, Eilat, Israel, 29 May - 3 Jun. 1994 Sponsored by Alfried Krupp von Bohlen und Halbach Foundation, Ist. Nazionale di Fisica Nucleare, Commissariat a l'Energie Atomique
(Contracts DE-AC02-76CH-00016; BMFT-06-HD-5541)
(DE95-005005; BNL-61120; CONF-9405216-3) Avail: CASI HC A02/MF A01

The gallium chloride detector operated by the GALLEX-collaboration in the Gran Sasso Underground Laboratory responds primarily to pp-neutrinos. They are produced in the primary fusion reaction of hydrogen into deuterium and directly coupled to the solar luminosity. Standard Solar Models predict ca. 58% of the total signal expected in GALLEX (123-132 SNU) to be due to pp-neutrinos. The relative pp-neutrino dominance becomes even larger if the deficit of higher energy neutrinos (as observed in the Homestake- and Kamiokande experiments) is considered. During the first data taking period, 15 solar runs had been performed within the exposure period 14.5.1991 - 29.4.1992. The result, 81 +/- 17 +/- 9 SNU provided the first experimental evidence for pp-neutrinos from the Sun. At the same time, it confirmed the depression of higher energy neutrino fluxes relative to the model predictions. Here the authors report the results of 15 more solar neutrino runs, covering the period 19.8.92 - 13.10.93. They obtain 78 +/- 13 +/- 5 SNU. Evaluated together, the result for all 30 runs is 79 +/- 10 +/- 6 SNU. While the SNU rate of GALLEX I is well reproduced the statistical error has been reduced so substantially that a value of signal +2 sigma is required to accommodate not only pp-and pep- but also the Be-7-neutrino induced Ge-71-production. Contrary, the fate of B-8-neutrinos has only little discernible effect on the GALLEX data. In conclusion, with the present errors GALLEX constitutes a 2.5 sigma problem for Be-7 neutrinos within the frame of 'astrophysical' solutions. Alternatively, the particle physics solution (MSW-effect) can consistently explain all available solar neutrino results, leading to a most probable mass scale with the muon-neutrino at approximately 3 meV (milli-eV). However, since the GALLEX result allows the presence of pp and pep neutrinos at full strength. the latter explanation of the data is not forced. DOE

N95-25576 National Geophysical Data Center, Boulder, CO.
SOLAR-GEOPHYSICAL DATA NUMBER 603, NOVEMBER 1994. PART 1: (PROMPT REPORTS). DATA FOR OCTOBER, SEPTEMBER 1994, AND LATE DATA
H. E. Coffey Nov. 1994 138 p Limited Reproducibility: More than 20% of this document may be affected by microfiche quality
(PB95-166393; SGD-603-Pt-1) Avail: CASI HC A07

Contents include the following: Detailed Index for 1994; Data for October 1994--Solar-Terrestrial Environment, IUWDS Alert Periods (Advance and Worldwide), Solar Activity Indices, Solar Flares, Solar Radio Emission, Stanford Mean Solar Magnetic Field, and GOES-7 Daily Electron Fluence; Data for September 1994--Solar Active Regions, Sudden Ionospheric Disturbances, Solar Radio Spectral Observations, Solar Radioheliograph-164 MHz-Nancay, Cosmic Ray Measurements by Neutron Monitor, Geomagnetic Indices, Principal Magnetic Storms, and Sudden Commencements/Solar Flare Effects; and Late Data--International Geophysical Calendar 1995--Explanations and Recommended Scientific Programs. NTIS

N95-25577# National Geophysical Data Center, Boulder, CO.
SOLAR-GEOPHYSICAL DATA NUMBER 603, NOVEMBER 1994. PART 2: (COMPREHENSIVE REPORTS). DATA FOR MAY 1994 AND MISCELLANEOUS
Helen E. Coffey, ed. Nov. 1994 42 p
(PB95-166401; SGD-603-Pt-2) Avail: CASI HC A03/MF A01

Contents include the following: Detailed Index for 1994; Data for May 1994 -- Solar Flares, Solar Radio Bursts at Fixed Frequencies, Solar X-Ray Radiation from GOES Satellite (Graphs), and Active Prominences and Filaments; Miscellaneous Data -- NOAASESC Solar Proton Events Jan. 1976-Oct. 1994, and International Geophysical Calendar 1995 (Explanations and Recommended Scientific Programs). NTIS

N95-25986# International Centre for Theoretical Physics, Trieste (Italy).
ESTIMATION AND ANALYSIS OF SPECTRAL SOLAR RADIATION OVER CAIRO
M. M. AbdelWahab and M. Omran (Egyptian Meteorological Authority, Cairo, Egypt.) May 1994 14 p
(DE95-606029; IC-94/101) Avail: CASI HC A03/MF A01 (US Sales Only)

This work presents a methodology to estimate spectral diffuse and global radiation on horizontal surface. This method is validated by comparing with measured direct and global spectral radiation in four bands. The results show a good performance in cloudless conditions. The analysis of the ratio of surface values to extraterrestrial ones revealed an over-all depletion in the summer months. Also there was no evidence for any tendency for conversion of radiational components through different bands. The model presents excellent agreement with the measured values for (UV/G) ratio. DOE

N95-26042# International Centre for Theoretical Physics, Trieste (Italy).
PREDICTING THE COMPONENTS OF THE TOTAL HEMISPHERICAL SOLAR RADIATION FROM SUNSHINE DURATION MEASUREMENTS IN LAGOS, NIGERIA
A. A. L. Maduekwe and M. A. C. Chendo Jun. 1994 16 p
(DE95-606030; IC-94/140) Avail: CASI HC A03/MF A01 (US Sales Only)

Correlations for the city of Lagos (latitude 6.58 deg N, longitude 3.33 deg E) have been found between the records of bright sunshine hours and the daily and monthly components of the total hemispherical solar radiation. Four new models have been developed which include H/H(sub 0) as a predictor in the Angstrom type models for the diffuse and beam fractions. They contain the quadratic term of the sunshine index, (n/N) and are given as follows: Q/H(sub 0)=a+b(H/H(sub 0))+c(n/N)+d(n/N)(sup 2) Q/H(sub 0)=a+b(H/H(sub 0))+d(n/N)(sup 2); Q/H(sub 0)=a+b(H/H(sub 0))+c(n/N)+d(n/N)(sup 2); Q/H(sub 0)=a+b(H/H(sub 0))+d(n/N)(sup 2); where Q is the diffuse or beam radiation on a horizontal plane. The statistical test carried out showed that the new equations generally improved the prediction of the beam or diffuse components from the Angstrom type equations by over 25%. DOE

93 SPACE RADIATION

Includes cosmic radiation; and inner and outer earth's radiation belts.

For biological effects of radiation see *52 Aerospace Medicine.* For theory see *73 Nuclear and High-Energy Physics.*

N95-24381*# Columbia Univ., New York, NY. Astrophysics Lab.
GAMMA-RAY EMISSION FROM GLOBULAR CLUSTERS. SHOCK HIGH ENERGY EMISSION FROM THE BE-STAR/PULSAR SYSTEM PSR 1259-63. ECHOES IN X-RAY NOVAE Annual Status Report, 15 Apr. 1994 - 14 Apr. 1995
Philip Kaaret Apr. 1995 16 p
(Grant NAG5-2235)
(NASA-CR-197994; NAS 1.26:197994) Avail: CASI HC A03/MF A01

This grant covers work on the Compton phase 3 investigation, 'Shock High Energy Emission from the Be- Star/Pulsar System PSR 1259-63' and cycle 4 investigations 'Diffuse Gamma-Ray Emission at High Latitudes' and 'Echoes in X-Ray Novae'. Work under the investigation 'Diffuse Gamma-Ray Emission at High Latitudes' has lead to the publication of a paper (attached), describing gamma-ray emissivity variations in the northern galactic hemisphere. Using archival EGRET data, we have found a large irregular region of enhanced gamma-ray emissivity at energies greater 100 MeV. This is the first observation of local structure in the gamma-ray emissivity. Work under the investigation 'Echoes in X-Ray Novae' is proceeding with analysis of data from OSSE from the transient source GRO J1655-40. The outburst of this source last fall triggered this Target of Opportunity investigation. Preliminary spectral analysis shows emission out to 600 keV and a pure power low spectrum with no evidence of an exponential cutoff. Work is complete on the analysis of BATSE data from the Be-Star/Pulsar Sustem PSR 1259-63. Derived from text

N95-25926*# National Aeronautics and Space Administration. Marshall Space Flight Center, Huntsville, AL.
LINEAR ENERGY TRANSFER (LET) SPECTRA OF COSMIC RADIATION IN LOW EARTH ORBIT
T. A. Parnell, J. W. Watts, Jr., A. B. Akopova (Academy of Sciences of the Armenian SSR, Erivan, Armenia.), N. V. Magradze (Academy of Sciences of the Armenian SSR, Erivan, Armenia.), V. E. Dudkin (Institute of Biomedical Problems, Moscow, USSR.), E. E. Kovalev (Institute of Biomedical Problems, Moscow, USSR.), Yu. V. Potapov (Institute of Biomedical Problems, Moscow, USSR.), E. V. Benton (San Francisco Univ., CA.), A. L. Frank (San Francisco Univ., CA.), and E. R. Benton (San Francisco Univ., CA.) *In* San Francisco Univ., High LET, Passive Space Radiation Dosimetry and Spectrometry Mar. 1995 6 p (For primary document see N95-25911 08-72)
(Contract NCC2-521; NAG8-071)
Copyright Avail: CASI HC A02/MF A03

N95-25931*# San Francisco Univ., CA.
COSMIC RAY PARTICLES WITH DIFFERENT LET VALUES UNDER VARIOUS THICKNESSES OF SHIELDING IN LOW ALTITUDE ORBITS: CALCULATIONS AND COSMOS-2044 MEASUREMENTS
E. V. Benton, A. L. Frank, E. R. Benton, A. M. Marenny (Research Center of Space Craft Radiation Safety, Moscow, Russia.), R. A. Nymmik (Moscow State Univ., Russia.), and A. A. Suslov (Moscow State Univ., Russia.) *In its* High LET, Passive Space Radiation Dosimetry and Spectrometry Mar. 1995 5 p (For primary document see N95-25911 08-72)
(Contract NCC2-521)
Avail: CASI HC A01/MF A03

99 GENERAL

N95-24870# European Space Agency. European Space Research and Technology Center, ESTEC, Noordwijk (Netherlands).
EUROPE IN SPACE, 1960-1973
John Krige (European Univ. Inst., Florence, Italy.), Arturo Russo (Palermo Univ., Italy.), N. Longdon, ed., and B. Battrick, ed. Sep. 1994 141 p Original contains color illustrations
(ESA-SP-1172; ISBN-92-9092-125-0) Avail: CASI HC A07/MF A02

This book describes the historical evolution of the European space program. It is divided into three main parts. The first narrates the background to Europe's entry into space and explores the circumstances surrounding the establishment of ESRO (European Space Research Organisation) and ELDO (European Space Vehicle Launcher Development Organisation) and the implementation of ESRO's first scientific program. The next major part describes first attempts to reorient the European space effort towards the development of telecommunication satellites. It then fleshes out the painful and divisive efforts to define the place of launchers in European space policy from the mid-1960s onwards, and discusses the new possibilities opened up by the American offer to participate in the post-Apollo program. The last part shows how the conflicts that characterized the latter part of the 1960s were resolved and the foundations laid for ESA (European Space Agency). The new scientific program that was approved and the 'package deals' that were arranged are described. In the conclusion, the historical period surveyed is summarized and the main changes characterizing the European space effort in this period are identified. Derived from text

N95-24871# European Space Agency. European Space Research and Technology Center, ESTEC, Noordwijk (Netherlands).
THE HISTORY OF ELDO. PART 1: 1961-1964
Michelangelo DeMaria (La Sapienza Univ., Rome, Italy.) Sep. 1993 44 p Original contains color illustrations
(ESA-HSR-10-Pt-1) Avail: CASI HC A03/MF A01

The ESA History Study Reports are preliminary reports of studies carried out within the framework of an ESA (European Space Agency) contract. They will form the basis of a comprehensive study of European Space activities covering the period 1959-1987. 'Blue Streak' and 'Veronique' -- the first and second stage of the proposed European launcher -- are reviewed in this volume as part of the origins of the ELDO launch vehicle, along with the international cooperation and participation in the project. CASI

N95-24908# Electrotechnical Lab., Ibaraki (Japan).
SUMMARIES OF REPORTS OF THE ELECTROTECHNICAL LABORATORY, NO. 48 Abstract Only
Mar. 1994 48 p
(ISSN 0388-080X)
(JTN-95-80825) Avail: CASI HC A03/MF A01

The report is the collection of the abstracts of the studies carried out at the Electrotechnical Laboratory, Agency of Industrial Science and Technology, Ministry of International Trade and Industry, between 1992 and 1993. The following topics are discussed: ozone jet generator, NO2 oxidation beam source, laser, plasma, film growth, superconductors, single-crystal fibers, Josephson tunnel junctions, electron system, ion irradiation, English articles, machine translation system, speech data base, three-dimensional object, image sequences, digital optical logic operation system, robot technology, spoken dialogue understanding system, natural language conversion system, computers, antennas, solar energy applications, lithium secondary batteries, global environmental problems, energy technologies, energy consumption, lenses, superconducting magnet, amorphous silicon, spectroscopy, photoemission, thin films, ionization, back-propagation algorithm, carp retina, space robots, and solar chemical heat pump system. Author (NASDA)

N95-25200# European Space Agency. European Space Research and Technology Center, ESTEC, Noordwijk (Netherlands).
ESA BULLETIN NO. 81
Bruce Battrick, ed., Duc Guyenne, ed., and Clare Mattok, ed. Feb. 1995 108 p Original contains color illustrations
(ISSN 0376-4265)
Avail: CASI HC A06/MF A02

European space science - in retrospect and in prospect; United Nations/ESA workshops on basic space science; ESA's participation in the International Microgravity Laboratory (IML-2) mission; land-surface analysis using ERS-1 SAR interferometry; a new approach to European space standards; implementation of a communications infrastructure for remote operations; using satellites for worldwide Tele-Health and education-the GATES proposal; the ECSL summer course on space law and policy-an example of ESA's role in space-law teaching; engineering

costing techniques in ESA; a photogrammetry system for use in thermal-vacuum testing; and programs under development and operations are discussed. Derived from text

N95-26335# Executive Office of the President, Washington, DC. Office of Science and Technology Policy.

SCIENCE IN THE NATIONAL INTEREST

William J. Clinton and Albert Gore, Jr. Aug. 1994 34 p Original contains color illustrations

(ISBN-0-16-045186-8) Avail: CASI HC A03/MF A01; SOD HC

The science and technology goals for the United States are addressed in this Presidential Report. The short and long range goals, methodology, and funding for these goals are discussed and several areas in science and technology are presented: (1) GPS-based navigation systems; (2) Molecular level and genetic cancer studies; (3) Buchminsterfullerence studies; (4) Information Superhighway technology; (5) Earth monitoring systems; (6) Genetic engineering of soil bacterium; (7) MRI; (8) Computer technology - Supercomputers; (9) Light-emitting plastics; and (10) Hubble Space Telescope. CASI

Typical Subject Index Listing

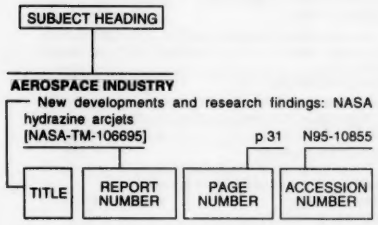

The subject heading is a key to the subject content of the document. Titles, report numbers, and accession numbers of pertinent documents are provided under each subject heading. When the title is insufficiently descriptive of the document content, a title extension is added, separated from the title by three hyphens. The report number helps to indicate the type of document cited (e.g., NASA report, NASA translation, NASA contractor report). The accession number is the number by which the document abstracts are arranged in this journal and by which the document is sold or requested. The page number helps you locate the citation in the abstract section. The titles, with title extensions if present, are arranged under each subject heading in ascending accession number order. The subject headings have been selected from the latest revision of the *NASA Thesaurus*.

A

ABEL FUNCTION
Intrinsic heights of stable varieties. Application to abelian varieties
[PB95-165577] p 2029 N95-24323

ABLATION
Experimental and theoretical study of plasma-water interaction in electrothermal guns
[DE94-628961] p 2078 N95-24706
Modeling plasma/material interactions during a tokamak disruption
[DE95-004247] p 2078 N95-24861
Results obtained using the pellet charge exchange diagnostic on TFTR
[DE95-003254] p 2079 N95-25120

ABSOLUTE ZERO
Asymptotics for the Kummer function of Bose plasmas
[DE95-607019] p 2096 N95-25428

ABSORBERS (EQUIPMENT)
Evaluation of commercial fuel tank water absorbers
[AD-A288361] p 1951 N95-25513

ABSORBERS (MATERIALS)
Distribution and nature of UV absorbers on Trition's surface
[NASA-CR-198008] p 2112 N95-26116

ABSORPTION
Staurosporine analysis and its pharmacokinetics in the blood of rats
[DE94-013857] p 2008 N95-24600

ABSORPTION SPECTRA
Temperature and dose dependence of metal colloid production in alpha-irradiated CaF2
[DE95-004907] p 2088 N95-25288
Dynamic Jahn-Teller-induced infrared absorption of a charged C60(-) molecule
[DE95-607577] p 2063 N95-25971
Distribution and nature of UV absorbers on Trition's surface
[NASA-CR-198008] p 2112 N95-26116

ABSORPTION SPECTROSCOPY
XAS studies of Ni(I), Ni(II), and Ni(III) complexes
[DE95-004844] p 1928 N95-24257
Tunable diode lasers as continuous emission monitors for thermal waste treatment processes
[DE95-004381] p 1972 N95-25549

ACCELERATION (PHYSICS)
Estimates of effects of residual acceleration on USML-1 experiments
[NASA-CR-197964] p 2084 N95-24261

ACCELERATION STRESSES (PHYSIOLOGY)
Motionsickness-seasickness: Summary of existing knowledge and suggested lines of development
[PB95-141495] p 2011 N95-24863

ACCIDENTS
The accident site portable integrated video system
[DE95-000539] p 1953 N95-24605
Cobalt release from PCA steel during possible fusion reactor accidents
[DE95-005019] p 2069 N95-25365

ACCLIMATIZATION
The effects on photosynthetic CO2 assimilation to long-term elevation of atmospheric CO2 concentration: An assessment of the response of Trifolium Repens L. CV. Blanca grown at F.A.C.E
[DE95-005687] p 2008 N95-25383

ACETYLACETONE
Effects of acetylacetone additions on PZT thin film processing
[DE95-006322] p 1941 N95-25370

ACIDS
Selective extraction of trivalent actinides from lanthanides with dithiophosphinic acids and tributylphosphate
[DE95-005249] p 1924 N95-25597

ACOUSTIC EMISSION
Emerging nondestructive inspection for aging aircraft
[PB95-143053] p 1905 N95-25401
An analysis of the feasibility of using the Hsu-Nielsen calibration method in systems for measuring acoustic emission from partial discharges
[IFTR-20/1994] p 2040 N95-26071
Measurements of acoustic emission on a laser ceramic treatment line
[IFTR-28/1994] p 2040 N95-26180

ACOUSTIC FATIGUE
Numerical simulation of the nonlinear response of composite plates under combined thermal and acoustic loading
[NASA-CR-197426] p 1981 N95-24907

ACOUSTIC FREQUENCIES
A study of the effect of voice pitch on the perception of synthetic Polish vowels
[IFTR-10/1994] p 1956 N95-26018

ACOUSTIC IMAGING
3-D seismic imaging of complex geologies
[DE95-006813] p 2004 N95-25476

ACOUSTIC LEVITATION
Stiffening of the ACES deployable space boom
p 1978 N95-26307

ACOUSTIC MEASUREMENT
An analysis of the feasibility of using the Hsu-Nielsen calibration method in systems for measuring acoustic emission from partial discharges
[IFTR-20/1994] p 2040 N95-26071

ACOUSTIC PROPAGATION
Atmospheric and terrain effects on acoustic propagation
[AD-A288727] p 2039 N95-25503

ACOUSTIC PROPERTIES
Effect of density gradients in confined supersonic shear layers, part 1
[NASA-CR-198029] p 1962 N95-24412
Effect of density gradients in confined supersonic shear layers. Part 2: 3-D modes
[NASA-CR-198030] p 1962 N95-24413
The use of acoustic surface waves to analyze gases apparatus and experiments p 2039 N95-25115

ACOUSTIC VELOCITY
Zero sound velocity in pi, rho mesons at different temperatures
[DE95-607145] p 2053 N95-25459
The phenomenon of non-linearity accompanying the action of acoustic pressure on a Helmholtz resonator
[IFTR-19/1994] p 2040 N95-26108

ACOUSTICS
Non-invasive detection of increased intracranial pressure using acoustical techniques
[AD-A279292] p 2010 N95-24309

ACRYLATES
Antioxidant and sensitizer effect on the stability of natural rubber latex vulcanized by gamma rays
[DE94-636061] p 1939 N95-24373

ACRYLONITRILES
Space shuttle propellant constitutive law verification tests
[NASA-CR-198047] p 1947 N95-24226

ACTINIDE SERIES
Selective extraction of trivalent actinides from lanthanides with dithiophosphinic acids and tributylphosphate
[DE95-005249] p 1924 N95-25597

ACTIVATION ENERGY
Study of very high temperature technology, 2
[DE95-730105] p 2088 N95-24900

ACTIVE CONTROL
Integrated passive/active vibration absorber for multi-story buildings
[NASA-TM-109178] p 1979 N95-24208
Actively controlled shaft seals for aerospace applications
[NASA-CR-198035] p 1974 N95-24218
Active weld control
[NASA-CR-196588] p 1976 N95-25595

ACTUATION
Actuating signals in adaptive control systems
[IFTR-13/1994] p 2027 N95-26330

ACTUATORS
Milli-robots for surgical teleoperation
[NASA-CR-197378] p 1974 N95-24204
The 1994 Fiber Optic Sensors for Aerospace Technology (FOSAT) Workshop
[NASA-CP-10166] p 1912 N95-24207
Tutorial on beam-based feedback systems for linacs
[DE95-006054] p 2067 N95-24573
Rotary actuator
[NASA-CASE-MFS-28581-1] p 1936 N95-25545
Actuating signals in adaptive control systems
[IFTR-13/1994] p 2027 N95-26330

ADA (PROGRAMMING LANGUAGE)
Towards a formal semantics for Ada 9X
[NASA-CR-195037] p 2020 N95-24634

ADAPTIVE CONTROL
Application of neural networks to unsteady aerodynamic control p 2024 N95-25264
Neural network technique for orbit correction in accelerators/storage rings
[DE95-005955] p 2026 N95-25368
Active weld control
[NASA-CR-196588] p 1976 N95-25595
Actuating signals in adaptive control systems
[IFTR-13/1994] p 2027 N95-26330

ADAPTIVE FILTERS
Adaptive projective filters
[DE94-628374] p 2030 N95-24645

ADDITIVES
The facility for commercial doping of silicon by thermal neutrons in channel 3 at the IBR-2
[DE94-636293] p 2085 N95-24374
Atom probe field ion microscopy of Type 308 CRE stainless steel welds
[DE94-019161] p 1938 N95-26064

ADHESIVE BONDING
Dynamic methods for determining the material characteristics of saturated permeable media
[IFTR-17/1993] p 1932 N95-26107

ADHESIVES
Development of a high temperature, high speed disc lubricant test machine
[AD-A288685] p 1977 N95-26050

ADIABATIC EQUATIONS
Quasiparticles in magnetized plasma
[DE95-607610] p 2081 N95-25632
Inelastic collisions of negative muons and hadrons with metastable hydrogen atoms
[DE95-607537] p 2056 N95-25668
ADSORPTION
Entropy and enthalpy of adsorption of gaseous chlorides of metals on quartz glass as a function of the molecular composition
[DE94-627162] p 2093 N95-24481
ADVANCED LAUNCH SYSTEM (STS)
Optimal guidance law development for an advanced launch system
[NASA-CR-4667] p 1917 N95-26205
ADVANCED TECHNOLOGY LABORATORY
STS-66 mission highlights resource tape
[NASA-TM-110550] p 1918 N95-24197
ADVANCED TEST REACTORS
Experimental and theoretical basis for advanced tokamaks
[DE95-003255] p 2077 N95-24646
AEROACOUSTICS
Effects of cavity dimensions, boundary layer, and temperature on cavity noise with emphasis on benchmark data to validate computational aeroacoustic codes
[NASA-CR-4653] p 2039 N95-24879
Noise impact of advanced high lift systems
[NASA-CR-195028] p 2040 N95-26160
Jet mixer noise suppressor using acoustic feedback
[NASA-CASE-LEW-15170-2] p 2040 N95-26187
AERODYNAMIC BALANCE
Balances for the measurement of multiple components of force in flows of a millisecond duration
p 1965 N95-25400
AERODYNAMIC CHARACTERISTICS
Performance of an aerodynamic yaw controller mounted on the space shuttle orbiter body flap at Mach 10
[NASA-TM-109179] p 1906 N95-24397
Experimental study of the effects of Reynolds number on high angle of attack aerodynamic characteristics of forebodies during rotary motion
[NASA-CR-195033] p 1907 N95-24443
Exploratory flow visualization investigation of mast-mounted sights in presence of a rotor
[NASA-TM-4634] p 1907 N95-24566
Low speed aerodynamic characteristics of delta wings with vortex flaps: 60 deg and 70 deg delta wings
[NAL-TR-1245] p 1907 N95-25105
AERODYNAMIC COEFFICIENTS
NREL airfoil families for HAWTs
[DE95-000267] p 1994 N95-24882
Measurements of longitudinal static aerodynamic coefficients by the cable mount system
[NAL-TR-1226] p 1908 N95-25761
AERODYNAMIC CONFIGURATIONS
Aerodynamic shape optimization of wing and wing-body configurations using control theory
[NASA-CR-198024] p 1911 N95-25334
Configuration and other differences between Black Hawk and Seahawk helicopters in military service in the USA and Australia
[AR-008-386] p 1911 N95-25935
AERODYNAMIC DRAG
Numerical and experimental study of drag characteristics of two-dimensional HLFC airfoils in high subsonic, high Reynolds number flow
[NAL-TR-1244T] p 1907 N95-24998
Thrust measurements of a complete axisymmetric scramjet in an impulse facility p 1914 N95-25395
A theoretical and experimental investigation of the flow over supersonic leading edge wing/body configurations
[DRA-TM-AERO-PROP-41] p 1907 N95-25649
Aerodynamic characteristics of the orbital reentry vehicle experimental probe fins in a supersonic flow
[NAL-TR-1232] p 1921 N95-25664
AERODYNAMIC HEATING
Heat transfer measurements in small scale wind tunnels
[AD-A288689] p 1915 N95-26053
AERODYNAMIC LOADS
Balances for the measurement of multiple components of force in flows of a millisecond duration
p 1965 N95-25400
AERODYNAMIC NOISE
Effects of cavity dimensions, boundary layer, and temperature on cavity noise with emphasis on benchmark data to validate computational aeroacoustic codes
[NASA-CR-4653] p 2039 N95-24879
Noise impact of advanced high lift systems
[NASA-CR-195028] p 2040 N95-26160
AERODYNAMICS
Aeronautical engineering: A continuing bibliography with indexes (supplement 316)
[NASA-SP-7037(316)] p 1905 N95-24465
Aerodynamic parameter estimation via Fourier modulating function techniques
[NASA-CR-4654] p 1911 N95-24630
Using digital filtering techniques as an aid in wind turbine data analysis
[DE94-011862] p 1993 N95-24853
Aeronautical engineering: A continuing bibliography with indexes (supplement 317)
[NASA-SP-7037(317)] p 1906 N95-25798
Cumulative reports and publications through December 31, 1994
[NASA-CR-195043] p 2014 N95-26085
AERONAUTICAL ENGINEERING
Aeronautical engineering: A continuing bibliography with indexes (supplement 316)
[NASA-SP-7037(316)] p 1905 N95-24465
JPRS report: Science and technology. Central Eurasia
[JPRS-UST-94-027] p 1957 N95-24470
JPRS report: Science and technology. Central Eurasia
[JPRS-UST-94-018] p 1950 N95-24472
Aeronautical engineering: A continuing bibliography with indexes (supplement 317)
[NASA-SP-7037(317)] p 1906 N95-25798
AERONAUTICS
NASA video catalog
[NASA-SP-7109(01)] p 2103 N95-24238
Aeronautical engineering: A continuing bibliography with indexes (supplement 316)
[NASA-SP-7037(316)] p 1905 N95-24465
AERONOMY
STEP: Satellite Test of the Equivalence Principle. Report on the phase A study
[NASA-TM-110598] p 1917 N95-26184
AEROSOLS
The atmospheric effects of stratospheric aircraft: A fourth program report
[NASA-RP-1359] p 1996 N95-24274
Microphysical and compositional influences on shortwave radiative forcing of climate by sulfate aerosols
[DE95-005999] p 1997 N95-24570
Evaluation of the performance of an annular diffusion denuder
[DE95-002258] p 1998 N95-24606
Report series in aerosol science
[DE95-737628] p 1999 N95-24904
Formation of thallium based high temperature superconductors using aerosol flow reacted precursor powders
[DE95-005901] p 2089 N95-25389
The whitehouse effect: Shortwave radiative forcing of climate by anthropogenic aerosols
[DE95-005998] p 2001 N95-25442
Effects of nitric acid vapor on the formation of cloud droplets in troposphere
[DE95-744869] p 2001 N95-25500
AEROSPACE ENGINEERING
NASA-UVA light aerospace alloy and structures technology program (LA2ST)
[NASA-CR-198041] p 1933 N95-24220
NASA video catalog
[NASA-SP-7109(01)] p 2103 N95-24238
JPRS report: Science and technology. Central Eurasia: Space
[JPRS-USP-94-008] p 1916 N95-24359
JPRS report: Science and technology. Central Eurasia
[JPRS-UST-94-035] p 2016 N95-24429
New approaches to optimization in aerospace conceptual design
[NASA-CR-196695] p 1910 N95-24436
Research in the service of the Swedish National Defence
[PB95-141941] p 1989 N95-24444
JPRS report: Science and technology. Central Eurasia
[JPRS-UST-95-009] p 1916 N95-24467
JPRS Report: Science and technology. Central Eurasia
[JPRS-UST-95-002] p 1916 N95-24621
Office of Space Science: Integrated technology strategy
[NASA-TM-110578] p 2108 N95-26183
Launch system design for access to space
p 1918 N95-26308
LH2 fuel tank design for SSTO p 1987 N95-26309
AEROSPACE ENVIRONMENTS
Go for EVA
[NASA-TM-110537] p 1918 N95-24195
Space basic
[NASA-TM-110540] p 2108 N95-24196
The natural space environment: Effects on spacecraft
[NASA-RP-1350] p 1921 N95-25875
Preliminary results of radiation measurements on EURECA p 2060 N95-25923
Journal of the Communications Research Laboratory, volume 41, number 1, March 1994
[PB95-177606] p 1956 N95-26008
AEROSPACE INDUSTRY
Actively controlled shaft seals for aerospace applications
[NASA-CR-198035] p 1974 N95-24218
AEROSPACE MEDICINE
STS-67 post flight presentation
[NASA-TM-110552] p 1918 N95-24198
Relation of motion sickness susceptibility to vestibular and behavioral measures of orientation
[NASA-CR-198048] p 2010 N95-24410
Aviation epidemiology data register
[AD-A279303] p 2010 N95-24423
Aerospace medicine and biology: A continuing bibliography with indexes (supplement 400)
[NASA-SP-7011(400)] p 2011 N95-24464
Motionsickness-seasickness: Summary of existing knowledge and suggested lines of development
[PB95-141495] p 2011 N95-24863
An assessment of aviation accident risk of aphakic civil airmen by class of medical certificate held and by age: 1982-1985
[DOT/FAA/AM-95/11] p 2011 N95-25336
Aerospace medicine and biology: A continuing bibliography with indexes (supplement 401)
[NASA-SP-7011(401)] p 2012 N95-25800
AEROSPACE PLANES
Measurements of longitudinal static aerodynamic coefficients by the cable mount system
[NAL-TR-1226] p 1908 N95-25761
AEROSPACE SAFETY
Aerospace safety advisory panel
[NASA-TM-110554] p 1920 N95-24505
AEROSPACE SCIENCES
NASA video catalog
[NASA-SP-7109(01)] p 2103 N95-24238
JPRS report: Science and technology. Central Eurasia: Space
[JPRS-USP-94-007] p 1915 N95-24358
JPRS report: Science and technology. Central Eurasia: Space
[JPRS-USP-94-008] p 1916 N95-24359
JPRS report: Science and technology. Central Eurasia
[JPRS-UST-95-009] p 1916 N95-24467
JPRS report: Science and technology. Central Eurasia. Otechestvennaya Geologiya: Studies in Aerospace and Remote Sensing
[JPRS-UST-95-004] p 1989 N95-24768
JPRS report: Science and technology. Central Eurasia: Space
[JPRS-USP-94-008] p 1916 N95-24847
ESA Bulletin No. 81 p 2114 N95-25200
AEROSPACE SYSTEMS
Applications of solid lubricant films in spacecraft
[AD-A288784] p 1947 N95-26188
AEROSPACE TECHNOLOGY TRANSFER
Office of Space Science: Integrated technology strategy
[NASA-TM-110578] p 2108 N95-26183
AEROTHERMODYNAMICS
DSMC calculations for 70-deg blunted cone at 3.2 km/s in nitrogen
[NASA-TM-109181] p 1961 N95-24396
AGE FACTOR
A longevity and survival analysis for a cohort of retired airline pilots
[DOT/FAA/AM-95/5] p 2012 N95-24237
An assessment of aviation accident risk of aphakic civil airmen by class of medical certificate held and by age: 1982-1985
[DOT/FAA/AM-95/11] p 2011 N95-25336
AGGREGATES
Adventures in the evolution of a high-bandwidth network for central servers
[DE95-006215] p 2020 N95-24597
Generation, detection and characterization of gas-phase transition metal aggregates and compounds
[DE95-004439] p 1930 N95-24686
AGING (MATERIALS)
Proceedings of the 2d USAF Aging Aircraft Conference
[AD-A288217] p 1911 N95-25578
AGRICULTURE
Clean fractionation of biomass
[DE95-000259] p 2007 N95-24307
AIR
Evaluation of the performance of an annular diffusion denuder
[DE95-002258] p 1998 N95-24606
AIR FLOW
Formation of thallium based high temperature superconductors using aerosol flow reacted precursor powders
[DE95-005901] p 2089 N95-25389

AIR LAND INTERACTIONS
Future emissions and concentrations of carbon dioxide: Key ocean/atmosphere/land analyses
[CSIRO-TP-31] p 1999 N95-25199
AIR NAVIGATION
Federal Aviation Administration plan for research, engineering and development, 1995
p 2102 N95-24202
AIR POLLUTION
The atmospheric effects of stratospheric aircraft: A fourth program report
[NASA-RP-1359] p 1996 N95-24274
Retrofit NOx control technologies for natural gas prime movers
[PB95-149290] p 1997 N95-24294
Responsibility means doing without: How to rescue the ozone-layer
[PB95-166807] p 1997 N95-24334
Optimized hydrogen piston engines
[DE95-003656] p 1975 N95-24550
Diesel fuel component contribution to engine emissions and performance
[DE95-000238] p 1998 N95-24604
Methods of valuing air pollution and estimated monetary values of air pollutants in various US regions
[DE95-006854] p 1998 N95-24618
Brayton-cycle solvent recovery heat pump. A technical brief
[DE94-000225] p 1991 N95-24666
Report series in aerosol science
[DE95-737628] p 1999 N95-24904
Spray characteristics of single- and three-hole nozzle injectors in ambient air and in a motored single-cylinder test engine
[PB95-166286] p 1976 N95-25574
Draft regulatory impact analysis: Control of air pollution emission standards for new nonroad spark-ignition marine engines
[PB95-166294] p 2001 N95-25575
Nuclear energy and the environment
[DE95-600438] p 2001 N95-25615
Carbon taxes and India
[DE95-005401] p 2001 N95-25629
Nitrogen oxide emissions and their control from uninstalled aircraft engines in enclosed test cells: Joint report to Congress on the Environmental Protection Agency - Department of Transportation study
[PB95-166237] p 2002 N95-26005
Disposal of electronic equipment
[PB95-177861] p 2002 N95-26047
Sector-specific issues and reporting methodologies supporting the general guidelines for the voluntary reporting of greenhouse gases under Section 1605(b) of the Energy Policy Act of 1992, Volume 2. Part 4: Transportation sector. Part 5: Forestry sector. Part 6: Agricultural sector
[DE95-003297] p 2003 N95-26065
Cross-flow, filter-sorbent-catalyst for particulate, SO2 and NO(x) control
[DE95-001934] p 2003 N95-26091
AIR QUALITY
Resolving the ambiguities: An industrial hygiene Indoor Air Quality (IAQ) symposium
[DE95-005391] p 2000 N95-25380
Nitrogen oxide emissions and their control from uninstalled aircraft engines in enclosed test cells: Joint report to Congress on the Environmental Protection Agency - Department of Transportation study
[PB95-166237] p 2002 N95-26005
AIR SAMPLING
Evaluation of the performance of an annular diffusion denuder
[DE95-002258] p 1998 N95-24606
AIR TRAFFIC
Aviation system capacity improvements through technology
[NASA-TM-109165] p 1909 N95-24633
AIR TRAFFIC CONTROL
Federal Aviation Administration plan for research, engineering and development, 1995
p 2102 N95-24202
Aviation system capacity improvements through technology
[NASA-TM-109165] p 1909 N95-24633
AIR TRAFFIC CONTROLLERS (PERSONNEL)
Sleep patterns in air traffic controllers working rapidly rotating shifts: A field study
[DOT/FAA/AM-95/12] p 2012 N95-26204
AIR TRANSPORTATION
Federal Aviation Administration plan for research, engineering and development, 1995
p 2102 N95-24202
Aviation system capacity improvements through technology
[NASA-TM-109165] p 1909 N95-24633
AIR WATER INTERACTIONS
Future emissions and concentrations of carbon dioxide: Key ocean/atmosphere/land analyses
[CSIRO-TP-31] p 1999 N95-25199
AIRBORNE EQUIPMENT
Use of voronoi diagrams for qualitative matching
[PB95-165445] p 1988 N95-24240
Airborne imaging of tropospheric emission at millimeter and submillimeter wavelengths
[NASA-TM-110498] p 2003 N95-24336
Replicator for characterization of cirrus and polar stratospheric cloud particles
[NASA-CR-197992] p 2005 N95-24411
AIRBORNE LASERS
Use of voronoi diagrams for qualitative matching
[PB95-165445] p 1988 N95-24240
AIRBORNE RADAR
Analysis of data from a radar warning receiver with the accent on association of sensor reports
[PB95-141768] p 1953 N95-24836
AIRBORNE/SPACEBORNE COMPUTERS
Missileborne Artificial Vision System (MAVIS)
p 2022 N95-25254
AIRCRAFT ACCIDENT INVESTIGATION
Aircraft accident report: Impact with blast fence upon landing rollout Action Air Charters flight 990 Piper PA-31-350, N990RA, Stratford, Connecticut,27 April 1994
[PB94-910410] p 1908 N95-24206
AIRCRAFT ACCIDENTS
Aircraft accident report: Impact with blast fence upon landing rollout Action Air Charters flight 990 Piper PA-31-350, N990RA, Stratford, Connecticut,27 April 1994
[PB94-910410] p 1908 N95-24206
An assessment of aviation accident risk of aphakic civil airmen by class of medical certificate held and by age: 1982-1985
[DOT/FAA/AM-95/11] p 2011 N95-25336
AIRCRAFT APPROACH SPACING
Characterizing the wake vortex signature for an active line of sight remote sensor
[NASA-CR-197697] p 1909 N95-24391
AIRCRAFT CONFIGURATIONS
Aerodynamics model for a generic ASTOVL lift-fan aircraft
[NASA-TM-110347] p 1908 N95-26302
AIRCRAFT CONSTRUCTION MATERIALS
NASA-UVa light aerospace alloy and structures technology program supplement: Aluminum-based materials for high speed aircraft
[NASA-CR-4645] p 1935 N95-24878
Investigation into the flammability properties of honeycomb composites
[PB95-143293] p 1941 N95-25342
Jet engine applications for materials with nanometer-scale dimensions p 1945 N95-26131
AIRCRAFT CONTROL
Application of neural networks to unsteady aerodynamic control p 2024 N95-25264
AIRCRAFT DESIGN
NASA video catalog
[NASA-SP-7109(01)] p 2103 N95-24238
Advanced subsonic airplane design and economic studies
[NASA-CR-195443] p 1913 N95-24304
A crew-centered flight deck design philosophy for High-Speed Civil Transport (HSCT) aircraft
[NASA-TM-109171] p 1910 N95-24582
Geometric analysis of wing sections
[NASA-TM-110346] p 1910 N95-24629
Aerodynamic shape optimization of wing and wing-body configurations using control theory
[NASA-CR-198024] p 1911 N95-25334
The coupling of fluids, dynamics, and controls on advanced architecture computers
[NASA-CR-197727] p 2017 N95-25797
A quiet STOL Research Aircraft Development program
[NAL-TR-1223] p 1911 N95-25862
Noise impact of advanced high lift systems
[NASA-CR-195028] p 2040 N95-26160
Aerodynamics model for a generic ASTOVL lift-fan aircraft
[NASA-TM-110347] p 1908 N95-26302
AIRCRAFT DETECTION
Visual contrast detection thresholds for aircraft contrails
[AD-A288618] p 1905 N95-25607
Orientation determination of aircraft using visual 3D matching and radar. Case study 2
[PB95-165791] p 1955 N95-25749
AIRCRAFT ENGINES
The effect of altitude conditions on the particle emissions of a J85-GE-5L turbojet engine
[NASA-TM-106669] p 1914 N95-24561
Bird ingestion into large turbofan engines
[DOT/FAA/CT-93/14] p 1909 N95-24631
Nitrogen oxide emissions and their control from uninstalled aircraft engines in enclosed test cells: Joint report to Congress on the Environmental Protection Agency - Department of Transportation study
[PB95-166237] p 2002 N95-26005
Thermal Barrier Coating Workshop
[NASA-CP-10170] p 1943 N95-26119
Thermal barrier coatings for aircraft engines: History and directions p 1943 N95-26121
Thermal barrier coatings issues in advanced land-based gas turbines p 1944 N95-26122
PVD TBC experience on GE aircraft engines
p 1944 N95-26126
Thermal barrier coating life modeling in aircraft gas turbine engines p 1947 N95-26140
AIRCRAFT EQUIPMENT
Analysis of warping effects on the static and dynamic response of a seat-type structure
[NIAR-94-12] p 1979 N95-24211
AIRCRAFT GUIDANCE
How to fly an aircraft with control theory and splines
p 2027 N95-25805
AIRCRAFT HAZARDS
Characterizing the wake vortex signature for an active line of sight remote sensor
[NASA-CR-197697] p 1909 N95-24391
Consistent approach to describing aircraft HIRF protection
[NASA-CR-195067] p 1909 N95-25341
AIRCRAFT LANDING
Aircraft accident report: Impact with blast fence upon landing rollout Action Air Charters flight 990 Piper PA-31-350, N990RA, Stratford, Connecticut,27 April 1994
[PB94-910410] p 1908 N95-24206
Characterizing the wake vortex signature for an active line of sight remote sensor
[NASA-CR-197697] p 1909 N95-24391
AIRCRAFT MAINTENANCE
An overview of Health and Usage Monitoring Systems (HUMS) for military helicopters
[DSTO-TR-0061] p 1905 N95-24200
Helicopter life substantiation: Review of some USA and UK initiatives
[DSTO-TR-0062] p 1905 N95-24201
Estimate of probability of crack detection from service difficulty report data
[PB95-149381] p 1905 N95-24295
Emerging nondestructive inspection for aging aircraft
[PB95-143053] p 1905 N95-25401
Proceedings of the 2d USAF Aging Aircraft Conference
[AD-A288217] p 1911 N95-25578
AIRCRAFT MODELS
Aspect estimation of an aircraft using library model silhouettes
[PB95-141834] p 2036 N95-25894
AIRCRAFT NOISE
Aviation system capacity improvements through technology
[NASA-TM-109165] p 1909 N95-24633
AIRCRAFT PARTS
JPRS report: Science and technology. Central Eurasia
[JPRS-UST-95-011] p 1910 N95-24541
AIRCRAFT PILOTS
A longevity and survival analysis for a cohort of retired airline pilots
[DOT/FAA/AM-95/5] p 2012 N95-24237
Aviation epidemiology data register
[AD-A279303] p 2010 N95-24423
Visual contrast detection thresholds for aircraft contrails
[AD-A288618] p 1905 N95-25607
AIRCRAFT PRODUCTION
Report to Congressional Committees. Tactical Aircraft: Concurrency in development and production of F-22 aircraft should be reduced
[GAO/NSIAD-95-59] p 1911 N95-26338
AIRCRAFT SAFETY
Federal Aviation Administration plan for research, engineering and development, 1995
p 2102 N95-24202
Development of an intervention program to encourage shoulder harness use and aircraft retrofit in general aviation aircraft, phases 1 and 2
[DOT/FAA/AM-95/2] p 1909 N95-24384
Quantity-distance requirements for earth-bermed aircraft shelters
[AD-A279692] p 1915 N95-24424
Bird ingestion into large turbofan engines
[DOT/FAA/CT-93/14] p 1909 N95-24631

AIRCRAFT STRUCTURES
NASA-UVA light aerospace alloy and structures technology program (LA2ST)
[NASA-CR-198041] p 1933 N95-24220
JPRS report: Science and technology. Central Eurasia
[JPRS-UST-95-011] p 1910 N95-24541
Proceedings of the 2d USAF Aging Aircraft Conference
[AD-A288217] p 1911 N95-25578
Design and evaluation of a foam-filled hat-stiffened panel concept for aircraft primary structural applications
[NASA-TM-109175] p 1928 N95-26251
AIRCRAFT WAKES
Three-dimensional interaction of wake/boundary-layer and vortex/boundary-layer data report
[CUED/A-AEREO/TR-23] p 1906 N95-24210
Characterizing the wake vortex signature for an active line of sight remote sensor
[NASA-CR-197697] p 1909 N95-24391
AIRFOIL PROFILES
Geometric analysis of wing sections
[NASA-TM-110346] p 1910 N95-24629
AIRFOILS
NREL airfoil families for HAWTs
[DE95-000267] p 1994 N95-24882
Wind technology development: Large and small turbines
[DE95-000286] p 1995 N95-26090
Thermal barrier coatings for aircraft engines: History and directions p 1943 N95-26121
AIRFRAMES
Advanced subsonic airplane design and economic studies
[NASA-CR-195443] p 1913 N95-24304
AIRPORT SECURITY
Federal Aviation Administration plan for research, engineering and development, 1995
p 2102 N95-24202
AIRPORTS
Federal Aviation Administration plan for research, engineering and development, 1995
p 2102 N95-24202
Aviation system capacity improvements through technology
[NASA-TM-109165] p 1909 N95-24633
AIRSHIPS
Long endurance stratospheric solar powered airship
[PB95-178729] p 1911 N95-26009
AIRSPACE
Aviation system capacity improvements through technology
[NASA-TM-109165] p 1909 N95-24633
ALGEBRA
Anionic construction of the sl(sub q, s)(2) algebra
[DE95-600838] p 2043 N95-24350
Quantum group gauge theories and covariant quantum algebras
[DE94-628524] p 2094 N95-24509
Central extension of a new W(infinity)-type algebra
[DE95-607086] p 2037 N95-25599
Singularly perturbed differential/algebraic equations
[AD-A288365] p 2033 N95-25601
On the Cohen-Macaulayness and Gorensteinness of integral closure filtrations Rees algebras of height-two equimultiple ideals
[DE95-607000] p 2034 N95-25989
The criteria for the Cohen-Macaulayness and Gorensteiness of Rees algebras of ideals having positive analytic deviation
[DE95-607003] p 2034 N95-25992
ALGORITHMS
Performance issues for iterative solvers in device simulation
[NASA-CR-197952] p 2027 N95-24214
Implementation of a parallel algorithm for thermo-chemical nonequilibrium flow simulations
[DE95-004758] p 1961 N95-24262
A parallel, portable and versatile treecode
[DE95-000842] p 2019 N95-24343
Parallel algorithms for dynamically partitioning unstructured grids
[DE95-001616] p 2015 N95-24346
SYSINT(SYSINTM)-program complex for numerical solution of the eigenvalue problem for system of integral equations
[DE94-636729] p 2029 N95-24375
Separation analysis, a tool for analyzing multigrid algorithms
[NASA-CR-195036] p 2029 N95-24389
Ice surface temperature retrieval from AVHRR, ATSR, and passive microwave satellite data: Algorithm development and application
[NASA-CR-198037] p 1989 N95-24441
The 24th Order high temperature expansion for the 3-D Ising model
[DE95-004952] p 2093 N95-24450
Software of a distributor of high voltage of the H C-600 hadronic calorimeter
[DE94-628255] p 1967 N95-24486
A tool for debugging internet multicast routing
[DE95-003433] p 2020 N95-24496
Passive microwave algorithm development and evaluation
[NASA-CR-197915] p 2005 N95-24535
Visibility ordering meshed polyhedra
[CSRD-1097] p 2030 N95-24557
Aerodynamic parameter estimation via Fourier modulating function techniques
[NASA-CR-4654] p 1911 N95-24630
Oscillator poly spheroidal functions
[DE94-628440] p 2030 N95-24636
Adaptive projective filters
[DE94-628374] p 2030 N95-24645
Introduction to the Monte Carlo methods
[DE94-628386] p 2035 N95-24693
A higher-order projection method for the simulation of unsteady turbulent nonpremixed combustion in an industrial burner
[DE95-005919] p 1931 N95-25291
Fast algorithms for transport models
[DE95-007064] p 2054 N95-25479
Numerical and symbolic algorithms for application specific signal processing
[AD-A288202] p 2017 N95-25507
On the numerical method for analysis of the dynamics of the classical Hamiltonian systems
[DE95-605218] p 2034 N95-25906
Numerical solution of the optimized random phase approximation
[DE95-605636] p 2034 N95-25982
Flexible architectures for sensor fusion in theater missile defense
[AD-A288666] p 2007 N95-26048
Splines in two-dimensional problems
[IFTR-2/1993] p 2035 N95-26106
CMM functional software evaluation (algorithm qualification)
[DE95-006178] p 2018 N95-26167
On convergence of the Nelder-Mead simplex algorithm for unconstrained stochastic optimization
[AD-A289453] p 2006 N95-26197
Optimal guidance law development for an advanced launch system
[NASA-CR-4667] p 1917 N95-26205
Numerical simulation of laminar flow in a curved duct
[DE95-005427] p 1966 N95-26240
ALKALIES
A study of the electrochemical behavior of tungsten in caustic solutions and platinum/iridium in ch loride solutions
[DE95-004951] p 1930 N95-25123
ALKANES
Pulse radiolysis of alkanes: A time-resolved electron paramagnetic resonance study
[DE95-005831] p 2045 N95-24459
ALKYL COMPOUNDS
Pulse radiolysis of alkanes: A time-resolved electron paramagnetic resonance study
[DE95-005831] p 2045 N95-24459
ALKYNES
The transformation of organic amines by transition metal cluster compounds
[DE95-004180] p 1923 N95-24851
ALPHA PARTICLES
Results obtained using the pellet charge exchange diagnostic on TFTR
[DE95-003254] p 2079 N95-25120
Energetic particle drive for toroidicity-induced Alfven eigenmodes and kinetic toroidicity-induced Alfven eigenmodes in a low-shear Tokamak
[DE95-003222] p 2079 N95-25216
ALTERNATIVES
Alternatives to traditional transportation fuels 1993
[DE95-005445] p 1947 N95-24273
ALTITUDE SICKNESS
Non-invasive detection of increased intracranial pressure using acoustical techniques
[AD-A279292] p 2010 N95-24309
ALTITUDE TESTS
The effect of altitude conditions on the particle emissions of a J85-GE-5L turbojet engine
[NASA-TM-106669] p 1914 N95-24561
ALUMINIDES
Synthesis of Ni3Al and NiAl intermetallics
[DE95-005897] p 1934 N95-24433
Localized corrosion and stress corrosion cracking characteristics of a low-aluminum-content iron-aluminum alloy
[DE95-003259] p 1934 N95-24647
Strengthening of NiAl matrix composites
[AD-A288923] p 1926 N95-25505
Stability and elastic properties of hydrogen loaded Ti(1-x)Al(x) alloys: An ab initio study
[AD-A288903] p 1936 N95-25529
Atomistic studies of grain boundaries in NiAl
[DE95-005208] p 1937 N95-26014
ALUMINUM
Characterization of ultradispersed aluminum
[DE95-006379] p 1933 N95-24329
Ignition of exploding aluminum droplets behind shock waves in water
[DE95-003975] p 1963 N95-24678
Decay of a laser generated shock wave in an aluminium target
[DE94-629014] p 1972 N95-24707
Synthesis and processing of Al2O3/Al composites by in situ reaction of aluminum and mullite
[DE95-006224] p 1937 N95-25775
ALUMINUM ALLOYS
The temperature and strain rate dependence of the flow stress of single crystal NiAl deformed along the zone group axes (110)
[DE95-003634] p 2083 N95-24233
Synthesis of Ni3Al and NiAl intermetallics
[DE95-005897] p 1934 N95-24433
Localized corrosion and stress corrosion cracking characteristics of a low-aluminum-content iron-aluminum alloy
[DE95-003259] p 1934 N95-24647
NASA-UVa light aerospace alloy and structures technology program supplement: Aluminum-based materials for high speed aircraft
[NASA-CR-4645] p 1935 N95-24878
The geometry of disorder: Theoretical investigations of quasicrystals and frustrated magnets
[DE95-006641] p 1936 N95-25560
A description of the cyclical properties of an aluminum alloy based on complex stress state tests
[IFTR-29/1994] p 1936 N95-25638
Atomistic studies of grain boundaries in NiAl
[DE95-005208] p 1937 N95-26014
ALUMINUM GALLIUM ARSENIDES
Optical determinations of energy-band dispersion curves in novel compound semiconductor materials
[DE95-006318] p 2089 N95-25353
ALUMINUM NITRIDES
Oxidation of ion-implanted NiAl
[DE95-005899] p 1935 N95-25388
ALUMINUM OXIDES
Au/Cr sputter coating for the protection of alumina during sliding at high temperatures
[NASA-TM-106853] p 1923 N95-24437
High octane ethers from synthesis gas-derived alcohols
[DE95-001146] p 1948 N95-24655
Processing and characterization of transformation-toughened ceramics with strength retention to elevated temperatures
[DE95-005758] p 1941 N95-25387
Strengthening of NiAl matrix composites
[AD-A288923] p 1926 N95-25505
Temperature-dependent growth of LaAlO3 films on YBa2CuO7 C-axis films for multilayer structures
[DE95-005257] p 2089 N95-25598
Synthesis and processing of Al2O3/Al composites by in situ reaction of aluminum and mullite
[DE95-006224] p 1937 N95-25775
LuAlO3: A high density, high speed scintillator for gamma detection
[DE95-004678] p 2064 N95-26256
AMBIGUITY
Resolving the ambiguities: An industrial hygiene Indoor Air Quality (IAQ) symposium
[DE95-005391] p 2000 N95-25380
AMINES
Simple chemical assays for presence of S2F10 in decomposed SF6
[DE95-001423] p 1929 N95-24345
The transformation of organic amines by transition metal cluster compounds
[DE95-004180] p 1923 N95-24851
AMINO ACIDS
Genetic and biophysical studies of the photosynthetic reaction center
[DE95-004179] p 2008 N95-24850
AMMONIA
Development of novel active transport membrane devices
[DE95-002658] p 1932 N95-26093
AMMONIUM COMPOUNDS
Effect of He pressure on the superconducting transition temperatures of Na2CsC60 and (NH3)4Na2CsC60
[DE95-006320] p 2087 N95-24616
AMORPHOUS MATERIALS
A solubility model for amorphous silica in concentrated electrolytes
[DE95-004896] p 1931 N95-25252

Proceedings of the Workshop on Dynamics and Structure of Disordered System
[DE94-792685] p 1931 N95-25356
Reciprocal space analysis of the microstructure of luminescent and nonluminescent porous silicon films
[DE95-005420] p 1941 N95-25382
In situ XAFS study of oxides formed on nickel thin film electrodes in KOH solution
[AD-A288735] p 1932 N95-26056

AMORPHOUS SILICON
Technical evaluation of a dual-junction same-band-gap amorphous silicon photovoltaic system at NREL
[DE95-000277] p 1996 N95-26285

AMPLIFICATION
Simulation study of tapered FEL amplifiers in Raman and Compton regimes
[DE94-785266] p 1971 N95-24340

AMPLIFIER DESIGN
Experimental and theoretical development towards a 500 MW, one-microsecond, L-band relativistic klystron amplifier
[DE95-003682] p 1958 N95-24589

AMPLIFIERS
Simulation study of tapered FEL amplifiers in Raman and Compton regimes
[DE94-785266] p 1971 N95-24340

AMPLITUDE MODULATION
Continuous phase and amplitude holographic elements
[NASA-CASE-NPO-18791-1] p 1971 N95-26340

ANALOG SIMULATION
New techniques to test fatigue properties of coined sheet specimens. Part 4: Development of experimental techniques
[PB95-165130] p 1982 N95-25445

ANALOG TO DIGITAL CONVERTERS
The impact of multiplexing on the dynamic requirements of analog-to-digital converters
[DE95-006302] p 1960 N95-25558

ANALOGS
Quantum symplectic geometry. 1: The matrix Hamiltonian formalism
[DE95-607009] p 2032 N95-25427

ANALYZING
Closed orbit related problems: Correction, feedback, and analysis
[DE95-005969] p 2070 N95-25441

ANGLE OF ATTACK
Experimental study of the effects of Reynolds number on high angle of attack aerodynamic characteristics of forebodies during rotary motion
[NASA-CR-195033] p 1907 N95-24443

ANGULAR CORRELATION
Angular displacement measuring device
[NASA-CASE-ARC-11937-1] p 2074 N95-26015

ANGULAR DISTRIBUTION
KORP-1: A program for calculating the direct (n, p) or (p, n) reaction by using DWBA method
[DE94-628768] p 2049 N95-24724
Study of properties of Ne - Al neutron rich isotopes at and near N = 20 magic shell using elastic scattering in inverse kinematics
[DE94-628655] p 2055 N95-25538

ANGULAR MOMENTUM
The determination of the main parameters of the backward spectrometer of the 0(sup 0) facility
[DE94-628385] p 2048 N95-24692
Matrix element and complex l-plane evaluation of two-loop vacuum amplitudes in QED on S4
[DE95-607099] p 2097 N95-25473

ANIMALS
Interaction mechanisms and biological effects of static magnetic fields
[DE95-004929] p 2009 N95-26169

ANIONS
Anionic construction of the sl(sub q, s)(2) algebra
[DE95-600838] p 2043 N95-24350
Study of radicals, clusters and transition state species by anion photoelectron spectroscopy
[DE95-003438] p 2045 N95-24533
Group transfer and electron transfer reactions of organometallic complexes
[DE95-003732] p 2050 N95-25112

ANISOTROPY
Temperature dependence of magnetic anisotropy and magnetostriction: Beyond the mean-field theory
[DE94-634529] p 2084 N95-24244
Tachyon condensates and anisotropic universe
[DE95-607074] p 2097 N95-25456
Anisotropy of dilepton emission from nuclear collisions
[DE95-004354] p 2070 N95-25634
Homogeneous anisotropic cosmological models in the minimum quadratic Poincare gauge theory of gravity
[DE95-607083] p 2110 N95-25647
On analysis of resonance neutron depolarization in uniaxial media
[DE95-703782] p 2057 N95-25669
On fractal structure of quantum gravity and relic radiation anisotropy
[DE95-605306] p 2099 N95-25966

ANNEALING
Copper transport on oxygen annealing of a superconducting film Y-Ba-Cu-O
[DE94-627566] p 2086 N95-24537
Pulsed laser annealing of P implanted diamond
[DE95-605947] p 2090 N95-25985

ANNIHILATION REACTIONS
Fractal studies on the positron annihilation in metals
[DE94-634488] p 2041 N95-24232
The left-right forward-backward asymmetry of heavy quarks measured with jet charge and with leptons at the SLD
[DE95-006145] p 2046 N95-24593
A study of K(sub s) (lambda) and (bar (lambda)) production in hadronic Z(sup 0) decays
[DE95-004280] p 2047 N95-24660
Annihilation diagrams in two-body nonleptonic decays of charmed mesons
[DE95-607181] p 2054 N95-25463
Quasi two body decays of charm mesons
[DE94-792634] p 2057 N95-25901

ANNOTATIONS
An annotation system for 3D fluid flow visualization
p 1966 N95-25869

ANNUAL VARIATIONS
Assessment of climate variability of the Greenland ice sheet: Integration of in situ and satellite data
[NASA-CR-198020] p 1998 N95-24846

ANNULAR FLOW
Studies of two-phase gas-liquid flow in microgravity
[NASA-CR-195434] p 1963 N95-24906

ANODES
Recent advances in lithium ion technology
[DE95-004769] p 2054 N95-25470

ANODIZING
Non-destructive characterization of porous silicon using x ray reflectivity
[DE95-004766] p 1942 N95-25898

ANOMALIES
The off-shell axial anomaly via the (gamma)*(pi)(sup 0) (yields) (gamma) transition
[DE95-004762] p 2057 N95-25896
Flexible architectures for sensor fusion in theater missile defense
[AD-A288666] p 2007 N95-26048

ANTARCTIC REGIONS
Ice surface temperature retrieval from AVHRR, ATSR, and passive microwave satellite data: Algorithm development and application
[NASA-CR-198037] p 1989 N95-24441

ANTENNA ARRAYS
Broadband uniplanar microstrip to slot-line transitions
[NASA-CR-195448] p 1957 N95-24476

ANTENNA COMPONENTS
Experimental study of tapered slot elements
[PB95-165163] p 1955 N95-25644

ANTENNA DESIGN
A satellite-tracking millimeter-wave reflector antenna system for mobile satellite-tracking
[NASA-CASE-NPO-18772-1-CU] p 1954 N95-25316
The effects of the environment on an experimental VHF radio Direction Finding antenna system
[AD-A288791] p 1956 N95-26191

ANTENNAS
Hidden Markov models and neural networks for fault detection in dynamic systems p 2024 N95-25261

ANTIFERROMAGNETISM
Spin correlations in percolating networks with fractal geometry
[DE95-001074] p 2037 N95-24479
Staggered magnetization in the Heisenberg antiferromagnet
[DE95-607102] p 2038 N95-25458

ANTINEUTRINOS
Search for the prompt muon antineutrino from charm particle decays at the IHEP-JINR Neutrino detector in 70 GeV proton beam-dump experiment
[DE94-628772] p 2049 N95-24889

ANTIOXIDANTS
Antioxidant and sensitizer effect on the stability of natural rubber latex vulcanized by gamma rays
[DE94-636061] p 1939 N95-24373

ANTIPARTICLES
The existence of antiparticles seems to forbid violations of statistics
[DE94-628523] p 2050 N95-25094

ANTIPROTONS
Theoretical motivation for gravitation experiments on ultra-low energy antiprotons and antihydrogen
[DE95-003662] p 2091 N95-24235
The emission of particle identification efficiency in the EXCHARM experiment
[DE94-628258] p 2047 N95-24644
Evidence for top quark production in 1.8 TeV p-bar p collisions
[DE95-003496] p 2068 N95-24728
Photon-charm production in p(anti p) collisions at radical s = 1.8 TeV
[DE95-004850] p 2052 N95-25377
A search for t(anti t) (yields) lepton + E(sub T) + jets signature in p(anti p) collisions at (radical)s = 1.8 TeV with the DO detector
[DE95-004239] p 2052 N95-25402

ANTIREFLECTION COATINGS
Spacecraft materials studies on The Aerospace Corporation Tray on EOIM-3
[AD-A288682] p 1942 N95-26049

APOGEE BOOST MOTORS
Development test of a liquid apogee engine for the ETS-4
[NAL-TR-1250] p 1922 N95-24999

APOLLO 12 FLIGHT
Apollo 12: Pinpoint for science
[NASA-TM-110576] p 1917 N95-25424

APOLLO 13 FLIGHT
Apollo 13: Houston, we've got a problem
[NASA-TM-110551] p 1918 N95-24215

APPLICATION SPECIFIC INTEGRATED CIRCUITS
ASIC implementation of a data-push architecture for silicon pixel readout
[DE95-003368] p 2015 N95-24648

APPLICATIONS OF MATHEMATICS
On corrections to the Nambu action
[NASA-CR-197625] p 2065 N95-24335
Cumulative reports and publications through December 31, 1994
[NASA-CR-195043] p 2014 N95-26085

APPLICATIONS PROGRAMS (COMPUTERS)
Structure and manual of radioisotope-production data base, ISOP
[DE94-785197] p 2043 N95-24337
Thermohydrodynamic analysis of cryogenic liquid turbulent flow fluid film bearings, phase 2
[NASA-CR-197412] p 1962 N95-24461
Software engineering and data management for automated payload experiment tool
[NASA-CR-196562] p 2104 N95-24477
Integration of design, structural, thermal and optical analysis: And user's guide for structural-to-optical translator (PATCOD)
[NASA-TM-110153] p 1950 N95-24559
A practical approach to portability and performance problems on massively parallel supercomputers
[DE95-005251] p 2020 N95-24612
Information management architecture for an integrated computing environment for the Environmental Restoration Program. Environmental Restoration Program, Volume 3: Interim technical architecture
[DE95-001386] p 2105 N95-24656
ASYS2: A new version of computer algebra package ASYS for analysis and simplification of polynomial systems
[DE94-628384] p 2030 N95-24691
Software engineering and data management for automated payload experiment tool
[NASA-CR-197703] p 2016 N95-24876
Benchmark testing and independent verification of the VS2DT computer code
[DE95-004386] p 1965 N95-25485
An FEL design code running on Mathcad(trademark)
[DE95-005279] p 1973 N95-25565
User's manual for FAROW: Fatigue and reliability of wind turbine components, version 1.1
[DE95-005530] p 1995 N95-26037
CMM functional software evaluation (algorithm qualification)
[DE95-006178] p 2018 N95-26167

APPROACH INDICATORS
Flight reference display for powered-lift STOL aircraft
[NAL-TR-1251] p 1912 N95-25005

APPROXIMATION
Finite quantum physics and noncommutative geometry
[DE94-634282] p 2027 N95-24228
The method of space-time conservation element and solution element: Development of a new implicit solver
[NASA-TM-106897] p 2029 N95-24474
Saddle-point method in path integrals
[DE94-628379] p 2036 N95-24688
Elastic form factors of hydrogen-like atoms in nS-states
[DE94-628437] p 2048 N95-24700
Exponentially accurate approximations to piece-wise smooth periodic functions
[NASA-CR-195059] p 2031 N95-24856

Numerical and symbolic algorithms for application specific signal processing
[AD-A288202] p 2017 N95-25507
Splines and control theory p 2026 N95-25802

AQUEOUS SOLUTIONS
Determination of trace elements in plutonium by solvent extraction and ICP-atomic emission spectrometry
[DE94-634887] p 2042 N95-24269
Cesium cobaltdicarbollide-solubility, precipitation, and reactivity in basic aqueous solution
[DE95-005881] p 1929 N95-24430
Experimental and theoretical study of plasma-water interaction in electrothermal guns
[DE94-628961] p 2078 N95-24706
A solubility model for amorphous silica in concentrated electrolytes
[DE95-004896] p 1931 N95-25252

AQUIFERS
Long-Term Flow Test number 1: Roosevelt Hot Springs, Utah
[DE95-004995] p 2004 N95-25666

ARCHITECTURE (COMPUTERS)
Workflow automation architecture standard
[DE95-004748] p 2035 N95-24248
DOLIB: Distributed Object Library
[DE95-004791] p 2019 N95-24250
Outline of fast analyzer for MHD equilibrium FAME
[DE94-777540] p 2076 N95-24311
ASIC implementation of a data-push architecture for silicon pixel readout
[DE95-003368] p 2015 N95-24648
Information management architecture for an integrated computing environment for the Environmental Restoration Program. Environmental Restoration Program, Volume 3: Interim technical architecture
[DE95-001386] p 2105 N95-24656
Proceedings of the 1994 Conference on Computing in Energy Physics
[DE95-004442] p 2068 N95-24665
VLSI neuroprocessors p 2023 N95-25258
Three-D Artificial Neural Network (3DANN) technology. Blueprint for the future p 2024 N95-25260
Proceedings of workshop on Future in HEP Computing
[DE94-792684] p 2021 N95-25303
Designing a stencil compiler for the Connection Machine model CM-5
[DE95-006861] p 2021 N95-25477
Design of Fusion Safety Data Base
[DE95-703897] p 2080 N95-25495
Naval network security requirements analysis
[AD-A288692] p 2022 N95-26054
Design documentation for the SINTRA preprocessor
[AD-A288804] p 2015 N95-26192

ARCTIC REGIONS
Ice surface temperature retrieval from AVHRR, ATSR, and passive microwave satellite data: Algorithm development and application
[NASA-CR-198037] p 1989 N95-24441

ARGON ISOTOPES
Multiplicities of secondaries in nuclear interactions, induced by Ne-20, Ar-40 and Fe-56 nuclei at 0.1-0.5 GeV/nucleon p 2060 N95-25920

ARTIFICIAL INTELLIGENCE
Study of composite zirconium oxide
[DE95-730104] p 1926 N95-25111
Innovation and application of ANN in Europe demonstrated by Kohonen maps p 2024 N95-25262
Grounding explanations in evolving, diagnostic situations
[NASA-CR-198027] p 2026 N95-25335
Proceedings of the 4th IEEE Workshop on Neural Networks for Signal Processing
[AD-A288383] p 2026 N95-25603
Instructable autonomous agents
[NASA-CR-197802] p 2019 N95-26206
Center for Computational Structures Technology
[NASA-CR-198028] p 1983 N95-26263

ARTIFICIAL SATELLITES
Small spacecraft power and thermal subsystems
[NASA-CR-195029] p 1921 N95-24216
JPRS report: Science and technology. Central Eurasia
[JPRS-UST-95-010] p 1953 N95-24539

ASCENT TRAJECTORIES
Optimal guidance law development for an advanced launch system
[NASA-CR-4667] p 1917 N95-26205

ASPECT RATIO
Formation of thallium based high temperature superconductors using aerosol flow reacted precursor powders
[DE95-005901] p 2089 N95-25389

ASSAYING
Simple chemical assays for presence of S2F10 in decomposed SF6
[DE95-001423] p 1929 N95-24345

ASSIMILATION
The effects on photosynthetic CO2 assimilation to long-term elevation of atmospheric CO2 concentration: An assessment of the response of Trifolium Repens L. CV. Blanca grown at F.A.C.E
[DE95-005687] p 2008 N95-25383

ASTEROIDS
The whistler-mode bow wave of an asteroid
[U-OF-IOWA-95-2] p 2111 N95-26195

ASTRODYNAMICS
Rich cluster simulation: Dynamics and mass estimates
[DE95-005233] p 2110 N95-25766

ASTRONAUTICS
NASA video catalog
[NASA-SP-7109(01)] p 2103 N95-24238

ASTRONOMICAL MODELS
Creation and development of the Universe (symmetry approach)
[DE94-628558] p 2109 N95-24884
Possible constraints on SUSY-model parameters from direct dark matter search
[DE94-628561] p 2109 N95-24885
On SUSY dark matter detection with spinless nuclei
[DE94-628562] p 2109 N95-24886
Homogeneous anisotropic cosmological models in the minimum quadratic Poincare gauge theory of gravity
[DE95-607083] p 2110 N95-25647
A survey of surveys
[DE95-004238] p 2111 N95-26284

ASTRONOMICAL SPECTROSCOPY
Far-infrared and submillimeter spectroscopy of photodissociation regions
[DE95-607520] p 2110 N95-25467

ASTRONOMY
NASA video catalog
[NASA-SP-7109(01)] p 2103 N95-24238
Perspectives from space: NASA classroom information and activities
[NASA-TM-110577] p 2100 N95-25643
Regge in the sky: Origin of the cosmic rotation
[DE95-607001] p 2111 N95-25990

ASTROPHYSICS
Core-collapse supernovae and nucleosynthesis
[NASA-CR-197731] p 2109 N95-25122
From superconductivity to supernovae: The Ginzburg symposium. Report on the symposium held in honor of Vitaly L. Ginzburg
[NASA-TM-110596] p 2108 N95-25746

ASYMMETRY
W-charge asymmetry at CDF, tests of structure functions
[DE95-004855] p 2041 N95-24256
Measurement of alpha(sub s)from hadronic event observables at the Z(sup 0) resonance
[DE95-005943] p 2045 N95-24434
A measurement of the left-right, forward-backward asymmetry for charm quarks using D(*+) and D(+) mesons
[DE95-006061] p 2046 N95-24575
Tau physics at future facilities
[DE95-006071] p 2046 N95-24591
The left-right forward-backward asymmetry of heavy quarks measured with jet charge and with leptons at the SLD
[DE95-006145] p 2046 N95-24593
On the Compton non-Abelian twist-3 asymmetry
[DE94-628586] p 2095 N95-24727
The twist-3 single spin asymmetries of pion production
[DE95-607144] p 2052 N95-25437
Neutrino mass and oscillation angle phenomena within the asymmetric left-right models
[DE95-607201] p 2054 N95-25466

ASYMPTOTIC METHODS
The diffraction of electromagnetic waves by screens placed at the boundaries of dielectric media
[IFTR-4/1994] p 1954 N95-25393

ASYMPTOTIC PROPERTIES
Semiclassical asymptotics on covering manifolds and morse inequalities
[PB95-165510] p 2028 N95-24251
Asymptotic properties of the oscillator poly spheroidal functions
[DE94-628441] p 2032 N95-24860

ASYMPTOTIC SERIES
Heat Kernel expansion on a cone and quantum fields near cosmic strings
[DE94-628520] p 2094 N95-24507
Asymptotics for the Kummer function of Bose plasmas
[DE95-607019] p 2096 N95-25428
Singularly perturbed differential/algebraic equations
[AD-A288365] p 2033 N95-25601

ATMOSPHERIC ATTENUATION
Wave-propagation aspects on VHF-radar applications
[PB95-141818] p 1953 N95-24649

ATMOSPHERIC CHEMISTRY
An investigation of the effect of surface impurities on the adsorption kinetics of hydrogen chemisorbed onto iron
[NASA-CR-197967] p 1933 N95-24400
Microphysical and compositional influences on shortwave radiative forcing of climate by sulfate aerosols
[DE95-005999] p 1997 N95-24570
Parallel processing of atmospheric chemistry calculations: Preliminary considerations
[DE95-005915] p 1999 N95-25198
Effects of nitric acid vapor on the formation of cloud droplets in troposphere
[DE95-744869] p 2001 N95-25500
Development of a model of atmospheric oxygen variations to estimate terrestrial carbon storage and release
[NASA-CR-198002] p 2002 N95-25955
Design and development of a cloud reference library and support for cloud and simulation communities. Summary report
[AD-A288704] p 2006 N95-26012

ATMOSPHERIC CIRCULATION
Parallel processing of atmospheric chemistry calculations: Preliminary considerations
[DE95-005915] p 1999 N95-25198

ATMOSPHERIC COMPOSITION
Preliminary analysis of University of North Dakota aircraft data from the FIRE Cirrus IFO-2
[NASA-CR-198038] p 2005 N95-24219
Replicator for characterization of cirrus and polar stratospheric cloud particles
[NASA-CR-197992] p 2005 N95-24411
Future emissions and concentrations of carbon dioxide: Key ocean/atmosphere/land analyses
[CSIRO-TP-31] p 1999 N95-25199
The effects on photosynthetic CO2 assimilation to long-term elevation of atmospheric CO2 concentration: An assessment of the response of Trifolium Repens L. CV. Blanca grown at F.A.C.E
[DE95-005687] p 2008 N95-25383
The whitehouse effect: Shortwave radiative forcing of climate by anthropogenic aerosols
[DE95-005998] p 2001 N95-25442

ATMOSPHERIC EFFECTS
Biospheric effects of a large extraterrestrial impact: Case study of the cretaceous/tertiary boundary crater
[NASA-CR-198015] p 1997 N95-24501

ATMOSPHERIC GENERAL CIRCULATION MODELS
Technical report series on global modeling and data assimilation. Volume 5: Documentation of the AIRES/GEOS dynamical core, version 2
[NASA-TM-104606-VOL-5] p 2003 N95-24766
Parallel processing of atmospheric chemistry calculations: Preliminary considerations
[DE95-005915] p 1999 N95-25198
Global ocean circulation and equator-pole heat transport as a function of ocean GCM resolution
[DE95-004198] p 2000 N95-25279
Impacts of microphysics, radiation and environmental winds in mid-latitude and tropical squall-line systems, and their climatic implications
[DE95-004965] p 2005 N95-25287
Intercomparison of hydrologic processes in global climate models
[NASA-TM-104617] p 2005 N95-26341

ATMOSPHERIC MODELS
Impacts of microphysics, radiation and environmental winds in mid-latitude and tropical squall-line systems, and their climatic implications
[DE95-004965] p 2005 N95-25287
A numerical prediction of the precipitation and hydrology of California
[DE95-004966] p 2006 N95-25635
Development of a model of atmospheric oxygen variations to estimate terrestrial carbon storage and release
[NASA-CR-198002] p 2002 N95-25955
Design and development of a cloud reference library and support for cloud and simulation communities. Summary report
[AD-A288704] p 2006 N95-26012

ATMOSPHERIC PHYSICS
Technical report series on global modeling and data assimilation. Volume 5: Documentation of the AIRES/GEOS dynamical core, version 2
[NASA-TM-104606-VOL-5] p 2003 N95-24766
Design and development of a cloud reference library and support for cloud and simulation communities. Summary report
[AD-A288704] p 2006 N95-26012

ATMOSPHERIC TURBULENCE
Laser beam log amplitude temporal scintillation spectrum due to crosswind. Part 1: Theory
[TR-1-FSRC-1994-PT-1] p 1971 N95-24371

Atmospheric and terrain effects on acoustic propagation
[AD-A288727] p 2039 N95-25503

ATOMIC BEAMS
On the possibility of obtaining the polarized protons by the method of direct optic pumping of a fast atomic beam
[DE94-634309] p 2041 N95-24267
Laser cooling of neutral atoms by red-shifted diffuse light in an optical integral sphere cavity
[DE94-634310] p 2041 N95-24268
Design study of a negative-ion based NBI system for JT-60U
[DE94-785265] p 2043 N95-24339

ATOMIC CLUSTERS
Nanostructured materials
[DE95-004595] p 2088 N95-25280

ATOMIC COLLISIONS
International bulletin on atomic and molecular data for fusion, no. 47
[DE94-634442] p 2040 N95-24230
Toward improved photon-atom scattering predictions
[DE95-003651] p 2046 N95-24549
Inelastic collisions of negative muons and hadrons with metastable hydrogen atoms
[DE95-607537] p 2056 N95-25668
Multiplicities of secondaries in interactions of 1.8 GeV/nucleon Fe-56 nuclei with photoemulsion and the cascade evaporation model p 2059 N95-25917
Target fragments in collisions of 1.8 GeV/nucleon Fe-56 nuclei with photoemulsion nuclei, and the cascade-evaporation model p 2059 N95-25918

ATOMIC ENERGY LEVELS
Superconducting in the near half-filling Hubbard model
[DE94-634857] p 2092 N95-24275

ATOMIC EXCITATIONS
Semiclassical hyperspherical matrix elements for helium doubly excited states
[DE94-628867] p 2048 N95-24718

ATOMIC FORCE MICROSCOPY
Atomic force microscopy as a process characterization tool for GaAs-based integrated circuit fabrication
[DE95-006223] p 2064 N95-26168

ATOMIC PHYSICS
Index of nuclear data libraries available from the IAEA Nuclear Data Section
[DE95-605213] p 2107 N95-25980

ATOMIC STRUCTURE
International bulletin on atomic and molecular data for fusion, no. 47
[DE94-634442] p 2040 N95-24230
Electronic structure and pairing of strongly correlated fermions: Fermi liquid versus spin liquid
[DE95-005929] p 2044 N95-24419
Theoretical and experimental studies on the C15 intermetallic compound NbCr2
[DE95-003665] p 2086 N95-24513
Ionization potential data library of atoms and ions
[DE94-628380] p 2048 N95-24689
Thermochemistry, kinetics and spectroscopy of Kr and Kr2F
[DE95-005732] p 1941 N95-25386
The geometry of disorder: Theoretical investigations of quasicrystals and frustrated magnets
[DE95-006641] p 1936 N95-25560
Electronic structure of (La,Sr)2CuO4 and Ba(0.6)K(0.4)BiO3
[DE95-004963] p 2091 N95-26170

ATOMIC WEIGHTS
Atomic masses 1993. The 1993 atomic mass evaluation
[DE94-634462] p 2040 N95-24231

ATOMS
Ionization potential data library of atoms and ions
[DE94-628380] p 2048 N95-24689
Elastic form factors of hydrogen-like atoms in nS-states
[DE94-628437] p 2048 N95-24700
Diagrammatic many-body perturbation expansion for atoms and molecules
[PB95-165221] p 2056 N95-25620

ATTENUATION
Flux attenuation at NREL's High-Flux Solar Furnace
[DE95-000219] p 1993 N95-24715

ATTITUDE INDICATORS
Flight reference display for powered-lift STOL aircraft
[NAL-TR-1251] p 1912 N95-25005

AUDITORY PERCEPTION
Psychophysical evaluation of three-dimensional auditory displays
[NASA-CR-198010] p 2011 N95-24564
Temporal pacing in visual attention
[AD-A289785] p 2013 N95-26041
Automatic classification of Polish fricatives on the basis of optimization of the parameter space
[IFTR-9/1994] p 1956 N95-26331

AUDITORY SIGNALS
Psychophysical evaluation of three-dimensional auditory displays
[NASA-CR-198010] p 2011 N95-24564

AUGMENTATION
Enhancement of thickness uniformity of thin films grown by pulsed laser deposition
[NASA-CR-197791] p 1943 N95-26081

AUSTENITE
Static recrystallization behavior of austenite in HSLA 100 during Thermomechanical Controlled Processing (TMCP)
[AD-A288737] p 1937 N95-26057

AUSTRALIA
The use of radioisotopes in human experiments: Comments in response to recent media articles
[DE95-605680] p 2012 N95-25981

AUTOIONIZATION
Na-like autoionizing levels: Plasma diagnostics and prospects for photopumped soft x-ray lasers
[DE95-004207] p 1972 N95-25100

AUTOMATIC CONTROL
A preview of a modular surface light scattering instrument with autotracking optics
[NASA-TM-110495] p 2072 N95-24386
Software of a distributor of high voltage of the H C-600 hadronic calorimeter
[DE94-628255] p 1967 N95-24486
Automation based on knowledge modeling theory and its applications in engine diagnostic systems using Space Shuttle Main Engine vibrational data
[NASA-CR-197983] p 1922 N95-24626
Controls concepts for next generation reuseable rocket engines
[NASA-TM-106902] p 1923 N95-25877
Partial camera automation in a simulated Unmanned Air Vehicle
[AD-A288786] p 1913 N95-26190
Automated protein crystal growth facility
p 1918 N95-26306

AUTOMATION
Workflow automation architecture standard
[DE95-004748] p 2035 N95-24248
Automated Procurement System (APS): Project management plan (DS-03), version 1.2
[NASA-CR-196576] p 2102 N95-24442

AUTOMOBILE ENGINES
Activities of the Ceramic Technology Project
[DE95-003394] p 1940 N95-24588
Development of a dedicated ethanol ultra-low emission vehicle (ULEV) system design
[DE95-004016] p 1975 N95-24880

AUTOMOBILE FUELS
Alternatives to traditional transportation fuels 1993
[DE95-005445] p 1947 N95-24273
Development of a dedicated ethanol ultra-low emission vehicle (ULEV) system design
[DE95-004016] p 1975 N95-24880

AUTOMOBILES
Liquid-fueled SOFC power sources for transportation
[DE95-002998] p 1991 N95-24607
Development of a dedicated ethanol ultra-low emission vehicle (ULEV) system design
[DE95-004016] p 1975 N95-24880
Developing a standardized test procedure for hybrid vehicles: The challenge of the SAE HEV task force
[DE95-000280] p 1978 N95-26286

AUTONOMOUS NAVIGATION
Interfacing a digital compass to a remote-controlled helicopter
[PB95-164927] p 1914 N95-24260

AUTONOMY
Instructable autonomous agents
[NASA-CR-197802] p 2019 N95-26206

AUXILIARY POWER SOURCES
Predictability in space launch vehicle anomaly detection using intelligent neuro-fuzzy systems
p 2025 N95-25266

AVAILABILITY
Availability analysis of a 100 kWh superconducting magnetic energy storage
[DE95-737621] p 2066 N95-24448

AVIONICS
Assessment of avionics technology in European aerospace organizations
[NASA-CR-189201] p 1912 N95-24624
Preload release mechanism
[NASA-CASE-MSC-22327-1] p 1976 N95-25592
Configuration and other differences between Black Hawk and Seahawk helicopters in military service in the USA and Australia
[AR-008-386] p 1911 N95-25935

AXIAL LOADS
Thermoelastic equations for multi-layered cylindrical shell
[NAL-TR-1222] p 1982 N95-25661

AXIAL STRESS
Thrust measurement in a 2-D scramjet nozzle
p 1914 N95-25397
Mechanical properties testing and results for thermal barrier coatings p 1946 N95-26134

AXISYMMETRIC BODIES
Sensitivity analysis of frictional contact response of axisymmetric composite structures p 1985 N95-26271
Dynamic sensitivity analysis of frictional contact/impact response of axisymmetric composite structures
p 1986 N95-26279

AXISYMMETRIC FLOW
A higher-order projection method for the simulation of unsteady turbulent nonpremixed combustion in an industrial burner
[DE95-005919] p 1931 N95-25291

AZIMUTH
Geomagnetic Polar Cap (PC) index, 1975-1993
[UAG-103] p 2004 N95-24897

B

BACKGROUND RADIATION
PC based analysis of gamma ray spectra generated by semiconductor detectors
[DE94-628381] p 1958 N95-24690
Further ways to distinguish single-lepton top quark signals from background at the Tevatron
[PB95-165395] p 2056 N95-25567
On fractal structure of quantum gravity and relic radiation anisotropy
[DE95-605306] p 2099 N95-25966

BACKSCATTERING
Diurnal variations of backscattering properties of pine trees at C- and X-bands
[PB95-149738] p 1988 N95-24299
Copper transport on oxygen annealing of a superconducting film Y-Ba-Cu-O
[DE94-627566] p 2086 N95-24537
Method and apparatus for non-destructive evaluation of composite materials with cloth surface impressions
[NASA-CASE-LAR-14535-1] p 1926 N95-25305

BACKWARD FACING STEPS
Solutions of turbulent backward-facing step flow with heat transfer using the finite volume method
[DE95-003360] p 1962 N95-24489

BAFFLES
Numerical simulation of flow and the effect of baffle arrangement on pressure drop and temperature pattern in a circular combustor p 1963 N95-24628

BALANCING
Dynamic load balancing for parallel finite element methods with adaptive h- and p-refinement
[DE95-004521] p 2021 N95-24681

BALL BEARINGS
Performance of solid lubricated ball bearings at high-temperatures in a vacuum
[NAL-TR-1243] p 1976 N95-25323

BALLISTIC MISSILES
Flexible architectures for sensor fusion in theater missile defense
[AD-A288666] p 2007 N95-26048

BALLOONING MODES
Maryland controlled fusion research program
[DE95-006642] p 2081 N95-25561
Self-sustained turbulence and L-mode confinement in toroidal plasmas 2
[NIFS-278] p 2082 N95-25759

BAND STRUCTURE OF SOLIDS
BCS-like gap structure of HgBa2CuO(4+delta) tunnel junctions
[DE95-004125] p 2087 N95-24855

BANDWIDTH
Adventures in the evolution of a high-bandwidth network for central servers
[DE95-006215] p 2020 N95-24597

BARIUM COMPOUNDS
Accurate determination of IC modulation parameter in Sr(x)Ba(1-x)Nb2O6 from second order satellites of neutron diffraction TOF (Time-Of-Flight) spectra
[DE94-629003] p 2090 N95-25851

BARIUM OXIDES
BCS-like gap structure of HgBa2CuO(4+delta) tunnel junctions
[DE95-004125] p 2087 N95-24855
Formation of thallium based high temperature superconductors using aerosol flow reacted precursor powders
[DE95-005901] p 2089 N95-25389
Electronic structure of (La,Sr)2CuO4 and Ba(0.6)K(0.4)BiO3
[DE95-004963] p 2091 N95-26170

BARIUM TITANATES
Solution based synthesis of perovskite-type oxide films and powders
[DE95-006170] p 2086 N95-24594
BARRIER LAYERS
Current-voltage characteristics of a tunnel junction with resonant centers
[DE94-634530] p 1956 N95-24245
BARYON RESONANCE
Investigation of the gross structure of spectra and mass distributions of hadronic resonances
[DE94-636799] p 2043 N95-24361
Baryon spectroscopy and the omega minus
[DE95-004838] p 2052 N95-25374
BARYONS
Deficiency of the Gross-Llewellyn Smith sum rule and QCD vacuum polarization effect
[DE94-636790] p 2042 N95-24315
Baryon spectroscopy and the omega minus
[DE95-004838] p 2052 N95-25374
Theoretical studies in hadronic and nuclear physics
[DE95-006643] p 2098 N95-25562
BATCH PROCESSING
SPEEDUP simulation of liquid waste batch processing, revision 1
[DE95-001240] p 1939 N95-24344
BAYES THEOREM
The hard truth --- a method to determine the reliability of a specific feature of a Bayesian solution
[DE95-005240] p 2033 N95-25767
BCS THEORY
BCS-like gap structure of HgBa2CuO(4+delta) tunnel junctions
[DE95-004125] p 2087 N95-24855
BEAM INJECTION
The AGS gamma(sub t)-jump system
[DE95-003170] p 2064 N95-24287
Design study of a negative-ion based NBI system for JT-60U
[DE94-785265] p 2043 N95-24339
High-beta discharges with neutral beam injection in CHS
[NIFS-280] p 2071 N95-26031
BEAM INTERACTIONS
The AGS gamma(sub t)-jump system
[DE95-003170] p 2064 N95-24287
Self-consistent beam halo studies & halo diagnostic development in a continuous linear focusing channel
[DE95-003706] p 2065 N95-24331
A high-energy high-luminosity (mu)(+) - (mu)(-) collider
[DE95-006097] p 2065 N95-24357
A fast tracking method using resonance basis Hamiltonians
[DE95-004292] p 2068 N95-24664
Emittance growth caused by nonuniform charge distribution of bunched beam in linac
[DE95-602121] p 2072 N95-26095
BEAMS (RADIATION)
The AGS gamma(sub t)-jump system
[DE95-003170] p 2064 N95-24287
Proceedings of the 21st Japan Conference on Radiation and Radioisotopes
[DE94-785275] p 2056 N95-25614
BEAMS (SUPPORTS)
An analytical study of the vibration of beams fitted with neutralizers. Part 3: Torsional wave motion
[ISVR-TR-238-PT-3] p 1982 N95-25003
BELARUS
Display technologies in Russia, Ukraine, and Belarus
[ISBN-1-883712-36-X] p 2085 N95-24460
BENDING FATIGUE
Thrust measurement in a 2-D scramjet nozzle
p 1914 N95-25397
New techniques to test fatigue properties of coined sheet specimens. Part 4: Development of experimental techniques
[PB95-165130] p 1982 N95-25445
New techniques to test fatigue properties of coined sheet specimens. Part 3: Fatigue testing and analysis of a component like coining in sheet steel materials
[PB95-165668] p 1982 N95-25569
BETATRONS
A normal form approach to the theory of nonlinear betatronic motion
[DE95-603831] p 2062 N95-25944
BETHE-SALPETER EQUATION
Numerical investigation of Schwinger-Dyson and Bethe-Salpeter equations with Gauss potential in the framework of the quarkonium model
[DE94-636730] p 2029 N95-24387
Heavy quark effective theory, interpolating fields and Bethe-Salpeter amplitudes
[DE95-607146] p 2053 N95-25460
BIAS
Device-quality tunnel junctions on the high (T(sub c)) super conductor HgBa2CuO(4+delta)
[DE95-004646] p 2084 N95-24279
BIBLIOGRAPHIES
International bulletin on atomic and molecular data for fusion, no. 47
[DE94-634442] p 2040 N95-24230
NASA video catalog
[NASA-SP-7109(01)] p 2103 N95-24238
Research in the service of the Swedish National Defence
[PB95-141941] p 1989 N95-24444
Aeronautical engineering: A continuing bibliography with indexes (supplement 316)
[NASA-SP-7037(316)] p 1905 N95-24465
Motionsickness-seasickness: Summary of existing knowledge and suggested lines of development
[PB95-141495] p 2011 N95-24863
NREL Photovoltaic Program FY 1994 bibliography
[DE95-000275] p 1993 N95-24865
Aeronautical engineering: A continuing bibliography with indexes (supplement 317)
[NASA-SP-7037(317)] p 1906 N95-25798
Aerospace medicine and biology: A continuing bibliography with indexes (supplement 401)
[NASA-SP-7011(401)] p 2012 N95-25800
Online nuclear data service
[DE95-602487] p 2107 N95-25941
The spacelab scientific missions: A comprehensive bibliography of scientific publications
[NASA-TM-108487] p 2107 N95-26084
Cumulative reports and publications through December 31, 1994
[NASA-CR-195043] p 2014 N95-26085
BIG BANG COSMOLOGY
Creation and development of the Universe (symmetry approach)
[DE94-628558] p 2109 N95-24884
BIHARMONIC EQUATIONS
Optical diffraction from fractals with a structural transition
[DE94-634311] p 2029 N95-24401
BINARY ALLOYS
The (lambda)-bar exponent for conservative systems
[DE95-607661] p 1937 N95-25977
BINARY DATA
A generic data exchange scheme between FITS format and C structures
[DE95-004849] p 2106 N95-25376
Heuristic approach to the path planning problem in a raster map
[PB95-141826] p 2034 N95-25893
BINARY SYSTEMS (MATERIALS)
Kinetics of diffusional droplet growth in a liquid/liquid two-phase system
[NASA-CR-198050] p 1961 N95-24221
BIOCONVERSION
XAS studies of Ni(I), Ni(II), and Ni(III) complexes
[DE95-004844] p 1928 N95-24257
Yearbook 1993: Bioenergy Research Programme. Utilization of bioenergy and biomass conversion
[DE95-717518] p 1993 N95-24862
JALO: Fuel conversion
[DE95-737597] p 1949 N95-25244
BIODYNAMICS
On producing sequential movements and actions. An integrative review and an update of the generalized motor program
[AD-A288628] p 2014 N95-25610
BIOLOGICAL EFFECTS
Aerospace medicine and biology: A continuing bibliography with indexes (supplement 400)
[NASA-SP-7011(400)] p 2011 N95-24464
Interim report of the advisory committee on human radiation experiments
[DE95-003265] p 2011 N95-24497
Human radiation experiments: The Department of Energy roadmap to the story and the records
[DE95-006364] p 2012 N95-25371
Biological effectiveness of neutrons: Research needs
[DE95-004795] p 2051 N95-25373
Interaction mechanisms and biological effects of static magnetic fields
[DE95-004929] p 2009 N95-26169
BIOLOGY
Overview of selected molecular biological databases
[DE95-005906] p 2008 N95-25181
Proceedings of the International Seminar on the Chemistry of High Energy Atoms
[DE95-709895] p 2072 N95-26162
BIOMASS
Biologically produced succinic acid: A new route to chemical intermediates
[DE95-000257] p 2007 N95-24306
Clean fractionation of biomass
[DE95-000259] p 2007 N95-24307
Appendix model performance: Model documentation. Renewable Fuels Module of the National Energy Modelling System
[DE95-006080] p 1991 N95-24355
Bioprocessing in nonaqueous media: Critical needs and opportunities
[DE95-004878] p 2008 N95-24843
JALO: Fuel conversion
[DE95-737597] p 1949 N95-25244
Carbon taxes and India
[DE95-005401] p 2001 N95-25629
BIOMASS ENERGY PRODUCTION
Yearbook 1993: Bioenergy Research Programme. Utilization of bioenergy and biomass conversion
[DE95-717518] p 1993 N95-24862
JALO: Fuel conversion
[DE95-737597] p 1949 N95-25244
BIONICS
Biological effectiveness of neutrons: Research needs
[DE95-004795] p 2051 N95-25373
BIOPHYSICS
Genetic and biophysical studies of the photosynthetic reaction center
[DE95-004179] p 2008 N95-24850
BIOPROCESSING
FNAS phase partitions
[NASA-CR-193855] p 1940 N95-24562
Bioprocessing in nonaqueous media: Critical needs and opportunities
[DE95-004878] p 2008 N95-24843
BIOREACTORS
Bioprocessing in nonaqueous media: Critical needs and opportunities
[DE95-004878] p 2008 N95-24843
BIOSATELLITES
Depth distribution of absorbed dose on the external surface of Cosmos 1887 biosatellite
p 2061 N95-25927
Cosmic ray LET spectra and doses on board Cosmos-2044 biosatellite p 2061 N95-25930
Cosmic ray particles with different LET values under various thicknesses of shielding in low altitude orbits: Calculations and Cosmos-2044 measurements
p 2062 N95-25931
Radiobiological experiments with plant seeds aboard the biosatellite Cosmos 1887 p 2009 N95-25933
BIOSPHERE
Biospheric effects of a large extraterrestrial impact: Case study of the cretaceous/tertiary boundary crater
[NASA-CR-198015] p 1997 N95-24501
Our changing planet: The FY 1995 U.S. Global Change Research Program p 2002 N95-25852
BIOTECHNOLOGY
Biologically produced succinic acid: A new route to chemical intermediates
[DE95-000257] p 2007 N95-24306
JPRS report: Science and technology. Central Eurasia
[JPRS-UST-94-035] p 2016 N95-24429
JPRS Report: Science and technology. Central Eurasia
[JPRS-UST-94-032] p 1950 N95-24759
BIRD-AIRCRAFT COLLISIONS
Bird ingestion into large turbofan engines
[DOT/FAA/CT-93/14] p 1909 N95-24631
BIRDS
Bird ingestion into large turbofan engines
[DOT/FAA/CT-93/14] p 1909 N95-24631
BIREFRINGENCE
Measurement of the magnetically-induced QED birefringence of the vacuum and an improved search for laboratory axions: Project definition study of the use of assets and facilities of the Superconducting Super Collider Laboratory
[DE95-005110] p 2065 N95-24317
BISMUTH OXIDES
Application of extended-crystal diffraction techniques to the symmetry and structure analysis of 221-PbBiSrCaCuO
[DE95-605913] p 2090 N95-25984
Electronic structure of (La,Sr)2CuO4 and Ba(0.6)K(0.4)BiO3
[DE95-004963] p 2091 N95-26170
BIVARIATE ANALYSIS
On the joint spectral density of bivariate random sequences
[NASA-CR-197698] p 2035 N95-24278
BLACK HOLES (ASTRONOMY)
String-loop corrections to effective action and black-hole instabilities
[DE95-607085] p 2110 N95-25433

BLANKETS (FISSION REACTORS)
Phase 3 experiments of the JAERI/USDOE collaborative program on fusion blanket neutronics. Volume 1: Experiment
[DE94-777528] p 2076 N95-24511
BLANKETS (FUSION REACTORS)
US technical report for the ITER blanket/shield
[DE95-004667] p 2079 N95-25283
Proceedings of the 2nd international workshop on electromagnetic forces and related effects on blankets and other structures surrounding the fusion plasma torus
[DE94-792667] p 2082 N95-25903
BLAST LOADS
Quantity-distance requirements for earth-bermed aircraft shelters
[AD-A279692] p 1915 N95-24424
BLOCH BAND
Nonlinearity induced nontrivial dynamics in the Jaynes-Cummings Hamiltonian
[DE95-607004] p 2032 N95-25452
BLOCK COPOLYMERS
Design of supramolecular ordered systems for mesoscopic colloids and molecular composites
[DE95-004448] p 2048 N95-24687
BLOCK DIAGRAMS
Nonlinear system analysis using slowly-varying complex frequency method
[NAL-TR-1217] p 2034 N95-25860
BLOOD
Staurosporine analysis and its pharmacokinetics in the blood of rats
[DE94-013857] p 2008 N95-24600
Measurement of blood nitrogen content after rapid compressions to assess the speed of nitrogen uptake during the compression phase of submarine escape. (Includes measurement of nitrogen concentration in blood following rapid compression to 5 bar)
[PB95-165726] p 2012 N95-25570
BLOOD CELLS
Staurosporine analysis and its pharmacokinetics in the blood of rats
[DE94-013857] p 2008 N95-24600
BLOOD PLASMA
Staurosporine analysis and its pharmacokinetics in the blood of rats
[DE94-013857] p 2008 N95-24600
BLUNT BODIES
DSMC calculations for 70-deg blunted cone at 3.2 km/s in nitrogen
[NASA-TM-109181] p 1961 N95-24396
BODY WEIGHT
Testing of experimental antileishmanial compounds
[AD-A288807] p 2009 N95-26193
BODY-WING CONFIGURATIONS
Aerodynamic shape optimization of wing and wing-body configurations using control theory
[NASA-CR-198024] p 1911 N95-25334
A theoretical and experimental investigation of the flow over supersonic leading edge wing/body configurations
[DRA-TM-AERO-PROP-41] p 1907 N95-25649
BOLOMETERS
Read out electronics for thermal detectors of bolometer type
[PB95-141842] p 1967 N95-24280
BOLTED JOINTS
Experimental analysis of thread movement in bolted connections due to vibrations
[NASA-CR-197705] p 1975 N95-24991
Static and fatigue properties of pin-joint specimens of a AS-4/PEEK thermoplastic composite material
[NAL-TR-1214] p 1927 N95-25859
BOLTS
Experimental analysis of thread movement in bolted connections due to vibrations
[NASA-CR-197705] p 1975 N95-24991
BOLTZMANN TRANSPORT EQUATION
Fast algorithms for transport models
[DE95-007064] p 2054 N95-25479
HZE beam transport in multilayered materials
p 2060 N95-25922
BONDING
Feasibility of ceramic joining with high energy electron beams
[DE95-004519] p 1940 N95-24717
BONE DEMINERALIZATION
Human parathyroid hormone-(1-38) restores cancellous bone to the immobilized, osteopenic proximal tibial metaphysis in rats
[NASA-CR-197709] p 2011 N95-24556
BONE MINERAL CONTENT
Human parathyroid hormone-(1-38) restores cancellous bone to the immobilized, osteopenic proximal tibial metaphysis in rats
[NASA-CR-197709] p 2011 N95-24556
BONES
Human parathyroid hormone-(1-38) restores cancellous bone to the immobilized, osteopenic proximal tibial metaphysis in rats
[NASA-CR-197709] p 2011 N95-24556
BOOMS (EQUIPMENT)
Stiffening of the ACES deployable space boom
p 1978 N95-26307
BOOSTER ROCKET ENGINES
BSM Delta Qualification 2, volume 2
[NASA-CR-196567] p 1922 N95-24844
BSA Delta Qualification 2, volume 3, book 1
[NASA-CR-196565] p 1922 N95-24845
BSM Delta Qualification 2, volume 3, book 2
[NASA-CR-196568] p 1922 N95-24854
BORN APPROXIMATION
KORP-1: A program for calculating the direct (n, p) or (p, n) reaction by using DWBA method
[DE94-628768] p 2049 N95-24724
Radiative corrections for pion polarizability experiments
[DE95-607177] p 2053 N95-25462
BORN-INFELD THEORY
Nonlinear theories of spin-2 field in terms of Fierz variables
[DE95-600854] p 2095 N95-24833
BORON
Atom probe field ion microscopy of Type 308 CRE stainless steel welds
[DE94-019161] p 1938 N95-26064
BORON CARBIDES
JPRS report: Science and technology. Central Eurasia
[JPRS-UST-95-012] p 1950 N95-24540
High heat flux experiment on B4C-converted carbon based materials for plasma facing materials of JT-60U
[DE94-777545] p 2077 N95-24585
BOROSILICATE GLASS
SPEEDUP simulation of liquid waste batch processing, revision 1
[DE95-001240] p 1939 N95-24344
BOSONS
W-charge asymmetry at CDF, tests of structure functions
[DE95-004855] p 2041 N95-24256
Investigation of the gross structure of spectra and mass distributions of hadronic resonances
[DE94-636799] p 2043 N95-24361
Extending the kinematic range for W(sub R) searches in e(-)e(-) collisions at the NLC
[DE95-005946] p 2044 N95-24415
A test of the flavor independence of strong interactions
[DE95-005948] p 2044 N95-24418
Electronic structure and pairing of strongly correlated fermions: Fermi liquid versus spin liquid
[DE95-005929] p 2044 N95-24419
Probing anomalous gauge boson couplings at LEP
[DE95-005934] p 2044 N95-24420
Measurement of alpha(sub s)from hadronic event observables at the Z(sup 0) resonance
[DE95-005943] p 2045 N95-24434
The left-right forward-backward asymmetry of heavy quarks measured with jet charge and with leptons at the SLD
[DE95-006145] p 2046 N95-24593
Measurement of the WW gamma, ZZ gamma and Z gamm a gamma couplings at the Fermilab Tevatron
[DE95-003495] p 2067 N95-24601
Measurement of alpha(sub s) from hadronic ev ent observables at the Z(sup 0) resonance
[DE95-005949] p 2047 N95-24622
A study of K(sub s) (lambda) and (bar (lambda)) production in hadronic Z(sup 0) decays
[DE95-004280] p 2047 N95-24660
Studies of strong electroweak symmetry breaking at future e(+)e(-) linear colliders
[DE95-004281] p 2067 N95-24661
q-bosons and the q-analogue quantized field
[DE95-005925] p 2051 N95-25294
Tau as a probe for new physics
[DE95-005928] p 2051 N95-25296
Testing supersymmetry at the next linear collider
[DE95-006064] p 2069 N95-25297
Extended gauge sectors
[DE95-006485] p 2052 N95-25407
String-loop corrections to effective action and black-hole instabilities
[DE95-607085] p 2110 N95-25433
Masses of heavy fermions and Higgs boson in four-generation fermion condensate scheme
[DE95-607124] p 2053 N95-25450
Anomalous WWZ couplings and K(sub L) yields mu(+) mu(-)
[DE95-607190] p 2054 N95-25464
Neutrino mass and oscillation angle phenomena within the asymmetric left-right models
[DE95-607201] p 2054 N95-25466
Statistical mechanics of relativistic spin-1 bosons in a magnetic field
[DE95-607100] p 2054 N95-25474
Electroweak boson pair production at the Tevatron
[DE95-004234] p 2056 N95-25563
Further ways to distinguish single-lepton top quark signals from background at the Tevatron
[PB95-165395] p 2056 N95-25567
Electroweak coupling measurements from polarized Bhabha scattering at the Z(exp 0) resonance
[DE95-006090] p 2057 N95-25768
BOTANY
The effects on photosynthetic CO2 assimilation to long-term elevation of atmospheric CO2 concentration: An assessment of the response of Trifolium Repens L. CV. Blanca grown at F.A.C.E
[DE95-005687] p 2008 N95-25383
BOUNDARY CONDITIONS
Bounds for departure from normality and the Frobenius norm of matrix eigenvalues
[DE95-006144] p 2030 N95-24592
Boundary dynamics in dilaton gravity
[DE95-607080] p 2098 N95-25526
Nonexistence of global solutions to some quasilinear hyperbolic equations with dynamic boundary conditions
[DE95-607010] p 2033 N95-25645
BOUNDARY ELEMENT METHOD
The dual boundary element formulation for elastoplastic fracture mechanics
[DRA-TR-93062] p 1980 N95-24383
BOUNDARY LAYER EQUATIONS
Supersonic quiet-tunnel development for laminar-turbulent transition research
[NASA-CR-198040] p 1915 N95-24302
BOUNDARY LAYER FLOW
Numerical calculations of shock-wave/boundary-layer flow interactions
[NASA-TM-106694] p 1966 N95-26077
BOUNDARY LAYER TRANSITION
Supersonic quiet-tunnel development for laminar-turbulent transition research
[NASA-CR-198040] p 1915 N95-24302
BOUNDARY LAYERS
Three-dimensional interaction of wake/boundary-layer and vortex/boundary-layer data report
[CUED/A-AEREO/TR-23] p 1906 N95-24210
BOUNDARY LUBRICATION
Development of a high temperature, high speed disc lubricant test machine
[AD-A288685] p 1977 N95-26050
BOUNDARY VALUE PROBLEMS
Numerical investigation of Schwinger-Dyson and Bethe-Salpeter equations with Gauss potential in the framework of the quarkonium model
[DE94-636730] p 2029 N95-24387
The diffraction of electromagnetic waves by screens placed at the boundaries of dielectric media
[IFTR-4/1994] p 1954 N95-25393
Friction on geological faults modelling and variational formulation of initial boundary value problems
[IFTR-31/1994] p 2004 N95-25958
BOW WAVES
The whistler-mode bow wave of an asteroid
[U-OF-IOWA-95-2] p 2111 N95-26195
On a remarkable similarity between the propagation of whistlers and the bow wave of a ship
[U-OF-IOWA-94-22] p 2111 N95-26196
BRANCHING (PHYSICS)
Tau physics 1994: A theoretical perspective
[DE95-004840] p 2052 N95-25375
Quasi two body decays of charm mesons
[DE94-792634] p 2057 N95-25901
Results/prospects in E777/851/865
[DE95-005959] p 2064 N95-26006
BRAYTON CYCLE
Brayton-cycle solvent recovery heat pump. A technical brief
[DE94-000225] p 1991 N95-24666
BREMSSTRAHLUNG
Bremsstrahlung scattering calculations for the beam stops and collimators in the APS insertion-device beamlines
[DE95-005471] p 2069 N95-25300
BRITTLE MATERIALS
An analysis of hypercritical states in elastic and inelastic systems
[IFTR-1/1994] p 2037 N95-25339
BRITTLENESS
Atomistic studies of grain boundaries in NiAl
[DE95-005208] p 1937 N95-26014
BROADCASTING
JPRS report: Science and technology. Central Eurasia
[JPRS-UST-95-010] p 1953 N95-24539

BROKEN SYMMETRY
Tau physics at future facilities
[DE95-006071] p 2046 N95-24591
Studies of strong electroweak symmetry breaking at future e(+)e(-) linear colliders
[DE95-004281] p 2067 N95-24661
Current status and future prospect of space and time reversal symmetry violation on low energy neutron reactions
[DE94-765589] p 2048 N95-24702
Light-front quantized field theory: An introduction. Spontaneous symmetry breaking. Phase transition in (phi)(sup 4) theory
[DE95-600856] p 2095 N95-24837
Tests for leptonic CP violation in tau decays
[DE95-005927] p 2050 N95-24902
Vortex solutions in two-Higgs-doublet systems
[DE94-634363] p 2096 N95-25107
R parity in standard-like superstring models
[DE94-628531] p 2096 N95-25215
Low energy properties of the heavy vector fermions
[DE94-634362] p 2051 N95-25290
CP violation tests for tau/top processes
[DE95-005924] p 2051 N95-25292
Tau as a probe for new physics
[DE95-005928] p 2051 N95-25296
Tau physics 1994: A theoretical perspective
[DE95-004840] p 2052 N95-25375
Study of the simplest realistic Higgs sector in quark-lepton symmetric models
[DE95-607159] p 2053 N95-25461
Anomalous WWZ couplings and K(sub L) yields mu(+) mu(-)
[DE95-607190] p 2054 N95-25464
Ten dimensional SO(10) G.U.T. models with dynamical symmetry breaking
[DE95-607093] p 2098 N95-25533
Cosmological constraints on perturbative supersymmetry breaking
[PB95-165361] p 2099 N95-25628
Dynamical chiral symmetry breaking in scale invariant quantum electrodynamics in sixth dimensions
[DE95-607133] p 2099 N95-25667
The off-shell axial anomaly via the (gamma)*(pi)(sup 0) (yields) (gamma) transition
[DE95-004762] p 2057 N95-25896
BRONZES
Accurate determination of IC modulation parameter in Sr(x)Ba(1-x)Nb2O6 from second order satellites of neutron diffraction TOF (Time-Of-Flight) spectra
[DE94-629003] p 2090 N95-25851
BROWNIAN MOVEMENTS
Quantum group random walks in strongly correlated 2+1 D spin systems
[DE95-607844] p 2091 N95-26103
BSCCO SUPERCONDUCTORS
Oxygen stoichiometry and its influence on superconductivity in Bi2Sr2CaCu2O(8+x)
[DE95-004660] p 2088 N95-25282
BUBBLES
Studies of two-phase gas-liquid flow in microgravity
[NASA-CR-195434] p 1963 N95-24906
BUCKLING
Design and evaluation of a foam-filled hat-stiffened panel concept for aircraft primary structural applications
[NASA-TM-109175] p 1928 N95-26251
Finite element buckling and postbuckling solutions for multilayered composite panels p 1983 N95-26264
Thermomechanical postbuckling of multilayered composite panels with cutouts p 1984 N95-26267
Nonlinear structural analysis on distributed-memory computers p 1985 N95-26272
Recent advances in the sensitivity analysis for the thermomechanical postbuckling of composite panels p 1985 N95-26274
Postbuckling and large-deflection nonlinear analyses on distributed-memory computers p 1986 N95-26276
Buckling and postbuckling of composite panels with cutouts subjected to combined edge shear and temperature change p 1987 N95-26280
Sensitivity analysis for large-deflection and postbuckling responses on distributed-memory computers p 1987 N95-26281
BUCKMINSTERFULLERENE
A photoemission study of the diamond and the single crystal C(60)
[DE95-006149] p 2085 N95-24463
BUDGETING
Integrated planning: A baseline development perspective
[DE95-004945] p 2102 N95-24905
BUILDINGS
Integrated passive/active vibration absorber for multi-story buildings
[NASA-TM-109178] p 1979 N95-24208
The fundamentals of modelling heat and moisture processes in structures
[IFTR-15/1994] p 1951 N95-26109
BUNCHING
Emittance growth caused by nonuniform charge distribution of bunched beam in linac
[DE95-602121] p 2072 N95-26095
BUOYANCY
Hydrodynamic instabilities in inertial confinement fusion
[DE95-003663] p 2078 N95-24667
BURGER EQUATION
Spectrum and energy transfer in steady Burgers turbulence
[NASA-CR-195047] p 1963 N95-24584
Nonlinear difference approximations for evolutionary PDE's
[DE95-005260] p 2033 N95-25676
BURNERS
A higher-order projection method for the simulation of unsteady turbulent nonpremixed combustion in an industrial burner
[DE95-005919] p 1931 N95-25291
User guide to the Burner Engineering Research Laboratory
[DE95-004191] p 1931 N95-25492
BUTANES
High octane ethers from synthesis gas-derived alcohols
[DE95-001146] p 1948 N95-24655

C

C BAND
Diurnal variations of backscattering properties of pine trees at C- and X-bands
[PB95-149738] p 1988 N95-24299
C++ (PROGRAMMING LANGUAGE)
Using and programming the SUPERCODE
[DE95-004342] p 2080 N95-25344
CABLES (ROPES)
Measurements of longitudinal static aerodynamic coefficients by the cable mount system
[NAL-TR-1226] p 1908 N95-25761
CALCIUM CHLORIDES
A study of the electrochemical behavior of tungsten in caustic solutions and platinum/iridium in ch loride solutions
[DE95-004951] p 1930 N95-25123
CALCIUM FLUORIDES
Temperature and dose dependence of metal colloid production in alpha-irradiated CaF2
[DE95-004907] p 2088 N95-25288
CALCIUM OXIDES
Processing and electrochemical properties of mixed conducting La(1-x)A(x)Co(1-y)Fe(y)O(3-delta) (A=Sr, Ca)
[DE95-004910] p 2088 N95-25002
Application of extended-crystal diffraction techniques to the symmetry and structure analysis of 221-PbBiSrCaCuO
[DE95-605913] p 2090 N95-25984
CALCULUS OF VARIATIONS
A brief survey of constrained mechanics and variational problems in terms of differential forms p 2026 N95-25803
CALIBRATING
A correction of the quantum efficiency of cesium iodide and other photocathodes due to the recalibration of the reference photomultipliers
[DE94-628177] p 1957 N95-24483
Metrology: Measurement assurance program guidelines
[NASA-RP-1364] p 1950 N95-24543
Absolute calibration and monitoring of a spectrometric channel using a photomultiplier
[DE94-628251] p 1968 N95-24635
Calibration of optical time domain reflectometers using time delay generator
[PB95-141776] p 2073 N95-24673
Hot-wire calibration in subsonic/transonic flow regimes
[NASA-CR-197725] p 1970 N95-25699
Video camera as a visual sensor, part 2
[NAL-TR-1231-PT-2] p 1970 N95-25763
Performance tests of air source heat pumps under frosting conditions. Quality of results
[PB95-141792] p 1995 N95-25892
Fission foil detector calibrations with high energy protons p 2060 N95-25924
Proton calibration of low energy neutron detectors containing (6)LiF p 2060 N95-25925
An analysis of the feasibility of using the Hsu-Nielsen calibration method in systems for measuring acoustic emission from partial discharges
[IFTR-20/1994] p 2040 N95-26071
Differential preamplifier and pre-emphasis network
[AD-A288780] p 1961 N95-26186
CALIFORNIA
Coso Monitoring Program, October 1992 through September 1993
[AD-A279147] p 1989 N95-24422
A numerical prediction of the precipitation and hydrology of California
[DE95-004966] p 2006 N95-25635
CALORIMETERS
Measurements of thermal conductivity of diamond thin films by the ac calorimetric method
[PB95-149746] p 1939 N95-24300
Test of an array of CsI(Tl) crystal towers for a low or medium energy e(+)e(-) collider calorimeter
[DE95-006068] p 2043 N95-24354
Energy resolution of a lead scintillating fiber electromagnetic calorimeter
[DE94-628253] p 1967 N95-24484
Software of a distributor of high voltage of the H C-600 hadronic calorimeter
[DE94-628255] p 1967 N95-24486
The KTeV PMT laser monitoring system
[DE95-004237] p 1972 N95-24869
Fire test of surface products: Comparison of data from the nordic box test and the cone calorimeter
[PB95-165239] p 1932 N95-26000
CAMERAS
Video camera as a visual sensor, part 2
[NAL-TR-1231-PT-2] p 1970 N95-25763
Partial camera automation in a simulated Unmanned Air Vehicle
[AD-A288786] p 1913 N95-26190
CANCER
Photonics: From target recognition to lesion detection p 2023 N95-25259
CANONICAL FORMS
Dissipative quantum mechanics: The generalization of the canonical quantization and von Neumann equation
[DE95-607008] p 2096 N95-25426
CAPACITANCE
The effect of the impedance of the generator and intermediate circuits on the impedance of plasma as it applies to magnetron sputtering of thin films in a radio-frequency field
[IFTR-8-1994] p 2083 N95-26019
CAPE KENNEDY LAUNCH COMPLEX
Study of launch site processing and facilities for future launch vehicles
[NASA-CR-198025] p 1918 N95-24579
CAPILLARY FLOW
Assessing capillary flow on printed wiring board surfaces
[DE94-015768] p 1959 N95-24712
Capillary flow on narrow strips and in V-shaped grooves
[DE95-000543] p 1935 N95-24716
CAPTURE EFFECT
Current status and future prospect of space and time reversal symmetry violation on low energy neutron reactions
[DE94-765589] p 2048 N95-24702
CARBENES
Group transfer and electron transfer reactions of organometallic complexes
[DE95-003732] p 2050 N95-25112
CARBOHYDRATES
Structural studies of complex carbohydrates of plant cell walls
[DE95-005545] p 2007 N95-24368
CARBON
Transmission electron microscope studies of extraterrestrial materials
[NASA-CR-188363] p 1928 N95-24222
Wear resistant composite structure of vitreous carbon containing convoluted fibers
[DE95-006255] p 1925 N95-24426
Characterization and performance of carbon films deposited by plasma and ion beam based techniques
[DE95-005213] p 1940 N95-24456
Carbons and hydrogen by persistent metal radicals
[DE95-003834] p 1929 N95-24553
Stainless steel recycle
[DE95-003905] p 1934 N95-24615
Disilene Addition to C70
[DE95-006321] p 2087 N95-24617
Recent advances in lithium ion technology
[DE95-004769] p 2054 N95-25470
Carbon taxes and India
[DE95-005401] p 2001 N95-25629
Development of a model of atmospheric oxygen variations to estimate terrestrial carbon storage and release
[NASA-CR-198002] p 2002 N95-25955
Surface plasmon observed for carbon nanotubes
[DE95-607769] p 2091 N95-26260

CARBON DIOXIDE
XAS studies of Ni(I), Ni(II), and Ni(III) complexes
[DE95-004844] p 1928 N95-24257
Study on the production of alternative fuels by carbon dioxide hydrogenation
[DE95-744284] p 1948 N95-24498
Investigation of technologies for CO2 separation, fixation and disposal for the prevention of global warming
[DE95-744285] p 1997 N95-24499
Supercritical carbon dioxide cleaning market assessment and commercialization/deployment plan
[DE94-017394] p 1998 N95-24653
Future emissions and concentrations of carbon dioxide: Key ocean/atmosphere/land analyses
[CSIRO-TP-31] p 1999 N95-25199
The effects on photosynthetic CO2 assimilation to long-term elevation of atmospheric CO2 concentration: An assessment of the response of Trifolium Repens L. CV. Blanca grown at F.A.C.E
[DE95-005687] p 2008 N95-25383
Heat release rate measurements in tunnel fires
[PB95-165106] p 1931 N95-25443
Development of novel active transport membrane devices
[DE95-002658] p 1932 N95-26093

CARBON DIOXIDE CONCENTRATION
Future emissions and concentrations of carbon dioxide: Key ocean/atmosphere/land analyses
[CSIRO-TP-31] p 1999 N95-25199
The effects on photosynthetic CO2 assimilation to long-term elevation of atmospheric CO2 concentration: An assessment of the response of Trifolium Repens L. CV. Blanca grown at F.A.C.E
[DE95-005687] p 2008 N95-25383
The whitehouse effect: Shortwave radiative forcing of climate by anthropogenic aerosols
[DE95-005998] p 2001 N95-25442

CARBON DIOXIDE LASERS
Engineering and design of a CO2 phase contrast interferometer system for DIII-D
[DE95-004249] p 1972 N95-24709

CARBON FIBER REINFORCED PLASTICS
Significance of varied thickness to damage tolerance of carbon fiber/epoxy laminates
[PB95-165460] p 1925 N95-24242
Study on tensile fatigue testing method of unidirectional fiber-resin matrix composites
[NAL-TR-1241] p 1926 N95-24989
Study on tensile fatigue testing method of unidirectional fiber-resin matrix composites
[NAL-TR-1241] p 1927 N95-25770

CARBON FIBERS
Significance of varied thickness to damage tolerance of carbon fiber/epoxy laminates
[PB95-165460] p 1925 N95-24242
Development of oxidation resistant SiC/C compositionally gradient materials
[DE94-785101] p 1925 N95-24365

CARBON ISOTOPES
Conductivity in insulators due to implantation of conducting species
[DE95-607773] p 1932 N95-26261

CARBON MONOXIDE
Heat release rate measurements in tunnel fires
[PB95-165106] p 1931 N95-25443

CARBON SUBOXIDES
Formation of thallium based high temperature superconductors using aerosol flow reacted precursor powders
[DE95-005901] p 2089 N95-25389

CARBON 13
The effect of O2 intercalation on the rotational Dynamics and the ordering transition of C60
[DE95-004765] p 2090 N95-25897

CARBON-CARBON COMPOSITES
Development of oxidation resistant SiC/C compositionally gradient materials
[DE94-785101] p 1925 N95-24365
Spacecraft materials studies on The Aerospace Corporation Tray on EOIM-3
[AD-A288682] p 1942 N95-26049

CARBONATES
Biospheric effects of a large extraterrestrial impact: Case study of the cretaceous/tertiary boundary crater
[NASA-CR-198015] p 1997 N95-24501
Intermediate-sized natural gas fueled carbonate fuel cell power plants
[DE95-004990] p 1996 N95-26171

CARBONYL COMPOUNDS
Group transfer and electron transfer reactions of organometallic complexes
[DE95-003732] p 2050 N95-25112

CARDIOVASCULAR SYSTEM
Thermal and vascular changes induced by the acclimation of the extremities to cold in man
[PB95-131587] p 2010 N95-24310

CARNOT CYCLE
Thermodynamic property evaluation and magnetic refrigeration cycle analysis for gadolinium gallium garnet
[DE95-005910] p 1951 N95-25367

CARRIER MOBILITY
Time-dependent numerical simulation of vertical cavity lasers
[DE95-006862] p 1973 N95-26112

CARTESIAN COORDINATES
On a generalized Kepler-Coulomb system: Inter basis expansions
[DE94-636739] p 2093 N95-24349

CASTING
Processing and properties of iridium alloys for space power applications
[DE95-005902] p 1935 N95-25390

CASTINGS
AMCC casting development, volume 2
[NASA-CR-197720] p 1938 N95-26068

CATALOGS (PUBLICATIONS)
NASA video catalog
[NASA-SP-7109(01)] p 2103 N95-24238
National Renewable Energy Laboratory Information Resources Catalogue. A collection of energy efficiency and renewable energy information resources
[DE94-011900] p 1990 N95-24305
Environment, 1980-1993
[DE95-605240] p 2002 N95-25779

CATALYSTS
Direct catalytic decomposition of nitric oxide
[DE95-005202] p 1928 N95-24286
Synthesis and characterization of Fe colloid catalysts in inverse micelle solutions
[DE95-006313] p 1929 N95-24614
Cross-flow, filter-sorbent-catalyst for particulate, SO2 and NO(x) control
[DE95-001934] p 2003 N95-26091

CATALYTIC ACTIVITY
Direct catalytic decomposition of nitric oxide
[DE95-005202] p 1928 N95-24286
High octane ethers from synthesis gas-derived alcohols
[DE95-001146] p 1948 N95-24655
Cross-flow, filter-sorbent-catalyst for particulate, SO2 and NO(x) control
[DE95-001934] p 2003 N95-26091

CATHODES
Recent advances in lithium ion technology
[DE95-004769] p 2054 N95-25470
A new method of emittance measurement for electron beams from the Micro-emitter
[DE94-792657] p 2070 N95-25631

CATHODIC COATINGS
Characterization and performance of carbon films deposited by plasma and ion beam based techniques
[DE95-005213] p 1940 N95-24456
Processing of LaCrO3 for solid oxide fuel cell applications
[DE95-000024] p 1992 N95-24683

CAUCHY PROBLEM
Saddle-point method in path integrals
[DE94-628379] p 2036 N95-24688
Behaviour at X= +/- infinity of solutions to a pr edator-prey model
[DE95-607049] p 2033 N95-25748

CAUCHY-RIEMANN EQUATIONS
Saddle-point method in path integrals
[DE94-628379] p 2036 N95-24688

CAVITIES
Effects of cavity dimensions, boundary layer, and temperature on cavity noise with emphasis on benchmark data to validate computational aeroacoustic codes
[NASA-CR-4653] p 2039 N95-24879

CAVITY FLOW
Effects of cavity dimensions, boundary layer, and temperature on cavity noise with emphasis on benchmark data to validate computational aeroacoustic codes
[NASA-CR-4653] p 2039 N95-24879

CD-ROM
CD-ROM in the age of internet
[DE95-005067] p 2104 N95-24454
Applications for electronic documents
[DE95-005036] p 2106 N95-25765

CELL MEMBRANES (BIOLOGY)
Contribution of ankyrin-band 3 complexes to the organization and mechanical properties of the membrane skeleton of human erythrocyte
[DE95-005835] p 2010 N95-24427

CELLS (BIOLOGY)
Structures and functions of oligosaccharins
[DE95-003140] p 2007 N95-24225
Structural studies of complex carbohydrates of plant cell walls
[DE95-005545] p 2007 N95-24368
Electrophoretic separation of cells and particles from rat pituitary --- analysis of pituitary cell electrophoresis experiment done on IML-2 (7/94)
[NASA-CR-197975] p 2008 N95-24475

CELLULOSE
Structural studies of complex carbohydrates of plant cell walls
[DE95-005545] p 2007 N95-24368

CENTRAL EUROPE
JPRS report: Science and technology. Central Eurasia
[JPRS-UST-95-006] p 1950 N95-24731

CENTRAL PROCESSING UNITS
Downsizing systems and expected opposition to introduction
[DE95-730186] p 2104 N95-24494
Parallel processing for scientific computations
[NASA-CR-198013] p 2020 N95-24563

CERAMIC COATINGS
PVD TBC experience on GE aircraft engines
p 1944 N95-26126
Properties of plasma sprayed bond coats
p 1946 N95-26135
Thermal fracture mechanisms in ceramic thermal barrier coatings p 1946 N95-26138
Thermal barrier coating life modeling in aircraft gas turbine engines p 1947 N95-26140

CERAMIC MATRIX COMPOSITES
Thermomechanical fatigue behavior of three CFCC's
[NASA-CR-195441] p 1927 N95-25880

CERAMICS
Investigation of properties and performance of ceramic composite components
[DE95-004737] p 1939 N95-24247
Au/Cr sputter coating for the protection of alumina during sliding at high temperatures
[NASA-TM-106853] p 1923 N95-24437
Development of sensors for ceramic components in advanced propulsion systems. Phase 2: Temperature sensor systems evaluation
[NASA-CR-195283] p 1967 N95-24473
Activities of the Ceramic Technology Project
[DE95-003394] p 1940 N95-24588
Feasibility of ceramic joining with high energy electron beams
[DE95-004519] p 1940 N95-24717
Study of composite zirconium oxide
[DE95-730104] p 1926 N95-25111
Processing and characterization of transformation-toughened ceramics with strength retention to elevated temperatures
[DE95-005758] p 1941 N95-25387
Whisker reinforced glass ceramic
[DE95-005568] p 1927 N95-25998
Measurements of acoustic emission on a laser ceramic treatment line
[IFTR-28/1994] p 2040 N95-26180

CEREBRUM
Non-invasive detection of increased intracranial pressure using acoustical techniques
[AD-A279292] p 2010 N95-24309

CERENKOV COUNTERS
Milagro: A low energy threshold extensive air shower array
[DE95-005246] p 2110 N95-25675

CERENKOV RADIATION
Field equipotentials of a fast-moving charge in medium
[DE94-636737] p 2065 N95-24348
Detector for transit time measurement of photomultiplier single-photoelectron pulses
[DE94-628256] p 2073 N95-24642
The emission of particle identification efficiency in the EXCHARM experiment
[DE94-628258] p 2047 N95-24644
Milagro: A low energy threshold extensive air shower array
[DE95-005246] p 2110 N95-25675
Nonlinear analysis of millimeter and sub-millimeter wave sources such as Cerenkov masers, orotrons, and ubitrons
[AD-A288777] p 1974 N95-26114

CERIUM
LuAlO3: A high density, high speed scintillator for gamma detection
[DE95-004678] p 2064 N95-26256

CERIUM OXIDES
Thin film ionic conductors based on cerium oxide
[DE95-003668] p 2086 N95-24514

CERTIFICATION
Consistent approach to describing aircraft HIRF protection
[NASA-CR-195067] p 1909 N95-25341

CESIUM COMPOUNDS
Cesium cobaltdicarbollide-solubility, precipitation, and reactivity in basic aqueous solution
[DE95-005881] p 1929 N95-24430

CESIUM IODIDES
Electric field effects on the quantum efficiency of Cesium-iodide photocathodes in gas media
[DE94-628176] p 1957 N95-24482
A correction of the quantum efficiency of cesium iodide and other photocathodes due to the recalibration of the reference photomultipliers
[DE94-628177] p 1957 N95-24483
CESIUM ISOTOPES
Test of an array of CsI(Tl) crystal towers for a low or medium energy e(+)e(-) collider calorimeter
[DE95-006068] p 2043 N95-24354
CHANNEL FLOW
A well-posed numerical method to track isolated conformal map singularities in Hele-Shaw flow
[NASA-CR-195035] p 2032 N95-25114
CHAOS
Decoherence, determinism and chaos revisited
[DE95-006070] p 2094 N95-24578
Flare stars and Pascal distribution
[DE95-607044] p 2110 N95-25431
Optical instabilities and chaos due to the virtual formation of biexcitons
[DE95-607664] p 2063 N95-25994
CHARACTER RECOGNITION
Document analysis with neural net circuits
p 2023 N95-25256
CHARACTERISTICS
Dynamic methods for determining the material characteristics of saturated permeable media
[IFTR-17/1993] p 1932 N95-26107
CHARACTERIZATION
Synthesis and characterization of Fe colloid catalysts in inverse micelle solutions
[DE95-006313] p 1929 N95-24614
CHARGE CARRIERS
A theoretical analysis of strain in GaN and its effects on carrier conductivity
[AD-A288769] p 2090 N95-26061
CHARGE COUPLED DEVICES
Stereo imaging velocimetry for microgravity applications
[NASA-TM-110494] p 1949 N95-24416
CHARGE DISTRIBUTION
On the central charge in 3 D-supersymmetry
[DE95-600851] p 2093 N95-24352
Over-compression, a method to shape the longitudinal bunch distribution for a reduced energy spread
[DE95-006052] p 2066 N95-24572
Emittance growth caused by nonuniform charge distribution of bunched beam in linac
[DE95-602121] p 2072 N95-26095
CHARGE EXCHANGE
Results obtained using the pellet charge exchange diagnostic on TFTR
[DE95-003254] p 2079 N95-25120
CHARGED PARTICLES
Advances and prospects in reversed field pinch research
[DE95-007017] p 2077 N95-24602
New physics effects on CP Violation in B decays
[DE94-628617] p 2049 N95-24722
Tests for leptonic CP violation in tau decays
[DE95-005927] p 2050 N95-24902
Neutrino optics
[DE95-004236] p 2073 N95-25239
Fast algorithms for transport models
[DE95-007064] p 2054 N95-25479
A superfield generalization of the classical action-at-a-distance theory
[DE95-607084] p 1955 N95-25648
Dynamics of nonadiabatic charged particles in the magnetic dipole field with imposed homogeneous magnetic field
[DE95-605222] p 2057 N95-25778
Charge-Dyon system as the reduced oscillator
[DE95-606998] p 2100 N95-25987
CHARM (PARTICLE PHYSICS)
On leading charmed meson production in pi-nucleon interactions
[DE94-636797] p 2043 N95-24360
A measurement of the left-right, forward-backward asymmetry for charm quarks using D(*+) and D(+) mesons
[DE95-006061] p 2046 N95-24575
The emission of particle identification efficiency in the EXCHARM experiment
[DE94-628258] p 2047 N95-24644
Search for the prompt muon antineutrino from charm particle decays at the IHEP-JINR Neutrino detector in 70 GeV proton beam-dump experiment
[DE94-628772] p 2049 N95-24889
Probing new physics in rare charm processes
[DE95-006067] p 2050 N95-24903
Elementary particle physics
[DE95-004376] p 2051 N95-25241
B physics with CDF: Recent results and future prospects
[DE95-004793] p 2051 N95-25372
Photon-charm production in p(anti p) collisions at radical s = 1.8 TeV
[DE95-004850] p 2052 N95-25377
Annihilation diagrams in two-body nonleptonic decays of charmed mesons
[DE95-607181] p 2054 N95-25463
CHARTS
Mapping, charting and geodesy handbook
[AD-A286558] p 1989 N95-24502
CHEBYSHEV APPROXIMATION
A conservative staggered-grid Chebyshev multidomain method for compressible flows
[NASA-CR-195060] p 2030 N95-24632
CHECKOUT
Debugging the virtual machine
[DE95-002193] p 2016 N95-24898
Reliability analysis of software based safety functions
[DE95-606516] p 2018 N95-26045
CHELATION
Effects of acetylacetone additions on PZT thin film processing
[DE95-006322] p 1941 N95-25370
CHEMICAL ANALYSIS
Gamma spectrum analysis including NAA with SAMPO for windows
[PB95-149720] p 2042 N95-24298
Simple chemical assays for presence of S2F10 in decomposed SF6
[DE95-001423] p 1929 N95-24345
Co-firing high sulfur coal with refuse derived fuels
[DE95-006243] p 1997 N95-24406
Standardization of equations for radiochemical calculations
[DE95-003028] p 1930 N95-25097
Field-usable portable analyzer for chlorinated organic compounds
[DE95-003127] p 1930 N95-25098
Use of mass spectrometric methods for field screening of VOC's
[DE95-004903] p 1999 N95-25249
Measurement of blood nitrogen content after rapid compressions to assess the speed of nitrogen uptake during the compression phase of submarine escape. (Includes measurement of nitrogen concentration in blood following rapid compression to 5 bar)
[PB95-165726] p 2012 N95-25570
Activities of the Radiation Laboratory Department of Nuclear Engineering Kyoto University
[DE95-709896] p 2072 N95-26163
Activities of the Radiation Laboratory Department of Nuclear Engineering Faculty of Engineering, Kyoto University
[DE95-709897] p 2072 N95-26164
CHEMICAL CLEANING
Parts washing alternatives study: United States Coast Guard. Project summary and report
[PB95-166146] p 1942 N95-26004
CHEMICAL COMPOSITION
Simple chemical assays for presence of S2F10 in decomposed SF6
[DE95-001423] p 1929 N95-24345
Entropy and enthalpy of adsorption of gaseous chlorides of metals on quartz glass as a function of the molecular composition
[DE94-627162] p 2093 N95-24481
CHEMICAL EXPLOSIONS
Explosive performance measurements on large, multiple-hole arrays and large masses of conventional explosive
[DE95-002718] p 1948 N95-24670
CHEMICAL FRACTIONATION
Development of novel active transport membrane devices
[DE95-002658] p 1932 N95-26093
CHEMICAL REACTIONS
Implementation of a parallel algorithm for thermo-chemical nonequilibrium flow simulations
[DE95-004758] p 1961 N95-24262
Simple chemical assays for presence of S2F10 in decomposed SF6
[DE95-001423] p 1929 N95-24345
Carbons and hydrogen by persistent metal radicals
[DE95-003834] p 1929 N95-24553
Bioprocessing in nonaqueous media: Critical needs and opportunities
[DE95-004878] p 2008 N95-24843
Some aspects of the hot corrosion of thermal barrier coatings p 1946 N95-26137
CHEMISORPTION
An investigation of the effect of surface impurities on the adsorption kinetics of hydrogen chemisorbed onto iron
[NASA-CR-197967] p 1933 N95-24400
CHEMISTRY
JPRS report: Science and technology. Central Eurasia
[JPRS-UST-95-017] p 1988 N95-26080
CHIPS (ELECTRONICS)
Smart vision chips: An overview p 2024 N95-25265
CHIRAL DYNAMICS
Chiral limit of QCD
[DE95-005245] p 2094 N95-24610
Parity doubling from thermodynamics of experimental hadron spectrum
[DE95-600934] p 2095 N95-24839
Chiral symmetry on the lattice
[DE95-003962] p 2087 N95-24849
Meson properties at finite temperature and density within Nambu-Jona-Lasinio model
[DE94-628630] p 2049 N95-24888
CHIRALITY
Update on B(sub K) with Wilson fermions
[DE95-004953] p 2085 N95-24451
Chiral symmetry on the lattice
[DE95-003962] p 2087 N95-24849
Dynamical chiral symmetry breaking in scale invariant quantum electrodynamics in sixth dimensions
[DE95-607133] p 2099 N95-25667
Heavy-neutrino chirality enhancement of the decay K(L) yields e(mu) in left-right symmetric models
[PB95-165387] p 2064 N95-26096
CHIRP
Type P dispersive delay lines p 1959 N95-25116
CHLORIDES
Entropy and enthalpy of adsorption of gaseous chlorides of metals on quartz glass as a function of the molecular composition
[DE94-627162] p 2093 N95-24481
CHLOROCARBONS
Field-usable portable analyzer for chlorinated organic compounds
[DE95-003127] p 1930 N95-25098
CHLOROFLUOROCARBONS
Responsibility means doing without: How to rescue the ozone-layer
[PB95-166807] p 1997 N95-24334
Materials Compatibility and Lubricants Research (MCLR) Program
[DE95-004862] p 1941 N95-25243
CHROMATOGRAPHY
Modeling of the simulated countercurrent moving-bed chromatographic reactor used for the oxidative coupling of methane
[DE95-004930] p 1924 N95-25286
CHROMIUM
Au/Cr sputter coating for the protection of alumina during sliding at high temperatures
[NASA-TM-106853] p 1923 N95-24437
Structural and thermodynamic properties of 3-d transition metals: Pseudopotential theory revisited
[DE95-605639] p 1937 N95-25983
CHROMIUM ALLOYS
Localized corrosion and stress corrosion cracking characteristics of a low-aluminum-content iron-aluminum alloy
[DE95-003259] p 1934 N95-24647
CHROMIUM OXIDES
Processing of LaCrO3 for solid oxide fuel cell applications
[DE95-000024] p 1992 N95-24683
CIRCLES (GEOMETRY)
Inversion of circular averages and application of backprojection methods to radar imaging
[PB95-141578] p 1955 N95-25891
Describing the macroscopic world: Closing the circle within the dynamical reduction program
[DE95-606997] p 2100 N95-26046
CIRCUIT BOARDS
Crosstalk on printed circuit boards
[PB95-165171] p 1960 N95-25472
The evaluation of potential limonene scavengers
[DE95-006853] p 2002 N95-25899
CIRCUIT RELIABILITY
Fifth European Symposium on Reliability of Electron Devices, Failure Physics and Analysis
[AD-A286614] p 1956 N95-24447
CIRCUITS
An optimized implementation of a fault-tolerant clock synchronization circuit
[NASA-TM-109176] p 2019 N95-24382
Differential preamplifier and pre-emphasis network
[AD-A288780] p 1961 N95-26186
CIRCULAR ORBITS
Neural network technique for orbit correction in accelerators/storage rings
[DE95-005955] p 2026 N95-25368
CIRCULAR POLARIZATION
Experimental study of tapered slot elements
[PB95-165163] p 1955 N95-25644

CIRRUS CLOUDS
Preliminary analysis of University of North Dakota aircraft data from the FIRE Cirrus IFO-2
[NASA-CR-198038] p 2005 N95-24219
Replicator for characterization of cirrus and polar stratospheric cloud particles
[NASA-CR-197992] p 2005 N95-24411
Nucleation and growth of crystals under cirrus and polar stratospheric cloud conditions
[NASA-CR-197991] p 2085 N95-24478

CIVIL DEFENSE
Planning for the unknown: Coping with uncertainty
[PB95-165114] p 2102 N95-25642

CLADDING
Processing and properties of iridium alloys for space power applications
[DE95-005902] p 1935 N95-25390

CLASSICAL MECHANICS
Elliptic deformed Newton mechanics in the three-dimensional phase space
[DE94-636741] p 2092 N95-24313
On q-deformed supersymmetric classical mechanical models
[DE95-600864] p 2095 N95-24838
Quantum symplectic geometry. 1: The matrix Hamiltonian formalism
[DE95-607009] p 2032 N95-25427
Testing quantum behaviour at the macroscopic level
[DE95-607005] p 2097 N95-25453

CLASSIFICATIONS
Neural network classification of clinical neurophysiological data for acute care monitoring
p 2024 N95-25263
Temporal pacing in visual attention
[AD-A289785] p 2013 N95-26041
National standard and code compliance for electrical equipment installed in hazardous locations for the void fraction instrument
[DE95-002158] p 1960 N95-26092

CLEAN ENERGY
Spray characteristics of single- and three-hole nozzle injectors in ambient air and in a motored single-cylinder test engine
[PB95-166286] p 1976 N95-25574

CLEAN FUELS
Alternatives to traditional transportation fuels 1993
[DE95-005445] p 1947 N95-24273

CLEANERS
Parts washing alternatives study: United States Coast Guard. Project summary and report
[PB95-166146] p 1942 N95-26004

CLEANING
Supercritical carbon dioxide cleaning market assessment and commercialization/deployment plan
[DE94-017394] p 1998 N95-24653

CLEBSCH-GORDAN COEFFICIENTS
On a generalized Kepler-Coulomb system: Inter basis expansions
[DE94-636739] p 2093 N95-24349

CLIMATE
Microphysical and compositional influences on shortwave radiative forcing of climate by sulfate aerosols
[DE95-005999] p 1997 N95-24570
Impacts of microphysics, radiation and environmental winds in mid-latitude and tropical squall-line systems, and their climatic implications
[DE95-004965] p 2005 N95-25287

CLIMATE CHANGE
Global ocean circulation and equator-pole heat transport as a function of ocean GCM resolution
[DE95-004198] p 2000 N95-25279
Impacts of microphysics, radiation and environmental winds in mid-latitude and tropical squall-line systems, and their climatic implications
[DE95-004965] p 2005 N95-25287
Sector-specific issues and reporting methodologies supporting the General Guidelines for the voluntary reporting of greenhouse gases under Section 1605(b) of the Energy Policy Act of 1992, volume 1. Part 1: Electricity supply sector. Part 2: Residential and commercial buildings sector. Part 3: Industrial sector
[DE95-003296] p 2000 N95-25362
The whitehouse effect: Shortwave radiative forcing of climate by anthropogenic aerosols
[DE95-005998] p 2001 N95-25442
Our changing planet: The FY 1995 U.S. Global Change Research Program p 2002 N95-25852

CLIMATE MODELS
Computational load in model physics of the parallel NCAR community climate model
[DE95-005410] p 2019 N95-24342
Use of cloud observations and mesoscale meteorology models to evaluate and improve cloud parameterizations
[DE95-006256] p 2005 N95-24613
Global ocean circulation and equator-pole heat transport as a function of ocean GCM resolution
[DE95-004198] p 2000 N95-25279
Intercomparison of hydrologic processes in global climate models
[NASA-TM-104617] p 2005 N95-26341

CLIMATOLOGY
Preliminary analysis of University of North Dakota aircraft data from the FIRE Cirrus IFO-2
[NASA-CR-198038] p 2005 N95-24219
Assessment of climate variability of the Greenland ice sheet: Integration of in situ and satellite data
[NASA-CR-198020] p 1998 N95-24846

CLINICAL MEDICINE
Neural network classification of clinical neurophysiological data for acute care monitoring
p 2024 N95-25263
Activities of the National Institute of Radiological Sciences
[DE95-709916] p 2072 N95-26165

CLOCKS
An optimized implementation of a fault-tolerant clock synchronization circuit
[NASA-TM-109176] p 2019 N95-24382

CLOUD COVER
Preliminary analysis of University of North Dakota aircraft data from the FIRE Cirrus IFO-2
[NASA-CR-198038] p 2005 N95-24219
Use of cloud observations and mesoscale meteorology models to evaluate and improve cloud parameterizations
[DE95-006256] p 2005 N95-24613
The whitehouse effect: Shortwave radiative forcing of climate by anthropogenic aerosols
[DE95-005998] p 2001 N95-25442

CLOUD PHYSICS
Preliminary analysis of University of North Dakota aircraft data from the FIRE Cirrus IFO-2
[NASA-CR-198038] p 2005 N95-24219
Report series in aerosol science
[DE95-737628] p 1999 N95-24904
Impacts of microphysics, radiation and environmental winds in mid-latitude and tropical squall-line systems, and their climatic implications
[DE95-004965] p 2005 N95-25287

CLOUDS (METEOROLOGY)
Airborne imaging of tropospheric emission at millimeter and submillimeter wavelengths
[NASA-TM-110498] p 2003 N95-24336
Use of cloud observations and mesoscale meteorology models to evaluate and improve cloud parameterizations
[DE95-006256] p 2005 N95-24613
Effects of nitric acid vapor on the formation of cloud droplets in troposphere
[DE95-744869] p 2001 N95-25500
Design and development of a cloud reference library and support for cloud and simulation communities. Summary report
[AD-A288704] p 2006 N95-26012

CLUSTER ANALYSIS
Clustering using winner-take-all units
[PB95-165403] p 2026 N95-25568

CLUTTER
Multispectral detection of ground targets in highly correlated backgrounds
[AD-A289292] p 1990 N95-26040
Implementation of scene shadows in the Target Acquisition TDA (TARGAC)
[AD-A288760] p 1912 N95-26060

COAL
Co-firing high sulfur coal with refuse derived fuels
[DE95-006243] p 1997 N95-24406
High octane ethers from synthesis gas-derived alcohols
[DE95-001146] p 1948 N95-24655

COALESCING
A mechanism of collisionless magnetic reconnection
[NIFS-274] p 2083 N95-26339

COATING
Robotic weld overlay coatings for erosion control
[DE95-005187] p 1939 N95-24285
Magnetically controlled deposition of metals using gas plasma
[DE95-003827] p 2077 N95-24552

COATINGS
FNAS phase partitions
[NASA-CR-193855] p 1940 N95-24562
Method for determining shear direction using liquid crystal coatings
[NASA-CASE-ARC-11995-1] p 2075 N95-26117

COBALT
Cobalt release from PCA steel during possible fusion reactor accidents
[DE95-005019] p 2069 N95-25365

COBALT COMPOUNDS
Cesium cobaltdicarbollide-solubility, precipitation, and reactivity in basic aqueous solution
[DE95-005881] p 1929 N95-24430

COBALT ISOTOPES
Cobalt release from PCA steel during possible fusion reactor accidents
[DE95-005019] p 2069 N95-25365

COBALT OXIDES
Processing and electrochemical properties of mixed conducting La(1-x)A(x)Co(1-y)Fe(y)O(3-delta) (A=Sr, Ca)
[DE95-004910] p 2088 N95-25002

COBALT 60
Antioxidant and sensitizer effect on the stability of natural rubber latex vulcanized by gamma rays
[DE94-636061] p 1939 N95-24373

COCKPITS
A crew-centered flight deck design philosophy for High-Speed Civil Transport (HSCT) aircraft
[NASA-TM-109171] p 1910 N95-24582

COEFFICIENT OF FRICTION
Wear-resistant, self-lubricating surfaces of diamond coatings
[NASA-TM-106887] p 1924 N95-25961

COEFFICIENTS
Numerical solution of the optimized random phase approximation
[DE95-605636] p 2034 N95-25982

COERCIVITY
Coercive field and domain wall properties in (Dy(x)Y(1-x))Fe2 and (Er(x)Y(1-x))Fe2
[DE95-601135] p 1937 N95-25751

COGENERATION
Small gas turbine component evaluation study
[PB95-147542] p 1913 N95-24293
Simulation of diurnal thermal energy storage systems: Preliminary results
[DE95-005751] p 1991 N95-24369

COGNITION
Cognitive diagnosis combined with latent trait theory and multiphase responses
[AD-A288701] p 2013 N95-26010
Instructable autonomous agents
[NASA-CR-197802] p 2019 N95-26206

COHERENT RADAR
Laser based methods for range, Doppler and vibration measurements
[PB95-141958] p 1952 N95-24445

COHERENT RADIATION
Automatic measurement system for measuring of the nonlinearity of photo detectors
[PB95-165197] p 2074 N95-25999

COHESION
Atomistic studies of grain boundaries in NiAl
[DE95-005208] p 1937 N95-26014

COINING
New techniques to test fatigue properties of coined sheet specimens. Part 2: Comparison of different materials, forming operations and life prediction techniques for a simple test geometry
[PB95-165122] p 1982 N95-25444
New techniques to test fatigue properties of coined sheet specimens. Part 4: Development of experimental techniques
[PB95-165130] p 1982 N95-25445
New techniques to test fatigue properties of coined sheet specimens. Part 3: Fatigue testing and analysis of a component like coining in sheet steel materials
[PB95-165668] p 1982 N95-25569

COLD ACCLIMATIZATION
Thermal and vascular changes induced by the acclimation of the extremities to cold in man
[PB95-131587] p 2010 N95-24310

COLD WATER
Thermal and vascular changes induced by the acclimation of the extremities to cold in man
[PB95-131587] p 2010 N95-24310

COLD WORKING
Creep properties of 20% cold worked hastelloy XR
[DE94-785198] p 1933 N95-24338

COLLAPSE
Core-collapse supernovae and nucleosynthesis
[NASA-CR-197731] p 2109 N95-25122
Strong phase correlations of solitons of nonlinear Schroedinger equation
[DE95-607002] p 2063 N95-25991

COLLIMATORS
Bremsstrahlung scattering calculations for the beam stops and collimators in the APS insertion-device beamlines
[DE95-005471] p 2069 N95-25300

COLLISION PARAMETERS
Measurement of the SS-OS Dijet cross-section ratio
[DE95-004852] p 2041 N95-24253

COLLISIONAL PLASMAS
Experimental and theoretical study of plasma-water interaction in electrothermal guns
| DE94-628961 | p 2078 N95-24706
COLLISIONLESS PLASMAS
Particle acceleration very near an x-line in a collisionless plasma
| ATR-92(7251)-4 | p 2080 N95-25325
Magnetic mirror effect as a trigger of collisionless magnetic reconnection
| NIFS-295 | p 2083 N95-26337
A mechanism of collisionless magnetic reconnection
| NIFS-274 | p 2083 N95-26339
COLLISIONS
Aircraft accident report: Impact with blast fence upon landing rollout Action Air Charters flight 980 Piper PA-31-350, N990RA, Stratford, Connecticut,27 April 1994
| PB94-910410 | p 1908 N95-24206
Measurement of the SS-OS Dijet cross-section ratio
| DE95-004852 | p 2041 N95-24253
Vacuum polarization effects in low-energy muonic atom collisions
| DE95-605393 | p 2058 N95-25910
COLLOIDS
Synthesis and characterization of Fe colloid catalysts in inverse micelle solutions
| DE95-006313 | p 1929 N95-24614
Design of supramolecular ordered systems for mesoscopic colloids and molecular composites
| DE95-004448 | p 2048 N95-24687
Temperature and dose dependence of metal colloid production in alpha-irradiated CaF2
| DE95-004907 | p 2088 N95-25288
COLOR
Colour vision deficiencies: Matching and confusion of computer colours
| PB95-141925 | p 2013 N95-24864
COLOR VISION
Colour vision deficiencies: Matching and confusion of computer colours
| PB95-141925 | p 2013 N95-24864
COLORIMETRY
Measurements of thermal conductivity of diamond thin films by the ac calorimetric method
| PB95-149746 | p 1939 N95-24300
COMBINATORIAL ANALYSIS
Measurement accuracy, bit-strings, Manthey's quaternions, and RRQM
| DE95-006211 | p 2098 N95-25530
COMBUSTION
Stratified charge rotary engine combustion studies
| NASA-CR-197985 | p 1974 N95-24223
Diesel fuel component contribution to engine emissions and performance
| DE95-000238 | p 1998 N95-24604
Nonequilibrium multiphase mixture modeling of energetic material response
| DE95-003353 | p 1948 N95-24608
Temperature bounds in a model of laminar flames
| DE95-607048 | p 1931 N95-25447
Workshop report: Measurement techniques in highly transient, spectrally rich combustion environments
| AD-A288395 | p 1969 N95-25606
Plasma burning and control in reactor core
| DE95-602882 | p 2082 N95-25942
COMBUSTION CHAMBERS
Stratified charge rotary engine combustion studies
| NASA-CR-197985 | p 1974 N95-24223
Effect of density gradients in confined supersonic shear layers, part 1
| NASA-CR-198029 | p 1962 N95-24412
Effect of density gradients in confined supersonic shear layers. Part 2: 3-D modes
| NASA-CR-198030 | p 1962 N95-24413
Numerical simulation of flow and the effect of baffle arrangement on pressure drop and temperature pattern in a circular combustor p 1963 N95-24628
A review of chemically reactive turbulent flow analysis, mixing mechanisms and modeling, and a new design of low NOx combustor for non-premixed reactants p 1963 N95-24762
Scaling in a scramjet combustor p 1933 N95-25398
TBC experience in land based gas turbines p 1944 N95-26127
Thick thermal barrier coatings for diesel engines p 1946 N95-26136
COMBUSTION CHEMISTRY
Combustion characteristics of metallized hydrocarbon fuels
| NAL-TR-1224 | p 1949 N95-25769
COMBUSTION PHYSICS
Report series in aerosol science
| DE95-737628 | p 1999 N95-24904
Temperature bounds in a model of laminar flames
| DE95-607048 | p 1931 N95-25447
Workshop report: Measurement techniques in highly transient, spectrally rich combustion environments
| AD-A288395 | p 1969 N95-25606
COMBUSTION PRODUCTS
Co-firing high sulfur coal with refuse derived fuels
| DE95-006243 | p 1997 N95-24406
Diesel fuel component contribution to engine emissions and performance
| DE95-000238 | p 1998 N95-24604
COMBUSTION STABILITY
A review of chemically reactive turbulent flow analysis, mixing mechanisms and modeling, and a new design of low NOx combustor for non-premixed reactants p 1963 N95-24762
COMBUSTION SYNTHESIS
Processing and electrochemical properties of mixed conducting La(1-x)A(x)Co(1-y)Fe(y)O(3-delta) (A = Sr, Ca)
| DE95-004910 | p 2088 N95-25002
COMMAND AND CONTROL
Flexible architectures for sensor fusion in theater missile defense
| AD-A288666 | p 2007 N95-26048
COMMAND MODULES
Apollo 13: Houston, we've got a problem
| NASA-TM-110551 | p 1918 N95-24215
Apollo 12: Pinpoint for science
| NASA-TM-110576 | p 1917 N95-25424
COMMERCIAL AIRCRAFT
Consistent approach to describing aircraft HIRF protection
| NASA-CR-195067 | p 1909 N95-25341
Emerging nondestructive inspection for aging aircraft
| PB95-143053 | p 1905 N95-25401
COMMERCIAL ENERGY
Sector-specific issues and reporting methodologies supporting the General Guidelines for the voluntary reporting of greenhouse gases under Section 1605(b) of the Energy Policy Act of 1992, volume 1. Part 1: Electricity supply sector. Part 2: Residential and commercial buildings sector. Part 3: Industrial sector
| DE95-003296 | p 2000 N95-25362
Nuclear energy and the environment
| DE95-600438 | p 2001 N95-25615
COMMERCIAL SPACECRAFT
Use of advanced solar cells for commercial communication satellites
| NASA-TM-106879 | p 1991 N95-24560
Assessment of Commercial Satellite Communications Initiative (CSCI) studies
| AD-A288357 | p 1920 N95-25508
COMMUNICATING
Final report and recommendations of the ESnet Authentication Pilot Project
| DE95-005755 | p 2103 N95-24370
COMMUNICATION NETWORKS
Discrete-event-dynamic-system-based approaches for control in integrated voice/data multihop Radio Networks
| AD-A288389 | p 1954 N95-25604
COMMUNICATION SATELLITES
Use of advanced solar cells for commercial communication satellites
| NASA-TM-106879 | p 1991 N95-24560
ESRO's telecommunications programme and the OTS project (1970-1974)
| ESA-HSR-13 | p 1953 N95-24893
Towards an era of global village: The dynamics of world telecommunications and its implications for the future of nation state
| PB95-165064 | p 1954 N95-25482
Assessment of Commercial Satellite Communications Initiative (CSCI) studies
| AD-A288357 | p 1920 N95-25508
COMMUTATION
On connection of q-deformed para oscillators with para oscillators
| DE95-607007 | p 2096 N95-25425
On D=2 (1/3, 1/3) supersymmetric theories 1
| DE95-607075 | p 2036 N95-25522
COMMUTATORS
Realistic NN potential for the Low approach
| DE94-628606 | p 2049 N95-24720
COMMUTER AIRCRAFT
Emerging nondestructive inspection for aging aircraft
| PB95-143053 | p 1905 N95-25401
COMPACTING
Nonequilibrium multiphase mixture modeling of energetic material response
| DE95-003353 | p 1948 N95-24608
COMPARISON
Feed system design for a reduced pressure tank p 1923 N95-26310
COMPASSES
Interfacing a digital compass to a remote-controlled helicopter
| PB95-164927 | p 1914 N95-24260
COMPILERS
Debugging the virtual machine
| DE95-002193 | p 2016 N95-24898
Designing a stencil compiler for the Connection Machine model CM-5
| DE95-006861 | p 2021 N95-25477
COMPLEX COMPOUNDS
Electron spin resonance of radicals and metal complexes
| DE95-605640 | p 2055 N95-25499
COMPLEX NUMBERS
A note on the total least squares problem for coplanar points
| DE95-004876 | p 2032 N95-25251
Monte Carlo simulations with indefinite and complex-valued measures
| DE95-607056 | p 2017 N95-25448
COMPONENT RELIABILITY
Fifth European Symposium on Reliability of Electron Devices, Failure Physics and Analysis
| AD-A286614 | p 1956 N95-24447
Background information to reliability stress screening of components: A guide for component users. Nordtest project 1140-93
| PB95-165775 | p 1978 N95-26002
Proposed Nordtest method: Reliability stress screening of components. A guide for component users. Nordtest project 1140-93
| PB95-165783 | p 1978 N95-26003
COMPOSITE MATERIALS
NASA-UVA light aerospace alloy and structures technology program (LA2ST)
| NASA-CR-198041 | p 1933 N95-24220
Investigation of properties and performance of ceramic composite components
| DE95-004737 | p 1939 N95-24247
Development of oxidation resistant SiC/C compositionally gradient materials
| DE94-785101 | p 1925 N95-24365
JPRS report: Science and technology. Central Eurasia
| JPRS-UST-94-018 | p 1950 N95-24472
Composite materials flown on the Long Duration Exposure Facility
| NASA-CR-4657 | p 1923 N95-24583
Optical properties of fractal nanocomposites
| DE95-005414 | p 1926 N95-25295
Method and apparatus for non-destructive evaluation of composite materials with cloth surface impressions
| NASA-CASE-LAR-14535-1 | p 1926 N95-25305
Processing and characterization of transformation-toughened ceramics with strength retention to elevated temperatures
| DE95-005758 | p 1941 N95-25387
Synthesis and processing of Al2O3/Al composites by in situ reaction of aluminum and mullite
| DE95-006224 | p 1937 N95-25775
LH2 fuel tank design for SSTO p 1987 N95-26309
COMPOSITE PROPELLANTS
Space shuttle propellant constitutive law verification tests
| NASA-CR-198047 | p 1947 N95-24226
COMPOSITE STRUCTURES
Investigation of properties and performance of ceramic composite components
| DE95-004737 | p 1939 N95-24247
Response to a localized impact loading of a composite multilayered rotational shell structure: Theory and numerical methods, volume 1
| ONERA-NT-1994-10-VOL-1 | p 1979 N95-24282
Response to a localized impact loading of a composite multilayered rotational shell structure: Theory and numerical methods, volume 2
| ONERA-NT-1994-10-VOL-2 | p 1980 N95-24283
Response to a localized impact loading of a composite multilayered rotational shell structure: Theory and numerical methods, Volume 3
| ONERA-NT-1994-10-VOL-3 | p 1980 N95-24284
Wear resistant composite structure of vitreous carbon containing convoluted fibers
| DE95-006255 | p 1925 N95-24426
Numerical simulation of the nonlinear response of composite plates under combined thermal and acoustic loading
| NASA-CR-197426 | p 1981 N95-24907
Thermoelastic equations for multi-layered cylindrical shell
| NAL-TR-1222 | p 1982 N95-25661
Method and apparatus for weaving curved material preforms
| NASA-CASE-LAR-14752-1 | p 1943 N95-26118
Finite element buckling and postbuckling solutions for multilayered composite panels p 1983 N95-26264
Thermomechanical postbuckling of multilayered composite panels with cutouts p 1984 N95-26267
Nonlinear vibrations of thin-walled composite frames p 1984 N95-26269

Effect of mesh distortion on the accuracy of transverse shear stresses and their sensitivity coefficients in multilayered composites p 1985 N95-26270
Sensitivity analysis of frictional contact response of axisymmetric composite structures p 1985 N95-26271
Recent advances in the sensitivity analysis for the thermomechanical postbuckling of composite panels p 1985 N95-26274
Dynamic sensitivity analysis of frictional contact/impact response of axisymmetric composite structures p 1986 N95-26279
Buckling and postbuckling of composite panels with cutouts subjected to combined edge shear and temperature change p 1987 N95-26280
Sensitivity analysis for large-deflection and postbuckling responses on distributed-memory computers p 1987 N95-26281

COMPOSITION (PROPERTY)
In situ XAFS study of oxides formed on nickel thin film electrodes in KOH solution
[AD-A288735] p 1932 N95-26056

COMPRESSED GAS
Inflatable rescue device
[NASA-CASE-MSC-22244-1] p 2014 N95-25306

COMPRESSIBILITY
Processing and characterization of transformation-toughened ceramics with strength retention to elevated temperatures
[DE95-005758] p 1941 N95-25387

COMPRESSIBILITY EFFECTS
A pseudo-sound constitutive relationship for the dilatational covariances in compressible turbulence: An analytical theory
[NASA-CR-195064] p 1966 N95-25964

COMPRESSIBLE FLOW
Implementation of a parallel algorithm for thermo-chemical nonequilibrium flow simulations
[DE95-004758] p 1961 N95-24262
Study of compressible flow through a rectangular-to-semiannular transition duct
[NASA-CR-4660] p 1914 N95-24392
Effect of density gradients in confined supersonic shear layers, part 1
[NASA-CR-198029] p 1962 N95-24412
A conservative staggered-grid Chebyshev multidomain method for compressible flows
[NASA-CR-195060] p 2030 N95-24632
A domain decomposition study of massively parallel computing in compressible gas dynamics
[DE95-004759] p 1965 N95-25895
A pseudo-sound constitutive relationship for the dilatational covariances in compressible turbulence: An analytical theory
[NASA-CR-195064] p 1966 N95-25964

COMPRESSING
Over-compression, a method to shape the longitudinal bunch distribution for a reduced energy spread
[DE95-006052] p 2066 N95-24572

COMPRESSION RATIO
Learning random networks for compression of still and moving images p 2025 N95-25268

COMPRESSION TESTS
Performance evaluation of LE-7 high pressure pumps
[NAL-TR-1212T] p 1977 N95-25672

COMPRESSION WAVES
Viscoelastic waves and multiple scales
[DE94-014130] p 1966 N95-26063

COMPRESSIVE STRENGTH
Mechanical properties testing and results for thermal barrier coatings p 1946 N95-26134
Effects of through-the-thickness stitching on impact and interlaminar fracture properties of textile graphite/epoxy laminates
[NASA-CR-195042] p 1928 N95-26203

COMPTON EFFECT
Simulation study of tapered FEL amplifiers in Raman and Compton regimes
[DE94-785266] p 1971 N95-24340
On the Compton non-Abelian twist-3 asymmetry
[DE94-628586] p 2095 N95-24727

COMPUTATION
Performance issues for iterative solvers in device simulation
[NASA-CR-197952] p 2027 N95-24214
Computational load in model physics of the parallel NCAR community climate model
[DE95-005410] p 2019 N95-24342
Postbuckling and large-deflection nonlinear analyses on distributed-memory computers p 1986 N95-26276
Reduction technique for tire contact problems p 1986 N95-26277
Sensitivity analysis for the dynamic response of thermoviscoplastic shells of revolution p 1986 N95-26278
Dynamic sensitivity analysis of frictional contact/impact response of axisymmetric composite structures p 1986 N95-26279
Sensitivity analysis for large-deflection and postbuckling responses on distributed-memory computers p 1987 N95-26281
Computational strategies for tire monitoring and analysis p 1978 N95-26282
Assessment of computational models for thermoelectroelastic multilayered plates p 1987 N95-26283

COMPUTATIONAL ASTROPHYSICS
Rich cluster simulation: Dynamics and mass estimates
[DE95-005233] p 2110 N95-25766

COMPUTATIONAL FLUID DYNAMICS
Verification of computational aerodynamic predictions for complex hypersonic vehicles using the INCA(trademark) code
[DE95-004757] p 1906 N95-24308
Aerodynamic optimization studies on advanced architecture computers
[NASA-CR-198045] p 1906 N95-24379
DSMC calculations for 70-deg blunted cone at 3.2 km/s in nitrogen
[NASA-TM-109181] p 1961 N95-24396
Investigation of convection and pressure treatment with splitting techniques
[NASA-TM-106868] p 1961 N95-24399
The method of space-time conservation element and solution element: Development of a new implicit solver
[NASA-TM-106897] p 2029 N95-24474
Solutions of turbulent backward-facing step flow with heat transfer using the finite volume method
[DE95-003360] p 1962 N95-24489
A conservative staggered-grid Chebyshev multidomain method for compressible flows
[NASA-CR-195060] p 2030 N95-24632
A review of chemically reactive turbulent flow analysis, mixing mechanisms and modeling, and a new design of low NOx combustor for non-premixed reactants p 1963 N95-24762
Multigrid solution strategies for adaptive meshing problems
[NASA-CR-195049] p 2031 N95-24857
Advanced multi-phase flow CFD model development for solid rocket motor flowfield analysis
[NASA-CR-198044] p 1923 N95-25103
Implementation of a parallel unstructured Euler solver on the CM-5
[NASA-CR-195056] p 2032 N95-25106
A well-posed numerical method to track isolated conformal map singularities in Hele-Shaw flow
[NASA-CR-195035] p 2032 N95-25114
The first ICASE/LARC industry roundtable: Session proceedings
[NASA-CR-195040] p 2014 N95-25119
A higher-order projection method for the simulation of unsteady turbulent nonpremixed combustion in an industrial burner
[DE95-005919] p 1931 N95-25291
Aerodynamic shape optimization of wing and wing-body configurations using control theory
[NASA-CR-198024] p 1911 N95-25334
The coupling of fluids, dynamics, and controls on advanced architecture computers
[NASA-CR-197727] p 2017 N95-25797
The 3D widgets for exploratory scientific visualization p 1966 N95-25868
An annotation system for 3D fluid flow visualization p 1966 N95-25869
Recent improvements to and validation of the one dimensional NASA wave rotor model
[NASA-TM-106913] p 1908 N95-25962
A combined geometric approach for solving the Navier-Stokes equations on dynamic grids
[NASA-TM-106919] p 1908 N95-26075
Numerical calculations of shock-wave/boundary-layer flow interactions
[NASA-TM-106694] p 1966 N95-26077
Particle-mesh techniques
[NASA-CR-4666] p 2083 N95-26082
Cumulative reports and publications through December 31, 1994
[NASA-CR-195043] p 2014 N95-26085
Numerical simulation of laminar flow in a curved duct
[DE95-005427] p 1966 N95-26240

COMPUTATIONAL GEOMETRY
Visibility ordering meshed polyhedra
[CSRD-1097] p 2030 N95-24557

COMPUTATIONAL GRIDS
Shell deformation states and the finite element method: A benchmark study of cylindrical shells
[PB95-149621] p 1980 N95-24296
Parallel algorithms for dynamically partitioning unstructured grids
[DE95-001616] p 2015 N95-24346
Covolume solutions of three dimensional div-curl equations
[NASA-CR-195031] p 2029 N95-24421
The method of space-time conservation element and solution element: Development of a new implicit solver
[NASA-TM-106897] p 2029 N95-24474
A conservative staggered-grid Chebyshev multidomain method for compressible flows
[NASA-CR-195060] p 2030 N95-24632
Dynamic load balancing for parallel finite element methods with adaptive h- and p-refinement
[DE95-004521] p 2021 N95-24681
Multigrid solution strategies for adaptive meshing problems
[NASA-CR-195049] p 2031 N95-24857
Implementation of a parallel unstructured Euler solver on the CM-5
[NASA-CR-195056] p 2032 N95-25106
Nonlinear difference approximations for evolutionary PDE's
[DE95-005260] p 2033 N95-25676
Numerical solution of the optimized random phase approximation
[DE95-605636] p 2034 N95-25982
A combined geometric approach for solving the Navier-Stokes equations on dynamic grids
[NASA-TM-106919] p 1908 N95-26075
Particle-mesh techniques
[NASA-CR-4666] p 2083 N95-26082
Holograpy machine HORN-1 for computer-aided retrieve of virtual three-dimensional image
[NIFS-218] p 1971 N95-26182
Summary report for ITER Task D10: Update and implementation of neutron transport and activation codes and processed libraries
[DE95-007631] p 2083 N95-26185
Numerical simulation of laminar flow in a curved duct
[DE95-005427] p 1966 N95-26240
Effect of mesh distortion on the accuracy of transverse shear stresses and their sensitivity coefficients in multilayered composites p 1985 N95-26270

COMPUTER AIDED DESIGN
Space shuttle propellant constitutive law verification tests
[NASA-CR-198047] p 1947 N95-24226
Aerodynamic optimization studies on advanced architecture computers
[NASA-CR-198045] p 1906 N95-24379
Integration of design, structural, thermal and optical analysis: And user's guide for structural-to-optical translator (PATCOD)
[NASA-TM-110153] p 1950 N95-24559
Data preparation requirements for modeling wind turbines with ADAMS(R)
[DE95-000266] p 1992 N95-24684
Understanding and improving materials processing through interpreting and manipulating predictive models
[DE95-004384] p 1930 N95-25242
Using and programming the SUPERCODE
[DE95-004342] p 2080 N95-25344
Computer analysis of graphics for the requirements of computer-aided design systems
[IPPT-29-1992] p 2016 N95-25392
An FEL design code running on Mathcad(trademark)
[DE95-005279] p 1973 N95-25565
Aspect estimation of an aircraft using library model silhouettes
[PB95-141834] p 2036 N95-25894
Dynamic matrices and their application to the concept of a semi-sparse matrix
[AD-A288688] p 2035 N95-26051
Computerized design and generation of low-noise gears with localized bearing contact
[NASA-TM-106880] p 1977 N95-26074
LH2 fuel tank design for SSTO p 1987 N95-26309
Feed system design for a reduced pressure tank p 1923 N95-26310
Continuous phase and amplitude holographic elements
[NASA-CASE-NPO-18791-1] p 1971 N95-26340

COMPUTER AIDED MAPPING
Stratified charge rotary engine combustion studies
[NASA-CR-197985] p 1974 N95-24223

COMPUTER AIDED TOMOGRAPHY
Neural networks: Application to medical imaging p 2025 N95-25267

COMPUTER ASSISTED INSTRUCTION
Activity Management System user reference manual
[DE95-000989] p 2105 N95-24654
Information management architecture for an integrated computing environment for the Environmental Restoration Program. Environmental Restoration Program, Volume 3: Interim technical architecture
[DE95-001386] p 2105 N95-24656
Instructable autonomous agents
[NASA-CR-197802] p 2019 N95-26206

COMPUTER COMPONENTS
An optimized implementation of a fault-tolerant clock synchronization circuit
| NASA-TM-109176 | p 2019 N95-24382

COMPUTER GRAPHICS
Visibility ordering meshed polyhedra
| CSRD-1097 | p 2030 N95-24557
Object-oriented parallel polygon rendering
| DE95-004909 | p 2021 N95-24881
Hardcopy extraction considerations for Vector Product Format (VPF) products
| AD-A288620 | p 2106 N95-25608
Three-dimensional user interfaces for scientific visualization
| NASA-CR-197923 | p 2017 N95-25867
The 3D widgets for exploratory scientific visualization p 1966 N95-25868
An annotation system for 3D fluid flow visualization p 1966 N95-25869
Scheduling time-critical graphics on multiple processors p 2018 N95-25870
Four-Dimensional Information Visualization and Analysis System
| DE95-004935 | p 2022 N95-26013

COMPUTER INFORMATION SECURITY
Final report and recommendations of the ESnet Authentication Pilot Project
| DE95-005755 | p 2103 N95-24370
Survey of methods for secure connection to the internet
| DE95-730185 | p 1952 N95-24493
JPRS report: Science and technology. Central Eurasia
| JPRS-UST-95-012 | p 1950 N95-24540
Naval network security requirements analysis
| AD-A288692 | p 2022 N95-26054

COMPUTER NETWORKS
ESnet Program Plan 1994
| DE95-005329 | p 2019 N95-24290
Raising the IQ in full-text searching via intelligent querying
| DE95-002981 | p 2103 N95-24330
Final report and recommendations of the ESnet Authentication Pilot Project
| DE95-005755 | p 2103 N95-24370
Downsizing systems and expected opposition to introduction
| DE95-730186 | p 2104 N95-24494
A tool for debugging internet multicast routing
| DE95-003433 | p 2020 N95-24496
Adventures in the evolution of a high-bandwidth network for central servers
| DE95-006215 | p 2020 N95-24597
Information management architecture for an integrated computing environment for the Environmental Restoration Program. Environmental Restoration Program, Volume 3: Interim technical architecture
| DE95-001386 | p 2105 N95-24656
Proceedings of workshop on Future in HEP Computing
| DE94-792684 | p 2021 N95-25303
Dynamics of TCP traffic over ATM networks
| DE95-004687 | p 2021 N95-25359
Wide-area traffic: The failure of Poisson modeling
| DE95-004685 | p 2015 N95-25773
The coupling of fluids, dynamics, and controls on advanced architecture computers
| NASA-CR-197727 | p 2017 N95-25797
Naval network security requirements analysis
| AD-A288692 | p 2022 N95-26054
Converting multiple OC-3c ATM streams to HIPPI to drive an HDTV frame buffer from a workstation cluster
| DE95-003638 | p 2022 N95-26066

COMPUTER PROGRAM INTEGRITY
Quarterly update
| AD-A288743 | p 2018 N95-26058

COMPUTER PROGRAMMING
Towards a formal semantics for Ada 9X
| NASA-CR-195037 | p 2020 N95-24634
Using and programming the SUPERCODE
| DE95-004342 | p 2080 N95-25344
Cumulative reports and publications through December 31, 1994
| NASA-CR-195043 | p 2014 N95-26085

COMPUTER PROGRAMS
DOLIB: Distributed Object Library
| DE95-004791 | p 2019 N95-24250
Lawrence Livermore pulsed sphere benchmark analysis of MCNP(trademark) ENDF/B-VI
| DE95-004864 | p 2041 N95-24258
Detvag-90: An implementation of Vogler's method for calculation of multiple knife-edge diffraction
| PB95-141859 | p 1951 N95-24281
Expert system for nuclide identification in gamma spectrum analysis
| PB95-149712 | p 2042 N95-24297
Gamma spectrum analysis including NAA with SAMPO for windows
| PB95-149720 | p 2042 N95-24298
Verification of computational aerodynamic predictions for complex hypersonic vehicles using the INCA(trademark) code
| DE95-004757 | p 1906 N95-24308
Outline of fast analyzer for MHD equilibrium FAME
| DE94-777540 | p 2076 N95-24311
A parallel, portable and versatile treecode
| DE95-000842 | p 2019 N95-24343
SPEEDUP simulation of liquid waste batch processing, revision 1
| DE95-001240 | p 1939 N95-24344
A computing program of sample magnetic moments recognition for SQUID-magnetometer measurements
| DE94-637073 | p 2037 N95-24363
Application of compartmental metabolic models for determination of retention and excretion functions
| DE95-600249 | p 2010 N95-24367
SYSINT(SYSINTM)-program complex for numerical solution of the eigenvalue problem for system of integral equations
| DE94-636729 | p 2029 N95-24375
Numerical investigation of Schwinger-Dyson and Bethe-Salpeter equations with Gauss potential in the framework of the quarkonium model
| DE94-636730 | p 2029 N95-24387
Nonequilibrium multiphase mixture modeling of energetic material response
| DE95-003353 | p 1948 N95-24608
Data preparation requirements for modeling wind turbines with ADAMS(R)
| DE95-000266 | p 1992 N95-24684
PC based analysis of gamma ray spectra generated by semiconductor detectors
| DE94-628381 | p 1958 N95-24690
Introduction to the Monte Carlo methods
| DE94-628386 | p 2035 N95-24693
Numerical analysis of electron cyclotron resonance heating on JT-60U and JFT-2M
| DE95-709766 | p 2080 N95-25471
Designing a stencil compiler for the Connection Machine model CM-5
| DE95-006861 | p 2021 N95-25477
The NJOY nuclear data processing system: Version 91
| DE95-006764 | p 2055 N95-25484
A numerical prediction of the precipitation and hydrology of California
| DE95-004966 | p 2006 N95-25635
HZE beam transport in multilayered materials p 2060 N95-25922
Cognitive diagnosis combined with latent trait theory and multiphase responses
| AD-A288701 | p 2013 N95-26010
Reliability analysis of software based safety functions
| DE95-606516 | p 2018 N95-26045
Quarterly update
| AD-A288743 | p 2018 N95-26058
A software tool to design thermal barrier coatings p 1946 N95-26139
A generic interface element for COMET-AR
| NASA-CR-195075 | p 1983 N95-26199
Instructable autonomous agents
| NASA-CR-197802 | p 2019 N95-26206

COMPUTER SYSTEMS DESIGN
The CDF silicon vertex detector SVX and its upgrades
| DE95-003743 | p 2050 N95-24901
Software fault tolerance in computer operating systems
| NASA-CR-197999 | p 2016 N95-24993

COMPUTER SYSTEMS PERFORMANCE
Computational load in model physics of the parallel NCAR community climate model
| DE95-005410 | p 2019 N95-24342
The emission of particle identification efficiency in the EXCHARM experiment
| DE94-628258 | p 2047 N95-24644
The CDF silicon vertex detector SVX and its upgrades
| DE95-003743 | p 2050 N95-24901
Software fault tolerance in computer operating systems
| NASA-CR-197999 | p 2016 N95-24993
FTAPE: A fault injection tool to measure fault tolerance
| NASA-CR-198000 | p 1978 N95-25333
Alpha(sub critical) for parallel processors
| PB95-165320 | p 2022 N95-25625
Use of multiple fronts in Gaussian elimination
| PB95-165353 | p 2033 N95-25627

COMPUTER SYSTEMS PROGRAMS
Information management architecture for an integrated computing environment for the Environmental Restoration Program. Environmental Restoration Program, Volume 3: Interim technical architecture
| DE95-001386 | p 2105 N95-24656

COMPUTER TECHNIQUES
ARMDAT: A brief description of a computerized test system for burst transmission
| PB95-165452 | p 1951 N95-24241
JPRS report: Science and technology. Central Eurasia
| JPRS-UST-94-035 | p 2016 N95-24429
EXODUS 2: A finite element data model
| DE95-004267 | p 2016 N95-24659
A Decade of Neural Networks: Practical Applications and Prospects
| NASA-CR-197334 | p 2022 N95-25253
Computer analysis of graphics for the requirements of computer-aided design systems
| IPPT-29-1992 | p 2016 N95-25392
Machine-aided indexing at NASA
| NASA-CR-197796 | p 2106 N95-25410
Applications for electronic documents
| DE95-005036 | p 2106 N95-25765
Computer support for cooperative tasks in Mission Operations Centers
| DE95-004928 | p 2102 N95-25771
Holograpy machine HORN-1 for computer-aided retrieve of virtual three-dimensional image
| NIFS-218 | p 1971 N95-26182

COMPUTER VISION
Missileborne Artificial Vision System (MAVIS) p 2022 N95-25254
Document analysis with neural net circuits p 2023 N95-25256
From neural-based object recognition toward microelectronic eyes p 2023 N95-25257
Smart vision chips: An overview p 2024 N95-25265
Video camera as a visual sensor, part 2
| NAL-TR-1231-PT-2 | p 1970 N95-25763
Aspect estimation of an aircraft using library model silhouettes
| PB95-141834 | p 2036 N95-25894

COMPUTERIZED SIMULATION
Performance issues for iterative solvers in device simulation
| NASA-CR-197952 | p 2027 N95-24214
Investigation of properties and performance of ceramic composite components
| DE95-004737 | p 1939 N95-24247
Lawrence Livermore pulsed sphere benchmark analysis of MCNP(trademark) ENDF/B-VI
| DE95-004864 | p 2041 N95-24258
Implementation of a parallel algorithm for thermo-chemical nonequilibrium flow simulations
| DE95-004758 | p 1961 N95-24262
Estimate of probability of crack detection from service difficulty report data
| PB95-149381 | p 1905 N95-24295
Simulation study of tapered FEL amplifiers in Raman and Compton regimes
| DE94-785266 | p 1971 N95-24340
Computational load in model physics of the parallel NCAR community climate model
| DE95-005410 | p 2019 N95-24342
SPEEDUP simulation of liquid waste batch processing, revision 1
| DE95-001240 | p 1939 N95-24344
Parallel algorithms for dynamically partitioning unstructured grids
| DE95-001616 | p 2015 N95-24346
Simulation of diurnal thermal energy storage systems: Preliminary results
| DE95-005751 | p 1991 N95-24369
Generation and computerized simulation of meshing and contact of modified involute helical gears
| NASA-CR-4644 | p 1952 N95-24395
The influence of CDM on the dynamical estimate of (Omega) in the local neighborhood
| DE95-005212 | p 2109 N95-24455
Recipes for high resolution time-of-flight detectors
| DE95-006196 | p 1967 N95-24596
Nonequilibrium multiphase mixture modeling of energetic material response
| DE95-003353 | p 1948 N95-24608
Activities of the Solid State Division
| DE95-003900 | p 2087 N95-24611
Numerical simulation of flow and the effect of baffle arrangement on pressure drop and temperature pattern in a circular combustor p 1963 N95-24628
Unfolding of true distributions from experimental data distorted by detectors with finite resolutions
| DE94-628372 | p 2035 N95-24643
The emission of particle identification efficiency in the EXCHARM experiment
| DE94-628258 | p 2047 N95-24644

EXODUS 2: A finite element data model
[DE95-004267] p 2016 N95-24659
Co-validation of three methods for optical characterization of point-focus concentrators
[DE95-001613] p 1992 N95-24674
Ionization potential data library of atoms and ions
[DE94-628380] p 2048 N95-24689
The role of shaping in achieving high performance in DIII-D
[DE95-003877] p 2078 N95-25102
A higher-order projection method for the simulation of unsteady turbulent nonpremixed combustion in an industrial burner
[DE95-005919] p 1931 N95-25291
Statistical mechanics of nonlinear coherent structures: Kinks in the Phi(sup 6) model
[DE95-005253] p 2096 N95-25293
Using and programming the SUPERCODE
[DE95-004342] p 2080 N95-25344
Radial electron-beam-breakup transit-time oscillator
[DE95-005731] p 1959 N95-25385
Computer analysis of graphics for the requirements of computer-aided design systems
[IPPT-29-1992] p 2016 N95-25392
Monte Carlo simulations with indefinite and complex-valued measures
[DE95-607056] p 2017 N95-25448
Fast algorithms for transport models
[DE95-007064] p 2054 N95-25479
Molecular dynamics calculation of shear viscosity for molten salt
[DE95-703970] p 2055 N95-25496
Finite element methods in a simulation code for offshore wind turbines
[PB95-164984] p 1994 N95-25501
Atmospheric and terrain effects on acoustic propagation
[AD-A288727] p 2039 N95-25503
Implementation of wave propagation model for windows
[PB95-165742] p 2017 N95-25571
Rich cluster simulation: Dynamics and mass estimates
[DE95-005233] p 2110 N95-25766
Multidimensional visualization and browsing for intelligence analysis
[DE95-004901] p 2106 N95-25774
The coupling of fluids, dynamics, and controls on advanced architecture computers
[NASA-CR-197727] p 2017 N95-25797
The 3D widgets for exploratory scientific visualization p 1966 N95-25868
Molecular dynamics simulation of a piston driven shock wave in a hard sphere gas
[NASA-CR-195463] p 2063 N95-25963
Design and development of a cloud reference library and support for cloud and simulation communities. Summary report
[AD-A288704] p 2006 N95-26012
Four-Dimensional Information Visualization and Analysis System
[DE95-004935] p 2022 N95-26013
Microscan simulation
[AD-A289139] p 2075 N95-26039
Simulating the dynamic interaction of a robotic arm and the Space Shuttle remote manipulator system
[NASA-CR-195076] p 2027 N95-26086
Time-dependent numerical simulation of vertical cavity lasers
[DE95-006862] p 1973 N95-26112
Average cosine meter and high spectral resolution measurements at the marine light mixed layer site
[AD-A288713] p 1970 N95-26113
Intermediate-sized natural gas fueled carbonate fuel cell power plants
[DE95-004990] p 1996 N95-26171
Summary report for ITER Task D10: Update and implementation of neutron transport and activation codes and processed libraries
[DE95-007631] p 2083 N95-26185

CONCATENATED CODES
On the Trellis structure of a (64,40,8) subcode of the (64,42,8) third-order Reed-Muller code
[NASA-CR-198019] p 2015 N95-24224

CONCENTRATION (COMPOSITION)
Measurement of blood nitrogen content after rapid compressions to assess the speed of nitrogen uptake during the compression phase of submarine escape. (Includes measurement of nitrogen concentration in blood following rapid compression to 5 bar)
[PB95-165726] p 2012 N95-25570

CONCENTRATORS
Co-validation of three methods for optical characterization of point-focus concentrators
[DE95-001613] p 1992 N95-24674
Mirror alignment and focus of point-focus solar concentrators
[DE95-002609] p 1992 N95-24676
Comparison of three methods for optical characterization of point-focus concentrators
[DE95-000282] p 1994 N95-25309

CONCURRENT ENGINEERING
Integration of design, structural, thermal and optical analysis: And user's guide for structural-to-optical translator (PATCOD)
[NASA-TM-110153] p 1950 N95-24559
Understanding and improving materials processing through interpreting and manipulating predictive models
[DE95-004384] p 1930 N95-25242

CONCURRENT PROCESSING
VLSI neuroprocessors p 2023 N95-25258

CONDENSATES
Low energy theorems in quark potential models
[DE94-636791] p 2042 N95-24316
Tachyon condensates and anisotropic universe
[DE95-607074] p 2097 N95-25456

CONDENSED MATTER PHYSICS
A functional integral approach without slave bosons to the Anderson model
[DE94-634858] p 2028 N95-24276
Nanostructured materials
[DE95-004595] p 2088 N95-25280

CONDUCTION BANDS
A theoretical analysis of strain in GaN and its effects on carrier conductivity
[AD-A288769] p 2090 N95-26061

CONDUCTORS
Thin film ionic conductors based on cerium oxide
[DE95-003668] p 2086 N95-24514
On the effects of gravitational fields on the electrical properties of matter
[DE95-607022] p 2038 N95-25430
Crosstalk on printed circuit boards
[PB95-165171] p 1960 N95-25472

CONES
Heat Kernel expansion on a cone and quantum fields near cosmic strings
[DE94-628520] p 2094 N95-24507

CONFERENCES
The 1994 Fiber Optic Sensors for Aerospace Technology (FOSAT) Workshop
[NASA-CP-10166] p 1912 N95-24207
Proceedings of the 1993 Symposium on Nuclear Data
[DE94-012554] p 2104 N95-24372
Fifth European Symposium on Reliability of Electron Devices, Failure Physics and Analysis
[AD-A286614] p 1956 N95-24447
Superconductivity Program for Electric Power Systems: 1994 Annual PEER Review. Volume 1, Meeting Proceedings
[DE95-005058] p 1956 N95-24452
Superconductivity Program for Electric Power Systems: 1994 Annual PEER Review. Volume 2, Meeting Proceedings
[DE95-005059] p 1957 N95-24453
Electromagnetic Devices and Processes in Environment Protection. Proceedings of International Conference ELMECO 1994
[AD-A286613] p 1952 N95-24503
Geometry of multihadron production
[DE95-004290] p 2047 N95-24663
Proceedings of the 1994 Conference on Computing in Energy Physics
[DE95-004442] p 2068 N95-24665
Report series in aerosol science
[DE95-737628] p 1999 N95-24904
The first ICASE/LARC industry roundtable: Session proceedings
[NASA-CR-195040] p 2014 N95-25119
A Decade of Neural Networks: Practical Applications and Prospects
[NASA-CR-197334] p 2022 N95-25253
Proceedings of workshop on Future in HEP Computing
[DE94-792684] p 2021 N95-25303
Proceedings of the Workshop on Dynamics and Structure of Disordered System
[DE94-792685] p 1931 N95-25356
Resolving the ambiguities: An industrial hygiene Indoor Air Quality (IAQ) symposium
[DE95-005391] p 2000 N95-25380
Conference on physics from large gamma-ray detec tor arrays. Volume 2: Proceedings
[DE95-006900] p 2070 N95-25478
The Third International Workshop on the Physics and Modern Applications of Lasers
[DE95-606395] p 1972 N95-25491
Electron spin resonance of radicals and metal complexes
[DE95-605640] p 2055 N95-25499
Physics in Ukraine International Conference. Volume 3: Statistical physics and phase transitions
[DE95-605765] p 2038 N95-25552
Physics in Ukraine International Conference. Volume 5: Low temperature physics
[DE95-605800] p 2038 N95-25553
Physics in Ukraine International Conference. Volume 1: Physics of elementary particles and quantum field theory. General problems
[DE95-606413] p 2056 N95-25554
Physics in Ukraine International Conference. Volume 6: Plasma physics
[DE95-606422] p 2081 N95-25555
Proceedings of the 2d USAF Aging Aircraft Conference
[AD-A288217] p 1911 N95-25578
Proceedings of the 4th IEEE Workshop on Neural Networks for Signal Processing
[AD-A288383] p 2026 N95-25603
Proceedings of the 21st Japan Conference on Radiation and Radioisotopes
[DE94-785275] p 2056 N95-25614
Physics in Ukraine International Conference. Volume 4: Radiophysics and Electronics
[DE95-605570] p 2038 N95-25616
From superconductivity to supernovae: The Ginzburg symposium. Report on the symposium held in honor of Vitaly L. Ginzburg
[NASA-TM-110596] p 2108 N95-25746
Fourth symposium of the geological survey of Japan on remote sensing of satellite geology
[PB95-178737] p 1917 N95-25750
Proceedings of the 2nd international workshop on electromagnetic forces and related effects on blankets and other structures surrounding the fusion plasma torus
[DE94-792667] p 2082 N95-25903
Thermal Barrier Coating Workshop
[NASA-CP-10170] p 1943 N95-26119
Proceedings of the International Seminar on the Chemistry of High Energy Atoms
[DE95-709895] p 2072 N95-26162

CONFIGURATION INTERACTION
Probing new physics in rare charm processes
[DE95-006067] p 2050 N95-24903

CONFINEMENT
Experimental and theoretical basis for advanced tokamaks
[DE95-003255] p 2077 N95-24646
Divertor design for the Tokamak Physics Experiment
[DE95-003653] p 2078 N95-24650
Mass splitting of the pseudoscalar and vector mesons induced by the homogeneous vacuum gluon field
[DE95-605322] p 2058 N95-25908
Excited states of mesons within the NJL model with the homogeneous vacuum gluon field
[DE95-605323] p 2058 N95-25909
Dynamics of phase ordering of nematics in a pore
[DE95-607662] p 2090 N95-25978
Isotope effect on confinement in DT plasmas
[NIFS-275] p 2083 N95-26326

CONFORMAL MAPPING
A well-posed numerical method to track isolated conformal map singularities in Hele-Shaw flow
[NASA-CR-195035] p 2032 N95-25114

CONGRESSIONAL REPORTS
Federal alternative motor fuels program: Light duty federal vehicles, trucks, and buses
[DE95-003982] p 1948 N95-24679
Nitrogen oxide emissions and their control from uninstalled aircraft engines in enclosed test cells: Joint report to Congress on the Environmental Protection Agency - Department of Transportation study
[PB95-166237] p 2002 N95-26005
Report to Congressional Committees. Tactical Aircraft: Concurrency in development and production of F-22 aircraft should be reduced
[GAO/NSIAD-95-59] p 1911 N95-26338

CONICAL BODIES
DSMC calculations for 70-deg blunted cone at 3.2 km/s in nitrogen
[NASA-TM-109181] p 1961 N95-24396

CONICS
Enhancement of thickness uniformity of thin films grown by pulsed laser deposition
[NASA-CR-197791] p 1943 N95-26081

CONJUGATES
A partial unification model in non-commutative geometry
[DE95-607129] p 2097 N95-25435

CONNECTION MACHINE
Implementation of a parallel unstructured Euler solver on the CM-5
[NASA-CR-195056] p 2032 N95-25106
Designing a stencil compiler for the Connection Machine model CM-5
[DE95-006861] p 2021 N95-25477

CONSERVATION
Statistical mechanics of magnetized pair Fermi gas
[DE95-607097] p 2063 N95-25969
CONSERVATION LAWS
The method of space-time conservation element and solution element: Development of a new implicit solver
[NASA-TM-106897] p 2029 N95-24474
CONSISTENCY
Metrology: Measurement assurance program guidelines
[NASA-RP-1364] p 1950 N95-24543
Quasi two body decays of charm mesons
[DE94-792634] p 2057 N95-25901
CONSTRAINTS
Evaluation of restraint system concepts for the Japanese Experiment Module flight demonstration
[NASA-TM-104808] p 2013 N95-24627
A brief survey of constrained mechanics and variational problems in terms of differential forms
p 2026 N95-25803
CONSTRUCTION
Recipes for high resolution time-of-flight detectors
[DE95-006196] p 1967 N95-24596
Construction of a nitrogen laser for plasma diagnostics
[DE95-607599] p 1973 N95-25973
On Segal-Wilson's construction for the (tau)-functions of the constrained KP hierarchies
[DE95-606999] p 2100 N95-25988
CONSTRUCTION MATERIALS
Fire test of surface products: Comparison of data from the nordic box test and the cone calorimeter
[PB95-165239] p 1932 N95-26000
CONTACT LOADS
Wear resistant composite structure of vitreous carbon containing convoluted fibers
[DE95-006255] p 1925 N95-24426
Reduction technique for tire contact problems
p 1986 N95-26277
Computational strategies for tire monitoring and analysis p 1978 N95-26282
CONTAMINANTS
Methods of valuing air pollution and estimated monetary values of air pollutants in various US regions
[DE95-006854] p 1998 N95-24618
Chelant extraction and REDOX manipulation for mobilization of heavy metals from contaminated soils
[DE95-004131] p 2000 N95-25363
CONTAMINATION
Characterizing pre-polished Type 304L stainless steel
[DE95-001241] p 1934 N95-24480
Stainless steel recycle
[DE95-003905] p 1934 N95-24615
Use of mass spectrometric methods for field screening of VOC's
[DE95-004903] p 1999 N95-25249
CONTINENTAL SHELVES
Shelf sediment dynamics and development of lithostratigraphy
[AD-A288886] p 2006 N95-25504
CONTINUITY (MATHEMATICS)
The lattice spinor QED Hamiltonian critique of the continuous space approach
[DE94-628521] p 2094 N95-24508
CONTINUOUS RADIATION
A vacuum window for a 1 MW CW 110 GHz gyrotron
[DE94-016584] p 2079 N95-25108
CONTINUOUS WAVE LASERS
Laser beam characterization results for a high power CW Nd:YAG laser
[DE95-006319] p 1971 N95-24408
Diode laser pumped solid state laser with 2 micrometer wavelength
[PB95-165270] p 1973 N95-25622
CONTINUOUS WAVE RADAR
Analysis of waveforms for bistatic radar systems
[PB95-165098] p 1955 N95-25641
CONTINUUM MECHANICS
Evolution of plastic anisotropy for high-strain-rate computations
[DE95-004220] p 1941 N95-25237
CONTRACT MANAGEMENT
Acquisition forecast: Fiscal year 1995
[NASA-TM-110575] p 2103 N95-25850
CONTRACTS
Crystal Growth Furnace (CGF)
[NASA-CR-196591] p 2089 N95-25409
Acquisition forecast: Fiscal year 1995
[NASA-TM-110575] p 2103 N95-25850
CONTRAILS
Visual contrast detection thresholds for aircraft contrails
[AD-A286618] p 1905 N95-25607
CONTROL
Tutorial on beam-based feedback systems for linacs
[DE95-006054] p 2067 N95-24573
CONTROL EQUIPMENT
Retrofit NOx control technologies for natural gas prime movers
[PB95-149290] p 1997 N95-24294
SPEEDUP simulation of liquid waste batch processing, revision 1
[DE95-001240] p 1939 N95-24344
CONTROL SYSTEMS DESIGN
Small spacecraft power and thermal subsystems
[NASA-CR-195029] p 1921 N95-24216
SPEEDUP simulation of liquid waste batch processing, revision 1
[DE95-001240] p 1939 N95-24344
Efficient eigenvalue assignment by state and output feedback with applications for large space structures
[NASA-TM-110155] p 1920 N95-24581
Application of neural networks to unsteady aerodynamic control p 2024 N95-25264
Flexible architectures for sensor fusion in theater missile defense
[AD-A288666] p 2007 N95-26048
Partial camera automation in a simulated Unmanned Air Vehicle
[AD-A288786] p 1913 N95-26190
Universal Test Facility p 1918 N95-26305
Stiffening of the ACES deployable space boom
p 1978 N95-26307
CONTROL THEORY
Aerodynamic shape optimization of wing and wing-body configurations using control theory
[NASA-CR-198024] p 1911 N95-25334
Splines and control theory p 2026 N95-25802
Control theory and splines, applied to signature storage p 2027 N95-25804
How to fly an aircraft with control theory and splines
p 2027 N95-25805
Controls concepts for next generation reuseable rocket engines
[NASA-TM-106902] p 1923 N95-25877
Actuating signals in adaptive control systems
[IFTR-13/1994] p 2027 N95-26330
CONTROLLED FUSION
Flow-through Z-pinch study for radiation generation and fusion energy production
[DE95-004209] p 2076 N95-24544
Magnetized target fusion: An ultra high energy approach in an unexplored parameter space
[DE95-005252] p 2080 N95-25289
Maryland controlled fusion research program
[DE95-006642] p 2081 N95-25561
CONTROLLERS
Learning to train neural networks for real-world control problems p 2025 N95-25269
Alternate method for achieving temperature control in the -160 to +90 Celcius range
[NASA-CASE-NPO-18995-1-CU] p 1969 N95-25547
Flexible architectures for sensor fusion in theater missile defense
[AD-A288666] p 2007 N95-26048
Actuating signals in adaptive control systems
[IFTR-13/1994] p 2027 N95-26330
CONVECTION
Investigation of convection and pressure treatment with splitting techniques
[NASA-TM-106868] p 1961 N95-24399
Core-collapse supernovae and nucleosynthesis
[NASA-CR-197731] p 2109 N95-25122
CONVECTIVE FLOW
Estimates of effects of residual acceleration on USML-1 experiments
[NASA-CR-197964] p 2084 N95-24261
Convective flow effects on protein crystal growth
[NASA-CR-197891] p 2086 N95-24534
CONVECTIVE HEAT TRANSFER
Heat release rate measurements in tunnel fires
[PB95-165106] p 1931 N95-25443
CONVERGENCE
Performance issues for iterative solvers in device simulation
[NASA-CR-197952] p 2027 N95-24214
Distribution of the error term for the number of lattice points inside a shifted ball
[PB95-165569] p 2029 N95-24325
Separation analysis, a tool for analyzing multigrid algorithms
[NASA-CR-195036] p 2029 N95-24389
Semi-infinite mathematical programming: A collocation approach
[DE94-634273] p 2016 N95-24708
Faster magnet sorting with a threshold acceptance algorithm
[DE95-006487] p 2038 N95-25408
Variational method for the calculation of the surface hyperspherical functions for the systems of ZH(mu)-type. The test calculation of the dt(mu)-system
[DE94-628905] p 2033 N95-25539
On convergence of the Nelder-Mead simplex algorithm for unconstrained stochastic optimization
[AD-A289453] p 2006 N95-26197
CONVERGENT-DIVERGENT NOZZLES
Internal performance characteristics of thrust-vectored axisymmetric ejector nozzles
[NASA-TM-4610] p 1907 N95-25338
COOLANTS
Effect of film cooling/regenerative cooling on scramjet engine performances
[NAL-TR-1242] p 1914 N95-24990
Heat removal capability of divertor coaxial tube assembly
[DE95-709770] p 1966 N95-26161
COOLING
Crystalline beams: Theory, experiments, and proposals
[DE95-003955] p 2068 N95-24685
Performance tests of air source heat pumps under frosting conditions. Quality of results
[PB95-141792] p 1995 N95-25892
COOLING FLOWS (ASTROPHYSICS)
Research in nuclear astrophysics: Stellar collapse and supernovae
[DE95-004300] p 2110 N95-25343
COOLING SYSTEMS
Effect of film cooling/regenerative cooling on scramjet engine performances
[NAL-TR-1242] p 1914 N95-24990
COPOLYMERS
Space shuttle propellant constitutive law verification tests
[NASA-CR-198047] p 1947 N95-24226
NMR and optical studies of piezoelectric polymers
[DE95-003836] p 1940 N95-24554
COPPER
PEP-2 vacuum system: Joining SS flanges to copper beam chambers
[DE95-006093] p 1974 N95-24356
Copper transport on oxygen annealing of a superconducting film Y-Ba-Cu-O
[DE94-627566] p 2086 N95-24537
Capillary flow on narrow strips and in V-shaped grooves
[DE95-000543] p 1935 N95-24716
Study of copper perovskite
[DE95-730106] p 2088 N95-24988
Na-like autoionizing levels: Plasma diagnostics and prospects for photopumped soft x-ray lasers
[DE95-004207] p 1972 N95-25100
The use of acoustic surface waves to analyze gases apparatus and experiments p 2039 N95-25115
Benchmark experiment on a copper slab assembly bombarded by D-T neutrons
[DE95-709764] p 2055 N95-25497
COPPER ALLOYS
NASA-UVa light aerospace alloy and structures technology program supplement: Aluminum-based materials for high speed aircraft
[NASA-CR-4645] p 1935 N95-24878
Evaluation of a diffusion/trapping model for hydrogen ingress in high-strength alloys
[AD-A288447] p 1936 N95-25502
COPPER OXIDES
Device-quality tunnel junctions on the high (T(sub c)) super conductor HgBa2CuO(4+delta)
[DE95-004646] p 2084 N95-24279
BCS-like gap structure of HgBa2CuO(4+delta) tunnel junctions
[DE95-004125] p 2087 N95-24855
Formation of thallium based high temperature superconductors using aerosol flow reacted precursor powders
[DE95-005901] p 2089 N95-25389
Polarization and intensity of dd-transitions in superconducting copper oxides
[DE95-605886] p 2090 N95-25776
Application of extended-crystal diffraction techniques to the symmetry and structure analysis of 221-PbBiSrCaCuO
[DE95-605913] p 2090 N95-25984
CORNER FLOW
Numerical calculations of shock-wave/boundary-layer flow interactions
[NASA-TM-106694] p 1966 N95-26077
CORRECTION
On corrections to the Nambu action
[NASA-CR-197625] p 2065 N95-24335
Creation of a scalar potential in 2D dilaton gravity
[DE95-006066] p 2003 N95-24577
Coupling correction using closed orbit measurements
[DE95-005957] p 2070 N95-25369
Closed orbit related problems: Correction, feedback, and analysis
[DE95-005969] p 2070 N95-25441

CORRELATION
Correlations for the NO A(sup 2)(Sigma)(+) electronic quenching cross-section
| DE95-006195 | p 2047 N95-24595
The hard truth --- a method to determine the reliability of a specific feature of a Bayesian solution
| DE95-005240 | p 2033 N95-25767
Strong phase correlations of solitons of nonlinear Schroedinger equation
| DE95-607002 | p 2063 N95-25991
Predicting the components of the total hemispherical solar radiation from sunshine duration measurements in Lagos, Nigeria
| DE95-606030 | p 2113 N95-26042
CORROSION
Localized corrosion and stress corrosion cracking characteristics of a low-aluminum-content iron-aluminum alloy
| DE95-003259 | p 1934 N95-24647
Proceedings of the 2d USAF Aging Aircraft Conference
| AD-A288217 | p 1911 N95-25578
CORROSION PREVENTION
The corrosion protection of AISI(TM) 1010 steel by organic and inorganic zinc-rich primers
| NASA-TP-3545 | p 1936 N95-25677
CORROSION RESISTANCE
Robotic weld overlay coatings for erosion control
| DE95-005187 | p 1939 N95-24285
Processing and properties of iridium alloys for space power applications
| DE95-005902 | p 1935 N95-25390
CORROSION TESTS
Localized corrosion and stress corrosion cracking characteristics of a low-aluminum-content iron-aluminum alloy
| DE95-003259 | p 1934 N95-24647
The corrosion protection of AISI(TM) 1010 steel by organic and inorganic zinc-rich primers
| NASA-TP-3545 | p 1936 N95-25677
COSMIC GASES
Far-infrared and submillimeter spectroscopy of photodissociation regions
| DE95-607520 | p 2110 N95-25467
COSMIC RAY SHOWERS
Milagro: A low energy threshold extensive air shower array
| DE95-005246 | p 2110 N95-25675
COSMIC RAYS
High LET, passive space radiation dosimetry and spectrometry
| NASA-CR-197694 | p 2058 N95-25911
Linear Energy Transfer (LET) spectra of cosmic radiation in low Earth orbit p 2061 N95-25926
Experimental and calculated LET distributions in the Cosmos-2044 biosatellite orbit p 2061 N95-25929
Cosmic ray LET spectra and doses on board Cosmos-2044 biosatellite p 2061 N95-25930
Cosmic ray particles with different LET values under various thicknesses of shielding in low altitude orbits: Calculations and Cosmos-2044 measurements p 2062 N95-25931
COSMOLOGY
Quantum corrections for a cosmological string solution
| DE95-006057 | p 2109 N95-24327
Heat Kernel expansion on a cone and quantum fields near cosmic strings
| DE94-628520 | p 2094 N95-24507
Creation of a scalar potential in 2D dilaton gravity
| DE95-006066 | p 2003 N95-24577
A quantum gravitational mechanism for exiting inflation
| DE95-003342 | p 2096 N95-24867
Relevance of induced gauge interactions in decoherence
| DE95-607082 | p 2097 N95-25432
Tachyon condensates and anisotropic universe
| DE95-607074 | p 2097 N95-25456
Valencia 1993: The summary of particle theory
| DE95-607121 | p 2110 N95-25469
Cosmological constraints on perturbative supersymmetry breaking
| PB95-165361 | p 2099 N95-25628
Homogeneous anisotropic cosmological models in the minimum quadratic Poincare gauge theory of gravity
| DE95-607083 | p 2110 N95-25647
Rich cluster simulation: Dynamics and mass estimates
| DE95-005233 | p 2110 N95-25766
A new formulation of quantum field theory on S4
| DE95-607098 | p 2099 N95-25970
COSMONAUTS
JPRS report: Science and technology. Central Eurasia: Space
| JPRS-USP-94-007 | p 1915 N95-24358
COSMOS SATELLITES
Cosmic ray LET spectra and doses on board Cosmos-2044 biosatellite p 2061 N95-25930
Radiobiological experiments with plant seeds aboard the biosatellite Cosmos 1887 p 2009 N95-25933
COST ANALYSIS
Small gas turbine component evaluation study
| PB95-147542 | p 1913 N95-24293
Monolithic solid oxide fuel cell technology advancement for coal-based power generation
| DE94-012258 | p 1990 N95-24318
COST EFFECTIVENESS
The physics design of the Tokamak Physics Experiment
| DE95-003649 | p 2076 N95-24548
Measuring the strategic value of information technology investments
| DE94-018160 | p 2104 N95-24603
Integrated planning: A baseline development perspective
| DE95-004945 | p 2102 N95-24905
Renewable Energy Demonstration Project by the National Renewable Energy Laboratory and the General Services Administration
| DE95-000261 | p 1995 N95-25995
COST ESTIMATES
Issues in NASA program and project management
| NASA-SP-6101(08) | p 2102 N95-24565
COST REDUCTION
Report of the Space Shuttle Management Independent Review Team
| NASA-TM-110579 | p 1919 N95-24466
Activities of the Ceramic Technology Project
| DE95-003394 | p 1940 N95-24588
Integrated planning: A baseline development perspective
| DE95-004945 | p 2102 N95-24905
COSTS
Methods of valuing air pollution and estimated monetary values of air pollutants in various US regions
| DE95-006854 | p 1998 N95-24618
Science in the national interest
| ISBN-0-16-045186-8 | p 2115 N95-26335
COULOMB COLLISIONS
Variational method for the calculation of the surface hyperspherical functions for the systems of ZH(mu)-type. The test calculation of the dt(mu)-system
| DE94-628905 | p 2033 N95-25539
Vacuum polarization effects in low-energy muonic atom collisions
| DE95-605393 | p 2058 N95-25910
COULOMB POTENTIAL
On a generalized Kepler-Coulomb system: Inter basis expansions
| DE94-636739 | p 2093 N95-24349
The Lienard-Wiechert potentials and relativistic length
| DE94-636733 | p 2093 N95-24376
Lienard-Wiechert potentials as a consequence of Lorentz transformation of Coulomb potential
| DE94-636734 | p 1952 N95-24377
Radiative corrections for pion polarizability experiments
| DE95-607177 | p 2053 N95-25462
COUPLING
A technique for the evaluation of strength of coupling between SEA subsystems
| ISVR-TR-241 | p 1981 N95-24997
A technique for the evaluation of strength of coupling between SEA subsystems: Experiments with two coupled plates and two coupled rooms
| ISVR-TR-242 | p 1982 N95-25332
Study of the simplest realistic Higgs sector in quark-lepton symmetric models
| DE95-607159 | p 2053 N95-25461
Anomalous WWZ couplings and K(sub L) yields mu(+) mu(-)
| DE95-607190 | p 2054 N95-25464
Electroweak coupling measurements from polarized Bhabha scattering at the Z(exp 0) resonance
| DE95-006090 | p 2057 N95-25768
COUPLING COEFFICIENTS
Coupling correction using closed orbit measurements
| DE95-005957 | p 2070 N95-25369
COUPLINGS
A test of the flavor independence of strong interactions
| DE95-005948 | p 2044 N95-24418
Probing anomalous gauge boson couplings at LEP
| DE95-005934 | p 2044 N95-24420
A test of the flavor independence of strong interactions
| DE95-006063 | p 2046 N95-24576
Decoherence, determinism and chaos revisited
| DE95-006070 | p 2094 N95-24578
Measurement of the WW gamma, ZZ gamma and Z gamm a gamma couplings at the Fermilab Tevatron
| DE95-003495 | p 2067 N95-24601
On a possible explanation of the origin of the quark mass spectrum
| DE95-605315 | p 2063 N95-25968
CRACK GEOMETRY
Stress analysis of a crack in the residual stress field by welding and its application to the fatigue crack propagation
| NAL-TR-1248 | p 1981 N95-25000
CRACK INITIATION
Estimate of probability of crack detection from service difficulty report data
| PB95-149381 | p 1905 N95-24295
Thermal fracture mechanisms in ceramic thermal barrier coatings p 1946 N95-26138
CRACK PROPAGATION
Estimate of probability of crack detection from service difficulty report data
| PB95-149381 | p 1905 N95-24295
Stress analysis of a crack in the residual stress field by welding and its application to the fatigue crack propagation
| NAL-TR-1248 | p 1981 N95-25000
Stress analysis of a crack in the residual stress field by welding and its application to the fatigue crack propagation
| NAL-TR-1248 | p 1983 N95-25796
Separation of crack extension modes in orthotropic delamination models
| NASA-TM-109180 | p 1927 N95-26083
CRACKING (FRACTURING)
An analysis of hypercritical states in elastic and inelastic systems
| IFTR-1/1994 | p 2037 N95-25339
New techniques to test fatigue properties of coined sheet specimens. Part 4: Development of experimental techniques
| PB95-165130 | p 1982 N95-25445
CRACKS
The dual boundary element formulation for elastoplastic fracture mechanics
| DRA-TR-93062 | p 1980 N95-24383
Processing and characterization of transformation-toughened ceramics with strength retention to elevated temperatures
| DE95-005758 | p 1941 N95-25387
New techniques to test fatigue properties of coined sheet specimens. Part 4: Development of experimental techniques
| PB95-165130 | p 1982 N95-25445
Separation of crack extension modes in orthotropic delamination models
| NASA-TM-109180 | p 1927 N95-26083
CRASHWORTHINESS
Analysis of warping effects on the static and dynamic response of a seat-type structure
| NIAR-94-12 | p 1979 N95-24211
CREEP PROPERTIES
Creep properties of 20% cold worked hastelloy XR
| DE94-785198 | p 1933 N95-24338
CREEP RUPTURE STRENGTH
Atom probe field ion microscopy of Type 308 CRE stainless steel welds
| DE94-019161 | p 1938 N95-26064
CREEP TESTS
Changes in the strength characteristics of 15HM boiler steel caused by initial plastic deformation under constant and monotonic loads
| IFTR-30/1994 | p 1938 N95-26333
CRETACEOUS-TERTIARY BOUNDARY
Biospheric effects of a large extraterrestrial impact: Case study of the cretaceous/tertiary boundary crater
| NASA-CR-198015 | p 1997 N95-24501
CREW WORKSTATIONS
A crew-centered flight deck design philosophy for High-Speed Civil Transport (HSCT) aircraft
| NASA-TM-109171 | p 1910 N95-24582
CRIME
How Captain Amerika uses neural networks to fight crime p 2025 N95-25272
CRITICAL FLOW
High frequency flow-structural interaction in dense subsonic fluids
| NASA-CR-4652 | p 1906 N95-24217
Electric field effects on a near-critical fluid in microgravity
| NASA-TM-106894 | p 2099 N95-25878
CRITICAL LOADING
Stability and elastic properties of hydrogen loaded Ti(1-x)Al(x) alloys: An ab initio study
| AD-A288903 | p 1936 N95-25529
CRITICAL TEMPERATURE
Critical parameters of Quark-Hadron phase transition with interacting and massive quarks
| DE95-607143 | p 2052 N95-25436
Statistical mechanics of the magnetized pair Bose gas
| DE95-607096 | p 2063 N95-25993

Condensate localization by mesoscale disorder in high-T(sub c) superconductors
[DE95-607819] p 1960 N95-26100

CROP GROWTH
The effects on photosynthetic CO2 assimilation to long-term elevation of atmospheric CO2 concentration: An assessment of the response of Trifolium Repens L. CV. Blanca grown at F.A.C.E
[DE95-005687] p 2008 N95-25383

CROSS FLOW
Three-dimensional interaction of wake/boundary-layer and vortex/boundary-layer data report
[CUED/A-AEREO/TR-23] p 1906 N95-24210
Laser beam log amplitude temporal scintillation spectrum due to crosswind. Part 1: Theory
[TR-1-FSRC-1994-PT-1] p 1971 N95-24371
Crossflow mixing of noncircular jets
[NASA-TM-106865] p 1913 N95-24390
Effect of density gradients in confined supersonic shear layers. Part 2: 3-D modes
[NASA-CR-198030] p 1962 N95-24413
Cross-flow, filter-sorbent-catalyst for particulate, SO2 and NO(x) control
[DE95-001934] p 2003 N95-26091

CROSS SECTIONS
Proceedings of the 1993 Symposium on Nuclear Data
[DE94-012554] p 2104 N95-24372
A Green's function method for hadrons in nuclei
[DE94-792620] p 2070 N95-25772

CROSSED FIELDS
Experimental constraints on transport
[DE95-004962] p 2050 N95-25180

CROSSLINKING
Pulse radiolysis of alkanes: A time-resolved electron paramagnetic resonance study
[DE95-005831] p 2045 N95-24459

CROSSTALK
Crosstalk on printed circuit boards
[PB95-165171] p 1960 N95-25472

CRYOGENIC EQUIPMENT
The measurement of the low frequency noise characteristics of the field effect transistors for cryogenic detectors
[DE94-628257] p 1957 N95-24487

CRYOGENIC FLUIDS
Thermohydrodynamic analysis of cryogenic liquid turbulent flow fluid film bearings, phase 2
[NASA-CR-197412] p 1962 N95-24461

CRYOGENICS
Simple chemical assays for presence of S2F10 in decomposed SF6
[DE95-001423] p 1929 N95-24345
Cryogenic helium gas convection research
[DE95-004372] p 1965 N95-25404
STEP: Satellite Test of the Equivalence Principle. Report on the phase A study
[NASA-TM-110598] p 1917 N95-26184

CRYSTAL DEFECTS
Melting of the moving vortex lattice in the presence of disorder
[DE95-004126] p 2087 N95-24868

CRYSTAL GROWTH
Estimates of effects of residual acceleration on USML-1 experiments
[NASA-CR-197964] p 2084 N95-24261
Nucleation and growth of crystals under cirrus and polar stratospheric cloud conditions
[NASA-CR-197991] p 2085 N95-24478
Convective flow effects on protein crystal growth
[NASA-CR-197891] p 2086 N95-24534
Development of optical systems — holographic technique for monitoring crystal growth
[NASA-CR-197702] p 2073 N95-24545
Crystal Growth Furnace (CGF)
[NASA-CR-196591] p 2089 N95-25409
Enhancement of thickness uniformity of thin films grown by pulsed laser deposition
[NASA-CR-197791] p 1943 N95-26081

CRYSTAL LATTICES
Test of an array of CsI(Tl) crystal towers for a low or medium energy e(+)e(-) collider calorimeter
[DE95-006068] p 2043 N95-24354
Melting of the moving vortex lattice in the presence of disorder
[DE95-004126] p 2087 N95-24868
Proceedings of the Workshop on Dynamics and Structure of Disordered System
[DE94-792685] p 1931 N95-25356
Coherent state path-integral representation of supersymmetric lattice models
[DE95-607820] p 2091 N95-26101
Rotational melting in displacive quantum paraelectrics
[DE95-607804] p 2091 N95-26252

CRYSTAL OSCILLATORS
Phase correction in two-crystal optical parametric oscillators
[DE95-006317] p 2074 N95-25559

CRYSTAL STRUCTURE
Design of supramolecular ordered systems for mesoscopic colloids and molecular composites
[DE95-004448] p 2048 N95-24687
Evolution of plastic anisotropy for high-strain-rate computations
[DE95-004220] p 1941 N95-25237
Reciprocal space analysis of the microstructure of luminescent and nonluminescent porous silicon films
[DE95-005420] p 1941 N95-25382
The geometry of disorder: Theoretical investigations of quasicrystals and frustrated magnets
[DE95-006641] p 1936 N95-25560
Atomistic studies of grain boundaries in NiAl
[DE95-005208] p 1937 N95-26014
Rotational melting in displacive quantum paraelectrics
[DE95-607804] p 2091 N95-26252

CRYSTALLINITY
Solution based synthesis of perovskite-type oxide films and powders
[DE95-006170] p 2086 N95-24594
Crystalline beams: Theory, experiments, and proposals
[DE95-003955] p 2068 N95-24685

CRYSTALLIZATION
Nucleation and growth of crystals under cirrus and polar stratospheric cloud conditions
[NASA-CR-197991] p 2085 N95-24478
Fusion proteins as alternate crystallization paths to difficult structure problems
[NASA-TM-110497] p 2008 N95-24531
Melting of the moving vortex lattice in the presence of disorder
[DE95-004126] p 2087 N95-24868
Domain growth in weakly disordered magnets: A coupled map lattice approach
[DE95-607663] p 2090 N95-25979

CRYSTALS
Kinetic modeling of the atomic layer epitaxy window in group 4 semiconductor growth
[DE95-005903] p 2089 N95-25391
Phase correction in two-crystal optical parametric oscillators
[DE95-006317] p 2074 N95-25559
The geometry of disorder: Theoretical investigations of quasicrystals and frustrated magnets
[DE95-006641] p 1936 N95-25560
Application of extended-crystal diffraction techniques to the symmetry and structure analysis of 221-PbBiSrCaCuO
[DE95-605913] p 2090 N95-25984

CUBES (MATHEMATICS)
Cyclic subgroups in class groups of real quadratic fields
[DE94-628407] p 2031 N95-24697

CUBIC LATTICES
On the calculation of lattice sums arising in Bose-Einstein statistics of quasiparticle excitations
[DE94-634531] p 2084 N95-24246

CURL (VECTORS)
Covolume solutions of three dimensional div-curl equations
[NASA-CR-195031] p 2029 N95-24421

CURRENT ALGEBRA
On the central charge in 3 D-supersymmetry
[DE95-600851] p 2093 N95-24352

CURVATURE
On corrections to the Nambu action
[NASA-CR-197625] p 2065 N95-24335
On squaring the primary constraints in a generalized Hamiltonian dynamics
[DE94-628500] p 2036 N95-24504

CYCLES
Modelling the day to day wind variability offshore central Chile at about 30 deg south
[DE95-606032] p 2006 N95-26043

CYCLIC ACCELERATORS
Eigenvector method for optimized orbit correction
[DE95-005967] p 2071 N95-25785

CYCLIC COMPOUNDS
Disilene Addition to C70
[DE95-006321] p 2087 N95-24617

CYCLIC LOADS
The effect of multidirectional cyclical deformation on the evolution of the plasticity surface of 18G2A steel
[IFTR-25/1994] p 1935 N95-25117
Oxidation of ion-implanted NiAl
[DE95-005899] p 1935 N95-25388
A description of the cyclical properties of an aluminum alloy based on complex stress state tests
[IFTR-29/1994] p 1936 N95-25638

CYCLOTRON RADIATION
Numerical analysis of electron cyclotron resonance heating on JT-60U and JFT-2M
[DE95-709766] p 2080 N95-25471

CYCLOTRON RESONANCE
Numerical analysis of electron cyclotron resonance heating on JT-60U and JFT-2M
[DE95-709766] p 2080 N95-25471

CYLINDRICAL SHELLS
Shell deformation states and the finite element method: A benchmark study of cylindrical shells
[PB95-149621] p 1980 N95-24296
Thermoelastic equations for multi-layered cylindrical shell
[NAL-TR-1222] p 1982 N95-25661
Three-dimensional solutions for thermomechanical stresses in sandwich panels and shells p 1984 N95-26265
Sensitivity analysis for the dynamic response of viscoplastic shells of revolution p 1984 N95-26268

CYTOLOGY
Activities of the National Institute of Radiological Sciences
[DE95-709916] p 2072 N95-26165

CZOCHRALSKI METHOD
Back surface cell structures for reducing recombination in CZ silicon solar cells
[DE95-005423] p 1995 N95-25566

D

DAMAGE
Reduction in fiber damage thresholds due to static fatigue
[DE95-004778] p 1979 N95-24263
Bird ingestion into large turbofan engines
[DOT/FAA/CT-93/14] p 1909 N95-24631
An overview of NDE methods for thick composites and a proposal for analysis of computed technology data
[AD-A288733] p 1979 N95-26055
Raman study of damage processes in Si(+)-implanted GaAs
[DE95-005898] p 2091 N95-26087

DAMAGE ASSESSMENT
Debris/ice/TPS assessment and integrated photographic analysis of shuttle mission STS-63
[NASA-TM-110649] p 1921 N95-25337
Emerging nondestructive inspection for aging aircraft
[PB95-143053] p 1905 N95-25401
Proceedings of the 2d USAF Aging Aircraft Conference
[AD-A288217] p 1911 N95-25578
Static and fatigue properties of pin-joint specimens of a AS-4/PEEK thermoplastic composite material
[NAL-TR-1214] p 1927 N95-25859
Transmission diagnostic research at NASA Lewis Research Center
[NASA-TM-106901] p 1977 N95-26076

DAMPING
The cooling of particle beams
[DE95-004669] p 2065 N95-24320

DARK MATTER
The influence of CDM on the dynamical estimate of (Omega) in the local neighborhood
[DE95-005212] p 2109 N95-24455
Possible constraints on SUSY-model parameters from direct dark matter search
[DE94-628561] p 2109 N95-24885
On SUSY dark matter detection with spinless nuclei
[DE94-628562] p 2109 N95-24886
Neutrino oscillations from discrete non-Abelian family symmetries
[DE95-004355] p 2052 N95-25403
Valencia 1993: The summary of particle theory
[DE95-607121] p 2110 N95-25469
Rich cluster simulation: Dynamics and mass estimates
[DE95-005233] p 2110 N95-25766

DATA ACQUISITION
An overview of Health and Usage Monitoring Systems (HUMS) for military helicopters
[DSTO-TR-0061] p 1905 N95-24200
Structure and manual of radioisotope-production data base, ISOP
[DE94-785197] p 2043 N95-24337
Activity Management System user reference manual
[DE95-000989] p 2105 N95-24654
Proceedings of the 1994 Conference on Computing in Energy Physics
[DE95-004442] p 2068 N95-24665
Directory of Energy Data Collection Forms: Forms in use as of October 1994
[DE95-004329] p 2105 N95-24710
Design of Fusion Safety Data Base
[DE95-703897] p 2080 N95-25495

The impact of multiplexing on the dynamic requirements of analog-to-digital converters
[DE95-006302] p 1960 N95-25558
Hardcopy extraction considerations for Vector Product Format (VPF) products
[AD-A288620] p 2106 N95-25608
The track system of the modernized Hyperon spectrometer
[DE95-604003] p 2058 N95-25905
Infrared multispectral sensor program, Phase 2. Field measurements, analysis and modeling. Volume 1: Fourier transform spectrometer sensor characterization
[AD-A288888] p 2075 N95-26173

DATA BASE MANAGEMENT SYSTEMS
Raising the IQ in full-text searching via intelligent querying
[DE95-002981] p 2103 N95-24330
CD-ROM in the age of internet
[DE95-005067] p 2104 N95-24454
Integrated resource management database for a distributed information system
[DE95-730180] p 2104 N95-24492
Current experiments in elementary particle physics. Revision
[DE95-003797] p 2067 N95-24652
Activity Management System user reference manual
[DE95-000989] p 2105 N95-24654
Information management architecture for an integrated computing environment for the Environmental Restoration Program. Environmental Restoration Program, Volume 3: Interim technical architecture
[DE95-001386] p 2105 N95-24656
Overview of selected molecular biological databases
[DE95-005906] p 2008 N95-25181
The use of DBMS and document oriented interface in the TPLAN-system
[DE95-605219] p 2106 N95-25907

DATA BASES
Space shuttle propellant constitutive law verification tests
[NASA-CR-198047] p 1947 N95-24226
Atomic masses 1993. The 1993 atomic mass evaluation
[DE94-634462] p 2040 N95-24231
Structure and manual of radioisotope-production data base, ISOP
[DE94-785197] p 2043 N95-24337
NLS Flight Simulation Laboratory (FSL) documentation
[NASA-CR-196564] p 2104 N95-24439
Integrated resource management database for a distributed information system
[DE95-730180] p 2104 N95-24492
Current experiments in elementary particle physics. Revision
[DE95-003797] p 2067 N95-24652
Activity Management System user reference manual
[DE95-000989] p 2105 N95-24654
Overview of selected molecular biological databases
[DE95-005906] p 2008 N95-25181
Integration of heterogeneous data bases for development of a large-scale environmental data atlas for multi-platform PC and workstation users
[DE95-002689] p 2000 N95-25278
The NJOY nuclear data processing system: Version 91
[DE95-006764] p 2055 N95-25484
Design of Fusion Safety Data Base
[DE95-703897] p 2080 N95-25495
Hardcopy extraction considerations for Vector Product Format (VPF) products
[AD-A288620] p 2106 N95-25608
The use of DBMS and document oriented interface in the TPLAN-system
[DE95-605219] p 2106 N95-25907
Online nuclear data service
[DE95-602487] p 2107 N95-25941
Index of nuclear data libraries available from the IAEA Nuclear Data Section
[DE95-605213] p 2107 N95-25980
Long Duration Exposure Facility mini-data base user's guide: IBM-compatible PC computer version
[NASA-CR-4655] p 1925 N95-26072
A software tool to design thermal barrier coatings
p 1946 N95-26139

DATA COLLECTION PLATFORMS
Long endurance stratospheric solar powered airship
[PB95-178729] p 1911 N95-26009

DATA COMPRESSION
Clustering using winner-take-all units
[PB95-165403] p 2026 N95-25568

DATA INTEGRATION
Discrete-event-dynamic-system-based approaches for control in integrated voice/data multihop Radio Networks
[AD-A288389] p 1954 N95-25604

DATA LINKS
Discrete-event-dynamic-system-based approaches for control in integrated voice/data multihop Radio Networks
[AD-A288389] p 1954 N95-25604

DATA MANAGEMENT
Software engineering and data management for automated payload experiment tool
[NASA-CR-196562] p 2104 N95-24477
Software engineering and data management for automated payload experiment tool
[NASA-CR-197703] p 2016 N95-24876

DATA PROCESSING
Theoretical and experimental studies on the C15 intermetallic compound NbCr2
[DE95-003665] p 2086 N95-24513
Thin film ionic conductors based on cerium oxide
[DE95-003668] p 2086 N95-24514
Technical report series on global modeling and data assimilation. Volume 5: Documentation of the AIRES/GEOS dynamical core, version 2
[NASA-TM-104606-VOL-5] p 2003 N95-24766
Assessment of climate variability of the Greenland ice sheet: Integration of in situ and satellite data
[NASA-CR-198020] p 1998 N95-24846
Using digital filtering techniques as an aid in wind turbine data analysis
[DE94-011862] p 1993 N95-24853
Multidimensional data analysis on the basis of integral nonparametric statistics and multilayer perceptrons
[DE94-628375] p 2035 N95-24858
The NJOY nuclear data processing system: Version 91
[DE95-006764] p 2055 N95-25484
Dynamic matrices and their application to the concept of a semi-sparse matrix
[AD-A288688] p 2035 N95-26051

DATA PROCESSING EQUIPMENT
The NJOY nuclear data processing system: Version 91
[DE95-006764] p 2055 N95-25484

DATA REDUCTION
Using digital filtering techniques as an aid in wind turbine data analysis
[DE94-011862] p 1993 N95-24853

DATA RETRIEVAL
A report: A plan to establish Internet access points at Minority Campus sites for connection to a central computing facility
[DE95-004374] p 2105 N95-25240
Holograpy machine HORN-1 for computer-aided retrieve of virtual three-dimensional image
[NIFS-218] p 1971 N95-26182

DATA SMOOTHING
A brief survey of constrained mechanics and variational problems in terms of differential forms
p 2026 N95-25803

DATA STORAGE
Dynamic matrices and their application to the concept of a semi-sparse matrix
[AD-A288688] p 2035 N95-26051

DATA STRUCTURES
A generic data exchange scheme between FITS format and C structures
[DE95-004849] p 2106 N95-25376

DATA SYSTEMS
The impact of multiplexing on the dynamic requirements of analog-to-digital converters
[DE95-006302] p 1960 N95-25558
Geographical information systems and other tools for spatial information management
[PB95-165759] p 2106 N95-25572

DATA TRANSMISSION
The accident site portable integrated video system
[DE95-000539] p 1953 N95-24605
Annual report 1992/93, FOA 38. Radio systems and wave propagation
[PB95-141735] p 1953 N95-24835
Dynamics of TCP traffic over ATM networks
[DE95-004687] p 2021 N95-25359
A generic data exchange scheme between FITS format and C structures
[DE95-004849] p 2106 N95-25376
Converting multiple OC-3c ATM streams to HIPPI to drive an HDTV frame buffer from a workstation cluster
[DE95-003638] p 2022 N95-26066

DE BROGLIE WAVELENGTHS
Observation of the scalar Aharonov-Bohm effect by neutron interferometry
[DE95-607020] p 2097 N95-25446

DEATH
A longevity and survival analysis for a cohort of retired airline pilots
[DOT/FAA/AM-95/5] p 2012 N95-24237

DEBRIS
Quantity-distance requirements for earth-bermed aircraft shelters
[AD-A279692] p 1915 N95-24424
Debris/ice/TPS assessment and integrated photographic analysis of shuttle mission STS-63
[NASA-TM-110649] p 1921 N95-25337

DECAY
The track system of the modernized Hyperon spectrometer
[DE95-604003] p 2058 N95-25905

DECAY RATES
Decay of a laser generated shock wave in an aluminium target
[DE94-629014] p 1972 N95-24707

DECELERATION
Laser cooling of neutral atoms by red-shifted diffuse light in an optical integral sphere cavity
[DE94-634310] p 2041 N95-24268

DECISION MAKING
The scientific programme between ESRO and ESA: Choosing new projects (1973-1977)
[ESA-HSR-16] p 1917 N95-24896
Planning for the unknown: Coping with uncertainty
[PB95-165114] p 2102 N95-25642

DECODING
On the Trellis structure of a (64,40,8) subcode of the (64,42,8) third-order Reed-Muller code
[NASA-CR-198019] p 2015 N95-24224
Circuit for high resolution decoding of multi-anode microchannel array detectors
[NASA-CASE-GSC-13478-1] p 1960 N95-25889

DECOMPOSITION
Direct catalytic decomposition of nitric oxide
[DE95-005202] p 1928 N95-24286
Simple chemical assays for presence of S2F10 in decomposed SF6
[DE95-001423] p 1929 N95-24345
A domain decomposition study of massively parallel computing in compressible gas dynamics
[DE95-004759] p 1965 N95-25895

DECONTAMINATION
SPEEDUP simulation of liquid waste batch processing, revision 1
[DE95-001240] p 1939 N95-24344
Characterizing pre-polished Type 304L stainless steel
[DE95-001241] p 1934 N95-24480
Stainless steel recycle
[DE95-003905] p 1934 N95-24615
Chelant extraction and REDOX manipulation for mobilization of heavy metals from contaminated soils
[DE95-004131] p 2000 N95-25363
Evaluation of commercial fuel tank water absorbers
[AD-A288361] p 1951 N95-25513

DEEP SPACE NETWORK
Hidden Markov models and neural networks for fault detection in dynamic systems p 2024 N95-25261

DEFECTS
Response to a localized impact loading of a composite multilayered rotational shell structure: Theory and numerical methods, volume 1
[ONERA-NT-1994-10-VOL-1] p 1979 N95-24282
Response to a localized impact loading of a composite multilayered rotational shell structure: Theory and numerical methods, volume 2
[ONERA-NT-1994-10-VOL-2] p 1980 N95-24283
Response to a localized impact loading of a composite multilayered rotational shell structure: Theory and numerical methods, Volume 3
[ONERA-NT-1994-10-VOL-3] p 1980 N95-24284
Dynamics of phase ordering of nematics in a pore
[DE95-607662] p 2090 N95-25978
An overview of NDE methods for thick composites and a proposal for analysis of computed technology data
[AD-A288733] p 1979 N95-26055

DEFENSE PROGRAM
Annual report 1992/93, FOA 38. Radio systems and wave propagation
[PB95-141735] p 1953 N95-24835
Assessment of Commercial Satellite Communications Initiative (CSCI) studies
[AD-A288357] p 1920 N95-25508
Planning for the unknown: Coping with uncertainty
[PB95-165114] p 2102 N95-25642

DEFLECTION
Shell deformation states and the finite element method: A benchmark study of cylindrical shells
[PB95-149621] p 1980 N95-24296

DEFORMATION
Analysis of warping effects on the static and dynamic response of a seat-type structure
[NIAR-94-12] p 1979 N95-24211
The temperature and strain rate dependence of the flow stress of single crystal NiAl deformed along the zone group axes (110)
[DE95-003634] p 2083 N95-24233

Shell deformation states and the finite element method: A benchmark study of cylindrical shells
[PB95-149621] p 1980 N95-24296
Elliptic deformed Newton mechanics in the three-dimensional phase space
[DE94-636741] p 2092 N95-24313
On the finite element implementation of the generalized method of cells micromechanics constitutive model
[NASA-CR-195451] p 1980 N95-24398
Temperature and strain-rate effects on deformation mechanisms in irradiated stainless steel
[DE95-004941] p 1934 N95-24449
Residual Stress Measurements with Laser Speckle Correlation Interferometry and Local Heat Treating
[DE95-060082] p 1981 N95-24598
A description of the cyclical properties of an aluminum alloy based on complex stress state tests
[IFTR-29/1994] p 1936 N95-25638
Thermoelastic equations for multi-layered cylindrical shell
[NAL-TR-1222] p 1982 N95-25661
Modelling the day to day wind variability offshore central Chile at about 30 deg south
[DE95-606032] p 2006 N95-26043
Static recrystallization behavior of austenite in HSLA 10C during Thermomechanical Controlled Processing (TMCP)
[AD-A288737] p 1937 N95-26057
A fully associative, nonisothermal, nonlinear kinematic, unified viscoplastic model for titanium alloys
[NASA-TM-106926] p 1983 N95-26078
Techniques for studying the mechanical properties of materials in complex stress states
[IFTR-34/1994] p 1983 N95-26178
An experimental determination of the plastic anisotropy of metal
[IFTR-33/1994] p 1938 N95-26179
The rotations of deformable bodies. Part 1: Geometry and Kinematics
[IFTR-7/1994] p 2039 N95-26332

DEFROSTING
Performance tests of air source heat pumps under frosting conditions. Quality of results
[PB95-141792] p 1995 N95-25892

DEGENERATION
Dynamic Jahn-Teller-induced infrared absorption of a charged C60(-) molecule
[DE95-607577] p 2063 N95-25971

DEGRADATION
Reduction in fiber damage thresholds due to static fatigue
[DE95-004778] p 1979 N95-24263
Differential preamplifier and pre-emphasis network
[AD-A288780] p 1961 N95-26186

DEGREES OF FREEDOM
Quantization of a Hamiltonian system with an infinite number of degrees of freedom
[DE95-605279] p 2034 N95-25783

DEHYDRATION
High octane ethers from synthesis gas-derived alcohols
[DE95-001146] p 1948 N95-24655

DELAMINATING
Separation of crack extension modes in orthotropic delamination models
[NASA-TM-109180] p 1927 N95-26083
Overview of thermal barrier coatings in diesel engines p 1945 N95-26129
Effects of through-the-thickness stitching on impact and interlaminar fracture properties of textile graphite/epoxy laminates
[NASA-CR-195042] p 1928 N95-26203

DELAY LINES
Large-format high resolution microchannel plate detectors for ultraviolet astronomy
[NASA-CR-197993] p 2108 N95-25104
Type P dispersive delay lines p 1959 N95-25116

DELTA FUNCTION
On an expansion of the Fermi function
[DE94-628494] p 2035 N95-24883

DELTA WINGS
Low speed aerodynamic characteristics of delta wings with vortex flaps: 60 deg and 70 deg delta wings
[NAL-TR-1245] p 1907 N95-25105

DENSITY (MASS/VOLUME)
Effect of density gradients in confined supersonic shear layers, part 1
[NASA-CR-198029] p 1962 N95-24412
Effect of density gradients in confined supersonic shear layers. Part 2: 3-D modes
[NASA-CR-198030] p 1962 N95-24413

DENSITY DISTRIBUTION
On the joint spectral density of bivariate random sequences
[NASA-CR-197698] p 2035 N95-24278
Aerodynamic characteristics of the orbital reentry vehicle experimental probe fins in a supersonic flow
[NAL-TR-1232] p 1921 N95-25664
Correlated density matrix theory of spatially inhomogeneous Bose fluids
[DE95-607840] p 2100 N95-26102
Calculating the thermodynamic properties of planar and spherical liquid-vapour interface
[DE95-608777] p 2100 N95-26105

DENSITY MEASUREMENT
Fischer Tropsch synthesis in supercritical fluids
[DE95-005206] p 1929 N95-24341

DEPOLARIZATION
Depolarization in the SLC Collider Arcs
[DE95-005942] p 2065 N95-24409
On analysis of resonance neutron depolarization in uniaxial media
[DE95-703782] p 2057 N95-25669

DEPOSITION
Characterization and performance of carbon films deposited by plasma and ion beam based techniques
[DE95-005213] p 1940 N95-24456
Magnetically controlled deposition of metals using gas plasma
[DE95-003827] p 2077 N95-24552

DEPOSITS
Biospheric effects of a large extraterrestrial impact: Case study of the cretaceous/tertiary boundary crater
[NASA-CR-198015] p 1997 N95-24501

DEPTH
Depth distribution of absorbed dose on the external surface of Cosmos 1887 biosatellite p 2061 N95-25927

DERIVATION
Testing of experimental antileishmanial compounds
[AD-A288807] p 2009 N95-26193

DESCENT
Space basic
[NASA-TM-110540] p 2108 N95-24196
STS-66 mission highlights resource tape
[NASA-TM-110550] p 1918 N95-24197

DESIGN ANALYSIS
Solar Eagle 2
[NASA-CR-198043] p 1990 N95-24199
Actively controlled shaft seals for aerospace applications
[NASA-CR-198035] p 1974 N95-24218
Optical generation of radio-frequency power
[DE95-005276] p 1951 N95-24289
Monolithic solid oxide fuel cell technology advancement for coal-based power generation
[DE94-012258] p 1990 N95-24318
Development of a model protection and dynamic response monitoring system for the national transonic facility
[NASA-CR-195041] p 1915 N95-24388
New approaches to optimization in aerospace conceptual design
[NASA-CR-196695] p 1910 N95-24436
Availability analysis of a 100 kWh superconducting magnetic energy storage
[DE95-737621] p 2066 N95-24448
Integration of design, structural, thermal and optical analysis: And user's guide for structural-to-optical translator (PATCOD)
[NASA-TM-110153] p 1950 N95-24559
Parallel processing for scientific computations
[NASA-CR-198013] p 2020 N95-24563
A crew-centered flight deck design philosophy for High-Speed Civil Transport (HSCT) aircraft
[NASA-TM-109171] p 1910 N95-24582
Recipes for high resolution time-of-flight detectors
[DE95-006196] p 1967 N95-24596
The development of a positron ionization gauge
[DE95-005958] p 1968 N95-24623
Engineering and design of a CO2 phase contrast interferometer system for DIII-D
[DE95-004249] p 1972 N95-24709
The KTeV PMT laser monitoring system
[DE95-004237] p 1972 N95-24869
The CDF silicon vertex detector SVX and its upgrades
[DE95-003743] p 2050 N95-24901
Tunable vibration absorbers: Key design parameters
[ISVR-TR-244] p 1981 N95-24995
A vacuum window for a 1 MW CW 110 GHz gyrotron
[DE94-016584] p 2079 N95-25108
Elise: The next step in development of induction heavy ion drivers for inertial fusion energy
[DE95-004679] p 2069 N95-25358
Spray characteristics of single- and three-hole nozzle injectors in ambient air and in a motored single-cylinder test engine
[PB95-166286] p 1976 N95-25574
An ion sensitive probe and its application to a mirror device
[DE95-602307] p 1970 N95-25940
Long endurance stratospheric solar powered airship
[PB95-178729] p 1911 N95-26009
Field-portable reflectance spectrometer
[AD-A288750] p 1970 N95-26059
A design perspective on thermal barrier coatings p 1943 N95-26120

DESTABILIZATION
Self-sustained turbulence and L-mode confinement in toroidal plasmas 2
[NIFS-278] p 2082 N95-25759

DESTRUCTION
Bound states of 'dressed' particles
[DE94-636773] p 2042 N95-24314

DESTRUCTIVE TESTS
Heat release rate measurements in tunnel fires
[PB95-165106] p 1931 N95-25443

DETECTION
Muon identifier efficiency of the GINES detecto r in the UNK neutrino beam
[DE94-628254] p 2045 N95-24485
Field-usable portable analyzer for chlorinated organic compounds
[DE95-003127] p 1930 N95-25098
An overview of NDE methods for thick composites and a proposal for analysis of computed technology data
[AD-A288733] p 1979 N95-26055

DETECTORS
Detector for transit time measurement of photomultiplier single-photoelectron pulses
[DE94-628256] p 2073 N95-24642
Unfolding of true distributions from experimental data distorted by detectors with finite resolutions
[DE94-628372] p 2035 N95-24643

DETONATION
The critical diameter, detonation velocity and shock sensitivity of Australian PBXW-115
[DSTO-TR-0076] p 1947 N95-24394
Explosive performance measurements on large, multiple-hole arrays and large masses of conventional explosive
[DE95-002718] p 1948 N95-24670

DEUTERIUM
Benchmark experiment on a copper slab assembly bombarded by D-T neutrons
[DE95-709764] p 2055 N95-25497

DEUTERIUM FLUORIDES
The effects of the environment on an experimental VHF radio Direction Finding antenna system
[AD-A288791] p 1956 N95-26191

DEUTERONS
Spin structure of the nucleon and polarization
[DE95-004282] p 2047 N95-24662

DEVELOPING NATIONS
Preparatory research for global warming precaution spread promotion manual and early spread plan research work
[DE95-730143] p 1996 N95-24291
Construction of a nitrogen laser for plasma diagnostics
[DE95-607599] p 1973 N95-25973

DIAGNOSIS
Neural network application to comprehensive engine diagnostics p 2023 N95-25255
Photonics: From target recognition to lesion detection p 2023 N95-25259
Neural networks: Application to medical imaging p 2025 N95-25267
Grounding explanations in evolving, diagnostic situations
[NASA-CR-198027] p 2026 N95-25335

DIAMAGNETISM
Transport suppression by diamagnetic phase shift as a possible mechanism to the L to H transition
[DE95-003345] p 2077 N95-24587

DIAMETERS
The critical diameter, detonation velocity and shock sensitivity of Australian PBXW-115
[DSTO-TR-0076] p 1947 N95-24394

DIAMOND FILMS
Measurements of thermal conductivity of diamond thin films by the ac calorimetric method
[PB95-149746] p 1939 N95-24300
Study of very high temperature technology, 2
[DE95-730105] p 2088 N95-24900
Wear-resistant, self-lubricating surfaces of diamond coatings
[NASA-TM-106887] p 1924 N95-25961

DIAMONDS
Measurements of thermal conductivity of diamond thin films by the ac calorimetric method
[PB95-149746] p 1939 N95-24300
A photoemission study of the diamond and the single crystal C(60)
[DE95-006149] p 2085 N95-24463
Potential of diamond for applications in microelectronics
[PB95-141446] p 1942 N95-25633

Pulsed laser annealing of P implanted diamond
[DE95-605947] p 2090 N95-25985

DICTIONARIES
Machine-aided indexing at NASA
[NASA-CR-197796] p 2106 N95-25410

DIELECTRIC PROPERTIES
Asymptotics for the Kummer function of Bose plasmas
[DE95-607019] p 2096 N95-25428

DIELECTRICS
The diffraction of electromagnetic waves by screens placed at the boundaries of dielectric media
[IFTR-4/1994] p 1954 N95-25393
Two dimensional Bose plasma in a magnetic field
[DE95-607629] p 2082 N95-25976

DIESEL ENGINES
Diesel fuel component contribution to engine emissions and performance
[DE95-000238] p 1998 N95-24604
Thermal Barrier Coating Workshop
[NASA-CP-10170] p 1943 N95-26119
Thermal barrier coatings application in diesel engines
p 1944 N95-26124
Overview of thermal barrier coatings in diesel engines
p 1945 N95-26129
Thick thermal barrier coatings for diesel engines
p 1946 N95-26136

DIESEL FUELS
Diesel fuel component contribution to engine emissions and performance
[DE95-000238] p 1998 N95-24604

DIFFERENTIAL AMPLIFIERS
Differential preamplifier and pre-emphasis network
[AD-A288780] p 1961 N95-26186

DIFFERENTIAL EQUATIONS
Periodic solutions of Hamiltonian perturbations of 2D linear Schroedinger equations
[PB95-165536] p 2028 N95-24301
Application of compartmental metabolic models for determination of retention and excretion functions
[DE95-600249] p 2010 N95-24367
Linear non-modal phenomena in numerical analysis and applied mathematics
[DE95-005495] p 2029 N95-24458
Aerodynamic parameter estimation via Fourier modulating function techniques
[NASA-CR-4654] p 1911 N95-24630
Symbolic dynamics of the Lorenz equations
[DE95-607045] p 2036 N95-25439
Singularly perturbed differential/algebraic equations
[AD-A288365] p 2033 N95-25601
Thermoelastic equations for multi-layered cylindrical shell
[NAL-TR-1222] p 1982 N95-25661

DIFFERENTIAL GEOMETRY
Quantum symplectic geometry. 1: The matrix Hamiltonian formalism
[DE95-607009] p 2032 N95-25427
A partial unification model in non-commutative geometry
[DE95-607129] p 2097 N95-25435

DIFFRACTION
On a possibility for a measurement of the transversal proton polarization in the diffractive pion production in pp and pe high energy collisions
[DE94-628598] p 2047 N95-24668
Application of extended-crystal diffraction techniques to the symmetry and structure analysis of 221-PbBiSrCaCuO
[DE95-605913] p 2090 N95-25984

DIFFRACTION PATTERNS
Limiting analytic form for Aharonov-Bohm diffraction pattern
[DE95-600839] p 2065 N95-24351

DIFFRACTION PROPAGATION
Optical diffraction from fractals with a structural transition
[DE94-634311] p 2029 N95-24401

DIFFRACTOMETERS
User guide for the Polaris powder diffractometer at ISIS. Version 2.1
[PB95-165767] p 2074 N95-25573

DIFFUSE RADIATION
Laser cooling of neutral atoms by red-shifted diffuse light in an optical integral sphere cavity
[DE94-634310] p 2041 N95-24268
Gamma-ray emission from globular clusters. Shock high energy emission from the Be-Star/Pulsar System PSR 1259-63. Echoes in x-ray novae
[NASA-CR-197994] p 2114 N95-24381
Estimation and analysis of spectral solar radiation over Cairo
[DE95-606029] p 2113 N95-25986

DIFFUSION
Fischer Tropsch synthesis in supercritical fluids
[DE95-005206] p 1929 N95-24341
Solution based synthesis of perovskite-type oxide films and powders
[DE95-006170] p 2086 N95-24594
Experimental constraints on transport
[DE95-004962] p 2050 N95-25180
Evaluation of a diffusion/trapping model for hydrogen ingress in high-strength alloys
[AD-A288447] p 1936 N95-25502
Viscoelastic waves and multiple scales
[DE94-014130] p 1966 N95-26063

DIFFUSION COEFFICIENT
A proposal to introduce a turbulence factor into a diffusion coefficient of a Tokamak plasma
[DE94-777533] p 2075 N95-24272
Fischer Tropsch synthesis in supercritical fluids
[DE95-005206] p 1929 N95-24341

DIFFUSION THEORY
Quantum group random walks in strongly correlated 2+1 D spin systems
[DE95-607844] p 2091 N95-26103

DIFFUSION WELDING
JPRS report: Science and technology. Central Eurasia
[JPRS-UST-95-012] p 1950 N95-24540

DIGITAL DATA
Study on propagation impairments, distortions and unavailability on digital microwave links
[DE95-723047] p 1953 N95-24848
Using digital filtering techniques as an aid in wind turbine data analysis
[DE94-011862] p 1993 N95-24853

DIGITAL ELECTRONICS
ASIC implementation of a data-push architecture for silicon pixel readout
[DE95-003368] p 2015 N95-24648

DIGITAL FILTERS
Adaptive projective filters
[DE94-628374] p 2030 N95-24645
Using digital filtering techniques as an aid in wind turbine data analysis
[DE94-011862] p 1993 N95-24853

DIGITAL NAVIGATION
Interfacing a digital compass to a remote-controlled helicopter
[PB95-164927] p 1914 N95-24260

DIGITAL SIMULATION
Finite element methods in a simulation code for offshore wind turbines
[PB95-164984] p 1994 N95-25501

DIGITAL SYSTEMS
ARMDAT: A brief description of a computerized test system for burst transmission
[PB95-165452] p 1951 N95-24241
Tutorial on beam-based feedback systems for linacs
[DE95-006054] p 2067 N95-24573
A generic data exchange scheme between FITS format and C structures
[DE95-004849] p 2106 N95-25376
Hardcopy extraction considerations for Vector Product Format (VPF) products
[AD-A288620] p 2106 N95-25608

DIGITAL TECHNIQUES
Numerical and symbolic algorithms for application specific signal processing
[AD-A288202] p 2017 N95-25507

DIMENSIONAL ANALYSIS
Simulation study of tapered FEL amplifiers in Raman and Compton regimes
[DE94-785266] p 1971 N95-24340
Evaluation of the performance of an annular diffusion denuder
[DE95-002258] p 1998 N95-24606

DIMERIZATION
Carbons and hydrogen by persistent metal radicals
[DE95-003834] p 1929 N95-24553

DIODES
Diode laser pumped solid state laser with 2 micrometer wavelength
[PB95-165270] p 1973 N95-25622

DIRAC EQUATION
On the field theory of the extended-type electron
[DE95-607069] p 2053 N95-25449

DIRECTION FINDING
The effects of the environment on an experimental VHF radio Direction Finding antenna system
[AD-A288791] p 1956 N95-26191

DIRECTIONAL ANTENNAS
A satellite-tracking millimeter-wave reflector antenna system for mobile satellite-tracking
[NASA-CASE-NPO-18772-1-CU] p 1954 N95-25316

DIRECTIONAL CONTROL
Performance of an aerodynamic yaw controller mounted on the space shuttle orbiter body flap at Mach 10
[NASA-TM-109179] p 1906 N95-24397

DIRECTIONAL STABILITY
Suspension system for gimbal supported scanning payloads
[NASA-CASE-MFS-28817-1] p 1969 N95-25544

DIRECTORIES
EOS Directory
[NASA-TM-110580] p 1989 N95-24542
Directory of Energy Data Collection Forms: Forms in use as of October 1994
[DE95-004329] p 2105 N95-24710
Directory of Defence and Aerospace Information Centers
[AGARD-R-802] p 2107 N95-26334

DISCOVERY (ORBITER)
Debris/ice/TPS assessment and integrated photographic analysis of shuttle mission STS-63
[NASA-TM-110649] p 1921 N95-25337

DISCRETE FUNCTIONS
A discrete variable representation for electron-hydrogen atom scattering
[DE95-003436] p 2045 N95-24512

DISCRIMINANT ANALYSIS (STATISTICS)
Automatic classification of Polish fricatives on the basis of optimization of the parameter space
[IFTR-9/1994] p 1956 N95-26331

DISORDERS
The geometry of disorder: Theoretical investigations of quasicrystals and frustrated magnets
[DE95-006641] p 1936 N95-25560

DISPLACEMENT
Separation of crack extension modes in orthotropic delamination models
[NASA-TM-109180] p 1927 N95-26083

DISPLACEMENT MEASUREMENT
X-ray based displacement and strain measurements for hostile environments
[NASA-CR-194451] p 1968 N95-25330
Angular displacement measuring device
[NASA-CASE-ARC-11937-1] p 2074 N95-26015

DISPLAY DEVICES
Display technologies in Russia, Ukraine, and Belarus
[ISBN-1-883712-36-X] p 2085 N95-24460
Psychophysical evaluation of three-dimensional auditory displays
[NASA-CR-198010] p 2011 N95-24564
Colour vision deficiencies: Matching and confusion of computer colours
[PB95-141925] p 2013 N95-24864
Preliminary experiments of an optical fiber display
[NAL-TR-1257] p 2073 N95-25004
Geographical information systems and other tools for spatial information management
[PB95-165759] p 2106 N95-25572
Temporal pacing in visual attention
[AD-A289785] p 2013 N95-26041

DISRUPTING
Modeling plasma/material interactions during a tokamak disruption
[DE95-004247] p 2078 N95-24861

DISSIPATION
A fully associative, nonisothermal, nonlinear kinematic, unified viscoplastic model for titanium alloys
[NASA-TM-106926] p 1983 N95-26078

DISSOCIATION
Fragmentation cross sections of O-16 between 0.9 and 200 GeV/nucleon p 2060 N95-25921

DISTANCE
Distances on a lattice from noncommutative geometry
[DE94-634327] p 2027 N95-24229

DISTORTION
Effect of mesh distortion on the accuracy of transverse shear stresses and their sensitivity coefficients in multilayered composites p 1985 N95-26270

DISTRIBUTED PROCESSING
Computational load in model physics of the parallel NCAR community climate model
[DE95-005410] p 2019 N95-24342
Integrated resource management database for a distributed information system
[DE95-730180] p 2104 N95-24492
Downsizing systems and expected opposition to introduction
[DE95-730186] p 2104 N95-24494
Proceedings of workshop on Future in HEP Computing
[DE94-792684] p 2021 N95-25303
Numerical and symbolic algorithms for application specific signal processing
[AD-A288202] p 2017 N95-25507
The coupling of fluids, dynamics, and controls on advanced architecture computers
[NASA-CR-197727] p 2017 N95-25797

DISTRIBUTION (PROPERTY)
Unfolding of true distributions from experimental data distorted by detectors with finite resolutions
[DE94-628372] p 2035 N95-24643

DISTRIBUTION FUNCTIONS
Multidimensional data analysis on the basis of integral nonparametric statistics and multilayer perceptrons
[DE94-628375] p 2035 N95-24858
Results obtained using the pellet charge exchange diagnostic on TFTR
[DE95-003254] p 2079 N95-25120
DISTRIBUTORS
Software of a distributor of high voltage of the H C-600 hadronic calorimeter
[DE94-628255] p 1967 N95-24486
DIURNAL VARIATIONS
Diurnal variations of backscattering properties of pine trees at C- and X-bands
[PB95-149738] p 1988 N95-24299
Simulation of diurnal thermal energy storage systems: Preliminary results
[DE95-005751] p 1991 N95-24369
Sleep patterns in air traffic controllers working rapidly rotating shifts: A field study
[DOT/FAA/AM-95/12] p 2012 N95-26204
DIVERGENCE
Covolume solutions of three dimensional div-curl equations
[NASA-CR-195031] p 2029 N95-24421
DIVERTERS
Divertor design for the Tokamak Physics Experiment
[DE95-003653] p 2078 N95-24650
Heat removal capability of divertor coaxial tube assembly
[DE95-709770] p 1966 N95-26161
DIVERTORS (FUSION REACTORS)
The physics design of the Tokamak Physics Experiment
[DE95-003649] p 2076 N95-24548
Modeling plasma/material interactions during a tokamak disruption
[DE95-004247] p 2078 N95-24861
New modular heliotron system compatible with closed helical divertor and good plasma confinement
[NIFS-279] p 2081 N95-25653
DOCUMENT STORAGE
NLS Flight Simulation Laboratory (FSL) documentation
[NASA-CR-196564] p 2104 N95-24439
DOCUMENTATION
NLS Flight Simulation Laboratory (FSL) documentation
[NASA-CR-196564] p 2104 N95-24439
Software engineering and data management for automated payload experiment tool
[NASA-CR-196562] p 2104 N95-24477
Directory of Energy Data Collection Forms: Forms in use as of October 1994
[DE95-004329] p 2105 N95-24710
Software engineering and data management for automated payload experiment tool
[NASA-CR-197703] p 2016 N95-24876
DOCUMENTS
Document analysis with neural net circuits
p 2023 N95-25256
Voluntary reporting of greenhouse gases under Section 1605(b) of the Energy Policy Act of 1992: General guidelines
[DE95-003295] p 2000 N95-25361
Applications for electronic documents
[DE95-005036] p 2106 N95-25765
DOMAIN WALL
Statistical mechanics of nonlinear coherent structures: Kinks in the Phi(sup 6) model
[DE95-005253] p 2096 N95-25293
Coercive field and domain wall properties in (Dy(x)Y(1-x))Fe2 and (Er(x)Y(1-x))Fe2
[DE95-601135] p 1937 N95-25751
DOMAINS
Domain growth in weakly disordered magnets: A coupled map lattice approach
[DE95-607663] p 2090 N95-25979
DONOR MATERIALS
Photoionization of shallow donor impurities in finite-barrier quantum wells
[DE95-607521] p 2097 N95-25468
DOPED CRYSTALS
The facility for commercial doping of silicon by thermal neutrons in channel 3 at the IBR-2
[DE94-636293] p 2085 N95-24374
Effect of He pressure on the superconducting transition temperatures of Na2CsC60 and (NH3)4Na2CsC60
[DE95-006320] p 2087 N95-24616
Fe-57 and Sn-119 Moessbauer studies on La(1.25)Nd(0.6)Sr(0.15)CuO4: Evidence for local magnetic ordering below (approx. equal) 32 K
[DE95-601210] p 1959 N95-25405
Back surface cell structures for reducing recombination in CZ silicon solar cells
[DE95-005423] p 1995 N95-25566
Diode laser pumped solid state laser with 2 micrometer wavelength
[PB95-165270] p 1973 N95-25622
LuAlO3: A high density, high speed scintillator for gamma detection
[DE95-004678] p 2064 N95-26256
DOPPLER EFFECT
The use of empirical models to investigate GPS derived total electron content
[DE95-606045] p 2111 N95-26044
DOPPLER RADAR
Laser based methods for range, Doppler and vibration measurements
[PB95-141958] p 1952 N95-24445
DOSAGE
Pulsed laser annealing of P implanted diamond
[DE95-605947] p 2090 N95-25985
DOSIMETERS
High LET, passive space radiation dosimetry and spectrometry
[NASA-CR-197694] p 2058 N95-25911
LET spectra measurements from the STS-35 CPDs
p 2058 N95-25912
Summary of LET spectra and dose measurements on ten STS missions p 2058 N95-25913
USF/Russian dosimetry on STS-57
p 2059 N95-25915
Dosimetry on STS-42 with the RME APD
p 2059 N95-25916
Proton calibration of low energy neutron detectors containing (6)LiF p 2060 N95-25925
DOUBLE BASE ROCKET PROPELLANTS
Space shuttle propellant constitutive law verification tests
[NASA-CR-198047] p 1947 N95-24226
DRAG REDUCTION
Numerical and experimental study of drag characteristics of two-dimensional HLFC airfoils in high subsonic, high Reynolds number flow
[NAL-TR-1244T] p 1907 N95-24998
A theoretical and experimental investigation of the flow over supersonic leading edge wing/body configurations
[DRA-TM-AERO-PROP-41] p 1907 N95-25649
DROPS (LIQUIDS)
Kinetics of diffusional droplet growth in a liquid/liquid two-phase system
[NASA-CR-198050] p 1961 N95-24221
Ignition of exploding aluminum droplets behind shock waves in water
[DE95-003975] p 1963 N95-24678
Effects of nitric acid vapor on the formation of cloud droplets in troposphere
[DE95-744869] p 2001 N95-25500
DRUGS
Motionsickness-seasickness: Summary of existing knowledge and suggested lines of development
[PB95-141495] p 2011 N95-24863
DRYING
Applications of solid lubricant films in spacecraft
[AD-A288784] p 1947 N95-26188
DUCTED FLOW
Study of compressible flow through a rectangular-to-semiannular transition duct
[NASA-CR-4660] p 1914 N95-24392
Recent improvements to and validation of the one dimensional NASA wave rotor model
[NASA-TM-106913] p 1908 N95-25962
Numerical simulation of laminar flow in a curved duct
[DE95-005427] p 1966 N95-26240
DUCTILE-BRITTLE TRANSITION
Processing and properties of iridium alloys for space power applications
[DE95-005902] p 1935 N95-25390
DUCTILITY
Composite ductility: The role of reinforcement and matrix
[DE95-003664] p 1925 N95-24590
DUCTS
Numerical simulation of laminar flow in a curved duct
[DE95-005427] p 1966 N95-26240
DWARF STARS
Resolution of the classical Hyades lithium problem
[DE95-003661] p 2109 N95-24234
DYADICS
Exact solution of 2 D Poincare gravity coupled with fermion matter
[DE95-605314] p 2099 N95-25967
DYNAMIC CHARACTERISTICS
High frequency flow-structural interaction in dense subsonic fluids
[NASA-CR-4652] p 1906 N95-24217
Experimental study of the effects of Reynolds number on high angle of attack aerodynamic characteristics of forebodies during rotary motion
[NASA-CR-195033] p 1907 N95-24443
Finite element methods in a simulation code for offshore wind turbines
[PB95-164984] p 1994 N95-25501
Dynamics of nonadiabatic charged particles in the magnetic dipole field with imposed homogeneous magnetic field
[DE95-605222] p 2057 N95-25778
DYNAMIC CONTROL
The transmission and control of vibrational power in a two stage isolation system with a water-loaded substructure
[ISVR-TR-235] p 1975 N95-24992
Understanding and improving materials processing through interpreting and manipulating predictive models
[DE95-004384] p 1930 N95-25242
High-beta discharges with neutral beam injection in CHS
[NIFS-280] p 2071 N95-26031
DYNAMIC LOADS
Dynamic load balancing for parallel finite element methods with adaptive h- and p-refinement
[DE95-004521] p 2021 N95-24681
Sensitivity analysis of the non-linear dynamic viscoplastic response of 2-d structures with respect to material parameters p 1984 N95-26266
DYNAMIC PROGRAMMING
Equivariant localization: BV-geometry and supersymmetric dynamics
[DE94-628436] p 2036 N95-24699
DYNAMIC RESPONSE
Analysis of warping effects on the static and dynamic response of a seat-type structure
[NIAR-94-12] p 1979 N95-24211
Development of a model protection and dynamic response monitoring system for the national transonic facility
[NASA-CR-195041] p 1915 N95-24388
Center for Computational Structures Technology
[NASA-CR-198028] p 1983 N95-26263
Sensitivity analysis of the non-linear dynamic viscoplastic response of 2-d structures with respect to material parameters p 1984 N95-26266
Sensitivity analysis for the dynamic response of viscoplastic shells of revolution p 1984 N95-26268
Sensitivity analysis for the dynamic response of thermoviscoplastic shells of revolution
p 1986 N95-26278
Dynamic sensitivity analysis of frictional contact/impact response of axisymmetric composite structures
p 1986 N95-26279
Sensitivity analysis for large-deflection and postbuckling responses on distributed-memory computers
p 1987 N95-26281
DYNAMIC STRUCTURAL ANALYSIS
A review of rolling element bearing vibration detection, diagnosis and prognosis
[DSTO-RR-0013] p 1975 N95-24393
Numerical simulation of the nonlinear response of composite plates under combined thermal and acoustic loading
[NASA-CR-197426] p 1981 N95-24907
The transmission and control of vibrational power in a two stage isolation system with a water-loaded substructure
[ISVR-TR-235] p 1975 N95-24992
Dynamic analysis of truss members using longitudinal waves
[IFTR-35/1994] p 1981 N95-24996
A technique for the evaluation of strength of coupling between SEA subsystems
[ISVR-TR-241] p 1981 N95-24997
An analytical study of the vibration of beams fitted with neutralizers. Part 3: Torsional wave motion
[ISVR-TR-238-PT-3] p 1982 N95-25003
A technique for the evaluation of strength of coupling between SEA subsystems: Experiments with two coupled plates and two coupled rooms
[ISVR-TR-242] p 1982 N95-25332
Dynamic methods for determining the material characteristics of saturated permeable media
[IFTR-17/1993] p 1932 N95-26107
Center for Computational Structures Technology
[NASA-CR-198028] p 1983 N95-26263
DYNAMIC TESTS
Analysis of warping effects on the static and dynamic response of a seat-type structure
[NIAR-94-12] p 1979 N95-24211
Experimental analysis of thread movement in bolted connections due to vibrations
[NASA-CR-197705] p 1975 N95-24991
The impact of multiplexing on the dynamic requirements of analog-to-digital converters
[DE95-006302] p 1960 N95-25558
DYNAMICAL SYSTEMS
Symbolic dynamics of the Lorenz equations
[DE95-607045] p 2036 N95-25439

Nonexistence of global solutions to some quasilinear hyperbolic equations with dynamic boundary conditions
[DE95-607010] p 2033 N95-25645
Actuating signals in adaptive control systems
[IFTR-13/1994] p 2027 N95-26330

E

EARTH ATMOSPHERE
Future emissions and concentrations of carbon dioxide: Key ocean/atmosphere/land analyses
[CSIRO-TP-31] p 1999 N95-25199
Environment, 1980-1993
[DE95-605240] p 2002 N95-25779
EARTH CRUST
3-D seismic imaging of complex geologies
[DE95-006813] p 2004 N95-25476
EARTH HYDROSPHERE
Environment, 1980-1993
[DE95-605240] p 2002 N95-25779
EARTH MAGNETOSPHERE
Dynamics Explorer 1, retarding ion mass spectrometer summary spectrograms-82/110 to 82/229 spin-time spectrograms for H(+), He(+), O(+), N(+), O(++), M/Z = 2, and molecular ions
[NASA-TM-108485] p 2003 N95-24763
Dynamics Explorer 1, retarding ion mass spectrometer summary spectrograms-82/230 to 82/265 spin-time spectrograms for H(+), He(+), O(+), N(+), O(++), M/Z = 2, and molecular ions
[NASA-TM-108486] p 2003 N95-24764
EARTH OBSERVATIONS (FROM SPACE)
STS-67 post flight presentation
[NASA-TM-110552] p 1918 N95-24198
EARTH OBSERVING SYSTEM (EOS)
EOS Directory
[NASA-TM-110580] p 1989 N95-24542
EARTH ORBITAL ENVIRONMENTS
Use of advanced solar cells for commercial communication satellites
[NASA-TM-106879] p 1991 N95-24560
Depth distribution of absorbed dose on the external surface of Cosmos 1887 biosatellite
p 2061 N95-25927
Neutron influences and energy spectra in the Cosmos-2044 biosatellite orbit p 2061 N95-25928
Experimental and calculated LET distributions in the Cosmos-2044 biosatellite orbit p 2061 N95-25929
Long Duration Exposure Facility mini-data base user's guide: IBM-compatible PC computer version
[NASA-CR-4655] p 1925 N95-26072
EARTH ORBITS
STS-66 mission highlights resource tape
[NASA-TM-110550] p 1918 N95-24197
EARTH SCIENCES
JPRS report: Science and technology. Central Eurasia
[JPRS-UST-95-009] p 1916 N95-24467
JPRS report: Science and technology. Central Eurasia
[JPRS-UST-94-018] p 1950 N95-24472
JPRS Report: Science and technology. Central Eurasia
[JPRS-UST-95-002] p 1916 N95-24621
JPRS report: Science and technology. Central Eurasia
[JPRS-UST-95-003] p 1988 N95-24730
JPRS Report: Science and technology. Central Eurasia
[JPRS-UST-94-031] p 1988 N95-24760
Summaries of FY 1994 geosciences research
[DE95-005657] p 1988 N95-25440
Perspectives from space: NASA classroom information and activities
[NASA-TM-110577] p 2100 N95-25643
Spaceborne synthetic aperture radar: Current status and future directions. A report to the Committee on Earth Sciences, Space Studies Board, National Research Council
[NASA-TM-4679] p 1955 N95-25710
JPRS report: Science and technology. Central Eurasia
[JPRS-UST-95-017] p 1988 N95-26080
EARTHQUAKE RESISTANT STRUCTURES
Integrated passive/active vibration absorber for multi-story buildings
[NASA-TM-109178] p 1979 N95-24208
ECOLOGY
A phase-transition induced by the struggle for life in a competitive coexistence model in ecology
[DE95-607047] p 2001 N95-25521
Quantum mechanical analogy for solving a competitive coexistence model in ecology
[DE95-607046] p 2001 N95-25531
Spaceborne synthetic aperture radar: Current status and future directions. A report to the Committee on Earth Sciences, Space Studies Board, National Research Council
[NASA-TM-4679] p 1955 N95-25710
Biological monitoring of national freshwaters, 1992
[PB95-166690] p 2002 N95-25745
ECONOMIC ANALYSIS
Small gas turbine component evaluation study
[PB95-147542] p 1913 N95-24293
Advanced subsonic airplane design and economic studies
[NASA-CR-195443] p 1913 N95-24304
Measuring the strategic value of information technology investments
[DE94-018160] p 2104 N95-24603
ECONOMICS
Construction of a nitrogen laser for plasma diagnostics
[DE95-607599] p 1973 N95-25973
ECOSYSTEMS
A phase-transition induced by the struggle for life in a competitive coexistence model in ecology
[DE95-607047] p 2001 N95-25521
Quantum mechanical analogy for solving a competitive coexistence model in ecology
[DE95-607046] p 2001 N95-25531
Biological monitoring of national freshwaters, 1992
[PB95-166690] p 2002 N95-25745
EDDY CURRENTS
Emerging nondestructive inspection for aging aircraft
[PB95-143053] p 1905 N95-25401
EDITING
Activities of the National Institute of Radiological Sciences
[DE95-709916] p 2072 N95-26165
EDUCATION
ESA Bulletin No. 81 p 2114 N95-25200
Perspectives from space: NASA classroom information and activities
[NASA-TM-110577] p 2100 N95-25643
Activities of the National Institute of Radiological Sciences
[DE95-709916] p 2072 N95-26165
EFFICIENCY
Muon identifier efficiency of the GINES detecto r in the UNK neutrino beam
[DE94-628254] p 2045 N95-24485
EIGENVALUES
SYSINT(SYSINTM)-program complex for numerical solution of the eigenvalue problem for system of integral equations
[DE94-636729] p 2029 N95-24375
Separation analysis, a tool for analyzing multigrid algorithms
[NASA-CR-195036] p 2029 N95-24389
Efficient eigenvalue assignment by state and output feedback with applications for large space structures
[NASA-TM-110155] p 1920 N95-24581
Bounds for departure from normality and the Frobenius norm of matrix eigenvalues
[DE95-006144] p 2030 N95-24592
Semiclassical hyperspherical matrix elements for helium doubly excited states
[DE94-628867] p 2048 N95-24718
Asymptotic properties of the oscillator poly spheroidal functions
[DE94-628441] p 2032 N95-24860
EIGENVECTORS
Asymptotic properties of the oscillator poly spheroidal functions
[DE94-628441] p 2032 N95-24860
Eigenvector method for optimized orbit correction
[DE95-005967] p 2071 N95-25785
EINSTEIN EQUATIONS
Relevance of induced gauge interactions in decoherence
[DE95-607082] p 2097 N95-25432
String-loop corrections to effective action and black-hole instabilities
[DE95-607085] p 2110 N95-25433
Wormhole on the Lobachevsky background
[DE95-605251] p 2099 N95-25780
EJECTA
Biospheric effects of a large extraterrestrial impact: Case study of the cretaceous/tertiary boundary crater
[NASA-CR-198015] p 1997 N95-24501
EJECTORS
Internal performance characteristics of thrust-vectored axisymmetric ejector nozzles
[NASA-TM-4610] p 1907 N95-25338
ELASTIC BENDING
New techniques to test fatigue properties of coined sheet specimens. Part 4: Development of experimental techniques
[PB95-165130] p 1982 N95-25445
ELASTIC PROPERTIES
An analysis of hypercritical states in elastic and inelastic systems
[IFTR-1/1994] p 2037 N95-25339
Stability and elastic properties of hydrogen loaded Ti(1-x)Al(x) alloys: An ab initio study
[AD-A288903] p 1936 N95-25529
Techniques for studying the mechanical properties of materials in complex stress states
[IFTR-34/1994] p 1983 N95-26178
ELASTIC SCATTERING
Polarization and N-N elastic scattering amplitudes
[DE95-004648] p 2042 N95-24292
New results in nucleon-nucleon scattering at intermediate energies
[DE95-004594] p 2043 N95-24332
Spin correlations in percolating networks with fractal geometry
[DE95-001074] p 2037 N95-24479
Toward improved photon-atom scattering predictions
[DE95-003651] p 2046 N95-24549
NMR and optical studies of piezoelectric polymers
[DE95-003836] p 1940 N95-24554
Elastic form factors of hydrogen-like atoms in nS-states
[DE94-628437] p 2048 N95-24700
On SUSY dark matter detection with spinless nuclei
[DE94-628562] p 2109 N95-24886
Neutral current neutrino-nucleon scattering
[DE95-005027] p 2069 N95-25366
Study of properties of Ne - Al neutron rich isotopes at and near N = 20 magic shell using elastic scattering in inverse kinematics
[DE94-628655] p 2055 N95-25538
ELASTIC WAVES
An analytical study of the vibration of beams fitted with neutralizers. Part 3: Torsional wave motion
[ISVR-TR-238-PT-3] p 1982 N95-25003
Modelling the day to day wind variability offshore central Chile at about 30 deg south
[DE95-606032] p 2006 N95-26043
ELASTOHYDRODYNAMICS
Development of a high temperature, high speed disc lubricant test machine
[AD-A288685] p 1977 N95-26050
ELASTOPLASTICITY
The dual boundary element formulation for elastoplastic fracture mechanics
[DRA-TR-93062] p 1980 N95-24383
ELDO LAUNCH VEHICLE
The history of ELDO. Part 1: 1961-1964
[ESA-HSR-10-PT-1] p 2114 N95-24871
ELECTRIC BATTERIES
Small spacecraft power and thermal subsystems
[NASA-CR-195029] p 1921 N95-24428
Summaries of reports of the Electrotechnical Laboratory, no. 48
[JTN-95-80825] p 2114 N95-24908
Recent advances in lithium ion technology
[DE95-004769] p 2054 N95-25470
In situ XAFS study of oxides formed on nickel thin film electrodes in KOH solution
[AD-A288735] p 1932 N95-26056
ELECTRIC CHARGE
Field equipotentials of a fast-moving charge in medium
[DE94-636737] p 2065 N95-24348
Lienard-Wiechert potentials as a consequence of Lorentz transformation of Coulomb potential
[DE94-636734] p 1952 N95-24377
Can the electric charges of elementary particles change with time?
[DE95-607194] p 2054 N95-25465
ELECTRIC CONDUCTORS
New evaluation method of superconductor characteristics for realizing the Large Helical Device
[NIFS-297] p 2071 N95-25855
ELECTRIC CONNECTORS
Preload release mechanism
[NASA-CASE-MSC-22327-1] p 1976 N95-25592
ELECTRIC EQUIPMENT
National standard and code compliance for electrical equipment installed in hazardous locations for the void fraction instrument
[DE95-002158] p 1960 N95-26092
ELECTRIC FIELDS
Electric field effects on the quantum efficiency of Cesium-iodide photocathodes in gas media
[DE94-628176] p 1957 N95-24482
Particle acceleration very near an x-line in a collisionless plasma
[ATR-92(7251)-4] p 2080 N95-25325
On the effects of gravitational fields on the electrical properties of matter
[DE95-607022] p 2038 N95-25430
Electric field effects on a near-critical fluid in microgravity
[NASA-TM-106894] p 2099 N95-25878
A mechanism of collisionless magnetic reconnection
[NIFS-274] p 2083 N95-26339

ELECTRIC GENERATORS
Wind technology development: Large and small turbines
[DE95-000286] p 1995 N95-26090
ELECTRIC HYBRID VEHICLES
Test plan/procedure for the DPHV system integration
[DE95-003414] p 1994 N95-25121
Developing a standardized test procedure for hybrid vehicles: The challenge of the SAE HEV task force
[DE95-000280] p 1978 N95-26286
ELECTRIC IGNITION
The railplug: A new ignitor for internal combustion engines
[DE95-005487] p 1977 N95-26172
ELECTRIC MOTOR VEHICLES
Solar Eagle 2
[NASA-CR-198043] p 1990 N95-24199
TITLE: Environmental, health, and safety issues offuel cells in transportation. Volume 1: Phosphoricacid fuel-cell buses
[DE95-000289] p 1993 N95-24866
ELECTRIC MOTORS
Piezoelectric motor development at AlliedSignal Inc., Kansas City Division
[DE95-003389] p 1958 N95-24532
Stiffening of the ACES deployable space boom
p 1978 N95-26307
ELECTRIC NETWORKS
From neural-based object recognition toward microelectronic eyes p 2023 N95-25257
ELECTRIC POTENTIAL
The impact of multiplexing on the dynamic requirements of analog-to-digital converters
[DE95-006302] p 1960 N95-25558
Hot-wire calibration in subsonic/transonic flow regimes
[NASA-CR-197725] p 1970 N95-25699
ELECTRIC POWER
Sector-specific issues and reporting methodologies supporting the General Guidelines for the voluntary reporting of greenhouse gases under Section 1605(b) of the Energy Policy Act of 1992, volume 1. Part 1: Electricity supply sector. Part 2: Residential and commercial buildings sector. Part 3: Industrial sector
[DE95-003296] p 2000 N95-25362
ELECTRIC POWER SUPPLIES
Superconductivity Program for Electric Power Systems: 1994 Annual PEER Review. Volume 1, Meeting Proceedings
[DE95-005058] p 1956 N95-24452
Superconductivity Program for Electric Power Systems: 1994 Annual PEER Review. Volume 2, Meeting Proceedings
[DE95-005059] p 1957 N95-24453
ELECTRIC PULSES
Detector for transit time measurement of photomultiplier single-photoelectron pulses
[DE94-628256] p 2073 N95-24642
The impact of multiplexing on the dynamic requirements of an alog-to-digital converters
[DE95-006302] p 1960 N95-25558
ELECTRICAL ENGINEERING
JPRS report: Science and technology. Central Eurasia
[JPRS-UST-95-008] p 1957 N95-24468
JPRS report: Science and technology. Central Eurasia
[JPRS-UST-94-027] p 1957 N95-24470
JPRS report: Science and technology. Central Eurasia
[JPRS-UST-94-018] p 1950 N95-24472
Electromagnetic Devices and Processes in Environment Protection. Proceedings of International Conference ELMECO 1994
[AD-A286613] p 1952 N95-24503
JPRS Report: Science and technology. Central Eurasia
[JPRS-UST-95-002] p 1916 N95-24621
JPRS report: Science and technology. Central Eurasia
[JPRS-UST-94-034] p 1987 N95-24729
JPRS report: Science and technology. Central Eurasia
[JPRS-UST-95-006] p 1950 N95-24731
ELECTRICAL IMPEDANCE
The effect of the impedance of the generator and intermediate circuits on the impedance of plasma as it applies to magnetron sputtering of thin films in a radio-frequency field
[IFTR-8-1994] p 2083 N95-26019
High input impedance amplifier
[NASA-CASE-GSC-13571-1] p 1960 N95-26038
ELECTRICAL MEASUREMENT
A new method of emittance measurement for electron beams from the Micro-emitter
[DE94-792657] p 2070 N95-25631
ELECTRICAL PROPERTIES
On the effects of gravitational fields on the electrical properties of matter
[DE95-607022] p 2038 N95-25430
ELECTRICAL RESISTIVITY
Current-voltage characteristics of a tunnel junction with resonant centers
[DE94-634530] p 1956 N95-24245
Processing and electrochemical properties of mixed conducting La(1-x)A(x)Co(1-y)Fe(y)O(3-delta) (A=Sr, Ca)
[DE95-004910] p 2088 N95-25002
Oxygen stoichiometry and its influence on superconductivity in Bi2Sr2CaCu2O(8+x)
[DE95-004660] p 2088 N95-25282
The effect of the impedance of the generator and intermediate circuits on the impedance of plasma as it applies to magnetron sputtering of thin films in a radio-frequency field
[IFTR-8-1994] p 2083 N95-26019
A theoretical analysis of strain in GaN and its effects on carrier conductivity
[AD-A288769] p 2090 N95-26061
Conductivity in insulators due to implantation of conducting species
[DE95-607773] p 1932 N95-26261
ELECTRICITY
Finite element methods in a simulation code for offshore wind turbines
[PB95-164984] p 1994 N95-25501
ELECTRO-OPTICS
Implementation of scene shadows in the Target Acquisition TDA (TARGAC)
[AD-A288760] p 1912 N95-26060
ELECTROCHEMICAL CORROSION
The corrosion protection of AlSi(TM) 1010 steel by organic and inorganic zinc-rich primers
[NASA-TP-3545] p 1936 N95-25677
ELECTROCHEMICAL MACHINING
A study of the electrochemical behavior of tungsten in caustic solutions and platinum/iridium in ch loride solutions
[DE95-004951] p 1930 N95-25123
ELECTROCHEMICAL OXIDATION
Electrochemical organic destruction in support of Hanford tank waste pretreatment
[DE95-002854] p 1924 N95-25248
ELECTROCHEMISTRY
Processing and electrochemical properties of mixed conducting La(1-x)A(x)Co(1-y)Fe(y)O(3-delta) (A=Sr, Ca)
[DE95-004910] p 2088 N95-25002
A study of the electrochemical behavior of tungsten in caustic solutions and platinum/iridium in ch loride solutions
[DE95-004951] p 1930 N95-25123
The corrosion protection of AlSi(TM) 1010 steel by organic and inorganic zinc-rich primers
[NASA-TP-3545] p 1936 N95-25677
ELECTRODES
Recent advances in lithium ion technology
[DE95-004769] p 2054 N95-25470
In situ XAFS study of oxides formed on nickel thin film electrodes in KOH solution
[AD-A288735] p 1932 N95-26056
ELECTRODYNAMICS
Nonlinear theories of spin-2 field in terms of Fierz variables
[DE95-600854] p 2095 N95-24833
Chiral symmetry on the lattice
[DE95-003962] p 2087 N95-24849
Selected problems of the interaction of electromagnetic waves and a turbulent plasma
[IFTR-9-1993] p 2080 N95-25340
Interaction mechanisms and biological effects of static magnetic fields
[DE95-004929] p 2009 N95-26169
ELECTROENCEPHALOGRAPHY
Neural network classification of clinical neurophysiological data for acute care monitoring
p 2024 N95-25263
ELECTROKINETICS
FNAS phase partitions
[NASA-CR-193855] p 1940 N95-24562
ELECTROLYSIS
Simple chemical assays for presence of S2F10 in decomposed SF6
[DE95-001423] p 1929 N95-24345
ELECTROLYTES
A solubility model for amorphous silica in concentrated electrolytes
[DE95-004896] p 1931 N95-25252
ELECTROLYTIC CELLS
Monolithic solid oxide fuel cell technology advancement for coal-based power generation
[DE94-012258] p 1990 N95-24318
Monolithic solid oxide fuel cell technology advancement for coal-based power generation
[DE95-006152] p 1991 N95-24425
Liquid-fueled SOFC power sources for transportation
[DE95-002998] p 1991 N95-24607
TITLE: Environmental, health, and safety issues offuel cells in transportation. Volume 1: Phosphoricacid fuel-cell buses
[DE95-000289] p 1993 N95-24866
ELECTROMAGNETIC COUPLING
On the problem of unboundedness from below of the spinor QED Hamiltonian
[DE94-628579] p 2094 N95-24638
Neutral current neutrino-nucleon scattering
[DE95-005027] p 2069 N95-25366
Impulsive Alfven coupling between the magnetosphere and ionosphere
[NIFS-276] p 2004 N95-26036
ELECTROMAGNETIC FIELDS
Selected problems of the interaction of electromagnetic waves and a turbulent plasma
[IFTR-9-1993] p 2080 N95-25340
Consistent approach to describing aircraft HIRF protection
[NASA-CR-195067] p 1909 N95-25341
A superfield generalization of the classical action-at-a-distance theory
[DE95-607084] p 1955 N95-25648
Fluctuations in macroscopically agitated plasma: Quasiparticles and effective temperature
[DE95-607611] p 2082 N95-25777
Proceedings of the 2nd international workshop on electromagnetic forces and related effects on blankets and other structures surrounding the fusion plasma torus
[DE94-792667] p 2082 N95-25903
ELECTROMAGNETIC INTERACTIONS
Lagrangian formulation of NJL model with se parable interaction
[DE94-628519] p 1952 N95-24506
ELECTROMAGNETIC INTERFERENCE
Read out electronics for thermal detectors of bolometer type
[PB95-141842] p 1967 N95-24280
ELECTROMAGNETIC RADIATION
Electromagnetic waves and photoacoustic transformation in gyrotropic superlattices
p 2083 N95-24205
Selected problems of the interaction of electromagnetic waves and a turbulent plasma
[IFTR-9-1993] p 2080 N95-25340
The diffraction of electromagnetic waves by screens placed at the boundaries of dielectric media
[IFTR-4/1994] p 1954 N95-25393
Phase correction in two-crystal optical parametric oscillators
[DE95-006317] p 2074 N95-25559
Fluctuations and electromagnetic wave scattering in macroscopically agitated plasma: Effects of turbulent diffusion
[DE95-607612] p 2081 N95-25617
Solitons in electron-positron plasma
[DE95-607608] p 2082 N95-25974
Self-focusing of electromagnetic radiation in electron-positron ion plasma
[DE95-607626] p 2082 N95-25975
ELECTROMAGNETIC WAVE FILTERS
Type P dispersive delay lines p 1959 N95-25116
ELECTROMAGNETIC WAVE TRANSMISSION
Laser beam log amplitude temporal scintillation spectrum due to crosswind. Part 1: Theory
[TR-1-FSRC-1994-PT-1] p 1971 N95-24371
Analysis of waveforms for bistatic radar systems
[PB95-165098] p 1955 N95-25641
ELECTROMAGNETISM
A superfield generalization of the classical action-at-a-distance theory
[DE95-607084] p 1955 N95-25648
ELECTRON BEAM WELDING
PEP-2 vacuum system: Joining SS flanges to copper beam chambers
[DE95-006093] p 1974 N95-24356
ELECTRON BEAMS
Simulation study of tapered FEL amplifiers in Raman and Compton regimes
[DE94-785266] p 1971 N95-24340
Limiting analytic form for Aharonov-Bohm diffraction pattern
[DE95-600839] p 2065 N95-24351
Depolarization in the SLC Collider Arcs
[DE95-005942] p 2065 N95-24409
A search for jet handedness in hadronic Z(sup 0) decays
[DE95-005944] p 2045 N95-24435
Characterization and performance of carbon films deposited by plasma and ion beam based techniques
[DE95-005213] p 1940 N95-24456
Energy resolution of a lead scintillating fiber electromagnetic calorimeter
[DE94-628253] p 1967 N95-24484

Over-compression, a method to shape the longitudinal bunch distribution for a reduced energy spread
[DE95-006052] p 2066 N95-24572
Tutorial on beam-based feedback systems for linacs
[DE95-006054] p 2067 N95-24573
A measurement of the left-right, forward-backward asymmetry for charm quarks using D(*+) and D(+) mesons
[DE95-006061] p 2046 N95-24575
Feasibility of ceramic joining with high energy electron beams
[DE95-004519] p 1940 N95-24717
Radial electron-beam-breakup transit-time oscillator
[DE95-005731] p 1959 N95-25385
A new method of emittance measurement for electron beams from the Micro-emitter
[DE94-792657] p 2070 N95-25631
A possibility of pi(-) Meson production by a low energy electron bunch and positive ion bunch
[NIFS-277] p 2071 N95-26029
Continuous phase and amplitude holographic elements
[NASA-CASE-NPO-18791-1] p 1971 N95-26340

ELECTRON BUNCHING

A possibility of pi(-) Meson production by a low energy electron bunch and positive ion bunch
[NIFS-277] p 2071 N95-26029

ELECTRON CYCLOTRON HEATING

Numerical analysis of electron cyclotron resonance heating on JT-60U and JFT-2M
[DE95-709766] p 2080 N95-25471
Report on the meeting on Chaotic Phenomena in Plasma
[DE94-792670] p 2082 N95-25904

ELECTRON DENSITY (CONCENTRATION)

Operating level of HT-6B tokamak device
[DE95-602999] p 2082 N95-25943
The use of empirical models to investigate GPS derived total electron content
[DE95-606045] p 2111 N95-26044

ELECTRON DIFFRACTION

Limiting analytic form for Aharonov-Bohm diffraction pattern
[DE95-600839] p 2065 N95-24351
Accurate determination of IC modulation parameter in Sr(x)Ba(1-x)Nb2O6 from second order satellites of neutron diffraction TOF (Time-Of-Flight) spectra
[DE94-629003] p 2090 N95-25851
Application of extended-crystal diffraction techniques to the symmetry and structure analysis of 221-PbBiSrCaCuO
[DE95-605913] p 2090 N95-25984

ELECTRON EMISSION

Physics in Ukraine International Conference. Volume 4: Radiophysics and Electronics
[DE95-605570] p 2038 N95-25616
Anisotropy of dilepton emission from nuclear collisions
[DE95-004354] p 2070 N95-25634

ELECTRON ENERGY

Experimental constraints on transport
[DE95-004962] p 2050 N95-25180
Self-sustained turbulence and L-mode confinement in toroidal plasmas 2
[NIFS-278] p 2082 N95-25759
An ion sensitive probe and its application to a mirror device
[DE95-602307] p 1970 N95-25940
Operating level of HT-6B tokamak device
[DE95-602999] p 2082 N95-25943
Surface plasmon observed for carbon nanotubes
[DE95-607769] p 2091 N95-26260

ELECTRON GUNS

A new method of emittance measurement for electron beams from the Micro-emitter
[DE94-792657] p 2070 N95-25631

ELECTRON MOBILITY

A theoretical analysis of strain in GaN and its effects on carrier conductivity
[AD-A288769] p 2090 N95-26061

ELECTRON PARAMAGNETIC RESONANCE

Pulse radiolysis of alkanes: A time-resolved electron paramagnetic resonance study
[DE95-005831] p 2045 N95-24459
Electron spin resonance of radicals and metal complexes
[DE95-605640] p 2055 N95-25499

ELECTRON PHONON INTERACTIONS

Electron-phonon interaction in the Hubbard model
[DE94-634859] p 2092 N95-24277

ELECTRON PLASMA

Transport reduction by current profile control in the reversed field pinch
[DE95-007016] p 2077 N95-24619

ELECTRON SCATTERING

A discrete variable representation for electron-hydrogen atom scattering
[DE95-003436] p 2045 N95-24512
Electroweak coupling measurements from polarized Bhabha scattering at the Z(exp 0) resonance
[DE95-006090] p 2057 N95-25768

ELECTRON SPIN

Depolarization in the SLC Collider Arcs
[DE95-005942] p 2065 N95-24409
On the field theory of the extended-type electron
[DE95-607069] p 2053 N95-25449
On D=2 (1/3, 1/3) supersymmetric theories 1
[DE95-607075] p 2036 N95-25522

ELECTRON STATES

Electronic structure and pairing of strongly correlated fermions: Fermi liquid versus spin liquid
[DE95-005929] p 2044 N95-24419
Study of radicals, clusters and transition state species by anion photoelectron spectroscopy
[DE95-003438] p 2045 N95-24533

ELECTRON TRANSFER

Correlations for the NO A(sup 2)(Sigma)(+) electronic quenching cross-section
[DE95-006195] p 2047 N95-24595
Group transfer and electron transfer reactions of organometallic complexes
[DE95-003732] p 2050 N95-25112

ELECTRON TRANSITIONS

Study of radicals, clusters and transition state species by anion photoelectron spectroscopy
[DE95-003438] p 2045 N95-24533
Quantum group random walks in strongly correlated 2+1 D spin systems
[DE95-607844] p 2091 N95-26103

ELECTRON TUNNELING

Current-voltage characteristics of a tunnel junction with resonant centers
[DE94-634530] p 1956 N95-24245

ELECTRON-POSITRON PAIRS

The discovery of the tau lepton: Part 1, The early history through 1975; Part 2, Confirmation of the discovery and measurement of major properties, 1976-1982
[DE95-005945] p 2044 N95-24414
Multiplicity moments in e(+)e(-) annihilation into hadrons at the Z(sup 0) resonance
[DE95-005950] p 2047 N95-24641
Present experimental data on cross channel deep-inelastic processes and the Gribov-Lipatov relation
[DE94-628605] p 2049 N95-24719
Neutrino mass and oscillation angle phenomena within the asymmetric left-right models
[DE95-607201] p 2054 N95-25466
Searching for exotic mesons in e(+)e(-) annihilation at DA(phi)NE
[PB95-165379] p 2064 N95-26001
Electronic structure of (La,Sr)2CuO4 and Ba(0.6)K(0.4)BiO3
[DE95-004963] p 2091 N95-26170

ELECTRON-POSITRON PLASMAS

Solitons in electron-positron plasma
[DE95-607608] p 2082 N95-25974
Self-focusing of electromagnetic radiation in electron-positron ion plasma
[DE95-607626] p 2082 N95-25975

ELECTRONIC CONTROL

Wind technology development: Large and small turbines
[DE95-000286] p 1995 N95-26090

ELECTRONIC EQUIPMENT

Fifth European Symposium on Reliability of Electron Devices, Failure Physics and Analysis
[AD-A286614] p 1956 N95-24447
Background information to reliability stress screening of components: A guide for component users. Nordtest project 1140-93
[PB95-165775] p 1978 N95-26002
Proposed Nordtest method: Reliability stress screening of components. A guide for component users. Nordtest project 1140-93
[PB95-165783] p 1978 N95-26003
Disposal of electronic equipment
[PB95-177861] p 2002 N95-26047

ELECTRONIC MAIL

Survey of methods for secure connection to the internet
[DE95-730185] p 1952 N95-24493

ELECTRONIC WARFARE

Analysis of data from a radar warning receiver with the accent on association of sensor reports
[PB95-141768] p 1953 N95-24836

ELECTRONS

Superconducting in the near half-filling Hubbard model
[DE94-634857] p 2092 N95-24275
Extending the kinematic range for W(sub R) searches in e(-)e(-) collisions at the NLC
[DE95-005946] p 2044 N95-24415
Electronic structure and pairing of strongly correlated fermions: Fermi liquid versus spin liquid
[DE95-005929] p 2044 N95-24419
Electroweak coupling measurements from polarized Bhabha scattering at the Z(sup 0) resonance
[DE95-006056] p 2067 N95-24574
The left-right forward-backward asymmetry of heavy quarks measured with jet charge and with leptons at the SLD
[DE95-006145] p 2046 N95-24593
Measurement of the WW gamma, ZZ gamma and Z gamm a gamma couplings at the Fermilab Tevatron
[DE95-003495] p 2067 N95-24601
Present experimental data on cross channel deep-inelastic processes and the Gribov-Lipatov relation
[DE94-628605] p 2049 N95-24719
Experimental constraints on transport
[DE95-004962] p 2050 N95-25180
On the effects of gravitational fields on the electrical properties of matter
[DE95-607022] p 2038 N95-25430
Photoionization of shallow donor impurities in finite-barrier quantum wells
[DE95-607521] p 2097 N95-25468
Theoretical studies in hadronic and nuclear physics
[DE95-006643] p 2098 N95-25562
Structural and thermodynamic properties of 3-d transition metals: Pseudopotential theory revisited
[DE95-605639] p 1937 N95-25983
Results/prospects in E777/851/865
[DE95-005959] p 2064 N95-26006

ELECTROPHORESIS

Electrophoretic separation of cells and particles from rat pituitary --- analysis of pituitary cell electrophoresis experiment done on IML-2 (7/94)
[NASA-CR-197975] p 2008 N95-24475
FNAS phase partitions
[NASA-CR-193855] p 1940 N95-24562

ELECTROPOLISHING

Characterizing pre-polished Type 304L stainless steel
[DE95-001241] p 1934 N95-24480

ELECTROSTATICS

Advances and prospects in reversed field pinch research
[DE95-007017] p 2077 N95-24602
Target injection methods for inertial fusion energy
[DE95-003654] p 2067 N95-24651

ELECTROSTRICTION

Electric field effects on a near-critical fluid in microgravity
[NASA-TM-106894] p 2099 N95-25878

ELECTROWEAK INTERACTIONS (FIELD THEORY)

Z flux-line lattices and self-dual equations in the standard model
[DE94-634364] p 2093 N95-24405
Probing anomalous gauge boson couplings at LEP
[DE95-005934] p 2044 N95-24420
Electroweak coupling measurements from polarized Bhabha scattering at the Z(sup 0) resonance
[DE95-006056] p 2067 N95-24574
Studies of strong electroweak symmetry breaking at future e(+)e(-) linear colliders
[DE95-004281] p 2067 N95-24661
Tau physics 1994: A theoretical perspective
[DE95-004840] p 2052 N95-25375
Anomalous WWZ couplings and K(sub L) yields mu(+) mu(-)
[DE95-607190] p 2054 N95-25464
Electroweak boson pair production at the Tevatron
[DE95-004234] p 2056 N95-25563

ELECTROWEAK MODEL

Studies of strong electroweak symmetry breaking at future e(+)e(-) linear colliders
[DE95-004281] p 2067 N95-24661
Low energy properties of the heavy vector fermions
[DE94-634362] p 2051 N95-25290
Study of the simplest realistic Higgs sector in quark-lepton symmetric models
[DE95-607159] p 2053 N95-25461
Neutrino mass and oscillation angle phenomena within the asymmetric left-right models
[DE95-607201] p 2054 N95-25466
A simple relation among the quark masses
[DE95-703783] p 2055 N95-25494

ELEMENTARY EXCITATIONS

On the calculation of lattice sums arising in Bose-Einstein statistics of quasiparticle excitations
[DE94-634531] p 2084 N95-24246
Fluctuations in macroscopically agitated plasma: Quasiparticles and effective temperature
[DE95-607611] p 2082 N95-25777

ELEMENTARY PARTICLE INTERACTIONS
Deficiency of the Gross-Llewellyn Smith sum rule and QCD vacuum polarization effect
[DE94-636790] p 2042 N95-24315
The discovery of the tau lepton: Part 1, The early history through 1975; Part 2, Confirmation of the discovery and measurement of major properties, 1976-1982
[DE95-005945] p 2044 N95-24414
A test of the flavor independence of strong interactions
[DE95-005948] p 2044 N95-24418
Measurement of alpha(sub s)from hadronic event observables at the Z(sup 0) resonance
[DE95-005943] p 2045 N95-24434
Measurement of the WW gamma, ZZ gamma and Z gamm a gamma couplings at the Fermilab Tevatron
[DE95-003495] p 2067 N95-24601
Measurement of alpha(sub s) from hadronic ev ent observables at the Z(sup 0) resonance
[DE95-005949] p 2047 N95-24622
Testing supersymmetry at the next linear collider
[DE95-006064] p 2069 N95-25297
Neutral current neutrino-nucleon scattering
[DE95-005027] p 2069 N95-25366
Photon-charm production in p(anti p) collisions at radical s = 1.8 TeV
[DE95-004850] p 2052 N95-25377
Masses of heavy fermions and Higgs boson in four-generation fermion condensate scheme
[DE95-607124] p 2053 N95-25450
Neutrino mass and oscillation angle phenomena within the asymmetric left-right models
[DE95-607201] p 2054 N95-25466
Inelastic collisions of negative muons and hadrons with Helium metastable atoms
[DE95-607538] p 2055 N95-25493
Ten dimensional SO(10) G.U.T. models with dynamical symmetry breaking
[DE95-607093] p 2098 N95-25533
Multichannel resonances and closed channels (scalar sector)
[DE94-628629] p 2055 N95-25537

ELEMENTARY PARTICLES
International bulletin on atomic and molecular data for fusion, no. 47
[DE94-634442] p 2040 N95-24230
DOE-High Energy Physics Contract with the University of Hawaii
[DE95-004214] p 2068 N95-24852
Can the electric charges of elementary particles change with time?
[DE95-607194] p 2054 N95-25465
Research in elementary particle physics
[DE95-007323] p 2054 N95-25481
Physics in Ukraine International Conference. Volume 1: Physics of elementary particles and quantum field theory. General problems
[DE95-606413] p 2056 N95-25554
On a new type of long-range forces
[DE95-605286] p 2063 N95-25965

ELLIPSOIDS
Field equipotentials of a fast-moving charge in medium
[DE94-636737] p 2065 N95-24348

ELLIPTIC DIFFERENTIAL EQUATIONS
Semiclassical asymptotics on covering manifolds and morse inequalities
[PB95-165510] p 2028 N95-24251

ELLIPTICITY
Ellipsoidal basis for isotropic oscillator
[DE95-605253] p 2034 N95-25782

ELONGATION
The Lienard-Wiechert potentials and relativistic length
[DE94-636733] p 2093 N95-24376

EMBEDDING
Two dimensional simplicial paths
[DE95-607087] p 2036 N95-25434

EMISSION SPECTRA
ASCA solid state imaging spectrometer observations of O stars
[NASA-CR-197281] p 2108 N95-24385
LuAlO3: A high density, high speed scintillator for gamma detection
[DE95-004678] p 2064 N95-26256

EMITTANCE
Depolarization in the SLC Collider Arcs
[DE95-005942] p 2065 N95-24409
Coupling correction using closed orbit measurements
[DE95-005957] p 2070 N95-25369
A new method of emittance measurement for electron beams from the Micro-emitter
[DE94-792657] p 2070 N95-25631
Emittance growth caused by nonuniform charge distribution of bunched beam in linac
[DE95-602121] p 2072 N95-26095

EMITTERS
Analysis of data from a radar warning receiver with the accent on association of sensor reports
[PB95-141768] p 1953 N95-24836
A new method of emittance measurement for electron beams from the Micro-emitter
[DE94-792657] p 2070 N95-25631

ENCAPSULATING
The effect of encapsulation on the reflectance of photovoltaic modules using textured multicrystalline-silicon solar cells
[DE95-004781] p 1996 N95-26166

END EFFECTORS
Milli-robots for surgical teleoperation
[NASA-CR-197378] p 1974 N95-24204

ENERGETIC PARTICLES
Energetic particle drive for toroidicity-induced Alfven eigenmodes and kinetic toroidicity-induced Alfven eigenmodes in a low-shear Tokamak
[DE95-003222] p 2079 N95-25216

ENERGY BANDS
Optical determinations of energy-band dispersion curves in novel compound semiconductor materials
[DE95-006318] p 2089 N95-25353

ENERGY BUDGETS
Assessment of climate variability of the Greenland ice sheet: Integration of in situ and satellite data
[NASA-CR-198020] p 1998 N95-24846

ENERGY CONSERVATION
National Renewable Energy Laboratory Information Resources Catalogue. A collection of energy efficiency and renewable energy information resources
[DE94-011900] p 1990 N95-24305
Brayton-cycle solvent recovery heat pump. A technical brief
[DE94-000225] p 1991 N95-24666
Federal alternative motor fuels program: Light duty federal vehicles, trucks, and buses
[DE95-003982] p 1948 N95-24679
The energy efficiency of passive solar heating systems
[IFTR-22/1994] p 1995 N95-25758
The fundamentals of modelling heat and moisture processes in structures
[IFTR-15/1994] p 1951 N95-26109

ENERGY CONSUMPTION
Summaries of reports of the Electrotechnical Laboratory, no. 48
[JTN-95-80825] p 2114 N95-24908
Nuclear energy and the environment
[DE95-600438] p 2001 N95-25615
Developing a standardized test procedure for hybrid vehicles: The challenge of the SAE HEV task force
[DE95-000280] p 1978 N95-26286

ENERGY CONVERSION
Bioprocessing in nonaqueous media: Critical needs and opportunities
[DE95-004878] p 2008 N95-24843
Innovative energy production in fusion reactors
[NIFS-250] p 2072 N95-26111
Direct energy conversion of radiation energy in fusion reactor
[NIFS-254] p 2072 N95-26250

ENERGY CONVERSION EFFICIENCY
Experimental and theoretical development towards a 500 MW, one-microsecond, L-band relativistic klystron amplifier
[DE95-003682] p 1958 N95-24589
NREL airfoil families for HAWTs
[DE95-000267] p 1994 N95-24882

ENERGY DISSIPATION
Energy resolution of a lead scintillating fiber electromagnetic calorimeter
[DE94-628253] p 1967 N95-24484
The transmission and control of vibrational power in a two stage isolation system with a water-loaded substructure
[ISVR-TR-235] p 1975 N95-24992
Dissipative quantum mechanics: The generalization of the canonical quantization and von Neumann equation
[DE95-607008] p 2096 N95-25426
Surface plasmon observed for carbon nanotubes
[DE95-607769] p 2091 N95-26260

ENERGY DISTRIBUTION
The AGS gamma(sub t)-jump system
[DE95-003170] p 2064 N95-24287

ENERGY LEVELS
Theoretical and experimental studies on the C15 intermetallic compound NbCr2
[DE95-003665] p 2086 N95-24513
Correlations for the NO A(sup 2)(Sigma)(+) electronic quenching cross-section
[DE95-006195] p 2047 N95-24595
Some remarks to the problem of neutrino oscillation
[DE94-628599] p 2048 N95-24669
Polarization and intensity of dd-transitions in superconducting copper oxides
[DE95-605886] p 2090 N95-25776

ENERGY METHODS
A technique for the evaluation of strength of coupling between SEA subsystems
[ISVR-TR-241] p 1981 N95-24997
A technique for the evaluation of strength of coupling between SEA subsystems: Experiments with two coupled plates and two coupled rooms
[ISVR-TR-242] p 1982 N95-25332

ENERGY POLICY
Preparatory research for global warming precaution spread promotion manual and early spread plan research work
[DE95-730143] p 1996 N95-24291
Study on the production of alternative fuels by carbon dioxide hydrogenation
[DE95-744284] p 1948 N95-24498
Federal alternative motor fuels program: Light duty federal vehicles, trucks, and buses
[DE95-003982] p 1948 N95-24679
Voluntary reporting of greenhouse gases under Section 1605(b) of the Energy Policy Act of 1992: General guidelines
[DE95-003295] p 2000 N95-25361
Sector-specific issues and reporting methodologies supporting the General Guidelines for the voluntary reporting of greenhouse gases under Section 1605(b) of the Energy Policy Act of 1992, volume 1. Part 1: Electricity supply sector. Part 2: Residential and commercial buildings sector. Part 3: Industrial sector
[DE95-003296] p 2000 N95-25362
Renewable Energy Demonstration Project by the National Renewable Energy Laboratory and the General Services Administration
[DE95-000261] p 1995 N95-25995
Sector-specific issues and reporting methodologies supporting the general guidelines for the voluntary reporting of greenhouse gases under Section 1605(b) of the Energy Policy Act of 1992, Volume 2. Part 4: Transportation sector. Part 5: Forestry sector. Part 6: Agricultural sector
[DE95-003297] p 2003 N95-26065
Wind technology development: Large and small turbines
[DE95-000286] p 1995 N95-26090

ENERGY SOURCES
Directory of Energy Data Collection Forms: Forms in use as of October 1994
[DE95-004329] p 2105 N95-24710

ENERGY SPECTRA
Anharmonic potential in the oscillator representation
[DE94-636740] p 2092 N95-24312
The facility for commercial doping of silicon by thermal neutrons in channel 3 at the IBR-2
[DE94-636293] p 2085 N95-24374
Energy resolution of a lead scintillating fiber electromagnetic calorimeter
[DE94-628253] p 1967 N95-24484
Statistical mechanics of relativistic spin-1 bosons in a magnetic field
[DE95-607100] p 2054 N95-25474
Linear Energy Transfer (LET) spectra of cosmic radiation in low Earth orbit p 2061 N95-25926
Neutron influences and energy spectra in the Cosmos-2044 biosatellite orbit p 2061 N95-25928
Cosmic ray LET spectra and doses on board Cosmos-2044 biosatellite p 2061 N95-25930
Differential neutron energy spectra measured on spacecraft low Earth orbit p 2062 N95-25932
LuAlO3: A high density, high speed scintillator for gamma detection
[DE95-004678] p 2064 N95-26256
Surface plasmon observed for carbon nanotubes
[DE95-607769] p 2091 N95-26260

ENERGY STORAGE
Solar thermal electric hybridization issues
[DE95-000217] p 1992 N95-24714
The transformation of organic amines by transition metal cluster compounds
[DE95-004180] p 1923 N95-24851

ENERGY TECHNOLOGY
ESnet Program Plan 1994
[DE95-005329] p 2019 N95-24290
National Renewable Energy Laboratory Information Resources Catalogue. A collection of energy efficiency and renewable energy information resources
[DE94-011900] p 1990 N95-24305
Biologically produced succinic acid: A new route to chemical intermediates
[DE95-000257] p 2007 N95-24306
Clean fractionation of biomass
[DE95-000259] p 2007 N95-24307
Proceedings of the 1993 Symposium on Nuclear Data
[DE94-012554] p 2104 N95-24372

Yearbook 1993: Bioenergy Research Programme. Utilization of bioenergy and biomass conversion
[DE95-717518] p 1993 N95-24862
NREL Photovoltaic Program FY 1994 bibliography
[DE95-000275] p 1993 N95-24865
JALO: Fuel conversion
[DE95-737597] p 1949 N95-25244
Benchmark experiment on a copper slab assembly bombarded by D-T neutrons
[DE95-709764] p 2055 N95-25497
Renewable Energy Demonstration Project by the National Renewable Energy Laboratory and the General Services Administration
[DE95-000261] p 1995 N95-25995
Intermediate-sized natural gas fueled carbonate fuel cell power plants
[DE95-004990] p 1996 N95-26171

ENERGY TRANSFER
Spectrum and energy transfer in steady Burgers turbulence
[NASA-CR-195047] p 1963 N95-24584
Experimental constraints on transport
[DE95-004962] p 2050 N95-25180
The interactions of high-energy, highly charged Xe ions with buckyballs
[DE95-004597] p 2069 N95-25281
Dynamics of structure formation in nonequilibrium systems (Wave Media)
[DE95-607609] p 2081 N95-25556
Magnetized target fusion: An overview of the concept
[DE95-005247] p 2070 N95-25594
HET mini-manual
[PB95-165338] p 2057 N95-25900

ENGINE AIRFRAME INTEGRATION
Advanced subsonic airplane design and economic studies
[NASA-CR-195443] p 1913 N95-24304

ENGINE ANALYZERS
Neural network application to comprehensive engine diagnostics p 2023 N95-25255

ENGINE DESIGN
Small gas turbine component evaluation study
[PB95-147542] p 1913 N95-24293
Development of a dedicated ethanol ultra-low emission vehicle (ULEV) system design
[DE95-004016] p 1975 N95-24880
Investigation of a rotary valving system with variable valve timing for internal combustion engines
[DE95-003831] p 1976 N95-25101

ENGINE INLETS
Study of compressible flow through a rectangular-to-semiannular transition duct
[NASA-CR-4660] p 1914 N95-24392

ENGINE MONITORING INSTRUMENTS
Predictability in space launch vehicle anomaly detection using intelligent neuro-fuzzy systems p 2025 N95-25266

ENGINE NOISE
Noise impact of advanced high lift systems
[NASA-CR-195028] p 2040 N95-26160
Jet mixer noise suppressor using acoustic feedback
[NASA-CASE-LEW-15170-2] p 2040 N95-26187

ENGINE PARTS
Small gas turbine component evaluation study
[PB95-147542] p 1913 N95-24293
Investigation of a rotary valving system with variable valve timing for internal combustion engines
[DE95-003831] p 1976 N95-25101
Waste minimization assessment for a manufacturer of parts for truck engines
[PB95-144481] p 1911 N95-26062

ENGINE TESTS
Diesel fuel component contribution to engine emissions and performance
[DE95-000238] p 1998 N95-24604
BSM Delta Qualification 2, volume 2
[NASA-CR-196567] p 1922 N95-24844
BSA Delta Qualification 2, volume 3, book 1
[NASA-CR-196565] p 1922 N95-24845
BSM Delta Qualification 2, volume 3, book 2
[NASA-CR-196568] p 1922 N95-24854
Turbine-engine applications of thermographic-phosphor temperature measurements
[DE95-003625] p 1989 N95-25110
Assessment of overhaul surge margin tests applied to the T53 engines in ADF Iroquois helicopters
[AR-008-389] p 1914 N95-25936
Nitrogen oxide emissions and their control from uninstalled aircraft engines in enclosed test cells: Joint report to Congress on the Environmental Protection Agency - Department of Transportation study
[PB95-166237] p 2002 N95-26005
Perspective on thermal barrier coatings for industrial gas turbine applications p 1945 N95-26128
Overview of thermal barrier coatings in diesel engines p 1945 N95-26129
Thick thermal barrier coatings for diesel engines p 1946 N95-26136

ENGINEERING
JPRS report: Science and technology. Central Eurasia
[JPRS-UST-94-030] p 1962 N95-24469
JPRS report: Science and technology. Central Eurasia
[JPRS-UST-95-003] p 1988 N95-24730
JPRS report: Science and technology. Central Eurasia
[JPRS-UST-94-033] p 2037 N95-24732
JPRS report: Science and technology. Central Eurasia
[JPRS-UST-95-018] p 2071 N95-26079

ENTHALPY
Entropy and enthalpy of adsorption of gaseous chlorides of metals on quartz glass as a function of the molecular composition
[DE94-627162] p 2093 N95-24481
Thermodynamic property evaluation and magnetic refrigeration cycle analysis for gadolinium gallium garnet
[DE95-005910] p 1951 N95-25367
The Superorbital Expansion Tube concept, experiment and analysis p 1915 N95-25399

ENTROPY
Entropy and enthalpy of adsorption of gaseous chlorides of metals on quartz glass as a function of the molecular composition
[DE94-627162] p 2093 N95-24481
Thermodynamic property evaluation and magnetic refrigeration cycle analysis for gadolinium gallium garnet
[DE95-005910] p 1951 N95-25367

ENVIRONMENT EFFECTS
Alternatives to traditional transportation fuels 1993
[DE95-005445] p 1947 N95-24273
The atmospheric effects of stratospheric aircraft: A fourth program report
[NASA-RP-1359] p 1996 N95-24274
Responsibility means doing without: How to rescue the ozone-layer
[PB95-166807] p 1997 N95-24334
Environment, 1980-1993
[DE95-605240] p 2002 N95-25779
Parts washing alternatives study: United States Coast Guard. Project summary and report
[PB95-166146] p 1942 N95-26004
Process, properties and environmental response of plasma sprayed thermal barrier coatings p 1945 N95-26132

ENVIRONMENT MANAGEMENT
Integrated planning: A baseline development perspective
[DE95-004945] p 2102 N95-24905

ENVIRONMENT POLLUTION
Nuclear energy and the environment
[DE95-600438] p 2001 N95-25615

ENVIRONMENT PROTECTION
JPRS report: Science and technology. Central Eurasia: Space
[JPRS-USP-94-008] p 1916 N95-24359
Electromagnetic Devices and Processes in Environment Protection. Proceedings of International Conference ELMECO 1994
[AD-A286613] p 1952 N95-24503
TITLE: Environmental, health, and safety issues offuel cells in transportation. Volume 1: Phosphoricacid fuel-cell buses
[DE95-000289] p 1993 N95-24866
Materials Compatibility and Lubricants Research (MCLR) Program
[DE95-004862] p 1941 N95-25243
Voluntary reporting of greenhouse gases under Section 1605(b) of the Energy Policy Act of 1992: General guidelines
[DE95-003295] p 2000 N95-25361
Sector-specific issues and reporting methodologies supporting the General Guidelines for the voluntary reporting of greenhouse gases under Section 1605(b) of the Energy Policy Act of 1992, volume 1. Part 1: Electricity supply sector. Part 2: Residential and commercial buildings sector. Part 3: Industrial sector
[DE95-003296] p 2000 N95-25362
Nitrogen oxide emissions and their control from uninstalled aircraft engines in enclosed test cells: Joint report to Congress on the Environmental Protection Agency - Department of Transportation study
[PB95-166237] p 2002 N95-26005

ENVIRONMENTAL CHEMISTRY
Cross-flow, filter-sorbent-catalyst for particulate, SO2 and NO(x) control
[DE95-001934] p 2003 N95-26091

ENVIRONMENTAL CONTROL
MuSR user guide
[PB95-165304] p 2056 N95-25624

ENVIRONMENTAL ENGINEERING
Preparatory research for global warming precaution spread promotion manual and early spread plan research work
[DE95-730143] p 1996 N95-24291

ENVIRONMENTAL MONITORING
Preparatory research for global warming precaution spread promotion manual and early spread plan research work
[DE95-730143] p 1996 N95-24291
Responsibility means doing without: How to rescue the ozone-layer
[PB95-166807] p 1997 N95-24334
Coso Monitoring Program, October 1992 through September 1993
[AD-A279147] p 1989 N95-24422
Integration of heterogeneous data bases for development of a large-scale environmental data atlas for multi-platform PC and workstation users
[DE95-002689] p 2000 N95-25278

ENVIRONMENTAL TESTS
BSM Delta qualification 2, volume 1
[NASA-CR-196566-VOL-1] p 1921 N95-24440
BSM Delta Qualification 2, volume 2
[NASA-CR-196567] p 1922 N95-24844
BSA Delta Qualification 2, volume 3, book 1
[NASA-CR-196565] p 1922 N95-24845
The effects of the environment on an experimental VHF radio Direction Finding antenna system
[AD-A288791] p 1956 N95-26191

ENVIRONMENTS
Prediction of humans in various environments using gas sensors and neural networks
[PB95-141560] p 2009 N95-24227

ENZYMES
Fusion proteins as alternate crystallization paths to difficult structure problems
[NASA-TM-110497] p 2008 N95-24531
Overview of selected molecular biological databases
[DE95-005906] p 2008 N95-25181

EPIDEMIOLOGY
Aviation epidemiology data register
[AD-A279303] p 2010 N95-24423

EPITAXY
Oxidation of ion-implanted NiAl
[DE95-005899] p 1935 N95-25388
Kinetic modeling of the atomic layer epitaxy window in group 4 semiconductor growth
[DE95-005903] p 2089 N95-25391
Temperature-dependent growth of LaAlO3 films on YBa2CuO7 C-axis films for multilayer structures
[DE95-005257] p 2089 N95-25598

EPOXY MATRIX COMPOSITES
Significance of varied thickness to damage tolerance of carbon fiber/epoxy laminates
[PB95-165460] p 1925 N95-24242

EQUATIONS OF MOTION
Nonlinear theories of spin-2 field in terms of Fierz variables
[DE95-600854] p 2095 N95-24833
A well-posed numerical method to track isolated conformal map singularities in Hele-Shaw flow
[NASA-CR-195035] p 2032 N95-25114
On the field theory of the extended-type electron
[DE95-607069] p 2053 N95-25449
Quasiparticles in magnetized plasma
[DE95-607610] p 2081 N95-25632
The geodesic motion in Kaluza-Klein spinning space
[DE95-607070] p 2039 N95-25646
On a new type of long-range forces
[DE95-605286] p 2063 N95-25965
Exact solution of 2 D Poincare gravity coupled with fermion matter
[DE95-605314] p 2099 N95-25967

EQUATIONS OF STATE
An analysis of hypercritical states in elastic and inelastic systems
[IFTR-1/1994] p 2037 N95-25339
Critical parameters of Quark-Hadron phase transition with interacting and massive quarks
[DE95-607143] p 2052 N95-25436

EQUIPMENT SPECIFICATIONS
Go for EVA
[NASA-TM-110537] p 1918 N95-24195

EQUIPOTENTIALS
Field equipotentials of a fast-moving charge in medium
[DE94-636737] p 2065 N95-24348

EQUIVALENCE
STEP: Satellite Test of the Equivalence Principle. Report on the phase A study
[NASA-TM-110598] p 1917 N95-26184

EROSION
Robotic weld overlay coatings for erosion control
[DE95-005187] p 1939 N95-24285
Modeling plasma/material interactions during a tokamak disruption
[DE95-004247] p 2078 N95-24861

ERROR ANALYSIS
Software fault tolerance in computer operating systems
[NASA-CR-197999] p 2016 N95-24993
Standardization of equations for radiochemical calculations
[DE95-003028] p 1930 N95-25097
A note on the total least squares problem for coplanar points
[DE95-004876] p 2032 N95-25251
Grounding explanations in evolving, diagnostic situations
[NASA-CR-198027] p 2026 N95-25335
Monte Carlo simulations with indefinite and complex-valued measures
[DE95-607056] p 2017 N95-25448
Adaptive finite element method 2: Error estimation
[AD-A288358] p 2033 N95-25509

ERROR CORRECTING CODES
Use of voronoi diagrams for qualitative matching
[PB95-165445] p 1988 N95-24240

ERRORS
Distribution of the error term for the number of lattice points inside a shifted ball
[PB95-165569] p 2029 N95-24325
Adaptive finite element method 2: Error estimation
[AD-A288358] p 2033 N95-25509
Aspect estimation of an aircraft using library model silhouettes
[PB95-141834] p 2036 N95-25894

ERS-1 (ESA SATELLITE)
ESA Bulletin No. 81 p 2114 N95-25200

ERYTHROCYTES
Contribution of ankyrin-band 3 complexes to the organization and mechanical properties of the membrane skeleton of human erythrocyte
[DE95-005835] p 2010 N95-24427

ESA SATELLITES
Europe in space, 1960-1973
[ESA-SP-1172] p 2114 N95-24870

ESSENTIALLY NON-OSCILLATORY SCHEMES
Essentially nonoscillatory (ENO) reconstructions via extrapolation
[NASA-TM-106907] p 2018 N95-25879

ESTIMATING
Aerodynamic parameter estimation via Fourier modulating function techniques
[NASA-CR-4654] p 1911 N95-24630

ETCHING
A study of the electrochemical behavior of tungsten in caustic solutions and platinum/iridium in ch loride solutions
[DE95-004951] p 1930 N95-25123

ETHERS
High octane ethers from synthesis gas-derived alcohols
[DE95-001146] p 1948 N95-24655
The transformation of organic amines by transition metal cluster compounds
[DE95-004180] p 1923 N95-24851

ETHICS
Interim report of the advisory committee on human radiation experiments
[DE95-003265] p 2011 N95-24497

ETHYL ALCOHOL
Development of a dedicated ethanol ultra-low emission vehicle (ULEV) system design
[DE95-004016] p 1975 N95-24880

ETHYLENE
Modeling of the simulated countercurrent moving-bed chromatographic reactor used for the oxidative coupling of methane
[DE95-004930] p 1924 N95-25286

EUCLIDEAN GEOMETRY
Construction of the moduli space of monopoles
[PB95-165528] p 2028 N95-24255
Saddle-point method in path integrals
[DE94-628379] p 2036 N95-24688
A new formulation of quantum field theory on S4
[DE95-607098] p 2099 N95-25970

EULER EQUATIONS OF MOTION
Investigation of convection and pressure treatment with splitting techniques
[NASA-TM-106868] p 1961 N95-24399
Effect of density gradients in confined supersonic shear layers, part 1
[NASA-CR-198029] p 1962 N95-24412
Implementation of a parallel unstructured Euler solver on the CM-5
[NASA-CR-195056] p 2032 N95-25106

EULER-LAGRANGE EQUATION
Correlated density matrix theory of spatially inhomogeneous Bose fluids
[DE95-607840] p 2100 N95-26102

EURECA (ESA)
Preliminary results of radiation measurements on EURECA p 2060 N95-25923

EUROPA LAUNCH VEHICLES
Europe in space, 1960-1973
[ESA-SP-1172] p 2114 N95-24870

EUROPE
Assessment of avionics technology in European aerospace organizations
[NASA-CR-189201] p 1912 N95-24624
Innovation and application of ANN in Europe demonstrated by Kohonen maps p 2024 N95-25262

EUROPEAN SPACE AGENCY
Europe in space, 1960-1973
[ESA-SP-1172] p 2114 N95-24870
The history of ELDO. Part 1: 1961-1964
[ESA-HSR-10-PT-1] p 2114 N95-24871
Reflections on Europe in space
[ESA-HSR-11] p 1916 N95-24872
The origins of the Federal Republic of Germany's space policy, 1959-1965: European and national dimensions
[ESA-HSR-12] p 1916 N95-24892
ESRO's telecommunications programme and the OTS project (1970-1974)
[ESA-HSR-13] p 1953 N95-24893
United States-European cooperation in space during the sixties
[ESA-HSR-14] p 2107 N95-24894
United States-European space cooperation in the post-Apollo programme
[ESA-HSR-15] p 2107 N95-24895
The scientific programme between ESRO and ESA: Choosing new projects (1973-1977)
[ESA-HSR-16] p 1917 N95-24896
ESA Bulletin No. 81 p 2114 N95-25200

EUROPEAN SPACE PROGRAMS
Europe in space, 1960-1973
[ESA-SP-1172] p 2114 N95-24870
ESA Bulletin No. 81 p 2114 N95-25200

EVALUATION
Technical evaluation of a dual-junction same-band-gap amorphous silicon photovoltaic system at NREL
[DE95-000277] p 1996 N95-26285

EVAPORATION
Intercomparison of hydrologic processes in global climate models
[NASA-TM-104617] p 2005 N95-26341

EXCITATION
Anharmonic potential in the oscillator representation
[DE94-636740] p 2092 N95-24312
Structure of liquid He-4 excitations spectrum
[DE94-637113] p 2043 N95-24364
Excited states of mesons within the NJL model with the homogeneous vacuum gluon field
[DE95-605323] p 2058 N95-25909

EXHAUST EMISSION
Alternatives to traditional transportation fuels 1993
[DE95-005445] p 1947 N95-24273
Small gas turbine component evaluation study
[PB95-147542] p 1913 N95-24293
Retrofit NOx control technologies for natural gas prime movers
[PB95-149290] p 1997 N95-24294
The effect of altitude conditions on the particle emissions of a J85-GE-5L turbojet engine
[NASA-TM-106669] p 1914 N95-24561
Diesel fuel component contribution to engine emissions and performance
[DE95-000238] p 1998 N95-24604
Methods of valuing air pollution and estimated monetary values of air pollutants in various US regions
[DE95-006854] p 1998 N95-24618
Development of a dedicated ethanol ultra-low emission vehicle (ULEV) system design
[DE95-004016] p 1975 N95-24880
Draft regulatory impact analysis: Control of air pollution emission standards for new nonroad spark-ignition marine engines
[PB95-166294] p 2001 N95-25575
Carbon taxes and India
[DE95-005401] p 2001 N95-25629
Sector-specific issues and reporting methodologies supporting the general guidelines for the voluntary reporting of greenhouse gases under Section 1605(b) of the Energy Policy Act of 1992, Volume 2. Part 4: Transportation sector. Part 5: Forestry sector. Part 6: Agricultural sector
[DE95-003297] p 2003 N95-26065
Developing a standardized test procedure for hybrid vehicles: The challenge of the SAE HEV task force
[DE95-000280] p 1978 N95-26286

EXHAUST GASES
Alternatives to traditional transportation fuels 1993
[DE95-005445] p 1947 N95-24273
The atmospheric effects of stratospheric aircraft: A fourth program report
[NASA-RP-1359] p 1996 N95-24274
Study on the production of alternative fuels by carbon dioxide hydrogenation
[DE95-744284] p 1948 N95-24498
Optimized hydrogen piston engines
[DE95-003656] p 1975 N95-24550
Heat release rate measurements in tunnel fires
[PB95-165106] p 1931 N95-25443
Tunable diode lasers as continuous emission monitors for thermal waste treatment processes
[DE95-004381] p 1972 N95-25549
Draft regulatory impact analysis: Control of air pollution emission standards for new nonroad spark-ignition marine engines
[PB95-166294] p 2001 N95-25575
Carbon taxes and India
[DE95-005401] p 2001 N95-25629

EXHAUST NOZZLES
Internal performance characteristics of thrust-vectored axisymmetric ejector nozzles
[NASA-TM-4610] p 1907 N95-25338

EXISTENCE THEOREMS
Nonexistence of global solutions to some quasilinear hyperbolic equations with dynamic boundary conditions
[DE95-607010] p 2033 N95-25645

EXOBIOLOGY
Aerospace medicine and biology: A continuing bibliography with indexes (supplement 400)
[NASA-SP-7011(400)] p 2011 N95-24464

EXOTHERMIC REACTIONS
Characterization of ultradispersed aluminum
[DE95-006379] p 1933 N95-24329

EXPANSION
Recoil effects in quantum topological solitons
[DE95-607006] p 2097 N95-25454

EXPECTATION
On a possible explanation of the origin of the quark mass spectrum
[DE95-605315] p 2063 N95-25968

EXPERIMENT DESIGN
Target injection methods for inertial fusion energy
[DE95-003654] p 2067 N95-24651
A software tool to design thermal barrier coatings p 1946 N95-26139
The 1994 NASA/USRA/ADP Design Projects
[NASA-CR-197415] p 2101 N95-26304
Universal Test Facility p 1918 N95-26305
Automated protein crystal growth facility p 1918 N95-26306

EXPERIMENTATION
Human radiation experiments: The Department of Energy roadmap to the story and the records
[DE95-006364] p 2012 N95-25371

EXPERT SYSTEMS
Workflow automation architecture standard
[DE95-004748] p 2035 N95-24248
Expert system for nuclide identification in gamma spectrum analysis
[PB95-149712] p 2042 N95-24297
Neural network technique for orbit correction in accelerators/storage rings
[DE95-005955] p 2026 N95-25368
Low-cost image analysis system
[DE95-005021] p 2021 N95-25378

EXPLOSIONS
Quantity-distance requirements for earth-bermed aircraft shelters
[AD-A279692] p 1915 N95-24424

EXPLOSIVE DEVICES
Explosive performance measurements on large, multiple-hole arrays and large masses of conventional explosive
[DE95-002718] p 1948 N95-24670

EXPLOSIVE FORMING
Evolution of plastic anisotropy for high-strain-rate computations
[DE95-004220] p 1941 N95-25237

EXPLOSIVES
The critical diameter, detonation velocity and shock sensitivity of Australian PBXW-115
[DSTO-TR-0076] p 1947 N95-24394
Characterization of plastic bonded explosives by pyrolysis-gas chromatography and multivariate data analysis. Applications of the procedure
[AD-A288761] p 1949 N95-25517
Characterization of plastic bonded explosives by pyrolysis-gas chromatography and multivariate data analysis. Development of the procedure
[AD-A288787] p 1949 N95-25528

EXPONENTIAL FUNCTIONS
Exponentially accurate approximations to piece-wise smooth periodic functions
[NASA-CR-195059] p 2031 N95-24856

EXPONENTS
The (lambda)-bar exponent for conservative systems
[DE95-607661] p 1937 N95-25977
EXTENSIONS
Central extension of a new W(infinity)-type algebra
[DE95-607086] p 2037 N95-25599
EXTERNAL TANKS
Debris/ice/TPS assessment and integrated photographic analysis of shuttle mission STS-63
[NASA-TM-110649] p 1921 N95-25337
EXTRACTION
Chelant extraction and REDOX manipulation for mobilization of heavy metals from contaminated soils
[DE95-004131] p 2000 N95-25363
Selective extraction of trivalent actinides from lanthanides with dithiophosphinic acids and tributylphosphate
[DE95-005249] p 1924 N95-25597
EXTRAPOLATION
Essentially nonoscillatory (ENO) reconstructions via extrapolation
[NASA-TM-106907] p 2018 N95-25879
EXTRATERRESTRIAL RADIATION
High LET, passive space radiation dosimetry and spectrometry
[NASA-CR-197694] p 2058 N95-25911
A study of the radiation environment on board the space shuttle flight STS-57 p 2059 N95-25914
USF/Russian dosimetry on STS-57 p 2059 N95-25915
Dosimetry on STS-42 with the RME APD p 2059 N95-25916
Neutron influences and energy spectra in the Cosmos-2044 biosatellite orbit p 2061 N95-25928
Space radiation dosimetry on US and Soviet manned missions p 2009 N95-25934
EXTRAVEHICULAR ACTIVITY
STS-66 mission highlights resource tape
[NASA-TM-110550] p 1918 N95-24197
EXTRAVEHICULAR MOBILITY UNITS
Go for EVA
[NASA-TM-110537] p 1918 N95-24195
EXTRUDING
Processing and properties of iridium alloys for space power applications
[DE95-005902] p 1935 N95-25390
EYE (ANATOMY)
An assessment of aviation accident risk of aphakic civil airmen by class of medical certificate held and by age: 1982-1985
[DOT/FAA/AM-95/11] p 2011 N95-25336

F

F-22 AIRCRAFT
Report to Congressional Committees. Tactical Aircraft: Concurrency in development and production of F-22 aircraft should be reduced
[GAO/NSIAD-95-59] p 1911 N95-26338
FABRICATION
Actively controlled shaft seals for aerospace applications
[NASA-CR-198035] p 1974 N95-24218
GaAsSb-based heterojunction tunnel diodes for tandem solar cell interconnects
[DE95-004779] p 1990 N95-24264
Monolithic solid oxide fuel cell technology advancement for coal-based power generation
[DE94-012258] p 1990 N95-24318
Energy resolution of a lead scintillating fiber electromagnetic calorimeter
[DE94-628253] p 1967 N95-24484
Piezoelectric motor development at AlliedSignal Inc., Kansas City Division
[DE95-003389] p 1958 N95-24532
The potential of vacuum microelectronics for space reactor applications
[DE95-000542] p 1958 N95-24586
Activities of the Ceramic Technology Project
[DE95-003394] p 1940 N95-24588
Back surface cell structures for reducing recombination in CZ silicon solar cells
[DE95-005423] p 1995 N95-25566
Atomic force microscopy as a process characterization tool for GaAs-based integrated circuit fabrication
[DE95-006223] p 2064 N95-26168
FABRICS
Method and apparatus for weaving curved material preforms
[NASA-CASE-LAR-14752-1] p 1943 N95-26118
FABRY-PEROT INTERFEROMETERS
Measurement of the magnetically-induced QED birefringence of the vacuum and an improved search for laboratory axions: Project definition study of the use of assets and facilities of the Superconducting Super Collider Laboratory
[DE95-005110] p 2065 N95-24317
FACE CENTERED CUBIC LATTICES
Temperature dependence of magnetic anisotropy and magnetostriction: Beyond the mean-field theory
[DE94-634529] p 2084 N95-24244
The effect of O2 intercalation on the rotational Dynamics and the ordering transition of C60
[DE95-004765] p 2090 N95-25897
FACTORIAL DESIGN
A software tool to design thermal barrier coatings p 1946 N95-26139
FACTORIZATION
Generators of matrix factorable representations of block-tridiagonal and inverse matrices
[DE94-628387] p 2031 N95-24694
Quasi-generalized matrix processes and representations of general block tridiagonal matrices
[DE94-628377] p 2031 N95-24704
Natural elementary factorization of general block-tridiagonal matrices in case of zero minors of both types
[DE94-628378] p 2031 N95-24705
Quasi two body decays of charm mesons
[DE94-792634] p 2057 N95-25901
FAILURE ANALYSIS
Fifth European Symposium on Reliability of Electron Devices, Failure Physics and Analysis
[AD-A286614] p 1956 N95-24447
Availability analysis of a 100 kWh superconducting magnetic energy storage
[DE95-737621] p 2066 N95-24448
New techniques to test fatigue properties of coined sheet specimens. Part 4: Development of experimental techniques
[PB95-165130] p 1982 N95-25445
Background information to reliability stress screening of components: A guide for component users. Nordtest project 1140-93
[PB95-165775] p 1978 N95-26002
Reliability analysis of software based safety functions
[DE95-606516] p 2018 N95-26045
Transmission diagnostic research at NASA Lewis Research Center
[NASA-TM-106901] p 1977 N95-26076
FAILURE MODES
A review of rolling element bearing vibration detection, diagnosis and prognosis
[DSTO-RR-0013] p 1975 N95-24393
Availability analysis of a 100 kWh superconducting magnetic energy storage
[DE95-737621] p 2066 N95-24448
Reliability analysis of software based safety functions
[DE95-606516] p 2018 N95-26045
Development of a high temperature, high speed disc lubricant test machine
[AD-A288685] p 1977 N95-26050
FAR INFRARED RADIATION
Far-infrared and submillimeter spectroscopy of photodissociation regions
[DE95-607520] p 2110 N95-25467
FARADAY EFFECT
Development of a fast response rotating polarimeter for a Faraday rotation measurement
[DE94-777532] p 2075 N95-24271
FATIGUE (BIOLOGY)
Sleep patterns in air traffic controllers working rapidly rotating shifts: A field study
[DOT/FAA/AM-95/12] p 2012 N95-26204
FATIGUE (MATERIALS)
Reduction in fiber damage thresholds due to static fatigue
[DE95-004778] p 1979 N95-24263
Stress analysis of a crack in the residual stress field by welding and its application to the fatigue crack propagation
[NAL-TR-1248] p 1981 N95-25000
Study on tensile fatigue testing method of unidirectional fiber-resin matrix composites
[NAL-TR-1241] p 1927 N95-25770
Thermomechanical fatigue behavior of three CFCC's
[NASA-CR-195441] p 1927 N95-25880
FATIGUE LIFE
Helicopter life substantiation: Review of some USA and UK initiatives
[DSTO-TR-0062] p 1905 N95-24201
New techniques to test fatigue properties of coined sheet specimens. Part 3: Fatigue testing and analysis of a component like coining in sheet steel materials
[PB95-165668] p 1982 N95-25569
Proceedings of the 2d USAF Aging Aircraft Conference
[AD-A288217] p 1911 N95-25578
User's manual for FAROW: Fatigue and reliability of wind turbine components, version 1.1
[DE95-005530] p 1995 N95-26037
FATIGUE TESTS
Study on tensile fatigue testing method of unidirectional fiber-resin matrix composites
[NAL-TR-1241] p 1926 N95-24989
New techniques to test fatigue properties of coined sheet specimens. Part 2: Comparison of different materials, forming operations and life prediction techniques for a simple test geometry
[PB95-165122] p 1982 N95-25444
New techniques to test fatigue properties of coined sheet specimens. Part 4: Development of experimental techniques
[PB95-165130] p 1982 N95-25445
New techniques to test fatigue properties of coined sheet specimens. Part 3: Fatigue testing and analysis of a component like coining in sheet steel materials
[PB95-165668] p 1982 N95-25569
A description of the cyclical properties of an aluminum alloy based on complex stress state tests
[IFTR-29/1994] p 1936 N95-25638
Study on tensile fatigue testing method of unidirectional fiber-resin matrix composites
[NAL-TR-1241] p 1927 N95-25770
Static and fatigue properties of pin-joint specimens of a AS-4/PEEK thermoplastic composite material
[NAL-TR-1214] p 1927 N95-25859
Transmission diagnostic research at NASA Lewis Research Center
[NASA-TM-106901] p 1977 N95-26076
Mechanical properties testing and results for thermal barrier coatings p 1946 N95-26134
FAULT DETECTION
A portable transmission vibration analysis system for the S-70A-9 Black Hawk helicopter
[DSTO-TR-0072] p 1966 N95-24203
A review of rolling element bearing vibration detection, diagnosis and prognosis
[DSTO-RR-0013] p 1975 N95-24393
Neural network application to comprehensive engine diagnostics p 2023 N95-25255
Hidden Markov models and neural networks for fault detection in dynamic systems p 2024 N95-25261
Predictability in space launch vehicle anomaly detection using intelligent neuro-fuzzy systems p 2025 N95-25266
Magnetic flaw detection studies: Methods and Equipment
[IFTR-38/1994] p 1978 N95-25957
Transmission diagnostic research at NASA Lewis Research Center
[NASA-TM-106901] p 1977 N95-26076
FAULT TOLERANCE
An optimized implementation of a fault-tolerant clock synchronization circuit
[NASA-TM-109176] p 2019 N95-24382
Software fault tolerance in computer operating systems
[NASA-CR-197999] p 2016 N95-24993
FTAPE: A fault injection tool to measure fault tolerance
[NASA-CR-198000] p 1978 N95-25333
FAULT TREES
Reliability analysis of software based safety functions
[DE95-606516] p 2018 N95-26045
FEASIBILITY
Measurement of the magnetically-induced QED birefringence of the vacuum and an improved search for laboratory axions: Project definition study of the use of assets and facilities of the Superconducting Super Collider Laboratory
[DE95-005110] p 2065 N95-24317
FEASIBILITY ANALYSIS
Cryogenic helium gas convection research
[DE95-004372] p 1965 N95-25404
FEDERAL BUDGETS
Our changing planet: The FY 1995 U.S. Global Change Research Program p 2002 N95-25852
FEED SYSTEMS
Simplified liquid oxygen propellant conditioning concepts
[NASA-TM-108482] p 1948 N95-24558
Feed system design for a reduced pressure tank p 1923 N95-26310
FEEDBACK
Aerospace safety advisory panel
[NASA-TM-110554] p 1920 N95-24505
Tutorial on beam-based feedback systems for linacs
[DE95-006054] p 2067 N95-24573

FEEDBACK CONTROL
Efficient eigenvalue assignment by state and output feedback with applications for large space structures
[NASA-TM-110155] p 1920 N95-24581
Adaptive projective filters
[DE94-628374] p 2030 N95-24645
Application of neural networks to unsteady aerodynamic control p 2024 N95-25264
Closed orbit related problems: Correction, feedback, and analysis
[DE95-005969] p 2070 N95-25441
FEEDFORWARD CONTROL
A neural network controller for automated composite manufacturing p 2025 N95-25271
FELTS
An examination of metal felt wicks for heat-pipe applications
[DE95-002608] p 1994 N95-25109
FENCES (BARRIERS)
Aircraft accident report: Impact with blast fence upon landing rollout Action Air Charters flight 990 Piper PA-31-350, N990RA, Stratford, Connecticut,27 April 1994
[PB94-910410] p 1908 N95-24206
FERMI LIQUIDS
Electronic structure and pairing of strongly correlated fermions: Fermi liquid versus spin liquid
[DE95-005929] p 2044 N95-24419
FERMI SURFACES
Theoretical and experimental studies on the C15 intermetallic compound NbCr2
[DE95-003665] p 2086 N95-24513
On an expansion of the Fermi function
[DE94-628494] p 2035 N95-24883
FERMI-DIRAC STATISTICS
On connection of q-deformed para oscillators with para oscillators
[DE95-607007] p 2096 N95-25425
FERMIONS
A functional integral approach without slave bosons to the Anderson model
[DE94-634858] p 2028 N95-24276
Bound states of 'dressed' particles
[DE94-636773] p 2042 N95-24314
Electronic structure and pairing of strongly correlated fermions: Fermi liquid versus spin liquid
[DE95-005929] p 2044 N95-24419
Update on B(sub K) with Wilson fermions
[DE95-004953] p 2085 N95-24451
Covariant single-time equations for a system of N spinor particles
[DE94-628587] p 2047 N95-24640
Chiral symmetry on the lattice
[DE95-003962] p 2087 N95-24849
TeV scale leptoquarks as a signature of standard-like superstring models
[DE94-628529] p 2096 N95-25095
Testing supersymmetry at the next linear collider
[DE95-006064] p 2069 N95-25297
Masses of heavy fermions and Higgs boson in four-generation fermion condensate scheme
[DE95-607124] p 2053 N95-25450
Ten dimensional SO(10) G.U.T. models with dynamical symmetry breaking
[DE95-607093] p 2098 N95-25533
Exact solution of 2 D Poincare gravity coupled with fermion matter
[DE95-605314] p 2099 N95-25967
Statistical mechanics of magnetized pair Fermi gas
[DE95-607097] p 2063 N95-25969
FERROELECTRICITY
Effects of acetylacetone additions on PZT thin film processing
[DE95-006322] p 1941 N95-25370
Rotational melting in displacive quantum paraelectrics
[DE95-607804] p 2091 N95-26252
FERROMAGNETIC MATERIALS
Proceedings of the 2nd international workshop on electromagnetic forces and related effects on blankets and other structures surrounding the fusion plasma torus
[DE94-792667] p 2082 N95-25903
FEYNMAN DIAGRAMS
Anomalous WWZ couplings and K(sub L) yields mu(+) mu(-)
[DE95-607190] p 2054 N95-25464
FIBER COMPOSITES
On the finite element implementation of the generalized method of cells micromechanics constitutive model
[NASA-CR-195451] p 1980 N95-24398
An evaluation of a coupled microstructural approach for the analysis of functionally graded composites via the finite-element method
[NASA-CR-195455] p 1925 N95-24438
A neural network controller for automated composite manufacturing p 2025 N95-25271
Apparatus for consolidating a pre-impregnated, filament-reinforced polymeric prepreg material
[NASA-CASE-LAR-15173-1-CU] p 1926 N95-25546
FIBER OPTICS
The 1994 Fiber Optic Sensors for Aerospace Technology (FOSAT) Workshop
[NASA-CP-10166] p 1912 N95-24207
Laser velocimeter for near-surface measurements
[NASA-CASE-ARC-11917-1] p 1967 N95-24236
A preview of a modular surface light scattering instrument with autotracking optics
[NASA-TM-110495] p 2072 N95-24386
The accident site portable integrated video system
[DE95-000539] p 1953 N95-24605
Towards an era of global village: The dynamics of world telecommunications and its implications for the future of nation state
[PB95-165064] p 1954 N95-25482
Workshop report: Measurement techniques in highly transient, spectrally rich combustion environments
[AD-A288395] p 1969 N95-25606
Average cosine meter and high spectral resolution measurements at the marine light mixed layer site
[AD-A288713] p 1970 N95-26113
FIBONACCI NUMBERS
Nonlinearity induced nontrivial dynamics in the Jaynes-Cummings Hamiltonian
[DE95-607004] p 2032 N95-25452
FIELD COILS
New modular heliotron system compatible with closed helical divertor and good plasma confinement
[NIFS-279] p 2081 N95-25653
New evaluation method of superconductor characteristics for realizing the Large Helical Device
[NIFS-297] p 2071 N95-25855
FIELD EFFECT TRANSISTORS
The measurement of the low frequency noise characteristics of the field effect transistors for cryogenic detectors
[DE94-628257] p 1957 N95-24487
FIELD EMISSION
The potential of vacuum microelectronics for space reactor applications
[DE95-000542] p 1958 N95-24586
A new method of emittance measurement for electron beams from the Micro-emitter
[DE94-792657] p 2070 N95-25631
FIELD OF VIEW
Preliminary experiments of an optical fiber display
[NAL-TR-1257] p 2073 N95-25004
FIELD THEORY (ALGEBRA)
Distances on a lattice from noncommutative geometry
[DE94-634327] p 2027 N95-24229
Matrix element and complex l-plane evaluation of two-loop vacuum amplitudes in QED on S4
[DE95-607099] p 2097 N95-25473
On exotic supersymmetries of the Phi(1,3) deformation of minimal models
[DE95-607088] p 2033 N95-25532
A covariant canonical description of Liouville field theory
[DE95-607094] p 2098 N95-25534
The space of solutions of Toda field theory
[DE95-607095] p 2099 N95-25650
FIELD THEORY (PHYSICS)
Theoretical motivation for gravitation experiments on ultra-low energy antiprotons and antihydrogen
[DE95-003662] p 2091 N95-24235
Construction of the moduli space of monopoles
[PB95-165528] p 2028 N95-24255
Anharmonic potential in the oscillator representation
[DE94-636740] p 2092 N95-24312
Relations among solutions for wave and Klein-Gordon equations for different dimensions
[DE95-600853] p 2093 N95-24446
Heat Kernel expansion on a cone and quantum fields near cosmic strings
[DE94-628520] p 2094 N95-24507
The lattice spinor QED Hamiltonian critique of the continuous space approach
[DE94-628521] p 2094 N95-24508
Dressing and bound states in quantum field theory
[DE94-628580] p 2095 N95-24639
Quantum group and quantum symmetry
[DE94-634329] p 2095 N95-24767
Probing the Froissart bound for models with charged vector fields in D = 3
[DE95-600855] p 2095 N95-24834
Light-front quantized field theory: An introduction. Spontaneous symmetry breaking. Phase transition in (phi)(sup 4) theory
[DE95-600856] p 2095 N95-24837
CP violation tests for tau/top processes
[DE95-005924] p 2051 N95-25292
q-bosons and the q-analogue quantized field
[DE95-005925] p 2051 N95-25294
On the field theory of the extended-type electron
[DE95-607069] p 2053 N95-25449
Heavy quark effective theory, interpolating fields and Bethe-Salpeter amplitudes
[DE95-607146] p 2053 N95-25460
On D=2 (1/3, 1/3) supersymmetric theories 1
[DE95-607075] p 2036 N95-25522
Physics in Ukraine International Conference. Volume 1: Physics of elementary particles and quantum field theory. General problems
[DE95-606413] p 2056 N95-25554
Physics in Ukraine International Conference. Volume 4: Radiophysics and Electronics
[DE95-605570] p 2038 N95-25616
Quantization of a Hamiltonian system with an infinite number of degrees of freedom
[DE95-605279] p 2034 N95-25783
Coherent state path-integral representation of supersymmetric lattice models
[DE95-607820] p 2091 N95-26101
FILM COOLING
Effect of film cooling/regenerative cooling on scramjet engine performances
[NAL-TR-1242] p 1914 N95-24990
FILM THICKNESS
Enhancement of thickness uniformity of thin films grown by pulsed laser deposition
[NASA-CR-197791] p 1943 N95-26081
FILTRATION
On the Cohen-Macaulayness and Gorensteinness of integral closure filtrations Rees algebras of height-two equimultiple ideals
[DE95-607000] p 2034 N95-25989
FINANCIAL MANAGEMENT
Integrated planning: A baseline development perspective
[DE95-004945] p 2102 N95-24905
FINE STRUCTURE
Far-infrared and submillimeter spectroscopy of photodissociation regions
[DE95-607520] p 2110 N95-25467
FINITE DIFFERENCE THEORY
Technical report series on global modeling and data assimilation. Volume 5: Documentation of the AIRES/GEOS dynamical core, version 2
[NASA-TM-104606-VOL-5] p 2003 N95-24766
Advanced multi-phase flow CFD model development for solid rocket motor flowfield analysis
[NASA-CR-198044] p 1923 N95-25103
Benchmark testing and independent verification of the VS2DT computer code
[DE95-004386] p 1965 N95-25485
Nonlinear difference approximations for evolutionary PDE's
[DE95-005260] p 2033 N95-25676
FINITE ELEMENT METHOD
Dynamic behavior of a magnetic bearing supported jet engine rotor with auxiliary bearings
[NASA-CR-197860] p 1913 N95-24213
Space shuttle propellant constitutive law verification tests
[NASA-CR-198047] p 1947 N95-24226
Shell deformation states and the finite element method: A benchmark study of cylindrical shells
[PB95-149621] p 1980 N95-24296
On the finite element implementation of the generalized method of cells micromechanics constitutive model
[NASA-CR-195451] p 1980 N95-24398
An evaluation of a coupled microstructural approach for the analysis of functionally graded composites via the finite-element method
[NASA-CR-195455] p 1925 N95-24438
EXODUS 2: A finite element data model
[DE95-004267] p 2016 N95-24659
Dynamic load balancing for parallel finite element methods with adaptive h- and p-refinement
[DE95-004521] p 2021 N95-24681
Numerical simulation of the nonlinear response of composite plates under combined thermal and acoustic loading
[NASA-CR-197426] p 1981 N95-24907
New techniques to test fatigue properties of coined sheet specimens. Part 2: Comparison of different materials, forming operations and life prediction techniques for a simple test geometry
[PB95-165122] p 1982 N95-25444
Finite element methods in a simulation code for offshore wind turbines
[PB95-164984] p 1994 N95-25501
Adaptive finite element method 2: Error estimation
[AD-A288358] p 2033 N95-25509
Issues related to prediction of residual stresses in titanium alloy matrix composites
[DE95-005243] p 1926 N95-25596
A software tool to design thermal barrier coatings p 1946 N95-26139

A generic interface element for COMET-AR
[NASA-CR-195075] p 1983 N95-26199
Center for Computational Structures Technology
[NASA-CR-198028] p 1983 N95-26263
Finite element buckling and postbuckling solutions for multilayered composite panels p 1983 N95-26264

FINITE VOLUME METHOD
Solutions of turbulent backward-facing step flow with heat transfer using the finite volume method
[DE95-003360] p 1962 N95-24489
Numerical simulation of laminar flow in a curved duct
[DE95-005427] p 1966 N95-26240

FINS
Aerodynamic characteristics of the orbital reentry vehicle experimental probe fins in a supersonic flow
[NAL-TR-1232] p 1921 N95-25664
Fundamental wind tunnel experiments on low-speed flutter of a tip-fin configuration wing
[NAL-TR-1228] p 1908 N95-25762

FIRE (CLIMATOLOGY)
Preliminary analysis of University of North Dakota aircraft data from the FIRE Cirrus IFO-2
[NASA-CR-198038] p 2005 N95-24219

FIRE PREVENTION
Heat release rate measurements in tunnel fires
[PB95-165106] p 1931 N95-25443
Fire test of surface products: Comparison of data from the nordic box test and the cone calorimeter
[PB95-165239] p 1932 N95-26000

FIRES
Heat release rate measurements in tunnel fires
[PB95-165106] p 1931 N95-25443
Fire test of surface products: Comparison of data from the nordic box test and the cone calorimeter
[PB95-165239] p 1932 N95-26000

FISCHER-TROPSCH PROCESS
Fischer Tropsch synthesis in supercritical fluids
[DE95-005206] p 1929 N95-24341

FISSION
Fission foil detector calibrations with high energy protons p 2060 N95-25924

FLAME SPRAYING
Thermal spray processing p 1945 N95-26130

FLAME TEMPERATURE
Temperature bounds in a model of laminar flames
[DE95-607048] p 1931 N95-25447

FLAMES
Temperature bounds in a model of laminar flames
[DE95-607048] p 1931 N95-25447
User guide to the Burner Engineering Research Laboratory
[DE95-004191] p 1931 N95-25492

FLAMMABILITY
Investigation into the flammability properties of honeycomb composites
[PB95-143293] p 1941 N95-25342
Fire test of surface products: Comparison of data from the nordic box test and the cone calorimeter
[PB95-165239] p 1932 N95-26000

FLANGES
PEP-2 vacuum system: Joining SS flanges to copper beam chambers
[DE95-006093] p 1974 N95-24356

FLAPS (CONTROL SURFACES)
Performance of an aerodynamic yaw controller mounted on the space shuttle orbiter body flap at Mach 10
[NASA-TM-109179] p 1906 N95-24397

FLARE STARS
Flare stars and Pascal distribution
[DE95-607044] p 2110 N95-25431

FLAVOR (PARTICLE PHYSICS)
Investigation of the gross structure of spectra and mass distributions of hadronic resonances
[DE94-636799] p 2043 N95-24361
A test of the flavor independence of strong interactions
[DE95-005948] p 2044 N95-24418
A test of the flavor independence of strong interactions
[DE95-006063] p 2046 N95-24576
Chiral symmetry on the lattice
[DE95-003962] p 2087 N95-24849
Critical parameters of Quark-Hadron phase transition with interacting and massive quarks
[DE95-607143] p 2052 N95-25436
Results/prospects in E777/851/865
[DE95-005959] p 2064 N95-26006

FLEXIBLE SPACECRAFT
Efficient eigenvalue assignment by state and output feedback with applications for large space structures
[NASA-TM-110155] p 1920 N95-24581

FLIGHT CHARACTERISTICS
Aerodynamic characteristics of the orbital reentry vehicle experimental probe fins in a supersonic flow
[NAL-TR-1232] p 1921 N95-25664

FLIGHT CONTROL
Assessment of avionics technology in European aerospace organizations
[NASA-CR-189201] p 1912 N95-24624

FLIGHT CREWS
A longevity and survival analysis for a cohort of retired airline pilots
[DOT/FAA/AM-95/5] p 2012 N95-24237
Aviation epidemiology data register
[AD-A279303] p 2010 N95-24423
A crew-centered flight deck design philosophy for High-Speed Civil Transport (HSCT) aircraft
[NASA-TM-109171] p 1910 N95-24582
An assessment of aviation accident risk of aphakic civil airmen by class of medical certificate held and by age: 1982-1985
[DOT/FAA/AM-95/11] p 2011 N95-25336

FLIGHT HAZARDS
Bird ingestion into large turbofan engines
[DOT/FAA/CT-93/14] p 1909 N95-24631

FLIGHT MECHANICS
NASA-UVA light aerospace alloy and structures technology program (LA2ST)
[NASA-CR-198041] p 1933 N95-24220

FLIGHT SAFETY
Evaluation of restraint system concepts for the Japanese Experiment Module flight demonstration
[NASA-TM-104808] p 2013 N95-24627

FLIGHT SIMULATION
NLS Flight Simulation Laboratory (FSL) documentation
[NASA-CR-196564] p 2104 N95-24439
Flight reference display for powered-lift STOL aircraft
[NAL-TR-1251] p 1912 N95-25005

FLIGHT SIMULATORS
Preliminary experiments of an optical fiber display
[NAL-TR-1257] p 2073 N95-25004
Visual contrast detection thresholds for aircraft contrails
[AD-A288618] p 1905 N95-25607

FLIGHT TEST VEHICLES
Reentry guidance for hypersonic Flight Experiment (HYFLEX) vehicle
[NAL-TR-1235] p 1910 N95-25764

FLIGHT TESTS
Flight reference display for powered-lift STOL aircraft
[NAL-TR-1251] p 1912 N95-25005

FLOW CHARACTERISTICS
Estimates of effects of residual acceleration on USML-1 experiments
[NASA-CR-197964] p 2084 N95-24261
Supersonic quiet-tunnel development for laminar-turbulent transition research
[NASA-CR-198040] p 1915 N95-24302
Studies of two-phase gas-liquid flow in microgravity
[NASA-CR-195434] p 1963 N95-24906
An examination of metal felt wicks for heat-pipe applications
[DE95-002608] p 1994 N95-25109
Aerodynamic characteristics of the orbital reentry vehicle experimental probe fins in a supersonic flow
[NAL-TR-1232] p 1921 N95-25664

FLOW CHARTS
Metrology measurement capability
[DE95-005411] p 1969 N95-25381

FLOW DISTRIBUTION
Exploratory flow visualization investigation of mast-mounted sights in presence of a rotor
[NASA-TM-4634] p 1907 N95-24566
Low speed aerodynamic characteristics of delta wings with vortex flaps: 60 deg and 70 deg delta wings
[NAL-TR-1245] p 1907 N95-25105
Predicting the transport properties of sedimentary rocks from microgeometry
[DE95-000129] p 2004 N95-26089

FLOW EQUATIONS
The method of space-time conservation element and solution element: Development of a new implicit solver
[NASA-TM-106897] p 2029 N95-24474
A review of Reynolds stress models for turbulent shear flows
[NASA-CR-195054] p 1962 N95-24580
Benchmark testing and independent verification of the VS2DT computer code
[DE95-004386] p 1965 N95-25485

FLOW MEASUREMENT
Supersonic quiet-tunnel development for laminar-turbulent transition research
[NASA-CR-198040] p 1915 N95-24302
Stereo imaging velocimetry for microgravity applications
[NASA-TM-110494] p 1949 N95-24416
Assessing capillary flow on printed wiring board surfaces
[DE94-015768] p 1959 N95-24712

FLOW VELOCITY
Capillary flow on narrow strips and in V-shaped grooves
[DE95-000543] p 1935 N95-24716

FLOW VISUALIZATION
Stratified charge rotary engine combustion studies
[NASA-CR-197985] p 1974 N95-24223
Exploratory flow visualization investigation of mast-mounted sights in presence of a rotor
[NASA-TM-4634] p 1907 N95-24566
Experimental and theoretical study of plasma-water interaction in electrothermal guns
[DE94-628961] p 2078 N95-24706

FLUE GASES
Co-firing high sulfur coal with refuse derived fuels
[DE95-006243] p 1997 N95-24406
Tunable diode lasers as continuous emission monitors for thermal waste treatment processes
[DE95-004381] p 1972 N95-25549

FLUID BOUNDARIES
A well-posed numerical method to track isolated conformal map singularities in Hele-Shaw flow
[NASA-CR-195035] p 2032 N95-25114

FLUID DYNAMICS
Report series in aerosol science
[DE95-737628] p 1999 N95-24904

FLUID FILMS
Thermohydrodynamic analysis of cryogenic liquid turbulent flow fluid film bearings, phase 2
[NASA-CR-197412] p 1962 N95-24461
Studies of two-phase gas-liquid flow in microgravity
[NASA-CR-195434] p 1963 N95-24906

FLUID FLOW
Benchmark testing and independent verification of the VS2DT computer code
[DE95-004386] p 1965 N95-25485
An annotation system for 3D fluid flow visualization p 1966 N95-25869
Predicting the transport properties of sedimentary rocks from microgeometry
[DE95-000129] p 2004 N95-26089

FLUID MECHANICS
NASA-UVA light aerospace alloy and structures technology program (LA2ST)
[NASA-CR-198041] p 1933 N95-24220
Linear non-modal phenomena in numerical analysis and applied mathematics
[DE95-005495] p 2029 N95-24458
JPRS report: Science and technology. Central Eurasia
[JPRS-UST-94-030] p 1962 N95-24469
JPRS report: Science and technology. Central Eurasia
[JPRS-UST-94-018] p 1950 N95-24472
A pseudo-sound constitutive relationship for the dilatational covariances in compressible turbulence: An analytical theory
[NASA-CR-195064] p 1966 N95-25964

FLUID-SOLID INTERACTIONS
High frequency flow-structural interaction in dense subsonic fluids
[NASA-CR-4652] p 1906 N95-24217

FLUIDIZED BED PROCESSORS
Co-firing high sulfur coal with refuse derived fuels
[DE95-006243] p 1997 N95-24406

FLUORESCENCE
On the uncertainty in single molecule fluorescent lifetime and energy emission measurements
[NASA-CR-198009] p 2049 N95-24877

FLUORIDES
NMR and optical studies of piezoelectric polymers
[DE95-003836] p 1940 N95-24554
Thermochemistry, kinetics and spectroscopy of Kr and Kr2F
[DE95-005732] p 1941 N95-25386

FLUORITE
Thin film ionic conductors based on cerium oxide
[DE95-003668] p 2086 N95-24514

FLUOROHYDROCARBONS
Materials Compatibility and Lubricants Research (MCLR) Program
[DE95-004862] p 1941 N95-25243

FLUTTER ANALYSIS
Fundamental wind tunnel experiments on low-speed flutter of a tip-fin configuration wing
[NAL-TR-1228] p 1908 N95-25762

FLUX (RATE)
User guide for the Polaris powder diffractometer at ISIS. Version 2.1
[PB95-165767] p 2074 N95-25573
Summary report for ITER Task D10: Update and implementation of neutron transport and activation codes and processed libraries
[DE95-007631] p 2083 N95-26185

FLUX DENSITY
Flux attenuation at NREL's High-Flux Solar Furnace
[DE95-000219] p 1993 N95-24715

Boundary dynamics in dilaton gravity
[DE95-607080] p 2098 N95-25526
Neutron influences and energy spectra in the Cosmos-2044 biosatellite orbit p 2061 N95-25928

FLUX VECTOR SPLITTING
Investigation of convection and pressure treatment with splitting techniques
[NASA-TM-106868] p 1961 N95-24399

FOAMS
Design and evaluation of a foam-filled hat-stiffened panel concept for aircraft primary structural applications
[NASA-TM-109175] p 1928 N95-26251

FOCAL PLANE DEVICES
Multi-spectral smart retina
[AD-A288950] p 2074 N95-25506

FOCUSING
Mirror alignment and focus of point-focus solar concentrators
[DE95-002609] p 1992 N95-24676

FOKKER-PLANCK EQUATION
A superfield generalization of the classical action-at-a-distance theory
[DE95-607084] p 1955 N95-25648

FOOD CHAIN
Activities of the National Institute of Radiological Sciences
[DE95-709916] p 2072 N95-26165

FORCE DISTRIBUTION
Thrust measurements of a complete axisymmetric scramjet in an impulse facility p 1914 N95-25395
Balances for the measurement of multiple components of force in flows of a millisecond duration p 1965 N95-25400

FOREBODIES
Experimental study of the effects of Reynolds number on high angle of attack aerodynamic characteristics of forebodies during rotary motion
[NASA-CR-195033] p 1907 N95-24443

FOREST MANAGEMENT
Sector-specific issues and reporting methodologies supporting the general guidelines for the voluntary reporting of greenhouse gases under Section 1605(b) of the Energy Policy Act of 1992, Volume 2. Part 4: Transportation sector. Part 5: Forestry sector. Part 6: Agricultural sector
[DE95-003297] p 2003 N95-26065

FORM FACTORS
Elastic form factors of hydrogen-like atoms in nS-states
[DE94-628437] p 2048 N95-24700
Annihilation diagrams in two-body nonleptonic decays of charmed mesons
[DE95-607181] p 2054 N95-25463
The off-shell axial anomaly via the (gamma)*(pi)(sup 0) (yields) (gamma) transition
[DE95-004762] p 2057 N95-25896

FORMALISM
Equivariant localization: BV-geometry and supersymmetric dynamics
[DE94-628436] p 2036 N95-24699
Quantum symplectic geometry. 1: The matrix Hamiltonian formalism
[DE95-607009] p 2032 N95-25427
Self-sustained turbulence and L-mode confinement in toroidal plasmas 2
[NIFS-278] p 2082 N95-25759
Describing the macroscopic world: Closing the circle within the dynamical reduction program
[DE95-606997] p 2100 N95-26046

FORMING TECHNIQUES
Apparatus for consolidating a pre-impregnated, filament-reinforced polymeric prepreg material
[NASA-CASE-LAR-15173-1-CU] p 1926 N95-25546

FORTRAN
Using and programming the SUPERCODE
[DE95-004342] p 2080 N95-25344

FOSSIL FUELS
Nuclear energy and the environment
[DE95-600438] p 2001 N95-25615

FOURIER ANALYSIS
A computing program of sample magnetic moments recognition for SQUID-magnetometer measurements
[DE94-637073] p 2037 N95-24363
Aerodynamic parameter estimation via Fourier modulating function techniques
[NASA-CR-4654] p 1911 N95-24630

FOURIER SERIES
Exponentially accurate approximations to piece-wise smooth periodic functions
[NASA-CR-195059] p 2031 N95-24856

FOURIER TRANSFORMATION
FT-IR microscopical analysis with synchrotron radiation: The microscope optics and system performance
[DE95-004834] p 1928 N95-24265
Techniques for the investigation of wave turbulence in water wave data
[AD-A288392] p 2007 N95-25605
Infrared multispectral sensor program, Phase 2. Field measurements, analysis and modeling. Volume 1: Fourier transform spectrometer sensor characterization
[AD-A288888] p 2075 N95-26173

FRACTALS
Fractal studies on the positron annihilation in metals
[DE94-634488] p 2041 N95-24232
Optical diffraction from fractals with a structural transition
[DE94-634311] p 2029 N95-24401
Spin correlations in percolating networks with fractal geometry
[DE95-001074] p 2037 N95-24479
Optical properties of fractal nanocomposites
[DE95-005414] p 1926 N95-25295
Proceedings of the Workshop on Dynamics and Structure of Disordered System
[DE94-792685] p 1931 N95-25356
On fractal structure of quantum gravity and relic radiation anisotropy
[DE95-605306] p 2099 N95-25966

FRACTIONATION
Clean fractionation of biomass
[DE95-000259] p 2007 N95-24307

FRACTURE MECHANICS
Significance of varied thickness to damage tolerance of carbon fiber/epoxy laminates
[PB95-165460] p 1925 N95-24242
The dual boundary element formulation for elastoplastic fracture mechanics
[DRA-TR-93062] p 1980 N95-24383
Separation of crack extension modes in orthotropic delamination models
[NASA-TM-109180] p 1927 N95-26083

FRACTURE STRENGTH
Composite ductility: The role of reinforcement and matrix
[DE95-003664] p 1925 N95-24590
Effects of through-the-thickness stitching on impact and interlaminar fracture properties of textile graphite/epoxy laminates
[NASA-CR-195042] p 1928 N95-26203

FRACTURING
Significance of varied thickness to damage tolerance of carbon fiber/epoxy laminates
[PB95-165460] p 1925 N95-24242
Thermal fracture mechanisms in ceramic thermal barrier coatings p 1946 N95-26138

FRAGMENTATION
Quantity-distance requirements for earth-bermed aircraft shelters
[AD-A279692] p 1915 N95-24424
The interactions of high-energy, highly charged Xe ions with buckyballs
[DE95-004597] p 2069 N95-25281
Fragmentation cross sections of O-16 between 0.9 and 200 GeV/nucleon p 2060 N95-25921

FRAMES
Analysis of warping effects on the static and dynamic response of a seat-type structure
[NIAR-94-12] p 1979 N95-24211
Nonlinear vibrations of thin-walled composite frames p 1984 N95-26269

FREE CONVECTION
Cryogenic helium gas convection research
[DE95-004372] p 1965 N95-25404

FREE ELECTRON LASERS
Simulation study of tapered FEL amplifiers in Raman and Compton regimes
[DE94-785266] p 1971 N95-24340
An FEL design code running on Mathcad(trademark)
[DE95-005279] p 1973 N95-25565
Nonlinear analysis of millimeter and sub-millimeter wave sources such as Cerenkov masers, orotrons, and ubitrons
[AD-A288777] p 1974 N95-26114

FREE ELECTRONS
On the field theory of the extended-type electron
[DE95-607069] p 2053 N95-25449

FREE ENERGY
The 24th Order high temperature expansion for the 3-D Ising model
[DE95-004952] p 2093 N95-24450
Thermodynamic property evaluation and magnetic refrigeration cycle analysis for gadolinium gallium garnet
[DE95-005910] p 1951 N95-25367
Correlated density matrix theory of spatially inhomogeneous Bose fluids
[DE95-607840] p 2100 N95-26102

FREE FLOW
Exploratory flow visualization investigation of mast-mounted sights in presence of a rotor
[NASA-TM-4634] p 1907 N95-24566

FREE RADICALS
Study of radicals, clusters and transition state species by anion photoelectron spectroscopy
[DE95-003438] p 2045 N95-24533

FREEZE DRYING
Solution based synthesis of perovskite-type oxide films and powders
[DE95-006170] p 2086 N95-24594

FREQUENCY DISTRIBUTION
The characteristics and design of an apparatus constructed by the Institute of Basic Problems of Technology to study relaxation phenomena in liquids at frequencies of 10-150 MHz
[IFTR-21/1994] p 1932 N95-25959
Intercomparison of hydrologic processes in global climate models
[NASA-TM-104617] p 2005 N95-26341

FREQUENCY MEASUREMENT
The measurement of the low frequency noise characteristics of the field effect transistors for cryogenic detectors
[DE94-628257] p 1957 N95-24487

FREQUENCY RANGES
Annual report 1992/93, FOA 38. Radio systems and wave propagation
[PB95-141735] p 1953 N95-24835
Experimental study of tapered slot elements
[PB95-165163] p 1955 N95-25644

FRESH WATER
Biological monitoring of national freshwaters, 1992
[PB95-166690] p 2002 N95-25745

FRESNEL INTEGRALS
The diffraction of electromagnetic waves by screens placed at the boundaries of dielectric media
[IFTR-4/1994] p 1954 N95-25393

FRICTION
Wear resistant composite structure of vitreous carbon containing convoluted fibers
[DE95-006255] p 1925 N95-24426
Friction on geological faults modelling and variational formulation of initial boundary value problems
[IFTR-31/1994] p 2004 N95-25958

FROST DAMAGE
Debris/ice/TPS assessment and integrated photographic analysis of shuttle mission STS-63
[NASA-TM-110649] p 1921 N95-25337

FUEL CELL POWER PLANTS
Intermediate-sized natural gas fueled carbonate fuel cell power plants
[DE95-004990] p 1996 N95-26171

FUEL CELLS
Monolithic solid oxide fuel cell technology advancement for coal-based power generation
[DE94-012258] p 1990 N95-24318
Monolithic solid oxide fuel cell technology advancement for coal-based power generation
[DE95-006152] p 1991 N95-24425
Liquid-fueled SOFC power sources for transportation
[DE95-002998] p 1991 N95-24607
Processing of LaCrO3 for solid oxide fuel cell applications
[DE95-000024] p 1992 N95-24683
Test plan/procedure for the DPHV system integration
[DE95-003414] p 1994 N95-25121

FUEL COMBUSTION
Shock tunnel studies of scramjet phenomena 1993
[NASA-CR-195038] p 1964 N95-25394
Nuclear energy and the environment
[DE95-600438] p 2001 N95-25615

FUEL CONSUMPTION
Alternatives to traditional transportation fuels 1993
[DE95-005445] p 1947 N95-24273
Small gas turbine component evaluation study
[PB95-147542] p 1913 N95-24293
Developing a standardized test procedure for hybrid vehicles: The challenge of the SAE HEV task force
[DE95-000280] p 1978 N95-26286

FUEL CONTAMINATION
Evaluation of commercial fuel tank water absorbers
[AD-A288361] p 1951 N95-25513

FUEL CONTROL
Predictability in space launch vehicle anomaly detection using intelligent neuro-fuzzy systems p 2025 N95-25266

FUEL FLOW
Simplified liquid oxygen propellant conditioning concepts
[NASA-TM-108482] p 1948 N95-24558

FUEL INJECTION
Stratified charge rotary engine combustion studies
[NASA-CR-197985] p 1974 N95-24223
Investigation of a rotary valving system with variable valve timing for internal combustion engines
[DE95-003831] p 1976 N95-25101
Shock tunnel studies of scramjet phenomena 1993
[NASA-CR-195038] p 1964 N95-25394

Scramjet thrust measurement in a shock tunnel
p 1914 N95-25396
Spray characteristics of single- and three-hole nozzle injectors in ambient air and in a motored single-cylinder test engine
[PB95-166286] p 1976 N95-25574
FUEL PRODUCTION
Study on the production of alternative fuels by carbon dioxide hydrogenation
[DE95-744284] p 1948 N95-24498
FUEL SYSTEMS
Simplified liquid oxygen propellant conditioning concepts
[NASA-TM-108482] p 1948 N95-24558
Development of a dedicated ethanol ultra-low emission vehicle (ULEV) system design
[DE95-004016] p 1975 N95-24880
Evaluation of commercial fuel tank water absorbers
[AD-A288361] p 1951 N95-25513
Feed system design for a reduced pressure tank
p 1923 N95-26310
FUEL TANKS
LH2 fuel tank design for SSTO p 1987 N95-26309
FUEL TESTS
Federal alternative motor fuels program: Light duty federal vehicles, trucks, and buses
[DE95-003982] p 1948 N95-24679
FULLERENES
Disilene Addition to C70
[DE95-006321] p 2087 N95-24617
FUNCTION GENERATORS
Optically-switched submillimeter-wave oscillator and radiator having a switch-to-switch propagation delay
[NASA-CASE-NPO-18547-1-CU] p 1959 N95-25307
FUNCTIONAL DESIGN SPECIFICATIONS
Test plan/procedure for the DPHV system integration
[DE95-003414] p 1994 N95-25121
The 1994 NASA/USRA/ADP Design Projects
[NASA-CR-197415] p 2101 N95-26304
Universal Test Facility p 1918 N95-26305
Automated protein crystal growth facility
p 1918 N95-26306
FUNCTIONALLY GRADIENT MATERIALS
An evaluation of a coupled microstructural approach for the analysis of functionally graded composites via the finite-element method
[NASA-CR-195455] p 1925 N95-24438
FUNCTIONALS
Unfolding of true distributions from experimental data distorted by detectors with finite resolutions
[DE94-628372] p 2035 N95-24643
FUNCTIONS (MATHEMATICS)
Splines in two-dimensional problems
[IFTR-2/1993] p 2035 N95-26106
FURNACES
Crystal Growth Furnace (CGF)
[NASA-CR-196591] p 2089 N95-25409
User guide to the Burner Engineering Research Laboratory
[DE95-004191] p 1931 N95-25492
FUSELAGES
Estimate of probability of crack detection from service difficulty report data
[PB95-149381] p 1905 N95-24295
FUSION REACTORS
Experimental and theoretical basis for advanced tokamaks
[DE95-003255] p 2077 N95-24646
Results obtained using the pellet charge exchange diagnostic on TFTR
[DE95-003254] p 2079 N95-25120
Cobalt release from PCA steel during possible fusion reactor accidents
[DE95-005019] p 2069 N95-25365
Design of Fusion Safety Data Base
[DE95-703897] p 2080 N95-25495
Benchmark experiment on a copper slab assembly bombarded by D-T neutrons
[DE95-709764] p 2055 N95-25497
Characteristics of D(-3)He fueled FRC reactor: ARTEMIS-L
[NIFS-251] p 2072 N95-26110
Innovative energy production in fusion reactors
[NIFS-250] p 2072 N95-26111
Direct energy conversion of radiation energy in fusion reactor
[NIFS-254] p 2072 N95-26250
FUSION WELDING
JPRS report: Science and technology. Central Eurasia
[JPRS-UST-95-011] p 1910 N95-24541
FUZZY SYSTEMS
Predictability in space launch vehicle anomaly detection using intelligent neuro-fuzzy systems
p 2025 N95-25266

G

G STARS
Resolution of the classical Hyades lithium problem
[DE95-003661] p 2109 N95-24234
GADOLINIUM-GALLIUM GARNET
Thermodynamic property evaluation and magnetic refrigeration cycle analysis for gadolinium gallium garnet
[DE95-005910] p 1951 N95-25367
GALACTIC CLUSTERS
Rich cluster simulation: Dynamics and mass estimates
[DE95-005233] p 2110 N95-25766
GALACTIC HALOS
Rich cluster simulation: Dynamics and mass estimates
[DE95-005233] p 2110 N95-25766
GALACTIC MASS
Rich cluster simulation: Dynamics and mass estimates
[DE95-005233] p 2110 N95-25766
GALACTIC RADIATION
Gamma-ray emission from globular clusters. Shock high energy emission from the Be-Star/Pulsar System PSR 1259-63. Echoes in x-ray novae
[NASA-CR-197994] p 2114 N95-24381
From superconductivity to supernovae: The Ginzburg symposium. Report on the symposium held in honor of Vitaly L. Ginzburg
[NASA-TM-110596] p 2108 N95-25746
GALACTIC STRUCTURE
A survey of surveys
[DE95-004238] p 2111 N95-26284
GALAXIES
The influence of CDM on the dynamical estimate of (Omega) in the local neighborhood
[DE95-005212] p 2109 N95-24455
GALERKIN METHOD
Semi-infinite mathematical programming: A collocation approach
[DE94-634273] p 2016 N95-24708
GALLIUM ARSENIDES
GaAsSb-based heterojunction tunnel diodes for tandem solar cell interconnects
[DE95-004779] p 1990 N95-24264
The measurement of the low frequency noise characteristics of the field effect transistors for cryogenic detectors
[DE94-628257] p 1957 N95-24487
High gain GaAs Photoconductive Semiconductor Switches (PCSS): Device lifetime, high current testing, optical pulse generators
[DE95-003354] p 1957 N95-24488
Optical determinations of energy-band dispersion curves in novel compound semiconductor materials
[DE95-006318] p 2089 N95-25353
Raman study of damage processes in Si(+)-implanted GaAs
[DE95-005898] p 2091 N95-26087
Atomic force microscopy as a process characterization tool for GaAs-based integrated circuit fabrication
[DE95-006223] p 2064 N95-26168
GALLIUM ISOTOPES
Update of GALLEX solar neutrino results and implications
[DE95-005005] p 2113 N95-25364
GALLIUM NITRIDES
A theoretical analysis of strain in GaN and its effects on carrier conductivity
[AD-A288769] p 2090 N95-26061
GAMMA RAY ASTRONOMY
Gamma-ray emission from globular clusters. Shock high energy emission from the Be-Star/Pulsar System PSR 1259-63. Echoes in x-ray novae
[NASA-CR-197994] p 2114 N95-24381
DOE-High Energy Physics Contract with the University of Hawaii
[DE95-004214] p 2068 N95-24852
From superconductivity to supernovae: The Ginzburg symposium. Report on the symposium held in honor of Vitaly L. Ginzburg
[NASA-TM-110596] p 2108 N95-25746
GAMMA RAY SPECTRA
Expert system for nuclide identification in gamma spectrum analysis
[PB95-149712] p 2042 N95-24297
Gamma spectrum analysis including NAA with SAMPO for windows
[PB95-149720] p 2042 N95-24298
PC based analysis of gamma ray spectra generated by semiconductor detectors
[DE94-628381] p 1958 N95-24690
GAMMA RAYS
Bremsstrahlung scattering calculations for the beam stops and collimators in the APS insertion-device beamlines
[DE95-005471] p 2069 N95-25300
Conference on physics from large gamma-ray detec tor arrays. Volume 2: Proceedings
[DE95-006900] p 2070 N95-25478
Benchmark experiment on a copper slab assembly bombarded by D-T neutrons
[DE95-709764] p 2055 N95-25497
Milagro: A low energy threshold extensive air shower array
[DE95-005246] p 2110 N95-25675
GAS ANALYSIS
Prediction of humans in various environments using gas sensors and neural networks
[PB95-141560] p 2009 N95-24227
Field-usable portable analyzer for chlorinated organic compounds
[DE95-003127] p 1930 N95-25098
The use of acoustic surface waves to analyze gases apparatus and experiments p 2039 N95-25115
GAS CHROMATOGRAPHY
Use of mass spectrometric methods for field screening of VOC's
[DE95-004903] p 1999 N95-25249
Characterization of plastic bonded explosives by pyrolysis-gas chromatography and multivariate data analysis. Applications of the procedure
[AD-A288761] p 1949 N95-25517
Characterization of plastic bonded explosives by pyrolysis-gas chromatography and multivariate data analysis. Development of the procedure
[AD-A288787] p 1949 N95-25528
GAS DENSITY
The development of a positron ionization gauge
[DE95-005958] p 1968 N95-24623
GAS DETECTORS
Prediction of humans in various environments using gas sensors and neural networks
[PB95-141560] p 2009 N95-24227
The track system of the modernized Hyperon spectrometer
[DE95-604003] p 2058 N95-25905
GAS DYNAMICS
Report series in aerosol science
[DE95-737628] p 1999 N95-24904
A domain decomposition study of massively parallel computing in compressible gas dynamics
[DE95-004759] p 1965 N95-25895
Molecular dynamics simulation of a piston driven shock wave in a hard sphere gas
[NASA-CR-195463] p 2063 N95-25963
GAS EXCHANGE
The effects on photosynthetic CO2 assimilation to long-term elevation of atmospheric CO2 concentration: An assessment of the response of Trifolium Repens L. CV. Blanca grown at F.A.C.E
[DE95-005687] p 2008 N95-25383
GAS GUNS
Target injection methods for inertial fusion energy
[DE95-003654] p 2067 N95-24651
GAS IONIZATION
The interactions of high-energy, highly charged Xe ions with buckyballs
[DE95-004597] p 2069 N95-25281
GAS MIXTURES
Electric field effects on the quantum efficiency of Cesium-iodide photocathodes in gas media
[DE94-628176] p 1957 N95-24482
Development of novel active transport membrane devices
[DE95-002658] p 1932 N95-26093
GAS PRESSURE
The development of a positron ionization gauge
[DE95-005958] p 1968 N95-24623
Target injection methods for inertial fusion energy
[DE95-003654] p 2067 N95-24651
GAS RECOVERY
Study on the production of alternative fuels by carbon dioxide hydrogenation
[DE95-744284] p 1948 N95-24498
GAS STREAMS
Development of novel active transport membrane devices
[DE95-002658] p 1932 N95-26093
GAS TEMPERATURE
Aerodynamic characteristics of the orbital reentry vehicle experimental probe fins in a supersonic flow
[NAL-TR-1232] p 1921 N95-25664
GAS TURBINE ENGINES
Small gas turbine component evaluation study
[PB95-147542] p 1913 N95-24293
Draft regulatory impact analysis: Control of air pollution emission standards for new nonroad spark-ignition marine engines
[PB95-166294] p 2001 N95-25575
Thermal barrier coatings for aircraft engines: History and directions p 1943 N95-26121

Thermal barrier coatings application in diesel engines p 1944 N95-26124
Thermal barrier coating experience in the gas turbine engine p 1944 N95-26125
PVD TBC experience on GE aircraft engines p 1944 N95-26126
Perspective on thermal barrier coatings for industrial gas turbine applications p 1945 N95-26128
Jet engine applications for materials with nanometer-scale dimensions p 1945 N95-26131
Thermal conductivity of zirconia thermal barrier coatings p 1945 N95-26133
Thermal barrier coating life modeling in aircraft gas turbine engines p 1947 N95-26140

GAS TURBINES
Retrofit NOx control technologies for natural gas prime movers
[PB95-149290] p 1997 N95-24294
Simulation of diurnal thermal energy storage systems: Preliminary results
[DE95-005751] p 1991 N95-24369
Thermal Barrier Coating Workshop
[NASA-CP-10170] p 1943 N95-26119
Thermal barrier coatings issues in advanced land-based gas turbines p 1944 N95-26122
TBC experience in land based gas turbines p 1944 N95-26127

GAS WELDING
Ternary gas plasma welding torch
[NASA-CASE-MFS-28857-1] p 1976 N95-25548

GAS-METAL INTERACTIONS
An investigation of the effect of surface impurities on the adsorption kinetics of hydrogen chemisorbed onto iron
[NASA-CR-197967] p 1933 N95-24400
Evaluation of a diffusion/trapping model for hydrogen ingress in high-strength alloys
[AD-A288447] p 1936 N95-25502

GASEOUS DIFFUSION
Development of novel active transport membrane devices
[DE95-002658] p 1932 N95-26093

GASES
Entropy and enthalpy of adsorption of gaseous chlorides of metals on quartz glass as a function of the molecular composition
[DE94-627162] p 2093 N95-24481

GASIFICATION
High octane ethers from synthesis gas-derived alcohols
[DE95-001146] p 1948 N95-24655
JALO: Fuel conversion
[DE95-737597] p 1949 N95-25244

GAUGE INVARIANCE
Finite quantum physics and noncommutative geometry
[DE94-634282] p 2027 N95-24228
Z flux-line lattices and self-dual equations in the standard model
[DE94-634364] p 2093 N95-24405
Quantum group gauge theories and covariant quantum algebras
[DE94-628524] p 2094 N95-24509
Relevance of induced gauge interactions in decoherence
[DE95-607082] p 2097 N95-25432
Equivariant Kaehler geometry and localization in the G/G model
[DE95-607073] p 2036 N95-25455
Geometric gauge fields in semiclassical gravity
[DE95-607079] p 2098 N95-25525
Boundary dynamics in dilaton gravity
[DE95-607080] p 2098 N95-25526
Semiglobal Alice strings
[DE95-607081] p 2098 N95-25527
The off-shell axial anomaly via the (gamma)*(pi)(sup 0) (yields) (gamma) transition
[DE95-004762] p 2057 N95-25896
On a new type of long-range forces
[DE95-605286] p 2063 N95-25965

GAUGE THEORY
Quantum group gauge theories and covariant quantum algebras
[DE94-628524] p 2094 N95-24509
Creation and development of the Universe (symmetry approach)
[DE94-628558] p 2109 N95-24884
Vortex solutions in two-Higgs-doublet systems
[DE94-634363] p 2096 N95-25107
Equivariant Kaehler geometry and localization in the G/G model
[DE95-607073] p 2036 N95-25455
The Hamiltonian of SU(2) lattice gauge theory in approximate tri-diagonal form
[DE95-607101] p 2098 N95-25475
Ten dimensional SO(10) G.U.T. models with dynamical symmetry breaking
[DE95-607093] p 2098 N95-25533
Homogeneous anisotropic cosmological models in the minimum quadratic Poincare gauge theory of gravity
[DE95-607083] p 2110 N95-25647
A superfield generalization of the classical action-at-a-distance theory
[DE95-607084] p 1955 N95-25648
Strong phase correlations of solitons of nonlinear Schroedinger equation
[DE95-607002] p 2063 N95-25991

GAUSS EQUATION
Numerical investigation of Schwinger-Dyson and Bethe-Salpeter equations with Gauss potential in the framework of the quarkonium model
[DE94-636730] p 2029 N95-24387

GAUSSIAN ELIMINATION
Use of multiple fronts in Gaussian elimination
[PB95-165353] p 2033 N95-25627

GEAR TEETH
Generation and computerized simulation of meshing and contact of modified involute helical gears
[NASA-CR-4644] p 1952 N95-24395

GEARS
Generation and computerized simulation of meshing and contact of modified involute helical gears
[NASA-CR-4644] p 1952 N95-24395
Computerized design and generation of low-noise gears with localized bearing contact
[NASA-TM-106880] p 1977 N95-26074

GENERAL AVIATION AIRCRAFT
Development of an intervention program to encourage shoulder harness use and aircraft retrofit in general aviation aircraft, phases 1 and 2
[DOT/FAA/AM-95/2] p 1909 N95-24384

GENERAL OVERVIEWS
Smart vision chips: An overview p 2024 N95-25265

GENETIC ALGORITHMS
New approaches to optimization in aerospace conceptual design
[NASA-CR-196695] p 1910 N95-24436

GENETICS
Genetic and biophysical studies of the photosynthetic reaction center
[DE95-004179] p 2008 N95-24850
The effects on photosynthetic CO2 assimilation to long-term elevation of atmospheric CO2 concentration: An assessment of the response of Trifolium Repens L. CV. Blanca grown at F.A.C.E
[DE95-005687] p 2008 N95-25383
Activities of the National Institute of Radiological Sciences
[DE95-709916] p 2072 N95-26165

GEOCHEMISTRY
Summaries of FY 1994 geosciences research
[DE95-005657] p 1988 N95-25440

GEODESIC LINES
The geodesic motion in Kaluza-Klein spinning space
[DE95-607070] p 2039 N95-25646

GEODESY
Mapping, charting and geodesy handbook
[AD-A286558] p 1989 N95-24502

GEOGRAPHIC INFORMATION SYSTEMS
Geographical information systems and other tools for spatial information management
[PB95-165759] p 2106 N95-25572

GEOLOGICAL FAULTS
Friction on geological faults modelling and variational formulation of initial boundary value problems
[IFTR-31/1994] p 2004 N95-25958

GEOLOGICAL SURVEYS
Distribution and nature of UV absorbers on Trition's surface
[NASA-CR-198008] p 2112 N95-26116

GEOMAGNETISM
Geomagnetic Polar Cap (PC) index, 1975-1993
[UAG-103] p 2004 N95-24897
Solar-geophysical data number 603, November 1994. Part 1: (Prompt reports). Data for October, September 1994, and late data
[PB95-166393] p 2113 N95-25576
The natural space environment: Effects on spacecraft
[NASA-RP-1350] p 1921 N95-25875
Impulsive Alfven coupling between the magnetosphere and ionosphere
[NIFS-276] p 2004 N95-26036

GEOMETRICAL OPTICS
The Third International Workshop on the Physics and Modern Applications of Lasers
[DE95-606395] p 1972 N95-25491

GEOMETRY
Finite quantum physics and noncommutative geometry
[DE94-634282] p 2027 N95-24228
Distances on a lattice from noncommutative geometry
[DE94-634327] p 2027 N95-24229

GEOMORPHOLOGY
Shelf sediment dynamics and development of lithostratigraphy
[AD-A288886] p 2006 N95-25504

GEOPHYSICS
Summaries of FY 1994 geosciences research
[DE95-005657] p 1988 N95-25440
3-D seismic imaging of complex geologies
[DE95-006813] p 2004 N95-25476
Solar-geophysical data number 603, November 1994. Part 1: (Prompt reports). Data for October, September 1994, and late data
[PB95-166393] p 2113 N95-25576
Solar-geophysical data number 603, November 1994. Part 2: (Comprehensive reports). Data for May 1994 and miscellaneous
[PB95-166401] p 2113 N95-25577

GEOSTROPHIC WIND
Modelling the day to day wind variability offshore central Chile at about 30 deg south
[DE95-606032] p 2006 N95-26043

GEOSYNCHRONOUS ORBITS
The use of empirical models to investigate GPS derived total electron content
[DE95-606045] p 2111 N95-26044

GEOTEMPERATURE
Coso Monitoring Program, October 1992 through September 1993
[AD-A279147] p 1989 N95-24422

GEOTHERMAL RESOURCES
Coso Monitoring Program, October 1992 through September 1993
[AD-A279147] p 1989 N95-24422
Long-Term Flow Test number 1: Roosevelt Hot Springs, Utah
[DE95-004995] p 2004 N95-25666

GERMANIUM COMPOUNDS
Proceedings of the Workshop on Dynamics and Structure of Disordered System
[DE94-792685] p 1931 N95-25356

GERMANY
The origins of the Federal Republic of Germany's space policy, 1959-1965: European and national dimensions
[ESA-HSR-12] p 1916 N95-24892

GETTERS
High-beta discharges with neutral beam injection in CHS
[NIFS-280] p 2071 N95-26031

GIMBALS
Suspension system for gimbal supported scanning payloads
[NASA-CASE-MFS-28817-1] p 1969 N95-25544

GLASS
Entropy and enthalpy of adsorption of gaseous chlorides of metals on quartz glass as a function of the molecular composition
[DE94-627162] p 2093 N95-24481
Proceedings of the Workshop on Dynamics and Structure of Disordered System
[DE94-792685] p 1931 N95-25356

GLASS FIBER REINFORCED PLASTICS
Study on tensile fatigue testing method of unidirectional fiber-resin matrix composites
[NAL-TR-1241] p 1926 N95-24989
Study on tensile fatigue testing method of unidirectional fiber-resin matrix composites
[NAL-TR-1241] p 1927 N95-25770

GLASS FIBERS
Thermomechanical fatigue behavior of three CFCC's
[NASA-CR-195441] p 1927 N95-25880

GLASS LASERS
Central Laser Facility. Annual report to the Laser Facility Committee
[PB95-160511] p 1973 N95-25640

GLOBAL AIR POLLUTION
Sector-specific issues and reporting methodologies supporting the General Guidelines for the voluntary reporting of greenhouse gases under Section 1605(b) of the Energy Policy Act of 1992, volume 1. Part 1: Electricity supply sector. Part 2: Residential and commercial buildings sector. Part 3: Industrial sector
[DE95-003296] p 2000 N95-25362

GLOBAL POSITIONING SYSTEM
Use of voronoi diagrams for qualitative matching
[PB95-165445] p 1988 N95-24240
Real-time testing and demonstration of the US Army Corps of Engineers' Real-Time On-The-Fly positioning system
[AD-A288624] p 1910 N95-25609
The use of empirical models to investigate GPS derived total electron content
[DE95-606045] p 2111 N95-26044

GLOBAL WARMING
Preparatory research for global warming precaution spread promotion manual and early spread plan research work
[DE95-730143] p 1996 N95-24291
Investigation of technologies for CO2 separation, fixation and disposal for the prevention of global warming
[DE95-744285] p 1997 N95-24499
Nuclear energy and the environment
[DE95-600438] p 2001 N95-25615
Our changing planet: The FY 1995 U.S. Global Change Research Program p 2002 N95-25852

GLUONS
Measurement of the SS-OS Dijet cross-section ratio
[DE95-004852] p 2041 N95-24253
A measurement of quark and gluon jet differences at the Z(sup 0) resonance
[DE95-005947] p 2044 N95-24417
On the Compton non-Abelian twist-3 asymmetry
[DE94-628586] p 2095 N95-24727
The twist-3 single spin asymmetries of pion production
[DE95-607144] p 2052 N95-25437
Mass splitting of the pseudoscalar and vector mesons induced by the homogeneous vacuum gluon field
[DE95-605322] p 2058 N95-25908
Excited states of mesons within the NJL model with the homogeneous vacuum gluon field
[DE95-605323] p 2058 N95-25909

GOES SATELLITES
Solar-geophysical data number 603, November 1994. Part 2: (Comprehensive reports). Data for May 1994 and miscellaneous
[PB95-166401] p 2113 N95-25577

GOGGLES
Visual performance with Omnibus 3: A comparative evaluation of enhanced generation three image intensifier technology
[PB95-141891] p 2013 N95-24510

GOLD
Au/Cr sputter coating for the protection of alumina during sliding at high temperatures
[NASA-TM-106853] p 1923 N95-24437
Formation of thallium based high temperature superconductors using aerosol flow reacted precursor powders
[DE95-005901] p 2089 N95-25389

GOODNESS OF FIT
Multidimensional data analysis on the basis of integral nonparametric statistics and multilayer perceptrons
[DE94-628375] p 2035 N95-24858

GOVERNMENT PROCUREMENT
Automated Procurement System (APS): Project management plan (DS-03), version 1.2
[NASA-CR-196576] p 2102 N95-24442
Acquisition forecast: Fiscal year 1995
[NASA-TM-110575] p 2103 N95-25850
Report to Congressional Committees. Tactical Aircraft: Concurrency in development and production of F-22 aircraft should be reduced
[GAO/NSIAD-95-59] p 1911 N95-26338

GOVERNMENT/INDUSTRY RELATIONS
Sector-specific issues and reporting methodologies supporting the General Guidelines for the voluntary reporting of greenhouse gases under Section 1605(b) of the Energy Policy Act of 1992, volume 1. Part 1: Electricity supply sector. Part 2: Residential and commercial buildings sector. Part 3: Industrial sector
[DE95-003296] p 2000 N95-25362
Assessment of Commercial Satellite Communications Initiative (CSCI) studies
[AD-A288357] p 1920 N95-25508
The 1994 NASA/USRA/ADP Design Projects
[NASA-CR-197415] p 2101 N95-26304

GRAIN BOUNDARIES
Atomistic studies of grain boundaries in NiAl
[DE95-005208] p 1937 N95-26014

GRAMMARS
The use of DBMS and document oriented interface in the TPLAN-system
[DE95-605219] p 2106 N95-25907

GRAND UNIFIED THEORY
Ten dimensional SO(10) G.U.T. models with dynamical symmetry breaking
[DE95-607093] p 2098 N95-25533
Heavy-neutrino effects on tau-lepton decays
[PB95-165346] p 2056 N95-25626

GRAPHICAL USER INTERFACE
Information management architecture for an integrated computing environment for the Environmental Restoration Program. Environmental Restoration Program, Volume 3: Interim technical architecture
[DE95-001386] p 2105 N95-24656
Three-dimensional user interfaces for scientific visualization
[NASA-CR-197923] p 2017 N95-25867
The 3D widgets for exploratory scientific visualization p 1966 N95-25868
An annotation system for 3D fluid flow visualization p 1966 N95-25869
Four-Dimensional Information Visualization and Analysis System
[DE95-004935] p 2022 N95-26013

GRAPHITE-EPOXY COMPOSITES
Effects of through-the-thickness stitching on impact and interlaminar fracture properties of textile graphite/epoxy laminates
[NASA-CR-195042] p 1928 N95-26203

GRASSES
The effects on photosynthetic CO2 assimilation to long-term elevation of atmospheric CO2 concentration: An assessment of the response of Trifolium Repens L. CV. Blanca grown at F.A.C.E
[DE95-005687] p 2008 N95-25383

GRAVITATION
Theoretical motivation for gravitation experiments on ultra-low energy antiprotons and antihydrogen
[DE95-003662] p 2091 N95-24235
Creation of a scalar potential in 2D dilaton gravity
[DE95-006066] p 2003 N95-24577
A quantum gravitational mechanism for exiting inflation
[DE95-003342] p 2096 N95-24867
Geometric gauge fields in semiclassical gravity
[DE95-607079] p 2098 N95-25525
Boundary dynamics in dilaton gravity
[DE95-607080] p 2098 N95-25526
Homogeneous anisotropic cosmological models in the minimum quadratic Poincare gauge theory of gravity
[DE95-607083] p 2110 N95-25647
On fractal structure of quantum gravity and relic radiation anisotropy
[DE95-605306] p 2099 N95-25966
Exact solution of 2 D Poincare gravity coupled with fermion matter
[DE95-605314] p 2099 N95-25967
A new formulation of quantum field theory on S4
[DE95-607098] p 2099 N95-25970

GRAVITATION THEORY
Tachyon condensates and anisotropic universe
[DE95-607074] p 2097 N95-25456
STEP: Satellite Test of the Equivalence Principle. Report on the phase A study
[NASA-TM-110598] p 1917 N95-26184

GRAVITATIONAL COLLAPSE
Research in nuclear astrophysics: Stellar collapse and supernovae
[DE95-004300] p 2110 N95-25343

GRAVITATIONAL EFFECTS
On the effects of gravitational fields on the electrical properties of matter
[DE95-607022] p 2038 N95-25430

GRAVITATIONAL FIELDS
Mars observer mission: Mapping the Martian world
[NASA-CR-110585] p 2112 N95-24672
On the effects of gravitational fields on the electrical properties of matter
[DE95-607022] p 2038 N95-25430

GRAVITATIONAL PHYSIOLOGY
STS-67 post flight presentation
[NASA-TM-110552] p 1918 N95-24198

GREEN'S FUNCTIONS
A functional integral approach without slave bosons to the Anderson model
[DE94-634858] p 2028 N95-24276
Relations among solutions for wave and Klein-Gordon equations for different dimensions
[DE95-600853] p 2093 N95-24446
Covariant single-time equations for a system of N spinor particles
[DE94-628587] p 2047 N95-24640
Dissipative quantum mechanics: The generalization of the canonical quantization and von Neumann equation
[DE95-607008] p 2096 N95-25426
A Green's function method for hadrons in nuclei
[DE94-792620] p 2070 N95-25772
HZE beam transport in multilayered materials p 2060 N95-25922

GREENHOUSE EFFECT
Responsibility means doing without: How to rescue the ozone-layer
[PB95-166807] p 1997 N95-24334
Investigation of technologies for CO2 separation, fixation and disposal for the prevention of global warming
[DE95-744285] p 1997 N95-24499
Microphysical and compositional influences on shortwave radiative forcing of climate by sulfate aerosols
[DE95-005999] p 1997 N95-24570
Voluntary reporting of greenhouse gases under Section 1605(b) of the Energy Policy Act of 1992: General guidelines
[DE95-003295] p 2000 N95-25361
Sector-specific issues and reporting methodologies supporting the General Guidelines for the voluntary reporting of greenhouse gases under Section 1605(b) of the Energy Policy Act of 1992, volume 1. Part 1: Electricity supply sector. Part 2: Residential and commercial buildings sector. Part 3: Industrial sector
[DE95-003296] p 2000 N95-25362
Carbon taxes and India
[DE95-005401] p 2001 N95-25629
Sector-specific issues and reporting methodologies supporting the general guidelines for the voluntary reporting of greenhouse gases under Section 1605(b) of the Energy Policy Act of 1992, Volume 2. Part 4: Transportation sector. Part 5: Forestry sector. Part 6: Agricultural sector
[DE95-003297] p 2003 N95-26065

GREENHOUSES
Preparatory research for global warming precaution spread promotion manual and early spread plan research work
[DE95-730143] p 1996 N95-24291

GREENLAND
Assessment of climate variability of the Greenland ice sheet: Integration of in situ and satellite data
[NASA-CR-198020] p 1998 N95-24846

GRID GENERATION (MATHEMATICS)
Parallel algorithms for dynamically partitioning unstructured grids
[DE95-001616] p 2015 N95-24346
Visibility ordering meshed polyhedra
[CSRD-1097] p 2030 N95-24557
Object-oriented parallel polygon rendering
[DE95-004909] p 2021 N95-24881
Aerodynamic shape optimization of wing and wing-body configurations using control theory
[NASA-CR-198024] p 1911 N95-25334
Adaptive finite element method 2: Error estimation
[AD-A288358] p 2033 N95-25509
A combined geometric approach for solving the Navier-Stokes equations on dynamic grids
[NASA-TM-106919] p 1908 N95-26075

GROUND STATE
Dressing and bound states in quantum field theory
[DE94-628580] p 2095 N95-24639
Quasi two body decays of charm mesons
[DE94-792634] p 2057 N95-25901

GROUND SUPPORT SYSTEMS
Apollo 13: Houston, we've got a problem
[NASA-TM-110551] p 1918 N95-24215
Study of launch site processing and facilities for future launch vehicles
[NASA-CR-198025] p 1918 N95-24579

GROUND TESTS
The Superorbital Expansion Tube concept, experiment and analysis p 1915 N95-25399

GROUND WATER
Identification of potential groundwater flow paths using geological and geophysical data
[DE95-006253] p 1988 N95-24407

GROUP DYNAMICS
Grounding explanations in evolving, diagnostic situations
[NASA-CR-198027] p 2026 N95-25335

GROUP THEORY
Quantum group gauge theories and covariant quantum algebras
[DE94-628524] p 2094 N95-24509
Equivariant localization: BV-geometry and supersymmetric dynamics
[DE94-628436] p 2036 N95-24699
Quantum group and quantum symmetry
[DE94-634329] p 2095 N95-24767
A partial unification model in non-commutative geometry
[DE95-607129] p 2097 N95-25435
On exotic supersymmetries of the Phi(1,3) deformation of minimal models
[DE95-607088] p 2033 N95-25532
Constraints, complex structures and quantization
[DE95-605252] p 2037 N95-25781

GROUP VELOCITY
On a remarkable similarity between the propagation of whistlers and the bow wave of a ship
[U-OF-IOWA-94-22] p 2111 N95-26196

GROUP 4A COMPOUNDS
Kinetic modeling of the atomic layer epitaxy window in group 4 semiconductor growth
[DE95-005903] p 2089 N95-25391

GROUP 4B COMPOUNDS
Kinetic modeling of the atomic layer epitaxy window in group 4 semiconductor growth
[DE95-005903] p 2089 N95-25391

GYROTROPISM
Electromagnetic waves and photoacoustic transformation in gyrotropic superlattices p 2083 N95-24205

H

H ALPHA LINE
Journal of the Communications Research Laboratory, volume 41, number 1, March 1994
[PB95-177606] p 1956 N95-26008

H-60 HELICOPTER
Configuration and other differences between Black Hawk and Seahawk helicopters in military service in the USA and Australia
[AR-008-386] p 1911 N95-25935

HADRONS
Investigation of the gross structure of spectra and mass distributions of hadronic resonances
[DE94-636799] p 2043 N95-24361
The discovery of the tau lepton: Part 1, The early history through 1975; Part 2, Confirmation of the discovery and measurement of major properties, 1976-1982
[DE95-005945] p 2044 N95-24414
A measurement of quark and gluon jet differences at the Z(sup 0) resonance
[DE95-005947] p 2044 N95-24417
A test of the flavor independence of strong interactions
[DE95-005948] p 2044 N95-24418
Measurement of alpha(sub s)from hadronic event observables at the Z(sup 0) resonance
[DE95-005943] p 2045 N95-24434
A search for jet handedness in hadronic Z(sup 0) decays
[DE95-005944] p 2045 N95-24435
Update on B(sub K) with Wilson fermions
[DE95-004953] p 2085 N95-24451
Software of a distributor of high voltage of the H C-600 hadronic calorimeter
[DE94-628255] p 1967 N95-24486
Lagrangian formulation of NJL model with se parable interaction
[DE94-628519] p 1952 N95-24506
Measurement of the charged multiplicity of Z(sup 0) (yields) b(bar b) events
[DE95-006051] p 2046 N95-24571
A test of the flavor independence of strong interactions
[DE95-006063] p 2046 N95-24576
Measurement of alpha(sub s) from hadronic ev ent observables at the Z(sup 0) resonance
[DE95-005949] p 2047 N95-24622
Multiplicity moments in e(+)e(-) annihilation into hadrons at the Z(sup 0) resonance
[DE95-005950] p 2047 N95-24641
The emission of particle identification efficiency in the EXCHARM experiment
[DE94-628258] p 2047 N95-24644
A study of K(sub s) (lambda) and (bar (lambda)) production in hadronic Z(sup 0) decays
[DE95-004280] p 2047 N95-24660
Geometry of multihadron production
[DE95-004290] p 2047 N95-24663
Parity doubling from thermodynamics of experimental hadron spectrum
[DE95-600934] p 2095 N95-24839
Critical parameters of Quark-Hadron phase transition with interacting and massive quarks
[DE95-607143] p 2052 N95-25436
Heavy quark effective theory, interpolating fields and Bethe-Salpeter amplitudes
[DE95-607146] p 2053 N95-25460
Inelastic collisions of negative muons and hadrons with Helium metastable atoms
[DE95-607538] p 2055 N95-25493
Inelastic collisions of negative muons and hadrons with metastable hydrogen atoms
[DE95-607537] p 2056 N95-25668
A Green's function method for hadrons in nuclei
[DE94-792620] p 2070 N95-25772

HAFNIUM OXIDES
Processing and characterization of transformation-toughened ceramics with strength retention to elevated temperatures
[DE95-005758] p 1941 N95-25387

HALL EFFECT
Complex scattering dynamics and the quantum Hall effect
[DE95-005239] p 2093 N95-24457

HALOS
Self-consistent beam halo studies & halo diagnostic development in a continuous linear focusing channel
[DE95-003706] p 2065 N95-24331

HAMILTON-JACOBI EQUATION
Semiclassical hyperspherical matrix elements for helium doubly excited states
[DE94-628867] p 2048 N95-24718

HAMILTONIAN FUNCTIONS
Periodic solutions of Hamiltonian perturbations of 2D linear Schroedinger equations
[PB95-165536] p 2028 N95-24301
Construction of quasi-periodic solutions for Hamiltonian perturbations of linear equations and applications to nonlinear PDE
[PB95-165551] p 2028 N95-24322
Constraints and Hamiltonian in light-front quantized field theory
[DE95-600852] p 2093 N95-24353
Complex scattering dynamics and the quantum Hall effect
[DE95-005239] p 2093 N95-24457
On squaring the primary constraints in a generalized Hamiltonian dynamics
[DE94-628500] p 2036 N95-24504
The lattice spinor QED Hamiltonian critique of the continuous space approach
[DE94-628521] p 2094 N95-24508
A discrete variable representation for electron-hydrogen atom scattering
[DE95-003436] p 2045 N95-24512
The geometry of weak solutions of certain integrable nonlinar PDE's
[DE95-005241] p 2030 N95-24609
On the problem of unboundedness from below of the spinor QED Hamiltonian
[DE94-628579] p 2094 N95-24638
A fast tracking method using resonance basis Hamiltonians
[DE95-004292] p 2068 N95-24664
Geometric quantization of symplectic manifolds with symmetry
[DE94-628435] p 2031 N95-24698
Quantum symplectic geometry. 1: The matrix Hamiltonian formalism
[DE95-607009] p 2032 N95-25427
Nonlinearity induced nontrivial dynamics in the Jaynes-Cummings Hamiltonian
[DE95-607004] p 2032 N95-25452
The Hamiltonian of SU(2) lattice gauge theory in approximate tri-diagonal form
[DE95-607101] p 2098 N95-25475
A covariant canonical description of Liouville field theory
[DE95-607094] p 2098 N95-25534
The space of solutions of Toda field theory
[DE95-607095] p 2099 N95-25650
Constraints, complex structures and quantization
[DE95-605252] p 2037 N95-25781
Quantization of a Hamiltonian system with an infinite number of degrees of freedom
[DE95-605279] p 2034 N95-25783
On the numerical method for analysis of the dynamics of the classical Hamiltonian systems
[DE95-605218] p 2034 N95-25906
Dynamics of phase ordering of nematics in a pore
[DE95-607662] p 2090 N95-25978
Charge-Dyon system as the reduced oscillator
[DE95-606998] p 2100 N95-25987

HANDBOOKS
Mapping, charting and geodesy handbook
[AD-A286558] p 1989 N95-24502
Metrology: Measurement assurance program guidelines
[NASA-RP-1364] p 1950 N95-24543

HANDEDNESS
A search for jet handedness in hadronic Z(sup 0) decays
[DE95-005944] p 2045 N95-24435

HANDWRITING
How Captain Amerika uses neural networks to fight crime p 2025 N95-25272

HARDNESS
Time dependent indentation testing at non-ambient temperatures utilizing the high temperature mechanical properties microprobe
[DE95-005895] p 1933 N95-24432

HARMONIC GENERATIONS
Nonlinear optics and organic materials
[DE95-004677] p 2074 N95-25357

HARMONIC OSCILLATION
Anionic construction of the sl(sub q, s)(2) algebra
[DE95-600838] p 2043 N95-24350

HARMONIC OSCILLATORS
Semiclassical asymptotics on covering manifolds and morse inequalities
[PB95-165510] p 2028 N95-24251
Anharmonic potential in the oscillator representation
[DE94-636740] p 2092 N95-24312
Elliptic deformed Newton mechanics in the three-dimensional phase space
[DE94-636741] p 2092 N95-24313
Oscillator poly spheroidal functions
[DE94-628440] p 2030 N95-24636
Asymptotic properties of the oscillator poly spheroidal functions
[DE94-628441] p 2032 N95-24860
On connection of q-deformed para oscillators with para oscillators
[DE95-607007] p 2096 N95-25425
Dissipative quantum mechanics: The generalization of the canonical quantization and von Neumann equation
[DE95-607008] p 2096 N95-25426
Ellipsoidal basis for isotropic oscillator
[DE95-605253] p 2034 N95-25782

HARNESSES
Development of an intervention program to encourage shoulder harness use and aircraft retrofit in general aviation aircraft, phases 1 and 2
[DOT/FAA/AM-95/2] p 1909 N95-24384

HARTREE APPROXIMATION
Disilene Addition to C70
[DE95-006321] p 2087 N95-24617

HASTELLOY (TRADEMARK)
Creep properties of 20% cold worked hastelloy XR
[DE94-785198] p 1933 N95-24338

HAZARDS
TITLE: Environmental, health, and safety issues offuel cells in transportation. Volume 1: Phosphoricacid fuel-cell buses
[DE95-000289] p 1993 N95-24866

HEAT ENGINES
Activities of the Ceramic Technology Project
[DE95-003394] p 1940 N95-24588
Thermal spray processing p 1945 N95-26130

HEAT FLUX
High heat flux experiment on B4C-converted carbon based materials for plasma facing materials of JT-60U
[DE94-777545] p 2077 N95-24585
Divertor design for the Tokamak Physics Experiment
[DE95-003653] p 2078 N95-24650
Turbine-engine applications of thermographic-phosphor temperature measurements
[DE95-003625] p 1989 N95-25110
Heat flux instrumentation for HYFLITE thermal protection system
[NASA-CR-197715] p 1968 N95-25118

HEAT PIPES
Felt-metal-wick heat-pipe solar receiver
[DE95-004535] p 1992 N95-24682
An examination of metal felt wicks for heat-pipe applications
[DE95-002608] p 1994 N95-25109

HEAT PUMPS
Brayton-cycle solvent recovery heat pump. A technical brief
[DE94-000225] p 1991 N95-24666
Performance tests of air source heat pumps under frosting conditions. Quality of results
[PB95-141792] p 1995 N95-25892

HEAT STORAGE
Simulation of diurnal thermal energy storage systems: Preliminary results
[DE95-005751] p 1991 N95-24369

HEAT TRANSFER
Solutions of turbulent backward-facing step flow with heat transfer using the finite volume method
[DE95-003360] p 1962 N95-24489
Heat Kernel expansion on a cone and quantum fields near cosmic strings
[DE94-628520] p 2094 N95-24507
Heat release rate measurements in tunnel fires
[PB95-165106] p 1931 N95-25443

HEATING
Residual Stress Measurements with Laser Speckle Correlation Interferometry and Local Heat Treating
[DE95-060082] p 1981 N95-24598
Transport reduction by current profile control in the reversed field pinch
[DE95-007016] p 2077 N95-24619

HEATING EQUIPMENT
Performance tests of air source heat pumps under frosting conditions. Quality of results
[PB95-141792] p 1995 N95-25892

HEAVY IONS
The physics and experimental program of the Relativistic Heavy Ion Collider (RHIC)
[DE95-003416] p 2066 N95-24495
Elise: The next step in development of induction heavy ion drivers for inertial fusion energy
[DE95-004679] p 2069 N95-25358
Conference on physics from large gamma-ray detec tor arrays. Volume 2: Proceedings
[DE95-006900] p 2070 N95-25478
Theoretical studies in hadronic and nuclear physics
[DE95-006643] p 2098 N95-25562
Anisotropy of dilepton emission from nuclear collisions
[DE95-004354] p 2070 N95-25634

Activities of the National Institute of Radiological Sciences
[DE95-709916] p 2072 N95-26165

HEISENBERG THEORY
Staggered magnetization in the Heisenberg antiferromagnet
[DE95-607102] p 2038 N95-25458

HELICOPTER PROPELLER DRIVE
A portable transmission vibration analysis system for the S-70A-9 Black Hawk helicopter
[DSTO-TR-0072] p 1966 N95-24203

HELICOPTERS
Interfacing a digital compass to a remote-controlled helicopter
[PB95-164927] p 1914 N95-24260

HELIOTRONS
New modular heliotron system compatible with closed helical divertor and good plasma confinement
[NIFS-279] p 2081 N95-25653
New evaluation method of superconductor characteristics for realizing the Large Helical Device
[NIFS-297] p 2071 N95-25855
High-beta discharges with neutral beam injection in CHS
[NIFS-280] p 2071 N95-26031

HELIUM ATOMS
Semiclassical hyperspherical matrix elements for helium doubly excited states
[DE94-628867] p 2048 N95-24718
Inelastic collisions of negative muons and hadrons with Helium metastable atoms
[DE95-607538] p 2055 N95-25493

HELIUM IONS
Copper transport on oxygen annealing of a superconducting film Y-Ba-Cu-O
[DE94-627566] p 2086 N95-24537
Dynamics Explorer 1, retarding ion mass spectrometer summary spectrograms-82/110 to 82/229 spin-time spectrograms for H(+), He(+), O(+), N(+), O(+ +), M/Z = 2, and molecular ions
[NASA-TM-108485] p 2003 N95-24763
Dynamics Explorer 1, retarding ion mass spectrometer summary spectrograms-82/230 to 82/265 spin-time spectrograms for H(+), He(+), O(+), N(+), O(+ +), M/Z = 2, and molecular ions
[NASA-TM-108486] p 2003 N95-24764

HELIUM ISOTOPES
Structure of liquid He-4 excitations spectrum
[DE94-637113] p 2043 N95-24364
Characteristics of D(-3)He fueled FRC reactor: ARTEMIS-L
[NIFS-251] p 2072 N95-26110
Innovative energy production in fusion reactors
[NIFS-250] p 2072 N95-26111

HELIUM-NEON LASERS
Decay of a laser generated shock wave in an aluminium target
[DE94-629014] p 1972 N95-24707

HELMHOLTZ EQUATIONS
Numerical simulation methods for wave propagation through optical waveguides
[DE94-634313] p 2073 N95-24402

HELMHOLTZ RESONATORS
The phenomenon of non-linearity accompanying the action of acoustic pressure on a Helmholtz resonator
[IFTR-19/1994] p 2040 N95-26108

HERMITIAN POLYNOMIAL
Intrinsic heights of stable varieties. Application to abelian varieties
[PB95-165577] p 2029 N95-24323

HETEROGENEITY
Integration of heterogeneous data bases for development of a large-scale environmental data atlas for multi-platform PC and workstation users
[DE95-002689] p 2000 N95-25278

HETEROJUNCTION DEVICES
GaAsSb-based heterojunction tunnel diodes for tandem solar cell interconnects
[DE95-004779] p 1990 N95-24264
Temperature-dependent growth of LaAlO3 films on YBa2CuO7 C-axis films for multilayer structures
[DE95-005257] p 2089 N95-25598

HEURISTIC METHODS
Cyclic subgroups in class groups of real quadratic fields
[DE94-628407] p 2031 N95-24697
The diffraction of electromagnetic waves by screens placed at the boundaries of dielectric media
[IFTR-4/1994] p 1954 N95-25393
Heuristic approach to the path planning problem in a raster map
[PB95-141826] p 2034 N95-25893

HIERARCHIES
On Segal-Wilson's construction for the (tau)-functions of the constrained KP hierarchies
[DE95-606999] p 2100 N95-25988

HIGGS BOSONS
Vortex solutions in two-Higgs-doublet systems
[DE94-634363] p 2096 N95-25107
Scalar three body decays and signals for new physics
[DE95-607188] p 2053 N95-25438
Study of the simplest realistic Higgs sector in quark-lepton symmetric models
[DE95-607159] p 2053 N95-25461

HIGH ALTITUDE
Non-invasive detection of increased intracranial pressure using acoustical techniques
[AD-A279292] p 2010 N95-24309

HIGH CURRENT
High gain GaAs Photoconductive Semiconductor Switches (PCSS): Device lifetime, high current testing, optical pulse generators
[DE95-003354] p 1957 N95-24488
Over-compression, a method to shape the longitudinal bunch distribution for a reduced energy spread
[DE95-006052] p 2066 N95-24572
Experimental and theoretical development towards a 500 MW, one-microsecond, L-band relativistic klystron amplifier
[DE95-003682] p 1958 N95-24589
New evaluation method of superconductor characteristics for realizing the Large Helical Device
[NIFS-297] p 2071 N95-25855

HIGH DEFINITION TELEVISION
Converting multiple OC-3c ATM streams to HIPPI to drive an HDTV frame buffer from a workstation cluster
[DE95-003638] p 2022 N95-26066

HIGH ENERGY ELECTRONS
Feasibility of ceramic joining with high energy electron beams
[DE95-004519] p 1940 N95-24717

HIGH ENERGY INTERACTIONS
Multiplicity moments in e(+)e(-) annihilation into hadrons at the Z(sup 0) resonance
[DE95-005950] p 2047 N95-24641
Current experiments in elementary particle physics. Revision
[DE95-003797] p 2067 N95-24652
Proceedings of the 1994 Conference on Computing in Energy Physics
[DE95-004442] p 2068 N95-24665
On a possibility for a measurement of the transversal proton polarization in the diffractive pion production in pp and pe high energy collisions
[DE94-628598] p 2047 N95-24668
Theory of ultra dense matter and the dynamics of high energy interactions involving nuclei
[DE95-004114] p 2048 N95-24671
Search for top in lepton + jets in D0 using a topological tag
[DE95-003929] p 2048 N95-24677
High Energy Physics Division research activities
[DE95-003985] p 2068 N95-24680
Introduction to the Monte Carlo methods
[DE94-628386] p 2035 N95-24693
DOE-High Energy Physics Contract with the University of Hawaii
[DE95-004214] p 2068 N95-24852
Notion of the inclusive spectra and cross sections of B-meson production in hadronic interactions of high energies
[DE94-628628] p 2049 N95-24887
High Energy Physics Advisory Panel's subpanel on vision for the future of high-energy physics
[DE94-013641] p 2068 N95-24899
Proceedings of workshop on Future in HEP Computing
[DE94-792684] p 2021 N95-25303
Baryon spectroscopy and the omega minus
[DE95-004838] p 2052 N95-25374
Radiative corrections for pion polarizability experiments
[DE95-607177] p 2053 N95-25462
A Green's function method for hadrons in nuclei
[DE94-792620] p 2070 N95-25772
Dependence of the multiplicities of secondary particles on the impact parameter in collisions of high-energy neon and iron nuclei with photoemulsion nuclei p 2059 N95-25919
Multiplicities of secondaries in nuclear interactions, induced by Ne-20, Ar-40 and Fe-56 nuclei at 0.1-0.5 GeV/nucleon p 2060 N95-25920
Fragmentation cross sections of O-16 between 0.9 and 200 GeV/nucleon p 2060 N95-25921

HIGH FREQUENCIES
ARMDAT: A brief description of a computerized test system for burst transmission
[PB95-165452] p 1951 N95-24241

HIGH POWER LASERS
Laser beam characterization results for a high power CW Nd:YAG laser
[DE95-006319] p 1971 N95-24408
Central Laser Facility. Annual report to the Laser Facility Committee
[PB95-160511] p 1973 N95-25640
Evolution of Spark plasma using nitrogen laser shadowgraphy system
[DE95-607598] p 2082 N95-25972

HIGH PRESSURE
The phenomenon of non-linearity accompanying the action of acoustic pressure on a Helmholtz resonator
[IFTR-19/1994] p 2040 N95-26108

HIGH RESOLUTION
Recipes for high resolution time-of-flight detectors
[DE95-006196] p 1967 N95-24596
Large-format high resolution microchannel plate detectors for ultraviolet astronomy
[NASA-CR-197993] p 2108 N95-25104
Circuit for high resolution decoding of multi-anode microchannel array detectors
[NASA-CASE-GSC-13478-1] p 1960 N95-25889

HIGH REYNOLDS NUMBER
Numerical and experimental study of drag characteristics of two-dimensional HLFC airfoils in high subsonic, high Reynolds number flow
[NAL-TR-1244T] p 1907 N95-24998

HIGH SPEED
Development of a high temperature, high speed disc lubricant test machine
[AD-A288685] p 1977 N95-26050

HIGH STRENGTH ALLOYS
Evaluation of a diffusion/trapping model for hydrogen ingress in high-strength alloys
[AD-A288447] p 1936 N95-25502

HIGH STRENGTH STEELS
Localized corrosion and stress corrosion cracking characteristics of a low-alurninum-content iron-aluminum alloy
[DE95-003259] p 1934 N95-24647
The effect of multidirectional cyclical deformation on the evolution of the plasticity surface of 18G2A steel
[IFTR-25/1994] p 1935 N95-25117
New techniques to test fatigue properties of coined sheet specimens. Part 2: Comparison of different materials, forming operations and life prediction techniques for a simple test geometry
[PB95-165122] p 1982 N95-25444
New techniques to test fatigue properties of coined sheet specimens. Part 4: Development of experimental techniques
[PB95-165130] p 1982 N95-25445

HIGH TEMPERATURE
Wear resistant composite structure of vitreous carbon containing convoluted fibers
[DE95-006255] p 1925 N95-24426
Neutron diffraction from HoNi2B2C, version 1
[DE95-005894] p 2085 N95-24431
Time dependent indentation testing at non-ambient temperatures utilizing the high temperature mechanical properties microprobe
[DE95-005895] p 1933 N95-24432
Solution based synthesis of perovskite-type oxide films and powders
[DE95-006170] p 2086 N95-24594
Study of very high temperature technology, 2
[DE95-730105] p 2088 N95-24900
Performance of solid lubricated ball bearings at high-temperatures in a vacuum
[NAL-TR-1243] p 1976 N95-25323
Statistical mechanics of the magnetized pair Bose gas
[DE95-607096] p 2063 N95-25993
Development of a high temperature, high speed disc lubricant test machine
[AD-A288685] p 1977 N95-26050

HIGH TEMPERATURE ENVIRONMENTS
Compensated high temperature strain gage
[NASA-CASE-LAR-14776-1] p 1968 N95-24625
Report series in aerosol science
[DE95-737628] p 1999 N95-24904
Aerodynamic characteristics of the orbital reentry vehicle experimental probe fins in a supersonic flow
[NAL-TR-1232] p 1921 N95-25664

HIGH TEMPERATURE GASES
High frequency flow-structural interaction in dense subsonic fluids
[NASA-CR-4652] p 1906 N95-24217

HIGH TEMPERATURE PLASMAS
Evidence for modified transport due to sheared E x B flows in high-temperature plasmas
[DE95-004870] p 2079 N95-25250
Maryland controlled fusion research program
[DE95-006642] p 2081 N95-25561

HIGH TEMPERATURE SUPERCONDUCTORS
Electron-phonon interaction in the Hubbard model
[DE94-634859] p 2092 N95-24277
Device-quality tunnel junctions on the high (T(sub c)) super conductor HgBa2CuO(4+delta)
[DE95-004646] p 2084 N95-24279

Electronic structure and pairing of strongly correlated fermions: Fermi liquid versus spin liquid
[DE95-005929] p 2044 N95-24419
Superconductivity Program for Electric Power Systems: 1994 Annual PEER Review. Volume 1, Meeting Proceedings
[DE95-005058] p 1956 N95-24452
Superconductivity Program for Electric Power Systems: 1994 Annual PEER Review. Volume 2, Meeting Proceedings
[DE95-005059] p 1957 N95-24453
Superconducting magnets, 1994
[DE95-003813] p 1958 N95-24551
Intrinsic magnetic torque at low magnetic induction
[DE95-601209] p 1959 N95-24842
BCS-like gap structure of HgBa2CuO(4 + delta) tunnel junctions
[DE95-004125] p 2087 N95-24855
Study of copper perovskite
[DE95-730106] p 2088 N95-24988
Formation of thallium based high temperature superconductors using aerosol flow reacted precursor powders
[DE95-005901] p 2089 N95-25389
Fe-57 and Sn-119 Moessbauer studies on La(1.25)Nd(0.6)Sr(0.15)CuO4: Evidence for local magnetic ordering below (approx. equal) 32 K
[DE95-601210] p 1959 N95-25405
Polarization and intensity of dd-transitions in superconducting copper oxides
[DE95-605886] p 2090 N95-25776
Condensate localization by mesoscale disorder in high-T(sub c) superconductors
[DE95-607819] p 1960 N95-26100
Coherent state path-integral representation of supersymmetric lattice models
[DE95-607820] p 2091 N95-26101

HIGH TEMPERATURE TESTS
Investigation of properties and performance of ceramic composite components
[DE95-004737] p 1939 N95-24247
Au/Cr sputter coating for the protection of alumina during sliding at high temperatures
[NASA-TM-106853] p 1923 N95-24437
Processing and characterization of transformation-toughened ceramics with strength retention to elevated temperatures
[DE95-005758] p 1941 N95-25387

HIGH VOLTAGES
Software of a distributor of high voltage of the H C-600 hadronic calorimeter
[DE94-628255] p 1967 N95-24486

HILBERT SPACE
Can we test the many-Hilbert-space approach to quantum mechanics?
[DE95-607021] p 2097 N95-25429
Describing the macroscopic world: Closing the circle within the dynamical reduction program
[DE95-606997] p 2100 N95-26046

HILBERT TRANSFORMATION
Techniques for the investigation of wave turbulence in water wave data
[AD-A288392] p 2007 N95-25605

HISTORIES
Space basic
[NASA-TM-110540] p 2108 N95-24196
Apollo 13: Houston, we've got a problem
[NASA-TM-110551] p 1918 N95-24215
Europe in space, 1960-1973
[ESA-SP-1172] p 2114 N95-24870
Reflections on Europe in space
[ESA-HSR-11] p 1916 N95-24872
The origins of the Federal Republic of Germany's space policy, 1959-1965: European and national dimensions
[ESA-HSR-12] p 1916 N95-24892
ESRO's telecommunications programme and the OTS project (1970-1974)
[ESA-HSR-13] p 1953 N95-24893
United States-European cooperation in space during the sixties
[ESA-HSR-14] p 2107 N95-24894
United States-European space cooperation in the post-Apollo programme
[ESA-HSR-15] p 2107 N95-24895
The scientific programme between ESRO and ESA: Choosing new projects (1973-1977)
[ESA-HSR-16] p 1917 N95-24896
Human radiation experiments: The Department of Energy roadmap to the story and the records
[DE95-006364] p 2012 N95-25371
Apollo 12: Pinpoint for science
[NASA-TM-110576] p 1917 N95-25424
Voyager: The grandest tour. The mission to the outer planets
[NASA-CR-197708] p 2112 N95-25854
The use of radioisotopes in human experiments: Comments in response to recent media articles
[DE95-605680] p 2012 N95-25981

HOHLRAUMS
Targets for laser-driven opacity measurements
[DE95-006172] p 1973 N95-25557

HOLOGRAPHY
Kinetics of diffusional droplet growth in a liquid/liquid two-phase system
[NASA-CR-198050] p 1961 N95-24221
Development of optical systems --- holographic technique for monitoring crystal growth
[NASA-CR-197702] p 2073 N95-24545
Holograpy machine HORN-1 for computer-aided retrieve of virtual three-dimensional image
[NIFS-218] p 1971 N95-26182
Continuous phase and amplitude holographic elements
[NASA-CASE-NPO-18791-1] p 1971 N95-26340

HOMING DEVICES
Missileborne Artificial Vision System (MAVIS)
p 2022 N95-25254

HOMOGENEITY
Solution based synthesis of perovskite-type oxide films and powders
[DE95-006170] p 2086 N95-24594
Homogeneous anisotropic cosmological models in the minimum quadratic Poincare gauge theory of gravity
[DE95-607083] p 2110 N95-25647

HOMOGENEOUS TURBULENCE
A review of Reynolds stress models for turbulent shear flows
[NASA-CR-195054] p 1962 N95-24580

HONEYCOMB STRUCTURES
Investigation into the flammability properties of honeycomb composites
[PB95-143293] p 1941 N95-25342
LH2 fuel tank design for SSTO p 1987 N95-26309

HORMONES
Human parathyroid hormone-(1-38) restores cancellous bone to the immobilized, osteopenic proximal tibial metaphysis in rats
[NASA-CR-197709] p 2011 N95-24556

HOT ATOMS
Proceedings of the International Seminar on the Chemistry of High Energy Atoms
[DE95-709895] p 2072 N95-26162

HOT CORROSION
Some aspects of the hot corrosion of thermal barrier coatings p 1946 N95-26137

HOT-WIRE ANEMOMETERS
Hot-wire calibration in subsonic/transonic flow regimes
[NASA-CR-197725] p 1970 N95-25699

HUBBLE CONSTANT
A quantum gravitational mechanism for exiting inflation
[DE95-003342] p 2096 N95-24867

HUMAN BEHAVIOR
On producing sequential movements and actions. An integrative review and an update of the generalized motor program
[AD-A288628] p 2014 N95-25610

HUMAN BEINGS
Prediction of humans in various environments using gas sensors and neural networks
[PB95-141560] p 2009 N95-24227
Human radiation experiments: The Department of Energy roadmap to the story and the records
[DE95-006364] p 2012 N95-25371
The use of radioisotopes in human experiments: Comments in response to recent media articles
[DE95-605680] p 2012 N95-25981

HUMAN BODY
Application of compartmental metabolic models for determination of retention and excretion functions
[DE95-600249] p 2010 N95-24367

HUMAN FACTORS ENGINEERING
A crew-centered flight deck design philosophy for High-Speed Civil Transport (HSCT) aircraft
[NASA-TM-109171] p 1910 N95-24582
Colour vision deficiencies: Matching and confusion of computer colours
[PB95-141925] p 2013 N95-24864
The dependence of human reliability upon task information content
[DE95-006645] p 2014 N95-25483
Aerospace medicine and biology: A continuing bibliography with indexes (supplement 401)
[NASA-SP-7011(401)] p 2012 N95-25800

HUMAN PERFORMANCE
Motionsickness-seasickness: Summary of existing knowledge and suggested lines of development
[PB95-141495] p 2011 N95-24863
The dependence of human reliability upon task information content
[DE95-006645] p 2014 N95-25483
On producing sequential movements and actions. An integrative review and an update of the generalized motor program
[AD-A288628] p 2014 N95-25610
Sleep patterns in air traffic controllers working rapidly rotating shifts: A field study
[DOT/FAA/AM-95/12] p 2012 N95-26204

HUMAN RESOURCES
Continual improvement plan
[NASA-TM-110574] p 2103 N95-25849

HUMAN-COMPUTER INTERFACE
Instructable autonomous agents
[NASA-CR-197802] p 2019 N95-26206

HYBRID COMPOSITES
Three-dimensional solutions for coupled thermoelectroelastic response of multilayered plates
p 1985 N95-26273
Assessment of computational models for thermoelectroelastic multilayered plates
p 1987 N95-26283

HYBRID PROPULSION
Solar thermal electric hybridization issues
[DE95-000217] p 1992 N95-24714

HYBRID STRUCTURES
Launch system design for access to space
p 1918 N95-26308

HYDRAULIC EQUIPMENT
Milli-robots for surgical teleoperation
[NASA-CR-197378] p 1974 N95-24204

HYDROCARBON COMBUSTION
User guide to the Burner Engineering Research Laboratory
[DE95-004191] p 1931 N95-25492

HYDROCARBON FUEL PRODUCTION
Yearbook 1993: Bioenergy Research Programme. Utilization of bioenergy and biomass conversion
[DE95-717518] p 1993 N95-24862

HYDROCARBON FUELS
Combustion characteristics of metallized hydrocarbon fuels
[NAL-TR-1224] p 1949 N95-25769

HYDROCARBONS
Responsibility means doing without: How to rescue the ozone-layer
[PB95-166807] p 1997 N95-24334
Continued computational evaluation of the feasibility of nitrating precursors to C12N12O12
[AD-A288369] p 1924 N95-25602
The evaluation of potential limonene scavengers
[DE95-006853] p 2002 N95-25899

HYDRODYNAMICS
Performance evaluation of LE-7 high pressure pumps
[NAL-TR-1212T] p 1977 N95-25672

HYDROELECTRICITY
Appendix model performance: Model documentation. Renewable Fuels Module of the National Energy Modelling System
[DE95-006080] p 1991 N95-24355

HYDROGEN
An investigation of the effect of surface impurities on the adsorption kinetics of hydrogen chemisorbed onto iron
[NASA-CR-197967] p 1933 N95-24400
Carbons and hydrogen by persistent metal radicals
[DE95-003834] p 1929 N95-24553
Elastic form factors of hydrogen-like atoms in nS-states
[DE94-628437] p 2048 N95-24700
Development of novel active transport membrane devices
[DE95-002658] p 1932 N95-26093

HYDROGEN ATOMS
A discrete variable representation for electron-hydrogen atom scattering
[DE95-003436] p 2045 N95-24512
Inelastic collisions of negative muons and hadrons with metastable hydrogen atoms
[DE95-607537] p 2056 N95-25668

HYDROGEN EMBRITTLEMENT
Evaluation of a diffusion/trapping model for hydrogen ingress in high-strength alloys
[AD-A288447] p 1936 N95-25502
Stability and elastic properties of hydrogen loaded Ti(1-x)Al(x) alloys: An ab initio study
[AD-A288903] p 1936 N95-25529

HYDROGEN ENGINES
Optimized hydrogen piston engines
[DE95-003656] p 1975 N95-24550

HYDROGEN FUELS
Test plan/procedure for the DPHV system integration
[DE95-003414] p 1994 N95-25121
Shock tunnel studies of scramjet phenomena 1993
[NASA-CR-195038] p 1964 N95-25394
LH2 fuel tank design for SSTO p 1987 N95-26309

HYDROGEN IONS
On the possibility of obtaining the polarized protons by the method of direct optic pumping of a fast atomic beam
[DE94-634309] p 2041 N95-24267
Design study of a negative-ion based NBI system for JT-60U
[DE94-785265] p 2043 N95-24339
Dynamics Explorer 1, retarding ion mass spectrometer summary spectrograms-82/110 to 82/229 spin-time spectrograms for H(+), He(+), O(+), N(+), O(++), M/Z = 2, and molecular ions
[NASA-TM-108485] p 2003 N95-24763
Dynamics Explorer 1, retarding ion mass spectrometer summary spectrograms-82/230 to 82/265 spin-time spectrograms for H(+), He(+), O(+), N(+), O(++), M/Z = 2, and molecular ions
[NASA-TM-108486] p 2003 N95-24764

HYDROGEN ISOTOPES
Mesic molecules of light nuclei in the oscillator representation
[DE94-628904] p 2050 N95-24890

HYDROGEN PLASMA
Isotope effect on confinement in DT plasmas
[NIFS-275] p 2083 N95-26326

HYDROGENATION
Study on the production of alternative fuels by carbon dioxide hydrogenation
[DE95-744284] p 1948 N95-24498

HYDROGEOLOGY
Identification of potential groundwater flow paths using geological and geophysical data
[DE95-006253] p 1988 N95-24407
Summaries of FY 1994 geosciences research
[DE95-005657] p 1988 N95-25440
Long-Term Flow Test number 1: Roosevelt Hot Springs, Utah
[DE95-004995] p 2004 N95-25666

HYDROGRAPHY
Use of voronoi diagrams for qualitative matching
[PB95-165445] p 1988 N95-24240
Real-time testing and demonstration of the US Army Corps of Engineers' Real-Time On-The-Fly positioning system
[AD-A288624] p 1910 N95-25609

HYDROLOGICAL CYCLE
Intercomparison of hydrologic processes in global climate models
[NASA-TM-104617] p 2005 N95-26341

HYDROLOGY
A numerical prediction of the precipitation and hydrology of California
[DE95-004966] p 2006 N95-25635
Spaceborne synthetic aperture radar: Current status and future directions. A report to the Committee on Earth Sciences, Space Studies Board, National Research Council
[NASA-TM-4679] p 1955 N95-25710

HYDROLOGY MODELS
Intercomparison of hydrologic processes in global climate models
[NASA-TM-104617] p 2005 N95-26341

HYDROTHERMAL SYSTEMS
Long-Term Flow Test number 1: Roosevelt Hot Springs, Utah
[DE95-004995] p 2004 N95-25666

HYDROXIDES
In situ XAFS study of oxides formed on nickel thin film electrodes in KOH solution
[AD-A288735] p 1932 N95-26056

HYDROXYL COMPOUNDS
Ion beam mixing of titanium overlayers with hydroxyapatite substrates
[DE95-005278] p 1935 N95-25379

HYGROSCOPICITY
Nucleation and growth of crystals under cirrus and polar stratospheric cloud conditions
[NASA-CR-197991] p 2085 N95-24478

HYPERBOLIC DIFFERENTIAL EQUATIONS
Nonexistence of global solutions to some quasilinear hyperbolic equations with dynamic boundary conditions
[DE95-607010] p 2033 N95-25645

HYPERGEOMETRIC FUNCTIONS
Asymptotics for the Kummer function of Bose plasmas
[DE95-607019] p 2096 N95-25428

HYPERNUCLEI
A Green's function method for hadrons in nuclei
[DE94-792620] p 2070 N95-25772

HYPERONS
The track system of the modernized Hyperon spectrometer
[DE95-604003] p 2058 N95-25905

HYPERSONIC FLOW
Verification of computational aerodynamic predictions for complex hypersonic vehicles using the INCA(trademark) code
[DE95-004757] p 1906 N95-24308
DSMC calculations for 70-deg blunted cone at 3.2 km/s in nitrogen
[NASA-TM-109181] p 1961 N95-24396

HYPERSONIC HEAT TRANSFER
Heat transfer measurements in small scale wind tunnels
[AD-A288689] p 1915 N95-26053

HYPERSONIC SPEED
Performance of an aerodynamic yaw controller mounted on the space shuttle orbiter body flap at Mach 10
[NASA-TM-109179] p 1906 N95-24397

HYPERSONIC VEHICLES
Verification of computational aerodynamic predictions for complex hypersonic vehicles using the INCA(trademark) code
[DE95-004757] p 1906 N95-24308
Reentry guidance for hypersonic Flight Experiment (HYFLEX) vehicle
[NAL-TR-1235] p 1910 N95-25764
Heat transfer measurements in small scale wind tunnels
[AD-A288689] p 1915 N95-26053

HYPOKINESIA
Human parathyroid hormone-(1-38) restores cancellous bone to the immobilized, osteopenic proximal tibial metaphysis in rats
[NASA-CR-197709] p 2011 N95-24556

HYPOTHESES
The Fitzgerald-Lorentz hypothesis from the viewpoint of relativity theory
[DE94-636735] p 2093 N95-24378
Temporal pacing in visual attention
[AD-A289785] p 2013 N95-26041

I

IBM PERSONAL COMPUTERS
The use of DBMS and document oriented interface in the TPLAN-system
[DE95-605219] p 2106 N95-25907

ICE
Assessment of climate variability of the Greenland ice sheet: Integration of in situ and satellite data
[NASA-CR-198020] p 1998 N95-24846

ICE CLOUDS
Nucleation and growth of crystals under cirrus and polar stratospheric cloud conditions
[NASA-CR-197991] p 2085 N95-24478

ICE ENVIRONMENTS
Spaceborne synthetic aperture radar: Current status and future directions. A report to the Committee on Earth Sciences, Space Studies Board, National Research Council
[NASA-TM-4679] p 1955 N95-25710

ICE FORMATION
Debris/ice/TPS assessment and integrated photographic analysis of shuttle mission STS-63
[NASA-TM-110649] p 1921 N95-25337

IDEAL GAS
Recent improvements to and validation of the one dimensional NASA wave rotor model
[NASA-TM-106913] p 1908 N95-25962

IDENTIFYING
Muon identifier efficiency of the GINES detecto r in the UNK neutrino beam
[DE94-628254] p 2045 N95-24485
The emission of particle identification efficiency in the EXCHARM experiment
[DE94-628258] p 2047 N95-24644

IGNITERS
The railplug: A new ignitor for internal combustion engines
[DE95-005487] p 1977 N95-26172

IGNITION
Ignition of exploding aluminum droplets behind shock waves in water
[DE95-003975] p 1963 N95-24678

IMAGE ANALYSIS
JPRS report: Science and technology. Central Eurasia
[JPRS-UST-95-013] p 1987 N95-24538
Low-cost image analysis system
[DE95-005021] p 2021 N95-25378
Inversion of circular averages and application of backprojection methods to radar imaging
[PB95-141578] p 1955 N95-25891
Heuristic anproach to the path planning problem in a raster map
[PB95-141826] p 2034 N95-25893
Aspect estimation of an aircraft using library model silhouettes
[PB95-141834] p 2036 N95-25894

IMAGE CONTRAST
Visual performance with Omnibus 3: A comparative evaluation of enhanced generation three image intensifier technology
[PB95-141891] p 2013 N95-24510
Implementation of scene shadows in the Target Acquisition TDA (TARGAC)
[AD-A288760] p 1912 N95-26060

IMAGE CORRELATORS
Relative orientation of multiple images using projective singular correlation
[PB95-149936] p 1967 N95-24259

IMAGE INTENSIFIERS
Visual performance with Omnibus 3: A comparative evaluation of enhanced generation three image intensifier technology
[PB95-141891] p 2013 N95-24510

IMAGE PROCESSING
Research in the service of the Swedish National Defence
[PB95-141941] p 1989 N95-24444
The Clementine Mission: Initial Results from lunar mapping
[NASA-TM-110555] p 2112 N95-24994
Document analysis with neural net circuits
p 2023 N95-25256
Photonics: From target recognition to lesion detection
p 2023 N95-25259
Low-cost image analysis system
[DE95-005021] p 2021 N95-25378
3-D seismic imaging of complex geologies
[DE95-006813] p 2004 N95-25476
Multi-spectral smart retina
[AD-A288950] p 2074 N95-25506
Proceedings of the 4th IEEE Workshop on Neural Networks for Signal Processing
[AD-A288383] p 2026 N95-25603
Multidimensional visualization and browsing for intelligence analysis
[DE95-004901] p 2106 N95-25774
Four-Dimensional Information Visualization and Analysis System
[DE95-004935] p 2022 N95-26013
Continuous phase and amplitude holographic elements
[NASA-CASE-NPO-18791-1] p 1971 N95-26340

IMAGE RECONSTRUCTION
Microscan simulation
[AD-A289139] p 2075 N95-26039
Holograpy machine HORN-1 for computer-aided retrieve of virtual three-dimensional image
[NIFS-218] p 1971 N95-26182

IMAGE RESOLUTION
Multi-spectral smart retina
[AD-A288950] p 2074 N95-25506
Microscan simulation
[AD-A289139] p 2075 N95-26039

IMAGES
Holograpy machine HORN-1 for computer-aided retrieve of virtual three-dimensional image
[NIFS-218] p 1971 N95-26182

IMAGING TECHNIQUES
Relative orientation of multiple images using projective singular correlation
[PB95-149936] p 1967 N95-24259
Read out electronics for thermal detectors of bolometer type
[PB95-141842] p 1967 N95-24280
Airborne imaging of tropospheric emission at millimeter and submillimeter wavelengths
[NASA-TM-110498] p 2003 N95-24336
Stereo imaging velocimetry for microgravity applications
[NASA-TM-110494] p 1949 N95-24416
Display technologies in Russia, Ukraine, and Belarus
[ISBN-1-883712-36-X] p 2085 N95-24460
Neural networks: Application to medical imaging
p 2025 N95-25267
Reciprocal space analysis of the microstructure of luminescent and nonluminescent porous silicon films
[DE95-005420] p 1941 N95-25382
3-D seismic imaging of complex geologies
[DE95-006813] p 2004 N95-25476
Multi-spectral smart retina
[AD-A288950] p 2074 N95-25506
Spray characteristics of single- and three-hole nozzle injectors in ambient air and in a motored single-cylinder test engine
[PB95-166286] p 1976 N95-25574
Inversion of circular averages and application of backprojection methods to radar imaging
[PB95-141578] p 1955 N95-25891

Continuous phase and amplitude holographic elements
[NASA-CASE-NPO-18791-1] p 1971 N95-26340
IMMOBILIZATION
Human parathyroid hormone-(1-38) restores cancellous bone to the immobilized, osteopenic proximal tibial metaphysis in rats
[NASA-CR-197709] p 2011 N95-24556
IMPACT
Dependence of the multiplicities of secondary particles on the impact parameter in collisions of high-energy neon and iron nuclei with photoemulsion nuclei p 2059 N95-25919
IMPACT LOADS
Analysis of warping effects on the static and dynamic response of a seat-type structure
[NIAR-94-12] p 1979 N95-24211
Significance of varied thickness to damage tolerance of carbon fiber/epoxy laminates
[PB95-165460] p 1925 N95-24242
Response to a localized impact loading of a composite multilayered rotational shell structure: Theory and numerical methods, volume 1
[ONERA-NT-1994-10-VOL-1] p 1979 N95-24282
Response to a localized impact loading of a composite multilayered rotational shell structure: Theory and numerical methods, volume 2
[ONERA-NT-1994-10-VOL-2] p 1980 N95-24283
Response to a localized impact loading of a composite multilayered rotational shell structure: Theory and numerical methods, Volume 3
[ONERA-NT-1994-10-VOL-3] p 1980 N95-24284
IMPACT RESISTANCE
Effects of through-the-thickness stitching on impact and interlaminar fracture properties of textile graphite/epoxy laminates
[NASA-CR-195042] p 1928 N95-26203
Design and evaluation of a foam-filled hat-stiffened panel concept for aircraft primary structural applications
[NASA-TM-109175] p 1928 N95-26251
IMPACT STRENGTH
Effects of through-the-thickness stitching on impact and interlaminar fracture properties of textile graphite/epoxy laminates
[NASA-CR-195042] p 1928 N95-26203
IMPLOSIONS
Pulsed power drivers for ICF and high energy density physics
[DE95-003361] p 2066 N95-24500
Hydrodynamic instabilities in inertial confinement fusion
[DE95-003663] p 2078 N95-24667
Magnetized target fusion: An ultra high energy approach in an unexplored parameter space
[DE95-005252] p 2080 N95-25289
IMPULSES
Thrust measurements of a complete axisymmetric scramjet in an impulse facility p 1914 N95-25395
The off-shell axial anomaly via the (gamma)*(pi)(sup 0) (yields) (gamma) transition
[DE95-004762] p 2057 N95-25896
IMPURITIES
Current-voltage characteristics of a tunnel junction with resonant centers
[DE94-634530] p 1956 N95-24245
Determination of trace elements in plutonium by solvent extraction and ICP-atomic emission spectrometry
[DE94-634887] p 2042 N95-24269
An investigation of the effect of surface impurities on the adsorption kinetics of hydrogen chemisorbed onto iron
[NASA-CR-197967] p 1933 N95-24400
Photoionization of shallow donor impurities in finite-barrier quantum wells
[DE95-607521] p 2097 N95-25468
IN-FLIGHT MONITORING
An overview of Health and Usage Monitoring Systems (HUMS) for military helicopters
[DSTO-TR-0061] p 1905 N95-24200
INCOMPRESSIBLE FLOW
A review of Reynolds stress models for turbulent shear flows
[NASA-CR-195054] p 1962 N95-24580
INCONEL (TRADEMARK)
Robotic weld overlay coatings for erosion control
[DE95-005187] p 1939 N95-24285
INDENTATION
Time dependent indentation testing at non-ambient temperatures utilizing the high temperature mechanical properties microprobe
[DE95-005895] p 1933 N95-24432
INDEPENDENT VARIABLES
Exact solution of 2 D Poincare gravity coupled with fermion matter
[DE95-605314] p 2099 N95-25967
Numerical solution of the optimized random phase approximation
[DE95-605636] p 2034 N95-25982
INDEXES
Aerospace medicine and biology: A continuing bibliography with indexes (supplement 401)
[NASA-SP-7011(401)] p 2012 N95-25800
Index of nuclear data libraries available from the IAEA Nuclear Data Section
[DE95-605213] p 2107 N95-25980
INDEXES (DOCUMENTATION)
Aeronautical engineering: A continuing bibliography with indexes (supplement 316)
[NASA-SP-7037(316)] p 1905 N95-24465
Machine-aided indexing at NASA
[NASA-CR-197796] p 2106 N95-25410
Aeronautical engineering: A continuing bibliography with indexes (supplement 317)
[NASA-SP-7037(317)] p 1906 N95-25798
INDEXES (RATIOS)
Geomagnetic Polar Cap (PC) index, 1975-1993
[UAG-103] p 2004 N95-24897
INDIA
Carbon taxes and India
[DE95-005401] p 2001 N95-25629
INDIUM
Time dependent indentation testing at non-ambient temperatures utilizing the high temperature mechanical properties microprobe
[DE95-005895] p 1933 N95-24432
INDIUM GALLIUM ARSENIDES
GaAsSb-based heterojunction tunnel diodes for tandem solar cell interconnects
[DE95-004779] p 1990 N95-24264
Optical determinations of energy-band dispersion curves in novel compound semiconductor materials
[DE95-006318] p 2089 N95-25353
INDOOR AIR POLLUTION
Resolving the ambiguities: An industrial hygiene Indoor Air Quality (IAQ) symposium
[DE95-005391] p 2000 N95-25380
INDUSTRIAL ENERGY
Sector-specific issues and reporting methodologies supporting the General Guidelines for the voluntary reporting of greenhouse gases under Section 1605(b) of the Energy Policy Act of 1992, volume 1. Part 1: Electricity supply sector. Part 2: Residential and commercial buildings sector. Part 3: Industrial sector
[DE95-003296] p 2000 N95-25362
INDUSTRIAL PLANTS
SPEEDUP simulation of liquid waste batch processing, revision 1
[DE95-001240] p 1939 N95-24344
Tau physics at future facilities
[DE95-006071] p 2046 N95-24591
INDUSTRIAL SAFETY
Resolving the ambiguities: An industrial hygiene Indoor Air Quality (IAQ) symposium
[DE95-005391] p 2000 N95-25380
National standard and code compliance for electrical equipment installed in hazardous locations for the void fraction instrument
[DE95-002158] p 1960 N95-26092
INDUSTRIAL WASTES
Supercritical carbon dioxide cleaning market assessment and commercialization/deployment plan
[DE94-017394] p 1998 N95-24653
Waste minimization assessment for a manufacturer of parts for truck engines
[PB95-144481] p 1911 N95-26062
INDUSTRIES
Commercial Space Transportation Study (CSTS)
[SSD94D0035] p 1919 N95-25747
INELASTIC COLLISIONS
Core-collapse supernovae and nucleosynthesis
[NASA-CR-197731] p 2109 N95-25122
Inelastic collisions of negative muons and hadrons with Helium metastable atoms
[DE95-607538] p 2055 N95-25493
Inelastic collisions of negative muons and hadrons with metastable hydrogen atoms
[DE95-607537] p 2056 N95-25668
Multiplicities of secondaries in interactions of 1.8 GeV/nucleon Fe-56 nuclei with photoemulsion and the cascade evaporation model p 2059 N95-25917
INELASTIC SCATTERING
Deficiency of the Gross-Llewellyn Smith sum rule and QCD vacuum polarization effect
[DE94-636790] p 2042 N95-24315
Structure of liquid He-4 excitations spectrum
[DE94-637113] p 2043 N95-24364
Present experimental data on cross channel deep-inelastic processes and the Gribov-Lipatov relation
[DE94-628605] p 2049 N95-24719
HET mini-manual
[PB95-165338] p 2057 N95-25900
INERTIAL CONFINEMENT FUSION
Pulsed power drivers for ICF and high energy density physics
[DE95-003361] p 2066 N95-24500
Target injection methods for inertial fusion energy
[DE95-003654] p 2067 N95-24651
Hydrodynamic instabilities in inertial confinement fusion
[DE95-003663] p 2078 N95-24667
Elise: The next step in development of induction heavy ion drivers for inertial fusion energy
[DE95-004679] p 2069 N95-25358
Targets for laser-driven opacity measurements
[DE95-006172] p 1973 N95-25557
Central Laser Facility. Annual report to the Laser Facility Committee
[PB95-160511] p 1973 N95-25640
INFERENCE
Performance tests of air source heat pumps under frosting conditions. Quality of results
[PB95-141792] p 1995 N95-25892
INFINITE SPAN WINGS
Three-dimensional interaction of wake/boundary-layer and vortex/boundary-layer data report
[CUED/A-AEREO/TR-23] p 1906 N95-24210
INFLATABLE STRUCTURES
Inflatable rescue device
[NASA-CASE-MSC-22244-1] p 2014 N95-25306
INFLATING
A quantum gravitational mechanism for exiting inflation
[DE95-003342] p 2096 N95-24867
INFORMATION
Measuring the strategic value of information technology investments
[DE94-018160] p 2104 N95-24603
INFORMATION DISSEMINATION
National Renewable Energy Laboratory Information Resources Catalogue. A collection of energy efficiency and renewable energy information resources
[DE94-011900] p 1990 N95-24305
CD-ROM in the age of internet
[DE95-005067] p 2104 N95-24454
Human radiation experiments: The Department of Energy roadmap to the story and the records
[DE95-006364] p 2012 N95-25371
Index of nuclear data libraries available from the IAEA Nuclear Data Section
[DE95-605213] p 2107 N95-25980
INFORMATION MANAGEMENT
National Renewable Energy Laboratory Information Resources Catalogue. A collection of energy efficiency and renewable energy information resources
[DE94-011900] p 1990 N95-24305
Raising the IQ in full-text searching via intelligent querying
[DE95-002981] p 2103 N95-24330
Final report and recommendations of the ESnet Authentication Pilot Project
[DE95-005755] p 2103 N95-24370
CD-ROM in the age of internet
[DE95-005067] p 2104 N95-24454
Integrated resource management database for a distributed information system
[DE95-730180] p 2104 N95-24492
Current experiments in elementary particle physics. Revision
[DE95-003797] p 2067 N95-24652
Activity Management System user reference manual
[DE95-000989] p 2105 N95-24654
Information management architecture for an integrated computing environment for the Environmental Restoration Program. Environmental Restoration Program, Volume 3: Interim technical architecture
[DE95-001386] p 2105 N95-24656
Geographical information systems and other tools for spatial information management
[PB95-165759] p 2106 N95-25572
Applications for electronic documents
[DE95-005036] p 2106 N95-25765
Multidimensional visualization and browsing for intelligence analysis
[DE95-004901] p 2106 N95-25774
INFORMATION RETRIEVAL
Raising the IQ in full-text searching via intelligent querying
[DE95-002981] p 2103 N95-24330
Current experiments in elementary particle physics. Revision
[DE95-003797] p 2067 N95-24652
Activity Management System user reference manual
[DE95-000989] p 2105 N95-24654
The energy intelligence information system
[DE95-002184] p 2105 N95-24675

A report: A plan to establish Internet access points at Minority Campus sites for connection to a central computing facility
[DE95-004374] p 2105 N95-25240
Multidimensional visualization and browsing for intelligence analysis
[DE95-004901] p 2106 N95-25774
Online nuclear data service
[DE95-602487] p 2107 N95-25941

INFORMATION SYSTEMS
Raising the IQ in full-text searching via intelligent querying
[DE95-002981] p 2103 N95-24330
Final report and recommendations of the ESnet Authentication Pilot Project
[DE95-005755] p 2103 N95-24370
NLS Flight Simulation Laboratory (FSL) documentation
[NASA-CR-196564] p 2104 N95-24439
Integrated resource management database for a distributed information system
[DE95-730180] p 2104 N95-24492
Downsizing systems and expected opposition to introduction
[DE95-730186] p 2104 N95-24494
Measuring the strategic value of information technology investments
[DE94-018160] p 2104 N95-24603
Information management architecture for an integrated computing environment for the Environmental Restoration Program. Environmental Restoration Program, Volume 3: Interim technical architecture
[DE95-001386] p 2105 N95-24656
The energy intelligence information system
[DE95-002184] p 2105 N95-24675
Integration of heterogeneous data bases for development of a large-scale environmental data atlas for multi-platform PC and workstation users
[DE95-002689] p 2000 N95-25278
Hardcopy extraction considerations for Vector Product Format (VPF) products
[AD-A288620] p 2106 N95-25608
Applications for electronic documents
[DE95-005036] p 2106 N95-25765
Index of nuclear data libraries available from the IAEA Nuclear Data Section
[DE95-605213] p 2107 N95-25980
Directory of Defence and Aerospace Information Centers
[AGARD-R-802] p 2107 N95-26334

INFRARED ABSORPTION
Simple chemical assays for presence of S2F10 in decomposed SF6
[DE95-001423] p 1929 N95-24345
Tunable diode lasers as continuous emission monitors for thermal waste treatment processes
[DE95-004381] p 1972 N95-25549
Dynamic Jahn-Teller-induced infrared absorption of a charged C60(-) molecule
[DE95-607577] p 2063 N95-25971

INFRARED DETECTORS
Read out electronics for thermal detectors of bolometer type
[PB95-141842] p 1967 N95-24280
Automatic measurement system for measuring of the nonlinearity of photo detectors
[PB95-165197] p 2074 N95-25999
Microscan simulation
[AD-A289139] p 2075 N95-26039
Infrared multispectral sensor program, Phase 2. Field measurements, analysis and modeling. Volume 1: Fourier transform spectrometer sensor characterization
[AD-A288888] p 2075 N95-26173

INFRARED IMAGERY
Microscan simulation
[AD-A289139] p 2075 N95-26039

INFRARED RADIATION
Multispectral detection of ground targets in highly correlated backgrounds
[AD-A289292] p 1990 N95-26040

INFRARED SPECTRA
Implementation of scene shadows in the Target Acquisition TDA (TARGAC)
[AD-A288760] p 1912 N95-26060

INFRARED SPECTROMETERS
Infrared multispectral sensor program, Phase 2. Field measurements, analysis and modeling. Volume 1: Fourier transform spectrometer sensor characterization
[AD-A288888] p 2075 N95-26173

INFRARED SPECTROSCOPY
Infrared spectroscopy of Jupiter and Saturn
[NASA-CR-198034] p 2111 N95-24239
FT-IR microscopical analysis with synchrotron radiation: The microscope optics and system performance
[DE95-004834] p 1928 N95-24265

INGESTION (ENGINES)
Bird ingestion into large turbofan engines
[DOT/FAA/CT-93/14] p 1909 N95-24631

INGOTS
The facility for commercial doping of silicon by thermal neutrons in channel 3 at the IBR-2
[DE94-636293] p 2085 N95-24374
Stainless steel recycle
[DE95-003905] p 1934 N95-24615

INHIBITORS
Staurosporine analysis and its pharmacokinetics in the blood of rats
[DE94-013857] p 2008 N95-24600
Genetic and biophysical studies of the photosynthetic reaction center
[DE95-004179] p 2008 N95-24850

INJECTION GUIDANCE
Optimal guidance law development for an advanced launch system
[NASA-CR-4667] p 1917 N95-26205

INJECTORS
Development test of a liquid apogee engine for the ETS-4
[NAL-TR-1250] p 1922 N95-24999
Spray characteristics of single- and three-hole nozzle injectors in ambient air and in a motored single-cylinder test engine
[PB95-166286] p 1976 N95-25574

INLET FLOW
Study of compressible flow through a rectangular-to-semiannular transition duct
[NASA-CR-4660] p 1914 N95-24392
Solutions of turbulent backward-facing step flow with heat transfer using the finite volume method
[DE95-003360] p 1962 N95-24489

INLET NOZZLES
Study of compressible flow through a rectangular-to-semiannular transition duct
[NASA-CR-4660] p 1914 N95-24392

INPUT/OUTPUT ROUTINES
DOLIB: Distributed Object Library
[DE95-004791] p 2019 N95-24250

INSPECTION
Estimate of probability of crack detection from service difficulty report data
[PB95-149381] p 1905 N95-24295
Debris/ice/TPS assessment and integrated photographic analysis of shuttle mission STS-63
[NASA-TM-110649] p 1921 N95-25337
Background information to reliability stress screening of components: A guide for component users. Nordtest project 1140-93
[PB95-165775] p 1978 N95-26002
An overview of NDE methods for thick composites and a proposal for analysis of computed technology data
[AD-A288733] p 1979 N95-26055

INSTALLING
National standard and code compliance for electrical equipment installed in hazardous locations for the void fraction instrument
[DE95-002158] p 1960 N95-26092

INSTRUMENT COMPENSATION
Compensated high temperature strain gage
[NASA-CASE-LAR-14776-1] p 1968 N95-24625

INSTRUMENT ERRORS
Suspension system for gimbal supported scanning payloads
[NASA-CASE-MFS-28817-1] p 1969 N95-25544

INSTRUMENT PACKAGES
Field-usable portable analyzer for chlorinated organic compounds
[DE95-003127] p 1930 N95-25098

INSULATORS
US technical report for the ITER blanket/shield
[DE95-004667] p 2079 N95-25283
Superconductivity, magnetism and metal-insulator transitions in some ternary and pseudoternary 3d-, 4d- and 5d-metal oxides
[DE95-005904] p 2038 N95-25600
Conductivity in insulators due to implantation of conducting species
[DE95-607773] p 1932 N95-26261

INTEGRAL EQUATIONS
SYSINT(SYSINTM)-program complex for numerical solution of the eigenvalue problem for system of integral equations
[DE94-636729] p 2029 N95-24375
Saddle-point method in path integrals
[DE94-628379] p 2036 N95-24688

INTEGRATED CIRCUITS
The potential of vacuum microelectronics for space reactor applications
[DE95-000542] p 1958 N95-24586
Using consumer IC packages in harsh high reliability applications
[DE94-016565] p 1959 N95-24713
Optically-switched submillimeter-wave oscillator and radiator having a switch-to-switch propagation delay
[NASA-CASE-NPO-18547-1-CU] p 1959 N95-25307
Multi-spectral smart retina
[AD-A288950] p 2074 N95-25506
Atomic force microscopy as a process characterization tool for GaAs-based integrated circuit fabrication
[DE95-006223] p 2064 N95-26168

INTEGRATED LIBRARY SYSTEMS
Information management architecture for an integrated computing environment for the Environmental Restoration Program. Environmental Restoration Program, Volume 3: Interim technical architecture
[DE95-001386] p 2105 N95-24656

INTERACTIONAL AERODYNAMICS
Three-dimensional interaction of wake/boundary-layer and vortex/boundary-layer data report
[CUED/A-AEREO/TR-23] p 1906 N95-24210
Spectrum and energy transfer in steady Burgers turbulence
[NASA-CR-195047] p 1963 N95-24584
A study of three-dimensional interaction flow fields between swept shock waves and turbulent boundary layers. Flow structures and effects of bleed
[NAL-TR-1227] p 1963 N95-25001
Numerical calculations of shock-wave/boundary-layer flow interactions
[NASA-TM-106694] p 1966 N95-26077

INTERACTIVE CONTROL
Gamma spectrum analysis including NAA with SAMPO for windows
[PB95-149720] p 2042 N95-24298
Instructable autonomous agents
[NASA-CR-197802] p 2019 N95-26206

INTERATOMIC FORCES
Atomistic studies of grain boundaries in NiAl
[DE95-005208] p 1937 N95-26014

INTERCALATION
The effect of O2 intercalation on the rotational Dynamics and the ordering transition of C60
[DE95-004765] p 2090 N95-25897

INTERDIGITAL TRANSDUCERS
Type P dispersive delay lines p 1959 N95-25116

INTERFACES
Ion beam mixing of titanium overlayers with hydroxyapaptite substrates
[DE95-005278] p 1935 N95-25379

INTERFEROMETERS
Engineering and design of a CO2 phase contrast interferometer system for DIII-D
[DE95-004249] p 1972 N95-24709
Liquid crystal point diffraction interferometer
[NASA-TM-106899] p 1970 N95-26073

INTERFEROMETRY
Emerging nondestructive inspection for aging aircraft
[PB95-143053] p 1905 N95-25401
Can we test the many Hilbert-space approach to quantum mechanics?
[DE95-607021] p 2097 N95-25429
Observation of the scalar Aharonov-Bohm effect by neutron interferometry
[DE95-607020] p 2097 N95-25446
Liquid crystal point diffraction interferometer
[NASA-TM-106899] p 1970 N95-26073

INTERGALACTIC MEDIA
Far-infrared and submillimeter spectroscopy of photodissociation regions
[DE95-607520] p 2110 N95-25467

INTERMETALLICS
Synthesis of Ni3Al and NiAl intermetallics
[DE95-005897] p 1934 N95-24433
Theoretical and experimental studies on the C15 intermetallic compound NbCr2
[DE95-003665] p 2086 N95-24513
Coercive field and domain wall properties in (Dy(x)Y(1-x))Fe2 and (Er(x)Y(1-x))Fe2
[DE95-601135] p 1937 N95-25751
Atomistic studies of grain boundaries in NiAl
[DE95-005208] p 1937 N95-26014

INTERMOLECULAR FORCES
Continued computational evaluation of the feasibility of nitrating precursors to C12N12O12
[AD-A288369] p 1924 N95-25602

INTERNAL COMBUSTION ENGINES
Investigation of a rotary valving system with variable valve timing for internal combustion engines
[DE95-003831] p 1976 N95-25101
The railplug: A new ignitor for internal combustion engines
[DE95-005487] p 1977 N95-26172

INTERNAL FLOW
High frequency flow-structural interaction in dense subsonic fluids
[NASA-CR-4652] p 1906 N95-24217

Advanced multi-phase flow CFD model development for solid rocket motor flowfield analysis
[NASA-CR-198044] p 1923 N95-25103

INTERNATIONAL COOPERATION
JPRS report: Science and technology. Central Eurasia: Space
[JPRS-USP-94-008] p 1916 N95-24359
Europe in space, 1960-1973
[ESA-SP-1172] p 2114 N95-24870
The history of ELDO. Part 1: 1961-1964
[ESA-HSR-10-PT-1] p 2114 .N95-24871
United States-European cooperation in space during the sixties
[ESA-HSR-14] p 2107 N95-24894
United States-European space cooperation in the post-Apollo programme
[ESA-HSR-15] p 2107 N95-24895
The scientific programme between ESRO and ESA: Choosing new projects (1973-1977)
[ESA-HSR-16] p 1917 N95-24896
Activities of the National Institute of Radiological Sciences
[DE95-709916] p 2072 N95-26165

INTERNATIONAL SPACE STATION
Evaluation of restraint system concepts for the Japanese Experiment Module flight demonstration
[NASA-TM-104808] p 2013 N95-24627

INTERNETS
CD-ROM in the age of internet
[DE95-005067] p 2104 N95-24454
Survey of methods for secure connection to the internet
[DE95-730185] p 1952 N95-24493
A tool for debugging internet multicast routing
[DE95-003433] p 2020 N95-24496
A report: A plan to establish Internet access points at Minority Campus sites for connection to a central computing facility
[DE95-004374] p 2105 N95-25240

INTERPLANETARY DUST
Transmission electron microscope studies of extraterrestrial materials
[NASA-CR-188363] p 1928 N95-24222

INTERPLANETARY MAGNETIC FIELDS
Geomagnetic Polar Cap (PC) index, 1975-1993
[UAG-103] p 2004 N95-24897

INTERPOLATION
Control theory and splines, applied to signature storage p 2027 N95-25804

INTERPROCESSOR COMMUNICATION
Downsizing systems and expected opposition to introduction
[DE95-730186] p 2104 N95-24494

INTERSTITIALS
The effect of O2 intercalation on the rotational Dynamics and the ordering transition of C60
[DE95-004765] p 2090 N95-25897

INTRACRANIAL PRESSURE
Non-invasive detection of increased intracranial pressure using acoustical techniques
[AD-A279292] p 2010 N95-24309

INVARIANCE
Moving scales contraction contradicts interval invariance
[DE94-636736] p 2092 N95-24347
The left-right forward-backward asymmetry of heavy quarks measured with jet charge and with leptons at the SLD
[DE95-006145] p 2046 N95-24593
Adaptive projective filters
[DE94-628374] p 2030 N95-24645
New physics effects on CP Violation in B decays
[DE94-628617] p 2049 N95-24722
Meson properties at finite temperature and density within Nambu-Jona-Lasinio model
[DE94-628630] p 2049 N95-24888
Tests for leptonic CP violation in tau decays
[DE95-005927] p 2050 N95-24902
Tau as a probe for new physics
[DE95-005928] p 2051 N95-25296
HyperKaehler metrics building and integrable models
[DE95-607077] p 2038 N95-25524
Strong phase correlations of solitons of nonlinear Schroedinger equation
[DE95-607002] p 2063 N95-25991
Results/prospects in E777/851/865
[DE95-005959] p 2064 N95-26006

INVENTIONS
Differential preamplifier and pre-emphasis network
[AD-A288780] p 1961 N95-26186

INVERSE KINEMATICS
Study of properties of Ne - Al neutron rich isotopes at and near N = 20 magic shell using elastic scattering in inverse kinematics
[DE94-628655] p 2055 N95-25538

INVERSE SCATTERING
Inversion of circular averages and application of backprojection methods to radar imaging
[PB95-141578] p 1955 N95-25891

INVERSIONS
On the structure of direct representations of inverse matrices to the block-tridiagonal ones in case of zero main block angular minors
[DE94-628376] p 2031 N95-24859
Inversion of circular averages and application of backprojection methods to radar imaging
[PB95-141578] p 1955 N95-25891

INVESTMENT CASTING
AMCC casting development, volume 2
[NASA-CR-197720] p 1938 N95-26068

INVISCID FLOW
Multigrid solution strategies for adaptive meshing problems
[NASA-CR-195049] p 2031 N95-24857

ION ACCELERATORS
Conference on physics from large gamma-ray detec tor arrays. Volume 2: Proceedings
[DE95-006900] p 2070 N95-25478
Annual report of National Institute of Radiological Sciences
[DE94-792664] p 2009 N95-25902

ION BEAMS
On the possibility of obtaining the polarized protons by the method of direct optic pumping of a fast atomic beam
[DE94-634309] p 2041 N95-24267
Characterization and performance of carbon films deposited by plasma and ion beam based techniques
[DE95-005213] p 1940 N95-24456
Activities of the Solid State Division
[DE95-003900] p 2087 N95-24611
Crystalline beams: Theory, experiments, and proposals
[DE95-003955] p 2068 N95-24685
Ion beam mixing of titanium overlayers with hydroxyapaptite substrates
[DE95-005278] p 1935 N95-25379
Measurement of profiles of the space potential in JIPP T-IIU Tokamak plasmas by slow poloidal and fast toroidal sweeps of a heavy ion beam
[NIFS-273] p 2081 N95-25651
HZE beam transport in multilayered materials p 2060 N95-25922
A possibility of pi(-) Meson production by a low energy electron bunch and positive ion bunch
[NIFS-277] p 2071 N95-26029

ION EXCHANGE MEMBRANE ELECTROLYTES
Cross-flow, filter-sorbent-catalyst for particulate, SO2 and NO(x) control
[DE95-001934] p 2003 N95-26091

ION IMPLANTATION
One-step in-diffusion as a result of multipulse laser irradiation of LiNbO3 single-crystalline substrates covered with thin Ti deposits on the effect of the radiation wavelength
[DE94-634524] p 2084 N95-24324
High-energy ionoluminescence of LiF
[DE94-629015] p 2087 N95-24891
Oxidation of ion-implanted NiAl
[DE95-005899] p 1935 N95-25388
Wear-resistant, self-lubricating surfaces of diamond coatings
[NASA-TM-106887] p 1924 N95-25961
Raman study of damage processes in Si(+)-implanted GaAs
[DE95-005898] p 2091 N95-26087
Activities of the Radiation Laboratory Department of Nuclear Engineering Kyoto University
[DE95-709896] p 2072 N95-26163
Activities of the Radiation Laboratory Department of Nuclear Engineering Faculty of Engineering, Kyoto University
[DE95-709897] p 2072 N95-26164
Conductivity in insulators due to implantation of conducting species
[DE95-607773] p 1932 N95-26261

ION IRRADIATION
Temperature and strain-rate effects on deformation mechanisms in irradiated stainless steel
[DE95-004941] p 1934 N95-24449
Summaries of reports of the Electrotechnical Laboratory, no. 48
[JTN-95-80825] p 2114 N95-24908
Ion beam mixing of titanium overlayers with hydroxyapaptite substrates
[DE95-005278] p 1935 N95-25379

ION MICROSCOPES
Atom probe field ion microscopy of Type 308 CRE stainless steel welds
[DE94-019161] p 1938 N95-26064

ION PROBES
An ion sensitive probe and its application to a mirror device
[DE95-602307] p 1970 N95-25940

ION TEMPERATURE
An ion sensitive probe and its application to a mirror device
[DE95-602307] p 1970 N95-25940
Operating level of HT-6B tokamak device
[DE95-602999] p 2082 N95-25943

IONIZATION
The cooling of particle beams
[DE95-004669] p 2065 N95-24320
Continued computational evaluation of the feasibility of nitrating precursors to C12N12O12
[AD-A288369] p 1924 N95-25602
Multiplicities of secondaries in interactions of 1.8 GeV/nucleon Fe-56 nuclei with photoemulsion and the cascade evaporation model p 2059 N95-25917

IONIZATION CROSS SECTIONS
The interactions of high-energy, highly charged Xe ions with buckyballs
[DE95-004597] p 2069 N95-25281

IONIZATION GAGES
The development of a positron ionization gauge
[DE95-005958] p 1968 N95-24623

IONIZATION POTENTIALS
Ionization potential data library of atoms and ions
[DE94-628380] p 2048 N95-24689

IONIZED GASES
Measurement of profiles of the space potential in JIPP T-IIU Tokamak plasmas by slow poloidal and fast toroidal sweeps of a heavy ion beam
[NIFS-273] p 2081 N95-25651
Aerodynamic characteristics of the orbital reentry vehicle experimental probe fins in a supersonic flow
[NAL-TR-1232] p 1921 N95-25664

IONIZING RADIATION
Dosimetry on STS-42 with the RME APD p 2059 N95-25916

IONS
Ionization potential data library of atoms and ions
[DE94-628380] p 2048 N95-24689
High-energy ionoluminescence of LiF
[DE94-629015] p 2087 N95-24891
Experimental constraints on transport
[DE95-004962] p 2050 N95-25180
Molecular dynamics calculation of shear viscosity for molten salt
[DE95-703970] p 2055 N95-25496
Measurement of kinetic energy of ions collected from laser resonance photoionized plasma by time-of-flight method
[DE95-709767] p 2081 N95-25498

IRIDIUM ALLOYS
A study of the electrochemical behavior of tungsten in caustic solutions and platinum/iridium in ch loride solutions
[DE95-004951] p 1930 N95-25123
Processing and properties of iridium alloys for space power applications
[DE95-005902] p 1935 N95-25390

IRON
An investigation of the effect of surface impurities on the adsorption kinetics of hydrogen chemisorbed onto iron
[NASA-CR-197967] p 1933 N95-24400
Synthesis and characterization of Fe colloid catalysts in inverse micelle solutions
[DE95-006313] p 1929 N95-24614

IRON ALLOYS
Robotic weld overlay coatings for erosion control
[DE95-005187] p 1939 N95-24285
Localized corrosion and stress corrosion cracking characteristics of a low-aluminum-content iron-aluminum alloy
[DE95-003259] p 1934 N95-24647
Mossbauer spectroscopy, x ray diffraction and magnetic measurements of iron-nickel ultrafine particles
[DE95-601136] p 1930 N95-24840
NASA-UVa light aerospace alloy and structures technology program supplement: Aluminum-based materials for high speed aircraft
[NASA-CR-4645] p 1935 N95-24878
Evaluation of a diffusion/trapping model for hydrogen ingress in high-strength alloys
[AD-A288447] p 1936 N95-25502
JPRS report: Science and technology. Central Eurasia
[JPRS-UST-95-018] p 2071 N95-26079

IRON COMPOUNDS
Synthesis and characterization of Fe colloid catalysts in inverse micelle solutions
[DE95-006313] p 1929 N95-24614
Coercive field and domain wall properties in (Dy(x)Y(1-x))Fe2 and (Er(x)Y(1-x))Fe2
[DE95-601135] p 1937 N95-25751

IRON ISOTOPES
Multiplicities of secondaries in interactions of 1.8 GeV/nucleon Fe-56 nuclei with photoemulsion and the cascade evaporation model p 2059 N95-25917
Target fragments in collisions of 1.8 GeV/nucleon Fe-56 nuclei with photoemulsion nuclei, and the cascade-evaporation model p 2059 N95-25918
Multiplicities of secondaries in nuclear interactions, induced by Ne-20, Ar-40 and Fe-56 nuclei at 0.1-0.5 GeV/nucleon p 2060 N95-25920
IRON OXIDES
Processing and electrochemical properties of mixed conducting La(1-x)A(x)Co(1-y)Fe(y)O(3-delta) (A=Sr, Ca) [DE95-004910] p 2088 N95-25002
IRON 57
Fe-57 and Sn-119 Moessbauer studies on La(1.25)Nd(0.6)Sr(0.15)CuO4: Evidence for local magnetic ordering below (approx. equal) 32 K [DE95-601210] p 1959 N95-25405
IRRADIATION
One-step in-diffusion as a result of multipulse laser irradiation of LiNbO3 single-crystalline substrates covered with thin Ti deposits on the effect of the radiation wavelength [DE94-634524] p 2084 N95-24324
High-energy ionoluminescence of LiF [DE94-629015] p 2087 N95-24891
Temperature and dose dependence of metal colloid production in alpha-irradiated CaF2 [DE95-004907] p 2088 N95-25288
Activities of the Radiation Laboratory Department of Nuclear Engineering Kyoto University [DE95-709896] p 2072 N95-26163
Activities of the Radiation Laboratory Department of Nuclear Engineering Faculty of Engineering, Kyoto University [DE95-709897] p 2072 N95-26164
ISCCP PROJECT
Preliminary analysis of University of North Dakota aircraft data from the FIRE Cirrus IFO-2 [NASA-CR-198038] p 2005 N95-24219
ISING MODEL
The 24th Order high temperature expansion for the 3-D Ising model [DE95-004952] p 2093 N95-24450
Monte Carlo simulations with indefinite and complex-valued measures [DE95-607056] p 2017 N95-25448
Domain growth in weakly disordered magnets: A coupled map lattice approach [DE95-607663] p 2090 N95-25979
ISOLATION
The transmission and control of vibrational power in a two stage isolation system with a water-loaded substructure [ISVR-TR-235] p 1975 N95-24992
ISOTHERMAL FLOW
Crossflow mixing of noncircular jets [NASA-TM-106865] p 1913 N95-24390
ISOTHERMAL PROCESSES
Oxidation of ion-implanted NiAl [DE95-005899] p 1935 N95-25388
ISOTOPE EFFECT
Isotope effect on confinement in DT plasmas [NIFS-275] p 2083 N95-26326
ISOTOPE RATIOS
Development of a portable mass spectrometric system for determination of isotopic composition of solid uranium samples using fluorine volatilization [DE95-005728] p 1969 N95-25384
ISOTOPE SEPARATION
Carbons and hydrogen by persistent metal radicals [DE95-003834] p 1929 N95-24553
Measurement of kinetic energy of ions collected from laser resonance photoionized plasma by time-of-flight method [DE95-709767] p 2081 N95-25498
ITERATIVE SOLUTION
Performance issues for iterative solvers in device simulation [NASA-CR-197952] p 2027 N95-24214
Users manual for KSP data-structure-neutral codes implementing Krylov space methods [DE95-004265] p 2020 N95-24658
Newton iterative methods for large scale nonlinear systems [DE95-007067] p 2032 N95-25480

J

J INTEGRAL
The dual boundary element formulation for elastoplastic fracture mechanics [DRA-TR-93062] p 1980 N95-24383
J-85 ENGINE
The effect of altitude conditions on the particle emissions of a J85-GE-5L turbojet engine [NASA-TM-106669] p 1914 N95-24561
JAHN-TELLER EFFECT
Dynamic Jahn-Teller-induced infrared absorption of a charged C60(-) molecule [DE95-607577] p 2063 N95-25971
JAMMING
Wave-propagation aspects on VHF-radar applications [PB95-141818] p 1953 N95-24649
JAPAN
Proceedings of the 1993 Symposium on Nuclear Data [DE94-012554] p 2104 N95-24372
Proceedings of the 21st Japan Conference on Radiation and Radioisotopes [DE94-785275] p 2056 N95-25614
Activities of the National Institute of Radiological Sciences [DE95-709916] p 2072 N95-26165
JAPANESE SPACE PROGRAM
Fourth symposium of the geological survey of Japan on remote sensing of satellite geology [PB95-178737] p 1917 N95-25750
JAPANESE SPACECRAFT
Evaluation of restraint system concepts for the Japanese Experiment Module flight demonstration [NASA-TM-104808] p 2013 N95-24627
JET AIRCRAFT NOISE
Noise impact of advanced high lift systems [NASA-CR-195028] p 2040 N95-26160
Jet mixer noise suppressor using acoustic feedback [NASA-CASE-LEW-15170-2] p 2040 N95-26187
JET ENGINES
Dynamic behavior of a magnetic bearing supported jet engine rotor with auxiliary bearings [NASA-CR-197860] p 1913 N95-24213
A design perspective on thermal barrier coatings p 1943 N95-26120
Jet engine applications for materials with nanometer-scale dimensions p 1945 N95-26131
JET FLOW
Jet mixer noise suppressor using acoustic feedback [NASA-CASE-LEW-15170-2] p 2040 N95-26187
JET MIXING FLOW
Crossflow mixing of noncircular jets [NASA-TM-106865] p 1913 N95-24390
Jet mixer noise suppressor using acoustic feedback [NASA-CASE-LEW-15170-2] p 2040 N95-26187
JET THRUST
Scramjet thrust measurement in a shock tunnel p 1914 N95-25396
JOSEPHSON JUNCTIONS
BCS-like gap structure of HgBa2CuO(4+delta) tunnel junctions [DE95-004125] p 2087 N95-24855
JOURNAL BEARINGS
Thermohydrodynamic analysis of cryogenic liquid turbulent flow fluid film bearings, phase 2 [NASA-CR-197412] p 1962 N95-24461
JUPITER (PLANET)
Voyager: The grandest tour. The mission to the outer planets [NASA-CR-197708] p 2112 N95-25854
JUPITER ATMOSPHERE
Infrared spectroscopy of Jupiter and Saturn [NASA-CR-198034] p 2111 N95-24239

K

K STARS
Resolution of the classical Hyades lithium problem [DE95-003661] p 2109 N95-24234
K-EPSILON TURBULENCE MODEL
Numerical calculations of shock-wave/boundary-layer flow interactions [NASA-TM-106694] p 1966 N95-26077
KAONS
The track system of the modernized Hyperon spectrometer [DE95-604003] p 2058 N95-25905
Preliminary results on the decays D(+) yields K(+)pi(+)pi(-), D(+) yields K(+)K(+)K(-) [DE95-004865] p 2071 N95-26011
KAWASAKI AIRCRAFT
A quiet STOL Research Aircraft Development program [NAL-TR-1223] p 1911 N95-25862
KERNEL FUNCTIONS
Heat Kernel expansion on a cone and quantum fields near cosmic strings [DE94-628520] p 2094 N95-24507
KINEMATICS
Top quark kinematics and mass determination [DE95-004853] p 2041 N95-24254
A review of rolling element bearing vibration detection, diagnosis and prognosis [DSTO-RR-0013] p 1975 N95-24393
A fully associative, nonisothermal, nonlinear kinematic, unified viscoplastic model for titanium alloys [NASA-TM-106926] p 1983 N95-26078
The rotations of deformable bodies. Part 1: Geometry and Kinematics [IFTR-7/1994] p 2039 N95-26332
KINETIC ENERGY
New results in nucleon-nucleon scattering at intermediate energies [DE95-004594] p 2043 N95-24332
A technique for the evaluation of strength of coupling between SEA subsystems [ISVR-TR-241] p 1981 N95-24997
A technique for the evaluation of strength of coupling between SEA subsystems: Experiments with two coupled plates and two coupled rooms [ISVR-TR-242] p 1982 N95-25332
Measurement of kinetic energy of ions collected from laser resonance photoionized plasma by time-of-flight method [DE95-709767] p 2081 N95-25498
KINETIC EQUATIONS
Kinetic modeling of the atomic layer epitaxy window in group 4 semiconductor growth [DE95-005903] p 2089 N95-25391
KINETIC THEORY
Energetic particle drive for toroidicity-induced Alfven eigenmodes and kinetic toroidicity-induced Alfven eigenmodes in a low-shear Tokamak [DE95-003222] p 2079 N95-25216
KINETICS
Kinetics of diffusional droplet growth in a liquid/liquid two-phase system [NASA-CR-198050] p 1961 N95-24221
Convective flow effects on protein crystal growth [NASA-CR-197891] p 2086 N95-24534
Dynamics of phase ordering of nematics in a pore [DE95-607662] p 2090 N95-25978
KLEIN-GORDON EQUATION
Relations among solutions for wave and Klein-Gordon equations for different dimensions [DE95-600853] p 2093 N95-24446
KLYSTRONS
Experimental and theoretical development towards a 500 MW, one-microsecond, L-band relativistic klystron amplifier [DE95-003682] p 1958 N95-24589
RF pulse compression in the NLC test accelerator at SLAC [DE95-006478] p 2070 N95-25406
KNOWLEDGE BASED SYSTEMS
Study of launch site processing and facilities for future launch vehicles [NASA-CR-198025] p 1918 N95-24579
Machine-aided indexing at NASA [NASA-CR-197796] p 2106 N95-25410
KNOWLEDGE BASES (ARTIFICIAL INTELLIGENCE)
Workflow automation architecture standard [DE95-004748] p 2035 N95-24248
KNOWLEDGE REPRESENTATION
Automation based on knowledge modeling theory and its applications in engine diagnostic systems using Space Shuttle Main Engine vibrational data [NASA-CR-197983] p 1922 N95-24626
KRYPTON
Thermochemistry, kinetics and spectroscopy of Kr and Kr2F [DE95-005732] p 1941 N95-25386
KVANT MODULES
JPRS report: Science and technology. Central Eurasia: Space [JPRS-USP-94-008] p 1916 N95-24359

L

LABOR
Partial camera automation in a simulated Unmanned Air Vehicle [AD-A288786] p 1913 N95-26190
LABORATORIES
NLS Flight Simulation Laboratory (FSL) documentation [NASA-CR-196564] p 2104 N95-24439
User guide to the Burner Engineering Research Laboratory [DE95-004191] p 1931 N95-25492
LAGRANGE MULTIPLIERS
Nonlinearity induced nontrivial dynamics in the Jaynes-Cummings Hamiltonian [DE95-607004] p 2032 N95-25452

LAGRANGIAN FUNCTION
Lagrangian formulation of NJL model with se parable interaction
[DE94-628519] p 1952 N95-24506
Quantum group gauge theories and covariant quantum algebras
[DE94-628524] p 2094 N95-24509
Evolution of plastic anisotropy for high-strain-rate computations
[DE95-004220] p 1941 N95-25237
Low energy properties of the heavy vector fermions
[DE94-634362] p 2051 N95-25290
Two dimensional simplicial paths
[DE95-607087] p 2036 N95-25434
LAMINAR FLOW
Numerical and experimental study of drag characteristics of two-dimensional HLFC airfoils in high subsonic, high Reynolds number flow
[NAL-TR-1244T] p 1907 N95-24998
Temperature bounds in a model of laminar flames
[DE95-607048] p 1931 N95-25447
Numerical simulation of laminar flow in a curved duct
[DE95-005427] p 1966 N95-26240
LAMINAR FLOW AIRFOILS
Numerical and experimental study of drag characteristics of two-dimensional HLFC airfoils in high subsonic, high Reynolds number flow
[NAL-TR-1244T] p 1907 N95-24998
LAMINATES
Significance of varied thickness to damage tolerance of carbon fiber/epoxy laminates
[PB95-165460] p 1925 N95-24242
Numerical simulation of the nonlinear response of composite plates under combined thermal and acoustic loading
[NASA-CR-197426] p 1981 N95-24907
Temperature-dependent growth of LaAlO3 films on YBa2CuO7 C-axis films for multilayer structures
[DE95-005257] p 2089 N95-25598
Thermoelastic equations for multi-layered cylindrical shell
[NAL-TR-1222] p 1982 N95-25661
Effects of through-the-thickness stitching on impact and interlaminar fracture properties of textile graphite/epoxy laminates
[NASA-CR-195042] p 1928 N95-26203
Sensitivity analysis for large-deflection and postbuckling responses on distributed-memory computers
p 1987 N95-26281
LANDAU FACTOR
Landau-Zener treatments of solar neutrino oscillations
[DE95-004761] p 2113 N95-24249
LANDAU-GINZBURG EQUATIONS
Intrinsic magnetic torque at low magnetic induction
[DE95-601209] p 1959 N95-24842
On D=2 (1/3,1/3) supersymmetric theories 2
[DE95-607076] p 2037 N95-25523
LANGEVIN FORMULA
Statistical mechanics of nonlinear coherent structures: Kinks in the Phi(sup 6) model
[DE95-005253] p 2096 N95-25293
LANTHANUM COMPOUNDS
Electronic structure of (La,Sr)2CuO4 and Ba(0.6)K(0.4)BiO3
[DE95-004963] p 2091 N95-26170
LANTHANUM OXIDES
Processing of LaCrO3 for solid oxide fuel cell applications
[DE95-000024] p 1992 N95-24683
Processing and electrochemical properties of mixed conducting La(1-x)A(x)Co(1-y)Fe(y)O(3-delta) (A=Sr, Ca)
[DE95-004910] p 2088 N95-25002
Fe-57 and Sn-119 Moessbauer studies on La(1.25)Nd(0.6)Sr(0.15)CuO4: Evidence for local magnetic ordering below (approx. equal) 32 K
[DE95-601210] p 1959 N95-25405
Temperature-dependent growth of LaAlO3 films on YBa2CuO7 C-axis films for multilayer structures
[DE95-005257] p 2089 N95-25598
LAP JOINTS
Estimate of probability of crack detection from service difficulty report data
[PB95-149381] p 1905 N95-24295
LARGE SCALE INTEGRATION
Holograpy machine HORN-1 for computer-aided retrieve of virtual three-dimensional image
[NIFS-218] p 1971 N95-26182
LARGE SPACE STRUCTURES
Efficient eigenvalue assignment by state and output feedback with applications for large space structures
[NASA-TM-110155] p 1920 N95-24581
LASER ABLATION
Summaries of reports of the Electrotechnical Laboratory, no. 48
[JTN-95-80825] p 2114 N95-24908
LASER ANNEALING
Pulsed laser annealing of P implanted diamond
[DE95-605947] p 2090 N95-25985
LASER APPLICATIONS
JPRS report: Science and technology. Central Eurasia
[JPRS-UST-94-030] p 1962 N95-24469
Residual Stress Measurements with Laser Speckle Correlation Interferometry and Local Heat Treating
[DE95-060082] p 1981 N95-24598
Activities of the Solid State Division
[DE95-003900] p 2087 N95-24611
Co-validation of three methods for optical characterization of point-focus concentrators
[DE95-001613] p 1992 N95-24674
Summaries of reports of the Electrotechnical Laboratory, no. 48
[JTN-95-80825] p 2114 N95-24908
The Third International Workshop on the Physics and Modern Applications of Lasers
[DE95-606395] p 1972 N95-25491
Targets for laser-driven opacity measurements
[DE95-006172] p 1973 N95-25557
LASER BEAMS
One-step in-diffusion as a result of multipulse laser irradiation of LiNbO3 single-crystalline substrates covered with thin Ti deposits on the effect of the radiation wavelength
[DE94-634524] p 2084 N95-24324
Laser beam log amplitude temporal scintillation spectrum due to crosswind. Part 1: Theory
[TR-1-FSRC-1994-PT-1] p 1971 N95-24371
Laser beam characterization results for a high power CW Nd:YAG laser
[DE95-006319] p 1971 N95-24408
Measurement of kinetic energy of ions collected from laser resonance photoionized plasma by time-of-flight method
[DE95-709767] p 2081 N95-25498
Measurements of acoustic emission on a laser ceramic treatment line
[IFTR-28/1994] p 2040 N95-26180
Holograpy machine HORN-1 for computer-aided retrieve of virtual three-dimensional image
[NIFS-218] p 1971 N95-26182
LASER CAVITIES
High gain GaAs Photoconductive Semiconductor Switches (PCSS): Device lifetime, high current testing, optical pulse generators
[DE95-003354] p 1957 N95-24488
Time-dependent numerical simulation of vertical cavity lasers
[DE95-006862] p 1973 N95-26112
LASER COOLING
Laser cooling of neutral atoms by red-shifted diffuse light in an optical integral sphere cavity
[DE94-634310] p 2041 N95-24268
The cooling of particle beams
[DE95-004669] p 2065 N95-24320
LASER DEPOSITION
Decay of a laser generated shock wave in an aluminium target
[DE94-629014] p 1972 N95-24707
LASER DOPPLER VELOCIMETERS
Stratified charge rotary engine combustion studies
[NASA-CR-197985] p 1974 N95-24223
Laser velocimeter for near-surface measurements
[NASA-CASE-ARC-11917-1] p 1967 N95-24236
LASER HEATING
A neural network controller for automated composite manufacturing p 2025 N95-25271
LASER INDUCED FLUORESCENCE
Thermochemistry, kinetics and spectroscopy of Kr and Kr2F
[DE95-005732] p 1941 N95-25386
LASER OUTPUTS
Laser velocimeter for near-surface measurements
[NASA-CASE-ARC-11917-1] p 1967 N95-24236
Laser beam characterization results for a high power CW Nd:YAG laser
[DE95-006319] p 1971 N95-24408
Laser light scattering, from an advanced technology development program to experiments in a reduced gravity environment
[NASA-TM-110496] p 1971 N95-24530
Measurement of kinetic energy of ions collected from laser resonance photoionized plasma by time-of-flight method
[DE95-709767] p 2081 N95-25498
An FEL design code running on Mathcad(trademark)
[DE95-005279] p 1973 N95-25565
Central Laser Facility. Annual report to the Laser Facility Committee
[PB95-160511] p 1973 N95-25640
LASER PLASMAS
Na-like autoionizing levels: Plasma diagnostics and prospects for photopumped soft x-ray lasers
[DE95-004207] p 1972 N95-25100
Central Laser Facility. Annual report to the Laser Facility Committee
[PB95-160511] p 1973 N95-25640
Construction of a nitrogen laser for plasma diagnostics
[DE95-607599] p 1973 N95-25973
LASER PUMPING
Diode laser pumped solid state laser with 2 micrometer wavelength
[PB95-165270] p 1973 N95-25622
LASER RANGE FINDERS
Laser based methods for range, Doppler and vibration measurements
[PB95-141958] p 1952 N95-24445
LASER TARGETS
Targets for laser-driven opacity measurements
[DE95-006172] p 1973 N95-25557
LASERS
Optical generation of radio-frequency power
[DE95-005276] p 1951 N95-24289
JPRS report: Science and technology. Central Eurasia
[JPRS-UST-94-024] p 1958 N95-24620
Decay of a laser generated shock wave in an aluminium target
[DE94-629014] p 1972 N95-24707
The Third International Workshop on the Physics and Modern Applications of Lasers
[DE95-606395] p 1972 N95-25491
Pulsed laser annealing of P implanted diamond
[DE95-605947] p 2090 N95-25985
LASING
Na-like autoionizing levels: Plasma diagnostics and prospects for photopumped soft x-ray lasers
[DE95-004207] p 1972 N95-25100
LATEX
Antioxidant and sensitizer effect on the stability of natural rubber latex vulcanized by gamma rays
[DE94-636061] p 1939 N95-24373
The use of DBMS and document oriented interface in the TPLAN-system
[DE95-605219] p 2106 N95-25907
LATITUDE
Impacts of microphysics, radiation and environmental winds in mid-latitude and tropical squall-line systems, and their climatic implications
[DE95-004965] p 2005 N95-25287
Predicting the components of the total hemispherical solar radiation from sunshine duration measurements in Lagos, Nigeria
[DE95-606030] p 2113 N95-26042
LATTICE PARAMETERS
On the calculation of lattice sums arising in Bose-Einstein statistics of quasiparticle excitations
[DE94-634531] p 2084 N95-24246
LATTICES
Update on B(sub K) with Wilson fermions
[DE95-004953] p 2085 N95-24451
LATTICES (MATHEMATICS)
Distances on a lattice from noncommutative geometry
[DE94-634327] p 2027 N95-24229
Distribution of the error term for the number of lattice points inside a shifted ball
[PB95-165569] p 2029 N95-24325
The lattice spinor QED Hamiltonian critique of the continuous space approach
[DE94-628521] p 2094 N95-24508
Zero sound velocity in pi, rho mesons at different temperatures
[DE95-607145] p 2053 N95-25459
The Hamiltonian of SU(2) lattice gauge theory in approximate tri-diagonal form
[DE95-607101] p 2098 N95-25475
LAUNCH VEHICLE CONFIGURATIONS
The 1994 NASA/USRA/ADP Design Projects
[NASA-CR-197415] p 2101 N95-26304
Launch system design for access to space
p 1918 N95-26308
LAUNCH VEHICLES
Study of launch site processing and facilities for future launch vehicles
[NASA-CR-198025] p 1918 N95-24579
Predictability in space launch vehicle anomaly detection using intelligent neuro-fuzzy systems
p 2025 N95-25266
Applications of solid lubricant films in spacecraft
[AD-A288784] p 1947 N95-26188
Optimal guidance law development for an advanced launch system
[NASA-CR-4667] p 1917 N95-26205
LAUNCHING SITES
Study of launch site processing and facilities for future launch vehicles
[NASA-CR-198025] p 1918 N95-24579

LAWS
Domain growth in weakly disordered magnets: A coupled map lattice approach
| DE95-607663 | p 2090 N95-25979
LEAD ACETATES
Experimental and theoretical study of plasma-water interaction in electrothermal guns
| DE94-628961 | p 2078 N95-24706
LEAD OXIDES
Application of extended-crystal diffraction techniques to the symmetry and structure analysis of 221-PbBiSrCaCuO
| DE95-605913 | p 2090 N95-25984
LEAD ZIRCONATE TITANATES
Effects of acetylacetone additions on PZT thin film processing
| DE95-006322 | p 1941 N95-25370
LEADERSHIP
Continual improvement plan
| NASA-TM-110574 | p 2103 N95-25849
LEADING EDGE SLATS
Three-dimensional interaction of wake/boundary-layer and vortex/boundary-layer data report
| CUED/A-AEREO/TR-23 | p 1906 N95-24210
LEADING EDGES
A theoretical and experimental investigation of the flow over supersonic leading edge wing/body configurations
| DRA-TM-AERO-PROP-41 | p 1907 N95-25649
LEARNING THEORY
Instructable autonomous agents
| NASA-CR-197802 | p 2019 N95-26206
LEAST SQUARES METHOD
Aerodynamic parameter estimation via Fourier modulating function techniques
| NASA-CR-4654 | p 1911 N95-24630
Unfolding of true distributions from experimental data distorted by detectors with finite resolutions
| DE94-628372 | p 2035 N95-24643
Adaptive projective filters
| DE94-628374 | p 2030 N95-24645
A note on the total least squares problem for coplanar points
| DE95-004876 | p 2032 N95-25251
LEAVES
The effects on photosynthetic CO2 assimilation to long-term elevation of atmospheric CO2 concentration: An assessment of the response of Trifolium Repens L. CV. Blanca grown at F.A.C.E
| DE95-005687 | p 2008 N95-25383
LENGTH
The Lienard-Wiechert potentials and relativistic length
| DE94-636733 | p 2093 N95-24376
Lienard-Wiechert potentials as a consequence of Lorentz transformation of Coulomb potential
| DE94-636734 | p 1952 N95-24377
LENSES
An assessment of aviation accident risk of aphakic civil airmen by class of medical certificate held and by age: 1982-1985
| DOT/FAA/AM-95/11 | p 2011 N95-25336
LEPTONS
Top quark kinematics and mass determination
| DE95-004853 | p 2041 N95-24254
The discovery of the tau lepton: Part 1, The early history through 1975; Part 2, Confirmation of the discovery and measurement of major properties, 1976-1982
| DE95-005945 | p 2044 N95-24414
Extending the kinematic range for W(sub R) searches in e(-)e(-) collisions at the NLC
| DE95-005946 | p 2044 N95-24415
Probing anomalous gauge boson couplings at LEP
| DE95-005934 | p 2044 N95-24420
The left-right forward-backward asymmetry of heavy quarks measured with jet charge and with leptons at the SLD
| DE95-006145 | p 2046 N95-24593
Search for top in lepton + jets in D0 using a topological tag
| DE95-003929 | p 2048 N95-24677
Tests for leptonic CP violation in tau decays
| DE95-005927 | p 2050 N95-24902
Low energy properties of the heavy vector fermions
| DE94-634362 | p 2051 N95-25290
CP violation tests for tau/top processes
| DE95-005924 | p 2051 N95-25292
Tau as a probe for new physics
| DE95-005928 | p 2051 N95-25296
A search for t(anti t) (yields) lepton + E(sub T) + jets signature in p(anti p) collisions at (radical)s = 1.8 TeV with the DO detector
| DE95-004239 | p 2052 N95-25402
Masses of heavy fermions and Higgs boson in four-generation fermion condensate scheme
| DE95-607124 | p 2053 N95-25450
Study of the simplest realistic Higgs sector in quark-lepton symmetric models
| DE95-607159 | p 2053 N95-25461
Can the electric charges of elementary particles change with time?
| DE95-607194 | p 2054 N95-25465
A simple relation among the quark masses
| DE95-703783 | p 2055 N95-25494
Further ways to distinguish single-lepton top quark signals from background at the Tevatron
| PB95-165395 | p 2056 N95-25567
Heavy-neutrino effects on tau-lepton decays
| PB95-165346 | p 2056 N95-25626
Anisotropy of dilepton emission from nuclear collisions
| DE95-004354 | p 2070 N95-25634
LEWIS NUMBERS
Temperature bounds in a model of laminar flames
| DE95-607048 | p 1931 N95-25447
LIBRARIES
Aspect estimation of an aircraft using library model silhouettes
| PB95-141834 | p 2036 N95-25894
Index of nuclear data libraries available from the IAEA Nuclear Data Section
| DE95-605213 | p 2107 N95-25980
Activities of the National Institute of Radiological Sciences
| DE95-709916 | p 2072 N95-26165
Directory of Defence and Aerospace Information Centers
| AGARD-R-802 | p 2107 N95-26334
LIE GROUPS
Geometric quantization of symplectic manifolds with symmetry
| DE94-628435 | p 2031 N95-24698
Quantum group and quantum symmetry
| DE94-634329 | p 2095 N95-24767
Nonlinearity induced nontrivial dynamics in the Jaynes-Cummings Hamiltonian
| DE95-607004 | p 2032 N95-25452
Equivariant Kaehler geometry and localization in the G/G model
| DE95-607073 | p 2036 N95-25455
On D = 2 (1/3,1/3) supersymmetric theories 2
| DE95-607076 | p 2037 N95-25523
Constraints, complex structures and quantization
| DE95-605252 | p 2037 N95-25781
The criteria for the Cohen-Macaulayness and Gorensteiness of Rees algebras of ideals having positive analytic deviation
| DE95-607003 | p 2034 N95-25992
LIENARD POTENTIAL
The Lienard-Wiechert potentials and relativistic length
| DE94-636733 | p 2093 N95-24376
Lienard-Wiechert potentials as a consequence of Lorentz transformation of Coulomb potential
| DE94-636734 | p 1952 N95-24377
LIFE (DURABILITY)
B physics with CDF: Recent results and future prospects
| DE95-004793 | p 2051 N95-25372
Properties of plasma sprayed bond coats
p 1946 N95-26135
Thermal barrier coating life modeling in aircraft gas turbine engines p 1947 N95-26140
LIFE SCIENCES
NASA video catalog
| NASA-SP-7109(01) | p 2103 N95-24238
Aerospace medicine and biology: A continuing bibliography with indexes (supplement 400)
| NASA-SP-7011(400) | p 2011 N95-24464
JPRS report: Science and technology. Central Eurasia
| JPRS-UST-94-024 | p 1958 N95-24620
JPRS Report: Science and technology. Central Eurasia
| JPRS-UST-95-002 | p 1916 N95-24621
JPRS report: Science and technology. Central Eurasia
| JPRS-UST-94-034 | p 1987 N95-24729
JPRS report: Science and technology. Central Eurasia
| JPRS-UST-95-003 | p 1988 N95-24730
JPRS report: Science and technology. Central Eurasia
| JPRS-UST-95-006 | p 1950 N95-24731
JPRS report: Science and technology. Central Eurasia
| JPRS-UST-94-033 | p 2037 N95-24732
JPRS Report: Science and technology. Central Eurasia
| JPRS-UST-94-032 | p 1950 N95-24759
JPRS Report: Science and technology. Central Eurasia
| JPRS-UST-94-031 | p 1988 N95-24760
Aerospace medicine and biology: A continuing bibliography with indexes (supplement 401)
| NASA-SP-7011(401) | p 2012 N95-25800
JPRS report: Science and technology. Central Eurasia
| JPRS-UST-95-018 | p 2071 N95-26079
LIFE SPAN
A longevity and survival analysis for a cohort of retired airline pilots
| DOT/FAA/AM-95/5 | p 2012 N95-24237
LIFE SUPPORT SYSTEMS
Aerospace medicine and biology: A continuing bibliography with indexes (supplement 400)
| NASA-SP-7011(400) | p 2011 N95-24464
LIFT
NREL airfoil families for HAWTs
| DE95-000267 | p 1994 N95-24882
Aerodynamic characteristics of the orbital reentry vehicle experimental probe fins in a supersonic flow
| NAL-TR-1232 | p 1921 N95-25664
Noise impact of advanced high lift systems
| NASA-CR-195028 | p 2040 N95-26160
LIFT DRAG RATIO
Low speed aerodynamic characteristics of delta wings with vortex flaps: 60 deg and 70 deg delta wings
| NAL-TR-1245 | p 1907 N95-25105
LIFT FANS
Aerodynamics model for a generic ASTOVL lift-fan aircraft
| NASA-TM-110347 | p 1908 N95-26302
LIFTOFF (LAUNCHING)
Apollo 12: Pinpoint for science
| NASA-TM-110576 | p 1917 N95-25424
LIGANDS
The transformation of organic amines by transition metal cluster compounds
| DE95-004180 | p 1923 N95-24851
Selective extraction of trivalent actinides from lanthanides with dithiophosphinic acids and tributylphosphate
| DE95-005249 | p 1924 N95-25597
LIGHT (VISIBLE RADIATION)
Laser cooling of neutral atoms by red-shifted diffuse light in an optical integral sphere cavity
| DE94-634310 | p 2041 N95-24268
LIGHT ALLOYS
NASA-UVA light aerospace alloy and structures technology program (LA2ST)
| NASA-CR-198041 | p 1933 N95-24220
LIGHT AMPLIFIERS
Application of optical fiber amplifier for wavelength division multiplexing communication system. Part 2: Design of four-channel transmission system using two EDFA repeaters
| DE95-730179 | p 1952 N95-24491
Phase correction in two-crystal optical parametric oscillators
| DE95-006317 | p 2074 N95-25559
LIGHT BEAMS
Laser velocimeter for near-surface measurements
| NASA-CASE-ARC-11917-1 | p 1967 N95-24236
Laser light scattering, from an advanced technology development program to experiments in a reduced gravity environment
| NASA-TM-110496 | p 1971 N95-24530
Method for determining shear direction using liquid crystal coatings
| NASA-CASE-ARC-11995-1 | p 2075 N95-26117
LIGHT EMISSION
The KTeV PMT laser monitoring system
| DE95-004237 | p 1972 N95-24869
LIGHT SCATTERING
A preview of a modular surface light scattering instrument with autotracking optics
| NASA-TM-110495 | p 2072 N95-24386
Laser light scattering, from an advanced technology development program to experiments in a reduced gravity environment
| NASA-TM-110496 | p 1971 N95-24530
Calculation of light scattering from a spherical particle on a surface by the multipole expansion method
| ATR-95(9558)-2 | p 2075 N95-26198
LIGHT SOURCES
FT-IR microscopical analysis with synchrotron radiation: The microscope optics and system performance
| DE95-004834 | p 1928 N95-24265
Optical generation of radio-frequency power
| DE95-005276 | p 1951 N95-24289
Advanced Light Source report
| DE95-003449 | p 2073 N95-24546
A quality monitor and monitoring technique employing optically stimulated electron emission
| NASA-CASE-LAR-15063-1-CU | p 1978 N95-25304
LIGHT TRANSMISSION
Laser beam characterization results for a high power CW Nd:YAG laser
| DE95-006319 | p 1971 N95-24408
LIGHT-CONE EXPANSION
Constraints and Hamiltonian in light-front quantized field theory
| DE95-600852 | p 2093 N95-24353

LINE OF SIGHT
Characterizing the wake vortex signature for an active line of sight remote sensor
[NASA-CR-197697] p 1909 N95-24391

LINEAR ACCELERATORS
Self-consistent beam halo studies & halo diagnostic development in a continuous linear focusing channel
[DE95-003706] p 2065 N95-24331
A high-energy high-luminosity (mu)(+) - (mu)(-) collider
[DE95-006097] p 2065 N95-24357
Over-compression, a method to shape the longitudinal bunch distribution for a reduced energy spread
[DE95-006052] p 2066 N95-24572
Tutorial on beam-based feedback systems for linacs
[DE95-006054] p 2067 N95-24573
Target injection methods for inertial fusion energy
[DE95-003654] p 2067 N95-24651
Studies of strong electroweak symmetry breaking at future e(+)e(-) linear colliders
[DE95-004281] p 2067 N95-24661
High-gradient experiment on X-band disk-loaded structures
[DE94-765446] p 1958 N95-24701
Testing supersymmetry at the next linear collider
[DE95-006064] p 2069 N95-25297
Elise: The next step in development of induction heavy ion drivers for inertial fusion energy
[DE95-004679] p 2069 N95-25358
RF pulse compression in the NLC test accelerator at SLAC
[DE95-006478] p 2070 N95-25406
Emittance growth caused by nonuniform charge distribution of bunched beam in linac
[DE95-602121] p 2072 N95-26095

LINEAR ARRAYS
Experimental study of tapered slot elements
[PB95-165163] p 1955 N95-25644

LINEAR ENERGY TRANSFER (LET)
High LET, passive space radiation dosimetry and spectrometry
[NASA-CR-197694] p 2058 N95-25911
LET spectra measurements from the STS-35 CPDs p 2058 N95-25912
Summary of LET spectra and dose measurements on ten STS missions p 2058 N95-25913
A study of the radiation environment on board the space shuttle flight STS-57 p 2059 N95-25914
Dosimetry on STS-42 with the RME APD p 2059 N95-25916
HZE beam transport in multilayered materials p 2060 N95-25922
Linear Energy Transfer (LET) spectra of cosmic radiation in low Earth orbit p 2061 N95-25926
Experimental and calculated LET distributions in the Cosmos-2044 biosatellite orbit p 2061 N95-25929
Cosmic ray LET spectra and doses on board Cosmos-2044 biosatellite p 2061 N95-25930
Cosmic ray particles with different LET values under various thicknesses of shielding in low altitude orbits: Calculations and Cosmos-2044 measurements p 2062 N95-25931
Space radiation dosimetry on US and Soviet manned missions p 2009 N95-25934

LINEAR EQUATIONS
Periodic solutions of Hamiltonian perturbations of 2D linear Schroedinger equations
[PB95-165536] p 2028 N95-24301
Construction of quasi-periodic solutions for Hamiltonian perturbations of linear equations and applications to nonlinear PDE
[PB95-165551] p 2028 N95-24322
Domain decomposition and generators of direct methods of the solution of linear equation systems with general block-tridiagonal matrices
[DE94-628388] p 2031 N95-24695
Behaviour at X= +/- infinity of solutions to a pr edator-prey model
[DE95-607049] p 2033 N95-25748

LINEAR OPERATORS
Construction of quasi-periodic solutions for Hamiltonian perturbations of linear equations and applications to nonlinear PDE
[PB95-165551] p 2028 N95-24322

LINEAR POLARIZATION
Depolarization in the SLC Collider Arcs
[DE95-005942] p 2065 N95-24409
Polarization and intensity of dd-transitions in superconducting copper oxides
[DE95-605886] p 2090 N95-25776

LINEAR SYSTEMS
Use of multiple fronts in Gaussian elimination
[PB95-165353] p 2033 N95-25627
The effects of the environment on an experimental VHF radio Direction Finding antenna system
[AD-A288791] p 1956 N95-26191

LIOUVILLE THEOREM
A covariant canonical description of Liouville field theory
[DE95-607094] p 2098 N95-25534

LIQUID CRYSTALS
NMR and optical studies of piezoelectric polymers
[DE95-003836] p 1940 N95-24554
Dynamics of phase ordering of nematics in a pore
[DE95-607662] p 2090 N95-25978
Liquid crystal point diffraction interferometer
[NASA-TM-106899] p 1970 N95-26073
Method for determining shear direction using liquid crystal coatings
[NASA-CASE-ARC-11995-1] p 2075 N95-26117

LIQUID FLOW
Thermohydrodynamic analysis of cryogenic liquid turbulent flow fluid film bearings, phase 2
[NASA-CR-197412] p 1962 N95-24461

LIQUID FUELS
Liquid-fueled SOFC power sources for transportation
[DE95-002998] p 1991 N95-24607

LIQUID HELIUM
Cryogenic helium gas convection research
[DE95-004372] p 1965 N95-25404
Performance evaluation of LE-7 high pressure pumps
[NAL-TR-1212T] p 1977 N95-25672

LIQUID HYDROGEN
LH2 fuel tank design for SSTO p 1987 N95-26309

LIQUID METALS
Heat removal capability of divertor coaxial tube assembly
[DE95-709770] p 1966 N95-26161

LIQUID NITROGEN
Alternate method for achieving temperature control in the -160 to + 90 Celcius range
[NASA-CASE-NPO-18995-1-CU] p 1969 N95-25547

LIQUID OXYGEN
Simplified liquid oxygen propellant conditioning concepts
[NASA-TM-108482] p 1948 N95-24558
Performance evaluation of LE-7 high pressure pumps
[NAL-TR-1212T] p 1977 N95-25672
Combustion characteristics of metallized hydrocarbon fuels
[NAL-TR-1224] p 1949 N95-25769

LIQUID PHASES
Kinetics of diffusional droplet growth in a liquid/liquid two-phase system
[NASA-CR-198050] p 1961 N95-24221

LIQUID PROPELLANT ROCKET ENGINES
Simplified liquid oxygen propellant conditioning concepts
[NASA-TM-108482] p 1948 N95-24558

LIQUID ROCKET PROPELLANTS
Development test of a liquid apogee engine for the ETS-4
[NAL-TR-1250] p 1922 N95-24999
Combustion characteristics of metallized hydrocarbon fuels
[NAL-TR-1224] p 1949 N95-25769

LIQUID SLOSHING
A preview of a modular surface light scattering instrument with autotracking optics
[NASA-TM-110495] p 2072 N95-24386

LIQUID WASTES
SPEEDUP simulation of liquid waste batch processing, revision 1
[DE95-001240] p 1939 N95-24344

LIQUID-GAS MIXTURES
Studies of two-phase gas-liquid flow in microgravity
[NASA-CR-195434] p 1963 N95-24906

LIQUID-SOLID INTERFACES
Dynamic methods for determining the material characteristics of saturated permeable media
[IFTR-17/1993] p 1932 N95-26107

LIQUID-VAPOR INTERFACES
Calculating the thermodynamic properties of planar and spherical liquid-vapour interface
[DE95-608777] p 2100 N95-26105

LIQUIDS
Structure of liquid He-4 excitations spectrum
[DE94-637113] p 2043 N95-24364
The characteristics and design of an apparatus constructed by the Institute of Basic Problems of Technology to study relaxation phenomena in liquids at frequencies of 10-150 MHz
[IFTR-21/1994] p 1932 N95-25959
Numerical solution of the optimized random phase approximation
[DE95-605636] p 2034 N95-25982

LISP (PROGRAMMING LANGUAGE)
Heuristic approach to the path planning problem in a raster map
[PB95-141826] p 2034 N95-25893

LITHIUM
Resolution of the classical Hyades lithium problem
[DE95-003661] p 2109 N95-24234
Summaries of reports of the Electrotechnical Laboratory, no. 48
[JTN-95-80825] p 2114 N95-24908

LITHIUM ALLOYS
NASA-UVa light aerospace alloy and structures technology program supplement: Aluminum-based materials for high speed aircraft
[NASA-CR-4645] p 1935 N95-24878

LITHIUM FLUORIDES
High-energy ionoluminescence of LiF
[DE94-629015] p 2087 N95-24891
Proton calibration of low energy neutron detectors containing (6)LiF p 2060 N95-25925

LITHIUM NIOBATES
One-step in-diffusion as a result of multipulse laser irradiation of LiNbO3 single-crystalline substrates covered with thin Ti deposits on the effect of the radiation wavelength
[DE94-634524] p 2084 N95-24324

LITHIUM OXIDES
Recent advances in lithium ion technology
[DE95-004769] p 2054 N95-25470

LITHOGRAPHY
Continuous phase and amplitude holographic elements
[NASA-CASE-NPO-18791-1] p 1971 N95-26340

LOAD TESTS
Techniques for studying the mechanical properties of materials in complex stress states
[IFTR-34/1994] p 1983 N95-26178

LOADS (FORCES)
Finite element buckling and postbuckling solutions for multilayered composite panels p 1983 N95-26264
Changes in the strength characteristics of 15HM boiler steel caused by initial plastic deformation under constant and monotonic loads
[IFTR-30/1994] p 1938 N95-26333

LOCAL AREA NETWORKS
NLS Flight Simulation Laboratory (FSL) documentation
[NASA-CR-196564] p 2104 N95-24439
CD-ROM in the age of internet
[DE95-005067] p 2104 N95-24454
Parallel processing for scientific computations
[NASA-CR-198013] p 2020 N95-24563

LOGIC CIRCUITS
ASIC implementation of a data-push architecture for silicon pixel readout
[DE95-003368] p 2015 N95-24648
Circuit for high resolution decoding of multi-anode microchannel array detectors
[NASA-CASE-GSC-13478-1] p 1960 N95-25889

LONG DURATION EXPOSURE FACILITY
Composite materials flown on the Long Duration Exposure Facility
[NASA-CR-4657] p 1923 N95-24583
Long Duration Exposure Facility mini-data base user's guide: IBM-compatible PC computer version
[NASA-CR-4655] p 1925 N95-26072

LONGITUDE
Predicting the components of the total hemispherical solar radiation from sunshine duration measurements in Lagos, Nigeria
[DE95-606030] p 2113 N95-26042

LONGITUDINAL WAVES
Dynamic analysis of truss members using longitudinal waves
[IFTR-35/1994] p 1981 N95-24996

LOOPS
Tutorial on beam-based feedback systems for linacs
[DE95-006054] p 2067 N95-24573

LORENTZ CONTRACTION
Moving scales contraction contradicts interval invariance
[DE94-636736] p 2092 N95-24347
The Fitzgerald-Lorentz hypothesis from the viewpoint of relativity theory
[DE94-636735] p 2093 N95-24378

LORENTZ FORCE
Meson properties at finite temperature and density within Nambu-Jona-Lasinio model
[DE94-628630] p 2049 N95-24888

LORENTZ TRANSFORMATIONS
The Lienard-Wiechert potentials and relativistic length
[DE94-636733] p 2093 N95-24376
Lienard-Wiechert potentials as a consequence of Lorentz transformation of Coulomb potential
[DE94-636734] p 1952 N95-24377
The Fitzgerald-Lorentz hypothesis from the viewpoint of relativity theory
[DE94-636735] p 2093 N95-24378

LOUVERS
Heat removal capability of divertor coaxial tube assembly
[DE95-709770] p 1966 N95-26161
LOW ALTITUDE
Cosmic ray particles with different LET values under various thicknesses of shielding in low altitude orbits: Calculations and Cosmos-2044 measurements
p 2062 N95-25931
LOW COST
Evolution of Spark plasma using nitrogen laser shadowgraphy system
[DE95-607598] p 2082 N95-25972
LOW EARTH ORBITS
Composite materials flown on the Long Duration Exposure Facility
[NASA-CR-4657] p 1923 N95-24583
Linear Energy Transfer (LET) spectra of cosmic radiation in low Earth orbit p 2061 N95-25926
Differential neutron energy spectra measured on spacecraft low Earth orbit p 2062 N95-25932
LOW SPEED
Low speed aerodynamic characteristics of delta wings with vortex flaps: 60 deg and 70 deg delta wings
[NAL-TR-1245] p 1907 N95-25105
LOW TEMPERATURE PHYSICS
Physics in Ukraine International Conference. Volume 5: Low temperature physics
[DE95-605800] p 2038 N95-25553
Correlated density matrix theory of spatially inhomogeneous Bose fluids
[DE95-607840] p 2100 N95-26102
LUBRICANT TESTS
Development of a high temperature, high speed disc lubricant test machine
[AD-A288685] p 1977 N95-26050
LUBRICANTS
Materials Compatibility and Lubricants Research (MCLR) Program
[DE95-004862] p 1941 N95-25243
Spacecraft materials studies on The Aerospace Corporation Tray on EOIM-3
[AD-A288682] p 1942 N95-26049
LUBRICATION
Information compendium on solid film lubricants
[AD-A288360] p 1942 N95-25510
Development of a high temperature, high speed disc lubricant test machine
[AD-A288685] p 1977 N95-26050
LUBRICATION SYSTEMS
Improved lubrication performance of sputtered MoS2 film by surface treatments of Ti-alloy substrate
[NAL-TR-1213] p 1942 N95-25760
LUMINESCENCE
Update of GALLEX solar neutrino results and implications
[DE95-005005] p 2113 N95-25364
LUMINOSITY
A high-energy high-luminosity (mu)(+) - (mu)(-) collider
[DE95-006097] p 2065 N95-24357
LUNAR EXPLORATION
Apollo 13: Houston, we've got a problem
[NASA-TM-110551] p 1918 N95-24215
The Clementine Mission: Initial Results from lunar mapping
[NASA-TM-110555] p 2112 N95-24994
Apollo 12: Pinpoint for science
[NASA-TM-110576] p 1917 N95-25424
LUNAR FLIGHT
Apollo 13: Houston, we've got a problem
[NASA-TM-110551] p 1918 N95-24215
LUNAR LANDING
Apollo 12: Pinpoint for science
[NASA-TM-110576] p 1917 N95-25424
LUNAR MAPS
The Clementine Mission: Initial Results from lunar mapping
[NASA-TM-110555] p 2112 N95-24994
LUNAR MODULE
Apollo 13: Houston, we've got a problem
[NASA-TM-110551] p 1918 N95-24215
Apollo 12: Pinpoint for science
[NASA-TM-110576] p 1917 N95-25424
LUNAR ORBITS
The Clementine Mission: Initial Results from lunar mapping
[NASA-TM-110555] p 2112 N95-24994
Apollo 12: Pinpoint for science
[NASA-TM-110576] p 1917 N95-25424
LUNAR ROCKS
Transmission electron microscope studies of extraterrestrial materials
[NASA-CR-188363] p 1928 N95-24222
LUNAR SOIL
Transmission electron microscope studies of extraterrestrial materials
[NASA-CR-188363] p 1928 N95-24222
Apollo 12: Pinpoint for science
[NASA-TM-110576] p 1917 N95-25424
LUNAR SURFACE
The Clementine Mission: Initial Results from lunar mapping
[NASA-TM-110555] p 2112 N95-24994
Apollo 12: Pinpoint for science
[NASA-TM-110576] p 1917 N95-25424
LUTETIUM COMPOUNDS
LuAlO3: A high density, high speed scintillator for gamma detection
[DE95-004678] p 2064 N95-26256
LYSOZYME
Convective flow effects on protein crystal growth
[NASA-CR-197891] p 2086 N95-24534

M

MACH NUMBER
A study of three-dimensional interaction flow fields between swept shock waves and turbulent boundary layers. Flow structures and effects of bleed
[NAL-TR-1227] p 1963 N95-25001
Molecular dynamics simulation of a piston driven shock wave in a hard sphere gas
[NASA-CR-195463] p 2063 N95-25963
MACHINE LEARNING
Reducing neural network training time with parallel processing
[NASA-TM-110154] p 2015 N95-24209
Learning to train neural networks for real-world control problems p 2025 N95-25269
Neural network applications in telecommunications
p 2025 N95-25270
Proceedings of the 4th IEEE Workshop on Neural Networks for Signal Processing
[AD-A288383] p 2026 N95-25603
Instructable autonomous agents
[NASA-CR-197802] p 2019 N95-26206
MACHINE ORIENTED LANGUAGES
Summaries of reports of the Electrotechnical Laboratory, no. 48
[JTN-95-80825] p 2114 N95-24908
MACROSCOPIC EQUATIONS
Testing quantum behaviour at the macroscopic level
[DE95-607005] p 2097 N95-25453
MAGELLAN PROJECT (NASA)
User guide to the Magellan synthetic aperture radar images
[NASA-RP-1356] p 2112 N95-24987
MAGNESIUM ALLOYS
NASA-UVa light aerospace alloy and structures technology program supplement: Aluminum-based materials for high speed aircraft
[NASA-CR-4645] p 1935 N95-24878
MAGNETIC BEARINGS
Dynamic behavior of a magnetic bearing supported jet engine rotor with auxiliary bearings
[NASA-CR-197860] p 1913 N95-24213
Development of a fast response rotating polarimeter for a Faraday rotation measurement
[DE94-777532] p 2075 N95-24271
MAGNETIC COILS
Superconductivity Program for Electric Power Systems: 1994 Annual PEER Review. Volume 1, Meeting Proceedings
[DE95-005058] p 1956 N95-24452
MAGNETIC COOLING
Superconductivity Program for Electric Power Systems: 1994 Annual PEER Review. Volume 1, Meeting Proceedings
[DE95-005058] p 1956 N95-24452
Superconductivity Program for Electric Power Systems: 1994 Annual PEER Review. Volume 2, Meeting Proceedings
[DE95-005059] p 1957 N95-24453
Thermodynamic property evaluation and magnetic refrigeration cycle analysis for gadolinium gallium garnet
[DE95-005910] p 1951 N95-25367
MAGNETIC DIPOLES
Dynamics of nonadiabatic charged particles in the magnetic dipole field with imposed homogeneous magnetic field
[DE95-605222] p 2057 N95-25778
MAGNETIC DOMAINS
On analysis of resonance neutron depolarization in uniaxial media
[DE95-703782] p 2057 N95-25669
MAGNETIC EFFECTS
Interaction mechanisms and biological effects of static magnetic fields
[DE95-004929] p 2009 N95-26169
MAGNETIC ENERGY STORAGE
Availability analysis of a 100 kWh superconducting magnetic energy storage
[DE95-737621] p 2066 N95-24448
MAGNETIC FIELD CONFIGURATIONS
Characteristics of D(-3)He fueled FRC reactor: ARTEMIS-L
[NIFS-251] p 2072 N95-26110
MAGNETIC FIELD RECONNECTION
Magnetic mirror effect as a trigger of collisionless magnetic reconnection
[NIFS-295] p 2083 N95-26337
A mechanism of collisionless magnetic reconnection
[NIFS-274] p 2083 N95-26339
MAGNETIC FIELDS
Measurement of the magnetically-induced QED birefringence of the vacuum and an improved search for laboratory axions: Project definition study of the use of assets and facilities of the Superconducting Super Collider Laboratory
[DE95-005110] p 2065 N95-24317
Complex scattering dynamics and the quantum Hall effect
[DE95-005239] p 2093 N95-24457
Toroidal response in magnetic resonance
[DE94-628406] p 2037 N95-24696
Magnetized target fusion: An ultra high energy approach in an unexplored parameter space
[DE95-005252] p 2080 N95-25289
Particle acceleration very near an x-line in a collisionless plasma
[ATR-92(7251)-4] p 2080 N95-25325
Asymptotics for the Kummer function of Bose plasmas
[DE95-607019] p 2096 N95-25428
Observation of the scalar Aharonov-Bohm effect by neutron interferometry
[DE95-607020] p 2097 N95-25446
Staggered magnetization in the Heisenberg antiferromagnet
[DE95-607102] p 2038 N95-25458
Statistical mechanics of relativistic spin-1 bosons in a magnetic field
[DE95-607100] p 2054 N95-25474
Fluctuations and electromagnetic wave scattering in macroscopically agitated plasma: Effects of turbulent diffusion
[DE95-607612] p 2081 N95-25617
Dynamics of nonadiabatic charged particles in the magnetic dipole field with imposed homogeneous magnetic field
[DE95-605222] p 2057 N95-25778
Report on the meeting on Chaotic Phenomena in Plasma
[DE94-792670] p 2062 N95-25904
A normal form approach to the theory of nonlinear betatronic motion
[DE95-603831] p 2062 N95-25944
Two dimensional Bose plasma in a magnetic field
[DE95-607629] p 2082 N95-25976
Statistical mechanics of the magnetized pair Bose gas
[DE95-607096] p 2063 N95-25993
A possibility of pi(-) Meson production by a low energy electron bunch and positive ion bunch
[NIFS-277] p 2071 N95-26029
Interaction mechanisms and biological effects of static magnetic fields
[DE95-004929] p 2009 N95-26169
Magnetic mirror effect as a trigger of collisionless magnetic reconnection
[NIFS-295] p 2083 N95-26337
A mechanism of collisionless magnetic reconnection
[NIFS-274] p 2083 N95-26339
MAGNETIC FLUX
Limiting analytic form for Aharonov-Bohm diffraction pattern
[DE95-600839] p 2065 N95-24351
MAGNETIC INDUCTION
Toroidal response in magnetic resonance
[DE94-628406] p 2037 N95-24696
Intrinsic magnetic torque at low magnetic induction
[DE95-601209] p 1959 N95-24842
MAGNETIC ISLANDS
A mechanism of collisionless magnetic reconnection
[NIFS-274] p 2083 N95-26339
MAGNETIC MEASUREMENT
Mossbauer spectroscopy, x ray diffraction and magnetic measurements of iron-nickel ultrafine particles
[DE95-601136] p 1930 N95-24840
Coercive field and domain wall properties in (Dy(x)Y(1-x))Fe2 and (Er(x)Y(1-x))Fe2
[DE95-601135] p 1937 N95-25751

MAGNETIC MIRRORS
An ion sensitive probe and its application to a mirror device
[DE95-602307] p 1970 N95-25940
Magnetic mirror effect as a trigger of collisionless magnetic reconnection
[NIFS-295] p 2083 N95-26337
MAGNETIC MOMENTS
A computing program of sample magnetic moments recognition for SQUID-magnetometer measurements
[DE94-637073] p 2037 N95-24363
Tau physics at future facilities
[DE95-006071] p 2046 N95-24591
MAGNETIC PROPERTIES
Neutron diffraction from HoNi2B2C, version 1
[DE95-005894] p 2085 N95-24431
Spin correlations in percolating networks with fractal geometry
[DE95-001074] p 2037 N95-24479
Superconductivity, magnetism and metal-insulator transitions in some ternary and pseudoternary 3d-, 4d- and 5d-metal oxides
[DE95-005904] p 2038 N95-25600
MAGNETIC RESONANCE
Toroidal response in magnetic resonance
[DE94-628406] p 2037 N95-24696
MAGNETIC SIGNALS
Wave-propagation aspects on VHF-radar applications
[PB95-141818] p 1953 N95-24649
MAGNETIC SPECTROSCOPY
The determination of the main parameters of the backward spectrometer of the 0(sup 0) facility
[DE94-628385] p 2048 N95-24692
The track system of the modernized Hyperon spectrometer
[DE95-604003] p 2058 N95-25905
MAGNETIC VARIATIONS
Geomagnetic Polar Cap (PC) index, 1975-1993
[UAG-103] p 2004 N95-24897
MAGNETIZATION
Magnetized target fusion: An ultra high energy approach in an unexplored parameter space
[DE95-005252] p 2080 N95-25289
Staggered magnetization in the Heisenberg antiferromagnet
[DE95-607102] p 2038 N95-25458
Statistical mechanics of relativistic spin-1 bosons in a magnetic field
[DE95-607100] p 2054 N95-25474
Magnetized target fusion: An overview of the concept
[DE95-005247] p 2070 N95-25594
Coercive field and domain wall properties in (Dy(x)Y(1-x))Fe2 and (Er(x)Y(1-x))Fe2
[DE95-601135] p 1937 N95-25751
Magnetic flaw detection studies: Methods and Equipment
[IFTR-38/1994] p 1978 N95-25957
The (lambda)-bar exponent for conservative systems
[DE95-607661] p 1937 N95-25977
Statistical mechanics of the magnetized pair Bose gas
[DE95-607096] p 2063 N95-25993
Magnetized pair Bose gas: Relativistic superconductor
[DE95-607846] p 2100 N95-26104
MAGNETO-OPTICS
Neutrino optics
[DE95-004236] p 2073 N95-25239
MAGNETOHYDRODYNAMIC FLOW
Evidence for modified transport due to sheared E x B flows in high-temperature plasmas
[DE95-004870] p 2079 N95-25250
MAGNETOHYDRODYNAMIC STABILITY
A proposal to introduce a turbulence factor into a diffusion coefficient of a Tokamak plasma
[DE94-777533] p 2075 N95-24272
Outline of fast analyzer for MHD equilibrium FAME
[DE94-777540] p 2076 N95-24311
Experimental and theoretical basis for advanced tokamaks
[DE95-003255] p 2077 N95-24646
Hydrodynamic instabilities in inertial confinement fusion
[DE95-003663] p 2078 N95-24667
The role of shaping in achieving high performance in DIII-D
[DE95-003877] p 2078 N95-25102
Evidence for modified transport due to sheared E x B flows in high-temperature plasmas
[DE95-004870] p 2079 N95-25250
Self-sustained turbulence and L-mode confinement in toroidal plasmas 2
[NIFS-278] p 2082 N95-25759
Isotope effect on confinement in DT plasmas
[NIFS-275] p 2083 N95-26326
MAGNETOHYDRODYNAMIC WAVES
Energetic particle drive for toroidicity-induced Alfven eigenmodes and kinetic toroidicity-induced Alfven eigenmodes in a low-shear Tokamak
[DE95-003222] p 2079 N95-25216
Self-sustained turbulence and L-mode confinement in toroidal plasmas 2
[NIFS-278] p 2082 N95-25759
Report on the meeting on Chaotic Phenomena in Plasma
[DE94-792670] p 2082 N95-25904
Impulsive Alfven coupling between the magnetosphere and ionosphere
[NIFS-276] p 2004 N95-26036
MAGNETOHYDRODYNAMICS
Flow-through Z-pinch study for radiation generation and fusion energy production
[DE95-004209] p 2076 N95-24544
Magnetically controlled deposition of metals using gas plasma
[DE95-003827] p 2077 N95-24552
Maryland controlled fusion research program
[DE95-006642] p 2081 N95-25561
Impulsive Alfven coupling between the magnetosphere and ionosphere
[NIFS-276] p 2004 N95-26036
Particle-mesh techniques
[NASA-CR-4666] p 2083 N95-26082
Magnetic mirror effect as a trigger of collisionless magnetic reconnection
[NIFS-295] p 2083 N95-26337
MAGNETOMECHANICS (PHYSICS)
Interaction mechanisms and biological effects of static magnetic fields
[DE95-004929] p 2009 N95-26169
MAGNETOMETERS
A computing program of sample magnetic moments recognition for SQUID-magnetometer measurements
[DE94-637073] p 2037 N95-24363
MAGNETOSPHERE-IONOSPHERE COUPLING
Impulsive Alfven coupling between the magnetosphere and ionosphere
[NIFS-276] p 2004 N95-26036
MAGNETOSPHERIC ION DENSITY
Dynamics Explorer 1, retarding ion mass spectrometer summary spectrograms-82/110 to 82/229 spin-time spectrograms for H(+), He(+), O(+), N(+), O(++), M/Z = 2, and molecular ions
[NASA-TM-108485] p 2003 N95-24763
Dynamics Explorer 1, retarding ion mass spectrometer summary spectrograms-82/230 to 82/265 spin-time spectrograms for H(+), He(+), O(+), N(+), O(++), M/Z = 2, and molecular ions
[NASA-TM-108486] p 2003 N95-24764
MAGNETOSTRICTION
Temperature dependence of magnetic anisotropy and magnetostriction: Beyond the mean-field theory
[DE94-634529] p 2084 N95-24244
MAGNETRON SPUTTERING
The effect of the impedance of the generator and intermediate circuits on the impedance of plasma as it applies to magnetron sputtering of thin films in a radio-frequency field
[IFTR-8-1994] p 2083 N95-26019
MAGNETS
Neutrino optics
[DE95-004236] p 2073 N95-25239
The geometry of disorder: Theoretical investigations of quasicrystals and frustrated magnets
[DE95-006641] p 1936 N95-25560
Domain growth in weakly disordered magnets: A coupled map lattice approach
[DE95-607663] p 2090 N95-25979
MAMMARY GLANDS
Photonics: From target recognition to lesion detection
p 2023 N95-25259
MAN ENVIRONMENT INTERACTIONS
Our changing planet: The FY 1995 U.S. Global Change Research Program p 2002 N95-25852
MAN MACHINE SYSTEMS
Aerospace medicine and biology: A continuing bibliography with indexes (supplement 400)
[NASA-SP-7011(400)] p 2011 N95-24464
A crew-centered flight deck design philosophy for High-Speed Civil Transport (HSCT) aircraft
[NASA-TM-109171] p 1910 N95-24582
Activity Management System user reference manual
[DE95-000989] p 2105 N95-24654
Aerospace medicine and biology: A continuing bibliography with indexes (supplement 401)
[NASA-SP-7011(401)] p 2012 N95-25800
MANAGEMENT
Computer support for cooperative tasks in Mission Operations Centers
[DE95-004928] p 2102 N95-25771
MANAGEMENT INFORMATION SYSTEMS
Workflow automation architecture standard
[DE95-004748] p 2035 N95-24248
MANAGEMENT METHODS
Issues in NASA program and project management
[NASA-SP-6101(08)] p 2102 N95-24565
NASA strategic plan
[NASA-TM-110592] p 2103 N95-26262
MANAGEMENT PLANNING
Automated Procurement System (APS): Project management plan (DS-03), version 1.2
[NASA-CR-196576] p 2102 N95-24442
Report of the Space Shuttle Management Independent Review Team
[NASA-TM-110579] p 1919 N95-24466
Continual improvement plan
[NASA-TM-110574] p 2103 N95-25849
NASA strategic plan
[NASA-TM-110592] p 2103 N95-26262
MANAGEMENT SYSTEMS
Integrated planning: A baseline development perspective
[DE95-004945] p 2102 N95-24905
MANGANESE ALLOYS
The geometry of disorder: Theoretical investigations of quasicrystals and frustrated magnets
[DE95-006641] p 1936 N95-25560
MANIFOLDS (MATHEMATICS)
Finite quantum physics and noncommutative geometry
[DE94-634282] p 2027 N95-24228
Distances on a lattice from noncommutative geometry
[DE94-634327] p 2027 N95-24229
Semiclassical asymptotics on covering manifolds and morse inequalities
[PB95-165510] p 2028 N95-24251
Construction of the moduli space of monopoles
[PB95-165528] p 2028 N95-24255
Geometric quantization of symplectic manifolds with symmetry
[DE94-628435] p 2031 N95-24698
Equivariant localization: BV-geometry and supersymmetric dynamics
[DE94-628436] p 2036 N95-24699
Two dimensional simplicial paths
[DE95-607087] p 2036 N95-25434
Equivariant Kaehler geometry and localization in the G/G model
[DE95-607073] p 2036 N95-25455
Involutive co-distributions preserved by transitive families of vector fields
[DE95-607078] p 2032 N95-25457
Constraints, complex structures and quantization
[DE95-605252] p 2037 N95-25781
The rotations of deformable bodies. Part 1: Geometry and Kinematics
[IFTR-7/1994] p 2039 N95-26332
MANIPULATORS
Simulating the dynamic interaction of a robotic arm and the Space Shuttle remote manipulator system
[NASA-CR-195076] p 2027 N95-26086
MANNED MARS MISSIONS
JPRS report: Science and technology. Central Eurasia: Space
[JPRS-USP-94-008] p 1916 N95-24359
MANNED SPACE FLIGHT
NASA video catalog
[NASA-SP-7109(01)] p 2103 N95-24238
Space radiation dosimetry on US and Soviet manned missions p 2009 N95-25934
MANNED SPACECRAFT
Apollo 12: Pinpoint for science
[NASA-TM-110576] p 1917 N95-25424
MANUALS
HET mini-manual
[PB95-165338] p 2057 N95-25900
MANUFACTURING
Display technologies in Russia, Ukraine, and Belarus
[ISBN-1-883712-36-X] p 2085 N95-24460
A neural network controller for automated composite manufacturing p 2025 N95-25271
An overview of NDE methods for thick composites and a proposal for analysis of computed technology data
[AD-A288733] p 1979 N95-26055
MANY BODY PROBLEM
The influence of CDM on the dynamical estimate of (Omega) in the local neighborhood
[DE95-005212] p 2109 N95-24455
Diagrammatic many-body perturbation expansion for atoms and molecules
[PB95-165221] p 2056 N95-25620
Atomistic studies of grain boundaries in NiAl
[DE95-005208] p 1937 N95-26014
MAPPING
A fast tracking method using resonance basis Hamiltonians
[DE95-004292] p 2068 N95-24664

Hardcopy extraction considerations for Vector Product Format (VPF) products
[AD-A288620] p 2106 N95-25608

MAPS

Geologic mapping of Argyre Planitia
[NASA-CR-197986] p 2112 N95-24303
Identification of potential groundwater flow paths using geological and geophysical data
[DE95-006253] p 1988 N95-24407
Mapping, charting and geodesy handbook
[AD-A286558] p 1989 N95-24502
Computer analysis of graphics for the requirements of computer-aided design systems
[IPPT-29-1992] p 2016 N95-25392

MARINE BIOLOGY

Spaceborne synthetic aperture radar: Current status and future directions. A report to the Committee on Earth Sciences, Space Studies Board, National Research Council
[NASA-TM-4679] p 1955 N95-25710

MARINE CHEMISTRY

Spaceborne synthetic aperture radar: Current status and future directions. A report to the Committee on Earth Sciences, Space Studies Board, National Research Council
[NASA-TM-4679] p 1955 N95-25710

MARKET RESEARCH

Supercritical carbon dioxide cleaning market assessment and commercialization/deployment plan
[DE94-017394] p 1998 N95-24653
Commercial Space Transportation Study (CSTS)
[SSD94D0035] p 1919 N95-25747

MARKOV PROCESSES

Hidden Markov models and neural networks for fault detection in dynamic systems p 2024 N95-25261

MARS (PLANET)

Mars observer mission: Mapping the Martian world
[NASA-CR-110585] p 2112 N95-24672
Return to the red planet: The Mars Observer Mission
[NASA-CR-197707] p 2113 N95-26336

MARS ENVIRONMENT

Return to the red planet: The Mars Observer Mission
[NASA-CR-197707] p 2113 N95-26336

MARS EXPLORATION

Mars observer mission: Mapping the Martian world
[NASA-CR-110585] p 2112 N95-24672
Return to the red planet: The Mars Observer Mission
[NASA-CR-197707] p 2113 N95-26336

MARS OBSERVER

Mars observer mission: Mapping the Martian world
[NASA-CR-110585] p 2112 N95-24672
Return to the red planet: The Mars Observer Mission
[NASA-CR-197707] p 2113 N95-26336

MARS SATELLITES

Mars observer mission: Mapping the Martian world
[NASA-CR-110585] p 2112 N95-24672

MARS SURFACE

Geologic mapping of Argyre Planitia
[NASA-CR-197986] p 2112 N95-24303
Mars observer mission: Mapping the Martian world
[NASA-CR-110585] p 2112 N95-24672

MARYLAND

Maryland controlled fusion research program
[DE95-006642] p 2081 N95-25561

MASERS

Nonlinear analysis of millimeter and sub-millimeter wave sources such as Cerenkov masers, orotrons, and ubitrons
[AD-A288777] p 1974 N95-26114

MASS DISTRIBUTION

Investigation of the gross structure of spectra and mass distributions of hadronic resonances
[DE94-636799] p 2043 N95-24361
Chiral limit of QCD
[DE95-005245] p 2094 N95-24610

MASS SPECTRA

The physics and experimental program of the Relativistic Heavy Ion Collider (RHIC)
[DE95-003416] p 2066 N95-24495
On a possible explanation of the origin of the quark mass spectrum
[DE95-605315] p 2063 N95-25968

MASS SPECTROMETERS

Development of a portable mass spectrometric system for determination of isotopic composition of solid uranium samples using fluorine volatilization
[DE95-005728] p 1969 N95-25384

MASS SPECTROSCOPY

Use of mass spectrometric methods for field screening of VOC's
[DE95-004903] p 1999 N95-25249
Development of a portable mass spectrometric system for determination of isotopic composition of solid uranium samples using fluorine volatilization
[DE95-005728] p 1969 N95-25384

MASSIVE STARS

Core-collapse supernovae and nucleosynthesis
[NASA-CR-197731] p 2109 N95-25122

MASSIVELY PARALLEL PROCESSORS

Implementation of a parallel algorithm for thermo-chemical nonequilibrium flow simulations
[DE95-004758] p 1961 N95-24262
A practical approach to portability and performance problems on massively parallel supercomputers
[DE95-005251] p 2020 N95-24612
From neural-based object recognition toward microelectronic eyes p 2023 N95-25257
Alpha(sub critical) for parallel processors
[PB95-165320] p 2022 N95-25625
A domain decomposition study of massively parallel computing in compressible gas dynamics
[DE95-004759] p 1965 N95-25895
Holograpy machine HORN-1 for computer-aided retrieve of virtual three-dimensional image
[NIFS-218] p 1971 N95-26182
Nonlinear structural analysis on distributed-memory computers p 1985 N95-26272

MATCHING

Orientation determination of aircraft using visual 3D matching and radar. Case study 2
[PB95-165791] p 1955 N95-25749

MATERIALS SCIENCE

JPRS report: Science and technology. Central Eurasia
[JPRS-UST-94-018] p 1950 N95-24472
Dynamic methods for determining the material characteristics of saturated permeable media
[IFTR-17/1993] p 1932 N95-26107

MATERIALS TESTS

An examination of metal felt wicks for heat-pipe applications
[DE95-002608] p 1994 N95-25109
Recent progress in shear punch testing
[DE95-005962] p 1937 N95-26007

MATHEMATICAL MODELS

Electromagnetic waves and photoacoustic transformation in gyrotropic superlattices p 2083 N95-24205
Actively controlled shaft seals for aerospace applications
[NASA-CR-198035] p 1974 N95-24218
Estimates of effects of residual acceleration on USML-1 experiments
[NASA-CR-197964] p 2084 N95-24261
Superconducting in the near half-filling Hubbard model
[DE94-634857] p 2092 N95-24275
A functional integral approach without slave bosons to the Anderson model
[DE94-634858] p 2028 N95-24276
Electron-phonon interaction in the Hubbard model
[DE94-634859] p 2092 N95-24277
Application of compartmental metabolic models for determination of retention and excretion functions
[DE95-600249] p 2010 N95-24367
Numerical investigation of Schwinger-Dyson and Bethe-Salpeter equations with Gauss potential in the framework of the quarkonium model
[DE94-636730] p 2029 N95-24387
On the finite element implementation of the generalized method of cells micromechanics constitutive model
[NASA-CR-195451] p 1980 N95-24398
Numerical simulation methods for wave propagation through optical waveguides
[DE94-634313] p 2073 N95-24402
Effect of density gradients in confined supersonic shear layers, part 1
[NASA-CR-198029] p 1962 N95-24412
Effect of density gradients in confined supersonic shear layers. Part 2: 3-D modes
[NASA-CR-198030] p 1962 N95-24413
The role of force measurements in advanced vibration test methods
[DE95-001833] p 1975 N95-24462
UEDGE and DEGAS modeling of the DIII-D scrape-off layer plasma
[DE95-003652] p 2076 N95-24490
Evaluation of the performance of an annular diffusion denuder
[DE95-002258] p 1998 N95-24606
Nonequilibrium multiphase mixture modeling of energetic material response
[DE95-003353] p 1948 N95-24608
Automation based on knowledge modeling theory and its applications in engine diagnostic systems using Space Shuttle Main Engine vibrational data
[NASA-CR-197983] p 1922 N95-24626
Aerodynamic parameter estimation via Fourier modulating function techniques
[NASA-CR-4654] p 1911 N95-24630
EXODUS 2: A finite element data model
[DE95-004267] p 2016 N95-24659
Capillary flow on narrow strips and in V-shaped grooves
[DE95-000543] p 1935 N95-24716
Technical report series on global modeling and data assimilation. Volume 5: Documentation of the AIRES/GEOS dynamical core, version 2
[NASA-TM-104606-VOL-5] p 2003 N95-24766
Modeling plasma/material interactions during a tokamak disruption
[DE95-004247] p 2078 N95-24861
On the uncertainty in single molecule fluorescent lifetime and energy emission measurements
[NASA-CR-198009] p 2049 N95-24877
Report series in aerosol science
[DE95-737628] p 1999 N95-24904
The transmission and control of vibrational power in a two stage isolation system with a water-loaded substructure
[ISVR-TR-235] p 1975 N95-24992
Software fault tolerance in computer operating systems
[NASA-CR-197999] p 2016 N95-24993
Future emissions and concentrations of carbon dioxide: Key ocean/atmosphere/land analyses
[CSIRO-TP-31] p 1999 N95-25199
A solubility model for amorphous silica in concentrated electrolytes
[DE95-004896] p 1931 N95-25252
Modeling of the simulated countercurrent moving-bed chromatographic reactor used for the oxidative coupling of methane
[DE95-004930] p 1924 N95-25286
An analysis of hypercritical states in elastic and inelastic systems
[IFTR-1/1994] p 2037 N95-25339
Kinetic modeling of the atomic layer epitaxy window in group 4 semiconductor growth
[DE95-005903] p 2089 N95-25391
The diffraction of electromagnetic waves by screens placed at the boundaries of dielectric media
[IFTR-4/1994] p 1954 N95-25393
Neutrino oscillations from discrete non-Abelian family symmetries
[DE95-004355] p 2052 N95-25403
Critical parameters of Quark-Hadron phase transition with interacting and massive quarks
[DE95-607143] p 2052 N95-25436
Closed orbit related problems: Correction, feedback, and analysis
[DE95-005969] p 2070 N95-25441
Equivariant Kaehler geometry and localization in the G/G model
[DE95-607073] p 2036 N95-25455
Fast algorithms for transport models
[DE95-007064] p 2054 N95-25479
A simple relation among the quark masses
[DE95-703783] p 2055 N95-25494
Atmospheric and terrain effects on acoustic propagation
[AD-A288727] p 2039 N95-25503
A phase-transition induced by the struggle for life in a competitive coexistence model in ecology
[DE95-607047] p 2001 N95-25521
HyperKaehler metrics building and integrable models
[DE95-607077] p 2038 N95-25524
Quantum mechanical analogy for solving a competitive coexistence model in ecology
[DE95-607046] p 2001 N95-25531
Theoretical studies in hadronic and nuclear physics
[DE95-006643] p 2098 N95-25562
New techniques to test fatigue properties of coined sheet specimens. Part 3: Fatigue testing and analysis of a component like coining in sheet steel materials
[PB95-165668] p 1982 N95-25569
Implementation of wave propagation model for windows
[PB95-165742] p 2017 N95-25571
Issues related to prediction of residual stresses in titanium alloy matrix composites
[DE95-005243] p 1926 N95-25596
Central extension of a new W(infinity)-type algebra
[DE95-607086] p 2037 N95-25599
A numerical prediction of the precipitation and hydrology of California
[DE95-004966] p 2006 N95-25635
Homogeneous anisotropic cosmological models in the minimum quadratic Poincare gauge theory of gravity
[DE95-607083] p 2110 N95-25647
A superfield generalization of the classical action-at-a-distance theory
[DE95-607084] p 1955 N95-25648
The energy efficiency of passive solar heating systems
[IFTR-22/1994] p 1995 N95-25758

The hard truth --- a method to determine the reliability of a specific feature of a Bayesian solution
[DE95-005240] p 2033 N95-25767
Wide-area traffic: The failure of Poisson modeling
[DE95-004685] p 2015 N95-25773
Recent improvements to and validation of the one dimensional NASA wave rotor model
[NASA-TM-106913] p 1908 N95-25962
Results/prospects in E777/851/865
[DE95-005959] p 2064 N95-26006
Cognitive diagnosis combined with latent trait theory and multiphase responses
[AD-A288701] p 2013 N95-26010
Describing the macroscopic world: Closing the circle within the dynamical reduction program
[DE95-606997] p 2100 N95-26046
Calculating the thermodynamic properties of planar and spherical liquid-vapour interface
[DE95-608777] p 2100 N95-26105
Splines in two-dimensional problems
[IFTR-2/1993] p 2035 N95-26106
Thermal barrier coating life modeling in aircraft gas turbine engines p 1947 N95-26140
Intermediate-sized natural gas fueled carbonate fuel cell power plants
[DE95-004990] p 1996 N95-26171
A generic interface element for COMET-AR
[NASA-CR-195075] p 1983 N95-26199
Assessment of computational models for thermoelectroelastic multilayered plates p 1987 N95-26283
Aerodynamics model for a generic ASTOVL lift-fan aircraft
[NASA-TM-110347] p 1908 N95-26302
Feed system design for a reduced pressure tank p 1923 N95-26310

MATHEMATICAL PROGRAMMING
New approaches to optimization in aerospace conceptual design
[NASA-CR-196695] p 1910 N95-24436
Semi-infinite mathematical programming: A collocation approach
[DE94-634273] p 2016 N95-24708

MATRICES (MATHEMATICS)
Bounds for departure from normality and the Frobenius norm of matrix eigenvalues
[DE95-006144] p 2030 N95-24592
Generators of matrix factorable representations of block-tridiagonal and inverse matrices
[DE94-628387] p 2031 N95-24694
Domain decomposition and generators of direct methods of the solution of linear equation systems with general block-tridiagonal matrices
[DE94-628388] p 2031 N95-24695
Quasi-generalized matrix processes and representations of general block tridiagonal matrices
[DE94-628377] p 2031 N95-24704
Natural elementary factorization of general block-tridiagonal matrices in case of zero minors of both types
[DE94-628378] p 2031 N95-24705
On the structure of direct representations of inverse matrices to the block-tridiagonal ones in case of zero main block angular minors
[DE94-628376] p 2031 N95-24859
Matrix element and complex l-plane evaluation of two-loop vacuum amplitudes in QED on S4
[DE95-607099] p 2097 N95-25473
Dynamic matrices and their application to the concept of a semi-sparse matrix
[AD-A288688] p 2035 N95-26051

MATRIX MATERIALS
LH2 fuel tank design for SSTO p 1987 N95-26309

MATRIX METHODS
Matrix element and complex l-plane evaluation of two-loop vacuum amplitudes in QED on S4
[DE95-607099] p 2097 N95-25473

MATRIX THEORY
On the structure of direct representations of inverse matrices to the block-tridiagonal ones in case of zero main block angular minors
[DE94-628376] p 2031 N95-24859

MATTER (PHYSICS)
Research in nuclear astrophysics: Stellar collapse and supernovae
[DE95-004300] p 2110 N95-25343
Anisotropy of dilepton emission from nuclear collisions
[DE95-004354] p 2070 N95-25634

MAXIMUM ENTROPY METHOD
Nonlinearity induced nontrivial dynamics in the Jaynes-Cummings Hamiltonian
[DE95-607004] p 2032 N95-25452

MAXIMUM LIKELIHOOD ESTIMATES
Estimate of probability of crack detection from service difficulty report data
[PB95-149381] p 1905 N95-24295

MAXWELL EQUATION
Decoherence, determinism and chaos revisited
[DE95-006070] p 2094 N95-24578

MEASUREMENT
Creation of a scalar potential in 2D dilaton gravity
[DE95-006066] p 2003 N95-24577
Geometric quantization of symplectic manifolds with symmetry
[DE94-628435] p 2031 N95-24698
Metrology measurement capability
[DE95-005411] p 1969 N95-25381
Constraints, complex structures and quantization
[DE95-605252] p 2037 N95-25781
Quantization of a Hamiltonian system with an infinite number of degrees of freedom
[DE95-605279] p 2034 N95-25783

MEASURING INSTRUMENTS
Probing anomalous gauge boson couplings at LEP
[DE95-005934] p 2044 N95-24420
Metrology measurement capability
[DE95-005411] p 1969 N95-25381
Workshop report: Measurement techniques in highly transient, spectrally rich combustion environments
[AD-A288395] p 1969 N95-25606
National standard and code compliance for electrical equipment installed in hazardous locations for the void fraction instrument
[DE95-002158] p 1960 N95-26092

MECHANICAL DEVICES
Rotary actuator
[NASA-CASE-MFS-28581-1] p 1936 N95-25545
Preload release mechanism
[NASA-CASE-MSC-22327-1] p 1976 N95-25592

MECHANICAL ENGINEERING
NASA-UVA light aerospace alloy and structures technology program (LA2ST)
[NASA-CR-198041] p 1933 N95-24220
JPRS report: Science and technology. Central Eurasia
[JPRS-UST-94-027] p 1957 N95-24470
The 1994 NASA/USRA/ADP Design Projects
[NASA-CR-197415] p 2101 N95-26304
LH2 fuel tank design for SSTO p 1987 N95-26309

MECHANICAL PROPERTIES
The temperature and strain rate dependence of the flow stress of single crystal NiAl deformed along the zone group axes (110)
[DE95-003634] p 2083 N95-24233
Time dependent indentation testing at non-ambient temperatures utilizing the high temperature mechanical properties microprobe
[DE95-005895] p 1933 N95-24432
Nonequilibrium multiphase mixture modeling of energetic material response
[DE95-003353] p 1948 N95-24608
Techniques for studying the mechanical properties of materials in complex stress states
[IFTR-34/1994] p 1983 N95-26178

MECHANICAL SHOCK
The critical diameter, detonation velocity and shock sensitivity of Australian PBXW-115
[DSTO-TR-0076] p 1947 N95-24394

MEDICAL EQUIPMENT
Annual report of National Institute of Radiological Sciences
[DE94-792664] p 2009 N95-25902

MEDICAL SCIENCE
JPRS report: Science and technology. Central Eurasia
[JPRS-UST-94-035] p 2016 N95-24429
JPRS report: Science and technology. Central Eurasia
[JPRS-UST-94-024] p 1958 N95-24620
JPRS Report: Science and technology. Central Eurasia
[JPRS-UST-94-032] p 1950 N95-24759
JPRS Report: Science and technology. Central Eurasia
[JPRS-UST-94-031] p 1988 N95-24760
Neural networks: Application to medical imaging p 2025 N95-25267

MEDICAL SERVICES
Aviation epidemiology data register
[AD-A279303] p 2010 N95-24423
Activities of the National Institute of Radiological Sciences
[DE95-709916] p 2072 N95-26165
Testing of experimental antileishmanial compounds
[AD-A288807] p 2009 N95-26193

MELLIN TRANSFORMS
Statistical mechanics of the magnetized pair Bose gas
[DE95-607096] p 2063 N95-25993

MELTING
Melting of the moving vortex lattice in the presence of disorder
[DE95-004126] p 2087 N95-24868
Rotational melting in displacive quantum paraelectrics
[DE95-607804] p 2091 N95-26252

MEMBRANES
Development of novel active transport membrane devices
[DE95-002658] p 1932 N95-26093

MEMORY (COMPUTERS)
DOLIB: Distributed Object Library
[DE95-004791] p 2019 N95-24250
CD-ROM in the age of internet
[DE95-005067] p 2104 N95-24454
Parallel processing for scientific computations
[NASA-CR-198013] p 2020 N95-24563

MENTAL PERFORMANCE
Cognitive diagnosis combined with latent trait theory and multiphase responses
[AD-A288701] p 2013 N95-26010
Sleep patterns in air traffic controllers working rapidly rotating shifts: A field study
[DOT/FAA/AM-95/12] p 2012 N95-26204

MERCURY OXIDES
Device-quality tunnel junctions on the high (T(sub c)) super conductor HgBa2CuO(4+delta)
[DE95-004646] p 2084 N95-24279
BCS-like gap structure of HgBa2CuO(4+delta) tunnel junctions
[DE95-004125] p 2087 N95-24855

MESOMETEOROLOGY
Use of cloud observations and mesoscale meteorology models to evaluate and improve cloud parameterizations
[DE95-006256] p 2005 N95-24613

MESON RESONANCE
Baryon spectroscopy and the omega minus
[DE95-004838] p 2052 N95-25374

MESON-NUCLEON INTERACTIONS
On leading charmed meson production in pi-nucleon interactions
[DE94-636797] p 2043 N95-24360
Radiative corrections for pion polarizability experiments
[DE95-607177] p 2053 N95-25462

MESONS
On leading charmed meson production in pi-nucleon interactions
[DE94-636797] p 2043 N95-24360
New physics effects on CP Violation in B decays
[DE94-628617] p 2049 N95-24722
Notion of the inclusive spectra and cross sections of B-meson production in hadronic interactions of high energies
[DE94-628628] p 2049 N95-24887
Probing new physics in rare charm processes
[DE95-006067] p 2050 N95-24903
B physics with CDF: Recent results and future prospects
[DE95-004793] p 2051 N95-25372
Zero sound velocity in pi, rho mesons at different temperatures
[DE95-607145] p 2053 N95-25459
Multichannel resonances and closed channels (scalar sector)
[DE94-628629] p 2055 N95-25537
Theoretical studies in hadronic and nuclear physics
[DE95-006643] p 2098 N95-25562
Anisotropy of dilepton emission from nuclear collisions
[DE95-004354] p 2070 N95-25634
Quasi two body decays of charm mesons
[DE94-792634] p 2057 N95-25901
Excited states of mesons within the NJL model with the homogeneous vacuum gluon field
[DE95-605323] p 2058 N95-25909
Preliminary results on the decays D(+) yields K(+)pi(+)pi(-), D(+) yields K(+)K(+)K(-)
[DE95-004865] p 2071 N95-26011

MESOSCALE PHENOMENA
Use of cloud observations and mesoscale meteorology models to evaluate and improve cloud parameterizations
[DE95-006256] p 2005 N95-24613
Global ocean circulation and equator-pole heat transport as a function of ocean GCM resolution
[DE95-004198] p 2000 N95-25279

MESSAGE PROCESSING
Dialogue transcription tools
[TN-94-1] p 2016 N95-24536

METAL CLUSTERS
The transformation of organic amines by transition metal cluster compounds
[DE95-004180] p 1923 N95-24851
Optical properties of fractal nanocomposites
[DE95-005414] p 1926 N95-25295

METAL COATINGS
Au/Cr sputter coating for the protection of alumina during sliding at high temperatures
[NASA-TM-106853] p 1923 N95-24437

METAL FATIGUE
New techniques to test fatigue properties of coined sheet specimens. Part 2: Comparison of different materials, forming operations and life prediction techniques for a simple test geometry
[PB95-165122] p 1982 N95-25444
New techniques to test fatigue properties of coined sheet specimens. Part 4: Development of experimental techniques
[PB95-165130] p 1982 N95-25445
New techniques to test fatigue properties of coined sheet specimens. Part 3: Fatigue testing and analysis of a component like coining in sheet steel materials
[PB95-165668] p 1982 N95-25569
Proceedings of the 2d USAF Aging Aircraft Conference
[AD-A288217] p 1911 N95-25578
A description of the cyclical properties of an aluminum alloy based on complex stress state tests
[IFTR-29/1994] p 1936 N95-25638
Stress analysis of a crack in the residual stress field by welding and its application to the fatigue crack propagation
[NAL-TR-1248] p 1983 N95-25796
Recent progress in shear punch testing
[DE95-005962] p 1937 N95-26007
Techniques for studying the mechanical properties of materials in complex stress states
[IFTR-34/1994] p 1983 N95-26178
Changes in the strength characteristics of 15HM boiler steel caused by initial plastic deformation under constant and monotonic loads
[IFTR-30/1994] p 1938 N95-26333

METAL FIBERS
Wear resistant composite structure of vitreous carbon containing convoluted fibers
[DE95-006255] p 1925 N95-24426

METAL FILMS
Performance of solid lubricated ball bearings at high-temperatures in a vacuum
[NAL-TR-1243] p 1976 N95-25323
Ion beam mixing of titanium overlayers with hydroxyapatite substrates
[DE95-005278] p 1935 N95-25379
In situ XAFS study of oxides formed on nickel thin film electrodes in KOH solution
[AD-A288735] p 1932 N95-26056
Continuous phase and amplitude holographic elements
[NASA-CASE-NPO-18791-1] p 1971 N95-26340

METAL FOILS
Fission foil detector calibrations with high energy protons p 2060 N95-25924

METAL IONS
Na-like autoionizing levels: Plasma diagnostics and prospects for photopumped soft x-ray lasers
[DE95-004207] p 1972 N95-25100
Recent advances in lithium ion technology
[DE95-004769] p 2054 N95-25470
Electron spin resonance of radicals and metal complexes
[DE95-605640] p 2055 N95-25499

METAL MATRIX COMPOSITES
Composite ductility: The role of reinforcement and matrix
[DE95-003664] p 1925 N95-24590
NASA-UVa light aerospace alloy and structures technology program supplement: Aluminum-based materials for high speed aircraft
[NASA-CR-4645] p 1935 N95-24878
Strengthening of NiAl matrix composites
[AD-A288923] p 1926 N95-25505
Issues related to prediction of residual stresses in titanium alloy matrix composites
[DE95-005243] p 1926 N95-25596

METAL SHEETS
New techniques to test fatigue properties of coined sheet specimens. Part 2: Comparison of different materials, forming operations and life prediction techniques for a simple test geometry
[PB95-165122] p 1982 N95-25444
New techniques to test fatigue properties of coined sheet specimens. Part 4: Development of experimental techniques
[PB95-165130] p 1982 N95-25445
New techniques to test fatigue properties of coined sheet specimens. Part 3: Fatigue testing and analysis of a component like coining in sheet steel materials
[PB95-165668] p 1982 N95-25569

METAL SURFACES
An investigation of the effect of surface impurities on the adsorption kinetics of hydrogen chemisorbed onto iron
[NASA-CR-197967] p 1933 N95-24400

METAL-METAL BONDING
The transformation of organic amines by transition metal cluster compounds
[DE95-004180] p 1923 N95-24851

METALLIC GLASSES
Whisker reinforced glass ceramic
[DE95-005568] p 1927 N95-25998

METALLURGY
Processing and properties of iridium alloys for space power applications
[DE95-005902] p 1935 N95-25390

METALS
Fractal studies on the positron annihilation in metals
[DE94-634488] p 2041 N95-24232
Entropy and enthalpy of adsorption of gaseous chlorides of metals on quartz glass as a function of the molecular composition
[DE94-627162] p 2093 N95-24481
Chelant extraction and REDOX manipulation for mobilization of heavy metals from contaminated soils
[DE95-004131] p 2000 N95-25363
Combustion characteristics of metallized hydrocarbon fuels
[NAL-TR-1224] p 1949 N95-25769
Structural and thermodynamic properties of 3-d transition metals: Pseudopotential theory revisited
[DE95-605639] p 1937 N95-25983
Disposal of electronic equipment
[PB95-177861] p 2002 N95-26047
An experimental determination of the plastic anisotropy of metal
[IFTR-33/1994] p 1938 N95-26179

METASTABLE ATOMS
Inelastic collisions of negative muons and hadrons with Helium metastable atoms
[DE95-607538] p 2055 N95-25493

METEORITE CRATERS
Biospheric effects of a large extraterrestrial impact: Case study of the cretaceous/tertiary boundary crater
[NASA-CR-198015] p 1997 N95-24501

METEORITIC COMPOSITION
Fourth symposium of the geological survey of Japan on remote sensing of satellite geology
[PB95-178737] p 1917 N95-25750

METEOROLOGICAL INSTRUMENTS
Replicator for characterization of cirrus and polar stratospheric cloud particles
[NASA-CR-197992] p 2005 N95-24411

METEOROLOGY
Design and development of a cloud reference library and support for cloud and simulation communities. Summary report
[AD-A288704] p 2006 N95-26012

METHANE
XAS studies of Ni(I), Ni(II), and Ni(III) complexes
[DE95-004844] p 1928 N95-24257
Modeling of the simulated countercurrent moving-bed chromatographic reactor used for the oxidative coupling of methane
[DE95-004930] p 1924 N95-25286

METHOD OF CHARACTERISTICS
New evaluation method of superconductor characteristics for realizing the Large Helical Device
[NIFS-297] p 2071 N95-25855

METHYL ALCOHOL
High octane ethers from synthesis gas-derived alcohols
[DE95-001146] p 1948 N95-24655

METROLOGY
Metrology: Measurement assurance program guidelines
[NASA-RP-1364] p 1950 N95-24543
Metrology measurement capability
[DE95-005411] p 1969 N95-25381

MICROANALYSIS
FT-IR microscopical analysis with synchrotron radiation: The microscope optics and system performance
[DE95-004834] p 1928 N95-24265
Time dependent indentation testing at non-ambient temperatures utilizing the high temperature mechanical properties microprobe
[DE95-005895] p 1933 N95-24432

MICROCHANNEL PLATES
Large-format high resolution microchannel plate detectors for ultraviolet astronomy
[NASA-CR-197993] p 2108 N95-25104

MICROCOMPUTERS
Introduction to the Monte Carlo methods
[DE94-628386] p 2035 N95-24693

MICROELECTRONICS
The potential of vacuum microelectronics for space reactor applications
[DE95-000542] p 1958 N95-24586
Physics in Ukraine International Conference. Volume 4: Radiophysics and Electronics
[DE95-605570] p 2038 N95-25616
Potential of diamond for applications in microelectronics
[PB95-141446] p 1942 N95-25633

MICROGRAVITY
STS-66 mission highlights resource tape
[NASA-TM-110550] p 1918 N95-24197
Laser light scattering, from an advanced technology development program to experiments in a reduced gravity environment
[NASA-TM-110496] p 1971 N95-24530
JPRS report: Science and technology. Central Eurasia: Seminar on materials science
[JPRS-UST-95-007] p 1920 N95-24761
Studies of two-phase gas-liquid flow in microgravity
[NASA-CR-195434] p 1963 N95-24906
ESA Bulletin No. 81 p 2114 N95-25200
Electric field effects on a near-critical fluid in microgravity
[NASA-TM-106894] p 2099 N95-25878
Universal Test Facility p 1918 N95-26305

MICROGRAVITY APPLICATIONS
Stereo imaging velocimetry for microgravity applications
[NASA-TM-110494] p 1949 N95-24416

MICROHARDNESS
Robotic weld overlay coatings for erosion control
[DE95-005187] p 1939 N95-24285

MICROMECHANICS
On the finite element implementation of the generalized method of cells micromechanics constitutive model
[NASA-CR-195451] p 1980 N95-24398
An evaluation of a coupled microstructural approach for the analysis of functionally graded composites via the finite-element method
[NASA-CR-195455] p 1925 N95-24438

MICROPROCESSORS
From neural-based object recognition toward microelectronic eyes p 2023 N95-25257
VLSI neuroprocessors p 2023 N95-25258
Smart vision chips: An overview p 2024 N95-25265

MICROSTRIP ANTENNAS
Broadband uniplanar microstrip to slot-line transitions
[NASA-CR-195448] p 1957 N95-24476
Experimental study of tapered slot elements
[PB95-165163] p 1955 N95-25644

MICROSTRIP TRANSMISSION LINES
Broadband uniplanar microstrip to slot-line transitions
[NASA-CR-195448] p 1957 N95-24476

MICROSTRUCTURE
NASA-UVA light aerospace alloy and structures technology program (LA2ST)
[NASA-CR-198041] p 1933 N95-24220
An evaluation of a coupled microstructural approach for the analysis of functionally graded composites via the finite-element method
[NASA-CR-195455] p 1925 N95-24438
Temperature and strain-rate effects on deformation mechanisms in irradiated stainless steel
[DE95-004941] p 1934 N95-24449
Nanostructured materials
[DE95-004595] p 2088 N95-25280
Optical properties of fractal nanocomposites
[DE95-005414] p 1926 N95-25295
Effects of acetylacetone additions on PZT thin film processing
[DE95-006322] p 1941 N95-25370
Reciprocal space analysis of the microstructure of luminescent and nonluminescent porous silicon films
[DE95-005420] p 1941 N95-25382
Processing and properties of iridium alloys for space power applications
[DE95-005902] p 1935 N95-25390
Synthesis and processing of Al2O3/Al composites by in situ reaction of aluminum and mullite
[DE95-006224] p 1937 N95-25775
Atom probe field ion microscopy of Type 308 CRE stainless steel welds
[DE94-019161] p 1938 N95-26064
Atomic force microscopy as a process characterization tool for GaAs-based integrated circuit fabrication
[DE95-006223] p 2064 N95-26168

MICROWAVE AMPLIFIERS
Experimental and theoretical development towards a 500 MW, one-microsecond, L-band relativistic klystron amplifier
[DE95-003682] p 1958 N95-24589
A vacuum window for a 1 MW CW 110 GHz gyrotron
[DE94-016584] p 2079 N95-25108
Radial electron-beam-breakup transit-time oscillator
[DE95-005731] p 1959 N95-25385

MICROWAVE ANTENNAS
Broadband uniplanar microstrip to slot-line transitions
[NASA-CR-195448] p 1957 N95-24476

MICROWAVE FREQUENCIES
Wave-propagation aspects on VHF-radar applications
[PB95-141818] p 1953 N95-24649

MICROWAVE IMAGERY
Airborne imaging of tropospheric emission at millimeter and submillimeter wavelengths
[NASA-TM-110498] p 2003 N95-24336
Passive microwave algorithm development and evaluation
[NASA-CR-197915] p 2005 N95-24535

MICROWAVE OSCILLATORS
Optically-switched submillimeter-wave oscillator and radiator having a switch-to-switch propagation delay
[NASA-CASE-NPO-18547-1-CU] p 1959 N95-25307
Radial electron-beam-breakup transit-time oscillator
[DE95-005731] p 1959 N95-25385

MICROWAVE SCATTERING
Diurnal variations of backscattering properties of pine trees at C- and X-bands
[PB95-149738] p 1988 N95-24299

MICROWAVE TRANSMISSION
Study on propagation impairments, distortions and unavailability on digital microwave links
[DE95-723047] p 1953 N95-24848

MICROWAVE TUBES
Nonlinear analysis of millimeter and sub-millimeter wave sources such as Cerenkov masers, orotrons, and ubitrons
[AD-A288777] p 1974 N95-26114

MICROWAVES
Fusion-neutron diagnostic on the Microwave Tokamak Experiment
[DE94-777530] p 2075 N95-24270
Study on propagation impairments, distortions and unavailability on digital microwave links
[DE95-723047] p 1953 N95-24848
Radial electron-beam-breakup transit-time oscillator
[DE95-005731] p 1959 N95-25385

MILITARY HELICOPTERS
An overview of Health and Usage Monitoring Systems (HUMS) for military helicopters
[DSTO-TR-0061] p 1905 N95-24200
Helicopter life substantiation: Review of some USA and UK initiatives
[DSTO-TR-0062] p 1905 N95-24201

MILITARY TECHNOLOGY
Mapping, charting and geodesy handbook
[AD-A286558] p 1989 N95-24502

MILLIMETER WAVES
Airborne imaging of tropospheric emission at millimeter and submillimeter wavelengths
[NASA-TM-110498] p 2003 N95-24336
Nonlinear analysis of millimeter and sub-millimeter wave sources such as Cerenkov masers, orotrons, and ubitrons
[AD-A288777] p 1974 N95-26114

MIMD (COMPUTERS)
Outline of fast analyzer for MHD equilibrium FAME
[DE94-777540] p 2076 N95-24311

MINKOWSKI SPACE
The space of solutions of Toda field theory
[DE95-607095] p 2099 N95-25650

MIR SPACE STATION
JPRS report: Science and technology. Central Eurasia: Space
[JPRS-USP-94-008] p 1916 N95-24359

MIRRORS
Mirror alignment and focus of point-focus solar concentrators
[DE95-002609] p 1992 N95-24676

MISALIGNMENT
Computerized design and generation of low-noise gears with localized bearing contact
[NASA-TM-106880] p 1977 N95-26074

MISSILE COMPONENTS
Missileborne Artificial Vision System (MAVIS)
p 2022 N95-25254

MISSILE DEFENSE
Flexible architectures for sensor fusion in theater missile defense
[AD-A288666] p 2007 N95-26048

MISSION PLANNING
Apollo 13: Houston, we've got a problem
[NASA-TM-110551] p 1918 N95-24215
Mars observer mission: Mapping the Martian world
[NASA-CR-110585] p 2112 N95-24672
An overview of the Nuclear Electric Propulsion Space Test Program (NEPSTP) satellite
[DE94-013121] p 1920 N95-24711
Return to the red planet: The Mars Observer Mission
[NASA-CR-197707] p 2113 N95-26336

MIXED CRYSTALS
Thermal diffuse scattering in time-of-flight neutron diffraction studied on SBN single crystals
[DE94-637054] p 2085 N95-24362

MIXERS
Jet mixer noise suppressor using acoustic feedback
[NASA-CASE-LEW-15170-2] p 2040 N95-26187

MOBILE COMMUNICATION SYSTEMS
JPRS report: Science and technology. Central Eurasia
[JPRS-UST-95-010] p 1953 N95-24539
Assessment of Commercial Satellite Communications Initiative (CSCI) studies
[AD-A288357] p 1920 N95-25508
Journal of the Communications Research Laboratory, volume 41, number 1, March 1994
[PB95-177606] p 1956 N95-26008

MODEMS
ARMDAT: A brief description of a computerized test system for burst transmission
[PB95-165452] p 1951 N95-24241

MODES (STANDING WAVES)
Effect of density gradients in confined supersonic shear layers. Part 2: 3-D modes
[NASA-CR-198030] p 1962 N95-24413

MODULATION
Aerodynamic parameter estimation via Fourier modulating function techniques
[NASA-CR-4654] p 1911 N95-24630
Application of extended-crystal diffraction techniques to the symmetry and structure analysis of 221-PbBiSrCaCuO
[DE95-605913] p 2090 N95-25984

MODULES
Appendix model performance: Model documentation. Renewable Fuels Module of the National Energy Modelling System
[DE95-006080] p 1991 N95-24355
Evaluation of restraint system concepts for the Japanese Experiment Module flight demonstration
[NASA-TM-104808] p 2013 N95-24627
Using and programming the SUPERCODE
[DE95-004342] p 2080 N95-25344

MODULUS OF ELASTICITY
Theoretical and experimental studies on the C15 intermetallic compound NbCr2
[DE95-003665] p 2086 N95-24513

MOISTURE
Using consumer IC packages in harsh high reliability applications
[DE94-016565] p 1959 N95-24713
The fundamentals of modelling heat and moisture processes in structures
[IFTR-15/1994] p 1951 N95-26109

MOLDING MATERIALS
Method for molding structural parts utilizing modified silicone rubber
[NASA-CASE-LAR-15217-1] p 1939 N95-24212

MOLECULAR BEAMS
Summaries of reports of the Electrotechnical Laboratory, no. 48
[JTN-95-80825] p 2114 N95-24908

MOLECULAR BIOLOGY
Structures and functions of oligosaccharins
[DE95-003140] p 2007 N95-24225
Annual report of National Institute of Radiological Sciences
[DE94-792664] p 2009 N95-25902

MOLECULAR CLOUDS
Far-infrared and submillimeter spectroscopy of photodissociation regions
[DE95-607520] p 2110 N95-25467

MOLECULAR CLUSTERS
Study of radicals, clusters and transition state species by anion photoelectron spectroscopy
[DE95-003438] p 2045 N95-24533

MOLECULAR COLLISIONS
International bulletin on atomic and molecular data for fusion, no. 47
[DE94-634442] p 2040 N95-24230

MOLECULAR DYNAMICS
A practical approach to portability and performance problems on massively parallel supercomputers
[DE95-005251] p 2020 N95-24612
Molecular dynamics calculation of shear viscosity for molten salt
[DE95-703970] p 2055 N95-25496
Stability and elastic properties of hydrogen loaded Ti(1-x)Al(x) alloys: An ab initio study
[AD-A288903] p 1936 N95-25529
Molecular dynamics simulation of a piston driven shock wave in a hard sphere gas
[NASA-CR-195463] p 2063 N95-25963

MOLECULAR EXCITATION
On the uncertainty in single molecule fluorescent lifetime and energy emission measurements
[NASA-CR-198009] p 2049 N95-24877
Thermochemistry, kinetics and spectroscopy of Kr and Kr2F
[DE95-005732] p 1941 N95-25386

MOLECULAR IONS
Dynamics Explorer 1, retarding ion mass spectrometer summary spectrograms-82/110 to 82/229 spin-time spectrograms for H(+), He(+), O(+), N(+), O(++), M/Z = 2, and molecular ions
[NASA-TM-108485] p 2003 N95-24763
Dynamics Explorer 1, retarding ion mass spectrometer summary spectrograms-82/230 to 82/265 spin-time spectrograms for H(+), He(+), O(+), N(+), O(++), M/Z = 2, and molecular ions
[NASA-TM-108486] p 2003 N95-24764

MOLECULAR ORBITALS
A photoemission study of the diamond and the single crystal C(60)
[DE95-006149] p 2085 N95-24463
Diagrammatic many-body perturbation expansion for atoms and molecules
[PB95-165221] p 2056 N95-25620

MOLECULAR SPECTRA
Infrared spectroscopy of Jupiter and Saturn
[NASA-CR-198034] p 2111 N95-24239

MOLECULAR SPECTROSCOPY
FT-IR microscopical analysis with synchrotron radiation: The microscope optics and system performance
[DE95-004834] p 1928 N95-24265

MOLECULAR STRUCTURE
Contribution of ankyrin-band 3 complexes to the organization and mechanical properties of the membrane skeleton of human erythrocyte
[DE95-005835] p 2010 N95-24427
A photoemission study of the diamond and the single crystal C(60)
[DE95-006149] p 2085 N95-24463
Fusion proteins as alternate crystallization paths to difficult structure problems
[NASA-TM-110497] p 2008 N95-24531
Design of supramolecular ordered systems for mesoscopic colloids and molecular composites
[DE95-004448] p 2048 N95-24687

MOLECULES
Infrared spectroscopy of Jupiter and Saturn
[NASA-CR-198034] p 2111 N95-24239
Correlations for the NO A(sup 2)(Sigma)(+) electronic quenching cross-section
[DE95-006195] p 2047 N95-24595
On the uncertainty in single molecule fluorescent lifetime and energy emission measurements
[NASA-CR-198009] p 2049 N95-24877
Mesic molecules of light nuclei in the oscillator representation
[DE94-628904] p 2050 N95-24890
Diagrammatic many-body perturbation expansion for atoms and molecules
[PB95-165221] p 2056 N95-25620
The effect of O2 intercalation on the rotational Dynamics and the ordering transition of C60
[DE95-004765] p 2090 N95-25897

MOLTEN SALTS
Molecular dynamics calculation of shear viscosity for molten salt
[DE95-703970] p 2055 N95-25496
Development of novel active transport membrane devices
[DE95-002658] p 1932 N95-26093

MOLYBDENUM
Feasibility of ceramic joining with high energy electron beams
[DE95-004519] p 1940 N95-24717

MOLYBDENUM ALLOYS
Localized corrosion and stress corrosion cracking characteristics of a low-aluminum-content iron-aluminum alloy
[DE95-003259] p 1934 N95-24647

MOLYBDENUM DISULFIDES
Improved lubrication performance of sputtered MoS2 film by surface treatments of Ti-alloy substrate
[NAL-TR-1213] p 1942 N95-25760

MOMENTUM
The determination of the main parameters of the backward spectrometer of the 0(sup 0) facility
[DE94-628385] p 2048 N95-24692
The track system of the modernized Hyperon spectrometer
[DE95-604003] p 2058 N95-25905
Electronic structure of (La,Sr)2CuO4 and Ba(0.6)K(0.4)BiO3
[DE95-004963] p 2091 N95-26170

MOMENTUM TRANSFER
HET mini-manual
[PB95-165338] p 2057 N95-25900

MONOPOLES
Construction of the moduli space of monopoles
[PB95-165528] p 2028 N95-24255
The geodesic motion in Kaluza-Klein spinning space
[DE95-607070] p 2039 N95-25646

MONTE CARLO METHOD
Lawrence Livermore pulsed sphere benchmark analysis of MCNP(trademark) ENDF/B-VI
[DE95-004864] p 2041 N95-24258
DSMC calculations for 70-deg blunted cone at 3.2 km/s in nitrogen
[NASA-TM-109181] p 1961 N95-24396
Phase 3 experiments of the JAERI/USDOE collaborative program on fusion blanket neutronics. Volume 1: Experiment
[DE94-777528] p 2076 N95-24511
Introduction to the Monte Carlo methods
[DE94-628386] p 2035 N95-24693
Notion of the inclusive spectra and cross sections of B-meson production in hadronic interactions of high energies
[DE94-628628] p 2049 N95-24887
Numerical simulation of the nonlinear response of composite plates under combined thermal and acoustic loading
[NASA-CR-197426] p 1981 N95-24907
Monte Carlo simulations with indefinite and complex-valued measures
[DE95-607056] p 2017 N95-25448
MOON
Apollo 12: Pinpoint for science
[NASA-TM-110576] p 1917 N95-25424
MORPHOLOGY
Characterization of ultradispersed aluminum
[DE95-006379] p 1933 N95-24329
MORTALITY
A longevity and survival analysis for a cohort of retired airline pilots
[DOT/FAA/AM-95/5] p 2012 N95-24237
Testing of experimental antileishmanial compounds
[AD-A288807] p 2009 N95-26193
MOSSBAUER EFFECT
Mossbauer spectroscopy, x ray diffraction and magnetic measurements of iron-nickel ultrafine particles
[DE95-601136] p 1930 N95-24840
Fe-57 and Sn-119 Moessbauer studies on La(1.25)Nd(0.6)Sr(0.15)CuO4: Evidence for local magnetic ordering below (approx. equal) 32 K
[DE95-601210] p 1959 N95-25405
MOTION
JPRS report: Science and technology. Central Eurasia
[JPRS-UST-95-010] p 1953 N95-24539
MOTION PERCEPTION
Relation of motion sickness susceptibility to vestibular and behavioral measures of orientation
[NASA-CR-198048] p 2010 N95-24410
MOTION PICTURES
NASA video catalog
[NASA-SP-7109(01)] p 2103 N95-24238
Learning random networks for compression of still and moving images p 2025 N95-25268
MOTION SICKNESS
Relation of motion sickness susceptibility to vestibular and behavioral measures of orientation
[NASA-CR-198048] p 2010 N95-24410
Motionsickness-seasickness: Summary of existing knowledge and suggested lines of development
[PB95-141495] p 2011 N95-24863
MOTION SIMULATORS
Simulating the dynamic interaction of a robotic arm and the Space Shuttle remote manipulator system
[NASA-CR-195076] p 2027 N95-26086
MOTIVATION
Creation of a scalar potential in 2D dilaton gravity
[DE95-006066] p 2003 N95-24577
MULLITES
Synthesis and processing of Al2O3/Al composites by in situ reaction of aluminum and mullite
[DE95-006224] p 1937 N95-25775
MULTI-ANODE MICROCHANNEL ARRAYS
Circuit for high resolution decoding of multi-anode microchannel array detectors
[NASA-CASE-GSC-13478-1] p 1960 N95-25889
MULTICHANNEL COMMUNICATION
The accident site portable integrated video system
[DE95-000539] p 1953 N95-24605
MULTIDISCIPLINARY DESIGN OPTIMIZATION
Aerodynamic optimization studies on advanced architecture computers
[NASA-CR-198045] p 1906 N95-24379
MULTIGRID METHODS
Separation analysis, a tool for analyzing multigrid algorithms
[NASA-CR-195036] p 2029 N95-24389
Multigrid solution strategies for adaptive meshing problems
[NASA-CR-195049] p 2031 N95-24857
MULTIMEDIA
Applications for electronic documents
[DE95-005036] p 2106 N95-25765
MULTIPATH TRANSMISSION
Study on propagation impairments, distortions and unavailability on digital microwave links
[DE95-723047] p 1953 N95-24848
MULTIPHASE FLOW
Advanced multi-phase flow CFD model development for solid rocket motor flowfield analysis
[NASA-CR-198044] p 1923 N95-25103
MULTIPOLES
Calculation of light scattering from a spherical particle on a surface by the multipole expansion method
[ATR-95(9558)-2] p 2075 N95-26198
MULTIPROCESSING (COMPUTERS)
DOLIB: Distributed Object Library
[DE95-004791] p 2019 N95-24250
Parallel processing for scientific computations
[NASA-CR-198013] p 2020 N95-24563
Scheduling time-critical graphics on multiple processors p 2018 N95-25870
MULTISENSOR FUSION
International bulletin on atomic and molecular data for fusion, no. 47
[DE94-634442] p 2040 N95-24230
Analysis of data from a radar warning receiver with the accent on association of sensor reports
[PB95-141768] p 1953 N95-24836
Clustering using winner-take-all units
[PB95-165403] p 2026 N95-25568
Flexible architectures for sensor fusion in theater missile defense
[AD-A288666] p 2007 N95-26048
MULTISTATIC RADAR
Multistatic radar: Synchronization and time reference system
[PB95-165288] p 1954 N95-25623
Analysis of waveforms for bistatic radar systems
[PB95-165098] p 1955 N95-25641
MULTIVARIABLE CONTROL
Controls concepts for next generation reuseable rocket engines
[NASA-TM-106902] p 1923 N95-25877
MULTIVARIATE STATISTICAL ANALYSIS
Characterization of plastic bonded explosives by pyrolysis-gas chromatography and multivariate data analysis. Applications of the procedure
[AD-A288761] p 1949 N95-25517
Characterization of plastic bonded explosives by pyrolysis-gas chromatography and multivariate data analysis. Development of the procedure
[AD-A288787] p 1949 N95-25528
MUON SPIN ROTATION
MuSR user guide
[PB95-165304] p 2056 N95-25624
MUONS
Low energy theorems in quark potential models
[DE94-636791] p 2042 N95-24316
A high-energy high-luminosity (mu)(+) - (mu)(-) collider
[DE95-006097] p 2065 N95-24357
Muon identifier efficiency of the GINES detecto r in the UNK neutrino beam
[DE94-628254] p 2045 N95-24485
Measurement of the WW gamma, ZZ gamma and Z gamm a gamma couplings at the Fermilab Tevatron
[DE95-003495] p 2067 N95-24601
Search for the prompt muon antineutrino from charm particle decays at the IHEP-JINR Neutrino detector in 70 GeV proton beam-dump experiment
[DE94-628772] p 2049 N95-24889
Mesic molecules of light nuclei in the oscillator representation
[DE94-628904] p 2050 N95-24890
Photon-charm production in p(anti p) collisions at radical s = 1.8 TeV
[DE95-004850] p 2052 N95-25377
Inelastic collisions of negative muons and hadrons with Helium metastable atoms
[DE95-607538] p 2055 N95-25493
Variational method for the calculation of the surface hyperspherical functions for the systems of ZH(mu)-type. The test calculation of the dt(mu)-system
[DE94-628905] p 2033 N95-25539
MuSR user guide
[PB95-165304] p 2056 N95-25624
Inelastic collisions of negative muons and hadrons with metastable hydrogen atoms
[DE95-607537] p 2056 N95-25668
MUTATIONS
Genetic and biophysical studies of the photosynthetic reaction center
[DE95-004179] p 2008 N95-24850

N

N-TYPE SEMICONDUCTORS
Optical determinations of energy-band dispersion curves in novel compound semiconductor materials
[DE95-006318] p 2089 N95-25353
NASA PROGRAMS
Automated Procurement System (APS): Project management plan (DS-03), version 1.2
[NASA-CR-196576] p 2102 N95-24442
Issues in NASA program and project management
[NASA-SP-6101(08)] p 2102 N95-24565
United States-European cooperation in space during the sixties
[ESA-HSR-14] p 2107 N95-24894
United States-European space cooperation in the post-Apollo programme
[ESA-HSR-15] p 2107 N95-24895
Continual improvement plan
[NASA-TM-110574] p 2103 N95-25849
Acquisition forecast: Fiscal year 1995
[NASA-TM-110575] p 2103 N95-25850
NASA strategic plan
[NASA-TM-110592] p 2103 N95-26262
NATIONAL AIRSPACE SYSTEM
Federal Aviation Administration plan for research, engineering and development, 1995
p 2102 N95-24202
Aviation system capacity improvements through technology
[NASA-TM-109165] p 1909 N95-24633
NATURAL GAS
Retrofit NOx control technologies for natural gas prime movers
[PB95-149290] p 1997 N95-24294
User guide to the Burner Engineering Research Laboratory
[DE95-004191] p 1931 N95-25492
Intermediate-sized natural gas fueled carbonate fuel cell power plants
[DE95-004990] p 1996 N95-26171
NATURAL LANGUAGE (COMPUTERS)
Dialogue transcription tools
[TN-94-1] p 2016 N95-24536
Instructable autonomous agents
[NASA-CR-197802] p 2019 N95-26206
NATURAL LANGUAGE PROCESSING
Machine-aided indexing at NASA
[NASA-CR-197796] p 2106 N95-25410
NATURAL SATELLITES
Fourth symposium of the geological survey of Japan on remote sensing of satellite geology
[PB95-178737] p 1917 N95-25750
NAVIER-STOKES EQUATION
Verification of computational aerodynamic predictions for complex hypersonic vehicles using the INCA(trademark) code
[DE95-004757] p 1906 N95-24308
Investigation of convection and pressure treatment with splitting techniques
[NASA-TM-106868] p 1961 N95-24399
Advanced multi-phase flow CFD model development for solid rocket motor flowfield analysis
[NASA-CR-198044] p 1923 N95-25103
A domain decomposition study of massively parallel computing in compressible gas dynamics
[DE95-004759] p 1965 N95-25895
Classical closure theory and Lam's interpretation of epsilon-RNG
[NASA-CR-195061] p 1965 N95-25960
A combined geometric approach for solving the Navier-Stokes equations on dynamic grids
[NASA-TM-106919] p 1908 N95-26075
Numerical simulation of laminar flow in a curved duct
[DE95-005427] p 1966 N95-26240
NAVIGATION AIDS
Mapping, charting and geodesy handbook
[AD-A286558] p 1989 N95-24502
NAVIGATION SATELLITES
The use of empirical models to investigate GPS derived total electron content
[DE95-606045] p 2111 N95-26044
NEAR INFRARED RADIATION
Distribution and nature of UV absorbers on Trition's surface
[NASA-CR-198008] p 2112 N95-26116
NEAR WAKES
DSMC calculations for 70-deg blunted cone at 3.2 km/s in nitrogen
[NASA-TM-109181] p 1961 N95-24396
NEGATIVE CONDUCTANCE
A theoretical analysis of strain in GaN and its effects on carrier conductivity
[AD-A288769] p 2090 N95-26061

NEGATIVE IONS
Design study of a negative-ion based NBI system for JT-60U
[DE94-785265] p 2043 N95-24339
Anionic construction of the sl(sub q, s)(2) algebra
[DE95-600838] p 2043 N95-24350
NEGATIVE MATTER
Theoretical studies in hadronic and nuclear physics
[DE95-006643] p 2098 N95-25562
NEODYMIUM
Measurement of kinetic energy of ions collected from laser resonance photoionized plasma by time-of-flight method
[DE95-709767] p 2081 N95-25498
NEODYMIUM LASERS
Reduction in fiber damage thresholds due to static fatigue
[DE95-004778] p 1979 N95-24263
Laser beam characterization results for a high power CW Nd:YAG laser
[DE95-006319] p 1971 N95-24408
NEON ISOTOPES
Multiplicities of secondaries in nuclear interactions, induced by Ne-20, Ar-40 and Fe-56 nuclei at 0.1-0.5 GeV/nucleon p 2060 N95-25920
NEPTUNE (PLANET)
Voyager: The grandest tour. The mission to the outer planets
[NASA-CR-197708] p 2112 N95-25854
NERNST-ETTINGSHAUSEN EFFECT
Direct energy conversion of radiation energy in fusion reactor
[NIFS-254] p 2072 N95-26250
NETHERLANDS
Biological monitoring of national freshwaters, 1992
[PB95-166690] p 2002 N95-25745
NEURAL NETS
Reducing neural network training time with parallel processing
[NASA-TM-110154] p 2015 N95-24209
Prediction of humans in various environments using gas sensors and neural networks
[PB95-141560] p 2009 N95-24227
Multidimensional data analysis on the basis of integral nonparametric statistics and multilayer perceptrons
[DE94-628375] p 2035 N95-24858
A Decade of Neural Networks: Practical Applications and Prospects
[NASA-CR-197334] p 2022 N95-25253
Missileborne Artificial Vision System (MAVIS) p 2022 N95-25254
Neural network application to comprehensive engine diagnostics p 2023 N95-25255
Document analysis with neural net circuits p 2023 N95-25256
From neural-based object recognition toward microelectronic eyes p 2023 N95-25257
VLSI neuroprocessors p 2023 N95-25258
Photonics: From target recognition to lesion detection p 2023 N95-25259
Three-D Artificial Neural Network (3DANN) technology. Blueprint for the future p 2024 N95-25260
Hidden Markov models and neural networks for fault detection in dynamic systems p 2024 N95-25261
Innovation and application of ANN in Europe demonstrated by Kohonen maps p 2024 N95-25262
Neural network classification of clinical neurophysiological data for acute care monitoring p 2024 N95-25263
Application of neural networks to unsteady aerodynamic control p 2024 N95-25264
Predictability in space launch vehicle anomaly detection using intelligent neuro-fuzzy systems p 2025 N95-25266
Neural networks: Application to medical imaging p 2025 N95-25267
Learning random networks for compression of still and moving images p 2025 N95-25268
Learning to train neural networks for real-world control problems p 2025 N95-25269
Neural network applications in telecommunications p 2025 N95-25270
A neural network controller for automated composite manufacturing p 2025 N95-25271
How Captain Amerika uses neural networks to fight crime p 2025 N95-25272
Neural network technique for orbit correction in accelerators/storage rings
[DE95-005955] p 2026 N95-25368
Proceedings of the 4th IEEE Workshop on Neural Networks for Signal Processing
[AD-A288383] p 2026 N95-25603
Discrete-event-dynamic-system-based approaches for control in integrated voice/data multihop Radio Networks
[AD-A288389] p 1954 N95-25604
A hybrid neurocomputing/numerical strategy for nonlinear structural analysis p 1986 N95-26275
NEUROPHYSIOLOGY
Neural network classification of clinical neurophysiological data for acute care monitoring p 2024 N95-25263
On producing sequential movements and actions. An integrative review and an update of the generalized motor program
[AD-A288628] p 2014 N95-25610
NEUTRAL ATOMS
Laser cooling of neutral atoms by red-shifted diffuse light in an optical integral sphere cavity
[DE94-634310] p 2041 N95-24268
NEUTRAL BEAMS
Design study of a negative-ion based NBI system for JT-60U
[DE94-785265] p 2043 N95-24339
Divertor design for the Tokamak Physics Experiment
[DE95-003653] p 2078 N95-24650
The role of shaping in achieving high performance in DIII-D
[DE95-003877] p 2078 N95-25102
High-beta discharges with neutral beam injection in CHS
[NIFS-280] p 2071 N95-26031
NEUTRAL CURRENTS
Tau as a probe for new physics
[DE95-005928] p 2051 N95-25296
Neutral current neutrino-nucleon scattering
[DE95-005027] p 2069 N95-25366
NEUTRAL PARTICLES
UEDGE and DEGAS modeling of the DIII-D scrape-off layer plasma
[DE95-003652] p 2076 N95-24490
NEUTRALIZERS
An analytical study of the vibration of beams fitted with neutralizers. Part 3: Torsional wave motion
[ISVR-TR-238-PT-3] p 1982 N95-25003
NEUTRINO BEAMS
Muon identifier efficiency of the GINES detecto r in the UNK neutrino beam
[DE94-628254] p 2045 N95-24485
Neutrino optics
[DE95-004236] p 2073 N95-25239
NEUTRINOS
Landau-Zener treatments of solar neutrino oscillations
[DE95-004761] p 2113 N95-24249
Neutrino masses and b - tau unification in the supersymmetric standard model
[DE94-634361] p 2043 N95-24404
Extending the kinematic range for W(sub R) searches in e(-)e(-) collisions at the NLC
[DE95-005946] p 2044 N95-24415
DOE-High Energy Physics Contract with the University of Hawaii
[DE95-004214] p 2068 N95-24852
Search for the prompt muon antineutrino from charm particle decays at the IHEP-JINR Neutrino detector in 70 GeV proton beam-dump experiment
[DE94-628772] p 2049 N95-24889
Neutrino optics
[DE95-004236] p 2073 N95-25239
Update of GALLEX solar neutrino results and implications
[DE95-005005] p 2113 N95-25364
Neutral current neutrino-nucleon scattering
[DE95-005027] p 2069 N95-25366
Neutrino oscillations from discrete non-Abelian family symmetries
[DE95-004355] p 2052 N95-25403
Scalar three body decays and signals for new physics
[DE95-607188] p 2053 N95-25438
Neutrino mass and oscillation angle phenomena within the asymmetric left-right models
[DE95-607201] p 2054 N95-25466
Heavy-neutrino effects on tau-lepton decays
[PB95-165346] p 2056 N95-25626
Statistical mechanics of magnetized pair Fermi gas
[DE95-607097] p 2063 N95-25969
Heavy-neutrino chirality enhancement of the decay K(L) yields e(mu) in left-right symmetric models
[PB95-165387] p 2064 N95-26096
NEUTRON ACTIVATION ANALYSIS
Gamma spectrum analysis including NAA with SAMPO for windows
[PB95-149720] p 2042 N95-24298
The facility for commercial doping of silicon by thermal neutrons in channel 3 at the IBR-2
[DE94-636293] p 2085 N95-24374
NEUTRON BEAMS
Proton calibration of low energy neutron detectors containing (6)LiF p 2060 N95-25925
NEUTRON COUNTERS
Fusion-neutron diagnostic on the Microwave Tokamak Experiment
[DE94-777530] p 2075 N95-24270
High LET, passive space radiation dosimetry and spectrometry
[NASA-CR-197694] p 2058 N95-25911
Preliminary results of radiation measurements on EURECA p 2060 N95-25923
Proton calibration of low energy neutron detectors containing (6)LiF p 2060 N95-25925
NEUTRON DIFFRACTION
Thermal diffuse scattering in time-of-flight neutron diffraction studied on SBN single crystals
[DE94-637054] p 2085 N95-24362
Neutron diffraction from HoNi2B2C, version 1
[DE95-005894] p 2085 N95-24431
NMR and optical studies of piezoelectric polymers
[DE95-003836] p 1940 N95-24554
User guide for the Polaris powder diffractometer at ISIS. Version 2.1
[PB95-165767] p 2074 N95-25573
Accurate determination of IC modulation parameter in Sr(x)Ba(1-x)Nb2O6 from second order satellites of neutron diffraction TOF (Time-Of-Flight) spectra
[DE94-629003] p 2090 N95-25851
NEUTRON EMISSION
Biological effectiveness of neutrons: Research needs
[DE95-004795] p 2051 N95-25373
NEUTRON IRRADIATION
The facility for commercial doping of silicon by thermal neutrons in channel 3 at the IBR-2
[DE94-636293] p 2085 N95-24374
NEUTRON RADIOGRAPHY
Benchmark experiment on a copper slab assembly bombarded by D-T neutrons
[DE95-709764] p 2055 N95-25497
NEUTRON SCATTERING
Spin correlations in percolating networks with fractal geometry
[DE95-001074] p 2037 N95-24479
Activities of the Solid State Division
[DE95-003900] p 2087 N95-24611
Current status and future prospect of space and time reversal symmetry violation on low energy neutron reactions
[DE94-765589] p 2048 N95-24702
HET mini-manual
[PB95-165338] p 2057 N95-25900
NEUTRON SPECTRA
Lawrence Livermore pulsed sphere benchmark analysis of MCNP(trademark) ENDF/B-VI
[DE95-004864] p 2041 N95-24258
The facility for commercial doping of silicon by thermal neutrons in channel 3 at the IBR-2
[DE94-636293] p 2085 N95-24374
A study of the radiation environment on board the space shuttle flight STS-57 p 2059 N95-25914
Neutron influences and energy spectra in the Cosmos-2044 biosatellite orbit p 2061 N95-25928
NEUTRON STARS
Research in nuclear astrophysics: Stellar collapse and supernovae
[DE95-004300] p 2110 N95-25343
NEUTRONS
Lawrence Livermore pulsed sphere benchmark analysis of MCNP(trademark) ENDF/B-VI
[DE95-004864] p 2041 N95-24258
Thermal diffuse scattering in time-of-flight neutron diffraction studied on SBN single crystals
[DE94-637054] p 2085 N95-24362
Current status and future prospect of space and time reversal symmetry violation on low energy neutron reactions
[DE94-765589] p 2048 N95-24702
Biological effectiveness of neutrons: Research needs
[DE95-004795] p 2051 N95-25373
Fast algorithms for transport models
[DE95-007064] p 2054 N95-25479
Benchmark experiment on a copper slab assembly bombarded by D-T neutrons
[DE95-709764] p 2055 N95-25497
Study of properties of Ne - Al neutron rich isotopes at and near N = 20 magic shell using elastic scattering in inverse kinematics
[DE94-628655] p 2055 N95-25538
On analysis of resonance neutron depolarization in uniaxial media
[DE95-703782] p 2057 N95-25669
Proton calibration of low energy neutron detectors containing (6)LiF p 2060 N95-25925
Differential neutron energy spectra measured on spacecraft low Earth orbit p 2062 N95-25932

Summary report for ITER Task D10: Update and implementation of neutron transport and activation codes and processed libraries
[DE95-007631] p 2083 N95-26185

NEWTON METHODS
SYSINT(SYSINTM)-program complex for numerical solution of the eigenvalue problem for system of integral equations
[DE94-636729] p 2029 N95-24375
Newton iterative methods for large scale nonlinear systems
[DE95-007067] p 2032 N95-25480

NICKEL
XAS studies of Ni(I), Ni(II), and Ni(III) complexes
[DE95-004844] p 1928 N95-24257
In situ XAFS study of oxides formed on nickel thin film electrodes in KOH solution
[AD-A288735] p 1932 N95-26056

NICKEL ALLOYS
The temperature and strain rate dependence of the flow stress of single crystal NiAl deformed along the zone group axes (110)
[DE95-003634] p 2083 N95-24233
Synthesis of Ni3Al and NiAl intermetallics
[DE95-005897] p 1934 N95-24433
Mossbauer spectroscopy, x ray diffraction and magnetic measurements of iron-nickel ultrafine particles
[DE95-601136] p 1930 N95-24840
Evaluation of a diffusion/trapping model for hydrogen ingress in high-strength alloys
[AD-A288447] p 1936 N95-25502
Strengthening of NiAl matrix composites
[AD-A288923] p 1926 N95-25505

NICKEL COMPOUNDS
Atomistic studies of grain boundaries in NiAl
[DE95-005208] p 1937 N95-26014

NIGERIA
Predicting the components of the total hemispherical solar radiation from sunshine duration measurements in Lagos, Nigeria
[DE95-606030] p 2113 N95-26042

NIGHT VISION
Visual performance with Omnibus 3: A comparative evaluation of enhanced generation three image intensifier technology
[PB95-141891] p 2013 N95-24510

NIOBATES
Accurate determination of IC modulation parameter in Sr(x)Ba(1-x)Nb2O6 from second order satellites of neutron diffraction TOF (Time-Of-Flight) spectra
[DE94-629003] p 2090 N95-25851

NIOBIUM ALLOYS
Theoretical and experimental studies on the C15 intermetallic compound NbCr2
[DE95-003665] p 2086 N95-24513

NITRATES
Solution based synthesis of perovskite-type oxide films and powders
[DE95-006170] p 2086 N95-24594

NITRATION
Continued computational evaluation of the feasibility of nitrating precursors to C12N12O12
[AD-A288369] p 1924 N95-25602

NITRIC ACID
Effects of nitric acid vapor on the formation of cloud droplets in troposphere
[DE95-744869] p 2001 N95-25500

NITRIC OXIDE
Direct catalytic decomposition of nitric oxide
[DE95-005202] p 1928 N95-24286
Correlations for the NO A(sup 2)(Sigma)(+) electronic quenching cross-section
[DE95-006195] p 2047 N95-24595

NITROGEN
DSMC calculations for 70-deg blunted cone at 3.2 km/s in nitrogen
[NASA-TM-109181] p 1961 N95-24396
Measurement of blood nitrogen content after rapid compressions to assess the speed of nitrogen uptake during the compression phase of submarine escape. (includes measurement of nitrogen concentration in blood following rapid compression to 5 bar)
[PB95-165726] p 2012 N95-25570

NITROGEN IONS
Dynamics Explorer 1, retarding ion mass spectrometer summary spectrograms-82/110 to 82/229 spin-time spectrograms for H(+), He(+), O(+), N(+), O(++), M/Z = 2, and molecular ions
[NASA-TM-108485] p 2003 N95-24763
Dynamics Explorer 1, retarding ion mass spectrometer summary spectrograms-82/230 to 82/265 spin-time spectrograms for H(+), He(+), O(+), N(+), O(++), M/Z = 2, and molecular ions
[NASA-TM-108486] p 2003 N95-24764

NITROGEN LASERS
Evolution of Spark plasma using nitrogen laser shadowgraphy system
[DE95-607598] p 2082 N95-25972
Construction of a nitrogen laser for plasma diagnostics
[DE95-607599] p 1973 N95-25973

NITROGEN OXIDES
Retrofit NOx control technologies for natural gas prime movers
[PB95-149290] p 1997 N95-24294
Nitrogen oxide emissions and their control from uninstalled aircraft engines in enclosed test cells: Joint report to Congress on the Environmental Protection Agency - Department of Transportation study
[PB95-166237] p 2002 N95-26005
Cross-flow, filter-sorbent-catalyst for particulate, SO2 and NO(x) control
[DE95-001934] p 2003 N95-26091

NITROGEN TETROXIDE
Development test of a liquid apogee engine for the ETS-4
[NAL-TR-1250] p 1922 N95-24999

NOISE MEASUREMENT
The measurement of the low frequency noise characteristics of the field effect transistors for cryogenic detectors
[DE94-628257] p 1957 N95-24487

NOISE REDUCTION
Computerized design and generation of low-noise gears with localized bearing contact
[NASA-TM-106880] p 1977 N95-26074
Noise impact of advanced high lift systems
[NASA-CR-195028] p 2040 N95-26160
Jet mixer noise suppressor using acoustic feedback
[NASA-CASE-LEW-15170-2] p 2040 N95-26187

NONADIABATIC CONDITIONS
Dynamics of nonadiabatic charged particles in the magnetic dipole field with imposed homogeneous magnetic field
[DE95-605222] p 2057 N95-25778

NONDESTRUCTIVE TESTS
Investigation of properties and performance of ceramic composite components
[DE95-004737] p 1939 N95-24247
Using consumer IC packages in harsh high reliability applications
[DE94-016565] p 1959 N95-24713
A quality monitor and monitoring technique employing optically stimulated electron emission
[NASA-CASE-LAR-15063-1-CU] p 1978 N95-25304
Method and apparatus for non-destructive evaluation of composite materials with cloth surface impressions
[NASA-CASE-LAR-14535-1] p 1926 N95-25305
Emerging nondestructive inspection for aging aircraft
[PB95-143053] p 1905 N95-25401
Proceedings of the 2d USAF Aging Aircraft Conference
[AD-A288217] p 1911 N95-25578
Static and fatigue properties of pin-joint specimens of a AS-4/PEEK thermoplastic composite material
[NAL-TR-1214] p 1927 N95-25859
An overview of NDE methods for thick composites and a proposal for analysis of computed technology data
[AD-A288733] p 1979 N95-26055

NONEQUILIBRIUM FLOW
Implementation of a parallel algorithm for thermo-chemical nonequilibrium flow simulations
[DE95-004758] p 1961 N95-24262

NONEQUILIBRIUM PLASMAS
Dynamics of structure formation in nonequilibrium systems (Wave Media)
[DE95-607609] p 2081 N95-25556

NONLINEAR EQUATIONS
Periodic solutions of Hamiltonian perturbations of 2D linear Schroedinger equations
[PB95-165536] p 2028 N95-24301
Construction of quasi-periodic solutions for Hamiltonian perturbations of linear equations and applications to nonlinear PDE
[PB95-165551] p 2028 N95-24322
The geometry of weak solutions of certain integrable nonlinar PDE's
[DE95-005241] p 2030 N95-24609
ASYS2: A new version of computer algebra package ASYS for analysis and simplification of polynomial systems
[DE94-628384] p 2030 N95-24691
Nonlinear theories of spin-2 field in terms of Fierz variables
[DE95-600854] p 2095 N95-24833
An analysis of hypercritical states in elastic and inelastic systems
[IFTR-1/1994] p 2037 N95-25339
Selected problems of the interaction of electromagnetic waves and a turbulent plasma
[IFTR-9-1993] p 2080 N95-25340
Nonlinearity induced nontrivial dynamics in the Jaynes-Cummings Hamiltonian
[DE95-607004] p 2032 N95-25452
Nonlinear difference approximations for evolutionary PDE's
[DE95-005260] p 2033 N95-25676
Nonlinear system analysis using slowly-varying complex frequency method
[NAL-TR-1217] p 2034 N95-25860
Strong phase correlations of solitons of nonlinear Schroedinger equation
[DE95-607002] p 2063 N95-25991
Optical instabilities and chaos due to the virtual formation of biexcitons
[DE95-607664] p 2063 N95-25994
Postbuckling and large-deflection nonlinear analyses on distributed-memory computers p 1986 N95-26276

NONLINEAR OPTICS
Optical properties of fractal nanocomposites
[DE95-005414] p 1926 N95-25295
Selected problems of the interaction of electromagnetic waves and a turbulent plasma
[IFTR-9-1993] p 2080 N95-25340
Nonlinear optics and organic materials
[DE95-004677] p 2074 N95-25357
Phase correction in two-crystal optical parametric oscillators
[DE95-006317] p 2074 N95-25559

NONLINEAR PROGRAMMING
Semi-infinite mathematical programming: A collocation approach
[DE94-634273] p 2016 N95-24708

NONLINEAR SYSTEMS
Numerical simulation of the nonlinear response of composite plates under combined thermal and acoustic loading
[NASA-CR-197426] p 1981 N95-24907
Newton iterative methods for large scale nonlinear systems
[DE95-007067] p 2032 N95-25480
Nonlinear system analysis using slowly-varying complex frequency method
[NAL-TR-1217] p 2034 N95-25860
Sensitivity analysis of the non-linear dynamic viscoplastic response of 2-d structures with respect to material parameters p 1984 N95-26266
Nonlinear structural analysis on distributed-memory computers p 1985 N95-26272
A hybrid neurocomputing/numerical strategy for nonlinear structural analysis p 1986 N95-26275

NONLINEARITY
Over-compression, a method to shape the longitudinal bunch distribution for a reduced energy spread
[DE95-006052] p 2066 N95-24572
Tutorial on beam-based feedback systems for linacs
[DE95-006054] p 2067 N95-24573
Adaptive projective filters
[DE94-628374] p 2030 N95-24645
Numerical simulation of the nonlinear response of composite plates under combined thermal and acoustic loading
[NASA-CR-197426] p 1981 N95-24907
Nonlinearity induced nontrivial dynamics in the Jaynes-Cummings Hamiltonian
[DE95-607004] p 2032 N95-25452
Quasiparticles in magnetized plasma
[DE95-607610] p 2081 N95-25632
A normal form approach to the theory of nonlinear betatronic motion
[DE95-603831] p 2062 N95-25944
Solitons in electron-positron plasma
[DE95-607608] p 2082 N95-25974
A fully associative, nonisothermal, nonlinear kinematic, unified viscoplastic model for titanium alloys
[NASA-TM-106926] p 1983 N95-26078
Nonlinear analysis of millimeter and sub-millimeter wave sources such as Cerenkov masers, orotrons, and ubitrons
[AD-A288777] p 1974 N95-26114
On convergence of the Nelder-Mead simplex algorithm for unconstrained stochastic optimization
[AD-A289453] p 2006 N95-26197
Nonlinear vibrations of thin-walled composite frames p 1984 N95-26269

NONPARAMETRIC STATISTICS
Multidimensional data analysis on the basis of integral nonparametric statistics and multilayer perceptrons
[DE94-628375] p 2035 N95-24858

NORMALITY
Bounds for departure from normality and the Frobenius norm of matrix eigenvalues
[DE95-006144] p 2030 N95-24592

NORMS
Behavior of a trigonometric polynomial with given number of terms on small subsets of the unit circumference (norm duplication problem)
[PB95-165544] p 2028 N95-24321
NORTH ATLANTIC TREATY ORGANIZATION (NATO)
Directory of Defence and Aerospace Information Centers
[AGARD-R-802] p 2107 N95-26334
NOVAE
Gamma-ray emission from globular clusters. Shock high energy emission from the Be-Star/Pulsar System PSR 1259-63. Echoes in x-ray novae
[NASA-CR-197994] p 2114 N95-24381
NOZZLE DESIGN
Internal performance characteristics of thrust-vectored axisymmetric ejector nozzles
[NASA-TM-4610] p 1907 N95-25338
NOZZLE EFFICIENCY
Internal performance characteristics of thrust-vectored axisymmetric ejector nozzles
[NASA-TM-4610] p 1907 N95-25338
NOZZLE FLOW
Scaling in a scramjet combustor p 1933 N95-25398
NOZZLE GEOMETRY
Thrust measurement in a 2-D scramjet nozzle
p 1914 N95-25397
NOZZLE WALLS
Supersonic quiet-tunnel development for laminar-turbulent transition research
[NASA-CR-198040] p 1915 N95-24302
NUCLEAR ASTROPHYSICS
Research in nuclear astrophysics: Stellar collapse and supernovae
[DE95-004300] p 2110 N95-25343
NUCLEAR BINDING ENERGY
Mesic molecules of light nuclei in the oscillator representation
[DE94-628904] p 2050 N95-24890
NUCLEAR ELECTRIC POWER GENERATION
Proceedings of the 1993 Symposium on Nuclear Data
[DE94-012554] p 2104 N95-24372
Environment, 1980-1993
[DE95-605240] p 2002 N95-25779
The use of radioisotopes in human experiments: Comments in response to recent media articles
[DE95-605680] p 2012 N95-25981
NUCLEAR ELECTRIC PROPULSION
An overview of the Nuclear Electric Propulsion Space Test Program (NEPSTP) satellite
[DE94-013121] p 1920 N95-24711
NUCLEAR EMULSIONS
Multiplicities of secondaries in interactions of 1.8 GeV/nucleon Fe-56 nuclei with photoemulsion and the cascade evaporation model p 2059 N95-25917
Target fragments in collisions of 1.8 GeV/nucleon Fe-56 nuclei with photoemulsion nuclei, and the cascade-evaporation model p 2059 N95-25918
Dependence of the multiplicities of secondary particles on the impact parameter in collisions of high-energy neon and iron nuclei with photoemulsion nuclei
p 2059 N95-25919
Multiplicities of secondaries in nuclear interactions, induced by Ne-20, Ar-40 and Fe-56 nuclei at 0.1-0.5 GeV/nucleon p 2060 N95-25920
NUCLEAR ENERGY
Nuclear energy and the environment
[DE95-600438] p 2001 N95-25615
NUCLEAR FUELS
The energy intelligence information system
[DE95-002184] p 2105 N95-24675
Magnetized target fusion: An ultra high energy approach in an unexplored parameter space
[DE95-005252] p 2080 N95-25289
Characteristics of D(-3)He fueled FRC reactor: ARTEMIS-L
[NIFS-251] p 2072 N95-26110
Innovative energy production in fusion reactors
[NIFS-250] p 2072 N95-26111
NUCLEAR FUSION
ESnet Program Plan 1994
[DE95-005329] p 2019 N95-24290
Proceedings of the 1993 Symposium on Nuclear Data
[DE94-012554] p 2104 N95-24372
Core-collapse supernovae and nucleosynthesis
[NASA-CR-197731] p 2109 N95-25122
Magnetized target fusion: An overview of the concept
[DE95-005247] p 2070 N95-25594
Construction of a nitrogen laser for plasma diagnostics
[DE95-607599] p 1973 N95-25973
Direct energy conversion of radiation energy in fusion reactor
[NIFS-254] p 2072 N95-26250
NUCLEAR INTERACTIONS
The physics and experimental program of the Relativistic Heavy Ion Collider (RHIC)
[DE95-003416] p 2066 N95-24495
Dependence of the multiplicities of secondary particles on the impact parameter in collisions of high-energy neon and iron nuclei with photoemulsion nuclei
p 2059 N95-25919
Multiplicities of secondaries in nuclear interactions, induced by Ne-20, Ar-40 and Fe-56 nuclei at 0.1-0.5 GeV/nucleon p 2060 N95-25920
NUCLEAR MAGNETIC RESONANCE
NMR and optical studies of piezoelectric polymers
[DE95-003836] p 1940 N95-24554
The effect of O2 intercalation on the rotational Dynamics and the ordering transition of C60
[DE95-004765] p 2090 N95-25897
NUCLEAR MODELS
HZE beam transport in multilayered materials
p 2060 N95-25922
NUCLEAR PHYSICS
ESnet Program Plan 1994
[DE95-005329] p 2019 N95-24290
Moving scales contraction contradicts interval invariance
[DE94-636736] p 2092 N95-24347
Proceedings of the 1993 Symposium on Nuclear Data
[DE94-012554] p 2104 N95-24372
JPRS report: Science and technology. Central Eurasia: Institute of General and Nuclear Physics: 1993 Status and Prospects
[JPRS-UST-94-025] p 2045 N95-24471
Current experiments in elementary particle physics. Revision
[DE95-003797] p 2067 N95-24652
Tau as a probe for new physics
[DE95-005928] p 2051 N95-25296
Theoretical studies in hadronic and nuclear physics
[DE95-006643] p 2098 N95-25562
Online nuclear data service
[DE95-602487] p 2107 N95-25941
NUCLEAR POWER PLANTS
The energy intelligence information system
[DE95-002184] p 2105 N95-24675
The dependence of human reliability upon task information content
[DE95-006645] p 2014 N95-25483
NUCLEAR POWER REACTORS
The energy intelligence information system
[DE95-002184] p 2105 N95-24675
NUCLEAR RADIATION SPECTROSCOPY
A high intensity slow positron facility for the Advanced Neutron Source
[DE94-014108] p 2050 N95-25099
NUCLEAR REACTIONS
Atomic masses 1993. The 1993 atomic mass evaluation
[DE94-634462] p 2040 N95-24231
Current status and future prospect of space and time reversal symmetry violation on low energy neutron reactions
[DE94-765589] p 2048 N95-24702
KORP-1: A program for calculating the direct (n, p) or (p, n) reaction by using DWBA method
[DE94-628768] p 2049 N95-24724
Anisotropy of dilepton emission from nuclear collisions
[DE95-004354] p 2070 N95-25634
Index of nuclear data libraries available from the IAEA Nuclear Data Section
[DE95-605213] p 2107 N95-25980
NUCLEAR REACTORS
Proceedings of the 1993 Symposium on Nuclear Data
[DE94-012554] p 2104 N95-24372
The facility for commercial doping of silicon by thermal neutrons in channel 3 at the IBR-2
[DE94-636293] p 2085 N95-24374
NUCLEAR RESEARCH
Cryogenic helium gas convection research
[DE95-004372] p 1965 N95-25404
Maryland controlled fusion research program
[DE95-006642] p 2081 N95-25561
NUCLEAR SCATTERING
Possible constraints on SUSY-model parameters from direct dark matter search
[DE94-628561] p 2109 N95-24885
On SUSY dark matter detection with spinless nuclei
[DE94-628562] p 2109 N95-24886
NUCLEAR SPIN
Spin structure of the nucleon and polarization
[DE95-004282] p 2047 N95-24662
Toroidal response in magnetic resonance
[DE94-628406] p 2037 N95-24696
On SUSY dark matter detection with spinless nuclei
[DE94-628562] p 2109 N95-24886
NUCLEAR STRUCTURE
On SUSY dark matter detection with spinless nuclei
[DE94-628562] p 2109 N95-24886
NUCLEATION
Nucleation and growth of crystals under cirrus and polar stratospheric cloud conditions
[NASA-CR-197991] p 2085 N95-24478
NUCLEI (NUCLEAR PHYSICS)
Mesic molecules of light nuclei in the oscillator representation
[DE94-628904] p 2050 N95-24890
Multiplicities of secondaries in interactions of 1.8 GeV/nucleon Fe-56 nuclei with photoemulsion and the cascade evaporation model p 2059 N95-25917
Target fragments in collisions of 1.8 GeV/nucleon Fe-56 nuclei with photoemulsion nuclei, and the cascade-evaporation model p 2059 N95-25918
Dependence of the multiplicities of secondary particles on the impact parameter in collisions of high-energy neon and iron nuclei with photoemulsion nuclei
p 2059 N95-25919
Multiplicities of secondaries in nuclear interactions, induced by Ne-20, Ar-40 and Fe-56 nuclei at 0.1-0.5 GeV/nucleon p 2060 N95-25920
Fragmentation cross sections of O-16 between 0.9 and 200 GeV/nucleon p 2060 N95-25921
NUCLEON-NUCLEON INTERACTIONS
Polarization and N-N elastic scattering amplitudes
[DE95-004648] p 2042 N95-24292
Bound states of 'dressed' particles
[DE94-636773] p 2042 N95-24314
New results in nucleon-nucleon scattering at intermediate energies
[DE95-004594] p 2043 N95-24332
Realistic NN potential for the Low approach
[DE94-628606] p 2049 N95-24720
NUCLEON-NUCLEON SCATTERING
New results in nucleon-nucleon scattering at intermediate energies
[DE95-004594] p 2043 N95-24332
NUCLEONS
Chiral limit of QCD
[DE95-005245] p 2094 N95-24610
Spin structure of the nucleon and polarization
[DE95-004282] p 2047 N95-24662
Realistic NN potential for the Low approach
[DE94-628606] p 2049 N95-24720
Neutral current neutrino-nucleon scattering
[DE95-005027] p 2069 N95-25366
Theoretical studies in hadronic and nuclear physics
[DE95-006643] p 2098 N95-25562
NUCLIDES
Expert system for nuclide identification in gamma spectrum analysis
[PB95-149712] p 2042 N95-24297
Gamma spectrum analysis including NAA with SAMPO for windows
[PB95-149720] p 2042 N95-24298
NUMERICAL ANALYSIS
Response to a localized impact loading of a composite multilayered rotational shell structure: Theory and numerical methods, volume 1
[ONERA-NT-1994-10-VOL-1] p 1979 N95-24282
Response to a localized impact loading of a composite multilayered rotational shell structure: Theory and numerical methods, volume 2
[ONERA-NT-1994-10-VOL-2] p 1980 N95-24283
Response to a localized impact loading of a composite multilayered rotational shell structure: Theory and numerical methods, Volume 3
[ONERA-NT-1994-10-VOL-3] p 1980 N95-24284
Covolume solutions of three dimensional div-curl equations
[NASA-CR-195031] p 2029 N95-24421
Linear non-modal phenomena in numerical analysis and applied mathematics
[DE95-005495] p 2029 N95-24458
An analysis of hypercritical states in elastic and inelastic systems
[IFTR-1/1994] p 2037 N95-25339
Numerical analysis of electron cyclotron resonance heating on JT-60U and JFT-2M
[DE95-709766] p 2080 N95-25471
On the numerical method for analysis of the dynamics of the classical Hamiltonian systems
[DE95-605218] p 2034 N95-25906
NUMERICAL CONTROL
Proceedings of the 1994 Conference on Computing in Energy Physics
[DE95-004442] p 2068 N95-24665
Calibration of optical time domain reflectometers using time delay generator
[PB95-141776] p 2073 N95-24673
MuSR user guide
[PB95-165304] p 2056 N95-25624

NUMERICAL FLOW VISUALIZATION
Three-dimensional user interfaces for scientific visualization
[NASA-CR-197923] p 2017 N95-25867
The 3D widgets for exploratory scientific visualization
p 1966 N95-25868
An annotation system for 3D fluid flow visualization
p 1966 N95-25869
NUMERICAL WEATHER FORECASTING
Technical report series on global modeling and data assimilation. Volume 5: Documentation of the AIRES/GEOS dynamical core, version 2
[NASA-TM-104606-VOL-5] p 2003 N95-24766
A numerical prediction of the precipitation and hydrology of California
[DE95-004966] p 2006 N95-25635

O

O STARS
ASCA solid state imaging spectrometer observations of O stars
[NASA-CR-197281] p 2108 N95-24385
OBJECT-ORIENTED PROGRAMMING
DOLIB: Distributed Object Library
[DE95-004791] p 2019 N95-24250
Parallel processing for scientific computations
[NASA-CR-198013] p 2020 N95-24563
Object-oriented parallel polygon rendering
[DE95-004909] p 2021 N95-24881
OBLIQUE SHOCK WAVES
A study of three-dimensional interaction flow fields between swept shock waves and turbulent boundary layers. Flow structures and effects of bleed
[NAL-TR-1227] p 1963 N95-25001
OBSERVATION
Dynamic Jahn-Teller-induced infrared absorption of a charged C60(-) molecule
[DE95-607577] p 2063 N95-25971
OCCURRENCES
Modelling the day to day wind variability offshore central Chile at about 30 deg south
[DE95-606032] p 2006 N95-26043
OCEAN BOTTOM
Shelf sediment dynamics and development of lithostratigraphy
[AD-A288886] p 2006 N95-25504
OCEAN CURRENTS
Global ocean circulation and equator-pole heat transport as a function of ocean GCM resolution
[DE95-004198] p 2000 N95-25279
OCEAN DYNAMICS
Global ocean circulation and equator-pole heat transport as a function of ocean GCM resolution
[DE95-004198] p 2000 N95-25279
OCEAN SURFACE
Techniques for the investigation of wave turbulence in water wave data
[AD-A288392] p 2007 N95-25605
OCEANOGRAPHY
JPRS report: Science and technology. Central Eurasia
[JPRS-UST-95-013] p 1987 N95-24538
OMEGA-MESONS
Baryon spectroscopy and the omega minus
[DE95-004838] p 2052 N95-25374
ON-LINE SYSTEMS
Proceedings of the 1994 Conference on Computing in Energy Physics
[DE95-004442] p 2068 N95-24665
Online nuclear data service
[DE95-602487] p 2107 N95-25941
Index of nuclear data libraries available from the IAEA Nuclear Data Section
[DE95-605213] p 2107 N95-25980
ONBOARD DATA PROCESSING
Missileborne Artificial Vision System (MAVIS)
p 2022 N95-25254
ONBOARD EQUIPMENT
Suspension system for gimbal supported scanning payloads
[NASA-CASE-MFS-28817-1] p 1969 N95-25544
ONE DIMENSIONAL FLOW
Recent improvements to and validation of the one dimensional NASA wave rotor model
[NASA-TM-106913] p 1908 N95-25962
OPACITY
Resolution of the classical Hyades lithium problem
[DE95-003661] p 2109 N95-24234
Targets for laser-driven opacity measurements
[DE95-006172] p 1973 N95-25557
OPENINGS
Thermomechanical postbuckling of multilayered composite panels with cutouts p 1984 N95-26267
Buckling and postbuckling of composite panels with cutouts subjected to combined edge shear and temperature change p 1987 N95-26280
OPERATING COSTS
Report of the Space Shuttle Management Independent Review Team
[NASA-TM-110579] p 1919 N95-24466
Downsizing systems and expected opposition to introduction
[DE95-730186] p 2104 N95-24494
OPERATING SYSTEMS (COMPUTERS)
Software fault tolerance in computer operating systems
[NASA-CR-197999] p 2016 N95-24993
OPERATIONAL AMPLIFIERS
High input impedance amplifier
[NASA-CASE-GSC-13571-1] p 1960 N95-26038
OPERATIONAL HAZARDS
Quantity-distance requirements for earth-bermed aircraft shelters
[AD-A279692] p 1915 N95-24424
OPERATIONS RESEARCH
Study of launch site processing and facilities for future launch vehicles
[NASA-CR-198025] p 1918 N95-24579
OPERATORS (MATHEMATICS)
Involutive co-distributions preserved by transitive families of vector fields
[DE95-607078] p 2032 N95-25457
Measurement accuracy, bit-strings, Manthey's quaternions, and RRQM
[DE95-006211] p 2098 N95-25530
OPHTHALMOLOGY
An assessment of aviation accident risk of aphakic civil airmen by class of medical certificate held and by age: 1982-1985
[DOT/FAA/AM-95/11] p 2011 N95-25336
OPTICAL COMMUNICATION
Optical space communication: An overview
[DE94-634314] p 1952 N95-24403
Application of optical fiber amplifier for wavelength division multiplexing communication system. Part 2: Design of four-channel transmission system using two EDFA repeaters
[DE95-730179] p 1952 N95-24491
The Third International Workshop on the Physics and Modern Applications of Lasers
[DE95-606395] p 1972 N95-25491
OPTICAL CORRECTION PROCEDURE
Phase correction in two-crystal optical parametric oscillators
[DE95-006317] p 2074 N95-25559
OPTICAL EQUIPMENT
Integration of design, structural, thermal and optical analysis: And user's guide for structural-to-optical translator (PATCOD)
[NASA-TM-110153] p 1950 N95-24559
OPTICAL FIBERS
Reduction in fiber damage thresholds due to static fatigue
[DE95-004778] p 1979 N95-24263
Energy resolution of a lead scintillating fiber electromagnetic calorimeter
[DE94-628253] p 1967 N95-24484
Application of optical fiber amplifier for wavelength division multiplexing communication system. Part 2: Design of four-channel transmission system using two EDFA repeaters
[DE95-730179] p 1952 N95-24491
Calibration of optical time domain reflectometers using time delay generator
[PB95-141776] p 2073 N95-24673
Preliminary experiments of an optical fiber display
[NAL-TR-1257] p 2073 N95-25004
Comparison of three methods for optical characterization of point-focus concentrators
[DE95-000282] p 1994 N95-25309
The Third International Workshop on the Physics and Modern Applications of Lasers
[DE95-606395] p 1972 N95-25491
OPTICAL MEASUREMENT
Development of optical systems — holographic technique for monitoring crystal growth
[NASA-CR-197702] p 2073 N95-24545
Targets for laser-driven opacity measurements
[DE95-006172] p 1973 N95-25557
Automatic measurement system for measuring of the nonlinearity of photo detectors
[PB95-165197] p 2074 N95-25999
Angular displacement measuring device
[NASA-CASE-ARC-11937-1] p 2074 N95-26015
Liquid crystal point diffraction interferometer
[NASA-TM-106899] p 1970 N95-26073
OPTICAL MEASURING INSTRUMENTS
The 1994 Fiber Optic Sensors for Aerospace Technology (FOSAT) Workshop
[NASA-CP-10166] p 1912 N95-24207
OPTICAL PROPERTIES
Electromagnetic waves and photoacoustic transformation in gyrotropic superlattices
p 2083 N95-24205
Integration of design, structural, thermal and optical analysis: And user's guide for structural-to-optical translator (PATCOD)
[NASA-TM-110153] p 1950 N95-24559
Composite materials flown on the Long Duration Exposure Facility
[NASA-CR-4657] p 1923 N95-24583
Optical properties of fractal nanocomposites
[DE95-005414] p 1926 N95-25295
Effects of acetylacetone additions on PZT thin film processing
[DE95-006322] p 1941 N95-25370
Metrology measurement capability
[DE95-005411] p 1989 N95-25381
OPTICAL PUMPING
On the possibility of obtaining the polarized protons by the method of direct optic pumping of a fast atomic beam
[DE94-634309] p 2041 N95-24267
OPTICAL RADAR
Laser based methods for range, Doppler and vibration measurements
[PB95-141958] p 1952 N95-24445
JPRS report: Science and technology. Central Eurasia
[JPRS-UST-95-013] p 1987 N95-24538
OPTICAL REFLECTION
Method for determining shear direction using liquid crystal coatings
[NASA-CASE-ARC-11995-1] p 2075 N95-26117
OPTICAL RESONANCE
Measurement of kinetic energy of ions collected from laser resonance photoionized plasma by time-of-flight method
[DE95-709767] p 2081 N95-25498
OPTICAL SCANNERS
Comparison of three methods for optical characterization of point-focus concentrators
[DE95-000282] p 1994 N95-25309
OPTICAL SWITCHING
Optically-switched submillimeter-wave oscillator and radiator having a switch-to-switch propagation delay
[NASA-CASE-NPO-18547-1-CU] p 1959 N95-25307
OPTICAL TRACKING
Orientation determination of aircraft using visual 3D matching and radar. Case study 2
[PB95-165791] p 1955 N95-25749
OPTICAL WAVEGUIDES
Numerical simulation methods for wave propagation through optical waveguides
[DE94-634313] p 2073 N95-24402
OPTICS
JPRS report: Science and technology. Central Eurasia
[JPRS-UST-94-018] p 1950 N95-24472
JPRS report: Science and technology. Central Eurasia
[JPRS-UST-94-024] p 1958 N95-24620
Neutrino optics
[DE95-004236] p 2073 N95-25239
OPTIMAL CONTROL
Optimal guidance law development for an advanced launch system
[NASA-CR-4667] p 1917 N95-26205
OPTIMIZATION
Reducing neural network training time with parallel processing
[NASA-TM-110154] p 2015 N95-24209
Aerodynamic optimization studies on advanced architecture computers
[NASA-CR-198045] p 1906 N95-24379
Geometric analysis of wing sections
[NASA-TM-110346] p 1910 N95-24629
Aerodynamic shape optimization of wing and wing-body configurations using control theory
[NASA-CR-198024] p 1911 N95-25334
Active weld control
[NASA-CR-196588] p 1976 N95-25595
ORBIT CALCULATION
Closed orbit related problems: Correction, feedback, and analysis
[DE95-005969] p 2070 N95-25441
ORBITAL POSITION ESTIMATION
Coupling correction using closed orbit measurements
[DE95-005957] p 2070 N95-25369
ORBITS
Symbolic dynamics of the Lorenz equations
[DE95-607045] p 2036 N95-25439
Eigenvector method for optimized orbit correction
[DE95-005967] p 2071 N95-25785

ORDER-DISORDER TRANSFORMATIONS
Melting of the moving vortex lattice in the presence of disorder
[DE95-004126] p 2087 N95-24868
Proceedings of the Workshop on Dynamics and Structure of Disordered System
[DE94-792685] p 1931 N95-25356
Domain growth in weakly disordered magnets: A coupled map lattice approach
[DE95-607663] p 2090 N95-25979
In situ XAFS study of oxides formed on nickel thin film electrodes in KOH solution
[AD-A288735] p 1932 N95-26056
ORGANIC COMPOUNDS
Composite materials flown on the Long Duration Exposure Facility
[NASA-CR-4657] p 1923 N95-24583
Field-usable portable analyzer for chlorinated organic compounds
[DE95-003127] p 1930 N95-25098
Electrochemical organic destruction in support of Hanford tank waste pretreatment
[DE95-002854] p 1924 N95-25248
ORGANIC MATERIALS
Nonlinear optics and organic materials
[DE95-004677] p 2074 N95-25357
ORGANIC SILICON COMPOUNDS
Disilene Addition to C70
[DE95-006321] p 2087 N95-24617
ORGANOMETALLIC COMPOUNDS
Generation, detection and characterization of gas-phase transition metal aggregates and compounds
[DE95-004439] p 1930 N95-24686
Group transfer and electron transfer reactions of organometallic complexes
[DE95-003732] p 2050 N95-25112
ORTHOTROPISM
Separation of crack extension modes in orthotropic delamination models
[NASA-TM-109180] p 1927 N95-26083
OSCILLATIONS
Some remarks to the problem of neutrino oscillation
[DE94-628599] p 2048 N95-24669
Mesic molecules of light nuclei in the oscillator representation
[DE94-628904] p 2050 N95-24890
Neutrino oscillations from discrete non-Abelian family symmetries
[DE95-004355] p 2052 N95-25403
Neutrino mass and oscillation angle phenomena within the asymmetric left-right models
[DE95-607201] p 2054 N95-25466
OSCILLATORS
An FEL design code running on Mathcad(trademark)
[DE95-005279] p 1973 N95-25565
Charge-Dyon system as the reduced oscillator
[DE95-606998] p 2100 N95-25987
OSMIUM
The transformation of organic amines by transition metal cluster compounds
[DE95-004180] p 1923 N95-24851
OSTEOPOROSIS
Human parathyroid hormone-(1-38) restores cancellous bone to the immobilized, osteopenic proximal tibial metaphysis in rats
[NASA-CR-197709] p 2011 N95-24556
OTOLITH ORGANS
Relation of motion sickness susceptibility to vestibular and behavioral measures of orientation
[NASA-CR-198048] p 2010 N95-24410
OXIDATION
Characterization of ultradispersed aluminum
[DE95-006379] p 1933 N95-24329
Development of oxidation resistant SiC/C compositionally gradient materials
[DE94-785101] p 1925 N95-24365
Ignition of exploding aluminum droplets behind shock waves in water
[DE95-003975] p 1963 N95-24678
Oxidation of ion-implanted NiAl
[DE95-005899] p 1935 N95-25388
Spacecraft materials studies on The Aerospace Corporation Tray on EOIM-3
[AD-A288682] p 1942 N95-26049
In situ XAFS study of oxides formed on nickel thin film electrodes in KOH solution
[AD-A288735] p 1932 N95-26056
OXIDATION RESISTANCE
Development of oxidation resistant SiC/C compositionally gradient materials
[DE94-785101] p 1925 N95-24365
Oxidation of ion-implanted NiAl
[DE95-005899] p 1935 N95-25388
Processing and properties of iridium alloys for space power applications
[DE95-005902] p 1935 N95-25390
Thermal barrier coating experience in the gas turbine engine p 1944 N95-26125
Properties of plasma sprayed bond coats p 1946 N95-26135
OXIDATION-REDUCTION REACTIONS
XAS studies of Ni(I), Ni(II), and Ni(III) complexes
[DE95-004844] p 1928 N95-24257
OXIDE FILMS
Solution based synthesis of perovskite-type oxide films and powders
[DE95-006170] p 2086 N95-24594
Oxidation of ion-implanted NiAl
[DE95-005899] p 1935 N95-25388
OXIDES
In situ XAFS study of oxides formed on nickel thin film electrodes in KOH solution
[AD-A288735] p 1932 N95-26056
OXYGEN
Copper transport on oxygen annealing of a superconducting film Y-Ba-Cu-O
[DE94-627566] p 2086 N95-24537
Oxygen stoichiometry and its influence on superconductivity in Bi2Sr2CaCu2O(8+x)
[DE95-004660] p 2088 N95-25282
The effect of O2 intercalation on the rotational Dynamics and the ordering transition of C60
[DE95-004765] p 2090 N95-25897
Development of a model of atmospheric oxygen variations to estimate terrestrial carbon storage and release
[NASA-CR-198002] p 2002 N95-25955
Spacecraft materials studies on The Aerospace Corporation Tray on EOIM-3
[AD-A288682] p 1942 N95-26049
OXYGEN ATOMS
Composite materials flown on the Long Duration Exposure Facility
[NASA-CR-4657] p 1923 N95-24583
OXYGEN CONSUMPTION
Heat release rate measurements in tunnel fires
[PB95-165106] p 1931 N95-25443
OXYGEN IONS
Dynamics Explorer 1, retarding ion mass spectrometer summary spectrograms-82/110 to 82/229 spin-time spectrograms for H(+), He(+), O(+), N(+), O(++), M/Z = 2, and molecular ions
[NASA-TM-108485] p 2003 N95-24763
Dynamics Explorer 1, retarding ion mass spectrometer summary spectrograms-82/230 to 82/265 spin-time spectrograms for H(+), He(+), O(+), N(+), O(++), M/Z = 2, and molecular ions
[NASA-TM-108486] p 2003 N95-24764
OXYGEN ISOTOPES
Fragmentation cross sections of O-16 between 0.9 and 200 GeV/nucleon p 2060 N95-25921
OXYGEN 18
Oxidation of ion-implanted NiAl
[DE95-005899] p 1935 N95-25388
OZONE
The atmospheric effects of stratospheric aircraft: A fourth program report
[NASA-RP-1359] p 1996 N95-24274
OZONE DEPLETION
Responsibility means doing without: How to rescue the ozone-layer
[PB95-166807] p 1997 N95-24334
Our changing planet: The FY 1995 U.S. Global Change Research Program p 2002 N95-25852
OZONOSPHERE
Responsibility means doing without: How to rescue the ozone-layer
[PB95-166807] p 1997 N95-24334

P

P-N JUNCTIONS
GaAsSb-based heterojunction tunnel diodes for tandem solar cell interconnects
[DE95-004779] p 1990 N95-24264
PACKET SWITCHING
A tool for debugging internet multicast routing
[DE95-003433] p 2020 N95-24496
Dynamics of TCP traffic over ATM networks
[DE95-004687] p 2021 N95-25359
PACKET TRANSMISSION
Dynamics of TCP traffic over ATM networks
[DE95-004687] p 2021 N95-25359
PACKETS (COMMUNICATION)
A tool for debugging internet multicast routing
[DE95-003433] p 2020 N95-24496
Dynamics of TCP traffic over ATM networks
[DE95-004687] p 2021 N95-25359
PAIR PRODUCTION
Search for top in lepton + jets in D0 using a topological tag
[DE95-003929] p 2048 N95-24677
Notion of the inclusive spectra and cross sections of B-meson production in hadronic interactions of high energies
[DE94-628628] p 2049 N95-24887
Scalar three body decays and signals for new physics
[DE95-607188] p 2053 N95-25438
Electroweak boson pair production at the Tevatron
[DE95-004234] p 2056 N95-25563
Anisotropy of dilepton emission from nuclear collisions
[DE95-004354] p 2070 N95-25634
Magnetized pair Bose gas: Relativistic superconductor
[DE95-607846] p 2100 N95-26104
PANELS
New techniques to test fatigue properties of coined sheet specimens. Part 2: Comparison of different materials, forming operations and life prediction techniques for a simple test geometry
[PB95-165122] p 1982 N95-25444
Design and evaluation of a foam-filled hat-stiffened panel concept for aircraft primary structural applications
[NASA-TM-109175] p 1928 N95-26251
Finite element buckling and postbuckling solutions for multilayered composite panels p 1983 N95-26264
Thermomechanical postbuckling of multilayered composite panels with cutouts p 1984 N95-26267
Effect of mesh distortion on the accuracy of transverse shear stresses and their sensitivity coefficients in multilayered composites p 1985 N95-26270
Recent advances in the sensitivity analysis for the thermomechanical postbuckling of composite panels p 1985 N95-26274
Buckling and postbuckling of composite panels with cutouts subjected to combined edge shear and temperature change p 1987 N95-26280
PARABOLIC BODIES
On a generalized Kepler-Coulomb system: Inter basis expansions
[DE94-636739] p 2093 N95-24349
PARABOLIC DIFFERENTIAL EQUATIONS
Atmospheric and terrain effects on acoustic propagation
[AD-A288727] p 2039 N95-25503
Adaptive finite element method 2: Error estimation
[AD-A288358] p 2033 N95-25509
Behaviour at X= +/- infinity of solutions to a predator-prey model
[DE95-607049] p 2033 N95-25748
PARABOLIC REFLECTORS
A satellite-tracking millimeter-wave reflector antenna system for mobile satellite-tracking
[NASA-CASE-NPO-18772-1-CU] p 1954 N95-25316
PARALLEL COMPUTERS
Outline of fast analyzer for MHD equilibrium FAME
[DE94-777540] p 2076 N95-24311
A domain decomposition study of massively parallel computing in compressible gas dynamics
[DE95-004759] p 1965 N95-25895
Postbuckling and large-deflection nonlinear analyses on distributed-memory computers p 1986 N95-26276
Sensitivity analysis for large-deflection and postbuckling responses on distributed-memory computers p 1987 N95-26281
PARALLEL PROCESSING (COMPUTERS)
Reducing neural network training time with parallel processing
[NASA-TM-110154] p 2015 N95-24209
Implementation of a parallel algorithm for thermo-chemical nonequilibrium flow simulations
[DE95-004758] p 1961 N95-24262
Outline of fast analyzer for MHD equilibrium FAME
[DE94-777540] p 2076 N95-24311
Computational load in model physics of the parallel NCAR community climate model
[DE95-005410] p 2019 N95-24342
A parallel, portable and versatile treecode
[DE95-000842] p 2019 N95-24343
Parallel algorithms for dynamically partitioning unstructured grids
[DE95-001616] p 2015 N95-24346
Aerodynamic optimization studies on advanced architecture computers
[NASA-CR-198045] p 1906 N95-24379
Parallel processing for scientific computations
[NASA-CR-198013] p 2020 N95-24563
A practical approach to portability and performance problems on massively parallel supercomputers
[DE95-005251] p 2020 N95-24612
Object-oriented parallel polygon rendering
[DE95-004909] p 2021 N95-24881
Implementation of a parallel unstructured Euler solver on the CM-5
[NASA-CR-195056] p 2032 N95-25106

Parallel processing of atmospheric chemistry calculations: Preliminary considerations
[DE95-005915] p 1999 N95-25198
A Decade of Neural Networks: Practical Applications and Prospects
[NASA-CR-197334] p 2022 N95-25253
Missileborne Artificial Vision System (MAVIS)
p 2022 N95-25254
VLSI neuroprocessors p 2023 N95-25258
Low-cost image analysis system
[DE95-005021] p 2021 N95-25378
Designing a stencil compiler for the Connection Machine model CM-5
[DE95-006861] p 2021 N95-25477
Alpha(sub critical) for parallel processors
[PB95-165320] p 2022 N95-25625
Use of multiple fronts in Gaussian elimination
[PB95-165353] p 2033 N95-25627
The coupling of fluids, dynamics, and controls on advanced architecture computers
[NASA-CR-197727] p 2017 N95-25797
A domain decomposition study of massively parallel computing in compressible gas dynamics
[DE95-004759] p 1965 N95-25895
Dynamic matrices and their application to the concept of a semi-sparse matrix
[AD-A288688] p 2035 N95-26051
Converting multiple OC-3c ATM streams to HIPPI to drive an HDTV frame buffer from a workstation cluster
[DE95-003638] p 2022 N95-26066
Nonlinear structural analysis on distributed-memory computers p 1985 N95-26272

PARALLEL PROGRAMMING

On the Trellis structure of a (64,40,8) subcode of the (64,42,8) third-order Reed-Muller code
[NASA-CR-198019] p 2015 N95-24224

PARAMETER IDENTIFICATION

Aerodynamic parameter estimation via Fourier modulating function techniques
[NASA-CR-4654] p 1911 N95-24630
Actuating signals in adaptive control systems
[IFTR-13/1994] p 2027 N95-26330

PARAMETERIZATION

The space of solutions of Toda field theory
[DE95-607095] p 2099 N95-25650

PARAMETRIC AMPLIFIERS

Phase correction in two-crystal optical parametric oscillators
[DE95-006317] p 2074 N95-25559

PARATHYROID GLAND

Human parathyroid hormone-(1-38) restores cancellous bone to the immobilized, osteopenic proximal tibial metaphysis in rats
[NASA-CR-197709] p 2011 N95-24556

PARITY

Parity doubling from thermodynamics of experimental hadron spectrum
[DE95-600934] p 2095 N95-24839
CP violation tests for tau/top processes
[DE95-005924] p 2051 N95-25292

PARTIAL DIFFERENTIAL EQUATIONS

Construction of quasi-periodic solutions for Hamiltonian perturbations of linear equations and applications to nonlinear PDE
[PB95-165551] p 2028 N95-24322
Covolume solutions of three dimensional div-curl equations
[NASA-CR-195031] p 2029 N95-24421
The geometry of weak solutions of certain integrable nonlinar PDE's
[DE95-005241] p 2030 N95-24609
Nonlinear difference approximations for evolutionary PDE's
[DE95-005260] p 2033 N95-25676

PARTIAL PRESSURE

Oxygen stoichiometry and its influence on superconductivity in Bi2Sr2CaCu2O(8+x)
[DE95-004660] p 2088 N95-25282
Structural and thermodynamic properties of 3-d transition metals: Pseudopotential theory revisited
[DE95-605639] p 1937 N95-25983

PARTICLE ACCELERATION

High Energy Physics Advisory Panel's subpanel on vision for the future of high-energy physics
[DE94-013641] p 2068 N95-24899
Particle acceleration very near an x-line in a collisionless plasma
[ATR-92(7251)-4] p 2080 N95-25325

PARTICLE ACCELERATOR TARGETS

Target injection methods for inertial fusion energy
[DE95-003654] p 2067 N95-24651
Anisotropy of dilepton emission from nuclear collisions
[DE95-004354] p 2070 N95-25634

PARTICLE ACCELERATORS

The AGS gamma(sub t)-jump system
[DE95-003170] p 2064 N95-24287
The physics and experimental program of the Relativistic Heavy Ion Collider (RHIC)
[DE95-003416] p 2066 N95-24495
Pulsed power drivers for ICF and high energy density physics
[DE95-003361] p 2066 N95-24500
Annual report of National Institute of Radiological Sciences
[DE94-792664] p 2009 N95-25902

PARTICLE BEAMS

The cooling of particle beams
[DE95-004669] p 2065 N95-24320
Pulsed power drivers for ICF and high energy density physics
[DE95-003361] p 2066 N95-24500
Search for the prompt muon antineutrino from charm particle decays at the IHEP-JINR Neutrino detector in 70 GeV proton beam-dump experiment
[DE94-628772] p 2049 N95-24889
A high intensity slow positron facility for the Advanced Neutron Source
[DE94-014108] p 2050 N95-25099
Testing supersymmetry at the next linear collider
[DE95-006064] p 2069 N95-25297
Neural network technique for orbit correction in accelerators/storage rings
[DE95-005955] p 2026 N95-25368
Coupling correction using closed orbit measurements
[DE95-005957] p 2070 N95-25369

PARTICLE CHARGING

W-charge asymmetry at CDF, tests of structure functions
[DE95-004855] p 2041 N95-24256
CP violation tests for tau/top processes
[DE95-005924] p 2051 N95-25292

PARTICLE COLLISIONS

W-charge asymmetry at CDF, tests of structure functions
[DE95-004855] p 2041 N95-24256
Proton-proton interactions using the RHIC polarized collider
[DE95-005839] p 2043 N95-24326
New results in nucleon-nucleon scattering at intermediate energies
[DE95-004594] p 2043 N95-24332
A high-energy high-luminosity (mu)(+) - (mu)(-) collider
[DE95-006097] p 2065 N95-24357
Extending the kinematic range for W(sub R) searches in e(-)e(-) collisions at the NLC
[DE95-005946] p 2044 N95-24415
The physics and experimental program of the Relativistic Heavy Ion Collider (RHIC)
[DE95-003416] p 2066 N95-24495
Accelerator physics R and D
[DE95-003624] p 2046 N95-24547
Toward improved photon-atom scattering predictions
[DE95-003651] p 2046 N95-24549
Multiplicity moments in e(+)e(-) annihilation into hadrons at the Z(sup 0) resonance
[DE95-005950] p 2047 N95-24641
On a possibility for a measurement of the transversal proton polarization in the diffractive pion production in pp and pe high energy collisions
[DE94-628598] p 2047 N95-24668
Evidence for top quark production in 1.8 TeV p-bar p collisions
[DE95-003496] p 2068 N95-24728
The interactions of high-energy, highly charged Xe ions with buckyballs
[DE95-004597] p 2069 N95-25281
Testing supersymmetry at the next linear collider
[DE95-006064] p 2069 N95-25297
A search for t(anti t) (yields) lepton + E(sub T) + jets signature in p(anti p) collisions at (radical)s = 1.8 TeV with the DO detector
[DE95-004239] p 2052 N95-25402
Fast algorithms for transport models
[DE95-007064] p 2054 N95-25479
Inelastic collisions of negative muons and hadrons with Helium metastable atoms
[DE95-607538] p 2055 N95-25493
Anisotropy of dilepton emission from nuclear collisions
[DE95-004354] p 2070 N95-25634
Dependence of the multiplicities of secondary particles on the impact parameter in collisions of high-energy neon and iron nuclei with photoemulsion nuclei
p 2059 N95-25919
Multiplicities of secondaries in nuclear interactions, induced by Ne-20, Ar-40 and Fe-56 nuclei at 0.1-0.5 GeV/nucleon p 2060 N95-25920
Fragmentation cross sections of O-16 between 0.9 and 200 GeV/nucleon p 2060 N95-25921

PARTICLE DECAY

Quantum mechanics with spontaneous localization and experiments
[DE94-634285] p 2092 N95-24266
Low energy theorems in quark potential models
[DE94-636791] p 2042 N95-24316
Investigation of the gross structure of spectra and mass distributions of hadronic resonances
[DE94-636799] p 2043 N95-24361
The discovery of the tau lepton: Part 1, The early history through 1975; Part 2, Confirmation of the discovery and measurement of major properties, 1976-1982
[DE95-005945] p 2044 N95-24414
Extending the kinematic range for W(sub R) searches in e(-)e(-) collisions at the NLC
[DE95-005946] p 2044 N95-24415
A measurement of quark and gluon jet differences at the Z(sup 0) resonance
[DE95-005947] p 2044 N95-24417
A test of the flavor independence of strong interactions
[DE95-005948] p 2044 N95-24418
Measurement of alpha(sub s)from hadronic event observables at the Z(sup 0) resonance
[DE95-005943] p 2045 N95-24434
A search for jet handedness in hadronic Z(sup 0) decays
[DE95-005944] p 2045 N95-24435
Lagrangian formulation of NJL model with se parable interaction
[DE94-628519] p 1952 N95-24506
Measurement of the charged multiplicity of Z(sup 0) (yields) b(bar b) events
[DE95-006051] p 2046 N95-24571
The left-right forward-backward asymmetry of heavy quarks measured with jet charge and with leptons at the SLD
[DE95-006145] p 2046 N95-24593
Measurement of alpha(sub s) from hadronic ev ent observables at the Z(sup 0) resonance
[DE95-005949] p 2047 N95-24622
A study of K(sub s) (lambda) and (bar (lambda)) production in hadronic Z(sup 0) decays
[DE95-004280] p 2047 N95-24660
New physics effects on CP Violation in B decays
[DE94-628617] p 2049 N95-24722
Evidence for top quark production in 1.8 TeV p-bar p collisions
[DE95-003496] p 2068 N95-24728
DOE-High Energy Physics Contract with the University of Hawaii
[DE95-004214] p 2068 N95-24852
Search for the prompt muon antineutrino from charm particle decays at the IHEP-JINR Neutrino detector in 70 GeV proton beam-dump experiment
[DE94-628772] p 2049 N95-24889
Elementary particle physics
[DE95-004376] p 2051 N95-25241
CP violation tests for tau/top processes
[DE95-005924] p 2051 N95-25292
B physics with CDF: Recent results and future prospects
[DE95-004793] p 2051 N95-25372
Tau physics 1994: A theoretical perspective
[DE95-004840] p 2052 N95-25375
A search for t(anti t) (yields) lepton + E(sub T) + jets signature in p(anti p) collisions at (radical)s = 1.8 TeV with the DO detector
[DE95-004239] p 2052 N95-25402
Heavy quark effective theory, interpolating fields and Bethe-Salpeter amplitudes
[DE95-607146] p 2053 N95-25460
Annihilation diagrams in two-body nonleptonic decays of charmed mesons
[DE95-607181] p 2054 N95-25463
Heavy-neutrino effects on tau-lepton decays
[PB95-165346] p 2056 N95-25626
Electroweak coupling measurements from polarized Bhabha scattering at the Z(exp 0) resonance
[DE95-006090] p 2057 N95-25768
Searching for exotic mesons in e(+)e(-) annihilation at DA(phi)NE
[PB95-165379] p 2064 N95-26001
Results/prospects in E777/851/865
[DE95-005959] p 2064 N95-26006
Preliminary results on the decays D(+) yields K(+)pi(+)pi(-), D(+) yields K(+)K(+)K(-)
[DE95-004865] p 2071 N95-26011
Heavy-neutrino chirality enhancement of the decay K(L) yields e(mu) in left-right symmetric models
[PB95-165387] p 2064 N95-26096

PARTICLE DENSITY (CONCENTRATION)

Replicator for characterization of cirrus and polar stratospheric cloud particles
[NASA-CR-197992] p 2005 N95-24411

Meson properties at finite temperature and density within Nambu-Jona-Lasinio model
[DE94-628630] p 2049 N95-24888

PARTICLE DIFFUSION

Transport suppression by diamagnetic phase shift as a possible mechanism to the L to H transition
[DE95-003345] p 2077 N95-24587

PARTICLE EMISSION

The emission of particle identification efficiency in the EXCHARM experiment
[DE94-628258] p 2047 N95-24644
Report series in aerosol science
[DE95-737628] p 1999 N95-24904

PARTICLE ENERGY

A high-energy high-luminosity (mu)(+) - (mu)(-) collider
[DE95-006097] p 2065 N95-24357
Scalar three body decays and signals for new physics
[DE95-607188] p 2053 N95-25438

PARTICLE IN CELL TECHNIQUE

Particle-mesh techniques
[NASA-CR-4666] p 2083 N95-26082

PARTICLE INTERACTIONS

Accelerator physics R and D
[DE95-003624] p 2046 N95-24547
Geometry of multihadron production
[DE95-004290] p 2047 N95-24663
Present experimental data on cross channel deep-inelastic processes and the Gribov-Lipatov relation
[DE94-628605] p 2049 N95-24719
Notion of the inclusive spectra and cross sections of B-meson production in hadronic interactions of high energies
[DE94-628628] p 2049 N95-24887
Probing new physics in rare charm processes
[DE95-006067] p 2050 N95-24903
Elementary particle physics
[DE95-004376] p 2051 N95-25241

PARTICLE MASS

Top quark kinematics and mass determination
[DE95-004853] p 2041 N95-24254
Neutrino masses and b - tau unification in the supersymmetric standard model
[DE94-634361] p 2043 N95-24404
Evidence for top quark production in 1.8 TeV p-bar p collisions
[DE95-003496] p 2068 N95-24728
Meson properties at finite temperature and density within Nambu-Jona-Lasinio model
[DE94-628630] p 2049 N95-24888
Supersymmetry and light quark masses in a realistic superstring model
[DE94-628530] p 2096 N95-25096
B physics with CDF: Recent results and future prospects
[DE95-004793] p 2051 N95-25372
Neutrino oscillations from discrete non-Abelian family symmetries
[DE95-004355] p 2052 N95-25403
Masses of heavy fermions and Higgs boson in four-generation fermion condensate scheme
[DE95-607124] p 2053 N95-25450
Neutrino mass and oscillation angle phenomena within the asymmetric left-right models
[DE95-607201] p 2054 N95-25466
A simple relation among the quark masses
[DE95-703783] p 2055 N95-25494
Electroweak coupling measurements from polarized Bhabha scattering at the Z(exp 0) resonance
[DE95-006090] p 2057 N95-25768
Results/prospects in E777/851/865
[DE95-005959] p 2064 N95-26006

PARTICLE MOTION

The geodesic motion in Kaluza-Klein spinning space
[DE95-607070] p 2039 N95-25646
Magnetic mirror effect as a trigger of collisionless magnetic reconnection
[NIFS-295] p 2083 N95-26337
A mechanism of collisionless magnetic reconnection
[NIFS-274] p 2083 N95-26339

PARTICLE PRECIPITATION

Report series in aerosol science
[DE95-737628] p 1999 N95-24904

PARTICLE PRODUCTION

Study of the structure of the events produced in soft (bar p)p interactions of (radical)s = 1800 GeV
[DE95-004851] p 2041 N95-24252
Top quark kinematics and mass determination
[DE95-004853] p 2041 N95-24254
Proton-proton interactions using the RHIC polarized collider
[DE95-005839] p 2043 N95-24326
On leading charmed meson production in pi-nucleon interactions
[DE94-636797] p 2043 N95-24360
Extending the kinematic range for W(sub R) searches in e(-)e(-) collisions at the NLC
[DE95-005946] p 2044 N95-24415
A measurement of quark and gluon jet differences at the Z(sup 0) resonance
[DE95-005947] p 2044 N95-24417
Tau physics at future facilities
[DE95-006071] p 2046 N95-24591
Measurement of the WW gamma, ZZ gamma and Z gamm a gamma couplings at the Fermilab Tevatron
[DE95-003495] p 2067 N95-24601
Multiplicity moments in e(+)e(-) annihilation into hadrons at the Z(sup 0) resonance
[DE95-005950] p 2047 N95-24641
A study of K(sub s) (lambda) and (bar (lambda)) production in hadronic Z(sup 0) decays
[DE95-004280] p 2047 N95-24660
Geometry of multihadron production
[DE95-004290] p 2047 N95-24663
Evidence for top quark production in 1.8 TeV p-bar p collisions
[DE95-003496] p 2068 N95-24728
DOE-High Energy Physics Contract with the University of Hawaii
[DE95-004214] p 2068 N95-24852
Search for the prompt muon antineutrino from charm particle decays at the IHEP-JINR Neutrino detector in 70 GeV proton beam-dump experiment
[DE94-628772] p 2049 N95-24889
Elementary particle physics
[DE95-004376] p 2051 N95-25241
B physics with CDF: Recent results and future prospects
[DE95-004793] p 2051 N95-25372
Photon-charm production in p(anti p) collisions at radical s = 1.8 TeV
[DE95-004850] p 2052 N95-25377
A search for t(anti t) (yields) lepton + E(sub T) + jets signature in p(anti p) collisions at (radical)s = 1.8 TeV with the DO detector
[DE95-004239] p 2052 N95-25402
Extended gauge sectors
[DE95-006485] p 2052 N95-25407
The twist-3 single spin asymmetries of pion production
[DE95-607144] p 2052 N95-25437
Ten dimensional SO(10) G.U.T. models with dynamical symmetry breaking
[DE95-607093] p 2098 N95-25533
Further ways to distinguish single-lepton top quark signals from background at the Tevatron
[PB95-165395] p 2056 N95-25567
Electroweak coupling measurements from polarized Bhabha scattering at the Z(exp 0) resonance
[DE95-006090] p 2057 N95-25768
A Green's function method for hadrons in nuclei
[DE94-792620] p 2070 N95-25772

PARTICLE SIZE DISTRIBUTION

Characterization of ultradispersed aluminum
[DE95-006379] p 1933 N95-24329
The effect of altitude conditions on the particle emissions of a J85-GE-5L turbojet engine
[NASA-TM-106669] p 1914 N95-24561

PARTICLE SPIN

Temperature dependence of magnetic anisotropy and magnetostriction: Beyond the mean-field theory
[DE94-634529] p 2084 N95-24244
Accelerator physics R and D
[DE95-003624] p 2046 N95-24547
Current status and future prospect of space and time reversal symmetry violation on low energy neutron reactions
[DE94-765589] p 2048 N95-24702
The twist-3 single spin asymmetries of pion production
[DE95-607144] p 2052 N95-25437
Scalar three body decays and signals for new physics
[DE95-607188] p 2053 N95-25438
The geodesic motion in Kaluza-Klein spinning space
[DE95-607070] p 2039 N95-25646
Quantum group random walks in strongly correlated 2 + 1 D spin systems
[DE95-607844] p 2091 N95-26103

PARTICLE THEORY

Self-consistent beam halo studies & halo diagnostic development in a continuous linear focusing channel
[DE95-003706] p 2065 N95-24331
Supersymmetry
[DE95-004670] p 2092 N95-24333
High Energy Physics Advisory Panel's subpanel on vision for the future of high-energy physics
[DE94-013641] p 2068 N95-24899
Neutrino mass and oscillation angle phenomena within the asymmetric left-right models
[DE95-607201] p 2054 N95-25466
Valencia 1993: The summary of particle theory
[DE95-607121] p 2110 N95-25469
A simple relation among the quark masses
[DE95-703783] p 2055 N95-25494

PARTICLE TRACKS

Adaptive projective filters
[DE94-628374] p 2030 N95-24645
Target injection methods for inertial fusion energy
[DE95-003654] p 2067 N95-24651
The CDF silicon vertex detector SVX and its upgrades
[DE95-003743] p 2050 N95-24901
Double-sided silicon microstrip sensors for the CDF SVX 2 detector
[DE95-004235] p 2068 N95-25238
Fission foil detector calibrations with high energy protons p 2060 N95-25924

PARTICLE TRAJECTORIES

Neural network technique for orbit correction in accelerators/storage rings
[DE95-005955] p 2026 N95-25368

PARTICLES

Existence domains and some properties of a particle bound state in fields with homogeneous dependence of its potential energy on coordinates
[DE95-605280] p 2057 N95-25784

PARTICULATE REINFORCED COMPOSITES

Strengthening of NiAl matrix composites
[AD-A288923] p 1926 N95-25505

PARTICULATES

Cross-flow, filter-sorbent-catalyst for particulate, SO2 and NO(x) control
[DE95-001934] p 2003 N95-26091

PARTITIONS (MATHEMATICS)

Parallel algorithms for dynamically partitioning unstructured grids
[DE95-001616] p 2015 N95-24346

PARTONS

Measurement of the SS-OS Dijet cross-section ratio
[DE95-004852] p 2041 N95-24253
W-charge asymmetry at CDF, tests of structure functions
[DE95-004855] p 2041 N95-24256
A search for jet handedness in hadronic Z(sup 0) decays
[DE95-005944] p 2045 N95-24435
The twist-3 single spin asymmetries of pion production
[DE95-607144] p 2052 N95-25437
Parton distributions for low Q2
[PB95-165213] p 2056 N95-25619

PASSENGER AIRCRAFT

Noise impact of advanced high lift systems
[NASA-CR-195028] p 2040 N95-26160

PATHOGENS

Structures and functions of oligosaccharins
[DE95-003140] p 2007 N95-24225

PATTERN RECOGNITION

Use of voronoi diagrams for qualitative matching
[PB95-165445] p 1988 N95-24240
Neural network application to comprehensive engine diagnostics p 2023 N95-25255
From neural-based object recognition toward microelectronic eyes p 2023 N95-25257
Photonics: From target recognition to lesion detection p 2023 N95-25259
Three-D Artificial Neural Network (3DANN) technology. Blueprint for the future p 2024 N95-25260
Neural network classification of clinical neurophysiological data for acute care monitoring p 2024 N95-25263
How Captain Amerika uses neural networks to fight crime p 2025 N95-25272

PAYLOAD DEPLOYMENT & RETRIEVAL SYSTEM

STS-67 post flight presentation
[NASA-TM-110552] p 1918 N95-24198

PAYLOAD RETRIEVAL (STS)

Evaluation of restraint system concepts for the Japanese Experiment Module flight demonstration
[NASA-TM-104808] p 2013 N95-24627

PAYLOAD TRANSFER

Shuttle to space station transfer of the materials exposure facility
[NASA-TM-110156] p 1919 N95-24765

PAYLOADS

Software engineering and data management for automated payload experiment tool
[NASA-CR-196562] p 2104 N95-24477
Shuttle to space station transfer of the materials exposure facility
[NASA-TM-110156] p 1919 N95-24765
Suspension system for gimbal supported scanning payloads
[NASA-CASE-MFS-28817-1] p 1969 N95-25544

PEEK

Static and fatigue properties of pin-joint specimens of a AS-4/PEEK thermoplastic composite material
[NAL-TR-1214] p 1927 N95-25859

PELLETS
Results obtained using the pellet charge exchange diagnostic on TFTR
[DE95-003254] p 2079 N95-25120
PEPTIDES
Fusion proteins as alternate crystallization paths to difficult structure problems
[NASA-TM-110497] p 2008 N95-24531
Genetic and biophysical studies of the photosynthetic reaction center
[DE95-004179] p 2008 N95-24850
PERCOLATION
Spin correlations in percolating networks with fractal geometry
[DE95-001074] p 2037 N95-24479
PERFORMANCE
Adventures in the evolution of a high-bandwidth network for central servers
[DE95-006215] p 2020 N95-24597
PERFORMANCE PREDICTION
Effect of film cooling/regenerative cooling on scramjet engine performances
[NAL-TR-1242] p 1914 N95-24990
New techniques to test fatigue properties of coined sheet specimens. Part 2: Comparison of different materials, forming operations and life prediction techniques for a simple test geometry
[PB95-165122] p 1982 N95-25444
PERFORMANCE TESTS
Actively controlled shaft seals for aerospace applications
[NASA-CR-198035] p 1974 N95-24218
Investigation of properties and performance of ceramic composite components
[DE95-004737] p 1939 N95-24247
Monolithic solid oxide fuel cell technology advancement for coal-based power generation
[DE94-012258] p 1990 N95-24318
AMC EN-1038: Reduced scale solar simulator supplementary test report
[NASA-CR-197988] p 1915 N95-24380
Visual performance with Omnibus 3: A comparative evaluation of enhanced generation three image intensifier technology
[PB95-141891] p 2013 N95-24510
Experimental and theoretical development towards a 500 MW, one-microsecond, L-band relativistic klystron amplifier
[DE95-003682] p 1958 N95-24589
High-gradient experiment on X-band disk-loaded structures
[DE94-765446] p 1958 N95-24701
BSA Delta Qualification 2, volume 3, book 1
[NASA-CR-196565] p 1922 N95-24845
Flight reference display for powered-lift STOL aircraft
[NAL-TR-1251] p 1912 N95-25005
Comparison of three methods for optical characterization of point-focus concentrators
[DE95-000282] p 1994 N95-25309
FTAPE: A fault injection tool to measure fault tolerance
[NASA-CR-198000] p 1978 N95-25333
Internal performance characteristics of thrust-vectored axisymmetric ejector nozzles
[NASA-TM-4610] p 1907 N95-25338
Thermodynamic property evaluation and magnetic refrigeration cycle analysis for gadolinium gallium garnet
[DE95-005910] p 1951 N95-25367
Development of a portable mass spectrometric system for determination of isotopic composition of solid uranium samples using fluorine volatilization
[DE95-005728] p 1969 N95-25384
Radial electron-beam-breakup transit-time oscillator
[DE95-005731] p 1959 N95-25385
Benchmark testing and independent verification of the VS2DT computer code
[DE95-004386] p 1965 N95-25485
Evaluation of commercial fuel tank water absorbers
[AD-A288361] p 1951 N95-25513
Performance evaluation of LE-7 high pressure pumps
[NAL-TR-1212T] p 1977 N95-25672
Facility for the evaluation of space communications and related systems
[NASA-TM-106904] p 1955 N95-25876
Performance tests of air source heat pumps under frosting conditions. Quality of results
[PB95-141792] p 1995 N95-25892
Wind technology development: Large and small turbines
[DE95-000286] p 1995 N95-26090
Developing a standardized test procedure for hybrid vehicles: The challenge of the SAE HEV task force
[DE95-000280] p 1978 N95-26286
PERIODIC FUNCTIONS
Exponentially accurate approximations to piece-wise smooth periodic functions
[NASA-CR-195059] p 2031 N95-24856
PERIODIC VARIATIONS
Modelling the day to day wind variability offshore central Chile at about 30 deg south
[DE95-606032] p 2006 N95-26043
PERMANENT MAGNETS
Faster magnet sorting with a threshold acceptance algorithm
[DE95-006487] p 2038 N95-25408
PERMEABILITY
Predicting the transport properties of sedimentary rocks from microgeometry
[DE95-000129] p 2004 N95-26089
Dynamic methods for determining the material characteristics of saturated permeable media
[IFTR-17/1993] p 1932 N95-26107
PERMUTATIONS
A partial unification model in non-commutative geometry
[DE95-607129] p 2097 N95-25435
PEROVSKITES
Thin film ionic conductors based on cerium oxide
[DE95-003668] p 2086 N95-24514
Study of copper perovskite
[DE95-730106] p 2088 N95-24988
Ion beam mixing of titanium overlayers with hydroxyapaptite substrates
[DE95-005278] p 1935 N95-25379
Rotational melting in displacive quantum paraelectrics
[DE95-607804] p 2091 N95-26252
LuAlO3: A high density, high speed scintillator for gamma detection
[DE95-004678] p 2064 N95-26256
PEROXIDES
Antioxidant and sensitizer effect on the stability of natural rubber latex vulcanized by gamma rays
[DE94-636061] p 1939 N95-24373
PERSONNEL
EOS Directory
[NASA-TM-110580] p 1989 N95-24542
PERTURBATION
Bounds for departure from normality and the Frobenius norm of matrix eigenvalues
[DE95-006144] p 2030 N95-24592
Transport reduction by current profile control in the reversed field pinch
[DE95-007016] p 2077 N95-24619
Modelling the day to day wind variability offshore central Chile at about 30 deg south
[DE95-606032] p 2006 N95-26043
On convergence of the Nelder-Mead simplex algorithm for unconstrained stochastic optimization
[AD-A289453] p 2006 N95-26197
PERTURBATION THEORY
Periodic solutions of Hamiltonian perturbations of 2D linear Schroedinger equations
[PB95-165536] p 2028 N95-24301
Bound states of 'dressed' particles
[DE94-636773] p 2042 N95-24314
Construction of quasi-periodic solutions for Hamiltonian perturbations of linear equations and applications to nonlinear PDE
[PB95-165551] p 2028 N95-24322
Recent progress in one-loop multi-parton calculations
[DE95-006062] p 2092 N95-24328
Chiral limit of QCD
[DE95-005245] p 2094 N95-24610
A quantum gravitational mechanism for exiting inflation
[DE95-003342] p 2096 N95-24867
Singularly perturbed differential/algebraic equations
[AD-A288365] p 2033 N95-25601
Diagrammatic many-body perturbation expansion for atoms and molecules
[PB95-165221] p 2056 N95-25620
Cosmological constraints on perturbative supersymmetry breaking
[PB95-165361] p 2099 N95-25628
The hard truth --- a method to determine the reliability of a specific feature of a Bayesian solution
[DE95-005240] p 2033 N95-25767
Optimal guidance law development for an advanced launch system
[NASA-CR-4667] p 1917 N95-26205
PETRI NETS
Reliability analysis of software based safety functions
[DE95-806516] p 2018 N95-26045
PHARMACOLOGY
Staurosporine analysis and its pharmacokinetics in the blood of rats
[DE94-013857] p 2008 N95-24600
JPRS Report: Science and technology. Central Eurasia
[JPRS-UST-94-031] p 1988 N95-24760
PHASE CONTRAST
Engineering and design of a CO2 phase contrast interferometer system for DIII-D
[DE95-004249] p 1972 N95-24709
PHASE CONTROL
Liquid crystal point diffraction interferometer
[NASA-TM-106899] p 1970 N95-26073
PHASE ERROR
Phase correction in two-crystal optical parametric oscillators
[DE95-006317] p 2074 N95-25559
Liquid crystal point diffraction interferometer
[NASA-TM-106899] p 1970 N95-26073
PHASE MODULATION
Accurate determination of IC modulation parameter in Sr(x)Ba(1-x)Nb2O6 from second order satellites of neutron diffraction TOF (Time-Of-Flight) spectra
[DE94-629003] p 2090 N95-25851
Continuous phase and amplitude holographic elements
[NASA-CASE-NPO-18791-1] p 1971 N95-26340
PHASE SEPARATION (MATERIALS)
FNAS phase partitions
[NASA-CR-193855] p 1940 N95-24562
PHASE SHIFT
Transport suppression by diamagnetic phase shift as a possible mechanism to the L to H transition
[DE95-003345] p 2077 N95-24587
Observation of the scalar Aharonov-Bohm effect by neutron interferometry
[DE95-607020] p 2097 N95-25446
PHASE STABILITY (MATERIALS)
Stability and elastic properties of hydrogen loaded Ti(1-x)Al(x) alloys: An ab initio study
[AD-A288903] p 1936 N95-25529
PHASE TRANSFORMATIONS
Kinetics of diffusional droplet growth in a liquid/liquid two-phase system
[NASA-CR-198050] p 1961 N95-24221
T=0 finite-size scaling for a quantum system with long-range interaction
[DE94-634528] p 2092 N95-24288
Theory of ultra dense matter and the dynamics of high energy interactions involving nuclei
[DE95-004114] p 2048 N95-24671
Report series in aerosol science
[DE95-737628] p 1999 N95-24904
Statistical mechanics of nonlinear coherent structures: Kinks in the Phi(sup 6) model
[DE95-005253] p 2096 N95-25293
Processing and characterization of transformation-toughened ceramics with strength retention to elevated temperatures
[DE95-005758] p 1941 N95-25387
Critical parameters of Quark-Hadron phase transition with interacting and massive quarks
[DE95-607143] p 2052 N95-25436
Zero sound velocity in pi, rho mesons at different temperatures
[DE95-607145] p 2053 N95-25459
Physics in Ukraine International Conference. Volume 3: Statistical physics and phase transitions
[DE95-605765] p 2038 N95-25552
Superconductivity, magnetism and metal-insulator transitions in some ternary and pseudoternary 3d-, 4d- and 5d-metal oxides
[DE95-005904] p 2038 N95-25600
Accurate determination of IC modulation parameter in Sr(x)Ba(1-x)Nb2O6 from second order satellites of neutron diffraction TOF (Time-Of-Flight) spectra
[DE94-629003] p 2090 N95-25851
PHASE-SPACE INTEGRAL
Elliptic deformed Newton mechanics in the three-dimensional phase space
[DE94-636741] p 2092 N95-24313
PHASED ARRAYS
Broadband uniplanar microstrip to slot-line transitions
[NASA-CR-195448] p 1957 N95-24476
PHENOL FORMALDEHYDE
Investigation into the flammability properties of honeycomb composites
[PB95-143293] p 1941 N95-25342
PHENOLIC RESINS
Investigation into the flammability properties of honeycomb composites
[PB95-143293] p 1941 N95-25342
PHENOMENOLOGY
Electronic structure and pairing of strongly correlated fermions: Fermi liquid versus spin liquid
[DE95-005929] p 2044 N95-24419
PHONETICS
A study of the effect of voice pitch on the perception of synthetic Polish vowels
[IFTR-10/1994] p 1956 N95-26018

PHONONS
Structure of liquid He-4 excitations spectrum
[DE94-637113] p 2043 N95-24364
PHOSPHINES
Selective extraction of trivalent actinides from lanthanides with dithiophosphinic acids and tributylphosphate
[DE95-005249] p 1924 N95-25597
PHOSPHORESCENCE
LuAlO3: A high density, high speed scintillator for gamma detection
[DE95-004678] p 2064 N95-26256
PHOSPHORIC ACID FUEL CELLS
TITLE: Environmental, health, and safety issues offuel cells in transportation. Volume 1: Phosphoricacid fuel-cell buses
[DE95-000289] p 1993 N95-24866
PHOSPHORUS
New techniques to test fatigue properties of coined sheet specimens. Part 2: Comparison of different materials, forming operations and life prediction techniques for a simple test geometry
[PB95-165122] p 1982 N95-25444
PHOTOACOUSTIC SPECTROSCOPY
Electromagnetic waves and photoacoustic transformation in gyrotropic superlattices p 2083 N95-24205
PHOTOCATHODES
Electric field effects on the quantum efficiency of Cesium-iodide photocathodes in gas media
[DE94-628176] p 1957 N95-24482
A correction of the quantum efficiency of cesium iodide and other photocathodes due to the recalibration of the reference photomultipliers
[DE94-628177] p 1957 N95-24483
PHOTOCHEMICAL REACTIONS
The atmospheric effects of stratospheric aircraft: A fourth program report
[NASA-RP-1359] p 1996 N95-24274
Overview of solar detoxification activities in the United States
[DE95-000264] p 1997 N95-24319
Disilene Addition to C70
[DE95-006321] p 2087 N95-24617
Genetic and biophysical studies of the photosynthetic reaction center
[DE95-004179] p 2008 N95-24850
Parallel processing of atmospheric chemistry calculations: Preliminary considerations
[DE95-005915] p 1999 N95-25198
PHOTOCONDUCTIVITY
High gain GaAs Photoconductive Semiconductor Switches (PCSS): Device lifetime, high current testing, optical pulse generators
[DE95-003354] p 1957 N95-24488
Back surface cell structures for reducing recombination in CZ silicon solar cells
[DE95-005423] p 1995 N95-25566
PHOTODIODES
The impact of multiplexing on the dynamic requirements of analog-to-digital converters
[DE95-006302] p 1960 N95-25558
PHOTODISSOCIATION
Far-infrared and submillimeter spectroscopy of photodissociation regions
[DE95-607520] p 2110 N95-25467
PHOTOELECTRIC EMISSION
A photoemission study of the diamond and the single crystal C(60)
[DE95-006149] p 2085 N95-24463
PHOTOELECTRON SPECTROSCOPY
A photoemission study of the diamond and the single crystal C(60)
[DE95-006149] p 2085 N95-24463
Study of radicals, clusters and transition state species by anion photoelectron spectroscopy
[DE95-003438] p 2045 N95-24533
PHOTOELECTRONS
Detector for transit time measurement of photomultiplier single-photoelectron pulses
[DE94-628256] p 2073 N95-24642
A quality monitor and monitoring technique employing optically stimulated electron emission
[NASA-CASE-LAR-15063-1-CU] p 1978 N95-25304
PHOTOGRAMMETRY
Relative orientation of multiple images using projective singular correlation
[PB95-149936] p 1967 N95-24259
ESA Bulletin No. 81 p 2114 N95-25200
PHOTOGRAPHIC FILM
Space basic
[NASA-TM-110540] p 2108 N95-24196
PHOTOGRAPHIC RECORDING
Debris/ice/TPS assessment and integrated photographic analysis of shuttle mission STS-63
[NASA-TM-110649] p 1921 N95-25337
PHOTOIONIZATION
Photoionization of shallow donor impurities in finite-barrier quantum wells
[DE95-607521] p 2097 N95-25468
Measurement of kinetic energy of ions collected from laser resonance photoionized plasma by time-of-flight method
[DE95-709767] p 2081 N95-25498
PHOTOLUMINESCENCE
Optical determinations of energy-band dispersion curves in novel compound semiconductor materials
[DE95-006318] p 2089 N95-25353
Reciprocal space analysis of the microstructure of luminescent and nonluminescent porous silicon films
[DE95-005420] p 1941 N95-25382
PHOTOMETERS
Optical generation of radio-frequency power
[DE95-005276] p 1951 N95-24289
Automatic measurement system for measuring of the nonlinearity of photo detectors
[PB95-165197] p 2074 N95-25999
Angular displacement measuring device
[NASA-CASE-ARC-11937-1] p 2074 N95-26015
PHOTOMULTIPLIER TUBES
A correction of the quantum efficiency of cesium iodide and other photocathodes due to the recalibration of the reference photomultipliers
[DE94-628177] p 1957 N95-24483
Absolute calibration and monitoring of a spectrometric channel using a photomultiplier
[DE94-628251] p 1968 N95-24635
Detector for transit time measurement of photomultiplier single-photoelectron pulses
[DE94-628256] p 2073 N95-24642
The KTeV PMT laser monitoring system
[DE95-004237] p 1972 N95-24869
PHOTON DENSITY
On the uncertainty in single molecule fluorescent lifetime and energy emission measurements
[NASA-CR-198009] p 2049 N95-24877
PHOTONS
The 1994 Fiber Optic Sensors for Aerospace Technology (FOSAT) Workshop
[NASA-CP-10166] p 1912 N95-24207
Photon-charm production in p(anti p) collisions at radical s = 1.8 TeV
[DE95-004850] p 2052 N95-25377
Radiative corrections for pion polarizability experiments
[DE95-607177] p 2053 N95-25462
Photoionization of shallow donor impurities in finite-barrier quantum wells
[DE95-607521] p 2097 N95-25468
Statistical mechanics of the magnetized pair Bose gas
[DE95-607096] p 2063 N95-25993
PHOTOSYNTHESIS
Genetic and biophysical studies of the photosynthetic reaction center
[DE95-004179] p 2008 N95-24850
The effects on photosynthetic CO2 assimilation to long-term elevation of atmospheric CO2 concentration: An assessment of the response of Trifolium Repens L. CV. Blanca grown at F.A.C.E
[DE95-005687] p 2008 N95-25383
PHOTOVOLTAIC CELLS
The effect of encapsulation on the reflectance of photovoltaic modules using textured multicrystalline-silicon solar cells
[DE95-004781] p 1996 N95-26166
Technical evaluation of a dual-junction same-band-gap amorphous silicon photovoltaic system at NREL
[DE95-000277] p 1996 N95-26285
PHOTOVOLTAIC CONVERSION
NREL Photovoltaic Program FY 1994 bibliography
[DE95-000275] p 1993 N95-24865
Wind technology development: Large and small turbines
[DE95-000286] p 1995 N95-26090
PHTHALOCYANIN
The use of acoustic surface waves to analyze gases apparatus and experiments p 2039 N95-25115
PHYSICAL PROPERTIES
Whisker reinforced glass ceramic
[DE95-005568] p 1927 N95-25998
PHYSICS
JPRS report: Science and technology. Central Eurasia
[JPRS-UST-95-017] p 1988 N95-26080
PHYSIOLOGICAL EFFECTS
Measurement of blood nitrogen content after rapid compressions to assess the speed of nitrogen uptake during the compression phase of submarine escape. (Includes measurement of nitrogen concentration in blood following rapid compression to 5 bar)
[PB95-165726] p 2012 N95-25570
PHYSIOLOGICAL TESTS
STS-67 post flight presentation
[NASA-TM-110552] p 1918 N95-24198
PIEZOELECTRIC CRYSTALS
NMR and optical studies of piezoelectric polymers
[DE95-003836] p 1940 N95-24554
PIEZOELECTRICITY
Piezoelectric motor development at AlliedSignal Inc., Kansas City Division
[DE95-003389] p 1958 N95-24532
Study of composite zirconium oxide
[DE95-730104] p 1926 N95-25111
PINNING
Coercive field and domain wall properties in (Dy(x)Y(1-x))Fe2 and (Er(x)Y(1-x))Fe2
[DE95-601135] p 1937 N95-25751
PIONS
Low energy theorems in quark potential models
[DE94-636791] p 2042 N95-24316
Numerical investigation of Schwinger-Dyson and Bethe-Salpeter equations with Gauss potential in the framework of the quarkonium model
[DE94-636730] p 2029 N95-24387
Lagrangian formulation of NJL model with se parable interaction
[DE94-628519] p 1952 N95-24506
On a possibility for a measurement of the transversal proton polarization in the diffractive pion production in pp and pe high energy collisions
[DE94-628598] p 2047 N95-24668
The twist-3 single spin asymmetries of pion production
[DE95-607144] p 2052 N95-25437
Radiative corrections for pion polarizability experiments
[DE95-607177] p 2053 N95-25462
A Green's function method for hadrons in nuclei
[DE94-792620] p 2070 N95-25772
The off-shell axial anomaly via the (gamma)*(pi)(sup 0) (yields) (gamma) transition
[DE95-004762] p 2057 N95-25896
Preliminary results on the decays D(+) yields K(+)pi(+)pi(-), D(+) yields K(+)K(+)K(-)
[DE95-004865] p 2071 N95-26011
A possibility of pi(-) Meson production by a low energy electron bunch and positive ion bunch
[NIFS-277] p 2071 N95-26029
PIPE FLOW
Studies of two-phase gas-liquid flow in microgravity
[NASA-CR-195434] p 1963 N95-24906
PIPER AIRCRAFT
Aircraft accident report: Impact with blast fence upon landing rollout Action Air Charters flight 990 Piper PA-31-350, N990RA, Stratford, Connecticut,27 April 1994
[PB94-910410] p 1908 N95-24206
PISTON ENGINES
Retrofit NOx control technologies for natural gas prime movers
[PB95-149290] p 1997 N95-24294
Optimized hydrogen piston engines
[DE95-003656] p 1975 N95-24550
PITUITARY GLAND
Electrophoretic separation of cells and particles from rat pituitary --- analysis of pituitary cell electrophoresis experiment done on IML-2 (7/94)
[NASA-CR-197975] p 2008 N95-24475
PITUITARY HORMONES
Electrophoretic separation of cells and particles from rat pituitary --- analysis of pituitary cell electrophoresis experiment done on IML-2 (7/94)
[NASA-CR-197975] p 2008 N95-24475
PIXELS
ASIC implementation of a data-push architecture for silicon pixel readout
[DE95-003368] p 2015 N95-24648
PLANE WAVES
Generalization of the Rayleigh formula to the model with ring-shaped potentials
[DE94-628578] p 2094 N95-24637
PLANETARY COMPOSITION
Infrared spectroscopy of Jupiter and Saturn
[NASA-CR-198034] p 2111 N95-24239
PLANETARY GEOLOGY
Geologic mapping of Argyre Planitia
[NASA-CR-197986] p 2112 N95-24303
Fourth symposium of the geological survey of Japan on remote sensing of satellite geology
[PB95-178737] p 1917 N95-25750
Distribution and nature of UV absorbers on Triton's surface
[NASA-CR-198008] p 2112 N95-26116
PLANETARY MAGNETIC FIELDS
Mars observer mission: Mapping the Martian world
[NASA-CR-110585] p 2112 N95-24672

PLANETARY MAPPING
Geologic mapping of Argyre Planitia
[NASA-CR-197986] p 2112 N95-24303
Mars observer mission: Mapping the Martian world
[NASA-CR-110585] p 2112 N95-24672
PLANETS
Regge in the sky: Origin of the cosmic rotation
[DE95-607001] p 2111 N95-25990
PLANNING
Planning for the unknown: Coping with uncertainty
[PB95-165114] p 2102 N95-25642
PLANTS (BOTANY)
Structures and functions of oligosaccharins
[DE95-003140] p 2007 N95-24225
Structural studies of complex carbohydrates of plant cell walls
[DE95-005545] p 2007 N95-24368
Radiobiological experiments with plant seeds aboard the biosatellite Cosmos 1887 p 2009 N95-25933
PLASMA ARC WELDING
Ternary gas plasma welding torch
[NASA-CASE-MFS-28857-1] p 1976 N95-25548
PLASMA CLOUDS
Results obtained using the pellet charge exchange diagnostic on TFTR
[DE95-003254] p 2079 N95-25120
PLASMA CONTROL
Flow-through Z-pinch study for radiation generation and fusion energy production
[DE95-004209] p 2076 N95-24544
The physics design of the Tokamak Physics Experiment
[DE95-003649] p 2076 N95-24548
Transport suppression by diamagnetic phase shift as a possible mechanism to the L to H transition
[DE95-003345] p 2077 N95-24587
Advances and prospects in reversed field pinch research
[DE95-007017] p 2077 N95-24602
Transport reduction by current profile control in the reversed field pinch
[DE95-007016] p 2077 N95-24619
Experimental and theoretical basis for advanced tokamaks
[DE95-003255] p 2077 N95-24646
Divertor design for the Tokamak Physics Experiment
[DE95-003653] p 2078 N95-24650
The role of shaping in achieving high performance in DIII-D
[DE95-003877] p 2078 N95-25102
Experimental constraints on transport
[DE95-004962] p 2050 N95-25180
Evidence for modified transport due to sheared E x B flows in high-temperature plasmas
[DE95-004870] p 2079 N95-25250
New modular heliotron system compatible with closed helical divertor and good plasma confinement
[NIFS-279] p 2081 N95-25653
Self-sustained turbulence and L-mode confinement in toroidal plasmas 2
[NIFS-278] p 2082 N95-25759
Plasma burning and control in reactor core
[DE95-602882] p 2082 N95-25942
High-beta discharges with neutral beam injection in CHS
[NIFS-280] p 2071 N95-26031
Isotope effect on confinement in DT plasmas
[NIFS-275] p 2083 N95-26326
PLASMA CURRENTS
Measurement of profiles of the space potential in JIPP T-IIU Tokamak plasmas by slow poloidal and fast toroidal sweeps of a heavy ion beam
[NIFS-273] p 2081 N95-25651
A mechanism of collisionless magnetic reconnection
[NIFS-274] p 2083 N95-26339
PLASMA DIAGNOSTICS
Fusion-neutron diagnostic on the Microwave Tokamak Experiment
[DE94-777530] p 2075 N95-24270
Development of a fast response rotating polarimeter for a Faraday rotation measurement
[DE94-777532] p 2075 N95-24271
Na-like autoionizing levels: Plasma diagnostics and prospects for photopumped soft x-ray lasers
[DE95-004207] p 1972 N95-25100
Central Laser Facility. Annual report to the Laser Facility Committee
[PB95-160511] p 1973 N95-25640
Construction of a nitrogen laser for plasma diagnostics
[DE95-607599] p 1973 N95-25973
PLASMA DIFFUSION
A proposal to introduce a turbulence factor into a diffusion coefficient of a Tokamak plasma
[DE94-777533] p 2075 N95-24272
PLASMA DYNAMICS
Particle acceleration very near an x-line in a collisionless plasma
[ATR-92(7251)-4] p 2080 N95-25325
Dynamics of structure formation in nonequilibrium systems (Wave Media)
[DE95-607609] p 2081 N95-25556
PLASMA EQUILIBRIUM
Experimental and theoretical basis for advanced tokamaks
[DE95-003255] p 2077 N95-24646
PLASMA HEATING
Design study of a negative-ion based NBI system for JT-60U
[DE94-785265] p 2043 N95-24339
Divertor design for the Tokamak Physics Experiment
[DE95-003653] p 2078 N95-24650
Magnetized target fusion: An ultra high energy approach in an unexplored parameter space
[DE95-005252] p 2080 N95-25289
Plasma burning and control in reactor core
[DE95-602882] p 2082 N95-25942
Operating level of HT-6B tokamak device
[DE95-602999] p 2082 N95-25943
PLASMA INTERACTIONS
Experimental and theoretical study of plasma-water interaction in electrothermal guns
[DE94-628961] p 2078 N95-24706
Modeling plasma/material interactions during a tokamak disruption
[DE95-004247] p 2078 N95-24861
Particle acceleration very near an x-line in a collisionless plasma
[ATR-92(7251)-4] p 2080 N95-25325
Using and programming the SUPERCODE
[DE95-004342] p 2080 N95-25344
Dynamics of structure formation in nonequilibrium systems (Wave Media)
[DE95-607609] p 2081 N95-25556
PLASMA JETS
A measurement of quark and gluon jet differences at the Z(sup 0) resonance
[DE95-005947] p 2044 N95-24417
The effect of the impedance of the generator and intermediate circuits on the impedance of plasma as it applies to magnetron sputtering of thin films in a radio-frequency field
[IFTR-8-1994] p 2083 N95-26019
High-beta discharges with neutral beam injection in CHS
[NIFS-280] p 2071 N95-26031
PLASMA LAYERS
UEDGE and DEGAS modeling of the DIII-D scrape-off layer plasma
[DE95-003652] p 2076 N95-24490
Two dimensional Bose plasma in a magnetic field
[DE95-607629] p 2082 N95-25976
PLASMA LOSS
Transport reduction by current profile control in the reversed field pinch
[DE95-007016] p 2077 N95-24619
PLASMA OSCILLATIONS
Maryland controlled fusion research program
[DE95-006642] p 2081 N95-25561
PLASMA PHYSICS
Experimental and theoretical basis for advanced tokamaks
[DE95-003255] p 2077 N95-24646
Physics in Ukraine International Conference. Volume 6: Plasma physics
[DE95-606422] p 2081 N95-25555
Central Laser Facility. Annual report to the Laser Facility Committee
[PB95-160511] p 1973 N95-25640
PLASMA POTENTIALS
Measurement of profiles of the space potential in JIPP T-IIU Tokamak plasmas by slow poloidal and fast toroidal sweeps of a heavy ion beam
[NIFS-273] p 2081 N95-25651
PLASMA RADIATION
Summaries of reports of the Electrotechnical Laboratory, no. 48
[JTN-95-80825] p 2114 N95-24908
PLASMA RESONANCE
Electroweak coupling measurements from polarized Bhabha scattering at the Z(exp 0) resonance
[DE95-006090] p 2057 N95-25768
PLASMA SPRAYING
Magnetically controlled deposition of metals using gas plasma
[DE95-003827] p 2077 N95-24552
Thermal spray processing p 1945 N95-26130
Process, properties and environmental response of plasma sprayed thermal barrier coatings p 1945 N95-26132
Thermal conductivity of zirconia thermal barrier coatings p 1945 N95-26133
Mechanical properties testing and results for thermal barrier coatings p 1946 N95-26134
Properties of plasma sprayed bond coats p 1946 N95-26135
PLASMA TEMPERATURE
Fluctuations in macroscopically agitated plasma: Quasiparticles and effective temperature
[DE95-607611] p 2082 N95-25777
PLASMA TORCHES
Ternary gas plasma welding torch
[NASA-CASE-MFS-28857-1] p 1976 N95-25548
PLASMA TURBULENCE
A proposal to introduce a turbulence factor into a diffusion coefficient of a Tokamak plasma
[DE94-777533] p 2075 N95-24272
Selected problems of the interaction of electromagnetic waves and a turbulent plasma
[IFTR-9-1993] p 2080 N95-25340
Cryogenic helium gas convection research
[DE95-004372] p 1965 N95-25404
Self-sustained turbulence and L-mode confinement in toroidal plasmas 2
[NIFS-278] p 2082 N95-25759
PLASMA WAVES
Dynamics of structure formation in nonequilibrium systems (Wave Media)
[DE95-607609] p 2081 N95-25556
Fluctuations and electromagnetic wave scattering in macroscopically agitated plasma: Effects of turbulent diffusion
[DE95-607612] p 2081 N95-25617
Fluctuations in macroscopically agitated plasma: Quasiparticles and effective temperature
[DE95-607611] p 2082 N95-25777
PLASMAS (PHYSICS)
Outline of fast analyzer for MHD equilibrium FAME
[DE94-777540] p 2076 N95-24311
Magnetically controlled deposition of metals using gas plasma
[DE95-003827] p 2077 N95-24552
Transport suppression by diamagnetic phase shift as a possible mechanism to the L to H transition
[DE95-003345] p 2077 N95-24587
Divertor design for the Tokamak Physics Experiment
[DE95-003653] p 2078 N95-24650
Results obtained using the pellet charge exchange diagnostic on TFTR
[DE95-003254] p 2079 N95-25120
Cobalt release from PCA steel during possible fusion reactor accidents
[DE95-005019] p 2069 N95-25365
Asymptotics for the Kummer function of Bose plasmas
[DE95-607019] p 2096 N95-25428
Numerical analysis of electron cyclotron resonance heating on JT-60U and JFT-2M
[DE95-709766] p 2080 N95-25471
Measurement of kinetic energy of ions collected from laser resonance photoionized plasma by time-of-flight method
[DE95-709767] p 2081 N95-25498
Physics in Ukraine International Conference. Volume 6: Plasma physics
[DE95-606422] p 2081 N95-25555
Quasiparticles in magnetized plasma
[DE95-607610] p 2081 N95-25632
New modular heliotron system compatible with closed helical divertor and good plasma confinement
[NIFS-279] p 2081 N95-25653
Report on the meeting on Chaotic Phenomena in Plasma
[DE94-792670] p 2082 N95-25904
Evolution of Spark plasma using nitrogen laser shadowgraphy system
[DE95-607598] p 2082 N95-25972
Construction of a nitrogen laser for plasma diagnostics
[DE95-607599] p 1973 N95-25973
Solitons in electron-positron plasma
[DE95-607608] p 2082 N95-25974
Self-focusing of electromagnetic radiation in electron-positron ion plasma
[DE95-607626] p 2082 N95-25975
Two dimensional Bose plasma in a magnetic field
[DE95-607629] p 2082 N95-25976
Direct energy conversion of radiation energy in fusion reactor
[NIFS-254] p 2072 N95-26250
PLASMONS
Surface plasmon observed for carbon nanotubes
[DE95-607769] p 2091 N95-26260
PLASTIC ANISOTROPY
Evolution of plastic anisotropy for high-strain-rate computations
[DE95-004220] p 1941 N95-25237

An experimental determination of the plastic anisotropy of metal
[IFTR-33/1994] p 1938 N95-26179

PLASTIC DEFORMATION
The effect of multidirectional cyclical deformation on the evolution of the plasticity surface of 18G2A steel
[IFTR-25/1994] p 1935 N95-25117
Changes in the strength characteristics of 15HM boiler steel caused by initial plastic deformation under constant and monotonic loads
[IFTR-30/1994] p 1938 N95-26333

PLASTIC PROPERTIES
The effect of multidirectional cyclical deformation on the evolution of the plasticity surface of 18G2A steel
[IFTR-25/1994] p 1935 N95-25117
An analysis of hypercritical states in elastic and inelastic systems
[IFTR-1/1994] p 2037 N95-25339
An experimental determination of the plastic anisotropy of metal
[IFTR-33/1994] p 1938 N95-26179
Changes in the strength characteristics of 15HM boiler steel caused by initial plastic deformation under constant and monotonic loads
[IFTR-30/1994] p 1938 N95-26333

PLASTICS
Using consumer IC packages in harsh high reliability applications
[DE94-016565] p 1959 N95-24713

PLATE THEORY
Numerical simulation of the nonlinear response of composite plates under combined thermal and acoustic loading
[NASA-CR-197426] p 1981 N95-24907

PLATES (STRUCTURAL MEMBERS)
Numerical simulation of the nonlinear response of composite plates under combined thermal and acoustic loading
[NASA-CR-197426] p 1981 N95-24907
The transmission and control of vibrational power in a two stage isolation system with a water-loaded substructure
[ISVR-TR-235] p 1975 N95-24992
A technique for the evaluation of strength of coupling between SEA subsystems: Experiments with two coupled plates and two coupled rooms
[ISVR-TR-242] p 1982 N95-25332
Three-dimensional solutions for coupled thermoelectroelastic response of multilayered plates
p 1985 N95-26273
Assessment of computational models for thermoelectroelastic multilayered plates
p 1987 N95-26283

PLATINUM
Feasibility of ceramic joining with high energy electron beams
[DE95-004519] p 1940 N95-24717

PLATINUM ALLOYS
A study of the electrochemical behavior of tungsten in caustic solutions and platinum/iridium in ch loride solutions
[DE95-004951] p 1930 N95-25123

PLUMES
The atmospheric effects of stratospheric aircraft: A fourth program report
[NASA-RP-1359] p 1996 N95-24274
Enhancement of thickness uniformity of thin films grown by pulsed laser deposition
[NASA-CR-197791] p 1943 N95-26081

PLUTONIUM
Determination of trace elements in plutonium by solvent extraction and ICP-atomic emission spectrometry
[DE94-634887] p 2042 N95-24269

PLUTONIUM 238
Processing and properties of iridium alloys for space power applications
[DE95-005902] p 1935 N95-25390

POINCARE PROBLEM
Homogeneous anisotropic cosmological models in the minimum quadratic Poincare gauge theory of gravity
[DE95-607083] p 2110 N95-25647
Exact solution of 2 D Poincare gravity coupled with fermion matter
[DE95-605314] p 2099 N95-25967

POINT IMPACT
Response to a localized impact loading of a composite multilayered rotational shell structure: Theory and numerical methods, volume 1
[ONERA-NT-1994-10-VOL-1] p 1979 N95-24282
Response to a localized impact loading of a composite multilayered rotational shell structure: Theory and numerical methods, volume 2
[ONERA-NT-1994-10-VOL-2] p 1980 N95-24283
Response to a localized impact loading of a composite multilayered rotational shell structure: Theory and numerical methods, Volume 3
[ONERA-NT-1994-10-VOL-3] p 1980 N95-24284

POINTING CONTROL SYSTEMS
Hidden Markov models and neural networks for fault detection in dynamic systems p 2024 N95-25261

POISSON DENSITY FUNCTIONS
Wide-area traffic: The failure of Poisson modeling
[DE95-004685] p 2015 N95-25773

POISSON EQUATION
Optical diffraction from fractals with a structural transition
[DE94-634311] p 2029 N95-24401

POLAR CAPS
Geomagnetic Polar Cap (PC) index, 1975-1993
[UAG-103] p 2004 N95-24897

POLAR ORBITS
Use of advanced solar cells for commercial communication satellites
[NASA-TM-106879] p 1991 N95-24560

POLARIMETERS
STS-67 post flight presentation
[NASA-TM-110552] p 1918 N95-24198
Development of a fast response rotating polarimeter for a Faraday rotation measurement
[DE94-777532] p 2075 N95-24271

POLARIMETRY
Tests for leptonic CP violation in tau decays
[DE95-005927] p 2050 N95-24902

POLARIZATION
On the possibility of obtaining the polarized protons by the method of direct optic pumping of a fast atomic beam
[DE94-634309] p 2041 N95-24267
On a possibility for a measurement of the transversal proton polarization in the diffractive pion production in pp and pe high energy collisions
[DE94-628598] p 2047 N95-24668
Radiative corrections for pion polarizability experiments
[DE95-607177] p 2053 N95-25462

POLARIZATION (SPIN ALIGNMENT)
Polarization and N-N elastic scattering amplitudes
[DE95-004648] p 2042 N95-24292
A search for jet handedness in hadronic Z(sup 0) decays
[DE95-005944] p 2045 N95-24435
Spin structure of the nucleon and polarization
[DE95-004282] p 2047 N95-24662

POLARIZATION (WAVES)
Deficiency of the Gross-Llewellyn Smith sum rule and QCD vacuum polarization effect
[DE94-636790] p 2042 N95-24315
Experimental study of tapered slot elements
[PB95-165163] p 1955 N95-25644

POLARIZED ELECTROMAGNETIC RADIATION
Experimental study of tapered slot elements
[PB95-165163] p 1955 N95-25644

POLARIZED LIGHT
Angular displacement measuring device
[NASA-CASE-ARC-11937-1] p 2074 N95-26015

POLARIZED RADIATION
Accelerator physics R and D
[DE95-003624] p 2046 N95-24547
Electroweak coupling measurements from polarized Bhabha scattering at the Z(exp 0) resonance
[DE95-006090] p 2057 N95-25768

POLICIES
JPRS report: Science and technology. Central Eurasia: Space
[JPRS-USP-94-008] p 1916 N95-24359
Interim report of the advisory committee on human radiation experiments
[DE95-003265] p 2011 N95-24497
JPRS report: Science and technology. Central Eurasia
[JPRS-UST-95-017] p 1988 N95-26080

POLLUTION
Effects of nitric acid vapor on the formation of cloud droplets in troposphere
[DE95-744869] p 2001 N95-25500

POLLUTION CONTROL
Small gas turbine component evaluation study
[PB95-147542] p 1913 N95-24293
Overview of solar detoxification activities in the United States
[DE95-000264] p 1997 N95-24319
Investigation of technologies for CO2 separation, fixation and disposal for the prevention of global warming
[DE95-744285] p 1997 N95-24499
Electromagnetic Devices and Processes in Environment Protection. Proceedings of International Conference ELMECO 1994
[AD-A286613] p 1952 N95-24503
Optimized hydrogen piston engines
[DE95-003656] p 1975 N95-24550
Brayton-cycle solvent recovery heat pump. A technical brief
[DE94-000225] p 1991 N95-24666
Development of a dedicated ethanol ultra-low emission vehicle (ULEV) system design
[DE95-004016] p 1975 N95-24880
Voluntary reporting of greenhouse gases under Section 1605(b) of the Energy Policy Act of 1992: General guidelines
[DE95-003295] p 2000 N95-25361
Draft regulatory impact analysis: Control of air pollution emission standards for new nonroad spark-ignition marine engines
[PB95-166294] p 2001 N95-25575
Parts washing alternatives study: United States Coast Guard. Project summary and report
[PB95-166146] p 1942 N95-26004
Waste minimization assessment for a manufacturer of parts for truck engines
[PB95-144481] p 1911 N95-26062
Cross-flow, filter-sorbent-catalyst for particulate, SO2 and NO(x) control
[DE95-001934] p 2003 N95-26091

POLLUTION MONITORING
Retrofit NOx control technologies for natural gas prime movers
[PB95-149290] p 1997 N95-24294
JPRS report: Science and technology. Central Eurasia: Space
[JPRS-USP-94-007] p 1915 N95-24358
Evaluation of the performance of an annular diffusion denuder
[DE95-002258] p 1998 N95-24606
Methods of valuing air pollution and estimated monetary values of air pollutants in various US regions
[DE95-006854] p 1998 N95-24618
Standardization of equations for radiochemical calculations
[DE95-003028] p 1930 N95-25097
Field-usable portable analyzer for chlorinated organic compounds
[DE95-003127] p 1930 N95-25098
Tunable diode lasers as continuous emission monitors for thermal waste treatment processes
[DE95-004381] p 1972 N95-25549
Nitrogen oxide emissions and their control from uninstalled aircraft engines in enclosed test cells: Joint report to Congress on the Environmental Protection Agency - Department of Transportation study
[PB95-166237] p 2002 N95-26005
Cross-flow, filter-sorbent-catalyst for particulate, SO2 and NO(x) control
[DE95-001934] p 2003 N95-26091

POLOIDAL FLUX
New evaluation method of superconductor characteristics for realizing the Large Helical Device
[NIFS-297] p 2071 N95-25855

POLYBENZIMIDAZOLE
Space shuttle propellant constitutive law verification tests
[NASA-CR-198047] p 1947 N95-24226

POLYBUTADIENE
Space shuttle propellant constitutive law verification tests
[NASA-CR-198047] p 1947 N95-24226

POLYCRYSTALS
BCS-like gap structure of HgBa2CuO(4+delta) tunnel junctions
[DE95-004125] p 2087 N95-24855
Temperature-dependent growth of LaAlO3 films on YBa2CuO7 C-axis films for multilayer structures
[DE95-005257] p 2089 N95-25598

POLYGONS
Object-oriented parallel polygon rendering
[DE95-004909] p 2021 N95-24881

POLYHEDRONS
Visibility ordering meshed polyhedra
[CSRD-1097] p 2030 N95-24557

POLYMER MATRIX COMPOSITES
Apparatus for consolidating a pre-impregnated, filament-reinforced polymeric prepreg material
[NASA-CASE-LAR-15173-1-CU] p 1926 N95-25546

POLYMERIC FILMS
FNAS phase partitions
[NASA-CR-193855] p 1940 N95-24562

POLYNOMIALS
Behavior of a trigonometric polynomial with given number of terms on small subsets of the unit circumference (norm duplication problem)
[PB95-165544] p 2028 N95-24321
PC based analysis of gamma ray spectra generated by semiconductor detectors
[DE94-628381] p 1958 N95-24690

ASYS2: A new version of computer algebra package ASYS for analysis and simplification of polynomial systems
[DE94-628384] p 2030 N95-24691
Cyclic subgroups in class groups of real quadratic fields
[DE94-628407] p 2031 N95-24697
Numerical solution of the optimized random phase approximation
[DE95-605636] p 2034 N95-25982

POLYURETHANE RESINS
Design of supramolecular ordered systems for mesoscopic colloids and molecular composites
[DE95-004448] p 2048 N95-24687

POMERANCHUK THEOREM
Notion of the inclusive spectra and cross sections of B-meson production in hadronic interactions of high energies
[DE94-628628] p 2049 N95-24887

POROSITY
Processing of LaCrO3 for solid oxide fuel cell applications
[DE95-000024] p 1992 N95-24683
Reciprocal space analysis of the microstructure of luminescent and nonluminescent porous silicon films
[DE95-005420] p 1941 N95-25382
Non-destructive characterization of porous silicon using x ray reflectivity
[DE95-004766] p 1942 N95-25898
Dynamic methods for determining the material characteristics of saturated permeable media
[IFTR-17/1993] p 1932 N95-26107

POROUS MATERIALS
Nonequilibrium multiphase mixture modeling of energetic material response
[DE95-003353] p 1948 N95-24608
Felt-metal-wick heat-pipe solar receiver
[DE95-004535] p 1992 N95-24682
Predicting the transport properties of sedimentary rocks from microgeometry
[DE95-000129] p 2004 N95-26089

PORTABLE EQUIPMENT
A portable transmission vibration analysis system for the S-70A-9 Black Hawk helicopter
[DSTO-TR-0072] p 1966 N95-24203
The accident site portable integrated video system
[DE95-000539] p 1953 N95-24605
Development of a portable mass spectrometric system for determination of isotopic composition of solid uranium samples using fluorine volatilization
[DE95-005728] p 1969 N95-25384

POSITION (LOCATION)
Equivariant localization: BV-geometry and supersymmetric dynamics
[DE94-628436] p 2036 N95-24699
Equivariant Kaehler geometry and localization in the G/G model
[DE95-607073] p 2036 N95-25455
Heuristic approach to the path planning problem in a raster map
[PB95-141826] p 2034 N95-25893
Temporal pacing in visual attention
[AD-A289785] p 2013 N95-26041
The use of empirical models to investigate GPS derived total electron content
[DE95-606045] p 2111 N95-26044

POSITION ERRORS
Use of voronoi diagrams for qualitative matching
[PB95-165445] p 1988 N95-24240

POSITION INDICATORS
Real-time testing and demonstration of the US Army Corps of Engineers' Real-Time On-The-Fly positioning system
[AD-A288624] p 1910 N95-25609

POSITIVE IONS
A possibility of pi(-) Meson production by a low energy electron bunch and positive ion bunch
[NIFS-277] p 2071 N95-26029

POSITRON ANNIHILATION
Fractal studies on the positron annihilation in metals
[DE94-634488] p 2041 N95-24232
Multiplicity moments in e(+)e(-) annihilation into hadrons at the Z(sup 0) resonance
[DE95-005950] p 2047 N95-24641
Electroweak coupling measurements from polarized Bhabha scattering at the Z(exp 0) resonance
[DE95-006090] p 2057 N95-25768
Searching for exotic mesons in e(+)e(-) annihilation at DA(phi)NE
[PB95-165379] p 2064 N95-26001

POSITRONIUM
The development of a positron ionization gauge
[DE95-005958] p 1968 N95-24623

POSITRONS
Supersymmetry
[DE95-004670] p 2092 N95-24333
The development of a positron ionization gauge
[DE95-005958] p 1968 N95-24623
A high intensity slow positron facility for the Advanced Neutron Source
[DE94-014108] p 2050 N95-25099
Bremsstrahlung scattering calculations for the beam stops and collimators in the APS insertion-device beamlines
[DE95-005471] p 2069 N95-25300

POSTFLIGHT ANALYSIS
Debris/ice/TPS assessment and integrated photographic analysis of shuttle mission STS-63
[NASA-TM-110649] p 1921 N95-25337

POSTMISSION ANALYSIS (SPACECRAFT)
STS-60 Space Shuttle mission report
[NASA-CR-197233] p 1919 N95-26189

POTASSIUM CHLORIDES
Molecular dynamics calculation of shear viscosity for molten salt
[DE95-703970] p 2055 N95-25496

POTASSIUM HYDROXIDES
Antioxidant and sensitizer effect on the stability of natural rubber latex vulcanized by gamma rays
[DE94-636061] p 1939 N95-24373
In situ XAFS study of oxides formed on nickel thin film electrodes in KOH solution
[AD-A288735] p 1932 N95-26056

POTASSIUM OXIDES
Electronic structure of (La,Sr)2CuO4 and Ba(0.6)K(0.4)BiO3
[DE95-004963] p 2091 N95-26170

POTENTIAL ENERGY
Complex scattering dynamics and the quantum Hall effect
[DE95-005239] p 2093 N95-24457
Existence domains and some properties of a particle bound state in fields with homogeneous dependence of its potential energy on coordinates
[DE95-605280] p 2057 N95-25784

POTENTIAL FIELDS
Observation of the scalar Aharonov-Bohm effect by neutron interferometry
[DE95-607020] p 2097 N95-25446
Statistical mechanics of relativistic spin-1 bosons in a magnetic field
[DE95-607100] p 2054 N95-25474

POWDER (PARTICLES)
Superconductivity Program for Electric Power Systems: 1994 Annual PEER Review. Volume 1, Meeting Proceedings
[DE95-005058] p 1956 N95-24452
Solution based synthesis of perovskite-type oxide films and powders
[DE95-006170] p 2086 N95-24594
Formation of thallium based high temperature superconductors using aerosol flow reacted precursor powders
[DE95-005901] p 2089 N95-25389

POWDERED ALUMINUM
Characterization of ultradispersed aluminum
[DE95-006379] p 1933 N95-24329

POWER PLANTS
Wind technology development: Large and small turbines
[DE95-000286] p 1995 N95-26090

POWER SPECTRA
On the joint spectral density of bivariate random sequences
[NASA-CR-197698] p 2035 N95-24278

POWER TRANSMISSION
The transmission and control of vibrational power in a two stage isolation system with a water-loaded substructure
[ISVR-TR-235] p 1975 N95-24992

POWERED LIFT AIRCRAFT
Flight reference display for powered-lift STOL aircraft
[NAL-TR-1251] p 1912 N95-25005
A quiet STOL Research Aircraft Development program
[NAL-TR-1223] p 1911 N95-25862

PRE-MAIN SEQUENCE STARS
Resolution of the classical Hyades lithium problem
[DE95-003661] p 2109 N95-24234

PREAMPLIFIERS
Optical space communication: An overview
[DE94-634314] p 1952 N95-24403
High input impedance amplifier
[NASA-CASE-GSC-13571-1] p 1960 N95-26038
Differential preamplifier and pre-emphasis network
[AD-A288780] p 1961 N95-26186

PRECIPITATES
Cesium cobaltdicarbollide-solubility, precipitation, and reactivity in basic aqueous solution
[DE95-005881] p 1929 N95-24430

PRECIPITATION (CHEMISTRY)
Cesium cobaltdicarbollide-solubility, precipitation, and reactivity in basic aqueous solution
[DE95-005881] p 1929 N95-24430

PRECIPITATION (METEOROLOGY)
Airborne imaging of tropospheric emission at millimeter and submillimeter wavelengths
[NASA-TM-110498] p 2003 N95-24336
A numerical prediction of the precipitation and hydrology of California
[DE95-004966] p 2006 N95-25635
Intercomparison of hydrologic processes in global climate models
[NASA-TM-104617] p 2005 N95-26341

PREDICTION ANALYSIS TECHNIQUES
On the finite element implementation of the generalized method of cells micromechanics constitutive model
[NASA-CR-195451] p 1980 N95-24398
Testing supersymmetry at the next linear collider
[DE95-006064] p 2069 N95-25297
Neutrino oscillations from discrete non-Abelian family symmetries
[DE95-004355] p 2052 N95-25403
New techniques to test fatigue properties of coined sheet specimens. Part 2: Comparison of different materials, forming operations and life prediction techniques for a simple test geometry
[PB95-165122] p 1982 N95-25444
A numerical prediction of the precipitation and hydrology of California
[DE95-004966] p 2006 N95-25635

PREDICTIONS
Predicting the components of the total hemispherical solar radiation from sunshine duration measurements in Lagos, Nigeria
[DE95-606030] p 2113 N95-26042
An overview of NDE methods for thick composites and a proposal for analysis of computed technology data
[AD-A288733] p 1979 N95-26055

PREFLIGHT ANALYSIS
Debris/ice/TPS assessment and integrated photographic analysis of shuttle mission STS-63
[NASA-TM-110649] p 1921 N95-25337

PREFORMS
Method for molding structural parts utilizing modified silicone rubber
[NASA-CASE-LAR-15217-1] p 1939 N95-24212
Method and apparatus for weaving curved material preforms
[NASA-CASE-LAR-14752-1] p 1943 N95-26118

PREPREGS
Apparatus for consolidating a pre-impregnated, filament-reinforced polymeric prepreg material
[NASA-CASE-LAR-15173-1-CU] p 1926 N95-25546

PREPROCESSING
Design documentation for the SINTRA preprocessor
[AD-A288804] p 2015 N95-26192

PRESIDENTIAL REPORTS
Apollo 13: Houston, we've got a problem
[NASA-TM-110551] p 1918 N95-24215
Science in the national interest
[ISBN-0-16-045186-8] p 2115 N95-26335

PRESSURE
Investigation of convection and pressure treatment with splitting techniques
[NASA-TM-106868] p 1961 N95-24399

PRESSURE DEPENDENCE
Oxygen stoichiometry and its influence on superconductivity in Bi2Sr2CaCu2O(8+x)
[DE95-004660] p 2088 N95-25282

PRESSURE DISTRIBUTION
Experimental study of the effects of Reynolds number on high angle of attack aerodynamic characteristics of forebodies during rotary motion
[NASA-CR-195033] p 1907 N95-24443
Scaling in a scramjet combustor p 1933 N95-25398
Modelling the day to day wind variability offshore central Chile at about 30 deg south
[DE95-606032] p 2006 N95-26043

PRESSURE DRAG
A theoretical and experimental investigation of the flow over supersonic leading edge wing/body configurations
[DRA-TM-AERO-PROP-41] p 1907 N95-25649

PRESSURE DROP
Numerical simulation of flow and the effect of baffle arrangement on pressure drop and temperature pattern in a circular combustor p 1963 N95-24626

PRESSURE EFFECTS
Effect of He pressure on the superconducting transition temperatures of Na2CsC60 and (NH3)4Na2CsC60
[DE95-006320] p 2087 N95-24616

PRESSURE GRADIENTS
Performance tests of air source heat pumps under frosting conditions. Quality of results
[PB95-141792] p 1995 N95-25892

Modelling the day to day wind variability offshore central Chile at about 30 deg south
[DE95-606032] p 2006 N95-26043

PRESSURE MEASUREMENT

Effect of He pressure on the superconducting transition temperatures of Na2CsC60 and (NH3)4Na2CsC60
[DE95-006320] p 2087 N95-24616
The development of a positron ionization gauge
[DE95-005958] p 1968 N95-24623
Workshop report: Measurement techniques in highly transient, spectrally rich combustion environments
[AD-A288395] p 1969 N95-25606
Performance evaluation of LE-7 high pressure pumps
[NAL-TR-1212T] p 1977 N95-25672

PRESSURE OSCILLATIONS

The phenomenon of non-linearity accompanying the action of acoustic pressure on a Helmholtz resonator
[IFTR-19/1994] p 2040 N95-26108

PRESSURE RATIO

Internal performance characteristics of thrust-vectored axisymmetric ejector nozzles
[NASA-TM-4610] p 1907 N95-25338

PRESSURE REDUCTION

A study of three-dimensional interaction flow fields between swept shock waves and turbulent boundary layers. Flow structures and effects of bleed
[NAL-TR-1227] p 1963 N95-25001
Measurement of blood nitrogen content after rapid compressions to assess the speed of nitrogen uptake during the compression phase of submarine escape. (Includes measurement of nitrogen concentration in blood following rapid compression to 5 bar)
[PB95-165726] p 2012 N95-25570

PRESSURE VESSEL DESIGN

The 1994 NASA/USRA/ADP Design Projects
[NASA-CR-197415] p 2101 N95-26304
Feed system design for a reduced pressure tank
p 1923 N95-26310

PRETREATMENT

Electrochemical organic destruction in support of Hanford tank waste pretreatment
[DE95-002854] p 1924 N95-25248

PRIMERS (COATINGS)

The corrosion protection of AISI(TM) 1010 steel by organic and inorganic zinc-rich primers
[NASA-TP-3545] p 1936 N95-25677

PRINCIPAL COMPONENTS ANALYSIS

Characterization of plastic bonded explosives by pyrolysis-gas chromatography and multivariate data analysis. Applications of the procedure
[AD-A288761] p 1949 N95-25517
Characterization of plastic bonded explosives by pyrolysis-gas chromatography and multivariate data analysis. Development of the procedure
[AD-A288787] p 1949 N95-25528

PRINTED CIRCUITS

Assessing capillary flow on printed wiring board surfaces
[DE94-015768] p 1959 N95-24712
Crosstalk on printed circuit boards
[PB95-165171] p 1960 N95-25472
Proposed Nordtest method: Reliability stress screening of components. A guide for component users. Nordtest project 1140-93
[PB95-165783] p 1978 N95-26003
Disposal of electronic equipment
[PB95-177861] p 2002 N95-26047

PRIVACY

Survey of methods for secure connection to the internet
[DE95-730185] p 1952 N95-24493

PROBABILITY DENSITY FUNCTIONS

Statistical mechanics of nonlinear coherent structures: Kinks in the Phi(sup 6) model
[DE95-005253] p 2096 N95-25293

PROBABILITY THEORY

Cyclic subgroups in class groups of real quadratic fields
[DE94-628407] p 2031 N95-24697
A new formulation of quantum field theory on S4
[DE95-607098] p 2099 N95-25970
On convergence of the Nelder-Mead simplex algorithm for unconstrained stochastic optimization
[AD-A289453] p 2006 N95-26197

PROBLEM SOLVING

On corrections to the Nambu action
[NASA-CR-197625] p 2065 N95-24335
Aerodynamic parameter estimation via Fourier modulating function techniques
[NASA-CR-4654] p 1911 N95-24630
Grounding explanations in evolving, diagnostic situations
[NASA-CR-198027] p 2026 N95-25335
Closed orbit related problems: Correction, feedback, and analysis
[DE95-005969] p 2070 N95-25441
Newton iterative methods for large scale nonlinear systems
[DE95-007067] p 2032 N95-25480
Splines in two-dimensional problems
[IFTR-2/1993] p 2035 N95-26106
Optimal guidance law development for an advanced launch system
[NASA-CR-4667] p 1917 N95-26205

PROCESS CONTROL (INDUSTRY)

Neural network application to comprehensive engine diagnostics p 2023 N95-25255
A neural network controller for automated composite manufacturing p 2025 N95-25271
Processing and properties of iridium alloys for space power applications
[DE95-005902] p 1935 N95-25390
AMCC casting development, volume 2
[NASA-CR-197720] p 1938 N95-26068

PROCUREMENT MANAGEMENT

Workflow automation architecture standard
[DE95-004748] p 2035 N95-24248
Integrated planning: A baseline development perspective
[DE95-004945] p 2102 N95-24905
Acquisition forecast: Fiscal year 1995
[NASA-TM-110575] p 2103 N95-25850

PRODUCT DEVELOPMENT

Targets for laser-driven opacity measurements
[DE95-006172] p 1973 N95-25557
A quiet STOL Research Aircraft Development program
[NAL-TR-1223] p 1911 N95-25862

PRODUCTION ENGINEERING

Processing and characterization of transformation-toughened ceramics with strength retention to elevated temperatures
[DE95-005758] p 1941 N95-25387

PROGRAM VERIFICATION (COMPUTERS)

Verification of computational aerodynamic predictions for complex hypersonic vehicles using the INCA(trademark) code
[DE95-004757] p 1906 N95-24308
A parallel, portable and versatile treecode
[DE95-000842] p 2019 N95-24343
Debugging the virtual machine
[DE95-002193] p 2016 N95-24898
FTAPE: A fault injection tool to measure fault tolerance
[NASA-CR-198000] p 1978 N95-25333

PROGRAMMERS

Design documentation for the SINTRA preprocessor
[AD-A288804] p 2015 N95-26192

PROGRAMMING ENVIRONMENTS

Debugging the virtual machine
[DE95-002193] p 2016 N95-24898

PROGRAMMING LANGUAGES

Debugging the virtual machine
[DE95-002193] p 2016 N95-24898

PROJECT MANAGEMENT

Automated Procurement System (APS): Project management plan (DS-03), version 1.2
[NASA-CR-196576] p 2102 N95-24442
Issues in NASA program and project management
[NASA-SP-6101(08)] p 2102 N95-24565
Continual improvement plan
[NASA-TM-110574] p 2103 N95-25849
Office of Space Science: Integrated technology strategy
[NASA-TM-110578] p 2108 N95-26183

PROJECT PLANNING

Integrated planning: A baseline development perspective
[DE95-004945] p 2102 N95-24905

PROJECTIVE GEOMETRY

Relative orientation of multiple images using projective singular correlation
[PB95-149936] p 1967 N95-24259

PROLATENESS

On a generalized Kepler-Coulomb system: Inter basis expansions
[DE94-636739] p 2093 N95-24349

PROPAGATION MODES

On a remarkable similarity between the propagation of whistlers and the bow wave of a ship
[U-OF-IOWA-94-22] p 2111 N95-26196

PROPELLANT ADDITIVES

Combustion characteristics of metallized hydrocarbon fuels
[NAL-TR-1224] p 1949 N95-25769

PROPELLANT COMBUSTION

Combustion characteristics of metallized hydrocarbon fuels
[NAL-TR-1224] p 1949 N95-25769

PROPELLANT PROPERTIES

Combustion characteristics of metallized hydrocarbon fuels
[NAL-TR-1224] p 1949 N95-25769

PROPELLANT TESTS

Space shuttle propellant constitutive law verification tests
[NASA-CR-198047] p 1947 N95-24226
Combustion characteristics of metallized hydrocarbon fuels
[NAL-TR-1224] p 1949 N95-25769

PROPORTIONAL COUNTERS

Fusion-neutron diagnostic on the Microwave Tokamak Experiment
[DE94-777530] p 2075 N95-24270

PROPOSALS

High Energy Physics Advisory Panel's subpanel on vision for the future of high-energy physics
[DE94-013641] p 2068 N95-24899

PROPULSION

Advanced subsonic airplane design and economic studies
[NASA-CR-195443] p 1913 N95-24304
Workshop report: Measurement techniques in highly transient, spectrally rich combustion environments
[AD-A288395] p 1969 N95-25606

PROPULSION SYSTEM CONFIGURATIONS

Development of sensors for ceramic components in advanced propulsion systems. Phase 2: Temperature sensor systems evaluation
[NASA-CR-195283] p 1967 N95-24473
Development test of a liquid apogee engine for the ETS-4
[NAL-TR-1250] p 1922 N95-24999

PROPULSION SYSTEM PERFORMANCE

Development of sensors for ceramic components in advanced propulsion systems. Phase 2: Temperature sensor systems evaluation
[NASA-CR-195283] p 1967 N95-24473
Development test of a liquid apogee engine for the ETS-4
[NAL-TR-1250] p 1922 N95-24999

PROTECTION

Development of a model protection and dynamic response monitoring system for the national transonic facility
[NASA-CR-195041] p 1915 N95-24388
Heat removal capability of divertor coaxial tube assembly
[DE95-709770] p 1966 N95-26161

PROTECTIVE CLOTHING

Aerospace medicine and biology: A continuing bibliography with indexes (supplement 400)
[NASA-SP-7011(400)] p 2011 N95-24464

PROTECTIVE COATINGS

Development of oxidation resistant SiC/C compositionally gradient materials
[DE94-785101] p 1925 N95-24365
Au/Cr sputter coating for the protection of alumina during sliding at high temperatures
[NASA-TM-106853] p 1923 N95-24437
High heat flux experiment on B4C-converted carbon based materials for plasma facing materials of JT-60U
[DE94-777545] p 2077 N95-24585
Ion beam mixing of titanium overlayers with hydroxyapaptite substrates
[DE95-005278] p 1935 N95-25379
Information compendium on solid film lubricants
[AD-A288360] p 1942 N95-25510

PROTEIN CRYSTAL GROWTH

Convective flow effects on protein crystal growth
[NASA-CR-197891] p 2086 N95-24534
Automated protein crystal growth facility
p 1918 N95-26306

PROTEINS

Fusion proteins as alternate crystallization paths to difficult structure problems
[NASA-TM-110497] p 2008 N95-24531
Overview of selected molecular biological databases
[DE95-005906] p 2008 N95-25181

PROTOCOL (COMPUTERS)

Dynamics of TCP traffic over ATM networks
[DE95-004687] p 2021 N95-25359

PROTON BEAMS

On the possibility of obtaining the polarized protons by the method of direct optic pumping of a fast atomic beam
[DE94-634309] p 2041 N95-24267
The determination of the main parameters of the backward spectrometer of the 0(sup 0) facility
[DE94-628385] p 2048 N95-24692
Fission foil detector calibrations with high energy protons p 2060 N95-25924

PROTON ENERGY

Fission foil detector calibrations with high energy protons p 2060 N95-25924

PROTON IRRADIATION

Fission foil detector calibrations with high energy protons p 2060 N95-25924

PROTON-PROTON REACTIONS
Study of the structure of the events produced in soft (bar p)p interactions of (radical)s = 1800 GeV
[DE95-004851] p 2041 N95-24252
W-charge asymmetry at CDF, tests of structure functions
[DE95-004855] p 2041 N95-24256
Proton-proton interactions using the RHIC polarized collider
[DE95-005839] p 2043 N95-24326
New results in nucleon-nucleon scattering at intermediate energies
[DE95-004594] p 2043 N95-24332
Accelerator physics R and D
[DE95-003624] p 2046 N95-24547
A search for t(anti t) (yields) lepton + E(sub T) + jets signature in p(anti p) collisions at (radical)s = 1.8 TeV with the DO detector
[DE95-004239] p 2052 N95-25402
PROTONS
On a possibility for a measurement of the transversal proton polarization in the diffractive pion production in pp and pe high energy collisions
[DE94-628598] p 2047 N95-24668
The determination of the main parameters of the backward spectrometer of the 0(sup 0) facility
[DE94-628385] p 2048 N95-24692
Evidence for top quark production in 1.8 TeV p-bar p collisions
[DE95-003496] p 2068 N95-24728
Search for the prompt muon antineutrino from charm particle decays at the IHEP-JINR Neutrino detector in 70 GeV proton beam-dump experiment
[DE94-628772] p 2049 N95-24889
Photon-charm production in p(anti p) collisions at radical s = 1.8 TeV
[DE95-004850] p 2052 N95-25377
PROTOTYPES
Space basic
[NASA-TM-110540] p 2108 N95-24196
PROVING
Space shuttle propellant constitutive law verification tests
[NASA-CR-198047] p 1947 N95-24226
Can we test the many-Hilbert-space approach to quantum mechanics?
[DE95-607021] p 2097 N95-25429
PSEUDOPOTENTIALS
Structural and thermodynamic properties of 3-d transition metals: Pseudopotential theory revisited
[DE95-605639] p 1937 N95-25983
PSYCHOLOGICAL TESTS
Cognitive diagnosis combined with latent trait theory and multiphase responses
[AD-A288701] p 2013 N95-26010
PSYCHOPHYSIOLOGY
Temporal pacing in visual attention
[AD-A289785] p 2013 N95-26041
PUBLIC HEALTH
JPRS report: Science and technology. Central Eurasia
[JPRS-UST-94-024] p 1958 N95-24620
JPRS Report: Science and technology. Central Eurasia
[JPRS-UST-94-032] p 1950 N95-24759
JPRS Report: Science and technology. Central Eurasia
[JPRS-UST-94-031] p 1988 N95-24760
TITLE: Environmental, health, and safety issues offuel cells in transportation. Volume 1: Phosphoricacid fuel-cell buses
[DE95-000289] p 1993 N95-24866
Biological effectiveness of neutrons: Research needs
[DE95-004795] p 2051 N95-25373
PULSARS
Gamma-ray emission from globular clusters. Shock high energy emission from the Be-Star/Pulsar System PSR 1259-63. Echoes in x-ray novae
[NASA-CR-197994] p 2114 N95-24381
PULSE COMMUNICATION
Facility for the evaluation of space communications and related systems
[NASA-TM-106904] p 1955 N95-25876
PULSE COMPRESSION
RF pulse compression in the NLC test accelerator at SLAC
[DE95-006478] p 2070 N95-25406
PULSE GENERATORS
Optical generation of radio-frequency power
[DE95-005276] p 1951 N95-24289
High gain GaAs Photoconductive Semiconductor Switches (PCSS): Device lifetime, high current testing, optical pulse generators
[DE95-003354] p 1957 N95-24488
PULSE RADAR
Analysis of waveforms for bistatic radar systems
[PB95-165098] p 1955 N95-25641
PULSED LASER DEPOSITION
Enhancement of thickness uniformity of thin films grown by pulsed laser deposition
[NASA-CR-197791] p 1943 N95-26081
PULSED LASERS
Reduction in fiber damage thresholds due to static fatigue
[DE95-004778] p 1979 N95-24263
Decay of a laser generated shock wave in an aluminium target
[DE94-629014] p 1972 N95-24707
The KTeV PMT laser monitoring system
[DE95-004237] p 1972 N95-24869
Diode laser pumped solid state laser with 2 micrometer wavelength
[PB95-165270] p 1973 N95-25622
Pulsed laser annealing of P implanted diamond
[DE95-605947] p 2090 N95-25985
PUNCHES
Recent progress in shear punch testing
[DE95-005962] p 1937 N95-26007
PURIFICATION
High octane ethers from synthesis gas-derived alcohols
[DE95-001146] p 1948 N95-24655
PYROLYSIS
Characterization of plastic bonded explosives by pyrolysis-gas chromatography and multivariate data analysis. Applications of the procedure
[AD-A288761] p 1949 N95-25517
Characterization of plastic bonded explosives by pyrolysis-gas chromatography and multivariate data analysis. Development of the procedure
[AD-A288787] p 1949 N95-25528
PYROTECHNICS
BSM Delta Qualification 2, volume 2
[NASA-CR-196567] p 1922 N95-24844

Q

Q SWITCHED LASERS
Reduction in fiber damage thresholds due to static fatigue
[DE95-004778] p 1979 N95-24263
Q VALUES
On connection of q-deformed para oscillators with para oscillators
[DE95-607007] p 2096 N95-25425
QUALIFICATIONS
BSM Delta Qualification 2, volume 2
[NASA-CR-196567] p 1922 N95-24844
BSA Delta Qualification 2, volume 3, book 1
[NASA-CR-196565] p 1922 N95-24845
BSM Delta Qualification 2, volume 3, book 2
[NASA-CR-196568] p 1922 N95-24854
QUALITATIVE ANALYSIS
Reliability analysis of software based safety functions
[DE95-606516] p 2018 N95-26045
QUALITY CONTROL
Metrology: Measurement assurance program guidelines
[NASA-RP-1364] p 1950 N95-24543
Neural network application to comprehensive engine diagnostics p 2023 N95-25255
Faster magnet sorting with a threshold acceptance algorithm
[DE95-006487] p 2038 N95-25408
Background information to reliability stress screening of components: A guide for component users. Nordtest project 1140-93
[PB95-165775] p 1978 N95-26002
QUANTITATIVE ANALYSIS
Reliability analysis of software based safety functions
[DE95-606516] p 2018 N95-26045
QUANTUM CHROMODYNAMICS
Deficiency of the Gross-Llewellyn Smith sum rule and QCD vacuum polarization effect
[DE94-636790] p 2042 N95-24315
Low energy theorems in quark potential models
[DE94-636791] p 2042 N95-24316
Recent progress in one-loop multi-parton calculations
[DE95-006062] p 2092 N95-24328
Measurement of alpha(sub s)from hadronic event observables at the Z(sup 0) resonance
[DE95-005943] p 2045 N95-24434
Lagrangian formulation of NJL model with se parable interaction
[DE94-628519] p 1952 N95-24506
Measurement of the charged multiplicity of Z(sup 0) (yields) b(bar b) events
[DE95-006051] p 2046 N95-24571
Chiral limit of QCD
[DE95-005245] p 2094 N95-24610
Measurement of alpha(sub s) from hadronic ev ent observables at the Z(sup 0) resonance
[DE95-005949] p 2047 N95-24622
Dressing and bound states in quantum field theory
[DE94-628580] p 2095 N95-24639
Multiplicity moments in e(+)e(-) annihilation into hadrons at the Z(sup 0) resonance
[DE95-005950] p 2047 N95-24641
Geometry of multihadron production
[DE95-004290] p 2047 N95-24663
Theory of ultra dense matter and the dynamics of high energy interactions involving nuclei
[DE95-004114] p 2048 N95-24671
The determination of V(sub cb) and QCD Sum Rules in Heavy Quark Effective theory
[DE94-628636] p 2095 N95-24723
On the Compton non-Abelian twist-3 asymmetry
[DE94-628586] p 2095 N95-24727
Notion of the inclusive spectra and cross sections of B-meson production in hadronic interactions of high energies
[DE94-628628] p 2049 N95-24887
Search for the prompt muon antineutrino from charm particle decays at the IHEP-JINR Neutrino detector in 70 GeV proton beam-dump experiment
[DE94-628772] p 2049 N95-24889
Tau physics 1994: A theoretical perspective
[DE95-004840] p 2052 N95-25375
Critical parameters of Quark-Hadron phase transition with interacting and massive quarks
[DE95-607143] p 2052 N95-25436
The twist-3 single spin asymmetries of pion production
[DE95-607144] p 2052 N95-25437
Zero sound velocity in pi, rho mesons at different temperatures
[DE95-607145] p 2053 N95-25459
Theoretical studies in hadronic and nuclear physics
[DE95-006643] p 2098 N95-25562
QUANTUM EFFICIENCY
Electric field effects on the quantum efficiency of Cesium-iodide photocathodes in gas media
[DE94-628176] p 1957 N95-24482
A correction of the quantum efficiency of cesium iodide and other photocathodes due to the recalibration of the reference photomultipliers
[DE94-628177] p 1957 N95-24483
QUANTUM ELECTRODYNAMICS
Measurement of the magnetically-induced QED birefringence of the vacuum and an improved search for laboratory axions: Project definition study of the use of assets and facilities of the Superconducting Super Collider Laboratory
[DE95-005110] p 2065 N95-24317
The lattice spinor QED Hamiltonian critique of the continuous space approach
[DE94-628521] p 2094 N95-24508
Generalization of the Rayleigh formula to the model with ring-shaped potentials
[DE94-628578] p 2094 N95-24637
On the problem of unboundedness from below of the spinor QED Hamiltonian
[DE94-628579] p 2094 N95-24638
Dressing and bound states in quantum field theory
[DE94-628580] p 2095 N95-24639
Matrix element and complex l-plane evaluation of two-loop vacuum amplitudes in QED on S4
[DE95-607099] p 2097 N95-25473
Dynamical chiral symmetry breaking in scale invariant quantum electrodynamics in sixth dimensions
[DE95-607133] p 2099 N95-25667
QUANTUM MECHANICS
Finite quantum physics and noncommutative geometry
[DE94-634282] p 2027 N95-24228
Theoretical motivation for gravitation experiments on ultra-low energy antiprotons and antihydrogen
[DE95-003662] p 2091 N95-24235
Quantum mechanics with spontaneous localization and experiments
[DE94-634285] p 2092 N95-24266
T=0 finite-size scaling for a quantum system with long-range interaction
[DE94-634528] p 2092 N95-24288
Anharmonic potential in the oscillator representation
[DE94-636740] p 2092 N95-24312
Elliptic deformed Newton mechanics in the three-dimensional phase space
[DE94-636741] p 2092 N95-24313
Bound states of 'dressed' particles
[DE94-636773] p 2042 N95-24314
On a generalized Kepler-Coulomb system: Inter basis expansions
[DE94-636739] p 2093 N95-24349
Constraints and Hamiltonian in light-front quantized field theory
[DE95-600852] p 2093 N95-24353

Numerical investigation of Schwinger-Dyson and Bethe-Salpeter equations with Gauss potential in the framework of the quarkonium model
[DE94-636730] p 2029 N95-24387
Complex scattering dynamics and the quantum Hall effect
[DE95-005239] p 2093 N95-24457
Quantum group gauge theories and covariant quantum algebras
[DE94-628524] p 2094 N95-24509
Decoherence, determinism and chaos revisited
[DE95-006070] p 2094 N95-24578
Saddle-point method in path integrals
[DE94-628379] p 2036 N95-24688
Nonlinear theories of spin-2 field in terms of Fierz variables
[DE95-600854] p 2095 N95-24833
Probing the Froissart bound for models with charged vector fields in D = 3
[DE95-600855] p 2095 N95-24834
On q-deformed supersymmetric classical mechanical models
[DE95-600864] p 2095 N95-24838
Meson properties at finite temperature and density within Nambu-Jona-Lasinio model
[DE94-628630] p 2049 N95-24888
Low energy properties of the heavy vector fermions
[DE94-634362] p 2051 N95-25290
CP violation tests for tau/top processes
[DE95-005924] p 2051 N95-25292
Dissipative quantum mechanics: The generalization of the canonical quantization and von Neumann equation
[DE95-607008] p 2096 N95-25426
Quantum symplectic geometry. 1: The matrix Hamiltonian formalism
[DE95-607009] p 2032 N95-25427
Can we test the many-Hilbert-space approach to quantum mechanics?
[DE95-607021] p 2097 N95-25429
On the effects of gravitational fields on the electrical properties of matter
[DE95-607022] p 2038 N95-25430
Relevance of induced gauge interactions in decoherence
[DE95-607082] p 2097 N95-25432
Observation of the scalar Aharonov-Bohm effect by neutron interferometry
[DE95-607020] p 2097 N95-25446
Testing quantum behaviour at the macroscopic level
[DE95-607005] p 2097 N95-25453
Recoil effects in quantum topological solitons
[DE95-607006] p 2097 N95-25454
Measurement accuracy, bit-strings, Manthey's quaternions, and RRQM
[DE95-006211] p 2098 N95-25530
On analysis of resonance neutron depolarization in uniaxial media
[DE95-703782] p 2057 N95-25669
Quantization of a Hamiltonian system with an infinite number of degrees of freedom
[DE95-605279] p 2034 N95-25783
Charge-Dyon system as the reduced oscillator
[DE95-606998] p 2100 N95-25987
On Segal-Wilson's construction for the (tau)-functions of the constrained KP hierarchies
[DE95-606999] p 2100 N95-25988
Describing the macroscopic world: Closing the circle within the dynamical reduction program
[DE95-606997] p 2100 N95-26046
Quantum group random walks in strongly correlated 2+1 D spin systems
[DE95-607844] p 2091 N95-26103
STEP: Satellite Test of the Equivalence Principle. Report on the phase A study
[NASA-TM-110598] p 1917 N95-26184
Rotational melting in displacive quantum paraelectrics
[DE95-607804] p 2091 N95-26252

QUANTUM NUMBERS

Recent progress in one-loop multi-parton calculations
[DE95-006062] p 2092 N95-24328
Ellipsoidal basis for isotropic oscillator
[DE95-605253] p 2034 N95-25782
Mass splitting of the pseudoscalar and vector mesons induced by the homogeneous vacuum gluon field
[DE95-605322] p 2058 N95-25908
Excited states of mesons within the NJL model with the homogeneous vacuum gluon field
[DE95-605323] p 2058 N95-25909
Statistical mechanics of magnetized pair Fermi gas
[DE95-607097] p 2063 N95-25969

QUANTUM OPTICS

The Third International Workshop on the Physics and Modern Applications of Lasers
[DE95-606395] p 1972 N95-25491

QUANTUM STATISTICS

On the calculation of lattice sums arising in Bose-Einstein statistics of quasiparticle excitations
[DE94-634531] p 2084 N95-24246
On an expansion of the Fermi function
[DE94-628494] p 2035 N95-24883
The existence of antiparticles seems to forbid violations of statistics
[DE94-628523] p 2050 N95-25094
q-bosons and the q-analogue quantized field
[DE95-005925] p 2051 N95-25294
On connection of q-deformed para oscillators with para oscillators
[DE95-607007] p 2096 N95-25425
Flare stars and Pascal distribution
[DE95-607044] p 2110 N95-25431
Correlated density matrix theory of spatially inhomogeneous Bose fluids
[DE95-607840] p 2100 N95-26102
Magnetized pair Bose gas: Relativistic superconductor
[DE95-607846] p 2100 N95-26104

QUANTUM THEORY

Anharmonic potential in the oscillator representation
[DE94-636740] p 2092 N95-24312
Bound states of 'dressed' particles
[DE94-636773] p 2042 N95-24314
Quantum corrections for a cosmological string solution
[DE95-006057] p 2109 N95-24327
Anionic construction of the sl(sub q, s)(2) algebra
[DE95-600838] p 2043 N95-24350
On the central charge in 3 D-supersymmetry
[DE95-600851] p 2093 N95-24352
Constraints and Hamiltonian in light-front quantized field theory
[DE95-600852] p 2093 N95-24353
Heat Kernel expansion on a cone and quantum fields near cosmic strings
[DE94-628520] p 2094 N95-24507
Dressing and bound states in quantum field theory
[DE94-628580] p 2095 N95-24639
Quantum group and quantum symmetry
[DE94-634329] p 2095 N95-24767
Probing the Froissart bound for models with charged vector fields in D = 3
[DE95-600855] p 2095 N95-24834
Light-front quantized field theory: An introduction. Spontaneous symmetry breaking. Phase transition in (phi)(sup 4) theory
[DE95-600856] p 2095 N95-24837
A quantum gravitational mechanism for exiting inflation
[DE95-003342] p 2096 N95-24867
The existence of antiparticles seems to forbid violations of statistics
[DE94-628523] p 2050 N95-25094
R parity in standard-like superstring models
[DE94-628531] p 2096 N95-25215
q-bosons and the q-analogue quantized field
[DE95-005925] p 2051 N95-25294
Tau as a probe for new physics
[DE95-005928] p 2051 N95-25296
Testing supersymmetry at the next linear collider
[DE95-006064] p 2069 N95-25297
On the field theory of the extended-type electron
[DE95-607069] p 2053 N95-25449
Equivariant Kaehler geometry and localization in the G/G model
[DE95-607073] p 2036 N95-25455
Tachyon condensates and anisotropic universe
[DE95-607074] p 2097 N95-25456
Matrix element and complex l-plane evaluation of two-loop vacuum amplitudes in QED on S4
[DE95-607099] p 2097 N95-25473
On D=2 (1/3, 1/3) supersymmetric theories 1
[DE95-607075] p 2036 N95-25522
On D=2 (1/3,1/3) supersymmetric theories 2
[DE95-607076] p 2037 N95-25523
A covariant canonical description of Liouville field theory
[DE95-607094] p 2098 N95-25534
Physics in Ukraine International Conference. Volume 1: Physics of elementary particles and quantum field theory. General problems
[DE95-606413] p 2056 N95-25554
A new formulation of quantum field theory on S4
[DE95-607098] p 2099 N95-25970

QUANTUM WELLS

Optical determinations of energy-band dispersion curves in novel compound semiconductor materials
[DE95-006318] p 2089 N95-25353
Photoionization of shallow donor impurities in finite-barrier quantum wells
[DE95-607521] p 2097 N95-25468

QUARK MODELS

Low energy theorems in quark potential models
[DE94-636791] p 2042 N95-24316
Numerical investigation of Schwinger-Dyson and Bethe-Salpeter equations with Gauss potential in the framework of the quarkonium model
[DE94-636730] p 2029 N95-24387
Lagrangian formulation of NJL model with se parable interaction
[DE94-628519] p 1952 N95-24506
TeV scale leptoquarks as a signature of standard-like superstring models
[DE94-628529] p 2096 N95-25095
Supersymmetry and light quark masses in a realistic superstring model
[DE94-628530] p 2096 N95-25096
Critical parameters of Quark-Hadron phase transition with interacting and massive quarks
[DE95-607143] p 2052 N95-25436
Zero sound velocity in pi, rho mesons at different temperatures
[DE95-607145] p 2053 N95-25459
Heavy quark effective theory, interpolating fields and Bethe-Salpeter amplitudes
[DE95-607146] p 2053 N95-25460
A simple relation among the quark masses
[DE95-703783] p 2055 N95-25494
Theoretical studies in hadronic and nuclear physics
[DE95-006643] p 2098 N95-25562

QUARKS

Top quark kinematics and mass determination
[DE95-004853] p 2041 N95-24254
W-charge asymmetry at CDF, tests of structure functions
[DE95-004855] p 2041 N95-24256
Low energy theorems in quark potential models
[DE94-636791] p 2042 N95-24316
On leading charmed meson production in pi-nucleon interactions
[DE94-636797] p 2043 N95-24360
Numerical investigation of Schwinger-Dyson and Bethe-Salpeter equations with Gauss potential in the framework of the quarkonium model
[DE94-636730] p 2029 N95-24387
A measurement of quark and gluon jet differences at the Z(sup 0) resonance
[DE95-005947] p 2044 N95-24417
A test of the flavor independence of strong interactions
[DE95-005948] p 2044 N95-24418
Lagrangian formulation of NJL model with se parable interaction
[DE94-628519] p 1952 N95-24506
A measurement of the left-right, forward-backward asymmetry for charm quarks using D(*+) and D(+) mesons
[DE95-006061] p 2046 N95-24575
A test of the flavor independence of strong interactions
[DE95-006063] p 2046 N95-24576
The left-right forward-backward asymmetry of heavy quarks measured with jet charge and with leptons at the SLD
[DE95-006145] p 2046 N95-24593
Chiral limit of QCD
[DE95-005245] p 2094 N95-24610
Theory of ultra dense matter and the dynamics of high energy interactions involving nuclei
[DE95-004114] p 2048 N95-24671
The determination of V(sub cb) and QCD Sum Rules in Heavy Quark Effective theory
[DE94-628636] p 2095 N95-24723
Evidence for top quark production in 1.8 TeV p-bar p collisions
[DE95-003496] p 2068 N95-24728
TeV scale leptoquarks as a signature of standard-like superstring models
[DE94-628529] p 2096 N95-25095
CP violation tests for tau/top processes
[DE95-005924] p 2051 N95-25292
q-bosons and the q-analogue quantized field
[DE95-005925] p 2051 N95-25294
Baryon spectroscopy and the omega minus
[DE95-004838] p 2052 N95-25374
Photon-charm production in p(anti p) collisions at radical s = 1.8 TeV
[DE95-004850] p 2052 N95-25377
Neutrino oscillations from discrete non-Abelian family symmetries
[DE95-004355] p 2052 N95-25403
Critical parameters of Quark-Hadron phase transition with interacting and massive quarks
[DE95-607143] p 2052 N95-25436
The twist-3 single spin asymmetries of pion production
[DE95-607144] p 2052 N95-25437
Masses of heavy fermions and Higgs boson in four-generation fermion condensate scheme
[DE95-607124] p 2053 N95-25450

Heavy quark effective theory, interpolating fields and Bethe-Salpeter amplitudes
[DE95-607146] p 2053 N95-25460
Study of the simplest realistic Higgs sector in quark-lepton symmetric models
[DE95-607159] p 2053 N95-25461
Can the electric charges of elementary particles change with time?
[DE95-607194] p 2054 N95-25465
A simple relation among the quark masses
[DE95-703783] p 2055 N95-25494
Theoretical studies in hadronic and nuclear physics
[DE95-006643] p 2098 N95-25562
Further ways to distinguish single-lepton top quark signals from background at the Tevatron
[PB95-165395] p 2056 N95-25567
Parton distributions for low Q2
[PB95-165213] p 2056 N95-25619
Mass splitting of the pseudoscalar and vector mesons induced by the homogeneous vacuum gluon field
[DE95-605322] p 2058 N95-25908
Excited states of mesons within the NJL model with the homogeneous vacuum gluon field
[DE95-605323] p 2058 N95-25909
On a possible explanation of the origin of the quark mass spectrum
[DE95-605315] p 2063 N95-25968

QUARTZ
Entropy and enthalpy of adsorption of gaseous chlorides of metals on quartz glass as a function of the molecular composition
[DE94-627162] p 2093 N95-24481
Conductivity in insulators due to implantation of conducting species
[DE95-607773] p 1932 N95-26261

QUASARS
From superconductivity to supernovae: The Ginzburg symposium. Report on the symposium held in honor of Vitaly L. Ginzburg
[NASA-TM-110596] p 2108 N95-25746

QUATERNIONS
Measurement accuracy, bit-strings, Manthey's quaternions, and RRQM
[DE95-006211] p 2098 N95-25530

QUINONES
Genetic and biophysical studies of the photosynthetic reaction center
[DE95-004179] p 2008 N95-24850

R

RADAR DETECTION
Characterizing the wake vortex signature for an active line of sight remote sensor
[NASA-CR-197697] p 1909 N95-24391
Laser based methods for range, Doppler and vibration measurements
[PB95-141958] p 1952 N95-24445
Wave-propagation aspects on VHF-radar applications
[PB95-141818] p 1953 N95-24649
Analysis of waveforms for bistatic radar systems
[PB95-165098] p 1955 N95-25641

RADAR IMAGERY
User guide to the Magellan synthetic aperture radar images
[NASA-RP-1356] p 2112 N95-24987
Inversion of circular averages and application of backprojection methods to radar imaging
[PB95-141578] p 1955 N95-25891

RADAR MAPS
User guide to the Magellan synthetic aperture radar images
[NASA-RP-1356] p 2112 N95-24987

RADAR RECEIVERS
Analysis of data from a radar warning receiver with the accent on association of sensor reports
[PB95-141768] p 1953 N95-24836

RADAR SCANNING
Analysis of waveforms for bistatic radar systems
[PB95-165098] p 1955 N95-25641

RADAR SCATTERING
Diurnal variations of backscattering properties of pine trees at C- and X-bands
[PB95-149738] p 1988 N95-24299

RADAR SIGNATURES
Characterizing the wake vortex signature for an active line of sight remote sensor
[NASA-CR-197697] p 1909 N95-24391

RADAR TRACKING
Orientation determination of aircraft using visual 3D matching and radar. Case study 2
[PB95-165791] p 1955 N95-25749
Aspect estimation of an aircraft using library model silhouettes
[PB95-141834] p 2036 N95-25894

RADAR TRANSMISSION
Wave-propagation aspects on VHF-radar applications
[PB95-141818] p 1953 N95-24649

RADIAL VELOCITY
Radial electron-beam-breakup transit-time oscillator
[DE95-005731] p 1959 N95-25385

RADIANCE
Multispectral detection of ground targets in highly correlated backgrounds
[AD-A289292] p 1990 N95-26040

RADIANT COOLING
The cooling of particle beams
[DE95-004669] p 2065 N95-24320

RADIATION ABSORPTION
Cosmic ray LET spectra and doses on board Cosmos-2044 biosatellite p 2061 N95-25930

RADIATION COUNTERS
The emission of particle identification efficiency in the EXCHARM experiment
[DE94-628258] p 2047 N95-24644
On SUSY dark matter detection with spinless nuclei
[DE94-628562] p 2109 N95-24886

RADIATION DAMAGE
Preliminary results of radiation measurements on EURECA p 2060 N95-25923

RADIATION DETECTORS
DOE-High Energy Physics Contract with the University of Hawaii
[DE95-004214] p 2068 N95-24852
The CDF silicon vertex detector SVX and its upgrades
[DE95-003743] p 2050 N95-24901
Double-sided silicon microstrip sensors for the CDF SVX 2 detector
[DE95-004235] p 2068 N95-25238
Update of GALLEX solar neutrino results and implications
[DE95-005005] p 2113 N95-25364
Conference on physics from large gamma-ray detec tor arrays. Volume 2: Proceedings
[DE95-006900] p 2070 N95-25478
Research in elementary particle physics
[DE95-007323] p 2054 N95-25481
Preliminary results of radiation measurements on EURECA p 2060 N95-25923
Cosmic ray LET spectra and doses on board Cosmos-2044 biosatellite p 2061 N95-25930
Space radiation dosimetry on US and Soviet manned missions p 2009 N95-25934

RADIATION DISTRIBUTION
Experimental and calculated LET distributions in the Cosmos-2044 biosatellite orbit p 2061 N95-25929
Enhancement of thickness uniformity of thin films grown by pulsed laser deposition
[NASA-CR-197791] p 1943 N95-26081

RADIATION DOSAGE
Temperature and dose dependence of metal colloid production in alpha-irradiated CaF2
[DE95-004907] p 2088 N95-25288
High LET, passive space radiation dosimetry and spectrometry
[NASA-CR-197694] p 2058 N95-25911
LET spectra measurements from the STS-35 CPDs p 2058 N95-25912
Summary of LET spectra and dose measurements on ten STS missions p 2058 N95-25913
A study of the radiation environment on board the space shuttle flight STS-57 p 2059 N95-25914
USF/Russian dosimetry on STS-57 p 2059 N95-25915
Dosimetry on STS-42 with the RME APD p 2059 N95-25916
Proton calibration of low energy neutron detectors containing (6)LiF p 2060 N95-25925
Linear Energy Transfer (LET) spectra of cosmic radiation in low Earth orbit p 2061 N95-25926
Depth distribution of absorbed dose on the external surface of Cosmos 1887 biosatellite p 2061 N95-25927
Experimental and calculated LET distributions in the Cosmos-2044 biosatellite orbit p 2061 N95-25929
Space radiation dosimetry on US and Soviet manned missions p 2009 N95-25934

RADIATION EFFECTS
One-step in-diffusion as a result of multipulse laser irradiation of LiNbO3 single-crystalline substrates covered with thin Ti deposits on the effect of the radiation wavelength
[DE94-634524] p 2084 N95-24324
Interim report of the advisory committee on human radiation experiments
[DE95-003265] p 2011 N95-24497
Use of advanced solar cells for commercial communication satellites
[NASA-TM-106879] p 1991 N95-24560
Temperature and dose dependence of metal colloid production in alpha-irradiated CaF2
[DE95-004907] p 2088 N95-25288
Consistent approach to describing aircraft HIRF protection
[NASA-CR-195067] p 1909 N95-25341
Human radiation experiments: The Department of Energy roadmap to the story and the records
[DE95-006364] p 2012 N95-25371
Biological effectiveness of neutrons: Research needs
[DE95-004795] p 2051 N95-25373
Preliminary results of radiation measurements on EURECA p 2060 N95-25923

RADIATION HAZARDS
Interim report of the advisory committee on human radiation experiments
[DE95-003265] p 2011 N95-24497
LET spectra measurements from the STS-35 CPDs p 2058 N95-25912

RADIATION INJURIES
Activities of the National Institute of Radiological Sciences
[DE95-709916] p 2072 N95-26165

RADIATION MEASUREMENT
High LET, passive space radiation dosimetry and spectrometry
[NASA-CR-197694] p 2058 N95-25911
LET spectra measurements from the STS-35 CPDs p 2058 N95-25912
Summary of LET spectra and dose measurements on ten STS missions p 2058 N95-25913
A study of the radiation environment on board the space shuttle flight STS-57 p 2059 N95-25914
USF/Russian dosimetry on STS-57 p 2059 N95-25915
Dosimetry on STS-42 with the RME APD p 2059 N95-25916
Neutron influences and energy spectra in the Cosmos-2044 biosatellite orbit p 2061 N95-25928
Experimental and calculated LET distributions in the Cosmos-2044 biosatellite orbit p 2061 N95-25929
Cosmic ray LET spectra and doses on board Cosmos-2044 biosatellite p 2061 N95-25930
Differential neutron energy spectra measured on spacecraft low Earth orbit p 2062 N95-25932
Space radiation dosimetry on US and Soviet manned missions p 2009 N95-25934

RADIATION MEASURING INSTRUMENTS
Proceedings of the 21st Japan Conference on Radiation and Radioisotopes
[DE94-785275] p 2056 N95-25614
Preliminary results of radiation measurements on EURECA p 2060 N95-25923

RADIATION PROTECTION
Consistent approach to describing aircraft HIRF protection
[NASA-CR-195067] p 1909 N95-25341

RADIATION SHIELDING
Bremsstrahlung scattering calculations for the beam stops and collimators in the APS insertion-device beamlines
[DE95-005471] p 2069 N95-25300
Biological effectiveness of neutrons: Research needs
[DE95-004795] p 2051 N95-25373
LET spectra measurements from the STS-35 CPDs p 2058 N95-25912
Summary of LET spectra and dose measurements on ten STS missions p 2058 N95-25913
Depth distribution of absorbed dose on the external surface of Cosmos 1887 biosatellite p 2061 N95-25927
Cosmic ray particles with different LET values under various thicknesses of shielding in low altitude orbits: Calculations and Cosmos-2044 measurements p 2062 N95-25931
Space radiation dosimetry on US and Soviet manned missions p 2009 N95-25934

RADIATION SOURCES
Optical generation of radio-frequency power
[DE95-005276] p 1951 N95-24289
Flow-through Z-pinch study for radiation generation and fusion energy production
[DE95-004209] p 2076 N95-24544
Automatic measurement system for measuring of the nonlinearity of photo detectors
[PB95-165197] p 2074 N95-25999

RADIATION TOLERANCE
Antioxidant and sensitizer effect on the stability of natural rubber latex vulcanized by gamma rays
[DE94-636061] p 1939 N95-24373

RADIATION TRANSPORT
Lawrence Livermore pulsed sphere benchmark analysis of MCNP(trademark) ENDF/B-VI
[DE95-004864] p 2041 N95-24258

RADIATIVE HEAT TRANSFER
Global ocean circulation and equator-pole heat transport as a function of ocean GCM resolution
[DE95-004198] p 2000 N95-25279
The whitehouse effect: Shortwave radiative forcing of climate by anthropogenic aerosols
[DE95-005998] p 2001 N95-25442
RADIATIVE TRANSFER
Radiative corrections for pion polarizability experiments
[DE95-607177] p 2053 N95-25462
RADIATORS
Optically-switched submillimeter-wave oscillator and radiator having a switch-to-switch propagation delay
[NASA-CASE-NPO-18547-1-CU] p 1959 N95-25307
RADICALS
Pulse radiolysis of alkanes: A time-resolved electron paramagnetic resonance study
[DE95-005831] p 2045 N95-24459
Carbons and hydrogen by persistent metal radicals
[DE95-003834] p 1929 N95-24553
Electron spin resonance of radicals and metal complexes
[DE95-605640] p 2055 N95-25499
RADII
Inversion of circular averages and application of backprojection methods to radar imaging
[PB95-141578] p 1955 N95-25891
Modelling the day to day wind variability offshore central Chile at about 30 deg south
[DE95-606032] p 2006 N95-26043
RADIO ASTRONOMY
From superconductivity to supernovae: The Ginzburg symposium. Report on the symposium held in honor of Vitaly L. Ginzburg
[NASA-TM-110596] p 2108 N95-25746
RADIO BURSTS
ARMDAT: A brief description of a computerized test system for burst transmission
[PB95-165452] p 1951 N95-24241
RADIO COMMUNICATION
STS-67 post flight presentation
[NASA-TM-110552] p 1918 N95-24198
Annual report 1992/93, FOA 38. Radio systems and wave propagation
[PB95-141735] p 1953 N95-24835
Discrete-event-dynamic-system-based approaches for control in integrated voice/data multihop Radio Networks
[AD-A288389] p 1954 N95-25604
RADIO ELECTRONICS
Physics in Ukraine International Conference. Volume 4: Radiophysics and Electronics
[DE95-605570] p 2038 N95-25616
RADIO EQUIPMENT
Discrete-event-dynamic-system-based approaches for control in integrated voice/data multihop Radio Networks
[AD-A288389] p 1954 N95-25604
RADIO FREQUENCIES
Optical generation of radio-frequency power
[DE95-005276] p 1951 N95-24289
Divertor design for the Tokamak Physics Experiment
[DE95-003653] p 2078 N95-24650
The effect of the impedance of the generator and intermediate circuits on the impedance of plasma as it applies to magnetron sputtering of thin films in a radio-frequency field
[IFTR-8-1994] p 2083 N95-26019
RADIO GALAXIES
From superconductivity to supernovae: The Ginzburg symposium. Report on the symposium held in honor of Vitaly L. Ginzburg
[NASA-TM-110596] p 2108 N95-25746
RADIO OBSERVATION
Solar-geophysical data number 603, November 1994. Part 1: (Prompt reports). Data for October, September 1994, and late data
[PB95-166393] p 2113 N95-25576
RADIO PHYSICS
Physics in Ukraine International Conference. Volume 4: Radiophysics and Electronics
[DE95-605570] p 2038 N95-25616
RADIO TRANSMISSION
ARMDAT: A brief description of a computerized test system for burst transmission
[PB95-165452] p 1951 N95-24241
Detvag-90: An implementation of Vogler's method for calculation of multiple knife-edge diffraction
[PB95-141859] p 1951 N95-24281
RADIO WAVES
Detvag-90: An implementation of Vogler's method for calculation of multiple knife-edge diffraction
[PB95-141859] p 1951 N95-24281
Optical generation of radio-frequency power
[DE95-005276] p 1951 N95-24289
RADIOACTIVE DECAY
Tests for leptonic CP violation in tau decays
[DE95-005927] p 2050 N95-24902
RADIOACTIVE ISOTOPES
Expert system for nuclide identification in gamma spectrum analysis
[PB95-149712] p 2042 N95-24297
Structure and manual of radioisotope-production data base, ISOP
[DE94-785197] p 2043 N95-24337
Cobalt release from PCA steel during possible fusion reactor accidents
[DE95-005019] p 2069 N95-25365
Fe-57 and Sn-119 Moessbauer studies on La(1.25)Nd(0.6)Sr(0.15)CuO4: Evidence for local magnetic ordering below (approx. equal) 32 K
[DE95-601210] p 1959 N95-25405
Proceedings of the 21st Japan Conference on Radiation and Radioisotopes
[DE94-785275] p 2056 N95-25614
The use of radioisotopes in human experiments: Comments in response to recent media articles
[DE95-605680] p 2012 N95-25981
RADIOACTIVE MATERIALS
Application of compartmental metabolic models for determination of retention and excretion functions
[DE95-600249] p 2010 N95-24367
RADIOACTIVE WASTES
SPEEDUP simulation of liquid waste batch processing, revision 1
[DE95-001240] p 1939 N95-24344
Standardization of equations for radiochemical calculations
[DE95-003028] p 1930 N95-25097
Electrochemical organic destruction in support of Hanford tank waste pretreatment
[DE95-002854] p 1924 N95-25248
National standard and code compliance for electrical equipment installed in hazardous locations for the void fraction instrument
[DE95-002158] p 1960 N95-26092
RADIOBIOLOGY
Biological effectiveness of neutrons: Research needs
[DE95-004795] p 2051 N95-25373
Radiobiological experiments with plant seeds aboard the biosatellite Cosmos 1887 p 2009 N95-25933
RADIOCHEMISTRY
Antioxidant and sensitizer effect on the stability of natural rubber latex vulcanized by gamma rays
[DE94-636061] p 1939 N95-24373
Standardization of equations for radiochemical calculations
[DE95-003028] p 1930 N95-25097
RADIOLOGY
Photonics: From target recognition to lesion detection p 2023 N95-25259
Annual report of National Institute of Radiological Sciences
[DE94-792664] p 2009 N95-25902
Activities of the National Institute of Radiological Sciences
[DE95-709916] p 2072 N95-26165
RADIOLYSIS
Antioxidant and sensitizer effect on the stability of natural rubber latex vulcanized by gamma rays
[DE94-636061] p 1939 N95-24373
Pulse radiolysis of alkanes: A time-resolved electron paramagnetic resonance study
[DE95-005831] p 2045 N95-24459
RADIOMETERS
Airborne imaging of tropospheric emission at millimeter and submillimeter wavelengths
[NASA-TM-110498] p 2003 N95-24336
Multispectral detection of ground targets in highly correlated backgrounds
[AD-A289292] p 1990 N95-26040
Average cosine meter and high spectral resolution measurements at the marine light mixed layer site
[AD-A288713] p 1970 N95-26113
RAILGUN ACCELERATORS
Target injection methods for inertial fusion energy
[DE95-003654] p 2067 N95-24651
RAIN
Passive microwave algorithm development and evaluation
[NASA-CR-197915] p 2005 N95-24535
RAMAN SPECTRA
Simulation study of tapered FEL amplifiers in Raman and Compton regimes
[DE94-785266] p 1971 N95-24340
Raman study of damage processes in Si(+)-implanted GaAs
[DE95-005898] p 2091 N95-26087
RAMAN SPECTROSCOPY
Raman study of damage processes in Si(+)-implanted GaAs
[DE95-005898] p 2091 N95-26087
RAMJET ENGINES
Workshop report: Measurement techniques in highly transient, spectrally rich combustion environments
[AD-A288395] p 1969 N95-25606
RAMSAUER EFFECT
Vacuum polarization effects in low-energy muonic atom collisions
[DE95-605393] p 2058 N95-25910
RANDOM ACCESS MEMORY
Three-D Artificial Neural Network (3DANN) technology. Blueprint for the future p 2024 N95-25260
RANDOM NUMBERS
Introduction to the Monte Carlo methods
[DE94-628386] p 2035 N95-24693
RANDOM PROCESSES
On the joint spectral density of bivariate random sequences
[NASA-CR-197698] p 2035 N95-24278
RANDOM WALK
Quantum group random walks in strongly correlated 2+1 D spin systems
[DE95-607844] p 2091 N95-26103
RARE EARTH COMPOUNDS
Neutron diffraction from HoNi2B2C, version 1
[DE95-005894] p 2085 N95-24431
RARE EARTH ELEMENTS
Selective extraction of trivalent actinides from lanthanides with dithiophosphinic acids and tributylphosphate
[DE95-005249] p 1924 N95-25597
RARE GAS COMPOUNDS
Thermochemistry, kinetics and spectroscopy of Kr and Kr2F
[DE95-005732] p 1941 N95-25386
RAREFIED GAS DYNAMICS
DSMC calculations for 70-deg blunted cone at 3.2 km/s in nitrogen
[NASA-TM-109181] p 1961 N95-24396
RAY TRACING
Co-validation of three methods for optical characterization of point-focus concentrators
[DE95-001613] p 1992 N95-24674
Numerical analysis of electron cyclotron resonance heating on JT-60U and JFT-2M
[DE95-709766] p 2080 N95-25471
RAYLEIGH EQUATIONS
Generalization of the Rayleigh formula to the model with ring-shaped potentials
[DE94-628578] p 2094 N95-24637
RAYLEIGH WAVES
Viscoelastic waves and multiple scales
[DE94-014130] p 1966 N95-26063
REACTING FLOW
A review of chemically reactive turbulent flow analysis, mixing mechanisms and modeling, and a new design of low NOx combustor for non-premixed reactants p 1963 N95-24762
Advanced multi-phase flow CFD model development for solid rocket motor flowfield analysis
[NASA-CR-198044] p 1923 N95-25103
REACTION KINETICS
Direct catalytic decomposition of nitric oxide
[DE95-005202] p 1928 N95-24286
An investigation of the effect of surface impurities on the adsorption kinetics of hydrogen chemisorbed onto iron
[NASA-CR-197967] p 1933 N95-24400
Cesium cobaltdicarbollide-solubility, precipitation, and reactivity in basic aqueous solution
[DE95-005881] p 1929 N95-24430
Study of radicals, clusters and transition state species by anion photoelectron spectroscopy
[DE95-003438] p 2045 N95-24533
Carbons and hydrogen by persistent metal radicals
[DE95-003834] p 1929 N95-24553
Generation, detection and characterization of gas-phase transition metal aggregates and compounds
[DE95-004439] p 1930 N95-24686
Report series in aerosol science
[DE95-737628] p 1999 N95-24904
Modeling of the simulated countercurrent moving-bed chromatographic reactor used for the oxidative coupling of methane
[DE95-004930] p 1924 N95-25286
A higher-order projection method for the simulation of unsteady turbulent nonpremixed combustion in an industrial burner
[DE95-005919] p 1931 N95-25291
Thermochemistry, kinetics and spectroscopy of Kr and Kr2F
[DE95-005732] p 1941 N95-25386

Anisotropy of dilepton emission from nuclear collisions
[DE95-004354] p 2070 N95-25634
Synthesis and processing of Al2O3/Al composites by in situ reaction of aluminum and mullite
[DE95-006224] p 1937 N95-25775

REACTION TIME
The critical diameter, detonation velocity and shock sensitivity of Australian PBXW-115
[DSTO-TR-0076] p 1947 N95-24394

REACTION WHEELS
Suspension system for gimbal supported scanning payloads
[NASA-CASE-MFS-28817-1] p 1969 N95-25544

REACTION-DIFFUSION EQUATIONS
Temperature bounds in a model of laminar flames
[DE95-607048] p 1931 N95-25447
Behaviour at X= +/- infinity of solutions to a predator-prey model
[DE95-607049] p 2033 N95-25748

REACTIVITY
Cesium cobaltdicarbollide-solubility, precipitation, and reactivity in basic aqueous solution
[DE95-005881] p 1929 N95-24430

REACTOR CORES
Plasma burning and control in reactor core
[DE95-602882] p 2082 N95-25942

REACTOR DESIGN
The physics design of the Tokamak Physics Experiment
[DE95-003649] p 2076 N95-24548
Divertor design for the Tokamak Physics Experiment
[DE95-003653] p 2078 N95-24650
A high intensity slow positron facility for the Advanced Neutron Source
[DE94-014108] p 2050 N95-25099
Understanding and improving materials processing through interpreting and manipulating predictive models
[DE95-004384] p 1930 N95-25242
US technical report for the ITER blanket/shield
[DE95-004667] p 2079 N95-25283
Modeling of the simulated countercurrent moving-bed chromatographic reactor used for the oxidative coupling of methane
[DE95-004930] p 1924 N95-25286
Using and programming the SUPERCODE
[DE95-004342] p 2080 N95-25344
Direct energy conversion of radiation energy in fusion reactor
[NIFS-254] p 2072 N95-26250

REACTOR MATERIALS
Modeling plasma/material interactions during a tokamak disruption
[DE95-004247] p 2078 N95-24861
Benchmark experiment on a copper slab assembly bombarded by D-T neutrons
[DE95-709764] p 2055 N95-25497

REACTOR PHYSICS
An overview of the Nuclear Electric Propulsion Space Test Program (NEPSTP) satellite
[DE94-013121] p 1920 N95-24711

REACTOR SAFETY
The dependence of human reliability upon task information content
[DE95-006645] p 2014 N95-25483

REACTOR TECHNOLOGY
Activities of the Radiation Laboratory Department of Nuclear Engineering Kyoto University
[DE95-709896] p 2072 N95-26163
Activities of the Radiation Laboratory Department of Nuclear Engineering Faculty of Engineering, Kyoto University
[DE95-709897] p 2072 N95-26164

READERS
Document analysis with neural net circuits
p 2023 N95-25256
Design documentation for the SINTRA preprocessor
[AD-A288804] p 2015 N95-26192

READOUT
ASIC implementation of a data-push architecture for silicon pixel readout
[DE95-003368] p 2015 N95-24648
The impact of multiplexing on the dynamic requirements of analog-to-digital converters
[DE95-006302] p 1960 N95-25558

REAL TIME OPERATION
Understanding and improving materials processing through interpreting and manipulating predictive models
[DE95-004384] p 1930 N95-25242
Real-time testing and demonstration of the US Army Corps of Engineers' Real-Time On-The-Fly positioning system
[AD-A288624] p 1910 N95-25609
Scheduling time-critical graphics on multiple processors p 2018 N95-25870
Optimal guidance law development for an advanced launch system
[NASA-CR-4667] p 1917 N95-26205

RECEIVERS
Optical space communication: An overview
[DE94-634314] p 1952 N95-24403

RECIPROCAL THEOREMS
Reciprocal space analysis of the microstructure of luminescent and nonluminescent porous silicon films
[DE95-005420] p 1941 N95-25382

RECOMMENDATIONS
Voluntary reporting of greenhouse gases under Section 1605(b) of the Energy Policy Act of 1992: General guidelines
[DE95-003295] p 2000 N95-25361

RECORDS
Human radiation experiments: The Department of Energy roadmap to the story and the records
[DE95-006364] p 2012 N95-25371

RECORDS MANAGEMENT
Integrated resource management database for a distributed information system
[DE95-730180] p 2104 N95-24492

RECRYSTALLIZATION
Static recrystallization behavior of austenite in HSLA 100 during Thermomechanical Controlled Processing (TMCP)
[AD-A288737] p 1937 N95-26057

RECYCLING
Stainless steel recycle
[DE95-003905] p 1934 N95-24615

REED-SOLOMON CODES
On the Trellis structure of a (64,40,8) subcode of the (64,42,8) third-order Reed-Muller code
[NASA-CR-198019] p 2015 N95-24224

REENTRY GUIDANCE
Reentry guidance for hypersonic Flight Experiment (HYFLEX) vehicle
[NAL-TR-1235] p 1910 N95-25764

REFERENCE SYSTEMS
The Fitzgerald-Lorentz hypothesis from the viewpoint of relativity theory
[DE94-636735] p 2093 N95-24378

REFINING
Diesel fuel component contribution to engine emissions and performance
[DE95-000238] p 1998 N95-24604

REFLECTANCE
Non-destructive characterization of porous silicon using x ray reflectivity
[DE95-004766] p 1942 N95-25898
Field-portable reflectance spectrometer
[AD-A288750] p 1970 N95-26059
The effect of encapsulation on the reflectance of photovoltaic modules using textured multicrystalline-silicon solar cells
[DE95-004781] p 1996 N95-26166

REFLECTOMETERS
Calibration of optical time domain reflectometers using time delay generator
[PB95-141776] p 2073 N95-24673

REFLECTOR ANTENNAS
A satellite-tracking millimeter-wave reflector antenna system for mobile satellite-tracking
[NASA-CASE-NPO-18772-1-CU] p 1954 N95-25316

REFRACTORY METAL ALLOYS
Processing and properties of iridium alloys for space power applications
[DE95-005902] p 1935 N95-25390

REFRIGERANTS
Materials Compatibility and Lubricants Research (MCLR) Program
[DE95-004862] p 1941 N95-25243

REFRIGERATING
Thermodynamic property evaluation and magnetic refrigeration cycle analysis for gadolinium gallium garnet
[DE95-005910] p 1951 N95-25367

REGENERATION (ENGINEERING)
Thermodynamic property evaluation and magnetic refrigeration cycle analysis for gadolinium gallium garnet
[DE95-005910] p 1951 N95-25367

REGENERATIVE COOLING
Effect of film cooling/regenerative cooling on scramjet engine performances
[NAL-TR-1242] p 1914 N95-24990

REINFORCEMENT (STRUCTURES)
Design and evaluation of a foam-filled hat-stiffened panel concept for aircraft primary structural applications
[NASA-TM-109175] p 1928 N95-26251

REINFORCING FIBERS
Thermomechanical fatigue behavior of three CFCC's
[NASA-CR-195441] p 1927 N95-25880

REINFORCING MATERIALS
Composite ductility: The role of reinforcement and matrix
[DE95-003664] p 1925 N95-24590
Strengthening of NiAl matrix composites
[AD-A288923] p 1926 N95-25505
Whisker reinforced glass ceramic
[DE95-005568] p 1927 N95-25998
Effects of through-the-thickness stitching on impact and interlaminar fracture properties of textile graphite/epoxy laminates
[NASA-CR-195042] p 1928 N95-26203

RELATIVISTIC EFFECTS
Field equipotentials of a fast-moving charge in medium
[DE94-636737] p 2065 N95-24348

RELATIVISTIC ELECTRON BEAMS
Electroweak coupling measurements from polarized Bhabha scattering at the Z(exp 0) resonance
[DE95-006090] p 2057 N95-25768

RELATIVISTIC PARTICLES
The physics and experimental program of the Relativistic Heavy Ion Collider (RHIC)
[DE95-003416] p 2066 N95-24495
On squaring the primary constraints in a generalized Hamiltonian dynamics
[DE94-628500] p 2036 N95-24504

RELATIVISTIC PLASMAS
Critical parameters of Quark-Hadron phase transition with interacting and massive quarks
[DE95-607143] p 2052 N95-25436

RELATIVISTIC THEORY
The Lienard-Wiechert potentials and relativistic length
[DE94-636733] p 2093 N95-24376
Lienard-Wiechert potentials as a consequence of Lorentz transformation of Coulomb potential
[DE94-636734] p 1952 N95-24377
The Fitzgerald-Lorentz hypothesis from the viewpoint of relativity theory
[DE94-636735] p 2093 N95-24378

RELATIVITY
Theoretical motivation for gravitation experiments on ultra-low energy antiprotons and antihydrogen
[DE95-003662] p 2091 N95-24235
Moving scales contraction contradicts interval invariance
[DE94-636736] p 2092 N95-24347
Wormhole on the Lobachevsky background
[DE95-605251] p 2099 N95-25780
Magnetized pair Bose gas: Relativistic superconductor
[DE95-607846] p 2100 N95-26104

RELAXATION (MECHANICS)
The characteristics and design of an apparatus constructed by the Institute of Basic Problems of Technology to study relaxation phenomena in liquids at frequencies of 10-150 MHz
[IFTR-21/1994] p 1932 N95-25959

RELIABILITY
Adventures in the evolution of a high-bandwidth network for central servers
[DE95-006215] p 2020 N95-24597
Using consumer IC packages in harsh high reliability applications
[DE94-016565] p 1959 N95-24713

RELIABILITY ANALYSIS
Fifth European Symposium on Reliability of Electron Devices, Failure Physics and Analysis
[AD-A286614] p 1956 N95-24447
Availability analysis of a 100 kWh superconducting magnetic energy storage
[DE95-737621] p 2066 N95-24448
Background information to reliability stress screening of components: A guide for component users. Nordtest project 1140-93
[PB95-165775] p 1978 N95-26002
Proposed Nordtest method: Reliability stress screening of components. A guide for component users. Nordtest project 1140-93
[PB95-165783] p 1978 N95-26003
Reliability analysis of software based safety functions
[DE95-606516] p 2018 N95-26045

RELIABILITY ENGINEERING
Fifth European Symposium on Reliability of Electron Devices, Failure Physics and Analysis
[AD-A286614] p 1956 N95-24447
Software fault tolerance in computer operating systems
[NASA-CR-197999] p 2016 N95-24993
Reliability analysis of software based safety functions
[DE95-606516] p 2018 N95-26045

RELIC RADIATION
On fractal structure of quantum gravity and relic radiation anisotropy
[DE95-605306] p 2099 N95-25966

REMOTE CONTROL
Interfacing a digital compass to a remote-controlled helicopter
[PB95-164927] p 1914 N95-24260

REMOTE MANIPULATOR SYSTEM
Simulating the dynamic interaction of a robotic arm and the Space Shuttle remote manipulator system
[NASA-CR-195076] p 2027 N95-26086
REMOTE SENSING
Preliminary analysis of University of North Dakota aircraft data from the FIRE Cirrus IFO-2
[NASA-CR-198038] p 2005 N95-24219
Ice surface temperature retrieval from AVHRR, ATSR, and passive microwave satellite data: Algorithm development and application
[NASA-CR-198037] p 1989 N95-24441
Research in the service of the Swedish National Defence
[PB95-141941] p 1989 N95-24444
JPRS report: Science and technology. Central Eurasia. Otechestvennaya Geologiya: Studies in Aerospace and Remote Sensing
[JPRS-UST-95-004] p 1989 N95-24768
Assessment of climate variability of the Greenland ice sheet: Integration of *in situ* and satellite data
[NASA-CR-198020] p 1998 N95-24846
Turbine-engine applications of thermographic-phosphor temperature measurements
[DE95-003625] p 1989 N95-25110
Low-cost image analysis system
[DE95-005021] p 2021 N95-25378
Fourth symposium of the geological survey of Japan on remote sensing of satellite geology
[PB95-178737] p 1917 N95-25750
Journal of the Communications Research Laboratory, volume 41, number 1, March 1994
[PB95-177606] p 1956 N95-26008
Field-portable reflectance spectrometer
[AD-A288750] p 1970 N95-26059
REMOTE SENSORS
Characterizing the wake vortex signature for an active line of sight remote sensor
[NASA-CR-197697] p 1909 N95-24391
REMOTELY PILOTED VEHICLES
Interfacing a digital compass to a remote-controlled helicopter
[PB95-164927] p 1914 N95-24260
RENORMALIZATION GROUP METHODS
Classical closure theory and Lam's interpretation of epsilon-RNG
[NASA-CR-195061] p 1965 N95-25960
REPEATERS
Application of optical fiber amplifier for wavelength division multiplexing communication system. Part 2: Design of four-channel transmission system using two EDFA repeaters
[DE95-730179] p 1952 N95-24491
RESCUE OPERATIONS
Inflatable rescue device
[NASA-CASE-MSC-22244-1] p 2014 N95-25306
RESEARCH AIRCRAFT
A quiet STOL Research Aircraft Development program
[NAL-TR-1223] p 1911 N95-25862
RESEARCH AND DEVELOPMENT
Federal Aviation Administration plan for research, engineering and development, 1995
p 2102 N95-24202
Biologically produced succinic acid: A new route to chemical intermediates
[DE95-000257] p 2007 N95-24306
Clean fractionation of biomass
[DE95-000259] p 2007 N95-24307
Monolithic solid oxide fuel cell technology advancement for coal-based power generation
[DE94-012258] p 1990 N95-24318
JPRS report: Science and technology. Central Eurasia: Space
[JPRS-USP-94-007] p 1915 N95-24358
JPRS report: Science and technology. Central Eurasia: Space
[JPRS-USP-94-008] p 1916 N95-24359
Display technologies in Russia, Ukraine, and Belarus
[ISBN-1-883712-36-X] p 2085 N95-24460
JPRS report: Science and technology. Central Eurasia
[JPRS-UST-95-009] p 1916 N95-24467
JPRS report: Science and technology. Central Eurasia
[JPRS-UST-95-008] p 1957 N95-24468
JPRS report: Science and technology. Central Eurasia
[JPRS-UST-94-030] p 1962 N95-24469
JPRS report: Science and technology. Central Eurasia
[JPRS-UST-94-027] p 1957 N95-24470
JPRS report: Science and technology. Central Eurasia: Institute of General and Nuclear Physics: 1993 Status and Prospects
[JPRS-UST-94-025] p 2045 N95-24471
JPRS report: Science and technology. Central Eurasia
[JPRS-UST-94-018] p 1950 N95-24472
Piezoelectric motor development at AlliedSignal Inc., Kansas City Division
[DE95-003389] p 1958 N95-24532
JPRS report: Science and technology. Central Eurasia
[JPRS-UST-95-013] p 1987 N95-24538
JPRS report: Science and technology. Central Eurasia
[JPRS-UST-95-010] p 1953 N95-24539
JPRS report: Science and technology. Central Eurasia
[JPRS-UST-95-012] p 1950 N95-24540
JPRS report: Science and technology. Central Eurasia
[JPRS-UST-95-011] p 1910 N95-24541
Advances and prospects in reversed field pinch research
[DE95-007017] p 2077 N95-24602
Activities of the Solid State Division
[DE95-003900] p 2087 N95-24611
JPRS Report: Science and technology. Central Eurasia
[JPRS-UST-95-002] p 1916 N95-24621
Assessment of avionics technology in European aerospace organizations
[NASA-CR-189201] p 1912 N95-24624
JPRS report: Science and technology. Central Eurasia
[JPRS-UST-94-034] p 1987 N95-24729
JPRS report: Science and technology. Central Eurasia
[JPRS-UST-95-003] p 1988 N95-24730
JPRS report: Science and technology. Central Eurasia
[JPRS-UST-95-006] p 1950 N95-24731
JPRS report: Science and technology. Central Eurasia
[JPRS-UST-94-033] p 2037 N95-24732
JPRS Report: Science and technology. Central Eurasia
[JPRS-UST-94-032] p 1950 N95-24759
JPRS Report: Science and technology. Central Eurasia
[JPRS-UST-94-031] p 1988 N95-24760
JPRS report: Science and technology. Central Eurasia: Seminar on materials science
[JPRS-UST-95-007] p 1920 N95-24761
JPRS report: Science and technology. Central Eurasia. Otechestvennaya Geologiya: Studies in Aerospace and Remote Sensing
[JPRS-UST-95-004] p 1989 N95-24768
Bioprocessing in nonaqueous media: Critical needs and opportunities
[DE95-004878] p 2008 N95-24843
JPRS report: Science and technology. Central Eurasia: Space
[JPRS-USP-94-008] p 1916 N95-24847
Yearbook 1993: Bioenergy Research Programme. Utilization of bioenergy and biomass conversion
[DE95-717518] p 1993 N95-24862
Study of very high temperature technology, 2
[DE95-730105] p 2088 N95-24900
Study of copper perovskite
[DE95-730106] p 2088 N95-24988
Study of composite zirconium oxide
[DE95-730104] p 1926 N95-25111
The first ICASE/LARC industry roundtable: Session proceedings
[NASA-CR-195040] p 2014 N95-25119
Summaries of FY 1994 geosciences research
[DE95-005657] p 1988 N95-25440
JPRS report: Science and technology. Central Eurasia
[JPRS-UST-95-018] p 2071 N95-26079
JPRS report: Science and technology. Central Eurasia
[JPRS-UST-95-017] p 1988 N95-26080
Development of novel active transport membrane devices
[DE95-002658] p 1932 N95-26093
Office of Space Science: Integrated technology strategy
[NASA-TM-110578] p 2108 N95-26183
Science in the national interest
[ISBN-0-16-045186-8] p 2115 N95-26335
RESEARCH FACILITIES
A high intensity slow positron facility for the Advanced Neutron Source
[DE94-014108] p 2050 N95-25099
User guide to the Burner Engineering Research Laboratory
[DE95-004191] p 1931 N95-25492
Automated protein crystal growth facility
p 1918 N95-26306
RESEARCH MANAGEMENT
High Energy Physics Advisory Panel's subpanel on vision for the future of high-energy physics
[DE94-013641] p 2068 N95-24899
Our changing planet: The FY 1995 U.S. Global Change Research Program p 2002 N95-25852
Office of Space Science: Integrated technology strategy
[NASA-TM-110578] p 2108 N95-26183
RESEARCH PROJECTS
JPRS report: Science and technology. Central Eurasia: Space
[JPRS-USP-94-008] p 1916 N95-24359
Current experiments in elementary particle physics. Revision
[DE95-003797] p 2067 N95-24652
High Energy Physics Division research activities
[DE95-003985] p 2068 N95-24680
Report series in aerosol science
[DE95-737628] p 1999 N95-24904
Renewable Energy Demonstration Project by the National Renewable Energy Laboratory and the General Services Administration
[DE95-000261] p 1995 N95-25995
RESIDENTIAL ENERGY
Sector-specific issues and reporting methodologies supporting the General Guidelines for the voluntary reporting of greenhouse gases under Section 1605(b) of the Energy Policy Act of 1992, volume 1. Part 1: Electricity supply sector. Part 2: Residential and commercial buildings sector. Part 3: Industrial sector
[DE95-003296] p 2000 N95-25362
RESIDUAL STRESS
Residual Stress Measurements with Laser Speckle Correlation Interferometry and Local Heat Treating
[DE95-060082] p 1981 N95-24598
Stress analysis of a crack in the residual stress field by welding and its application to the fatigue crack propagation
[NAL-TR-1248] p 1981 N95-25000
Processing and characterization of transformation-toughened ceramics with strength retention to elevated temperatures
[DE95-005758] p 1941 N95-25387
Issues related to prediction of residual stresses in titanium alloy matrix composites
[DE95-005243] p 1926 N95-25596
Stress analysis of a crack in the residual stress field by welding and its application to the fatigue crack propagation
[NAL-TR-1248] p 1983 N95-25796
RESIN MATRIX COMPOSITES
Investigation into the flammability properties of honeycomb composites
[PB95-143293] p 1941 N95-25342
Study on tensile fatigue testing method of unidirectional fiber-resin matrix composites
[NAL-TR-1241] p 1927 N95-25770
Static and fatigue properties of pin-joint specimens of a AS-4/PEEK thermoplastic composite material
[NAL-TR-1214] p 1927 N95-25859
RESOLUTION
Resolving the ambiguities: An industrial hygiene Indoor Air Quality (IAQ) symposium
[DE95-005391] p 2000 N95-25380
RESONANCE
A measurement of quark and gluon jet differences at the Z(sup 0) resonance
[DE95-005947] p 2044 N95-24417
Measurement of alpha(sub s)from hadronic event observables at the Z(sup 0) resonance
[DE95-005943] p 2045 N95-24434
Measurement of alpha(sub s) from hadronic ev ent observables at the Z(sup 0) resonance
[DE95-005949] p 2047 N95-24622
A fast tracking method using resonance basis Hamiltonians
[DE95-004292] p 2068 N95-24664
Multichannel resonances and closed channels (scalar sector)
[DE94-628629] p 2055 N95-25537
On analysis of resonance neutron depolarization in uniaxial media
[DE95-703782] p 2057 N95-25669
RESONANCE SCATTERING
Electroweak coupling measurements from polarized Bhabha scattering at the Z(sup 0) resonance
[DE95-006056] p 2067 N95-24574
RESONANT FREQUENCIES
The transmission and control of vibrational power in a two stage isolation system with a water-loaded substructure
[ISVR-TR-235] p 1975 N95-24992
RESONANT TUNNELING
Current-voltage characteristics of a tunnel junction with resonant centers
[DE94-634530] p 1956 N95-24245
RESOURCES MANAGEMENT
Integrated resource management database for a distributed information system
[DE95-730180] p 2104 N95-24492
Issues in NASA program and project management
[NASA-SP-6101(08)] p 2102 N95-24565
RESPONSES
Cognitive diagnosis combined with latent trait theory and multiphase responses
[AD-A288701] p 2013 N95-26010

RESTORATION
Information management architecture for an integrated computing environment for the Environmental Restoration Program. Environmental Restoration Program, Volume 3: Interim technical architecture
[DE95-001386] p 2105 N95-24656
REVERSE FIELD PINCH
Advances and prospects in reversed field pinch research
[DE95-007017] p 2077 N95-24602
Transport reduction by current profile control in the reversed field pinch
[DE95-007016] p 2077 N95-24619
REYNOLDS NUMBER
Experimental study of the effects of Reynolds number on high angle of attack aerodynamic characteristics of forebodies during rotary motion
[NASA-CR-195033] p 1907 N95-24443
REYNOLDS STRESS
A review of Reynolds stress models for turbulent shear flows
[NASA-CR-195054] p 1962 N95-24580
RHENIUM COMPOUNDS
Carbons and hydrogen by persistent metal radicals
[DE95-003834] p 1929 N95-24553
RHO-MESONS
Searching for exotic mesons in e(+)e(-) annihilation at DA(phi)NE
[PB95-165379] p 2064 N95-26001
RHODAMINE
On the uncertainty in single molecule fluorescent lifetime and energy emission measurements
[NASA-CR-198009] p 2049 N95-24877
RIEMANN MANIFOLD
The geometry of weak solutions of certain integrable nonlinar PDE's
[DE95-005241] p 2030 N95-24609
RIGID STRUCTURES
The transmission and control of vibrational power in a two stage isolation system with a water-loaded substructure
[ISVR-TR-235] p 1975 N95-24992
The rotations of deformable bodies. Part 1: Geometry and Kinematics
[IFTR-7/1994] p 2039 N95-26332
RINGS (MATHEMATICS)
On the Cohen-Macaulayness and Gorensteinness of integral closure filtrations Rees algebras of height-two equimultiple ideals
[DE95-607000] p 2034 N95-25989
The criteria for the Cohen-Macaulayness and Gorensteiness of Rees algebras of ideals having positive analytic deviation
[DE95-607003] p 2034 N95-25992
RISK
Aerospace safety advisory panel
[NASA-TM-110554] p 1920 N95-24505
An assessment of aviation accident risk of aphakic civil airmen by class of medical certificate held and by age: 1982-1985
[DOT/FAA/AM-95/11] p 2011 N95-25336
Report to Congressional Committees. Tactical Aircraft: Concurrency in development and production of F-22 aircraft should be reduced
[GAO/NSIAD-95-59] p 1911 N95-26338
RIVETED JOINTS
Estimate of probability of crack detection from service difficulty report data
[PB95-149381] p 1905 N95-24295
ROASTING
Preparation of stabilized zirconia (ZrO2) with ytteria (Y2O3) by simultaneous precipitation
[DE95-600163] p 1933 N95-24366
ROBOT ARMS
Simulating the dynamic interaction of a robotic arm and the Space Shuttle remote manipulator system
[NASA-CR-195076] p 2027 N95-26086
ROBOT DYNAMICS
Simulating the dynamic interaction of a robotic arm and the Space Shuttle remote manipulator system
[NASA-CR-195076] p 2027 N95-26086
ROBOTICS
Shuttle to space station transfer of the materials exposure facility
[NASA-TM-110156] p 1919 N95-24765
ROBOTS
Milli-robots for surgical teleoperation
[NASA-CR-197378] p 1974 N95-24204
Summaries of reports of the Electrotechnical Laboratory, no. 48
[JTN-95-80825] p 2114 N95-24908
ROCKET ENGINE CONTROL
Controls concepts for next generation reuseable rocket engines
[NASA-TM-106902] p 1923 N95-25877
ROCKET ENGINE DESIGN
BSM Delta qualification 2, volume 1
[NASA-CR-196566-VOL-1] p 1921 N95-24440
ROCKET ENGINES
Controls concepts for next generation reuseable rocket engines
[NASA-TM-106902] p 1923 N95-25877
ROLLER BEARINGS
A review of rolling element bearing vibration detection, diagnosis and prognosis
[DSTO-RR-0013] p 1975 N95-24393
ROLLERS
A review of rolling element bearing vibration detection, diagnosis and prognosis
[DSTO-RR-0013] p 1975 N95-24393
ROOMS
A technique for the evaluation of strength of coupling between SEA subsystems: Experiments with two coupled plates and two coupled rooms
[ISVR-TR-242] p 1982 N95-25332
ROTARY ENGINES
Stratified charge rotary engine combustion studies
[NASA-CR-197985] p 1974 N95-24223
ROTARY STABILITY
Experimental study of the effects of Reynolds number on high angle of attack aerodynamic characteristics of forebodies during rotary motion
[NASA-CR-195033] p 1907 N95-24443
ROTATING PLASMAS
Maryland controlled fusion research program
[DE95-006642] p 2081 N95-25561
ROTATING SHAFTS
Rotary actuator
[NASA-CASE-MFS-28581-1] p 1936 N95-25545
ROTATION
Response to a localized impact loading of a composite multilayered rotational shell structure: Theory and numerical methods, volume 2
[ONERA-NT-1994-10-VOL-2] p 1980 N95-24283
Suspension system for gimbal supported scanning payloads
[NASA-CASE-MFS-28817-1] p 1969 N95-25544
Aspect estimation of an aircraft using library model silhouettes
[PB95-141834] p 2036 N95-25894
Regge in the sky: Origin of the cosmic rotation
[DE95-607001] p 2111 N95-25990
The rotations of deformable bodies. Part 1: Geometry and Kinematics
[IFTR-7/1994] p 2039 N95-26332
ROTATIONAL SPECTRA
Method for determining shear direction using liquid crystal coatings
[NASA-CASE-ARC-11995-1] p 2075 N95-26117
ROTOR AERODYNAMICS
Recent improvements to and validation of the one dimensional NASA wave rotor model
[NASA-TM-106913] p 1908 N95-25962
ROTOR DYNAMICS
Dynamic behavior of a magnetic bearing supported jet engine rotor with auxiliary bearings
[NASA-CR-197860] p 1913 N95-24213
Thermohydrodynamic analysis of cryogenic liquid turbulent flow fluid film bearings, phase 2
[NASA-CR-197412] p 1962 N95-24461
ROTORS
Dynamic behavior of a magnetic bearing supported jet engine rotor with auxiliary bearings
[NASA-CR-197860] p 1913 N95-24213
Exploratory flow visualization investigation of mast-mounted sights in presence of a rotor
[NASA-TM-4634] p 1907 N95-24566
Recent improvements to and validation of the one dimensional NASA wave rotor model
[NASA-TM-106913] p 1908 N95-25962
Dynamics of phase ordering of nematics in a pore
[DE95-607662] p 2090 N95-25978
RUNWAYS
Aircraft accident report: Impact with blast fence upon landing rollout Action Air Charters flight 990 Piper PA-31-350, N990RA, Stratford, Connecticut,27 April 1994
[PB94-910410] p 1908 N95-24206
RUSSIAN FEDERATION
Display technologies in Russia, Ukraine, and Belarus
[ISBN-1-883712-36-X] p 2085 N95-24460
JPRS report: Science and technology. Central Eurasia
[JPRS-UST-95-009] p 1916 N95-24467
JPRS report: Science and technology. Central Eurasia
[JPRS-UST-95-008] p 1957 N95-24468
JPRS report: Science and technology. Central Eurasia
[JPRS-UST-94-030] p 1962 N95-24469
JPRS report: Science and technology. Central Eurasia
[JPRS-UST-94-027] p 1957 N95-24470
JPRS report: Science and technology. Central Eurasia: Institute of General and Nuclear Physics: 1993 Status and Prospects
[JPRS-UST-94-025] p 2045 N95-24471
JPRS report: Science and technology. Central Eurasia
[JPRS-UST-94-018] p 1950 N95-24472
JPRS report: Science and technology. Central Eurasia
[JPRS-UST-94-024] p 1958 N95-24620
JPRS Report: Science and technology. Central Eurasia
[JPRS-UST-95-002] p 1916 N95-24621
JPRS report: Science and technology. Central Eurasia
[JPRS-UST-94-034] p 1987 N95-24729
JPRS report: Science and technology. Central Eurasia
[JPRS-UST-95-003] p 1988 N95-24730
JPRS report: Science and technology. Central Eurasia
[JPRS-UST-95-006] p 1950 N95-24731
JPRS report: Science and technology. Central Eurasia
[JPRS-UST-94-033] p 2037 N95-24732
JPRS Report: Science and technology. Central Eurasia
[JPRS-UST-94-032] p 1950 N95-24759
JPRS Report: Science and technology. Central Eurasia
[JPRS-UST-94-031] p 1988 N95-24760
JPRS report: Science and technology. Central Eurasia: Seminar on materials science
[JPRS-UST-95-007] p 1920 N95-24761
JPRS report: Science and technology. Central Eurasia. Otechestvennaya Geologiya: Studies in Aerospace and Remote Sensing
[JPRS-UST-95-004] p 1989 N95-24768
JPRS report: Science and technology. Central Eurasia: Space
[JPRS-USP-94-008] p 1916 N95-24847
JPRS report: Science and technology. Central Eurasia
[JPRS-UST-95-018] p 2071 N95-26079
JPRS report: Science and technology. Central Eurasia
[JPRS-UST-95-017] p 1988 N95-26080
RUSSIAN SPACE PROGRAM
JPRS report: Science and technology. Central Eurasia: Space
[JPRS-USP-94-008] p 1916 N95-24359
JPRS report: Science and technology. Central Eurasia
[JPRS-UST-95-013] p 1987 N95-24538
JPRS report: Science and technology. Central Eurasia
[JPRS-UST-95-010] p 1953 N95-24539
JPRS report: Science and technology. Central Eurasia
[JPRS-UST-95-012] p 1950 N95-24540

S

S MATRIX THEORY
A discrete variable representation for electron-hydrogen atom scattering
[DE95-003436] p 2045 N95-24512
Toward improved photon-atom scattering predictions
[DE95-003651] p 2046 N95-24549
S WAVES
Creation of a scalar potential in 2D dilaton gravity
[DE95-006066] p 2003 N95-24577
Vacuum polarization effects in low-energy muonic atom collisions
[DE95-605393] p 2058 N95-25910
Viscoelastic waves and multiple scales
[DE94-014130] p 1986 N95-26063
SADDLE POINTS
Saddle-point method in path integrals
[DE94-628379] p 2036 N95-24688
SAFETY
Interim report of the advisory committee on human radiation experiments
[DE95-003265] p 2011 N95-24497
TITLE: Environmental, health, and safety issues offuel cells in transportation. Volume 1: Phosphoricacid fuel-cell buses
[DE95-000289] p 1993 N95-24866
Cobalt release from PCA steel during possible fusion reactor accidents
[DE95-005019] p 2069 N95-25365
Design of Fusion Safety Data Base
[DE95-703897] p 2080 N95-25495
SAFETY DEVICES
Inflatable rescue device
[NASA-CASE-MSC-22244-1] p 2014 N95-25306
SAFETY FACTORS
The energy intelligence information system
[DE95-002184] p 2105 N95-24675
SAFETY MANAGEMENT
Software engineering and data management for automated payload experiment tool
[NASA-CR-196562] p 2104 N95-24477

SAMPLING
Standardization of equations for radiochemical calculations
[DE95-003028] p 1930 N95-25097
SANDWICH STRUCTURES
The transmission and control of vibrational power in a two stage isolation system with a water-loaded substructure
[ISVR-TR-235] p 1975 N95-24992
Three-dimensional solutions for thermomechanical stresses in sandwich panels and shells
p 1984 N95-26265
SATELLITE ATMOSPHERES
Infrared spectroscopy of Jupiter and Saturn
[NASA-CR-198034] p 2111 N95-24239
SATELLITE COMMUNICATION
ESRO's telecommunications programme and the OTS project (1970-1974)
[ESA-HSR-13] p 1953 N95-24893
Assessment of Commercial Satellite Communications Initiative (CSCI) studies
[AD-A288357] p 1920 N95-25508
Journal of the Communications Research Laboratory, volume 41, number 1, March 1994
[PB95-177606] p 1956 N95-26008
SATELLITE DESIGN
Small spacecraft power and thermal subsystems
[NASA-CR-195029] p 1921 N95-24216
Small spacecraft power and thermal subsystems
[NASA-CR-195029] p 1921 N95-24428
An overview of the Nuclear Electric Propulsion Space Test Program (NEPSTP) satellite
[DE94-013121] p 1920 N95-24711
SATELLITE IMAGERY
Research in the service of the Swedish National Defence
[PB95-141941] p 1989 N95-24444
SATELLITE INSTRUMENTS
User guide for the Polaris powder diffractometer at ISIS. Version 2.1
[PB95-165767] p 2074 N95-25573
SATELLITE NETWORKS
Assessment of Commercial Satellite Communications Initiative (CSCI) studies
[AD-A288357] p 1920 N95-25508
SATELLITE OBSERVATION
JPRS report: Science and technology. Central Eurasia: Space
[JPRS-USP-94-007] p 1915 N95-24358
Ice surface temperature retrieval from AVHRR, ATSR, and passive microwave satellite data: Algorithm development and application
[NASA-CR-198037] p 1989 N95-24441
Assessment of climate variability of the Greenland ice sheet: Integration of in situ and satellite data
[NASA-CR-198020] p 1998 N95-24846
SATELLITE SURFACES
Distribution and nature of UV absorbers on Trition's surface
[NASA-CR-198008] p 2112 N95-26116
SATELLITE TRACKING
A satellite-tracking millimeter-wave reflector antenna system for mobile satellite-tracking
[NASA-CASE-NPO-18772-1-CU] p 1954 N95-25316
SATELLITE-BORNE INSTRUMENTS
Return to the red planet: The Mars Observer Mission
[NASA-CR-197707] p 2113 N95-26336
SATELLITE-BORNE PHOTOGRAPHY
Mars observer mission: Mapping the Martian world
[NASA-CR-110585] p 2112 N95-24672
SATURATION (CHEMISTRY)
Dynamic methods for determining the material characteristics of saturated permeable media
[IFTR-17/1993] p 1932 N95-26107
SATURN (PLANET)
Voyager: The grandest tour. The mission to the outer planets
[NASA-CR-197708] p 2112 N95-25854
SATURN ATMOSPHERE
Infrared spectroscopy of Jupiter and Saturn
[NASA-CR-198034] p 2111 N95-24239
SCALARS
On the central charge in 3 D-supersymmetry
[DE95-600851] p 2093 N95-24352
Constraints and Hamiltonian in light-front quantized field theory
[DE95-600852] p 2093 N95-24353
Creation of a scalar potential in 2D dilaton gravity
[DE95-006066] p 2003 N95-24577
Scalar three body decays and signals for new physics
[DE95-607188] p 2053 N95-25438
SCALE EFFECT
Moving scales contraction contradicts interval invariance
[DE94-636736] p 2092 N95-24347
SCALE MODELS
On the central charge in 3 D-supersymmetry
[DE95-600851] p 2093 N95-24352
AMC EN-1038: Reduced scale solar simulator supplementary test report
[NASA-CR-197988] p 1915 N95-24380
Scaling in a scramjet combustor p 1933 N95-25398
Heat transfer measurements in small scale wind tunnels
[AD-A288689] p 1915 N95-26053
SCALING LAWS
Experimental constraints on transport
[DE95-004962] p 2050 N95-25180
SCANNERS
Suspension system for gimbal supported scanning payloads
[NASA-CASE-MFS-28817-1] p 1969 N95-25544
SCATTERING
Thermal diffuse scattering in time-of-flight neutron diffraction studied on SBN single crystals
[DE94-637054] p 2085 N95-24362
Bremsstrahlung scattering calculations for the beam stops and collimators in the APS insertion-device beamlines
[DE95-005471] p 2069 N95-25300
Radiative corrections for pion polarizability experiments
[DE95-607177] p 2053 N95-25462
Vacuum polarization effects in low-energy muonic atom collisions
[DE95-605393] p 2058 N95-25910
SCATTERING AMPLITUDE
Polarization and N-N elastic scattering amplitudes
[DE95-004648] p 2042 N95-24292
Calculation of light scattering from a spherical particle on a surface by the multipole expansion method
[ATR-95(9558)-2] p 2075 N95-26198
SCATTERING COEFFICIENTS
Diurnal variations of backscattering properties of pine trees at C- and X-bands
[PB95-149738] p 1988 N95-24299
SCATTERING CROSS SECTIONS
Polarization and N-N elastic scattering amplitudes
[DE95-004648] p 2042 N95-24292
Toward improved photon-atom scattering predictions
[DE95-003651] p 2046 N95-24549
Notion of the inclusive spectra and cross sections of B-meson production in hadronic interactions of high energies
[DE94-628628] p 2049 N95-24887
Calculation of light scattering from a spherical particle on a surface by the multipole expansion method
[ATR-95(9558)-2] p 2075 N95-26198
SCAVENGING
The evaluation of potential limonene scavengers
[DE95-006853] p 2002 N95-25899
SCHEDULES
Sleep patterns in air traffic controllers working rapidly rotating shifts: A field study
[DOT/FAA/AM-95/12] p 2012 N95-26204
SCHEDULING
Integrated planning: A baseline development perspective
[DE95-004945] p 2102 N95-24905
Scheduling time-critical graphics on multiple processors p 2018 N95-25870
SCHROEDINGER EQUATION
Semiclassical asymptotics on covering manifolds and morse inequalities
[PB95-165510] p 2028 N95-24251
Periodic solutions of Hamiltonian perturbations of 2D linear Schroedinger equations
[PB95-165536] p 2028 N95-24301
Anharmonic potential in the oscillator representation
[DE94-636740] p 2092 N95-24312
On a generalized Kepler-Coulomb system: Inter basis expansions
[DE94-636739] p 2093 N95-24349
Numerical simulation methods for wave propagation through optical waveguides
[DE94-634313] p 2073 N95-24402
Oscillator poly spheroidal functions
[DE94-628440] p 2030 N95-24636
Generalization of the Rayleigh formula to the model with ring-shaped potentials
[DE94-628578] p 2094 N95-24637
On the problem of unboundedness from below of the spinor QED Hamiltonian
[DE94-628579] p 2094 N95-24638
Toroidal response in magnetic resonance
[DE94-628406] p 2037 N95-24696
Quantum group and quantum symmetry
[DE94-634329] p 2095 N95-24767
Ellipsoidal basis for isotropic oscillator
[DE95-605253] p 2034 N95-25782
Existence domains and some properties of a particle bound state in fields with homogeneous dependence of its potential energy on coordinates
[DE95-605280] p 2057 N95-25784
Strong phase correlations of solitons of nonlinear Schroedinger equation
[DE95-607002] p 2063 N95-25991
Condensate localization by mesoscale disorder in high-T(sub c) superconductors
[DE95-607819] p 1960 N95-26100
SCHWARZSCHILD METRIC
Wormhole on the Lobachevsky background
[DE95-605251] p 2099 N95-25780
SCIENTIFIC VISUALIZATION
Object-oriented parallel polygon rendering
[DE95-004909] p 2021 N95-24881
Multidimensional visualization and browsing for intelligence analysis
[DE95-004901] p 2106 N95-25774
Three-dimensional user interfaces for scientific visualization
[NASA-CR-197923] p 2017 N95-25867
The 3D widgets for exploratory scientific visualization
p 1966 N95-25868
An annotation system for 3D fluid flow visualization
p 1966 N95-25869
Scheduling time-critical graphics on multiple processors p 2018 N95-25870
Four-Dimensional Information Visualization and Analysis System
[DE95-004935] p 2022 N95-26013
SCINTILLATING FIBERS
Energy resolution of a lead scintillating fiber electromagnetic calorimeter
[DE94-628253] p 1967 N95-24484
SCINTILLATION
Laser beam log amplitude temporal scintillation spectrum due to crosswind. Part 1: Theory
[TR-1-FSRC-1994-PT-1] p 1971 N95-24371
LuAlO3: A high density, high speed scintillator for gamma detection
[DE95-004678] p 2064 N95-26256
SCINTILLATION COUNTERS
Fusion-neutron diagnostic on the Microwave Tokamak Experiment
[DE94-777530] p 2075 N95-24270
Absolute calibration and monitoring of a spectrometric channel using a photomultiplier
[DE94-628251] p 1968 N95-24635
SEA ICE
Ice surface temperature retrieval from AVHRR, ATSR, and passive microwave satellite data: Algorithm development and application
[NASA-CR-198037] p 1989 N95-24441
SEALS (STOPPERS)
Actively controlled shaft seals for aerospace applications
[NASA-CR-198035] p 1974 N95-24218
SEAT BELTS
Development of an intervention program to encourage shoulder harness use and aircraft retrofit in general aviation aircraft, phases 1 and 2
[DOT/FAA/AM-95/2] p 1909 N95-24384
SEATS
Analysis of warping effects on the static and dynamic response of a seat-type structure
[NIAR-94-12] p 1979 N95-24211
SECONDARY FLOW
Internal performance characteristics of thrust-vectored axisymmetric ejector nozzles
[NASA-TM-4610] p 1907 N95-25338
SECURITY
How Captain Amerika uses neural networks to fight crime p 2025 N95-25272
Towards an era of global village: The dynamics of world telecommunications and its implications for the future of nation state
[PB95-165064] p 1954 N95-25482
SEDIMENT TRANSPORT
Shelf sediment dynamics and development of lithostratigraphy
[AD-A288886] p 2006 N95-25504
SEDIMENTARY ROCKS
Predicting the transport properties of sedimentary rocks from microgeometry
[DE95-000129] p 2004 N95-26089
SEEDS
Radiobiological experiments with plant seeds aboard the biosatellite Cosmos 1887 p 2009 N95-25933
SEISMOLOGY
3-D seismic imaging of complex geologies
[DE95-006813] p 2004 N95-25476
SELECTION
Adventures in the evolution of a high-bandwidth network for central servers
[DE95-006215] p 2020 N95-24597

SELECTIVE DISSEMINATION OF INFORMATION
Survey of methods for secure connection to the internet
[DE95-730185] p 1952 N95-24493
Naval network security requirements analysis
[AD-A288692] p 2022 N95-26054
SELENIUM COMPOUNDS
Proceedings of the Workshop on Dynamics and Structure of Disordered System
[DE94-792685] p 1931 N95-25356
SELF ERECTING DEVICES
Efficient eigenvalue assignment by state and output feedback with applications for large space structures
[NASA-TM-110155] p 1920 N95-24581
SELF FOCUSING
Self-focusing of electromagnetic radiation in electron-positron ion plasma
[DE95-607626] p 2082 N95-25975
SELF LUBRICATING MATERIALS
Wear-resistant, self-lubricating surfaces of diamond coatings
[NASA-TM-106887] p 1924 N95-25961
SELF ORGANIZING SYSTEMS
Multidimensional data analysis on the basis of integral nonparametric statistics and multilayer perceptrons
[DE94-628375] p 2035 N95-24858
Innovation and application of ANN in Europe demonstrated by Kohonen maps p 2024 N95-25262
SEMANTICS
Towards a formal semantics for Ada 9X
[NASA-CR-195037] p 2020 N95-24634
SEMICIRCULAR CANALS
Relation of motion sickness susceptibility to vestibular and behavioral measures of orientation
[NASA-CR-198048] p 2010 N95-24410
SEMICONDUCTOR DEVICES
Performance issues for iterative solvers in device simulation
[NASA-CR-197952] p 2027 N95-24214
Fifth European Symposium on Reliability of Electron Devices, Failure Physics and Analysis
[AD-A286614] p 1956 N95-24447
The CDF silicon vertex detector SVX and its upgrades
[DE95-003743] p 2050 N95-24901
Potential of diamond for applications in microelectronics
[PB95-141446] p 1942 N95-25633
SEMICONDUCTOR JUNCTIONS
Photoionization of shallow donor impurities in finite-barrier quantum wells
[DE95-607521] p 2097 N95-25468
SEMICONDUCTOR LASERS
High gain GaAs Photoconductive Semiconductor Switches (PCSS): Device lifetime, high current testing, optical pulse generators
[DE95-003354] p 1957 N95-24488
SEMICONDUCTORS (MATERIALS)
JPRS report: Science and technology. Central Eurasia
[JPRS-UST-95-008] p 1957 N95-24468
High gain GaAs Photoconductive Semiconductor Switches (PCSS): Device lifetime, high current testing, optical pulse generators
[DE95-003354] p 1957 N95-24488
ASIC implementation of a data-push architecture for silicon pixel readout
[DE95-003368] p 2015 N95-24648
PC based analysis of gamma ray spectra generated by semiconductor detectors
[DE94-628381] p 1958 N95-24690
Double-sided silicon microstrip sensors for the CDF SVX 2 detector
[DE95-004235] p 2068 N95-25238
Kinetic modeling of the atomic layer epitaxy window in group 4 semiconductor growth
[DE95-005903] p 2089 N95-25391
Photoionization of shallow donor impurities in finite-barrier quantum wells
[DE95-607521] p 2097 N95-25468
Optical instabilities and chaos due to the virtual formation of biexcitons
[DE95-607664] p 2063 N95-25994
Automatic measurement system for measuring of the nonlinearity of photo detectors
[PB95-165197] p 2074 N95-25999
SENSITIVITY
Measurement of the SS-OS Dijet cross-section ratio
[DE95-004852] p 2041 N95-24253
Sensitivity analysis of the non-linear dynamic viscoplastic response of 2-d structures with respect to material parameters p 1984 N95-26266
Sensitivity analysis for the dynamic response of viscoplastic shells of revolution p 1984 N95-26268
Effect of mesh distortion on the accuracy of transverse shear stresses and their sensitivity coefficients in multilayered composites p 1985 N95-26270
Sensitivity analysis of frictional contact response of axisymmetric composite structures p 1985 N95-26271
Recent advances in the sensitivity analysis for the thermomechanical postbuckling of composite panels p 1985 N95-26274
Reduction technique for tire contact problems p 1986 N95-26277
Sensitivity analysis for the dynamic response of thermoviscoplastic shells of revolution p 1986 N95-26278
Dynamic sensitivity analysis of frictional contact/impact response of axisymmetric composite structures p 1986 N95-26279
Sensitivity analysis for large-deflection and postbuckling responses on distributed-memory computers p 1987 N95-26281
SENSORS
The 1994 Fiber Optic Sensors for Aerospace Technology (FOSAT) Workshop
[NASA-CP-10166] p 1912 N95-24207
SEQUENCING
On producing sequential movements and actions. An integrative review and an update of the generalized motor program
[AD-A288628] p 2014 N95-25610
SERIES (MATHEMATICS)
Behavior of a trigonometric polynomial with given number of terms on small subsets of the unit circumference (norm duplication problem)
[PB95-165544] p 2028 N95-24321
Distribution of the error term for the number of lattice points inside a shifted ball
[PB95-165569] p 2029 N95-24325
SERIES EXPANSION
Heat Kernel expansion on a cone and quantum fields near cosmic strings
[DE94-628520] p 2094 N95-24507
On an expansion of the Fermi function
[DE94-628494] p 2035 N95-24883
Asymptotics for the Kummer function of Bose plasmas
[DE95-607019] p 2096 N95-25428
SERVICE LIFE
An overview of Health and Usage Monitoring Systems (HUMS) for military helicopters
[DSTO-TR-0061] p 1905 N95-24200
Helicopter life substantiation: Review of some USA and UK initiatives
[DSTO-TR-0062] p 1905 N95-24201
A review of rolling element bearing vibration detection, diagnosis and prognosis
[DSTO-RR-0013] p 1975 N95-24393
High gain GaAs Photoconductive Semiconductor Switches (PCSS): Device lifetime, high current testing, optical pulse generators
[DE95-003354] p 1957 N95-24488
Proceedings of the 2d USAF Aging Aircraft Conference
[AD-A288217] p 1911 N95-25578
PVD TBC experience on GE aircraft engines p 1944 N95-26126
SET THEORY
Uniform rectifiability and singular sets
[PB95-165502] p 2028 N95-24243
Behavior of a trigonometric polynomial with given number of terms on small subsets of the unit circumference (norm duplication problem)
[PB95-165544] p 2028 N95-24321
Intrinsic heights of stable varieties. Application to abelian varieties
[PB95-165577] p 2029 N95-24323
SHADOWS
Implementation of scene shadows in the Target Acquisition TDA (TARGAC)
[AD-A288760] p 1912 N95-26060
SHAFTS (MACHINE ELEMENTS)
Actively controlled shaft seals for aerospace applications
[NASA-CR-198035] p 1974 N95-24218
SHAPE FUNCTIONS
Geometric analysis of wing sections
[NASA-TM-110346] p 1910 N95-24629
SHAPE MEMORY ALLOYS
Rotary actuator
[NASA-CASE-MFS-28581-1] p 1936 N95-25545
SHAPES
Over-compression, a method to shape the longitudinal bunch distribution for a reduced energy spread
[DE95-006052] p 2066 N95-24572
SHEAR FLOW
A review of Reynolds stress models for turbulent shear flows
[NASA-CR-195054] p 1962 N95-24580
Evidence for modified transport due to sheared E x B flows in high-temperature plasmas
[DE95-004870] p 2079 N95-25250
Self-sustained turbulence and L-mode confinement in toroidal plasmas 2
[NIFS-278] p 2082 N95-25759
Method for determining shear direction using liquid crystal coatings
[NASA-CASE-ARC-11995-1] p 2075 N95-26117
SHEAR LAYERS
Effect of density gradients in confined supersonic shear layers, part 1
[NASA-CR-198029] p 1962 N95-24412
Effect of density gradients in confined supersonic shear layers. Part 2: 3-D modes
[NASA-CR-198030] p 1962 N95-24413
SHEAR STRENGTH
Recent progress in shear punch testing
[DE95-005962] p 1937 N95-26007
SHEAR STRESS
Effect of mesh distortion on the accuracy of transverse shear stresses and their sensitivity coefficients in multilayered composites p 1985 N95-26270
SHELL THEORY
Sensitivity analysis for the dynamic response of viscoplastic shells of revolution p 1984 N95-26268
SHELLS (STRUCTURAL FORMS)
Response to a localized impact loading of a composite multilayered rotational shell structure: Theory and numerical methods, volume 1
[ONERA-NT-1994-10-VOL-1] p 1979 N95-24282
Response to a localized impact loading of a composite multilayered rotational shell structure: Theory and numerical methods, volume 2
[ONERA-NT-1994-10-VOL-2] p 1980 N95-24283
Response to a localized impact loading of a composite multilayered rotational shell structure: Theory and numerical methods, Volume 3
[ONERA-NT-1994-10-VOL-3] p 1980 N95-24284
The transmission and control of vibrational power in a two stage isolation system with a water-loaded substructure
[ISVR-TR-235] p 1975 N95-24992
SHELTERS
Quantity-distance requirements for earth-bermed aircraft shelters
[AD-A279692] p 1915 N95-24424
SHIELDING
HZE beam transport in multilayered materials p 2060 N95-25922
SHOCK HEATING
The Superorbital Expansion Tube concept, experiment and analysis p 1915 N95-25399
SHOCK TESTS
BSM Delta Qualification 2, volume 2
[NASA-CR-196567] p 1922 N95-24844
Shock tunnel studies of scramjet phenomena 1993
[NASA-CR-195038] p 1964 N95-25394
The Superorbital Expansion Tube concept, experiment and analysis p 1915 N95-25399
SHOCK TUBES
The Superorbital Expansion Tube concept, experiment and analysis p 1915 N95-25399
SHOCK TUNNELS
Shock tunnel studies of scramjet phenomena 1993
[NASA-CR-195038] p 1964 N95-25394
Thrust measurements of a complete axisymmetric scramjet in an impulse facility p 1914 N95-25395
Scramjet thrust measurement in a shock tunnel p 1914 N95-25396
Scaling in a scramjet combustor p 1933 N95-25398
Balances for the measurement of multiple components of force in flows of a millisecond duration p 1965 N95-25400
SHOCK WAVE INTERACTION
A study of three-dimensional interaction flow fields between swept shock waves and turbulent boundary layers. Flow structures and effects of bleed
[NAL-TR-1227] p 1963 N95-25001
Numerical calculations of shock-wave/boundary-layer flow interactions
[NASA-TM-106694] p 1966 N95-26077
SHOCK WAVE PROFILES
Molecular dynamics simulation of a piston driven shock wave in a hard sphere gas
[NASA-CR-195463] p 2063 N95-25963
SHOCK WAVE PROPAGATION
Molecular dynamics simulation of a piston driven shock wave in a hard sphere gas
[NASA-CR-195463] p 2063 N95-25963
SHOCK WAVES
The critical diameter, detonation velocity and shock sensitivity of Australian PBXW-115
[DSTO-TR-0076] p 1947 N95-24394
Ignition of exploding aluminum droplets behind shock waves in water
[DE95-003975] p 1963 N95-24678

Decay of a laser generated shock wave in an aluminium target
[DE94-629014] p 1972 N95-24707
Shock tunnel studies of scramjet phenomena 1993
[NASA-CR-195038] p 1964 N95-25394
Scramjet thrust measurement in a shock tunnel
p 1914 N95-25396
Molecular dynamics simulation of a piston driven shock wave in a hard sphere gas
[NASA-CR-195463] p 2063 N95-25963

SHORT TAKEOFF AIRCRAFT
Flight reference display for powered-lift STOL aircraft
[NAL-TR-1251] p 1912 N95-25005
A quiet STOL Research Aircraft Development program
[NAL-TR-1223] p 1911 N95-25862

SHROUDS
TBC experience in land based gas turbines
p 1944 N95-26127

SIGNAL ANALYSIS
A computing program of sample magnetic moments recognition for SQUID-magnetometer measurements
[DE94-637073] p 2037 N95-24363
Techniques for the investigation of wave turbulence in water wave data
[AD-A288392] p 2007 N95-25605

SIGNAL ANALYZERS
ARMDAT: A brief description of a computerized test system for burst transmission
[PB95-165452] p 1951 N95-24241

SIGNAL DETECTION
Wave-propagation aspects on VHF-radar applications
[PB95-141818] p 1953 N95-24649
Analysis of data from a radar warning receiver with the accent on association of sensor reports
[PB95-141768] p 1953 N95-24836
Further ways to distinguish single-lepton top quark signals from background at the Tevatron
[PB95-165395] p 2056 N95-25567
Analysis of waveforms for bistatic radar systems
[PB95-165098] p 1955 N95-25641

SIGNAL DISTORTION
Unfolding of true distributions from experimental data distorted by detectors with finite resolutions
[DE94-628372] p 2035 N95-24643
Study on propagation impairments, distortions and unavailability on digital microwave links
[DE95-723047] p 1953 N95-24848

SIGNAL FADING
Study on propagation impairments, distortions and unavailability on digital microwave links
[DE95-723047] p 1953 N95-24848

SIGNAL MEASUREMENT
Techniques for the investigation of wave turbulence in water wave data
[AD-A288392] p 2007 N95-25605

SIGNAL PROCESSING
ARMDAT: A brief description of a computerized test system for burst transmission
[PB95-165452] p 1951 N95-24241
A review of rolling element bearing vibration detection, diagnosis and prognosis
[DSTO-RR-0013] p 1975 N95-24393
PC based analysis of gamma ray spectra generated by semiconductor detectors
[DE94-628381] p 1958 N95-24690
Multi-spectral smart retina
[AD-A288950] p 2074 N95-25506
Numerical and symbolic algorithms for application specific signal processing
[AD-A288202] p 2017 N95-25507
Proceedings of the 4th IEEE Workshop on Neural Networks for Signal Processing
[AD-A288383] p 2026 N95-25603
Techniques for the investigation of wave turbulence in water wave data
[AD-A288392] p 2007 N95-25605
Inversion of circular averages and application of backprojection methods to radar imaging
[PB95-141578] p 1955 N95-25891

SIGNAL TRANSMISSION
Application of optical fiber amplifier for wavelength division multiplexing communication system. Part 2: Design of four-channel transmission system using two EDFA repeaters
[DE95-730179] p 1952 N95-24491

SILICA GLASS
Reduction in fiber damage thresholds due to static fatigue
[DE95-004778] p 1979 N95-24263

SILICON
The facility for commercial doping of silicon by thermal neutrons in channel 3 at the IBR-2
[DE94-636293] p 2085 N95-24374
The measurement of the low frequency noise characteristics of the field effect transistors for cryogenic detectors
[DE94-628257] p 1957 N95-24487
ASIC implementation of a data-push architecture for silicon pixel readout
[DE95-003368] p 2015 N95-24648
The CDF silicon vertex detector SVX and its upgrades
[DE95-003743] p 2050 N95-24901
Double-sided silicon microstrip sensors for the CDF SVX 2 detector
[DE95-004235] p 2068 N95-25238
Back surface cell structures for reducing recombination in CZ silicon solar cells
[DE95-005423] p 1995 N95-25566
Non-destructive characterization of porous silicon using x ray reflectivity
[DE95-004766] p 1942 N95-25898
Raman study of damage processes in Si(+)-implanted GaAs
[DE95-005898] p 2091 N95-26087

SILICON ALLOYS
New techniques to test fatigue properties of coined sheet specimens. Part 2: Comparison of different materials, forming operations and life prediction techniques for a simple test geometry
[PB95-165122] p 1982 N95-25444

SILICON CARBIDES
Development of oxidation resistant SiC/C compositionally gradient materials
[DE94-785101] p 1925 N95-24365
Thermomechanical fatigue behavior of three CFCC's
[NASA-CR-195441] p 1927 N95-25880

SILICON DIOXIDE
A solubility model for amorphous silica in concentrated electrolytes
[DE95-004896] p 1931 N95-25252

SILICON FILMS
Reciprocal space analysis of the microstructure of luminescent and nonluminescent porous silicon films
[DE95-005420] p 1941 N95-25382

SILICON NITRIDES
Feasibility of ceramic joining with high energy electron beams
[DE95-004519] p 1940 N95-24717
Performance of solid lubricated ball bearings at high-temperatures in a vacuum
[NAL-TR-1243] p 1976 N95-25323
A statistical analysis of the effect of PECVD deposition parameters on surface and bulk recombination in silicon solar cells
[DE95-004780] p 1994 N95-25360

SILICON OXIDES
A statistical analysis of the effect of PECVD deposition parameters on surface and bulk recombination in silicon solar cells
[DE95-004780] p 1994 N95-25360

SILICONE RUBBER
Method for molding structural parts utilizing modified silicone rubber
[NASA-CASE-LAR-15217-1] p 1939 N95-24212

SILVER ALLOYS
NASA-UVa light aerospace alloy and structures technology program supplement: Aluminum-based materials for high speed aircraft
[NASA-CR-4645] p 1935 N95-24878

SIMD (COMPUTERS)
Implementation of a parallel unstructured Euler solver on the CM-5
[NASA-CR-195056] p 2032 N95-25106

SIMPLEX METHOD
On convergence of the Nelder-Mead simplex algorithm for unconstrained stochastic optimization
[AD-A289453] p 2006 N95-26197

SIMPLIFICATION
ASYS2: A new version of computer algebra package ASYS for analysis and simplification of polynomial systems
[DE94-628384] p 2030 N95-24691

SIMULATED ANNEALING
Clustering using winner-take-all units
[PB95-165403] p 2026 N95-25568

SIMULATORS
Evaluation of the performance of an annular diffusion denuder
[DE95-002258] p 1998 N95-24606

SINGLE CRYSTALS
The temperature and strain rate dependence of the flow stress of single crystal NiAl deformed along the zone group axes (110)
[DE95-003634] p 2083 N95-24233
One-step in-diffusion as a result of multipulse laser irradiation of LiNbO3 single-crystalline substrates covered with thin Ti deposits on the effect of the radiation wavelength
[DE94-634524] p 2084 N95-24324
Thermal diffuse scattering in time-of-flight neutron diffraction studied on SBN single crystals
[DE94-637054] p 2085 N95-24362
The facility for commercial doping of silicon by thermal neutrons in channel 3 at the IBR-2
[DE94-636293] p 2085 N95-24374
A photoemission study of the diamond and the single crystal C(60)
[DE95-006149] p 2085 N95-24463
High-energy ionoluminescence of LiF
[DE94-629015] p 2087 N95-24891
Temperature and dose dependence of metal colloid production in alpha-irradiated CaF2
[DE95-004907] p 2088 N95-25288
Reciprocal space analysis of the microstructure of luminescent and nonluminescent porous silicon films
[DE95-005420] p 1941 N95-25382
Oxidation of ion-implanted NiAl
[DE95-005899] p 1935 N95-25388

SINGLE STAGE TO ORBIT VEHICLES
The 1994 NASA/USRA/ADP Design Projects
[NASA-CR-197415] p 2101 N95-26304
Launch system design for access to space
p 1918 N95-26308
LH2 fuel tank design for SSTO p 1987 N95-26309
Feed system design for a reduced pressure tank
p 1923 N95-26310

SINGULARITY (MATHEMATICS)
Uniform rectifiability and singular sets
[PB95-165502] p 2028 N95-24243
Recent progress in one-loop multi-parton calculations
[DE95-006062] p 2092 N95-24328
A well-posed numerical method to track isolated conformal map singularities in Hele-Shaw flow
[NASA-CR-195035] p 2032 N95-25114

SINTERING
Preparation of stabilized zirconia (ZrO2) with ytteria (Y2O3) by simultaneous precipitation
[DE95-600163] p 1933 N95-24366
Processing of LaCrO3 for solid oxide fuel cell applications
[DE95-000024] p 1992 N95-24683

SIS (SEMICONDUCTORS)
A theoretical analysis of strain in GaN and its effects on carrier conductivity
[AD-A288769] p 2090 N95-26061

SIS (SUPERCONDUCTORS)
Device-quality tunnel junctions on the high (T(sub c)) super conductor HgBa2CuO(4+delta)
[DE95-004646] p 2084 N95-24279
BCS-like gap structure of HgBa2CuO(4+delta) tunnel junctions
[DE95-004125] p 2087 N95-24855

SKIN TEMPERATURE (BIOLOGY)
Thermal and vascular changes induced by the acclimation of the extremities to cold in man
[PB95-131587] p 2010 N95-24310

SKULL
Non-invasive detection of increased intracranial pressure using acoustical techniques
[AD-A279292] p 2010 N95-24309

SKY SURVEYS (ASTRONOMY)
A generic data exchange scheme between FITS format and C structures
[DE95-004849] p 2106 N95-25376
A survey of surveys
[DE95-004238] p 2111 N95-26284

SLEEP
Sleep patterns in air traffic controllers working rapidly rotating shifts: A field study
[DOT/FAA/AM-95/12] p 2012 N95-26204

SLIDING
Au/Cr sputter coating for the protection of alumina during sliding at high temperatures
[NASA-TM-106853] p 1923 N95-24437

SLOT ANTENNAS
Broadband uniplanar microstrip to slot-line transitions
[NASA-CR-195448] p 1957 N95-24476
Experimental study of tapered slot elements
[PB95-165163] p 1955 N95-25644

SLURRIES
Whisker reinforced glass ceramic
[DE95-005568] p 1927 N95-25998

SNOW
Assessment of climate variability of the Greenland ice sheet: Integration of in situ and satellite data
[NASA-CR-198020] p 1998 N95-24846

SODIUM CHLORIDES
Localized corrosion and stress corrosion cracking characteristics of a low-aluminum-content iron-aluminum alloy
[DE95-003259] p 1934 N95-24647

SODIUM COMPOUNDS
Effect of He pressure on the superconducting transition temperatures of Na2CsC60 and (NH3)4Na2CsC60
[DE95-006320] p 2087 N95-24616

Accurate determination of IC modulation parameter in Sr(x)Ba(1-x)Nb2O6 from second order satellites of neutron diffraction TOF (Time-Of-Flight) spectra
[DE94-629003] p 2090 N95-25851

SODIUM HYDROXIDES
Localized corrosion and stress corrosion cracking characteristics of a low-aluminum-content iron-aluminum alloy
[DE95-003259] p 1934 N95-24647

SODIUM ISOTOPES
Study of properties of Ne - Al neutron rich isotopes at and near N = 20 magic shell using elastic scattering in inverse kinematics
[DE94-628655] p 2055 N95-25538

SOFTWARE ENGINEERING
Software engineering and data management for automated payload experiment tool
[NASA-CR-196562] p 2104 N95-24477
Software engineering and data management for automated payload experiment tool
[NASA-CR-197703] p 2016 N95-24876
Software fault tolerance in computer operating systems
[NASA-CR-197999] p 2016 N95-24993
Proceedings of workshop on Future in HEP Computing
[DE94-792684] p 2021 N95-25303
Numerical and symbolic algorithms for application specific signal processing
[AD-A288202] p 2017 N95-25507
Quarterly update
[AD-A288743] p 2018 N95-26058
CMM functional software evaluation (algorithm qualification)
[DE95-006178] p 2018 N95-26167
Design documentation for the SINTRA preprocessor
[AD-A288804] p 2015 N95-26192

SOFTWARE RELIABILITY
Reliability analysis of software based safety functions
[DE95-606516] p 2018 N95-26045

SOFTWARE TOOLS
Software of a distributor of high voltage of the H C-600 hadronic calorimeter
[DE94-628255] p 1967 N95-24486
Users manual for KSP data-structure-neutral codes implementing Krylov space methods
[DE95-004265] p 2020 N95-24658
Software engineering and data management for automated payload experiment tool
[NASA-CR-197703] p 2016 N95-24876
Understanding and improving materials processing through interpreting and manipulating predictive models
[DE95-004384] p 1930 N95-25242
FTAPE: A fault injection tool to measure fault tolerance
[NASA-CR-198000] p 1978 N95-25333
A software tool to design thermal barrier coatings
p 1946 N95-26139

SOIL SAMPLING
Field-usable portable analyzer for chlorinated organic compounds
[DE95-003127] p 1930 N95-25098

SOILS
Use of mass spectrometric methods for field screening of VOC's
[DE95-004903] p 1999 N95-25249
Chelant extraction and REDOX manipulation for mobilization of heavy metals from contaminated soils
[DE95-004131] p 2000 N95-25363

SOL-GEL PROCESSES
Effects of acetylacetone additions on PZT thin film processing
[DE95-006322] p 1941 N95-25370

SOLAR ACTIVITY
Solar-geophysical data number 603, November 1994. Part 1: (Prompt reports). Data for October, September 1994, and late data
[PB95-166393] p 2113 N95-25576
Solar-geophysical data number 603, November 1994. Part 2: (Comprehensive reports). Data for May 1994 and miscellaneous
[PB95-166401] p 2113 N95-25577

SOLAR ARRAYS
Solar Eagle 2
[NASA-CR-198043] p 1990 N95-24199
Small spacecraft power and thermal subsystems
[NASA-CR-195029] p 1921 N95-24428
Technical evaluation of a dual-junction same-band-gap amorphous silicon photovoltaic system at NREL
[DE95-000277] p 1996 N95-26285

SOLAR CELLS
GaAsSb-based heterojunction tunnel diodes for tandem solar cell interconnects
[DE95-004779] p 1990 N95-24264
Preparatory research for global warming precaution spread promotion manual and early spread plan research work
[DE95-730143] p 1996 N95-24291
Use of advanced solar cells for commercial communication satellites
[NASA-TM-106879] p 1991 N95-24560
NREL Photovoltaic Program FY 1994 bibliography
[DE95-000275] p 1993 N95-24865
A statistical analysis of the effect of PECVD deposition parameters on surface and bulk recombination in silicon solar cells
[DE95-004780] p 1994 N95-25360
Back surface cell structures for reducing recombination in CZ silicon solar cells
[DE95-005423] p 1995 N95-25566

SOLAR COLLECTORS
Co-validation of three methods for optical characterization of point-focus concentrators
[DE95-001613] p 1992 N95-24674
Mirror alignment and focus of point-focus solar concentrators
[DE95-002609] p 1992 N95-24676
Felt-metal-wick heat-pipe solar receiver
[DE95-004535] p 1992 N95-24682
An examination of metal felt wicks for heat-pipe applications
[DE95-002608] p 1994 N95-25109
Comparison of three methods for optical characterization of point-focus concentrators
[DE95-000282] p 1994 N95-25309

SOLAR ENERGY
Solar Eagle 2
[NASA-CR-198043] p 1990 N95-24199
Overview of solar detoxification activities in the United States
[DE95-000264] p 1997 N95-24319
Appendix model performance: Model documentation. Renewable Fuels Module of the National Energy Modelling System
[DE95-006080] p 1991 N95-24355
Renewable Energy Demonstration Project by the National Renewable Energy Laboratory and the General Services Administration
[DE95-000261] p 1995 N95-25995
Field-portable reflectance spectrometer
[AD-A288750] p 1970 N95-26059

SOLAR FURNACES
Flux attenuation at NREL's High-Flux Solar Furnace
[DE95-000219] p 1993 N95-24715

SOLAR HEATING
The energy efficiency of passive solar heating systems
[IFTR-22/1994] p 1995 N95-25758

SOLAR MAGNETIC FIELD
Solar-geophysical data number 603, November 1994. Part 1: (Prompt reports). Data for October, September 1994, and late data
[PB95-166393] p 2113 N95-25576

SOLAR NEUTRINOS
Some remarks to the problem of neutrino oscillation
[DE94-628599] p 2048 N95-24669
DOE-High Energy Physics Contract with the University of Hawaii
[DE95-004214] p 2068 N95-24852
Update of GALLEX solar neutrino results and implications
[DE95-005005] p 2113 N95-25364

SOLAR OSCILLATIONS
Landau-Zener treatments of solar neutrino oscillations
[DE95-004761] p 2113 N95-24249

SOLAR PHYSICS
Solar-geophysical data number 603, November 1994. Part 1: (Prompt reports). Data for October, September 1994, and late data
[PB95-166393] p 2113 N95-25576
Solar-geophysical data number 603, November 1994. Part 2: (Comprehensive reports). Data for May 1994 and miscellaneous
[PB95-166401] p 2113 N95-25577

SOLAR POWERED AIRCRAFT
Long endurance stratospheric solar powered airship
[PB95-178729] p 1911 N95-26009

SOLAR RADIATION
Microphysical and compositional influences on shortwave radiative forcing of climate by sulfate aerosols
[DE95-005999] p 1997 N95-24570
Estimation and analysis of spectral solar radiation over Cairo
[DE95-606029] p 2113 N95-25986
Predicting the components of the total hemispherical solar radiation from sunshine duration measurements in Lagos, Nigeria
[DE95-606030] p 2113 N95-26042

SOLAR SIMULATORS
AMC EN-1038: Reduced scale solar simulator supplementary test report
[NASA-CR-197988] p 1915 N95-24380

SOLAR SYSTEM
Voyager: The grandest tour. The mission to the outer planets
[NASA-CR-197708] p 2112 N95-25854

SOLAR TERRESTRIAL INTERACTIONS
Solar-geophysical data number 603, November 1994. Part 1: (Prompt reports). Data for October, September 1994, and late data
[PB95-166393] p 2113 N95-25576
Solar-geophysical data number 603, November 1994. Part 2: (Comprehensive reports). Data for May 1994 and miscellaneous
[PB95-166401] p 2113 N95-25577

SOLAR THERMAL ELECTRIC POWER PLANTS
Solar thermal electric hybridization issues
[DE95-000217] p 1992 N95-24714

SOLAR THERMAL PROPULSION
Solar thermal electric hybridization issues
[DE95-000217] p 1992 N95-24714

SOLAR WIND
Geomagnetic Polar Cap (PC) index, 1975-1993
[UAG-103] p 2004 N95-24897
The whistler-mode bow wave of an asteroid
[U-OF-IOWA-95-2] p 2111 N95-26195

SOLAR WIND VELOCITY
Geomagnetic Polar Cap (PC) index, 1975-1993
[UAG-103] p 2004 N95-24897

SOLDERING
Assessing capillary flow on printed wiring board surfaces
[DE94-015768] p 1959 N95-24712
Capillary flow on narrow strips and in V-shaped grooves
[DE95-000543] p 1935 N95-24716

SOLDERS
Assessing capillary flow on printed wiring board surfaces
[DE94-015768] p 1959 N95-24712

SOLID ELECTROLYTES
Monolithic solid oxide fuel cell technology advancement for coal-based power generation
[DE94-012258] p 1990 N95-24318
Monolithic solid oxide fuel cell technology advancement for coal-based power generation
[DE95-006152] p 1991 N95-24425

SOLID LUBRICANTS
Au/Cr sputter coating for the protection of alumina during sliding at high temperatures
[NASA-TM-106853] p 1923 N95-24437
Performance of solid lubricated ball bearings at high-temperatures in a vacuum
[NAL-TR-1243] p 1976 N95-25323
Information compendium on solid film lubricants
[AD-A288360] p 1942 N95-25510
Improved lubrication performance of sputtered MoS2 film by surface treatments of Ti-alloy substrate
[NAL-TR-1213] p 1942 N95-25760
Applications of solid lubricant films in spacecraft
[AD-A288784] p 1947 N95-26188

SOLID MECHANICS
NASA-UVA light aerospace alloy and structures technology program (LA2ST)
[NASA-CR-198041] p 1933 N95-24220

SOLID PROPELLANT ROCKET ENGINES
Advanced multi-phase flow CFD model development for solid rocket motor flowfield analysis
[NASA-CR-198044] p 1923 N95-25103

SOLID ROCKET PROPELLANTS
Space shuttle propellant constitutive law verification tests
[NASA-CR-198047] p 1947 N95-24226

SOLID STATE
Solution based synthesis of perovskite-type oxide films and powders
[DE95-006170] p 2086 N95-24594

SOLID STATE LASERS
Diode laser pumped solid state laser with 2 micrometer wavelength
[PB95-165270] p 1973 N95-25622

SOLID STATE PHYSICS
Activities of the Solid State Division
[DE95-003900] p 2087 N95-24611

SOLID WASTES
Co-firing high sulfur coal with refuse derived fuels
[DE95-006243] p 1997 N95-24406
Chelant extraction and REDOX manipulation for mobilization of heavy metals from contaminated soils
[DE95-004131] p 2000 N95-25363

SOLIDIFICATION
Estimates of effects of residual acceleration on USML-1 experiments
[NASA-CR-197964] p 2084 N95-24261

AMCC casting development, volume 2
[NASA-CR-197720] p 1938 N95-26068
SOLIDS
On the effects of gravitational fields on the electrical properties of matter
[DE95-607022] p 2038 N95-25430
SOLITARY WAVES
The geometry of weak solutions of certain integrable nonlinar PDE's
[DE95-005241] p 2030 N95-24609
Recoil effects in quantum topological solitons
[DE95-607006] p 2097 N95-25454
On Segal-Wilson's construction for the (tau)-functions of the constrained KP hierarchies
[DE95-606999] p 2100 N95-25988
SOLUBILITY
A solubility model for amorphous silica in concentrated electrolytes
[DE95-004896] p 1931 N95-25252
Dynamic methods for determining the material characteristics of saturated permeable media
[IFTR-17/1993] p 1932 N95-26107
SOLVENT EXTRACTION
Determination of trace elements in plutonium by solvent extraction and ICP-atomic emission spectrometry
[DE94-634887] p 2042 N95-24269
SOLVENTS
Brayton-cycle solvent recovery heat pump. A technical brief
[DE94-000225] p 1991 N95-24666
The evaluation of potential limonene scavengers
[DE95-006853] p 2002 N95-25899
SOOT
The effect of altitude conditions on the particle emissions of a J85-GE-5L turbojet engine
[NASA-TM-106669] p 1914 N95-24561
SORBENTS
Cross-flow, filter-sorbent-catalyst for particulate, SO2 and NO(x) control
[DE95-001934] p 2003 N95-26091
SORTING ALGORITHMS
Faster magnet sorting with a threshold acceptance algorithm
[DE95-006487] p 2038 N95-25408
SOUND PRESSURE
The phenomenon of non-linearity accompanying the action of acoustic pressure on a Helmholtz resonator
[IFTR-19/1994] p 2040 N95-26108
SOUND TRANSMISSION
Atmospheric and terrain effects on acoustic propagation
[AD-A288727] p 2039 N95-25503
SOUND WAVES
3-D seismic imaging of complex geologies
[DE95-006813] p 2004 N95-25476
SOVIET SATELLITES
JPRS report: Science and technology. Central Eurasia: Space
[JPRS-USP-94-007] p 1915 N95-24358
SPACE ADAPTATION SYNDROME
Relation of motion sickness susceptibility to vestibular and behavioral measures of orientation
[NASA-CR-198048] p 2010 N95-24410
SPACE CHARGE
Emittance growth caused by nonuniform charge distribution of bunched beam in linac
[DE95-602121] p 2072 N95-26095
SPACE COMMERCIALIZATION
Assessment of Commercial Satellite Communications Initiative (CSCI) studies
[AD-A288357] p 1920 N95-25508
Commercial Space Transportation Study (CSTS)
[SSD94D0035] p 1919 N95-25747
SPACE COMMUNICATION
Optical space communication: An overview
[DE94-634314] p 1952 N95-24403
Facility for the evaluation of space communications and related systems
[NASA-TM-106904] p 1955 N95-25876
SPACE DEBRIS
The natural space environment: Effects on spacecraft
[NASA-RP-1350] p 1921 N95-25875
SPACE EXPLORATION
Go for EVA
[NASA-TM-110537] p 1918 N95-24195
Space basic
[NASA-TM-110540] p 2108 N95-24196
NASA video catalog
[NASA-SP-7109(01)] p 2103 N95-24238
Perspectives from space: NASA classroom information and activities
[NASA-TM-110577] p 2100 N95-25643
Fourth symposium of the geological survey of Japan on remote sensing of satellite geology
[PB95-178737] p 1917 N95-25750
SPACE HEATING (BUILDINGS)
The fundamentals of modelling heat and moisture processes in structures
[IFTR-15/1994] p 1951 N95-26109
SPACE INDUSTRIALIZATION
Commercial Space Transportation Study (CSTS)
[SSD94D0035] p 1919 N95-25747
SPACE LAW
ESA Bulletin No. 81 p 2114 N95-25200
SPACE MISSIONS
Apollo 13: Houston, we've got a problem
[NASA-TM-110551] p 1918 N95-24215
The scientific programme between ESRO and ESA: Choosing new projects (1973-1977)
[ESA-HSR-16] p 1917 N95-24896
Return to the red planet: The Mars Observer Mission
[NASA-CR-197707] p 2113 N95-26336
SPACE OBSERVATIONS (FROM EARTH)
Milagro: A low energy threshold extensive air shower array
[DE95-005246] p 2110 N95-25675
SPACE PLASMAS
Fluctuations and electromagnetic wave scattering in macroscopically agitated plasma: Effects of turbulent diffusion
[DE95-607612] p 2081 N95-25617
The natural space environment: Effects on spacecraft
[NASA-RP-1350] p 1921 N95-25875
SPACE POWER REACTORS
The potential of vacuum microelectronics for space reactor applications
[DE95-000542] p 1958 N95-24586
An overview of the Nuclear Electric Propulsion Space Test Program (NEPSTP) satellite
[DE94-013121] p 1920 N95-24711
SPACE PROCESSING
Estimates of effects of residual acceleration on USML-1 experiments
[NASA-CR-197964] p 2084 N95-24261
Development of optical systems --- holographic technique for monitoring crystal growth
[NASA-CR-197702] p 2073 N95-24545
JPRS report: Science and technology. Central Eurasia: Seminar on materials science
[JPRS-UST-95-007] p 1920 N95-24761
SPACE PROGRAMS
Space basic
[NASA-TM-110540] p 2108 N95-24196
Issues in NASA program and project management
[NASA-SP-6101(08)] p 2102 N95-24565
The origins of the Federal Republic of Germany's space policy, 1959-1965: European and national dimensions
[ESA-HSR-12] p 1916 N95-24892
SPACE SHUTTLE BOOSTERS
BSM Delta qualification 2, volume 1
[NASA-CR-196566-VOL-1] p 1921 N95-24440
Debris/ice/TPS assessment and integrated photographic analysis of shuttle mission STS-63
[NASA-TM-110649] p 1921 N95-25337
STS-60 Space Shuttle mission report
[NASA-CR-197233] p 1919 N95-26189
SPACE SHUTTLE MAIN ENGINE
Automation based on knowledge modeling theory and its applications in engine diagnostic systems using Space Shuttle Main Engine vibrational data
[NASA-CR-197983] p 1922 N95-24626
STS-60 Space Shuttle mission report
[NASA-CR-197233] p 1919 N95-26189
SPACE SHUTTLE MISSIONS
STS-66 mission highlights resource tape
[NASA-TM-110550] p 1918 N95-24197
STS-67 post flight presentation
[NASA-TM-110552] p 1918 N95-24198
USF/Russian dosimetry on STS-57
p 2059 N95-25915
Dosimetry on STS-42 with the RME APD
p 2059 N95-25916
The spacelab scientific missions: A comprehensive bibliography of scientific publications
[NASA-TM-108487] p 2107 N95-26084
SPACE SHUTTLE ORBITERS
Performance of an aerodynamic yaw controller mounted on the space shuttle orbiter body flap at Mach 10
[NASA-TM-109179] p 1906 N95-24397
Predictability in space launch vehicle anomaly detection using intelligent neuro-fuzzy systems
p 2025 N95-25266
A study of the radiation environment on board the space shuttle flight STS-57 p 2059 N95-25914
USF/Russian dosimetry on STS-57
p 2059 N95-25915
STS-60 Space Shuttle mission report
[NASA-CR-197233] p 1919 N95-26189
SPACE SHUTTLE PAYLOADS
Go for EVA
[NASA-TM-110537] p 1918 N95-24195
STS-67 post flight presentation
[NASA-TM-110552] p 1918 N95-24198
Software engineering and data management for automated payload experiment tool
[NASA-CR-197703] p 2016 N95-24876
STS-60 Space Shuttle mission report
[NASA-CR-197233] p 1919 N95-26189
Automated protein crystal growth facility
p 1918 N95-26306
SPACE SHUTTLES
Space basic
[NASA-TM-110540] p 2108 N95-24196
STS-66 mission highlights resource tape
[NASA-TM-110550] p 1918 N95-24197
Space shuttle propellant constitutive law verification tests
[NASA-CR-198047] p 1947 N95-24226
Report of the Space Shuttle Management Independent Review Team
[NASA-TM-110579] p 1919 N95-24466
Aerospace safety advisory panel
[NASA-TM-110554] p 1920 N95-24505
STS-63 mission highlights resource tape
[NASA-TM-110562] p 1919 N95-25874
STS-60 Space Shuttle mission report
[NASA-CR-197233] p 1919 N95-26189
SPACE STATION FREEDOM
Universal Test Facility p 1918 N95-26305
Automated protein crystal growth facility
p 1918 N95-26306
SPACE STATIONS
Shuttle to space station transfer of the materials exposure facility
[NASA-TM-110156] p 1919 N95-24765
JPRS report: Science and technology. Central Eurasia: Space
[JPRS-USP-94-008] p 1916 N95-24847
SPACE TRANSPORTATION
Shuttle to space station transfer of the materials exposure facility
[NASA-TM-110156] p 1919 N95-24765
Commercial Space Transportation Study (CSTS)
[SSD94D0035] p 1919 N95-25747
SPACE TRANSPORTATION SYSTEM
Study of launch site processing and facilities for future launch vehicles
[NASA-CR-198025] p 1918 N95-24579
SPACE TRANSPORTATION SYSTEM FLIGHTS
STS-66 mission highlights resource tape
[NASA-TM-110550] p 1918 N95-24197
STS-67 post flight presentation
[NASA-TM-110552] p 1918 N95-24198
STS-63 mission highlights resource tape
[NASA-TM-110562] p 1919 N95-25874
A study of the radiation environment on board the space shuttle flight STS-57 p 2059 N95-25914
STS-60 Space Shuttle mission report
[NASA-CR-197233] p 1919 N95-26189
SPACE-TIME FUNCTIONS
On squaring the primary constraints in a generalized Hamiltonian dynamics
[DE94-628500] p 2036 N95-24504
Decoherence, determinism and chaos revisited
[DE95-006070] p 2094 N95-24578
Creation and development of the Universe (symmetry approach)
[DE94-628558] p 2109 N95-24884
A covariant canonical description of Liouville field theory
[DE95-607094] p 2098 N95-25534
The space of solutions of Toda field theory
[DE95-607095] p 2099 N95-25650
SPACEBORNE ASTRONOMY
STS-67 post flight presentation
[NASA-TM-110552] p 1918 N95-24198
SPACEBORNE EXPERIMENTS
Go for EVA
[NASA-TM-110537] p 1918 N95-24195
STS-66 mission highlights resource tape
[NASA-TM-110550] p 1918 N95-24197
STS-67 post flight presentation
[NASA-TM-110552] p 1918 N95-24198
Electrophoretic separation of cells and particles from rat pituitary --- analysis of pituitary cell electrophoresis experiment done on IML-2 (7/94)
[NASA-CR-197975] p 2008 N95-24475
Software engineering and data management for automated payload experiment tool
[NASA-TM-196562] p 2104 N95-24477
A study of the radiation environment on board the space shuttle flight STS-57 p 2059 N95-25914
Radiobiological experiments with plant seeds aboard the biosatellite Cosmos 1887 p 2009 N95-25933
STEP: Satellite Test of the Equivalence Principle. Report on the phase A study
[NASA-TM-110598] p 1917 N95-26184

Universal Test Facility p 1918 N95-26305
Automated protein crystal growth facility p 1918 N95-26306
Stiffening of the ACES deployable space boom p 1978 N95-26307
Return to the red planet: The Mars Observer Mission [NASA-CR-197707] p 2113 N95-26336

SPACEBORNE TELESCOPES
STS-66 mission highlights resource tape [NASA-TM-110550] p 1918 N95-24197

SPACECRAFT
Space basic [NASA-TM-110540] p 2108 N95-24196
Computer support for cooperative tasks in Mission Operations Centers [DE95-004928] p 2102 N95-25771

SPACECRAFT COMPONENTS
Small spacecraft power and thermal subsystems [NASA-CR-195029] p 1921 N95-24216
Computer support for cooperative tasks in Mission Operations Centers [DE95-004928] p 2102 N95-25771

SPACECRAFT CONSTRUCTION MATERIALS
Composite materials flown on the Long Duration Exposure Facility [NASA-CR-4657] p 1923 N95-24583
Shuttle to space station transfer of the materials exposure facility [NASA-TM-110156] p 1919 N95-24765
Long Duration Exposure Facility mini-data base user's guide: IBM-compatible PC computer version [NASA-CR-4655] p 1925 N95-26072

SPACECRAFT CONTROL
Performance of an aerodynamic yaw controller mounted on the space shuttle orbiter body flap at Mach 10 [NASA-TM-109179] p 1906 N95-24397

SPACECRAFT DESIGN
Small spacecraft power and thermal subsystems [NASA-CR-195029] p 1921 N95-24216
An overview of the Nuclear Electric Propulsion Space Test Program (NEPSTP) satellite [DE94-013121] p 1920 N95-24711
The natural space environment: Effects on spacecraft [NASA-RP-1350] p 1921 N95-25875
The 1994 NASA/USRA/ADP Design Projects [NASA-CR-197415] p 2101 N95-26304
Launch system design for access to space p 1918 N95-26308

SPACECRAFT ENVIRONMENTS
STS-63 mission highlights resource tape [NASA-TM-110562] p 1919 N95-25874
A study of the radiation environment on board the space shuttle flight STS-57 p 2059 N95-25914
USF/Russian dosimetry on STS-57 p 2059 N95-25915

SPACECRAFT GUIDANCE
Optimal guidance law development for an advanced launch system [NASA-CR-4667] p 1917 N95-26205

SPACECRAFT INSTRUMENTS
The Clementine Mission: Initial Results from lunar mapping [NASA-TM-110555] p 2112 N95-24994

SPACECRAFT LAUNCHING
Space basic [NASA-TM-110540] p 2108 N95-24196
STS-66 mission highlights resource tape [NASA-TM-110550] p 1918 N95-24197
Study of launch site processing and facilities for future launch vehicles [NASA-CR-198025] p 1918 N95-24579
Debris/ice/TPS assessment and integrated photographic analysis of shuttle mission STS-63 [NASA-TM-110649] p 1921 N95-25337
STS-63 mission highlights resource tape [NASA-TM-110562] p 1919 N95-25874
Launch system design for access to space p 1918 N95-26308

SPACECRAFT MAINTENANCE
Go for EVA [NASA-TM-110537] p 1918 N95-24195

SPACECRAFT ORBITS
Space basic [NASA-TM-110540] p 2108 N95-24196
STS-66 mission highlights resource tape [NASA-TM-110550] p 1918 N95-24197
JPRS report: Science and technology. Central Eurasia: Space [JPRS-USP-94-008] p 1916 N95-24359
Linear Energy Transfer (LET) spectra of cosmic radiation in low Earth orbit p 2061 N95-25926
Differential neutron energy spectra measured on spacecraft low Earth orbit p 2062 N95-25932

SPACECRAFT POWER SUPPLIES
Small spacecraft power and thermal subsystems [NASA-CR-195029] p 1921 N95-24216
Small spacecraft power and thermal subsystems [NASA-CR-195029] p 1921 N95-24428
Use of advanced solar cells for commercial communication satellites [NASA-TM-106879] p 1991 N95-24560

SPACECRAFT REENTRY
The Superorbital Expansion Tube concept, experiment and analysis p 1915 N95-25399

SPACECRAFT SHIELDING
Debris/ice/TPS assessment and integrated photographic analysis of shuttle mission STS-63 [NASA-TM-110649] p 1921 N95-25337

SPACECRAFT STRUCTURES
Efficient eigenvalue assignment by state and output feedback with applications for large space structures [NASA-TM-110155] p 1920 N95-24581

SPACELAB
The spacelab scientific missions: A comprehensive bibliography of scientific publications [NASA-TM-108487] p 2107 N95-26084

SPACING
Reciprocal space analysis of the microstructure of luminescent and nonluminescent porous silicon films [DE95-005420] p 1941 N95-25382

SPALLING
Thermal barrier coating life modeling in aircraft gas turbine engines p 1947 N95-26140

SPARK IGNITION
Draft regulatory impact analysis: Control of air pollution emission standards for new nonroad spark-ignition marine engines [PB95-166294] p 2001 N95-25575

SPARKS
Evolution of Spark plasma using nitrogen laser shadowgraphy system [DE95-607598] p 2082 N95-25972

SPATIAL DISTRIBUTION
Temporal pacing in visual attention [AD-A289785] p 2013 N95-26041
Distribution and nature of UV absorbers on Trition's surface [NASA-CR-198008] p 2112 N95-26116

SPATIAL RESOLUTION
Unfolding of true distributions from experimental data distorted by detectors with finite resolutions [DE94-628372] p 2035 N95-24643

SPECIFIC HEAT
Statistical mechanics of the magnetized pair Bose gas [DE95-607096] p 2063 N95-25993

SPECIFIC IMPULSE
Combustion characteristics of metallized hydrocarbon fuels [NAL-TR-1224] p 1949 N95-25769

SPECKLE HOLOGRAPHY
Development of optical systems --- holographic technique for monitoring crystal growth [NASA-CR-197702] p 2073 N95-24545

SPECKLE INTERFEROMETRY
Residual Stress Measurements with Laser Speckle Correlation Interferometry and Local Heat Treating [DE95-060082] p 1981 N95-24598

SPECKLE PATTERNS
Residual Stress Measurements with Laser Speckle Correlation Interferometry and Local Heat Treating [DE95-060082] p 1981 N95-24598

SPECTRA
Spectrum and energy transfer in steady Burgers turbulence [NASA-CR-195047] p 1963 N95-24584
Estimation and analysis of spectral solar radiation over Cairo [DE95-606029] p 2113 N95-25986

SPECTRAL BANDS
Estimation and analysis of spectral solar radiation over Cairo [DE95-606029] p 2113 N95-25986
Multispectral detection of ground targets in highly correlated backgrounds [AD-A289292] p 1990 N95-26040

SPECTRAL CORRELATION
Multispectral detection of ground targets in highly correlated backgrounds [AD-A289292] p 1990 N95-26040

SPECTRAL EMISSION
Gamma-ray emission from globular clusters. Shock high energy emission from the Be-Star/Pulsar System PSR 1259-63. Echoes in x-ray novae [NASA-CR-197994] p 2114 N95-24381

SPECTRAL METHODS
Linear non-modal phenomena in numerical analysis and applied mathematics [DE95-005495] p 2029 N95-24458
A conservative staggered-grid Chebyshev multidomain method for compressible flows [NASA-CR-195060] p 2030 N95-24632

SPECTRAL REFLECTANCE
Method for determining shear direction using liquid crystal coatings [NASA-CASE-ARC-11995-1] p 2075 N95-26117

SPECTRAL RESOLUTION
Field-portable reflectance spectrometer [AD-A288750] p 1970 N95-26059
Average cosine meter and high spectral resolution measurements at the marine light mixed layer site [AD-A288713] p 1970 N95-26113

SPECTRAL SIGNATURES
A search for t(anti t) (yields) lepton + E(sub T) + jets signature in p(anti p) collisions at (radical)s = 1.8 TeV with the DO detector [DE95-004239] p 2052 N95-25402

SPECTROGRAMS
Dynamics Explorer 1, retarding ion mass spectrometer summary spectrograms-82/110 to 82/229 spin-time spectrograms for H(+), He(+), O(+), N(+), O(++), M/Z = 2, and molecular ions [NASA-TM-108485] p 2003 N95-24763
Dynamics Explorer 1, retarding ion mass spectrometer summary spectrograms-82/230 to 82/285 spin-time spectrograms for H(+), He(+), O(+), N(+), O(++), M/Z = 2, and molecular ions [NASA-TM-108486] p 2003 N95-24764

SPECTROMETERS
Recipes for high resolution time-of-flight detectors [DE95-006196] p 1967 N95-24596
Absolute calibration and monitoring of a spectrometric channel using a photomultiplier [DE94-628251] p 1968 N95-24635
HET mini-manual [PB95-165338] p 2057 N95-25900

SPECTRORADIOMETERS
Field-portable reflectance spectrometer [AD-A288750] p 1970 N95-26059

SPECTROSCOPIC ANALYSIS
Determination of trace elements in plutonium by solvent extraction and ICP-atomic emission spectrometry [DE94-634887] p 2042 N95-24269
Thermal and vascular changes induced by the acclimation of the extremities to cold in man [PB95-131587] p 2010 N95-24310

SPECTROSCOPY
Baryon spectroscopy and the omega minus [DE95-004838] p 2052 N95-25374
High LET, passive space radiation dosimetry and spectrometry [NASA-CR-197694] p 2058 N95-25911

SPECTRUM ANALYSIS
Expert system for nuclide identification in gamma spectrum analysis [PB95-149712] p 2042 N95-24297
Gamma spectrum analysis including NAA with SAMPO for windows [PB95-149720] p 2042 N95-24298
Structure of liquid He-4 excitations spectrum [DE94-637113] p 2043 N95-24364
PC based analysis of gamma ray spectra generated by semiconductor detectors [DE94-628381] p 1958 N95-24690
Accurate determination of IC modulation parameter in Sr(x)Ba(1-x)Nb2O6 from second order satellites of neutron diffraction TOF (Time-Of-Flight) spectra [DE94-629003] p 2090 N95-25851
LET spectra measurements from the STS-35 CPDs p 2058 N95-25912
Distribution and nature of UV absorbers on Trition's surface [NASA-CR-198008] p 2112 N95-26116

SPEECH
Dialogue transcription tools [TN-94-1] p 2016 N95-24536
Automatic classification of Polish fricatives on the basis of optimization of the parameter space [IFTR-9/1994] p 1956 N95-26331

SPEECH RECOGNITION
How Captain Amerika uses neural networks to fight crime p 2025 N95-25272
A study of the effect of voice pitch on the perception of synthetic Polish vowels [IFTR-10/1994] p 1956 N95-26018
Automatic classification of Polish fricatives on the basis of optimization of the parameter space [IFTR-9/1994] p 1956 N95-26331

SPEED INDICATORS
Flight reference display for powered-lift STOL aircraft [NAL-TR-1251] p 1912 N95-25005

SPHERICAL COORDINATES
On a generalized Kepler-Coulomb system: Inter basis expansions [DE94-636739] p 2093 N95-24349

SPHERICAL WAVES
Generalization of the Rayleigh formula to the model with ring-shaped potentials
[DE94-628578] p 2094 N95-24637
SPHEROIDS
On a generalized Kepler-Coulomb system: Inter basis expansions
[DE94-636739] p 2093 N95-24349
Oscillator poly spheroidal functions
[DE94-628440] p 2030 N95-24636
SPIN
On a new type of long-range forces
[DE95-605286] p 2063 N95-25965
SPIN DYNAMICS
Proton-proton interactions using the RHIC polarized collider
[DE95-005839] p 2043 N95-24326
Toroidal response in magnetic resonance
[DE94-628406] p 2037 N95-24696
Statistical mechanics of relativistic spin-1 bosons in a magnetic field
[DE95-607100] p 2054 N95-25474
On exotic supersymmetries of the Phi(1,3) deformation of minimal models
[DE95-607088] p 2033 N95-25532
SPIN TESTS
Spin structure of the nucleon and polarization
[DE95-004282] p 2047 N95-24662
SPIN-SPIN COUPLING
Tau as a probe for new physics
[DE95-005928] p 2051 N95-25296
SPINDLES
Development of a fast response rotating polarimeter for a Faraday rotation measurement
[DE94-777532] p 2075 N95-24271
SPINOR GROUPS
The lattice spinor QED Hamiltonian critique of the continuous space approach
[DE94-628521] p 2094 N95-24508
Covariant single-time equations for a system of N spinor particles
[DE94-628587] p 2047 N95-24640
SPLINE FUNCTIONS
Hierarchical Control and Trajectory Planning
[NASA-CR-197922] p 2026 N95-25801
Splines and control theory p 2026 N95-25802
Control theory and splines, applied to signature storage p 2027 N95-25804
SPLINES
How to fly an aircraft with control theory and splines
p 2027 N95-25805
Splines in two-dimensional problems
[IFTR-2/1993] p 2035 N95-26106
SPRAY CHARACTERISTICS
Spray characteristics of single- and three-hole nozzle injectors in ambient air and in a motored single-cylinder test engine
[PB95-166286] p 1976 N95-25574
SPRAYED COATINGS
JPRS report: Science and technology. Central Eurasia
[JPRS-UST-95-011] p 1910 N95-24541
Magnetically controlled deposition of metals using gas plasma
[DE95-003827] p 2077 N95-24552
Properties of plasma sprayed bond coats
p 1946 N95-26135
Thick thermal barrier coatings for diesel engines
p 1946 N95-26136
SPRAYING
Measurement methods and standards for processing and application of thermal barrier coatings
p 1944 N95-26123
SPRINGS (WATER)
Long-Term Flow Test number 1: Roosevelt Hot Springs, Utah
[DE95-004995] p 2004 N95-25666
SQUID (DETECTORS)
A computing program of sample magnetic moments recognition for SQUID-magnetometer measurements
[DE94-637073] p 2037 N95-24363
Testing quantum behaviour at the macroscopic level
[DE95-607005] p 2097 N95-25453
STABILITY
Optical instabilities and chaos due to the virtual formation of biexcitons
[DE95-607664] p 2063 N95-25994
Describing the macroscopic world: Closing the circle within the dynamical reduction program
[DE95-606997] p 2100 N95-26046
STABILITY TESTS
Optical instabilities and chaos due to the virtual formation of biexcitons
[DE95-607664] p 2063 N95-25994
STABILIZATION
Tutorial on beam-based feedback systems for linacs
[DE95-006054] p 2067 N95-24573
STAGE SEPARATION
BSM Delta qualification 2, volume 1
[NASA-CR-196566-VOL-1] p 1921 N95-24440
STAINLESS STEELS
Temperature and strain-rate effects on deformation mechanisms in irradiated stainless steel
[DE95-004941] p 1934 N95-24449
Characterizing pre-polished Type 304L stainless steel
[DE95-001241] p 1934 N95-24480
Stainless steel recycle
[DE95-003905] p 1934 N95-24615
Localized corrosion and stress corrosion cracking characteristics of a low-aluminum-content iron-aluminum alloy
[DE95-003259] p 1934 N95-24647
Cobalt release from PCA steel during possible fusion reactor accidents
[DE95-005019] p 2069 N95-25365
Evaluation of a diffusion/trapping model for hydrogen ingress in high-strength alloys
[AD-A288447] p 1936 N95-25502
Atom probe field ion microscopy of Type 308 CRE stainless steel welds
[DE94-019161] p 1938 N95-26064
STANDARD MODEL (PARTICLE PHYSICS)
Neutrino masses and b - tau unification in the supersymmetric standard model
[DE94-634361] p 2043 N95-24404
Z flux-line lattices and self-dual equations in the standard model
[DE94-634364] p 2093 N95-24405
Probing anomalous gauge boson couplings at LEP
[DE95-005934] p 2044 N95-24420
Chiral symmetry on the lattice
[DE95-003962] p 2087 N95-24849
Meson properties at finite temperature and density within Nambu-Jona-Lasinio model
[DE94-628630] p 2049 N95-24888
Vortex solutions in two-Higgs-doublet systems
[DE94-634363] p 2096 N95-25107
R parity in standard-like superstring models
[DE94-628531] p 2096 N95-25215
Extended gauge sectors
[DE95-006485] p 2052 N95-25407
A partial unification model in non-commutative geometry
[DE95-607129] p 2097 N95-25435
Anomalous WWZ couplings and K(sub L) yields mu(+) mu(-)
[DE95-607190] p 2054 N95-25464
Electroweak coupling measurements from polarized Bhabha scattering at the Z(exp 0) resonance
[DE95-006090] p 2057 N95-25768
STANDARDIZATION
Standardization of equations for radiochemical calculations
[DE95-003028] p 1930 N95-25097
Resolving the ambiguities: An industrial hygiene Indoor Air Quality (IAQ) symposium
[DE95-005391] p 2000 N95-25380
STANDARDS
Metrology measurement capability
[DE95-005411] p 1969 N95-25381
Draft regulatory impact analysis: Control of air pollution emission standards for new nonroad spark-ignition marine engines
[PB95-166294] p 2001 N95-25575
STATIC AERODYNAMIC CHARACTERISTICS
Measurements of longitudinal static aerodynamic coefficients by the cable mount system
[NAL-TR-1226] p 1908 N95-25761
STATIC FIRING
BSM Delta qualification 2, volume 1
[NASA-CR-196566-VOL-1] p 1921 N95-24440
STATIC FRICTION
Sensitivity analysis of frictional contact response of axisymmetric composite structures p 1985 N95-26271
Dynamic sensitivity analysis of frictional contact/impact response of axisymmetric composite structures
p 1986 N95-26279
STATIC TESTS
Analysis of warping effects on the static and dynamic response of a seat-type structure
[NIAR-94-12] p 1979 N95-24211
Static and fatigue properties of pin-joint specimens of a AS-4/PEEK thermoplastic composite material
[NAL-TR-1214] p 1927 N95-25859
STATICS
Static recrystallization behavior of austenite in HSLA 100 during Thermomechanical Controlled Processing (TMCP)
[AD-A288737] p 1937 N95-26057
STATISTICAL ANALYSIS
Geomagnetic Polar Cap (PC) index, 1975-1993
[UAG-103] p 2004 N95-24897
Report series in aerosol science
[DE95-737628] p 1999 N95-24904
A technique for the evaluation of strength of coupling between SEA subsystems
[ISVR-TR-241] p 1981 N95-24997
A statistical analysis of the effect of PECVD deposition parameters on surface and bulk recombination in silicon solar cells
[DE95-004780] p 1994 N95-25360
STATISTICAL DISTRIBUTIONS
Introduction to the Monte Carlo methods
[DE94-628386] p 2035 N95-24693
Flare stars and Pascal distribution
[DE95-607044] p 2110 N95-25431
STATISTICAL MECHANICS
Quantum group and quantum symmetry
[DE94-634329] p 2095 N95-24767
Statistical mechanics of nonlinear coherent structures: Kinks in the Phi(sup 6) model
[DE95-005253] p 2096 N95-25293
Statistical mechanics of relativistic spin-1 bosons in a magnetic field
[DE95-607100] p 2054 N95-25474
Physics in Ukraine International Conference. Volume 3: Statistical physics and phase transitions
[DE95-605765] p 2038 N95-25552
A pseudo-sound constitutive relationship for the dilatational covariances in compressible turbulence: An analytical theory
[NASA-CR-195064] p 1966 N95-25964
Statistical mechanics of magnetized pair Fermi gas
[DE95-607097] p 2063 N95-25969
Statistical mechanics of the magnetized pair Bose gas
[DE95-607096] p 2063 N95-25993
Magnetized pair Bose gas: Relativistic superconductor
[DE95-607846] p 2100 N95-26104
STEADY STATE
Experimental and theoretical basis for advanced tokamaks
[DE95-003255] p 2077 N95-24646
Divertor design for the Tokamak Physics Experiment
[DE95-003653] p 2078 N95-24650
Multigrid solution strategies for adaptive meshing problems
[NASA-CR-195049] p 2031 N95-24857
Tunable vibration absorbers: Key design parameters
[ISVR-TR-244] p 1981 N95-24995
Optical instabilities and chaos due to the virtual formation of biexcitons
[DE95-607664] p 2063 N95-25994
STEAM FLOW
Coso Monitoring Program, October 1992 through September 1993
[AD-A279147] p 1989 N95-24422
STEELS
JPRS report: Science and technology. Central Eurasia
[JPRS-UST-95-011] p 1910 N95-24541
The corrosion protection of AISI(TM) 1010 steel by organic and inorganic zinc-rich primers
[NASA-TP-3545] p 1936 N95-25677
Static recrystallization behavior of austenite in HSLA 100 during Thermomechanical Controlled Processing (TMCP)
[AD-A288737] p 1937 N95-26057
Changes in the strength characteristics of 15HM boiler steel caused by initial plastic deformation under constant and monotonic loads
[IFTR-30/1994] p 1938 N95-26333
STELLAR ACTIVITY
Research in nuclear astrophysics: Stellar collapse and supernovae
[DE95-004300] p 2110 N95-25343
STELLAR EVOLUTION
Resolution of the classical Hyades lithium problem
[DE95-003661] p 2109 N95-24234
Research in nuclear astrophysics: Stellar collapse and supernovae
[DE95-004300] p 2110 N95-25343
STELLAR FLARES
Flare stars and Pascal distribution
[DE95-607044] p 2110 N95-25431
STELLAR SPECTRA
ASCA solid state imaging spectrometer observations of O stars
[NASA-CR-197281] p 2108 N95-24385
STELLAR WINDS
ASCA solid state imaging spectrometer observations of O stars
[NASA-CR-197281] p 2108 N95-24385
STEREOPHONICS
A study of the effect of voice pitch on the perception of synthetic Polish vowels
[IFTR-10/1994] p 1956 N95-26018
STEREOSCOPY
Stereo imaging velocimetry for microgravity applications
[NASA-TM-110494] p 1949 N95-24416

STIFFENING
Stiffening of the ACES deployable space boom
p 1978 N95-26307
STIFFNESS
Design and evaluation of a foam-filled hat-stiffened panel concept for aircraft primary structural applications
[NASA-TM-109175] p 1928 N95-26251
STIMULATED EMISSION
A quality monitor and monitoring technique employing optically stimulated electron emission
[NASA-CASE-LAR-15063-1-CU] p 1978 N95-25304
STIMULATED EMISSION DEVICES
A quality monitor and monitoring technique employing optically stimulated electron emission
[NASA-CASE-LAR-15063-1-CU] p 1978 N95-25304
STIRLING ENGINES
Felt-metal-wick heat-pipe solar receiver
[DE95-004535] p 1992 N95-24682
STOCHASTIC PROCESSES
The cooling of particle beams
[DE95-004669] p 2065 N95-24320
Describing the macroscopic world: Closing the circle within the dynamical reduction program
[DE95-606997] p 2100 N95-26046
On convergence of the Nelder-Mead simplex algorithm for unconstrained stochastic optimization
[AD-A289453] p 2006 N95-26197
STOICHIOMETRY
Oxygen stoichiometry and its influence on superconductivity in Bi2Sr2CaCu2O(8+x)
[DE95-004660] p 2088 N95-25282
In situ XAFS study of oxides formed on nickel thin film electrodes in KOH solution
[AD-A288735] p 1932 N95-26056
STORAGE RINGS (PARTICLE ACCELERATORS)
PEP-2 vacuum system: Joining SS flanges to copper beam chambers
[DE95-006093] p 1974 N95-24356
Crystalline beams: Theory, experiments, and proposals
[DE95-003955] p 2068 N95-24685
Elementary particle physics
[DE95-004376] p 2051 N95-25241
Bremsstrahlung scattering calculations for the beam stops and collimators in the APS insertion-device beamlines
[DE95-005471] p 2069 N95-25300
Neural network technique for orbit correction in accelerators/storage rings
[DE95-005955] p 2026 N95-25368
Coupling correction using closed orbit measurements
[DE95-005957] p 2070 N95-25369
Closed orbit related problems: Correction, feedback, and analysis
[DE95-005969] p 2070 N95-25441
Eigenvector method for optimized orbit correction
[DE95-005967] p 2071 N95-25785
STORAGE TANKS
National standard and code compliance for electrical equipment installed in hazardous locations for the void fraction instrument
[DE95-002158] p 1960 N95-26092
STOVL AIRCRAFT
Aerodynamics model for a generic ASTOVL lift-fan aircraft
[NASA-TM-110347] p 1908 N95-26302
STRAIN DISTRIBUTION
Shell deformation states and the finite element method: A benchmark study of cylindrical shells
[PB95-149621] p 1980 N95-24296
An evaluation of a coupled microstructural approach for the analysis of functionally graded composites via the finite-element method
[NASA-CR-195455] p 1925 N95-24438
STRAIN GAGES
Compensated high temperature strain gage
[NASA-CASE-LAR-14776-1] p 1968 N95-24625
STRAIN HARDENING
Composite ductility: The role of reinforcement and matrix
[DE95-003664] p 1925 N95-24590
STRAIN MEASUREMENT
Compensated high temperature strain gage
[NASA-CASE-LAR-14776-1] p 1968 N95-24625
X-ray based displacement and strain measurements for hostile environments
[NASA-CR-194451] p 1968 N95-25330
Scramjet thrust measurement in a shock tunnel
p 1914 N95-25396
Angular displacement measuring device
[NASA-CASE-ARC-11937-1] p 2074 N95-26015
STRAIN RATE
The temperature and strain rate dependence of the flow stress of single crystal NiAl deformed along the zone group axes (110)
[DE95-003634] p 2083 N95-24233
Time dependent indentation testing at non-ambient temperatures utilizing the high temperature mechanical properties microprobe
[DE95-005895] p 1933 N95-24432
Temperature and strain-rate effects on deformation mechanisms in irradiated stainless steel
[DE95-004941] p 1934 N95-24449
Evolution of plastic anisotropy for high-strain-rate computations
[DE95-004220] p 1941 N95-25237
STRATIGRAPHY
Shelf sediment dynamics and development of lithostratigraphy
[AD-A288886] p 2006 N95-25504
STRATOSPHERE
The atmospheric effects of stratospheric aircraft: A fourth program report
[NASA-RP-1359] p 1996 N95-24274
Replicator for characterization of cirrus and polar stratospheric cloud particles
[NASA-CR-197992] p 2005 N95-24411
Nucleation and growth of crystals under cirrus and polar stratospheric cloud conditions
[NASA-CR-197991] p 2085 N95-24478
Long endurance stratospheric solar powered airship
[PB95-178729] p 1911 N95-26009
STREAK CAMERAS
Characteristics of an ultrafast x-ray streak camera
[DE95-004210] p 1968 N95-24657
STREAMS
Temporal pacing in visual attention
[AD-A289785] p 2013 N95-26041
STRESS ANALYSIS
Residual Stress Measurements with Laser Speckle Correlation Interferometry and Local Heat Treating
[DE95-060082] p 1981 N95-24598
Stress analysis of a crack in the residual stress field by welding and its application to the fatigue crack propagation
[NAL-TR-1248] p 1981 N95-25000
New techniques to test fatigue properties of coined sheet specimens. Part 3: Fatigue testing and analysis of a component like coining in sheet steel materials
[PB95-165668] p 1982 N95-25569
Thermoelastic equations for multi-layered cylindrical shell
[NAL-TR-1222] p 1982 N95-25661
Stress analysis of a crack in the residual stress field by welding and its application to the fatigue crack propagation
[NAL-TR-1248] p 1983 N95-25796
Center for Computational Structures Technology
[NASA-CR-198028] p 1983 N95-26263
Three-dimensional solutions for thermomechanical stresses in sandwich panels and shells
p 1984 N95-26265
STRESS CONCENTRATION
New techniques to test fatigue properties of coined sheet specimens. Part 3: Fatigue testing and analysis of a component like coining in sheet steel materials
[PB95-165668] p 1982 N95-25569
STRESS CORROSION CRACKING
Localized corrosion and stress corrosion cracking characteristics of a low-aluminum-content iron-aluminum alloy
[DE95-003259] p 1934 N95-24647
STRESS CYCLES
A description of the cyclical properties of an aluminum alloy based on complex stress state tests
[IFTR-29/1994] p 1936 N95-25638
STRESS DISTRIBUTION
An evaluation of a coupled microstructural approach for the analysis of functionally graded composites via the finite-element method
[NASA-CR-195455] p 1925 N95-24438
Stress analysis of a crack in the residual stress field by welding and its application to the fatigue crack propagation
[NAL-TR-1248] p 1981 N95-25000
STRESS FUNCTIONS
Stress analysis of a crack in the residual stress field by welding and its application to the fatigue crack propagation
[NAL-TR-1248] p 1981 N95-25000
STRESS INTENSITY FACTORS
Stress analysis of a crack in the residual stress field by welding and its application to the fatigue crack propagation
[NAL-TR-1248] p 1981 N95-25000
STRESS MEASUREMENT
Residual Stress Measurements with Laser Speckle Correlation Interferometry and Local Heat Treating
[DE95-060082] p 1981 N95-24598
Techniques for studying the mechanical properties of materials in complex stress states
[IFTR-34/1994] p 1983 N95-26178
STRESS TENSORS
Molecular dynamics calculation of shear viscosity for molten salt
[DE95-703970] p 2055 N95-25496
STRESS WAVES
Thrust measurement in a 2-D scramjet nozzle
p 1914 N95-25397
STRESSES
The temperature and strain rate dependence of the flow stress of single crystal NiAl deformed along the zone group axes (110)
[DE95-003634] p 2083 N95-24233
Proposed Nordtest method: Reliability stress screening of components. A guide for component users. Nordtest project 1140-93
[PB95-165783] p 1978 N95-26003
STRING THEORY
Quantum corrections for a cosmological string solution
[DE95-006057] p 2109 N95-24327
Z flux-line lattices and self-dual equations in the standard model
[DE94-634364] p 2093 N95-24405
Heat Kernel expansion on a cone and quantum fields near cosmic strings
[DE94-628520] p 2094 N95-24507
TeV scale leptoquarks as a signature of standard-like superstring models
[DE94-628529] p 2096 N95-25095
String-loop corrections to effective action and black-hole instabilities
[DE95-607085] p 2110 N95-25433
Tachyon condensates and anisotropic universe
[DE95-607074] p 2097 N95-25456
Semiglobal Alice strings
[DE95-607081] p 2098 N95-25527
Central extension of a new W(infinity)-type algebra
[DE95-607086] p 2037 N95-25599
Cosmological constraints on perturbative supersymmetry breaking
[PB95-165361] p 2099 N95-25628
A superfield generalization of the classical action-at-a-distance theory
[DE95-607084] p 1955 N95-25648
STRONG INTERACTIONS (FIELD THEORY)
A test of the flavor independence of strong interactions
[DE95-006063] p 2046 N95-24576
STRONTIUM COMPOUNDS
Accurate determination of IC modulation parameter in Sr(x)Ba(1-x)Nb2O6 from second order satellites of neutron diffraction TOF (Time-Of-Flight) spectra
[DE94-629003] p 2090 N95-25851
Electronic structure of (La,Sr)2CuO4 and Ba(0.6)K(0.4)BiO3
[DE95-004963] p 2091 N95-26170
STRONTIUM OXIDES
Thermal diffuse scattering in time-of-flight neutron diffraction studied on SBN single crystals
[DE94-637054] p 2085 N95-24362
Processing and electrochemical properties of mixed conducting La(1-x)A(x)Co(1-y)Fe(y)O(3-delta) (A=Sr, Ca)
[DE95-004910] p 2088 N95-25002
STRUCTURAL ANALYSIS
Shell deformation states and the finite element method: A benchmark study of cylindrical shells
[PB95-149621] p 1980 N95-24296
An evaluation of a coupled microstructural approach for the analysis of functionally graded composites via the finite-element method
[NASA-CR-195455] p 1925 N95-24438
Integration of design, structural, thermal and optical analysis: And user's guide for structural-to-optical translator (PATCOD)
[NASA-TM-110153] p 1950 N95-24559
BSM Delta Qualification 2, volume 3, book 2
[NASA-CR-196568] p 1922 N95-24854
Finite element methods in a simulation code for offshore wind turbines
[PB95-164984] p 1994 N95-25501
Nonlinear structural analysis on distributed-memory computers p 1985 N95-26272
A hybrid neurocomputing/numerical strategy for nonlinear structural analysis p 1986 N95-26275
LH2 fuel tank design for SSTO p 1987 N95-26309
STRUCTURAL BASINS
Geologic mapping of Argyre Planitia
[NASA-CR-197986] p 2112 N95-24303
STRUCTURAL DESIGN
Go for EVA
[NASA-TM-110537] p 1918 N95-24195
Reducing neural network training time with parallel processing
[NASA-TM-110154] p 2015 N95-24209
Design and evaluation of a foam-filled hat-stiffened panel concept for aircraft primary structural applications
[NASA-TM-109175] p 1928 N95-26251

The 1994 NASA/USRA/ADP Design Projects
[NASA-CR-197415] p 2101 N95-26304
Universal Test Facility p 1918 N95-26305
Automated protein crystal growth facility p 1918 N95-26306
LH2 fuel tank design for SSTO p 1987 N95-26309
Feed system design for a reduced pressure tank p 1923 N95-26310

STRUCTURAL ENGINEERING
NASA-UVA light aerospace alloy and structures technology program (LA2ST)
[NASA-CR-198041] p 1933 N95-24220
JPRS report: Science and technology. Central Eurasia
[JPRS-UST-94-027] p 1957 N95-24470
Center for Computational Structures Technology
[NASA-CR-198028] p 1983 N95-26263

STRUCTURAL RELIABILITY
User's manual for FAROW: Fatigue and reliability of wind turbine components, version 1.1
[DE95-005530] p 1995 N95-26037

STRUCTURAL STABILITY
Structural and thermodynamic properties of 3-d transition metals: Pseudopotential theory revisited
[DE95-605639] p 1937 N95-25983

STRUCTURAL VIBRATION
Integrated passive/active vibration absorber for multi-story buildings
[NASA-TM-109178] p 1979 N95-24208
The transmission and control of vibrational power in a two stage isolation system with a water-loaded substructure
[ISVR-TR-235] p 1975 N95-24992
A technique for the evaluation of strength of coupling between SEA subsystems
[ISVR-TR-241] p 1981 N95-24997
Computerized design and generation of low-noise gears with localized bearing contact
[NASA-TM-106880] p 1977 N95-26074

SUBGROUPS
Cyclic subgroups in class groups of real quadratic fields
[DE94-628407] p 2031 N95-24697

SUBMILLIMETER WAVES
Airborne imaging of tropospheric emission at millimeter and submillimeter wavelengths
[NASA-TM-110498] p 2003 N95-24336
Optically-switched submillimeter-wave oscillator and radiator having a switch-to-switch propagation delay
[NASA-CASE-NPO-18547-1-CU] p 1959 N95-25307
Far-infrared and submillimeter spectroscopy of photodissociation regions
[DE95-607520] p 2110 N95-25467

SUBROUTINES
On the Trellis structure of a (64,40,8) subcode of the (64,42,8) third-order Reed-Muller code
[NASA-CR-198019] p 2015 N95-24224
Software fault tolerance in computer operating systems
[NASA-CR-197999] p 2016 N95-24993

SUBSONIC AIRCRAFT
Advanced subsonic airplane design and economic studies
[NASA-CR-195443] p 1913 N95-24304

SUBSONIC FLOW
High frequency flow-structural interaction in dense subsonic fluids
[NASA-CR-4652] p 1906 N95-24217
Effects of cavity dimensions, boundary layer, and temperature on cavity noise with emphasis on benchmark data to validate computational aeroacoustic codes
[NASA-CR-4653] p 2039 N95-24879
Numerical and experimental study of drag characteristics of two-dimensional HLFC airfoils in high subsonic, high Reynolds number flow
[NAL-TR-1244T] p 1907 N95-24998
Hot-wire calibration in subsonic/transonic flow regimes
[NASA-CR-197725] p 1970 N95-25699

SUBSONIC FLUTTER
Fundamental wind tunnel experiments on low-speed flutter of a tip-fin configuration wing
[NAL-TR-1228] p 1908 N95-25762

SUBSONIC SPEED
Noise impact of advanced high lift systems
[NASA-CR-195028] p 2040 N95-26160

SUBSTITUTES
Federal alternative motor fuels program: Light duty federal vehicles, trucks, and buses
[DE95-003982] p 1948 N95-24679

SUBSTRATES
Thin film ionic conductors based on cerium oxide
[DE95-003668] p 2086 N95-24514
Ion beam mixing of titanium overlayers with hydroxyapaptite substrates
[DE95-005278] p 1935 N95-25379
Back surface cell structures for reducing recombination in CZ silicon solar cells
[DE95-005423] p 1995 N95-25566
Improved lubrication performance of sputtered MoS2 film by surface treatments of Ti-alloy substrate
[NAL-TR-1213] p 1942 N95-25760

SULFATES
Biospheric effects of a large extraterrestrial impact: Case study of the cretaceous/tertiary boundary crater
[NASA-CR-198015] p 1997 N95-24501
Microphysical and compositional influences on shortwave radiative forcing of climate by sulfate aerosols
[DE95-005999] p 1997 N95-24570

SULFUR DIOXIDES
Cross-flow, filter-sorbent-catalyst for particulate, SO2 and NO(x) control
[DE95-001934] p 2003 N95-26091

SULFUR FLUORIDES
Simple chemical assays for presence of S2F10 in decomposed SF6
[DE95-001423] p 1929 N95-24345

SULFUR HEXAFLUORIDE
Electric field effects on a near-critical fluid in microgravity
[NASA-TM-106894] p 2099 N95-25878

SULFUR OXIDES
Biospheric effects of a large extraterrestrial impact: Case study of the cretaceous/tertiary boundary crater
[NASA-CR-198015] p 1997 N95-24501

SULFURIC ACID
High octane ethers from synthesis gas-derived alcohols
[DE95-001146] p 1948 N95-24655

SUM RULES
Deficiency of the Gross-Llewellyn Smith sum rule and QCD vacuum polarization effect
[DE94-636790] p 2042 N95-24315
The determination of V(sub cb) and QCD Sum Rules in Heavy Quark Effective theory
[DE94-628636] p 2095 N95-24723

SUNLIGHT
Predicting the components of the total hemispherical solar radiation from sunshine duration measurements in Lagos, Nigeria
[DE95-606030] p 2113 N95-26042

SUPERCOMPUTERS
A practical approach to portability and performance problems on massively parallel supercomputers
[DE95-005251] p 2020 N95-24612
Parallel processing of atmospheric chemistry calculations: Preliminary considerations
[DE95-005915] p 1999 N95-25198
Designing a stencil compiler for the Connection Machine model CM-5
[DE95-006861] p 2021 N95-25477
Converting multiple OC-3c ATM streams to HIPPI to drive an HDTV frame buffer from a workstation cluster
[DE95-003638] p 2022 N95-26066

SUPERCONDUCTING DEVICES
Device-quality tunnel junctions on the high (T(sub c)) super conductor HgBa2CuO(4+delta)
[DE95-004646] p 2084 N95-24279

SUPERCONDUCTING FILMS
Copper transport on oxygen annealing of a superconducting film Y-Ba-Cu-O
[DE94-627566] p 2086 N95-24537
Summaries of reports of the Electrotechnical Laboratory, no. 48
[JTN-95-80825] p 2114 N95-24908
Temperature-dependent growth of LaAlO3 films on YBa2CuO7 C-axis films for multilayer structures
[DE95-005257] p 2089 N95-25598
New evaluation method of superconductor characteristics for realizing the Large Helical Device
[NIFS-297] p 2071 N95-25855

SUPERCONDUCTING MAGNETS
Measurement of the magnetically-induced QED birefringence of the vacuum and an improved search for laboratory axions: Project definition study of the use of assets and facilities of the Superconducting Super Collider Laboratory
[DE95-005110] p 2065 N95-24317
Availability analysis of a 100 kWh superconducting magnetic energy storage
[DE95-737621] p 2066 N95-24448
Superconducting magnets, 1994
[DE95-003813] p 1958 N95-24551
Benchmark experiment on a copper slab assembly bombarded by D-T neutrons
[DE95-709764] p 2055 N95-25497
New evaluation method of superconductor characteristics for realizing the Large Helical Device
[NIFS-297] p 2071 N95-25855

SUPERCONDUCTING SUPER COLLIDER
Measurement of the magnetically-induced QED birefringence of the vacuum and an improved search for laboratory axions: Project definition study of the use of assets and facilities of the Superconducting Super Collider Laboratory
[DE95-005110] p 2065 N95-24317
Superconducting magnets, 1994
[DE95-003813] p 1958 N95-24551
Cryogenic helium gas convection research
[DE95-004372] p 1965 N95-25404

SUPERCONDUCTIVITY
Superconducting in the near half-filling Hubbard model
[DE94-634857] p 2092 N95-24275
Electron-phonon interaction in the Hubbard model
[DE94-634859] p 2092 N95-24277
Device-quality tunnel junctions on the high (T(sub c)) super conductor HgBa2CuO(4+delta)
[DE95-004646] p 2084 N95-24279
Neutron diffraction from HoNi2B2C, version 1
[DE95-005894] p 2085 N95-24431
Superconductivity Program for Electric Power Systems: 1994 Annual PEER Review. Volume 1, Meeting Proceedings
[DE95-005058] p 1956 N95-24452
Superconductivity Program for Electric Power Systems: 1994 Annual PEER Review. Volume 2, Meeting Proceedings
[DE95-005059] p 1957 N95-24453
Activities of the Solid State Division
[DE95-003900] p 2087 N95-24611
Effect of He pressure on the superconducting transition temperatures of Na2CsC60 and (NH3)4Na2CsC60
[DE95-006320] p 2087 N95-24616
Intrinsic magnetic torque at low magnetic induction
[DE95-601209] p 1959 N95-24842
BCS-like gap structure of HgBa2CuO(4+delta) tunnel junctions
[DE95-004125] p 2087 N95-24855
Oxygen stoichiometry and its influence on superconductivity in Bi2Sr2CaCu2O(8+x)
[DE95-004660] p 2088 N95-25282
Superconductivity, magnetism and metal-insulator transitions in some ternary and pseudoternary 3d-, 4d- and 5d-metal oxides
[DE95-005904] p 2038 N95-25600
From superconductivity to supernovae: The Ginzburg symposium. Report on the symposium held in honor of Vitaly L. Ginzburg
[NASA-TM-110596] p 2108 N95-25746
New evaluation method of superconductor characteristics for realizing the Large Helical Device
[NIFS-297] p 2071 N95-25855
Application of extended-crystal diffraction techniques to the symmetry and structure analysis of 221-PbBiSrCaCuO
[DE95-605913] p 2090 N95-25984
Condensate localization by mesoscale disorder in high-T(sub c) superconductors
[DE95-607819] p 1960 N95-26100
Coherent state path-integral representation of supersymmetric lattice models
[DE95-607820] p 2091 N95-26101
Magnetized pair Bose gas: Relativistic superconductor
[DE95-607846] p 2100 N95-26104

SUPERCONDUCTORS (MATERIALS)
Superconductivity Program for Electric Power Systems: 1994 Annual PEER Review. Volume 2, Meeting Proceedings
[DE95-005059] p 1957 N95-24453
Effect of He pressure on the superconducting transition temperatures of Na2CsC60 and (NH3)4Na2CsC60
[DE95-006320] p 2087 N95-24616
Summaries of reports of the Electrotechnical Laboratory, no. 48
[JTN-95-80825] p 2114 N95-24908
New evaluation method of superconductor characteristics for realizing the Large Helical Device
[NIFS-297] p 2071 N95-25855

SUPERCRITICAL FLUIDS
Fischer Tropsch synthesis in supercritical fluids
[DE95-005206] p 1929 N95-24341
Supercritical carbon dioxide cleaning market assessment and commercialization/deployment plan
[DE94-017394] p 1998 N95-24653

SUPERHIGH FREQUENCIES
Diurnal variations of backscattering properties of pine trees at C- and X-bands
[PB95-149738] p 1988 N95-24299
High-gradient experiment on X-band disk-loaded structures
[DE94-765446] p 1958 N95-24701
Annual report 1992/93, FOA 38. Radio systems and wave propagation
[PB95-141735] p 1953 N95-24835

RF pulse compression in the NLC test accelerator at SLAC
[DE95-006478] p 2070 N95-25406

SUPERLATTICES
Electromagnetic waves and photoacoustic transformation in gyrotropic superlattices p 2083 N95-24205
JPRS report: Science and technology. Central Eurasia
[JPRS-UST-95-008] p 1957 N95-24468
Application of extended-crystal diffraction techniques to the symmetry and structure analysis of 221-PbBiSrCaCuO
[DE95-605913] p 2090 N95-25984

SUPERNOVAE
Core-collapse supernovae and nucleosynthesis
[NASA-CR-197731] p 2109 N95-25122
Research in nuclear astrophysics: Stellar collapse and supernovae
[DE95-004300] p 2110 N95-25343
From superconductivity to supernovae: The Ginzburg symposium. Report on the symposium held in honor of Vitaly L. Ginzburg
[NASA-TM-110596] p 2108 N95-25746

SUPERSONIC COMBUSTION
Effect of density gradients in confined supersonic shear layers, part 1
[NASA-CR-198029] p 1962 N95-24412
Effect of density gradients in confined supersonic shear layers. Part 2: 3-D modes
[NASA-CR-198030] p 1962 N95-24413

SUPERSONIC COMBUSTION RAMJET ENGINES
Effect of film cooling/regenerative cooling on scramjet engine performances
[NAL-TR-1242] p 1914 N95-24990
Shock tunnel studies of scramjet phenomena 1993
[NASA-CR-195038] p 1964 N95-25394
Thrust measurements of a complete axisymmetric scramjet in an impulse facility p 1914 N95-25395
Scramjet thrust measurement in a shock tunnel p 1914 N95-25396
Thrust measurement in a 2-D scramjet nozzle p 1914 N95-25397
Scaling in a scramjet combustor p 1933 N95-25398
Balances for the measurement of multiple components of force in flows of a millisecond duration p 1965 N95-25400

SUPERSONIC FLOW
Effect of film cooling/regenerative cooling on scramjet engine performances
[NAL-TR-1242] p 1914 N95-24990
A study of three-dimensional interaction flow fields between swept shock waves and turbulent boundary layers. Flow structures and effects of bleed
[NAL-TR-1227] p 1963 N95-25001
A theoretical and experimental investigation of the flow over supersonic leading edge wing/body configurations
[DRA-TM-AERO-PROP-41] p 1907 N95-25649
Aerodynamic characteristics of the orbital reentry vehicle experimental probe fins in a supersonic flow
[NAL-TR-1232] p 1921 N95-25664
Numerical calculations of shock-wave/boundary-layer flow interactions
[NASA-TM-106694] p 1966 N95-26077

SUPERSONIC SPEED
Effect of density gradients in confined supersonic shear layers, part 1
[NASA-CR-198029] p 1962 N95-24412

SUPERSONIC TRANSPORTS
The atmospheric effects of stratospheric aircraft: A fourth program report
[NASA-RP-1359] p 1996 N95-24274
Study of compressible flow through a rectangular-to-semiannular transition duct
[NASA-CR-4660] p 1914 N95-24392
A crew-centered flight deck design philosophy for High-Speed Civil Transport (HSCT) aircraft
[NASA-TM-109171] p 1910 N95-24582
NASA-UVa light aerospace alloy and structures technology program supplement: Aluminum-based materials for high speed aircraft
[NASA-CR-4645] p 1935 N95-24878

SUPERSONIC WIND TUNNELS
Supersonic quiet-tunnel development for laminar-turbulent transition research
[NASA-CR-198040] p 1915 N95-24302

SUPERSYMMETRY
Supersymmetry
[DE95-004670] p 2092 N95-24333
On the central charge in 3 D-supersymmetry
[DE95-600851] p 2093 N95-24352
Equivariant localization: BV-geometry and supersymmetric dynamics
[DE94-628436] p 2036 N95-24699
On q-deformed supersymmetric classical mechanical models
[DE95-600864] p 2095 N95-24838
Possible constraints on SUSY-model parameters from direct dark matter search
[DE94-628561] p 2109 N95-24885
On SUSY dark matter detection with spinless nuclei
[DE94-628562] p 2109 N95-24886
Supersymmetry and light quark masses in a realistic superstring model
[DE94-628530] p 2096 N95-25096
R parity in standard-like superstring models
[DE94-628531] p 2096 N95-25215
Testing supersymmetry at the next linear collider
[DE95-006064] p 2069 N95-25297
Neutrino oscillations from discrete non-Abelian family symmetries
[DE95-004355] p 2052 N95-25403
A partial unification model in non-commutative geometry
[DE95-607129] p 2097 N95-25435
Scalar three body decays and signals for new physics
[DE95-607188] p 2053 N95-25438
Equivariant Kaehler geometry and localization in the G/G model
[DE95-607073] p 2036 N95-25455
On D=2 (1/3, 1/3) supersymmetric theories 1
[DE95-607075] p 2036 N95-25522
On D=2 (1/3,1/3) supersymmetric theories 2
[DE95-607076] p 2037 N95-25523
HyperKaehler metrics building and integrable models
[DE95-607077] p 2038 N95-25524
On exotic supersymmetries of the Phi(1,3) deformation of minimal models
[DE95-607088] p 2033 N95-25532
Cosmological constraints on perturbative supersymmetry breaking
[PB95-165361] p 2099 N95-25628
A superfield generalization of the classical action-at-a-distance theory
[DE95-607084] p 1955 N95-25648
Coherent state path-integral representation of supersymmetric lattice models
[DE95-607820] p 2091 N95-26101

SUPPORTS
Measurements of longitudinal static aerodynamic coefficients by the cable mount system
[NAL-TR-1226] p 1908 N95-25761

SUPPRESSORS
Jet mixer noise suppressor using acoustic feedback
[NASA-CASE-LEW-15170-2] p 2040 N95-26187

SURFACE ACOUSTIC WAVE DEVICES
The use of acoustic surface waves to analyze gases apparatus and experiments p 2039 N95-25115
Type P dispersive delay lines p 1959 N95-25116

SURFACE CRACKS
Thermal fracture mechanisms in ceramic thermal barrier coatings p 1946 N95-26138

SURFACE DIFFUSION
One-step in-diffusion as a result of multipulse laser irradiation of LiNbO3 single-crystalline substrates covered with thin Ti deposits on the effect of the radiation wavelength
[DE94-634524] p 2084 N95-24324

SURFACE EMITTING LASERS
Time-dependent numerical simulation of vertical cavity lasers
[DE95-006862] p 1973 N95-26112

SURFACE PROPERTIES
An investigation of the effect of surface impurities on the adsorption kinetics of hydrogen chemisorbed onto iron
[NASA-CR-197967] p 1933 N95-24400
Assessment of climate variability of the Greenland ice sheet: Integration of in situ and satellite data
[NASA-CR-198020] p 1998 N95-24846
Fire test of surface products: Comparison of data from the nordic box test and the cone calorimeter
[PB95-165239] p 1932 N95-26000
Calculating the thermodynamic properties of planar and spherical liquid-vapour interface
[DE95-608777] p 2100 N95-26105

SURFACE REACTIONS
International bulletin on atomic and molecular data for fusion, no. 47
[DE94-634442] p 2040 N95-24230
Spacecraft materials studies on The Aerospace Corporation Tray on EOIM-3
[AD-A288682] p 1942 N95-26049

SURFACE ROUGHNESS
Method and apparatus for non-destructive evaluation of composite materials with cloth surface impressions
[NASA-CASE-LAR-14535-1] p 1926 N95-25305
Non-destructive characterization of porous silicon using x ray reflectivity
[DE95-004766] p 1942 N95-25898

SURFACE TEMPERATURE
Ice surface temperature retrieval from AVHRR, ATSR, and passive microwave satellite data: Algorithm development and application
[NASA-CR-198037] p 1989 N95-24441

SURFACE TREATMENT
High heat flux experiment on B4C-converted carbon based materials for plasma facing materials of JT-60U
[DE94-777545] p 2077 N95-24585
Improved lubrication performance of sputtered MoS2 film by surface treatments of Ti-alloy substrate
[NAL-TR-1213] p 1942 N95-25760

SURFACE WATER
Coso Monitoring Program, October 1992 through September 1993
[AD-A279147] p 1989 N95-24422
Biological monitoring of national freshwaters, 1992
[PB95-166690] p 2002 N95-25745

SURFACE WAVES
The use of acoustic surface waves to analyze gases apparatus and experiments p 2039 N95-25115

SURFACTANTS
Synthesis and characterization of Fe colloid catalysts in inverse micelle solutions
[DE95-006313] p 1929 N95-24614

SURGICAL INSTRUMENTS
Milli-robots for surgical teleoperation
[NASA-CR-197378] p 1974 N95-24204

SURVEYS
Development of an intervention program to encourage shoulder harness use and aircraft retrofit in general aviation aircraft, phases 1 and 2
[DOT/FAA/AM-95/2] p 1909 N95-24384
Metrology measurement capability
[DE95-005411] p 1969 N95-25381

SURVIVAL
A longevity and survival analysis for a cohort of retired airline pilots
[DOT/FAA/AM-95/5] p 2012 N95-24237

SWEDEN
Planning for the unknown: Coping with uncertainty
[PB95-165114] p 2102 N95-25642

SWEPT WINGS
Three-dimensional interaction of wake/boundary-layer and vortex/boundary-layer data report
[CUED/A-AEREO/TR-23] p 1906 N95-24210
Aerodynamic shape optimization of wing and wing-body configurations using control theory
[NASA-CR-198024] p 1911 N95-25334

SWITCHES
High gain GaAs Photoconductive Semiconductor Switches (PCSS): Device lifetime, high current testing, optical pulse generators
[DE95-003354] p 1957 N95-24488
Adventures in the evolution of a high-bandwidth network for central servers
[DE95-006215] p 2020 N95-24597

SYLLABLES
Automatic classification of Polish fricatives on the basis of optimization of the parameter space
[IFTR-9/1994] p 1958 N95-26331

SYMMETRY
Response to a localized impact loading of a composite multilayered rotational shell structure: Theory and numerical methods, volume 1
[ONERA-NT-1994-10-VOL-1] p 1979 N95-24282
Response to a localized impact loading of a composite multilayered rotational shell structure: Theory and numerical methods, volume 2
[ONERA-NT-1994-10-VOL-2] p 1980 N95-24283
Response to a localized impact loading of a composite multilayered rotational shell structure: Theory and numerical methods, Volume 3
[ONERA-NT-1994-10-VOL-3] p 1980 N95-24284
Geometric quantization of symplectic manifolds with symmetry
[DE94-628435] p 2031 N95-24698
Quantum group and quantum symmetry
[DE94-634329] p 2095 N95-24767
Parity doubling from thermodynamics of experimental hadron spectrum
[DE95-600934] p 2095 N95-24839
Creation and development of the Universe (symmetry approach)
[DE94-628558] p 2109 N95-24884
Extended gauge sectors
[DE95-006485] p 2052 N95-25407
Heavy quark effective theory, interpolating fields and Bethe-Salpeter amplitudes
[DE95-607146] p 2053 N95-25460
The off-shell axial anomaly via the (gamma)*(pi)(sup 0) (yields) (gamma) transition
[DE95-004762] p 2057 N95-25896

Application of extended-crystal diffraction techniques to the symmetry and structure analysis of 221-PbBiSrCaCuO
[DE95-605913] p 2090 N95-25984
Calculation of light scattering from a spherical particle on a surface by the multipole expansion method
[ATR-95(9558)-2] p 2075 N95-26198

SYNCHRONISM
An optimized implementation of a fault-tolerant clock synchronization circuit
[NASA-TM-109176] p 2019 N95-24382
Multistatic radar: Synchronization and time reference system
[PB95-165288] p 1954 N95-25623

SYNCHRONOUS PLATFORMS
The use of empirical models to investigate GPS derived total electron content
[DE95-606045] p 2111 N95-26044

SYNCHROTRON RADIATION
FT-IR microscopical analysis with synchrotron radiation: The microscope optics and system performance
[DE95-004834] p 1928 N95-24265
Proceedings of the 21st Japan Conference on Radiation and Radioisotopes
[DE94-785275] p 2056 N95-25614

SYNCHROTRONS
The determination of the main parameters of the backward spectrometer of the 0(sup 0) facility
[DE94-628385] p 2048 N95-24692

SYNTHESIS (CHEMISTRY)
Study on the production of alternative fuels by carbon dioxide hydrogenation
[DE95-744284] p 1948 N95-24498
Synthesis and characterization of Fe colloid catalysts in inverse micelle solutions
[DE95-006313] p 1929 N95-24614
High octane ethers from synthesis gas-derived alcohols
[DE95-001146] p 1948 N95-24655
Study of copper perovskite
[DE95-730106] p 2088 N95-24988
Ion beam mixing of titanium overlayers with hydroxyapaptite substrates
[DE95-005278] p 1935 N95-25379
Synthesis and processing of Al2O3/Al composites by in situ reaction of aluminum and mullite
[DE95-006224] p 1937 N95-25775
Whisker reinforced glass ceramic
[DE95-005568] p 1927 N95-25998

SYNTHETIC APERTURE RADAR
User guide to the Magellan synthetic aperture radar images
[NASA-RP-1356] p 2112 N95-24987
ESA Bulletin No. 81 p 2114 N95-25200
Spaceborne synthetic aperture radar: Current status and future directions. A report to the Committee on Earth Sciences, Space Studies Board, National Research Council
[NASA-TM-4679] p 1955 N95-25710

SYSTEM EFFECTIVENESS
Felt-metal-wick heat-pipe solar receiver
[DE95-004535] p 1992 N95-24682
Development of a portable mass spectrometric system for determination of isotopic composition of solid uranium samples using fluorine volatilization
[DE95-005728] p 1969 N95-25384

SYSTEM FAILURES
Software fault tolerance in computer operating systems
[NASA-CR-197999] p 2016 N95-24993
Proposed Nordtest method: Reliability stress screening of components. A guide for component users. Nordtest project 1140-93
[PB95-165783] p 1978 N95-26003

SYSTEMS ANALYSIS
Nonlinear system analysis using slowly-varying complex frequency method
[NAL-TR-1217] p 2034 N95-25860
Facility for the evaluation of space communications and related systems
[NASA-TM-106904] p 1955 N95-25876
Feed system design for a reduced pressure tank
p 1923 N95-26310

SYSTEMS ENGINEERING
Development of a portable mass spectrometric system for determination of isotopic composition of solid uranium samples using fluorine volatilization
[DE95-005728] p 1969 N95-25384
On the numerical method for analysis of the dynamics of the classical Hamiltonian systems
[DE95-605218] p 2034 N95-25906
Launch system design for access to space
p 1918 N95-26308
Feed system design for a reduced pressure tank
p 1923 N95-26310

SYSTEMS INTEGRATION
Simulation of diurnal thermal energy storage systems: Preliminary results
[DE95-005751] p 1991 N95-24369
Test plan/procedure for the DPHV system integration
[DE95-003414] p 1994 N95-25121

SYSTEMS SIMULATION
Facility for the evaluation of space communications and related systems
[NASA-TM-106904] p 1955 N95-25876

SYSTEMS STABILITY
Unfolding of true distributions from experimental data distorted by detectors with finite resolutions
[DE94-628372] p 2035 N95-24643
Experimental and theoretical basis for advanced tokamaks
[DE95-003255] p 2077 N95-24646
New evaluation method of superconductor characteristics for realizing the Large Helical Device
[NIFS-297] p 2071 N95-25855
Actuating signals in adaptive control systems
[IFTR-13/1994] p 2027 N95-26330

T

T-53 ENGINE
Assessment of overhaul surge margin tests applied to the T53 engines in ADF Iroquois helicopters
[AR-008-389] p 1914 N95-25936

TABLES (DATA)
Metrology measurement capability
[DE95-005411] p 1969 N95-25381

TACHYONS
Tachyon condensates and anisotropic universe
[DE95-607074] p 2097 N95-25456

TARGET ACQUISITION
Implementation of scene shadows in the Target Acquisition TDA (TARGAC)
[AD-A288760] p 1912 N95-26060
Infrared multispectral sensor program, Phase 2. Field measurements, analysis and modeling. Volume 1: Fourier transform spectrometer sensor characterization
[AD-A288888] p 2075 N95-26173

TARGET RECOGNITION
Three-D Artificial Neural Network (3DANN) technology. Blueprint for the future p 2024 N95-25260
Low-cost image analysis system
[DE95-005021] p 2021 N95-25378

TARGET SIMULATORS
Neural network technique for orbit correction in accelerators/storage rings
[DE95-005955] p 2026 N95-25368

TARGETS
Magnetized target fusion: An overview of the concept
[DE95-005247] p 2070 N95-25594
Multispectral detection of ground targets in highly correlated backgrounds
[AD-A289292] p 1990 N95-26040
Heat removal capability of divertor coaxial tube assembly
[DE95-709770] p 1966 N95-26161

TASKS
On producing sequential movements and actions. An integrative review and an update of the generalized motor program
[AD-A288628] p 2014 N95-25610

TECHNOLOGIES
JPRS report: Science and technology. Central Eurasia
[JPRS-UST-95-009] p 1916 N95-24467
JPRS report: Science and technology. Central Eurasia
[JPRS-UST-95-008] p 1957 N95-24468
JPRS report: Science and technology. Central Eurasia
[JPRS-UST-94-030] p 1962 N95-24469
JPRS report: Science and technology. Central Eurasia
[JPRS-UST-94-027] p 1957 N95-24470
JPRS report: Science and technology. Central Eurasia: Institute of General and Nuclear Physics: 1993 Status and Prospects
[JPRS-UST-94-025] p 2045 N95-24471
JPRS report: Science and technology. Central Eurasia
[JPRS-UST-94-018] p 1950 N95-24472
JPRS report: Science and technology. Central Eurasia
[JPRS-UST-94-024] p 1958 N95-24620
JPRS Report: Science and technology. Central Eurasia
[JPRS-UST-95-002] p 1916 N95-24621
JPRS report: Science and technology. Central Eurasia
[JPRS-UST-94-034] p 1987 N95-24729
JPRS report: Science and technology. Central Eurasia
[JPRS-UST-95-003] p 1988 N95-24730
JPRS report: Science and technology. Central Eurasia
[JPRS-UST-95-006] p 1950 N95-24731
JPRS report: Science and technology. Central Eurasia
[JPRS-UST-94-033] p 2037 N95-24732
JPRS Report: Science and technology. Central Eurasia
[JPRS-UST-94-032] p 1950 N95-24759
JPRS Report: Science and technology. Central Eurasia
[JPRS-UST-94-031] p 1988 N95-24760
JPRS report: Science and technology. Central Eurasia: Seminar on materials science
[JPRS-UST-95-007] p 1920 N95-24761
JPRS report: Science and technology. Central Eurasia. Otechestvennaya Geologiya: Studies in Aerospace and Remote Sensing
[JPRS-UST-95-004] p 1989 N95-24768
JPRS report: Science and technology. Central Eurasia: Space
[JPRS-USP-94-008] p 1916 N95-24847
JPRS report: Science and technology. Central Eurasia
[JPRS-UST-95-018] p 2071 N95-26079
JPRS report: Science and technology. Central Eurasia
[JPRS-UST-95-017] p 1988 N95-26080
Science in the national interest
[ISBN-0-16-045186-8] p 2115 N95-26335

TECHNOLOGY ASSESSMENT
Display technologies in Russia, Ukraine, and Belarus
[ISBN-1-883712-36-X] p 2085 N95-24460
Assessment of avionics technology in European aerospace organizations
[NASA-CR-189201] p 1912 N95-24624
TITLE: Environmental, health, and safety issues offuel cells in transportation. Volume 1: Phosphoricacid fuel-cell buses
[DE95-000289] p 1993 N95-24866
Innovation and application of ANN in Europe demonstrated by Kohonen maps p 2024 N95-25262
Metrology measurement capability
[DE95-005411] p 1969 N95-25381
Cryogenic helium gas convection research
[DE95-004372] p 1965 N95-25404
Wind technology development: Large and small turbines
[DE95-000286] p 1995 N95-26090
The railplug: A new ignitor for internal combustion engines
[DE95-005487] p 1977 N95-26172
Science in the national interest
[ISBN-0-16-045186-8] p 2115 N95-26335

TECHNOLOGY TRANSFER
National Renewable Energy Laboratory Information Resources Catalogue. A collection of energy efficiency and renewable energy information resources
[DE94-011900] p 1990 N95-24305
Proceedings of the 1993 Symposium on Nuclear Data
[DE94-012554] p 2104 N95-24372
Three-D Artificial Neural Network (3DANN) technology. Blueprint for the future p 2024 N95-25260
Neural networks: Application to medical imaging
p 2025 N95-25267
Science in the national interest
[ISBN-0-16-045186-8] p 2115 N95-26335

TECHNOLOGY UTILIZATION
Piezoelectric motor development at AlliedSignal Inc., Kansas City Division
[DE95-003389] p 1958 N95-24532
The potential of vacuum microelectronics for space reactor applications
[DE95-000542] p 1958 N95-24586
Liquid-fueled SOFC power sources for transportation
[DE95-002998] p 1991 N95-24607
Aviation system capacity improvements through technology
[NASA-TM-109165] p 1909 N95-24633
Yearbook 1993: Bioenergy Research Programme. Utilization of bioenergy and biomass conversion
[DE95-717518] p 1993 N95-24862
A Decade of Neural Networks: Practical Applications and Prospects
[NASA-CR-197334] p 2022 N95-25253
Cryogenic helium gas convection research
[DE95-004372] p 1965 N95-25404
Science in the national interest
[ISBN-0-16-045186-8] p 2115 N95-26335

TELECOMMUNICATION
Study on propagation impairments, distortions and unavailability on digital microwave links
[DE95-723047] p 1953 N95-24848
Neural network applications in telecommunications
p 2025 N95-25270
Towards an era of global village: The dynamics of world telecommunications and its implications for the future of nation state
[PB95-165064] p 1954 N95-25482

TELEOPERATORS
Milli-robots for surgical teleoperation
[NASA-CR-197378] p 1974 N95-24204

TELESCOPES
Journal of the Communications Research Laboratory, volume 41, number 1, March 1994
[PB95-177606] p 1956 N95-26008
TEMPERATE REGIONS
Impacts of microphysics, radiation and environmental winds in mid-latitude and tropical squall-line systems, and their climatic implications
[DE95-004965] p 2005 N95-25287
TEMPERATURE CONTROL
Small spacecraft power and thermal subsystems
[NASA-CR-195029] p 1921 N95-24216
Small spacecraft power and thermal subsystems
[NASA-CR-195029] p 1921 N95-24428
Alternate method for achieving temperature control in the -160 to +90 Celcius range
[NASA-CASE-NPO-18995-1-CU] p 1969 N95-25547
AMCC casting development, volume 2
[NASA-CR-197720] p 1938 N95-26068
TEMPERATURE DEPENDENCE
The temperature and strain rate dependence of the flow stress of single crystal NiAl deformed along the zone group axes (110)
[DE95-003634] p 2083 N95-24233
Temperature dependence of magnetic anisotropy and magnetostriction: Beyond the mean-field theory
[DE94-634529] p 2084 N95-24244
Creep properties of 20% cold worked hastelloy XR
[DE94-785198] p 1933 N95-24338
Neutron diffraction from HoNi2B2C, version 1
[DE95-005894] p 2085 N95-24431
The measurement of the low frequency noise characteristics of the field effect transistors for cryogenic detectors
[DE94-628257] p 1957 N95-24487
Meson properties at finite temperature and density within Nambu-Jona-Lasinio model
[DE94-628630] p 2049 N95-24888
Oxygen stoichiometry and its influence on superconductivity in Bi2Sr2CaCu2O(8+x)
[DE95-004660] p 2088 N95-25282
Temperature and dose dependence of metal colloid production in alpha-irradiated CaF2
[DE95-004907] p 2088 N95-25288
Zero sound velocity in pi, rho mesons at different temperatures
[DE95-607145] p 2053 N95-25459
Temperature-dependent growth of LaAlO3 films on YBa2CuO7 C-axis films for multilayer structures
[DE95-005257] p 2089 N95-25598
Coercive field and domain wall properties in (Dy(x)Y(1-x))Fe2 and (Er(x)Y(1-x))Fe2
[DE95-601135] p 1937 N95-25751
Fluctuations in macroscopically agitated plasma: Quasiparticles and effective temperature
[DE95-607611] p 2082 N95-25777
TEMPERATURE DISTRIBUTION
Numerical simulation of flow and the effect of baffle arrangement on pressure drop and temperature pattern in a circular combustor p 1963 N95-24628
TEMPERATURE EFFECTS
Method for molding structural parts utilizing modified silicone rubber
[NASA-CASE-LAR-15217-1] p 1939 N95-24212
Temperature and strain-rate effects on deformation mechanisms in irradiated stainless steel
[DE95-004941] p 1934 N95-24449
Effects of cavity dimensions, boundary layer, and temperature on cavity noise with emphasis on benchmark data to validate computational aeroacoustic codes
[NASA-CR-4653] p 2039 N95-24879
Numerical simulation of the nonlinear response of composite plates under combined thermal and acoustic loading
[NASA-CR-197426] p 1981 N95-24907
Hot-wire calibration in subsonic/transonic flow regimes
[NASA-CR-197725] p 1970 N95-25699
Static recrystallization behavior of austenite in HSLA 100 during Thermomechanical Controlled Processing (TMCP)
[AD-A288737] p 1937 N95-26057
Correlated density matrix theory of spatially inhomogeneous Bose fluids
[DE95-607840] p 2100 N95-26102
Buckling and postbuckling of composite panels with cutouts subjected to combined edge shear and temperature change p 1987 N95-26280
Intercomparison of hydrologic processes in global climate models
[NASA-TM-104617] p 2005 N95-26341
TEMPERATURE GRADIENTS
AMCC casting development, volume 2
[NASA-CR-197720] p 1938 N95-26068
TEMPERATURE MEASUREMENT
Measurements of thermal conductivity of diamond thin films by the ac calorimetric method
[PB95-149746] p 1939 N95-24300
Coso Monitoring Program, October 1992 through September 1993
[AD-A279147] p 1989 N95-24422
Turbine-engine applications of thermographic-phosphor temperature measurements
[DE95-003625] p 1989 N95-25110
Heat flux instrumentation for HYFLITE thermal protection system
[NASA-CR-197715] p 1968 N95-25118
Performance evaluation of LE-7 high pressure pumps
[NAL-TR-1212T] p 1977 N95-25672
TEMPERATURE SENSORS
Development of sensors for ceramic components in advanced propulsion systems. Phase 2: Temperature sensor systems evaluation
[NASA-CR-195283] p 1967 N95-24473
Heat flux instrumentation for HYFLITE thermal protection system
[NASA-CR-197715] p 1968 N95-25118
TENSILE PROPERTIES
Synthesis of Ni3Al and NiAl intermetallics
[DE95-005897] p 1934 N95-24433
Composite materials flown on the Long Duration Exposure Facility
[NASA-CR-4657] p 1923 N95-24583
A fully associative, nonisothermal, nonlinear kinematic, unified viscoplastic model for titanium alloys
[NASA-TM-106926] p 1983 N95-26078
TENSILE STRENGTH
Antioxidant and sensitizer effect on the stability of natural rubber latex vulcanized by gamma rays
[DE94-636061] p 1939 N95-24373
Study on tensile fatigue testing method of unidirectional fiber-resin matrix composites
[NAL-TR-1241] p 1926 N95-24989
Study on tensile fatigue testing method of unidirectional fiber-resin matrix composites
[NAL-TR-1241] p 1927 N95-25770
Recent progress in shear punch testing
[DE95-005962] p 1937 N95-26007
Mechanical properties testing and results for thermal barrier coatings p 1946 N95-26134
TENSILE STRESS
Stability and elastic properties of hydrogen loaded Ti(1-x)Al(x) alloys: An ab initio study
[AD-A288903] p 1936 N95-25529
TENSILE TESTS
Study on tensile fatigue testing method of unidirectional fiber-resin matrix composites
[NAL-TR-1241] p 1927 N95-25770
Recent progress in shear punch testing
[DE95-005962] p 1937 N95-26007
An experimental determination of the plastic anisotropy of metal
[IFTR-33/1994] p 1938 N95-26179
TENSORS
Two dimensional Bose plasma in a magnetic field
[DE95-607629] p 2082 N95-25976
The rotations of deformable bodies. Part 1: Geometry and Kinematics
[IFTR-7/1994] p 2039 N95-26332
TERMINAL BALLISTICS
Significance of varied thickness to damage tolerance of carbon fiber/epoxy laminates
[PB95-165460] p 1925 N95-24242
TERNARY ALLOYS
Superconductivity, magnetism and metal-insulator transitions in some ternary and pseudoternary 3d-, 4d- and 5d-metal oxides
[DE95-005904] p 2038 N95-25600
TERRAIN
Atmospheric and terrain effects on acoustic propagation
[AD-A288727] p 2039 N95-25503
Partial camera automation in a simulated Unmanned Air Vehicle
[AD-A288786] p 1913 N95-26190
TEST FACILITIES
The Superorbital Expansion Tube concept, experiment and analysis p 1915 N95-25399
Universal Test Facility p 1918 N95-26305
TEST STANDS
Facility for the evaluation of space communications and related systems
[NASA-TM-106904] p 1955 N95-25876
TEST VEHICLES
Developing a standardized test procedure for hybrid vehicles: The challenge of the SAE HEV task force
[DE95-000280] p 1978 N95-26286
TEXTURES
Evolution of plastic anisotropy for high-strain-rate computations
[DE95-004220] p 1941 N95-25237
The effect of encapsulation on the reflectance of photovoltaic modules using textured multicrystalline-silicon solar cells
[DE95-004781] p 1996 N95-26166
THALLIUM COMPOUNDS
Formation of thallium based high temperature superconductors using aerosol flow reacted precursor powders
[DE95-005901] p 2089 N95-25389
THEOREMS
Uniform rectifiability and singular sets
[PB95-165502] p 2028 N95-24243
Low energy theorems in quark potential models
[DE94-636791] p 2042 N95-24316
Involutive co-distributions preserved by transitive families of vector fields
[DE95-607078] p 2032 N95-25457
THEORETICAL PHYSICS
High Energy Physics Division research activities
[DE95-003985] p 2068 N95-24680
Probing new physics in rare charm processes
[DE95-006067] p 2050 N95-24903
A partial unification model in non-commutative geometry
[DE95-607129] p 2097 N95-25435
Research in elementary particle physics
[DE95-007323] p 2054 N95-25481
Physics in Ukraine International Conference. Volume 3: Statistical physics and phase transitions
[DE95-605765] p 2038 N95-25552
Theoretical studies in hadronic and nuclear physics
[DE95-006643] p 2098 N95-25562
Dynamical chiral symmetry breaking in scale invariant quantum electrodynamics in sixth dimensions
[DE95-607133] p 2099 N95-25667
Inelastic collisions of negative muons and hadrons with metastable hydrogen atoms
[DE95-607537] p 2056 N95-25668
THERAPY
Annual report of National Institute of Radiological Sciences
[DE94-792664] p 2009 N95-25902
THERMAL ANALYSIS
Thermohydrodynamic analysis of cryogenic liquid turbulent flow fluid film bearings, phase 2
[NASA-CR-197412] p 1962 N95-24461
Integration of design, structural, thermal and optical analysis: And user's guide for structural-to-optical translator (PATCOD)
[NASA-TM-110153] p 1950 N95-24559
LH2 fuel tank design for SSTO p 1987 N95-26309
THERMAL CONDUCTIVITY
Measurements of thermal conductivity of diamond thin films by the ac calorimetric method
[PB95-149746] p 1939 N95-24300
Magnetized target fusion: An overview of the concept
[DE95-005247] p 2070 N95-25594
Thermal conductivity of zirconia thermal barrier coatings p 1945 N95-26133
THERMAL CONTROL COATINGS
Thermal Barrier Coating Workshop
[NASA-CP-10170] p 1943 N95-26119
A design perspective on thermal barrier coatings p 1943 N95-26120
Thermal barrier coatings for aircraft engines: History and directions p 1943 N95-26121
Thermal barrier coatings issues in advanced land-based gas turbines p 1944 N95-26122
Measurement methods and standards for processing and application of thermal barrier coatings p 1944 N95-26123
Thermal barrier coatings application in diesel engines p 1944 N95-26124
Thermal barrier coating experience in the gas turbine engine p 1944 N95-26125
PVD TBC experience on GE aircraft engines p 1944 N95-26126
TBC experience in land based gas turbines p 1944 N95-26127
Perspective on thermal barrier coatings for industrial gas turbine applications p 1945 N95-26128
Overview of thermal barrier coatings in diesel engines p 1945 N95-26129
Thermal spray processing p 1945 N95-26130
Process, properties and environmental response of plasma sprayed thermal barrier coatings p 1945 N95-26132
Thermal conductivity of zirconia thermal barrier coatings p 1945 N95-26133
Mechanical properties testing and results for thermal barrier coatings p 1946 N95-26134

Thick thermal barrier coatings for diesel engines
p 1946 N95-26136
Some aspects of the hot corrosion of thermal barrier coatings p 1946 N95-26137
Thermal fracture mechanisms in ceramic thermal barrier coatings p 1946 N95-26138
A software tool to design thermal barrier coatings
p 1946 N95-26139
Thermal barrier coating life modeling in aircraft gas turbine engines p 1947 N95-26140

THERMAL CYCLING TESTS
BSA Delta Qualification 2, volume 3, book 1
[NASA-CR-196565] p 1922 N95-24845

THERMAL DEGRADATION
Using consumer IC packages in harsh high reliability applications
[DE94-016565] p 1959 N95-24713

THERMAL DIFFUSION
Thermal diffuse scattering in time-of-flight neutron diffraction studied on SBN single crystals
[DE94-637054] p 2085 N95-24362

THERMAL DIFFUSIVITY
NMR and optical studies of piezoelectric polymers
[DE95-003836] p 1940 N95-24554

THERMAL ENERGY
Differential neutron energy spectra measured on spacecraft low Earth orbit p 2062 N95-25932

THERMAL ENVIRONMENTS
The natural space environment: Effects on spacecraft
[NASA-RP-1350] p 1921 N95-25875

THERMAL EXPANSION
Method for molding structural parts utilizing modified silicone rubber
[NASA-CASE-LAR-15217-1] p 1939 N95-24212
The 24th Order high temperature expansion for the 3-D Ising model
[DE95-004952] p 2093 N95-24450

THERMAL INSULATION
Thermal barrier coating experience in the gas turbine engine p 1944 N95-26125

THERMAL NEUTRONS
Proceedings of the 1993 Symposium on Nuclear Data
[DE94-012554] p 2104 N95-24372
The facility for commercial doping of silicon by thermal neutrons in channel 3 at the IBR-2
[DE94-636293] p 2085 N95-24374
Observation of the scalar Aharonov-Bohm effect by neutron interferometry
[DE95-607020] p 2097 N95-25446

THERMAL NOISE
Read out electronics for thermal detectors of bolometer type
[PB95-141842] p 1967 N95-24280

THERMAL PLASMAS
Study of very high temperature technology, 2
[DE95-730105] p 2088 N95-24900

THERMAL PROTECTION
Heat flux instrumentation for HYFLITE thermal protection system
[NASA-CR-197715] p 1968 N95-25118
Debris/ice/TPS assessment and integrated photographic analysis of shuttle mission STS-63
[NASA-TM-110649] p 1921 N95-25337

THERMAL STABILITY
Characterization of ultradispersed aluminum
[DE95-006379] p 1933 N95-24329

THERMAL STRESSES
An evaluation of a coupled microstructural approach for the analysis of functionally graded composites via the finite-element method
[NASA-CR-195455] p 1925 N95-24438
Compensated high temperature strain gage
[NASA-CASE-LAR-14776-1] p 1968 N95-24625
Thermal fracture mechanisms in ceramic thermal barrier coatings p 1946 N95-26138

THERMAL VACUUM TESTS
Alternate method for achieving temperature control in the -160 to +90 Celcius range
[NASA-CASE-NPO-18995-1-CU] p 1969 N95-25547

THERMOCHEMISTRY
JALO: Fuel conversion
[DE95-737597] p 1949 N95-25244
Thermochemistry, kinetics and spectroscopy of Kr and Kr2F
[DE95-005732] p 1941 N95-25386

THERMOCOUPLES
Heat flux instrumentation for HYFLITE thermal protection system
[NASA-CR-197715] p 1968 N95-25118

THERMODYNAMIC EFFICIENCY
Optimized hydrogen piston engines
[DE95-003656] p 1975 N95-24550

THERMODYNAMIC PROPERTIES
High heat flux experiment on B4C-converted carbon based materials for plasma facing materials of JT-60U
[DE94-777545] p 2077 N95-24585
Performance evaluation of LE-7 high pressure pumps
[NAL-TR-1212T] p 1977 N95-25672
Structural and thermodynamic properties of 3-d transition metals: Pseudopotential theory revisited
[DE95-605639] p 1937 N95-25983
Calculating the thermodynamic properties of planar and spherical liquid-vapour interface
[DE95-608777] p 2100 N95-26105

THERMODYNAMICS
Parity doubling from thermodynamics of experimental hadron spectrum
[DE95-600934] p 2095 N95-24839
A solubility model for amorphous silica in concentrated electrolytes
[DE95-004896] p 1931 N95-25252
Statistical mechanics of nonlinear coherent structures: Kinks in the Phi(sup 6) model
[DE95-005253] p 2096 N95-25293
Ion beam mixing of titanium overlayers with hydroxyapaptite substrates
[DE95-005278] p 1935 N95-25379
Statistical mechanics of relativistic spin-1 bosons in a magnetic field
[DE95-607100] p 2054 N95-25474
Thermomechanical fatigue behavior of three CFCC's
[NASA-CR-195441] p 1927 N95-25880
Statistical mechanics of magnetized pair Fermi gas
[DE95-607097] p 2063 N95-25969
Statistical mechanics of the magnetized pair Bose gas
[DE95-607096] p 2063 N95-25993
Static recrystallization behavior of austenite in HSLA 100 during Thermomechanical Controlled Processing (TMCP)
[AD-A288737] p 1937 N95-26057
Center for Computational Structures Technology
[NASA-CR-198028] p 1983 N95-26263
Three-dimensional solutions for thermomechanical stresses in sandwich panels and shells
p 1984 N95-26265
Thermomechanical postbuckling of multilayered composite panels with cutouts p 1984 N95-26267
Recent advances in the sensitivity analysis for the thermomechanical postbuckling of composite panels
p 1985 N95-26274

THERMOELASTICITY
Thermoelastic equations for multi-layered cylindrical shell
[NAL-TR-1222] p 1982 N95-25661
Three-dimensional solutions for thermomechanical stresses in sandwich panels and shells
p 1984 N95-26265
Three-dimensional solutions for coupled thermoelectroelastic response of multilayered plates
p 1985 N95-26273
Assessment of computational models for thermoelectroelastic multilayered plates
p 1987 N95-26283

THERMOELECTRICITY
Direct energy conversion of radiation energy in fusion reactor
[NIFS-254] p 2072 N95-26250

THERMOGRAPHY
Turbine-engine applications of thermographic-phosphor temperature measurements
[DE95-003625] p 1989 N95-25110
Emerging nondestructive inspection for aging aircraft
[PB95-143053] p 1905 N95-25401

THERMOLUMINESCENCE
High-energy ionoluminescence of LiF
[DE94-629015] p 2087 N95-24891
Depth distribution of absorbed dose on the external surface of Cosmos 1887 biosatellite
p 2061 N95-25927

THERMOMECHANICAL TREATMENT
Study of very high temperature technology, 2
[DE95-730105] p 2088 N95-24900

THERMONUCLEAR REACTIONS
Proceedings of the 1993 Symposium on Nuclear Data
[DE94-012554] p 2104 N95-24372
Design of Fusion Safety Data Base
[DE95-703897] p 2080 N95-25495

THERMOSPHERE
The natural space environment: Effects on spacecraft
[NASA-RP-1350] p 1921 N95-25875

THICKNESS
Back surface cell structures for reducing recombination in CZ silicon solar cells
[DE95-005423] p 1995 N95-25566

THIN FILMS
Measurements of thermal conductivity of diamond thin films by the ac calorimetric method
[PB95-149746] p 1939 N95-24300
Characterization and performance of carbon films deposited by plasma and ion beam based techniques
[DE95-005213] p 1940 N95-24456
Thin film ionic conductors based on cerium oxide
[DE95-003668] p 2086 N95-24514
Heat flux instrumentation for HYFLITE thermal protection system
[NASA-CR-197715] p 1968 N95-25118
Effects of acetylacetone additions on PZT thin film processing
[DE95-006322] p 1941 N95-25370
Reciprocal space analysis of the microstructure of luminescent and nonluminescent porous silicon films
[DE95-005420] p 1941 N95-25382
Information compendium on solid film lubricants
[AD-A288360] p 1942 N95-25510
Temperature-dependent growth of LaAlO3 films on YBa2CuO7 C-axis films for multilayer structures
[DE95-005257] p 2089 N95-25598
In situ XAFS study of oxides formed on nickel thin film electrodes in KOH solution
[AD-A288735] p 1932 N95-26056
Applications of solid lubricant films in spacecraft
[AD-A288784] p 1947 N95-26188

THIN WALLS
An experimental determination of the plastic anisotropy of metal
[IFTR-33/1994] p 1938 N95-26179

THREADS
Experimental analysis of thread movement in bolted connections due to vibrations
[NASA-CR-197705] p 1975 N95-24991

THREAT EVALUATION
Analysis of data from a radar warning receiver with the accent on association of sensor reports
[PB95-141768] p 1953 N95-24836
Consistent approach to describing aircraft HIRF protection
[NASA-CR-195067] p 1909 N95-25341

THREE BODY PROBLEM
Generators of matrix factorable representations of block-tridiagonal and inverse matrices
[DE94-628387] p 2031 N95-24694
Domain decomposition and generators of direct methods of the solution of linear equation systems with general block-tridiagonal matrices
[DE94-628388] p 2031 N95-24695
Quasi-generalized matrix processes and representations of general block tridiagonal matrices
[DE94-628377] p 2031 N95-24704
Natural elementary factorization of general block-tridiagonal matrices in case of zero minors of both types
[DE94-628378] p 2031 N95-24705
Variational method for the calculation of the surface hyperspherical functions for the systems of ZH(mu)-type. The test calculation of the dt(mu)-system
[DE94-628905] p 2033 N95-25539

THREE DIMENSIONAL FLOW
Three-dimensional interaction of wake/boundary-layer and vortex/boundary-layer data report
[CUED/A-AEREO/TR-23] p 1906 N95-24210
Stereo imaging velocimetry for microgravity applications
[NASA-TM-110494] p 1949 N95-24416
A study of three-dimensional interaction flow fields between swept shock waves and turbulent boundary layers. Flow structures and effects of bleed
[NAL-TR-1227] p 1963 N95-25001
An annotation system for 3D fluid flow visualization
p 1966 N95-25869
Numerical simulation of laminar flow in a curved duct
[DE95-005427] p 1966 N95-26240

THREE DIMENSIONAL MODELS
On the central charge in 3 D-supersymmetry
[DE95-600851] p 2093 N95-24352
The 24th Order high temperature expansion for the 3-D Ising model
[DE95-004952] p 2093 N95-24450
Psychophysical evaluation of three-dimensional auditory displays
[NASA-CR-198010] p 2011 N95-24564
Parallel processing of atmospheric chemistry calculations: Preliminary considerations
[DE95-005915] p 1999 N95-25198
Orientation determination of aircraft using visual 3D matching and radar. Case study 2
[PB95-165791] p 1955 N95-25749
Three-dimensional user interfaces for scientific visualization
[NASA-CR-197923] p 2017 N95-25867
The 3D widgets for exploratory scientific visualization
p 1966 N95-25868
Impulsive Alfven coupling between the magnetosphere and ionosphere
[NIFS-276] p 2004 N95-26036
Time-dependent numerical simulation of vertical cavity lasers
[DE95-006862] p 1973 N95-26112

Three-dimensional solutions for thermomechanical stresses in sandwich panels and shells
p 1984 N95-26265
Three-dimensional solutions for coupled thermoelectroelastic response of multilayered plates
p 1985 N95-26273

THREE DIMENSIONAL MOTION
Effect of density gradients in confined supersonic shear layers. Part 2: 3-D modes
[NASA-CR-198030] p 1962 N95-24413

THRESHOLDS (PERCEPTION)
Visual contrast detection thresholds for aircraft contrails
[AD-A288618] p 1905 N95-25607

THRUST
Thrust measurement in a 2-D scramjet nozzle
p 1914 N95-25397

THRUST MEASUREMENT
Thrust measurements of a complete axisymmetric scramjet in an impulse facility p 1914 N95-25395
Scramjet thrust measurement in a shock tunnel
p 1914 N95-25396
Thrust measurement in a 2-D scramjet nozzle
p 1914 N95-25397
Balances for the measurement of multiple components of force in flows of a millisecond duration
p 1965 N95-25400

THRUST VECTOR CONTROL
Internal performance characteristics of thrust-vectored axisymmetric ejector nozzles
[NASA-TM-4610] p 1907 N95-25338

TIME DEPENDENCE
Time dependent indentation testing at non-ambient temperatures utilizing the high temperature mechanical properties microprobe
[DE95-005895] p 1933 N95-24432
Characteristics of an ultrafast x-ray streak camera
[DE95-004210] p 1968 N95-24657
Can the electric charges of elementary particles change with time?
[DE95-607194] p 2054 N95-25465
Plasma burning and control in reactor core
[DE95-602882] p 2082 N95-25942
Dynamics of phase ordering of nematics in a pore
[DE95-607662] p 2090 N95-25978

TIME DIVISION MULTIPLEXING
The impact of multiplexing on the dynamic requirements of analog-to-digital converters
[DE95-006302] p 1960 N95-25558

TIME LAG
Calibration of optical time domain reflectometers using time delay generator
[PB95-141776] p 2073 N95-24673
Tunable vibration absorbers: Key design parameters
[ISVR-TR-244] p 1981 N95-24995
A technique for the evaluation of strength of coupling between SEA subsystems
[ISVR-TR-241] p 1981 N95-24997

TIME MEASUREMENT
Recipes for high resolution time-of-flight detectors
[DE95-006196] p 1967 N95-24596
Detector for transit time measurement of photomultiplier single-photoelectron pulses
[DE94-628256] p 2073 N95-24642
Calibration of optical time domain reflectometers using time delay generator
[PB95-141776] p 2073 N95-24673
Multistatic radar: Synchronization and time reference system
[PB95-165288] p 1954 N95-25623

TIME SIGNALS
Multistatic radar: Synchronization and time reference system
[PB95-165288] p 1954 N95-25623

TIN ISOTOPES
Fe-57 and Sn-119 Moessbauer studies on La(1.25)Nd(0.6)Sr(0.15)CuO4: Evidence for local magnetic ordering below (approx. equal) 32 K
[DE95-601210] p 1959 N95-25405

TIRES
Reduction technique for tire contact problems
p 1986 N95-26277
Computational strategies for tire monitoring and analysis p 1978 N95-26282

TITAN
Infrared spectroscopy of Jupiter and Saturn
[NASA-CR-198034] p 2111 N95-24239

TITANATES
Solution based synthesis of perovskite-type oxide films and powders
[DE95-006170] p 2086 N95-24594

TITANIUM
One-step in-diffusion as a result of multipulse laser irradiation of LiNbO3 single-crystalline substrates covered with thin Ti deposits on the effect of the radiation wavelength
[DE94-634524] p 2084 N95-24324
JPRS report: Science and technology. Central Eurasia
[JPRS-UST-95-012] p 1950 N95-25540
Ion beam mixing of titanium overlayers with hydroxyapaptite substrates
[DE95-005278] p 1935 N95-25379

TITANIUM ALLOYS
Stability and elastic properties of hydrogen loaded Ti(1-x)Al(x) alloys: An ab initio study
[AD-A288903] p 1936 N95-25529
Issues related to prediction of residual stresses in titanium alloy matrix composites
[DE95-005243] p 1926 N95-25596
Improved lubrication performance of sputtered MoS2 film by surface treatments of Ti-alloy substrate
[NAL-TR-1213] p 1942 N95-25760
A fully associative, nonisothermal, nonlinear kinematic, unified viscoplastic model for titanium alloys
[NASA-TM-106926] p 1983 N95-26078

TITANIUM BORIDES
Strengthening of NiAl matrix composites
[AD-A288923] p 1926 N95-25505

TOKAMAK DEVICES
Fusion-neutron diagnostic on the Microwave Tokamak Experiment
[DE94-777530] p 2075 N95-24270
A proposal to introduce a turbulence factor into a diffusion coefficient of a Tokamak plasma
[DE94-777533] p 2075 N95-24272
Outline of fast analyzer for MHD equilibrium FAME
[DE94-777540] p 2076 N95-24311
Design study of a negative-ion based NBI system for JT-60U
[DE94-785265] p 2043 N95-24339
UEDGE and DEGAS modeling of the DIII-D scrape-off layer plasma
[DE95-003652] p 2076 N95-24490
Phase 3 experiments of the JAERI/USDOE collaborative program on fusion blanket neutronics. Volume 1: Experiment
[DE94-777528] p 2076 N95-24511
The physics design of the Tokamak Physics Experiment
[DE95-003649] p 2076 N95-24548
High heat flux experiment on B4C-converted carbon based materials for plasma facing materials of JT-60U
[DE94-777545] p 2077 N95-24585
Transport suppression by diamagnetic phase shift as a possible mechanism to the L to H transition
[DE95-003345] p 2077 N95-24587
Experimental and theoretical basis for advanced tokamaks
[DE95-003255] p 2077 N95-24646
Divertor design for the Tokamak Physics Experiment
[DE95-003653] p 2078 N95-24650
Modeling plasma/material interactions during a tokamak disruption
[DE95-004247] p 2078 N95-24861
The role of shaping in achieving high performance in DIII-D
[DE95-003877] p 2078 N95-25102
A vacuum window for a 1 MW CW 110 GHz gyrotron
[DE94-016584] p 2079 N95-25108
Results obtained using the pellet charge exchange diagnostic on TFTR
[DE95-003254] p 2079 N95-25120
Energetic particle drive for toroidicity-induced Alfven eigenmodes and kinetic toroidicity-induced Alfven eigenmodes in a low-shear Tokamak
[DE95-003222] p 2079 N95-25216
US technical report for the ITER blanket/shield
[DE95-004667] p 2079 N95-25283
Using and programming the SUPERCODE
[DE95-004342] p 2080 N95-25344
Numerical analysis of electron cyclotron resonance heating on JT-60U and JFT-2M
[DE95-709766] p 2080 N95-25471
Maryland controlled fusion research program
[DE95-006642] p 2081 N95-25561
Measurement of profiles of the space potential in JIPP T-IIU Tokamak plasmas by slow poloidal and fast toroidal sweeps of a heavy ion beam
[NIFS-273] p 2081 N95-25651
Operating level of HT-6B tokamak device
[DE95-602999] p 2082 N95-25943

TOMOGRAPHY
Emerging nondestructive inspection for aging aircraft
[PB95-143053] p 1905 N95-25401

TOPOGRAPHY
Mars observer mission: Mapping the Martian world
[NASA-CR-110585] p 2112 N95-24672
Partial camera automation in a simulated Unmanned Air Vehicle
[AD-A288786] p 1913 N95-26190

TOPOLOGY
Finite quantum physics and noncommutative geometry
[DE94-634282] p 2027 N95-24228
The geometry of weak solutions of certain integrable nonlinar PDE's
[DE95-005241] p 2030 N95-24609
Symbolic dynamics of the Lorenz equations
[DE95-607045] p 2036 N95-25439
Recoil effects in quantum topological solitons
[DE95-607006] p 2097 N95-25454
Semiglobal Alice strings
[DE95-607081] p 2098 N95-25527

TOROIDAL PLASMAS
A proposal to introduce a turbulence factor into a diffusion coefficient of a Tokamak plasma
[DE94-777533] p 2075 N95-24272
Transport reduction by current profile control in the reversed field pinch
[DE95-007016] p 2077 N95-24619
Energetic particle drive for toroidicity-induced Alfven eigenmodes and kinetic toroidicity-induced Alfven eigenmodes in a low-shear Tokamak
[DE95-003222] p 2079 N95-25216
Self-sustained turbulence and L-mode confinement in toroidal plasmas 2
[NIFS-278] p 2082 N95-25759
Proceedings of the 2nd international workshop on electromagnetic forces and related effects on blankets and other structures surrounding the fusion plasma torus
[DE94-792667] p 2082 N95-25903
A normal form approach to the theory of nonlinear betatronic motion
[DE95-603831] p 2062 N95-25944

TOROIDS
Toroidal response in magnetic resonance
[DE94-628406] p 2037 N95-24696

TORQUE
Intrinsic magnetic torque at low magnetic induction
[DE95-601209] p 1959 N95-24842

TORSION
On squaring the primary constraints in a generalized Hamiltonian dynamics
[DE94-628500] p 2036 N95-24504

TORSIONAL VIBRATION
An analytical study of the vibration of beams fitted with neutralizers. Part 3: Torsional wave motion
[ISVR-TR-238-PT-3] p 1982 N95-25003

TORUSES
Construction of quasi-periodic solutions for Hamiltonian perturbations of linear equations and applications to nonlinear PDE
[PB95-165551] p 2028 N95-24322

TOTAL QUALITY MANAGEMENT
Continual improvement plan
[NASA-TM-110574] p 2103 N95-25849

TOUGHNESS
Processing and characterization of transformation-toughened ceramics with strength retention to elevated temperatures
[DE95-005758] p 1941 N95-25387

TOXIC HAZARDS
SPEEDUP simulation of liquid waste batch processing, revision 1
[DE95-001240] p 1939 N95-24344
Resolving the ambiguities: An industrial hygiene Indoor Air Quality (IAQ) symposium
[DE95-005391] p 2000 N95-25380
Nuclear energy and the environment
[DE95-600438] p 2001 N95-25615
National standard and code compliance for electrical equipment installed in hazardous locations for the void fraction instrument
[DE95-002158] p 1960 N95-26092

TOXICITY
The evaluation of potential limonene scavengers
[DE95-006853] p 2002 N95-25899
Disposal of electronic equipment
[PB95-177861] p 2002 N95-26047
Testing of experimental antileishmanial compounds
[AD-A288807] p 2009 N95-26193

TRACE ELEMENTS
Determination of trace elements in plutonium by solvent extraction and ICP-atomic emission spectrometry
[DE94-634887] p 2042 N95-24269

TRACKING (POSITION)
A preview of a modular surface light scattering instrument with autotracking optics
[NASA-TM-110495] p 2072 N95-24386
A fast tracking method using resonance basis Hamiltonians
[DE95-004292] p 2068 N95-24664

TRACKING PROBLEM
Adaptive projective filters
[DE94-628374] p 2030 N95-24645
Control theory and splines, applied to signature storage p 2027 N95-25804
TRAJECTORIES
Regge in the sky: Origin of the cosmic rotation
[DE95-607001] p 2111 N95-25990
TRAJECTORY CONTROL
Hierarchical Control and Trajectory Planning
[NASA-CR-197922] p 2026 N95-25801
TRAJECTORY OPTIMIZATION
Eigenvector method for optimized orbit correction
[DE95-005967] p 2071 N95-25785
Optimal guidance law development for an advanced launch system
[NASA-CR-4667] p 1917 N95-26205
TRAJECTORY PLANNING
Hierarchical Control and Trajectory Planning
[NASA-CR-197922] p 2026 N95-25801
Heuristic approach to the path planning problem in a raster map
[PB95-141826] p 2034 N95-25893
TRANSDUCERS
Workshop report: Measurement techniques in highly transient, spectrally rich combustion environments
[AD-A288395] p 1969 N95-25606
TRANSEARTH INJECTION
Optimal guidance law development for an advanced launch system
[NASA-CR-4667] p 1917 N95-26205
TRANSFER FUNCTIONS
Aerodynamic parameter estimation via Fourier modulating function techniques
[NASA-CR-4654] p 1911 N95-24630
TRANSFORMATIONS (MATHEMATICS)
Dissipative quantum mechanics: The generalization of the canonical quantization and von Neumann equation
[DE95-607008] p 2096 N95-25426
Splines in two-dimensional problems
[IFTR-2/1993] p 2035 N95-26106
TRANSIENT RESPONSE
Tunable vibration absorbers: Key design parameters
[ISVR-TR-244] p 1981 N95-24995
A higher-order projection method for the simulation of unsteady turbulent nonpremixed combustion in an industrial burner
[DE95-005919] p 1931 N95-25291
TRANSIT TIME
Detector for transit time measurement of photomultiplier single-photoelectron pulses
[DE94-628256] p 2073 N95-24642
Radial electron-beam-breakup transit-time oscillator
[DE95-005731] p 1959 N95-25385
TRANSITION FLOW
Study of compressible flow through a rectangular-to-semiannular transition duct
[NASA-CR-4660] p 1914 N95-24392
TRANSITION METALS
Generation, detection and characterization of gas-phase transition metal aggregates and compounds
[DE95-004439] p 1930 N95-24686
The transformation of organic amines by transition metal cluster compounds
[DE95-004180] p 1923 N95-24851
The geometry of disorder: Theoretical investigations of quasicrystals and frustrated magnets
[DE95-006641] p 1936 N95-25560
Structural and thermodynamic properties of 3-d transition metals: Pseudopotential theory revisited
[DE95-605639] p 1937 N95-25983
TRANSITION TEMPERATURE
Effect of He pressure on the superconducting transition temperatures of Na2CsC60 and (NH3)4Na2CsC60
[DE95-006320] p 2087 N95-24616
Statistical mechanics of the magnetized pair Bose gas
[DE95-607096] p 2063 N95-25993
TRANSLATING
Dialogue transcription tools
[TN-94-1] p 2016 N95-24536
Partial camera automation in a simulated Unmanned Air Vehicle
[AD-A288786] p 1913 N95-26190
TRANSMISSION ELECTRON MICROSCOPY
Transmission electron microscope studies of extraterrestrial materials
[NASA-CR-188363] p 1928 N95-24222
TRANSMISSION LINES
Application of optical fiber amplifier for wavelength division multiplexing communication system. Part 2: Design of four-channel transmission system using two EDFA repeaters
[DE95-730179] p 1952 N95-24491
Crosstalk on printed circuit boards
[PB95-165171] p 1960 N95-25472
Towards an era of global village: The dynamics of world telecommunications and its implications for the future of nation state
[PB95-165064] p 1954 N95-25482
TRANSMISSIONS (MACHINE ELEMENTS)
A portable transmission vibration analysis system for the S-70A-9 Black Hawk helicopter
[DSTO-TR-0072] p 1966 N95-24203
Computerized design and generation of low-noise gears with localized bearing contact
[NASA-TM-106880] p 1977 N95-26074
Transmission diagnostic research at NASA Lewis Research Center
[NASA-TM-106901] p 1977 N95-26076
TRANSONIC FLOW
Hot-wire calibration in subsonic/transonic flow regimes
[NASA-CR-197725] p 1970 N95-25699
TRANSONIC WIND TUNNELS
Development of a model protection and dynamic response monitoring system for the national transonic facility
[NASA-CR-195041] p 1915 N95-24388
TRANSPORT AIRCRAFT
Emerging nondestructive inspection for aging aircraft
[PB95-143053] p 1905 N95-25401
A quiet STOL Research Aircraft Development program
[NAL-TR-1223] p 1911 N95-25862
TRANSPORT PROPERTIES
Copper transport on oxygen annealing of a superconducting film Y-Ba-Cu-O
[DE94-627566] p 2086 N95-24537
Experimental constraints on transport
[DE95-004962] p 2050 N95-25180
Evidence for modified transport due to sheared E x B flows in high-temperature plasmas
[DE95-004870] p 2079 N95-25250
Fast algorithms for transport models
[DE95-007064] p 2054 N95-25479
Benchmark testing and independent verification of the VS2DT computer code
[DE95-004386] p 1965 N95-25485
Self-sustained turbulence and L-mode confinement in toroidal plasmas 2
[NIFS-278] p 2082 N95-25759
HZE beam transport in multilayered materials p 2060 N95-25922
Predicting the transport properties of sedimentary rocks from microgeometry
[DE95-000129] p 2004 N95-26089
TRANSPORT THEORY
Transport suppression by diamagnetic phase shift as a possible mechanism to the L to H transition
[DE95-003345] p 2077 N95-24587
Plasma burning and control in reactor core
[DE95-602882] p 2082 N95-25942
Development of novel active transport membrane devices
[DE95-002658] p 1932 N95-26093
Isotope effect on confinement in DT plasmas
[NIFS-275] p 2083 N95-26326
TRANSPORTATION
Heat release rate measurements in tunnel fires
[PB95-165106] p 1931 N95-25443
Sector-specific issues and reporting methodologies supporting the general guidelines for the voluntary reporting of greenhouse gases under Section 1605(b) of the Energy Policy Act of 1992, Volume 2. Part 4: Transportation sector. Part 5: Forestry sector. Part 6: Agricultural sector
[DE95-003297] p 2003 N95-26065
TRANSPUTERS
Low-cost image analysis system
[DE95-005021] p 2021 N95-25378
TRANSVERSE WAVES
The diffraction of electromagnetic waves by screens placed at the boundaries of dielectric media
[IFTR-4/1994] p 1954 N95-25393
TRAPPED PARTICLES
Maryland controlled fusion research program
[DE95-006642] p 2081 N95-25561
TRAPPING
Magnetized target fusion: An overview of the concept
[DE95-005247] p 2070 N95-25594
TRAYS
Spacecraft materials studies on The Aerospace Corporation Tray on EOIM-3
[AD-A288682] p 1942 N95-26049
TREES (MATHEMATICS)
A parallel, portable and versatile treecode
[DE95-000842] p 2019 N95-24343
TREES (PLANTS)
Diurnal variations of backscattering properties of pine trees at C- and X-bands
[PB95-149738] p 1988 N95-24299
TRELLIS CODING
On the Trellis structure of a (64,40,8) subcode of the (64,42,8) third-order Reed-Muller code
[NASA-CR-198019] p 2015 N95-24224
TRIBOLOGY
Characterization and performance of carbon films deposited by plasma and ion beam based techniques
[DE95-005213] p 1940 N95-24456
Information compendium on solid film lubricants
[AD-A288360] p 1942 N95-25510
Wear-resistant, self-lubricating surfaces of diamond coatings
[NASA-TM-106887] p 1924 N95-25961
TRIGONOMETRIC FUNCTIONS
Behavior of a trigonometric polynomial with given number of terms on small subsets of the unit circumference (norm duplication problem)
[PB95-165544] p 2028 N95-24321
TRITIUM
Carbons and hydrogen by persistent metal radicals
[DE95-003834] p 1929 N95-24553
Benchmark experiment on a copper slab assembly bombarded by D-T neutrons
[DE95-709764] p 2055 N95-25497
TRITON
Distribution and nature of UV absorbers on Trition's surface
[NASA-CR-198008] p 2112 N95-26116
TROPICAL REGIONS
Impacts of microphysics, radiation and environmental winds in mid-latitude and tropical squall-line systems, and their climatic implications
[DE95-004965] p 2005 N95-25287
TROPOSPHERE
Airborne imaging of tropospheric emission at millimeter and submillimeter wavelengths
[NASA-TM-110498] p 2003 N95-24336
Nucleation and growth of crystals under cirrus and polar stratospheric cloud conditions
[NASA-CR-197991] p 2085 N95-24478
JPRS report: Science and technology. Central Eurasia
[JPRS-UST-95-013] p 1987 N95-24538
The whitehouse effect: Shortwave radiative forcing of climate by anthropogenic aerosols
[DE95-005998] p 2001 N95-25442
Effects of nitric acid vapor on the formation of cloud droplets in troposphere
[DE95-744869] p 2001 N95-25500
TROPOSPHERIC RADIATION
The whitehouse effect: Shortwave radiative forcing of climate by anthropogenic aerosols
[DE95-005998] p 2001 N95-25442
TRUCKS
Waste minimization assessment for a manufacturer of parts for truck engines
[PB95-144481] p 1911 N95-26062
TRUNCATION ERRORS
On the numerical method for analysis of the dynamics of the classical Hamiltonian systems
[DE95-605218] p 2034 N95-25906
TRUSSES
Dynamic analysis of truss members using longitudinal waves
[IFTR-35/1994] p 1981 N95-24996
TUMBLING MOTION
Flexible architectures for sensor fusion in theater missile defense
[AD-A288666] p 2007 N95-26048
TUNABLE LASERS
Tunable diode lasers as continuous emission monitors for thermal waste treatment processes
[DE95-004381] p 1972 N95-25549
TUNGSTEN
Accurate determination of IC modulation parameter in Sr(x)Ba(1-x)Nb2O6 from second order satellites of neutron diffraction TOF (Time-Of-Flight) spectra
[DE94-629003] p 2090 N95-25851
TUNGSTEN ALLOYS
A study of the electrochemical behavior of tungsten in caustic solutions and platinum/iridium in ch loride solutions
[DE95-004951] p 1930 N95-25123
TUNNEL DIODES
Current-voltage characteristics of a tunnel junction with resonant centers
[DE94-634530] p 1956 N95-24245
GaAsSb-based heterojunction tunnel diodes for tandem solar cell interconnects
[DE95-004779] p 1990 N95-24264
TUNNEL JUNCTIONS
Current-voltage characteristics of a tunnel junction with resonant centers
[DE94-634530] p 1956 N95-24245
GaAsSb-based heterojunction tunnel diodes for tandem solar cell interconnects
[DE95-004779] p 1990 N95-24264

Device-quality tunnel junctions on the high (T(sub c)) super conductor HgBa2CuO(4+delta)
[DE95-004646] p 2084 N95-24279
BCS-like gap structure of HgBa2CuO(4+delta) tunnel junctions
[DE95-004125] p 2087 N95-24855

TUNNELS
Heat release rate measurements in tunnel fires
[PB95-165106] p 1931 N95-25443

TURBINE BLADES
Using digital filtering techniques as an aid in wind turbine data analysis
[DE94-011862] p 1993 N95-24853
NREL airfoil families for HAWTs
[DE95-000267] p 1994 N95-24882

TURBINE ENGINES
Turbine-engine applications of thermographic-phosphor temperature measurements
[DE95-003625] p 1989 N95-25110
A design perspective on thermal barrier coatings
p 1943 N95-26120

TURBINE EXHAUST NOZZLES
TBC experience in land based gas turbines
p 1944 N95-26127

TURBINE PUMPS
Simplified liquid oxygen propellant conditioning concepts
[NASA-TM-108482] p 1948 N95-24558
Performance evaluation of LE-7 high pressure pumps
[NAL-TR-1212T] p 1977 N95-25672

TURBOFAN ENGINES
Bird ingestion into large turbofan engines
[DOT/FAA/CT-93/14] p 1909 N95-24631

TURBULENCE
Spectrum and energy transfer in steady Burgers turbulence
[NASA-CR-195047] p 1963 N95-24584
Techniques for the investigation of wave turbulence in water wave data
[AD-A288392] p 2007 N95-25605
Classical closure theory and Lam's interpretation of epsilon-RNG
[NASA-CR-195061] p 1965 N95-25960
A pseudo-sound constitutive relationship for the dilatational covariances in compressible turbulence: An analytical theory
[NASA-CR-195064] p 1966 N95-25964
The phenomenon of non-linearity accompanying the action of acoustic pressure on a Helmholtz resonator
[IFTR-19/1994] p 2040 N95-26108

TURBULENCE EFFECTS
Laser beam log amplitude temporal scintillation spectrum due to crosswind. Part 1: Theory
[TR-1-FSRC-1994-PT-1] p 1971 N95-24371

TURBULENCE MODELS
A review of Reynolds stress models for turbulent shear flows
[NASA-CR-195054] p 1962 N95-24580
Spectrum and energy transfer in steady Burgers turbulence
[NASA-CR-195047] p 1963 N95-24584
A higher-order projection method for the simulation of unsteady turbulent nonpremixed combustion in an industrial burner
[DE95-005919] p 1931 N95-25291
Classical closure theory and Lam's interpretation of epsilon-RNG
[NASA-CR-195061] p 1965 N95-25960

TURBULENT BOUNDARY LAYER
Effects of cavity dimensions, boundary layer, and temperature on cavity noise with emphasis on benchmark data to validate computational aeroacoustic codes
[NASA-CR-4653] p 2039 N95-24879
A study of three-dimensional interaction flow fields between swept shock waves and turbulent boundary layers. Flow structures and effects of bleed
[NAL-TR-1227] p 1963 N95-25001

TURBULENT COMBUSTION
A higher-order projection method for the simulation of unsteady turbulent nonpremixed combustion in an industrial burner
[DE95-005919] p 1931 N95-25291

TURBULENT DIFFUSION
Transport suppression by diamagnetic phase shift as a possible mechanism to the L to H transition
[DE95-003345] p 2077 N95-24587
Fluctuations and electromagnetic wave scattering in macroscopically agitated plasma: Effects of turbulent diffusion
[DE95-607612] p 2081 N95-25617

TURBULENT FLOW
Thermohydrodynamic analysis of cryogenic liquid turbulent flow fluid film bearings, phase 2
[NASA-CR-197412] p 1962 N95-24461
Solutions of turbulent backward-facing step flow with heat transfer using the finite volume method
[DE95-003360] p 1962 N95-24489
A review of Reynolds stress models for turbulent shear flows
[NASA-CR-195054] p 1962 N95-24580
A review of chemically reactive turbulent flow analysis, mixing mechanisms and modeling, and a new design of low NOx combustor for non-premixed reactants
p 1963 N95-24762
A higher-order projection method for the simulation of unsteady turbulent nonpremixed combustion in an industrial burner
[DE95-005919] p 1931 N95-25291
A pseudo-sound constitutive relationship for the dilatational covariances in compressible turbulence: An analytical theory
[NASA-CR-195064] p 1966 N95-25964
Numerical calculations of shock-wave/boundary-layer flow interactions
[NASA-TM-106694] p 1966 N95-26077

TURBULENT JETS
Crossflow mixing of noncircular jets
[NASA-TM-106865] p 1913 N95-24390

TURBULENT MIXING
A review of chemically reactive turbulent flow analysis, mixing mechanisms and modeling, and a new design of low NOx combustor for non-premixed reactants
p 1963 N95-24762

TVD SCHEMES
Investigation of convection and pressure treatment with splitting techniques
[NASA-TM-106868] p 1961 N95-24399

TWINNING
Temperature and strain-rate effects on deformation mechanisms in irradiated stainless steel
[DE95-004941] p 1934 N95-24449

TWO DIMENSIONAL FLOW
Thrust measurement in a 2-D scramjet nozzle
p 1914 N95-25397
Benchmark testing and independent verification of the VS2DT computer code
[DE95-004386] p 1965 N95-25485
A combined geometric approach for solving the Navier-Stokes equations on dynamic grids
[NASA-TM-106919] p 1908 N95-26075

TWO DIMENSIONAL MODELS
Exact solution of 2 D Poincare gravity coupled with fermion matter
[DE95-605314] p 2099 N95-25967
Splines in two-dimensional problems
[IFTR-2/1993] p 2035 N95-26106
Sensitivity analysis of the non-linear dynamic viscoplastic response of 2-d structures with respect to material parameters p 1984 N95-26266

TWO PHASE FLOW
Studies of two-phase gas-liquid flow in microgravity
[NASA-CR-195434] p 1963 N95-24906

U

U.S.S.R. SPACE PROGRAM
JPRS report: Science and technology. Central Eurasia: Space
[JPRS-USP-94-007] p 1915 N95-24358

UH-1 HELICOPTER
Assessment of overhaul surge margin tests applied to the T53 engines in ADF Iroquois helicopters
[AR-008-389] p 1914 N95-25936

UH-60A HELICOPTER
A portable transmission vibration analysis system for the S-70A-9 Black Hawk helicopter
[DSTO-TR-0072] p 1966 N95-24203

UKRAINE
Display technologies in Russia, Ukraine, and Belarus
[ISBN-1-883712-36-X] p 2085 N95-24460
Physics in Ukraine International Conference. Volume 3: Statistical physics and phase transitions
[DE95-605765] p 2038 N95-25552
Physics in Ukraine International Conference. Volume 5: Low temperature physics
[DE95-605800] p 2038 N95-25553
Physics in Ukraine International Conference. Volume 1: Physics of elementary particles and quantum field theory. General problems
[DE95-606413] p 2056 N95-25554
Physics in Ukraine International Conference. Volume 6: Plasma physics
[DE95-606422] p 2081 N95-25555

ULTRASONIC TESTS
Method and apparatus for non-destructive evaluation of composite materials with cloth surface impressions
[NASA-CASE-LAR-14535-1] p 1926 N95-25305
Emerging nondestructive inspection for aging aircraft
[PB95-143053] p 1905 N95-25401

ULTRASONICS
The characteristics and design of an apparatus constructed by the Institute of Basic Problems of Technology to study relaxation phenomena in liquids at frequencies of 10-150 MHz
[IFTR-21/1994] p 1932 N95-25959

ULTRAVIOLET ASTRONOMY
Large-format high resolution microchannel plate detectors for ultraviolet astronomy
[NASA-CR-197993] p 2108 N95-25104

ULTRAVIOLET DETECTORS
Large-format high resolution microchannel plate detectors for ultraviolet astronomy
[NASA-CR-197993] p 2108 N95-25104
A quality monitor and monitoring technique employing optically stimulated electron emission
[NASA-CASE-LAR-15063-1-CU] p 1978 N95-25304
Automatic measurement system for measuring of the nonlinearity of photo detectors
[PB95-165197] p 2074 N95-25999

ULTRAVIOLET RADIATION
One-step in-diffusion as a result of multipulse laser irradiation of LiNbO3 single-crystalline substrates covered with thin Ti deposits on the effect of the radiation wavelength
[DE94-634524] p 2084 N95-24324
Advanced Light Source report
[DE95-003449] p 2073 N95-24546
A quality monitor and monitoring technique employing optically stimulated electron emission
[NASA-CASE-LAR-15063-1-CU] p 1978 N95-25304
Distribution and nature of UV absorbers on Triton's surface
[NASA-CR-198008] p 2112 N95-26116

ULTRAVIOLET TELESCOPES
STS-67 post flight presentation
[NASA-TM-110552] p 1918 N95-24198

UMBILICAL CONNECTORS
Go for EVA
[NASA-TM-110537] p 1918 N95-24195

UNCONTROLLED REENTRY (SPACECRAFT)
Space basic
[NASA-TM-110540] p 2108 N95-24196

UNDERGROUND STORAGE
Electrochemical organic destruction in support of Hanford tank waste pretreatment
[DE95-002854] p 1924 N95-25248
National standard and code compliance for electrical equipment installed in hazardous locations for the void fraction instrument
[DE95-002158] p 1960 N95-26092

UNDERWATER OPTICS
Average cosine meter and high spectral resolution measurements at the marine light mixed layer site
[AD-A288713] p 1970 N95-26113

UNIQUENESS
Numerical solution of the optimized random phase approximation
[DE95-605636] p 2034 N95-25982

UNITED KINGDOM
Helicopter life substantiation: Review of some USA and UK initiatives
[DSTO-TR-0062] p 1905 N95-24201

UNITED STATES
Helicopter life substantiation: Review of some USA and UK initiatives
[DSTO-TR-0062] p 1905 N95-24201
Science in the national interest
[ISBN-0-16-045186-8] p 2115 N95-26335

UNIVERSE
A quantum gravitational mechanism for exiting inflation
[DE95-003342] p 2096 N95-24867
Creation and development of the Universe (symmetry approach)
[DE94-628558] p 2109 N95-24884
Tachyon condensates and anisotropic universe
[DE95-607074] p 2097 N95-25456

UNIVERSITIES
A report: A plan to establish Internet access points at Minority Campus sites for connection to a central computing facility
[DE95-004374] p 2105 N95-25240

UNIVERSITY PROGRAM
Maryland controlled fusion research program
[DE95-006642] p 2081 N95-25561
The 1994 NASA/USRA/ADP Design Projects
[NASA-CR-197415] p 2101 N95-26304

UNSTEADY AERODYNAMICS
Application of neural networks to unsteady aerodynamic control p 2024 N95-25264

UNSTEADY FLOW
High frequency flow-structural interaction in dense subsonic fluids
[NASA-CR-4652] p 1906 N95-24217

Thermohydrodynamic analysis of cryogenic liquid turbulent flow fluid film bearings, phase 2
[NASA-CR-197412] p 1962 N95-24461
A higher-order projection method for the simulation of unsteady turbulent nonpremixed combustion in an industrial burner
[DE95-005919] p 1931 N95-25291
Benchmark testing and independent verification of the VS2DT computer code
[DE95-004386] p 1965 N95-25485
Recent improvements to and validation of the one dimensional NASA wave rotor model
[NASA-TM-106913] p 1908 N95-25962
A combined geometric approach for solving the Navier-Stokes equations on dynamic grids
[NASA-TM-106919] p 1908 N95-26075

UNSTRUCTURED GRIDS (MATHEMATICS)
Parallel algorithms for dynamically partitioning unstructured grids
[DE95-001616] p 2015 N95-24346

UPPER SURFACE BLOWING
A quiet STOL Research Aircraft Development program
[NAL-TR-1223] p 1911 N95-25862

URANIUM
Development of a portable mass spectrometric system for determination of isotopic composition of solid uranium samples using fluorine volatilization
[DE95-005728] p 1969 N95-25384

URANIUM FLUORIDES
Development of a portable mass spectrometric system for determination of isotopic composition of solid uranium samples using fluorine volatilization
[DE95-005728] p 1969 N95-25384

URANIUM ISOTOPES
Development of a portable mass spectrometric system for determination of isotopic composition of solid uranium samples using fluorine volatilization
[DE95-005728] p 1969 N95-25384

URANIUM OXIDES
Development of a portable mass spectrometric system for determination of isotopic composition of solid uranium samples using fluorine volatilization
[DE95-005728] p 1969 N95-25384

URANUS (PLANET)
Voyager: The grandest tour. The mission to the outer planets
[NASA-CR-197708] p 2112 N95-25854

USER MANUALS (COMPUTER PROGRAMS)
Structure and manual of radioisotope-production data base, ISOP
[DE94-785197] p 2043 N95-24337
Activity Management System user reference manual
[DE95-000989] p 2105 N95-24654
Users manual for KSP data-structure-neutral codes implementing Krylov space methods
[DE95-004265] p 2020 N95-24658
Using and programming the SUPERCODE
[DE95-004342] p 2080 N95-25344
User's manual for FAROW: Fatigue and reliability of wind turbine components, version 1.1
[DE95-005530] p 1995 N95-26037
Long Duration Exposure Facility mini-data base user's guide: IBM-compatible PC computer version
[NASA-CR-4655] p 1925 N95-26072

UTAH
Long-Term Flow Test number 1: Roosevelt Hot Springs, Utah
[DE95-004995] p 2004 N95-25666

V

VACUUM
A vacuum window for a 1 MW CW 110 GHz gyrotron
[DE94-016584] p 2079 N95-25108
Performance of solid lubricated ball bearings at high-temperatures in a vacuum
[NAL-TR-1243] p 1976 N95-25323
Mass splitting of the pseudoscalar and vector mesons induced by the homogeneous vacuum gluon field
[DE95-605322] p 2058 N95-25908
Excited states of mesons within the NJL model with the homogeneous vacuum gluon field
[DE95-605323] p 2058 N95-25909
Vacuum polarization effects in low-energy muonic atom collisions
[DE95-605393] p 2058 N95-25910
On a possible explanation of the origin of the quark mass spectrum
[DE95-605315] p 2063 N95-25968

VACUUM CHAMBERS
PEP-2 vacuum system: Joining SS flanges to copper beam chambers
[DE95-006093] p 1974 N95-24356
Target injection methods for inertial fusion energy
[DE95-003654] p 2067 N95-24651

VACUUM EFFECTS
The potential of vacuum microelectronics for space reactor applications
[DE95-000542] p 1958 N95-24586
Matrix element and complex l-plane evaluation of two-loop vacuum amplitudes in QED on S4
[DE95-607099] p 2097 N95-25473
Vacuum polarization effects in low-energy muonic atom collisions
[DE95-605393] p 2058 N95-25910

VACUUM SYSTEMS
Measurement of the magnetically-induced QED birefringence of the vacuum and an improved search for laboratory axions: Project definition study of the use of assets and facilities of the Superconducting Super Collider Laboratory
[DE95-005110] p 2065 N95-24317
PEP-2 vacuum system: Joining SS flanges to copper beam chambers
[DE95-006093] p 1974 N95-24356

VALENCE
Optical determinations of energy-band dispersion curves in novel compound semiconductor materials
[DE95-006318] p 2089 N95-25353

VALVES
Investigation of a rotary valving system with variable valve timing for internal combustion engines
[DE95-003831] p 1976 N95-25101

VAPOR DEPOSITION
A statistical analysis of the effect of PECVD deposition parameters on surface and bulk recombination in silicon solar cells
[DE95-004780] p 1994 N95-25360
Potential of diamond for applications in microelectronics
[PB95-141446] p 1942 N95-25633
Measurement methods and standards for processing and application of thermal barrier coatings
p 1944 N95-26123
PVD TBC experience on GE aircraft engines
p 1944 N95-26126
Thermal conductivity of zirconia thermal barrier coatings p 1945 N95-26133
Mechanical properties testing and results for thermal barrier coatings p 1946 N95-26134

VAPOR PHASES
Generation, detection and characterization of gas-phase transition metal aggregates and compounds
[DE95-004439] p 1930 N95-24686
Use of mass spectrometric methods for field screening of VOC's
[DE95-004903] p 1999 N95-25249
Cryogenic helium gas convection research
[DE95-004372] p 1965 N95-25404

VAPORS
Effects of nitric acid vapor on the formation of cloud droplets in troposphere
[DE95-744869] p 2001 N95-25500
The evaluation of potential limonene scavengers
[DE95-006853] p 2002 N95-25899

VARIABILITY
Development of a model of atmospheric oxygen variations to estimate terrestrial carbon storage and release
[NASA-CR-198002] p 2002 N95-25955
Modelling the day to day wind variability offshore central Chile at about 30 deg south
[DE95-606032] p 2006 N95-26043

VARIATIONAL PRINCIPLES
Dissipative quantum mechanics: The generalization of the canonical quantization and von Neumann equation
[DE95-607008] p 2096 N95-25426

VECTOR MESONS
Meson properties at finite temperature and density within Nambu-Jona-Lasinio model
[DE94-628630] p 2049 N95-24888
Annihilation diagrams in two-body nonleptonic decays of charmed mesons
[DE95-607181] p 2054 N95-25463
Mass splitting of the pseudoscalar and vector mesons induced by the homogeneous vacuum gluon field
[DE95-605322] p 2058 N95-25908
Searching for exotic mesons in e(+)e(-) annihilation at DA(phi)NE
[PB95-165379] p 2064 N95-26001

VECTOR QUANTIZATION
Clustering using winner-take-all units
[PB95-165403] p 2026 N95-25568

VECTORS (MATHEMATICS)
Covolume solutions of three dimensional div-curl equations
[NASA-CR-195031] p 2029 N95-24421
Involutive co-distributions preserved by transitive families of vector fields
[DE95-607078] p 2032 N95-25457

VEGETATION GROWTH
Structures and functions of oligosaccharins
[DE95-003140] p 2007 N95-24225

VELOCITY DISTRIBUTION
Laser beam log amplitude temporal scintillation spectrum due to crosswind. Part 1: Theory
[TR-1-FSRC-1994-PT-1] p 1971 N95-24371
Particle acceleration very near an x-line in a collisionless plasma
[ATR-92(7251)-4] p 2080 N95-25325

VELOCITY MEASUREMENT
Laser velocimeter for near-surface measurements
[NASA-CASE-ARC-11917-1] p 1967 N95-24236
Stereo imaging velocimetry for microgravity applications
[NASA-TM-110494] p 1949 N95-24416

VENUS SURFACE
User guide to the Magellan synthetic aperture radar images
[NASA-RP-1356] p 2112 N95-24987

VERTICAL DISTRIBUTION
Coupling correction using closed orbit measurements
[DE95-005957] p 2070 N95-25369

VERY HIGH FREQUENCIES
Wave-propagation aspects on VHF-radar applications
[PB95-141818] p 1953 N95-24649
The effects of the environment on an experimental VHF radio Direction Finding antenna system
[AD-A288791] p 1956 N95-26191

VERY LARGE SCALE INTEGRATION
VLSI neuroprocessors p 2023 N95-25258
Smart vision chips: An overview p 2024 N95-25265

VESTIBULES
Relation of motion sickness susceptibility to vestibular and behavioral measures of orientation
[NASA-CR-198048] p 2010 N95-24410

VIBRATION
A review of rolling element bearing vibration detection, diagnosis and prognosis
[DSTO-RR-0013] p 1975 N95-24393
Exploratory flow visualization investigation of mast-mounted sights in presence of a rotor
[NASA-TM-4634] p 1907 N95-24566
Tunable vibration absorbers: Key design parameters
[ISVR-TR-244] p 1981 N95-24995
Nonlinear vibrations of thin-walled composite frames
p 1984 N95-26269

VIBRATION DAMPING
Integrated passive/active vibration absorber for multi-story buildings
[NASA-TM-109178] p 1979 N95-24208
An analytical study of the vibration of beams fitted with neutralizers. Part 3: Torsional wave motion
[ISVR-TR-238-PT-3] p 1982 N95-25003
A technique for the evaluation of strength of coupling between SEA subsystems: Experiments with two coupled plates and two coupled rooms
[ISVR-TR-242] p 1982 N95-25332

VIBRATION EFFECTS
Experimental analysis of thread movement in bolted connections due to vibrations
[NASA-CR-197705] p 1975 N95-24991

VIBRATION ISOLATORS
Integrated passive/active vibration absorber for multi-story buildings
[NASA-TM-109178] p 1979 N95-24208
JPRS report: Science and technology. Central Eurasia: Seminar on materials science
[JPRS-UST-95-007] p 1920 N95-24761
Tunable vibration absorbers: Key design parameters
[ISVR-TR-244] p 1981 N95-24995

VIBRATION MEASUREMENT
A portable transmission vibration analysis system for the S-70A-9 Black Hawk helicopter
[DSTO-TR-0072] p 1966 N95-24203
Laser based methods for range, Doppler and vibration measurements
[PB95-141958] p 1952 N95-24445
Automation based on knowledge modeling theory and its applications in engine diagnostic systems using Space Shuttle Main Engine vibrational data
[NASA-CR-197983] p 1922 N95-24626

VIBRATION MODE
The transmission and control of vibrational power in a two stage isolation system with a water-loaded substructure
[ISVR-TR-235] p 1975 N95-24992

VIBRATION SIMULATORS
A portable transmission vibration analysis system for the S-70A-9 Black Hawk helicopter
[DSTO-TR-0072] p 1966 N95-24203

VIBRATION TESTS
The role of force measurements in advanced vibration test methods
[DE95-001833] p 1975 N95-24462

BSM Delta Qualification 2, volume 2
[NASA-CR-196567] p 1922 N95-24844
Experimental analysis of thread movement in bolted connections due to vibrations
[NASA-CR-197705] p 1975 N95-24991

VIBRATORY LOADS
The role of force measurements in advanced vibration test methods
[DE95-001833] p 1975 N95-24462

VIDEO COMMUNICATION
Learning random networks for compression of still and moving images p 2025 N95-25268

VIDEO COMPRESSION
Learning random networks for compression of still and moving images p 2025 N95-25268

VIDEO DATA
The accident site portable integrated video system
[DE95-000539] p 1953 N95-24605

VIDEO EQUIPMENT
The accident site portable integrated video system
[DE95-000539] p 1953 N95-24605
Video camera as a visual sensor, part 2
[NAL-TR-1231-PT-2] p 1970 N95-25763

VIDEO SIGNALS
Video camera as a visual sensor, part 2
[NAL-TR-1231-PT-2] p 1970 N95-25763

VIDEO TAPES
NASA video catalog
[NASA-SP-7109(01)] p 2103 N95-24238

VINYLIDENE
NMR and optical studies of piezoelectric polymers
[DE95-003836] p 1940 N95-24554

VIRIAL THEOREM
Existence domains and some properties of a particle bound state in fields with homogeneous dependence of its potential energy on coordinates
[DE95-605280] p 2057 N95-25784

VIRTUAL MEMORY SYSTEMS
DOLIB: Distributed Object Library
[DE95-004791] p 2019 N95-24250

VISCOELASTIC DAMPING
The transmission and control of vibrational power in a two stage isolation system with a water-loaded substructure
[ISVR-TR-235] p 1975 N95-24992

VISCOELASTICITY
Viscoelastic waves and multiple scales
[DE94-014130] p 1966 N95-26063

VISCOPLASTICITY
On the finite element implementation of the generalized method of cells micromechanics constitutive model
[NASA-CR-195451] p 1980 N95-24398
A fully associative, nonisothermal, nonlinear kinematic, unified viscoplastic model for titanium alloys
[NASA-TM-106926] p 1983 N95-26078
Sensitivity analysis of the non-linear dynamic viscoplastic response of 2-d structures with respect to material parameters p 1984 N95-26266
Sensitivity analysis for the dynamic response of viscoplastic shells of revolution p 1984 N95-26268
Sensitivity analysis for the dynamic response of thermoviscoplastic shells of revolution p 1986 N95-26278

VISCOSITY
Molecular dynamics calculation of shear viscosity for molten salt
[DE95-703970] p 2055 N95-25496
Self-sustained turbulence and L-mode confinement in toroidal plasmas 2
[NIFS-278] p 2082 N95-25759

VISCOUS FLOW
Multigrid solution strategies for adaptive meshing problems
[NASA-CR-195049] p 2031 N95-24857
Numerical simulation of laminar flow in a curved duct
[DE95-005427] p 1966 N95-26240

VISIBLE SPECTRUM
Implementation of scene shadows in the Target Acquisition TDA (TARGAC)
[AD-A288760] p 1912 N95-26060

VISION
An assessment of aviation accident risk of aphakic civil airmen by class of medical certificate held and by age: 1982-1985
[DOT/FAA/AM-95/11] p 2011 N95-25336

VISUAL AIDS
Perspectives from space: NASA classroom information and activities
[NASA-TM-110577] p 2100 N95-25643

VISUAL OBSERVATION
Use of cloud observations and mesoscale meteorology models to evaluate and improve cloud parameterizations
[DE95-006256] p 2005 N95-24613

VISUAL PERCEPTION
Visual performance with Omnibus 3: A comparative evaluation of enhanced generation three image intensifier technology
[PB95-141891] p 2013 N95-24510
Visual contrast detection thresholds for aircraft contrails
[AD-A288618] p 1905 N95-25607
Temporal pacing in visual attention
[AD-A289785] p 2013 N95-26041

VITERBI DECODERS
On the Trellis structure of a (64,40,8) subcode of the (64,42,8) third-order Reed-Muller code
[NASA-CR-198019] p 2015 N95-24224

VOICE COMMUNICATION
Automatic classification of Polish fricatives on the basis of optimization of the parameter space
[IFTR-9/1994] p 1956 N95-26331

VOICE DATA PROCESSING
Discrete-event-dynamic-system-based approaches for control in integrated voice/data multihop Radio Networks
[AD-A288389] p 1954 N95-25604
Automatic classification of Polish fricatives on the basis of optimization of the parameter space
[IFTR-9/1994] p 1956 N95-26331

VOIDS
Studies of two-phase gas-liquid flow in microgravity
[NASA-CR-195434] p 1963 N95-24906
National standard and code compliance for electrical equipment installed in hazardous locations for the void fraction instrument
[DE95-002158] p 1960 N95-26092

VOLT-AMPERE CHARACTERISTICS
Current-voltage characteristics of a tunnel junction with resonant centers
[DE94-634530] p 1956 N95-24245

VORTEX AVOIDANCE
Characterizing the wake vortex signature for an active line of sight remote sensor
[NASA-CR-197697] p 1909 N95-24391

VORTEX FLAPS
Low speed aerodynamic characteristics of delta wings with vortex flaps: 60 deg and 70 deg delta wings
[NAL-TR-1245] p 1907 N95-25105

VORTEX LATTICE METHOD
Melting of the moving vortex lattice in the presence of disorder
[DE95-004126] p 2087 N95-24868

VORTEX SHEDDING
High frequency flow-structural interaction in dense subsonic fluids
[NASA-CR-4652] p 1906 N95-24217

VORTEX SHEETS
Effect of density gradients in confined supersonic shear layers. Part 2: 3-D modes
[NASA-CR-198030] p 1962 N95-24413

VORTICES
Three-dimensional interaction of wake/boundary-layer and vortex/boundary-layer data report
[CUED/A-AEREO/TR-23] p 1906 N95-24210
The atmospheric effects of stratospheric aircraft: A fourth program report
[NASA-RP-1359] p 1996 N95-24274
Characterizing the wake vortex signature for an active line of sight remote sensor
[NASA-CR-197697] p 1909 N95-24391
Vortex solutions in two-Higgs-doublet systems
[DE94-634363] p 2096 N95-25107
Numerical simulation of laminar flow in a curved duct
[DE95-005427] p 1966 N95-26240

VOWELS
A study of the effect of voice pitch on the perception of synthetic Polish vowels
[IFTR-10/1994] p 1956 N95-26018

VOYAGER 1 SPACECRAFT
Voyager: The grandest tour. The mission to the outer planets
[NASA-CR-197708] p 2112 N95-25854

VOYAGER 1977 MISSION
Voyager: The grandest tour. The mission to the outer planets
[NASA-CR-197708] p 2112 N95-25854

VOYAGER 2 SPACECRAFT
Voyager: The grandest tour. The mission to the outer planets
[NASA-CR-197708] p 2112 N95-25854

VULCANIZING
Antioxidant and sensitizer effect on the stability of natural rubber latex vulcanized by gamma rays
[DE94-636061] p 1939 N95-24373

W

WALL FLOW
Supersonic quiet-tunnel development for laminar-turbulent transition research
[NASA-CR-198040] p 1915 N95-24302

WALL JETS
Effects of cavity dimensions, boundary layer, and temperature on cavity noise with emphasis on benchmark data to validate computational aeroacoustic codes
[NASA-CR-4653] p 2039 N95-24879

WALLS
Structures and functions of oligosaccharins
[DE95-003140] p 2007 N95-24225
Heat removal capability of divertor coaxial tube assembly
[DE95-709770] p 1966 N95-26161

WARNING SYSTEMS
Analysis of data from a radar warning receiver with the accent on association of sensor reports
[PB95-141768] p 1953 N95-24836

WARPAGE
Analysis of warping effects on the static and dynamic response of a seat-type structure
[NIAR-94-12] p 1979 N95-24211

WASHING
Chelant extraction and REDOX manipulation for mobilization of heavy metals from contaminated soils
[DE95-004131] p 2000 N95-25363

WASTE DISPOSAL
Overview of solar detoxification activities in the United States
[DE95-000264] p 1997 N95-24319
SPEEDUP simulation of liquid waste batch processing, revision 1
[DE95-001240] p 1939 N95-24344
The energy intelligence information system
[DE95-002184] p 2105 N95-24675
Waste minimization assessment for a manufacturer of parts for truck engines
[PB95-144481] p 1911 N95-26062

WASTE TREATMENT
SPEEDUP simulation of liquid waste batch processing, revision 1
[DE95-001240] p 1939 N95-24344
Electrochemical organic destruction in support of Hanford tank waste pretreatment
[DE95-002854] p 1924 N95-25248
Chelant extraction and REDOX manipulation for mobilization of heavy metals from contaminated soils
[DE95-004131] p 2000 N95-25363
Disposal of electronic equipment
[PB95-177861] p 2002 N95-26047
Waste minimization assessment for a manufacturer of parts for truck engines
[PB95-144481] p 1911 N95-26062

WASTE UTILIZATION
Co-firing high sulfur coal with refuse derived fuels
[DE95-006243] p 1997 N95-24406

WATER
Evaluation of commercial fuel tank water absorbers
[AD-A288361] p 1951 N95-25513
Fourth symposium of the geological survey of Japan on remote sensing of satellite geology
[PB95-178737] p 1917 N95-25750

WATER IMMERSION
Thermal and vascular changes induced by the acclimation of the extremities to cold in man
[PB95-131587] p 2010 N95-24310

WATER QUALITY
Biological monitoring of national freshwaters, 1992
[PB95-166690] p 2002 N95-25745

WATER TREATMENT
Electromagnetic Devices and Processes in Environment Protection. Proceedings of International Conference ELMECO 1994
[AD-A286613] p 1952 N95-24503

WATER VAPOR
Direct catalytic decomposition of nitric oxide
[DE95-005202] p 1928 N95-24286
Airborne imaging of tropospheric emission at millimeter and submillimeter wavelengths
[NASA-TM-110498] p 2003 N95-24336
Passive microwave algorithm development and evaluation
[NASA-CR-197915] p 2005 N95-24535
Effects of nitric acid vapor on the formation of cloud droplets in troposphere
[DE95-744869] p 2001 N95-25500

WATER WAVES
Techniques for the investigation of wave turbulence in water wave data
[AD-A288392] p 2007 N95-25605

On a remarkable similarity between the propagation of whistlers and the bow wave of a ship
[U-OF-IOWA-94-22] p 2111 N95-26196

WATERSHEDS
A numerical prediction of the precipitation and hydrology of California
[DE95-004966] p 2006 N95-25635

WAVE DIFFRACTION
Detvag-90: An implementation of Vogler's method for calculation of multiple knife-edge diffraction
[PB95-141859] p 1951 N95-24281
The diffraction of electromagnetic waves by screens placed at the boundaries of dielectric media
[IFTR-4/1994] p 1954 N95-25393

WAVE DISPERSION
On a remarkable similarity between the propagation of whistlers and the bow wave of a ship
[U-OF-IOWA-94-22] p 2111 N95-26196

WAVE EQUATIONS
Numerical simulation methods for wave propagation through optical waveguides
[DE94-634313] p 2073 N95-24402
Relations among solutions for wave and Klein-Gordon equations for different dimensions
[DE95-600853] p 2093 N95-24446

WAVE FUNCTIONS
Covariant single-time equations for a system of N spinor particles
[DE94-628587] p 2047 N95-24640
Elastic form factors of hydrogen-like atoms in nS-states
[DE94-628437] p 2048 N95-24700
Quantum group and quantum symmetry
[DE94-634329] p 2095 N95-24767
Geometric gauge fields in semiclassical gravity
[DE95-607079] p 2098 N95-25525
Existence domains and some properties of a particle bound state in fields with homogeneous dependence of its potential energy on coordinates
[DE95-605280] p 2057 N95-25784
Describing the macroscopic world: Closing the circle within the dynamical reduction program
[DE95-606997] p 2100 N95-26046
Condensate localization by mesoscale disorder in high-T(sub c) superconductors
[DE95-607819] p 1960 N95-26100

WAVE GENERATION
Optically-switched submillimeter-wave oscillator and radiator having a switch-to-switch propagation delay
[NASA-CASE-NPO-18547-1-CU] p 1959 N95-25307

WAVE PROPAGATION
Numerical simulation methods for wave propagation through optical waveguides
[DE94-634313] p 2073 N95-24402
Wave-propagation aspects on VHF-radar applications
[PB95-141818] p 1953 N95-24649
Decay of a laser generated shock wave in an aluminium target
[DE94-629014] p 1972 N95-24707
Annual report 1992/93, FOA 38. Radio systems and wave propagation
[PB95-141735] p 1953 N95-24835
Study on propagation impairments, distortions and unavailability on digital microwave links
[DE95-723047] p 1953 N95-24848
An analytical study of the vibration of beams fitted with neutralizers. Part 3: Torsional wave motion
[ISVR-TR-238-PT-3] p 1982 N95-25003
Implementation of wave propagation model for windows
[PB95-165742] p 2017 N95-25571
Solitons in electron-positron plasma
[DE95-607608] p 2082 N95-25974
Viscoelastic waves and multiple scales
[DE94-014130] p 1966 N95-26063
The whistler-mode bow wave of an asteroid
[U-OF-IOWA-95-2] p 2111 N95-26195
On a remarkable similarity between the propagation of whistlers and the bow wave of a ship
[U-OF-IOWA-94-22] p 2111 N95-26196

WAVE RESISTANCE
The phenomenon of non-linearity accompanying the action of acoustic pressure on a Helmholtz resonator
[IFTR-19/1994] p 2040 N95-26108

WAVE SCATTERING
Complex scattering dynamics and the quantum Hall effect
[DE95-005239] p 2093 N95-24457
Fluctuations and electromagnetic wave scattering in macroscopically agitated plasma: Effects of turbulent diffusion
[DE95-607612] p 2081 N95-25617

WAVEFORMS
Analysis of waveforms for bistatic radar systems
[PB95-165098] p 1955 N95-25641

WAVEGUIDES
High-gradient experiment on X-band disk-loaded structures
[DE94-765446] p 1958 N95-24701
Self-focusing of electromagnetic radiation in electron-positron ion plasma
[DE95-607626] p 2082 N95-25975

WAVELENGTH DIVISION MULTIPLEXING
Application of optical fiber amplifier for wavelength division multiplexing communication system. Part 2: Design of four-channel transmission system using two EDFA repeaters
[DE95-730179] p 1952 N95-24491

WEAK INTERACTIONS (FIELD THEORY)
A search for t(anti t) (yields) lepton + E(sub T) + jets signature in p(anti p) collisions at (radical)s = 1.8 TeV with the DO detector
[DE95-004239] p 2052 N95-25402
Study of the simplest realistic Higgs sector in quark-lepton symmetric models
[DE95-607159] p 2053 N95-25461
Can the electric charges of elementary particles change with time?
[DE95-607194] p 2054 N95-25465
The Hamiltonian of SU(2) lattice gauge theory in approximate tri-diagonal form
[DE95-607101] p 2098 N95-25475

WEAPONS DEVELOPMENT
Report to Congressional Committees. Tactical Aircraft: Concurrency in development and production of F-22 aircraft should be reduced
[GAO/NSIAD-95-59] p 1911 N95-26338

WEAR
Improved lubrication performance of sputtered MoS2 film by surface treatments of Ti-alloy substrate
[NAL-TR-1213] p 1942 N95-25760
Transmission diagnostic research at NASA Lewis Research Center
[NASA-TM-106901] p 1977 N95-26076

WEAR RESISTANCE
Wear resistant composite structure of vitreous carbon containing convoluted fibers
[DE95-006255] p 1925 N95-24426
Wear-resistant, self-lubricating surfaces of diamond coatings
[NASA-TM-106887] p 1924 N95-25961

WEAR TESTS
Au/Cr sputter coating for the protection of alumina during sliding at high temperatures
[NASA-TM-106853] p 1923 N95-24437

WEATHER FORECASTING
Journal of the Communications Research Laboratory, volume 41, number 1, March 1994
[PB95-177606] p 1956 N95-26008

WEAVING
Method and apparatus for weaving curved material preforms
[NASA-CASE-LAR-14752-1] p 1943 N95-26118

WEDGE FLOW
A study of three-dimensional interaction flow fields between swept shock waves and turbulent boundary layers. Flow structures and effects of bleed
[NAL-TR-1227] p 1963 N95-25001

WEIGHTING FUNCTIONS
Aerodynamic parameter estimation via Fourier modulating function techniques
[NASA-CR-4654] p 1911 N95-24630

WEIGHTLESSNESS
Go for EVA
[NASA-TM-110537] p 1918 N95-24195

WELDED JOINTS
Active weld control
[NASA-CR-196588] p 1976 N95-25595
Stress analysis of a crack in the residual stress field by welding and its application to the fatigue crack propagation
[NAL-TR-1248] p 1983 N95-25796
Atom probe field ion microscopy of Type 308 CRE stainless steel welds
[DE94-019161] p 1938 N95-26064

WELDED STRUCTURES
JPRS report: Science and technology. Central Eurasia
[JPRS-UST-95-011] p 1910 N95-24541

WELDING
Stress analysis of a crack in the residual stress field by welding and its application to the fatigue crack propagation
[NAL-TR-1248] p 1981 N95-25000
Active weld control
[NASA-CR-196588] p 1976 N95-25595

WHISKER COMPOSITES
Strengthening of NiAl matrix composites
[AD-A288923] p 1926 N95-25505
Whisker reinforced glass ceramic
[DE95-005568] p 1927 N95-25998

WHISTLERS
The whistler-mode bow wave of an asteroid
[U-OF-IOWA-95-2] p 2111 N95-26195
On a remarkable similarity between the propagation of whistlers and the bow wave of a ship
[U-OF-IOWA-94-22] p 2111 N95-26196

WICKS
Felt-metal-wick heat-pipe solar receiver
[DE95-004535] p 1992 N95-24682
An examination of metal felt wicks for heat-pipe applications
[DE95-002608] p 1994 N95-25109

WIGGLER MAGNETS
Simulation study of tapered FEL amplifiers in Raman and Compton regimes
[DE94-785266] p 1971 N95-24340
Faster magnet sorting with a threshold acceptance algorithm
[DE95-006487] p 2038 N95-25408
Nonlinear analysis of millimeter and sub-millimeter wave sources such as Cerenkov masers, orotrons, and ubitrons
[AD-A288777] p 1974 N95-26114

WIND EFFECTS
Laser beam log amplitude temporal scintillation spectrum due to crosswind. Part 1: Theory
[TR-1-FSRC-1994-PT-1] p 1971 N95-24371
Impacts of microphysics, radiation and environmental winds in mid-latitude and tropical squall-line systems, and their climatic implications
[DE95-004965] p 2005 N95-25287

WIND TUNNEL MODELS
Development of a model protection and dynamic response monitoring system for the national transonic facility
[NASA-CR-195041] p 1915 N95-24388
Angular displacement measuring device
[NASA-CASE-ARC-11937-1] p 2074 N95-26015

WIND TUNNEL NOZZLES
Supersonic quiet-tunnel development for laminar-turbulent transition research
[NASA-CR-198040] p 1915 N95-24302

WIND TUNNEL TESTS
Three-dimensional interaction of wake/boundary-layer and vortex/boundary-layer data report
[CUED/A-AEREO/TR-23] p 1906 N95-24210
Supersonic quiet-tunnel development for laminar-turbulent transition research
[NASA-CR-198040] p 1915 N95-24302
Study of compressible flow through a rectangular-to-semiannular transition duct
[NASA-CR-4660] p 1914 N95-24392
DSMC calculations for 70-deg blunted cone at 3.2 km/s in nitrogen
[NASA-TM-109181] p 1961 N95-24396
Performance of an aerodynamic yaw controller mounted on the space shuttle orbiter body flap at Mach 10
[NASA-TM-109179] p 1906 N95-24397
Experimental study of the effects of Reynolds number on high angle of attack aerodynamic characteristics of forebodies during rotary motion
[NASA-CR-195033] p 1907 N95-24443
Exploratory flow visualization investigation of mast-mounted sights in presence of a rotor
[NASA-TM-4634] p 1907 N95-24566
Using digital filtering techniques as an aid in wind turbine data analysis
[DE94-011862] p 1993 N95-24853
Effects of cavity dimensions, boundary layer, and temperature on cavity noise with emphasis on benchmark data to validate computational aeroacoustic codes
[NASA-CR-4653] p 2039 N95-24879
Numerical and experimental study of drag characteristics of two-dimensional HLFC airfoils in high subsonic, high Reynolds number flow
[NAL-TR-1244T] p 1907 N95-24998
A study of three-dimensional interaction flow fields between swept shock waves and turbulent boundary layers. Flow structures and effects of bleed
[NAL-TR-1227] p 1963 N95-25001
Low speed aerodynamic characteristics of delta wings with vortex flaps: 60 deg and 70 deg delta wings
[NAL-TR-1245] p 1907 N95-25105
Thrust measurements of a complete axisymmetric scramjet in an impulse facility p 1914 N95-25395
Scramjet thrust measurement in a shock tunnel p 1914 N95-25396
Scaling in a scramjet combustor p 1933 N95-25398
Balances for the measurement of multiple components of force in flows of a millisecond duration p 1965 N95-25400
Aerodynamic characteristics of the orbital reentry vehicle experimental probe fins in a supersonic flow
[NAL-TR-1232] p 1921 N95-25664

Measurements of longitudinal static aerodynamic coefficients by the cable mount system
[NAL-TR-1226] p 1908 N95-25761
Fundamental wind tunnel experiments on low-speed flutter of a tip-fin configuration wing
[NAL-TR-1228] p 1908 N95-25762
Heat transfer measurements in small scale wind tunnels
[AD-A286689] p 1915 N95-26053

WIND TURBINES
Data preparation requirements for modeling wind turbines with ADAMS(R)
[DE95-000266] p 1992 N95-24684
Using digital filtering techniques as an aid in wind turbine data analysis
[DE94-011862] p 1993 N95-24853
NREL airfoil families for HAWTs
[DE95-000267] p 1994 N95-24882
Finite element methods in a simulation code for offshore wind turbines
[PB95-164984] p 1994 N95-25501
User's manual for FAROW: Fatigue and reliability of wind turbine components, version 1.1
[DE95-005530] p 1995 N95-26037
Wind technology development: Large and small turbines
[DE95-000286] p 1995 N95-26090

WIND VELOCITY
Laser beam log amplitude temporal scintillation spectrum due to crosswind. Part 1: Theory
[TR-1-FSRC-1994-PT-1] p 1971 N95-24371
Passive microwave algorithm development and evaluation
[NASA-CR-197915] p 2005 N95-24535

WINDOWS (COMPUTER PROGRAMS)
Implementation of wave propagation model for windows
[PB95-165742] p 2017 N95-25571

WINDPOWER UTILIZATION
Appendix model performance: Model documentation. Renewable Fuels Module of the National Energy Modelling System
[DE95-006080] p 1991 N95-24355
Wind technology development: Large and small turbines
[DE95-000286] p 1995 N95-26090

WING OSCILLATIONS
Fundamental wind tunnel experiments on low-speed flutter of a tip-fin configuration wing
[NAL-TR-1228] p 1908 N95-25762

WING PROFILES
A theoretical and experimental investigation of the flow over supersonic leading edge wing/body configurations
[DRA-TM-AERO-PROP-41] p 1907 N95-25649

WING TIPS
Fundamental wind tunnel experiments on low-speed flutter of a tip-fin configuration wing
[NAL-TR-1228] p 1908 N95-25762

WINGLETS
Fundamental wind tunnel experiments on low-speed flutter of a tip-fin configuration wing
[NAL-TR-1228] p 1908 N95-25762

WINGS
Geometric analysis of wing sections
[NASA-TM-110346] p 1910 N95-24629
Fundamental wind tunnel experiments on low-speed flutter of a tip-fin configuration wing
[NAL-TR-1228] p 1908 N95-25762

WIRE
Superconductivity Program for Electric Power Systems: 1994 Annual PEER Review. Volume 2, Meeting Proceedings
[DE95-005059] p 1957 N95-24453
A study of the electrochemical behavior of tungsten in caustic solutions and platinum/iridium in ch loride solutions
[DE95-004951] p 1930 N95-25123

WIRE WINDING
Rotary actuator
[NASA-CASE-MFS-28581-1] p 1936 N95-25545

WORKSTATIONS
Parallel processing for scientific computations
[NASA-CR-198013] p 2020 N95-24563

WROUGHT ALLOYS
Robotic weld overlay coatings for erosion control
[DE95-005187] p 1939 N95-24285

X

X RAY ABSORPTION
ASCA solid state imaging spectrometer observations of O stars
[NASA-CR-197281] p 2108 N95-24385

X RAY ANALYSIS
Neural networks: Application to medical imaging
p 2025 N95-25267

X RAY DETECTORS
X-ray based displacement and strain measurements for hostile environments
[NASA-CR-194451] p 1968 N95-25330

X RAY DIFFRACTION
Mossbauer spectroscopy, x ray diffraction and magnetic measurements of iron-nickel ultrafine particles
[DE95-601136] p 1930 N95-24840
Accurate determination of IC modulation parameter in Sr(x)Ba(1-x)Nb2O6 from second order satellites of neutron diffraction TOF (Time-Of-Flight) spectra
[DE94-629003] p 2090 N95-25851

X RAY IMAGERY
Characteristics of an ultrafast x-ray streak camera
[DE95-004210] p 1968 N95-24657

X RAY INSPECTION
Emerging nondestructive inspection for aging aircraft
[PB95-143053] p 1905 N95-25401

X RAY LASERS
Na-like autoionizing levels: Plasma diagnostics and prospects for photopumped soft x-ray lasers
[DE95-004207] p 1972 N95-25100
Targets for laser-driven opacity measurements
[DE95-006172] p 1973 N95-25557

X RAY SOURCES
Pulsed power drivers for ICF and high energy density physics
[DE95-003361] p 2066 N95-24500

X RAY SPECTRA
ASCA solid state imaging spectrometer observations of O stars
[NASA-CR-197281] p 2108 N95-24385

X RAY SPECTROSCOPY
XAS studies of Ni(I), Ni(II), and Ni(III) complexes
[DE95-004844] p 1928 N95-24257
Non-destructive characterization of porous silicon using x ray reflectivity
[DE95-004766] p 1942 N95-25898

X RAYS
Advanced Light Source report
[DE95-003449] p 2073 N95-24546
Characteristics of an ultrafast x-ray streak camera
[DE95-004210] p 1968 N95-24657
Design of supramolecular ordered systems for mesoscopic colloids and molecular composites
[DE95-004448] p 2048 N95-24687
Coupling correction using closed orbit measurements
[DE95-005957] p 2070 N95-25369
Proceedings of the 21st Japan Conference on Radiation and Radioisotopes
[DE94-785275] p 2056 N95-25614
Non-destructive characterization of porous silicon using x ray reflectivity
[DE95-004766] p 1942 N95-25898

XENON
The interactions of high-energy, highly charged Xe ions with buckyballs
[DE95-004597] p 2069 N95-25281

XENON COMPOUNDS
Thermochemistry, kinetics and spectroscopy of Kr and Kr2F
[DE95-005732] p 1941 N95-25386

Y

YAG LASERS
Reduction in fiber damage thresholds due to static fatigue
[DE95-004778] p 1979 N95-24263
Laser beam characterization results for a high power CW Nd:YAG laser
[DE95-006319] p 1971 N95-24408

YANG-MILLS THEORY
Construction of the moduli space of monopoles
[PB95-165528] p 2028 N95-24255
Research in elementary particle physics
[DE95-007323] p 2054 N95-25481

YARNS
Effects of through-the-thickness stitching on impact and interlaminar fracture properties of textile graphite/epoxy laminates
[NASA-CR-195042] p 1928 N95-26203

YBCO SUPERCONDUCTORS
Copper transport on oxygen annealing of a superconducting film Y-Ba-Cu-O
[DE94-627566] p 2086 N95-24537
Temperature-dependent growth of LaAlO3 films on YBa2CuO7 C-axis films for multilayer structures
[DE95-005257] p 2089 N95-25598

YIELD
Modeling of the simulated countercurrent moving-bed chromatographic reactor used for the oxidative coupling of methane
[DE95-004930] p 1924 N95-25286

YIELD STRENGTH
Evolution of plastic anisotropy for high-strain-rate computations
[DE95-004220] p 1941 N95-25237
Recent progress in shear punch testing
[DE95-005962] p 1937 N95-26007

YTTRIUM OXIDES
Preparation of stabilized zirconia (ZrO2) with ytteria (Y2O3) by simultaneous precipitation
[DE95-600163] p 1933 N95-24366

YUKAWA POTENTIAL
The existence of antiparticles seems to forbid violations of statistics
[DE94-628523] p 2050 N95-25094
Low energy properties of the heavy vector fermions
[DE94-634362] p 2051 N95-25290
Recoil effects in quantum topological solitons
[DE95-607006] p 2097 N95-25454
On a possible explanation of the origin of the quark mass spectrum
[DE95-605315] p 2063 N95-25968

Z

ZENER EFFECT
Landau-Zener treatments of solar neutrino oscillations
[DE95-004761] p 2113 N95-24249

ZERO SOUND
Zero sound velocity in pi, rho mesons at different temperatures
[DE95-607145] p 2053 N95-25459

ZETA PINCH
Pulsed power drivers for ICF and high energy density physics
[DE95-003361] p 2066 N95-24500
Flow-through Z-pinch study for radiation generation and fusion energy production
[DE95-004209] p 2076 N95-24544

ZIRCONIUM OXIDES
Preparation of stabilized zirconia (ZrO2) with ytteria (Y2O3) by simultaneous precipitation
[DE95-600163] p 1933 N95-24366
High octane ethers from synthesis gas-derived alcohols
[DE95-001146] p 1948 N95-24655
Study of composite zirconium oxide
[DE95-730104] p 1926 N95-25111
Processing and characterization of transformation-toughened ceramics with strength retention to elevated temperatures
[DE95-005758] p 1941 N95-25387
Process, properties and environmental response of plasma sprayed thermal barrier coatings
p 1945 N95-26132
Thermal conductivity of zirconia thermal barrier coatings
p 1945 N95-26133

Typical Personal Author Index Listing

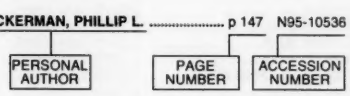

Listings in this index are arranged alphabetically by personal author. The page number helps you locate the citation in the abstract section. The accession number denotes the number by which the citation is identified.

A

AALFS, DAVID D. ..... p 2035 N95-24278
AARNIO, P. A. ..... p 2042 N95-24297
p 2042 N95-24298
ABANI, M. C. ..... p 1958 N95-24690
ABBOTT, TERENCE S. ..... p 1910 N95-24582
ABD-ELEMGUID, M. M. ..... p 1959 N95-25405
ABDALATI, W. ..... p 1998 N95-24846
ABDELWAHAB, M. M. ..... p 2113 N95-25986
ABDOU, MOHAMED A. ..... p 2076 N95-24511
ABEL, S. A. ..... p 2099 N95-25628
ABUALAZM, S. M. ..... p 2087 N95-24891
ACTON, C. ..... p 2112 N95-24994
ADACHI, K. ..... p 2081 N95-25651
ADAMCZYK, EUGENIUSZ ..... p 2039 N95-25115
ADAMOVSKY, GRIGORY ..... p 1912 N95-24207
ADAMS, RICHARD D. ..... p 1923 N95-24851
ADHIKARI, RATHIN ..... p 2053 N95-25438
ADKINS, DOUGLAS R. ..... p 1992 N95-24682
p 1994 N95-25109
AFANASEV, L. G. ..... p 2048 N95-24700
AGARWAL, DEBORAH ..... p 2020 N95-24496
AGUILERA-NAVARRO, V. C. ..... p 2065 N95-24351
AHMADI, GOODARZ ..... p 1979 N95-24208
AHRENS, L. ..... p 2064 N95-24287
AHUJA, K. K. ..... p 2039 N95-24879
AIKAWA, HIROSHI ..... p 2075 N95-24272
AIKAWA, TOSHIHIKO ..... p 1942 N95-25760
AISHIMA, YUKINORI ..... p 2081 N95-25498
AKATOV, YU. A. ..... p 2061 N95-25927
p 2009 N95-25933
AKGERMAN, A. ..... p 1929 N95-24341
AKHUNDOV, A. A. ..... p 2053 N95-25462
AKIBA, MASATO ..... p 2077 N95-24585
AKINLADE, O. ..... p 2034 N95-25982
AKINO, NOBORU ..... p 2043 N95-24339
AKISHIN, P. G. ..... p 2048 N95-24692
p 2034 N95-25906
AKIYAMA, R. ..... p 2071 N95-26031
AKOPOVA, A. B. ..... p 2059 N95-25914
p 2061 N95-25926
p 2061 N95-25928
p 2061 N95-25929
p 2062 N95-25932
ALA-HEIKKILAE, J. J. ..... p 2042 N95-24297
ALAKANGAS, EIJA ..... p 1993 N95-24862
ALBER, M. S. ..... p 2030 N95-24609
ALBERSHEIM, P. ..... p 2007 N95-24225
ALBINSSON, M. ..... p 1951 N95-24241
ALDABE, FERMIN ..... p 2097 N95-25454
ALEXANDER, MARGARET B. ..... p 1921 N95-25875
ALFORD, T. L. ..... p 1935 N95-25379
ALFORD, W. J. ..... p 2074 N95-25559
ALI, R. ..... p 2069 N95-25281
ALIABADI, M. H. ..... p 1980 N95-24383
ALIAGA, J. ..... p 2032 N95-25452
ALKHATIB, HASAN S. ..... p 2020 N95-24563
ALLEN, JAMES F. ..... p 2016 N95-24536
ALLEN, M. G. ..... p 2090 N95-25985
ALLEN, S. L. ..... p 2076 N95-24490
ALLENDORF, S. W. ..... p 1972 N95-25549
ALLISON, S. ..... p 2067 N95-24573
ALLISON, STEPHEN W. ..... p 1989 N95-25110
ALLMAN, B. E. ..... p 2097 N95-25446
ALMAGRI, A. F. ..... p 2077 N95-24619
ALMGREN, A. S. ..... p 1931 N95-25291
ALPERT, L. K. ..... p 2093 N95-24481
ALSPECTOR, JOSHUA ..... p 2025 N95-25270
ALTAJSKIJ, M. V. ..... p 2099 N95-25966
ALVES, K. M. B. ..... p 1937 N95-25751
AMAI, W. A. ..... p 1953 N95-24605
AMAKO, KATSUYA ..... p 2021 N95-25303
AMBUR, DAMODAR R. ..... p 1928 N95-26251
AMI, T. ..... p 2038 N95-25600
AMINPOUR, MOHAMMAD A. ..... p 1983 N95-26199
AMIRKHANOV, I. V. ..... p 2029 N95-24387
p 2057 N95-25778
AMUNDSEN, R. M. ..... p 1950 N95-24559
ANDERSEN, N. H. ..... p 2085 N95-24431
ANDERSEN, V. G. ..... p 2004 N95-24897
ANDERSON, HARLEN U. ..... p 1992 N95-24683
ANDERSSON, ROLAND ..... p 2073 N95-24673
ANDES, DAVID K. ..... p 2022 N95-25254
ANDO, TOSHIRO ..... p 2077 N95-24585
ANDRAKA, CHARLES E. ..... p 1992 N95-24682
p 1994 N95-25109
ANDRASTEK, DONALD A. ..... p 1913 N95-24304
ANDREAS, NICOS H. ..... p 1992 N95-24682
p 1994 N95-25109
ANDRICEVIC, R. ..... p 1988 N95-24407
ANIKEEVA, I. D. ..... p 2009 N95-25933
ANIKIN, I. ..... p 1952 N95-24506
ANSARI, RAFAT R. ..... p 1971 N95-24530
ANTONCHIK, V. A. ..... p 2059 N95-25917
p 2059 N95-25918
p 2059 N95-25919
p 2060 N95-25920
ANTONIAN, V. ..... p 2100 N95-25987
ANTONSEN, T. M., JR. ..... p 2081 N95-25561
ANZ, S. J. ..... p 1967 N95-24596
AOKI, ISAO ..... p 2080 N95-25495
AOYAGI, TETSUO ..... p 2076 N95-24311
APEL, J. ..... p 1955 N95-25710
APPLEBY, J. W., JR. ..... p 1945 N95-26131
ARAI, M. ..... p 1931 N95-25356
ARAKI, MASANORI ..... p 2043 N95-24339
p 2077 N95-24585
ARBUZOV, A. B. ..... p 2047 N95-24668
ARENSBURG, ALEX ..... p 2078 N95-24706
ARITA, MASASHI ..... p 1942 N95-25760
ARMSTRON, D. J. ..... p 2074 N95-25559
ARMSTRONG, F. E. ..... p 2067 N95-24652
ARMSTRONG, R. ..... p 1926 N95-25295
ARMSTRONG, T. R. ..... p 2088 N95-25002
ARNOLD, DON WESLEY ..... p 2045 N95-24533
ARNOLD, S. M. ..... p 1983 N95-26078
ARSENAULT, R. J. ..... p 1925 N95-24590
p 1926 N95-25505
ARTYUKH, A. G. ..... p 2055 N95-25538
ARVIDSON, R. ..... p 1955 N95-25710
ASH, ROBERT L. ..... p 1970 N95-25699
ASHILL, P. R. ..... p 1907 N95-25649
ASLANOV, V. ..... p 2064 N95-26256
ASSINK, R. A. ..... p 1941 N95-25370
p 2090 N95-25897
ATAMANIUK, BARBARA ..... p 2080 N95-25340
ATHEY, C. L. ..... p 2103 N95-24370
ATKINSON, W. H. ..... p 1967 N95-24473
ATTAYA, HOSNY ..... p 2083 N95-26185
ATTENBERGER, S. E. ..... p 2078 N95-25102
ATWELL, W. ..... p 2059 N95-25914
ATWOOD, CHRISTOPHER ..... p 2017 N95-25797
ATWOOD, JIM D. ..... p 2050 N95-25112
AUDI, G. ..... p 2040 N95-24231
AUH, J. M. ..... p 1997 N95-24499
AULL, J. E. ..... p 1939 N95-24344
AUSTIN, M. E. ..... p 2078 N95-25102
p 2079 N95-25250
AUSTIN, RICHARD S. ..... p 2112 N95-24987
AZEVEDO, I. S. ..... p 1959 N95-25405
AZUMI, M. ..... p 2082 N95-25759
p 2083 N95-26326
AZUMI, MASAFUMI ..... p 2080 N95-25471

B

BABU, S. S. ..... p 1938 N95-26064
BACA, A. G. ..... p 1957 N95-24488
p 2064 N95-26168
BACKEMEYER, LYNN A. ..... p 2013 N95-24627
BADAMDAMDIN, R. ..... p 2056 N95-25668
BADAVI, F. F. ..... p 2060 N95-25922
BADHWAR, G. D. ..... p 2059 N95-25914
BADIRKHAN, Z. ..... p 2034 N95-25982
BADRAOUI, S. ..... p 1931 N95-25447
p 2033 N95-25748
BAER, M. R. ..... p 1948 N95-24608
BAGGIO-SAITOVITCH, E. ..... p 1959 N95-25405
BAILEY, SHEILA G. ..... p 1991 N95-24560
BAIRD, K. G. ..... p 2047 N95-24660
BAKER, D. ..... p 2112 N95-24994
BAKER, GREGORY ..... p 2032 N95-25114
BAKER, M. R. ..... p 1929 N95-24345
BAKOS, R. J. ..... p 1964 N95-25394
BALACHANDRAN, A. P. ..... p 2027 N95-24228
BALACHANDRAN, U. ..... p 2088 N95-25282
BALAGUROV, A. M. ..... p 2085 N95-24382
p 2090 N95-25851
BALAKRISHNA, S. ..... p 1915 N95-24388
BALAKRISHNAN, A. V. ..... p 1971 N95-24371
BALCZERAK, A. ..... p 1932 N95-25959
BALEANU, DUMITRU ..... p 2039 N95-25646
BANERJEE, MANOJ K. ..... p 2098 N95-25562
BANERJEE, SAHEB ..... p 2031 N95-24856
BANG, HA HUY ..... p 2096 N95-25425
BANG, SA HYUN ..... p 2023 N95-25257
BANGERTER, R. O. ..... p 2069 N95-25358
BANILOWER, HOWARD ..... p 1909 N95-24631
BARABASH, L. S. ..... p 2049 N95-24889
BARANOV, S. A. ..... p 2049 N95-24889
BARASHENKOV, V. S. ..... p 2063 N95-25965
BARBOUR, J. C. ..... p 1941 N95-25382
BARDOS, D. C. ..... p 2082 N95-25976
BARGER, V. ..... p 2056 N95-25567
BARHEN, JACOB ..... p 2025 N95-25266
BARKLOW, T. L. ..... p 2067 N95-24661
BARNES, CORBIN ..... p 1918 N95-26308
BARRANS, R. ..... p 1924 N95-25597
BARTHOLOMEW, C. H. ..... p 1929 N95-24614
BARTZ, A. ..... p 1944 N95-26126
BATCHELOR, D. B. ..... p 2076 N95-24548
BATTRICK, B. ..... p 2114 N95-24870
BATTRICK, BRUCE ..... p 2114 N95-25200
BATUSOV, YU. A. ..... p 2049 N95-24889
BAUCOM, ROBERT M. ..... p 1939 N95-24212
BAUER, JACEK ..... p 2035 N95-26106
BAUMBICK, ROBERT ..... p 1912 N95-24207
p 1912 N95-24624
BAYLESS, W. R. ..... p 2087 N95-24816
BAZDENKOV, SERGEY ..... p 2083 N95-26337
BAZZANI, A. ..... p 2062 N95-25944
BEARDSLEY, M. B. ..... p 1946 N95-26136
BEATTIE, ALLAN ..... p 1905 N95-25401
BEAUJEAN, R. ..... p 2061 N95-25930
BEAZLEY, D. M. ..... p 2020 N95-24612
BEDAQUE, P. ..... p 2054 N95-25463
BEDNYAKOV, V. A. ..... p 2043 N95-24360
p 2109 N95-24885
p 2109 N95-24886
p 2099 N95-25966
BEECHER, S. C. ..... p 1945 N95-26133
BEHEIM, GLENN ..... p 1912 N95-24207
BEHRINGER, ROBERT P. ..... p 1965 N95-25404
BEHRNDT, K. ..... p 2109 N95-24327
p 2003 N95-24577
BEITEL, GEORGE A. ..... p 2106 N95-25765
BELHOUAS, M. ..... p 2016 N95-24708
BELL, J. B. ..... p 1931 N95-25291
BELL, R. ..... p 1948 N95-24608
BELLAMY, E. H. ..... p 1968 N95-24635
BELLETTINI, G. ..... p 1968 N95-24635
BELOKUROV, V. V. ..... p 2110 N95-25433

BELYAEV, V. B. ..... p 2033 N95-25539
BENATTI, F. ..... p 2092 N95-24266
p 2100 N95-26046
BENEDEK, KAREN ..... p 2003 N95-26091
BENGTSSON, M. ..... p 1955 N95-25749
BENGTSSON, MATS ..... p 2026 N95-25568
BENOY, PATRICIA A. ..... p 1923 N95-24437
BENSINGER, JAMES R. ..... p 2054 N95-25481
BENTON, E. R. ..... p 2058 N95-25911
p 2060 N95-25922
p 2061 N95-25926
p 2061 N95-25930
p 2062 N95-25931
BENTON, E. V. ..... p 2058 N95-25911
p 2059 N95-25914
p 2059 N95-25917
p 2059 N95-25918
p 2059 N95-25919
p 2060 N95-25920
p 2060 N95-25921
p 2060 N95-25922
p 2060 N95-25923
p 2060 N95-25924
p 2060 N95-25925
p 2061 N95-25926
p 2061 N95-25927
p 2061 N95-25929
p 2061 N95-25930
p 2062 N95-25931
p 2062 N95-25932
p 2009 N95-25933
p 2009 N95-25934
BENTON, E, V. ..... p 2061 N95-25928
BERATAN, KATHI K. ..... p 2112 N95-24987
BEREZHIANI, V. I. ..... p 2082 N95-25974
p 2082 N95-25975
BERGER, KIMBERLY H. ..... p 2106 N95-25608
BERN, Z. ..... p 2092 N95-24328
BERNARD, C. ..... p 2085 N95-24451
BERNDT, C. C. ..... p 1945 N95-26130
BERRY, H. G. ..... p 2069 N95-25281
BERTOLOTTI, M. ..... p 2084 N95-24324
BESCO, ROBERT O. ..... p 2012 N95-24237
BESHTOEV, KH. M. ..... p 2048 N95-24669
BETHEA, MARK D. ..... p 1949 N95-24416
BEUTH, JACK L. ..... p 1927 N95-26083
BHANOT, G. ..... p 2093 N95-24450
BHATTACHARJEE, A. ..... p 2028 N95-24276
BHATTACHARYA, A. ..... p 2090 N95-25978
BIALEK, J. ..... p 2076 N95-24548
BIELSKI, WLODZIMIERZ ROBERT
p 2004 N95-25958
BIERING, ROBERT C. ..... p 1915 N95-24380
BILAK, S. V. ..... p 2067 N95-24652
BILLINGSLEY, CHARLES E. ..... p 2089 N95-25409
BIMONTE, G. ..... p 2027 N95-24228
p 2027 N95-24229
p 2093 N95-24405
p 2096 N95-25107
BINDSCHADLER, R. ..... p 1955 N95-25710
BINGHAM, CARL E. ..... p 1993 N95-24715
BINKLEY, K. ..... p 1911 N95-26062
BIRCKELBAW, LOURDES G. ..... p 1908 N95-26302
BISHOP, A. R. ..... p 2063 N95-25971
BISWAL, B. ..... p 2090 N95-25979
BITTEL, J. ..... p 2010 N95-24310
BJOERCK, E. B. ..... p 1989 N95-24444
BJORKEN, JAMES D. ..... p 2047 N95-24663
BJORNSTAD, S. C. ..... p 1989 N95-24422
BLAGOVESHCHENSKIJ, N. M. ..... p 2043 N95-24364
BLAIR, KYM ..... p 2022 N95-26054
BLAMONT, J. ..... p 2112 N95-24994
BLANCH, H. W. ..... p 2008 N95-24843
BLASER, J. P. ..... p 1917 N95-26184
BLAU, MATTHIAS ..... p 2036 N95-25455
BLINOWSKI, ANDRZEJ ..... p 2039 N95-26332
BLOCKER, CRAIG A. ..... p 2054 N95-25481
BLOOM, P. ..... p 2015 N95-24648
BLOTTNER, F. G. ..... p 1961 N95-24262
p 1965 N95-25895
BLUNT, D. M. ..... p 1966 N95-24203
BOCKSTEINER, G. ..... p 1947 N95-24394
BOCZAR, T. ..... p 2040 N95-26071
BOERJESSON, A. ..... p 1978 N95-26002
p 1978 N95-26003
BOGDANOV, S. D. ..... p 2059 N95-25917
p 2059 N95-25918
p 2059 N95-25919
p 2060 N95-25920
BOGOYAVLENSKIJ, I. V. ..... p 2043 N95-24364
BOHN, MARK S. ..... p 1992 N95-24714
BOHNHOFF-HLAVACEK, GAIL ..... p 1925 N95-26072
BONI, A. A. ..... p 1972 N95-25549
BONLIE, JIM ..... p 1968 N95-24657
BOOTH, REX ..... p 1968 N95-24657
BORSA, F. ..... p 2038 N95-25600
BOSE, S. ..... p 1944 N95-26125
BOST, J. B. ..... p 2029 N95-24323
BOTERO, JAVIER ..... p 2040 N95-24230
BOUCHER, FRANCOIS ..... p 1971 N95-24530
BOURGAIN, J. ..... p 2028 N95-24301
p 2028 N95-24322
p 2029 N95-24325
BOURN, G. ..... p 1975 N95-24880
BOUSMAN, WILLIAM SCOTT ..... p 1963 N95-24906
BOWEN, BARRY C. ..... p 1921 N95-25337
BOWERS, MARK ..... p 1968 N95-24657
BOYARKIN, O. ..... p 2054 N95-25466
BOYD, R. E. ..... p 2012 N95-25981
BOYLE, T. J. ..... p 1941 N95-25370
BOZOKI, E. ..... p 2026 N95-25368
BOZOKI, E. S. ..... p 2070 N95-25441
BOZOKI, EVA ..... p 2071 N95-25785
BRAAMS, B. ..... p 2078 N95-24650
BRABY, L. A. ..... p 2051 N95-25373
BRADBURY, E. M. ..... p 2008 N95-24600
BRAMA, A. ..... p 2106 N95-25572
BRATKOVSKAYA, E. L. ..... p 2070 N95-25634
BRAVO, VICTOR AYALA ..... p 2032 N95-25457
BREIZMAN, B. N. ..... p 2079 N95-25216
BRENNAN, J. M. ..... p 2064 N95-24287
BRENNAN, M. J. ..... p 1981 N95-24995
BRENNAN, T. M. ..... p 1951 N95-24289
BRENTNALL, W. D. ..... p 1945 N95-26128
BRESKIN, A. ..... p 1957 N95-24482
p 1957 N95-24483
BRESNAHAM, P. J. ..... p 2000 N95-25278
BREUER, M. ..... p 1959 N95-25405
BREWER, J. C. ..... p 1905 N95-24295
BREWSTER, MICHAEL D. ..... p 2000 N95-25363
BRICKNER, RALPH G. ..... p 2021 N95-25477
BRIMHALL, J. L. ..... p 1934 N95-24449
BRINDLEY, W. J. ..... p 1943 N95-26119
p 1946 N95-26135
BRINKPETER, C. B. ..... p 1941 N95-25387
BROCKHOFF, R. C. ..... p 2041 N95-24258
BROERSE, J. J. ..... p 2051 N95-25373
BROMLEY, BENJAMIN ..... p 2110 N95-25766
BROOKS, J. N. ..... p 2078 N95-24650
BROWN, D. R. ..... p 2086 N95-24514
BROWN, EMERY N. ..... p 2049 N95-24877
BROWN, J. J., JR. ..... p 1927 N95-25998
BROWN, JAMES E. ..... p 1941 N95-25342
BROWN, S. R. ..... p 2056 N95-25624
BRUDNICKI, MYRON ..... p 1936 N95-25545
BRUEMMER, S. M. ..... p 1934 N95-24449
BRUGGEN, M. ..... p 2113 N95-24249
BRYDON, G. M. ..... p 1956 N95-24447
BRYNESTAD, J. ..... p 2089 N95-25389
BUCHANAN, R. A. ..... p 1934 N95-24647
BUCHHEIT, C. D. ..... p 1941 N95-25370
BUDAGOV, J. ..... p 1967 N95-24484
BUDAGOV, YURY ..... p 1968 N95-24635
BUDD, H. S. ..... p 2041 N95-24256
BUECHNER, B. ..... p 1959 N95-25405
BUEHLER, M. F. ..... p 1924 N95-25248
BUHL, MARSHALL L., JR. ..... p 1992 N95-24684
BUKUR, D. B. ..... p 1929 N95-24341
BURDANOV, YA. V. ..... p 2058 N95-25908
p 2058 N95-25909
BURDICK, M. B. ..... p 2105 N95-24654
BURGESON, JOHN ..... p 2006 N95-26012
BURLINGAME, E. ..... p 2015 N95-24648
BURRATTI, B. ..... p 2112 N95-24994
BURRELL, K. H. ..... p 2078 N95-25102
p 2050 N95-25180
p 2079 N95-25250
BURROUGHS, IVAN A. ..... p 1976 N95-25595
BURROWS, P. N. ..... p 2046 N95-24571
BURROWS, T. W. ..... p 2107 N95-25941
BURSILL, L. A. ..... p 2091 N95-26260
BURTON, R. G. ..... p 1925 N95-24426
BURTON, W. SCOTT ..... p 1984 N95-26265
BUSH, H., JR. ..... p 1973 N95-25557
BUSSELL, J. H. ..... p 1960 N95-26092
BUTTNER, WILLIAM J. ..... p 1930 N95-25098
BUZULUTSKOV, A. ..... p 1957 N95-24482
BYCZUK, K. ..... p 2044 N95-24419
BYE, M. ..... p 1917 N95-26184
BZOWSKA, DOROTA ..... p 1951 N95-26109

C

CAHILL, P. A. ..... p 2087 N95-24617
CAI, WEIQUAN ..... p 2041 N95-24268
CALISE, ANTHONY J. ..... p 1917 N95-26205
CALLAHAN, T. ..... p 1975 N95-24880
CALLENAS, A. ..... p 1973 N95-25622
CAMASSA, R. ..... p 2030 N95-24609
CAMPBELL, M. ..... p 1973 N95-26112
CAMPBELL, R. ..... p 2078 N95-24650
CANAVEL, V. ..... p 1939 N95-24373
CANESSA, E. ..... p 2029 N95-24401
CANISTRARO, HOWARD A. ..... p 1968 N95-25330
CAPONERO, M. A. ..... p 2084 N95-24324
CARASSITTI, F. ..... p 2084 N95-24324
CARDER, KENDALL L. ..... p 1970 N95-26113
CAREY, DAVID C. ..... p 2073 N95-25239
CARLEGRIM, B. ..... p 1955 N95-25644
CARLINI, G. ..... p 2082 N95-25974
CARLISLE, NANCY ..... p 1995 N95-25995
CARLSSON, JAN ..... p 1960 N95-25472
CARLSTEN, BRUCE E. ..... p 1958 N95-24589
CARR, R. ..... p 2038 N95-25408
CARR, ROBERT W. ..... p 1924 N95-25286
CARROLL, ERNEST A. ..... p 1912 N95-26060
CARSEY, F. ..... p 1955 N95-25710
CARSON, JOHN ..... p 2024 N95-25260
CARTER, C. D. ..... p 2047 N95-24595
CARTER, DANIEL C. ..... p 2008 N95-24531
CASARETT, G. W. ..... p 2051 N95-25373
CASPER, T. A. ..... p 2078 N95-25102
CASSANDRAS, CHRISTOS G. ..... p 1954 N95-25604
CASTALDINI, C. ..... p 1997 N95-24294
CASTELLI, M. G. ..... p 1983 N95-26078
CAVALLO, G. ..... p 1917 N95-26184
CEDERQUIST, J. N. ..... p 2075 N95-26173
CEKIC, M. ..... p 2077 N95-24619
CELATA, C. ..... p 2069 N95-25358
CERDEIRA, HILDA A. ..... p 2032 N95-25452
CHAKRABARTI, A. ..... p 2090 N95-25978
CHAKRABORTY, DHIMAN ..... p 2052 N95-25402
CHAMATI, H. ..... p 2092 N95-24288
CHAN, V. S. ..... p 2077 N95-24646
CHANCE, JOHN E. ..... p 1910 N95-25609
CHANG, C. I. ..... p 1911 N95-25578
CHANG, DAVID ..... p 2102 N95-24905
CHANG, I.-CHUNG ..... p 1910 N95-24629
CHANG, L. J. ..... p 2085 N95-24431
CHANG, S. C. ..... p 2029 N95-24474
CHANG, ZHE ..... p 2095 N95-24767
p 2091 N95-26101
CHAPELL, P. ..... p 1920 N95-25508
CHARMLEY, BILL ..... p 2001 N95-25575
CHASON, E. ..... p 1942 N95-25898
CHATRCHYAN, T. A. ..... p 2094 N95-24637
CHATTAM, DAVID ..... p 2104 N95-24477
p 2016 N95-24876
CHAU, JOHNNY ..... p 1913 N95-24304
CHAWLA, KALPANA ..... p 1906 N95-24379
CHECHIK, R. ..... p 1957 N95-24482
p 1957 N95-24483
CHELIDZE, A. J. ..... p 2049 N95-24720
CHEN, HONGXIN ..... p 2041 N95-24268
CHEN, J. ..... p 2084 N95-24279
p 2087 N95-24855
CHEN, JUI-SHENG ..... p 1977 N95-26074
CHEN, NINGXIN ..... p 1952 N95-24395
p 1977 N95-26074
CHEN, S. P. ..... p 2086 N95-24513
p 1937 N95-26014
CHEN, T. ..... p 2068 N95-24664
CHEN, W. ..... p 2108 N95-24385
CHEN, X. ..... p 1963 N95-24678
CHEN, YEN-SEN ..... p 1923 N95-25103
CHEN, YINBAO ..... p 2072 N95-26095
CHEN, YIPING ..... p 2082 N95-25942
CHENDO, M. A. C. ..... p 2113 N95-26042
CHENG, S. ..... p 2069 N95-25281
CHENG, Y. S. ..... p 1998 N95-24606
CHEPLAKOV, A. P. ..... p 2045 N95-24485
CHERNENKO, L. P. ..... p 2086 N95-24537
CHEUNG, H. MICHAEL ..... p 2072 N95-24386
CHIKARAISHI, H. ..... p 2071 N95-25855
CHIN, STEVE HUNG-NENG ..... p 2005 N95-25287
CHIRIKOV-ZORIN, I. ..... p 1967 N95-24484
p 1968 N95-24635
CHOUINARD, E. ..... p 1974 N95-24223
CHOULES, B. D. ..... p 1946 N95-26138
CHOW, C. Y. ..... p 2029 N95-24474
CHOWDHURY, D. ..... p 2090 N95-25979
CHRISTENSEN, DAVID ..... p 1978 N95-26286
CHRISTENSEN, DIANE G. ..... p 1909 N95-24384
CHU, F. ..... p 2086 N95-24513
CHU, M. S. ..... p 2078 N95-25102
CHUBURKOV, YURY T. ..... p 2093 N95-24481
CHUDAKOV, E. A. ..... p 2047 N95-24644
CHUONG, NGUYEN HONG ..... p 2110 N95-25647
CHYRCZAKOWSKI, STANISLAW ..... p 1951 N95-26109
CIARKOWSKI, ADAM ..... p 1954 N95-25393
CIECWIERZ, WOJCIECH ..... p 2083 N95-26019
CIMMINO, A. ..... p 2097 N95-25446
CLADIS, PATRICIA E. ..... p 2085 N95-24460
CLARK, ALAN F. ..... p 2108 N95-25746
CLARK, J. W. ..... p 2100 N95-26102
CLARK, P. ..... p 1982 N95-25003
CLARKE, LAURENCE P. ..... p 2025 N95-25267

CLAUSS, LLOYD ..... p 2102 N95-24905
CLAYTON, C. ..... p 2103 N95-24330
CLAYTOR, LLOYD ..... p 1931 N95-25492
CLEARY, N. L. ..... p 1948 N95-24558
CLERC, L. ..... p 2010 N95-24310
CLIFFORD, J. R. ..... p 1940 N95-24717
CLINTON, WILLIAM J. ..... p 2115 N95-26335
CLOSE, F. E. ..... p 2064 N95-26001
COCHRAN, R. J. ..... p 1962 N95-24489
CODA, S. ..... p 1972 N95-24709
COFFEY, H. E. ..... p 2113 N95-25576
COFFEY, HELEN E. ..... p 2113 N95-25577
COFFEY, L. ..... p 2087 N95-24855
COHEN, THOMAS D. ..... p 2098 N95-25562
COLATTO, L. P. ..... p 2093 N95-24352
p 2095 N95-24838
COLE, HOWARD M. ..... p 1992 N95-24682
p 1994 N95-25109
COLE, J. I. ..... p 1934 N95-24449
COLELLA, P. ..... p 1931 N95-25291
CONRAD, B. ..... p 2104 N95-24454
CONRAD, KURT W. ..... p 2104 N95-24603
COOK, RICHARD I. ..... p 2026 N95-25335
COOPER, R. ..... p 1934 N95-24433
COQBLIN, B. ..... p 2028 N95-24276
CORCORAN, M. F. ..... p 2108 N95-24385
CORDS, D. ..... p 2015 N95-24648
COSTINER, SORIN ..... p 2029 N95-24389
COTTRELL, L. ..... p 2020 N95-24597
COTTRELL, S. P. ..... p 2056 N95-25624
COURT, J. D. ..... p 2041 N95-24258
COVEY, C. ..... p 2000 N95-25279
COWEN, D. J. ..... p 2000 N95-25278
COYLE, J. M. ..... p 2033 N95-25509
CRAMER, CHRISTOPHER ..... p 2025 N95-25268
CRAWFORD, H. J. ..... p 2059 N95-25917
p 2059 N95-25918
p 2059 N95-25919
p 2060 N95-25920
CRAWFORD, M. K. ..... p 2038 N95-25600
CREUTZ, M. ..... p 2093 N95-24450
CREUTZ, MICHAEL ..... p 2087 N95-24849
CROSS, PAUL C. ..... p 1976 N95-25101
CROW, VERN ..... p 2106 N95-25774
CRUSE, T. A. ..... p 1946 N95-26134
CRUSE, THOMAS ..... p 2101 N95-26304
CRUZ, CRYSTAL E. ..... p 2012 N95-26204
CSANAK, G. ..... p 1973 N95-26112
CSIGE, I. ..... p 2060 N95-25922
CUMMINGS, U. ..... p 1974 N95-24356
CUMMINS, J. L. ..... p 2018 N95-26167
CUNNINGHAM, GREGORY S. ..... p 2033 N95-25767
CURTIN, CHRISTOPHER ..... p 2085 N95-24460
CURTIN, W. A. ..... p 1939 N95-24247
CURTISS, BRIAN ..... p 1970 N95-26059
CUSTER, J. S. ..... p 1941 N95-25382
CUTHBERTSON, J. W. ..... p 2078 N95-25102
CUTLER, R. A. ..... p 1941 N95-25387
CYR, M. A. ..... p 1967 N95-24473

D

DACUNHA, S. F. ..... p 1937 N95-25751
DAHLBERG, MARTIN ..... p 1931 N95-25443
DAHLKE, LUTZ ..... p 1905 N95-25401
DAICIC, J. ..... p 2054 N95-25474
p 2063 N95-25969
p 2063 N95-25993
p 2100 N95-26104
DAIRAKUM, MASAYUKI ..... p 2077 N95-24585
DALEY, E. W. ..... p 1911 N95-26062
DALEY, R. S. ..... p 1967 N95-24596
DAMOUR, T. ..... p 1917 N95-26184
DAN, NGUYEN TRUNG ..... p 2063 N95-25994
DANAHY, RAYMOND J. ..... p 1930 N95-25097
DANFORD, M. D. ..... p 1936 N95-25677
DANICKI, EUGENIUSZ ..... p 1959 N95-25116
DANIEL, W. J. ..... p 1965 N95-25400
DANIELSON, KENT T. ..... p 1978 N95-26282
DAPKUNAS, S. J. ..... p 1943 N95-26119
p 1944 N95-26123
DARDEN, M. H. ..... p 1977 N95-26172
DARLING, D. H. ..... p 1933 N95-24329
DART, M. ..... p 2020 N95-24597
DARVILL, A. G. ..... p 2007 N95-24368
DAS, A. ..... p 2054 N95-25463
DAS, SUMIT R. ..... p 2098 N95-25526
DASILVA, E. G. ..... p 1930 N95-24840
DATTA, DHUJATI PRASAD ..... p 2098 N95-25525
DATTA, DHURJATI PRASAD ..... p 2097 N95-25432
DAUD, TAHER ..... p 2025 N95-25266
DAUTET, HENRI ..... p 1971 N95-24530
DAVID, G. ..... p 2028 N95-24243
DAVID, S. A. ..... p 1938 N95-26064
DAVIES, JOHN P. ..... p 2007 N95-25605
DAVIES, M. ..... p 2112 N95-24994
DAVIS, J. BRADLEY ..... p 1921 N95-25337
DAVIS, L. I., JR. ..... p 2025 N95-25269
DAVYDOV, YU. I. ..... p 2058 N95-25905
DAWSON, S. ..... p 2044 N95-24420
DAZEVEDO, E. F. ..... p 2019 N95-24250
DEARAUJO, CARLOS F., JR. ..... p 2053 N95-25459
DEBENEDICTIS, DANIEL A. ..... p 1912 N95-26060
DECAMPOS, M. ..... p 1933 N95-24366
DECESARE, C. ..... p 2084 N95-24324
DECKER, F. J. ..... p 2066 N95-24572
DECKER, H. J. ..... p 1977 N95-26076
DECYK, V. K. ..... p 2081 N95-25632
DEFREITAS, L. R. ..... p 2095 N95-24833
DEHAAS, J. C.M. ..... p 2050 N95-25180
DEJ, E. A. ..... p 2047 N95-24640
DELCIMA, O. M. ..... p 2095 N95-24834
DELLACORTE, CHRISTOPHER .. p 1923 N95-24437
DELLAROCCO, PAMELA S. ..... p 2012 N95-26204
DEMARIA, MICHELANGELO ..... p 2114 N95-24871
DEMASI-MARCIN, J. ..... p 1944 N95-26125
DENG, CHUANBAO ..... p 2082 N95-25943
DENSMORE, ARTHUR C. ..... p 1954 N95-25316
DEOLIVIERA, I. G. ..... p 1959 N95-24842
DEPP, D. ..... p 2104 N95-24454
DEREFELDT, G. ..... p 2013 N95-24864
DERENZO, S. E. ..... p 2064 N95-26256
DESCHAMPS, PIERRE ..... p 1971 N95-24530
DESNICA, U. V. ..... p 2091 N95-26087
DEVINE, KAREN D. ..... p 2021 N95-24681
DEY, J. ..... p 2095 N95-24839
DEY, JISHNU ..... p 2053 N95-25459
DEY, MIRA ..... p 2053 N95-25459
DIAMOND, P. H. ..... p 2077 N95-24587
DIB, NIHAD I. ..... p 1957 N95-24476
DICKES, E. ..... p 1907 N95-24443
DIDYK, A. YU. ..... p 2087 N95-24891
DIETRICH, LECH ..... p 1936 N95-25638
p 1983 N95-26178
p 1938 N95-26179
DIKUSAR, N. D. ..... p 2030 N95-24645
DILLER, T. E. ..... p 1968 N95-25118
DIMARTINO, M. ..... p 2079 N95-25108
DIMENNA, R. A. ..... p 1939 N95-24344
DIMOS, D. ..... p 1941 N95-25370
DINEJKHAN, M. ..... p 2050 N95-24890
DINESCU, M. ..... p 2084 N95-24324
DINEYKHAN, M. ..... p 2092 N95-24312
DINIZ, P. ..... p 2015 N95-24346
DINWIDDIE, R. B. ..... p 1945 N95-26133
DIPIAZZA, P. ..... p 1963 N95-24678
DIVER, RICHARD B. ..... p 1992 N95-24676
DIXON, L. ..... p 2092 N95-24328
DJEMAI, A. E. F. ..... p 2032 N95-25427
DOANE, J. L. ..... p 2079 N95-25108
DOANE, WILLIAM J. ..... p 2085 N95-24460
DODGE, L. ..... p 1975 N95-24880
DOGRA, V. K. ..... p 1961 N95-24396
DOMAGALA, PIOTR ..... p 1956 N95-26331
DONALD, STACEY ..... p 1918 N95-26306
DONNELLY, RUSSELL J. ..... p 1965 N95-25404
DORIA, M. M. ..... p 1959 N95-24842
DORNHOFF, A. G. ..... p 2022 N95-26066
DOROKHOV, A. E. ..... p 2042 N95-24315
DOSANJH, SUDIP S. ..... p 2004 N95-25476
DOSHI, R. ..... p 1991 N95-24607
DOYAL, JEFFREY A. ..... p 1905 N95-25607
DOYLE, E. J. ..... p 2078 N95-25102
DOZIER, J. ..... p 1955 N95-25710
DRAKE, J. F. ..... p 2081 N95-25561
DREBORG, K. H. ..... p 2102 N95-25642
DUBOIS, A. J. ..... p 2022 N95-26066
DUBOVIK, V. M. ..... p 2037 N95-24696
DUDKIN, E. V. ..... p 2062 N95-25932
DUDKIN, V. E ..... p 2059 N95-25917
DUDKIN, V. E. ..... p 2059 N95-25914
p 2059 N95-25918
p 2059 N95-25919
p 2060 N95-25920
p 2061 N95-25926
p 2061 N95-25927
p 2061 N95-25928
p 2061 N95-25929
p 2061 N95-25930
DUFF, I. S. ..... p 2033 N95-25627
DUGAN, THOMAS J. ..... p 1930 N95-25097
DUNBAR, D. C. ..... p 2092 N95-24328
DUNFORD, C. L. ..... p 2107 N95-25941
DUNLAP, K. ..... p 2103 N95-24330
DUNN, A. M. ..... p 2109 N95-24455
DUNN, J. ..... p 1972 N95-25100
DUNN, JIM ..... p 1968 N95-24657
DUNN, PATRICK ..... p 1925 N95-24438
DUONG, H. H. ..... p 2079 N95-25120
DUPONT, J. N. ..... p 1939 N95-24285
DURANT, J. L., JR. ..... p 2047 N95-24595
DURSCH, HARRY ..... p 1925 N95-26072
DURSCH, HARRY W. ..... p 1923 N95-24583
DUXBURY, T. ..... p 2112 N95-24994
DVALI, G. ..... p 2098 N95-25527
DYKES, J. W. ..... p 2091 N95-26170
DZHINCHARADZE, D. G. ..... p 2058 N95-25905
DZIANKOWSKI, ZYGMUNT ..... p 1983 N95-26178
DZIENISZEWSKI, WOJCIECH ..... p 1951 N95-26109
DZYUBA, YU. G. ..... p 2057 N95-25778

E

EAKMAN, D. ..... p 1921 N95-24216
p 1921 N95-24428
EBERLE, C. C. ..... p 2050 N95-25099
EBERT, DAVID ..... p 2002 N95-25899
EBISAWA, NOBORU ..... p 2043 N95-24339
ECCLESTON, R. S. ..... p 2057 N95-25900
EDDLEMAN, JAMES L. ..... p 2076 N95-24544
EDMONDS, J. A. ..... p 2001 N95-25629
EFIMOV, G. V. ..... p 2092 N95-24312
p 2050 N95-24890
p 2058 N95-25908
p 2058 N95-25909
EFREMOV, A. ..... p 2052 N95-25437
EGOSHI, M. ..... p 2108 N95-24385
EHLER, G. B. ..... p 2000 N95-25278
EICKE, W. G. ..... p 1950 N95-24543
EILERS, DONALD D. ..... p 1948 N95-24670
EISMANN, M. T. ..... p 2075 N95-26173
EKSTROEM, C. ..... p 1914 N95-24260
p 2017 N95-25571
ELIASON, E. ..... p 2112 N95-24994
ELKIND, M. M. ..... p 2051 N95-25373
ELLIOTT, S. ..... p 1999 N95-25198
ELLISON, JOHN ..... p 2067 N95-24601
ELMASSALAMI, M. ..... p 1930 N95-24840
ELMER, KEVIN R. ..... p 2040 N95-26160
EMELYANENKO, G. A. ..... p 2031 N95-24694
p 2031 N95-24695
p 2031 N95-24704
p 2031 N95-24705
p 2031 N95-24859
EMERGY, A. F. ..... p 1962 N95-24489
EMERY, KEITH ..... p 1996 N95-26285
EMMA, P. ..... p 2065 N95-24409
ENDO, SHUJI ..... p 1982 N95-25661
ENGERT, D. E. ..... p 2103 N95-24370
ENQVIST, PER ..... p 2027 N95-25804
ENTING, I. G. ..... p 1999 N95-25199
ERAENEN, S. ..... p 1942 N95-25633
ERCOLESSI, E. ..... p 2027 N95-24228
ERES, G. ..... p 2089 N95-25391
ERICKSON, DAVID J., III ..... p 2002 N95-25955
ERIKSSON, E. A. ..... p 2102 N95-25642
ERIKSSON, G. ..... p 1953 N95-24649
EROR, N. G. ..... p 2088 N95-25282
ERREDE, STEVEN M. ..... p 2056 N95-25563
ERSHOV, S. N. ..... p 2055 N95-25538
ERWIN, JIMELL ..... p 1998 N95-24604
EVANS, D. L. ..... p 1955 N95-25710
EVANS, JOHN C. ..... p 1999 N95-25249
EVERITT, C. W. F. ..... p 1917 N95-26184
EWSUK, K. G. ..... p 1937 N95-25775
EXARHOS, G. J. ..... p 2088 N95-25288

F

FADEEV, N. G. ..... p 2045 N95-24485
FAEHNLE, M. ..... p 2084 N95-24244
p 2084 N95-24246
FAENOV, A. YA. ..... p 1972 N95-25100
FAHEY, JAMES ..... p 2085 N95-24478
FAHLEN, P. ..... p 1995 N95-25892
FAHRENHOLTZ, W. G. ..... p 1937 N95-25775
FAHY, F. J. ..... p 1981 N95-24997
p 1982 N95-25332
FAIDLEY, R. W. ..... p 1977 N95-26172
FAIRBANK, W. M., JR. ..... p 2065 N95-24317
FAIRBANKS, J. W. ..... p 1944 N95-26124
FALLER, WILLIAM E. ..... p 2024 N95-25264
FALTENS, A. ..... p 2069 N95-25358
FAN, B. J. ..... p 1998 N95-24606
FAN, QING ..... p 2027 N95-24214
FANG, HAI-PING ..... p 2036 N95-25439
FANNING, J. C. ..... p 1929 N95-24430
FARLEY, GARY L. ..... p 1943 N95-26118
FAULDER, D. D. ..... p 2004 N95-25666
FAULKNER, J. ..... p 2109 N95-24234
FAZIO, MICHAEL V. ..... p 1958 N95-24589
FELDHAUS, W. S. ..... p 1950 N95-24559
FELDKAMP, LEE A. ..... p 2025 N95-25269
FELMY, A. R. ..... p 1931 N95-25252
FELTER, T. E. ..... p 1967 N95-24596

FENG, J. L. p 2069 N95-25297
FERGUSON, B. L. p 1946 N95-26139
FERNANDEZ-BACA, J. A. p 2038 N95-25600
FERNANDEZ, F. N. p 2106 N95-25907
FERNANDEZ, FELIX E. p 1943 N95-26081
FERNANDEZBACA, J. A. p 2037 N95-24479
FERRARI, A. p 2084 N95-24324
FERRELL, R. A. p 2099 N95-25878
FESSENDEN, T. p 2069 N95-25358
FETZKO, S. p 1974 N95-24356
FIEGEL, TARRA p 2106 N95-25774
FINN, J. M. p 2081 N95-25561
FISCHER, J. E. p 2087 N95-24616
FISCHER, PETER p 1916 N95-24892
FISHER-VANDEN, K. A. p 2001 N95-25629
FISHER, R. K. p 2079 N95-25120
FLACHBART, R. H. p 1948 N95-24558
FLAHERTY, J. E. p 2033 N95-25509
FLAHERTY, JOSEPH E. p 2021 N95-24681
FLEDDERMANN, C. B. p 1994 N95-25360
FLEISCHAUER, PAUL D. p 1947 N95-26188
FLEMING, DONALD K. p 1996 N95-26171
FLEMING, JAMES G. p 1958 N95-24586
FLEMING, R. M. p 2087 N95-24616
FLEMING, TERENCE F. p 2013 N95-24627
FLOOK, V. p 2012 N95-25570
FLOWERS, G. T. p 1913 N95-24213
FLOYD, S. p 2021 N95-25359
FLOYD, SALLY p 2020 N95-24496
p 2015 N95-25773
FLUSS, M. J. p 2091 N95-26170
FLYTZANI-STEPHANOPOULOS, M. p 1928 N95-24286
FLYTZANI-STEPHANOPOULOS, MARIA p 2003 N95-26091
FOCHT, E. M. p 1937 N95-26057
FOREST, C. B. p 2050 N95-25180
FORNACIARI, NEAL p 1931 N95-25492
FORRESTER, B. D. p 1966 N95-24203
FORSBERG, L. p 2013 N95-24510
FORSYTH, P. A. p 2027 N95-24214
FOSTER, JEFFRY p 1914 N95-24392
FOX, JEFFREY p 2102 N95-25771
FRADKOV, V. E. p 1961 N95-24221
FRANK, A. L. p 2058 N95-25911
p 2059 N95-25914
p 2060 N95-25922
p 2060 N95-25923
p 2060 N95-25924
p 2060 N95-25925
p 2061 N95-25926
p 2061 N95-25927
p 2061 N95-25928
p 2061 N95-25929
p 2061 N95-25930
p 2062 N95-25931
p 2062 N95-25932
FRANK, M. R. p 2057 N95-25896
FRANKEL, N. E. p 2096 N95-25428
p 2054 N95-25474
p 2063 N95-25969
p 2082 N95-25976
p 2063 N95-25993
p 2100 N95-26104
FRASER, KEN F. p 1905 N95-24200
p 1905 N95-24201
FREDERICK, LARRY p 2089 N95-25409
FREDERICO, T. p 2095 N95-24839
FREISER, H. p 1924 N95-25597
FRENCH, BEVAN M. p 2113 N95-26336
FRENKEL, GABRIEL p 2007 N95-26048
FRICKE, ROBERT W., JR. p 1919 N95-26189
FRIEDMAN, A. p 2026 N95-25368
FRIEDMAN, AHARON p 2071 N95-25785
FRIGO, L. A. p 2058 N95-25911
FRIIS-CHRISTENSEN, E. p 2004 N95-24897
FRISH, M. D. p 1972 N95-25549
FRITH, P. C. W. p 1914 N95-25936
FRODGE, SALLY L. p 1910 N95-25609
FROSCH, R. p 2067 N95-24652
FUJIEDA, HIROTOSHI p 1907 N95-25105
FUJII, KIMIO p 1925 N95-24365
FUJISAWA, A. p 2081 N95-25651
FUJITA, E. p .928 N95-24257
FUJITA, TOSHIMI p 1907 N95-25105
FUKAHORI, T. p 2104 N95-24372
FUKUYAMA, A. p 2082 N95-25759
p 2083 N95-26326
FULKER, J. L. p 1907 N95-25649
FUNABIKI, KOHEI p 1912 N95-25005
FURENLID, L. R. p 1928 N95-24257
FURLANETTO, M. R. p 2047 N95-24595
FURSAEV, D. V. p 2094 N95-24507
FUTAKATA, ATSUSHI p 2104 N95-24492
FYODOROV, A. p 2064 N95-26256

G

GAASTERLAND, T. p 2008 N95-25181
GAGE, PETER J. p 1910 N95-24436
GAGUNASHVILI, N. D. p 2035 N95-24643
GAGYI-PALFFY, Z. p 2064 N95-26096
GAILIS, R. M. p 2063 N95-25993
GALIC, H. p 2067 N95-24652
GALLEGOS, R. R. p 1957 N95-24488
GAMMAGE, R. B. p 2000 N95-25380
GANGLOFF, RICHARD P. p 1933 N95-24220
GARCIA, F. p 1933 N95-24329
GAREEV, F. A. p 2043 N95-24361
p 2055 N95-25538
GARRAHAN, STEVEN L. p 2027 N95-26086
GARVEY, G. T. p 2069 N95-25366
GARZON, F. H. p 2086 N95-24514
p 2089 N95-25598
GASIEWSKI, A. J. p 2003 N95-24336
GATES, T. A. p 2105 N95-24654
GAUCHER, LIONEL FRANCIS p 2045 N95-24512
GEE, J. M. p 1995 N95-25566
GEE, JAMES M. p 1996 N95-26166
GEKTIN, A. p 2064 N95-26256
GELENBE, EROL p 2025 N95-25268
GENEROLI, ROBERT M. p 1976 N95-25592
GENNSER, M. p 2012 N95-25570
GENSTERMACHER, M. E. p 2076 N95-24490
GENUARDI, MICHAEL T. p 2106 N95-25410
GEORGE, PETE E. p 1923 N95-24583
GEORGETON, G. K. p 1939 N95-24344
GERDT, V. P. p 2030 N95-24691
GERNOTH, K. A. p 2100 N95-26102
GERVAIS, K. L. p 1924 N95-25248
GERVELLI, F. p 1968 N95-24635
GERZON, S. p 2053 N95-25462
GHEE, TERENCE A. p 1907 N95-24566
GHIRARDI, G. C. p 2092 N95-24266
p 2100 N95-26046
GHIRARDI, GIANCARLO p 2097 N95-25453
GHORASHI, BAHMAN p 1963 N95-24628
p 1963 N95-24762
GIAMBIAGI, J. J. p 2093 N95-24446
GIERMAN, S. M. p 1973 N95-25565
GIESKE, JOHN p 1905 N95-25401
GILLILAND, GARY p 2008 N95-24531
GINDAHL, K. p 2009 N95-24227
GINZBURG, VITALY L. p 2108 N95-25746
GIRIMAJI, SHARATH p 2014 N95-25119
GIRIMAJI, SHARATH S. p 1963 N95-24584
GIRVIN, RAQUEL p 1913 N95-24304
GLAESSNER, U. p 2093 N95-24450
GLAGOLEV, V. p 1967 N95-24484
GLASS, S. J. p 1940 N95-24717
GLICKMAN, M. E. p 1961 N95-24221
GOBBY, P. L. p 1973 N95-25557
GOEDJEN, J. G. p 1943 N95-26119
GOETZ, ALEXANDER F. p 1970 N95-26059
GOHIL, P. p 2050 N95-25180
GOLAY, M. W. p 2014 N95-25483
GOLDMAN, P. p 1995 N95-26090
GOLDSTEIN, W. H. p 1972 N95-25100
GOLDSTON, R. p 2078 N95-24650
GOLIKOV, V. V. p 2085 N95-24374
GOMEZ, V. M. p 1973 N95-25557
GOMI, HIROMI p 1970 N95-25763
GOODALL, COLIN p 1909 N95-24631
GOODHEAD, D. T. p 2051 N95-25373
GOODMAN, P. p 2090 N95-25984
GOODRICH, MICHAEL T. p 1965 N95-25485
GORBAR, EH. V. p 2099 N95-25667
GORE, ALBERT, JR. p 2115 N95-26335
GORKOV, L. P. p 2108 N95-25746
GORSLINE, DONN S. p 2112 N95-24303
GOSER, KARL p 2024 N95-25262
GOUNARIS, G. J. p 2064 N95-26001
GOUVEIA, MELANIE J. p 1912 N95-26060
GOVORKOV, A. B. p 2050 N95-25094
GOYAL, A. p 2089 N95-25389
GRAF, HANS PETER p 2023 N95-25256
GRAHN, K. p 1942 N95-25633
GRASSI, R. p 2092 N95-24266
p 2100 N95-26046
GRAY, G. T., III p 2083 N95-24233
GRAY, J. A. p 2047 N95-24595
GRAY, K. E. p 2084 N95-24279
p 2087 N95-24855
GREBER, ISAAC p 2063 N95-25963
GREEN, JAMES S. p 1978 N95-26282
GREEN, P. H. p 2087 N95-24611
GREENBERG, DAVID S. p 2004 N95-25476
GREER, JAMES p 2031 N95-24856
GREGORY, M. Y. p 1939 N95-24344
GRESILLON, D. p 2081 N95-25617
p 2082 N95-25777
GRICE, M. EDWARD p 1924 N95-25602
GRIFFIN, C. J. p 2017 N95-25448
GRIFFIN, G. D. p 1929 N95-24345
GROEBNER, R. J. p 2050 N95-25180
p 2079 N95-25250
GROMME, T. p 2067 N95-24573
GROPP, WILLIAM p 2020 N95-24658
GROSE, WILLIAM L. p 1996 N95-24274
GROSSBERG, P. p 2067 N95-24573
GROSSMAN, J. W. p 1992 N95-24674
GROSSMAN, JAMES W. p 1994 N95-25309
GRUVER, J. L. p 2032 N95-25452
GUASPARI, DAVID p 2020 N95-24634
GUEDDA, M. p 2033 N95-25748
GUILINGER, T. R. p 1942 N95-25898
GUIMARAES, A. P. p 1937 N95-25751
GULAMOV, T. I. p 2049 N95-24888
GULATI, SANDEEP p 2025 N95-25266
GUNN, WALTER J. p 1909 N95-24384
GUO, DEQUAN p 2082 N95-25943
GUPTA, R. p 2094 N95-24610
GURLEY, L. R. p 2008 N95-24600
GURNETT, DONALD A. p 2111 N95-26195
p 2111 N95-26196
GURULE, V. A. p 1973 N95-25557
GUSTAVSSON, A. p 1982 N95-25444
p 1982 N95-25569
GUSTAVSSON, ANDERS p 1982 N95-25445
GUSTAVSSON, SOREN p 1931 N95-25443
GUYENNE, DUC p 2114 N95-25200
GUZDAR, P. N. p 2081 N95-25561
GYULASSY, MIKLOS p 2048 N95-24671

H

HABIB, S. p 2096 N95-25293
HAEFFNER, D. R. p 2069 N95-25300
HAEMERI, K. p 1999 N95-24904
HAGERTY, JAMES D. p 1961 N95-26186
HAGINOYA, HIROFUMI p 2076 N95-24311
HAGRMAN, D. L. p 2069 N95-25365
HAHN, J. P. p 1976 N95-25574
HAKULINEN, T. T. p 2042 N95-24297
HALBLEIB, J. A. p 1940 N95-24717
HALL, J. L. p 2065 N95-24317
HALLETT, JOHN p 2005 N95-24411
p 2085 N95-24478
HALLIKAINEN, M. p 1988 N95-24299
HALYO, EDI p 2096 N95-25095
p 2096 N95-25096
p 2096 N95-25215
HAMADA, Y. p 2081 N95-25651
HAMADY, F. p 1974 N95-24223
HAMADY, F. J. p 1976 N95-25574
HAMAGUCHI, YASUMASA p 1927 N95-25859
HAMAMATSU, KIYOTAKA p 2080 N95-25471
HAMANN, DONALD J. p 1912 N95-26060
HAMILTON, M. L. p 1937 N95-26007
HAMILTON, R. T. p 2052 N95-25377
HAMMONS, B. E. p 1951 N95-24289
HANCOCK, ED p 1995 N95-25995
HANDSCHUH, R. F. p 1977 N95-26076
HANDSCHUH, ROBERT F. p 1977 N95-26074
HANEY, SCOTT W. p 2080 N95-25344
HANG, T. p 1939 N95-24344
HANLON, B. E. p 2097 N95-25435
p 2098 N95-25533
HANNIQUET, A. M. p 2010 N95-24310
HANRAHAN, R. J., JR. p 1935 N95-25388
HANSCHE, BRUCE p 1905 N95-25401
HANSEN, CRAIG N. p 1976 N95-25101
HANSEN, ROBERT p 1996 N95-26285
HANSON, KENNETH M. p 2033 N95-25767
HANSON, WILLIAM L. p 2009 N95-26193
HANSSON, G. p 1973 N95-25622
HAO, BAI-LIN p 2036 N95-25439
HAO, H. p 2099 N95-25878
HARADA, HIROO p 2076 N95-24311
HARDEN, JOHN H., JR. p 1989 N95-24502
HARIDOSS, P. p 2086 N95-24514
HARLOW, R. L. p 2038 N95-25600
HARRIS, B. A. p 2097 N95-25473
p 2099 N95-25970
HARRIS, JOHN W. p 2066 N95-24495
HARTMAN, CHARLES W. p 2076 N95-24544
HARTMANN, I. p 2091 N95-26087
HARVEY, W. DON p 1909 N95-24633
HASAN, J. p 2060 N95-25920
HASEGAWA, MASAJI p 1976 N95-25323
HASSAM, A. p 2081 N95-25561
HASSANEIN, AHMED p 2078 N95-24861
HATA, KENTARO p 2043 N95-24337
HAWLEY, M. p 2086 N95-24514
HAWLEY, M. E. p 2089 N95-25598
HAXTON, W. C. p 2113 N95-24249
p 2109 N95-25122

HAYES, JAMES R. p 1915 N95-26053
HAYNES, T. E. p 2091 N95-26087
HAYNES, W. BRIAN p 1958 N95-24589
HE, XIAO-GANG p 2054 N95-25464
HE, Y. p 2086 N95-24513
HEADLEY, T. J. p 1942 N95-25898
HEATHERLY, D. E. p 2089 N95-25389
HEDIN, A. p 1917 N95-26184
HEDIN, C. E. p 2013 N95-24864
HEDSTROM, GERALD p 1966 N95-26063
HEEMAN, PETER A. p 2016 N95-24536
HEFNER, BILL BRYAN, JR. p 1978 N95-25304
HEIL, ROBERT MILTON p 1909 N95-24391
HEILAND, RANDY W. p 2021 N95-24881
HEILMANN, C. p 2061 N95-25930
HEIMANN, M. p 1999 N95-25199
HEINRICH, W. p 2060 N95-25921
HEISKA, K. p 1988 N95-24299
HELGESON, W. D. p 1957 N95-24488
HELLINGS, R. W. p 1917 N95-26184
HELLSTROM, E. p 2086 N95-24514
HELMICH, D. R. p 1940 N95-24717
HEMMINGER, C. S. p 1942 N95-26049
HENDRICKS, J. S. p 2041 N95-24258
HENDRICKSON, B. p 2015 N95-24346
HENDRICKSON, L. p 2067 N95-24573
HENLEY, C. L. p 1936 N95-25560
HENNEKE, B. F. p 1973 N95-25557
HENRY, E. MICHAEL p 2023 N95-25259
HERAKOVICH, CARL T. p 1933 N95-24220
HERBERT, DEXTER p 2108 N95-24196
HERMAN, H. p 1945 N95-26130
HERMAN, RICHARD G. p 1948 N95-24655
HERMANN, ROBERT p 2026 N95-25803
HERMANSON, E. M. p 2014 N95-25483
HERNANDEZ, C. L. p 1959 N95-24712
HERNDON, KENNETH P. p 1966 N95-25868
HERTEL, E. p 1948 N95-24608
HESS, B. V. p 1967 N95-24596
HEWETT, J. L. p 2050 N95-24903
HICKS, M. p 1929 N95-24614
HIETALA, V. M. p 1951 N95-24289
HIGO, T. p 1958 N95-24701
HILDRETH, M. D. p 2044 N95-24418
HILL, D. N. p 2076 N95-24490
p 2078 N95-24650
HILLS, M. M. p 1942 N95-26049
HILTON, M. R. p 1942 N95-26049
HILTON, MICHAEL R. p 1947 N95-26188
HILTON, PAUL F. p 1912 N95-26060
HIMANSU, A. p 2029 N95-24474
HIMEL, T. p 2067 N95-24573
HINES, D. F. p 2082 N95-25976
HINKS, D. G. p 2084 N95-24279
p 2087 N95-24855
HINTON, L. W. p 2087 N95-24611
HIRZEBRUCH, S. E. p 2060 N95-25921
HITT, ELLIS p 1912 N95-24624
HJALMARSON, H. P. p 1957 N95-24488
HO, JOSEPH X. p 2008 N95-24531
HOANG, ANH TUAN p 2092 N95-24275
p 2028 N95-24276
p 2092 N95-24277
HOANG, NGUYEN VAN p 2110 N95-25647
HOCK, S. M. p 1995 N95-26090
HODGES, DONALD B. p 1912 N95-26060
HOFFMAN, A. p 1932 N95-26261
HOFFMAN, EDWARD J. p 2102 N95-24565
HOFFMAN, N. M. p 2078 N95-24667
HOLBROOK, B. p 2015 N95-24648
HOLDEMAN, J. D. p 1913 N95-24390
HOLIAN, KATHY p 2021 N95-25477
HOLLENBERG, LLOYD C. L. p 2038 N95-25458
p 2098 N95-25475
HOLM, D. D. p 2030 N95-24609
HOLM, E. A. p 1935 N95-24716
HOLMEN, I. M. p 2012 N95-25570
HOLMSTEN, MAGNUS p 2073 N95-24673
HOLT, K. A. p 1948 N95-24558
HOLTZAPPLE, R. p 2066 N95-24572
HOMAIFAR, ABDOLLAH p 1913 N95-24213
HONAMI, SHINJI p 1963 N95-25001
HOO, ED p 1995 N95-25995
HOOPER, STEVEN J. p 1979 N95-24211
HORIUCHI, RITOKU p 2083 N95-26337
HORN, P. W. p 2026 N95-25801
HORSTMAN, R. H. p 1962 N95-24489
HORTA, LUCAS G. p 1979 N95-24208
HOSHINO, KATSUMICHI p 2075 N95-24270
HOSKING, F. M. p 1959 N95-24712
HOULTON, R. J. p 2089 N95-25598
HOWARD, A. J. p 1942 N95-25898
p 2064 N95-26168
HOWARD, G. p 1924 N95-25597
HOWARD, IAN M. p 1975 N95-24393
HOWELL, L. p 1931 N95-25291
HOWELL, R. H. p 2091 N95-26170
HOYT, E. p 1974 N95-24356
HSU, L. L. p 1945 N95-26128
HSU, ROBERT H. p 1934 N95-24480
HUANG, P. G. p 1966 N95-26077
HUEBNER, WAYNE p 1992 N95-24683
HUEY, S. p 1997 N95-24294
HUFFMAN, SCOTT BRADLEY p 2019 N95-26206
HUGG, L. A. p 1929 N95-24430
HUGHES, JOHN F. p 1966 N95-25869
p 2018 N95-25870
HULETT, L. D., JR. p 2050 N95-25099
HULL, S. p 2074 N95-25573
HULTMAN, F. p 2013 N95-24510
HUND, THOMAS D. p 1996 N95-26166
HUNTRESS, WESLEY T., JR. p 2108 N95-26183
HUSSAIN, F. p 2053 N95-25460
HWANG, JENQ-NENG p 2026 N95-25603
HYATT, A. W. p 2078 N95-25102
HYMER, W. C. p 2008 N95-24475

I

IGNATIEV, A. YU. p 2054 N95-25465
IGUCHI, H. p 2081 N95-25651
IIYOSHI, A. p 2072 N95-26110
p 2072 N95-26111
p 2072 N95-26250
IKEDA, H. p 2037 N95-24479
p 1931 N95-25356
IKEDA, YUJIRO p 2076 N95-24511
p 2055 N95-25497
IKEHATA, TAKASHI p 2081 N95-25498
ILAIWI, K. F. p 2097 N95-25468
ILIN, V. D. p 2057 N95-25778
ILINA, A. N. p 2057 N95-25778
ILLARIONOVA, N. S. p 2067 N95-24652
IMAGAWA, S. p 2071 N95-25855
IMRICH, K. J. p 1934 N95-24615
INAGAKI, TOSHIHARU p 1912 N95-25005
INCAGLI, M. p 1968 N95-24635
INGASON, HAUKUR p 1931 N95-25443
IOFA, M. Z. p 2110 N95-25433
IRWIN, J. p 2068 N95-24664
ISAACS, H. S. p 1930 N95-25123
ISAEV, A. P. p 2094 N95-24509
ISAWA, KIYOYUKI p 1952 N95-24491
ISHIDA, YOJI p 1907 N95-24998
ISHIEKWENE, G. C. p 2082 N95-25972
p 1973 N95-25973
ISHIKAWA, HIROSHI p 2077 N95-24585
ISHIZUKA, HIROSHI p 2070 N95-25631
ISICHENKO, M. B. p 2077 N95-24587
ISOTALO, H. p 1939 N95-24300
ITO, T. p 1971 N95-26182
ITOH, K. p 2082 N95-25759
p 2083 N95-26326
ITOH, S. I. p 2083 N95-26326
ITOH, S.-I. p 2082 N95-25759
IVANDA, M. p 2091 N95-26087
IVANOV, M. p 1952 N95-24506
IVANOV, T. p 1956 N95-24245
IVANOV, V. V. p 2035 N95-24858
IWAMOTO, A. p 2071 N95-25855
IWANOW, ZDZISLAW p 2035 N95-26106
IWASA, K. p 2037 N95-24479
IWASAKI, AKIHITO p 1907 N95-25105
IWASAKI, KAZUO p 1908 N95-25762
IWASAKI, YOSHIHITO p 2044 N95-24417
IYER, RAVISHANKAR K. p 2016 N95-24993
p 1978 N95-25333
IZEN, JOSEPH M. p 2051 N95-25241

J

JACKSON, D. M. p 2003 N95-24336
JACKSON, R. W. p 1911 N95-25935
JACOB, MARY p 2042 N95-24269
JACOBS, S. J. p 2087 N95-24617
JACOBSEN, F. p 1968 N95-24623
JAFRY, Y. p 1917 N95-26184
JAIN, V. K. p 1952 N95-24403
JAKUBIK, WIESLAW p 2039 N95-25115
JAMEISON, D. N. p 2090 N95-25985
JAMES, BONNIE F. p 1921 N95-25875
JAMES, P. p 1981 N95-24997
JAMES, P. J. p 1982 N95-25332
JAMES, R. A. p 2050 N95-25180
JAMESON, ANTONY p 1911 N95-25334
JAMESON, R. A. p 2065 N95-24331
JAMNEJAD, VAHRAZ p 1954 N95-25316
JANECKI, DARIUSZ p 2027 N95-26330
JARVINEN, G. p 1924 N95-25597
JASPER, S. A., JR. p 1929 N95-24430
JAYARAMAN, N. p 1926 N95-25596
JEDRZEJEWSKI, ANDRZEJ p 1978 N95-25957
JEDRZEJUK, HANA p 1951 N95-26109
JEE, W. S. S. p 2011 N95-24556
JENDRUCKO, R. J. p 1911 N95-26062
JENKINS, ROBERT C. p 1975 N95-24991
JENSEN, HANS B. p 2068 N95-24728
JENSEN, J. R. p 2000 N95-25278
JEPPSSON, U. p 2102 N95-25642
JEZEK, K. p 1955 N95-25710
JI, XINHUA p 2008 N95-24531
JOB, P. K. p 2069 N95-25300
JOE, EDMOND J. p 1978 N95-25304
JOENSSON, L. p 1953 N95-24836
JOHANNESEN, LEILA J. p 2026 N95-25335
JOHNSEN, B. P. p 1946 N95-26134
JOHNSEN, H. A. p 1972 N95-25549
JOHNSON, B. R. p 2075 N95-26198
JOHNSON, D. R. p 1940 N95-24588
JOHNSON, DENNIS A. p 1967 N95-24236
JOHNSON, G. R. p 2103 N95-24370
JOHNSON, KENNETH R. p 1969 N95-25547
JOHNSSON, S. LENNART p 2021 N95-25477
JOHNSTON, D. C. p 2038 N95-25600
JOHNSTON, S. D. p 2056 N95-25624
JONES, D. P. p 1953 N95-24605
JONES, DONALD A. p 2033 N95-25676
JONES, E. D. p 2089 N95-25353
JONES, HOBERT W. p 1930 N95-25097
JONES, M. p 1924 N95-25597
JONES, MARI R. p 2013 N95-26041
JONES, P. p 1999 N95-25198
JONES, R. L. p 1946 N95-26137
JORDAN, ERIC H. p 1968 N95-25330
JORDANOV, A. p 1967 N95-24484
JORGENSON, PHILIP C. E. p 2018 N95-25879
JOSHI, G. p 2099 N95-25970
JOSHI, G. C. p 2097 N95-25435
p 2054 N95-25465
p 2097 N95-25473
p 2098 N95-25533
JOSHI, M. V. p 2042 N95-24269
JOSHI, MAHENDRA C. p 2040 N95-26160
JUBRINK, H. G. p 1954 N95-25623
JULKA, VIBHOR p 1954 N95-25604
JUNGERT, E. p 1988 N95-24240
JUNGMAR, M. p 2102 N95-25642

K

KAARET, PHILIP p 2114 N95-24381
KABRISKY, MATTHEW p 2025 N95-25272
KACHMAR, BRIAN A. p 1955 N95-25876
KACZMAREK, MARIUSZ p 1932 N95-26107
KADIRI, A. p 2033 N95-25532
KADYKOV, M. G. p 1967 N95-24486
KAISER, H. p 2097 N95-25446
KAISER, J. H. p 2091 N95-26170
KAISER, T. p 2078 N95-24650
KAITILA, J. p 1939 N95-24300
p 1942 N95-25633
KAITO, C. p 1930 N95-24840
KAKUTA, YOSHIAKI p 1927 N95-25859
KALISH, R. p 2090 N95-25985
p 1932 N95-26261
KALLIES, W. p 2042 N95-24316
p 2034 N95-25782
KAMBURYAN, A. F. p 2047 N95-24644
KAMIJO, KENJIRO p 1977 N95-25672
KAMIONSKIJ, V. L. p 2085 N95-24374
KANANOV, S. p 2053 N95-25462
KANDA, HIROSHI p 1907 N95-24998
KANDA, TAKESHI p 1914 N95-24990
KANEKO, H. p 2071 N95-25855
KANG, MYONG H. p 2015 N95-26192
KANIA, EDMUND p 1978 N95-25957
KAPISHIN, M. N. p 2047 N95-24644
KAPSHAJ, V. N. p 2047 N95-24640
KARAOGLAN, I. p 1985 N95-26271
KARAOGLAN, LEVENT p 1986 N95-26279
KARBOWSKI, J. p 2044 N95-24419
KARITA, YUKIO p 2021 N95-25303
KARLSSON, ANDERS p 2027 N95-25805
KARNATSEVICH, L. V. p 2043 N95-24364
KARPOV, O. N. p 2059 N95-25914
p 2061 N95-25929
KARTAL, S. p 2111 N95-26044
KARTAVTSEV, O. I. p 2033 N95-25539
KASISCHKE, E. p 1955 N95-25710
KASLE, DAVID B. p 1960 N95-25889
KATEHI, LINDA P. B. p 1957 N95-24476
KATIPAMULA, S. p 1991 N95-24369
KATNIK, GREGORY N. p 1921 N95-25337
KAUPPINEN, E. p 1999 N95-24904
KAWAHARA, HIROYASU p 2073 N95-25004
p 1912 N95-25005

KAWAI, M. p 2104 N95-24372
KAWASAKI, SUNAO p 1971 N95-24340
p 2070 N95-25631
KAWASUMI, Y. p 2081 N95-25651
KAWOLA, J. S. p 1929 N95-24614
KAY, R. REX p 1960 N95-25558
KAZACHA, G. S. p 2043 N95-24361
KAZAKOV, D. I. p 2063 N95-25968
KE, H. Z. p 2011 N95-24556
KEARNS, W. p 1920 N95-25508
KEE, ROBERT J. p 1930 N95-25242
KEEGAN, R. P. p 2058 N95-25911
p 2059 N95-25914
KEELING, KIM p 2008 N95-24531
KEELING, RALPH F. p 2002 N95-25955
KEICHER, D. M. p 1971 N95-24408
KEKELIDZE, V. D. p 2047 N95-24644
KELLER, LINDSAY P. p 1928 N95-24222
KELLERMANN, K. p 2108 N95-25746
KELLEY, HENRY L. p 1907 N95-24566
KELLY, JOHN C., JR. p 1913 N95-24213
KELLY, M. J. p 1942 N95-25898
KELLY, R. E. p 1962 N95-24412
p 1962 N95-24413
KEMENY, SABRINA E. p 2022 N95-25253
p 2023 N95-25258
KENNY, SEAN P. p 1920 N95-24581
KENT, S. M. p 2111 N95-26284
KERBER, THIERRY p 1979 N95-24282
p 1980 N95-24283
p 1980 N95-24284
KERCZEWSKI, ROBERT J. p 1955 N95-25876
KERO, R. p 2103 N95-24330
KESSELI, J. B. p 1913 N95-24293
KEY, J. p 1998 N95-24846
KEY, JEFF p 1989 N95-24441
KHARZHEEV, YU p 1967 N95-24484
KHUTORNOJ, N. V. p 2030 N95-24691
KHVASTUNOV, M. S. p 2092 N95-24347
KIBLER, M. p 2093 N95-24349
KIEFER, W. p 2091 N95-26087
KIEU, T. D. p 2017 N95-25448
KILCOYNE, S. H. p 2056 N95-25624
KILGORE, W. ALLEN p 1915 N95-24388
KIM, J. G. p 1934 N95-24647
KIM, J. M. p 2008 N95-24600
KIM, J. W. p 1948 N95-24498
p 1997 N95-24499
KIM, J.-H. p 2005 N95-26341
KIM, JINWON p 2006 N95-25635
KIM, JONNATHAN H. p 1922 N95-24626
KIM, K. H. p 2038 N95-25600
KIM, M. p 2050 N95-24902
KIM, S. H. p 1997 N95-24499
p 2001 N95-25629
KIM, W. p 1926 N95-25295
KIM, Y. S. p 1948 N95-24498
KIM, YONG H. p 1985 N95-26270
p 1987 N95-26280
KING, DONALD B. p 1958 N95-24586
KING, M. E. p 2043 N95-24354
p 2046 N95-24575
KING, R. R. p 1995 N95-25566
KIRANE, M. p 1931 N95-25447
p 2033 N95-25645
p 2033 N95-25748
KIRICHOK, A. V. p 2081 N95-25556
KIRKPATRICK, RONALD C. p 2070 N95-25594
KIRSCH, LAWRENCE E. p 2054 N95-25481
KIRSTEN, T. p 2113 N95-25364
KIRYK, ROMUALD p 1983 N95-26178
KISHI, KATSUHIRO p 1942 N95-25760
KISHIMOTO, YASUAKI p 1971 N95-24340
KISSEL, LYNN p 2046 N95-24549
KITAMOTO, S. p 2108 N95-24385
KITAZAWA, K. p 2091 N95-26170
KLAPDOR-KLEINGROTHAUS, H. V. p 2109 N95-24885
p 2109 N95-24886
KLEIN, A. G. p 2097 N95-25446
KLEINBERG, LEONARD L. p 1960 N95-26038
KLEM, J. F. p 1990 N95-24264
KLIBANOV, A. M. p 2008 N95-24843
KLICH, PHILLIP J. p 1919 N95-24765
KLIER, KAMIL p 1948 N95-24655
KLINGBIEL, PAUL H. p 2106 N95-25410
KLYUKHIN, V. I. p 2067 N95-24652
KNACKE, ROGER F. p 2111 N95-24239
KOBZEV, A. P. p 2086 N95-24537
KOCH, CHRISTOF p 2024 N95-25265
KOCHKIN, V. I. p 2033 N95-25539
KOJIMA, H. p 2091 N95-26170
KOKINI, K. p 1946 N95-26138
KOLIAS, JOHN H. p 2030 N95-24632
KOLOBRODOV, p 2043 N95-24364
KOMAROV, V. I. p 2048 N95-24692
KONKASHBAEV, ISAK K. p 2078 N95-24861
KONNO, CHIKARA p 2076 N95-24511
p 2055 N95-25497
KONOPLYANIKOV, V. F. p 2049 N95-24719
KOPRIVA, DAVID A. p 2030 N95-24632
KORENMAN, G. YA. p 2055 N95-25493
p 2056 N95-25668
KORHONEN, PEKKA p 2001 N95-25500
KORNEEV, D. A. p 2086 N95-24537
KOROBEJNIKOV, V. A. p 1957 N95-24487
KOROTKIYAN, V. p 2052 N95-25437
KOROTKIYAN, V. M. p 2095 N95-24727
KORTELING, J. E. p 1913 N95-26190
KORZHIK, M. p 2064 N95-26256
KOSAKO, KAZUAKI p 2076 N95-24511
p 2055 N95-25497
KOSHELEV, A. E. p 2087 N95-24868
KOSHKAROV, A. L. p 2036 N95-24688
KOSMACH, V. F. p 2059 N95-25919
p 2060 N95-25920
KOSOWER, D. A. p 2092 N95-24328
KOSSECKA, ELZBIETA p 1951 N95-26109
KOSTERMAN, J. p 1974 N95-24223
KOSTINA, L. N. p 2009 N95-25933
KOUACHI, S. p 2033 N95-25645
KOUZNETSOV, K. p 2087 N95-24855
KOVALENKO, A. D. p 2060 N95-25921
KOVALENKO, S. G. p 2109 N95-24885
p 2109 N95-24886
p 2099 N95-25966
KOVALEV, E. E. p 2059 N95-25917
p 2059 N95-25918
p 2059 N95-25919
p 2060 N95-25920
p 2061 N95-25926
p 2061 N95-25927
p 2061 N95-25930
KOWALCZK, MACIEJ p 2037 N95-25339
KOWALENKO, V. p 2063 N95-25969
p 2063 N95-25993
KOWALENKO, VICTOR p 2100 N95-26104
KOWALEWSKI, ZBIGNIEW L. p 2096 N95-25428
p 1935 N95-25117
p 1936 N95-25638
p 1938 N95-26333
KRAUTER, K. p 2067 N95-24573
KREIN, G. p 2095 N95-24839
KRESIN, V. Z. p 2108 N95-25746
KRIGE, JOHN p 2114 N95-24870
p 1916 N95-24872
KRINSKY, S. p 2070 N95-25369
KRISCH, A. D. p 2046 N95-24547
KRISHNARAJ, P. p 2088 N95-25282
KROEGER, D. M. p 2089 N95-25389
KRUMPELT, M. p 1991 N95-24607
KRUPA, D. p 2055 N95-25537
KUBIK, JOZEF p 1932 N95-26107
KUIVALAINEN, P. p 1939 N95-24300
p 1942 N95-25633
KUKLIN, V. M. p 2081 N95-25556
KULAGIN, E. N. p 2085 N95-24374
KULIMANOVA, N. p 1952 N95-24506
KULKARNI, MAKARAND p 1984 N95-26266
p 1984 N95-26268
p 1986 N95-26278
KULKARNI, V. T. p 2042 N95-24269
KULKOV, A. A. p 2073 N95-24642
KUMAR, ANIL p 2076 N95-24511
KUMAR, N. p 1960 N95-26100
KUMAR, R. p 1991 N95-24607
KUNG, H. p 1940 N95-24456
KUPERMAN, M. N. p 2001 N95-25521
KUPERMAN, MARCELO N. p 2001 N95-25531
KURAEV, EH. A. p 2047 N95-24668
KURATA, YUJI p 1933 N95-24338
KURFESS, J. D. p 2108 N95-25746
KURIBARA, MASAYUKI p 1952 N95-24491
KURONO, MASAHIRO p 1952 N95-24491
KURZ, WOLFGANG p 1994 N95-25501
KWAN, T. J. T. p 1959 N95-25385
p 1973 N95-26112

L

LACIAK, DANIEL V. p 1932 N95-26093
LADING, LARS p 2072 N95-24386
LAFLAMME, R. p 2109 N95-24455
LAI, M. p 1931 N95-25291
LAMARSH, WILLIAM J., II p 2015 N95-24209
LAMB, MILTON p 1907 N95-25338
LAMBECK, R. p 1921 N95-24216
p 1921 N95-24428
LAMBETH, M. p 1974 N95-24223
LANDI, G. p 2027 N95-24228
LANDIS, GEOFFREY A. p 1991 N95-24560
LANGE, CLIFFORD H. p 1995 N95-26037
LANTRIP, DAVID p 2106 N95-25774
LAPUCHA, DARIUSZ p 1910 N95-25609
LARIMER, JAMES p 2085 N95-24460
LARSSON, M. p 1982 N95-25444
p 1982 N95-25569
LASKOWSKI, LESZEK p 1995 N95-25758
p 1951 N95-26109
LASNIER, C. J. p 2076 N95-24490
LASSAHN, G. D. p 2021 N95-25378
LATORELLA, KARA A. p 1910 N95-24582
LATTIMER, JAMES M. p 2110 N95-25343
LAU, W. K.-M. p 2005 N95-26341
LAUBERTS, A. p 2036 N95-25894
LAUGHERY, MIKE p 1918 N95-26305
LAURANCE, R. p 1917 N95-26184
LAVINE, T. L. p 2070 N95-25406
LAWRENCE, W. E. p 1924 N95-25248
LAZARUS, D. M. p 2064 N95-26006
LAZARUS, E. A. p 2078 N95-25102
LEE-GLAUSER, GINA J. p 1979 N95-24208
LEE, E. p 2069 N95-25358
LEE, INHWAN p 2016 N95-24993
LEE, M. p 1917 N95-26184
LEE, S. A. p 2065 N95-24317
LEE, S. L. p 2030 N95-24592
p 2032 N95-25251
LEE, S. R. p 1941 N95-25382
LEE, T. K. p 1997 N95-24499
LEE, W. Y. p 1943 N95-26119
p 1944 N95-26122
LEFF, CRAIG E. p 2112 N95-24987
LEHAR, F. p 2067 N95-24652
LEHNERT, B. E. p 2008 N95-24600
LEINO, Y. p 1980 N95-24296
LEITAO, V. p 1980 N95-24383
LELAND, R. p 2015 N95-24346
LELOVIC, M. p 2088 N95-25282
LEMMEL, H. D. p 2107 N95-25980
LEONARD, T. p 2076 N95-24490
LEONDES, CORNELIUS p 1912 N95-24624
LEUNG, MARTIN S. K. p 1917 N95-26205
LEVIN, B. F. p 1939 N95-24285
LEVIN, Y. p 2053 N95-25461
LEVINE, T. p 1940 N95-24456
LEVINE, T. E. p 1935 N95-25379
LEVY, S. C. p 2054 N95-25470
LEWANDOWSKI, ALLAN A. p 1993 N95-24715
LEWICKI, D. G. p 1977 N95-26076
LEWIS, C. E. p 2008 N95-25383
LI, F. p 1955 N95-25710
LI, FOSHENG p 2041 N95-24268
LI, LINZHONG p 2082 N95-25943
LI, M. p 2011 N95-24556
LIANG, X. G. p 2011 N95-24556
LIAW, PAUL p 1923 N95-25103
LIBA, I. p 1967 N95-24484
LIBBY, S. B. p 1972 N95-25100
LICHTENWALNER, PETER F. p 2025 N95-25271
LIDIA, S. p 2038 N95-25408
LIEBECK, ROBERT H. p 1913 N95-24304
LIGETI, ZOLTAN p 2095 N95-24723
LIKHACHEV, A. YU. p 2059 N95-25919
p 2060 N95-25920
LIM, KAP p 2008 N95-24531
LIMBERG, T. p 2065 N95-24409
LIN, B. Y. p 2011 N95-24556
LIN, F. p 2015 N95-24648
LIN, SHU p 2015 N95-24224
LINDEMUTH, I. R. p 2080 N95-25289
LIOU, MENG-SING p 1961 N95-24399
LIOU, W. W. p 1966 N95-26077
LISCINSKY, D. S. p 1913 N95-24390
LITTLE, A. D. p 1950 N95-24559
LITTLE, W. A. p 2108 N95-25746
LITVAK, A. G. p 2063 N95-25991
LITVIN, FAYDOR L. p 1952 N95-24395
p 1977 N95-26074
LITVINENKO, E. I. p 2037 N95-24363
LIU, BAW-LIN p 1906 N95-24217
LIU, C. S. p 2081 N95-25561
LIU, LIANG p 2041 N95-24268
LIVECCHI-GONNOT, G. p 2010 N95-24310
LIZZI, F. p 2027 N95-24228
p 2027 N95-24229
LKHAGVA, O. p 2055 N95-25493
p 2056 N95-25668
LLOYD, W. G. p 1997 N95-24406
LOEHMAN, R. E. p 1940 N95-24717
p 1937 N95-25775
LOGE, G. p 1969 N95-25384
LOKEN, S. C. p 2068 N95-24665
LOKTEV, V. M. p 2090 N95-25776
LOLL, V. p 1978 N95-26002
p 1978 N95-26003
LOMDAHL, P. S. p 2020 N95-24612

LONGDON, N. p 2114 N95-24870
LOOBY, G. P. p 1911 N95-26062
LOOSE, R. R. p 1995 N95-26090
LOPEZ, AMALIA R. p 1966 N95-26240
LORENC, M. p 2040 N95-26071
LORENZO, CARL F. p 1923 N95-25877
LOUBRIEL, G. M. p 1957 N95-24488
LOUGHLIN, MARIA M. p 1966 N95-25869
LOY, D. A. p 2090 N95-25897
LOZANO, G. p 2093 N95-24405
p 2096 N95-25107
LU, J. p 1995 N95-25995
LU, JIAN p 1952 N95-24395
p 1977 N95-26074
LU, YU p 2063 N95-25971
LUBECK, CHRISTI p 1931 N95-25492
LUCAS, B. N. p 1933 N95-24432
LUCAS, G. E. p 1937 N95-26007
LUCCHESI, D. p 1968 N95-24635
LUCE, T. C. p 2050 N95-25180
LUCHES, A. p 2084 N95-24324
LUDWIG, DAVID E. p 2074 N95-25506
LUHANDJULA, M. K. p 2016 N95-24708
LUI, HURBERT p 1923 N95-26310
LUKAC, I. p 2034 N95-25782
LUKYANOV, V. K. p 2035 N95-24883
LUNEGOV, I. V. p 2037 N95-24696
LUNG, C. W. p 2041 N95-24232
LUPTAK, K. p 1935 N95-25379
LUSHCHIKOV, V. I. p 2085 N95-24374
LUTTGES, MARVIN W. p 2024 N95-25264
LYON, ROGER p 1913 N95-24304
LYONS, J. p 2056 N95-25620
LYONS, L. R. p 2080 N95-25325
LYUBOVITSKIJ, V. p 1952 N95-24506

M

MA, Y. F. p 2011 N95-24556
MACCALLA, AYANNA p 2025 N95-25266
MACFARLANE, J. J. p 2108 N95-24385
MACFARLANE, R. E. p 2055 N95-25484
MACGREGOR, ANDREW D. p 1971 N95-24530
MACKENZIE, R. p 2067 N95-24573
MACKEY, H. E., JR. p 2000 N95-25278
MACKOWSKI, M. p 1921 N95-24216
p 1921 N95-24428
MACNEICE, PETER p 2083 N95-26082
MADAN, V. K. p 1958 N95-24690
MADDOCKS, JAMES p 1965 N95-25404
MADDUX, GARY A. p 2104 N95-24477
p 2016 N95-24876
MADEJ, DARIUSZ p 2016 N95-25392
MADRAS, ERIC I. p 1926 N95-25305
MADUEKWE, A. A. L. p 2113 N95-26042
MAEDA, HIKOSUKE p 2075 N95-24270
MAEKAWA, FUJIO p 2076 N95-24511
p 2055 N95-25497
MAEKAWA, HIROSHI p 2076 N95-24511
p 2055 N95-25497
MAEKINEN, H. p 2066 N95-24448
MAENO, MASAKI p 2075 N95-24271
MAGHAMI, PEIMAN G. p 1920 N95-24581
MAGNUSSON, M. p 2011 N95-24863
MAGRADZE, N. V. p 2059 N95-25914
p 2061 N95-25926
p 2061 N95-25929
MAHAJAN, S. M. p 2082 N95-25975
MAHAPATRA, SWAPNA p 2097 N95-25456
MAHECHAGOMEZ, J. p 2048 N95-24718
MAIA, M. D. p 2065 N95-24335
MAIELLO, G. p 2084 N95-24324
MAIENSCHEIN, J. L. p 1933 N95-24329
MAKER, PAUL D. p 1971 N95-26340
MAKOWSKI, M. A. p 2050 N95-25180
MALAMUD, G. p 1957 N95-24482
p 1957 N95-24483
MALCZYNSKI, LEONARD p 2105 N95-24675
MALOY, S. A. p 2083 N95-24233
MALYUKOV, S. p 1967 N95-24484
MANAJAN, A. V. p 2038 N95-25600
MANI, S. p 2015 N95-24648
MANN, J. ADIN, JR. p 2072 N95-24386
MANSFIELD, D. K. p 2079 N95-25120
MANSOUR, A. N. p 1932 N95-26056
MANTEUFFEL, TOM p 2054 N95-25479
MARCIANO, W. J. p 2052 N95-25375
MARDER, A. R. p 1939 N95-24285
MARDOYAN, L. G. p 2093 N95-24349
p 2094 N95-24637
MARENNY, A. p 2009 N95-25933
MARENNY, A. M. p 2062 N95-25931
MARGOLIN, LEN G. p 2033 N95-25676
MARIOCCHI, A. p 1944 N95-26126
MARKEL, V. A. p 1926 N95-25295
MARKIEWICZ, T. W. p 2046 N95-24576
MARKO, KENNETH A. p 2023 N95-25255
MARSDEN, J. E. p 2030 N95-24609
MARTIN, A. D. p 2056 N95-25619
MARTIN, CHRISTOPHER p 2108 N95-25104
MARTIN, CLYDE p 2026 N95-25802
MARTIN, CLYDE F. p 2026 N95-25801
MARTIN, J. D. p 1960 N95-26092
MARTINEC, D. A. p 1912 N95-24624
MARTINO, A. p 1929 N95-24614
MARTINO, LOUIS E. p 2000 N95-25363
MARTINO, M. p 2084 N95-24324
MARTINSSON, C. p 2074 N95-25999
MARTOGLIO, P. A. p 1928 N95-24265
MARTONAK, R. p 2091 N95-26252
MARTSENYUK, M. A. p 2037 N95-24696
MASE, HIROSHI p 2081 N95-25498
MASERJIAN, JOSEPH p 1959 N95-25307
MASLANIK, JAMES p 1989 N95-24441
MASON, M. J. p 1931 N95-25252
MASUDA, YASUHIRO p 2048 N95-24702
MASUYA, GORO p 1914 N95-24990
MATHESON, LEIGH N. p 1912 N95-26060
MATHEUS-VALLE, J. L. p 2043 N95-24350
p 2095 N95-24838
MATHUR, V. S. p 2054 N95-25463
MATORA, I. M. p 2057 N95-25784
MATSUDA, TOSHIAKI p 2075 N95-24271
MATSUI, SHOUICHI p 1952 N95-24493
MATSUOKA, K. p 2071 N95-26031
MATTHEWS, F. p 2034 N95-25982
MATTOK, CLARE p 2114 N95-25200
MATZEN, M. KEITH p 2066 N95-24500
MAUDLIN, PAUL J. p 1941 N95-25237
MAVRIPLIS, D. J. p 2032 N95-25106
MAVRIPLIS, DIMITRI J. p 2031 N95-24857
MAYER, J. p 1935 N95-25379
MAYTON, MONICA p 1912 N95-24624
MCASHAN, MICHAEL p 1965 N95-25404
MCBETH, GIORGIO p 1963 N95-24762
MCCABE, D. J. p 1929 N95-24430
MCCARTHY, K. A. p 2069 N95-25365
MCCHESNEY, J. M. p 2079 N95-25120
MCCLEARY, SUSAN L. p 1983 N95-26199
MCCOLLOM, ALEX D. p 2049 N95-24877
MCCONNELL, SHANNON L. p 2112 N95-24987
MCCORD, JAMES T. p 1965 N95-25485
MCDANIEL, DILLON H. p 2066 N95-24500
MCDOWELL, D. L. p 1982 N95-25444
MCELFRESH, M. p 1930 N95-24840
MCGEE, WILLIAM F. p 1976 N95-25548
MCHALE, J. M., JR. p 2086 N95-24594
MCHUGH, JOHN p 2020 N95-24634
MCKAY, STEVEN J. p 1912 N95-26060
MCKOWN, THOMAS O. p 1948 N95-24670
MCMACKEN, J. R. F. p 2027 N95-24214
MCNEIL, WALTER E. p 1908 N95-26302
MCNEW, E. B. p 2069 N95-25365
MEDERNACH, J. W. p 1941 N95-25382
MEDLEY, S. S. p 2079 N95-25120
MEE, D. p 1964 N95-25394
p 1914 N95-25395
MEE, D. J. p 1914 N95-25396
p 1965 N95-25400
MEHOS, M. p 1997 N95-24319
MEI, CHUH p 1981 N95-24907
MEISSNER, MIROSLAW p 2040 N95-26108
MELACK, J. p 1955 N95-25710
MELANDER, A. p 1982 N95-25444
p 1982 N95-25569
MELANDER, ARNE p 1982 N95-25445
MELENDRES, C. A. p 1932 N95-26056
MELEZHIK, V. S. p 2058 N95-25910
MELKUMYAN, L. V. p 2061 N95-25928
p 2062 N95-25932
MENDOZA, J. p 2039 N95-24879
MENDREK, M. J. p 1936 N95-25677
MENTESANA, CHARLES P. p 1958 N95-24532
MERCER, CAROLYN R. p 1970 N95-26073
MEROLA, S. p 2019 N95-24290
MERRILL, WALTER C. p 1923 N95-25877
MESHCHERYAKOV, V. A. p 2055 N95-25537
MEYER, MARYJO B. p 1949 N95-24416
MEYER, TOM p 1966 N95-25868
MEYER, TOM W. p 2018 N95-25870
MEYER, W. J. p 1951 N95-24289
MEYER, WILLIAM V. p 2072 N95-24386
p 1971 N95-24530
MICHALAKES, J. G. p 2019 N95-24342
MICKLITZ, H. p 1959 N95-25405
MIKKANEN, P. p 1999 N95-24904
MIKKONEN, R. p 2066 N95-24448
MILDH, I. M. p 1953 N95-24835
MILES, MICHAEL D. p 2022 N95-25254
MILLER, BRIAN B. p 1949 N95-24416
MILLER, GREGORY A. p 2000 N95-25363
MILLER, L. L. p 2038 N95-25600
MILLER, M. K. p 1938 N95-26064
MILLER, NORMAN p 2006 N95-25635
MILLER, P. p 2016 N95-24898
p 2090 N95-25984
MILLER, R. A. p 1943 N95-26121
MILLER, R. F. p 1981 N95-24598
MILLEV, Y. p 2084 N95-24246
MILLEV, YONKO p 2084 N95-24244
MILLS, J. p 1924 N95-25597
MIN, B. M. p 1997 N95-24499
MINE, P. p 1957 N95-24482
p 1957 N95-24483
MINKEVICH, A. V. p 2110 N95-25647
MINKOV, B. p 2064 N95-26256
MIRKES, E. p 2056 N95-25567
MIRONOV, V. A. p 2063 N95-25991
MITCHELL, K. L. p 2057 N95-25896
MITCHELL, K. W. p 1995 N95-25566
MITCHELL, T. E. p 2086 N95-24513
MITCHUM, M. V. p 1950 N95-24559
MITO, T. p 2071 N95-25855
MITYURICH, G. S. p 2083 N95-24205
MIYOSHI, KAZUHISA p 1924 N95-25961
MIZUNO, H. p 1958 N95-24701
MOELLER, C. P. p 2079 N95-25108
MOINESTER, M. A. p 2053 N95-25462
MOIR, RALPH p 2076 N95-24544
MOIR, RALPH W. p 2067 N95-24651
MOISEENKO, A. A. p 2061 N95-25929
MOLDACH, JOANNA p 1951 N95-26109
MOLDOVER, M. R. p 2099 N95-25878
MOMOTA, H. p 2072 N95-26110
p 2072 N95-26111
MONACO, LISA A. p 2086 N95-24534
MONAHAN, J. H. p 1989 N95-24422
MONCRIEFF, D. p 2056 N95-25620
p 2022 N95-25625
MONEY, JOHN MARSHALL p 2090 N95-26061
MONTEIRO, M. R. p 2043 N95-24350
MONTGOMERY, BRAD p 1942 N95-26004
MONTGOMERY, RONALD W. p 2011 N95-25336
MOORE, C. S. p 1945 N95-26133
MOORE, J. E. p 1973 N95-25557
MOORE, J. P. p 2103 N95-24370
MOORE, MIKE p 2102 N95-25771
MOORTHY, HARI T. p 2015 N95-24224
MOORTHY, JAYASHREE p 1981 N95-24907
MORANO, ERIC p 2032 N95-25106
MORGAN, C. p 2103 N95-24330
MORGAN, R. G. p 1964 N95-25394
p 1915 N95-25399
MORIMATSU, OSAMU p 2070 N95-25772
MORISAKI, T. p 2071 N95-26031
MORITA, S. p 2071 N95-26031
MORIYAMA, MINORU p 1976 N95-25323
MOSES, W. W. p 2064 N95-26256
MOSHOFSKY, R. P. p 2035 N95-24248
MOSLEY, W. D. p 2091 N95-26170
MOSS, J. N. p 1961 N95-24396
MOSS, TIMOTHY A. p 1992 N95-24682
p 1994 N95-25109
MOSTROM, M. A. p 1959 N95-25385
MOTOJIMA, O. p 2071 N95-25855
p 2072 N95-26110
p 2072 N95-26111
p 2072 N95-26250
MOULTON, DAVID S. p 1998 N95-24604
MRIG, LAXMI p 1996 N95-26285
MUELLER, J. A. p 2051 N95-25372
MUIR, D. W. p 2055 N95-25484
MUIRA, N. p 2108 N95-24385
MUJIBURRAHMAN, S. M. p 1937 N95-25983
MUKHERJI, SUDIPTA p 2097 N95-25456
p 2098 N95-25526
MUKHOPADHYAYA, BISWARUP p 2053 N95-25438
MULE, K. p 2048 N95-24689
MULIK, J. p 1975 N95-24880
MULLER, RICHARD E. p 1971 N95-26340
MURADIAN, R. p 2110 N95-25431
p 2111 N95-25990
MURAKAMI, AKIRA p 1963 N95-25001
MURALIDHARAN, S. p 1924 N95-25597
MURAYAMA, HITOSHI p 2092 N95-24333
MUROTA, KATSUICHI p 1908 N95-25761
MURPHY, D. p 2087 N95-24616
MURPHY, DIANE R. p 2102 N95-24442
MURPHY, R. W. p 1951 N95-25367
MUSGRAVE, JEFFEREY L. p 1923 N95-25877
MUSYOKI, STEPHEN p 2070 N95-25631
MUTASIM, Z. Z. p 1945 N95-26128
MYERS, S. A. p 2090 N95-25897
MYLES, K. M. p 1991 N95-24607
MYONG, K. S. p 1948 N95-24498

N

NADOLSKI, WLADYSLAW ..... p 1981 N95-24996
NAEGELI, D. ..... p 1975 N95-24880
NAGABUSHANA, K. A. ..... p 1970 N95-25699
NAGAJTSEV, A. P. ..... p 2045 N95-24485
NAGAO, TAKAHARU ..... p 1977 N95-25672
NAGARAJ, B. A. ..... p 1945 N95-26133
NAJJAR, RAYMOND G. ..... p 2002 N95-25955
NAKAGAWARA, VAN B. ..... p 2011 N95-25336
NAKAHARA, YURIKO ..... p 2070 N95-25631
NAKAHIRA, MASATAKA ..... p 1966 N95-26161
NAKAISHI, CURTIS V. ..... p 1930 N95-25098
NAKAJIMA, HAJIME ..... p 1933 N95-24338
NAKAJIMA, N. ..... p 2071 N95-26031
NAKAMURA, KAZUYUKI ..... p 2077 N95-24585
NAKAMURA, MASARU ..... p 1912 N95-25005
NAKAMURA, TOMOO ..... p 2076 N95-24511
NAKANO, JUNICHI ..... p 1925 N95-24365
NAM, KHO SEB ..... p 2093 N95-24481
NANJUNDIAH, R. S. ..... p 2019 N95-24342
NARIHARA, K. ..... p 2081 N95-25651
NASTASI, M. ..... p 1935 N95-25379
NAUMANN, ROBERT J. ..... p 2084 N95-24261
NAZAROV, F. ..... p 2028 N95-24321
NEDELKO, S. N. ..... p 2058 N95-25908
p 2058 N95-25909
NEELY, A. J. ..... p 1915 N95-25399
NEFEDOV, N. A. ..... p 2059 N95-25917
p 2059 N95-25918
p 2059 N95-25919
p 2060 N95-25920
NELLSON, G. H. ..... p 2078 N95-24650
NELSON, C. A. ..... p 2050 N95-24902
p 2051 N95-25292
p 2051 N95-25294
p 2051 N95-25296
NELSON, W. A. ..... p 1944 N95-26127
NEMESURE, S. ..... p 1997 N95-24570
NERSESSIAN, A. ..... p 2100 N95-25987
NERSESYAN, A. P. ..... p 2036 N95-24699
NESTERENKO, V. V. ..... p 2036 N95-24504
NESTHUS, THOMAS E. ..... p 2012 N95-24237
NEUFFER, D. V. ..... p 2065 N95-24357
NGUYEN, D. C. ..... p 1973 N95-25565
NGUYEN, HOGAN H. ..... p 1972 N95-24869
NGUYEN, NGOC THUAN ..... p 2092 N95-24275
p 2028 N95-24276
NGUYEN, TOAN THANG ..... p 2092 N95-24277
p 2092 N95-24275
p 2028 N95-24276
p 2092 N95-24277
NICINSKI, T. ..... p 2106 N95-25376
NICKLOW, R. M. ..... p 2037 N95-24479
NICOLAIDES, R. A. ..... p 2029 N95-24421
NICOLSON, DAVID M. ..... p 1977 N95-26050
NIETO, M. M. ..... p 2091 N95-24235
NIINI, I. ..... p 1967 N95-24259
NIKITIN, V. A. ..... p 2047 N95-24668
NIKKINEN, M. T. ..... p 2042 N95-24296
NILSSON, S. ..... p 1955 N95-25891
NIR, YOSEF ..... p 2049 N95-24722
NISHIGUCHI, I. ..... p 2082 N95-25903
NISHIMURA, K. ..... p 2071 N95-26031
NISHIMURA, MAKOTO ..... p 1976 N95-25323
p 1942 N95-25760
NISHIZAWA, A. ..... p 2081 N95-25651
NISSLEY, D. M. ..... p 1947 N95-26140
NITTROUER, CHARLES A. ..... p 2006 N95-25504
NODA, JUNICHI ..... p 1921 N95-25664
NOEL, BRUCE W. ..... p 1989 N95-25110
NOGUCHI, MASAYOSHI ..... p 1907 N95-24998
NOGUCHI, YOSHIO ..... p 1926 N95-24989
NOGUCHI, YOUSHOI ..... p 1927 N95-25770
NOLIN, A. ..... p 1998 N95-24846
NOOR, A. K. ..... p 1985 N95-26271
NOOR, AHMED K. ..... p 1983 N95-26263
p 1983 N95-26264
p 1984 N95-26265
p 1984 N95-26266
p 1984 N95-26267
p 1984 N95-26268
p 1984 N95-26269
p 1985 N95-26270
p 1985 N95-26272
p 1985 N95-26273
p 1985 N95-26274
p 1986 N95-26275
p 1986 N95-26276
p 1986 N95-26277
p 1986 N95-26278
p 1986 N95-26279
p 1987 N95-26280
p 1987 N95-26281
p 1978 N95-26282
p 1987 N95-26283
NORRMAN, S. ..... p 1988 N95-24240
NORTH, DEANNE R. ..... p 2001 N95-25575
NORTON, O. W. ..... p 1921 N95-25875
NOVAK, R. C. ..... p 1945 N95-26132
NOVELLO, M. ..... p 2095 N95-24833
NOYES, H. P. ..... p 2094 N95-24578
p 2098 N95-25530
NYDEN, MARC R. ..... p 1941 N95-25342
NYMMIK, R. A. ..... p 2062 N95-25931

O

OASA, KAZUMI ..... p 2075 N95-24270
OBERKAMPF, WILLIAM L. ..... p 1966 N95-26240
OBERLATZ, MICHAEL J. ..... p 1912 N95-26060
OBUKHOV, YU. V. ..... p 2037 N95-24363
ODAGIRI, J. ..... p 1958 N95-24701
ODAJIMA, KAZUO ..... p 2075 N95-24270
OEDMAN, S. ..... p 2009 N95-24227
OERNHAGEN, H. ..... p 2011 N95-24863
p 2012 N95-25570
OESTMAN, B. ..... p 1932 N95-26000
OFARRELL, J. M. ..... p 1906 N95-24217
OGAWA, HIROAKI ..... p 2075 N95-24271
OGAWA, TORU ..... p 2055 N95-25496
OGAWA, TOSHIHIDE ..... p 2075 N95-24270
OGIWARA, NORIO ..... p 2075 N95-24271
OGURA, KOICHI ..... p 2081 N95-25498
OHNEMUS, J. ..... p 2056 N95-25567
OHNISHI, M. ..... p 2072 N95-26110
p 2072 N95-26111
p 2072 N95-26250
OHNISHI, YUKIYOSHI ..... p 2047 N95-24622
OHNO, Y. ..... p 2108 N95-24385
OHRINER, E. K. ..... p 1935 N95-25390
OKAMOTO, M. ..... p 2072 N95-26110
p 2072 N95-26111
p 2072 N95-26250
OKAMOTO, YOSHIHIRO ..... p 2055 N95-25496
OKAMURA, S. ..... p 2071 N95-26031
OKAZAKI, M. ..... p 1971 N95-26182
OKIISHI, THEODORE H. ..... p 1914 N95-24392
OLBRICH, C. ..... p 1974 N95-24223
OLDFIELD, RON A. ..... p 2004 N95-25476
OLEINICK, N. L. ..... p 2051 N95-25373
OLEKSUK, L. L. S. ..... p 1939 N95-24247
OLIVER, W. C. ..... p 1933 N95-24432
OLSSON, H. A. ..... p 1955 N95-25749
OMALLEY, M. W. ..... p 1957 N95-24488
OMRAN, M. ..... p 2113 N95-25986
ONO, FUMIEI ..... p 1914 N95-24990
ONO, TAKATSUGU ..... p 1912 N95-25005
ONOZUKA, M. ..... p 2072 N95-26110
p 2072 N95-26111
p 2072 N95-26250
OPAT, G. I. ..... p 2097 N95-25446
OPAT, GEOFFREY I. ..... p 2038 N95-25430
OPILSKI, ALEKSANDER ..... p 2039 N95-25115
OPPENHEIM, ALAN V. ..... p 2017 N95-25507
ORERORN, U. ..... p 1955 N95-25641
ORENSTEIN, R. M. ..... p 1944 N95-26127
ORHAUG, T. ..... p 1989 N95-24444
OSBORN, R. ..... p 2057 N95-25900
OSBORNE, T. H. ..... p 2078 N95-25102
OSHEA, P. G. ..... p 1973 N95-25565
OSMAN, S. M. ..... p 1937 N95-25983
p 2100 N95-26105
OSTERHELD, A. L. ..... p 1972 N95-25100
OSTROUMOV, V. I. ..... p 2059 N95-25917
p 2059 N95-25918
OTT, E. ..... p 2081 N95-25561
OTTESEN, D. K. ..... p 1972 N95-25549
OUANES, M. ..... p 2016 N95-24708
OVASKAINEN, O. ..... p 1980 N95-24296
OVERILL, R. E. ..... p 2022 N95-25625
OWSIANNY, MARIUSZ ..... p 1956 N95-26018
OXLEY, MARK E. ..... p 2025 N95-25272
OYAMA, YUKIO ..... p 2076 N95-24511
p 2055 N95-25497

P

PAGLIARONE, C. ..... p 1968 N95-24635
PALMER, DAVID W. ..... p 1959 N95-24713
PALMER, MICHAEL T. ..... p 1910 N95-24582
PALMER, R. ..... p 2065 N95-24357
PAN, WEI-PING ..... p 1997 N95-24406
PANCHENKO, I. P. ..... p 2081 N95-25556
PAPADOPOULOS, G. ..... p 2098 N95-25534
p 2099 N95-25650
PARANTHAMAN, M. ..... p 2089 N95-25389
PARK, S. C. ..... p 1997 N95-24499
PARKER, JAMES F., JR. ..... p 1909 N95-24384
PARKER, TIMOTHY J. ..... p 2112 N95-24303
PARKS, P. B. ..... p 2079 N95-25120
PARKS, W. P. ..... p 1944 N95-26122
PARNELL, T. A. ..... p 2061 N95-25926
p 2061 N95-25927
p 2061 N95-25930
p 2009 N95-25934
PASTORE, G. ..... p 2034 N95-25982
PATE, T. E. ..... p 1939 N95-24344
PATRA, B. K. ..... p 2052 N95-25436
PATTON, TERRY L. ..... p 2000 N95-25363
PATWARDHAN, A. B. ..... p 2042 N95-24269
PAUL, D. M. ..... p 2085 N95-24431
PAUL, P. H. ..... p 2047 N95-24595
PAUL, P. K. ..... p 1939 N95-24344
PAUL, PHILLIP ..... p 1931 N95-25492
PAULEY, H. ..... p 1907 N95-24443
PAULL, A. ..... p 1964 N95-25394
p 1914 N95-25395
p 1914 N95-25396
PAXSON, DANIEL E. ..... p 1908 N95-25962
PAXSON, VERN ..... p 2015 N95-25773
PAYNE, J. L. ..... p 1961 N95-24262
p 1906 N95-24308
p 1965 N95-25895
PEARSON, A. E. ..... p 1911 N95-24630
PEASE, DOUGLAS M. ..... p 1968 N95-25330
PECHERSKY, M. J. ..... p 1981 N95-24598
PEDERSON, L. R. ..... p 2088 N95-25002
PEMBER, R. B. ..... p 1931 N95-25291
PENG, J. L. ..... p 2091 N95-26260
PENNEY, TERRY ..... p 1978 N95-26286
PENNOCK, KELLY ..... p 2106 N95-25774
PEREPEZKO, J. H. ..... p 2086 N95-24513
PEREZRODRIGUEZ, F. ..... p 2029 N95-24401
PERL, M. L. ..... p 2044 N95-24414
p 2046 N95-24591
PEROOMIAN, OSHIN ..... p 1962 N95-24412
p 1962 N95-24413
PERRY, FERMAN W. ..... p 1983 N95-26263
PERVUSHIN, V. N. ..... p 2042 N95-24316
p 2029 N95-24387
PESTOV, A. B. ..... p 2063 N95-25965
PETERKA, ROBERT J. ..... p 2010 N95-24410
PETERS, C. ..... p 2069 N95-25358
PETERS, JEANNE M. ..... p 1983 N95-26264
p 1984 N95-26267
p 1984 N95-26269
p 1986 N95-26277
PETERS, ROBERT W. ..... p 2000 N95-25363
PETRAVIC, M. ..... p 1932 N95-26261
PETRIE, T. ..... p 2076 N95-24490
PETROV, M. P. ..... p 2079 N95-25120
PETRUS, G. ..... p 1946 N95-26139
PETTERSSON, L. ..... p 1955 N95-25644
PETTY, GRANT W. ..... p 2005 N95-24535
PETTY, K. H. ..... p 2050 N95-25180
PETZOLDT, RONALD W. ..... p 2067 N95-24651
PEYTON, RODNEY ..... p 2015 N95-26192
PHELPS, R. D. ..... p 1972 N95-24709
PHILLIPS, R. J. N. ..... p 2056 N95-25567
PHIPPS, GARY ..... p 1905 N95-25401
PICKRELL, G. R. ..... p 1927 N95-25998
PICKRELL, J. ..... p 2069 N95-25358
PIELORZ, AMALIA ..... p 1981 N95-24996
PIILA, J. ..... p 1980 N95-24296
PILAFTSIS, A. ..... p 2056 N95-25626
p 2064 N95-26096
PILLAY, G. ..... p 1924 N95-25248
PINDERA, MAREK-JERZY ..... p 1925 N95-24438
PINTO-NETO, N. ..... p 2095 N95-24833
PIPPIN, GARY ..... p 1925 N95-26072
PIPPIN, H. GARY ..... p 1923 N95-24583
PISKUNOVA, O. I. ..... p 2049 N95-24887
PISO, M. I. ..... p 2036 N95-25434
PITCHER, H. M. ..... p 2001 N95-25629
PITKAERANTA, J. ..... p 1980 N95-24296
PITTS, K. T. ..... p 2067 N95-24574
PITTS, KEVIN T. ..... p 2057 N95-25768
PIWOWAR, TOM ..... p 2006 N95-26012
PIZZI, R. ..... p 2016 N95-24898
PIZZICONI, V. ..... p 1935 N95-25379
PLIMPTON, S. ..... p 2015 N95-24346
PLOWIEC, R. ..... p 1932 N95-25959
PLOWIEC, RYSZARD ..... p 2083 N95-26019
PLUT, T. A. ..... p 1990 N95-24264
p 1957 N95-24488
PLYASHKEVICH, S. N. ..... p 2045 N95-24485
POELLOT, MICHAEL R. ..... p 2005 N95-24219
POGOSYAN, G. S. ..... p 2093 N95-24349
p 2034 N95-25782
POHLMANN, K. ..... p 1988 N95-24407
POJE, ANDREW C. ..... p 2033 N95-25676
POLITES, MICHAEL E. ..... p 1969 N95-25544
POLITZEER, PETER ..... p 1924 N95-25602
POLLOCK, A. M. T. ..... p 2108 N95-24385
POPE, KEVIN O. ..... p 1997 N95-24501

POPOV, A. D. ..... p 2031 N95-24698
p 2037 N95-25781
POPOWICZ, Z. ..... p 2094 N95-24509
PORTER, G. D. ..... p 2076 N95-24490
PORTER, L. ..... p 1964 N95-25394
PORTMAN, A. I. ..... p 2009 N95-25933
POTAPOV, V. ..... p 2059 N95-25914
POTAPOV, YU. V. ..... p 2061 N95-25926
p 2061 N95-25928
p 2061 N95-25929
p 2061 N95-25930
p 2062 N95-25932
POTREBENNIKOV, YURY K. ..... p 2047 N95-24644
POTTIER, MARC ..... p 2106 N95-25774
POULOS, STEPHEN ..... p 1978 N95-26286
POUND, BRUCE G. ..... p 1936 N95-25502
POWELL, BRADLEY W. ..... p 1976 N95-25595
PRAGER, S. C. ..... p 2077 N95-24602
PRAWER, S. ..... p 2090 N95-25985
p 2091 N95-26260
p 1932 N95-26261
PRESCOTT, CHARLES Y. ..... p 2047 N95-24662
PRESS, HAYES N. ..... p 1910 N95-24582
PRESSEL, DANIEL M. ..... p 2035 N95-26051
PRESSLY, ROBERT B. ..... p 1958 N95-24532
PRICE, DWIGHT ..... p 1968 N95-24657
PRICE, HENRY W. ..... p 1992 N95-24714
PRICE, J. M. ..... p 1961 N95-24396
PRIDMORE-BROWN, D. C. ..... p 2080 N95-25325
PROKERT, F. ..... p 2085 N95-24362
p 2090 N95-25851
PROTO, A. N. ..... p 2032 N95-25452
PROTOGENOV, A. P. ..... p 2063 N95-25991
p 2091 N95-26103
PROTOPOPESCU, SERBAN ..... p 2048 N95-24677
PROVANCHA, ANNA ..... p 2104 N95-24477
p 2016 N95-24876
PUCHKOV, A. V. ..... p 2043 N95-24364
PULKKINEN, U. ..... p 2018 N95-26045
PULSONETTI, M. V. ..... p 1933 N95-25398
PURCELL, RICHARD G. ..... p 2005 N95-24411
PURDY, ELLEN M. ..... p 1942 N95-25510
PURI, S. ..... p 2090 N95-25979
PUROHIT, MILIND ..... p 2071 N95-26011
PURVIS, BRADLEY D. ..... p 1905 N95-25607
PUSKORIUS, G. V. ..... p 2025 N95-25269
PUZYNIN, A. I. ..... p 2048 N95-24692
PUZYNIN, I. V. ..... p 2029 N95-24387
p 2034 N95-25906
PUZYNINA, T. B. ..... p 2029 N95-24387

Q

QAIYUM, ABDUL ..... p 2110 N95-25467
QIAN, Y. Z. ..... p 2113 N95-24249
QUEEN, BRIAN ..... p 2085 N95-24478
QUICK, R. M. ..... p 2065 N95-24351
QUINN, P. J. ..... p 2110 N95-25766

R

RACETTE, P. E. ..... p 2003 N95-24336
RACHAL, T. ..... p 1974 N95-24223
RADHAKRISHNAN ..... p 2042 N95-24269
RADICELLA, S. M. ..... p 2111 N95-26044
RAHEMATPURA, MANOJ ..... p 1979 N95-24211
RAISTRICK, I. A. ..... p 2089 N95-25598
RAKHMONOV, T. T. ..... p 2031 N95-24694
p 2031 N95-24695
p 2031 N95-24704
p 2031 N95-24705
p 2031 N95-24859
RALSTON, J. ..... p 1907 N95-24443
RAMATY, R. ..... p 2108 N95-25746
RAMER, DAVID P. ..... p 1905 N95-25607
RAMIREZ, JUAN J. ..... p 2066 N95-24500
RAMSEY, G. ED ..... p 1975 N95-24991
RAMSEY, G. P. ..... p 2042 N95-24292
RAMUS, J. E. ..... p 2103 N95-24370
RANACHOWSKI, J. ..... p 2083 N95-24205
RANACHOWSKI, JERZY ..... p 2039 N95-25115
p 1978 N95-25957
p 2040 N95-26180
RANACHOWSKI, ZBIGNIEW ..... p 2040 N95-26071
p 2040 N95-26180
RANGASWAMY, P. ..... p 1926 N95-25596
RANKIN, W. NEVYN ..... p 1934 N95-24480
RAO, M. ..... p 1937 N95-25977
p 2090 N95-25978
RAPPOPORT, KEVIN J. ..... p 1912 N95-26060
RATIS, YU. L. ..... p 2043 N95-24361
RAUBENHEIMER, T. ..... p 2066 N95-24572
RAVISHANKARA, A. R. ..... p 1996 N95-24274
RAWDON, BLAINE K. ..... p 1913 N95-24304
RAY, ASOK ..... p 1923 N95-25877
RAYL, K. D. ..... p 2008 N95-25181
RAYMOND, T. D. ..... p 2074 N95-25559
READ, WILLIAM J. L. ..... p 1956 N95-26191
REBBECHI, B. ..... p 1966 N95-24203
REBER, CATHLEEN A. ..... p 1959 N95-24713
RECAMI, ERASMO ..... p 2053 N95-25449
RECK, GREGORY M. ..... p 2108 N95-26183
REDA, DANIEL C. ..... p 2075 N95-26117
REDDY, R. V. ..... p 2004 N95-26036
REFFNER, J. A. ..... p 1928 N95-24265
REGINATO, L. ..... p 2069 N95-25358
REICHERT, BRUCE A. ..... p 1914 N95-24392
REIFSNIDER, K. L. ..... p 1939 N95-24247
REIN, D. ..... p 2054 N95-25466
REMONDI, BENJAMIN W. ..... p 1910 N95-25609
RENHORN, I. ..... p 1952 N95-24445
RENNER, M. W. ..... p 1928 N95-24257
RENSINK, M. E. ..... p 2076 N95-24490
REUTHER, JAMES ..... p 1911 N95-25334
REX, BRUCE ..... p 2022 N95-26013
REYNOLDS, EDWARD L. ..... p 1920 N95-24711
RHEA, OWEN ..... p 2006 N95-25635
RICE, EDWARD J. ..... p 2040 N95-26187
RICHARDSON, JOSEPH ..... p 2101 N95-26304
RICHTER, LUTOSLAWA ..... p 1956 N95-26331
RICKEY, JUNE ELIZABETH ..... p 1914 N95-24561
RIEGER, D. J. ..... p 2064 N95-26168
RIETJENS, M. ..... p 1949 N95-25517
p 1949 N95-25528
RILEY, J. P. ..... p 1950 N95-24543
RILEY, J. T. ..... p 1997 N95-24406
RILEY, K. J. ..... p 1950 N95-24543
RIMBEY, P. R. ..... p 1909 N95-25341
RIMONDI, F. ..... p 2041 N95-24252
RING, SHAN ..... p 1993 N95-24866
RINGH, U. ..... p 1967 N95-24280
RINOIE, KENICHI ..... p 1907 N95-25105
RISTIG, M. L. ..... p 2100 N95-26102
RISTORCELLI, J. R. ..... p 1966 N95-25964
RIZZO, T. G. ..... p 2044 N95-24415
p 2052 N95-25407
ROACH, DENNIS ..... p 1905 N95-25401
ROBERTO, RICHARD D. ..... p 1990 N95-24199
ROBERTS, C. D. ..... p 2057 N95-25896
ROBERTS, M. L. ..... p 1967 N95-24596
ROBERTS, R. G. ..... p 2056 N95-25619
ROBISON, GARY ..... p 1996 N95-26166
RODRIGUESJUNIOR, O. ..... p 2010 N95-24367
RODRIGUEZ, JOSE M. ..... p 1996 N95-24274
ROE, MERRY M. ..... p 2013 N95-26041
ROGERS, JAMES L., JR. ..... p 2015 N95-24209
ROGERS, RICHARD B. ..... p 2072 N95-24386
p 1971 N95-24530
ROGERS, STEVEN K. ..... p 2025 N95-25272
ROGERS, WILLIAM H. ..... p 1910 N95-24582
ROGNLIEN, T. D. ..... p 2076 N95-24490
ROHEN, W. T. ..... p 2035 N95-24248
ROHLFING, C. M. ..... p 2087 N95-24617
ROIVAINEN, P. ..... p 1955 N95-25749
ROIVAINEN, PERTTI ..... p 2026 N95-25568
ROJAS, S. ..... p 2015 N95-24648
ROKEY, MARK J. ..... p 2112 N95-24987
ROLDAN-PRADO, R. ..... p 1953 N95-24836
ROMANO, P. ..... p 2084 N95-24279
ROMANOW, A. ..... p 2021 N95-25359
ROMINE, C. H. ..... p 2019 N95-24250
RONDA, JACEK ..... p 2035 N95-26106
ROOKE, D. P. ..... p 1980 N95-24383
ROQUEMORE, A. L. ..... p 2079 N95-25120
ROSENBERGER, FRANZ ..... p 2086 N95-24534
ROSENBERGER, TODD E. ..... p 1969 N95-25606
ROSS, M. ..... p 2067 N95-24573
ROSSEINSKY, M. J. ..... p 2087 N95-24616
ROSSMANITH, R. ..... p 2065 N95-24409
ROSTOVTSEV, YU. V. ..... p 2091 N95-26103
ROTH, ROBERT ..... p 2002 N95-25899
ROUTTI, J. T. ..... p 2042 N95-24297
p 2042 N95-24298
ROWE, V. ..... p 2058 N95-25911
RSHTUNI, SH. B. ..... p 2061 N95-25928
RUBY, D. S. ..... p 1994 N95-25360
RUCK, DENNIS W. ..... p 2025 N95-25272
RUCKMAN, M. ..... p 1968 N95-24623
RUEKER, FLORIAN ..... p 2008 N95-24531
RUGGIERO, ALESSANDRO G. ..... p 2068 N95-24685
RUSIN, S. V. ..... p 2009 N95-25933
RUSSAKOVICH, N. A. ..... p 1967 N95-24484
RUSSAKOVICH, N. L. ..... p 1967 N95-24484
RUSSELL, A. J. ..... p 2008 N95-24843
RUSSELL, L. ..... p 2103 N95-24330
RUSSELL, S. ..... p 1935 N95-25379
RUSSO, ARTURO ..... p 2114 N95-24870
p 1916 N95-24872
p 1953 N95-24893
p 1917 N95-24896
RUTLLANT, J. ..... p 2006 N95-26043
RUZIC, D. N. ..... p 2078 N95-24650
RYABOV, YU. G. ..... p 2067 N95-24652
RYAN, THOMAS W., III ..... p 1998 N95-24604
RYBICKI, DANIEL J. ..... p 1976 N95-25548
RZESZOTARSKA, JADWIGA ..... p 2039 N95-25115

S

SAALTINK, MARK ..... p 2020 N95-24634
SACKINGER, S. J. ..... p 1959 N95-24712
SAFRANEK, J. ..... p 2070 N95-25369
SAIDI, E. H. ..... p 2036 N95-25522
p 2037 N95-25523
p 2038 N95-25524
p 2033 N95-25532
SAITO, NAOYUKI ..... p 2076 N95-24311
SAITO, TOSHIHITO ..... p 1914 N95-24990
SAITO, Y. ..... p 1930 N95-24840
SAKAKIBARA, S. ..... p 2071 N95-26031
SAKAMOTO, HIROSHI ..... p 1949 N95-25769
SAKAMOTO, KEISHI ..... p 1971 N95-24340
SAKATA, KIMIO ..... p 1963 N95-25001
SAKATA, SHINYA ..... p 2076 N95-24311
SALANT, RICHARD F. ..... p 1974 N95-24218
SALEEB, A. F. ..... p 1983 N95-26078
SALESI, GIOVANNI ..... p 2053 N95-25449
SALMON, J. K. ..... p 2019 N95-24343
SAMEJIMA, FUMIKO ..... p 2013 N95-26010
SAMIOS, N. P. ..... p 2052 N95-25374
SAMPAIO, CARLOS E. ..... p 2013 N95-24627
SAMPAIO, L. C. ..... p 1937 N95-25751
SAMULSKI, MICHAEL ..... p 2001 N95-25575
SANANDRES, LUIS ..... p 1962 N95-24461
SANDBERG, S. ..... p 2013 N95-24510
SANDUSKY, DONALD A. ..... p 1926 N95-25546
SANFORD, ROBERT ..... p 1931 N95-25492
SANGAL, SATYA P. ..... p 2012 N95-24237
SANKAR, BHAVANI V. ..... p 1928 N95-26203
SANNER, D. ..... p 2058 N95-25911
SANTINI, D. J. ..... p 1998 N95-24618
SARFF, J. S. ..... p 2077 N95-24619
SARIKOV, N. A. ..... p 2042 N95-24316
p 2029 N95-24387
SARKAR, S. ..... p 2099 N95-25628
SAROFIM, A. F. ..... p 1928 N95-24286
SASS, R. ..... p 2067 N95-24573
SATO, K. ..... p 2081 N95-25651
SATO, KAZUO ..... p 1949 N95-25769
SATO, MAMORU ..... p 1907 N95-24998
SATO, T. ..... p 2004 N95-26036
SATO, TETSUYA ..... p 2083 N95-26337
SATOH, KAZUYOSHI ..... p 2077 N95-24585
SAUERS, I. ..... p 1929 N95-24345
SAULT, A. G. ..... p 1929 N95-24614
SAUNDERS, CHRIS ..... p 2074 N95-25506
SAUSEDO, EH. ..... p 2099 N95-25667
SAVENKO, B. N. ..... p 2085 N95-24362
p 2090 N95-25851
SAVOUREY, G. ..... p 2010 N95-24310
SAXENA, A. ..... p 2096 N95-25293
SAYLES, RICHARD S. ..... p 1977 N95-26050
SCALLION, W. I. ..... p 1906 N95-24397
SCHAEFER, R. M. ..... p 1976 N95-25574
SCHEFER, ROBERT ..... p 1931 N95-25492
SCHIFERL, SHEILA K. ..... p 1941 N95-25237
SCHILCHER, K. ..... p 2064 N95-26096
SCHILLING, K. ..... p 2093 N95-24450
SCHIRBER, J. E. ..... p 2087 N95-24516
p 2090 N95-25897
SCHIRONE, L. ..... p 2084 N95-24324
SCHLUETER, E. M. ..... p 2004 N95-26089
SCHMALTZ, MARTIN ..... p 2052 N95-25403
SCHMIDT, A. J. ..... p 1924 N95-25248
SCHMIDT, V. HUGO ..... p 1940 N95-24554
SCHNEIDER, STEVEN P. ..... p 1915 N95-24302
SCHNITZER, HOWARD J. ..... p 2054 N95-25481
SCHOLL, KENT L. ..... p 1993 N95-24715
SCHOOF, LARRY A. ..... p 2016 N95-24659
SCHRECK, SCOTT J. ..... p 2024 N95-25264
SCHRIMSHER, ROBERT H. ..... p 2010 N95-24423
SCHROEDER, C. C. ..... p 1931 N95-25252
SCHROEDER, N. ..... p 1924 N95-25597
SCHROEDER, V. ..... p 1930 N95-25123
SCHUBERT, W. KENT ..... p 1996 N95-26166
SCHUR, ANNE ..... p 2106 N95-25774
SCHWARTZ, C. R. ..... p 2075 N95-26173
SCHWARTZ, R. W. ..... p 1941 N95-25370
SCHWARTZ, S. E. ..... p 1997 N95-24570
p 2001 N95-25442
SCHWIND, JOSEPH ..... p 1912 N95-24624
SCORZELLI, R. B. ..... p 1930 N95-24840
p 1959 N95-25405
SCOTT, C. A. ..... p 2056 N95-25624
SCOTT, C. D. ..... p 2008 N95-24843

SCOTT, J. A.	p 2033	N95-25627
SCOTT, PAUL W.	p 1913	N95-24304
SCOTT, T. C.	p 2008	N95-24843
SCULLY, JOHN R.	p 1933	N95-24220
SEBESTA, LORENZA	p 2107	N95-24894
	p 2107	N95-24895
SEDRA, M. B.	p 2036	N95-25522
	p 2037	N95-25523
	p 2038	N95-25524
	p 2033	N95-25532
SEEGMILLER, H. LEE B.	p 2074	N95-26015
SEIDE, TONIE S.	p 1942	N95-25510
SEIDEL, SALLY	p 2050	N95-24901
	p 2068	N95-25238
SEIDL, P.	p 2069	N95-25358
SEKI, KATSUMI	p 1976	N95-25323
SEKI, T.	p 2081	N95-25651
SEKI, YASUSHI	p 2080	N95-25495
SEKINE, HIDEO	p 1921	N95-25664
SELDING, J. H.	p 2075	N95-26173
SEMMES, S.	p 2028	N95-24243
SENJANOVIC, G.	p 2098	N95-25527
SENJANOVIC, GORAN	p 2110	N95-25469
SEO, J. M.	p 1948	N95-24498
SERIZAWA, YOSHIZUMI	p 1953	N95-24848
SESSLER, A. M.	p 2065	N95-24320
SETCHELL, R. E.	p 1979	N95-24263
SETSER, D. W.	p 1941	N95-25386
SEVERANCE, R.	p 1972	N95-25549
SGRO, JOSEPH	p 2024	N95-25263
SHABALIN, E. P.	p 2085	N95-24374
SHAFFER, REX	p 1918	N95-24579
SHAGAM, RICH	p 1905	N95-25401
SHALAEV, V.	p 1926	N95-25295
SHAMOVSKY, V. G.	p 2041	N95-24267
SHANABARGER, MICKEY R.	p 1933	N95-24400
SHANNAHAN, K. L.	p 1939	N95-24344
SHANNON, DAVID T., JR.	p 1919	N95-24765
SHAPIRO, S.	p 2015	N95-24648
SHARAPOV, E. I.	p 2057	N95-25669
SHARAPOV, S. E.	p 2079	N95-25216
SHARMA, A.	p 2073	N95-24402
SHARMA, SURESH K.	p 1928	N95-26203
SHCHELEV, A. S.	p 1967	N95-24486
SHELTON, R. N.	p 2091	N95-26170
SHEN, B. W.	p 2010	N95-24427
SHEN, S.	p 1975	N95-24992
SHEN, Y. R.	p 2074	N95-25357
SHEPARD, WILLIAM T.	p 1909	N95-24384
SHEPHERD, RONNIE	p 1968	N95-24657
SHEPODD, TIMOTHY J.	p 2002	N95-25899
SHERWIN, M. E.	p 2064	N95-26168
SHETTY, D. K.	p 1941	N95-25387
SHEU, BING J.	p 2023	N95-25257
SHI, N.	p 1925	N95-24590
SHIBATA, K.	p 1931	N95-25356
SHIBATA, TAKEMASA	p 2081	N95-25498
SHIBUI, MASANAO	p 1966	N95-26161
SHIFLET, GARY J.	p 1933	N95-24220
SHIHO, MAKOTO	p 1971	N95-24340
	p 2070	N95-25631
SHIMIZU, HIROSHI	p 2070	N95-25631
SHIMOKAWA, TOSHIYUKI	p 1927	N95-25859
SHINDO, MASAMI	p 1925	N95-24365
SHINDO, SHIGEMI	p 1963	N95-25001
SHINN, J. L.	p 2060	N95-25922
SHIRES, A.	p 1907	N95-25649
SHIREY, D. L.	p 1953	N95-24605
SHIRKOV, G. D.	p 2048	N95-24689
SHIRKOVA, E. EH.	p 2048	N95-24689
SHIROKOV, D. M.	p 2086	N95-24537
SHIROKOV, M. I.	p 2042	N95-24314
	p 2095	N95-24639
SHKROB, I. A.	p 2045	N95-24459
SHOAEE, H.	p 2067	N95-24573
SHOCK, H.	p 1974	N95-24223
SHOEMAKER, E.	p 2112	N95-24994
SHOSTAK, DAVID R.	p 2074	N95-25506
SHOUSE, K.	p 1975	N95-24880
SHROYER, K.	p 1969	N95-25381
SHU, D.	p 2069	N95-25300
SHU, WEI	p 2041	N95-24266
SHUBIN, M. A.	p 2028	N95-24251
SHUKLA, P. R.	p 2001	N95-25629
SHUL, R. J.	p 2064	N95-26168
SHUMLAK, U.	p 2076	N95-24544
SHUR, MICHAEL	p 2090	N95-26061
SHUYUN, DUAN	p 1970	N95-25940
SHYY, WEI	p 1961	N95-24399
SIDOROV, A. V.	p 2094	N95-24508
SIDWELL, VINCE	p 1978	N95-26307
SIEGEL, MICHAEL	p 2032	N95-25114
SIEGEL, R. W.	p 2088	N95-25280
SIKKA, V. K.	p 1934	N95-24433
SILVEIRA, VANDA	p 2065	N95-24335
SILVESTER, JUNE P.	p 2106	N95-25410
SIM, K. S.	p 1948	N95-24498
	p 1997	N95-24499
SIMMONS, J. M.	p 1964	N95-25394
	p 1965	N95-25400
SIMONS, RAINEE N.	p 1957	N95-24476
SIMPSON, R. L.	p 1933	N95-24329
SINCLAIR, M. B.	p 1941	N95-25370
SINGH, C. P.	p 2052	N95-25436
SINHA, S. C.	p 1913	N95-24213
SINNIS, C.	p 2110	N95-25675
SIPILAE, KAI	p 1949	N95-25244
SISAKYAN, A. N.	p 2094	N95-24637
	p 2034	N95-25782
SITENKO, A.	p 2038	N95-25552
	p 2038	N95-25553
	p 2056	N95-25554
	p 2081	N95-25555
	p 2038	N95-25616
SKACHKOV, N. B.	p 2047	N95-24640
	p 2049	N95-24719
SKELLY, JUNE J.	p 2013	N95-26041
SKINNER, K.	p 1964	N95-25394
SKJOELDEBRAND, R.	p 2001	N95-25615
SKOBELEV, I. YU.	p 1972	N95-25100
SKOMOROKHOV, A. N.	p 2043	N95-24364
SKOOG, K. O.	p 2013	N95-24864
SKUBIS, JERZY	p 2040	N95-26071
SKURATOV, V. A.	p 2087	N95-24891
SLATER, JOHN W.	p 1908	N95-26075
SLEPCHENKO, L. A.	p 2049	N95-24720
SLIFER, L., JR.	p 1921	N95-24216
	p 1921	N95-24428
SLIWOWSKI, MAREK	p 1935	N95-25117
	p 1936	N95-25638
SLUSARCZUK, MARKO	p 2085	N95-24460
SMALLWOOD, D. O.	p 1975	N95-24462
SMIRNOV, A. YU.	p 2043	N95-24404
SMITH, A. V.	p 2074	N95-25559
SMITH, B. F.	p 1924	N95-25597
SMITH, BARRY	p 2020	N95-24658
SMITH, D.	p 2112	N95-24994
SMITH, F. G.	p 1939	N95-24344
SMITH, J. R.	p 1975	N95-24550
SMITH, L.	p 1975	N95-24880
SMITH, N.	p 1920	N95-25508
SMITH, R. I.	p 2074	N95-25573
SMITH, W. A.	p 1929	N95-24430
SMOLIK, G. R.	p 2069	N95-25365
SMYTH, PADHRAIC	p 2024	N95-25261
SNOHA, JOHN J.	p 1939	N95-24212
SNOWDEN-SWAN, L. J.	p 1998	N95-24653
SO, L. L.	p 1973	N95-26112
SOBERING, TIM J.	p 1960	N95-25558
SOCHA, GRZEGORZ	p 1935	N95-25117
	p 1936	N95-25638
SOECHTING, F. O.	p 1943	N95-26120
SOETRISNO, M.	p 1961	N95-24262
	p 1965	N95-25895
SOLODUKHIN, S. N.	p 2099	N95-25967
SOLOVEV, M. I.	p 2045	N95-24485
SOLOVYEV, A.	p 1967	N95-24484
SOLUNIN, S. A.	p 2058	N95-25908
	p 2058	N95-25909
SOMASUNDARAM, S.	p 1991	N95-24369
SOMERS, D. M.	p 1994	N95-24882
SOMERTON, C.	p 1974	N95-24223
SON, J. E.	p 1997	N95-24499
SON, Y. M.	p 1948	N95-24498
	p 1997	N95-24499
SONI, A.	p 2085	N95-24451
SOONG, S. T.	p 2006	N95-25635
SOSENKO, P. P.	p 2081	N95-25617
	p 2081	N95-25632
	p 2082	N95-25777
SOTOMAYOR, JORGE	p 1912	N95-24207
SOTOZAKI, TOKUO	p 1908	N95-25762
SPALEK, J.	p 2044	N95-24419
SPALLA, P.	p 2111	N95-26044
SPARANO, G.	p 2027	N95-24228
	p 2027	N95-24229
SPENCE, B.	p 2098	N95-25534
	p 2099	N95-25650
SPENCE, PAUL A.	p 1930	N95-25242
SPENCER, MICHAEL G.	p 1959	N95-25307
SPEZIALE, CHARLES G.	p 1962	N95-24580
SPINKA, H.	p 2043	N95-24332
SPIVEY, KATHY H.	p 1915	N95-24424
SPROUSE, J. K.	p 1989	N95-24422
SPUDIS, P. D.	p 2112	N95-24994
SQUIRE, L. C.	p 1906	N95-24210
SREENIVASAN, KATEPALLI	p 1965	N95-25404
SRIVASTAVA, P. P.	p 2093	N95-24353
	p 2095	N95-24837
SRIVASTAVA, SUJAN	p 2001	N95-25575
STADELMANN, P. A.	p 2091	N95-26260
STALKER, R. J.	p 1964	N95-25394
	p 1914	N95-25395
	p 1914	N95-25396
	p 1933	N95-25398
STARKE, E. A., JR.	p 1935	N95-24878
STARKE, EDGAR A., JR.	p 1933	N95-24220
STARKOV, V. V.	p 2034	N95-25906
STARNES, JAMES H., JR.	p 1984	N95-26267
STARODUBTESEV, E. G.	p 2083	N95-24205
STECHEL, E. B.	p 1926	N95-25295
STECKEL, G. L.	p 1942	N95-26049
STEFFEN, K.	p 1998	N95-24846
STEFFEN, KONRAD	p 1989	N95-24441
STEIMLE, TIMOTHY C.	p 1930	N95-24686
STERN, S. ALAN	p 2112	N95-26116
STERNE, P. A.	p 2091	N95-26170
STETTER, JOSEPH R.	p 1930	N95-25098
STEVENSON, J. O.	p 1941	N95-25382
STEVENSON, J. W.	p 2088	N95-25002
STEWART, R. E.	p 1972	N95-25100
STEWART, RICHARD	p 1968	N95-24657
STINCHCOMB, W. W.	p 1939	N95-24247
STIRLING, W. J.	p 2056	N95-25619
STOBER, M.	p 1998	N95-24846
STOCKER, A. D.	p 2075	N95-26173
STOILOV, M. N.	p 2037	N95-25599
STOKER, M.	p 1929	N95-24614
STOKES, T. I.	p 1960	N95-26092
STOLARSKI, RICHARD S.	p 1996	N95-24274
STONER, GLENN E.	p 1933	N95-24220
STRAND, TROY	p 1996	N95-26285
STRANGE, R. R.	p 1967	N95-24473
STRATTON, MICHAEL D.	p 1905	N95-25607
STRELTSOV, V. N.	p 2092	N95-24347
	p 2065	N95-24348
	p 2093	N95-24376
	p 1952	N95-24377
	p 2093	N95-24378
STRINGFIELD, RAY M.	p 1958	N95-24589
STRIZH, T. A.	p 2029	N95-24387
STROEVE, J.	p 1998	N95-24846
STROKOVSKIJ, E. A.	p 2043	N95-24361
STRONGIN, M.	p 1968	N95-24623
STRUBLE, CRAIG	p 2106	N95-25774
STUART, MARK A.	p 2013	N95-24627
STUCKEY, W. K.	p 1942	N95-26049
STUECKEN, T.	p 1974	N95-24223
SUAREZ, MAX J.	p 2003	N95-24766
SUBRAMANIAN, M. A.	p 2038	N95-25600
SUCHICITAL, C.	p 1935	N95-25379
SUD, Y. C.	p 2005	N95-26341
SUDHOFF, FREDERICK A.	p 1996	N95-26171
SUDO, S.	p 2072	N95-26110
	p 2072	N95-26111
	p 2072	N95-26250
SUMATHI, S.	p 2042	N95-24269
SUMMER, MIKE E.	p 1934	N95-24480
SUNGUR, MERT	p 2025	N95-25268
SUNI, I.	p 1942	N95-25633
SURESH, AMBADY	p 2018	N95-25879
SURMA, J. E.	p 1924	N95-25248
SUROVTSEV, YU. S.	p 2055	N95-25537
SUSLOV, A. A.	p 2062	N95-25931
SUZUKI, HIROKAZU	p 1910	N95-25764
SUZUKI, MINEO	p 1976	N95-25323
	p 1942	N95-25760
SUZUKI, SATOSHI	p 2077	N95-24585
SVENSSON, I.	p 1951	N95-24281
SVENSSON, L.	p 1925	N95-24242
SVOBODA, JAMES S.	p 1955	N95-25876
SWAN, DON	p 1968	N95-24657
SWAN, SCOTT A.	p 2014	N95-25306
SWANSIGER, R. W.	p 1933	N95-24329
SWANSON, CHRIS	p 1965	N95-25404
SWARTLING, T.	p 2013	N95-24864
SWARTZ, K. L.	p 2020	N95-24597
SWENSON, F. J.	p 2109	N95-24234
SWIETLIK, C.	p 2103	N95-24330
SYPHERS, M. J.	p 2064	N95-24287
SZEWCZYK, Z. PETER	p 1986	N95-26275
SZOKE, A.	p 1972	N95-25100
SZYMURSKI, S. R.	p 1941	N95-25243

T

TAASAN, SHLOMO	p 2029	N95-24389
TADA, EISUKE	p 1966	N95-26161
TAKACS, LAWRENCE L.	p 2003	N95-24766
TAKAGI, T.	p 2082	N95-25903
TAKAHASHI, MAYUKO	p 1971	N95-24340
TAKAHATA, K.	p 2071	N95-25855
TAKATA, K.	p 1958	N95-24701
TAKATSU, HIDEYUKI	p 1966	N95-26161
TAKEUCHI, Y. R.	p 1946	N95-26138
TALBOT, JAN B.	p 2085	N95-24460
TAMAYAMA, MASATO	p 1963	N95-25001
TANAKA, KEIJI	p 1912	N95-25005

TANAKA, MOTOHIKO p 2083 N95-26339
TANDY, P. C. p 2057 N95-25896
TANG, WEI-PAI p 2027 N95-24214
TANG, YVETTE T. p 1987 N95-26283
TANG, YVETTE Y. p 1985 N95-26273
TANGLER, J. L. p 1994 N95-24882
TANI, KEIJI p 2076 N95-24311
TANIUCHI, T. p 1958 N95-24701
TANVEER, SALEH p 2032 N95-25114
TARASOV, A. V. p 2048 N95-24700
TARASOV, VASILY E. p 2096 N95-25426
TARDY, HERBERT L. p 1996 N95-26166
TARUVAI, SASTRY p 1963 N95-24628
TATAR, N. p 2033 N95-25645
TATE, ATSUSHI p 1921 N95-25564
TAWEL, RAOUL p 2025 N95-25266
TAYLOR, G. A. p 1939 N95-24344
TEETS, EDWARD p 2085 N95-24478
TELEGA, JOZEF JOACHIM p 2004 N95-25958
TENFORDE, T. S. p 2009 N95-26169
TENTYUKOV, M. N. p 2099 N95-25780
TEOTONIO-SOBRINHO, P. p 2027 N95-24228
TER-ANTONYAN, V. M. p 2094 N95-24637
TERADA, HIROYUKI p 1981 N95-25000
p 1983 N95-25796
TERASAKI, K. p 2057 N95-25901
TERAZAWA, HIDEZUMI p 2055 N95-25494
TERRELL, A. S. p 1929 N95-24430
TERUI, YUSHI p 1912 N95-25005
TERUNUMA, KUSUO p 2043 N95-24337
TERYAEV, O. p 2052 N95-25437
TERYAEV, O. V. p 2095 N95-24727
p 2070 N95-25634
THAKOOR, ANIL p 2025 N95-25266
THAKUR, SIDDHARTH p 1961 N95-24399
THEOFANOUS, T. G. p 1963 N95-24678
THIAGARAJAN, BALAJI p 2021 N95-25477
THODE, L. E. p 1973 N95-26112
THOMA, D. J. p 2086 N95-24513
THOMAN, J. W. p 2047 N95-24595
THOMAS, JASON E. p 1990 N95-26040
THOMAS, JIM p 2106 N95-25774
THOMAS, T. p 1911 N95-26062
THOMASSEN, K. I. p 2076 N95-24548
THOMPSON, GEORGE p 2036 N95-25455
THOMPSON, JAMES R. p 1947 N95-24226
THOMPSON, KYLE p 1905 N95-25401
THOMSON, MARK J. p 2097 N95-25429
THOMSPON, G. p 2053 N95-25460
THRESHER, R. W. p 1995 N95-26090
TIGGES, C. P. p 1990 N95-24264
TIN, PADETHA p 2072 N95-24386
p 1971 N95-24530
TING, AILI p 1930 N95-25242
TITOV, A. I. p 2049 N95-24888
TODD, L. J. p 1929 N95-24430
TODESCO, E. p 2062 N95-25944
TOI, K. p 2081 N95-25651
TOKAR, S. p 1968 N95-24635
TOKI, W. H. p 2065 N95-24317
TOKORO, KEN-ICHI p 2104 N95-24494
TOKUMOTO, S. p 1958 N95-24701
TOLLER, E. p 2034 N95-25893
TOLMIE, D. E. p 2022 N95-26066
TOLOCZKO, M. B. p 1937 N95-26007
TOLSON, ROBERT H. p 2027 N95-26086
TOLSTOV, K. D. p 2060 N95-25921
TOMANEK, DAVID p 1936 N95-25529
TOMICK, JOHN J. p 2006 N95-26197
TOMIO, L. p 2095 N95-24839
TOMIO, LAURO p 2053 N95-25459
TOMITA, Y. p 2072 N95-26110
p 2072 N95-26111
TOMLINSON, F. KEITH p 1930 N95-25097
TOMLINSON, JOHN p 2026 N95-25802
TOMLINSON, MICHAEL J. p 2038 N95-25458
TOMSIA, A. P. p 1937 N95-25775
TOMY, C. V. p 2085 N95-24431
TONEEV, V. D. p 2070 N95-25634
TONKOVICH, ANNA LEE Y. p 1924 N95-25286
TOOMARIAN, NIKZAD p 2025 N95-25266
TORR, MARSHA p 2107 N95-26084
TORRES-POMALES, WILFREDO p 2019 N95-24382
TORRES, FRANCISCO J. p 1910 N95-24629
TORRII, K. p 2108 N95-24385
TOSATTI, E. p 2091 N95-26252
TOWNSEND, D. P. p 1977 N95-26076
TRAYBAR, JOSEPH p 1912 N95-24624
TREFETHEN, L. N. p 2029 N95-24458
TREMBLEY, D. G. p 1972 N95-25549
TRIFUNAC, A. D. p 2045 N95-24459
TROSHICHEV, O. A. p 2004 N95-24897
TRUE, B. p 1913 N95-24390
TRUGMAN, S. A. p 2093 N95-24457
TRUSKOVA, N. F. p 2030 N95-24636
p 2032 N95-24860
TRY, PAUL D. p 2006 N95-26012
TRYON, ROBERT p 2101 N95-26304
TSAI, TIMOTHY K. p 1978 N95-25333
TSANTARIDIS, L. p 1932 N95-26000
TSCHARNUTER, WALTHER W. p 1971 N95-24530
TSOOKHUU, KH. p 2055 N95-25493
p 2056 N95-25668
TSUKANO, YUKICHI p 1912 N95-25005
TSUMORI, K. p 2071 N95-26031
TSURUOKA, TAKUYA p 2076 N95-24311
TUGAI, V. V. p 1955 N95-25648
TUMA, MEG p 1912 N95-24207
TUNG, CHEE p 1910 N95-24629
TURCHI, C. p 1997 N95-24319
TURLEY, W. DALE p 1989 N95-25110
TURMAN, B. N. p 1940 N95-24717
TURNER, KATHRYN p 2032 N95-25480
TURNER, W. C. p 1968 N95-24623
TURSKI, KAROL p 1983 N95-26178
TUTHILL, GEORGE F. p 1940 N95-24554
TUTTLE, S. p 1964 N95-25394
TUTTLE, S. L. p 1965 N95-25400
TUTTLE, SEAN p 1914 N95-25397
TWITCHELL, PAUL F. p 2006 N95-26012

U

UEDA, TETSUHIKO p 1908 N95-25762
UEHARA, GREGORY p 2015 N95-24224
UENOSONO, C. p 2072 N95-26110
p 2072 N95-26111
p 2072 N95-26250
ULRICKSON, M. p 2078 N95-24650
UMBARGER, K. O. p 2008 N95-24600
URAMOTO, JOSHIN p 2071 N95-26029
URBANCZYK, MARIAN p 2039 N95-25115
USTAD, A. L. p 2012 N95-25570
UZHINSKIJ, V. V. p 2035 N95-24693

V

VALENCIA, G. p 2044 N95-24420
VALTCHINOV, V. p 1956 N95-24245
VANALSTINE, JAMES M. p 1940 N95-24562
VANASSELT, W. p 2064 N95-24287
VANDAM, ANDRIES p 2017 N95-25867
VANDERBORG, W. p 1913 N95-26190
VANDYCK, O. B. p 2067 N95-24652
VANDYKE, JOHN P. p 2004 N95-25476
VANNELL, ERIC C. p 1920 N95-24581
VARTSKY, D. p 1957 N95-24482
p 1957 N95-24483
VASENDINA, V. A. p 2047 N95-24668
VAUGHAN, K. W. p 1966 N95-24203
VAULINA, E. N. p 2009 N95-25933
VAWTER, G. A. p 1951 N95-24289
VEERS, PAUL S. p 1995 N95-26037
VENNERSTROM, S. p 2004 N95-24897
VERBUS, V. A. p 2091 N95-26103
VERINK, E. D., JR. p 1935 N95-25388
VERONNEAU, STEPHEN J. H. p 2012 N95-24237
VERWEY, W. B. p 2014 N95-25610
VETRANO, J. S. p 1934 N95-24449
VIET, DUONG QUOC p 2034 N95-25989
p 2034 N95-25992
VIKRAM, C. S. p 1981 N95-24598
VIKRAM, CHANDRA S. p 2073 N95-24545
VINITSKIJ, S. I. p 2034 N95-25906
VINOKUR, V. M. p 2087 N95-24868
VIRCAR, A. V. p 1941 N95-25387
VISSANI, F. p 2043 N95-24404
VITEK, J. M. p 1938 N95-26064
VITEK, V. p 1937 N95-26014
VITUS, C. M. p 1930 N95-25123
VLONTZOS, JOHN p 2026 N95-25603
VOGEL, A. p 1955 N95-25644
VOLKAS, R. R. p 2053 N95-25461
VOLODKO, A. G. p 2058 N95-25905
VONHAEFTEN, BERNARDO p 2001 N95-25531
VONPRZEWOSKI, B. p 2067 N95-24652
VOSS, SUSAN S. p 1920 N95-24711

W

WADE, K. p 1924 N95-25597
WAGENER, R. p 1997 N95-24570
WAGNER, J. L. p 2084 N95-24279
p 2087 N95-24855
WAKAIRO, KAORU p 2073 N95-25004
WAKAMATSU, YOSHIO p 1914 N95-24990
WALCEK, C. J. p 2005 N95-24613
WALDRON, DOUGLAS J. p 1976 N95-25548
WALDRON, W. L. p 2108 N95-24385
WALEN, D. B. p 1909 N95-25341
WALKER, HOMER F. p 2032 N95-25480
WALKER, M. A. p 1906 N95-24308
WALKO, ROBERT J. p 1958 N95-24586
WALL, STEPHEN D. p 2112 N95-24987
WALLING, R. S. p 1972 N95-25100
WALTER, K. C. p 1940 N95-24456
WANG, J. p 1972 N95-25549
WANG, J. R. p 2003 N95-24336
WANG, L. M. p 2088 N95-25288
WANG, M. Q. p 1998 N95-24618
WANG, R. G. p 2028 N95-24255
WANG, WEI p 2029 N95-24401
WANG, WEN-ZHENG p 2063 N95-25971
WANG, X. Y. p 2029 N95-24474
WANG, YUZHU p 2041 N95-24268
WANIEWSKI, MACIEJ p 1983 N95-26178
WAPSTRA, A. H. p 2040 N95-24231
WARDWELL, DOUGLAS A. p 1908 N95-26302
WARINNER, S. A. p 1998 N95-24618
WARREN, M. S. p 2019 N95-24343
WARREN, MICHAEL p 2110 N95-25766
WASHINGTON, LAWRENCE C. p 2031 N95-24697
WATANABE, AKIHIKO p 1971 N95-24340
p 2070 N95-25631
WATANABE, AKIRA p 2073 N95-25004
WATANABE, HIDETO p 2076 N95-24311
WATANABE, K. p 2004 N95-26036
WATANABE, K. Y. p 2081 N95-25653
WATANABE, KUNIHIKO p 2083 N95-26337
WATANABE, MITSUNORI p 1921 N95-25664
WATANABE, T. H. p 2004 N95-26036
WATASE, YOSHIYUKI p 2021 N95-25303
WATSON, BRIAN C. p 1985 N95-26272
p 1986 N95-26276
p 1987 N95-26281
WATTS, J. W., JR. p 2061 N95-25926
p 2061 N95-25927
p 2061 N95-25929
p 2061 N95-25930
WEBER, W. J. p 2088 N95-25002
p 2088 N95-25288
WEI, PENG p 2106 N95-25376
WEIDERYD, M. p 2013 N95-24510
WEIGHT, KRISTEN p 1979 N95-26055
WEISNER, ERIK S. p 1939 N95-24212
WELCH, CHRISTOPHER S. p 1978 N95-25304
WELDON, W. F. p 1977 N95-26172
WENDELIN, T. J. p 1992 N95-24674
WENDELIN, TIMOTHY J. p 1994 N95-25309
WENDT, BRUCE J. p 1914 N95-24392
WENDT, M. p 1964 N95-25394
WERDIGER, MEIR p 1972 N95-24707
WERLEY, K. A. p 2078 N95-24650
WERNER, S. A. p 2097 N95-25446
WERT, JOHN A. p 1933 N95-24220
WESOKY, HOWARD L. p 1996 N95-24274
WEST, M. p 2039 N95-25503
WESTBY, ROBERT p 1995 N95-25995
WHELAN, DAN J. p 1947 N95-24394
WHITE, BILL p 1968 N95-24657
WHITE, R. G. p 1975 N95-24992
p 1982 N95-25003
WHITNEY, K. p 1975 N95-24880
WHITNEY, MARK G. p 1915 N95-24424
WIENER, JAMES p 2071 N95-26011
WIESS, A. p 1968 N95-24623
WIGHTMAN, FREDERIC L. p 2011 N95-24564
WIGLEY, T. M. L. p 1999 N95-25199
WILBANKS, W. L. p 1994 N95-25360
WILKINSON, R. A. p 2099 N95-25878
WILLIAMS, D. C. p 2046 N95-24593
WILLIAMS, G. P. p 1928 N95-24265
WILLIAMS, H. H. p 2041 N95-24254
WILLIAMS, H. R. p 1991 N95-24369
WILLIAMS, PETER L. p 2030 N95-24557
WILLIAMS, PHARIS E. p 1948 N95-24670
WILLIAMS, R. S. p 1967 N95-24598
WILLIAMS, ROBERT L., II p 2027 N95-26086
WILLIAMS, T. p 1997 N95-24319
WILLIAMS, TOM A. p 1992 N95-24714
WILLIAMS, WILLIAM R. p 1951 N95-25513
WILSON, ELIZABETH p 2026 N95-25603
WILSON, I. p 1958 N95-24701
WILSON, J. W. p 2060 N95-25922
WILSON, JACK p 1908 N95-25962
WILSON, S. p 2056 N95-25620
p 2022 N95-25625
p 1911 N95-26062
WILSON, TRACY A. p 1995 N95-26037
WILT, T. E. p 1980 N95-24398
WINQUIST, F. p 2009 N95-24227
WINTERSTEIN, STEVEN R. p 1995 N95-26037
WIO, HORACIO S. p 2001 N95-25521
p 2001 N95-25531
WISE, JIM p 2106 N95-25774
WITHAM, JAMES C. p 2022 N95-25254

WITHROW, S. P. ..... p 1935 N95-25388
WODICKA, GEORGE R. ..... p 2010 N95-24309
WOFSY, STEVEN C. ..... p 1996 N95-24274
WOJCIK, W. ..... p 2044 N95-24419
WOLFGANG, POLAK ..... p 2020 N95-24634
WOLFSON, MIKE G. ..... p 1947 N95-24394
WOMBLE, DAVID E. ..... p 2004 N95-25476
WONG, C. C. ..... p 1961 N95-24262
p 1965 N95-25895
WOO, KENNETH E. ..... p 1954 N95-25316
WOO, MYEUNG-JOUH ..... p 2063 N95-25963
WOOD, KATHRYN J. ..... p 2011 N95-25336
WOODARD, R. P. ..... p 2096 N95-24867
WOODS, DAVID D. ..... p 2026 N95-25335
WORTHEM, DENNIS W. ..... p 1927 N95-25880
WORTMAN, D. J. ..... p 1944 N95-26126
WRIGHT, GEOFF ..... p 1987 N95-26309
WRIGHT, I. G. ..... p 1944 N95-26122
WRIGHT, ROBERT A. ..... p 1913 N95-24304
WU, JIN ..... p 2085 N95-24463
WU, X. ..... p 2029 N95-24421
WU, XAIO-ZHONG ..... p 1965 N95-25404
WUENSCH, W. ..... p 1958 N95-24701

X

XIANKE, ZHANG ..... p 2031 N95-24697
XIE, H. ..... p 1913 N95-24213
XU, KANGMING ..... p 1985 N95-26273
p 1987 N95-26283
XU, QIANG ..... p 2082 N95-25942

Y

YABE, T. ..... p 1971 N95-26182
YADONG, WANG ..... p 1954 N95-25482
YAGI, M. ..... p 2082 N95-25759
p 2083 N95-26326
YAHIL, AMOS ..... p 2110 N95-25343
YAMADA, H. ..... p 2071 N95-26031
YAMADA, HIROSHI ..... p 2034 N95-25860
YAMADA, S. ..... p 2071 N95-25855
YAMAGUCHI, S. ..... p 2072 N95-26110
p 2072 N95-26111
p 2072 N95-26250
YAMALEEV, R. M. ..... p 2092 N95-24313
YAMAMOTO, J. ..... p 2071 N95-25855
YAMAMOTO, M. ..... p 1958 N95-24701
YAMAMOTO, N. ..... p 2011 N95-24556
YAMAZAKI, K. ..... p 2081 N95-25653
YAN, M. ..... p 1937 N95-26014
YAN, XIAOPU ..... p 2033 N95-25601
YAN, Y. T. ..... p 2068 N95-24664
YANAGI, N. ..... p 2071 N95-25855
YANAGI, RYOUJI ..... p 1963 N95-25001
YANAGIHARA, MASAAKI ..... p 1908 N95-25761
YANG, HUI-CHUN ..... p 2050 N95-24902
YANIV, ZIV ..... p 2085 N95-24460
YARBERRY, VICTOR R. ..... p 2016 N95-24659
YASINSAC, L. ..... p 1929 N95-24430
YASUDA, BRIAN ..... p 2075 N95-26039
YATSUYANAGI, NOBUYUKI ..... p 1949 N95-25769
YAZAKI, KOICHI ..... p 2070 N95-25772
YEH, HSU-CHI ..... p 1998 N95-24606
YETHIRAJ, M. ..... p 2085 N95-24431
YEUNG, C. P. ..... p 1906 N95-24210
YOKOKAWA, MITSUO ..... p 2055 N95-25496
YOKOSAWA, A. ..... p 2043 N95-24326
YOKOYAMA, KENJI ..... p 2077 N95-24585
YONUSHONIS, T. M. ..... p 1945 N95-26129
YORK, JEREMY ..... p 2106 N95-25774
YOSHIDA, MAKOTO ..... p 1977 N95-25672
YOSHIDA, Y. ..... p 2082 N95-25903
YOST, F. G. ..... p 1959 N95-24712
p 1935 N95-24716
YOST, WILLIAM T. ..... p 1978 N95-25304
YOUNG, B. K. F. ..... p 1972 N95-25100
YOUNG, BRUCE ..... p 1968 N95-24657
YOUNG, CAROLYNN ..... p 2113 N95-26336
YOUNG, CLARENCE P., JR. ..... p 1915 N95-24388
YOUNG, HARRY J. ..... p 1976 N95-25592
YOUNG, TERESA ..... p 1993 N95-24853
YOUSSEF, MAHMOUD Z. ..... p 2076 N95-24511
YOUVAN, DOUGLAS C. ..... p 2008 N95-24850
YU, S. ..... p 2069 N95-25358
YU, ZIQIANG ..... p 2049 N95-24724
YUAN, F. ..... p 2025 N95-25269
YUREV, M. Z. ..... p 2063 N95-25965

Z

ZABOKLICKI, ADAM ..... p 2040 N95-26180
ZACHARIAS, D. S. ..... p 2003 N95-24336
ZAGORODNIJ, A. G. ..... p 2081 N95-25556
ZAIKOV, R. P. ..... p 2037 N95-25599
ZAJMIDOROGA, O. A. ..... p 2073 N95-24642
ZAKRAJSEK, J. J. ..... p 1977 N95-26076
ZANG, ZHENHAI ..... p 2072 N95-26095
ZASADZINSKI, J. ..... p 2084 N95-24279
ZASADZINSKI, J. F. ..... p 2087 N95-24855
ZASTAVENKO, L. G. ..... p 2094 N95-24508
p 2094 N95-24638
ZEMLYANAYA, E. V. ..... p 2029 N95-24375
p 2029 N95-24387
ZERAFA, KEN ..... p 2001 N95-25575
ZEROUAOUI, J. ..... p 2036 N95-25522
p 2037 N95-25523
ZEROUAOUI, S. J. ..... p 2033 N95-25532
ZETTI, F. ..... p 1968 N95-24635
ZHANG, Y. ..... p 1928 N95-24286
ZHANG, YOU-JIN ..... p 2100 N95-25988
ZHANG, ZHENHUA ..... p 2049 N95-24877
ZHANG, ZHIMIN ..... p 2026 N95-25802
ZHARKOV, A. YURY ..... p 2030 N95-24691
ZHELTUKHIN, A. A. ..... p 1955 N95-25648
ZHELUDEV, I. S. ..... p 2109 N95-24884
ZHENG, HANQING ..... p 2051 N95-25290
ZHIDKOV, E. P. ..... p 2057 N95-25778
ZHIDKOV, P. E. ..... p 2034 N95-25783
ZHIGANG, YANG ..... p 1970 N95-25940
ZHOU, BANG-RONG ..... p 2053 N95-25450
ZHOU, J. ..... p 2047 N95-24641
ZHOU, O. ..... p 2087 N95-24616
ZHOU, SHANYU ..... p 2041 N95-24268
ZHOU, YE ..... p 1963 N95-24584
p 1965 N95-25960
ZIMMERLI, G. ..... p 2099 N95-25878
ZOLPER, J. C. ..... p 1990 N95-24264
p 2064 N95-26168
ZUH, JIXIANG ..... p 1971 N95-24530
ZUO, YIXIN ..... p 2049 N95-24724
ZUREK, WOJCIECH ..... p 2110 N95-25766
ZUTAVERN, F. J. ..... p 1957 N95-24488
ZVARA, I. ..... p 2093 N95-24481

Typical Corporate Source Index Listing

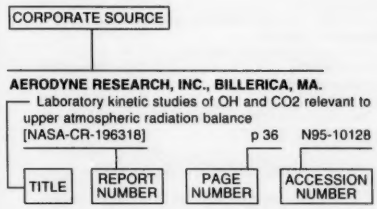

Listings in this index are arranged alphabetically by corporate source. The title of the document provides the user with a brief description of the subject matter. The report number helps to indicate the type of document cited (e.g., NASA report, translation, NASA contractor report). The accession number denotes the number by which the citation is identified. The page number helps you locate the citation in the abstract section. The titles are arranged under each corporate source in ascending accession number order.

A

ACADEMY OF SCIENCES OF THE UKRAINE, KIEV (UKRAINE).
Physics in Ukraine International Conference. Volume 3: Statistical physics and phase transitions
[DE95-605765] p 2038 N95-25552
Physics in Ukraine International Conference. Volume 5: Low temperature physics
[DE95-605800] p 2038 N95-25553
Physics in Ukraine International Conference. Volume 1: Physics of elementary particles and quantum field theory. General problems
[DE95-606413] p 2056 N95-25554
Physics in Ukraine International Conference. Volume 6: Plasma physics
[DE95-606422] p 2081 N95-25555
Dynamics of structure formation in nonequilibrium systems (Wave Media)
[DE95-607609] p 2081 N95-25556
Physics in Ukraine International Conference. Volume 4: Radiophysics and Electronics
[DE95-605570] p 2038 N95-25616
Fluctuations and electromagnetic wave scattering in macroscopically agitated plasma: Effects of turbulent diffusion
[DE95-607612] p 2081 N95-25617
Quasiparticles in magnetized plasma
[DE95-607610] p 2081 N95-25632
Dynamical chiral symmetry breaking in scale invariant quantum electrodynamics in sixth dimensions
[DE95-607133] p 2099 N95-25667
Polarization and intensity of dd-transitions in superconducting copper oxides
[DE95-605886] p 2090 N95-25776
Fluctuations in macroscopically agitated plasma: Quasiparticles and effective temperature
[DE95-607611] p 2082 N95-25777

ACADEMY OF SCIENCES (USSR), NOVOSIBIRSK (USSR).
On the possibility of obtaining the polarized protons by the method of direct optic pumping of a fast atomic beam
[DE94-634309] p 2041 N95-24267

ADVISORY GROUP FOR AEROSPACE RESEARCH AND DEVELOPMENT, NEUILLY-SUR-SEINE (FRANCE).
Directory of Defence and Aerospace Information Centers
[AGARD-R-802] p 2107 N95-26334

AERONAUTICAL RESEARCH LABS., MELBOURNE (AUSTRALIA).
Configuration and other differences between Black Hawk and Seahawk helicopters in military service in the USA and Australia
[AR-008-386] p 1911 N95-25935
Assessment of overhaul surge margin tests applied to the T53 engines in ADF Iroquois helicopters
[AR-008-389] p 1914 N95-25936

AEROSPACE CORP., EL SEGUNDO, CA.
Particle acceleration very near an x-line in a collisionless plasma
[ATR-92(7251)-4] p 2080 N95-25325
Spacecraft materials studies on The Aerospace Corporation Tray on EOIM-3
[AD-A288682] p 1942 N95-26049
Applications of solid lubricant films in spacecraft
[AD-A288784] p 1947 N95-26188
Calculation of light scattering from a spherical particle on a surface by the multipole expansion method
[ATR-95(9558)-2] p 2075 N95-26198

AEROSPACE MEDICAL RESEARCH LABS., WRIGHT-PATTERSON AFB, OH.
Temporal pacing in visual attention
[AD-A289785] p 2013 N95-26041

AIR-CONDITIONING AND REFRIGERATION TECHNOLOGY INST., INC., ARLINGTON, VA.
Materials Compatibility and Lubricants Research (MCLR) Program
[DE95-004862] p 1941 N95-25243

AIR FORCE ACADEMY, CO.
Application of neural networks to unsteady aerodynamic control p 2024 N95-25264

AIR FORCE INST. OF TECH., WRIGHT-PATTERSON AFB, OH.
How Captain Amerika uses neural networks to fight crime p 2025 N95-25272
Multispectral detection of ground targets in highly correlated backgrounds
[AD-A289292] p 1990 N95-26040
On convergence of the Nelder-Mead simplex algorithm for unconstrained stochastic optimization
[AD-A289453] p 2006 N95-26197

AIR PRODUCTS AND CHEMICALS, INC., ALLENTOWN, PA.
Development of novel active transport membrane devices
[DE95-002658] p 1932 N95-26093

AKRON UNIV., AKRON, OH.
On the finite element implementation of the generalized method of cells micromechanics constitutive model
[NASA-CR-195451] p 1980 N95-24398

ALABAMA UNIV., HUNTSVILLE, AL.
Estimates of effects of residual acceleration on USML-1 experiments
[NASA-CR-197964] p 2084 N95-24261
Software engineering and data management for automated payload experiment tool
[NASA-CR-196562] p 2104 N95-24477
Convective flow effects on protein crystal growth
[NASA-CR-197891] p 2086 N95-24534
Development of optical systems
[NASA-CR-197702] p 2073 N95-24545
FNAS phase partitions
[NASA-CR-193855] p 1940 N95-24562
Automation based on knowledge modeling theory and its applications in engine diagnostic systems using Space Shuttle Main Engine vibrational data
[NASA-CR-197983] p 1922 N95-24626
Software engineering and data management for automated payload experiment tool
[NASA-CR-197703] p 2016 N95-24876

ALACRON, INC., NASHUA, NH.
Neural network classification of clinical neurophysiological data for acute care monitoring p 2024 N95-25263

ALLIED-SIGNAL AEROSPACE CO., KANSAS CITY, MO.
Piezoelectric motor development at AlliedSignal Inc., Kansas City Division
[DE95-003389] p 1958 N95-24532
Metrology measurement capability
[DE95-005411] p 1969 N95-25381
CMM functional software evaluation (algorithm qualification)
[DE95-006178] p 2018 N95-26167

ALLIED-SIGNAL AEROSPACE CO., TORRANCE, CA.
Monolithic solid oxide fuel cell technology advancement for coal-based power generation
[DE94-012258] p 1990 N95-24318

ANALYTICAL SERVICES AND MATERIALS, INC., HAMPTON, VA.
A generic interface element for COMET-AR
[NASA-CR-195075] p 1983 N95-26199

ANALYTICAL SPECTRA DEVICE, INC., BOULDER, CO.
Field-portable reflectance spectrometer
[AD-A288750] p 1970 N95-26059

APPLIED RESEARCH, INC., HUNTSVILLE, AL.
Active weld control
[NASA-CR-196588] p 1976 N95-25595

APPLIED RESEARCH CORP., LANDOVER, MD.
ASCA solid state imaging spectrometer observations of O stars
[NASA-CR-197281] p 2108 N95-24385

ARGONNE NATIONAL LAB., IDAHO FALLS, ID.
Modeling plasma/material interactions during a tokamak disruption
[DE95-004247] p 2078 N95-24861

ARGONNE NATIONAL LAB., IL.
Device-quality tunnel junctions on the high (T(sub c)) super conductor HgBa2CuO(4+delta)
[DE95-004646] p 2084 N95-24279
Polarization and N-N elastic scattering amplitudes
[DE95-004648] p 2042 N95-24292
Proton-proton interactions using the RHIC polarized collider
[DE95-005839] p 2043 N95-24326
Raising the IQ in full-text searching via intelligent querying
[DE95-002981] p 2103 N95-24330
New results in nucleon-nucleon scattering at intermediate energies
[DE95-004594] p 2043 N95-24332
Computational load in model physics of the parallel NCAR community climate model
[DE95-005410] p 2019 N95-24342
Contribution of ankyrin-band 3 complexes to the organization and mechanical properties of the membrane skeleton of human erythrocyte
[DE95-005835] p 2010 N95-24427
Pulse radiolysis of alkanes: A time-resolved electron paramagnetic resonance study
[DE95-005831] p 2045 N95-24459
Liquid-fueled SOFC power sources for transportation
[DE95-002998] p 1991 N95-24607
Methods of valuing air pollution and estimated monetary values of air pollutants in various US regions
[DE95-006854] p 1998 N95-24618
Users manual for KSP data-structure-neutral codes implementing Krylov space methods
[DE95-004265] p 2020 N95-24658
High Energy Physics Division research activities
[DE95-003985] p 2068 N95-24680
BCS-like gap structure of HgBa2CuO(4+delta) tunnel junctions
[DE95-004125] p 2087 N95-24855
Melting of the moving vortex lattice in the presence of disorder
[DE95-004126] p 2087 N95-24868
Overview of selected molecular biological databases
[DE95-005906] p 2008 N95-25181

Nanostructured materials
[DE95-004595] p 2088 N95-25280
The interactions of high-energy, highly charged Xe ions with buckyballs
[DE95-004597] p 2069 N95-25281
Oxygen stoichiometry and its influence on superconductivity in Bi2Sr2CaCu2O(8+x)
[DE95-004660] p 2088 N95-25282
US technical report for the ITER blanket/shield
[DE95-004667] p 2079 N95-25283
Bremsstrahlung scattering calculations for the beam stops and collimators in the APS insertion-device beamlines
[DE95-005471] p 2069 N95-25300
Chelant extraction and REDOX manipulation for mobilization of heavy metals from contaminated soils
[DE95-004131] p 2000 N95-25363
Summary report for ITER Task D10: Update and implementation of neutron transport and activation codes and processed libraries
[DE95-007631] p 2083 N95-26185

ARIZONA STATE UNIV., TEMPE, AZ.
Generation, detection and characterization of gas-phase transition metal aggregates and compounds
[DE95-004439] p 1930 N95-24686

ARMY ARMAMENT RESEARCH, DEVELOPMENT AND ENGINEERING CENTER, WATERVLIET, NY.
Adaptive finite element method 2: Error estimation
[AD-A288358] p 2033 N95-25509

ARMY AVIATION SYSTEMS COMMAND, HAMPTON, VA.
Exploratory flow visualization investigation of mast-mounted sights in presence of a rotor
[NASA-TM-4634] p 1907 N95-24566

ARMY ENGINEER WATERWAYS EXPERIMENT STATION, VICKSBURG, MS.
Real-time testing and demonstration of the US Army Corps of Engineers' Real-Time On-The-Fly positioning system
[AD-A288624] p 1910 N95-25609

ARMY RESEARCH LAB., ABERDEEN PROVING GROUND, MD.
Workshop report: Measurement techniques in highly transient, spectrally rich combustion environments
[AD-A288395] p 1969 N95-25606
Dynamic matrices and their application to the concept of a semi-sparse matrix
[AD-A288688] p 2035 N95-26051

ARMY RESEARCH LAB., WATERTOWN, MA.
An overview of NDE methods for thick composites and a proposal for analysis of computed technology data
[AD-A288733] p 1979 N95-26055

ARMY TANK-AUTOMOTIVE SYSTEMS DEVELOPMENT CENTER, WARREN, MI.
Information compendium on solid film lubricants
[AD-A288360] p 1942 N95-25510
Evaluation of commercial fuel tank water absorbers
[AD-A288361] p 1951 N95-25513

AUBURN UNIV., AL.
Dynamic behavior of a magnetic bearing supported jet engine rotor with auxiliary bearings
[NASA-CR-197860] p 1913 N95-24213
Experimental analysis of thread movement in bolted connections due to vibrations
[NASA-CR-197705] p 1975 N95-24991

AUSTRALIAN NATIONAL UNIV., CANBERRA (AUSTRALIA).
Asymptotics for the Kummer function of Bose plasmas
[DE95-607019] p 2096 N95-25428

AUSTRALIAN NUCLEAR SCIENCE AND TECHNOLOGY ORGANISATION, CANBERRA (AUSTRALIA).
The use of radioisotopes in human experiments: Comments in response to recent media articles
[DE95-605680] p 2012 N95-25981

B

BAKER (WILFRED) ENGINEERING, INC., SAN ANTONIO, TX.
Quantity-distance requirements for earth-bermed aircraft shelters
[AD-A279692] p 1915 N95-24424

BELL COMMUNICATIONS RESEARCH, INC., MORRISTOWN, NJ.
Neural network applications in telecommunications
p 2025 N95-25270

BELL TELEPHONE LABS., INC., HOLMDEL, NJ.
Document analysis with neural net circuits
p 2023 N95-25256

BHABHA ATOMIC RESEARCH CENTRE, BOMBAY (INDIA).
Determination of trace elements in plutonium by solvent extraction and ICP-atomic emission spectrometry
[DE94-634887] p 2042 N95-24269
PC based analysis of gamma ray spectra generated by semiconductor detectors
[DE94-628381] p 1958 N95-24690

BIHRLE APPLIED RESEARCH, INC., HAMPTON, VA.
Experimental study of the effects of Reynolds number on high angle of attack aerodynamic characteristics of forebodies during rotary motion
[NASA-CR-195033] p 1907 N95-24443

BOEING CO., SEATTLE, WA.
Commercial Space Transportation Study (CSTS)
[SSD94D0035] p 1919 N95-25747

BOEING COMMERCIAL AIRPLANE CO., SEATTLE, WA.
Consistent approach to describing aircraft HIRF protection
[NASA-CR-195067] p 1909 N95-25341

BOEING DEFENSE AND SPACE GROUP, SEATTLE, WA.
Composite materials flown on the Long Duration Exposure Facility
[NASA-CR-4657] p 1923 N95-24583
Long Duration Exposure Facility mini-data base user's guide: IBM-compatible PC computer version
[NASA-CR-4655] p 1925 N95-26072

BRANDEIS UNIV., WALTHAM, MA.
Research in elementary particle physics
[DE95-007323] p 2054 N95-25481

BROOKHAVEN NATIONAL LAB., UPTON, NY.
XAS studies of Ni(I), Ni(II), and Ni(III) complexes
[DE95-004844] p 1928 N95-24257
FT-IR microscopical analysis with synchrotron radiation: The microscope optics and system performance
[DE95-004834] p 1928 N95-24265
The AGS gamma(sub t)-jump system
[DE95-003170] p 2064 N95-24287
A high-energy high-luminosity (mu)(+) - (mu)(-) collider
[DE95-006097] p 2065 N95-24357
Probing anomalous gauge boson couplings at LEP
[DE95-005934] p 2044 N95-24420
The 24th Order high temperature expansion for the 3-D Ising model
[DE95-004952] p 2093 N95-24450
Update on B(sub K) with Wilson fermions
[DE95-004953] p 2085 N95-24451
Microphysical and compositional influences on shortwave radiative forcing of climate by sulfate aerosols
[DE95-005999] p 1997 N95-24570
The development of a positron ionization gauge
[DE95-005958] p 1968 N95-24623
Search for top in lepton + jets in D0 using a topological tag
[DE95-003929] p 2048 N95-24677
Crystalline beams: Theory, experiments, and proposals
[DE95-003955] p 2068 N95-24685
Chiral symmetry on the lattice
[DE95-003962] p 2087 N95-24849
A study of the electrochemical behavior of tungsten in caustic solutions and platinum/iridium in ch loride solutions
[DE95-004951] p 1930 N95-25123
Update of GALLEX solar neutrino results and implications
[DE95-005005] p 2113 N95-25364
Neural network technique for orbit correction in accelerators/storage rings
[DE95-005955] p 2026 N95-25368
Coupling correction using closed orbit measurements
[DE95-005957] p 2070 N95-25369
Baryon spectroscopy and the omega minus
[DE95-004838] p 2052 N95-25374
Tau physics 1994: A theoretical perspective
[DE95-004840] p 2052 N95-25375
The effects on photosynthetic CO2 assimilation to long-term elevation of atmospheric CO2 concentration: An assessment of the response of Trifolium Repens L. CV. Blanca grown at F.A.C.E
[DE95-005687] p 2008 N95-25383
Closed orbit related problems: Correction, feedback, and analysis
[DE95-005969] p 2070 N95-25441
The whitehouse effect: Shortwave radietive forcing of climate by anthropogenic aerosols
[DE95-005998] p 2001 N95-25442
Eigenvector method for optimized orbit correction
[DE95-005967] p 2071 N95-25785
Results/prospects in E777/851/865
[DE95-005959] p 2064 N95-26006

BROWN UNIV., PROVIDENCE, RI.
Aerodynamic parameter estimation via Fourier modulating function techniques
[NASA-CR-4654] p 1911 N95-24630
Three-dimensional user interfaces for scientific visualization
[NASA-CR-197923] p 2017 N95-25867
The 3D widgets for exploratory scientific visualization
p 1966 N95-25868
Scheduling time-critical graphics on multiple processors p 2018 N95-25870

BURTON TECHNOLOGIES, INC., RALEIGH, NC.
Wear resistant composite structure of vitreous carbon containing convoluted fibers
[DE95-006255] p 1925 N95-24426

C

CALIFORNIA INST. OF TECH., PASADENA, CA.
Smart vision chips: An overview p 2024 N95-25265

CALIFORNIA STATE UNIV., LOS ANGELES, CA.
Solar Eagle 2
[NASA-CR-198043] p 1990 N95-24199

CALIFORNIA UNIV., BERKELEY, CA.
Predicting the transport properties of sedimentary rocks from microgeometry
[DE95-000129] p 2004 N95-26089

CALIFORNIA UNIV., BERKELEY. LAWRENCE BERKELEY LAB, CA.
The cooling of particle beams
[DE95-004669] p 2065 N95-24320
Supersymmetry
[DE95-004670] p 2092 N95-24333
The physics and experimental program of the Relativistic Heavy Ion Collider (RHIC)
[DE95-003416] p 2066 N95-24495
A tool for debugging internet multicast routing
[DE95-003433] p 2020 N95-24496
A discrete variable representation for electron-hydrogen atom scattering
[DE95-003436] p 2045 N95-24512
Study of radicals, clusters and transition state species by anion photoelectron spectroscopy
[DE95-003438] p 2045 N95-24533
Advanced Light Source report
[DE95-003449] p 2073 N95-24546
Superconducting magnets, 1994
[DE95-003813] p 1958 N95-24551
Current experiments in elementary particle physics. Revision
[DE95-003797] p 2067 N95-24652
Proceedings of the 1994 Conference on Computing in Energy Physics
[DE95-004442] p 2068 N95-24665
Nonlinear optics and organic materials
[DE95-004677] p 2074 N95-25357
Elise: The next step in development of induction heavy ion drivers for inertial fusion energy
[DE95-004679] p 2069 N95-25358
Dynamics of TCP traffic over ATM networks
[DE95-004687] p 2021 N95-25359
Conference on physics from large gamma-ray detec tor arrays. Volume 2: Proceedings
[DE95-006900] p 2070 N95-25478
Wide-area traffic: The failure of Poisson modeling
[DE95-004685] p 2015 N95-25773
Predicting the transport properties of sedimentary rocks from microgeometry
[DE95-000129] p 2004 N95-26089
LuAlO3: A high density, high speed scintillator for gamma detection
[DE95-004678] p 2064 N95-26256

CALIFORNIA UNIV., DAVIS, CA.
Further ways to distinguish single-lepton top quark signals from background at the Tevatron
[PB95-165395] p 2056 N95-25567

CALIFORNIA UNIV., LOS ANGELES, CA.
Laser beam log amplitude temporal scintillation spectrum due to crosswind. Part 1: Theory
[TR-1-FSRC-1994-PT-1] p 1971 N95-24371
Effect of density gradients in confined supersonic shear layers, part 1
[NASA-CR-198029] p 1962 N95-24412
Effect of density gradients in confined supersonic shear layers. Part 2: 3-D modes
[NASA-CR-198030] p 1962 N95-24413

CALIFORNIA UNIV., SANTA BARBARA, CA.
An investigation of the effect of surface impurities on the adsorption kinetics of hydrogen chemisorbed onto iron
[NASA-CR-197967] p 1933 N95-24400
Ignition of exploding aluminum droplets behind shock waves in water
[DE95-003975] p 1963 N95-24678

CAMBRIDGE UNIV., CAMBRIDGE (ENGLAND).
Three-dimensional interaction of wake/boundary-layer and vortex/boundary-layer data report
[CUED/A-AEREO/TR-23] p 1906 N95-24210

CAPE COAST UNIV. (GHANA).
The Third International Workshop on the Physics and Modern Applications of Lasers
[DE95-606395] p 1972 N95-25491

CARNEGIE-MELLON UNIV., PITTSBURGH, PA.
Quarterly update
[AD-A288743] p 2018 N95-26058
CASE WESTERN RESERVE UNIV., CLEVELAND, OH.
Molecular dynamics simulation of a piston driven shock wave in a hard sphere gas
[NASA-CR-195463] p 2063 N95-25963
CATERPILLAR TRACTOR CO., PEORIA, IL.
Thick thermal barrier coatings for diesel engines
p 1946 N95-26136
CENTRAL RESEARCH INST. OF ELECTRIC POWER INDUSTRY, TOKYO (JAPAN).
Application of optical fiber amplifier for wavelength division multiplexing communication system. Part 2: Design of four-channel transmission system using two EDFA repeaters
[DE95-730179] p 1952 N95-24491
Integrated resource management database for a distributed information system
[DE95-730180] p 2104 N95-24492
Survey of methods for secure connection to the internet
[DE95-730185] p 1952 N95-24493
Downsizing systems and expected opposition to introduction
[DE95-730186] p 2104 N95-24494
Study on propagation impairments, distortions and unavailability on digital microwave links
[DE95-723047] p 1953 N95-24848
CENTRE DE RECHERCHES DU SERVICE DE SANTE DES ARMEES, LA TRONCHE (FRANCE).
Thermal and vascular changes induced by the acclimation of the extremities to cold in man
[PB95-131587] p 2010 N95-24310
CENTRO BRASILEIRO DE PESQUISAS FISICAS, RIO DE JANEIRO.
Anionic construction of the sl(sub q, s)(2) algebra
[DE95-600838] p 2043 N95-24350
On the central charge in 3 D-supersymmetry
[DE95-600851] p 2093 N95-24352
Constraints and Hamiltonian in light-front quantized field theory
[DE95-600852] p 2093 N95-24353
Relations among solutions for wave and Klein-Gordon equations for different dimensions
[DE95-600853] p 2093 N95-24446
Nonlinear theories of spin-2 field in terms of Fierz variables
[DE95-600854] p 2095 N95-24833
Probing the Froissart bound for models with charged vector fields in D = 3
[DE95-600855] p 2095 N95-24834
Light-front quantized field theory: An introduction. Spontaneous symmetry breaking. Phase transition in (phi)(sup 4) theory
[DE95-600856] p 2095 N95-24837
On q-deformed supersymmetric classical mechanical models
[DE95-600864] p 2095 N95-24838
Mossbauer spectroscopy, x ray diffraction and magnetic measurements of iron-nickel ultrafine particles
[DE95-601136] p 1930 N95-24840
Intrinsic magnetic torque at low magnetic induction
[DE95-601209] p 1959 N95-24842
Fe-57 and Sn-119 Moessbauer studies on La(1.25)Nd(0.6)Sr(0.15)CuO4: Evidence for local magnetic ordering below (approx. equal) 32 K
[DE95-601210] p 1959 N95-25405
Coercive field and domain wall properties in (Dy(x)Y(1-x))Fe2 and (Er(x)Y(1-x))Fe2
[DE95-601135] p 1937 N95-25751
CHEMSYN SCIENCE LABS., LENEXA, KS.
The evaluation of potential limonene scavengers
[DE95-006853] p 2002 N95-25899
CHINA NUCLEAR INFORMATION CENTRE, BEIJING (CHINA).
KORP-1: A program for calculating the direct (n, p) or (p, n) reaction by using DWBA method
[DE94-628768] p 2049 N95-24724
An ion sensitive probe and its application to a mirror device
[DE95-602307] p 1970 N95-25940
Plasma burning and control in reactor core
[DE95-602882] p 2082 N95-25942
Operating level of HT-6B tokamak device
[DE95-602999] p 2082 N95-25943
Emittance growth caused by nonuniform charge distribution of bunched beam in linac
[DE95-602121] p 2072 N95-26095
CIVIL AEROMEDICAL INST., OKLAHOMA CITY, OK.
A longevity and survival analysis for a cohort of retired airline pilots
[DOT/FAA/AM-95/5] p 2012 N95-24237
Development of an intervention program to encourage shoulder harness use and aircraft retrofit in general aviation aircraft, phases 1 and 2
[DOT/FAA/AM-95/2] p 1909 N95-24384
An assessment of aviation accident risk of aphakic civil airmen by class of medical certificate held and by age: 1982-1985
[DOT/FAA/AM-95/11] p 2011 N95-25336
Sleep patterns in air traffic controllers working rapidly rotating shifts: A field study
[DOT/FAA/AM-95/12] p 2012 N95-26204
CLEMSON UNIV., SC.
On the joint spectral density of bivariate random sequences
[NASA-CR-197698] p 2035 N95-24278
Characterizing the wake vortex signature for an active line of sight remote sensor
[NASA-CR-197697] p 1909 N95-24391
CLEVELAND STATE UNIV., OH.
AMC EN-1038: Reduced scale solar simulator supplementary test report
[NASA-CR-197988] p 1915 N95-24380
Numerical simulation of flow and the effect of baffle arrangement on pressure drop and temperature pattern in a circular combustor p 1963 N95-24628
A review of chemically reactive turbulent flow analysis, mixing mechanisms and modeling, and a new design of low NOx combustor for non-premixed reactants
p 1963 N95-24762
COLORADO STATE UNIV., FORT COLLINS, CO.
Measurement of the magnetically-induced QED birefringence of the vacuum and an improved search for laboratory axions: Project definition study of the use of assets and facilities of the Superconducting Super Collider Laboratory
[DE95-005110] p 2065 N95-24317
COLORADO UNIV., BOULDER, CO.
Ice surface temperature retrieval from AVHRR, ATSR, and passive microwave satellite data: Algorithm development and application
[NASA-CR-198037] p 1989 N95-24441
Assessment of climate variability of the Greenland ice sheet: Integration of in situ and satellite data
[NASA-CR-198020] p 1998 N95-24846
COLORADO UNIV., DENVER, CO.
Fast algorithms for transport models
[DE95-007064] p 2054 N95-25479
COLUMBIA UNIV., NEW YORK, NY.
Gamma-ray emission from globular clusters. Shock high energy emission from the Be-Star/Pulsar System PSR 1259-63. Echoes in x-ray novae
[NASA-CR-197994] p 2114 N95-24381
Theory of ultra dense matter and the dynamics of high energy interactions involving nuclei
[DE95-004114] p 2048 N95-24671
Large-format high resolution microchannel plate detectors for ultraviolet astronomy
[NASA-CR-197993] p 2108 N95-25104
COMMONWEALTH SCIENTIFIC AND INDUSTRIAL RESEARCH ORGANIZATION, MORDIALOC (AUSTRALIA).
Future emissions and concentrations of carbon dioxide: Key ocean/atmosphere/land analyses
[CSIRO-TP-31] p 1999 N95-25199
COMMUNICATIONS RESEARCH LAB., TOKYO (JAPAN).
Journal of the Communications Research Laboratory, volume 41, number 1, March 1994
[PB95-177606] p 1956 N95-26008
CONNECTICUT UNIV., STORRS, CT.
X-ray based displacement and strain measurements for hostile environments
[NASA-CR-194451] p 1968 N95-25330
CORNELL UNIV., ITHACA, NY.
Linear non-modal phenomena in numerical analysis and applied mathematics
[DE95-005495] p 2029 N95-24458
The geometry of disorder: Theoretical investigations of quasicrystals and frustrated magnets
[DE95-006641] p 1936 N95-25560
CUMMINS ENGINE CO., INC., COLUMBUS, IN.
Overview of thermal barrier coatings in diesel engines
p 1945 N95-26129

D

DEFENCE RESEARCH AGENCY, FARNBOROUGH, HAMPSHIRE (ENGLAND).
The dual boundary element formulation for elastoplastic fracture mechanics
[DRA-TR-93062] p 1980 N95-24383
A theoretical and experimental investigation of the flow over supersonic leading edge wing/body configurations
[DRA-TM-AERO-PROP-41] p 1907 N95-25649
DEFENCE RESEARCH ESTABLISHMENT OTTAWA, OTTAWA (ONTARIO).
The effects of the environment on an experimental VHF radio Direction Finding antenna system
[AD-A288791] p 1956 N95-26191
DEFENCE SCIENCE AND TECHNOLOGY ORGANISATION, MELBOURNE (AUSTRALIA).
An overview of Health and Usage Monitoring Systems (HUMS) for military helicopters
[DSTO-TR-0061] p 1905 N95-24200
Helicopter life substantiation: Review of some USA and UK initiatives
[DSTO-TR-0062] p 1905 N95-24201
A portable transmission vibration analysis system for the S-70A-9 Black Hawk helicopter
[DSTO-TR-0072] p 1966 N95-24203
A review of rolling element bearing vibration detection, diagnosis and prognosis
[DSTO-RR-0013] p 1975 N95-24393
The critical diameter, detonation velocity and shock sensitivity of Australian PBXW-115
[DSTO-TR-0076] p 1947 N95-24394
DEFENSE MAPPING AGENCY AEROSPACE CENTER, SAINT LOUIS, MO.
Hardcopy extraction considerations for Vector Product Format (VPF) products
[AD-A288620] p 2106 N95-25608
DEFORMATION CONTROL TECHNOLOGY, INC., CLEVELAND, OH.
A software tool to design thermal barrier coatings
p 1946 N95-26139
DEPARTMENT OF ENERGY, MORGANTOWN, WV.
Monolithic solid oxide fuel cell technology advancement for coal-based power generation
[DE95-006152] p 1991 N95-24425
DEPARTMENT OF ENERGY, WASHINGTON, DC.
Alternatives to traditional transportation fuels 1993
[DE95-005445] p 1947 N95-24273
ESnet Program Plan 1994
[DE95-005329] p 2019 N95-24290
Appendix model performance: Model documentation. Renewable Fuels Module of the National Energy Modelling System
[DE95-006080] p 1991 N95-24355
Identification of potential groundwater flow paths using geological and geophysical data
[DE95-006253] p 1988 N95-24407
Superconductivity Program for Electric Power Systems: 1994 Annual PEER Review. Volume 1, Meeting Proceedings
[DE95-005058] p 1956 N95-24452
Superconductivity Program for Electric Power Systems: 1994 Annual PEER Review. Volume 2, Meeting Proceedings
[DE95-005059] p 1957 N95-24453
Carbons and hydrogen by persistent metal radicals
[DE95-003834] p 1929 N95-24553
Federal alternative motor fuels program: Light duty federal vehicles, trucks, and buses
[DE95-003982] p 1948 N95-24679
High Energy Physics Advisory Panel's subpanel on vision for the future of high-energy physics
[DE94-013641] p 2068 N95-24899
Voluntary reporting of greenhouse gases under Section 1605(b) of the Energy Policy Act of 1992: General guidelines
[DE95-003295] p 2000 N95-25361
Sector-specific issues and reporting methodologies supporting the General Guidelines for the voluntary reporting of greenhouse gases under Section 1605(b) of the Energy Policy Act of 1992, volume 1. Part 1: Electricity supply sector. Part 2: Residential and commercial buildings sector. Part 3: Industrial sector
[DE95-003296] p 2000 N95-25362
Human radiation experiments: The Department of Energy roadmap to the story and the records
[DE95-006364] p 2012 N95-25371
Summaries of FY 1994 geosciences research
[DE95-005657] p 1988 N95-25440
Further ways to distinguish single-lepton top quark signals from background at the Tevatron
[PB95-165395] p 2056 N95-25567
Sector-specific issues and reporting methodologies supporting the general guidelines for the voluntary reporting of greenhouse gases under Section 1605(b) of the Energy Policy Act of 1992, Volume 2. Part 4: Transportation sector. Part 5: Forestry sector. Part 6: Agricultural sector
[DE95-003297] p 2003 N95-26065
Thermal barrier coatings issues in advanced land-based gas turbines p 1944 N95-26122
Thermal barrier coatings application in diesel engines
p 1944 N95-26124

DESERT RESEARCH INST., RENO, NV.
Replicator for characterization of cirrus and polar stratospheric cloud particles
[NASA-CR-197992] p 2005 N95-24411
Nucleation and growth of crystals under cirrus and polar stratospheric cloud conditions
[NASA-CR-197991] p 2085 N95-24478
DIGITAL EQUIPMENT CORP., CAMBRIDGE, MA.
An annotation system for 3D fluid flow visualization
p 1966 N95-25869
DORTMUND UNIV. (GERMANY).
Innovation and application of ANN in Europe demonstrated by Kohonen maps p 2024 N95-25262
DUKE UNIV., DURHAM, NC.
Learning random networks for compression of still and moving images p 2025 N95-25268
DURHAM UNIV. (ENGLAND).
Parton distributions for low Q2
[PB95-165213] p 2056 N95-25619

E

ECOLE POLYTECHNIQUE FEDERALE DE LAUSANNE (SWITZERLAND).
Surface plasmon observed for carbon nanotubes
[DE95-607769] p 2091 N95-26260
EG AND G ENERGY MEASUREMENTS, INC., GOLETA, CA.
Turbine-engine applications of thermographic-phosphor temperature measurements
[DE95-003625] p 1989 N95-25110
ELECTROTECHNICAL LAB., IBARAKI (JAPAN).
Summaries of reports of the Electrotechnical Laboratory, no. 48
[JTN-95-80825] p 2114 N95-24908
ENDOROBOTICS CORP., WARREN, NJ.
Milli-robots for surgical teleoperation
[NASA-CR-197378] p 1974 N95-24204
ENERGETICS, INC., COLUMBIA, MD.
Brayton-cycle solvent recovery heat pump. A technical brief
[DE94-000225] p 1991 N95-24666
ENERGY AND ENVIRONMENTAL RESEARCH CORP., DURHAM, NC.
Nitrogen oxide emissions and their control from uninstalled aircraft engines in enclosed test cells: Joint report to Congress on the Environmental Protection Agency - Department of Transportation study
[PB95-166237] p 2002 N95-26005
ENERGY INFORMATION ADMINISTRATION, WASHINGTON, DC.
Directory of Energy Data Collection Forms: Forms in use as of October 1994
[DE95-004329] p 2105 N95-24710
ENGINEERING-SCIENCE, INC., HUNTSVILLE, AL.
Advanced multi-phase flow CFD model development for solid rocket motor flowfield analysis
[NASA-CR-198044] p 1923 N95-25103
ENVIRONMENTAL PROTECTION AGENCY, ANN ARBOR, MI.
Spray characteristics of single- and three-hole nozzle injectors in ambient air and in a motored single-cylinder test engine
[PB95-166286] p 1976 N95-25574
Draft regulatory impact analysis: Control of air pollution emission standards for new nonroad spark-ignition marine engines
[PB95-166294] p 2001 N95-25575
ENVIRONMENTAL RESEARCH INST. OF MICHIGAN, ANN ARBOR, MI.
Infrared multispectral sensor program, Phase 2. Field measurements, analysis and modeling. Volume 1: Fourier transform spectrometer sensor characterization
[AD-A288888] p 2075 N95-26173
EUROPEAN ORGANIZATION FOR NUCLEAR RESEARCH, GENEVA (SWITZERLAND).
A normal form approach to the theory of nonlinear betatronic motion
[DE95-603831] p 2062 N95-25944
EUROPEAN SPACE AGENCY. EUROPEAN SPACE RESEARCH AND TECHNOLOGY CENTER, ESTEC, NOORDWIJK (NETHERLANDS).
Europe in space, 1960-1973
[ESA-SP-1172] p 2114 N95-24870
The history of ELDO. Part 1: 1961-1964
[ESA-HSR-10-PT-1] p 2114 N95-24871
Reflections on Europe in space
[ESA-HSR-11] p 1916 N95-24872
The origins of the Federal Republic of Germany's space policy, 1959-1965: European and national dimensions
[ESA-HSR-12] p 1916 N95-24892
ESRO's telecommunications programme and the OTS project (1970-1974)
[ESA-HSR-13] p 1953 N95-24893
United States-European cooperation in space during the sixties
[ESA-HSR-14] p 2107 N95-24894
United States-European space cooperation in the post-Apollo programme
[ESA-HSR-15] p 2107 N95-24895
The scientific programme between ESRO and ESA: Choosing new projects (1973-1977)
[ESA-HSR-16] p 1917 N95-24896
ESA Bulletin No. 81 p 2114 N95-25200
EXECUTIVE OFFICE OF THE PRESIDENT, WASHINGTON, DC.
Our changing planet: The FY 1995 U.S. Global Change Research Program p 2002 N95-25852
Science in the national interest
[ISBN-0-16-045186-8] p 2115 N95-26335

F

FEDERAL AVIATION ADMINISTRATION, ATLANTIC CITY, NJ.
Bird ingestion into large turbofan engines
[DOT/FAA/CT-93/14] p 1909 N95-24631
FEDERAL AVIATION ADMINISTRATION, CAMBRIDGE, MA.
Estimate of probability of crack detection from service difficulty report data
[PB95-149381] p 1905 N95-24295
FEDERAL AVIATION ADMINISTRATION, WASHINGTON, DC.
Federal Aviation Administration plan for research, engineering and development, 1995
p 2102 N95-24202
FERMI NATIONAL ACCELERATOR LAB., BATAVIA, IL.
Study of the structure of the events produced in soft (bar p)p interactions of (radical)s = 1800 GeV
[DE95-004851] p 2041 N95-24252
Measurement of the SS-OS Dijet cross-section ratio
[DE95-004852] p 2041 N95-24253
Top quark kinematics and mass determination
[DE95-004853] p 2041 N95-24254
W-charge asymmetry at CDF, tests of structure functions
[DE95-004855] p 2041 N95-24256
On corrections to the Nambu action
[NASA-CR-197625] p 2065 N95-24335
Measurement of the WW gamma, ZZ gamma and Z gamm a gamma couplings at the Fermilab Tevatron
[DE95-003495] p 2067 N95-24601
Evidence for top quark production in 1.8 TeV p-bar p collisions
[DE95-003496] p 2068 N95-24728
The KTeV PMT laser monitoring system
[DE95-004237] p 1972 N95-24869
The CDF silicon vertex detector SVX and its upgrades
[DE95-003743] p 2050 N95-24901
Double-sided silicon microstrip sensors for the CDF SVX 2 detector
[DE95-004235] p 2068 N95-25238
Neutrino optics
[DE95-004236] p 2073 N95-25239
B physics with CDF: Recent results and future prospects
[DE95-004793] p 2051 N95-25372
A generic data exchange scheme between FITS format and C structures
[DE95-004849] p 2106 N95-25376
Photon-charm production in p(anti p) collisions at radical s = 1.8 TeV
[DE95-004850] p 2052 N95-25377
A search for t(anti t) (yields) lepton + E(sub T) + jets signature in p(anti p) collisions at (radical)s = 1.8 TeV with the DO detector
[DE95-004239] p 2052 N95-25402
Electroweak boson pair production at the Tevatron
[DE95-004234] p 2056 N95-25563
Preliminary results on the decays D(+) yields K(+)pi(+)pi(-), D(+) yields K(+)K(+)K(-)
[DE95-004865] p 2071 N95-26011
A survey of surveys
[DE95-004238] p 2111 N95-26284
FERNALD ENVIRONMENTAL RESTORATION MANAGEMENT CORP., CINCINNATI, OH.
Integrated planning: A baseline development perspective
[DE95-004945] p 2102 N95-24905
Standardization of equations for radiochemical calculations
[DE95-003028] p 1930 N95-25097
FINNISH ASSOCIATION FOR AEROSOL RESEARCH, ESPOO (FINLAND).
Report series in aerosol science
[DE95-737628] p 1999 N95-24904
Effects of nitric acid vapor on the formation of cloud droplets in troposphere
[DE95-744869] p 2001 N95-25500
FINNISH CENTRE FOR RADIATION AND NUCLEAR SAFETY, HELSINKI (FINLAND).
Reliability analysis of software based safety functions
[DE95-606516] p 2018 N95-26045
FLORIDA STATE UNIV., TALLAHASSEE, FL.
Diagrammatic many-body perturbation expansion for atoms and molecules
[PB95-165221] p 2056 N95-25620
Alpha(sub critical) for parallel processors
[PB95-165320] p 2022 N95-25625
FLORIDA UNIV., GAINESVILLE, FL.
A quantum gravitational mechanism for exiting inflation
[DE95-003342] p 2096 N95-24867
Effects of through-the-thickness stitching on impact and interlaminar fracture properties of textile graphite/epoxy laminates
[NASA-CR-195042] p 1928 N95-26203
FOERENADE FABRIKSVERKEN, LINKOEPING (SWEDEN).
Prediction of humans in various environments using gas sensors and neural networks
[PB95-141560] p 2009 N95-24227
Visual performance with Omnibus 3: A comparative evaluation of enhanced generation three image intensifier technology
[PB95-141891] p 2013 N95-24510
FORD MOTOR CO., DEARBORN, MI.
Neural network application to comprehensive engine diagnostics p 2023 N95-25255
Learning to train neural networks for real-world control problems p 2025 N95-25269

G

GAS RESEARCH INST., CHICAGO, IL.
Retrofit NOx control technologies for natural gas prime movers
[PB95-149290] p 1997 N95-24294
GENERAL ACCOUNTING OFFICE, WASHINGTON, DC.
Report to Congressional Committees. Tactical Aircraft: Concurrency in development and production of F-22 aircraft should be reduced
[GAO/NSIAD-95-59] p 1911 N95-26338
GENERAL ATOMICS CO., SAN DIEGO, CA.
Experimental and theoretical basis for advanced tokamaks
[DE95-003255] p 2077 N95-24646
Engineering and design of a CO2 phase contrast interferometer system for DIII-D
[DE95-004249] p 1972 N95-24709
The role of shaping in achieving high performance in DIII-D
[DE95-003877] p 2078 N95-25102
A vacuum window for a 1 MW CW 110 GHz gyrotron
[DE94-016584] p 2079 N95-25108
Results obtained using the pellet charge exchange diagnostic on TFTR
[DE95-003254] p 2079 N95-25120
Experimental constraints on transport
[DE95-004962] p 2050 N95-25180
Evidence for modified transport due to sheared E x B flows in high-temperature plasmas
[DE95-004870] p 2079 N95-25250
GENERAL DYNAMICS CORP., SAINT LOUIS, MO.
Commercial Space Transportation Study (CSTS)
[SSD94D0035] p 1919 N95-25747
GENERAL ELECTRIC CO., CINCINNATI, OH.
PVD TBC experience on GE aircraft engines
p 1944 N95-26126
GENERAL ELECTRIC CO., SCHENECTADY, NY.
TBC experience in land based gas turbines
p 1944 N95-26127
GEO ECO ARC RESEARCH, LA CANADA, CA.
Biospheric effects of a large extraterrestrial impact: Case study of the cretaceous/tertiary boundary crater
[NASA-CR-198015] p 1997 N95-24501
GEORGIA INST. OF TECH., ATLANTA, GA.
Actively controlled shaft seals for aerospace applications
[NASA-CR-198035] p 1974 N95-24218
Optimal guidance law development for an advanced launch system
[NASA-CR-4667] p 1917 N95-26205
GEORGIA TECH RESEARCH INST., ATLANTA, GA.
Effects of cavity dimensions, boundary layer, and temperature on cavity noise with emphasis on benchmark data to validate computational aeroacoustic codes
[NASA-CR-4653] p 2039 N95-24879
GEORGIA UNIV., ATHENS, GA.
Structures and functions of oligosaccharins
[DE95-003140] p 2007 N95-24225

Structural studies of complex carbohydrates of plant cell walls
[DE95-005545] p 2007 N95-24368
Testing of experimental antileishmanial compounds
[AD-A288807] p 2009 N95-26193

H

HANSEN ENGINE CORP., MINNETONKA, MN.
Investigation of a rotary valving system with variable valve timing for internal combustion engines
[DE95-003831] p 1976 N95-25101
HAWAII UNIV., HONOLULU, HI.
On the Trellis structure of a (64,40,8) subcode of the (64,42,8) third-order Reed-Muller code
[NASA-CR-198019] p 2015 N95-24224
DOE-High Energy Physics Contract with the University of Hawaii
[DE95-004214] p 2068 N95-24852
HELSINKI UNIV. OF TECHNOLOGY, ESPOO (FINLAND).
Relative orientation of multiple images using projective singular correlation
[PB95-149936] p 1967 N95-24259
Shell deformation states and the finite element method: A benchmark study of cylindrical shells
[PB95-149621] p 1980 N95-24296
Expert system for nuclide identification in gamma spectrum analysis
[PB95-149712] p 2042 N95-24297
Gamma spectrum analysis including NAA with SAMPO for windows
[PB95-149720] p 2042 N95-24298
Diurnal variations of backscattering properties of pine trees at C- and X-bands
[PB95-149738] p 1988 N95-24299
Measurements of thermal conductivity of diamond thin films by the ac calorimetric method
[PB95-149746] p 1939 N95-24300
Potential of diamond for applications in microelectronics
[PB95-141446] p 1942 N95-25633
HOKKAIDO NATIONAL INDUSTRIAL RESEARCH INST., SAPPORO (JAPAN).
Disposal of electronic equipment
[PB95-177861] p 2002 N95-26047
HOUSTON UNIV., TX.
Studies of two-phase gas-liquid flow in microgravity
[NASA-CR-195434] p 1963 N95-24906
HOWARD UNIV., WASHINGTON, DC.
A report: A plan to establish Internet access points at Minority Campus sites for connection to a central computing facility
[DE95-004374] p 2105 N95-25240
HUGHES STX, INC., LANHAM, MD.
Particle-mesh techniques
[NASA-CR-4666] p 2083 N95-26082
HUGHES STX, INC., LEXINGTON, MA.
Implementation of scene shadows in the Target Acquisition TDA (TARGAC)
[AD-A288760] p 1912 N95-26060

I

IDAHO NATIONAL ENGINEERING LAB., IDAHO FALLS, ID.
Magnetically controlled deposition of metals using gas plasma
[DE95-003827] p 2077 N95-24552
Cobalt release from PCA steel during possible fusion reactor accidents
[DE95-005019] p 2069 N95-25365
Low-cost image analysis system
[DE95-005021] p 2021 N95-25378
Long-Term Flow Test number 1: Roosevelt Hot Springs, Utah
[DE95-004995] p 2004 N95-25666
Applications for electronic documents
[DE95-005036] p 2106 N95-25765
ILLINOIS UNIV., CHICAGO, IL.
Generation and computerized simulation of meshing and contact of modified involute helical gears
[NASA-CR-4644] p 1952 N95-24395
ILLINOIS UNIV., URBANA, IL.
FTAPE: A fault injection tool to measure fault tolerance
[NASA-CR-198000] p 1978 N95-25333
ILLINOIS UNIV., URBANA-CHAMPAIGN, IL.
Visibility ordering meshed polyhedra
[CSRD-1097] p 2030 N95-24557
Software fault tolerance in computer operating systems
[NASA-CR-197999] p 2016 N95-24993
IMPERIAL COLL. OF SCIENCE AND TECHNOLOGY, LONDON (ENGLAND).
Development of a high temperature, high speed disc lubricant test machine
[AD-A288685] p 1977 N95-26050
INSTITUT DES HAUTES ETUDES SCIENTIFIQUES, BURES-SUR-YVETTE (FRANCE).
Uniform rectifiability and singular sets
[PB95-165502] p 2028 N95-24243
Semiclassical asymptotics on covering manifolds and morse inequalities
[PB95-165510] p 2028 N95-24251
Construction of the moduli space of monopoles
[PB95-165528] p 2028 N95-24255
Periodic solutions of Hamiltonian perturbations of 2D linear Schroedinger equations
[PB95-165536] p 2028 N95-24301
Behavior of a trigonometric polynomial with given number of terms on small subsets of the unit circumference (norm duplication problem)
[PB95-165544] p 2028 N95-24321
Construction of quasi-periodic solutions for Hamiltonian perturbations of linear equations and applications to nonlinear PDE
[PB95-165551] p 2028 N95-24322
Intrinsic heights of stable varieties. Application to abelian varieties
[PB95-165577] p 2029 N95-24323
Distribution of the error term for the number of lattice points inside a shifted ball
[PB95-165569] p 2029 N95-24325
INSTITUTE FOR COMPUTER APPLICATIONS IN SCIENCE AND ENGINEERING, HAMPTON, VA.
Separation analysis, a tool for analyzing multigrid algorithms
[NASA-CR-195036] p 2029 N95-24389
Covolume solutions of three dimensional div-curl equations
[NASA-CR-195031] p 2029 N95-24421
A review of Reynolds stress models for turbulent shear flows
[NASA-CR-195054] p 1962 N95-24580
Spectrum and energy transfer in steady Burgers turbulence
[NASA-CR-195047] p 1963 N95-24584
Exponentially accurate approximations to piece-wise smooth periodic functions
[NASA-CR-195059] p 2031 N95-24856
Multigrid solution strategies for adaptive meshing problems
[NASA-CR-195049] p 2031 N95-24857
Implementation of a parallel unstructured Euler solver on the CM-5
[NASA-CR-195056] p 2032 N95-25106
A well-posed numerical method to track isolated conformal map singularities in Hele-Shaw flow
[NASA-CR-195035] p 2032 N95-25114
The first ICASE/LARC industry roundtable: Session proceedings
[NASA-CR-195040] p 2014 N95-25119
Classical closure theory and Lam's interpretation of epsilon-RNG
[NASA-CR-195061] p 1965 N95-25960
A pseudo-sound constitutive relationship for the dilatational covariances in compressible turbulence: An analytical theory
[NASA-CR-195064] p 1966 N95-25964
Cumulative reports and publications through December 31, 1994
[NASA-CR-195043] p 2014 N95-26085
INSTITUTE FOR DEFENSE ANALYSES, ALEXANDRIA, VA.
Flexible architectures for sensor fusion in theater missile defense
[AD-A288666] p 2007 N95-26048
INSTITUTE FOR HUMAN FACTORS TNO, SOESTERBERG (NETHERLANDS).
On producing sequential movements and actions. An integrative review and an update of the generalized motor program
[AD-A288628] p 2014 N95-25610
INSTITUTE OF ELECTRICAL AND ELECTRONICS ENGINEERS, NEW YORK, NY.
Proceedings of the 4th IEEE Workshop on Neural Networks for Signal Processing
[AD-A288383] p 2026 N95-25603
INSTITUTE OF NUCLEAR CHEMISTRY AND TECHNOLOGY, WARSAW (POLAND).
Electron spin resonance of radicals and metal complexes
[DE95-605640] p 2055 N95-25499
INSTITUTE OF SOUND AND VIBRATION RESEARCH, SOUTHAMPTON (ENGLAND).
The transmission and control of vibrational power in a two stage isolation system with a water-loaded substructure
[ISVR-TR-235] p 1975 N95-24992
Tunable vibration absorbers: Key design parameters
[ISVR-TR-244] p 1981 N95-24995
A technique for the evaluation of strength of coupling between SEA subsystems
[ISVR-TR-241] p 1981 N95-24997
An analytical study of the vibration of beams fitted with neutralizers. Part 3: Torsional wave motion
[ISVR-TR-238-PT-3] p 1982 N95-25003
A technique for the evaluation of strength of coupling between SEA subsystems: Experiments with two coupled plates and two coupled rooms
[ISVR-TR-242] p 1982 N95-25332
INSTITUTO DE FISICA TEORICA, SAO PAULO (BRAZIL).
Limiting analytic form for Aharonov-Bohm diffraction pattern
[DE95-600839] p 2065 N95-24351
Parity doubling from thermodynamics of experimental hadron spectrum
[DE95-600934] p 2095 N95-24839
INSTITUTO DE PESQUISAS ENERGETICAS E NUCLEARES, SAO PAULO (BRAZIL).
Preparation of stabilized zirconia (ZrO_2) with ytteria (Y_2O_3) by simultaneous precipitation
[DE95-600163] p 1933 N95-24366
Application of compartmental metabolic models for determination of retention and excretion functions
[DE95-600249] p 2010 N95-24367
Antioxidant and sensitizer effect on the stability of natural rubber latex vulcanized by gamma rays
[DE94-636061] p 1939 N95-24373
INTERNATIONAL ATOMIC ENERGY AGENCY, VIENNA (AUSTRIA).
International bulletin on atomic and molecular data for fusion, no. 47
[DE94-634442] p 2040 N95-24230
Atomic masses 1993. The 1993 atomic mass evaluation
[DE94-634462] p 2040 N95-24231
Environment, 1980-1993
[DE95-605240] p 2002 N95-25779
Online nuclear data service
[DE95-602487] p 2107 N95-25941
Index of nuclear data libraries available from the IAEA Nuclear Data Section
[DE95-605213] p 2107 N95-25980
INTERNATIONAL CENTRE FOR THEORETICAL PHYSICS, TRIESTE (ITALY).
Finite quantum physics and noncommutative geometry
[DE94-634282] p 2027 N95-24228
Distances on a lattice from noncommutative geometry
[DE94-634327] p 2027 N95-24229
Fractal studies on the positron annihilation in metals
[DE94-634488] p 2041 N95-24232
Temperature dependence of magnetic anisotropy and magnetostriction: Beyond the mean-field theory
[DE94-634529] p 2084 N95-24244
Current-voltage characteristics of a tunnel junction with resonant centers
[DE94-634530] p 1956 N95-24245
On the calculation of lattice sums arising in Bose-Einstein statistics of quasiparticle excitations
[DE94-634531] p 2084 N95-24246
Quantum mechanics with spontaneous localization and experiments
[DE94-634285] p 2092 N95-24266
Laser cooling of neutral atoms by red-shifted diffuse light in an optical integral sphere cavity
[DE94-634310] p 2041 N95-24268
Superconducting in the near half-filling Hubbard model
[DE94-634857] p 2092 N95-24275
A functional integral approach without slave bosons to the Anderson model
[DE94-634858] p 2028 N95-24276
Electron-phonon interaction in the Hubbard model
[DE94-634859] p 2092 N95-24277
$T=0$ finite-size scaling for a quantum system with long-range interaction
[DE94-634528] p 2092 N95-24288
One-step in-diffusion as a result of multipulse laser irradiation of $LiNbO_3$ single-crystalline substrates covered with thin Ti deposits on the effect of the radiation wavelength
[DE94-634524] p 2084 N95-24324
Optical diffraction from fractals with a structural transition
[DE94-634311] p 2029 N95-24401
Numerical simulation methods for wave propagation through optical waveguides
[DE94-634313] p 2073 N95-24402

Optical space communication: An overview
[DE94-634314] p 1952 N95-24403
Neutrino masses and b - tau unification in the supersymmetric standard model
[DE94-634361] p 2043 N95-24404
Z flux-line lattices and self-dual equations in the standard model
[DE94-634364] p 2093 N95-24405
Cyclic subgroups in class groups of real quadratic fields
[DE94-628407] p 2031 N95-24697
Semi-infinite mathematical programming: A collocation approach
[DE94-634273] p 2016 N95-24708
Semiclassical hyperspherical matrix elements for helium doubly excited states
[DE94-628867] p 2048 N95-24718
Quantum group and quantum symmetry
[DE94-634329] p 2095 N95-24767
Creation and development of the Universe (symmetry approach)
[DE94-628558] p 2109 N95-24884
Vortex solutions in two-Higgs-doublet systems
[DE94-634363] p 2096 N95-25107
Low energy properties of the heavy vector fermions
[DE94-634362] p 2051 N95-25290
On connection of q-deformed para oscillators with para oscillators
[DE95-607007] p 2096 N95-25425
Dissipative quantum mechanics: The generalization of the canonical quantization and von Neumann equation
[DE95-607008] p 2096 N95-25426
Quantum symplectic geometry. 1: The matrix Hamiltonian formalism
[DE95-607009] p 2032 N95-25427
Flare stars and Pascal distribution
[DE95-607044] p 2110 N95-25431
Relevance of induced gauge interactions in decoherence
[DE95-607082] p 2097 N95-25432
String-loop corrections to effective action and black-hole instabilities
[DE95-607085] p 2110 N95-25433
Two dimensional simplicial paths
[DE95-607087] p 2036 N95-25434
Critical parameters of Quark-Hadron phase transition with interacting and massive quarks
[DE95-607143] p 2052 N95-25436
The twist-3 single spin asymmetries of pion production
[DE95-607144] p 2052 N95-25437
Scalar three body decays and signals for new physics
[DE95-607188] p 2053 N95-25438
Symbolic dynamics of the Lorenz equations
[DE95-607045] p 2036 N95-25439
Temperature bounds in a model of laminar flames
[DE95-607048] p 1931 N95-25447
On the field theory of the extended-type electron
[DE95-607069] p 2053 N95-25449
Masses of heavy fermions and Higgs boson in four-generation fermion condensate scheme
[DE95-607124] p 2053 N95-25450
Nonlinearity induced nontrivial dynamics in the Jaynes-Cummings Hamiltonian
[DE95-607004] p 2032 N95-25452
Testing quantum behaviour at the macroscopic level
[DE95-607005] p 2097 N95-25453
Recoil effects in quantum topological solitons
[DE95-607006] p 2097 N95-25454
Equivariant Kaehler geometry and localization in the G/G model
[DE95-607073] p 2036 N95-25455
Tachyon condensates and anisotropic universe
[DE95-607074] p 2097 N95-25456
Involutive co-distributions preserved by transitive families of vector fields
[DE95-607078] p 2032 N95-25457
Zero sound velocity in pi, rho mesons at different temperatures
[DE95-607145] p 2053 N95-25459
Heavy quark effective theory, interpolating fields and Bethe-Salpeter amplitudes
[DE95-607146] p 2053 N95-25460
Radiative corrections for pion polarizability experiments
[DE95-607177] p 2053 N95-25462
Annihilation diagrams in two-body nonleptonic decays of charmed mesons
[DE95-607181] p 2054 N95-25463
Neutrino mass and oscillation angle phenomena within the asymmetric left-right models
[DE95-607201] p 2054 N95-25466
Far-infrared and submillimeter spectroscopy of photodissociation regions
[DE95-607520] p 2110 N95-25467
Photoionization of shallow donor impurities in finite-barrier quantum wells
[DE95-607521] p 2097 N95-25468
Valencia 1993: The summary of particle theory
[DE95-607121] p 2110 N95-25469
A phase-transition induced by the struggle for life in a competitive coexistence model in ecology
[DE95-607047] p 2001 N95-25521
On D=2 (1/3, 1/3) supersymmetric theories 1
[DE95-607075] p 2036 N95-25522
On D=2 (1/3,1/3) supersymmetric theories 2
[DE95-607076] p 2037 N95-25523
HyperKaehler metrics building and integrable models
[DE95-607077] p 2038 N95-25524
Geometric gauge fields in semiclassical gravity
[DE95-607079] p 2098 N95-25525
Boundary dynamics in dilaton gravity
[DE95-607080] p 2098 N95-25526
Semiglobal Alice strings
[DE95-607081] p 2098 N95-25527
Quantum mechanical analogy for solving a competitive coexistence model in ecology
[DE95-607046] p 2001 N95-25531
On exotic supersymmetries of the Phi(1,3) deformation of minimal models
[DE95-607088] p 2033 N95-25532
Central extension of a new W(infinity)-type algebra
[DE95-607086] p 2037 N95-25599
Nonexistence of global solutions to some quasilinear hyperbolic equations with dynamic boundary conditions
[DE95-607010] p 2033 N95-25645
The geodesic motion in Kaluza-Klein spinning space
[DE95-607070] p 2039 N95-25646
Homogeneous anisotropic cosmological models in the minimum quadratic Poincare gauge theory of gravity
[DE95-607083] p 2110 N95-25647
A superfield generalization of the classical action-at-a-distance theory
[DE95-607084] p 1955 N95-25648
Behaviour at X= +/- infinity of solutions to a predator-prey model
[DE95-607049] p 2033 N95-25748
Dynamic Jahn-Teller-induced infrared absorption of a charged C60(-) molecule
[DE95-607577] p 2063 N95-25971
Evolution of Spark plasma using nitrogen laser shadowgraphy system
[DE95-607598] p 2082 N95-25972
Construction of a nitrogen laser for plasma diagnostics
[DE95-607599] p 1973 N95-25973
Solitons in electron-positron plasma
[DE95-607608] p 2082 N95-25974
Self-focusing of electromagnetic radiation in electron-positron ion plasma
[DE95-607626] p 2082 N95-25975
The (lambda)-bar exponent for conservative systems
[DE95-607661] p 1937 N95-25977
Dynamics of phase ordering of nematics in a pore
[DE95-607662] p 2090 N95-25978
Domain growth in weakly disordered magnets: A coupled map lattice approach
[DE95-607663] p 2090 N95-25979
Numerical solution of the optimized random phase approximation
[DE95-605636] p 2034 N95-25982
Structural and thermodynamic properties of 3-d transition metals: Pseudopotential theory revisited
[DE95-605639] p 1937 N95-25983
Estimation and analysis of spectral solar radiation over Cairo
[DE95-606029] p 2113 N95-25986
Charge-Dyon system as the reduced oscillator
[DE95-606998] p 2100 N95-25987
On Segal-Wilson's construction for the (tau)-functions of the constrained KP hierarchies
[DE95-606999] p 2100 N95-25988
On the Cohen-Macaulayness and Gorensteinness of integral closure filtrations Rees algebras of height-two equimultiple ideals
[DE95-607000] p 2034 N95-25989
Regge in the sky: Origin of the cosmic rotation
[DE95-607001] p 2111 N95-25990
Strong phase correlations of solitons of nonlinear Schroedinger equation
[DE95-607002] p 2063 N95-25991
The criteria for the Cohen-Macaulayness and Gorensteiness of Rees algebras of ideals having positive analytic deviation
[DE95-607003] p 2034 N95-25992
Optical instabilities and chaos due to the virtual formation of biexcitons
[DE95-607664] p 2063 N95-25994
Predicting the components of the total hemispherical solar radiation from sunshine duration measurements in Lagos, Nigeria
[DE95-606030] p 2113 N95-26042
Modelling the day to day wind variability offshore central Chile at about 30 deg south
[DE95-606032] p 2006 N95-26043
The use of empirical models to investigate GPS derived total electron content
[DE95-606045] p 2111 N95-26044
Describing the macroscopic world: Closing the circle within the dynamical reduction program
[DE95-606997] p 2100 N95-26046
Condensate localization by mesoscale disorder in high-T(sub c) superconductors
[DE95-607819] p 1960 N95-26100
Coherent state path-integral representation of supersymmetric lattice models
[DE95-607820] p 2091 N95-26101
Correlated density matrix theory of spatially inhomogeneous Bose fluids
[DE95-607840] p 2100 N95-26102
Quantum group random walks in strongly correlated 2+1 D spin systems
[DE95-607844] p 2091 N95-26103
Calculating the thermodynamic properties of planar and spherical liquid-vapour interface
[DE95-608777] p 2100 N95-26105
Rotational melting in displacive quantum paraelectrics
[DE95-607804] p 2091 N95-26252

IOWA STATE UNIV. OF SCIENCE AND TECHNOLOGY, AMES, IA.
Study of compressible flow through a rectangular-to-semiannular transition duct
[NASA-CR-4660] p 1914 N95-24392

IOWA UNIV., IOWA CITY, IA.
The whistler-mode bow wave of an asteroid
[U-OF-IOWA-95-2] p 2111 N95-26195
On a remarkable similarity between the propagation of whistlers and the bow wave of a ship
[U-OF-IOWA-94-22] p 2111 N95-26196

IRVINE SENSORS CORP., COSTA MESA, CA.
Three-D Artificial Neural Network (3DANN) technology. Blueprint for the future p 2024 N95-25260
Multi-spectral smart retina
[AD-A288950] p 2074 N95-25506

ISHIKAWAJIMA-HARIMA HEAVY INDUSTRIES CO. LTD., TOKYO (JAPAN).
Development test of a liquid apogee engine for the ETS-4
[NAL-TR-1250] p 1922 N95-24999

ISRAEL ATOMIC ENERGY COMMISSION, TEL AVIV (ISRAEL).
Decay of a laser generated shock wave in an aluminium target
[DE94-629014] p 1972 N95-24707

ISRAEL ATOMIC ENERGY COMMISSION, YAVNEH (ISRAEL).
Experimental and theoretical study of plasma-water interaction in electrothermal guns
[DE94-628961] p 2078 N95-24706

J

JAGELLONIAN UNIV., CRACOW (POLAND).
Electronic structure and pairing of strongly correlated fermions: Fermi liquid versus spin liquid
[DE95-005929] p 2044 N95-24419

JAPAN ATOMIC ENERGY RESEARCH INST., NAKA (JAPAN).
Fusion-neutron diagnostic on the Microwave Tokamak Experiment
[DE94-777530] p 2075 N95-24270
Development of a fast response rotating polarimeter for a Faraday rotation measurement
[DE94-777532] p 2075 N95-24271
A proposal to introduce a turbulence factor into a diffusion coefficient of a Tokamak plasma
[DE94-777533] p 2075 N95-24272
Outline of fast analyzer for MHD equilibrium FAME
[DE94-777540] p 2076 N95-24311

JAPAN ATOMIC ENERGY RESEARCH INST., TOKYO (JAPAN).
Structure and manual of radioisotope-production data base, ISOP
[DE94-785197] p 2043 N95-24337
Creep properties of 20% cold worked hastelloy XR
[DE94-785198] p 1933 N95-24338
Design study of a negative-ion based NBI system for JT-60U
[DE94-785265] p 2043 N95-24339
Simulation study of tapered FEL amplifiers in Raman and Compton regimes
[DE94-785266] p 1971 N95-24340
Development of oxidation resistant SiC/C compositionally gradient materials
[DE94-785101] p 1925 N95-24365
Proceedings of the 1993 Symposium on Nuclear Data
[DE94-012554] p 2104 N95-24372

Phase 3 experiments of the JAERI/USDOE collaborative program on fusion blanket neutronics. Volume 1: Experiment
[DE94-777528] p 2076 N95-24511

High heat flux experiment on B4C-converted carbon based materials for plasma facing materials of JT-60U
[DE94-777545] p 2077 N95-24585

Numerical analysis of electron cyclotron resonance heating on JT-60U and JFT-2M
[DE95-709766] p 2080 N95-25471

Design of Fusion Safety Data Base
[DE95-703897] p 2080 N95-25495

Molecular dynamics calculation of shear viscosity for molten salt
[DE95-703970] p 2055 N95-25496

Benchmark experiment on a copper slab assembly bombarded by D-T neutrons
[DE95-709764] p 2055 N95-25497

Measurement of kinetic energy of ions collected from laser resonance photoionized plasma by time-of-flight method
[DE95-709767] p 2081 N95-25498

Proceedings of the 21st Japan Conference on Radiation and Radioisotopes
[DE94-785275] p 2056 N95-25614

A new method of emittance measurement for electron beams from the Micro-emitter
[DE94-792657] p 2070 N95-25631

Heat removal capability of divertor coaxial tube assembly
[DE95-709770] p 1966 N95-26161

JAPAN ATOMIC INDUSTRIAL FORUM, INC. (JAPAN).

Proceedings of the 21st Japan Conference on Radiation and Radioisotopes
[DE94-785275] p 2056 N95-25614

JAPAN INDUSTRIAL TECHNOLOGY ASSOCIATION, TOKYO (JAPAN).

Fourth symposium of the geological survey of Japan on remote sensing of satellite geology
[PB95-178737] p 1917 N95-25750

JAPAN RADIOISOTOPE ASSOCIATION, INC. (JAPAN).

Proceedings of the 21st Japan Conference on Radiation and Radioisotopes
[DE94-785275] p 2056 N95-25614

JET PROPULSION LAB., CALIFORNIA INST. OF TECH., PASADENA, CA.

Mars observer mission: Mapping the Martian world
[NASA-CR-110585] p 2112 N95-24672

User guide to the Magellan synthetic aperture radar images
[NASA-RP-1356] p 2112 N95-24987

A Decade of Neural Networks: Practical Applications and Prospects
[NASA-CR-197334] p 2022 N95-25253

VLSI neuroprocessors p 2023 N95-25258

Hidden Markov models and neural networks for fault detection in dynamic systems p 2024 N95-25261

Predictability in space launch vehicle anomaly detection using intelligent neuro-fuzzy systems p 2025 N95-25266

Optically-switched submillimeter-wave oscillator and radiator having a switch-to-switch propagation delay
[NASA-CASE-NPO-18547-1-CU] p 1959 N95-25307

A satellite-tracking millimeter-wave reflector antenna system for mobile satellite-tracking
[NASA-CASE-NPO-18772-1-CU] p 1954 N95-25316

Alternate method for achieving temperature control in the -160 to +90 Celcius range
[NASA-CASE-NPO-18995-1-CU] p 1969 N95-25547

Spaceborne synthetic aperture radar: Current status and future directions. A report to the Committee on Earth Sciences, Space Studies Board, National Research Council
[NASA-TM-4679] p 1955 N95-25710

Voyager: The grandest tour. The mission to the outer planets
[NASA-CR-197708] p 2112 N95-25854

Return to the red planet: The Mars Observer Mission
[NASA-CR-197707] p 2113 N95-26336

JOHNS HOPKINS UNIV., BALTIMORE, MD.

A report: A plan to establish Internet access points at Minority Campus sites for connection to a central computing facility
[DE95-004374] p 2105 N95-25240

JOINT INST. FOR ADVANCEMENT OF FLIGHT SCIENCES, HAMPTON, VA.

Simulating the dynamic interaction of a robotic arm and the Space Shuttle remote manipulator system
[NASA-CR-195076] p 2027 N95-26086

JOINT INST. FOR NUCLEAR RESEARCH, DUBNA (USSR).

Anharmonic potential in the oscillator representation
[DE94-636740] p 2092 N95-24312

Elliptic deformed Newton mechanics in the three-dimensional phase space
[DE94-636741] p 2092 N95-24313

Bound states of 'dressed' particles
[DE94-636773] p 2042 N95-24314

Deficiency of the Gross-Llewellyn Smith sum rule and QCD vacuum polarization effect
[DE94-636790] p 2042 N95-24315

Low energy theorems in quark potential models
[DE94-636791] p 2042 N95-24316

Moving scales contraction contradicts interval invariance
[DE94-636736] p 2092 N95-24347

Field equipotentials of a fast-moving charge in medium
[DE94-636737] p 2065 N95-24348

On a generalized Kepler-Coulomb system: Inter basis expansions
[DE94-636739] p 2093 N95-24349

On leading charmed meson production in pi-nucleon interactions
[DE94-636797] p 2043 N95-24360

Investigation of the gross structure of spectra and mass distributions of hadronic resonances
[DE94-636799] p 2043 N95-24361

Thermal diffuse scattering in time-of-flight neutron diffraction studied on SBN single crystals
[DE94-637054] p 2085 N95-24362

A computing program of sample magnetic moments recognition for SQUID-magnetometer measurements
[DE94-637073] p 2037 N95-24363

Structure of liquid He-4 excitations spectrum
[DE94-637113] p 2043 N95-24364

The facility for commercial doping of silicon by thermal neutrons in channel 3 at the IBR-2
[DE94-636293] p 2085 N95-24374

SYSINT(SYSINTM)-program complex for numerical solution of the eigenvalue problem for system of integral equations
[DE94-636729] p 2029 N95-24375

The Lienard-Wiechert potentials and relativistic length
[DE94-636733] p 2093 N95-24376

Lienard-Wiechert potentials as a consequence of Lorentz transformation of Coulomb potential
[DE94-636734] p 1952 N95-24377

The Fitzgerald-Lorentz hypothesis from the viewpoint of relativity theory
[DE94-636735] p 2093 N95-24378

Numerical investigation of Schwinger-Dyson and Bethe-Salpeter equations with Gauss potential in the framework of the quarkonium model
[DE94-636730] p 2029 N95-24387

Entropy and enthalpy of adsorption of gaseous chlorides of metals on quartz glass as a function of the molecular composition
[DE94-627162] p 2093 N95-24481

Energy resolution of a lead scintillating fiber electromagnetic calorimeter
[DE94-628253] p 1967 N95-24484

Muon identifier efficiency of the GINES detecto r in the UNK neutrino beam
[DE94-628254] p 2045 N95-24485

Software of a distributor of high voltage of the H C-600 hadronic calorimeter
[DE94-628255] p 1967 N95-24486

The measurement of the low frequency noise characteristics of the field effect transistors for cryogenic detectors
[DE94-628257] p 1957 N95-24487

On squaring the primary constraints in a generalized Hamiltonian dynamics
[DE94-628500] p 2036 N95-24504

Lagrangian formulation of NJL model with se parable interaction
[DE94-628519] p 1952 N95-24506

Heat Kernel expansion on a cone and quantum fields near cosmic strings
[DE94-628520] p 2094 N95-24507

The lattice spinor QED Hamiltonian critique of the continuous space approach
[DE94-628521] p 2094 N95-24508

Quantum group gauge theories and covariant quantum algebras
[DE94-628524] p 2094 N95-24509

Copper transport on oxygen annealing of a superconducting film Y-Ba-Cu-O
[DE94-627566] p 2086 N95-24537

Absolute calibration and monitoring of a spectrometric channel using a photomultiplier
[DE94-628251] p 1968 N95-24635

Oscillator poly spheroidal functions
[DE94-628440] p 2030 N95-24636

Generalization of the Rayleigh formula to the model with ring-shaped potentials
[DE94-628578] p 2094 N95-24637

On the problem of unboundedness from below of the spinor QED Hamiltonian
[DE94-628579] p 2094 N95-24638

Dressing and bound states in quantum field theory
[DE94-628580] p 2095 N95-24639

Covariant single-time equations for a system of N spinor particles
[DE94-628587] p 2047 N95-24640

Detector for transit time measurement of photomultiplier single-photoelectron pulses
[DE94-628256] p 2073 N95-24642

Unfolding of true distributions from experimental data distorted by detectors with finite resolutions
[DE94-628372] p 2035 N95-24643

The emission of particle identification efficiency in the EXCHARM experiment
[DE94-628258] p 2047 N95-24644

Adaptive projective filters
[DE94-628374] p 2030 N95-24645

On a possibility for a measurement of the transversal proton polarization in the diffractive pion production in pp and pe high energy collisions
[DE94-628598] p 2047 N95-24668

Some remarks to the problem of neutrino oscillation
[DE94-628599] p 2048 N95-24669

Saddle-point method in path integrals
[DE94-628379] p 2036 N95-24688

Ionization potential data library of atoms and ions
[DE94-628380] p 2048 N95-24689

ASYS2: A new version of computer algebra package ASYS for analysis and simplification of polynomial systems
[DE94-628384] p 2030 N95-24691

The determination of the main parameters of the backward spectrometer of the 0(sup 0) facility
[DE94-628385] p 2048 N95-24692

Introduction to the Monte Carlo methods
[DE94-628386] p 2035 N95-24693

Generators of matrix factorable representations of block-tridiagonal and inverse matrices
[DE94-628387] p 2031 N95-24694

Domain decomposition and generators of direct methods of the solution of linear equation systems with general block-tridiagonal matrices
[DE94-628388] p 2031 N95-24695

Toroidal response in magnetic resonance
[DE94-628406] p 2037 N95-24696

Geometric quantization of symplectic manifolds with symmetry
[DE94-628435] p 2031 N95-24698

Equivariant localization: BV-geometry and supersymmetric dynamics
[DE94-628436] p 2036 N95-24699

Elastic form factors of hydrogen-like atoms in nS-states
[DE94-628437] p 2048 N95-24700

Quasi-generalized matrix processes and representations of general block tridiagonal matrices
[DE94-628377] p 2031 N95-24704

Natural elementary factorization of general block-tridiagonal matrices in case of zero minors of both types
[DE94-628378] p 2031 N95-24705

Present experimental data on cross channel deep-inelastic processes and the Gribov-Lipatov relation
[DE94-628605] p 2049 N95-24719

Realistic NN potential for the Low approach
[DE94-628606] p 2049 N95-24720

On the Compton non-Abelian twist-3 asymmetry
[DE94-628586] p 2095 N95-24727

Multidimensional data analysis on the basis of integral nonparametric statistics and multilayer perceptrons
[DE94-628375] p 2035 N95-24858

On the structure of direct representations of inverse matrices to the block-tridiagonal ones in case of zero main block angular minors
[DE94-628376] p 2031 N95-24859

Asymptotic properties of the oscillator poly spheroidal functions
[DE94-628441] p 2032 N95-24860

On an expansion of the Fermi function
[DE94-628494] p 2035 N95-24883

Possible constraints on SUSY-model parameters from direct dark matter search
[DE94-628561] p 2109 N95-24885

On SUSY dark matter detection with spinless nuclei
[DE94-628562] p 2109 N95-24886

Notion of the inclusive spectra and cross sections of B-meson production in hadronic interactions of high energies
[DE94-628628] p 2049 N95-24887

Meson properties at finite temperature and density within Nambu-Jona-Lasinio model
[DE94-628630] p 2049 N95-24888

Search for the prompt muon antineutrino from charm particle decays at the IHEP-JINR Neutrino detector in 70 GeV proton beam-dump experiment
[DE94-628772] p 2049 N95-24889

Mesic molecules of light nuclei in the oscillator representation
[DE94-628904] p 2050 N95-24890
High-energy ionoluminescence of LiF
[DE94-629015] p 2087 N95-24891
The existence of antiparticles seems to forbid violations of statistics
[DE94-628523] p 2050 N95-25094
Inelastic collisions of negative muons and hadrons with Helium metastable atoms
[DE95-607538] p 2055 N95-25493
Multichannel resonances and closed channels (scalar sector)
[DE94-628629] p 2055 N95-25537
Study of properties of Ne - Al neutron rich isotopes at and near N = 20 magic shell using elastic scattering in inverse kinematics
[DE94-628655] p 2055 N95-25538
Variational method for the calculation of the surface hyperspherical functions for the systems of ZH(mu)-type. The test calculation of the dt(mu)-system
[DE94-628905] p 2033 N95-25539
Anisotropy of dilepton emission from nuclear collisions
[DE95-004354] p 2070 N95-25634
Inelastic collisions of negative muons and hadrons with metastable hydrogen atoms
[DE95-607537] p 2056 N95-25668
Dynamics of nonadiabatic charged particles in the magnetic dipole field with imposed homogeneous magnetic field
[DE95-605222] p 2057 N95-25778
Wormhole on the Lobachevsky background
[DE95-605251] p 2099 N95-25780
Constraints, complex structures and quantization
[DE95-605252] p 2037 N95-25781
Ellipsoidal basis for isotropic oscillator
[DE95-605253] p 2034 N95-25782
Quantization of a Hamiltonian system with an infinite number of degrees of freedom
[DE95-605279] p 2034 N95-25783
Existence domains and some properties of a particle bound state in fields with homogeneous dependence of its potential energy on coordinates
[DE95-605280] p 2057 N95-25784
Accurate determination of IC modulation parameter in Sr(x)Ba(1-x)Nb2O6 from second order satellites of neutron diffraction TOF (Time-Of-Flight) spectra
[DE94-629003] p 2090 N95-25851
The track system of the modernized Hyperon spectrometer
[DE95-604003] p 2058 N95-25905
On the numerical method for analysis of the dynamics of the classical Hamiltonian systems
[DE95-605218] p 2034 N95-25906
The use of DBMS and document oriented interface in the TPLAN-system
[DE95-605219] p 2106 N95-25907
Mass splitting of the pseudoscalar and vector mesons induced by the homogeneous vacuum gluon field
[DE95-605322] p 2058 N95-25908
Excited states of mesons within the NJL model with the homogeneous vacuum gluon field
[DE95-605323] p 2058 N95-25909
Vacuum polarization effects in low-energy muonic atom collisions
[DE95-605393] p 2058 N95-25910
On a new type of long-range forces
[DE95-605286] p 2063 N95-25965
On fractal structure of quantum gravity and relic radiation anisotropy
[DE95-605306] p 2099 N95-25966
Exact solution of 2 D Poincare gravity coupled with fermion matter
[DE95-605314] p 2099 N95-25967
On a possible explanation of the origin of the quark mass spectrum
[DE95-605315] p 2063 N95-25968

JOINT PUBLICATIONS RESEARCH SERVICE, ARLINGTON, VA.
JPRS report: Science and technology. Central Eurasia
[JPRS-UST-95-013] p 1987 N95-24538
JPRS report: Science and technology. Central Eurasia
[JPRS-UST-95-010] p 1953 N95-24539
JPRS report: Science and technology. Central Eurasia
[JPRS-UST-95-012] p 1950 N95-24540
JPRS report: Science and technology. Central Eurasia
[JPRS-UST-95-011] p 1910 N95-24541
JPRS report: Science and technology. Central Eurasia: Space
[JPRS-USP-94-008] p 1916 N95-24847

JOINT PUBLICATIONS RESEARCH SERVICE, WASHINGTON, DC.
JPRS report: Science and technology. Central Eurasia: Space
[JPRS-USP-94-007] p 1915 N95-24358
JPRS report: Science and technology. Central Eurasia: Space
[JPRS-USP-94-008] p 1916 N95-24359
JPRS report: Science and technology. Central Eurasia
[JPRS-UST-94-035] p 2016 N95-24429
JPRS report: Science and technology. Central Eurasia
[JPRS-UST-95-009] p 1916 N95-24467
JPRS report: Science and technology. Central Eurasia
[JPRS-UST-95-008] p 1957 N95-24468
JPRS report: Science and technology. Central Eurasia
[JPRS-UST-94-030] p 1962 N95-24469
JPRS report: Science and technology. Central Eurasia
[JPRS-UST-94-027] p 1957 N95-24470
JPRS report: Science and technology. Central Eurasia: Institute of General and Nuclear Physics: 1993 Status and Prospects
[JPRS-UST-94-025] p 2045 N95-24471
JPRS report: Science and technology. Central Eurasia
[JPRS-UST-94-018] p 1950 N95-24472
JPRS report: Science and technology. Central Eurasia
[JPRS-UST-94-024] p 1958 N95-24620
JPRS Report: Science and technology. Central Eurasia
[JPRS-UST-95-002] p 1916 N95-24621
JPRS report: Science and technology. Central Eurasia
[JPRS-UST-94-034] p 1987 N95-24729
JPRS report: Science and technology. Central Eurasia
[JPRS-UST-95-003] p 1988 N95-24730
JPRS report: Science and technology. Central Eurasia
[JPRS-UST-95-006] p 1950 N95-24731
JPRS report: Science and technology. Central Eurasia
[JPRS-UST-94-033] p 2037 N95-24732
JPRS Report: Science and technology. Central Eurasia
[JPRS-UST-94-032] p 1950 N95-24759
JPRS Report: Science and technology. Central Eurasia
[JPRS-UST-94-031] p 1988 N95-24760
JPRS report: Science and technology. Central Eurasia: Seminar on materials science
[JPRS-UST-95-007] p 1920 N95-24761
JPRS report: Science and technology. Central Eurasia. Otechestvennaya Geologiya: Studies in Aerospace and Remote Sensing
[JPRS-UST-95-004] p 1989 N95-24768
JPRS report: Science and technology. Central Eurasia
[JPRS-UST-95-018] p 2071 N95-26079
JPRS report: Science and technology. Central Eurasia
[JPRS-UST-95-017] p 1988 N95-26080

K

KAUPPA-JA TEOLLISUUSMINISTERIO, HELSINKI, UUDENMAA (FINLAND).
JALO: Fuel conversion
[DE95-737597] p 1949 N95-25244

KINGS COLL., LONDON (ENGLAND).
A covariant canonical description of Liouville field theory
[DE95-607094] p 2098 N95-25534
Alpha(sub critical) for parallel processors
[PB95-165320] p 2022 N95-25625
The space of solutions of Toda field theory
[DE95-607095] p 2099 N95-25650

KOREA INST. OF ENERGY AND RESOURCES, TAEJON, CHUNGCHONGNAM (REPUBLIC OF KOREA).
Study on the production of alternative fuels by carbon dioxide hydrogenation
[DE95-744284] p 1948 N95-24498
Investigation of technologies for CO2 separation, fixation and disposal for the prevention of global warming
[DE95-744285] p 1997 N95-24499

KYOTO UNIV. (JAPAN).
Activities of the Radiation Laboratory Department of Nuclear Engineering Kyoto University
[DE95-709896] p 2072 N95-26163
Activities of the Radiation Laboratory Department of Nuclear Engineering Faculty of Engineering, Kyoto University
[DE95-709897] p 2072 N95-26164

KYOTO UNIV., UJI (JAPAN).
Quasi two body decays of charm mesons
[DE94-792634] p 2057 N95-25901

L

LAWRENCE LIVERMORE NATIONAL LAB., LIVERMORE, CA.
Characterization of ultradispersed aluminum
[DE95-006379] p 1933 N95-24329
UEDGE and DEGAS modeling of the DIII-D scrape-off layer plasma
[DE95-003652] p 2076 N95-24490
Flow-through Z-pinch study for radiation generation and fusion energy production
[DE95-004209] p 2076 N95-24544
The physics design of the Tokamak Physics Experiment
[DE95-003649] p 2076 N95-24548
Toward improved photon-atom scattering predictions
[DE95-003651] p 2046 N95-24549
Optimized hydrogen piston engines
[DE95-003656] p 1975 N95-24550
Divertor design for the Tokamak Physics Experiment
[DE95-003653] p 2078 N95-24650
Target injection methods for inertial fusion energy
[DE95-003654] p 2067 N95-24651
Characteristics of an ultrafast x-ray streak camera
[DE95-004210] p 1968 N95-24657
Debugging the virtual machine
[DE95-002193] p 2016 N95-24898
Na-like autoionizing levels: Plasma diagnostics and prospects for photopumped soft x-ray lasers
[DE95-004207] p 1972 N95-25100
Global ocean circulation and equator-pole heat transport as a function of ocean GCM resolution
[DE95-004198] p 2000 N95-25279
Impacts of microphysics, radiation and environmental winds in mid-latitude and tropical squall-line systems, and their climatic implications
[DE95-004965] p 2005 N95-25287
A higher-order projection method for the simulation of unsteady turbulent nonpremixed combustion in an industrial burner
[DE95-005919] p 1931 N95-25291
Using and programming the SUPERCODE
[DE95-004342] p 2080 N95-25344
A numerical prediction of the precipitation and hydrology of California
[DE95-004966] p 2006 N95-25635
Viscoelastic waves and multiple scales
[DE94-014130] p 1966 N95-26063
Electronic structure of (La,Sr)2CuO4 and Ba(0.6)K(0.4)BiO3
[DE95-004963] p 2091 N95-26170

LEGACY GOOD SAMARITAN HOSPITAL, PORTLAND, OR.
Relation of motion sickness susceptibility to vestibular and behavioral measures of orientation
[NASA-CR-198048] p 2010 N95-24410

LEHIGH UNIV., BETHLEHEM, PA.
Robotic weld overlay coatings for erosion control
[DE95-005187] p 1939 N95-24285
High octane ethers from synthesis gas-derived alcohols
[DE95-001146] p 1948 N95-24655

LINKOEPING UNIV. (SWEDEN).
Inversion of circular averages and application of backprojection methods to radar imaging
[PB95-141578] p 1955 N95-25891
Heuristic approach to the path planning problem in a raster map
[PB95-141826] p 2034 N95-25893
Aspect estimation of an aircraft using library model silhouettes
[PB95-141834] p 2036 N95-25894

LITTLE (ARTHUR D.), INC., CAMBRIDGE, MA.
Cross-flow, filter-sorbent-catalyst for particulate, SO2 and NO(x) control
[DE95-001934] p 2003 N95-26091

LOCKHEED CORP., CALABASAS, CA.
Commercial Space Transportation Study (CSTS)
[SSD94D0035] p 1919 N95-25747

LOCKHEED ENGINEERING AND MANAGEMENT SERVICES CO., INC., HOUSTON, TX.
STS-60 Space Shuttle mission report
[NASA-CR-197233] p 1919 N95-26189

LOCKHEED ENGINEERING AND SCIENCES CO., HAMPTON, VA.
A generic interface element for COMET-AR
[NASA-CR-195075] p 1983 N95-26199

LOCKHEED ENVIRONMENTAL SYSTEMS AND TECHNOLOGIES CO., LAS VEGAS, NV.
Parts washing alternatives study: United States Coast Guard. Project summary and report
[PB95-166146] p 1942 N95-26004

LOCKHEED MISSILES AND SPACE CO., PALO ALTO, CA.
Predictability in space launch vehicle anomaly detection using intelligent neuro-fuzzy systems
p 2025 N95-25266

LOS ALAMOS NATIONAL LAB., NM.
The temperature and strain rate dependence of the flow stress of single crystal NiAl deformed along the zone group axes (110)
[DE95-003634] p 2083 N95-24233
Resolution of the classical Hyades lithium problem
[DE95-003661] p 2109 N95-24234

Theoretical motivation for gravitation experiments on ultra-low energy antiprotons and antihydrogen
[DE95-003662] p 2091 N95-24235
Lawrence Livermore pulsed sphere benchmark analysis of MCNP(trademark) ENDF/B-VI
[DE95-004864] p 2041 N95-24258
Self-consistent beam halo studies & halo diagnostic development in a continuous linear focusing channel
[DE95-003706] p 2065 N95-24331
A parallel, portable and versatile treecode
[DE95-000842] p 2019 N95-24343
The influence of CDM on the dynamical estimate of (Omega) in the local neighborhood
[DE95-005212] p 2109 N95-24455
Characterization and performance of carbon films deposited by plasma and ion beam based techniques
[DE95-005213] p 1940 N95-24456
Complex scattering dynamics and the quantum Hall effect
[DE95-005239] p 2093 N95-24457
Interim report of the advisory committee on human radiation experiments
[DE95-003265] p 2011 N95-24497
Theoretical and experimental studies on the C15 intermetallic compound NbCr2
[DE95-003665] p 2086 N95-24513
Thin film ionic conductors based on cerium oxide
[DE95-003668] p 2086 N95-24514
Experimental and theoretical development towards a 500 MW, one-microsecond, L-band relativistic klystron amplifier
[DE95-003682] p 1958 N95-24589
Composite ductility: The role of reinforcement and matrix
[DE95-003664] p 1925 N95-24590
Solution based synthesis of perovskite-type oxide films and powders
[DE95-006170] p 2086 N95-24594
Correlations for the NO A(sup 2)(Sigma)(+) electronic quenching cross-section
[DE95-006195] p 2047 N95-24595
Staurosporine analysis and its pharmacokinetics in the blood of rats
[DE94-013857] p 2008 N95-24600
The geometry of weak solutions of certain integrable nonlinar PDE's
[DE95-005241] p 2030 N95-24609
Chiral limit of QCD
[DE95-005245] p 2094 N95-24610
A practical approach to portability and performance problems on massively parallel supercomputers
[DE95-005251] p 2020 N95-24612
Hydrodynamic instabilities in inertial confinement fusion
[DE95-003663] p 2078 N95-24667
Explosive performance measurements on large, multiple-hole arrays and large masses of conventional explosive
[DE95-002718] p 1948 N95-24670
An overview of the Nuclear Electric Propulsion Space Test Program (NEPSTP) satellite
[DE94-013121] p 1920 N95-24711
Parallel processing of atmospheric chemistry calculations: Preliminary considerations
[DE95-005915] p 1999 N95-25198
Evolution of plastic anisotropy for high-strain-rate computations
[DE95-004220] p 1941 N95-25237
Magnetized target fusion: An ultra high energy approach in an unexplored parameter space
[DE95-005252] p 2080 N95-25289
Statistical mechanics of nonlinear coherent structures: Kinks in the Phi(sup 6) model
[DE95-005253] p 2096 N95-25293
Neutral current neutrino-nucleon scattering
[DE95-005027] p 2069 N95-25366
Ion beam mixing of titanium overlayers with hydroxyapatite substrates
[DE95-005278] p 1935 N95-25379
Development of a portable mass spectrometric system for determination of isotopic composition of solid uranium samples using fluorine volatilization
[DE95-005728] p 1969 N95-25384
Radial electron-beam-breakup transit-time oscillator
[DE95-005731] p 1959 N95-25385
Thermochemistry, kinetics and spectroscopy of Kr and Kr2F
[DE95-005732] p 1941 N95-25386
Designing a stencil compiler for the Connection Machine model CM-5
[DE95-006861] p 2021 N95-25477
The NJOY nuclear data processing system: Version 91
[DE95-006764] p 2055 N95-25484
Targets for laser-driven opacity measurements
[DE95-006172] p 1973 N95-25557
An FEL design code running on Mathcad(trademark)
[DE95-005279] p 1973 N95-25565
Magnetized target fusion: An overview of the concept
[DE95-005247] p 2070 N95-25594
Issues related to prediction of residual stresses in titanium alloy matrix composites
[DE95-005243] p 1926 N95-25596
Selective extraction of trivalent actinides from lanthanides with dithiophosphinic acids and tributylphosphate
[DE95-005249] p 1924 N95-25597
Temperature-dependent growth of LaAlO3 films on YBa2CuO7 C-axis films for multilayer structures
[DE95-005257] p 2089 N95-25598
Milagro: A low energy threshold extensive air shower array
[DE95-005246] p 2110 N95-25675
Nonlinear difference approximations for evolutionary PDE's
[DE95-005260] p 2033 N95-25676
Rich cluster simulation: Dynamics and mass estimates
[DE95-005233] p 2110 N95-25766
The hard truth
[DE95-005240] p 2033 N95-25767
Atomistic studies of grain boundaries in NiAl
[DE95-005208] p 1937 N95-26014
Converting multiple OC-3c ATM streams to HIPPI to drive an HDTV frame buffer from a workstation cluster
[DE95-003638] p 2022 N95-26066
Time-dependent numerical simulation of vertical cavity lasers
[DE95-006862] p 1973 N95-26112

LOVELACE BIOMEDICAL AND ENVIRONMENTAL RESEARCH INST., ALBUQUERQUE, NM.
Evaluation of the performance of an annular diffusion denuder
[DE95-002258] p 1998 N95-24606

LOYOLA COLL., BALTIMORE, MD.
Display technologies in Russia, Ukraine, and Belarus
[ISBN-1-883712-36-X] p 2085 N95-24460

LUND UNIV. (SWEDEN).
Towards an era of global village: The dynamics of world telecommunications and its implications for the future of nation state
[PB95-165064] p 1954 N95-25482

LUNDS LASARETT (SWEDEN).
Motionsickness-seasickness: Summary of existing knowledge and suggested lines of development
[PB95-141495] p 2011 N95-24863

M

M-C POWER CORP., BURR RIDGE, IL.
Intermediate-sized natural gas fueled carbonate fuel cell power plants
[DE95-004990] p 1996 N95-26171

MAINZ UNIV. (GERMANY).
Heavy-neutrino chirality enhancement of the decay K(L) yields e(mu) in left-right symmetric models
[PB95-165387] p 2064 N95-26096

MARTIN MARIETTA CORP., BETHESDA, MD.
Commercial Space Transportation Study (CSTS)
[SSD94D0035] p 1919 N95-25747

MARTIN MARIETTA CORP., DENVER, CO.
Photonics: From target recognition to lesion detection
p 2023 N95-25259

MARYLAND UNIV., COLLEGE PARK, MD.
A report: A plan to establish Internet access points at Minority Campus sites for connection to a central computing facility
[DE95-004374] p 2105 N95-25240
Strengthening of NiAl matrix composites
[AD-A288923] p 1926 N95-25505
Maryland controlled fusion research program
[DE95-006642] p 2081 N95-25561
Theoretical studies in hadronic and nuclear physics
[DE95-006643] p 2098 N95-25562

MASSACHUSETTS GENERAL HOSPITAL, BOSTON, MA.
On the uncertainty in single molecule fluorescent lifetime and energy emission measurements
[NASA-CR-198009] p 2049 N95-24877

MASSACHUSETTS INST. OF TECH., CAMBRIDGE, MA.
Direct catalytic decomposition of nitric oxide
[DE95-005202] p 1928 N95-24286
Genetic and biophysical studies of the photosynthetic reaction center
[DE95-004179] p 2008 N95-24850
The dependence of human reliability upon task information content
[DE95-006645] p 2014 N95-25483
Numerical and symbolic algorithms for application specific signal processing
[AD-A288202] p 2017 N95-25507

MASSACHUSETTS UNIV., AMHERST, MA.
Discrete-event-dynamic-system-based approaches for control in integrated voice/data multihop Radio Networks
[AD-A288389] p 1954 N95-25604

MATERIALS TECHNOLOGIES OF VIRGINIA, BLACKSBURG, VA.
Whisker reinforced glass ceramic
[DE95-005568] p 1927 N95-25998

MCDONNELL-DOUGLAS AEROSPACE, LONG BEACH, CA.
Advanced subsonic airplane design and economic studies
[NASA-CR-195443] p 1913 N95-24304
Noise impact of advanced high lift systems
[NASA-CR-195028] p 2040 N95-26160

MCDONNELL-DOUGLAS AEROSPACE, SAINT LOUIS, MO.
A neural network controller for automated composite manufacturing p 2025 N95-25271

MCDONNELL-DOUGLAS AEROSPACE, SEABROOK, MD.
Small spacecraft power and thermal subsystems
[NASA-CR-195029] p 1921 N95-24216
Small spacecraft power and thermal subsystems
[NASA-CR-195029] p 1921 N95-24428

MCDONNELL-DOUGLAS CORP., SAINT LOUIS, MO.
Predictability in space launch vehicle anomaly detection using intelligent neuro-fuzzy systems
p 2025 N95-25266
Commercial Space Transportation Study (CSTS)
[SSD94D0035] p 1919 N95-25747

MCDONNELL-DOUGLAS SPACE SYSTEMS CO., COCOA BEACH, FL.
Study of launch site processing and facilities for future launch vehicles
[NASA-CR-198025] p 1918 N95-24579

MECHANICAL ENGINEERING LAB., SAKURA (JAPAN).
Long endurance stratospheric solar powered airship
[PB95-178729] p 1911 N95-26009

MELBOURNE UNIV., PARKVILLE (AUSTRALIA).
Can we test the many-Hilbert-space approach to quantum mechanics?
[DE95-607021] p 2097 N95-25429
On the effects of gravitational fields on the electrical properties of matter
[DE95-607022] p 2038 N95-25430
A partial unification model in non-commutative geometry
[DE95-607129] p 2097 N95-25435
Observation of the scalar Aharonov-Bohm effect by neutron interferometry
[DE95-607020] p 2097 N95-25446
Monte Carlo simulations with indefinite and complex-valued measures
[DE95-607056] p 2017 N95-25448
Staggered magnetization in the Heisenberg antiferromagnet
[DE95-607102] p 2038 N95-25458
Study of the simplest realistic Higgs sector in quark-lepton symmetric models
[DE95-607159] p 2053 N95-25461
Anomalous WWZ couplings and K(sub L) yields mu(+) mu(-)
[DE95-607190] p 2054 N95-25464
Can the electric charges of elementary particles change with time?
[DE95-607194] p 2054 N95-25465
Matrix element and complex l-plane evaluation of two-loop vacuum amplitudes in QED on S4
[DE95-607099] p 2097 N95-25473
Statistical mechanics of relativistic spin-1 bosons in a magnetic field
[DE95-607100] p 2054 N95-25474
The Hamiltonian of SU(2) lattice gauge theory in approximate tri-diagonal form
[DE95-607101] p 2098 N95-25475
Ten dimensional SO(10) G.U.T. models with dynamical symmetry breaking
[DE95-607093] p 2098 N95-25533
Statistical mechanics of magnetized pair Fermi gas
[DE95-607097] p 2063 N95-25969
A new formulation of quantum field theory on S4
[DE95-607098] p 2099 N95-25970
Two dimensional Bose plasma in a magnetic field
[DE95-607629] p 2082 N95-25976
Application of extended-crystal diffraction techniques to the symmetry and structure analysis of 221-PbBiSrCaCuO
[DE95-605913] p 2090 N95-25984
Pulsed laser annealing of P implanted diamond
[DE95-605947] p 2090 N95-25985
Statistical mechanics of the magnetized pair Bose gas
[DE95-607096] p 2063 N95-25993
Magnetized pair Bose gas: Relativistic superconductor
[DE95-607846] p 2100 N95-26104

Conductivity in insulators due to implantation of conducting species
[DE95-007773] p 1932 N95-26261
MICHIGAN STATE UNIV., EAST LANSING, MI.
Stratified charge rotary engine combustion studies
[NASA-CR-197985] p 1974 N95-24223
Stability and elastic properties of hydrogen loaded Ti(1-x)Al(x) alloys: An ab initio study
[AD-A288903] p 1936 N95-25529
MICHIGAN UNIV., ANN ARBOR, MI.
Accelerator physics R and D
[DE95-003624] p 2046 N95-24547
Instructable autonomous agents
[NASA-CR-197802] p 2019 N95-26206
MISSOURI UNIV., ROLLA, MO.
Processing of LaCrO3 for solid oxide fuel cell applications
[DE95-000024] p 1992 N95-24683
MITSUBISHI RESEARCH INST., INC., TOKYO (JAPAN).
Preparatory research for global warming precaution spread promotion manual and early spread plan research work
[DE95-730143] p 1996 N95-24291
MONTANA STATE UNIV., BOZEMAN, MT.
NMR and optical studies of piezoelectric polymers
[DE95-003836] p 1940 N95-24554
MOORE (THOMAS C., SR.), POQUOSON, VA.
Compensated high temperature strain gage
[NASA-CASE-LAR-14776-1] p 1968 N95-24625
MORGAN STATE UNIV., BALTIMORE, MD.
A report: A plan to establish Internet access points at Minority Campus sites for connection to a central computing facility
[DE95-004374] p 2105 N95-25240
MORGANTOWN TECHNOLOGY CENTER, WV.
Intermediate-sized natural gas fueled carbonate fuel cell power plants
[DE95-004990] p 1996 N95-26171
MVA, INC., NORCROSS, GA.
Transmission electron microscope studies of extraterrestrial materials
[NASA-CR-188363] p 1928 N95-24222

N

NASA CENTER FOR AEROSPACE INFORMATION, LINTHICUM HEIGHTS, MD.
Machine-aided indexing at NASA
[NASA-CR-197796] p 2106 N95-25410
NATIONAL AERONAUTICS AND SPACE ADMINISTRATION, WASHINGTON, DC.
NASA video catalog
[NASA-SP-7109(01)] p 2103 N95-24238
The atmospheric effects of stratospheric aircraft: A fourth program report
[NASA-RP-1359] p 1996 N95-24274
Aerospace medicine and biology: A continuing bibliography with indexes (supplement 400)
[NASA-SP-7011(400)] p 2011 N95-24464
Aeronautical engineering: A continuing bibliography with indexes (supplement 316)
[NASA-SP-7037(316)] p 1905 N95-24465
Report of the Space Shuttle Management Independent Review Team
[NASA-TM-110579] p 1919 N95-24466
Aerospace safety advisory panel
[NASA-TM-110554] p 1920 N95-24505
Issues in NASA program and project management
[NASA-SP-6101(08)] p 2102 N95-24565
Perspectives from space: NASA classroom information and activities
[NASA-TM-110577] p 2100 N95-25643
Aeronautical engineering: A continuing bibliography with indexes (supplement 317)
[NASA-SP-7037(317)] p 1906 N95-25798
Aerospace medicine and biology: A continuing bibliography with indexes (supplement 401)
[NASA-SP-7011(401)] p 2012 N95-25800
Continual improvement plan
[NASA-TM-110574] p 2103 N95-25849
Acquisition forecast: Fiscal year 1995
[NASA-TM-110575] p 2103 N95-25850
Office of Space Science: Integrated technology strategy
[NASA-TM-110578] p 2108 N95-26183
NASA strategic plan
[NASA-TM-110592] p 2103 N95-26262
NATIONAL AERONAUTICS AND SPACE ADMINISTRATION. AMES RESEARCH CENTER, MOFFETT FIELD, CA.
Laser velocimeter for near-surface measurements
[NASA-CASE-ARC-11917-1] p 1967 N95-24236
Geometric analysis of wing sections
[NASA-TM-110346] p 1910 N95-24629
Aerodynamic shape optimization of wing and wing-body configurations using control theory
[NASA-CR-198024] p 1911 N95-25334
Angular displacement measuring device
[NASA-CASE-ARC-11937-1] p 2074 N95-26015
Method for determining shear direction using liquid crystal coatings
[NASA-CASE-ARC-11995-1] p 2075 N95-26117
Aerodynamics model for a generic ASTOVL lift-fan aircraft
[NASA-TM-110347] p 1908 N95-26302
NATIONAL AERONAUTICS AND SPACE ADMINISTRATION. GODDARD SPACE FLIGHT CENTER, GREENBELT, MD.
Airborne imaging of tropospheric emission at millimeter and submillimeter wavelengths
[NASA-TM-110498] p 2003 N95-24336
EOS Directory
[NASA-TM-110580] p 1989 N95-24542
Technical report series on global modeling and data assimilation. Volume 5: Documentation of the AIRES/GEOS dynamical core, version 2
[NASA-TM-104606-VOL-5] p 2003 N95-24766
The Clementine Mission: Initial Results from lunar mapping
[NASA-TM-110555] p 2112 N95-24994
From superconductivity to supernovae: The Ginzburg symposium. Report on the symposium held in honor of Vitaly L. Ginzburg
[NASA-TM-110596] p 2108 N95-25746
Computer support for cooperative tasks in Mission Operations Centers
[DE95-004928] p 2102 N95-25771
Circuit for high resolution decoding of multi-anode microchannel array detectors
[NASA-CASE-GSC-13478-1] p 1960 N95-25889
High input impedance amplifier
[NASA-CASE-GSC-13571-1] p 1960 N95-26038
STEP: Satellite Test of the Equivalence Principle. Report on the phase A study
[NASA-TM-110598] p 1917 N95-26184
Intercomparison of hydrologic processes in global climate models
[NASA-TM-104617] p 2005 N95-26341
NATIONAL AERONAUTICS AND SPACE ADMINISTRATION. JOHN F. KENNEDY SPACE CENTER, COCOA BEACH, FL.
Metrology: Measurement assurance program guidelines
[NASA-RP-1364] p 1950 N95-24543
NATIONAL AERONAUTICS AND SPACE ADMINISTRATION. JOHN F. KENNEDY SPACE CENTER, LOMPOC, CA.
Debris/ice/TPS assessment and integrated photographic analysis of shuttle mission STS-63
[NASA-TM-110649] p 1921 N95-25337
NATIONAL AERONAUTICS AND SPACE ADMINISTRATION. LYNDON B. JOHNSON SPACE CENTER, HOUSTON, TX.
Go for EVA
[NASA-TM-110537] p 1918 N95-24195
Space basic
[NASA-TM-110540] p 2108 N95-24196
STS-66 mission highlights resource tape
[NASA-TM-110550] p 1918 N95-24197
STS-67 post flight presentation
[NASA-TM-110552] p 1918 N95-24198
Apollo 13: Houston, we've got a problem
[NASA-TM-110551] p 1918 N95-24215
Evaluation of restraint system concepts for the Japanese Experiment Module flight demonstration
[NASA-TM-104808] p 2013 N95-24627
Predictability in space launch vehicle anomaly detection using intelligent neuro-fuzzy systems
p 2025 N95-25266
Inflatable rescue device
[NASA-CASE-MSC-22244-1] p 2014 N95-25306
Apollo 12: Pinpoint for science
[NASA-TM-110576] p 1917 N95-25424
Preload release mechanism
[NASA-CASE-MSC-22327-1] p 1976 N95-25592
STS-63 mission highlights resource tape
[NASA-TM-110562] p 1919 N95-25874
A study of the radiation environment on board the space shuttle flight STS-57 p 2059 N95-25914
NATIONAL AERONAUTICS AND SPACE ADMINISTRATION. LANGLEY RESEARCH CENTER, HAMPTON, VA.
Integrated passive/active vibration absorber for multi-story buildings
[NASA-TM-109178] p 1979 N95-24208
Reducing neural network training time with parallel processing
[NASA-TM-110154] p 2015 N95-24209
Method for molding structural parts utilizing modified silicone rubber
[NASA-CASE-LAR-15217-1] p 1939 N95-24212
An optimized implementation of a fault-tolerant clock synchronization circuit
[NASA-TM-109176] p 2019 N95-24382
DSMC calculations for 70-deg blunted cone at 3.2 km/s in nitrogen
[NASA-TM-109181] p 1961 N95-24396
Performance of an aerodynamic yaw controller mounted on the space shuttle orbiter body flap at Mach 10
[NASA-TM-109179] p 1906 N95-24397
Integration of design, structural, thermal and optical analysis: And user's guide for structural-to-optical translator (PATCOD)
[NASA-TM-110153] p 1950 N95-24559
Efficient eigenvalue assignment by state and output feedback with applications for large space structures
[NASA-TM-110155] p 1920 N95-24581
A crew-centered flight deck design philosophy for High-Speed Civil Transport (HSCT) aircraft
[NASA-TM-109171] p 1910 N95-24582
A conservative staggered-grid Chebyshev multidomain method for compressible flows
[NASA-CR-195060] p 2030 N95-24632
Aviation system capacity improvements through technology
[NASA-TM-109165] p 1909 N95-24633
Shuttle to space station transfer of the materials exposure facility
[NASA-TM-110156] p 1919 N95-24765
A quality monitor and monitoring technique employing optically stimulated electron emission
[NASA-CASE-LAR-15063-1-CU] p 1978 N95-25304
Method and apparatus for non-destructive evaluation of composite materials with cloth surface impressions
[NASA-CASE-LAR-14535-1] p 1926 N95-25305
Internal performance characteristics of thrust-vectored axisymmetric ejector nozzles
[NASA-TM-4610] p 1907 N95-25338
Apparatus for consolidating a pre-impregnated, filament-reinforced polymeric prepreg material
[NASA-CASE-LAR-15173-1-CU] p 1926 N95-25546
HZE beam transport in multilayered materials
p 2060 N95-25922
Separation of crack extension modes in orthotropic delamination models
[NASA-TM-109180] p 1927 N95-26083
Method and apparatus for weaving curved material preforms
[NASA-CASE-LAR-14752-1] p 1943 N95-26118
Design and evaluation of a foam-filled hat-stiffened panel concept for aircraft primary structural applications
[NASA-TM-109175] p 1928 N95-26251
Thermomechanical postbuckling of multilayered composite panels with cutouts p 1984 N95-26267
NATIONAL AERONAUTICS AND SPACE ADMINISTRATION. LEWIS RESEARCH CENTER, CLEVELAND, OH.
The 1994 Fiber Optic Sensors for Aerospace Technology (FOSAT) Workshop
[NASA-CP-10166] p 1912 N95-24207
A preview of a modular surface light scattering instrument with autotracking optics
[NASA-TM-110495] p 2072 N95-24386
Crossflow mixing of noncircular jets
[NASA-TM-106865] p 1913 N95-24390
Investigation of convection and pressure treatment with splitting techniques
[NASA-TM-106868] p 1961 N95-24399
Stereo imaging velocimetry for microgravity applications
[NASA-TM-110494] p 1949 N95-24416
Au/Cr sputter coating for the protection of alumina during sliding at high temperatures
[NASA-TM-106853] p 1923 N95-24437
The method of space-time conservation element and solution element: Development of a new implicit solver
[NASA-TM-106897] p 2029 N95-24474
Laser light scattering, from an advanced technology development program to experiments in a reduced gravity environment
[NASA-TM-110496] p 1971 N95-24530
Use of advanced solar cells for commercial communication satellites
[NASA-TM-106879] p 1991 N95-24560
The effect of altitude conditions on the particle emissions of a J85-GE-5L turbojet engine
[NASA-TM-106669] p 1914 N95-24561
Assessment of avionics technology in European aerospace organizations
[NASA-CR-189201] p 1912 N95-24624
Facility for the evaluation of space communications and related systems
[NASA-TM-106904] p 1955 N95-25876

Controls concepts for next generation reuseable rocket engines
[NASA-TM-106902] p 1923 N95-25877
Electric field effects on a near-critical fluid in microgravity
[NASA-TM-106894] p 2099 N95-25878
Essentially nonoscillatory (ENO) reconstructions via extrapolation
[NASA-TM-106907] p 2018 N95-25879
Wear-resistant, self-lubricating surfaces of diamond coatings
[NASA-TM-106887] p 1924 N95-25961
Recent improvements to and validation of the one dimensional NASA wave rotor model
[NASA-TM-106913] p 1908 N95-25962
Liquid crystal point diffraction interferometer
[NASA-TM-106899] p 1970 N95-26073
Computerized design and generation of low-noise gears with localized bearing contact
[NASA-TM-106880] p 1977 N95-26074
A combined geometric approach for solving the Navier-Stokes equations on dynamic grids
[NASA-TM-106919] p 1908 N95-26075
Transmission diagnostic research at NASA Lewis Research Center
[NASA-TM-106901] p 1977 N95-26076
Numerical calculations of shock-wave/boundary-layer flow interactions
[NASA-TM-106694] p 1966 N95-26077
A fully associative, nonisothermal, nonlinear kinematic, unified viscoplastic model for titanium alloys
[NASA-TM-106926] p 1983 N95-26078
Thermal Barrier Coating Workshop
[NASA-CP-10170] p 1943 N95-26119
Thermal barrier coatings for aircraft engines: History and directions p 1943 N95-26121
Properties of plasma sprayed bond coats p 1946 N95-26135
Jet mixer noise suppressor using acoustic feedback
[NASA-CASE-LEW-15170-2] p 2040 N95-26187

NATIONAL AERONAUTICS AND SPACE ADMINISTRATION. MARSHALL SPACE FLIGHT CENTER, HUNTSVILLE, AL.

Fusion proteins as alternate crystallization paths to difficult structure problems
[NASA-TM-110497] p 2008 N95-24531
Simplified liquid oxygen propellant conditioning concepts
[NASA-TM-108482] p 1948 N95-24558
Dynamics Explorer 1, retarding ion mass spectrometer summary spectrograms-82/110 to 82/229 spin-time spectrograms for H(+), He(+), O(+), N(+), O(++), M/Z = 2, and molecular ions
[NASA-TM-108485] p 2003 N95-24763
Dynamics Explorer 1, retarding ion mass spectrometer summary spectrograms-82/230 to 82/265 spin-time spectrograms for H(+), He(+), O(+), N(+), O(++), M/Z = 2, and molecular ions
[NASA-TM-108486] p 2003 N95-24764
Suspension system for gimbal supported scanning payloads
[NASA-CASE-MFS-28817-1] p 1969 N95-25544
Rotary actuator
[NASA-CASE-MFS-28581-1] p 1936 N95-25545
Ternary gas plasma welding torch
[NASA-CASE-MFS-28857-1] p 1976 N95-25548
The corrosion protection of AISI(TM) 1010 steel by organic and inorganic zinc-rich primers
[NASA-TP-3545] p 1936 N95-25677
The natural space environment: Effects on spacecraft
[NASA-RP-1350] p 1921 N95-25875
Linear Energy Transfer (LET) spectra of cosmic radiation in low Earth orbit p 2061 N95-25926
Depth distribution of absorbed dose on the external surface of Cosmos 1887 biosatellite p 2061 N95-25927
Experimental and calculated LET distributions in the Cosmos-2044 biosatellite orbit p 2061 N95-25929
Cosmic ray LET spectra and doses on board Cosmos-2044 biosatellite p 2061 N95-25930
Space radiation dosimetry on US and Soviet manned missions p 2009 N95-25934
The spacelab scientific missions: A comprehensive bibliography of scientific publications
[NASA-TM-108487] p 2107 N95-26084

NATIONAL AERONAUTICS AND SPACE ADMINISTRATION. PASADENA OFFICE, CA.

Optically-switched submillimeter-wave oscillator and radiator having a switch-to-switch propagation delay
[NASA-CASE-NPO-18547-1-CU] p 1959 N95-25307
A satellite-tracking millimeter-wave reflector antenna system for mobile satellite-tracking
[NASA-CASE-NPO-18772-1-CU] p 1954 N95-25316
Alternate method for achieving temperature control in the -160 to +90 Celcius range
[NASA-CASE-NPO-18995-1-CU] p 1969 N95-25547
Continuous phase and amplitude holographic elements
[NASA-CASE-NPO-18791-1] p 1971 N95-26340

NATIONAL AEROSPACE LAB., TOKYO (JAPAN).

Study on tensile fatigue testing method of unidirectional fiber-resin matrix composites
[NAL-TR-1241] p 1926 N95-24989
Effect of film cooling/regenerative cooling on scramjet engine performances
[NAL-TR-1242] p 1914 N95-24990
Numerical and experimental study of drag characteristics of two-dimensional HLFC airfoils in high subsonic, high Reynolds number flow
[NAL-TR-1244T] p 1907 N95-24998
Development test of a liquid apogee engine for the ETS-4
[NAL-TR-1250] p 1922 N95-24999
Stress analysis of a crack in the residual stress field by welding and its application to the fatigue crack propagation
[NAL-TR-1248] p 1981 N95-25000
A study of three-dimensional interaction flow fields between swept shock waves and turbulent boundary layers. Flow structures and effects of bleed
[NAL-TR-1227] p 1983 N95-25001
Preliminary experiments of an optical fiber display
[NAL-TR-1257] p 2073 N95-25004
Flight reference display for powered-lift STOL aircraft
[NAL-TR-1251] p 1912 N95-25005
Low speed aerodynamic characteristics of delta wings with vortex flaps: 60 deg and 70 deg delta wings
[NAL-TR-1245] p 1907 N95-25105
Performance of solid lubricated ball bearings at high-temperatures in a vacuum
[NAL-TR-1243] p 1976 N95-25323
Thermoelastic equations for multi-layered cylindrical shell
[NAL-TR-1222] p 1982 N95-25661
Aerodynamic characteristics of the orbital reentry vehicle experimental probe fins in a supersonic flow
[NAL-TR-1232] p 1921 N95-25664
Performance evaluation of LE-7 high pressure pumps
[NAL-TR-1212T] p 1977 N95-25672
Improved lubrication performance of sputtered MoS2 film by surface treatments of Ti-alloy substrate
[NAL-TR-1213] p 1942 N95-25760
Measurements of longitudinal static aerodynamic coefficients by the cable mount system
[NAL-TR-1226] p 1908 N95-25761
Fundamental wind tunnel experiments on low-speed flutter of a tip-fin configuration wing
[NAL-TR-1228] p 1908 N95-25762
Video camera as a visual sensor, part 2
[NAL-TR-1231-PT-2] p 1970 N95-25763
Reentry guidance for hypersonic Flight Experiment (HYFLEX) vehicle
[NAL-TR-1235] p 1910 N95-25764
Combustion characteristics of metallized hydrocarbon fuels
[NAL-TR-1224] p 1949 N95-25769
Study on tensile fatigue testing method of unidirectional fiber-resin matrix composites
[NAL-TR-1241] p 1927 N95-25770
Stress analysis of a crack in the residual stress field by welding and its application to the fatigue crack propagation
[NAL-TR-1248] p 1983 N95-25796
Static and fatigue properties of pin-joint specimens of a AS-4/PEEK thermoplastic composite material
[NAL-TR-1214] p 1927 N95-25859
Nonlinear system analysis using slowly-varying complex frequency method
[NAL-TR-1217] p 2034 N95-25860
A quiet STOL Research Aircraft Development program
[NAL-TR-1223] p 1911 N95-25862

NATIONAL DEFENCE RESEARCH ESTABLISHMENT, LINKOEPING (SWEDEN).

Use of voronoi diagrams for qualitative matching
[PB95-165445] p 1988 N95-24240
ARMDAT: A brief description of a computerized test system for burst transmission
[PB95-165452] p 1951 N95-24241
Significance of varied thickness to damage tolerance of carbon fiber/epoxy laminates
[PB95-165460] p 1925 N95-24242
Interfacing a digital compass to a remote-controlled helicopter
[PB95-164927] p 1914 N95-24260
Research in the service of the Swedish National Defence
[PB95-141941] p 1989 N95-24444
Laser based methods for range, Doppler and vibration measurements
[PB95-141958] p 1952 N95-24445
Wave-propagation aspects on VHF-radar applications
[PB95-141818] p 1953 N95-24649
Annual report 1992/93, FOA 38. Radio systems and wave propagation
[PB95-141735] p 1953 N95-24835
Analysis of data from a radar warning receiver with the accent on association of sensor reports
[PB95-141768] p 1953 N95-24836
Analysis of waveforms for bistatic radar systems
[PB95-165098] p 1955 N95-25641
Experimental study of tapered slot elements
[PB95-165163] p 1955 N95-25644

NATIONAL DEFENCE RESEARCH ESTABLISHMENT, STOCKHOLM (SWEDEN).

Read out electronics for thermal detectors of bolometer type
[PB95-141842] p 1967 N95-24280
Detvag-90: An implementation of Vogler's method for calculation of multiple knife-edge diffraction
[PB95-141859] p 1951 N95-24281
Motionsickness-seasickness: Summary of existing knowledge and suggested lines of development
[PB95-141495] p 2011 N95-24863
Planning for the unknown: Coping with uncertainty
[PB95-165114] p 2102 N95-25642

NATIONAL GEOPHYSICAL DATA CENTER, BOULDER, CO.

Geomagnetic Polar Cap (PC) index, 1975-1993
[UAG-103] p 2004 N95-24897
Solar-geophysical data number 603, November 1994. Part 1: (Prompt reports). Data for October, September 1994, and late data
[PB95-166393] p 2113 N95-25576
Solar-geophysical data number 603, November 1994. Part 2: (Comprehensive reports). Data for May 1994 and miscellaneous
[PB95-166401] p 2113 N95-25577

NATIONAL INST. FOR FUSION SCIENCE, NAGOYA (JAPAN).

Measurement of profiles of the space potential in JIPP T-IIU Tokamak plasmas by slow poloidal and fast toroidal sweeps of a heavy ion beam
[NIFS-273] p 2081 N95-25651
New modular heliotron system compatible with closed helical divertor and good plasma confinement
[NIFS-279] p 2081 N95-25653
Self-sustained turbulence and L-mode confinement in toroidal plasmas 2
[NIFS-278] p 2082 N95-25759
New evaluation method of superconductor characteristics for realizing the Large Helical Device
[NIFS-297] p 2071 N95-25855
Report on the meeting on Chaotic Phenomena in Plasma
[DE94-792670] p 2082 N95-25904
A possibility of pi(-) Meson production by a low energy electron bunch and positive ion bunch
[NIFS-277] p 2071 N95-26029
High-beta discharges with neutral beam injection in CHS
[NIFS-280] p 2071 N95-26031
Impulsive Alfven coupling between the magnetosphere and ionosphere
[NIFS-276] p 2004 N95-26036
Characteristics of D(-3)He fueled FRC reactor: ARTEMIS-L
[NIFS-251] p 2072 N95-26110
Innovative energy production in fusion reactors
[NIFS-250] p 2072 N95-26111
Holograpy machine HORN-1 for computer-aided retrieve of virtual three-dimensional image
[NIFS-218] p 1971 N95-26182
Direct energy conversion of radiation energy in fusion reactor
[NIFS-254] p 2072 N95-26250
Isotope effect on confinement in DT plasmas
[NIFS-275] p 2083 N95-26326
Magnetic mirror effect as a trigger of collisionless magnetic reconnection
[NIFS-295] p 2083 N95-26337
A mechanism of collisionless magnetic reconnection
[NIFS-274] p 2083 N95-26339

NATIONAL INST. FOR RESEARCH IN INORGANIC MATERIALS, TSUKUBA (JAPAN).

Study of very high temperature technology, 2
[DE95-730105] p 2088 N95-24900
Study of copper perovskite
[DE95-730106] p 2088 N95-24988
Study of composite zirconium oxide
[DE95-730104] p 1926 N95-25111

NATIONAL INST. OF RADIOLOGICAL SCIENCES, CHIBA (JAPAN).

Annual report of National Institute of Radiological Sciences
[DE94-792664] p 2009 N95-25902
Activities of the National Institute of Radiological Sciences
[DE95-709916] p 2072 N95-26165

NATIONAL INST. OF STANDARDS AND TECHNOLOGY, GAITHERSBURG, MD.
Investigation into the flammability properties of honeycomb composites
[PB95-143293] p 1941 N95-25342
Measurement methods and standards for processing and application of thermal barrier coatings
p 1944 N95-26123

NATIONAL LAB. FOR HIGH ENERGY PHYSICS, TSUKUBA (JAPAN).
High-gradient experiment on X-band disk-loaded structures
[DE94-765446] p 1958 N95-24701
Current status and future prospect of space and time reversal symmetry violation on low energy neutron reactions
[DE94-765589] p 2048 N95-24702
Proceedings of workshop on Future in HEP Computing
[DE94-792684] p 2021 N95-25303
Proceedings of the Workshop on Dynamics and Structure of Disordered System
[DE94-792685] p 1931 N95-25356

NATIONAL RENEWABLE ENERGY LAB., GOLDEN, CO.
National Renewable Energy Laboratory Information Resources Catalogue. A collection of energy efficiency and renewable energy information resources
[DE94-011900] p 1990 N95-24305
Biologically produced succinic acid: A new route to chemical intermediates
[DE95-000257] p 2007 N95-24306
Clean fractionation of biomass
[DE95-000259] p 2007 N95-24307
Overview of solar detoxification activities in the United States
[DE95-000264] p 1997 N95-24319
Diesel fuel component contribution to engine emissions and performance
[DE95-000238] p 1998 N95-24604
Brayton-cycle solvent recovery heat pump. A technical brief
[DE94-000225] p 1991 N95-24666
Data preparation requirements for modeling wind turbines with ADAMS(R)
[DE95-000266] p 1992 N95-24684
Solar thermal electric hybridization issues
[DE95-000217] p 1992 N95-24714
Flux attenuation at NREL's High-Flux Solar Furnace
[DE95-000219] p 1993 N95-24715
Using digital filtering techniques as an aid in wind turbine data analysis
[DE94-011862] p 1993 N95-24853
NREL Photovoltaic Program FY 1994 bibliography
[DE95-000275] p 1993 N95-24865
TITLE: Environmental, health, and safety issues offuel cells in transportation. Volume 1: Phosphoricacid fuel-cell buses
[DE95-000289] p 1993 N95-24866
Development of a dedicated ethanol ultra-low emission vehicle (ULEV) system design
[DE95-004016] p 1975 N95-24880
NREL airfoil families for HAWTs
[DE95-000267] p 1994 N95-24882
Comparison of three methods for optical characterization of point-focus concentrators
[DE95-000282] p 1994 N95-25309
Renewable Energy Demonstration Project by the National Renewable Energy Laboratory and the General Services Administration
[DE95-000261] p 1995 N95-25995
Wind technology development: Large and small turbines
[DE95-000286] p 1995 N95-26090
Technical evaluation of a dual-junction same-band-gap amorphous silicon photovoltaic system at NREL
[DE95-000277] p 1996 N95-26285
Developing a standardized test procedure for hybrid vehicles: The challenge of the SAE HEV task force
[DE95-000280] p 1978 N95-26286

NATIONAL SPACE DEVELOPMENT AGENCY, TOKYO (JAPAN).
Development test of a liquid apogee engine for the ETS-4
[NAL-TR-1250] p 1922 N95-24999

NATIONAL TRANSPORTATION SAFETY BOARD, WASHINGTON, DC.
Aircraft accident report: Impact with blast fence upon landing rollout Action Air Charters flight 990 Piper PA-31-350, N990RA, Stratford, Connecticut,27 April 1994
[PB94-910410] p 1908 N95-24206

NATIVE AMERICAN SERVICES, HUNTSVILLE, AL.
NLS Flight Simulation Laboratory (FSL) documentation
[NASA-CR-196564] p 2104 N95-24439

NAVAL AIR WARFARE CENTER, CHINA LAKE, CA.
Missileborne Artificial Vision System (MAVIS)
p 2022 N95-25254

NAVAL AIR WEAPONS STATION, CHINA LAKE, CA.
Coso Monitoring Program, October 1992 through September 1993
[AD-A279147] p 1989 N95-24422

NAVAL AVIATION SYSTEMS TEAM, ARLINGTON, VA.
Mapping, charting and geodesy handbook
[AD-A286558] p 1989 N95-24502

NAVAL POSTGRADUATE SCHOOL, MONTEREY, CA.
Techniques for the investigation of wave turbulence in water wave data
[AD-A288392] p 2007 N95-25605

NAVAL RESEARCH LAB., WASHINGTON, DC.
Some aspects of the hot corrosion of thermal barrier coatings p 1946 N95-26137
Design documentation for the SINTRA preprocessor
[AD-A288804] p 2015 N95-26192

NAVAL SURFACE WARFARE CENTER, BETHESDA, MD.
Static recrystallization behavior of austenite in HSLA 100 during Thermomechanical Controlled Processing (TMCP)
[AD-A288737] p 1937 N95-26057

NAVAL SURFACE WARFARE CENTER, SILVER SPRING, MD.
In situ XAFS study of oxides formed on nickel thin film electrodes in KOH solution
[AD-A288735] p 1932 N95-26056

NEUROLOGICAL INST. OF NEW YORK, NEW YORK, NY.
Neural network classification of clinical neurophysiological data for acute care monitoring
p 2024 N95-25263

NEW ORLEANS UNIV., LA.
Continued computational evaluation of the feasibility of nitrating precursors to C12N12O12
[AD-A288369] p 1924 N95-25602

NORTH CAROLINA STATE UNIV., RALEIGH, NC.
Development of a model protection and dynamic response monitoring system for the national transonic facility
[NASA-CR-195041] p 1915 N95-24388

NORTH DAKOTA UNIV., GRAND FORKS, ND.
Preliminary analysis of University of North Dakota aircraft data from the FIRE Cirrus IFO-2
[NASA-CR-198038] p 2005 N95-24219

NORTHERN RESEARCH AND ENGINEERING CORP., WOBURN, MA.
Small gas turbine component evaluation study
[PB95-147542] p 1913 N95-24293

NYMA, INC., BROOK PARK, OH.
Broadband uniplanar microstrip to slot-line transitions
[NASA-CR-195448] p 1957 N95-24476
Thermomechanical fatigue behavior of three CFCC's
[NASA-CR-195441] p 1927 N95-25880

O

OAK RIDGE ASSOCIATED UNIVERSITIES, INC., TN.
Biological effectiveness of neutrons: Research needs
[DE95-004795] p 2051 N95-25373

OAK RIDGE NATIONAL LAB., TN.
Investigation of properties and performance of ceramic composite components
[DE95-004737] p 1939 N95-24247
DOLIB: Distributed Object Library
[DE95-004791] p 2019 N95-24250
Simple chemical assays for presence of S2F10 in decomposed SF6
[DE95-001423] p 1929 N95-24345
Neutron diffraction from HoNi2B2C, version 1
[DE95-005894] p 2085 N95-24431
Time dependent indentation testing at non-ambient temperatures utilizing the high temperature mechanical properties microprobe
[DE95-005895] p 1933 N95-24432
Synthesis of Ni3Al and NiAl intermetallics
[DE95-005897] p 1934 N95-24433
CD-ROM in the age of internet
[DE95-005067] p 2104 N95-24454
Spin correlations in percolating networks with fractal geometry
[DE95-001074] p 2037 N95-24479
Activities of the Ceramic Technology Project
[DE95-003394] p 1940 N95-24588
Bounds for departure from normality and the Frobenius norm of matrix eigenvalues
[DE95-006144] p 2030 N95-24592
Activities of the Solid State Division
[DE95-003900] p 2087 N95-24611
Localized corrosion and stress corrosion cracking characteristics of a low-aluminum-content iron-aluminum alloy
[DE95-003259] p 1934 N95-24647
Information management architecture for an integrated computing environment for the Environmental Restoration Program. Environmental Restoration Program, Volume 3: Interim technical architecture
[DE95-001386] p 2105 N95-24656
Bioprocessing in nonaqueous media: Critical needs and opportunities
[DE95-004878] p 2008 N95-24843
A high intensity slow positron facility for the Advanced Neutron Source
[DE94-014108] p 2050 N95-25099
A note on the total least squares problem for coplanar points
[DE95-004876] p 2032 N95-25251
Thermodynamic property evaluation and magnetic refrigeration cycle analysis for gadolinium gallium garnet
[DE95-005910] p 1951 N95-25367
Resolving the ambiguities: An industrial hygiene Indoor Air Quality (IAQ) symposium
[DE95-005391] p 2000 N95-25380
Processing and characterization of transformation-toughened ceramics with strength retention to elevated temperatures
[DE95-005758] p 1941 N95-25387
Oxidation of ion-implanted NiAl
[DE95-005899] p 1935 N95-25388
Formation of thallium based high temperature superconductors using aerosol flow reacted precursor powders
[DE95-005901] p 2089 N95-25389
Processing and properties of iridium alloys for space power applications
[DE95-005902] p 1935 N95-25390
Kinetic modeling of the atomic layer epitaxy window in group 4 semiconductor growth
[DE95-005903] p 2089 N95-25391
Superconductivity, magnetism and metal-insulator transitions in some ternary and pseudoternary 3d-, 4d- and 5d-metal oxides
[DE95-005904] p 2038 N95-25600
Atom probe field ion microscopy of Type 308 CRE stainless steel welds
[DE94-019161] p 1938 N95-26064
Raman study of damage processes in Si(+)-implanted GaAs
[DE95-005898] p 2091 N95-26087
Thermal conductivity of zirconia thermal barrier coatings p 1945 N95-26133

ODYSSEY RESEARCH ASSOCIATES, INC., ITHACA, NY.
Towards a formal semantics for Ada 9X
[NASA-CR-195037] p 2020 N95-24634

OFFICE NATIONAL D'ETUDES ET DE RECHERCHES AEROSPATIALES, CHATILLON (FRANCE).
Response to a localized impact loading of a composite multilayered rotational shell structure: Theory and numerical methods, volume 1
[ONERA-NT-1994-10-VOL-1] p 1979 N95-24282
Response to a localized impact loading of a composite multilayered rotational shell structure: Theory and numerical methods, volume 2
[ONERA-NT-1994-10-VOL-2] p 1980 N95-24283
Response to a localized impact loading of a composite multilayered rotational shell structure: Theory and numerical methods, Volume 3
[ONERA-NT-1994-10-VOL-3] p 1980 N95-24284

OFFICE OF NAVAL RESEARCH, ARLINGTON, VA.
Differential preamplifier and pre-emphasis network
[AD-A288780] p 1961 N95-26186

OHIO STATE UNIV., COLUMBUS, OH.
Grounding explanations in evolving, diagnostic situations
[NASA-CR-198027] p 2026 N95-25335

OKLAHOMA CITY AIR LOGISTICS CENTER, TINKER AFB, OK.
Proceedings of the 2d USAF Aging Aircraft Conference
[AD-A288217] p 1911 N95-25578

OLD DOMINION UNIV., NORFOLK, VA.
Numerical simulation of the nonlinear response of composite plates under combined thermal and acoustic loading
[NASA-CR-197426] p 1981 N95-24907
Hot-wire calibration in subsonic/transonic flow regimes
[NASA-CR-197725] p 1970 N95-25699

OREGON UNIV., EUGENE, OR.
Cryogenic helium gas convection research
[DE95-004372] p 1965 N95-25404

ORGANISATIE VOOR TOEGEPAST NATUURWETENSCHAPPELIJK ONDERZOEK, DELFT (NETHERLANDS).
Partial camera automation in a simulated Unmanned Air Vehicle
[AD-A288786] p 1913 N95-26190

OVERSET METHODS, INC., LOS ALTOS, CA.
Aerodynamic optimization studies on advanced architecture computers
[NASA-CR-198045] p 1906 N95-24379
The coupling of fluids, dynamics, and controls on advanced architecture computers
[NASA-CR-197727] p 2017 N95-25797
OXFORD UNIV., OXFORD (ENGLAND).
Cosmological constraints on perturbative supersymmetry breaking
[PB95-165361] p 2099 N95-25628

P

PACIFIC NORTHWEST LAB., RICHLAND, WA.
Simulation of diurnal thermal energy storage systems: Preliminary results
[DE95-005751] p 1991 N95-24369
Final report and recommendations of the ESnet Authentication Pilot Project
[DE95-005755] p 2103 N95-24370
Temperature and strain-rate effects on deformation mechanisms in irradiated stainless steel
[DE95-004941] p 1934 N95-24449
Supercritical carbon dioxide cleaning market assessment and commercialization/deployment plan
[DE94-017394] p 1998 N95-24653
Object-oriented parallel polygon rendering
[DE95-004909] p 2021 N95-24881
Processing and electrochemical properties of mixed conducting La(1-x)A(x)Co(1-y)Fe(y)O(3-delta) (A=Sr, Ca)
[DE95-004910] p 2088 N95-25002
Electrochemical organic destruction in support of Hanford tank waste pretreatment
[DE95-002854] p 1924 N95-25248
Use of mass spectrometric methods for field screening of VOC's
[DE95-004903] p 1999 N95-25249
A solubility model for amorphous silica in concentrated electrolytes
[DE95-004896] p 1931 N95-25252
Modeling of the simulated countercurrent moving-bed chromatographic reactor used for the oxidative coupling of methane
[DE95-004930] p 1924 N95-25286
Temperature and dose dependence of metal colloid production in alpha-irradiated CaF2
[DE95-004907] p 2088 N95-25288
Carbon taxes and India
[DE95-005401] p 2001 N95-25629
Multidimensional visualization and browsing for intelligence analysis
[DE95-004901] p 2106 N95-25774
Recent progress in shear punch testing
[DE95-005962] p 1937 N95-26007
Four-Dimensional Information Visualization and Analysis System
[DE95-004935] p 2022 N95-26013
Interaction mechanisms and biological effects of static magnetic fields
[DE95-004929] p 2009 N95-26169
PACIFIC-SIERRA RESEARCH CORP., ARLINGTON, VA.
Implementation of scene shadows in the Target Acquisition TDA (TARGAC)
[AD-A288760] p 1912 N95-26060
PENNSYLVANIA STATE UNIV., ERIE, PA.
Infrared spectroscopy of Jupiter and Saturn
[NASA-CR-198034] p 2111 N95-24239
PENNSYLVANIA STATE UNIV., UNIVERSITY PARK, PA.
Electrophoretic separation of cells and particles from rat pituitary
[NASA-CR-197975] p 2008 N95-24475
Development of a model of atmospheric oxygen variations to estimate terrestrial carbon storage and release
[NASA-CR-198002] p 2002 N95-25955
PENTASTAR ELECTRONICS, INC., HUNTSVILLE, AL.
Test plan/procedure for the DPHV system integration
[DE95-003414] p 1994 N95-25121
PITTSBURGH UNIV., PITTSBURGH, PA.
Singularly perturbed differential/algebraic equations
[AD-A288365] p 2033 N95-25601
POLISH ACADEMY OF SCIENCES, WARSAW (POLAND).
Electromagnetic waves and photoacoustic transformation in gyrotropic superlattices
p 2083 N95-24205
Dynamic analysis of truss members using longitudinal waves
[IFTR-35/1994] p 1981 N95-24996
The use of acoustic surface waves to analyze gases apparatus and experiments p 2039 N95-25115
Type P dispersive delay lines p 1959 N95-25116
The effect of multidirectional cyclical deformation on the evolution of the plasticity surface of 18G2A steel
[IFTR-25/1994] p 1935 N95-25117
An analysis of hypercritical states in elastic and inelastic systems
[IFTR-1/1994] p 2037 N95-25339
Selected problems of the interaction of electromagnetic waves and a turbulent plasma
[IFTR-9-1993] p 2080 N95-25340
Computer analysis of graphics for the requirements of computer-aided design systems
[IPPT-29-1992] p 2016 N95-25392
The diffraction of electromagnetic waves by screens placed at the boundaries of dielectric media
[IFTR-4/1994] p 1954 N95-25393
A description of the cyclical properties of an aluminum alloy based on complex stress state tests
[IFTR-29/1994] p 1936 N95-25638
The energy efficiency of passive solar heating systems
[IFTR-22/1994] p 1995 N95-25758
Magnetic flaw detection studies: Methods and Equipment
[IFTR-38/1994] p 1978 N95-25957
Friction on geological faults modelling and variational formulation of initial boundary value problems
[IFTR-31/1994] p 2004 N95-25958
The characteristics and design of an apparatus constructed by the Institute of Basic Problems of Technology to study relaxation phenomena in liquids at frequencies of 10-150 MHz
[IFTR-21/1994] p 1932 N95-25959
A study of the effect of voice pitch on the perception of synthetic Polish vowels
[IFTR-10/1994] p 1956 N95-26018
The effect of the impedance of the generator and intermediate circuits on the impedance of plasma as it applies to magnetron sputtering of thin films in a radio-frequency field
[IFTR-8-1994] p 2083 N95-26019
An analysis of the feasibility of using the Hsu-Nielsen calibration method in systems for measuring acoustic emission from partial discharges
[IFTR-20/1994] p 2040 N95-26071
Splines in two-dimensional problems
[IFTR-2/1993] p 2035 N95-26106
Dynamic methods for determining the material characteristics of saturated permeable media
[IFTR-17/1993] p 1932 N95-26107
The phenomenon of non-linearity accompanying the action of acoustic pressure on a Helmholtz resonator
[IFTR-19/1994] p 2040 N95-26108
The fundamentals of modelling heat and moisture processes in structures
[IFTR-15/1994] p 1951 N95-26109
Techniques for studying the mechanical properties of materials in complex stress states
[IFTR-34/1994] p 1983 N95-26178
An experimental determination of the plastic anisotropy of metal
[IFTR-33/1994] p 1938 N95-26179
Measurements of acoustic emission on a laser ceramic treatment line
[IFTR-28/1994] p 2040 N95-26180
Actuating signals in adaptive control systems
[IFTR-13/1994] p 2027 N95-26330
Automatic classification of Polish fricatives on the basis of optimization of the parameter space
[IFTR-9/1994] p 1956 N95-26331
The rotations of deformable bodies. Part 1: Geometry and Kinematics
[IFTR-7/1994] p 2039 N95-26332
Changes in the strength characteristics of 15HM boiler steel caused by initial plastic deformation under constant and monotonic loads
[IFTR-30/1994] p 1938 N95-26333
PRAIRIE VIEW AGRICULTURAL AND MECHANICAL COLL., TX.
A report: A plan to establish Internet access points at Minority Campus sites for connection to a central computing facility
[DE95-004374] p 2105 N95-25240
PRATT AND WHITNEY AIRCRAFT, EAST HARTFORD, CT.
Thermal barrier coating experience in the gas turbine engine p 1944 N95-26125
Process, properties and environmental response of plasma sprayed thermal barrier coatings
p 1945 N95-26132
Thermal barrier coating life modeling in aircraft gas turbine engines p 1947 N95-26140
PRATT AND WHITNEY AIRCRAFT, WEST PALM BEACH, FL.
A design perspective on thermal barrier coatings
p 1943 N95-26120

Jet engine applications for materials with nanometer-scale dimensions p 1945 N95-26131
PRECISION CASTPARTS CORP., PORTLAND, OR.
AMCC casting development, volume 2
[NASA-CR-197720] p 1938 N95-26068
PRIME TECHNOLOGY, INC., DAYTON, OH.
Aviation epidemiology data register
[AD-A279303] p 2010 N95-24423
PRINS MAURITS LAB. TNO, RIJSWIJK (NETHERLANDS).
Characterization of plastic bonded explosives by pyrolysis-gas chromatography and multivariate data analysis. Applications of the procedure
[AD-A288761] p 1949 N95-25517
Characterization of plastic bonded explosives by pyrolysis-gas chromatography and multivariate data analysis. Development of the procedure
[AD-A288787] p 1949 N95-25528
PROCUREMENT AUTOMATION INST., ARLINGTON, VA.
Automated Procurement System (APS): Project management plan (DS-03), version 1.2
[NASA-CR-196576] p 2102 N95-24442
PSI TECHNOLOGY CO., ANDOVER, MA.
Tunable diode lasers as continuous emission monitors for thermal waste treatment processes
[DE95-004381] p 1972 N95-25549
PUERTO RICO UNIV., MAYAGUEZ.
Enhancement of thickness uniformity of thin films grown by pulsed laser deposition
[NASA-CR-197791] p 1943 N95-26081
PURDUE UNIV., WEST LAFAYETTE, IN.
Supersonic quiet-tunnel development for laminar-turbulent transition research
[NASA-CR-198040] p 1915 N95-24302
Non-invasive detection of increased intracranial pressure using acoustical techniques
[AD-A279292] p 2010 N95-24309
Passive microwave algorithm development and evaluation
[NASA-CR-197915] p 2005 N95-24535
Thermal fracture mechanisms in ceramic thermal barrier coatings p 1946 N95-26138

Q

QAREL ASSOCIATES, NORTHAMPTON (ENGLAND).
Fifth European Symposium on Reliability of Electron Devices, Failure Physics and Analysis
[AD-A286614] p 1956 N95-24447
QUEENSLAND UNIV., SAINT LUCIA (AUSTRALIA).
Shock tunnel studies of scramjet phenomena 1993
[NASA-CR-195038] p 1964 N95-25394
Thrust measurements of a complete axisymmetric scramjet in an impulse facility p 1914 N95-25395
Scramjet thrust measurement in a shock tunnel
p 1914 N95-25396
Thrust measurement in a 2-D scramjet nozzle
p 1914 N95-25397
Scaling in a scramjet combustor p 1933 N95-25398
The Superorbital Expansion Tube concept, experiment and analysis p 1915 N95-25399
Balances for the measurement of multiple components of force in flows of a millisecond duration
p 1965 N95-25400

R

RADIAN CORP., RESEARCH TRIANGLE PARK, NC.
Nitrogen oxide emissions and their control from uninstalled aircraft engines in enclosed test cells: Joint report to Congress on the Environmental Protection Agency - Department of Transportation study
[PB95-166237] p 2002 N95-26005
RENSSELAER POLYTECHNIC INST., TROY, NY.
Kinetics of diffusional droplet growth in a liquid/liquid two-phase system
[NASA-CR-198050] p 1961 N95-24221
RESEARCH INST. FOR ADVANCED COMPUTER SCIENCE, MOFFETT FIELD, CA.
Performance issues for iterative solvers in device simulation
[NASA-CR-197952] p 2027 N95-24214
RESEARCH INST. OF NATIONAL DEFENCE, LINKOEPING (SWEDEN).
Clustering using winner-take-all units
[PB95-165403] p 2026 N95-25568
Implementation of wave propagation model for windows
[PB95-165742] p 2017 N95-25571
Geographical information systems and other tools for spatial information management
[PB95-165759] p 2106 N95-25572

Diode laser pumped solid state laser with 2 micrometer wavelength
[PB95-165270] p 1973 N95-25622
Multistatic radar: Synchronization and time reference system
[PB95-165288] p 1954 N95-25623
Orientation determination of aircraft using visual 3D matching and radar. Case study 2
[PB95-165791] p 1955 N95-25749

RESEARCH INST. OF NATIONAL DEFENCE, STOCKHOLM (SWEDEN).
Colour vision deficiencies: Matching and confusion of computer colours
[PB95-141925] p 2013 N95-24864
Measurement of blood nitrogen content after rapid compressions to assess the speed of nitrogen uptake during the compression phase of submarine escape. (Includes measurement of nitrogen concentration in blood following rapid compression to 5 bar)
[PB95-165726] p 2012 N95-25570

RICE UNIV., HOUSTON, TX.
A report: A plan to establish Internet access points at Minority Campus sites for connection to a central computing facility
[DE95-004374] p 2105 N95-25240

RIJKSINSTITUUT VOOR ZUIVERING AFVALWATER, LELYSTAD (NETHERLANDS).
Biological monitoring of national freshwaters, 1992
[PB95-166690] p 2002 N95-25745

RIKKYO UNIV., YOKOSUKA (JAPAN).
Proceedings of the International Seminar on the Chemistry of High Energy Atoms
[DE95-709895] p 2072 N95-26162

ROCHESTER UNIV., NY.
Dialogue transcription tools
[TN-94-1] p 2016 N95-24536

ROCKWELL INTERNATIONAL CORP., HUNTSVILLE, AL.
High frequency flow-structural interaction in dense subsonic fluids
[NASA-CR-4652] p 1906 N95-24217

ROCKWELL INTERNATIONAL CORP., PITTSBURGH, PA.
Commercial Space Transportation Study (CSTS)
[SSD94D0035] p 1919 N95-25747

ROSE MEDICAL CENTER, DENVER, CO.
Photonics: From target recognition to lesion detection p 2023 N95-25259

RUTHERFORD APPLETON LAB., CHILTON (ENGLAND).
Parton distributions for low Q2
[PB95-165213] p 2056 N95-25619
Diagrammatic many-body perturbation expansion for atoms and molecules
[PB95-165221] p 2056 N95-25620
Use of multiple fronts in Gaussian elimination
[PB95-165353] p 2033 N95-25627
Central Laser Facility. Annual report to the Laser Facility Committee
[PB95-160511] p 1973 N95-25640

RUTHERFORD APPLETON LAB., OXFORD (ENGLAND).
Further ways to distinguish single-lepton top quark signals from background at the Tevatron
[PB95-165395] p 2056 N95-25567
User guide for the Polaris powder diffractometer at ISIS. Version 2.1
[PB95-165767] p 2074 N95-25573
MuSR user guide
[PB95-165304] p 2056 N95-25624
Alpha(sub critical) for parallel processors
[PB95-165320] p 2022 N95-25625
Heavy-neutrino effects on tau-lepton decays
[PB95-165346] p 2056 N95-25626
Cosmological constraints on perturbative supersymmetry breaking
[PB95-165361] p 2099 N95-25628
HET mini-manual
[PB95-165338] p 2057 N95-25900
Searching for exotic mesons in e(+)e(-) annihilation at DA(phi)NE
[PB95-165379] p 2064 N95-26001
Heavy-neutrino chirality enhancement of the decay K(L) yields e(mu) in left-right symmetric models
[PB95-165387] p 2064 N95-26096

S

SALFORD UNIV. (ENGLAND).
Atmospheric and terrain effects on acoustic propagation
[AD-A288727] p 2039 N95-25503

SAN FRANCISCO UNIV., CA.
High LET, passive space radiation dosimetry and spectrometry
[NASA-CR-197694] p 2058 N95-25911
LET spectra measurements from the STS-35 CPDs p 2058 N95-25912
Summary of LET spectra and dose measurements on ten STS missions p 2058 N95-25913
USF/Russian dosimetry on STS-57 p 2059 N95-25915
Dosimetry on STS-42 with the RME APD p 2059 N95-25916
Multiplicities of secondaries in interactions of 1.8 GeV/nucleon Fe-56 nuclei with photoemulsion and the cascade evaporation model p 2059 N95-25917
Target fragments in collisions of 1.8 GeV/nucleon Fe-56 nuclei with photoemulsion nuclei, and the cascade-evaporation model p 2059 N95-25918
Dependence of the multiplicities of secondary particles on the impact parameter in collisions of high-energy neon and iron nuclei with photoemulsion nuclei p 2059 N95-25919
Multiplicities of secondaries in nuclear interactions, induced by Ne-20, Ar-40 and Fe-56 nuclei at 0.1-0.5 GeV/nucleon p 2060 N95-25920
Fragmentation cross sections of O-16 between 0.9 and 200 GeV/nucleon p 2060 N95-25921
Preliminary results of radiation measurements on EURECA p 2060 N95-25923
Fission foil detector calibrations with high energy protons p 2060 N95-25924
Proton calibration of low energy neutron detectors containing (6)LiF p 2060 N95-25925
Neutron influences and energy spectra in the Cosmos-2044 biosatellite orbit p 2061 N95-25928
Cosmic ray particles with different LET values under various thicknesses of shielding in low altitude orbits: Calculations and Cosmos-2044 measurements p 2062 N95-25931
Differential neutron energy spectra measured on spacecraft low Earth orbit p 2062 N95-25932
Radiobiological experiments with plant seeds aboard the biosatellite Cosmos 1887 p 2009 N95-25933

SANDIA LABS., LIVERMORE, CA.
User guide to the Burner Engineering Research Laboratory
[DE95-004191] p 1931 N95-25492

SANDIA NATIONAL LABS., ALBUQUERQUE, NM.
Implementation of a parallel algorithm for thermo-chemical nonequilibrium flow simulations
[DE95-004758] p 1961 N95-24262
Reduction in fiber damage thresholds due to static fatigue
[DE95-004778] p 1979 N95-24263
GaAsSb-based heterojunction tunnel diodes for tandem solar cell interconnects
[DE95-004779] p 1990 N95-24264
Optical generation of radio-frequency power
[DE95-005276] p 1951 N95-24289
Verification of computational aerodynamic predictions for complex hypersonic vehicles using the INCA(trademark) code
[DE95-004757] p 1906 N95-24308
Parallel algorithms for dynamically partitioning unstructured grids
[DE95-001616] p 2015 N95-24346
Laser beam characterization results for a high power CW Nd:YAG laser
[DE95-006319] p 1971 N95-24408
The role of force measurements in advanced vibration test methods
[DE95-001833] p 1975 N95-24462
High gain GaAs Photoconductive Semiconductor Switches (PCSS): Device lifetime, high current testing, optical pulse generators
[DE95-003354] p 1957 N95-24488
Solutions of turbulent backward-facing step flow with heat transfer using the finite volume method
[DE95-003360] p 1962 N95-24489
Pulsed power drivers for ICF and high energy density physics
[DE95-003361] p 2066 N95-24500
The potential of vacuum microelectronics for space reactor applications
[DE95-000542] p 1958 N95-24586
Recipes for high resolution time-of-flight detectors
[DE95-006196] p 1967 N95-24596
The accident site portable integrated video system
[DE95-000539] p 1953 N95-24605
Nonequilibrium multiphase mixture modeling of energetic material response
[DE95-003353] p 1948 N95-24608
Synthesis and characterization of Fe colloid catalysts in inverse micelle solutions
[DE95-006313] p 1929 N95-24614
Effect of He pressure on the superconducting transition temperatures of Na2CsC60 and (NH3)4Na2CsC60
[DE95-006320] p 2087 N95-24616
Disilene Addition to C70
[DE95-006321] p 2087 N95-24617
EXODUS 2: A finite element data model
[DE95-004267] p 2016 N95-24659
Co-validation of three methods for optical characterization of point-focus concentrators
[DE95-001613] p 1992 N95-24674
The energy intelligence information system
[DE95-002184] p 2105 N95-24675
Mirror alignment and focus of point-focus solar concentrators
[DE95-002609] p 1992 N95-24676
Dynamic load balancing for parallel finite element methods with adaptive h- and p-refinement
[DE95-004521] p 2021 N95-24681
Felt-metal-wick heat-pipe solar receiver
[DE95-004535] p 1992 N95-24682
Assessing capillary flow on printed wiring board surfaces
[DE94-015768] p 1959 N95-24712
Using consumer IC packages in harsh high reliability applications
[DE94-016565] p 1959 N95-24713
Capillary flow on narrow strips and in V-shaped grooves
[DE95-000543] p 1935 N95-24716
Feasibility of ceramic joining with high energy electron beams
[DE95-004519] p 1940 N95-24717
An examination of metal felt wicks for heat-pipe applications
[DE95-002608] p 1994 N95-25109
Optical properties of fractal nanocomposites
[DE95-005414] p 1926 N95-25295
Optical determinations of energy-band dispersion curves in novel compound semiconductor materials
[DE95-006318] p 2089 N95-25353
A statistical analysis of the effect of PECVD deposition parameters on surface and bulk recombination in silicon solar cells
[DE95-004780] p 1994 N95-25360
Effects of acetylacetone additions on PZT thin film processing
[DE95-006322] p 1941 N95-25370
Reciprocal space analysis of the microstructure of luminescent and nonluminescent porous silicon films
[DE95-005420] p 1941 N95-25382
Emerging nondestructive inspection for aging aircraft
[PB95-143053] p 1905 N95-25401
Recent advances in lithium ion technology
[DE95-004769] p 2054 N95-25470
3-D seismic imaging of complex geologies
[DE95-006813] p 2004 N95-25476
Benchmark testing and independent verification of the VS2DT computer code
[DE95-004386] p 1965 N95-25485
The impact of multiplexing on the dynamic requirements of analog-to-digital converters
[DE95-006302] p 1960 N95-25558
Phase correction in two-crystal optical parametric oscillators
[DE95-006317] p 2074 N95-25559
Back surface cell structures for reducing recombination in CZ silicon solar cells
[DE95-005423] p 1995 N95-25566
Synthesis and processing of Al2O3/Al composites by in situ reaction of aluminum and mullite
[DE95-006224] p 1937 N95-25775
A domain decomposition study of massively parallel computing in compressible gas dynamics
[DE95-004759] p 1965 N95-25895
The effect of O2 intercalation on the rotational Dynamics and the ordering transition of C60
[DE95-004765] p 2090 N95-25897
Non-destructive characterization of porous silicon using x ray reflectivity
[DE95-004766] p 1942 N95-25898
User's manual for FAROW: Fatigue and reliability of wind turbine components, version 1.1
[DE95-005530] p 1995 N95-26037
The effect of encapsulation on the reflectance of photovoltaic modules using textured multicrystalline-silicon solar cells
[DE95-004781] p 1996 N95-26166
Atomic force microscopy as a process characterization tool for GaAs-based integrated circuit fabrication
[DE95-006223] p 2064 N95-26168
Numerical simulation of laminar flow in a curved duct
[DE95-005427] p 1966 N95-26240

SANDIA NATIONAL LABS., LIVERMORE, CA.
Understanding and improving materials processing through interpreting and manipulating predictive models
[DE95-004384] p 1930 N95-25242
Tunable diode lasers as continuous emission monitors for thermal waste treatment processes
[DE95-004381] p 1972 N95-25549

SANTA CLARA UNIV., CA.
Parallel processing for scientific computations
[NASA-CR-198013] p 2020 N95-24563
SCIENCE AND TECHNOLOGY CORP., HAMPTON, VA.
Design and development of a cloud reference library and support for cloud and simulation communities. Summary report
[AD-A288704] p 2006 N95-26012
SCIENCE APPLICATIONS INTERNATIONAL CORP., DAYTON, OH.
Visual contrast detection thresholds for aircraft contrails
[AD-A288618] p 1905 N95-25607
SCIENCE APPLICATIONS INTERNATIONAL CORP., HUNTSVILLE, AL.
Active weld control
[NASA-CR-196588] p 1976 N95-25595
SCIENCE APPLICATIONS INTERNATIONAL CORP., MCLEAN, VA.
Assessment of Commercial Satellite Communications Initiative (CSCI) studies
[AD-A288357] p 1920 N95-25508
Nonlinear analysis of millimeter and sub-millimeter wave sources such as Cerenkov masers, orotrons, and ubitrons
[AD-A288777] p 1974 N95-26114
SECURE SOLUTIONS, INC., LA JOLLA, CA.
Naval network security requirements analysis
[AD-A288692] p 2022 N95-26054
SELSKAPET FOR INDUSTRIELL OG TEKNISK FORSKNING, TRONDHEIM (NORWAY).
Measurement of blood nitrogen content after rapid compressions to assess the speed of nitrogen uptake during the compression phase of submarine escape. (Includes measurement of nitrogen concentration in blood following rapid compression to 5 bar)
[PB95-165726] p 2012 N95-25570
SKJOELDEBRAND (R.).
Nuclear energy and the environment
[DE95-600438] p 2001 N95-25615
SOLAR TURBINES, INC. SAN DIEGO, CA.
Perspective on thermal barrier coatings for industrial gas turbine applications p 1945 N95-26128
SOUTH CAROLINA UNIV., COLUMBIA, SC.
The transformation of organic amines by transition metal cluster compounds
[DE95-004180] p 1923 N95-24851
SOUTHWEST RESEARCH INST., BOULDER, CO.
Distribution and nature of UV absorbers on Triton's surface
[NASA-CR-198008] p 2112 N95-26116
SRI INTERNATIONAL CORP., MENLO PARK, CA.
Evaluation of a diffusion/trapping model for hydrogen ingress in high-strength alloys
[AD-A288447] p 1936 N95-25502
STANFORD LINEAR ACCELERATOR CENTER, CA.
Quantum corrections for a cosmological string solution
[DE95-006057] p 2109 N95-24327
Recent progress in one-loop multi-parton calculations
[DE95-006062] p 2092 N95-24328
Test of an array of CsI(Tl) crystal towers for a low or medium energy e(+)e(-) collider calorimeter
[DE95-006068] p 2043 N95-24354
PEP-2 vacuum system: Joining SS flanges to copper beam chambers
[DE95-006093] p 1974 N95-24356
Depolarization in the SLC Collider Arcs
[DE95-005942] p 2065 N95-24409
The discovery of the tau lepton: Part 1, The early history through 1975; Part 2, Confirmation of the discovery and measurement of major properties, 1976-1982
[DE95-005945] p 2044 N95-24414
Extending the kinematic range for W(sub R) searches in e(-)e(-) collisions at the NLC
[DE95-005946] p 2044 N95-24415
A measurement of quark and gluon jet differences at the Z(sup 0) resonance
[DE95-005947] p 2044 N95-24417
A test of the flavor independence of strong interactions
[DE95-005948] p 2044 N95-24418
A search for jet handedness in hadronic Z(sup 0) decays
[DE95-005944] p 2045 N95-24435
A photoemission study of the diamond and the single crystal C(60)
[DE95-006149] p 2085 N95-24463
Measurement of the charged multiplicity of Z(sup 0) (yields) b(bar b) events
[DE95-006051] p 2046 N95-24571
Over-compression, a method to shape the longitudinal bunch distribution for a reduced energy spread
[DE95-006052] p 2066 N95-24572
Tutorial on beam-based feedback systems for linacs
[DE95-006054] p 2067 N95-24573
Electroweak coupling measurements from polarized Bhabha scattering at the Z(sup 0) resonance
[DE95-006056] p 2067 N95-24574
A measurement of the left-right, forward-backward asymmetry for charm quarks using D(*+) and D(+) mesons
[DE95-006061] p 2046 N95-24575
A test of the flavor independence of strong interactions
[DE95-006063] p 2046 N95-24576
Creation of a scalar potential in 2D dilaton gravity
[DE95-006066] p 2003 N95-24577
Decoherence, determinism and chaos revisited
[DE95-006070] p 2094 N95-24578
Tau physics at future facilities
[DE95-006071] p 2046 N95-24591
The left-right forward-backward asymmetry of heavy quarks measured with jet charge and with leptons at the SLD
[DE95-006145] p 2046 N95-24593
Adventures in the evolution of a high-bandwidth network for central servers
[DE95-006215] p 2020 N95-24597
Measurement of alpha(sub s) from hadronic ev ent observables at the Z(sup 0) resonance
[DE95-005949] p 2047 N95-24622
Multiplicity moments in e(+)e(-) annihilation into hadrons at the Z(sup 0) resonance
[DE95-005950] p 2047 N95-24641
ASIC implementation of a data-push architecture for silicon pixel readout
[DE95-003368] p 2015 N95-24648
A study of K(sub s) (lambda) and (bar (lambda)) production in hadronic Z(sup 0) decays
[DE95-004280] p 2047 N95-24660
Studies of strong electroweak symmetry breaking at future e(+)e(-) linear colliders
[DE95-004281] p 2067 N95-24661
Spin structure of the nucleon and polarization
[DE95-004282] p 2047 N95-24662
Geometry of multihadron production
[DE95-004290] p 2047 N95-24663
A fast tracking method using resonance basis Hamiltonians
[DE95-004292] p 2068 N95-24664
Probing new physics in rare charm processes
[DE95-006067] p 2050 N95-24903
RF pulse compression in the NLC test accelerator at SLAC
[DE95-006478] p 2070 N95-25406
Extended gauge sectors
[DE95-006485] p 2052 N95-25407
Faster magnet sorting with a threshold acceptance algorithm
[DE95-006487] p 2038 N95-25408
Measurement accuracy, bit-strings, Manthey's quaternions, and RRQM
[DE95-006211] p 2098 N95-25530
STANFORD UNIV., CA.
Measurement of alpha(sub s)from hadronic event observables at the Z(sup 0) resonance
[DE95-005943] p 2045 N95-24434
New approaches to optimization in aerospace conceptual design
[NASA-CR-196695] p 1910 N95-24436
Testing supersymmetry at the next linear collider
[DE95-006064] p 2069 N95-25297
Electroweak coupling measurements from polarized Bhabha scattering at the Z(exp 0) resonance
[DE95-006090] p 2057 N95-25768
STATE UNIV. OF NEW YORK, ALBANY, NY.
Use of cloud observations and mesoscale meteorology models to evaluate and improve cloud parameterizations
[DE95-006256] p 2005 N95-24613
STATE UNIV. OF NEW YORK, BINGHAMTON, NY.
Tests for leptonic CP violation in tau decays
[DE95-005927] p 2050 N95-24902
CP violation tests for tau/top processes
[DE95-005924] p 2051 N95-25292
q-bosons and the q-analogue quantized field
[DE95-005925] p 2051 N95-25294
Tau as a probe for new physics
[DE95-005928] p 2051 N95-25296
STATE UNIV. OF NEW YORK, BUFFALO, NY.
Group transfer and electron transfer reactions of organometallic complexes
[DE95-003732] p 2050 N95-25112
STATE UNIV. OF NEW YORK, STONY BROOK, NY.
Design of supramolecular ordered systems for mesoscopic colloids and molecular composites
[DE95-004448] p 2048 N95-24687
Research in nuclear astrophysics: Stellar collapse and supernovae
[DE95-004300] p 2110 N95-25343
A search for t(anti t) (yields) lepton + E(sub T) + jets signature in p(anti p) collisions at (radical)s = 1.8 TeV with the DO detector
[DE95-004239] p 2052 N95-25402
Shelf sediment dynamics and development of lithostratigraphy
[AD-A288886] p 2006 N95-25504
Thermal spray processing p 1945 N95-26130
SWEDISH INST. FOR MATERIALS TESTING, BORAS (SWEDEN).
Calibration of optical time domain reflectometers using time delay generator
[PB95-141776] p 2073 N95-24673
Heat release rate measurements in tunnel fires
[PB95-165106] p 1931 N95-25443
Crosstalk on printed circuit boards
[PB95-165171] p 1960 N95-25472
Performance tests of air source heat pumps under frosting conditions. Quality of results
[PB95-141792] p 1995 N95-25892
SWEDISH INST. FOR METALS RESEARCH, STOCKHOLM (SWEDEN).
New techniques to test fatigue properties of coined sheet specimens. Part 2: Comparison of different materials, forming operations and life prediction techniques for a simple test geometry
[PB95-165122] p 1982 N95-25444
New techniques to test fatigue properties of coined sheet specimens. Part 4: Development of experimental techniques
[PB95-165130] p 1982 N95-25445
New techniques to test fatigue properties of coined sheet specimens. Part 3: Fatigue testing and analysis of a component like coining in sheet steel materials
[PB95-165668] p 1982 N95-25569
SWEDISH NATIONAL TESTING AND RESEARCH INST., TSORAS (SWEDEN).
Automatic measurement system for measuring of the nonlinearity of photo detectors
[PB95-165197] p 2074 N95-25999
Background information to reliability stress screening of components: A guide for component users. Nordtest project 1140-93
[PB95-165775] p 1978 N95-26002
Proposed Nordtest method: Reliability stress screening of components. A guide for component users. Nordtest project 1140-93
[PB95-165783] p 1978 N95-26003

T

TAMPERE UNIV. OF TECHNOLOGY (FINLAND).
Availability analysis of a 100 kWh superconducting magnetic energy storage
[DE95-737621] p 2066 N95-24448
TECHNICAL RESEARCH CENTRE OF FINLAND, ESPOO (FINLAND).
Report series in aerosol science
[DE95-737628] p 1999 N95-24904
TECHNICAL RESEARCH CENTRE OF FINLAND, JYVASKYLA (FINLAND).
Yearbook 1993: Bioenergy Research Programme. Utilization of bioenergy and biomass conversion
[DE95-717518] p 1993 N95-24862
TECHNICAL UNIV. OF LUBLIN, LUBLIN (POLAND).
Electromagnetic Devices and Processes in Environment Protection. Proceedings of International Conference ELMECO 1994
[AD-A286613] p 1952 N95-24503
TECHNISCHE UNIV., DELFT (NETHERLANDS).
Finite element methods in a simulation code for offshore wind turbines
[PB95-164984] p 1994 N95-25501
TELEDYNE BROWN ENGINEERING, HUNTSVILLE, AL.
Crystal Growth Furnace (CGF)
[NASA-CR-196591] p 2089 N95-25409
TENNESSEE UNIV., KNOXVILLE, TN.
Localized corrosion and stress corrosion cracking characteristics of a low-aluminum-content iron-aluminum alloy
[DE95-003259] p 1934 N95-24647
Cognitive diagnosis combined with latent trait theory and multiphase responses
[AD-A288701] p 2013 N95-26010
TEXAS A&I UNIV., KINGSVILLE, TX.
A report: A plan to establish Internet access points at Minority Campus sites for connection to a central computing facility
[DE95-004374] p 2105 N95-25240
TEXAS A&M UNIV., COLLEGE STATION, TX.
Fischer Tropsch synthesis in supercritical fluids
[DE95-005206] p 1929 N95-24341
Thermohydrodynamic analysis of cryogenic liquid turbulent flow fluid film bearings, phase 2
[NASA-CR-197412] p 1962 N95-24461

TEXAS TECHNOLOGICAL UNIV., LUBBOCK, TX.
Hierarchical Control and Trajectory Planning
[NASA-CR-197922] p 2026 N95-25801
Splines and control theory p 2026 N95-25802
A brief survey of constrained mechanics and variational problems in terms of differential forms
p 2026 N95-25803
Control theory and splines, applied to signature storage p 2027 N95-25804
How to fly an aircraft with control theory and splines
p 2027 N95-25805

TEXAS UNIV., AUSTIN, TX.
Transport suppression by diamagnetic phase shift as a possible mechanism to the L to H transition
[DE95-003345] p 2077 N95-24587
Energetic particle drive for toroidicity-induced Alfven eigenmodes and kinetic toroidicity-induced Alfven eigenmodes in a low-shear Tokamak
[DE95-003222] p 2079 N95-25216
The railplug: A new ignitor for internal combustion engines
[DE95-005487] p 1977 N95-26172

TEXAS UNIV. AT DALLAS, RICHARDSON, TX.
Elementary particle physics
[DE95-004376] p 2051 N95-25241

THESSALONIKI UNIV., SALONIKA (GREECE).
Searching for exotic mesons in e(+)e(-) annihilation at DA(phi)NE
[PB95-165379] p 2064 N95-26001

THIOKOL CORP., HUNTSVILLE, AL.
Space shuttle propellant constitutive law verification tests
[NASA-CR-198047] p 1947 N95-24226

TOKYO UNIV. (JAPAN).
A Green's function method for hadrons in nuclei
[DE94-792620] p 2070 N95-25772
Proceedings of the 2nd international workshop on electromagnetic forces and related effects on blankets and other structures surrounding the fusion plasma torus
[DE94-792667] p 2082 N95-25903

TOKYO UNIV., TANASHI (JAPAN).
A simple relation among the quark masses
[DE95-703783] p 2055 N95-25494
On analysis of resonance neutron depolarization in uniaxial media
[DE95-703782] p 2057 N95-25669

TRAETEKNIK CENTRUM, STOCKHOLM (SWEDEN).
Fire test of surface products: Comparison of data from the nordic box test and the cone calorimeter
[PB95-165239] p 1932 N95-26000

TRANSDUCER RESEARCH, INC., NAPERVILLE, IL.
Field-usable portable analyzer for chlorinated organic compounds
[DE95-003127] p 1930 N95-25098

U

UMWELTBUNDESAMT, BERLIN (GERMANY).
Responsibility means doing without: How to rescue the ozone-layer
[PB95-166807] p 1997 N95-24334

UNITED SPACE BOOSTERS, INC., HUNTSVILLE, AL.
BSM Delta qualification 2, volume 1
[NASA-CR-196566-VOL-1] p 1921 N95-24440

UNITED TECHNOLOGIES CORP., EAST HARTFORD, CT.
Development of sensors for ceramic components in advanced propulsion systems. Phase 2: Temperature sensor systems evaluation
[NASA-CR-195283] p 1967 N95-24473

UNITED TECHNOLOGIES CORP., SAN JOSE, CA.
BSM Delta qualification 2, volume 1
[NASA-CR-196566-VOL-1] p 1921 N95-24440
BSM Delta Qualification 2, volume 2
[NASA-CR-196567] p 1922 N95-24844
BSA Delta Qualification 2, volume 3, book 1
[NASA-CR-196565] p 1922 N95-24845
BSM Delta Qualification 2, volume 3, book 2
[NASA-CR-196568] p 1922 N95-24854

UNIVERSITY CITY SCIENCE CENTER, PHILADELPHIA, PA.
Waste minimization assessment for a manufacturer of parts for truck engines
[PB95-144481] p 1911 N95-26062

UNIVERSITY OF SOUTH FLORIDA, SAINT PETERSBURG, FL.
Average cosine meter and high spectral resolution measurements at the marine light mixed layer site
[AD-A288713] p 1970 N95-26113

UNIVERSITY OF SOUTH FLORIDA, TAMPA, FL.
Neural networks: Application to medical imaging
p 2025 N95-25267

UNIVERSITY OF SOUTHERN CALIFORNIA, LOS ANGELES, CA.
Geologic mapping of Argyre Planitia
[NASA-CR-197986] p 2112 N95-24303
From neural-based object recognition toward microelectronic eyes p 2023 N95-25257

UNIVERSITY OF WESTERN KENTUCKY, BOWLING GREEN, KY.
Co-firing high sulfur coal with refuse derived fuels
[DE95-006243] p 1997 N95-24406

UTAH STATE UNIV., LOGAN, UT.
Newton iterative methods for large scale nonlinear systems
[DE95-007067] p 2032 N95-25480

UTAH UNIV., SALT LAKE CITY, UT.
Human parathyroid hormone-(1-38) restores cancellous bone to the immobilized, osteopenic proximal tibial metaphysis in rats
[NASA-CR-197709] p 2011 N95-24556

V

VANDERBILT UNIV., NASHVILLE, TN.
Mechanical properties testing and results for thermal barrier coatings p 1946 N95-26134
The 1994 NASA/USRA/ADP Design Projects
[NASA-CR-197415] p 2101 N95-26304
Universal Test Facility p 1918 N95-26305
Automated protein crystal growth facility
p 1918 N95-26306
Stiffening of the ACES deployable space boom
p 1978 N95-26307
Launch system design for access to space
p 1918 N95-26308
LH2 fuel tank design for SSTO p 1987 N95-26309
Feed system design for a reduced pressure tank
p 1923 N95-26310

VIRGINIA POLYTECHNIC INST., BLACKSBURG, VA.
Heat flux instrumentation for HYFLITE thermal protection system
[NASA-CR-197715] p 1968 N95-25118

VIRGINIA UNIV., CHARLOTTESVILLE, VA.
NASA-UVA light aerospace alloy and structures technology program (LA2ST)
[NASA-CR-198041] p 1933 N95-24220
A theoretical analysis of strain in GaN and its effects on carrier conductivity
[AD-A288769] p 2090 N95-26061

VIRGINIA UNIV., HAMPTON, VA.
Center for Computational Structures Technology
[NASA-CR-198028] p 1983 N95-26263
Finite element buckling and postbuckling solutions for multilayered composite panels p 1983 N95-26264
Three-dimensional solutions for thermomechanical stresses in sandwich panels and shells
p 1984 N95-26265
Sensitivity analysis of the non-linear dynamic viscoplastic response of 2-d structures with respect to material parameters p 1984 N95-26266
Sensitivity analysis for the dynamic response of viscoplastic shells of revolution p 1984 N95-26268
Nonlinear vibrations of thin-walled composite frames
p 1984 N95-26269
Effect of mesh distortion on the accuracy of transverse shear stresses and their sensitivity coefficients in multilayered composites p 1985 N95-26270
Sensitivity analysis of frictional contact response of axisymmetric composite structures p 1985 N95-26271
Nonlinear structural analysis on distributed-memory computers p 1985 N95-26272
Three-dimensional solutions for coupled thermoelectroelastic response of multilayered plates
p 1985 N95-26273
Recent advances in the sensitivity analysis for the thermomechanical postbuckling of composite panels
p 1985 N95-26274
A hybrid neurocomputing/numerical strategy for nonlinear structural analysis p 1986 N95-26275
Postbuckling and large-deflection nonlinear analyses on distributed-memory computers p 1986 N95-26276
Reduction technique for tire contact problems
p 1986 N95-26277
Sensitivity analysis for the dynamic response of thermoviscoplastic shells of revolution
p 1986 N95-26278
Dynamic sensitivity analysis of frictional contact/impact response of axisymmetric composite structures
p 1986 N95-26279
Buckling and postbuckling of composite panels with cutouts subjected to combined edge shear and temperature change p 1987 N95-26280
Sensitivity analysis for large-deflection and postbuckling responses on distributed-memory computers
p 1987 N95-26281
Computational strategies for tire monitoring and analysis p 1978 N95-26282
Assessment of computational models for thermoelectroelastic multilayered plates
p 1987 N95-26283

VIRGINIA UNIV. HOSPITAL, CHARLOTTESVILLE, VA.
An evaluation of a coupled microstructural approach for the analysis of functionally graded composites via the finite-element method
[NASA-CR-195455] p 1925 N95-24438
NASA-UVa light aerospace alloy and structures technology program supplement: Aluminum-based materials for high speed aircraft
[NASA-CR-4645] p 1935 N95-24878

W

WASHINGTON UNIV., SEATTLE, WA.
Landau-Zener treatments of solar neutrino oscillations
[DE95-004761] p 2113 N95-24249
Core-collapse supernovae and nucleosynthesis
[NASA-CR-197731] p 2109 N95-25122
Neutrino oscillations from discrete non-Abelian family symmetries
[DE95-004355] p 2052 N95-25403
The off-shell axial anomaly via the (gamma)*(pi)(sup 0) (yields) (gamma) transition
[DE95-004762] p 2057 N95-25896

WEIZMANN INST. OF SCIENCE, REHOVOT (ISRAEL).
Electric field effects on the quantum efficiency of Cesium-iodide photocathodes in gas media
[DE94-628176] p 1957 N95-24482
A correction of the quantum efficiency of cesium iodide and other photocathodes due to the recalibration of the reference photomultipliers
[DE94-628177] p 1957 N95-24483
New physics effects on CP Violation in B decays
[DE94-628617] p 2049 N95-24722
The determination of V(sub cb) and QCD Sum Rules in Heavy Quark Effective theory
[DE94-628636] p 2095 N95-24723
TeV scale leptoquarks as a signature of standard-like superstring models
[DE94-628529] p 2096 N95-25095
Supersymmetry and light quark masses in a realistic superstring model
[DE94-628530] p 2096 N95-25096
R parity in standard-like superstring models
[DE94-628531] p 2096 N95-25215

WESTINGHOUSE HANFORD CO., RICHLAND, WA.
Workflow automation architecture standard
[DE95-004748] p 2035 N95-24248
Measuring the strategic value of information technology investments
[DE94-018160] p 2104 N95-24603
Activity Management System user reference manual
[DE95-000989] p 2105 N95-24654
Electrochemical organic destruction in support of Hanford tank waste pretreatment
[DE95-002854] p 1924 N95-25248
National standard and code compliance for electrical equipment installed in hazardous locations for the void fraction instrument
[DE95-002158] p 1960 N95-26092

WESTINGHOUSE SAVANNAH RIVER CO., AIKEN, SC.
SPEEDUP simulation of liquid waste batch processing, revision 1
[DE95-001240] p 1939 N95-24344
Cesium cobaltdicarbollide-solubility, precipitation, and reactivity in basic aqueous solution
[DE95-005881] p 1929 N95-24430
Characterizing pre-polished Type 304L stainless steel
[DE95-001241] p 1934 N95-24480
Residual Stress Measurements with Laser Speckle Correlation Interferometry and Local Heat Treating
[DE95-060082] p 1981 N95-24598
Stainless steel recycle
[DE95-003905] p 1934 N95-24615
Integration of heterogeneous data bases for development of a large-scale environmental data atlas for multi-platform PC and workstation users
[DE95-002689] p 2000 N95-25278

WICHITA STATE UNIV., WICHITA, KS.
Analysis of warping effects on the static and dynamic response of a seat-type structure
[NIAR-94-12] p 1979 N95-24211

WISCONSIN UNIV., MADISON, WI.
Psychophysical evaluation of three-dimensional auditory displays
[NASA-CR-198010] p 2011 N95-24564
Advances and prospects in reversed field pinch research
[DE95-007017] p 2077 N95-24602

Transport reduction by current profile control in the reversed field pinch
[DE95-007016] p 2077 N95-24619
Further ways to distinguish single-lepton top quark signals from background at the Tevatron
[PB95-165395] p 2056 N95-25567

WRIGHT LAB., WRIGHT-PATTERSON AFB, OH.

Microscan simulation
[AD-A289139] p 2075 N95-26039
Heat transfer measurements in small scale wind tunnels
[AD-A288689] p 1915 N95-26053

Typical Contract Number Index Listing

AF- AFOSR-0090-93 ..... p 173 N95-10812

CONTRACT NUMBER | PAGE NUMBER | ACCESSION NUMBER

Listings in this index are arranged alphanumerically by contract number. Under each contract number the accession numbers denoting documents that have been produced as a result of research done under that contract are arranged in ascending order. The page number helps to locate the citation in the abstract section. The accession number denotes the number by which the citation is identified.

AF PROJ. ILIR ..... p 2013 N95-26041
AF PROJ. 2004 ..... p 2075 N95-26039
AF PROJ. 2404 ..... p 1915 N95-26053
AF PROJ. 3048 ..... p 1977 N95-26050
AF-AFOSR-0044-91 ..... p 2030 N95-24557
ARPA ORDER 8225 ..... p 1966 N95-25868
BMFT-06-HD-5541 ..... p 2113 N95-25364
CDDF PROJ. 92-12 ..... p 1922 N95-24626
CSL PROJ. 1061 ..... p 2002 N95-25899
DA PROJ. 1L1-62211-A-47-A ..... p 1952 N95-24395
p 1977 N95-26074
p 1977 N95-26076
DAAL01-93-C-2002 ..... p 1912 N95-26060
DAAL03-G-0213 ..... p 1943 N95-26081
DABT63-94-C-0045 ..... p 1978 N95-25333
DACA33-94-C-0033 ..... p 1970 N95-26059
DAJA45-93-C-0033 ..... p 2039 N95-25503
DAMD17-92-C-2062 ..... p 2010 N95-24423
DAMD17-92-J-2025 ..... p 2010 N95-24309
DAMD17-94-V-4004 ..... p 2009 N95-26193
DCA100-90-C-0056 ..... p 1920 N95-25508
DE-AC01-87CE-40762 ..... p 1991 N95-24666
DE-AC02-76CH-00016 ..... p 1928 N95-24257
p 1928 N95-24265
p 2064 N95-24287
p 2065 N95-24357
p 2044 N95-24420
p 2093 N95-24450
p 2085 N95-24451
p 1997 N95-24570
p 1968 N95-24623
p 2048 N95-24677
p 2068 N95-24685
p 2087 N95-24849
p 1930 N95-25123
p 2113 N95-25364
p 2026 N95-25368
p 2070 N95-25369
p 2052 N95-25374
p 2052 N95-25375
p 2008 N95-25383
p 2070 N95-25441
p 2001 N95-25442
p 2071 N95-25785
p 2064 N95-26006
DE-AC02-76CH-03000 ..... p 2041 N95-24252
p 2041 N95-24253
p 2041 N95-24254
p 2041 N95-24256
p 2067 N95-24601
p 2068 N95-24728
p 1972 N95-24869
p 2050 N95-24901
p 2068 N95-25238
p 2073 N95-25239
p 2051 N95-25372
p 2106 N95-25376
p 2052 N95-25377
p 2052 N95-25402
p 2056 N95-25563
p 2071 N95-26011
p 2111 N95-26284
DE-AC02-76CH-03073 ..... p 2078 N95-24650
p 2079 N95-25120
DE-AC02-76ER-00881 ..... p 2056 N95-25567
DE-AC02-76ER-02945 ..... p 1924 N95-25286
DE-AC02-76EV-00119 ..... p 2011 N95-24556
DE-AC02-94CE-50390 ..... p 1994 N95-25121
DE-AC03-76SF-00098 ..... p 2065 N95-24320
p 2092 N95-24333
p 2045 N95-24434
p 2045 N95-24435
p 2066 N95-24495
p 2020 N95-24496
p 2045 N95-24512
p 2045 N95-24533
p 2073 N95-24546
p 1958 N95-24551
p 2067 N95-24652
p 2068 N95-24665
p 2074 N95-25357
p 2069 N95-25358
p 2021 N95-25359
p 2070 N95-25478
p 2015 N95-25773
p 2004 N95-26089
p 2064 N95-26256
DE-AC03-76SF-00515 ..... p 2109 N95-24327
p 2043 N95-24354
p 1974 N95-24356
p 2065 N95-24409
p 2044 N95-24414
p 2044 N95-24415
p 2044 N95-24417
p 2044 N95-24418
p 2045 N95-24434
p 2045 N95-24435
p 2085 N95-24463
p 2046 N95-24571
p 2066 N95-24572
p 2067 N95-24573
p 2067 N95-24574
p 2046 N95-24575
p 2046 N95-24576
p 2003 N95-24577
p 2094 N95-24578
p 2046 N95-24591
p 2046 N95-24593
p 2020 N95-24597
p 2047 N95-24622
p 2047 N95-24641
p 2015 N95-24648
p 2067 N95-24652
p 2047 N95-24660
p 2067 N95-24661
p 2047 N95-24662
p 2047 N95-24663
p 2068 N95-24664
p 2050 N95-24903
p 2069 N95-25297
p 2070 N95-25406
p 2052 N95-25407
p 2038 N95-25408
p 2098 N95-25530
p 2057 N95-25768
DE-AC03-83ER-40103 ..... p 2068 N95-24852
DE-AC03-89ER-51114 ..... p 2076 N95-24490
p 2077 N95-24646
p 1972 N95-24709
p 2078 N95-25102
p 2079 N95-25108
p 2050 N95-25180
p 2079 N95-25250
DE-AC03-89ER-52153 ..... p 2079 N95-25108
DE-AC04-76DP-00613 ..... p 1958 N95-24532
p 1969 N95-25381
p 2018 N95-26167
DE-AC04-76DP-00789 ..... p 1930 N95-25242
p 2079 N95-25250
DE-AC04-76DR-00789 ..... p 1972 N95-25549
DE-AC04-76EV-01013 ..... p 1998 N95-24606
DE-AC04-94AL-85000 ..... p 1961 N95-24262
p 1979 N95-24263
p 1990 N95-24264
p 1951 N95-24289
p 1906 N95-24308
p 2015 N95-24346
p 1971 N95-24408
p 1975 N95-24462
p 1957 N95-24488
p 1962 N95-24489
p 2066 N95-24500
p 1958 N95-24586
p 2047 N95-24595
p 1967 N95-24596
p 1953 N95-24605
p 1948 N95-24608
p 1929 N95-24614
p 2087 N95-24616
p 2087 N95-24617
p 2016 N95-24659
p 1992 N95-24674
p 2105 N95-24675
p 1992 N95-24676
p 2021 N95-24681
p 1992 N95-24682
p 1959 N95-24712
p 1959 N95-24713
p 1935 N95-24716
p 1940 N95-24717
p 2078 N95-25102
p 1994 N95-25109
p 1926 N95-25295
p 1994 N95-25309
p 2089 N95-25353
p 1994 N95-25360
p 1941 N95-25370
p 1941 N95-25382
p 2054 N95-25470
p 2004 N95-25476
p 1965 N95-25485
p 1931 N95-25492
p 1960 N95-25558
p 2074 N95-25559
p 1995 N95-25566
p 1937 N95-25775
p 1965 N95-25895
p 2090 N95-25897
p 1942 N95-25898
p 2002 N95-25899
p 1995 N95-26037
p 1996 N95-26166
p 2064 N95-26168
p 1966 N95-26240
DE-AC04-95DP-85000 ..... p 1992 N95-24674
DE-AC05-76OR-00033 ..... p 2051 N95-25373
DE-AC05-84ER-40150 ..... p 2065 N95-24409
DE-AC05-84OR-21400 ..... p 1939 N95-24247
p 2019 N95-24250
p 1929 N95-24345
p 2085 N95-24431
p 1933 N95-24432
p 1934 N95-24433
p 2104 N95-24454
p 2037 N95-24479
p 1940 N95-24588
p 2030 N95-24592
p 2087 N95-24611
p 2077 N95-24646
p 1934 N95-24647
p 2105 N95-24656
p 2008 N95-24843
p 2050 N95-25099
p 2078 N95-25102
p 2079 N95-25250
p 2032 N95-25251
p 2079 N95-25283
p 1951 N95-25367
p 2000 N95-25380
p 1941 N95-25387
p 1935 N95-25388
p 2089 N95-25389
p 1935 N95-25390
p 2089 N95-25391
p 2038 N95-25600
p 1938 N95-26064
p 2091 N95-26087

DE-AC05-92OR-21972 p 2102 N95-24905
DE-AC06-76RL-01830 p 1991 N95-24369
p 2103 N95-24370
p 1934 N95-24449
p 1998 N95-24653
p 2021 N95-24881
p 2088 N95-25002
p 1924 N95-25248
p 1999 N95-25249
p 1931 N95-25252
p 1924 N95-25286
p 2088 N95-25288
p 2001 N95-25629
p 2102 N95-25771
p 2106 N95-25774
p 1937 N95-26007
p 2022 N95-26013
p 2009 N95-26169
DE-AC06-87RL-10930 p 2035 N95-24248
p 2104 N95-24603
p 2105 N95-24654
p 1960 N95-26092
DE-AC07-76ID-01570 p 2069 N95-25365
p 2021 N95-25378
p 2004 N95-25666
p 2106 N95-25765
DE-AC08-90NV-10845 p 1988 N95-24407
DE-AC08-93NV-11265 p 1989 N95-25110
DE-AC09-89SR-18035 p 1939 N95-24344
p 1929 N95-24430
p 1934 N95-24480
p 1981 N95-24598
p 1934 N95-24615
p 2000 N95-25278
DE-AC21-89MC-26006 p 1990 N95-24318
p 1991 N95-24425
DE-AC21-92MC-29118 p 1930 N95-25098
DE-AC22-89BC-14475 p 2004 N95-26089
DE-AC22-89PC-89805 p 2003 N95-26091
DE-AC22-90PC-90044 p 1948 N95-24655
DE-AC24-92OR-21972 p 1930 N95-25097
DE-AC35-89ER-40486 p 1968 N95-24623
DE-AC36-83CH-10093 p 1990 N95-24305
p 2007 N95-24306
p 2007 N95-24307
p 1997 N95-24319
p 1998 N95-24604
p 1991 N95-24666
p 1992 N95-24684
p 1992 N95-24714
p 1993 N95-24715
p 1993 N95-24853
p 1993 N95-24865
p 1993 N95-24866
p 1975 N95-24880
p 1994 N95-24882
p 1994 N95-25309
p 1995 N95-25995
p 1995 N95-26090
p 1996 N95-26285
p 1978 N95-26286
DE-AG03-76SF-00515 p 2092 N95-24328
DE-AI01-91CE-50306 p 1923 N95-24437
DE-FC05-85ER-25000 p 2030 N95-24632
p 2056 N95-25620
DE-FC36-89ID-12779 p 1932 N95-26093
DE-FG01-89CE-90049 p 1976 N95-25101
DE-FG01-94CE-15599 p 1927 N95-25998
DE-FG01-94CE-15613 p 1925 N95-24426
DE-FG02-85ER-25001 p 2030 N95-24557
DE-FG02-85ER-53198 p 2077 N95-24602
p 2077 N95-24619
DE-FG02-86ER-40291 p 2050 N95-24902
p 2051 N95-25292
p 2051 N95-25294
p 2051 N95-25296
DE-FG02-86ER-45237 p 2048 N95-24687
DE-FG02-87ER-13775 p 2050 N95-25112
DE-FG02-87ER-40317 p 2110 N95-25343
DE-FG02-89ER-45405 p 1936 N95-25560
DE-FG02-90ER-20019 p 2008 N95-24850
DE-FG02-90ER-45427 p 2044 N95-24419
DE-FG02-91CE-23810 p 1941 N95-25243
DE-FG02-91ER-14227 p 1930 N95-24686
DE-FG02-91ER-40628 p 2085 N95-24451
DE-FG02-91ER-40672 p 2045 N95-24434
p 2045 N95-24435
DE-FG02-91ER-40676 p 2045 N95-24434
p 2045 N95-24435
DE-FG02-91ER-40677 p 2045 N95-24434
p 2045 N95-24435
p 2056 N95-25563
DE-FG02-91ER-40685 p 2054 N95-25483
DE-FG02-91ER-54109 p 2079 N95-25250
DE-FG02-92ER-25136 p 2032 N95-25480
DE-FG02-92ER-40706 p 2054 N95-25481
DE-FG02-92ER-40715 p 2045 N95-24434
p 2045 N95-24435
DE-FG02-92ER-61364 p 2005 N95-24613
DE-FG02-92ER-75787 p 2014 N95-25483
DE-FG02-93ER-40762 p 2098 N95-25562
DE-FG02-93ER-40764 p 2048 N95-24671
DE-FG02-93ER-54197 p 2081 N95-25561
DE-FG02-94ER-25199 p 2029 N95-24458
DE-FG02-94ER-40822 p 2046 N95-24547
DE-FG03-86ER-53225 p 2079 N95-25250
DE-FG03-89ER-51121 p 2078 N95-25102
DE-FG03-91ER-40618 p 2045 N95-24434
p 2045 N95-24435
DE-FG03-91ER-40662 p 2092 N95-24328
DE-FG03-91ER-40674 p 2015 N95-24648
DE-FG03-92ER-40689 p 2045 N95-24434
p 2045 N95-24435
DE-FG03-92ER-40701 p 2045 N95-24434
p 2045 N95-24435
DE-FG03-92ER-54150 p 2077 N95-24646
p 2079 N95-25120
DE-FG03-93ER-25165 p 2054 N95-25479
DE-FG03-93ER-40788 p 2045 N95-24434
p 2045 N95-24435
DE-FG03-94ER-54241 p 2077 N95-24587
DE-FG05-80ET-53088 p 2079 N95-25216
DE-FG05-86ER-40272 p 2096 N95-24867
DE-FG05-88ER-53266 p 2077 N95-24587
DE-FG05-91ER-12115 p 1977 N95-26172
DE-FG05-92ER-40736 p 2051 N95-25241
DE-FG05-94ER-40876 p 1965 N95-25404
DE-FG05-94ER-40877 p 1965 N95-25404
DE-FG05-94ER-40878 p 1965 N95-25404
DE-FG05-94ER-40879 p 2105 N95-25240
DE-FG05-94ER-40880 p 2065 N95-24317
DE-FG06-85ER-40224 p 2067 N95-24574
p 2047 N95-24641
p 2057 N95-25768
DE-FG06-87ER-45292 p 1940 N95-24554
DE-FG06-90ER-40561 p 2113 N95-24249
p 2109 N95-25122
p 2052 N95-25403
p 2070 N95-25634
p 2057 N95-25896
DE-FG06-92ER-14254 p 1929 N95-24553
DE-FG07-93ID-13220 p 2077 N95-24552
DE-FG08-90ER-61012 p 2005 N95-24411
DE-FG09-84ER-13296 p 1923 N95-24851
DE-FG09-85ER-13425 p 2007 N95-24225
DE-FG09-85ER-13426 p 2007 N95-24368
DE-FG21-93MC-29224 p 1992 N95-24683
DE-FG22-91PC-91293 p 1928 N95-24286
DE-FG22-92PC-92542 p 1939 N95-24285
DE-FG22-92PC-92545 p 1929 N95-24341
DE-FG22-94PC-94211 p 1997 N95-24406
DE-PS05-94ER-40863 p 2105 N95-25240
DOT-FA4H2/A4044 p 1905 N95-24295
DTFA03-91-A-00018 p 1905 N95-25401
EPA-R-914903 p 1911 N95-26062
EPA-68-C4-0020 p 1942 N95-26004
EPA-68-D1-0177 p 2002 N95-26005
FAA TASK AM-A-91-PHY-144 p 2011 N95-25336
F04701-88-C-0089 p 1947 N95-26188
F04701-93-C-0094 p 1942 N95-26049
F08635-91-C-0189 p 1915 N95-24424
F19628-89-C-0190 p 2006 N95-26012
F205/BSF p 2084 N95-24244
p 2084 N95-24246
F33615-90-C-1441 p 2075 N95-26173
F33615-92-D-2293 p 1905 N95-25607
F49620-87-C-0084 p 1977 N95-26050
F49620-92-J-0133 p 2029 N95-24421
p 2029 N95-24421
GA PROJ. 3466 p 2078 N95-25102
GRI-5089-291-2077 p 1913 N95-24293
GRI-5091-254-2209 p 1997 N95-24294
KC-05-01 p 2092 N95-24275
p 2092 N95-24277
KT-04 p 2028 N95-24276
MDA903-89-C-0003 p 2007 N95-26048
NAGW-2126 p 2080 N95-25325
NAGW-2158 p 1998 N95-24846
NAGW-2194 p 2111 N95-24239
NAGW-2381 p 2065 N95-24335
NAGW-2523 p 2109 N95-25122
NAGW-2572 p 2085 N95-24478
NAGW-2593 p 2108 N95-25104
NAGW-2902 p 2112 N95-24303
NAGW-3402 p 2112 N95-26116
NAGW-3437 p 1989 N95-24441
NAGW-3782 p 2010 N95-24410
NAGW-3929 p 2002 N95-25955
NAGW-3944 p 2005 N95-24535
NAGW-4061 p 2049 N95-24877
NAGW-674 p 1964 N95-25394
NAG1-1065 p 1911 N95-24630
NAG1-1226 p 1928 N95-26203
NAG1-1351 p 2005 N95-24219
NAG1-1358 p 1981 N95-24907
NAG1-1455 p 1990 N95-24199
NAG1-1494 p 1910 N95-24436
NAG1-1552 p 1970 N95-25699
NAG1-1558 p 1910 N95-24436
NAG1-1607 p 1915 N95-24302
NAG1-613 p 2016 N95-24993
p 1978 N95-25333
NAG1-745 p 1933 N95-24220
p 1935 N95-24878
NAG1-928 p 2035 N95-24278
NAG1-939 p 1917 N95-26205
NAG2-435 p 2011 N95-24556
NAG2-640 p 1910 N95-24436
NAG2-663 p 2005 N95-24411
NAG2-830 p 2017 N95-25867
NAG2-902 p 2026 N95-25801
NAG3-1377 p 1925 N95-24438
NAG3-1395 p 2099 N95-25878
NAG3-1434 p 1962 N95-24461
NAG3-1507 p 1913 N95-24213
NAG3-1561 p 1914 N95-24392
NAG3-1643 p 1968 N95-25118
NAG3-510 p 1963 N95-24906
NAG3-795 p 2063 N95-25963
NAG3-853 p 1974 N95-24223
NAG3-974 p 1974 N95-24218
NAG5-1490 p 2003 N95-24336
NAG5-2188 p 1943 N95-26081
NAG5-2235 p 2114 N95-24381
NAG5-2613 p 2015 N95-24224
NAG8-071 p 2061 N95-25926
p 2009 N95-25934
NAG8-864 p 1961 N95-24221
NAG8-950 p 2086 N95-24534
NAG8-953 p 2008 N95-24475
NAG9-235 p 2058 N95-25911
NAG9-390 p 2026 N95-25335
NASA ORDER S-14626-F p 2108 N95-24385
NASA ORDER S-14645-F p 2108 N95-24385
NASA ORDER S-14648-F p 2108 N95-24385
NASW-4435 p 2101 N95-26304
NASW-4812 p 1997 N95-24501
NAS1-14101 p 2014 N95-26085
NAS1-14472 p 2014 N95-26085
NAS1-15810 p 2014 N95-26085
NAS1-16394 p 2014 N95-26085
NAS1-17070 p 2014 N95-26085
NAS1-17130 p 2014 N95-26085
NAS1-18224 p 1923 N95-24583
p 1925 N95-26072
NAS1-18605 p 2029 N95-24389
p 2014 N95-26085
NAS1-18972 p 2020 N95-24634
NAS1-19000 p 1983 N95-26199
NAS1-19061 p 2039 N95-24879
NAS1-19244 p 1921 N95-24216
p 1921 N95-24428
NAS1-19247 p 1923 N95-24583
p 1925 N95-26072
NAS1-19360 p 1909 N95-25341
NAS1-19480 p 2029 N95-24389
p 2029 N95-24421
p 1962 N95-24580
p 1963 N95-24584
p 2030 N95-24632
p 2031 N95-24856
p 2031 N95-24857
p 2032 N95-25106
p 2032 N95-25114
p 2014 N95-25119
p 1965 N95-25960
p 1966 N95-25964
p 2014 N95-26085
NAS1-19700 p 1983 N95-26199
NAS1-20103 p 2040 N95-26160
NAS1-20228 p 1907 N95-24443
NAS1-20288 p 1974 N95-24204
NAS10-11999 p 1918 N95-24579
NAS2-13721 p 2027 N95-24214
p 1911 N95-25334
NAS3-25141 p 1967 N95-24473
NAS3-25266 p 1991 N95-24560
p 2018 N95-25879
p 1927 N95-25880
p 1908 N95-25962
NAS3-25776 p 1955 N95-25876
NAS3-25954 p 1913 N95-24390
NAS3-25965 p 1913 N95-24304
NAS3-26619 p 1968 N95-25330
NAS3-27186 p 1957 N95-24476
p 1955 N95-25876
p 2099 N95-25878
p 1983 N95-26078

NAS3-88622 ..... p 1912 N95-24624
NAS5-32332 ..... p 2003 N95-24766
NAS5-32350 ..... p 2083 N95-26082
NAS7-1260 ..... p 2112 N95-24987
NAS7-918 ..... p 2022 N95-25253
p 1959 N95-25307
p 1954 N95-25316
p 1969 N95-25547
NAS8-36300 ..... p 1921 N95-24440
p 1922 N95-24844
p 1922 N95-24845
p 1922 N95-24854
NAS8-36637 ..... p 2089 N95-25409
NAS8-36955 ..... p 2084 N95-24261
p 1940 N95-24562
NAS8-37925 ..... p 2104 N95-24439
NAS8-38187 ..... p 1906 N95-24217
NAS8-38551 ..... p 1976 N95-25595
NAS8-38609 ..... p 2104 N95-24477
p 2073 N95-24545
p 2016 N95-24876
NAS8-39027 ..... p 1938 N95-26068
NAS8-39131 ..... p 1975 N95-24991
NAS8-39398 ..... p 1923 N95-25103
NAS8-39619 ..... p 1947 N95-24226
NAS8-39897 ..... p 2102 N95-24442
NAS9-17389 ..... p 2009 N95-25934
NAS9-18800 ..... p 2013 N95-24627
NAS9-18992 ..... p 1928 N95-24222
NATO-CRG-910627 ..... p 2096 N95-24867
NCCW-11 ..... p 1983 N95-26263
NCC1-104 ..... p 2027 N95-26086
NCC1-141 ..... p 1915 N95-24388
NCC2-374 ..... p 1962 N95-24412
p 1962 N95-24413
NCC2-517 ..... p 2019 N95-26206
NCC2-521 ..... p 2061 N95-25926
p 2061 N95-25927
p 2061 N95-25928
p 2061 N95-25929
p 2061 N95-25930
p 2062 N95-25931
p 2009 N95-25933
NCC2-542 ..... p 2011 N95-24564
NCC2-63 ..... p 1933 N95-24400
NCC2-644 ..... p 2020 N95-24563
NCC2-799 ..... p 2017 N95-25797
NCC2-806 ..... p 1906 N95-24379
NCC3-143 ..... p 1915 N95-24380
NCC3-166 ..... p 1971 N95-24530
NCC3-208 ..... p 2072 N95-24386
p 1971 N95-24530
NCC3-233 ..... p 1966 N95-26077
NCC3-266 ..... p 2072 N95-24386
NCC3-269 ..... p 2072 N95-24386
p 1971 N95-24530
NCC3-330 ..... p 1923 N95-24437
NCC3-368 ..... p 1980 N95-24398
NCC3-370 ..... p 1961 N95-24399
NGT-50414 ..... p 2035 N95-24278
NGT-50975 ..... p 1909 N95-24391
NIH-AR-38346 ..... p 2011 N95-24556
NSF DMR-91-20000 ..... p 2087 N95-24868
NSF DMS-92-22491 ..... p 2028 N95-24251
NSF DMS-94-04322 ..... p 2030 N95-24632
NSF EHR-91-08775 ..... p 1943 N95-26081
NSF ENG-92-17849 ..... p 2085 N95-24460
NSF IRI-90-13160 ..... p 2016 N95-24536
NSF MIP-84-10110 ..... p 2030 N95-24557
NSF OCR-92-03488 ..... p 2033 N95-25601
NSF PHY-90-24608 ..... p 2097 N95-25446
NSF PHY-93-07484 ..... p 2100 N95-26102
N00014-89-J-1091 ..... p 1970 N95-26113
N00014-90-J-1025 ..... p 2033 N95-25601
N00014-90-J-1396 ..... p 1936 N95-25529
N00014-90-J-1456 ..... p 2013 N95-26010
N00014-91-C-0263 ..... p 1936 N95-25502
N00014-91-J-1116 ..... p 2016 N95-24993
N00014-91-J-4052 ..... p 1966 N95-25868
N00014-92-J-1512 ..... p 2016 N95-24536
N00014-92-J-1580 ..... p 2090 N95-26061
N00014-92-J-2017 ..... p 1954 N95-25604
N00014-93-1-0686 ..... p 2017 N95-25507
N00014-93-1-0799 ..... p 2006 N95-25504
N00014-94-WX-23074 ..... p 1932 N95-26056
N00014-94-1-0088 ..... p 1962 N95-24580
N00014-94-1-0118 ..... p 1926 N95-25505
N00014-95-1-0028 ..... p 1924 N95-25602
N00039-93-C-0099 ..... p 2022 N95-26054
N68171-94-M-6201 ..... p 1952 N95-24503
ONR PROJ. RR015-09-41 ..... p 1954 N95-25604
PROJ. BRANDFORSK 723-924 .... p 1931 N95-25443
PROJ. EUREKA-337 ..... p 1982 N95-25444
p 1982 N95-25445
p 1982 N95-25569
PROJ. FOA-518372 ..... p 2017 N95-25571
PROJ. MTX ..... p 2075 N95-24270
PROJ. SOLAR EAGLE 2 ..... p 1990 N95-24199
RF PROJ. 760678/727376 ..... p 2026 N95-25335
RR04204 ..... p 2013 N95-26010
RTOP 232-01-04-05 ..... p 1917 N95-26205
RTOP 233-01-0E ..... p 2063 N95-25963
RTOP 233-01-00 ..... p 1991 N95-24560
RTOP 233-01-01-03 ..... p 1920 N95-24581
RTOP 233-01-03 ..... p 1979 N95-24208
RTOP 233-03-02-04 ..... p 1923 N95-24583
p 1925 N95-26072
RTOP 233-03-03-02 ..... p 2027 N95-26086
RTOP 235-01-1E ..... p 1955 N95-25876
RTOP 242-80-01-01 ..... p 1961 N95-24396
p 1906 N95-24397
RTOP 243-10-01-01 ..... p 1950 N95-24559
RTOP 282-10-01-01 ..... p 1907 N95-24566
RTOP 323-36-19 ..... p 1950 N95-24543
RTOP 477-50-00 ..... p 1921 N95-24216
p 1921 N95-24428
RTOP 505-10-11 ..... p 1910 N95-24629
RTOP 505-53-50-12 ..... p 2015 N95-24209
RTOP 505-59-30-04 ..... p 1907 N95-25338
RTOP 505-59-36-01 ..... p 1907 N95-24566
RTOP 505-59-52-01 ..... p 2039 N95-24879
RTOP 505-59-85-01 ..... p 1915 N95-24388
RTOP 505-60-00 ..... p 1912 N95-24207
RTOP 505-62-00 ..... p 1914 N95-24561
RTOP 505-62-36 ..... p 1952 N95-24395
p 1977 N95-26074
p 1977 N95-26076
RTOP 505-62-50 ..... p 1967 N95-24473
p 1923 N95-25877
p 1908 N95-25962
p 1970 N95-26073
RTOP 505-62-52 ..... p 2029 N95-24474
p 2018 N95-25879
p 1908 N95-26075
RTOP 505-63-12 ..... p 1980 N95-24398
p 1925 N95-24438
p 1983 N95-26078
RTOP 505-63-5A ..... p 1923 N95-24437
p 1924 N95-25961
RTOP 505-63-5B ..... p 1927 N95-25880
RTOP 505-63-50-04 ..... p 1927 N95-26083
p 1928 N95-26203
RTOP 505-63-50-08 ..... p 1928 N95-26251
RTOP 505-63-52 ..... p 1943 N95-26119
RTOP 505-63-53-01 ..... p 1983 N95-26199
RTOP 505-64-10-13 ..... p 2019 N95-24382
RTOP 505-64-10-56 ..... p 2020 N95-24634
RTOP 505-64-52-01 ..... p 1911 N95-24630
RTOP 505-68-30-01 ..... p 1907 N95-24443
RTOP 505-68-32 ..... p 1908 N95-26302
RTOP 505-69-20-01 ..... p 1909 N95-24633
RTOP 505-69-50 ..... p 1910 N95-24436
RTOP 505-70-62-04 ..... p 1964 N95-25394
RTOP 505-90-5K ..... p 1961 N95-24399
p 1966 N95-26077
RTOP 505-90-52-01 ..... p 2029 N95-24389
p 2029 N95-24421
p 1962 N95-24580
p 1963 N95-24584
p 2030 N95-24632
p 2031 N95-24856
p 2031 N95-24857
p 2032 N95-25106
p 2032 N95-25114
p 2014 N95-25119
p 1965 N95-25960
p 1966 N95-25964
p 2014 N95-26085
RTOP 506-43-61-02 ..... p 1923 N95-24583
p 1925 N95-26072
RTOP 506-44-2C ..... p 1957 N95-24476
RTOP 510-01-50 ..... p 1968 N95-25330
RTOP 537-06-20-06 ..... p 1935 N95-24878
RTOP 537-08-21-01 ..... p 1910 N95-24582
RTOP 538-01-13-01 ..... p 1909 N95-25341
RTOP 538-03-15-01 ..... p 2040 N95-26160
RTOP 538-08-11 ..... p 1913 N95-24304
RTOP 578-41-45-20 ..... p 2003 N95-24766
RTOP 644-11-00 ..... p 2022 N95-25253
RTOP 963-25-0A ..... p 1963 N95-24906
RTOP 963-50-0A ..... p 2099 N95-25678
RTOP 963-89-00-01 ..... p 1919 N95-24765
SANDIA-LA-3971 ..... p 2002 N95-25899
SWRI PROJ. 15-5653 ..... p 2112 N95-26116
W-31-109-ENG-38 ..... p 2084 N95-24279
p 2042 N95-24292
p 2043 N95-24326
p 2103 N95-24330
p 2043 N95-24332
p 2019 N95-24342
p 2010 N95-24427
p 2045 N95-24459
W-7405-ENG-36 ..... p 1991 N95-24607
p 1998 N95-24618
p 2020 N95-24658
p 2068 N95-24680
p 2087 N95-24855
p 2078 N95-24861
p 2087 N95-24868
p 2008 N95-25181
p 2088 N95-25280
p 2069 N95-25281
p 2088 N95-25282
p 2079 N95-25283
p 2069 N95-25300
p 2000 N95-25363
p 2057 N95-25896
p 2083 N95-26185
p 2083 N95-24233
p 2109 N95-24234
p 2091 N95-24235
p 2041 N95-24258
p 2065 N95-24331
p 2019 N95-24343
p 2109 N95-24455
p 1940 N95-24456
p 2093 N95-24457
p 2086 N95-24513
p 2086 N95-24514
p 1958 N95-24589
p 1925 N95-24590
p 2086 N95-24594
p 2008 N95-24600
p 2030 N95-24609
p 2094 N95-24610
p 2020 N95-24612
p 2078 N95-24667
p 1948 N95-24670
p 1920 N95-24711
p 1999 N95-25198
p 1941 N95-25237
p 2080 N95-25289
p 2096 N95-25293
p 2069 N95-25366
p 1935 N95-25379
p 1969 N95-25384
p 1959 N95-25385
p 1941 N95-25386
p 2021 N95-25477
p 2055 N95-25484
p 1973 N95-25557
p 1973 N95-25565
p 2070 N95-25594
p 1926 N95-25596
p 1924 N95-25597
p 2089 N95-25598
p 2110 N95-25675
p 2033 N95-25676
p 2110 N95-25766
p 2033 N95-25767
p 1937 N95-26014
p 2022 N95-26066
p 1973 N95-26112
W-7405-ENG-48 ..... p 2075 N95-24270
p 1933 N95-24329
p 2076 N95-24490
p 2076 N95-24544
p 2076 N95-24548
p 2046 N95-24549
p 1975 N95-24550
p 2077 N95-24646
p 2078 N95-24650
p 2067 N95-24651
p 1968 N95-24657
p 2016 N95-24898
p 1972 N95-25100
p 2078 N95-25102
p 2079 N95-25250
p 2000 N95-25279
p 2005 N95-25287
p 1931 N95-25291
p 2080 N95-25344
p 2006 N95-25635
p 1966 N95-26063
p 2091 N95-26170

Typical Report Number Index Listing

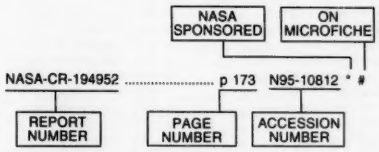

Listings in this index are arranged alphanumerically by report number. The accession number denotes the number by which the citation is identified. The page number helps to locate the citation in the abstract section. An asterisk (*) indicates that the item is a NASA report. A pound sign (#) indicates that the item is available on microfiche.

A-950044 ..... p 1910 N95-24436 * #
A-950049 ..... p 1910 N95-24629 * #
A-950051 ..... p 1908 N95-26302 * #

ACHRE-95003265 ..... p 2011 N95-24497 #

AD-A279147 ..... p 1989 N95-24422
AD-A279292 ..... p 2010 N95-24309
AD-A279303 ..... p 2010 N95-24423
AD-A279692 ..... p 1915 N95-24424
AD-A286558 ..... p 1989 N95-24502 #
AD-A286613 ..... p 1952 N95-24503
AD-A286614 ..... p 1956 N95-24447 #
AD-A288202 ..... p 2017 N95-25507
AD-A288217 ..... p 1911 N95-25578
AD-A288357 ..... p 1920 N95-25508
AD-A288358 ..... p 2033 N95-25509
AD-A288360 ..... p 1942 N95-25510
AD-A288361 ..... p 1951 N95-25513
AD-A288365 ..... p 2033 N95-25601
AD-A288369 ..... p 1924 N95-25602
AD-A288383 ..... p 2026 N95-25603
AD-A288389 ..... p 1954 N95-25604
AD-A288392 ..... p 2007 N95-25605
AD-A288395 ..... p 1969 N95-25606
AD-A288447 ..... p 1936 N95-25502
AD-A288618 ..... p 1905 N95-25607
AD-A288620 ..... p 2106 N95-25608
AD-A288624 ..... p 1910 N95-25609
AD-A288628 ..... p 2014 N95-25610
AD-A288666 ..... p 2007 N95-26048
AD-A288682 ..... p 1942 N95-26049
AD-A288685 ..... p 1977 N95-26050
AD-A288688 ..... p 2035 N95-26051
AD-A288689 ..... p 1915 N95-26053
AD-A288692 ..... p 2022 N95-26054
AD-A288701 ..... p 2013 N95-26010
AD-A288704 ..... p 2006 N95-26012
AD-A288713 ..... p 1970 N95-26113
AD-A288727 ..... p 2039 N95-25503
AD-A288733 ..... p 1979 N95-26055
AD-A288735 ..... p 1932 N95-26056
AD-A288737 ..... p 1937 N95-26057
AD-A288743 ..... p 2018 N95-26058
AD-A288750 ..... p 1970 N95-26059
AD-A288760 ..... p 1912 N95-26060
AD-A288761 ..... p 1949 N95-25517
AD-A288769 ..... p 2090 N95-26061
AD-A288777 ..... p 1974 N95-26114
AD-A288780 ..... p 1961 N95-26186
AD-A288784 ..... p 1947 N95-26188
AD-A288786 ..... p 1913 N95-26190
AD-A288787 ..... p 1949 N95-25528
AD-A288791 ..... p 1956 N95-26191
AD-A288804 ..... p 2015 N95-26192
AD-A288807 ..... p 2009 N95-26193
AD-A288886 ..... p 2006 N95-25504
AD-A288888 ..... p 2075 N95-26173
AD-A288903 ..... p 1936 N95-25529
AD-A288923 ..... p 1926 N95-25505
AD-A288950 ..... p 2074 N95-25506
AD-A289139 ..... p 2075 N95-26039
AD-A289292 ..... p 1990 N95-26040
AD-A289453 ..... p 2006 N95-26197
AD-A289785 ..... p 2013 N95-26041

AFCESA/ESL-TR-92-25 ..... p 1915 N95-24424

AFIT/CI/CIA-94-151 ..... p 2006 N95-26197

AFIT/GEO/ENP/94D-06 ..... p 1990 N95-26040

AFOSR-94-0756TR ..... p 1911 N95-25578

AGARD-R-802 ..... p 2107 N95-26334 #

AGS/AD-94-5 ..... p 2064 N95-24287 #

AIAA PAPER 95-0467 ..... p 2018 N95-25879 * #
AIAA PAPER 95-0732 ..... p 1913 N95-24390 * #

AL-TR-1994-0116 ..... p 1905 N95-25607

AL/CF-TR-1994-0087 ..... p 2013 N95-26041

ANL-HEP-CP-94-66 ..... p 2042 N95-24292 #
ANL-HEP-CP-94-68 ..... p 2043 N95-24326 #
ANL-HEP-CP-94-76 ..... p 2043 N95-24332 #

ANL-HEP-TR-94-60 ..... p 2068 N95-24680 #

ANL-93/30 ..... p 2020 N95-24658 #

ANL/APS/TB-20 ..... p 2069 N95-25300 #

ANL/BIM/PP-78964 ..... p 2010 N95-24427 #

ANL/CHM/PP-82180 ..... p 2045 N95-24459 #

ANL/CMT/CP-84099 ..... p 1991 N95-24607 #

ANL/DIS/CP-84374 ..... p 2103 N95-24330 #

ANL/ES/CP-84872 ..... p 2000 N95-25363 #

ANL/ESD-26 ..... p 1998 N95-24618 #

ANL/ET/CP-84649 ..... p 2088 N95-25282 #

ANL/FPP/TM-271 ..... p 2078 N95-24861 #
ANL/FPP/TM-277 ..... p 2083 N95-26185 #

ANL/MCS-TM-186 ..... p 2019 N95-24342 #
ANL/MCS-TM-200 ..... p 2008 N95-25181 #

ANL/MSD/CP-83118 ..... p 2087 N95-24855 #
ANL/MSD/CP-84398 ..... p 2084 N95-24279 #
ANL/MSD/CP-84768 ..... p 2088 N95-25280 #
ANL/MSD/CP-84784 ..... p 2087 N95-24868 #

ANL/PHY/CP-84104 ..... p 2069 N95-25281 #

AR-008-386 ..... p 1911 N95-25935
AR-008-389 ..... p 1914 N95-25936
AR-008-399 ..... p 1975 N95-24393
AR-008-923 ..... p 1905 N95-24200
AR-008-924 ..... p 1905 N95-24201
AR-008-938 ..... p 1966 N95-24203
AR-008-944 ..... p 1947 N95-24394

ARCCB-TR-94034 ..... p 2033 N95-25509

ARL-CR-194 ..... p 1912 N95-26060
ARL-CR-221 ..... p 1952 N95-24395 * #

ARL-GD-43 ..... p 1911 N95-25935

ARL-MR-198 ..... p 2035 N95-26051

ARL-SR-18 ..... p 1969 N95-25606

ARL-TN-48 ..... p 1914 N95-25936

ARL-TR-516 ..... p 1979 N95-26055
ARL-TR-748 ..... p 1977 N95-26076 * #
ARL-TR-760 ..... p 1977 N95-26074 * #

ASIPP-0038 ..... p 2082 N95-25943 #
ASIPP-0039 ..... p 2082 N95-25942 #

ATCOM-TR-95-A-001 ..... p 1907 N95-24566 * #

ATR-92(7251)-4 ..... p 2080 N95-25325 * #
ATR-95(9558)-2 ..... p 2075 N95-26198 #

AVC-92-193 ..... p 2112 N95-24672 *

B-259204 ..... p 1911 N95-26338 #

BARC-1993/E/025 ..... p 1958 N95-24690 #
BARC-1993/E/027 ..... p 2042 N95-24269 #

BNL-60824 ..... p 2064 N95-24287 #
BNL-60981 ..... p 2048 N95-24677 #
BNL-61007 ..... p 2068 N95-24685
BNL-61011 ..... p 2087 N95-24849 #
BNL-61078 ..... p 2008 N95-25383 #
BNL-61083 ..... p 1928 N95-24265
BNL-61084 ..... p 1928 N95-24257 #
BNL-61099 ..... p 2052 N95-25374 #
BNL-61120 ..... p 2113 N95-25364 #
BNL-61136 ..... p 1930 N95-25123 #
BNL-61139 ..... p 2085 N95-24451 #
BNL-61141 ..... p 2052 N95-25375 #
BNL-61142 ..... p 2093 N95-24450 #
BNL-61179 ..... p 2044 N95-24420 #
BNL-61220 ..... p 2001 N95-25442 #
BNL-61230 ..... p 1997 N95-24570 #
BNL-61246 ..... p 2070 N95-25369 #
BNL-61251 ..... p 2070 N95-25441 #
BNL-61252 ..... p 2071 N95-25785 #
BNL-61253 ..... p 2026 N95-25368 #
BNL-61258 ..... p 2064 N95-26006 #
BNL-61267 ..... p 2065 N95-24357 #
BNL-61272 ..... p 1968 N95-24623 #

BUDKERINP-93-40 ..... p 2041 N95-24267 #

CAL-2294 ..... p 2108 N95-25104 * #

CAP-109-MUON-94C ..... p 2085 N95-24357 #

CARDIVNSWC-TR-61-94/28 ..... p 1937 N95-26057

CBPF-NF-008/94 ..... p 2095 N95-24838 #
CBPF-NF-010/94 ..... p 2093 N95-24352 #
CBPF-NF-020/93 ..... p 1937 N95-25751 #
CBPF-NF-032/93 ..... p 2093 N95-24353 #
CBPF-NF-043/93 ..... p 2093 N95-24446 #
CBPF-NF-044/93 ..... p 1959 N95-24842 #
CBPF-NF-046/93 ..... p 1959 N95-25405 #
CBPF-NF-055/93 ..... p 2095 N95-24833 #
CBPF-NF-062/93 ..... p 2043 N95-24350 #
CBPF-NF-064/93 ..... p 2095 N95-24834 #
CBPF-NF-067/93 ..... p 1930 N95-24840 #
CBPF-NF-075/93 ..... p 2095 N95-24837 #

CERN-94-02 ..... p 2062 N95-25944 #

CMOTT-94-4 ..... p 1966 N95-26077 * #

CNIC-00736 ..... p 2049 N95-24724 #
CNIC-00789 ..... p 2082 N95-25943 #
CNIC-00797 ..... p 2072 N95-26095 #
CNIC-00808 ..... p 2082 N95-25942 #
CNIC-00817 ..... p 1970 N95-25940 #

CONF-9204102-11 ..... p 1977 N95-26172 #
CONF-9210482 ..... p 2072 N95-26162 #
CONF-9303297 ..... p 2021 N95-25303 #
CONF-9303298 ..... p 1931 N95-25356 #
CONF-9304280-1 ..... p 1993 N95-24853 #

CONF-9305384 ..... p 2055 N95-25499 #
CONF-9306258 ..... p 2049 N95-24722 #
CONF-9306388 ..... p 2038 N95-25552
CONF-9306388 ..... p 2038 N95-25553
CONF-9306388 ..... p 2056 N95-25554
CONF-9306388 ..... p 2081 N95-25555
CONF-9306388 ..... p 2038 N95-25616
CONF-9306398-1 ..... p 2050 N95-24901 #
CONF-9306401 ..... p 1999 N95-24904 #
CONF-930761-1 ..... p 2043 N95-24354 #
CONF-9309405 ..... p 2082 N95-25903 #
CONF-931077-1 ..... p 2044 N95-24419 #
CONF-9311139 ..... p 2104 N95-24372 #
CONF-931254-10 ..... p 2026 N95-25368 #
CONF-931254-11 ..... p 2071 N95-25785 #
CONF-931254-8 ..... p 2070 N95-25441 #
CONF-931254-9 ..... p 2070 N95-25369 #
CONF-940142-48 ..... p 1973 N95-26112 #
CONF-940268 ..... p 2056 N95-25614 #
CONF-940301-45 ..... p 1924 N95-25597 #
CONF-9403122-4 ..... p 2092 N95-24333 #
CONF-9403132-2 ..... p 2020 N95-24496 #
CONF-9403139-2 ..... p 2051 N95-25294 #
CONF-9403198-1 ..... p 2051 N95-25292 #
CONF-940399-2 ..... p 1926 N95-25596 #
CONF-940414-6 ..... p 1929 N95-24345 #
CONF-9404228-1 ..... p 2051 N95-25372 #
CONF-940492 ..... p 2068 N95-24665 #
CONF-9405162-2 ..... p 2109 N95-24327 #
CONF-9405170-3 ..... p 2050 N95-25099 #
CONF-9405170-8 ..... p 2091 N95-26170 #
CONF-9405204-3 ..... p 2093 N95-24457 #
CONF-9405216-3 ..... p 2113 N95-25364 #
CONF-9405264-1 ..... p 2109 N95-24234 #
CONF-9405275-1 ..... p 2074 N95-25357 #
CONF-940528-7 ..... p 1972 N95-25549 #
CONF-940536-2 ..... p 2021 N95-25378 #
CONF-940552-33 ..... p 2079 N95-25120 #
CONF-940580-22 ..... p 2078 N95-24650 #
CONF-940580-23 ..... p 2076 N95-24490 #
CONF-940592-10 ..... p 1972 N95-25100 #
CONF-940618-114 ..... p 1974 N95-24356 #
CONF-940618-115 ..... p 2065 N95-24409 #
CONF-940618-116 ..... p 2065 N95-24357 #
CONF-9406207-2 ..... p 2009 N95-26169 #
CONF-9406248-5 ..... p 2096 N95-24867 #
CONF-9406263 ..... p 2001 N95-25615 #
CONF-9406269-4 ..... p 2001 N95-25629
CONF-9406274-2 ..... p 2066 N95-24495 #
CONF-9406275-1 ..... p 1998 N95-24606 #
CONF-9406292-1 ..... p 2068 N95-24685
CONF-9406297-1 ..... p 2106 N95-25765 #
CONF-940630-51 ..... p 2076 N95-24544 #
CONF-940630-52 ..... p 2067 N95-24651 #
CONF-940693-5 ..... p 2047 N95-24662 #
CONF-9407701-22 ..... p 2087 N95-24868 #
CONF-9407129-4 ..... p 2003 N95-24577 #
CONF-9407135-2 ..... p 2092 N95-24328 #
CONF-9407135-3 ..... p 2046 N95-24576 #
CONF-940714-47 ..... p 1928 N95-24265
CONF-940714-48 ..... p 2038 N95-25408 #
CONF-9407142-5 ..... p 2041 N95-24254 #
CONF-9407142-6 ..... p 2041 N95-24256 #
CONF-9407142-7 ..... p 2041 N95-24253 #
CONF-9407153-VOL-1 ..... p 1956 N95-24452 #
CONF-9407153-VOL-2 ..... p 1957 N95-24453 #
CONF-9407156-1 ..... p 2088 N95-25282 #
CONF-9407157-1 ..... p 2052 N95-25374 #
CONF-9407157-2 ..... p 2044 N95-24414 #
CONF-9407158-1 ..... p 2094 N95-24578 #
CONF-9407160-1 ..... p 1931 N95-25291 #
CONF-940722-33 ..... p 2068 N95-24728 #
CONF-940722-35 ..... p 2056 N95-25563 #
CONF-940722-36 ..... p 2048 N95-24677 #
CONF-940722-37 ..... p 2045 N95-24435 #
CONF-940722-38 ..... p 2045 N95-24434 #
CONF-940722-40 ..... p 2050 N95-24902 #
CONF-940723-32 ..... p 1968 N95-24657 #
CONF-940812-4 ..... p 1920 N95-24711 #
CONF-9408125-46 ..... p 2066 N95-24572 #
CONF-9408125-48 ..... p 2067 N95-24573 #
CONF-9408127-5 ..... p 2078 N95-24667 #
CONF-940813-33 ..... p 1931 N95-25252 #
CONF-9408131-5 ..... p 1928 N95-24257 #
CONF-940815-101 ..... p 1930 N95-25098 #
CONF-940816-50 ..... p 2015 N95-24648 #
CONF-940816-53 ..... p 2067 N95-24661 #
CONF-940816-54 ..... p 2047 N95-24660 #
CONF-940816-59 ..... p 2067 N95-24601 #
CONF-940816-65 ..... p 2052 N95-25402 #
CONF-940816-66 ..... p 2068 N95-25238 #
CONF-940816-69 ..... p 2050 N95-24903 #
CONF-940816-70 ..... p 2069 N95-25297 #
CONF-940816-71 ..... p 2046 N95-24593 #
CONF-940816-73 ..... p 2046 N95-24575 #
CONF-940816-75 ..... p 2046 N95-24571 #
CONF-940816-76 ..... p 2044 N95-24418 #
CONF-940816-77 ..... p 2047 N95-24622 #
CONF-940816-78 ..... p 2047 N95-24641 #
CONF-940816-79 ..... p 2044 N95-24417 #
CONF-940816-80 ..... p 2044 N95-24415 #
CONF-940816-81 ..... p 2067 N95-24574 #
CONF-940816-82 ..... p 2052 N95-25377 #
CONF-940816-83 ..... p 2071 N95-26011
CONF-940816-88 ..... p 2044 N95-24420 #
CONF-9408186 ..... p 1972 N95-25491 #
CONF-9408189-1 ..... p 2077 N95-24646 #
CONF-9408196-2 ..... p 1973 N95-25565 #
CONF-9408198-1 ..... p 2111 N95-26284 #
CONF-9408202-1 ..... p 2021 N95-25359 #
CONF-9408202-2 ..... p 2015 N95-25773 #
CONF-9408207-1 ..... p 2033 N95-25767 #
CONF-940843-13 ..... p 2069 N95-25365 #
CONF-940873-3 ..... p 2104 N95-24603 #
CONF-940888-VOL-2 ..... p 2070 N95-25478 #
CONF-940903-1 ..... p 2091 N95-26087 #
CONF-9409103-12 ..... p 2043 N95-24332 #
CONF-9409103-9 ..... p 2042 N95-24292 #
CONF-9409186-2 ..... p 2020 N95-24597 #
CONF-940920-2 ..... p 1924 N95-25286 #
CONF-9409241-5 ..... p 2030 N95-24609 #
CONF-9409241-6 ..... p 2033 N95-25676 #
CONF-9409241-7 ..... p 2096 N95-25293 #
CONF-9409255-2 ..... p 2001 N95-25442 #
CONF-9409257-1 ..... p 2047 N95-24663 #
CONF-9409257-3 ..... p 2041 N95-24252 #
CONF-9409258-1 ..... p 2068 N95-24664 #
CONF-940926-3 ..... p 2084 N95-24279 #
CONF-9409264-1 ..... p 2091 N95-24235 #
CONF-9409268-2 ..... p 1972 N95-24869 #
CONF-9409269-1 ..... p 2087 N95-24849 #
CONF-9409269-2 ..... p 2085 N95-24451 #
CONF-9409269-3 ..... p 2093 N95-24450 #
CONF-9409269-4 ..... p 2094 N95-24610 #
CONF-9409270-1 ..... p 2109 N95-25122 * #
CONF-9409270-2 ..... p 2069 N95-25366 #
CONF-9409277-1 ..... p 2046 N95-24591 #
CONF-9409277-2 ..... p 2052 N95-25375 #
CONF-9409277-3 ..... p 2051 N95-25296 #
CONF-9409278-1 ..... p 2022 N95-26013 #
CONF-9409278-2 ..... p 2106 N95-25774 #
CONF-9409278-3 ..... p 2021 N95-24881 #
CONF-9409280-1 ..... p 2106 N95-25376 #
CONF-9409283-1 ..... p 2098 N95-25530 #
CONF-9409284-1 ..... p 2110 N95-25675 #
CONF-9409286-1 ..... p 1937 N95-26007 #
CONF-9409287-1 ..... p 2044 N95-24420 #
CONF-940933-16 ..... p 2076 N95-24548 #
CONF-940933-23 ..... p 2078 N95-25102 #
CONF-940933-24 ..... p 2050 N95-25180 #
CONF-940963-1 ..... p 2043 N95-24326 #
CONF-941006-3 ..... p 1957 N95-24488 #
CONF-941007-2 ..... p 1934 N95-24480 #
CONF-9410113-16 ..... p 2087 N95-24855 #
CONF-9410141-4 ..... p 2103 N95-24330 #
CONF-9410141-6 ..... p 2104 N95-24454 #
CONF-9410155-1 ..... p 1979 N95-24263 #
CONF-941016-3 ..... p 1935 N95-25388 #
CONF-941016-5 ..... p 1934 N95-24433 #
CONF-9410163-1 ..... p 2079 N95-25108 #
CONF-9410165-10 ..... p 2085 N95-24431 #
CONF-9410165-6 ..... p 2037 N95-24479 #
CONF-9410170-2 ..... p 1991 N95-24607 #
CONF-9410193-1 ..... p 1931 N95-25492 #
CONF-9410213-4 ..... p 1935 N95-25390 #
CONF-9410218-4 ..... p 1958 N95-24589 #
CONF-9410218-6 ..... p 2070 N95-25406 #
CONF-9410229-2 ..... p 2073 N95-25239 #
CONF-9410237-1 ..... p 2105 N95-24675 #
CONF-9410237-2 ..... p 2000 N95-25278 #
CONF-9410249-2 ..... p 2079 N95-25250 #
CONF-9410254-1 ..... p 1948 N95-24608 #
CONF-9410256-1 ..... p 1975 N95-24550 #
CONF-9410256-2 ..... p 1978 N95-26286 #
CONF-9410259-1 ..... p 1989 N95-25110
CONF-9410275-1 ..... p 2069 N95-25281 #
CONF-9410283-1 ..... p 2038 N95-25600 #
CONF-9410285-1 ..... p 2064 N95-26006 #
CONF-9410287-1 ..... p 2110 N95-25766 #
CONF-9410287-3 ..... p 2109 N95-24455 #
CONF-9410291-1 ..... p 2020 N95-24612 #
CONF-941041-1 ..... p 1973 N95-25557 #
CONF-941043-7 ..... p 2004 N95-25666 #
CONF-941070-2 ..... p 2102 N95-25771 * #
CONF-9411105-1 ..... p 1930 N95-25097 #
CONF-9411120-3 ..... p 2065 N95-24320 #
CONF-9411135-1-REV-1 ..... p 1939 N95-24344 #
CONF-9411151-1 ..... p 1958 N95-24532
CONF-9411152-1 ..... p 2066 N95-24500 #
CONF-9411152-3 ..... p 2069 N95-25358 #
CONF-9411172-1 ..... p 2088 N95-25280 #
CONF-9411173-2 ..... p 2064 N95-26256 #
CONF-9411180-1 ..... p 1999 N95-25249 #
CONF-9411182-1 ..... p 2070 N95-25594 #
CONF-9411182-2 ..... p 2080 N95-25289 #
CONF-941129-10 ..... p 2046 N95-24549 #
CONF-941139-1 ..... p 2000 N95-25380 #
CONF-941142-26 ..... p 1962 N95-24489 #
CONF-941144-10 ..... p 2086 N95-24513 #
CONF-941144-19 ..... p 1930 N95-25242 #
CONF-941144-24 ..... p 1942 N95-25898 #
CONF-941144-26 ..... p 2088 N95-25288 #
CONF-941144-27 ..... p 2090 N95-25897 #
CONF-941144-31 ..... p 1934 N95-24449 #
CONF-941144-32 ..... p 2088 N95-25002 #
CONF-941144-33 ..... p 2087 N95-24616 #
CONF-941144-34 ..... p 2089 N95-25598 #
CONF-941144-35 ..... p 1941 N95-25370 #
CONF-941144-37 ..... p 2087 N95-24617 #
CONF-941144-38 ..... p 1937 N95-26014
CONF-941144-39 ..... p 1935 N95-25379 #
CONF-941144-42 ..... p 1941 N95-25382 #
CONF-941144-43 ..... p 1926 N95-25295 #
CONF-941144-53 ..... p 1933 N95-24432 #
CONF-941144-54 ..... p 1940 N95-24456 #
CONF-941144-6 ..... p 2083 N95-24233 #
CONF-941144-9 ..... p 2086 N95-24514 #
CONF-941182-1 ..... p 2077 N95-24602 #
CONF-941186-1 ..... p 2065 N95-24331 #
CONF-941203-13 ..... p 1990 N95-24264 #
CONF-941203-15 ..... p 1996 N95-26166 #
CONF-941203-16 ..... p 1994 N95-25360 #
CONF-941203-17 ..... p 1996 N95-26285 #
CONF-941203-19 ..... p 1995 N95-25566 #
CONF-941210-2 ..... p 1995 N95-26090 #
CONF-941218-2 ..... p 1995 N95-25995 #
CONF-941245-1 ..... p 2000 N95-25363 #
CONF-941246-6 ..... p 2102 N95-24905 #
CONF-941250-1 ..... p 1941 N95-25243 #
CONF-941251-1 ..... p 2052 N95-25407 #
CONF-950110-3 ..... p 1958 N95-24586 #
CONF-950117-2 ..... p 2064 N95-26168 #
CONF-950124-3 ..... p 2006 N95-25635 #
CONF-950124-4 ..... p 2005 N95-25287 #
CONF-950129-1 ..... p 1940 N95-24717 #
CONF-950130-2 ..... p 1961 N95-24262 #
CONF-950130-3 ..... p 1906 N95-24308 #
CONF-950130-4 ..... p 1965 N95-25895 #
CONF-950130-6 ..... p 1966 N95-26240
CONF-950201-1 ..... p 1925 N95-24590 #
CONF-950212-1 ..... p 2019 N95-24343 #
CONF-950212-2 ..... p 2015 N95-24346 #
CONF-950212-4 ..... p 2021 N95-24681 #
CONF-950226-1 ..... p 1971 N95-24408 #
CONF-950226-2 ..... p 2089 N95-25353 #
CONF-950226-3 ..... p 1981 N95-24598 #
CONF-950226-5 ..... p 2074 N95-25559 #
CONF-950232-2 ..... p 1953 N95-24605 #
CONF-950240-2 ..... p 1975 N95-24462 #
CONF-950242-1 ..... p 2016 N95-24898 #
CONF-950247-1 ..... p 1948 N95-24670 #
CONF-950259-1 ..... p 2054 N95-25470 #
CONF-950262-1 ..... p 2089 N95-25391 #
CONF-950263-1 ..... p 1937 N95-25775 #
CONF-950265-1 ..... p 2089 N95-25389 #
CONF-950336-13 ..... p 1992 N95-24682 #
CONF-950336-18 ..... p 1994 N95-25309 #
CONF-950336-2 ..... p 1992 N95-24674 #
CONF-950336-3 ..... p 1992 N95-24714 #
CONF-950336-6 ..... p 1994 N95-25109 #
CONF-950336-7 ..... p 1992 N95-24676 #
CONF-950336-9 ..... p 1993 N95-24715 #
CONF-950344-1 ..... p 1959 N95-24712 #
CONF-950344-2 ..... p 1959 N95-24713 #
CONF-950344-3 ..... p 1935 N95-24716 #
CONF-950402-2 ..... p 1929 N95-24614 #
CONF-950402-3 ..... p 1997 N95-24570 #
CONF-950413-1 ..... p 1966 N95-26063 #
CONF-950436-1 ..... p 1960 N95-25558 #
CONF-950439-6 ..... p 2004 N95-25476 #
CONF-950443-2 ..... p 1938 N95-26064 #
CONF-950484-1 ..... p 2022 N95-26066 #

CRAD-9310-TR-0127 ..... p 2040 N95-26160 * #

CRIE-R-01 ..... p 1953 N95-24848 #
CRIE-R-93009 ..... p 1952 N95-24491 #
CRIE-R-93015 ..... p 2104 N95-24492 #
CRIE-R-94001 ..... p 1952 N95-24493 #
CRIE-R-94002 ..... p 2104 N95-24494 #

CRSSA-8/FH/TP ..... p 2010 N95-24310

CSD-5597-93-2 ..... p 1921 N95-24440 * #
CSD-5597-93-2 ..... p 1922 N95-24844 * #
CSD-5597-93-2 ..... p 1922 N95-24845 * #
CSD-5597-93-2 ..... p 1922 N95-24854 * #

CSE-TR-193-94 ..... p 2019 N95-26206 * #

CSEL-1994-TR-03 ..... p 2026 N95-25335 * #

CSIRO-TP-31 ..... p 1999 N95-25199

CSRD-1097 ..... p 2030 N95-24557 #

CUED/A-AEREO/TR-23 ..... p 1906 N95-24210 #

DE94-000225 ..... p 1991 N95-24666 #
DE94-011862 ..... p 1993 N95-24853 #
DE94-011900 ..... p 1990 N95-24305 #
DE94-012258 ..... p 1990 N95-24318 #
DE94-012554 ..... p 2104 N95-24372 #
DE94-013121 ..... p 1920 N95-24711 #
DE94-013641 ..... p 2068 N95-24899 #
DE94-013857 ..... p 2008 N95-24600 #
DE94-014108 ..... p 2050 N95-25099 #
DE94-014130 ..... p 1966 N95-26063 #
DE94-015768 ..... p 1959 N95-24712 #
DE94-016565 ..... p 1959 N95-24713 #
DE94-016584 ..... p 2079 N95-25108 #
DE94-017394 ..... p 1998 N95-24653 #
DE94-018160 ..... p 2104 N95-24603 #
DE94-019161 ..... p 1938 N95-26064 #
DE94-627162 ..... p 2093 N95-24481 #
DE94-627566 ..... p 2086 N95-24537 #
DE94-628176 ..... p 1957 N95-24482 #
DE94-628177 ..... p 1957 N95-24483 #
DE94-628251 ..... p 1968 N95-24635 #
DE94-628253 ..... p 1967 N95-24484 #
DE94-628254 ..... p 2045 N95-24485 #
DE94-628255 ..... p 1967 N95-24486 #
DE94-628256 ..... p 2073 N95-24642 #
DE94-628257 ..... p 1957 N95-24487 #
DE94-628258 ..... p 2047 N95-24644 #
DE94-628372 ..... p 2035 N95-24643 #
DE94-628374 ..... p 2030 N95-24645 #
DE94-628375 ..... p 2035 N95-24858 #
DE94-628376 ..... p 2031 N95-24859 #
DE94-628377 ..... p 2031 N95-24704 #
DE94-628378 ..... p 2031 N95-24705 #
DE94-628379 ..... p 2036 N95-24688 #
DE94-628380 ..... p 2048 N95-24689 #
DE94-628381 ..... p 1958 N95-24690 #
DE94-628384 ..... p 2030 N95-24691 #
DE94-628385 ..... p 2048 N95-24692 #
DE94-628386 ..... p 2035 N95-24693 #
DE94-628387 ..... p 2031 N95-24694 #
DE94-628388 ..... p 2031 N95-24695 #
DE94-628406 ..... p 2037 N95-24696 #
DE94-628407 ..... p 2031 N95-24697 #
DE94-628435 ..... p 2031 N95-24698 #
DE94-628436 ..... p 2036 N95-24699 #
DE94-628437 ..... p 2048 N95-24700 #
DE94-628440 ..... p 2030 N95-24636 #
DE94-628441 ..... p 2032 N95-24860 #
DE94-628494 ..... p 2035 N95-24883 #
DE94-628500 ..... p 2036 N95-24504 #
DE94-628519 ..... p 1952 N95-24506 #
DE94-628520 ..... p 2094 N95-24507 #
DE94-628521 ..... p 2094 N95-24508 #
DE94-628523 ..... p 2050 N95-25094 #
DE94-628524 ..... p 2094 N95-24509 #
DE94-628529 ..... p 2096 N95-25095 #
DE94-628530 ..... p 2096 N95-25096 #
DE94-628531 ..... p 2096 N95-25215 #
DE94-628558 ..... p 2109 N95-24884 #
DE94-628561 ..... p 2109 N95-24885 #
DE94-628562 ..... p 2109 N95-24886 #
DE94-628578 ..... p 2094 N95-24637 #
DE94-628579 ..... p 2094 N95-24638 #
DE94-628580 ..... p 2095 N95-24639 #
DE94-628586 ..... p 2095 N95-24727 #
DE94-628587 ..... p 2047 N95-24640 #
DE94-628598 ..... p 2047 N95-24668 #
DE94-628599 ..... p 2048 N95-24669 #
DE94-628605 ..... p 2049 N95-24719 #
DE94-628606 ..... p 2049 N95-24720 #
DE94-628617 ..... p 2049 N95-24722 #
DE94-628628 ..... p 2049 N95-24887 #
DE94-628629 ..... p 2055 N95-25537
DE94-628630 ..... p 2049 N95-24888 #
DE94-628636 ..... p 2095 N95-24723 #
DE94-628655 ..... p 2055 N95-25538
DE94-628768 ..... p 2049 N95-24724 #
DE94-628772 ..... p 2049 N95-24889 #
DE94-628867 ..... p 2048 N95-24718 #
DE94-628904 ..... p 2050 N95-24890 #
DE94-628905 ..... p 2033 N95-25539
DE94-628961 ..... p 2078 N95-24706 #
DE94-629003 ..... p 2090 N95-25851
DE94-629014 ..... p 1972 N95-24707 #
DE94-629015 ..... p 2087 N95-24891 #
DE94-634273 ..... p 2016 N95-24708 #
DE94-634282 ..... p 2027 N95-24228 #
DE94-634285 ..... p 2092 N95-24266 #
DE94-634309 ..... p 2041 N95-24267 #
DE94-634310 ..... p 2041 N95-24268 #
DE94-634311 ..... p 2029 N95-24401 #
DE94-634313 ..... p 2073 N95-24402 #
DE94-634314 ..... p 1952 N95-24403 #
DE94-634327 ..... p 2027 N95-24229 #
DE94-634329 ..... p 2095 N95-24767 #
DE94-634361 ..... p 2043 N95-24404 #
DE94-634362 ..... p 2051 N95-25290 #
DE94-634363 ..... p 2096 N95-25107 #
DE94-634364 ..... p 2093 N95-24405 #
DE94-634442 ..... p 2040 N95-24230 #
DE94-634462 ..... p 2040 N95-24231 #
DE94-634488 ..... p 2041 N95-24232 #
DE94-634524 ..... p 2084 N95-24324 #
DE94-634528 ..... p 2092 N95-24288 #
DE94-634529 ..... p 2084 N95-24244 #
DE94-634530 ..... p 1956 N95-24245 #
DE94-634531 ..... p 2084 N95-24246 #
DE94-634857 ..... p 2092 N95-24275 #
DE94-634858 ..... p 2028 N95-24276 #
DE94-634859 ..... p 2092 N95-24277 #
DE94-634887 ..... p 2042 N95-24269 #
DE94-636061 ..... p 1939 N95-24373 #
DE94-636293 ..... p 2085 N95-24374 #
DE94-636729 ..... p 2029 N95-24375 #
DE94-636730 ..... p 2029 N95-24387 #
DE94-636733 ..... p 2093 N95-24376 #
DE94-636734 ..... p 1952 N95-24377 #
DE94-636735 ..... p 2093 N95-24378 #
DE94-636736 ..... p 2092 N95-24347 #
DE94-636737 ..... p 2065 N95-24348 #
DE94-636739 ..... p 2093 N95-24349 #
DE94-636740 ..... p 2092 N95-24312 #
DE94-636741 ..... p 2092 N95-24313 #
DE94-636773 ..... p 2042 N95-24314 #
DE94-636790 ..... p 2042 N95-24315 #
DE94-636791 ..... p 2042 N95-24316 #
DE94-636797 ..... p 2043 N95-24360 #
DE94-636799 ..... p 2043 N95-24361 #
DE94-637054 ..... p 2085 N95-24362 #
DE94-637073 ..... p 2037 N95-24363 #
DE94-637113 ..... p 2043 N95-24364 #
DE94-765446 ..... p 1958 N95-24701 #
DE94-765589 ..... p 2048 N95-24702 #
DE94-777528 ..... p 2076 N95-24511 #
DE94-777530 ..... p 2075 N95-24270 #
DE94-777532 ..... p 2075 N95-24271 #
DE94-777533 ..... p 2075 N95-24272 #
DE94-777540 ..... p 2076 N95-24311 #
DE94-777545 ..... p 2077 N95-24585 #
DE94-785101 ..... p 1925 N95-24365 #
DE94-785197 ..... p 2043 N95-24337 #
DE94-785198 ..... p 1933 N95-24338 #
DE94-785265 ..... p 2043 N95-24339 #
DE94-785266 ..... p 1971 N95-24340 #
DE94-785275 ..... p 2056 N95-25614 #
DE94-792620 ..... p 2070 N95-25772 #
DE94-792634 ..... p 2057 N95-25901 #
DE94-792657 ..... p 2070 N95-25631 #
DE94-792664 ..... p 2009 N95-25902 #
DE94-792667 ..... p 2082 N95-25903 #
DE94-792670 ..... p 2082 N95-25904 #
DE94-792684 ..... p 2021 N95-25303 #
DE94-792685 ..... p 1931 N95-25356 #
DE95-000024 ..... p 1992 N95-24683 #
DE95-000129 ..... p 2004 N95-26089 #
DE95-000217 ..... p 1992 N95-24714 #
DE95-000219 ..... p 1993 N95-24715 #
DE95-000238 ..... p 1998 N95-24604
DE95-000257 ..... p 2007 N95-24306 #
DE95-000259 ..... p 2007 N95-24307 #
DE95-000261 ..... p 1995 N95-25995 #
DE95-000264 ..... p 1997 N95-24319 #
DE95-000266 ..... p 1992 N95-24684 #
DE95-000267 ..... p 1994 N95-24882 #
DE95-000275 ..... p 1993 N95-24865 #
DE95-000277 ..... p 1996 N95-26285 #
DE95-000280 ..... p 1978 N95-26286 #
DE95-000282 ..... p 1994 N95-25309 #
DE95-000286 ..... p 1995 N95-26090 #
DE95-000289 ..... p 1993 N95-24866 #
DE95-000539 ..... p 1953 N95-24605 #
DE95-000542 ..... p 1958 N95-24586 #
DE95-000543 ..... p 1935 N95-24716 #
DE95-000842 ..... p 2019 N95-24343 #
DE95-000989 ..... p 2105 N95-24654 #
DE95-001074 ..... p 2037 N95-24479 #
DE95-001146 ..... p 1948 N95-24655 #
DE95-001240 ..... p 1939 N95-24344 #
DE95-001241 ..... p 1934 N95-24480 #
DE95-001386 ..... p 2105 N95-24656 #
DE95-001423 ..... p 1929 N95-24345 #
DE95-001613 ..... p 1992 N95-24674 #
DE95-001616 ..... p 2015 N95-24346 #
DE95-001833 ..... p 1975 N95-24462 #
DE95-001934 ..... p 2003 N95-26091 #
DE95-002158 ..... p 1960 N95-26092 #
DE95-002184 ..... p 2105 N95-24675 #
DE95-002193 ..... p 2016 N95-24898 #
DE95-002258 ..... p 1998 N95-24606 #
DE95-002608 ..... p 1994 N95-25109 #
DE95-002609 ..... p 1992 N95-24676 #
DE95-002658 ..... p 1932 N95-26093 #
DE95-002689 ..... p 2000 N95-25278 #
DE95-002718 ..... p 1948 N95-24670 #
DE95-002854 ..... p 1924 N95-25248 #
DE95-002981 ..... p 2103 N95-24330 #
DE95-002998 ..... p 1991 N95-24607 #
DE95-003028 ..... p 1930 N95-25097 #
DE95-003127 ..... p 1930 N95-25098 #
DE95-003140 ..... p 2007 N95-24225 #
DE95-003170 ..... p 2064 N95-24287 #
DE95-003222 ..... p 2079 N95-25216 #
DE95-003254 ..... p 2079 N95-25120 #
DE95-003255 ..... p 2077 N95-24646 #
DE95-003259 ..... p 1934 N95-24647 #
DE95-003265 ..... p 2011 N95-24497 #
DE95-003295 ..... p 2000 N95-25361 #
DE95-003296 ..... p 2000 N95-25362 #
DE95-003297 ..... p 2003 N95-26065 #
DE95-003342 ..... p 2096 N95-24867 #
DE95-003345 ..... p 2077 N95-24587 #
DE95-003353 ..... p 1948 N95-24608 #
DE95-003354 ..... p 1957 N95-24488 #
DE95-003360 ..... p 1962 N95-24489 #
DE95-003361 ..... p 2066 N95-24500 #
DE95-003368 ..... p 2015 N95-24648 #
DE95-003389 ..... p 1958 N95-24532
DE95-003394 ..... p 1940 N95-24588 #
DE95-003414 ..... p 1994 N95-25121 #
DE95-003416 ..... p 2066 N95-24495 #
DE95-003433 ..... p 2020 N95-24496 #
DE95-003436 ..... p 2045 N95-24512 #
DE95-003438 ..... p 2045 N95-24533 #
DE95-003449 ..... p 2073 N95-24546 #
DE95-003495 ..... p 2067 N95-24601 #
DE95-003496 ..... p 2068 N95-24728 #
DE95-003624 ..... p 2046 N95-24547 #
DE95-003625 ..... p 1989 N95-25110
DE95-003634 ..... p 2083 N95-24233 #
DE95-003638 ..... p 2022 N95-26066 #
DE95-003649 ..... p 2076 N95-24548 #
DE95-003651 ..... p 2046 N95-24549 #
DE95-003652 ..... p 2076 N95-24490 #
DE95-003653 ..... p 2078 N95-24650 #
DE95-003654 ..... p 2067 N95-24651 #
DE95-003656 ..... p 1975 N95-24550 #
DE95-003661 ..... p 2109 N95-24234 #
DE95-003662 ..... p 2091 N95-24235 #
DE95-003663 ..... p 2078 N95-24667 #
DE95-003664 ..... p 1925 N95-24590 #
DE95-003665 ..... p 2086 N95-24513 #
DE95-003668 ..... p 2086 N95-24514 #
DE95-003682 ..... p 1958 N95-24589 #
DE95-003706 ..... p 2065 N95-24331 #
DE95-003732 ..... p 2050 N95-25112 #
DE95-003743 ..... p 2050 N95-24901 #
DE95-003797 ..... p 2067 N95-24652 #
DE95-003813 ..... p 1958 N95-24551 #
DE95-003827 ..... p 2077 N95-24552 #
DE95-003831 ..... p 1976 N95-25101 #
DE95-003834 ..... p 1929 N95-24553 #
DE95-003836 ..... p 1940 N95-24554 #
DE95-003877 ..... p 2078 N95-25102 #
DE95-003900 ..... p 2087 N95-24611 #
DE95-003905 ..... p 1934 N95-24615 #
DE95-003929 ..... p 2048 N95-24677 #
DE95-003955 ..... p 2068 N95-24685
DE95-003962 ..... p 2087 N95-24849 #
DE95-003975 ..... p 1963 N95-24678 #
DE95-003982 ..... p 1948 N95-24679 #
DE95-003985 ..... p 2068 N95-24680 #
DE95-004016 ..... p 1975 N95-24880 #
DE95-004114 ..... p 2048 N95-24671 #
DE95-004125 ..... p 2087 N95-24855 #
DE95-004126 ..... p 2087 N95-24868 #
DE95-004131 ..... p 2000 N95-25363 #
DE95-004179 ..... p 2008 N95-24850 #
DE95-004180 ..... p 1923 N95-24851 #
DE95-004191 ..... p 1931 N95-25492 #
DE95-004198 ..... p 2000 N95-25279 #
DE95-004207 ..... p 1972 N95-25100 #
DE95-004209 ..... p 2076 N95-24544 #
DE95-004210 ..... p 1968 N95-24657 #
DE95-004214 ..... p 2068 N95-24852 #
DE95-004220 ..... p 1941 N95-25237 #
DE95-004234 ..... p 2056 N95-25563 #
DE95-004235 ..... p 2068 N95-25238 #
DE95-004236 ..... p 2073 N95-25239 #

DE95-004237 ..... p 1972 N95-24869 #
DE95-004238 ..... p 2111 N95-26284 #
DE95-004239 ..... p 2052 N95-25402 #
DE95-004247 ..... p 2078 N95-24861 #
DE95-004249 ..... p 1972 N95-24709 #
DE95-004265 ..... p 2020 N95-24658 #
DE95-004267 ..... p 2016 N95-24659 #
DE95-004280 ..... p 2047 N95-24660 #
DE95-004281 ..... p 2067 N95-24661 #
DE95-004282 ..... p 2047 N95-24662 #
DE95-004290 ..... p 2047 N95-24663 #
DE95-004292 ..... p 2068 N95-24664 #
DE95-004300 ..... p 2110 N95-25343 #
DE95-004329 ..... p 2105 N95-24710 #
DE95-004342 ..... p 2080 N95-25344 #
DE95-004354 ..... p 2070 N95-25634 #
DE95-004355 ..... p 2052 N95-25403 #
DE95-004357 ..... p 2109 N95-25122 * #
DE95-004372 ..... p 1965 N95-25404 #
DE95-004374 ..... p 2105 N95-25240 #
DE95-004376 ..... p 2051 N95-25241 #
DE95-004381 ..... p 1972 N95-25549 #
DE95-004384 ..... p 1930 N95-25242 #
DE95-004386 ..... p 1965 N95-25485 #
DE95-004439 ..... p 1930 N95-24686 #
DE95-004442 ..... p 2068 N95-24665 #
DE95-004448 ..... p 2048 N95-24687 #
DE95-004519 ..... p 1940 N95-24717 #
DE95-004521 ..... p 2021 N95-24681 #
DE95-004535 ..... p 1992 N95-24682 #
DE95-004594 ..... p 2043 N95-24332 #
DE95-004595 ..... p 2088 N95-25280 #
DE95-004597 ..... p 2069 N95-25281 #
DE95-004646 ..... p 2084 N95-24279 #
DE95-004648 ..... p 2042 N95-24292 #
DE95-004660 ..... p 2088 N95-25282 #
DE95-004667 ..... p 2079 N95-25283 #
DE95-004669 ..... p 2065 N95-24320 #
DE95-004670 ..... p 2092 N95-24333 #
DE95-004677 ..... p 2074 N95-25357 #
DE95-004678 ..... p 2064 N95-26256 #
DE95-004679 ..... p 2069 N95-25358 #
DE95-004685 ..... p 2015 N95-25773 #
DE95-004687 ..... p 2021 N95-25359 #
DE95-004737 ..... p 1939 N95-24247 #
DE95-004748 ..... p 2035 N95-24248 #
DE95-004757 ..... p 1906 N95-24308 #
DE95-004758 ..... p 1961 N95-24262 #
DE95-004759 ..... p 1965 N95-25895 #
DE95-004761 ..... p 2113 N95-24249 #
DE95-004762 ..... p 2057 N95-25896 #
DE95-004765 ..... p 2090 N95-25897 #
DE95-004766 ..... p 1942 N95-25898 #
DE95-004769 ..... p 2054 N95-25470 #
DE95-004778 ..... p 1979 N95-24263 #
DE95-004779 ..... p 1990 N95-24264 #
DE95-004780 ..... p 1994 N95-25360 #
DE95-004781 ..... p 1996 N95-26166 #
DE95-004791 ..... p 2019 N95-24250 #
DE95-004793 ..... p 2051 N95-25372 #
DE95-004795 ..... p 2051 N95-25373 #
DE95-004834 ..... p 1928 N95-24265
DE95-004838 ..... p 2052 N95-25374 #
DE95-004840 ..... p 2052 N95-25375 #
DE95-004844 ..... p 1928 N95-24257 #
DE95-004849 ..... p 2106 N95-25376 #
DE95-004850 ..... p 2052 N95-25377 #
DE95-004851 ..... p 2041 N95-24252 #
DE95-004852 ..... p 2041 N95-24253 #
DE95-004853 ..... p 2041 N95-24254 #
DE95-004855 ..... p 2041 N95-24256 #
DE95-004862 ..... p 1941 N95-25243 #
DE95-004864 ..... p 2041 N95-24258 #
DE95-004865 ..... p 2071 N95-26011
DE95-004870 ..... p 2079 N95-25250 #
DE95-004876 ..... p 2032 N95-25251 #
DE95-004878 ..... p 2008 N95-24843 #
DE95-004896 ..... p 1931 N95-25252 #
DE95-004901 ..... p 2106 N95-25774 #
DE95-004903 ..... p 1999 N95-25249 #
DE95-004907 ..... p 2088 N95-25288 #
DE95-004909 ..... p 2021 N95-24881 #
DE95-004910 ..... p 2088 N95-25002 #
DE95-004928 ..... p 2102 N95-25771 * #
DE95-004929 ..... p 2009 N95-26169 #
DE95-004930 ..... p 1924 N95-25286 #
DE95-004935 ..... p 2022 N95-26013 #
DE95-004941 ..... p 1934 N95-24449 #
DE95-004945 ..... p 2102 N95-24905 #
DE95-004951 ..... p 1930 N95-25123 #
DE95-004952 ..... p 2093 N95-24450 #
DE95-004953 ..... p 2085 N95-24451 #
DE95-004962 ..... p 2050 N95-25180 #
DE95-004963 ..... p 2091 N95-26170 #
DE95-004965 ..... p 2005 N95-25287 #
DE95-004966 ..... p 2006 N95-25635 #
DE95-004990 ..... p 1996 N95-26171 #
DE95-004995 ..... p 2004 N95-25666 #
DE95-005005 ..... p 2113 N95-25364 #
DE95-005019 ..... p 2069 N95-25365 #
DE95-005021 ..... p 2021 N95-25378 #
DE95-005027 ..... p 2069 N95-25366 #
DE95-005036 ..... p 2106 N95-25765 #
DE95-005058 ..... p 1956 N95-24452 #
DE95-005059 ..... p 1957 N95-24453 #
DE95-005067 ..... p 2104 N95-24454 #
DE95-005110 ..... p 2065 N95-24317 #
DE95-005187 ..... p 1939 N95-24285 #
DE95-005202 ..... p 1928 N95-24286 #
DE95-005206 ..... p 1929 N95-24341
DE95-005208 ..... p 1937 N95-26014
DE95-005212 ..... p 2109 N95-24455 #
DE95-005213 ..... p 1940 N95-24456 #
DE95-005233 ..... p 2110 N95-25766 #
DE95-005239 ..... p 2093 N95-24457 #
DE95-005240 ..... p 2033 N95-25767 #
DE95-005241 ..... p 2030 N95-24609 #
DE95-005243 ..... p 1926 N95-25596 #
DE95-005245 ..... p 2094 N95-24610 #
DE95-005246 ..... p 2110 N95-25675 #
DE95-005247 ..... p 2070 N95-25594 #
DE95-005249 ..... p 1924 N95-25597 #
DE95-005251 ..... p 2020 N95-24612 #
DE95-005252 ..... p 2080 N95-25289 #
DE95-005253 ..... p 2096 N95-25293 #
DE95-005257 ..... p 2089 N95-25598 #
DE95-005260 ..... p 2033 N95-25676 #
DE95-005276 ..... p 1951 N95-24289 #
DE95-005278 ..... p 1935 N95-25379 #
DE95-005279 ..... p 1973 N95-25565 #
DE95-005329 ..... p 2019 N95-24290 #
DE95-005391 ..... p 2000 N95-25380 #
DE95-005401 ..... p 2001 N95-25629
DE95-005410 ..... p 2019 N95-24342 #
DE95-005411 ..... p 1969 N95-25381 #
DE95-005414 ..... p 1926 N95-25295 #
DE95-005420 ..... p 1941 N95-25382 #
DE95-005423 ..... p 1995 N95-25566 #
DE95-005427 ..... p 1966 N95-26240
DE95-005445 ..... p 1947 N95-24273 #
DE95-005471 ..... p 2069 N95-25300 #
DE95-005487 ..... p 1977 N95-26172 #
DE95-005495 ..... p 2029 N95-24458 #
DE95-005530 ..... p 1995 N95-26037 #
DE95-005545 ..... p 2007 N95-24368
DE95-005568 ..... p 1927 N95-25998 #
DE95-005657 ..... p 1988 N95-25440 #
DE95-005687 ..... p 2008 N95-25383 #
DE95-005728 ..... p 1969 N95-25384 #
DE95-005731 ..... p 1959 N95-25385 #
DE95-005732 ..... p 1941 N95-25386 #
DE95-005751 ..... p 1991 N95-24369 #
DE95-005755 ..... p 2103 N95-24370 #
DE95-005758 ..... p 1941 N95-25387 #
DE95-005831 ..... p 2045 N95-24459 #
DE95-005835 ..... p 2010 N95-24427 #
DE95-005839 ..... p 2043 N95-24326 #
DE95-005881 ..... p 1929 N95-24430 #
DE95-005894 ..... p 2085 N95-24431 #
DE95-005895 ..... p 1933 N95-24432 #
DE95-005897 ..... p 1934 N95-24433 #
DE95-005898 ..... p 2091 N95-26087 #
DE95-005899 ..... p 1935 N95-25388 #
DE95-005901 ..... p 2089 N95-25389 #
DE95-005902 ..... p 1935 N95-25390 #
DE95-005903 ..... p 2089 N95-25391 #
DE95-005904 ..... p 2038 N95-25600 #
DE95-005906 ..... p 2008 N95-25181 #
DE95-005910 ..... p 1951 N95-25367 #
DE95-005915 ..... p 1999 N95-25198 #
DE95-005919 ..... p 1931 N95-25291 #
DE95-005924 ..... p 2051 N95-25292 #
DE95-005925 ..... p 2051 N95-25294 #
DE95-005927 ..... p 2050 N95-24902 #
DE95-005928 ..... p 2051 N95-25296 #
DE95-005929 ..... p 2044 N95-24419 #
DE95-005934 ..... p 2044 N95-24420 #
DE95-005942 ..... p 2065 N95-24409 #
DE95-005943 ..... p 2045 N95-24434 #
DE95-005944 ..... p 2045 N95-24435 #
DE95-005945 ..... p 2044 N95-24414 #
DE95-005946 ..... p 2044 N95-24415 #
DE95-005947 ..... p 2044 N95-24417 #
DE95-005948 ..... p 2044 N95-24418 #
DE95-005949 ..... p 2047 N95-24622 #
DE95-005950 ..... p 2047 N95-24641 #
DE95-005955 ..... p 2026 N95-25368 #
DE95-005957 ..... p 2070 N95-25369 #
DE95-005958 ..... p 1968 N95-24623 #
DE95-005959 ..... p 2064 N95-26006 #
DE95-005962 ..... p 1937 N95-26007 #
DE95-005967 ..... p 2071 N95-25785 #
DE95-005969 ..... p 2070 N95-25441 #
DE95-005998 ..... p 2001 N95-25442 #
DE95-005999 ..... p 1997 N95-24570 #
DE95-006051 ..... p 2046 N95-24571 #
DE95-006052 ..... p 2066 N95-24572 #
DE95-006054 ..... p 2067 N95-24573 #
DE95-006056 ..... p 2067 N95-24574 #
DE95-006057 ..... p 2109 N95-24327 #
DE95-006061 ..... p 2046 N95-24575 #
DE95-006062 ..... p 2092 N95-24328 #
DE95-006063 ..... p 2046 N95-24576 #
DE95-006064 ..... p 2069 N95-25297 #
DE95-006066 ..... p 2003 N95-24577 #
DE95-006067 ..... p 2050 N95-24903 #
DE95-006068 ..... p 2043 N95-24354 #
DE95-006070 ..... p 2094 N95-24578 #
DE95-006071 ..... p 2046 N95-24591 #
DE95-006080 ..... p 1991 N95-24355 #
DE95-006090 ..... p 2057 N95-25768 #
DE95-006093 ..... p 1974 N95-24356 #
DE95-006097 ..... p 2065 N95-24357 #
DE95-006144 ..... p 2030 N95-24592 #
DE95-006145 ..... p 2046 N95-24593 #
DE95-006149 ..... p 2085 N95-24463 #
DE95-006152 ..... p 1991 N95-24425 #
DE95-006170 ..... p 2086 N95-24594 #
DE95-006172 ..... p 1973 N95-25557 #
DE95-006178 ..... p 2018 N95-26167 #
DE95-006195 ..... p 2047 N95-24595 #
DE95-006196 ..... p 1967 N95-24596 #
DE95-006211 ..... p 2098 N95-25530 #
DE95-006215 ..... p 2020 N95-24597 #
DE95-006223 ..... p 2064 N95-26168 #
DE95-006224 ..... p 1937 N95-25775 #
DE95-006243 ..... p 1997 N95-24406 #
DE95-006253 ..... p 1988 N95-24407 #
DE95-006255 ..... p 1925 N95-24426 #
DE95-006256 ..... p 2005 N95-24613 #
DE95-006302 ..... p 1960 N95-25558 #
DE95-006313 ..... p 1929 N95-24614 #
DE95-006317 ..... p 2074 N95-25559 #
DE95-006318 ..... p 2089 N95-25353 #
DE95-006319 ..... p 1971 N95-24408 #
DE95-006320 ..... p 2087 N95-24616 #
DE95-006321 ..... p 2087 N95-24617 #
DE95-006322 ..... p 1941 N95-25370 #
DE95-006364 ..... p 2012 N95-25371 #
DE95-006379 ..... p 1933 N95-24329 #
DE95-006478 ..... p 2070 N95-25406 #
DE95-006485 ..... p 2052 N95-25407 #
DE95-006487 ..... p 2038 N95-25408 #
DE95-006641 ..... p 1936 N95-25560 #
DE95-006642 ..... p 2081 N95-25561 #
DE95-006643 ..... p 2098 N95-25562 #
DE95-006645 ..... p 2014 N95-25483 #
DE95-006764 ..... p 2055 N95-25484 #
DE95-006813 ..... p 2004 N95-25476 #
DE95-006853 ..... p 2002 N95-25899 #
DE95-006854 ..... p 1998 N95-24618 #
DE95-006861 ..... p 2021 N95-25477 #
DE95-006862 ..... p 1973 N95-26112 #
DE95-006900 ..... p 2070 N95-25478 #
DE95-007016 ..... p 2077 N95-24619 #
DE95-007017 ..... p 2077 N95-24602 #
DE95-007064 ..... p 2054 N95-25479 #
DE95-007067 ..... p 2032 N95-25480 #
DE95-007323 ..... p 2054 N95-25481 #
DE95-007631 ..... p 2083 N95-26185 #
DE95-060082 ..... p 1981 N95-24598 #
DE95-600163 ..... p 1933 N95-24366 #
DE95-600249 ..... p 2010 N95-24367 #
DE95-600438 ..... p 2001 N95-25615 #
DE95-600838 ..... p 2043 N95-24350 #
DE95-600839 ..... p 2065 N95-24351 #
DE95-600851 ..... p 2093 N95-24352 #
DE95-600852 ..... p 2093 N95-24353 #
DE95-600853 ..... p 2093 N95-24446 #
DE95-600854 ..... p 2095 N95-24833 #
DE95-600855 ..... p 2095 N95-24834 #
DE95-600856 ..... p 2095 N95-24837 #
DE95-600864 ..... p 2095 N95-24838 #
DE95-600934 ..... p 2095 N95-24839 #
DE95-601135 ..... p 1937 N95-25751 #
DE95-601136 ..... p 1930 N95-24840 #
DE95-601209 ..... p 1959 N95-24842 #
DE95-601210 ..... p 1959 N95-25405 #
DE95-602121 ..... p 2072 N95-26095 #
DE95-602307 ..... p 1970 N95-25940 #
DE95-602487 ..... p 2107 N95-25941 #
DE95-602882 ..... p 2082 N95-25942 #
DE95-602999 ..... p 2082 N95-25943 #
DE95-603831 ..... p 2062 N95-25944 #
DE95-604003 ..... p 2058 N95-25905 #
DE95-605213 ..... p 2107 N95-25980 #
DE95-605218 ..... p 2034 N95-25906 #
DE95-605219 ..... p 2106 N95-25907 #

DE95-605222 ..... p 2057 N95-25778 #
DE95-605240 ..... p 2002 N95-25779 #
DE95-605251 ..... p 2099 N95-25780 #
DE95-605252 ..... p 2037 N95-25781 #
DE95-605253 ..... p 2034 N95-25782 #
DE95-605279 ..... p 2034 N95-25783 #
DE95-605280 ..... p 2057 N95-25784 #
DE95-605286 ..... p 2063 N95-25965 #
DE95-605306 ..... p 2099 N95-25966 #
DE95-605314 ..... p 2099 N95-25967 #
DE95-605315 ..... p 2063 N95-25968 #
DE95-605322 ..... p 2058 N95-25908 #
DE95-605323 ..... p 2058 N95-25909 #
DE95-605393 ..... p 2058 N95-25910 #
DE95-605570 ..... p 2038 N95-25616 #
DE95-605636 ..... p 2034 N95-25982 #
DE95-605639 ..... p 1937 N95-25983 #
DE95-605640 ..... p 2055 N95-25499 #
DE95-605680 ..... p 2012 N95-25981 #
DE95-605765 ..... p 2038 N95-25552
DE95-605800 ..... p 2038 N95-25553
DE95-605886 ..... p 2090 N95-25776 #
DE95-605913 ..... p 2090 N95-25984 #
DE95-605947 ..... p 2090 N95-25985 #
DE95-606029 ..... p 2113 N95-25986 #
DE95-606030 ..... p 2113 N95-26042 #
DE95-606032 ..... p 2006 N95-26043 #
DE95-606045 ..... p 2111 N95-26044 #
DE95-606395 ..... p 1972 N95-25491 #
DE95-606413 ..... p 2056 N95-25554
DE95-606422 ..... p 2081 N95-25555
DE95-606516 ..... p 2018 N95-26045 #
DE95-606997 ..... p 2100 N95-26046 #
DE95-606998 ..... p 2100 N95-25987 #
DE95-606999 ..... p 2100 N95-25988 #
DE95-607000 ..... p 2034 N95-25989 #
DE95-607001 ..... p 2111 N95-25990 #
DE95-607002 ..... p 2063 N95-25991 #
DE95-607003 ..... p 2034 N95-25992 #
DE95-607004 ..... p 2032 N95-25452 #
DE95-607005 ..... p 2097 N95-25453 #
DE95-607006 ..... p 2097 N95-25454 #
DE95-607007 ..... p 2096 N95-25425 #
DE95-607008 ..... p 2096 N95-25426 #
DE95-607009 ..... p 2032 N95-25427 #
DE95-607010 ..... p 2033 N95-25645 #
DE95-607019 ..... p 2096 N95-25428 #
DE95-607020 ..... p 2097 N95-25446 #
DE95-607021 ..... p 2097 N95-25429 #
DE95-607022 ..... p 2038 N95-25430 #
DE95-607044 ..... p 2110 N95-25431 #
DE95-607045 ..... p 2036 N95-25439 #
DE95-607046 ..... p 2001 N95-25531 #
DE95-607047 ..... p 2001 N95-25521 #
DE95-607048 ..... p 1931 N95-25447 #
DE95-607049 ..... p 2033 N95-25748 #
DE95-607056 ..... p 2017 N95-25448 #
DE95-607069 ..... p 2053 N95-25449 #
DE95-607070 ..... p 2039 N95-25646 #
DE95-607073 ..... p 2036 N95-25455 #
DE95-607074 ..... p 2097 N95-25456 #
DE95-607075 ..... p 2036 N95-25522 #
DE95-607076 ..... p 2037 N95-25523 #
DE95-607077 ..... p 2038 N95-25524 #
DE95-607078 ..... p 2032 N95-25457 #
DE95-607079 ..... p 2098 N95-25525 #
DE95-607080 ..... p 2098 N95-25526 #
DE95-607081 ..... p 2098 N95-25527 #
DE95-607082 ..... p 2097 N95-25432 #
DE95-607083 ..... p 2110 N95-25647 #
DE95-607084 ..... p 1955 N95-25648 #
DE95-607085 ..... p 2110 N95-25433 #
DE95-607086 ..... p 2037 N95-25599 #
DE95-607087 ..... p 2036 N95-25434 #
DE95-607088 ..... p 2033 N95-25532 #
DE95-607093 ..... p 2098 N95-25533 #
DE95-607094 ..... p 2098 N95-25534 #
DE95-607095 ..... p 2099 N95-25650 #
DE95-607096 ..... p 2063 N95-25993 #
DE95-607097 ..... p 2063 N95-25969 #
DE95-607098 ..... p 2099 N95-25970 #
DE95-607099 ..... p 2097 N95-25473 #
DE95-607100 ..... p 2054 N95-25474 #
DE95-607101 ..... p 2098 N95-25475 #
DE95-607102 ..... p 2038 N95-25458 #
DE95-607121 ..... p 2110 N95-25469 #
DE95-607124 ..... p 2053 N95-25450 #
DE95-607129 ..... p 2097 N95-25435 #
DE95-607133 ..... p 2099 N95-25667 #
DE95-607143 ..... p 2052 N95-25436 #
DE95-607144 ..... p 2052 N95-25437 #
DE95-607145 ..... p 2053 N95-25459 #
DE95-607146 ..... p 2053 N95-25460 #
DE95-607159 ..... p 2053 N95-25461 #
DE95-607177 ..... p 2053 N95-25462 #
DE95-607181 ..... p 2054 N95-25463 #
DE95-607188 ..... p 2053 N95-25438 #
DE95-607190 ..... p 2054 N95-25464 #
DE95-607194 ..... p 2054 N95-25465 #
DE95-607201 ..... p 2054 N95-25466 #
DE95-607520 ..... p 2110 N95-25467 #
DE95-607521 ..... p 2097 N95-25468 #
DE95-607537 ..... p 2056 N95-25668 #
DE95-607538 ..... p 2055 N95-25493 #
DE95-607577 ..... p 2063 N95-25971 #
DE95-607598 ..... p 2082 N95-25972 #
DE95-607599 ..... p 1973 N95-25973 #
DE95-607608 ..... p 2082 N95-25974 #
DE95-607609 ..... p 2081 N95-25556
DE95-607610 ..... p 2081 N95-25632
DE95-607611 ..... p 2082 N95-25777
DE95-607612 ..... p 2081 N95-25617
DE95-607626 ..... p 2082 N95-25975 #
DE95-607629 ..... p 2082 N95-25976 #
DE95-607661 ..... p 1937 N95-25977 #
DE95-607662 ..... p 2090 N95-25978 #
DE95-607663 ..... p 2090 N95-25979 #
DE95-607664 ..... p 2063 N95-25994 #
DE95-607769 ..... p 2091 N95-26260 #
DE95-607773 ..... p 1932 N95-26261 #
DE95-607804 ..... p 2091 N95-26252 #
DE95-607819 ..... p 1960 N95-26100 #
DE95-607820 ..... p 2091 N95-26101 #
DE95-607840 ..... p 2100 N95-26102 #
DE95-607844 ..... p 2091 N95-26103 #
DE95-607846 ..... p 2100 N95-26104 #
DE95-608777 ..... p 2100 N95-26105 #
DE95-703782 ..... p 2057 N95-25669 #
DE95-703783 ..... p 2055 N95-25494 #
DE95-703897 ..... p 2080 N95-25495 #
DE95-703970 ..... p 2055 N95-25496 #
DE95-709764 ..... p 2055 N95-25497 #
DE95-709766 ..... p 2080 N95-25471 #
DE95-709767 ..... p 2081 N95-25498 #
DE95-709770 ..... p 1966 N95-26161 #
DE95-709895 ..... p 2072 N95-26162 #
DE95-709896 ..... p 2072 N95-26163 #
DE95-709897 ..... p 2072 N95-26164 #
DE95-709916 ..... p 2072 N95-26165 #
DE95-717518 ..... p 1993 N95-24862 #
DE95-723047 ..... p 1953 N95-24848 #
DE95-730104 ..... p 1926 N95-25111 #
DE95-730105 ..... p 2088 N95-24900 #
DE95-730106 ..... p 2088 N95-24988 #
DE95-730143 ..... p 1996 N95-24291 #
DE95-730179 ..... p 1952 N95-24491 #
DE95-730180 ..... p 2104 N95-24492 #
DE95-730185 ..... p 1952 N95-24493 #
DE95-730186 ..... p 2104 N95-24494 #
DE95-737597 ..... p 1949 N95-25244 #
DE95-737621 ..... p 2066 N95-24448 #
DE95-737628 ..... p 1999 N95-24904 #
DE95-744284 ..... p 1948 N95-24498 #
DE95-744285 ..... p 1997 N95-24499 #
DE95-744869 ..... p 2001 N95-25500 #

DFPF-92/TH/58 ..... p 2093 N95-24353 #

DOE/BC-95000129 ..... p 2004 N95-26089 #

DOE/CE-15599/T1 ..... p 1927 N95-25998 #
DOE/CE-15613/T3 ..... p 1925 N95-24426 #
DOE/CE-23810/49 ..... p 1941 N95-25243 #
DOE/CE-50390/3 ..... p 1994 N95-25121 #
DOE/CE-90049/T1 ..... p 1976 N95-25101 #

DOE/CH-10093/251 ..... p 1991 N95-24666 #

DOE/EE-0033 ..... p 1948 N95-24679 #

DOE/EH-0445 ..... p 2012 N95-25371 #

DOE/EIA-M069-A ..... p 1991 N95-24355 #

DOE/EIA-0249(94) ..... p 2105 N95-24710 #
DOE/EIA-0585(93) ..... p 1947 N95-24273 #

DOE/ER-0614P ..... p 2068 N95-24899 #
DOE/ER-0632 ..... p 2019 N95-24290 #
DOE/ER-0636 ..... p 1988 N95-25440 #
DOE/ER-13296/11 ..... p 1923 N95-24851 #
DOE/ER-13425/T3 ..... p 2007 N95-24225 #
DOE/ER-13426/T4 ..... p 2007 N95-24368
DOE/ER-13775/6 ..... p 2050 N95-25112 #
DOE/ER-14227/3 ..... p 1930 N95-24686 #
DOE/ER-14254/2 ..... p 1929 N95-24553 #
DOE/ER-20019/T1 ..... p 2008 N95-24850 #
DOE/ER-25136/2 ..... p 2032 N95-25480 #
DOE/ER-25165/T1 ..... p 2054 N95-25479 #
DOE/ER-25199/T1 ..... p 2029 N95-24458 #
DOE/ER-40103/T6 ..... p 2068 N95-24852 #
DOE/ER-40272/206 ..... p 2096 N95-24867 #
DOE/ER-40291/22 ..... p 2051 N95-25292 #
DOE/ER-40291/23 ..... p 2051 N95-25294 #
DOE/ER-40291/25 ..... p 2050 N95-24902 #
DOE/ER-40291/26 ..... p 2051 N95-25296 #
DOE/ER-40317/13 ..... p 2110 N95-25343 #
DOE/ER-40561/164 ..... p 2113 N95-24249 #
DOE/ER-40561/167 ..... p 2070 N95-25634 #
DOE/ER-40561/168 ..... p 2052 N95-25403 #
DOE/ER-40561/170 ..... p 2109 N95-25122 * #
DOE/ER-40561/172 ..... p 2057 N95-25896 #
DOE/ER-40706/2 ..... p 2054 N95-25481 #
DOE/ER-40736/T1 ..... p 2051 N95-25241 #
DOE/ER-40762/042 ..... p 2098 N95-25562 #
DOE/ER-40764/3 ..... p 2048 N95-24671 #
DOE/ER-40822/1 ..... p 2046 N95-24547 #
DOE/ER-40878/T1 ..... p 1965 N95-25404 #
DOE/ER-40879/T1 ..... p 2105 N95-25240 #
DOE/ER-40880/1 ..... p 2065 N95-24317 #
DOE/ER-45237/T3 ..... p 2048 N95-24687 #
DOE/ER-45292/15 ..... p 1940 N95-24554 #
DOE/ER-45405/8 ..... p 1936 N95-25560 #
DOE/ER-53198/253 ..... p 2077 N95-24619 #
DOE/ER-53198/254 ..... p 2077 N95-24602 #
DOE/ER-53266/48 ..... p 2077 N95-24587 #
DOE/ER-54197/2 ..... p 2081 N95-25561 #
DOE/ER-61364/3 ..... p 2005 N95-24613 #
DOE/ER-75787/3 ..... p 2014 N95-25483 #

DOE/ET-53088/671 ..... p 2079 N95-25216 #

DOE/GO-10094-037 ..... p 2007 N95-24306 #
DOE/GO-10094-039 ..... p 2007 N95-24307 #

DOE/ID-10456 ..... p 1963 N95-24678 #
DOE/ID-12779/3 ..... p 1932 N95-26093 #
DOE/ID-13220/T2 ..... p 2077 N95-24552 #

DOE/MC-26006/3824 ..... p 1990 N95-24318 #
DOE/MC-26006/3960 ..... p 1991 N95-24425 #
DOE/MC-29224/3931 ..... p 1992 N95-24683 #

DOE/METC-C/95/7163 ..... p 1930 N95-25098 #

DOE/METC-95-7169 ..... p 1996 N95-26171 #

DOE/NASA/50306-7 ..... p 1923 N95-24437 * #

DOE/NV-10845/49 ..... p 1988 N95-24407 #

DOE/PC-89805/T9 ..... p 2003 N95-26091 #
DOE/PC-90044/T2 ..... p 1948 N95-24655 #
DOE/PC-91293/12 ..... p 1928 N95-24286 #
DOE/PC-92542/T8 ..... p 1939 N95-24285 #
DOE/PC-92545/8 ..... p 1929 N95-24341
DOE/PC-94211/T1 ..... p 1997 N95-24406 #

DOE/PO-0028-VOL-1 ..... p 2000 N95-25361 #
DOE/PO-0028-VOL-1 ..... p 2000 N95-25362 #
DOE/PO-0028-VOL-3 ..... p 2003 N95-26065 #

DOT-VNTSC-FAA-94-4 ..... p 1905 N95-24295 #

DOT/FAA/AM-95/11 ..... p 2011 N95-25336 #
DOT/FAA/AM-95/12 ..... p 2012 N95-26204 #
DOT/FAA/AM-95/2 ..... p 1909 N95-24384 #
DOT/FAA/AM-95/5 ..... p 2012 N95-24237 #

DOT/FAA/CT-93/14 ..... p 1909 N95-24631 #
DOT/FAA/CT-94/11 ..... p 1905 N95-25401
DOT/FAA/CT-94/90 ..... p 1905 N95-24295 #

DRA-TM-AERO-PROP-41 ..... p 1907 N95-25649 #

DRA-TR-93062 ..... p 1980 N95-24383 #

DRA/AP/TM9341/1.0 ..... p 1907 N95-25649 #

DREO-1226 ..... p 1956 N95-26191

DSF-T-1/94 ..... p 2096 N95-25107 #
DSF-T-2/94 ..... p 2027 N95-24228 #
DSF-T-5/94 ..... p 2093 N95-24405 #
DSF-T-7/94 ..... p 2027 N95-24229 #

DSTO-RR-0013 ..... p 1975 N95-24393

DSTO-TR-0061 ..... p 1905 N95-24200
DSTO-TR-0062 ..... p 1905 N95-24201
DSTO-TR-0072 ..... p 1966 N95-24203
DSTO-TR-0076 ..... p 1947 N95-24394

E-8627 ..... p 1967 N95-24473 * #
E-9049 ..... p 1966 N95-26077 * #
E-9143 ..... p 1914 N95-24561 * #
E-9410 ..... p 1952 N95-24395 * #
E-9426 ..... p 1912 N95-24207 * #

E-9442 ..... p 1923 N95-24437 * #
E-9445 ..... p 1963 N95-24906 * #
E-9477 ..... p 1913 N95-24390 * #
E-9483 ..... p 1961 N95-24399 * #
E-9484 ..... p 1927 N95-25880 * #
E-9488 ..... p 1913 N95-24304 * #
E-95-25 ..... p 1924 N95-25961 * #
E-9509 ..... p 1943 N95-26119 * #
E-9512 ..... p 1957 N95-24476 * #
E-9515 ..... p 1991 N95-24560 * #
E-9516 ..... p 1977 N95-26074 * #
E-9531 ..... p 1980 N95-24398 * #
E-9540 ..... p 2099 N95-25878 * #
E-9545 ..... p 2029 N95-24474 * #
E-9546 ..... p 1925 N95-24438 * #
E-9547 ..... p 1970 N95-26073 * #
E-9582 ..... p 1914 N95-24392 * #
E-9590 ..... p 1977 N95-26076 * #
E-9592 ..... p 1912 N95-24624 * #
E-9594 ..... p 1923 N95-25877 * #
E-9600 ..... p 1955 N95-25876 * #
E-9603 ..... p 2063 N95-25963 * #
E-9607 ..... p 2018 N95-25879 * #
E-9621 ..... p 1908 N95-25962 * #
E-9630 ..... p 1908 N95-26075 * #
E-9644 ..... p 1983 N95-26078 * #

EGG-M-94071 ..... p 2106 N95-25765 #
EGG-M-94084 ..... p 2021 N95-25378 #
EGG-M-94129 ..... p 2069 N95-25365 #
EGG-M-94230 ..... p 2004 N95-25666 #

EGG-11265-3011 ..... p 1989 N95-25110

ENSLAPP-L-469/94 ..... p 2036 N95-25455 #

EPA/AA/TDG-94/04 ..... p 1976 N95-25574

EPA/453/R-94/068 ..... p 2002 N95-26005 #
EPA/600/R-95/006 ..... p 1942 N95-26004 #
EPA/600/S-94/019 ..... p 1911 N95-26062 #

ER-40685-766 ..... p 2054 N95-25463 #

ERIM-232300-54-F-VOL-1 ..... p 2075 N95-26173

ES/ER/TM-120/V3 ..... p 2105 N95-24656 #

ESA-HSR-10-PT-1 ..... p 2114 N95-24871 #
ESA-HSR-11 ..... p 1916 N95-24872 #
ESA-HSR-12 ..... p 1916 N95-24892 #
ESA-HSR-13 ..... p 1953 N95-24893 #
ESA-HSR-14 ..... p 2107 N95-24894 #
ESA-HSR-15 ..... p 2107 N95-24895 #
ESA-HSR-16 ..... p 1917 N95-24896 #

ESA-SP-1170 ..... p 2112 N95-24994 * #
ESA-SP-1172 ..... p 2114 N95-24870 #

ETDE/JP-MF-95730104 ..... p 1926 N95-25111 #
ETDE/JP-MF-95730105 ..... p 2088 N95-24900 #
ETDE/JP-MF-95730106 ..... p 2088 N95-24988 #
ETDE/JP-MF-95730143 ..... p 1996 N95-24291 #

FAAR-23/1993 ..... p 1999 N95-24904 #
FAAR-24/1993 ..... p 2001 N95-25500 #

FEMP-2387 ..... p 1930 N95-25097 #
FEMP-2396 ..... p 2102 N95-24905 #

FERMILAB-PUB-94/027-A ..... p 2065 N95-24335 * #

FNAL/C-94/144-E ..... p 2041 N95-24253 #
FNAL/C-94/209-E ..... p 2052 N95-25377 #
FNAL/C-94/252-E ..... p 2051 N95-25372 #
FNAL/C-94/294-E ..... p 2052 N95-25402 #
FNAL/C-94/306-E ..... p 2056 N95-25563 #
FNAL/C-94/329-E ..... p 2067 N95-24601 #
FNAL/C-94/337-E ..... p 2041 N95-24256 #
FNAL/C-94/339-E ..... p 2068 N95-24728 #
FNAL/C-94/356-E ..... p 2073 N95-25239 #
FNAL/C-94/368-E ..... p 2041 N95-24254 #
FNAL/C-94/373 ..... p 2111 N95-26284 #
FNAL/C-94/375-E ..... p 2068 N95-25238 #
FNAL/C-94/377-E ..... p 2050 N95-24901 #
FNAL/C-94/397 ..... p 2106 N95-25376 #
FNAL/C-94/398 ..... p 1972 N95-24869 #
FNAL/C-94/404-E ..... p 2041 N95-24252 #
FNAL/C-94/408-E ..... p 2071 N95-26011

FOA-A-50024-5.2 ..... p 2013 N95-24864
FOA-A-50025-5.2 ..... p 2013 N95-24510

FOA-C-30723-3.4 ..... p 2026 N95-25568 #
FOA-C-30743-3.5 ..... p 1951 N95-24281
FOA-C-30746-3.5 ..... p 1953 N95-24835
FOA-C-30748-3.4 ..... p 2034 N95-25893 #
FOA-C-30749-3.3 ..... p 1955 N95-25891 #
FOA-C-30750-3.4 ..... p 1989 N95-24444
FOA-C-30751-3.4 ..... p 1953 N95-24836
FOA-C-30754-3.5 ..... p 1953 N95-24649
FOA-C-30756-3.1 ..... p 1973 N95-25622
FOA-C-30757-3.1 ..... p 2009 N95-24227
FOA-C-30758-3.2 ..... p 1955 N95-25644
FOA-C-30759-3.1 ..... p 1952 N95-24445
FOA-C-30761-3.4 ..... p 1988 N95-24240 #
FOA-C-30763-8.4,3.4 ..... p 2036 N95-25894 #
FOA-C-30764-3.1 ..... p 1967 N95-24280
FOA-C-30765-3.3 ..... p 1955 N95-25641
FOA-C-30766-3.4 ..... p 2106 N95-25572
FOA-C-30767-3.6 ..... p 2017 N95-25571
FOA-C-30768-3.6 ..... p 1914 N95-24260
FOA-C-50107-5.1 ..... p 2011 N95-24863

FOA-R-00013-3.5-SE ..... p 1951 N95-24241
FOA-R-94-00005-1.2-SE ..... p 2102 N95-25642
FOA-R-94-00008-5.1-SE ..... p 2012 N95-25570 #
FOA-R-94-00015-3.2-SE ..... p 1954 N95-25623
FOA-R-94-00019-S.4-SE ..... p 1925 N95-24242

FRCR-451 ..... p 2077 N95-24587 #

GA-A-21709 ..... p 2079 N95-25120 #
GA-A-21741 ..... p 2079 N95-25108 #
GA-A-21807 ..... p 2078 N95-25102 #
GA-A-21813 ..... p 2077 N95-24646 #
GA-A-21834 ..... p 2050 N95-25180 #
GA-A-21839 ..... p 1972 N95-24709 #
GA-A-21872 ..... p 2079 N95-25250 #

GAO/NSIAD-95-59 ..... p 1911 N95-26338 #

GRI-94/0329 ..... p 1997 N95-24294 #
GRI-94/0350 ..... p 1913 N95-24293

HEP-PH-9407330 ..... p 2053 N95-25460 #

HEP-TH-9306088 ..... p 2099 N95-25650 #
HEP-TH-9407015 ..... p 2098 N95-25526 #
HEP-TH-9408137 ..... p 2109 N95-24327 #

HEPTH-9408063 ..... p 2097 N95-25456 #

IA-1479 ..... p 2078 N95-24706 #
IA-1482 ..... p 1972 N95-24707 #

IAE-0127 ..... p 2072 N95-26095 #

IAEA-CN-60-I-2 ..... p 2076 N95-24548 #
IAEA-CN-60/A-5-I-1 ..... p 2078 N95-25102 #
IAEA-CN-60/F-P-3 ..... p 2071 N95-25855 #

IAEA-NDS-150-(REV-94/3) ..... p 2107 N95-25941 #
IAEA-NDS-47-REV-2 ..... p 2040 N95-24231 #
IAEA-NDS-7(REV-94/3) ..... p 2107 N95-25980 #

IAERU-9304 ..... p 2072 N95-26162 #

IBAMD-47 ..... p 2040 N95-24230 #

IC-92/332 ..... p 2109 N95-24884 #
IC-92/393 ..... p 2031 N95-24697 #
IC-93/216 ..... p 2054 N95-25463 #
IC-93/424 ..... p 2110 N95-25467 #
IC-94/100 ..... p 2084 N95-24324 #
IC-94/101 ..... p 2113 N95-25986 #
IC-94/102 ..... p 2043 N95-24404 #
IC-94/103 ..... p 2092 N95-24288 #
IC-94/106 ..... p 2084 N95-24244 #
IC-94/107 ..... p 2100 N95-26046 #
IC-94/108 ..... p 2036 N95-25455 #
IC-94/109 ..... p 2092 N95-24275 #
IC-94/110 ..... p 2028 N95-24276 #
IC-94/111 ..... p 2092 N95-24277 #
IC-94/116 ..... p 2097 N95-25456 #
IC-94/119 ..... p 2052 N95-25436 #
IC-94/121 ..... p 2051 N95-25290 #
IC-94/125 ..... p 2041 N95-24232 #
IC-94/128 ..... p 2100 N95-25987 #
IC-94/129 ..... p 2100 N95-26102 #
IC-94/130 ..... p 2036 N95-25522 #
IC-94/131 ..... p 2037 N95-25523 #
IC-94/132 ..... p 2038 N95-25524 #
IC-94/133 ..... p 1960 N95-26100 #
IC-94/134 ..... p 2082 N95-25975 #
IC-94/135 ..... p 2100 N95-25988 #
IC-94/136 ..... p 2034 N95-25989 #
IC-94/137 ..... p 1937 N95-25977 #
IC-94/138 ..... p 2090 N95-25978 #
IC-94/139 ..... p 2091 N95-26252 #
IC-94/140 ..... p 2113 N95-26042 #
IC-94/142 ..... p 2082 N95-25972 #
IC-94/143 ..... p 2111 N95-25990 #
IC-94/144 ..... p 2032 N95-25457 #
IC-94/145 ..... p 2090 N95-25979 #
IC-94/146 ..... p 2098 N95-25525 #
IC-94/147 ..... p 2098 N95-25526 #
IC-94/148 ..... p 2063 N95-25971 #
IC-94/149 ..... p 1937 N95-25983 #
IC-94/150 ..... p 2100 N95-26105 #
IC-94/151 ..... p 2091 N95-26103 #
IC-94/152 ..... p 2063 N95-25991 #
IC-94/153 ..... p 2034 N95-25992 #
IC-94/155 ..... p 2110 N95-25469 #
IC-94/156 ..... p 2098 N95-25527 #
IC-94/157 ..... p 2082 N95-25974 #
IC-94/158 ..... p 2032 N95-25452 #
IC-94/159 ..... p 2091 N95-26101 #
IC-94/163 ..... p 2054 N95-25466 #
IC-94/165 ..... p 2097 N95-25453 #
IC-94/166 ..... p 2006 N95-26043 #
IC-94/168 ..... p 2097 N95-25432 #
IC-94/169 ..... p 2052 N95-25437 #
IC-94/171 ..... p 2097 N95-25454 #
IC-94/173 ..... p 2110 N95-25647 #
IC-94/174 ..... p 2053 N95-25438 #
IC-94/175 ..... p 2110 N95-25431 #
IC-94/177 ..... p 2097 N95-25468 #
IC-94/179 ..... p 1955 N95-25648 #
IC-94/180 ..... p 2111 N95-26044 #
IC-94/184 ..... p 2036 N95-25439 #
IC-94/185 ..... p 2053 N95-25449 #
IC-94/186 ..... p 2001 N95-25531 #
IC-94/189 ..... p 2096 N95-25425 #
IC-94/18 ..... p 2096 N95-25107 #
IC-94/190 ..... p 2063 N95-25994 #
IC-94/191 ..... p 2053 N95-25459 #
IC-94/192 ..... p 2096 N95-25426 #
IC-94/193 ..... p 2110 N95-25433 #
IC-94/195 ..... p 2001 N95-25521 #
IC-94/196 ..... p 2034 N95-25982 #
IC-94/200 ..... p 1973 N95-25973 #
IC-94/201 ..... p 2037 N95-25599 #
IC-94/202 ..... p 2053 N95-25450 #
IC-94/203 ..... p 2053 N95-25462 #
IC-94/204 ..... p 2032 N95-25427 #
IC-94/207 ..... p 2036 N95-25434 #
IC-94/216 ..... p 2033 N95-25532 #
IC-94/38 ..... p 2027 N95-24228 #
IC-94/46 ..... p 2016 N95-24708 #
IC-94/53 ..... p 2033 N95-25645 #
IC-94/54 ..... p 1931 N95-25447 #
IC-94/55 ..... p 2033 N95-25748 #
IC-94/64 ..... p 2053 N95-25460 #
IC-94/65 ..... p 2093 N95-24405 #
IC-94/76 ..... p 2027 N95-24229 #
IC-94/77 ..... p 2029 N95-24401 #
IC-94/84 ..... p 2039 N95-25646 #
IC-94/89 ..... p 2095 N95-24767 #
IC-94/93 ..... p 2092 N95-24266 #
IC-94/95 ..... p 1956 N95-24245 #
IC-94/99 ..... p 2084 N95-24246 #

ICAF-1949 ..... p 1980 N95-24383 #

ICASE-26 ..... p 2014 N95-25119 * #
ICASE-95-13 ..... p 1963 N95-24584 * #
ICASE-95-14 ..... p 2031 N95-24857 * #
ICASE-95-15 ..... p 1962 N95-24580 * #
ICASE-95-16 ..... p 2032 N95-25106 * #
ICASE-95-17 ..... p 2031 N95-24856 * #
ICASE-95-18 ..... p 2030 N95-24632 * #
ICASE-95-19 ..... p 1965 N95-25960 * #
ICASE-95-22 ..... p 1966 N95-25964 * #
ICASE-95-4 ..... p 2029 N95-24421 * #
ICASE-95-7 ..... p 2032 N95-25114 * #
ICASE-95-8 ..... p 2029 N95-24389 * #

ICOMP-94-16 ..... p 1966 N95-26077 * #
ICOMP-95-3 ..... p 1961 N95-24399 * #

IDA-PAPER-P-2935 ..... p 2007 N95-26048

IFSR-671 ..... p 2079 N95-25216 #

IFT-P-012/94 ..... p 2095 N95-24839 #
IFT-P-014/94 ..... p 2065 N95-24351 #

IFTR-1/1994 ..... p 2037 N95-25339
IFTR-10/1994 ..... p 1956 N95-26018
IFTR-13/1994 ..... p 2027 N95-26330
IFTR-15/1994 ..... p 1951 N95-26109
IFTR-17/1993 ..... p 1932 N95-26107
IFTR-19/1994 ..... p 2040 N95-26108
IFTR-2/1993 ..... p 2035 N95-26106
IFTR-20/1994 ..... p 2040 N95-26071
IFTR-21/1994 ..... p 1932 N95-25959
IFTR-22/1994 ..... p 1995 N95-25758

IFTR-25/1994 ..... p 1935 N95-25117
IFTR-28/1994 ..... p 2040 N95-26180
IFTR-29/1994 ..... p 1936 N95-25638
IFTR-30/1994 ..... p 1938 N95-26333
IFTR-31/1994 ..... p 2004 N95-25958
IFTR-33/1994 ..... p 1938 N95-26179
IFTR-34/1994 ..... p 1983 N95-26178
IFTR-35/1994 ..... p 1981 N95-24996
IFTR-38/1994 ..... p 1978 N95-25957
IFTR-4/1994 ..... p 1954 N95-25393
IFTR-7/1994 ..... p 2039 N95-26332
IFTR-8-1994 ..... p 2083 N95-26019
IFTR-9-1993 ..... p 2080 N95-25340
IFTR-9/1994 ..... p 1956 N95-26331

IFUP-TH-39/94 ..... p 2098 N95-25527 #

IHES/M/94/45 ..... p 2029 N95-24325
IHES/M/94/46 ..... p 2028 N95-24322
IHES/M/94/47 ..... p 2028 N95-24321
IHES/M/94/48 ..... p 2028 N95-24301
IHES/M/94/49 ..... p 2029 N95-24323
IHES/M/94/50 ..... p 2028 N95-24255 #
IHES/M/94/51 ..... p 2028 N95-24251
IHES/M/94/52 ..... p 2028 N95-24243 #

IM-3145 ..... p 1982 N95-25444
IM-3146-PT-3 ..... p 1982 N95-25569 #
IM-3147-PT-4 ..... p 1982 N95-25445 #

IMSC-94-31 ..... p 2097 N95-25456 #

INDC(JPN)-169/L ..... p 2104 N95-24372 #

INFN-NA-IV-1/94 ..... p 2096 N95-25107 #
INFN-NA-IV-5/94 ..... p 2093 N95-24405 #

INIS-BR-3395 ..... p 1939 N95-24373 #
INIS-BR-3399 ..... p 1933 N95-24366 #
INIS-BR-3412 ..... p 2010 N95-24367 #

INIS-JP-024 ..... p 2056 N95-25614 #
INIS-JP-028 ..... p 2072 N95-26164 #
INIS-JP-029 ..... p 2072 N95-26163 #

INIS-MF-13983 ..... p 2001 N95-25615 #
INIS-MF-14358 ..... p 2002 N95-25779 #
INIS-MF-14376 ..... p 1972 N95-25491 #
INIS-MF-14385 ..... p 2012 N95-25981 #
INIS-MF-14387 ..... p 2055 N95-25499 #

INIS-UA-004-VOL-1 ..... p 2056 N95-25554
INIS-UA-004-VOL-3 ..... p 2038 N95-25552
INIS-UA-004-VOL-4 ..... p 2038 N95-25616
INIS-UA-004-VOL-5 ..... p 2038 N95-25553
INIS-UA-004-VOL-6 ..... p 2081 N95-25555

INS-1026 ..... p 2070 N95-25772 #
INS-1027 ..... p 2057 N95-25669 #
INS-1028 ..... p 2055 N95-25494 #

INT-PATENT-CLASS-B01P-3/36 . p 1967 N95-24236 *
INT-PATENT-CLASS-B23K-10/00 p 1976 N95-25548 *
INT-PATENT-CLASS-B25J-1/00 .. p 2014 N95-25306 *
INT-PATENT-CLASS-B64G-1/66 . p 1969 N95-25544 *

INT-PATENT-CLASS-C09K-19/00 p 2075 N95-26117 *

INT-PATENT-CLASS-D03D-3/08 . p 1943 N95-26118 *
INT-PATENT-CLASS-D03D-41/00 p 1943 N95-26118 *

INT-PATENT-CLASS-F02C-7/00 . p 2040 N95-26187 *
INT-PATENT-CLASS-F03G-7/00 . p 1936 N95-25545 *
INT-PATENT-CLASS-F16H-33/20 p 1969 N95-25544 *
INT-PATENT-CLASS-F17C-9/02 . p 1969 N95-25547 *
INT-PATENT-CLASS-F25B-19/00 p 1969 N95-25547 *

INT-PATENT-CLASS-G01B-11/16 p 2074 N95-26015 *
INT-PATENT-CLASS-G01B-11/16 p 2075 N95-26117 *
INT-PATENT-CLASS-G01B-7/16 . p 1968 N95-24625 *
INT-PATENT-CLASS-G01N-23/227 p 1978 N95-25304 *
INT-PATENT-CLASS-G01N-9/24 . p 1926 N95-25305 *
INT-PATENT-CLASS-G01T-1/18 . p 1960 N95-25889 *

INT-PATENT-CLASS-H01J-40/14 p 1959 N95-25307 *
INT-PATENT-CLASS-H01Q-19/12 p 1954 N95-25316 *
INT-PATENT-CLASS-H01R-13/629 p 1976 N95-25592 *
INT-PATENT-CLASS-H03H-3/00 . p 1960 N95-26038 *

IPPT-29-1992 ..... p 2016 N95-25392

ISBN-0-16-045186-8 ..... p 2115 N95-26335 #
ISBN-0-643-05256-9 ..... p 1999 N95-25199
ISBN-1-883712-36-X ..... p 2085 N95-24460 #
ISBN-91-7848-414-6 ..... p 2073 N95-24673
ISBN-91-7848-473-1 ..... p 1960 N95-25472 #

ISBN-92-836-1015-6 ..... p 2107 N95-26334 #
ISBN-92-9092-125-0 ..... p 2114 N95-24870 #
ISBN-951-22-1921-2 ..... p 1942 N95-25633
ISBN-951-22-2149-7 ..... p 1988 N95-24299
ISBN-951-22-2185-3 ..... p 1939 N95-24300 #
ISBN-951-22-2205-1 ..... p 1967 N95-24259

ISVR-TR-235 ..... p 1975 N95-24992
ISVR-TR-238-PT-3 ..... p 1982 N95-25003
ISVR-TR-241 ..... p 1981 N95-24997
ISVR-TR-242 ..... p 1982 N95-25332
ISVR-TR-244 ..... p 1981 N95-24995

ITER-TN-BL-5-0-3 ..... p 2079 N95-25283 #

ITER/US-95/IV-BL-17 ..... p 2083 N95-26185 #

ITF-93-38 ..... p 2099 N95-25667 #
ITF-94-4 ..... p 2081 N95-25556

ITP-94-10 ..... p 2081 N95-25632
ITP-94-1 ..... p 2090 N95-25776 #
ITP-94-8 ..... p 2082 N95-25777
ITP-94-9 ..... p 2081 N95-25617

IW-94075R ..... p 1994 N95-25501 #

IYAF-93-40 ..... p 2041 N95-24267 #

JAERI-M-93-242 ..... p 2055 N95-25496 #
JAERI-M-94-001 ..... p 1925 N95-24365 #
JAERI-M-94-012 ..... p 2043 N95-24337 #
JAERI-M-94-015-VOL-1 ..... p 2076 N95-24511 #
JAERI-M-94-019 ..... p 2104 N95-24372 #
JAERI-M-94-021 ..... p 2075 N95-24270 #
JAERI-M-94-022 ..... p 1933 N95-24338 #
JAERI-M-94-035 ..... p 2075 N95-24272 #
JAERI-M-94-038 ..... p 2055 N95-25497 #
JAERI-M-94-039 ..... p 2075 N95-24271 #
JAERI-M-94-044 ..... p 2080 N95-25495 #
JAERI-M-94-046 ..... p 2077 N95-24585 #
JAERI-M-94-047 ..... p 2070 N95-25631 #
JAERI-M-94-048 ..... p 1971 N95-24340 #
JAERI-M-94-050 ..... p 2076 N95-24311 #
JAERI-M-94-056 ..... p 2081 N95-25498 #
JAERI-M-94-062 ..... p 2080 N95-25471 #
JAERI-M-94-072 ..... p 2043 N95-24339 #
JAERI-M-94-073 ..... p 1966 N95-26161 #

JINR-D-2-93-381 ..... p 2093 N95-24376 #
JINR-D-2-93-437 ..... p 1952 N95-24377 #
JINR-D-2-94-11 ..... p 2093 N95-24378 #
JINR-D-2-94-72 ..... p 2092 N95-24347 #
JINR-D-2-94-85 ..... p 2065 N95-24348 #

JINR-E-10-93-311 ..... p 2035 N95-24643 #
JINR-E-11-93-468 ..... p 2030 N95-24691 #
JINR-E-11-94-140 ..... p 2034 N95-25906 #
JINR-E-11-94-204 ..... p 2106 N95-25907 #
JINR-E-13-93-295 ..... p 1968 N95-24635 #
JINR-E-13-93-308 ..... p 1967 N95-24484 #
JINR-E-13-93-339 ..... p 2048 N95-24692 #
JINR-E-14-93-279 ..... p 2090 N95-25851
JINR-E-14-94-20 ..... p 2087 N95-24891 #
JINR-E-14-94-99 ..... p 2085 N95-24362 #
JINR-E-2-93-257 ..... p 1952 N95-24506 #
JINR-E-2-93-286 ..... p 2095 N95-24727 #
JINR-E-2-93-290 ..... p 2094 N95-24637 #
JINR-E-2-93-291 ..... p 2094 N95-24507 #
JINR-E-2-93-292 ..... p 2031 N95-24698 #
JINR-E-2-93-294 ..... p 2049 N95-24719 #
JINR-E-2-93-297 ..... p 2048 N95-24669 #
JINR-E-2-93-309 ..... p 2049 N95-24887 #
JINR-E-2-93-315 ..... p 2094 N95-24508 #
JINR-E-2-93-328 ..... p 2036 N95-24504 #
JINR-E-2-93-340 ..... p 2047 N95-24640 #
JINR-E-2-93-357 ..... p 2049 N95-24720 #
JINR-E-2-93-358 ..... p 2036 N95-24699 #
JINR-E-2-93-447 ..... p 2109 N95-24885 #
JINR-E-2-93-448 ..... p 2109 N95-24886 #
JINR-E-2-93-461 ..... p 2055 N95-25537
JINR-E-2-93-462 ..... p 2035 N95-24693 #
JINR-E-2-93-53 ..... p 2050 N95-25094 #
JINR-E-2-93-54 ..... p 2094 N95-24509 #
JINR-E-2-93-71 ..... p 2094 N95-24638 #
JINR-E-2-94-103 ..... p 2042 N95-24315 #
JINR-E-2-94-107 ..... p 2093 N95-24349 #
JINR-E-2-94-117 ..... p 2099 N95-25967 #
JINR-E-2-94-131 ..... p 2043 N95-24361 #
JINR-E-2-94-132 ..... p 2063 N95-25965 #
JINR-E-2-94-153 ..... p 2099 N95-25780 #
JINR-E-2-94-162 ..... p 2063 N95-25968 #
JINR-E-2-94-170 ..... p 2099 N95-25966 #
JINR-E-2-94-174 ..... p 2037 N95-25781 #
JINR-E-2-94-230 ..... p 2034 N95-25782 #
JINR-E-2-94-42 ..... p 2042 N95-24316 #

JINR-E-2-94-79 ..... p 2043 N95-24360 #
JINR-E-2-94-82 ..... p 2042 N95-24314 #
JINR-E-2-94-88 ..... p 2058 N95-25908 #
JINR-E-2-94-89 ..... p 2058 N95-25909 #
JINR-E-4-93-293 ..... p 2048 N95-24700 #
JINR-E-4-93-465 ..... p 2050 N95-24890 #
JINR-E-4-93-55 ..... p 2095 N95-24639 #
JINR-E-4-94-141 ..... p 2058 N95-25910 #
JINR-E-4-94-75 ..... p 2092 N95-24312 #
JINR-E-5-93-314 ..... p 2030 N95-24645 #
JINR-E-5-94-172 ..... p 2034 N95-25783 #
JINR-E-7-93-74 ..... p 2055 N95-25538

JINR-R-1-93-285 ..... p 2045 N95-24485 #
JINR-R-1-93-327 ..... p 2049 N95-24889 #
JINR-R-10-93-243 ..... p 1967 N95-24486 #
JINR-R-10-93-348 ..... p 2035 N95-24858 #
JINR-R-10-94-105 ..... p 2057 N95-25778 #
JINR-R-10-94-44 ..... p 2037 N95-24363 #
JINR-R-11-93-248 ..... p 2031 N95-24859 #
JINR-R-11-93-249 ..... p 2031 N95-24704 #
JINR-R-11-93-250 ..... p 2031 N95-24705 #
JINR-R-11-93-265 ..... p 2031 N95-24694 #
JINR-R-11-93-266 ..... p 2031 N95-24695 #
JINR-R-11-94-120 ..... p 2029 N95-24375 #
JINR-R-11-94-74 ..... p 2029 N95-24387 #
JINR-R-13-93-326 ..... p 2073 N95-24642 #
JINR-R-13-93-331 ..... p 1957 N95-24487 #
JINR-R-13-93-362 ..... p 2047 N95-24644 #
JINR-R-13-94-114 ..... p 2058 N95-25905 #
JINR-R-2-93-304 ..... p 2047 N95-24668 #
JINR-R-2-93-321 ..... p 2036 N95-24688 #
JINR-R-2-93-463 ..... p 2049 N95-24888 #
JINR-R-2-94-109 ..... p 2092 N95-24313 #
JINR-R-3-93-242 ..... p 2086 N95-24537 #
JINR-R-3-94-125 ..... p 2043 N95-24364 #
JINR-R-4-93-300 ..... p 2035 N95-24883 #
JINR-R-4-93-460 ..... p 2033 N95-25539
JINR-R-4-94-115 ..... p 2057 N95-25784 #
JINR-R-4-94-143 ..... p 2056 N95-25668 #
JINR-R-4-94-146 ..... p 2055 N95-25493 #
JINR-R-5-93-169 ..... p 2030 N95-24636 #
JINR-R-5-93-170 ..... p 2032 N95-24860 #
JINR-R-6-93-244 ..... p 2037 N95-24696 #
JINR-R-6-93-289 ..... p 2093 N95-24481 #
JINR-R-9-93-307 ..... p 2048 N95-24689 #

JINR-18-94-108 ..... p 2085 N95-24374 #

JPL-PUBL-94-10 ..... p 2022 N95-25253 * #

JPL-400-445 ..... p 2112 N95-25854 * #
JPL-400-504 ..... p 2113 N95-26336 * #

JPRS-USP-94-007 ..... p 1915 N95-24358 #
JPRS-USP-94-008 ..... p 1916 N95-24359 #
JPRS-USP-94-008 ..... p 1916 N95-24847 #

JPRS-UST-94-018 ..... p 1950 N95-24472 #
JPRS-UST-94-024 ..... p 1958 N95-24620 #
JPRS-UST-94-025 ..... p 2045 N95-24471 #
JPRS-UST-94-027 ..... p 1957 N95-24470 #
JPRS-UST-94-030 ..... p 1962 N95-24469 #
JPRS-UST-94-031 ..... p 1988 N95-24760 #
JPRS-UST-94-032 ..... p 1950 N95-24759 #
JPRS-UST-94-033 ..... p 2037 N95-24732 #
JPRS-UST-94-034 ..... p 1987 N95-24729 #
JPRS-UST-94-035 ..... p 2016 N95-24429 #
JPRS-UST-95-002 ..... p 1916 N95-24621 #
JPRS-UST-95-003 ..... p 1988 N95-24730 #
JPRS-UST-95-004 ..... p 1989 N95-24768 #
JPRS-UST-95-006 ..... p 1950 N95-24731 #
JPRS-UST-95-007 ..... p 1920 N95-24761 #
JPRS-UST-95-008 ..... p 1957 N95-24468 #
JPRS-UST-95-009 ..... p 1916 N95-24467 #
JPRS-UST-95-010 ..... p 1953 N95-24539 #
JPRS-UST-95-011 ..... p 1910 N95-24541 #
JPRS-UST-95-012 ..... p 1950 N95-24540 #
JPRS-UST-95-013 ..... p 1987 N95-24538 #
JPRS-UST-95-017 ..... p 1988 N95-26080 #
JPRS-UST-95-018 ..... p 2071 N95-26079 #

JP9407200 ..... p 2070 N95-25772 #

JSC-08289 ..... p 1919 N95-26189 * #
JSC-1472 ..... p 1919 N95-25874 *
JSC-1477 ..... p 1918 N95-24198 *
JSC-536 ..... p 1917 N95-25424 *
JSC-548 ..... p 1918 N95-24215 *

JTN-95-80825 ..... p 2114 N95-24908 #

KCL-93/7 ..... p 2099 N95-25650 #

KCP-613-5411 ..... p 1969 N95-25381 #
KCP-613-5452 ..... p 2018 N95-26167 #

KCP-613-5515 ..... p 1958 N95-24532

KE-93006B ..... p 1997 N95-24499 #
KE-93016G ..... p 1948 N95-24498 #

KEK-PROC-92-18 ..... p 2048 N95-24702 #
KEK-PROC-93-14 ..... p 1931 N95-25356 #
KEK-PROC-93-16 ..... p 2021 N95-25303 #

KEK-93-9 ..... p 1958 N95-24701 #

KTM/E-B-155 ..... p 1949 N95-25244 #

L-17386 ..... p 1907 N95-25338 * #
L-17409 ..... p 1907 N95-24566 * #

LA-SUB-94-136 ..... p 1941 N95-25386 #
LA-SUB-94-169 ..... p 1959 N95-25385 #
LA-SUB-95-1 ..... p 1969 N05-25384 #

LA-UR-94-1688 ..... p 1920 N95-24711 #
LA-UR-94-3152 ..... p 2021 N95-25477 #
LA-UR-94-3301 ..... p 2019 N95-24343 #
LA-UR-94-3490 ..... p 1948 N95-24670 #
LA-UR-94-3753 ..... p 2065 N95-24331 #
LA-UR-94-378 ..... p 1973 N95-26112 #
LA-UR-94-3937 ..... p 2109 N95-24234 #
LA-UR-94-3945 ..... p 2078 N95-24667 #
LA-UR-94-3953 ..... p 2091 N95-24235 #
LA-UR-94-3956 ..... p 2086 N95-24513 #
LA-UR-94-3958 ..... p 1925 N95-24590 #
LA-UR-94-3966 ..... p 2086 N95-24514 #
LA-UR-94-4035 ..... p 2033 N95-25676 #
LA-UR-94-4061 ..... p 1958 N95-24589 #
LA-UR-94-4081 ..... p 2083 N95-24233 #
LA-UR-94-4124 ..... p 2069 N95-25366 #
LA-UR-94-4127 ..... p 2022 N95-26066 #
LA-UR-94-4163 ..... p 2110 N95-25766 #
LA-UR-94-4168 ..... p 1973 N95-25565 #
LA-UR-94-4179 ..... p 1940 N95-24456 #
LA-UR-94-4196 ..... p 2109 N95-24455 #
LA-UR-94-4218 ..... p 1937 N95-26014
LA-UR-94-4295 ..... p 2089 N95-25598 #
LA-UR-94-4318 ..... p 2096 N95-25293 #
LA-UR-94-4333 ..... p 2080 N95-25289 #
LA-UR-94-4339 ..... p 2020 N95-24612 #
LA-UR-94-4350 ..... p 1924 N95-25597 #
LA-UR-94-4354 ..... p 2070 N95-25594 #
LA-UR-94-4361 ..... p 2110 N95-25675 #
LA-UR-94-4364 ..... p 1935 N95-25379 #
LA-UR-94-4365 ..... p 2094 N95-24610 #
LA-UR-94-4374 ..... p 1926 N95-25596 #
LA-UR-94-4382 ..... p 2030 N95-24609 #
LA-UR-94-4385 ..... p 2033 N95-25767 #
LA-UR-94-4386 ..... p 2093 N95-24457 #
LA-UR-95-426 ..... p 1973 N95-25557 #
LA-UR-95-440 ..... p 2086 N95-24594 #

LA-12740-M ..... p 2055 N95-25484 #
LA-12788-MS ..... p 2008 N95-24600 #
LA-12814-MS ..... p 1999 N95-25198 #
LA-12858-MS ..... p 1941 N95-25237 #
LA-12885 ..... p 2041 N95-24258 #

LAMP-93/4 ..... p 2073 N95-24402 #
LAMP-94/1 ..... p 2048 N95-24718 #
LAMP-94/3 ..... p 1952 N95-24403 #
LAMP-94/5 ..... p 2041 N95-24268 #

LBL-PUB-601-VOL-7-NO-1 ..... p 2073 N95-24546 #

LBL-34780 ..... p 2020 N95-24496 #
LBL-35179 ..... p 2021 N95-25359 #
LBL-35238 ..... p 2015 N95-25773 #
LBL-35476 ..... p 1958 N95-24551 #
LBL-35635 ..... p 2069 N95-25358 #
LBL-35687-VOL-2 ..... p 2070 N95-25478 #
LBL-35822 ..... p 2068 N95-24665 #
LBL-36050 ..... p 2074 N95-25357 #
LBL-36079 ..... p 2045 N95-24533 #
LBL-36080 ..... p 2045 N95-24512 #
LBL-36175 ..... p 2092 N95-24333 #
LBL-36250 ..... p 2066 N95-24495 #
LBL-36273 ..... p 2064 N95-26256 #
LBL-36302 ..... p 2065 N95-24320 #
LBL-91-REV-8/94 ..... p 2067 N95-24652 #

M-763 ..... p 1921 N95-25875 * #
M-773 ..... p 1906 N95-24217 * #
M-776 ..... p 1936 N95-25677 * #

MIT-ANP-TR-026 ..... p 2014 N95-25483 #

MML-1-1994 ..... p 1926 N95-25505

NAL-TR-1212T ..... p 1977 N95-25672 #

NAL-TR-1213 ..... p 1942 N95-25760 #
NAL-TR-1214 ..... p 1927 N95-25859 #
NAL-TR-1217 ..... p 2034 N95-25860 #
NAL-TR-1222 ..... p 1982 N95-25661 #
NAL-TR-1223 ..... p 1911 N95-25862 #
NAL-TR-1224 ..... p 1949 N95-25769 #
NAL-TR-1226 ..... p 1908 N95-25761 #
NAL-TR-1227 ..... p 1963 N95-25001 #
NAL-TR-1228 ..... p 1908 N95-25762 #
NAL-TR-1231-PT-2 ..... p 1970 N95-25763 #
NAL-TR-1232 ..... p 1921 N95-25664 #
NAL-TR-1235 ..... p 1910 N95-25764 #
NAL-TR-1241 ..... p 1926 N95-24989 #
NAL-TR-1241 ..... p 1927 N95-25770 #
NAL-TR-1242 ..... p 1914 N95-24990 #
NAL-TR-1243 ..... p 1976 N95-25323 #
NAL-TR-1244T ..... p 1907 N95-24998 #
NAL-TR-1245 ..... p 1907 N95-25105 #
NAL-TR-1248 ..... p 1981 N95-25000 #
NAL-TR-1248 ..... p 1983 N95-25796 #
NAL-TR-1250 ..... p 1922 N95-24999 #
NAL-TR-1251 ..... p 1912 N95-25005 #
NAL-TR-1257 ..... p 2073 N95-25004 #

NAS 1.15:104606-VOL-5 ..... p 2003 N95-24766 * #
NAS 1.15:104617 ..... p 2005 N95-26341 * #
NAS 1.15:104808 ..... p 2013 N95-24627 * #
NAS 1.15:106669 ..... p 1914 N95-24561 * #
NAS 1.15:106694 ..... p 1966 N95-26077 * #
NAS 1.15:106853 ..... p 1923 N95-24437 * #
NAS 1.15:106865 ..... p 1913 N95-24390 * #
NAS 1.15:106868 ..... p 1961 N95-24399 * #
NAS 1.15:106879 ..... p 1991 N95-24560 * #
NAS 1.15:106880 ..... p 1977 N95-26074 * #
NAS 1.15:106887 ..... p 1924 N95-25961 * #
NAS 1.15:106894 ..... p 2099 N95-25878 * #
NAS 1.15:106897 ..... p 2029 N95-24474 * #
NAS 1.15:106899 ..... p 1970 N95-26073 * #
NAS 1.15:106901 ..... p 1977 N95-26076 * #
NAS 1.15:106902 ..... p 1923 N95-25877 * #
NAS 1.15:106904 ..... p 1955 N95-25876 * #
NAS 1.15:106907 ..... p 2018 N95-25879 * #
NAS 1.15:106913 ..... p 1908 N95-25962 * #
NAS 1.15:106919 ..... p 1908 N95-26075 * #
NAS 1.15:106926 ..... p 1983 N95-26078 * #
NAS 1.15:108482 ..... p 1948 N95-24558 * #
NAS 1.15:108485 ..... p 2003 N95-24763 * #
NAS 1.15:108486 ..... p 2003 N95-24764 * #
NAS 1.15:108487 ..... p 2107 N95-26084 * #
NAS 1.15:109165 ..... p 1909 N95-24633 * #
NAS 1.15:109171 ..... p 1910 N95-24582 * #
NAS 1.15:109175 ..... p 1928 N95-26251 * #
NAS 1.15:109176 ..... p 2019 N95-24382 * #
NAS 1.15:109178 ..... p 1979 N95-24208 * #
NAS 1.15:109179 ..... p 1906 N95-24397 * #
NAS 1.15:109180 ..... p 1927 N95-26083 * #
NAS 1.15:109181 ..... p 1961 N95-24396 * #
NAS 1.15:110153 ..... p 1950 N95-24559 * #
NAS 1.15:110154 ..... p 2015 N95-24209 * #
NAS 1.15:110155 ..... p 1920 N95-24581 * #
NAS 1.15:110156 ..... p 1919 N95-24765 * #
NAS 1.15:110346 ..... p 1910 N95-24629 * #
NAS 1.15:110347 ..... p 1908 N95-26302 * #
NAS 1.15:110494 ..... p 1949 N95-24416 * #
NAS 1.15:110495 ..... p 2072 N95-24386 * #
NAS 1.15:110496 ..... p 1971 N95-24530 * #
NAS 1.15:110497 ..... p 2008 N95-24531 * #
NAS 1.15:110498 ..... p 2003 N95-24336 * #
NAS 1.15:110554 ..... p 1920 N95-24505 * #
NAS 1.15:110555 ..... p 2112 N95-24994 * #
NAS 1.15:110574 ..... p 2103 N95-25849 * #
NAS 1.15:110575 ..... p 2103 N95-25850 * #
NAS 1.15:110577 ..... p 2100 N95-25643 * #
NAS 1.15:110578 ..... p 2108 N95-26183 * #
NAS 1.15:110579 ..... p 1919 N95-24466 * #
NAS 1.15:110580 ..... p 1989 N95-24542 * #
NAS 1.15:110592 ..... p 2103 N95-26262 * #
NAS 1.15:110596 ..... p 2108 N95-25746 * #
NAS 1.15:110598 ..... p 1917 N95-26184 * #
NAS 1.15:110649 ..... p 1921 N95-25337 * #
NAS 1.15:4610 ..... p 1907 N95-25338 * #
NAS 1.15:4634 ..... p 1907 N95-24566 * #
NAS 1.15:4679 ..... p 1955 N95-25710 * #
NAS 1.21:6101(08) ..... p 2102 N95-24565 * #
NAS 1.21:7011(400) ..... p 2011 N95-24464 *
NAS 1.21:7011(401) ..... p 2012 N95-25800 *
NAS 1.21:7037(316) ..... p 1905 N95-24465 *
NAS 1.21:7037(317) ..... p 1906 N95-25798 *
NAS 1.21:7109(01) ..... p 2103 N95-24238 * #
NAS 1.26;195061 ..... p 1965 N95-25960 * #
NAS 1.26:188363 ..... p 1928 N95-24222 * #
NAS 1.26:189201 ..... p 1912 N95-24624 * #
NAS 1.26:193855 ..... p 1940 N95-24562 * #
NAS 1.26:194451 ..... p 1968 N95-25330 * #
NAS 1.26:195026 ..... p 2040 N95-26160 * #
NAS 1.26:195029 ..... p 1921 N95-24216 * #

NAS 1.26:195029 ..... p 1921 N95-24428 * #
NAS 1.26:195031 ..... p 2029 N95-24421 * #
NAS 1.26:195033 ..... p 1907 N95-24443 * #
NAS 1.26:195035 ..... p 2032 N95-25114 * #
NAS 1.26:195036 ..... p 2029 N95-24389 * #
NAS 1.26:195037 ..... p 2020 N95-24634 * #
NAS 1.26:195038 ..... p 1964 N95-25394 * #
NAS 1.26:195040 ..... p 2014 N95-25119 * #
NAS 1.26:195041 ..... p 1915 N95-24388 * #
NAS 1.26:195042 ..... p 1928 N95-26203 * #
NAS 1.26:195043 ..... p 2014 N95-26085 * #
NAS 1.26:195047 ..... p 1963 N95-24584 * #
NAS 1.26:195049 ..... p 2031 N95-24857 * #
NAS 1.26:195054 ..... p 1962 N95-24580 * #
NAS 1.26:195056 ..... p 2032 N95-25106 * #
NAS 1.26:195059 ..... p 2031 N95-24856 * #
NAS 1.26:195060 ..... p 2030 N95-24632 * #
NAS 1.26:195064 ..... p 1966 N95-25964 * #
NAS 1.26:195075 ..... p 1983 N95-26199 * #
NAS 1.26:195076 ..... p 2027 N95-26086 * #
NAS 1.26:195283 ..... p 1967 N95-24473 * #
NAS 1.26:195434 ..... p 1963 N95-24906 * #
NAS 1.26:195441 ..... p 1927 N95-25880 * #
NAS 1.26:195443 ..... p 1913 N95-24304 * #
NAS 1.26:195448 ..... p 1957 N95-24476 * #
NAS 1.26:195451 ..... p 1980 N95-24398 * #
NAS 1.26:195455 ..... p 1925 N95-24438 * #
NAS 1.26:195463 ..... p 2063 N95-25963 * #
NAS 1.26:196562 ..... p 2104 N95-24477 * #
NAS 1.26:196564 ..... p 2104 N95-24439 * #
NAS 1.26:196565 ..... p 1922 N95-24845 * #
NAS 1.26:196566-VOL-1 ..... p 1921 N95-24440 * #
NAS 1.26:196567 ..... p 1922 N95-24844 * #
NAS 1.26:196568 ..... p 1922 N95-24854 * #
NAS 1.26:196576 ..... p 2102 N95-24442 * #
NAS 1.26:196588 ..... p 1976 N95-25595 * #
NAS 1.26:196591 ..... p 2089 N95-25409 * #
NAS 1.26:196695 ..... p 1910 N95-24436 * #
NAS 1.26:197233 ..... p 1919 N95-26189 * #
NAS 1.26:197281 ..... p 2108 N95-24385 * #
NAS 1.26:197334 ..... p 2022 N95-25253 * #
NAS 1.26:197378 ..... p 1974 N95-24204 * #
NAS 1.26:197412 ..... p 1962 N95-24461 * #
NAS 1.26:197415 ..... p 2101 N95-26304 * #
NAS 1.26:197426 ..... p 1981 N95-24907 * #
NAS 1.26:197625 ..... p 2065 N95-24335 * #
NAS 1.26:197694 ..... p 2058 N95-25911 * #
NAS 1.26:197697 ..... p 1909 N95-24391 * #
NAS 1.26:197698 ..... p 2035 N95-24278 * #
NAS 1.26:197702 ..... p 2073 N95-24545 * #
NAS 1.26:197703 ..... p 2016 N95-24876 * #
NAS 1.26:197705 ..... p 1975 N95-24991 * #
NAS 1.26:197707 ..... p 2113 N95-26336 * #
NAS 1.26:197708 ..... p 2112 N95-25854 * #
NAS 1.26:197709 ..... p 2011 N95-24556 * #
NAS 1.26:197715 ..... p 1968 N95-25118 * #
NAS 1.26:197720 ..... p 1938 N95-26068 * #
NAS 1.26:197725 ..... p 1970 N95-25699 * #
NAS 1.26:197727 ..... p 2017 N95-25797 * #
NAS 1.26:197731 ..... p 2109 N95-25122 * #
NAS 1.26:197791 ..... p 1943 N95-26081 * #
NAS 1.26:197796 ..... p 2106 N95-25410 * #
NAS 1.26:197802 ..... p 2019 N95-26206 * #
NAS 1.26:197860 ..... p 1913 N95-24213 * #
NAS 1.26:197891 ..... p 2086 N95-24534 * #
NAS 1.26:197915 ..... p 2005 N95-24535 * #
NAS 1.26:197922 ..... p 2026 N95-25801 * #
NAS 1.26:197923 ..... p 2017 N95-25867 * #
NAS 1.26:197952 ..... p 2027 N95-24214 * #
NAS 1.26:197964 ..... p 2084 N95-24261 * #
NAS 1.26:197967 ..... p 1933 N95-24400 * #
NAS 1.26:197975 ..... p 2008 N95-24475 * #
NAS 1.26:197983 ..... p 1922 N95-24626 * #
NAS 1.26:197985 ..... p 1974 N95-24223 * #
NAS 1.26:197986 ..... p 2112 N95-24303 * #
NAS 1.26:197988 ..... p 1915 N95-24380 * #
NAS 1.26:197991 ..... p 2085 N95-24478 * #
NAS 1.26:197992 ..... p 2005 N95-24411 * #
NAS 1.26:197993 ..... p 2108 N95-25104 * #
NAS 1.26:197994 ..... p 2114 N95-24381 * #
NAS 1.26:197999 ..... p 2016 N95-24993 * #
NAS 1.26:198000 ..... p 1978 N95-25333 * #
NAS 1.26:198002 ..... p 2002 N95-25955 * #
NAS 1.26:198008 ..... p 2112 N95-26116 * #
NAS 1.26:198009 ..... p 2049 N95-24877 * #
NAS 1.26:198010 ..... p 2011 N95-24564 * #
NAS 1.26:198013 ..... p 2020 N95-24563 * #
NAS 1.26:198015 ..... p 1997 N95-24501 * #
NAS 1.26:198019 ..... p 2015 N95-24224 * #
NAS 1.26:198020 ..... p 1998 N95-24846 * #
NAS 1.26:198024 ..... p 1911 N95-25334 * #
NAS 1.26:198025 ..... p 1918 N95-24579 * #
NAS 1.26:198027 ..... p 2026 N95-25335 * #
NAS 1.26:198028 ..... p 1983 N95-26263 * #
NAS 1.26:198029 ..... p 1962 N95-24412 * #
NAS 1.26:198030 ..... p 1962 N95-24413 * #

NAS 1.26:198034 ..... p 2111 N95-24239 * #
NAS 1.26:198035 ..... p 1974 N95-24218 * #
NAS 1.26:198037 ..... p 1989 N95-24441 * #
NAS 1.26:198038 ..... p 2005 N95-24219 * #
NAS 1.26:198040 ..... p 1915 N95-24302 * #
NAS 1.26:198041 ..... p 1933 N95-24220 * #
NAS 1.26:198043 ..... p 1990 N95-24199 * #
NAS 1.26:198044 ..... p 1923 N95-25103 * #
NAS 1.26:198045 ..... p 1906 N95-24379 * #
NAS 1.26:198047 ..... p 1947 N95-24226 * #
NAS 1.26:198048 ..... p 2010 N95-24410 * #
NAS 1.26:198050 ..... p 1961 N95-24221 * #
NAS 1.26:4644 ..... p 1952 N95-24395 * #
NAS 1.26:4645 ..... p 1935 N95-24878 * #
NAS 1.26:4652 ..... p 1906 N95-24217 * #
NAS 1.26:4653 ..... p 2039 N95-24879 * #
NAS 1.26:4654 ..... p 1911 N95-24630 * #
NAS 1.26:4655 ..... p 1925 N95-26072 * #
NAS 1.26:4657 ..... p 1923 N95-24583 * #
NAS 1.26:4660 ..... p 1914 N95-24392 * #
NAS 1.26:4666 ..... p 2083 N95-26082 * #
NAS 1.26:4667 ..... p 1917 N95-26205 * #
NAS 1.55:10166 ..... p 1912 N95-24207 * #
NAS 1.55:10170 ..... p 1943 N95-26119 * #
NAS 1.60:3545 ..... p 1936 N95-25677 * #
NAS 1.61:1350 ..... p 1921 N95-25875 * #
NAS 1.61:1356 ..... p 2112 N95-24987 * #
NAS 1.61:1359 ..... p 1996 N95-24274 * #
NAS 1.61:1364 ..... p 1950 N95-24543 * #
NAS 1.71:LAR-15217-1 ..... p 1939 N95-24212 * #

NASA-CASE-ARC-11917-1 ..... p 1967 N95-24236 *
NASA-CASE-ARC-11937-1 ..... p 2074 N95-26015 *
NASA-CASE-ARC-11995-1 ..... p 2075 N95-26117 *

NASA-CASE-GSC-13478-1 ..... p 1960 N95-25889 *
NASA-CASE-GSC-13571-1 ..... p 1960 N95-26038 *

NASA-CASE-LAR-14535-1 ..... p 1926 N95-25305 *
NASA-CASE-LAR-14752-1 ..... p 1943 N95-26118 *
NASA-CASE-LAR-14776-1 ..... p 1968 N95-24625 *
NASA-CASE-LAR-15063-1-CU ..... p 1978 N95-25304 *
NASA-CASE-LAR-15173-1-CU ..... p 1926 N95-25546 *
NASA-CASE-LAR-15217-1 ..... p 1939 N95-24212 * #

NASA-CASE-LEW-15170-2 ..... p 2040 N95-26187 *

NASA-CASE-MFS-28581-1 ..... p 1936 N95-25545 *
NASA-CASE-MFS-28817-1 ..... p 1969 N95-25544 *
NASA-CASE-MFS-28857-1 ..... p 1976 N95-25548 *

NASA-CASE-MSC-22244-1 ..... p 2014 N95-25306 *
NASA-CASE-MSC-22327-1 ..... p 1976 N95-25592 *

NASA-CASE-NPO-18547-1-CU ..... p 1959 N95-25307 *
NASA-CASE-NPO-18772-1-CU ..... p 1954 N95-25316 *
NASA-CASE-NPO-18791-1 ..... p 1971 N95-26340 *
NASA-CASE-NPO-18995-1-CU ..... p 1969 N95-25547 *

NASA-CP-10166 ..... p 1912 N95-24207 * #
NASA-CP-10170 ..... p 1943 N95-26119 * #

NASA-CR-110585 ..... p 2112 N95-24672 *
NASA-CR-188363 ..... p 1928 N95-24222 * #
NASA-CR-189201 ..... p 1912 N95-24624 * #
NASA-CR-193855 ..... p 1940 N95-24562 * #
NASA-CR-194451 ..... p 1968 N95-25330 * #
NASA-CR-195028 ..... p 2040 N95-26160 * #
NASA-CR-195029 ..... p 1921 N95-24216 * #
NASA-CR-195029 ..... p 1921 N95-24428 * #
NASA-CR-195031 ..... p 2029 N95-24421 * #
NASA-CR-195033 ..... p 1907 N95-24443 * #
NASA-CR-195035 ..... p 2032 N95-25114 * #
NASA-CR-195036 ..... p 2029 N95-24389 * #
NASA-CR-195037 ..... p 2020 N95-24634 * #
NASA-CR-195038 ..... p 1964 N95-25394 * #
NASA-CR-195040 ..... p 2014 N95-25119 * #
NASA-CR-195041 ..... p 1915 N95-24388 * #
NASA-CR-195042 ..... p 1928 N95-26203 * #
NASA-CR-195043 ..... p 2014 N95-26085 * #
NASA-CR-195047 ..... p 1963 N95-24584 * #
NASA-CR-195049 ..... p 2031 N95-24857 * #
NASA-CR-195054 ..... p 1962 N95-24580 * #
NASA-CR-195056 ..... p 2032 N95-25106 * #
NASA-CR-195059 ..... p 2031 N95-24856 * #
NASA-CR-195060 ..... p 2030 N95-24632 * #
NASA-CR-195061 ..... p 1965 N95-25960 * #
NASA-CR-195064 ..... p 1966 N95-25964 * #
NASA-CR-195067 ..... p 1909 N95-25341 * #
NASA-CR-195075 ..... p 1983 N95-26199 * #
NASA-CR-195076 ..... p 2027 N95-26086 * #
NASA-CR-195283 ..... p 1967 N95-24473 * #
NASA-CR-195434 ..... p 1963 N95-24906 * #
NASA-CR-195441 ..... p 1927 N95-25880 * #
NASA-CR-195443 ..... p 1913 N95-24304 * #
NASA-CR-195448 ..... p 1957 N95-24476 * #
NASA-CR-195451 ..... p 1980 N95-24398 * #
NASA-CR-195455 ..... p 1925 N95-24438 * #
NASA-CR-195463 ..... p 2063 N95-25963 * #
NASA-CR-196562 ..... p 2104 N95-24477 * #
NASA-CR-196564 ..... p 2104 N95-24439 * #
NASA-CR-196565 ..... p 1922 N95-24845 * #
NASA-CR-196566-VOL-1 ..... p 1921 N95-24440 * #
NASA-CR-196567 ..... p 1922 N95-24844 * #
NASA-CR-196568 ..... p 1922 N95-24854 * #
NASA-CR-196576 ..... p 2102 N95-24442 * #
NASA-CR-196588 ..... p 1976 N95-25595 * #
NASA-CR-196591 ..... p 2089 N95-25409 * #
NASA-CR-196695 ..... p 1910 N95-24436 * #
NASA-CR-197233 ..... p 1919 N95-26189 * #
NASA-CR-197281 ..... p 2108 N95-24385 * #
NASA-CR-197334 ..... p 2022 N95-25253 * #
NASA-CR-197378 ..... p 1974 N95-24204 * #
NASA-CR-197412 ..... p 1962 N95-24461 * #
NASA-CR-197415 ..... p 2101 N95-26304 * #
NASA-CR-197426 ..... p 1981 N95-24907 * #
NASA-CR-197625 ..... p 2065 N95-24335 * #
NASA-CR-197694 ..... p 2058 N95-25911 * #
NASA-CR-197697 ..... p 1909 N95-24391 * #
NASA-CR-197698 ..... p 2035 N95-24278 * #
NASA-CR-197702 ..... p 2073 N95-24545 * #
NASA-CR-197703 ..... p 2016 N95-24876 * #
NASA-CR-197705 ..... p 1975 N95-24991 * #
NASA-CR-197707 ..... p 2113 N95-26336 * #
NASA-CR-197708 ..... p 2112 N95-25854 * #
NASA-CR-197709 ..... p 2011 N95-24556 * #
NASA-CR-197715 ..... p 1968 N95-25118 * #
NASA-CR-197720 ..... p 1938 N95-26068 * #
NASA-CR-197725 ..... p 1970 N95-25699 * #
NASA-CR-197727 ..... p 2017 N95-25797 * #
NASA-CR-197731 ..... p 2109 N95-25122 * #
NASA-CR-197791 ..... p 1943 N95-26081 * #
NASA-CR-197796 ..... p 2106 N95-25410 * #
NASA-CR-197802 ..... p 2019 N95-26206 * #
NASA-CR-197860 ..... p 1913 N95-24213 * #
NASA-CR-197891 ..... p 2086 N95-24534 * #
NASA-CR-197915 ..... p 2005 N95-24535 * #
NASA-CR-197922 ..... p 2026 N95-25801 * #
NASA-CR-197923 ..... p 2017 N95-25867 * #
NASA-CR-197952 ..... p 2027 N95-24214 * #
NASA-CR-197964 ..... p 2084 N95-24261 * #
NASA-CR-197967 ..... p 1933 N95-24400 * #
NASA-CR-197975 ..... p 2008 N95-24475 * #
NASA-CR-197983 ..... p 1922 N95-24626 * #
NASA-CR-197985 ..... p 1974 N95-24223 * #
NASA-CR-197986 ..... p 2112 N95-24303 * #
NASA-CR-197988 ..... p 1915 N95-24380 * #
NASA-CR-197991 ..... p 2085 N95-24478 * #
NASA-CR-197992 ..... p 2005 N95-24411 * #
NASA-CR-197993 ..... p 2108 N95-25104 * #
NASA-CR-197994 ..... p 2114 N95-24381 * #
NASA-CR-197999 ..... p 2016 N95-24993 * #
NASA-CR-198000 ..... p 1978 N95-25333 * #
NASA-CR-198002 ..... p 2002 N95-25955 * #
NASA-CR-198008 ..... p 2112 N95-26116 * #
NASA-CR-198009 ..... p 2049 N95-24877 * #
NASA-CR-198010 ..... p 2011 N95-24564 * #
NASA-CR-198013 ..... p 2020 N95-24563 * #
NASA-CR-198015 ..... p 1997 N95-24501 * #
NASA-CR-198019 ..... p 2015 N95-24224 * #
NASA-CR-198020 ..... p 1998 N95-24846 * #
NASA-CR-198024 ..... p 1911 N95-25334 * #
NASA-CR-198025 ..... p 1918 N95-24579 * #
NASA-CR-198027 ..... p 2026 N95-25335 * #
NASA-CR-198028 ..... p 1983 N95-26263 * #
NASA-CR-198029 ..... p 1962 N95-24412 * #
NASA-CR-198030 ..... p 1962 N95-24413 * #
NASA-CR-198034 ..... p 2111 N95-24239 * #
NASA-CR-198035 ..... p 1974 N95-24218 * #
NASA-CR-198037 ..... p 1989 N95-24441 * #
NASA-CR-198038 ..... p 2005 N95-24219 * #
NASA-CR-198040 ..... p 1915 N95-24302 * #
NASA-CR-198041 ..... p 1933 N95-24220 * #
NASA-CR-198043 ..... p 1990 N95-24199 * #
NASA-CR-198044 ..... p 1923 N95-25103 * #
NASA-CR-198045 ..... p 1906 N95-24379 * #
NASA-CR-198047 ..... p 1947 N95-24226 * #
NASA-CR-198048 ..... p 2010 N95-24410 * #
NASA-CR-198050 ..... p 1961 N95-24221 * #
NASA-CR-4644 ..... p 1952 N95-24395 * #
NASA-CR-4645 ..... p 1935 N95-24878 * #
NASA-CR-4652 ..... p 1906 N95-24217 * #
NASA-CR-4653 ..... p 2039 N95-24879 * #
NASA-CR-4654 ..... p 1911 N95-24630 * #
NASA-CR-4655 ..... p 1925 N95-26072 * #
NASA-CR-4657 ..... p 1923 N95-24583 * #
NASA-CR-4660 ..... p 1914 N95-24392 * #
NASA-CR-4666 ..... p 2083 N95-26082 * #
NASA-CR-4667 ..... p 1917 N95-26205 * #

NASA-RP-1350 ..... p 1921 N95-25875 * #
NASA-RP-1356 ..... p 2112 N95-24987 * #
NASA-RP-1359 ..... p 1996 N95-24274 * #
NASA-RP-1364 ..... p 1950 N95-24543 * #

NASA-SP-6101(08) ..... p 2102 N95-24565 * #
NASA-SP-7011(400) ..... p 2011 N95-24464 *
NASA-SP-7011(401) ..... p 2012 N95-25800 *
NASA-SP-7037(316) ..... p 1905 N95-24465 *
NASA-SP-7037(317) ..... p 1906 N95-25798 *
NASA-SP-7109(01) ..... p 2103 N95-24238 * #

NASA-TM-104606-VOL-5 ..... p 2003 N95-24786 * #
NASA-TM-104617 ..... p 2005 N95-26341 * #
NASA-TM-104808 ..... p 2013 N95-24627 * #
NASA-TM-106669 ..... p 1914 N95-24561 * #
NASA-TM-106694 ..... p 1966 N95-26077 * #
NASA-TM-106853 ..... p 1923 N95-24437 * #
NASA-TM-106865 ..... p 1913 N95-24390 * #
NASA-TM-106868 ..... p 1961 N95-24399 * #
NASA-TM-106879 ..... p 1991 N95-24560 * #
NASA-TM-106880 ..... p 1977 N95-26074 * #
NASA-TM-106887 ..... p 1924 N95-25961 * #
NASA-TM-106894 ..... p 2099 N95-25878 * #
NASA-TM-106897 ..... p 2029 N95-24474 * #
NASA-TM-106899 ..... p 1970 N95-26073 * #
NASA-TM-106901 ..... p 1977 N95-26076 * #
NASA-TM-106902 ..... p 1923 N95-25877 * #
NASA-TM-106904 ..... p 1955 N95-25876 * #
NASA-TM-106907 ..... p 2018 N95-25879 * #
NASA-TM-106913 ..... p 1908 N95-25962 * #
NASA-TM-106919 ..... p 1908 N95-26075 * #
NASA-TM-106926 ..... p 1983 N95-26078 * #
NASA-TM-108482 ..... p 1948 N95-24558 * #
NASA-TM-108485 ..... p 2003 N95-24763 * #
NASA-TM-108486 ..... p 2003 N95-24764 * #
NASA-TM-108487 ..... p 2107 N95-26084 * #
NASA-TM-109165 ..... p 1909 N95-24633 * #
NASA-TM-109171 ..... p 1910 N95-24582 * #
NASA-TM-109175 ..... p 1928 N95-26251 * #
NASA-TM-109176 ..... p 2019 N95-24382 * #
NASA-TM-109178 ..... p 1979 N95-24208 * #
NASA-TM-109179 ..... p 1906 N95-24397 * #
NASA-TM-109180 ..... p 1927 N95-26083 * #
NASA-TM-109181 ..... p 1961 N95-24396 * #
NASA-TM-110153 ..... p 1950 N95-24559 * #
NASA-TM-110154 ..... p 2015 N95-24209 * #
NASA-TM-110155 ..... p 1920 N95-24581 * #
NASA-TM-110156 ..... p 1919 N95-24765 * #
NASA-TM-110346 ..... p 1910 N95-24629 * #
NASA-TM-110347 ..... p 1908 N95-26302 * #
NASA-TM-110494 ..... p 1949 N95-24416 * #
NASA-TM-110495 ..... p 2072 N95-24386 * #
NASA-TM-110496 ..... p 1971 N95-24530 * #
NASA-TM-110497 ..... p 2008 N95-24531 * #
NASA-TM-110498 ..... p 2003 N95-24336 * #
NASA-TM-110537 ..... p 1918 N95-24195 *
NASA-TM-110540 ..... p 2108 N95-24196 *
NASA-TM-110550 ..... p 1918 N95-24197 *
NASA-TM-110551 ..... p 1918 N95-24215 *
NASA-TM-110552 ..... p 1918 N95-24198 *
NASA-TM-110554 ..... p 1920 N95-24505 * #
NASA-TM-110555 ..... p 2112 N95-24994 * #
NASA-TM-110562 ..... p 1919 N95-25874 *
NASA-TM-110574 ..... p 2103 N95-25849 * #
NASA-TM-110575 ..... p 2103 N95-25850 * #
NASA-TM-110576 ..... p 1917 N95-25424 *
NASA-TM-110577 ..... p 2100 N95-25643 * #
NASA-TM-110578 ..... p 2108 N95-26183 * #
NASA-TM-110579 ..... p 1919 N95-24466 * #
NASA-TM-110580 ..... p 1989 N95-24542 * #
NASA-TM-110592 ..... p 2103 N95-26262 * #
NASA-TM-110596 ..... p 2108 N95-25746 * #
NASA-TM-110598 ..... p 1917 N95-26184 * #
NASA-TM-110649 ..... p 1921 N95-25337 * #
NASA-TM-4610 ..... p 1907 N95-25338 * #
NASA-TM-4634 ..... p 1907 N95-24566 * #
NASA-TM-4679 ..... p 1955 N95-25710 * #

NASA-TP-3545 ..... p 1936 N95-25677 * #

NAVY-CASE-75409 ..... p 1961 N95-26186

NAWS-CL-TP-003 ..... p 1989 N95-24422

NIAR-94-12 ..... p 1979 N95-24211 #

NIFS-PROC-16 ..... p 2082 N95-25904 #

NIFS-218 ..... p 1971 N95-26182 #
NIFS-250 ..... p 2072 N95-26111 #
NIFS-251 ..... p 2072 N95-26110 #
NIFS-254 ..... p 2072 N95-26250 #
NIFS-273 ..... p 2081 N95-25651 #
NIFS-274 ..... p 2083 N95-26339 #
NIFS-275 ..... p 2083 N95-26326 #
NIFS-276 ..... p 2004 N95-26036 #
NIFS-277 ..... p 2071 N95-26029 #

NIFS-278 ..... p 2082 N95-25759 #
NIFS-279 ..... p 2081 N95-25653 #
NIFS-280 ..... p 2071 N95-26031 #
NIFS-295 ..... p 2083 N95-26337 #
NIFS-297 ..... p 2071 N95-25855 #

NIRS-AR-36 ..... p 2072 N95-26165 #

NIRS-32 ..... p 2009 N95-25902 #

NISTIR-5509 ..... p 1941 N95-25342
NISTIR-5556 ..... p 2108 N95-25746 * #

NKU-0002 ..... p 2049 N95-24724 #

NNDC/ONL-94/3 ..... p 2107 N95-25941 #

NONP-NASA-DK-95-48160 ..... p 1925 N95-26072 * #

NONP-NASA-VT-95-43940 ..... p 1918 N95-24195 *
NONP-NASA-VT-95-43943 ..... p 2108 N95-24196 *
NONP-NASA-VT-95-44678 ..... p 1918 N95-24215 *
NONP-NASA-VT-95-44679 ..... p 1918 N95-24197 *
NONP-NASA-VT-95-45307 ..... p 1918 N95-24198 *
NONP-NASA-VT-95-45997 ..... p 1919 N95-25874 *
NONP-NASA-VT-95-46065 ..... p 1917 N95-25424 *
NONP-NASA-VT-95-47244 ..... p 2112 N95-24672 *

NREC-1762 ..... p 1913 N95-24293

NREL/SP-336-7233 ..... p 1990 N95-24305 #

NREL/TP-410-7408 ..... p 1993 N95-24865 #
NREL/TP-411-7402 ..... p 1996 N95-26285 #
NREL/TP-425-6054 ..... p 1998 N95-24604
NREL/TP-425-6722 ..... p 1975 N95-24880 #
NREL/TP-440-7224 ..... p 1995 N95-26090 #
NREL/TP-441-7077 ..... p 1993 N95-24853 #
NREL/TP-442-7109 ..... p 1994 N95-24882 #
NREL/TP-442-7228 ..... p 1992 N95-24684 #
NREL/TP-463-6831 ..... p 1993 N95-24866 #
NREL/TP-471-7019 ..... p 1992 N95-24714 #
NREL/TP-471-7262 ..... p 1997 N95-24319 #
NREL/TP-471-7294 ..... p 1993 N95-24715 #
NREL/TP-471-7296 ..... p 1994 N95-25309 #
NREL/TP-472-7023 ..... p 1995 N95-25995 #
NREL/TP-473-7026 ..... p 1978 N95-26286 #

NRL-MR/5520-94-7601 ..... p 1954 N95-25604

NRL/MR/5540-94-7640 ..... p 2015 N95-26192

NSTS-08289 ..... p 1919 N95-26189 * #

NTSB/AAR-94/08 ..... p 1908 N95-24206 #

OMI-02-93 ..... p 1906 N95-24379 * #

ONERA-NT-1994-10-VOL-1 ..... p 1979 N95-24282 #
ONERA-NT-1994-10-VOL-2 ..... p 1980 N95-24283 #
ONERA-NT-1994-10-VOL-3 ..... p 1980 N95-24284 #

ORA-TM-95-0044 ..... p 2020 N95-24634 * #

ORAU-94/D-58 ..... p 2051 N95-25373 #

ORD-57810 ..... p 1936 N95-25529

ORNL-6816 ..... p 2087 N95-24611 #

ORNL/SUB-85-22028/2 ..... p 1941 N95-25387 #
ORNL/SUB-87-SA946C/04 ..... p 1939 N95-24247 #
ORNL/SUB-88-07685CT92/04 ..... p 1934 N95-24647 #

ORNL/TM-12664 ..... p 1951 N95-25367 #
ORNL/TM-12744 ..... p 2019 N95-24250 #
ORNL/TM-12776 ..... p 1940 N95-24588 #
ORNL/TM-12849 ..... p 2008 N95-24843 #
ORNL/TM-12852 ..... p 2032 N95-25251 #
ORNL/TM-12853 ..... p 2030 N95-24592 #

OZ-93/01 ..... p 2098 N95-25533 #
OZ-93/11 ..... p 2053 N95-25461 #
OZ-93/12 ..... p 2097 N95-25435 #
OZ-93/13 ..... p 2054 N95-25464 #
OZ-93/15 ..... p 2098 N95-25475 #

PAPER-2210-21 ..... p 1971 N95-24530 * #
PAPER-2210-29 ..... p 2072 N95-24386 * #

PB94-910410 ..... p 1908 N95-24206 #
PB95-131587 ..... p 2010 N95-24310
PB95-141446 ..... p 1942 N95-25633
PB95-141495 ..... p 2011 N95-24863
PB95-141560 ..... p 2009 N95-24227
PB95-141578 ..... p 1955 N95-25891 #
PB95-141735 ..... p 1953 N95-24835
PB95-141768 ..... p 1953 N95-24836
PB95-141776 ..... p 2073 N95-24673
PB95-141792 ..... p 1995 N95-25892 #
PB95-141818 ..... p 1953 N95-24649
PB95-141826 ..... p 2034 N95-25893 #
PB95-141834 ..... p 2036 N95-25894 #
PB95-141842 ..... p 1967 N95-24280
PB95-141859 ..... p 1951 N95-24281
PB95-141891 ..... p 2013 N95-24510
PB95-141925 ..... p 2013 N95-24864
PB95-141941 ..... p 1989 N95-24444
PB95-141958 ..... p 1952 N95-24445
PB95-143053 ..... p 1905 N95-25401
PB95-143293 ..... p 1941 N95-25342
PB95-144481 ..... p 1911 N95-26062 #
PB95-147542 ..... p 1913 N95-24293
PB95-149290 ..... p 1997 N95-24294 #
PB95-149381 ..... p 1905 N95-24295 #
PB95-149621 ..... p 1980 N95-24296 #
PB95-149712 ..... p 2042 N95-24297
PB95-149720 ..... p 2042 N95-24298
PB95-149738 ..... p 1988 N95-24299
PB95-149746 ..... p 1939 N95-24300 #
PB95-149936 ..... p 1967 N95-24259
PB95-160511 ..... p 1973 N95-25640
PB95-164927 ..... p 1914 N95-24260
PB95-164984 ..... p 1994 N95-25501 #
PB95-165064 ..... p 1954 N95-25482 #
PB95-165098 ..... p 1955 N95-25641
PB95-165106 ..... p 1931 N95-25443 #
PB95-165114 ..... p 2102 N95-25642
PB95-165122 ..... p 1982 N95-25444
PB95-165130 ..... p 1982 N95-25445 #
PB95-165163 ..... p 1955 N95-25644
PB95-165171 ..... p 1960 N95-25472 #
PB95-165197 ..... p 2074 N95-25999
PB95-165213 ..... p 2056 N95-25619
PB95-165221 ..... p 2056 N95-25620
PB95-165239 ..... p 1932 N95-26000
PB95-165270 ..... p 1973 N95-25622
PB95-165288 ..... p 1954 N95-25623
PB95-165304 ..... p 2056 N95-25624
PB95-165320 ..... p 2022 N95-25625
PB95-165338 ..... p 2057 N95-25900
PB95-165346 ..... p 2056 N95-25626
PB95-165353 ..... p 2033 N95-25627
PB95-165361 ..... p 2099 N95-25628
PB95-165379 ..... p 2064 N95-26001
PB95-165387 ..... p 2064 N95-26096
PB95-165395 ..... p 2056 N95-25567
PB95-165403 ..... p 2026 N95-25568 #
PB95-165445 ..... p 1988 N95-24240 #
PB95-165452 ..... p 1951 N95-24241
PB95-165460 ..... p 1925 N95-24242
PB95-165502 ..... p 2028 N95-24243 #
PB95-165510 ..... p 2028 N95-24251
PB95-165528 ..... p 2028 N95-24255 #
PB95-165536 ..... p 2028 N95-24301
PB95-165544 ..... p 2028 N95-24321
PB95-165551 ..... p 2028 N95-24322
PB95-165569 ..... p 2029 N95-24325
PB95-165577 ..... p 2029 N95-24323
PB95-165668 ..... p 1982 N95-25569 #
PB95-165726 ..... p 2012 N95-25570 #
PB95-165742 ..... p 2017 N95-25571
PB95-165759 ..... p 2106 N95-25572
PB95-165767 ..... p 2074 N95-25573
PB95-165775 ..... p 1978 N95-26002 #
PB95-165783 ..... p 1978 N95-26003 #
PB95-165791 ..... p 1955 N95-25749
PB95-166146 ..... p 1942 N95-26004 #
PB95-166237 ..... p 2002 N95-26005 #
PB95-166286 ..... p 1976 N95-25574
PB95-166294 ..... p 2001 N95-25575 #
PB95-166393 ..... p 2113 N95-25576
PB95-166401 ..... p 2113 N95-25577 #
PB95-166690 ..... p 2002 N95-25745
PB95-166807 ..... p 1997 N95-24334
PB95-171963 ..... p 2108 N95-25746 * #
PB95-177606 ..... p 1956 N95-26008
PB95-177861 ..... p 2002 N95-26047
PB95-178729 ..... p 1911 N95-26009
PB95-178737 ..... p 1917 N95-25750

PL-TR-94-2248 ..... p 2006 N95-26012

PML-1992-A78 ..... p 1949 N95-25528
PML-1992-A79 ..... p 1949 N95-25517

PNL-SA-23824 ..... p 2102 N95-25771 * #
PNL-SA-24416 ..... p 1924 N95-25286 #
PNL-SA-24801 ..... p 1937 N95-26007 #
PNL-SA-24842 ..... p 2001 N95-25629
PNL-SA-24870 ..... p 2106 N95-25774 #
PNL-SA-24930 ..... p 2009 N95-26169 #
PNL-SA-24993 ..... p 2022 N95-26013 #
PNL-SA-25031 ..... p 2021 N95-24881 #
PNL-SA-25345 ..... p 1931 N95-25252 #
PNL-SA-25362 ..... p 1999 N95-25249 #
PNL-SA-25425 ..... p 2088 N95-25288 #
PNL-SA-25465 ..... p 2088 N95-25002 #
PNL-SA-25518 ..... p 1934 N95-24449 #

PNL-10044 ..... p 1998 N95-24653 #
PNL-10131 ..... p 1924 N95-25248 #
PNL-10222 ..... p 1991 N95-24369 #
PNL-10382 ..... p 2103 N95-24370 #

PWA-6113-55 ..... p 1967 N95-24473 * #

R/D-6968-EN-01 ..... p 2039 N95-25503
R/D-7463-CH-O2 ..... p 1952 N95-24503

RAL-94-040 ..... p 2033 N95-25627
RAL-94-042 ..... p 1973 N95-25640
RAL-94-090 ..... p 2064 N95-26096
RAL-94-094 ..... p 2099 N95-25628
RAL-94-099 ..... p 2056 N95-25567
RAL-94-103 ..... p 2022 N95-25625
RAL-94-104 ..... p 2056 N95-25619
RAL-94-107 ..... p 2064 N95-26001
RAL-94-108 ..... p 2056 N95-25620
RAL-94-109 ..... p 2056 N95-25624
RAL-94-113 ..... p 2056 N95-25626
RAL-94-115 ..... p 2074 N95-25573
RAL-94-117 ..... p 2057 N95-25900

REPT-E13-93-308 ..... p 1967 N95-24484 #

REPT-P1-93-285 ..... p 2045 N95-24485 #
REPT-P10-93-243 ..... p 1967 N95-24486 #
REPT-P13-93-331 ..... p 1957 N95-24487 #
REPT-P6-93-289 ..... p 2093 N95-24481 #

REPT-102-94-022U ..... p 2022 N95-26054
REPT-210RPT0046 ..... p 2089 N95-25409 * #
REPT-94-4 ..... p 1907 N95-24443 * #
REPT-95-001 ..... p 2015 N95-24224 * #
REPT-95B00069-VOL-5 ..... p 2003 N95-24766 * #
REPT-95B00072 ..... p 2083 N95-26082 * #

RIACS-TR-94-21 ..... p 2027 N95-24214 * #
RIACS-TR-95-01 ..... p 1911 N95-25334 * #

RIZA-93.028 ..... p 2002 N95-25745

RR-A333 ..... p 1980 N95-24296 #

R01-1069-25-001-95 ..... p 2013 N95-26010
R95-232 ..... p 2108 N95-24385 * #

S-791 ..... p 2013 N95-24627 * #

SAIC-MSO-93-205 ..... p 1920 N95-25508

SAIC-94/1150 ..... p 1974 N95-26114

SAND-91-1526 ..... p 1965 N95-25485 #
SAND-92-2137 ..... p 2016 N95-24659 #
SAND-94-0657C ..... p 1994 N95-25109 #
SAND-94-1112C ..... p 1959 N95-24712 #
SAND-94-1186C ..... p 1957 N95-24488 #
SAND-94-1402C ..... p 1965 N95-25895 #
SAND-94-1403C ..... p 1961 N95-24262 #
SAND-94-1419C ..... p 2066 N95-24500 #
SAND-94-1557C ..... p 1994 N95-25360 #
SAND-94-1571C ..... p 1996 N95-26166 #
SAND-94-1597C ..... p 1990 N95-24264 #
SAND-94-1613C ..... p 1995 N95-25566 #
SAND-94-1653C ..... p 1942 N95-25898 #
SAND-94-1693C ..... p 2087 N95-24617 #
SAND-94-1703C ..... p 2087 N95-24616 #
SAND-94-1736C ..... p 1941 N95-25382 #
SAND-94-1839C ..... p 1992 N95-24674 #
SAND-94-1982C ..... p 1959 N95-24713 #
SAND-94-2056C ..... p 1940 N95-24717 #
SAND-94-2206C ..... p 1971 N95-24408 #
SAND-94-2215C ..... p 1935 N95-24716 #
SAND-94-2264C ..... p 1962 N95-24489 #
SAND-94-2322C ..... p 1958 N95-24586 #
SAND-94-2394C ..... p 1953 N95-24605 #
SAND-94-2420C ..... p 2021 N95-24681 #
SAND-94-2426C ..... p 2064 N95-26168 #
SAND-94-2444C ..... p 2015 N95-24346 #
SAND-94-2460 ..... p 1995 N95-26037 #
SAND-94-2577C ..... p 1960 N95-25558 #
SAND-94-2617C ..... p 1979 N95-24263 #
SAND-94-2638C ..... p 1992 N95-24676 #
SAND-94-2639C ..... p 1948 N95-24608 #
SAND-94-2681C ..... p 1975 N95-24462 #
SAND-94-2682C ..... p 1992 N95-24682 #

SAND-94-2761 ..... p 1951 N95-24289 #
SAND-94-2763C ..... p 2054 N95-25470 #
SAND-94-2764C ..... p 2105 N95-24675 #
SAND-94-2833C ..... p 1937 N95-25775 #
SAND-94-3070C ..... p 1926 N95-25295 #
SAND-94-3147C ..... p 2090 N95-25897 #
SAND-94-3183C ..... p 1929 N95-24614 #
SAND-94-3190C ..... p 1906 N95-24308 #
SAND-94-8237 ..... p 2047 N95-24595 #
SAND-94-8238 ..... p 2002 N95-25899 #
SAND-94-8251 ..... p 1967 N95-24596 #
SAND-94-8556 ..... p 1931 N95-25492 #
SAND-94-8699C ..... p 1972 N95-25549 #
SAND-95-0012C ..... p 1966 N95-26240
SAND-95-0091C ..... p 1941 N95-25370 #
SAND-95-0093C ..... p 2074 N95-25559 #
SAND-95-0094C ..... p 2089 N95-25353 #
SAND-95-0169C ..... p 2004 N95-25476 #
SAND-95-8455C ..... p 1930 N95-25242 #

SCI(93)4 ..... p 1917 N95-26184 * #

SEI-94-CDRL-103-3 ..... p 2018 N95-26058

SGD-603-PT-1 ..... p 2113 N95-25576
SGD-603-PT-2 ..... p 2113 N95-25577 #

SIP-0068 ..... p 1970 N95-25940 #

SISSA-63/94/EP ..... p 2043 N95-24404 #

SLAC-PUB-6640 ..... p 2109 N95-24327 #
SLAC-PUB-6658 ..... p 2092 N95-24328 #

SLAC/SSRL-0089 ..... p 2085 N95-24463 #
SLAC/SSRL-0091 ..... p 2038 N95-25408 #

SMC-TR-94-41 ..... p 1942 N95-26049
SMC-TR-94-45 ..... p 1947 N95-26188

SP-RAPP-1994:08 ..... p 1931 N95-25443 #
SP-RAPP-1994:14 ..... p 1960 N95-25472 #
SP-RAPP-1994:30 ..... p 1978 N95-26003 #
SP-RAPP-1994:31 ..... p 1978 N95-26002 #
SP-RAPP-1994:37 ..... p 2074 N95-25999

SP-RAPPORT-1993:29 ..... p 2073 N95-24673
SP-RAPPORT-1994:01 ..... p 1995 N95-25892 #

SRI-PYU-2969 ..... p 1936 N95-25502

SSCL-N-846 ..... p 1968 N95-24623 #

SSD94D0035 ..... p 1919 N95-25747 #

STC-TR-2855 ..... p 2006 N95-26012

STUK-YTO-TR-53 ..... p 2018 N95-26045 #

SU-SLAC-PUB-6527 ..... p 2065 N95-24409 #
SU-SLAC-PUB-6549 ..... p 2045 N95-24434 #
SU-SLAC-PUB-6550 ..... p 2045 N95-24435 #
SU-SLAC-PUB-6566 ..... p 1974 N95-24356 #
SU-SLAC-PUB-6567 ..... p 2020 N95-24597 #
SU-SLAC-PUB-6584 ..... p 2044 N95-24414 #
SU-SLAC-PUB-6591 ..... p 2044 N95-24415 #
SU-SLAC-PUB-6597 ..... p 2044 N95-24417 #
SU-SLAC-PUB-6598 ..... p 2044 N95-24418 #
SU-SLAC-PUB-6599 ..... p 2047 N95-24622 #
SU-SLAC-PUB-6600 ..... p 2047 N95-24641 #
SU-SLAC-PUB-6601 ..... p 2047 N95-24660 #
SU-SLAC-PUB-6602 ..... p 2046 N95-24571 #
SU-SLAC-PUB-6604 ..... p 2066 N95-24572 #
SU-SLAC-PUB-6618 ..... p 2067 N95-24661 #
SU-SLAC-PUB-6620 ..... p 2047 N95-24662 #
SU-SLAC-PUB-6621 ..... p 2067 N95-24573 #
SU-SLAC-PUB-6632 ..... p 2038 N95-25408 #
SU-SLAC-PUB-6639 ..... p 2067 N95-24574 #
SU-SLAC-PUB-6648 ..... p 2046 N95-24593 #
SU-SLAC-PUB-6653 ..... p 2046 N95-24575 #
SU-SLAC-PUB-6659 ..... p 2046 N95-24576 #
SU-SLAC-PUB-6662 ..... p 2069 N95-25297 #
SU-SLAC-PUB-6673 ..... p 2003 N95-24577 #
SU-SLAC-PUB-6674 ..... p 2050 N95-24903 #
SU-SLAC-PUB-6680 ..... p 2015 N95-24648 #
SU-SLAC-PUB-6701 ..... p 2043 N95-24354 #
SU-SLAC-PUB-6707 ..... p 2047 N95-24663 #
SU-SLAC-PUB-6718 ..... p 2094 N95-24578 #
SU-SLAC-PUB-6727 ..... p 2068 N95-24664 #
SU-SLAC-PUB-6730 ..... p 2046 N95-24591 #
SU-SLAC-PUB-95-6741 ..... p 2052 N95-25407 #
SU-SLAC-PUB-95-6742 ..... p 2070 N95-25406 #
SU-SLAC-PUB-95-6750 ..... p 2098 N95-25530 #

SU-SLAC-446 ..... p 2057 N95-25768 #
SU-SLAC-450 ..... p 2085 N95-24463 #

SU-4240-567 ..... p 2027 N95-24228 #

TARDEC-TR-13609 ..... p 1942 N95-25510
TARDEC-TR-13615 ..... p 1951 N95-25513

TAUP-2183-94 ..... p 2053 N95-25462 #

TDCK-TD94-0076 ..... p 2014 N95-25610

TDCK-92-2398 ..... p 1949 N95-25528
TDCK-92-2406 ..... p 1949 N95-25517
TDCK-94-2179 ..... p 1913 N95-26190

TIFR/TH-94-24 ..... p 2098 N95-25526 #

TKK-F-A730 ..... p 2042 N95-24298
TKK-F-A731 ..... p 2042 N95-24297

TN-94-1 ..... p 2016 N95-24536 #

TNO-TM-1994-B-14 ..... p 2014 N95-25610
TNO-TM-1994-B-16 ..... p 1913 N95-26190

TR-ICMA-94-192 ..... p 2033 N95-25601

TR-011795-3570P ..... p 2035 N95-24278 * #
TR-080594-4871F ..... p 1909 N95-24391 * #
TR-1-FSRC-1994-PT-1 ..... p 1971 N95-24371 #
TR-76 ..... p 1924 N95-25602
TR-92(2935)-6 ..... p 1947 N95-26188
TR-94(4935)-1 ..... p 1942 N95-26049
TR-94-03-REV ..... p 2049 N95-24877 * #

TRAETEK-R-94/040-SE ..... p 1932 N95-26000

TTKK/TST-2/94 ..... p 2066 N95-24448 #

U-OF-IOWA-94-22 ..... p 2111 N95-26196 #
U-OF-IOWA-95-2 ..... p 2111 N95-26195 #

U-95-7007 ..... p 1947 N95-24226 * #

UAG-103 ..... p 2004 N95-24897 #

UAH-TR-5-33534 ..... p 2016 N95-24876 * #

UAH-5-33475 ..... p 2073 N95-24545 * #
UAH-5-33477 ..... p 2073 N95-24545 * #
UAH-5-33534 ..... p 2104 N95-24477 * #

UC-1210 ..... p 1995 N95-26037 #
UC-403 ..... p 1965 N95-25485 #
UC-414 ..... p 2057 N95-25768 #
UC-420 ..... p 1972 N95-24709 #
UC-706 ..... p 1989 N95-25110
UC-800 ..... p 1924 N95-25248 #

UCR/DO/94-20 ..... p 2067 N95-24601 #

UCRL-ID-117401 ..... p 2000 N95-25279 #
UCRL-ID-118982 ..... p 2080 N95-25344 #
UCRL-ID-119235 ..... p 1933 N95-24329 #

UCRL-JC-115491 ..... p 2076 N95-24490 #
UCRL-JC-115492 ..... p 2078 N95-24650 #
UCRL-JC-116030 ..... p 2067 N95-24651 #
UCRL-JC-116456 ..... p 1968 N95-24657 #
UCRL-JC-116558 ..... p 2091 N95-26170 #
UCRL-JC-116569 ..... p 1966 N95-26063 #
UCRL-JC-116574 ..... p 2005 N95-25287 #
UCRL-JC-116575 ..... p 2006 N95-25635 #
UCRL-JC-116894 ..... p 1975 N95-24550 #
UCRL-JC-117669 ..... p 2076 N95-24544 #
UCRL-JC-117928 ..... p 1972 N95-25100 #
UCRL-JC-117932 ..... p 2046 N95-24549 #
UCRL-JC-118448 ..... p 2016 N95-24898 #
UCRL-JC-118496 ..... p 2076 N95-24548 #
UCRL-JC-118634 ..... p 1931 N95-25291 #

UM-P-91/50 ..... p 2099 N95-25970 #
UM-P-92/72 ..... p 2099 N95-25970 #
UM-P-92/77 ..... p 1932 N95-26261 #
UM-P-93/01 ..... p 2098 N95-25533 #
UM-P-93/04 ..... p 2082 N95-25976 #
UM-P-93/33 ..... p 2098 N95-25534 #
UM-P-93/38 ..... p 2099 N95-25650 #
UM-P-93/42 ..... p 2054 N95-25465 #
UM-P-93/44 ..... p 2063 N95-25993 #
UM-P-93/45 ..... p 2063 N95-25969 #
UM-P-93/46 ..... p 2096 N95-25428 #
UM-P-93/49 ..... p 2090 N95-25985 #
UM-P-93/50 ..... p 2097 N95-25446 #
UM-P-93/51 ..... p 2053 N95-25461 #
UM-P-93/53 ..... p 2097 N95-25429 #
UM-P-93/54 ..... p 2097 N95-25435 #
UM-P-93/56 ..... p 2100 N95-26104 #

UM-P-93/58 ..... p 2054 N95-25464 #
UM-P-93/61 ..... p 2038 N95-25430 #
UM-P-93/62 ..... p 2099 N95-25970 #
UM-P-93/63 ..... p 2097 N95-25473 #
UM-P-93/64 ..... p 2090 N95-25984 #
UM-P-93/65 ..... p 2054 N95-25474 #
UM-P-93/70 ..... p 2017 N95-25448 #
UM-P-93/71 ..... p 2098 N95-25475 #
UM-P-93/72 ..... p 2038 N95-25458 #
UM-P-93/73 ..... p 2091 N95-26260 #

UR-1316 ..... p 2054 N95-25463 #

US-PATENT-APPL-SN-017205 ..... p 1943 N95-26118 *
US-PATENT-APPL-SN-031972 ..... p 2075 N95-26117 *
US-PATENT-APPL-SN-046256 ..... p 2040 N95-26187 *
US-PATENT-APPL-SN-060617 ..... p 1978 N95-25304 *
US-PATENT-APPL-SN-066274 ..... p 2014 N95-25306 *
US-PATENT-APPL-SN-071131 ..... p 1971 N95-26340 *
US-PATENT-APPL-SN-110278 ..... p 1926 N95-25305 *
US-PATENT-APPL-SN-113373 ..... p 1960 N95-26038 *
US-PATENT-APPL-SN-123629 ..... p 1969 N95-25544 *
US-PATENT-APPL-SN-125966 ..... p 1959 N95-25307 *
US-PATENT-APPL-SN-134441 ..... p 1936 N95-25545 *
US-PATENT-APPL-SN-141292 ..... p 1926 N95-25546 *
US-PATENT-APPL-SN-152631 ..... p 1969 N95-25547 *
US-PATENT-APPL-SN-172961 ..... p 1976 N95-25548 *
US-PATENT-APPL-SN-194654 ..... p 2040 N95-26187 *
US-PATENT-APPL-SN-230571 ..... p 1976 N95-25592 *
US-PATENT-APPL-SN-292621 ..... p 1939 N95-24212 * #
US-PATENT-APPL-SN-319688 ..... p 1961 N95-26186
US-PATENT-APPL-SN-596105 ..... p 1967 N95-24236 *
US-PATENT-APPL-SN-774490 ..... p 2074 N95-26015 *
US-PATENT-APPL-SN-880099 ..... p 1960 N95-25889 *
US-PATENT-APPL-SN-928865 ..... p 1968 N95-24625 *
US-PATENT-APPL-SN-999794 ..... p 1954 N95-25316 *

US-PATENT-CLASS-118-124 ..... p 1926 N95-25546 *
US-PATENT-CLASS-139-11 ..... p 1943 N95-26118 *
US-PATENT-CLASS-139-192 ..... p 1943 N95-26118 *
US-PATENT-CLASS-139-305 ..... p 1943 N95-26118 *
US-PATENT-CLASS-139-384 ..... p 1943 N95-26118 *
US-PATENT-CLASS-156-180 ..... p 1926 N95-25546 *
US-PATENT-CLASS-156-181 ..... p 1926 N95-25546 *
US-PATENT-CLASS-156-433 ..... p 1926 N95-25546 *
US-PATENT-CLASS-156-441 ..... p 1926 N95-25546 *
US-PATENT-CLASS-219-121.45 .. p 1976 N95-25548 *
US-PATENT-CLASS-219-121.48 .. p 1976 N95-25548 *
US-PATENT-CLASS-219-121.51 .. p 1976 N95-25548 *
US-PATENT-CLASS-219-121.5 .... p 1976 N95-25548 *
US-PATENT-CLASS-244-158R .... p 2014 N95-25306 *
US-PATENT-CLASS-244-158R .... p 1969 N95-25544 *
US-PATENT-CLASS-250-208.4 .... p 1959 N95-25307 *
US-PATENT-CLASS-250-214.1 .... p 1959 N95-25307 *
US-PATENT-CLASS-250-214VT .. p 1960 N95-25889 *
US-PATENT-CLASS-250-225 ..... p 2074 N95-26015 *
US-PATENT-CLASS-250-305 ..... p 1978 N95-25304 *
US-PATENT-CLASS-250-306 ..... p 1978 N95-25304 *
US-PATENT-CLASS-250-307 ..... p 1978 N95-25304 *
US-PATENT-CLASS-250-310 ..... p 1978 N95-25304 *
US-PATENT-CLASS-250-385.1 .... p 1960 N95-25889 *
US-PATENT-CLASS-250-492.22 .. p 1971 N95-26340 *
US-PATENT-CLASS-250-492.3 .... p 1971 N95-26340 *
US-PATENT-CLASS-264-136 ..... p 1926 N95-25546 *
US-PATENT-CLASS-264-174 ..... p 1926 N95-25546 *
US-PATENT-CLASS-29-621.1 ..... p 1968 N95-24625 *
US-PATENT-CLASS-294-1.1 ..... p 2014 N95-25306 *
US-PATENT-CLASS-294-19.1 ..... p 2014 N95-25306 *
US-PATENT-CLASS-330-109 ..... p 1960 N95-26038 *
US-PATENT-CLASS-330-291 ..... p 1960 N95-26038 *
US-PATENT-CLASS-330-292 ..... p 1960 N95-26038 *
US-PATENT-CLASS-330-293 ..... p 1960 N95-26038 *
US-PATENT-CLASS-330-294 ..... p 1960 N95-26038 *
US-PATENT-CLASS-330-4.5 ..... p 1959 N95-25307 *
US-PATENT-CLASS-343-713 ..... p 1954 N95-25316 *
US-PATENT-CLASS-343-765 ..... p 1969 N95-25544 *
US-PATENT-CLASS-343-766 ..... p 1969 N95-25544 *
US-PATENT-CLASS-343-786 ..... p 1954 N95-25316 *
US-PATENT-CLASS-343-840 ..... p 1954 N95-25316 *
US-PATENT-CLASS-356-152 ..... p 2074 N95-26015 *
US-PATENT-CLASS-356-28.5 ..... p 1967 N95-24236 *
US-PATENT-CLASS-356-28 ..... p 1967 N95-24236 *
US-PATENT-CLASS-356-32 ..... p 2075 N95-26117 *
US-PATENT-CLASS-356-34 ..... p 2074 N95-26015 *
US-PATENT-CLASS-364-413.13 .. p 1960 N95-25889 *
US-PATENT-CLASS-372-4 ..... p 1959 N95-25307 *
US-PATENT-CLASS-428-175 ..... p 1943 N95-26118 *
US-PATENT-CLASS-430-1 ..... p 1971 N95-26340 *
US-PATENT-CLASS-430-296 ..... p 1971 N95-26340 *
US-PATENT-CLASS-430-2 ..... p 1971 N95-26340 *
US-PATENT-CLASS-430-320 ..... p 1971 N95-26340 *
US-PATENT-CLASS-430-942 ..... p 1971 N95-26340 *
US-PATENT-CLASS-439-248 ..... p 1976 N95-25592 *
US-PATENT-CLASS-60-204 ..... p 2040 N95-26187 *
US-PATENT-CLASS-60-271 ..... p 2040 N95-26187 *
US-PATENT-CLASS-60-527 ..... p 1936 N95-25545 *

US-PATENT-CLASS-60-528 ..... p 1936 N95-25545 *
US-PATENT-CLASS-62-122 ..... p 1969 N95-25547 *
US-PATENT-CLASS-62-159 ..... p 1969 N95-25547 *
US-PATENT-CLASS-62-50.2 ..... p 1969 N95-25547 *
US-PATENT-CLASS-62-50.4 ..... p 1969 N95-25547 *
US-PATENT-CLASS-62-51.1 ..... p 1969 N95-25547 *
US-PATENT-CLASS-73-766 ..... p 1968 N95-24625 *
US-PATENT-CLASS-73-775 ..... p 1968 N95-24625 *
US-PATENT-CLASS-73-800 ..... p 2075 N95-26117 *
US-PATENT-CLASS-73/602 ..... p 1926 N95-25305 *
US-PATENT-CLASS-74-61 ..... p 1969 N95-25544 *
US-PATENT-CLASS-74-87 ..... p 1969 N95-25544 *

US-PATENT-5,090,801 ..... p 1967 N95-24236 *
US-PATENT-5,137,353 ..... p 2074 N95-26015 *
US-PATENT-5,375,474 ..... p 1968 N95-24625 *
US-PATENT-5,390,544 ..... p 1926 N95-25305 *
US-PATENT-5,392,597 ..... p 2040 N95-26187 *
US-PATENT-5,393,634 ..... p 1971 N95-26340 *
US-PATENT-5,393,980 ..... p 1978 N95-25304 *
US-PATENT-5,394,704 ..... p 1969 N95-25547 *
US-PATENT-5,394,752 ..... p 2075 N95-26117 *
US-PATENT-5,394,906 ..... p 1943 N95-26118 *
US-PATENT-5,395,477 ..... p 1926 N95-25546 *
US-PATENT-5,396,073 ..... p 1960 N95-25889 *
US-PATENT-5,396,769 ..... p 1936 N95-25545 *
US-PATENT-5,396,815 ..... p 1969 N95-25544 *
US-PATENT-5,397,244 ..... p 1976 N95-25592 *
US-PATENT-5,398,035 ..... p 1954 N95-25316 *
US-PATENT-5,399,831 ..... p 1976 N95-25548 *
US-PATENT-5,399,993 ..... p 1960 N95-26038 *
US-PATENT-5,401,069 ..... p 2014 N95-25306 *
US-PATENT-5,401,953 ..... p 1959 N95-25307 *

USARL/O3 ..... p 2039 N95-25503

USF-TR-82 ..... p 2058 N95-25911 * #

UTNL-R-0302 ..... p 2082 N95-25903 #

UVA/525467/EE95/101 ..... p 2090 N95-26061
UVA/528266/MSE94/117 ..... p 1933 N95-24220 * #

VJSC-1448 ..... p 1918 N95-24197 *

VTT-BIOENERGIA-3-PT-3 ..... p 1993 N95-24862 #

WBE-228-001 ..... p 1915 N95-24424

WES/TN/DRP-4-10 ..... p 1910 N95-25609

WHC-SA-2594 ..... p 2104 N95-24603 #

WHC-SD-HWV-UM-004-REV-1 ..... p 2105 N95-24654 #

WHC-SD-TD-CSWD-002 ..... p 2035 N95-24248 #

WHC-SD-WM-DA-159 ..... p 1960 N95-26092 #

WIS-PH-93-103 ..... p 2095 N95-24723 #
WIS-PH-93-114 ..... p 2096 N95-25095 #
WIS-PH-93-115 ..... p 1957 N95-24482 #
WIS-PH-93-116 ..... p 1957 N95-24483 #
WIS-PH-93-94 ..... p 2049 N95-24722 #
WIS-PH-93-98 ..... p 2096 N95-25096 #
WIS-PH-94-4 ..... p 2096 N95-25215 #

WL-TR-94-1095-VOL-1 ..... p 2075 N95-26173
WL-TR-94-1149 ..... p 2075 N95-26039
WL-TR-94-2069 ..... p 1977 N95-26050
WL-TR-94-3097 ..... p 1915 N95-26053

WSRC-MS-94-0246-REV-1 ..... p 1939 N95-24344 #
WSRC-MS-94-0418 ..... p 2000 N95-25278 #
WSRC-MS-94-0437 ..... p 1934 N95-24480 #
WSRC-MS-94-0632 ..... p 1981 N95-24598 #

WSRC-RP-94-1272 ..... p 1929 N95-24430 #

WSRC-TR-94-0527 ..... p 1934 N95-24615 #

YITP/U-94-10 ..... p 2057 N95-25901 #

APPENDIX

NASA SCIENTIFIC AND TECHNICAL INFORMATION OFFICE PRODUCTS AND SERVICES

The NASA Scientific and Technical Information (STI) Office provides for the collection and announcement of aerospace-related reports and literature obtained worldwide through agreements and exchanges. The result of the collection is the comprehensive NASA STI Database that covers aeronautics, space, and supporting disciplines.

The STI Database, documents generated or obtained by NASA, and products and services derived from or supporting the database are made available to the NASA research community and to the public. Descriptions and sources of these items are presented in the following pages.

Scientific and Technical Aerospace Reports (STAR) is an abstract journal, listing citations with abstracts for aerospace-related reports obtained from worldwide sources. *STAR* is issued on the first of each month, and announces current documents that have been entered into the NASA STI Database during the previous month. The reports are of the following types:

- NASA, NASA contractor, and NASA grantee reports;
- Reports issued by other U.S. Government agencies, domestic and foreign institutions, universities, and private firms;
- Translations in report form;
- NASA-owned patents and patent applications
- Other U.S. Government agency and foreign patents and patent applications
- Domestic and foreign dissertations and theses.

Journal, book, and conference literature, journal translations, and certain foreign dissertations having the same subject scope as *STAR* are announced in a companion journal, *NASA Open Volumes on Aerospace (NOVA). NOVA* is issued on the 15th of each month and is available from the NASA Center for AeroSpace Information, at the address below.

ELIGIBILITY AND REGISTRATION FOR NASA STI PRODUCTS AND SERVICES

Organizations of the type listed below that have registered with NASA can receive products and services.

- NASA offices and installations, contractors, subcontractors, grantees, and consultants;
- Other U.S. Government agencies and their contractors;
- Libraries in the United States that have arrangements with NASA to maintain collections of NASA documents for public reference;
- Other organizations in the United States having a need for NASA documents in work related to aeronautics and space research;
- Organizations abroad that have established reciprocal documents exchange arrangements with NASA.

The central service points—central points of document acquisition and control within qualified organizations—or individuals are eligible to register for NASA STI products and services. Domestic organizations or individuals may be eligible to receive various classes of NASA publications and services and should address their requests for registration or further information to:

ATTN: Registration Services
NASA Center for AeroSpace Information
800 Elkridge Landing Road
Linthicum Heights, MD 21090-2934
301-621-0390

Organizations abroad should direct requests to:

National Aeronautics and Space Administration
Scientific and Technical Information Office (JT)
International STI Office
Washington, DC 20546-0001
USA
703-271-5640

SUBJECT SCOPE

The subject scope of *STAR* and *NOVA* includes all aspects of aeronautics and space research and development, supporting basic and applied research, and applications. Aerospace aspects of Earth resources, energy development, conservation, oceanography, environmental protection, urban transportation, and other topics of high national priority are also covered.

HOW TO USE *STAR* SUBJECT CATEGORIES

Abstracts in *STAR* are categorized by 10 major subject divisions that are divided further into 76 specific subject categories. The subject divisions and categories are listed in the Table of Contents together with a note for each that defines its scope and provides any cross-references. For example:

16 SPACE TRANSPORTATION

Includes passenger and cargo space transportation, e.g., shuttle operations; and space rescue techniques. For related information see also *03 Air Transportation and Safety* and *18 Spacecraft Design, Testing and Performance.* For space suits see *54 Man/System Technology and Life Support.*

CROSS-REFERENCES

Individual *STAR* abstracts are not ordinarily cross-referenced, except for certain conference reports or book translations that have had separate abstracts written for their component papers or chapters. Citations and abstracts of the components follow immediately after those of the parent document. When the subject content of a component differs sufficiently from the general content of the parent, a cross-reference citation also is printed at the end of the category to which it normally would have been assigned if it were independent.

DOCUMENTS ON MICROFICHE

Documents available on microfiche are designated by a pound sign (#) following the accession number.

LIMITED REPRODUCIBILITY

A note of limited reproducibility appears in the citation, if there are factors affecting the reproducibility of more than 20% of the document. These factors include faint or broken type, color photographs, black and white photographs, foldouts, dot matrix print, or some other factor that limits the reproducibility of the document. This notation also appears on the microfiche header.

NASA PATENTS AND PATENT APPLICATIONS

Patents and patent applications owned by NASA are announced in *STAR* under appropriate subject categories and are referenced in the *STAR* indexes. In the Report Number Index, patents are indexed by the NASA Case Number, and the U.S. Patent Class. Patent applications are indexed by the NASA Case Number and the U.S. Patent Application Serial Number.

Printed copies of patents (which are not microfiched) are available for purchase from the U.S. Patent and Trademark Office.

When ordering patents, the U.S. Patent Number should be used, and payment must be remitted in advance, by money order or check payable to the Commissioner of Patents and Trademarks. Prepaid purchase coupons for ordering are also available from the U.S. Patent and Trademark Office.

NASA patent application specifications are sold in both paper copy and microfiche by the NASA Center for AeroSpace Information (CASI). The N accession number should be used in ordering either paper copy or microfiche from CASI.

The patents and patent applications announced in *STAR* are owned by NASA and are available for royalty-free licensing. Requests for licensing terms and further information should be addressed to:

National Aeronautics and Space Administration
Associate General Counsel for Intellectual Property
Code GP
Washington, DC 20546-0001

SOURCES FOR DOCUMENTS

One or more sources from which a document announced in *STAR* is available to the public is ordinarily given on the last line of the citation. The most commonly indicated sources and their acronyms or abbreviations are listed below, and their addresses are listed on page A-6. If the publication is available from a source other than those listed, the publisher and his address will be displayed on the availability line or in combination with the corporate source line.

Avail: CASI. Sold by the NASA Center for AeroSpace Information. Prices for hard copy (HC) and microfiche (MF) are indicated by a price code following the letters HC or MF in the *STAR* citation. Current values for the price codes are given in the tables on page A-7.

NOTE ON ORDERING DOCUMENTS: When ordering publications from NASA CASI, use the N accession number or other report number. It is also advisable to cite the title and other bibliographic identification.

Avail: SOD (or GPO). Sold by the Superintendent of Documents, U.S. Government Printing Office, in hard copy.

Avail: BLL (formerly NLL): British Library Lending Division, Boston Spa, Wetherby, Yorkshire, England. Photocopies available from this organization at the price shown. (If none is given, inquiry should be addressed to the BLL.)

Avail: DOE Depository Libraries. Organizations in U.S. cities and abroad that maintain collections of Department of Energy reports, usually in microfiche form, are listed in *Energy Research Abstracts*. Services available from the DOE and its depositories are described in a booklet, *DOE Technical Information Center - Its Functions and Services* (TID-4660), which may be obtained without charge from the DOE Technical Information Center.

Avail: ESDU. Pricing information on specific data, computer programs, and details on Engineering Sciences Data Unit (ESDU) topic categories can be obtained from ESDU International Ltd. Requesters in North America should use the Virginia address while all other requesters should use the London address, both of which are on page A-6.

Avail: Fachinformationszentrum Karlsruhe. Gesellschaft für wissenschaftlich-technische Information mbH 76344 Eggenstein-Leopoldshafen, Germany.

Avail: HMSO. Publications of Her Majesty's Stationery Office are sold in the U.S. by Pendragon House, Inc. (PHI), Redwood City, CA. The U.S. price (including a service and mailing charge) is given, or a conversion table may be obtained from PHI.

Avail: Issuing Activity, or Corporate Author, or no indication of availability. Inquiries as to the availability of these documents should be addressed to the organization shown in the citation as the corporate author of the document.

Avail: NASA Public Document Rooms. Documents so indicated may be examined at or purchased from the National Aeronautics and Space Administration (JBD-4), Public Documents Room (Room 1H23), Washington, DC 20546-0001, or public document rooms located at NASA installations, and the NASA Pasadena Office at the Jet Propulsion Laboratory.

Avail: NTIS. Sold by the National Technical Information Service. Initially distributed microfiche under the NTIS SRIM (Selected Research in Microfiche) are available. For information concerning this service, consult the NTIS Subscription Section, Springfield, VA 22161.

Avail: Univ. Microfilms. Documents so indicated are dissertations selected from *Dissertation Abstracts* and are sold by University Microfilms as xerographic copy (HC) and microfilm. All requests should cite the author and the Order Number as they appear in the citation.

Avail: US Patent and Trademark Office. Sold by Commissioner of Patents and Trademarks, U.S. Patent and Trademark Office, at the standard price of $1.50 each, postage free. (See discussion of NASA patents and patent applications on page A-3.)

Avail: (US Sales Only). These foreign documents are available to users within the United States from the National Technical Information Service (NTIS). They are available to users outside the United States through the International Nuclear Information Service (INIS) representative in their country, or by applying directly to the issuing organization.

Avail: USGS. Originals of many reports from the U.S. Geological Survey, which may contain color illustrations, or otherwise may not have the quality of illustrations preserved in the microfiche or facsimile reproduction, may be examined by the public at the libraries of the USGS field offices whose addresses are listed on page A-6. The libraries may be queried concerning the availability of specific documents and the possible utilization of local copying services, such as color reproduction.

FEDERAL DEPOSITORY LIBRARY PROGRAM

In order to provide the general public with greater access to U.S. Government publications, Congress established the Federal Depository Library Program under the Government Printing Office (GPO), with 53 regional depositories responsible for permanent retention of material, inter-library loan, and reference services. At least one copy of nearly every NASA and NASA-sponsored publication, either in printed or microfiche format, is received and retained by the 53 regional depositories. A list of the regional GPO libraries, arranged alphabetically by state, appears on page A-8. These libraries are *not* sales outlets. A local library can contact a regional depository to help locate specific reports, or direct contact may be made by an individual.

PUBLIC COLLECTION OF NASA DOCUMENTS

An extensive collection of NASA and NASA-sponsored publications is maintained by the British Library Lending Division, Boston Spa, Wetherby, Yorkshire, England for public access. The British Library Lending Division also has available many of the non-NASA publications cited in *STAR*. European requesters may purchase facsimile copy or microfiche of NASA and NASA-sponsored documents, those identified by both the symbols # and * from ESA — Information Retrieval Service European Space Agency, 8-10 rue Mario-Nikis, 75738 CEDEX 15, France.

SUBMITTING DOCUMENTS

All users of this abstract service are urged to forward reports to be considered for announcement in *STAR*. This will aid NASA in its efforts to provide the fullest possible coverage of all scientific and technical publications that might support aeronautics and space research and development. If you have prepared relevant reports (other than those you will transmit to NASA, DOD, or DOE through the

usual contract- or grant-reporting channels), please send them for consideration to the NASA Center for AeroSpace Information, 800 Elkridge Landing Road, Linthicum Heights, MD 21090-2934.

Reprints of journal articles, book chapters, and conference papers are also welcome. These will be considered for announcement in *STAR's* companion journal, *NOVA*.

You may specify a particular source to be included in a report announcement if you wish; otherwise the report will be placed on a public sale at the NASA Center for AeroSpace Information. Copyrighted publications will be announced but not distributed or sold.

PURCHASE OF *STAR*

STAR is publicly available on annual subscription from the NASA Center for AeroSpace Information (CASI). 1995 *STAR* subscription prices are $100.00/domestic and $125.00/foreign. Single copy prices: $33.00/domestic, $41.00/foreign.

An annual, cumulative *STAR Index* is also available at $70.00/domestic and foreign.

STAR is available to registered users on annual subscription from the NASA Center for AeroSpace Information, ATTN: Registration Services, 800 Elkridge Landing Road, Linthicum Heights, MD 21090-2934.

ADDRESSES OF ORGANIZATIONS

British Library Lending Division
Boston Spa, Wetherby, Yorkshire
England

Commissioner of Patents and Trademarks
U.S. Patent and Trademark Office
Washington, DC 20231

Department of Energy
Technical Information Center
P.O. Box 62
Oak Ridge, TN 37830

European Space Agency-
Information Retrieval Service ESRIN
Via Galileo Galilei
00044 Frascati (Rome) Italy

Engineering Sciences Data Unit International
P.O. Box 1633
Manassas, VA 22110

Engineering Sciences Data Unit
International, Ltd.
251-259 Regent Street
London, W1R 7AD, England

Fachinformationszentrum Karlsruhe
Gesellschaft für wissenschaftlich-technische
Information mbH
76344 Eggenstein-Leopoldshafen, Germany

Her Majesty's Stationery Office
P.O. Box 569, S.E. 1
London, England

NASA Center for AeroSpace Information
800 Elkridge Landing Road
Linthicum Heights, MD 21090-2934

National Aeronautics and Space Administration
Scientific and Technical Information Office
(JT)
Washington, DC 20546-0001

National Technical Information Service
5285 Port Royal Road
Springfield, VA 22161

Pendragon House, Inc.
899 Broadway Avenue
Redwood City, CA 94063

Superintendent of Documents
U.S. Government Printing Office
Washington, DC 20402

University Microfilms
A Xerox Company
300 North Zeeb Road
Ann Arbor, MI 48106

University Microfilms, Ltd.
Tylers Green
London, England

U.S. Geological Survey Library National Center
MS 950
12201 Sunrise Valley Drive
Reston, VA 22092

U.S. Geological Survey Library
2255 North Gemini Drive
Flagstaff, AZ 86001

U.S. Geological Survey
345 Middlefield Road
Menlo Park, CA 94025

U.S. Geological Survey Library
Box 25046
Denver Federal Center, MS914
Denver, CO 80225

NASA CASI PRICE CODE TABLE

(Effective January 1, 1995)

CASI PRICE CODE	NORTH AMERICAN PRICE	FOREIGN PRICE
A01	$ 6.00	$ 12.00
A02	9.00	18.00
A03	17.50	35.00
A04-A05	19.50	39.00
A06-A09	27.00	54.00
A10-A13	36.50	73.00
A14-A17	44.50	89.00
A18-A21	52.00	104.00
A22-A25	61.00	122.00
A99	Call For Price	Call For Price

IMPORTANT NOTICE

For users not registered at the NASA CASI, prepayment is required. Additionally, a shipping and handling fee of $1.00 per document for delivery within the United States and $9.00 per document for delivery outside the United States is charged.

For users registered at the NASA CASI, document orders may be invoiced at the end of the month, charged against a deposit account, or paid by check or credit card. NASA CASI accepts American Express, Diners' Club, MasterCard, and VISA credit cards. There are no shipping and handling charges. To register at the NASA CASI, please request a registration form through the NASA Access Help Desk at the numbers or addresses below.

RETURN POLICY

Effective June 1, 1995, the NASA Center for AeroSpace Information will gladly replace or make full refund on items you have requested if we have made an error in your order, if the item is defective, or if it was received in damaged condition and you contact us within 30 days of your original request. Just contact our NASA Access Help Desk at the numbers or addresses listed below.

NASA Center for AeroSpace Information
800 Elkridge Landing Road
Linthicum Heights, MD 21090-2934
Telephone: (301) 621-0390
E-mail: help@sti.nasa.gov
Fax: (301) 621-0134

FEDERAL REGIONAL DEPOSITORY LIBRARIES

ALABAMA

AUBURN UNIV. AT MONTGOMERY LIBRARY
Documents Dept.
7300 University Dr.
Montgomery, AL 36117-3596
(205) 244-3650 Fax: (205) 244-0678

UNIV. OF ALABAMA
Amelia Gayle Gorgas Library
Govt. Documents
P.O. Box 870266
Tuscaloosa, AL 35487-0266
(205) 348-6046 Fax: (205) 348-0760

ARIZONA

DEPT. OF LIBRARY, ARCHIVES, AND PUBLIC RECORDS
Research Division
Third Floor, State Capitol
1700 West Washington
Phoenix, AZ 85007
(602) 542-3701 Fax: (602) 542-4400

ARKANSAS

ARKANSAS STATE LIBRARY
State Library Service Section
Documents Service Section
One Capitol Mall
Little Rock, AR 72201-1014
(501) 682-2053 Fax: (501) 682-1529

CALIFORNIA

CALIFORNIA STATE LIBRARY
Govt. Publications Section
P.O. Box 942837 - 914 Capitol Mall
Sacramento, CA 94337-0091
(916) 654-0069 Fax: (916) 654-0241

COLORADO

UNIV. OF COLORADO - BOULDER
Libraries - Govt. Publications
Campus Box 184
Boulder, CO 80309-0184
(303) 492-8834 Fax: (303) 492-1881

DENVER PUBLIC LIBRARY
Govt. Publications Dept. BSG
1357 Broadway
Denver, CO 80203-2165
(303) 640-8846 Fax: (303) 640-8817

CONNECTICUT

CONNECTICUT STATE LIBRARY
231 Capitol Avenue
Hartford, CT 06106
(203) 566-4971 Fax: (203) 566-3322

FLORIDA

UNIV. OF FLORIDA LIBRARIES
Documents Dept.
240 Library West
Gainesville, FL 32611-2048
(904) 392-0366 Fax: (904) 392-7251

GEORGIA

UNIV. OF GEORGIA LIBRARIES
Govt. Documents Dept.
Jackson Street
Athens, GA 30602-1645
(706) 542-8949 Fax: (706) 542-4144

HAWAII

UNIV. OF HAWAII
Hamilton Library
Govt. Documents Collection
2550 The Mall
Honolulu, HI 96822
(808) 948-8230 Fax: (808) 956-5968

IDAHO

UNIV. OF IDAHO LIBRARY
Documents Section
Rayburn Street
Moscow, ID 83844-2353
(208) 885-6344 Fax: (208) 885-6817

ILLINOIS

ILLINOIS STATE LIBRARY
Federal Documents Dept.
300 South Second Street
Springfield, IL 62701-1796
(217) 782-7596 Fax: (217) 782-6437

INDIANA

INDIANA STATE LIBRARY
Serials/Documents Section
140 North Senate Avenue
Indianapolis, IN 46204-2296
(317) 232-3679 Fax: (317) 232-3728

IOWA

UNIV. OF IOWA LIBRARIES
Govt. Publications
Washington & Madison Streets
Iowa City, IA 52242-1166
(319) 335-5926 Fax: (319) 335-5900

KANSAS

UNIV. OF KANSAS
Govt. Documents & Maps Library
6001 Malott Hall
Lawrence, KS 66045-2800
(913) 864-4660 Fax: (913) 864-3855

KENTUCKY

UNIV. OF KENTUCKY
King Library South
Govt. Publications/Maps Dept.
Patterson Drive
Lexington, KY 40506-0039
(606) 257-3139 Fax: (606) 257-3139

LOUISIANA

LOUISIANA STATE UNIV.
Middleton Library
Govt. Documents Dept.
Baton Rouge, LA 70803-3312
(504) 388-2570 Fax: (504) 388-6992

LOUISIANA TECHNICAL UNIV.
Prescott Memorial Library
Govt. Documents Dept.
Ruston, LA 71272-0046
(318) 257-4962 Fax: (318) 257-2447

MAINE

UNIV. OF MAINE
Raymond H. Fogler Library
Govt. Documents Dept.
Orono, ME 04469-5729
(207) 581-1673 Fax: (207) 581-1653

MARYLAND

UNIV. OF MARYLAND - COLLEGE PARK
McKeldin Library
Govt. Documents/Maps Unit
College Park, MD 20742
(301) 405-9165 Fax: (301) 314-9416

MASSACHUSETTS

BOSTON PUBLIC LIBRARY
Govt. Documents
666 Boylston Street
Boston, MA 02117-0286
(617) 536-5400, ext. 226
Fax: (617) 536-7758

MICHIGAN

DETROIT PUBLIC LIBRARY
5201 Woodward Avenue
Detroit, MI 48202-4093
(313) 833-1025 Fax: (313) 833-0156

LIBRARY OF MICHIGAN
Govt. Documents Unit
P.O. Box 30007
717 West Allegan Street
Lansing, MI 48909
(517) 373-1300 Fax: (517) 373-3381

MINNESOTA

UNIV. OF MINNESOTA
Govt. Publications
409 Wilson Library
309 19th Avenue South
Minneapolis, MN 55455
(612) 624-5073 Fax: (612) 626-9353

MISSISSIPPI

UNIV. OF MISSISSIPPI
J.D. Williams Library
106 Old Gym Bldg.
University, MS 38677
(601) 232-5857 Fax: (601) 232-7465

MISSOURI

UNIV. OF MISSOURI - COLUMBIA
106B Ellis Library
Govt. Documents Sect.
Columbia, MO 65201-5149
(314) 882-6733 Fax: (314) 882-8044

MONTANA

UNIV. OF MONTANA
Mansfield Library
Documents Division
Missoula, MT 59812-1195
(406) 243-6700 Fax: (406) 243-2060

NEBRASKA

UNIV. OF NEBRASKA - LINCOLN
D.L. Love Memorial Library
Lincoln, NE 68588-0410
(402) 472-2562 Fax: (402) 472-5131

NEVADA

THE UNIV. OF NEVADA LIBRARIES
Business and Govt. Information Center
Reno, NV 89557-0044
(702) 784-6579 Fax: (702) 784-1751

NEW JERSEY

NEWARK PUBLIC LIBRARY
Science Div. - Public Access
P.O. Box 630
Five Washington Street
Newark, NJ 07101-7812
(201) 733-7782 Fax: (201) 733-5648

NEW MEXICO

UNIV. OF NEW MEXICO
General Library
Govt. Information Dept.
Albuquerque, NM 87131-1466
(505) 277-5441 Fax: (505) 277-6019

NEW MEXICO STATE LIBRARY
325 Don Gaspar Avenue
Santa Fe, NM 87503
(505) 827-3824 Fax: (505) 827-3888

NEW YORK

NEW YORK STATE LIBRARY
Cultural Education Center
Documents/Gift & Exchange Section
Empire State Plaza
Albany, NY 12230-0001
(518) 474-5355 Fax: (518) 474-5786

NORTH CAROLINA

UNIV. OF NORTH CAROLINA - CHAPEL HILL
Walter Royal Davis Library
CB 3912, Reference Dept.
Chapel Hill, NC 27514-8890
(919) 962-1151 Fax: (919) 962-4451

NORTH DAKOTA

NORTH DAKOTA STATE UNIV. LIB.
Documents
P.O. Box 5599
Fargo, ND 58105-5599
(701) 237-8886 Fax: (701) 237-7138

UNIV. OF NORTH DAKOTA
Chester Fritz Library
University Station
P.O. Box 9000 - Centennial and University Avenue
Grand Forks, ND 58202-9000
(701) 777-4632 Fax: (701) 777-3319

OHIO

STATE LIBRARY OF OHIO
Documents Dept.
65 South Front Street
Columbus, OH 43215-4163
(614) 644-7051 Fax: (614) 752-9178

OKLAHOMA

OKLAHOMA DEPT. OF LIBRARIES
U.S. Govt. Information Division
200 Northeast 18th Street
Oklahoma City, OK 73105-3298
(405) 521-2502, ext. 253
Fax: (405) 525-7804

OKLAHOMA STATE UNIV.
Edmon Low Library
Stillwater, OK 74078-0375
(405) 744-6546 Fax: (405) 744-5183

OREGON

PORTLAND STATE UNIV.
Branford P. Millar Library
934 Southwest Harrison
Portland, OR 97207-1151
(503) 725-4123 Fax: (503) 725-4524

PENNSYLVANIA

STATE LIBRARY OF PENN.
Govt. Publications Section
116 Walnut & Commonwealth Ave.
Harrisburg, PA 17105-1601
(717) 787-3752 Fax: (717) 783-2070

SOUTH CAROLINA

CLEMSON UNIV.
Robert Muldrow Cooper Library
Public Documents Unit
P.O. Box 343001
Clemson, SC 29634-3001
(803) 656-5174 Fax: (803) 656-3025

UNIV. OF SOUTH CAROLINA
Thomas Cooper Library
Green and Sumter Streets
Columbia, SC 29208
(803) 777-4841 Fax: (803) 777-9503

TENNESSEE

UNIV. OF MEMPHIS LIBRARIES
Govt. Publications Dept.
Memphis, TN 38152-0001
(901) 678-2206 Fax: (901) 678-2511

TEXAS

TEXAS STATE LIBRARY
United States Documents
P.O. Box 12927 - 1201 Brazos
Austin, TX 78701-0001
(512) 463-5455 Fax: (512) 463-5436

TEXAS TECH. UNIV. LIBRARIES
Documents Dept.
Lubbock, TX 79409-0002
(806) 742-2282 Fax: (806) 742-1920

UTAH

UTAH STATE UNIV.
Merrill Library Documents Dept.
Logan, UT 84322-3000
(801) 797-2678 Fax: (801) 797-2677

VIRGINIA

UNIV. OF VIRGINIA
Alderman Library
Govt. Documents
University Ave. & McCormick Rd.
Charlottesville, VA 22903-2498
(804) 824-3133 Fax: (804) 924-4337

WASHINGTON

WASHINGTON STATE LIBRARY
Govt. Publications
P.O. Box 42478
16th and Water Streets
Olympia, WA 98504-2478
(206) 753-4027 Fax: (206) 586-7575

WEST VIRGINIA

WEST VIRGINIA UNIV. LIBRARY
Govt. Documents Section
P.O. Box 6069 - 1549 University Ave.
Morgantown, WV 26506-6069
(304) 293-3051 Fax: (304) 293-6638

WISCONSIN

ST. HIST. SOC. OF WISCONSIN LIBRARY
Govt. Publication Section
816 State Street
Madison, WI 53706
(608) 264-6525 Fax: (608) 264-6520

MILWAUKEE PUBLIC LIBRARY
Documents Division
814 West Wisconsin Avenue
Milwaukee, WI 53233
(414) 286-3073 Fax: (414) 286-8074

•U.S. GOVERNMENT PRINTING OFFICE: 1995-387-253/20010

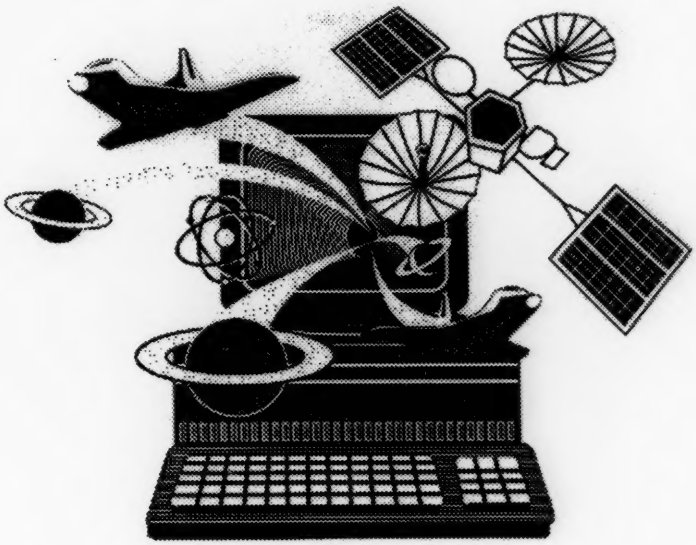

SCAN Goes Electronic!

If you have NASA Mail or if you can access the Internet, you can get biweekly issues of *SCAN* delivered to your desk—top absolutely free!

Electronic SCAN takes advantage of computer technology to alert you to the latest aerospace-related, worldwide scientific and technical information that has been published.

No more waiting while the paper copy is printed and mailed to you. You can review *Electronic SCAN* the same day it is released! And you get all 191—or any combination of—subject areas of announcements with abstracts to browse at your leisure. When you locate a publication of interest, you can print the announcement or electronically add it to your publication order list.

Electronic SCAN
Timely
Flexible
Complete
Free!

Start your free access to *Electronic SCAN* today. Over 1,000 announcements of new reports, books, conference proceedings, journal articles . . . and more—delivered to your computer every two weeks.

For instant access via Internet:
ftp.sti.nasa.gov
gopher.sti.nasa.gov
listserv@sti.nasa.gov

For additional information:
e-mail: help@sti.nasa.gov
scan@sti.nasa.gov
(Enter this address on the "To" line. Leave the subject line blank and send. You will receive an automatic reply with instructions in minutes.)

Phone: (301) 621-0390 Fax: (301) 621-0134

Write: NASA Access Help Desk
NASA STI Office
NASA Center for AeroSpace Information
800 Elkridge Landing Road
Linthicum Heights, MD 21090-2934

National Aeronautics and Space Administration
Scientific and Technical Information Office

4/95

National Aeronautics and
Space Administration
Code JT
Washington, DC 20546-0001

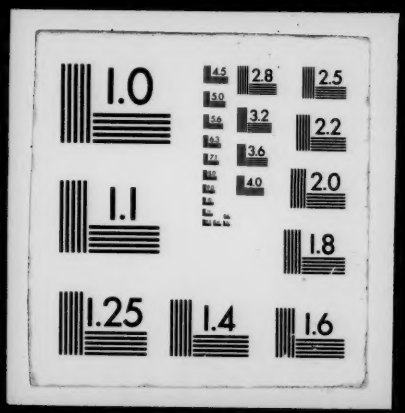
1.0
1.1
1.25
1.4
1.6
1.8
2.0
2.2
2.5
2.8
3.2
3.6
4.0
4.5
5.0
5.6
6.3
7.1
8.0
9.0